Traditional Poster

Motion Correction

Exhibition Hall 1272-1296 Monday 8:15 - 10:15

1272 

Joint Reconstruction of Simultaneous PET/MR Imaging with Motion Correction Using a B-spline Motion Model

Junshen Xu[1], Yibo Zhao[1], and Kui Ying[2]

[1]Department of Engineering Physics, Tsinghua University, Beijing, People's Republic of China, [2]Key Laboratory of Particle and Radiation Imaging, Ministry of Education, Medical Physics and Engineering Institute, Department of Engineering Physics, Tsinghua University, Beijing, People's Republic of China

Joint Reconstruction (JR) is an important approach to utilize the similarity of PET and MRI in simultaneous PET/MR imaging. For now, almost all the JR models ignore the effect of motion during scan, leading to blurring in images. We propose a motion correction method under the framework of JR, assuming that PET images and MRI images share exactly the same motion field and using a B-spline free deformation model to describe the motion. Both simulation and patient study show that the proposed method can reduce the blurring caused by motion in PET and MR images.

1273 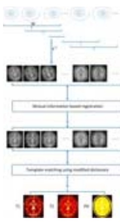

Motion Correction for Magnetic Resonance Fingerprinting by Using Sliding-Window Reconstruction and Image Registration

Zhongbiao Xu[1], Mengye Lyu[2,3], Edward Hui[4], Yingjie Mei[1,5], Zhifeng Chen[6], Wufan Chen[1], Ed X. Wu[2,3], and Yanqiu Feng[1]

[1]School of Biomedical Engineering, Guangdong Provincial Key Laboratory of Medical Image Processing, Southern Medical University, Guangzhou, People's Republic of China, [2]laboratory of Biomedical Imaging and Signal Processing, The University of Hong Kong, Hong Kong SAR, People's Republic of China, [3]Department of Electrical and Electronic Engineering,The University of Hong Kong, Hong Kong SAR, People's Republic of China, [4]Department of Diagnostic Radiology, The University of Hong Kong, Hong Kong SAR, People's Republic of China, [5]Philips Healthcare, Guangzhou, People's Republic of China, [6]Department of Biomedical Engineering, Zhejiang University, Hangzhou, People's Republic of China

The recently proposed magnetic resonance fingerprinting (MRF) technique demonstrates to be motion insensitive, but the early motion during the acquisition can still lead to severe errors in parameter quantification. In this study, we present a novel motion correct method for MRF based on sliding-window reconstruction and image registration.

1274 

Quantitative evaluation of prospective motion correction for structural imaging at 7T

Alessandro Sciarra[1], Hendrik Mattern[1], Renat Yakupov[1], Daniel Stucht[1], Peter Schulze[1], Frank Godenschweger[1], and Oliver Speck[1,2,3,4]

[1]Department of Biomedical Magnetic Resonance, Otto-von-Guericke University, Magdeburg, Germany, [2]German Center for Neurodegenerative Diseases, Magdeburg, Germany, [3]Center for Behavioral Brain Sciences, Magdeburg, Germany, [4]Leibniz Institute for Neurobiology, Magdeburg, Germany

The problem of motion in MRI scan still remains prevalent for many applications and numerous solutions for motion correction in MRI have been proposed to improve the image quality in presence of motion. Prospective motion correction using an optical tracking system has the advantage that it allows to eliminate motion artifacts without prolonging the overall scan time. In this study, we scanned healthy subjects at 7T with high resolution structural imaging sequences for diverse range of contrasts, which are commonly used in neuroscience applications. The final results show an improved image quality and a great potential of prospective motion correction.

1275 

Validating the accuracy and effectiveness of Prospective Motion Correction on rsfMRI

Pei Huang[1], David Hayes[1], and Marta Correia[1]

[1]Cognition and Brain Science Unit, MRC, Cambridge, United Kingdom

Prospective motion correction for MRI has been shown to greatly improve image quality for structural scans but its impact on fMRI data is still unclear. In this work, we studied the effectiveness of prospective motion correction by analysing the accuracy of the tracking system and looking at the effects of motion correction on resting-state fMRI with no instructed subject motion.

1276 

Quantifying the effectiveness of Prospective Motion Correction using a Visual fMRI task

Pei Huang[1], Nikolaus Kriegeskorte[1], Richard Henson[1], Arjen Alink[2], and Marta Correia[1]

[1]Cognition and Brain Science Unit, MRC, Cambridge, United Kingdom, [2]Department of Systems Neuroscience, University Medical Centre Hamburg-Eppendorf, Hamburg, Germany

Prospective Motion Correction (PMC) using an optical tracking system has been shown to improve data quality. We conducted a study on 18 subjects using robust visual stimuli to quantify the effectiveness of PMC on task-based fMRI. Our results show that PMC improves voxel-to-voxel registration across time and leads to better contrast-to-noise ratio. This is particularly evident in analyses which are more sensitive to inaccurate voxel registration and motion-induced noise.

1277 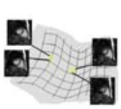

Free breathing & ungated cardiac cine MRI using joint smoothness regularization on image and patch manifolds (j-STORM)

Ankit Parekh[1], Sunrita Poddar[1], Xiaoming Bi[2], Dingxin Wang[2], and Mathews Jacob[1]

[1]Electrical and Computer Engineering, University of Iowa, Iowa City, IA, United States, [2]MR R&D, Siemens Healthcare, United States

A joint manifold smoothness regularization scheme (j-STORM) is proposed for free-breathing and ungated cardiac CINE imaging. The proposed method assumes that the images and square shaped image patches of the dynamic dataset live on a smooth, but separate, low-dimensional manifolds. We compare the reconstruction of two datasets from their highly undersampled measurements with the proposed j-STORM method to the image manifold smoothness scheme (STORM). The proposed scheme considerably reduces the streaking-artifacts present when only image manifold smoothness regularization is used and not the patch manifold smoothness.

1278 

Automatic reference-free detection and quantification of MR image artifacts in human examinations due to motion

Thomas Küstner[1,2], Annika Liebgott[1,2], Lukas Mauch[2], Petros Martirosian[3], Konstantin Nikolaou[1], Fritz Schick[3], Bin Yang[2], and Sergios Gatidis[1]

[1]Department of Radiology, University of Tuebingen, Tuebingen, Germany, [2]Institute of Signal Processing and System Theory, University of Stuttgart, Stuttgart, Germany, [3]Section on Experimental Radiology, University of Tuebingen, Tuebingen, Germany

MRI has a broad range of applications due to its flexible acquisition capabilities. This demands profound knowledge and careful parameter adjustment to identify stable sets which guarantee a high image quality for various and, especially in examinations of patients, unpredictable conditions. This complex nature and long examination times make it susceptible to artifacts which can markedly reduce the diagnostic image quality. An early detection and possible correction of these artifacts is desired. In this work we propose a convolutional neural network to automatically detect, localize and quantify motion artifacts. Initial results in the head and abdomen demonstrate the method's potential.

1279 

Gating PET data for cardiac imaging with radial MRI data

Daniel Spitzer[1], Klaus Schaefers[2], Lynn Frohwein[2], Bjoern Czekalla[2], Florian Buether[2,3], and Cornelius Faber[1]

[1]Department of Clinical Radiology, University of Muenster, Muenster, Germany, [2]European Institute for Molecular Imaging, University of Muenster, Muenster, Germany, [3]Department of Nuclear Medicine, University Hospital Muenster, Muenster, Germany

The increasing availability of MR/PET scanners opens new perspectives for cardiac imaging. However, technical issues for the reconstruction of signal from the moving myocardium remain to be solved. Using the k-space center in radial cardiac MRI data allows for generating a robust gating signal. Here, MR data acquired with a radial FLASH sequence in a 3 T MR/PET scanner continuously during a 15 minutes PET acquisition were used for retrospective gating. The k-space center magnitude was used to sort MRI and PET data into different cardiac phases while respiration-corrupted data were excluded, resulting in well separated cardiac phases.

1280 

Subject-specific 3D Modeling of Macaque Brain via Automatic Tissue Registration Based on in vivo MR Images Acquired at 7T

Weidao Chen[1,2], Bo Peng[3], Yi Sun[4], Gang Chen[1,2], Anna Wang Roe[1,2], Yakang Dai[3], and Xiaotong Zhang[1,2]

[1]Interdisciplinary Institute of Neuroscience and Technology, Zhejiang University, Hangzhou, People's Republic of China, [2]College of Biomedical Engineering & Instrument Science, Zhejiang University, Hangzhou, People's Republic of China, [3]Medical Imaging Department, Suzhou Institute of Biomedical Engineering and Technology, Chinese Academy of Sciences, Suzhou, People's Republic of China, [4]MR Collaboration Northeast Asia, Siemens Healthcare, Shanghai, People's Republic of China

Accurate subject-specific 3D modeling of macaque brain with anatomical subdivisions is important for neuroscience, neurophysiology and engineering researches. In this study, we have proposed a feasible approach for automatically creating 3D models of macaque brain based on in vivo MR images. A 3D template of macaque brain, consisting of scalp, skull, grey matter, white matter, and cerebrospinal fluid, was firstly constructed from 7T T1w images over an anesthetized macaque; then, by implementing symmetric feature-based pairwise registration method, this template was used to register another in vivo 7T dataset of macaque brain, which enables automatic and subject-specific 3D macaque brain modeling.

1281 

Estimating the bias associated with image registration in MRI

Riccardo Metere[1], Pierre-Louis Bazin[1], and Harald E. Möller[1]

[1]NMR Unit, Max Planck Institute for Human Cognitive and Brain Sciences, Leipzig, Germany

The most promising techniques for understanding the biophysical basis of the MRI signals rely on combining multi-modal quantitative maps as a source of spatially-resolved information. If the MRI maps are not obtained from simultaneous acquisitions, they need to be co-registered in order to ensure a consistent localization of the signal sources for pixel-by-pixel fitting. However, the effects of the co-registration step are notoriously difficult to quantify. Here, we present a method for investigating the bias associated with co-registration for different quantitative MRI acquisitions, and outline the relevance of these biases for multi-parameter analysis.

1282 

A Retrospective Cardiac Gating Method using Simultaneously Acquired Navigator

Byungjai Kim[1], Hyunseok Seo[1], Dongchan Kim[1], Jaejin Cho[1], Kinam Kwon[1], Seohee So[1], Kyungtak Min[1], Yoonmee Lee[1], Youngwoo Park[1], and Hyunwook Park[1]

[1]Korea Advanced Institute of Science and Technology, Daejeon, Korea, Republic of

A cardiac gating method using a navigator MR signal requires the additional acquisition steps interleaved with the acquisition of image signals. To eliminate the additional acquisitions for navigators, the proposed method obtains an image signal and a navigator signal at the same time, and separates them in post-processing. Cardiac motion information estimated from the separated navigators is used for retrospective cardiac gating. To demonstrate the feasibility of the proposed method, in-vivo experiments were performed for cardiac MRI with short axis view.

1283

Prospective Self-Gating For Cardio-Respiratory Synchronised Imaging in the Mouse.

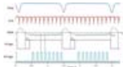

Paul Kinchesh[1], Boris Vojnovic[1], Stuart Gilchrist[1], Robert Newman[1], and Sean Smart[1]

[1]Oxford Institute for Radiation Oncology, University of Oxford, Oxford, United Kingdom

Prospective cardio-respiratory self-gating is demonstrated in the mouse. A gradient echo scan operating at constant TR enabled acquisition of CINE data blocks or maintenance of the NMR steady state depending on the level of a gating control signal that was evaluated within each TR. A portion of the FID during each TR was submitted to a signal processor chain for streaming into a pseudo-continuous analogue cardio-respiratory signal trace and conversion to a series of logic control signals for gating.

1284 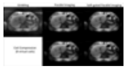

Fast motion robust abdominal stack of stars imaging using coil compression and soft gating

Tao Zhang[1], Ty A Cashen[2], Kang Wang[2], André Fischer[3,4], and Ersin Bayram[1]

[1]Global MR Applications and Workflow, GE Healthcare, Houston, TX, United States, [2]Global MR Applications and Workflow, GE Healthcare, Madison, WI, United States, [3]GE Global Research Europe, Garching bei München, Germany, [4]Cardiac Center of Excellence, GE Healthcare, Garching bei München, Germany

Stack of stars trajectory with golden angle ordering provides better motion robustness than Cartesian imaging for abdominal MRI. However, image reconstruction for non-Cartesian datasets is usually time-consuming, especially for datasets with high-density coil arrays. While additional motion correction methods can improve image quality for stack of stars, they often further increase the reconstruction time. In this work, we aim to reduce the reconstruction time for stack of stars using coil compression and improve motion robustness with a similar reconstruction time using soft gating.

1285 

Golden-angle Sparse Liver Imaging: Radial or Cartesian Sampling?

Li Feng[1], Hersh Chandarana[1], Tiejun Zhao[2], Mary Bruno[1], Daniel K Sodickson[1], and Ricardo Otazo[1]

[1]Center for Advanced Imaging Innovation and Research (CAI2R), New York University School of Medicine, New York, NY, United States, [2]Siemens Healthineers, New York, USA

This work compares golden-angle stack-of-stars sampling and golden-angle Cartesian sampling for free-breathing liver MRI with eXtra-Dimensional (XD) compressed sensing reconstruction. For Cartesian sampling, the phase-encoding steps in the k_y-k_z plane are segmented into multiple interleaves that rotate at a golden angle. Each interleave starts from the center (k_y=k_z=0) of k-space and follows a pseudo-radial pattern on a Cartesian grid. Results from this initial study suggest that golden-angle Cartesian sampling achieves higher effective spatial resolution than radial sampling, but it still suffers from residual ghosting artifacts due to respiratory motion for free-breathing liver imaging.

1286 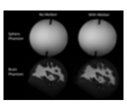

Motion-Correction Testing with an Anthropomorphic Brain Phantom

Kyoko Fujimoto[1,2], Trent V. Robertson[2], Vanessa Douet[2], Thomas Ernst[1,2], David G. Garmire[1], and V.Andrew Stenger[1,2]

[1]Department of Electrical Engineering, University of Hawaii at Manoa, Honolulu, HI, United States, [2]Department of Medicine, John A. Burns School of Medicine, University of Hawaii, Honolulu, HI, United States

Motion-correction (MoCo) techniques enable clinicians to obtain high-quality MR images with decreased artifact from patient movement. MoCo methods can be tested on a phantom, but it is difficult to fully observe the benefits of MoCo on a simple phantom. In this study, we propose an anthropomorphic brain phantom with white matter and gray matter structure to work with a pneumatic motion simulator and demonstrate a practical application in a simulated motion study.

1287 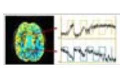

How to correct block design task-induced coherent head motion; Evaluation of retrospective motion correction methods in HCP fMRI

Wanyong Shin[1], Erik Beall[1], and Mark J Lowe[1]

[1]Radiology, Cleveland Clinic, Cleveland, OH, United States

Participants in block design finger tapping fMRI have a tendency to have paradigm coherent head motion. This finding appears to be very strong in HCP data, which utilizes spatially and temporally accelerated SMS sequence. We have introduced slice-oriented motion correction method (SLOMOCO[1]), and found SLOMOCO removed the head motion efficiently in HCP data, especially in the case that head motion pattern is synchronized to task paradigm. In this study, we compared the various motion correction methods in finger tapping fMRI HCP data.

1288 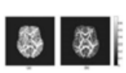

Phase-based Motion Detection for Diffusion Magnetic Resonance Imaging

Nahla M H Elsaid[1], Steven Roys[1], Maureen Stone[2], Rao P Gullapalli[1], Jerry L Prince[3], and Jiachen Zhuo[1]

[1]Diagnostic Radiology, University of Maryland School of Medicine, Baltimore, MD, United States, [2]Neural and Pain Sciences and Orthodontics, University of Maryland Dental School, Baltimore, MD, United States, [3]Electrical and Computer Engineering, Johns Hopkins University, Baltimore, MD, United States

Diffusion-weighted imaging is sensitive to subject motion. Even small subject motion induces dramatic spin phase changes, allowing phase map to have higher sensitivity than the magnitude images to detect subtle motion. In this study, we derived metrics based on the Haralick features in DWI phase maps for automatic motion detection and data rejection in diffusion-weighted imaging data. The motion detection method is validated against motion tracked by an external electromagnetic motion tracking sensor.

1289 

Motion Artifacts Reduction by Parallel Acquisition with Non-prolonged Deghosting Algorithm (PANDA)

Gaojie Zhu[1], Xiang Zhou[1], Hai Luo[1], Bin Wang[1], Xia Liu[1], Ziyue Wu[2], Leping Zha[1,2], and Qing-San Xiang[3]

[1]Advanced Applications, Alltech Medical Systems, Chengdu, People's Republic of China, [2]Advanced Applications, Alltech Medical Systems America, Solon, OH, United States, [3]Radiology, University of British Columbia, Vancouver, BC, Canada

Patient motion produces artifacts in MRI due to k-space data corruption. Ghosted images can be considered as a combination of ghost-free images and ghost masks. If two ghosted images contain the same ghost-free image component and different ghost components, the images and the ghost components can be separated. For images fully sampled with array coils, multiple images can be produced with parallel reconstruction with differently selected raw data subsets. In this work, we propose a new motion artifacts reduction algorithm, which regenerates a new k-space dataset based on data consistency, and then decomposes images into mostly ghost-free images and ghost masks.

1290

A Hybrid ECG/Self-Navigation Technique

Artan Kaso[1], Bernd Juergen Wintersperger[1,2], Mariana Lamacie[1], and Marshall Stephen Sussman[1,2]

[1]Medical Imaging, University Health Network, Toronto, ON, Canada, [2]Medical Imaging, University of Toronto, Toronto, ON, Canada

In self-navigation, cardiac and respiratory information is extracted from the MR signal. ECG and conventional navigator echoes are not required. Conventional navigators disrupt the steady state and add delays. Thus, self-navigation provides a clear advantage. However, ECG is monitored independently of the MR acquisition. Therefore, eliminating the ECG needlessly throws away information. In this study, a hybrid ECG/self-navigated sequence is developed. ECG is used for cardiac triggering. Self-navigation is used for respiratory compensation, and to provide additional cardiac gating. In 10 healthy volunteers, the ECG/self-navigation sequence provided equivalent image quality and quantitative cardiac metrics as a reference breath-hold scan.

1291

Correction of Ghosting Due to Respiration-induced B0 Variation in Double Echo Steady State (DESS) Breast Imaging: Initial Validation

Catherine J Moran[1], Brady Quist[1], Marcus T Alley[1], Akshay S Chaudhari[1], Bruce L Daniel[1], and Brian A Hargreaves[1]

[1]Radiology, Stanford University, Stanford, CA, United States

Double Echo Steady State (DESS) breast imaging for T2 and diffusion-weighted imaging in the breast is limited due to prominent ghosting artifacts. While actual respiratory motion of the breast tissue is minimal due to the prone position of the patient as well as immobilization paddles on the coil, respiratory-induced B0-variation is a source of ghosting. A method based on a per-TR off-resonance estimate and simulated phase data for correction of ghosting artifacts in DESS in the breast is described and validated in eight breast cancer patients. The new method effectively reduces ghosting artifact greatly improving image quality.

1292

Markerless Optical Tracking for Motion Correction in MR and PET/MR Imaging of the Brain

Julian Maclaren[1], Andre Kyme[2], Murat Aksoy[1], Benjamin Zahneisen[1], and Roland Bammer[1]

[1]Department of Radiology, Stanford University, Stanford, CA, United States, [2]Brain and Mind Centre, University of Sydney, Sydney, Australia

Optical prospective motion correction using markers attached to the patient’s head has been widely demonstrated to improve image quality in MRI of the brain. To simplify patient workflow, it would be helpful to remove the need for the marker. We have previously demonstrated markerless tracking using a stereo camera system, but this was done outside of the MR environment and used a 6-axis robot to validate tracking. In this work, we demonstrate markerless optical tracking in two volunteers during simultaneous MRI and use the markerless tracking data to retrospectively realign images.

1293

Image registration with structuralized Mutual Information: application to CEST

Bian Li[1], Huajun She[1], Shu Zhang[1], Jochen Keupp[2], Ivan Dimitrov[3], Albert Montillo[1], Ananth Madhuranthakam[1], Robert Lenkinski[1], and Elena Vinogradov[1]

[1]Department of Radiology, Advanced Imaging Research Center, UT Southwestern Medical Center, Dallas, TX, United States, [2]Philips Research, Hamburg, Germany, [3]Philips Healthcare, Gainesville, FL, United States

In image registration, mutual information (MI) has proved to be an effective similarity measure and is widely used for medical image registration. However, the MI algorithm does not consider spatial dependencies of voxels and introduces significant errors when registering images with large intensity changes, like in Z-spectral images of CEST-MRI. This abstract shows that by the incorporation of structural information the SMI algorithm demonstrates robust performance registering Z-spectral images with large and complex intensity variations.

1294

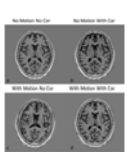

Synthetic MRI with Prospective Motion Correction

Murat Aksoy[1], Julian Maclaren[1], Dan Rettmann[2], Roland Bammer[1], and Ajit Shankaranarayanan[3]

[1]Radiology, Stanford University, Stanford, CA, United States, [2]Global MR Applications & Workflow, GE Healthcare, Rochester, MN, United States, [3]Global MR Applications & Workflow, GE Healthcare, Menlo Park, CA, United States

Quantification of tissue parameters such as T1, T2 and PD has gained significant interest due to potential applications in characterization of certain pathologies (Alzheimer’s, multiple sclerosis, etc.). One such technique, called “Synthetic MRI”, utilizes a fast spin echo (FSE) readout with inversion recovery in order to simultaneously get T1, T2 and PD maps using a single scan. In this abstract, we demonstrated that application of optical motion correction to simultaneous T1, T2 and PD quantification.

1295

Motion-corrected image reconstruction of abdominal DCE-MRI images

Adam Johansson[1], James Balter[1], and Yue Cao[1,2,3]

[1]Department of Radiation Oncology, University of Michigan, Ann Arbor, MI, United States, [2]Department of Radiology, University of Michigan, Ann Arbor, MI, United States, [3]Department of Biomedical Engineering, University of Michigan, Ann Arbor, MI, United States

Respiratory motion of abdominal organs causes motion artifacts, blur and signal loss in DCE-MRI images which can confound liver perfusion quantification. To correct for respiratory motion a motion signal derived using rigid-body image registration was used to group acquired data from a golden-angle stack-of-stars sequence into motion states. These were then aligned using deformable image registration and the resulting deformation vector fields were used to deform complex projection images reconstructed from individual spokes. Deformed projections were finally combined using view-sharing into an image time series. The resulting portal-venous input function exhibited a higher signal enhancement and no breathing-induced intensity ripples.

1296

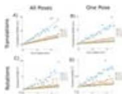

From Hand-Eye Calibration of Optical Tracking Cameras to Motion Correction

James A. Smith[1], Olivier E. Mougin[1], Maxim Zaitsev[2], Benjamin Knowles[2], Richard W. Bowtell[1], Paul M. Glover[1], and Penny A. Gowland[1]

[1]Sir Peter Mansfield Imaging Centre, University of Nottingham, Nottingham, United Kingdom, [2]Department of Radiology, University Medical Center Freiburg, Freiburg, Germany

For motion correction using an optical tracking camera, movements must be converted from the camera reference frame to the MR reference frame. This calibration transform is determined by matching poses recorded in both reference frames. We investigated the impact that errors in one or more of these poses has on the resulting calibration. We then investigated the impact that errors in calibration has upon the apparent motion recorded. Thus we outline the necessary precision in the calibration poses to achieve motion correction of different precisions.

Traditional Poster

More Motion

Exhibition Hall 1297-1316 — Monday 8:15 - 10:15

1297

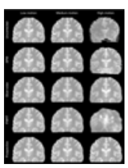

Evaluation of prospective and retrospective motion correction exploiting the slice-based acquisition of fMRI

Malte Hoffmann[1] and Stephen J Sawiak[1,2]

[1]Wolfson Brain Imaging Centre, Department of Clinical Neurosciences, University of Cambridge, Cambridge, United Kingdom, [2]Behavioural and Clinical Neuroscience Institute, Department of Psychology, University of Cambridge, Cambridge, United Kingdom

Motion artefacts are damaging to fMRI studies, masking real effects or forcing data to be discarded. Standard processing pipelines include linear registration steps between frames, though some groups proposed prospectively exploiting the slice-based nature of acquisition. The improvement this offers is rarely quantified as no “baseline” is available. Here, we simulated MRI acquisitions with a general slice-based navigation method to quantify the accuracy of prospective correction over retrospective registration. Compared to retrospective linear and non-linear techniques, registration of individual slices most accurately matched trial motion trajectories with better image quality than linear methods.

1298

Measuring the accuracy of prospective motion correction through retroactive application of estimates

Henric Rydén[1], Enrico Avventi[1,2], Ola Norbeck[1,2], and Stefan Skare[1,2]

[1]Neuroradiology, Karolinska University Hospital, Stockholm, Sweden, [2]Department of Clinical Neuroscience, Karolinska Institutet, Stockholm, Sweden

Several prospective motion correction methods have been presented to address the issue of motion induced artifacts in MRI. We present a method to determine the accuracy of prospective motion correction methods by applying estimates to a PROPELLER reconstruction.

1299

Correcting diffusion data for off-resonace effects, movement-induced signal loss and intra-volume movement.

Jesper L. R. Andersson[1], Mark S. Graham[2], Ivana Drobnjak[2], Hui Zhang[2], Nicola Filippini[1], and Matteo Bastiani[1]

[1]Oxford University, Oxford, United Kingdom, [2]University College London

An intra-volume movement model was added to an existing framework for correcting off-resonance distortions, movement-induced signal dropout and subject movement in diffusion data. It was validated on highly realistic simulated data with "normal" and "high" levels of subject movement. The results show that slice-wise movement parameters can be estimated with an accuracy of ~0.2mm and ~0.2degrees for translations and rotations respectively. The simulations also show that the method substantially decreases the difference in fidelity of FA between subjects who move a lot and subjects who move a little. We finally demonstrate how the method corrects telltale signs of intra-volume movement in real data.

1300

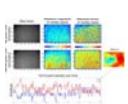

On the importance of skin color phase variations for video measurement of cardiac activity in MRI

Nicolai Spicher[1], Stephan Orzada[2], Stefan Maderwald[2], Markus Kukuk[1], and Mark E Ladd[2,3]

[1]University of Applied Sciences and Arts Dortmund, Dortmund, Germany, [2]Erwin L. Hahn Institute for Magnetic Resonance Imaging, University Duisburg-Essen, Essen, Germany, [3]Division of Medical Physics in Radiology, German Cancer Research Center, Heidelberg, Germany

The limitations of contact-based hardware for cardiac activity measurement in MRI (e.g. electrocardiography, pulse oximetry) might eventually be overcome by using videos of the skin. Currently, a limitation for practical usage is the poor signal-to-noise ratio of the acquired signals, especially in an MR environment. We analyzed pixel intensity variations over time measured on the forehead and observed that 15%-25% of pixels exhibit a different signal morphology and phase than the remaining pixels. This effect is a limitation for many algorithms related and unrelated to MRI: If all pixels within a region-of-interest are used for averaging, different signal types are mixed which biases results.

1301 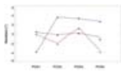 3D Motion Estimation of Head Using Three Orthogonal Navigator Echoes and Coil Sensitivity Profiles

Jiaen Liu[1], Peter van Gelderen[1], Jacco de Zwart[1], and Jeff Duyn[1]

[1]National Institute of Neurological Disorders and Stroke, National Institutes of Health, Bethesda, MD, United States

Subject motion is a common source of artifact in MRI scans. Various navigator techniques have been developed to monitor motion and correct motion artifacts. In this study, a new approach was developed to extract 3D motion information of the head based on three orthogonal 1D gradient-encoded echoes acquired in about 2 ms. Complementary positional information carried by the individual sensitivity profiles of a receive array was exploited. The method was evaluated in experiments. It suggested the estimated motion parameters were within ±0.5° and ±0.5 mm accuracy in reference to co-registered head images in various positions with rotations up to ±4°.

1302  Motion-induced Magnetic Field Changes Inside the Brain

Jiaen Liu[1], Jacco de Zwart[1], Peter van Gelderen[1], and Jeff Duyn[1]

[1]National Institute of Neurological Disorders and Stroke, National Institutes of Health, Bethesda, MD, United States

In this study, changes of the B_0 field inside the brain due to head motion were measured and analyzed. The sources contributing to this change include a static field introduced by the relative position of the head to the body and the shim coils, and a dynamic one from the head's orientation and its susceptibility. The experimental results suggest that the component from the head and/or body has a strong magnitude and complex spatial pattern, which makes it difficult to be measured with simple navigators. This B_0 field change should be properly taken into account for motion correction.

1303  High resolution free breathing abdominal imaging

Jan Hendrik Wülbern[1], Sven Kabus[1], Holger Eggers[1], and Peter Börnert[1]

[1]Philips Research Europe, Hamburg, Germany

The scan resolution of abdominal MR imaging using Cartesian sampling is generally limited by the breath-holding capability of the patient, as the respiratory motion would introduce ghosting artefacts. Here we show that golden-angle stack-of-stars sampling in combination with retrospective motion state binning and elastic registration enables sub millimeter in-plane scan resolutions. The technique allows the patient to breathe freely during the examination, hence improving the patient's comfort, and simultaneously increasing the achievable scan resolution.

1304  A Comparison of Prospective Motion Correction with 19F NMR Field Probes and an Optical Camera

Martin Eschelbach[1], Ali Aghaeifar[1], Jonas Bause[1], Jonas Handwerker[2], Jens Anders[2], Axel Thielscher[1,3], and Klaus Scheffler[1,4]

[1]High Field Magnetic Resonance Center, Max Planck Institute for Biological Cybernetics, Tuebingen, Germany, [2]Institute for Microelectronics, University of Ulm, Ulm, Germany, [3]Danish Research Centre for Magnetic Resonance, Copenhagen University Hospital Hvidovre, Copenhagen, Denmark, [4]Department of Biomedical Magnetic Resonance, University Clinic Tuebingen, Tuebingen, Germany

This work shows a comparison of prospective motion correction using NMR field probes and an optical tracking system in a phantom with induced motion as well as in an initial in vivo experiment. Tracking results for both systems were recorded concurrently to compare the motion estimates. The prospectively corrected images of a moving phantom and a moving human subject show a comparable correction ability for both systems. However, the lower precision of the field probe based system might prevent an application in highest-resolution imaging.

1305 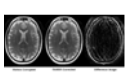 Retrospective motion correction of head rotations in 2D RARE brain images using TArgeted Motion Estimation and Reduction (TAMER)

Melissa W. Haskell[1,2], Stephen F. Cauley[1,3], and Lawrence L. Wald[1,3,4]

[1]A. A. Martinos Center for Biomedical Imaging, Department of Radiology, MGH, Charlestown, MA, United States, [2]Graduate Program in Biophysics, Harvard University, Cambridge, MA, United States, [3]Harvard Medical School, Boston, MA, United States, [4]Harvard-MIT Division of Health Sciences and Technology, MIT, Cambridge, MA, United States

RARE/TSE/FSE imaging is the most common brain sequence, but can be severely degraded by patient motion. While 2D navigated versions (PROPELLER) and motion-tracking approaches exist, they are not widely used. We introduced a data-consistency based retrospective method, TAMER, whereby the image and motion parameters are jointly estimated by minimizing data consistency error of a SENSE+motion forward model. We employ reduced modeling techniques which assess only a few targeted voxels at each step to make the large non-linear estimation problem computationally achievable. We demonstrate the approach to mitigating rotations in phantom and human scans in addition to previously reported translation mitigation.

1306  Impact of image registration on renal T1 mapping in children with chronic kidney disease

Fabio Nery[1], Enrico De Vita[2,3], Chris A. Clark[1], Isky Gordon[1], and David L. Thomas[3]

[1]UCL Great Ormond Street Institute of Child Health, Developmental Imaging and Biophysics Section, London, United Kingdom, [2]National Hospital for Neurology and Neurosurgery, Lysholm Department of Neuroradiology;, [3]UCL Institute of Neurology, Department of Brain Repair and Rehabilitation

Renal longitudinal relaxation time (T_1) is an established indicator of pathophysiological tissue status. We have applied image registration techniques to correct for motion during saturation recovery (SR) acquisitions with multiple recovery times used for T_1 mapping in kidneys of paediatric patients. All registration techniques were successful in improving the intra and inter-session repeatability of the T_1 estimates, as well as the quality of the underlying saturation recovery fits on a challenging patient population, as assessed by intra- and inter-scan repeatability and analysis of the root mean squared error of the SR fits.

1307

Ultrasound Monitoring of a Respiratory Phantom for the Development andValidation of Segmented EPI Reconstruction Methods

W. Scott Hoge[1], Frank R Preiswerk[1], Jonathan R Polimeni[2,3], Sanjay Yengul[1,4], Pelin Aksit Ciris[5], and Bruno Madore[1,3]

[1]Radiology, Brigham and Women's Hospital, Boston, MA, United States, [2]Radiology, Massachusetts General Hospital, MA, United States, [3]Harvard Medical School, Boston, MA, United States, [4]Boston University, Boston, MA, United States, [5]Dept. of Biomedical Engineering, Akdeniz University, Antalya, Turkey

In MRI, changes in lung volume can affect the static encoding field during brain imaging, inducing phase modulations in the acquired signal. In segmented EPI, these phase modulations manifest as ghost artifacts. To enable rapid development of new segmented EPI image formation methods, this work presents a respiratory phantom that can be monitored using an ultrasound transducer. Using inexpensive materials, the transducer tracks the thickness of a flexible water bottle as the respiratory phantom inflates/deflates. Results verify that phase changes induced by the changing air volume can be observed in both MR and ultrasound data, and are well correlated.

1308

Comparison of Multishot Readout-Segmented EPI and Interleaved-EPI for Motion Correction

Zijing Dong[1], Fuyixue Wang[1,2], Yishi Wang[1], and Hua Guo[1]

[1]Center for Biomedical Imaging Research, Department of Biomedical Engineering, School of Medicine, Tsinghua University, Beijing, People's Republic of China, [2]Harvard-MIT Health Sciences and Technology, MIT, Cambridge, MA, United States

Readout-segmented EPI (RS-EPI) and interleaved-EPI (iEPI) are the two most widely used multishot EPI techniques for high resolution DWI. Many methods have been proposed to correct the motion-induced phase variations and rigid-motion in RS-EPI and iEPI. To compare the performance of motion correction in RS-EPI and iEPI, DWI and DTI simulations were designed. The correction methods we implemented for RS-EPI and iEPI take account of motion-induced phase variation, bulk motion and altered diffusion gradient orientation due to rotation. In our test, iEPI show less artifacts, however the b-matrix correction of RS-EPI is more straightforward with better accuracy.

1309

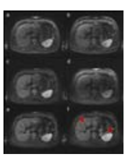

Readout-Segmented EPI with 2D-PACE for the Abdominal Diffusion Weighted Imaging

Wei Liu[1], Kun Zhou[1], and Fang Dong[1]

[1]Siemens Shenzhen Magnetic Resonance Ltd, Shenzhen, People's Republic of China

The 2D-PACE technique has been proved to be superior to conventional respiratory triggering techniques for imaging the abdominal region because it could detect more accurate respiratory waveform, which is already widely used in single shot EPI for high quality abdominal diffusion weighted imaging. The readout-segmented EPI features much shorter echo spacing compared with single shot EPI and consequently enjoys less distortion. In this study, the 2D-PACE technique is integrated into a readout-segmented EPI sequence and makes high resolution abdominal diffusion images with less distortion and image blurring.

1310

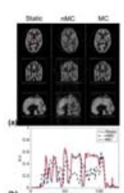

Unified Rigid Motion Compensation Using Wireless MR Active Markers for Simultaneous PET/MR Imaging of the Brain

Chang Gao[1], Chao Ma[2], Yibo Zhao[1], Kui Ying[1], Yoann Petibon[2], Jerome L. Ackerman[3], Chuan Huang[4], Georges El Fakhri[2], and Jinsong Ouyang[2]

[1]Engineering Physics, Tsinghua University, Beijing, People's Republic of China, [2]Gordon Center for Medical Imaging, Radiology, Massachusetts General Hospital, Harvard Medical School, Boston, MA, United States, [3]Athinoula A. Martinos Centerfor BiomedicalImaging, Radiology, Massachusetts General Hospital, Boston, MA, United States, [4]Radiology and Psychiatry, Stony Brook Medicine, Stony Brook, NY, United States

Head motion degrades image quality through loss of resolution in brain PET/MR. This work presents a wireless MR active marker based method to track and correct head motion for both PET and MRI. The proposed rigid motion correction method has been validated using a phantom study on a clinical PET/MR scanner.

1311

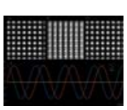

Motion simulation and correction validation using MR tagging

Ali Aghaeifar[1,2], Abbas Nasiraei Moghaddam[3], and Klaus Scheffler[1,4]

[1]Max Planck Institute for Biological Cybernetics, Tübingen, Germany, [2]IMPRS for Cognitive and Systems Neuroscience, University of Tübingen, Tübingen, Germany, [3]Biomedical engineering, Amirkabir University of Technology (Tehran Polytechnic), Tehran, Iran, [4]Department of Biomedical Magnetic Resonance, University of Tübingen, Tübingen, Germany

Involuntary subject motion is a well-known problem in MR imaging. Motion simulation is an important step to evaluate correction performance and motion induced artifacts. Here we introduce a new approach based on MR tagging to simulate desired motion pattern on a plain phantom. We employed SPAMM method to generate grid tags with a specified orientation and position. Grid tags were rotated and shifted with a desired pattern per TR. Correspondingly, the imaging slice followed the pattern to compensate the rotation and translation of the tags. Employing this approach, we could simulate motion in 5 DOF.

1312

Repeatability and motion-invariance of Zero Echo Time bone maps

Gaspar Delso[1], Florian Wiesinger[2], Yiqiang Jian[3], Shrikant Chikhalkar[3], Zhe Wang[3], Chad Bobb[3], David Goldhaber[3], and Floris Jansen[3]

[1]GE Healthcare, Cambridge, United Kingdom, [2]GE Global Research, Germany, [3]GE Healthcare, United States

The goal of the present study was to evaluate the repeatability of a ZTE-based bone imaging method with respect to clinically realistic variations of the ideal acquisition conditions.

1313

Rapid continuous multiarterial MRI of the hepatic arterial dominant phase during free-breathing.

Ahmed E Othman[1], Jakob Weiss[2], Christer Ruff[2], Manuel Kolb[2], Marcel Dominik Nickel[3], Peros Martirosian[2], Konstantin Nikolaou[2], and Mike Notohamiprodjo[2]

[1]Radiology, University Hospital Tübingen, Tübingen, Germany, [2]Radiology, University Hospital Tübingen, [3]Siemens Healthineers

Acquisition of continuous multiarterial MRI of hepatic arterial dominant phase during free-breathing using a free-breathing self-gated spoiled gradient-echo sequence with compressed sensing is feasible and yields excellent arterial enhancement with good compensation of respiratory artifacts and can improve robustness of arterial Phase liver MRI

1314

19F imaging with physiologic motion using UTE sequence with randomized spokes ordering

Bijaya Thapa[1,2], Kyle Jeong[1,3], Insun Lee[1], and Eun-Kee Jeong[1,4]

[1]Utah Center for Advanced Imaging Research, University of Utah, Salt Lake City, UT, United States, [2]Department of Physics and Astronomy, University of Utah, Salt Lake City, UT, United States, [3]Department of Biomedical Engeneering, Salt Lake City, UT, United States, [4]Department of Radiology and Imaging Sciences, University of Utah, Salt Lake City, UT, United States

3D radial, such as ultra-short TE (UTE) MRI, is insensitive to motion-related ghosting artifact, mainly because of heavy over-sampling at the k-space origin. However, using the smooth view ordering, of which direction of the readout gradient smoothly changes, any small portion of FID data with motion-corruption tends to be clustered, while directions of random view ordering are spread out over the entire 3D surface. In this work, we will compare the artifact induced by both motion and missing lines in 3D UTE MRI for smooth and random view orderings.

1315

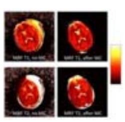

Application of retrospective motion correction to magnetic resonance fingerprinting

Mauro Costagli[1], Michela Tosetti[2,3], Graziella Donatelli[4], and Guido Buonincontri[2]

[1]IMAGO7 Research Institute, Pisa, Italy, [2]IMAGO7 Research Institute, [3]IRCCS Stella Maris, Pisa Italy, [4]Università di Pisa, Italy

The image quality of MRI exams is often poor in patients that cannot lay still or are unable to follow instructions. MR Fingerprinting is a novel technique with a greatly reduced sensitivity to patient motion and a short scan time. However, its images can still have artifacts when the degree of head movement is substantial. Here, we evaluate a novel motion correction scheme for MRF. Five subjects were instructed to intentionally move their head. In post-processing an iterative motion-correction algorithm was used on the anti-aliased image frames. When using our algorithm, we observed clearer images in all subjects, indicating that our technique can further increase the motion robustness of MRF.

1316

Motion detection in spectroscopy using FID navigators

Ryan Kalmoe[1], Edward J Auerbach[1], Malgorzata Marjańska[1], Patrick J Bolan[1], Ivan Tkac[1], Tobias Kober[2,3,4], and Gregory J Metzger[1]

[1]Center for Magnetic Resonance Research and Department of Radiology, University of Minnesota, Minneapolis, MN, United States, [2]Advanced Clinical Imaging Technology, Siemens Healthcare AG, Lausanne, Switzerland, [3]Department of Radiology, University Hospital (CHUV), Lausanne, Switzerland, [4]LTS5, École Polytechnique Fédérale de Lausanne, Lausanne, Switzerland

A free induction decay navigator (FIDnav) was implemented in a spectroscopic sequence to identify motion-corrupted spectra for retrospective rejection. An optimal channel combination of a weighted sum of channels based on the magnitude of a localized water reference signal allowed for improved identification of motion events. The FID navigator successfully detected motion events in both phantom studies and *in vivo* for both single voxel spectroscopy (SVS) and 2D chemical shift imaging (CSI). Removal of the motion-corrupted data based on the FIDnav is demonstrated to show improved spectral quality.

Traditional Poster

RF Pulse Design

Exhibition Hall 1317-1331 Monday 8:15 - 10:15

1317

Analytic description of the magnetisation phase during excitation

Bahman Tahayori[1,2], Zhaolin Chen[2], Gary Egan[2], and N. Jon Shah[1,2,3]

[1]Dept. Electrical and Computer Systems Engineering, Monash Institute of Medical Engineering, Monash University, Clayton, Australia, [2]Monash Biomedical Imaging, Monash University, Clayton, Australia, [3]Faculty of Medicine, Department of Neurology, JARA, RWTH Aachen University, Aachen, Germany

An approximate analytic expression is calculated for the phase of the transverse magnetisation during the excitation period. A spherical Bloch equation is used to find this expression. Simulation results are in agreement with the analytic solution. This analytic solution can be used where the phase information is required and, therefore, may be used to improve the performance of imaging through optimal pulse sequence design.

1318

Sheared 2DRF Excitation for Improved Off-resonance Robustness in Reduced FOV Imaging

Cagla Deniz Bahadir[1,2], Suchandrima Banerjee[3], Ajit Shankaranarayanan[3], and Emine Ulku Saritas[1,2]

[1]Department of Electrical and Electronics Engineering, Bilkent University, Ankara, Turkey, [2]National Magnetic Resonance Research Center (UMRAM), Bilkent University, Ankara, Turkey, [3]Global MR Applications & Workflow, GE Healthcare, Menlo Park, CA, United States

Reduced field-of-view (FOV) using two-dimensional spatially selective radio frequency (2DRF) excitation has been widely used for targeted, high-resolution diffusion weighted imaging (DWI). This work proposes a sheared 2DRF excitation scheme to rapidly and efficiently cover the excitation k-space. This approach not only enables extended slice coverage and preserves fat suppression capabilities, but also significantly improves the robustness against off-resonance-induced signal losses of 2DRF pulses.

1319

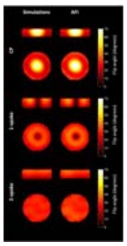

Double-Spoke Slab-Selective Ramp Pulse Design for UHF TOF MR Angiography

Gaël Saïb[1], Vincent Gras[1], Franck Mauconduit[2], Nicolas Boulant[1], Alexandre Vignaud[1], Denis Le Bihan[3], Laurent Le Brusquet[4], and Alexis Amadon[1]

[1]CEA/DRF/I2BM/NeuroSpin/UNIRS, Gif-Sur-Yvette, France, [2]Siemens Healthineers France, Saint-Denis, France, [3]CEA/DRF/I2BM/NeuroSpin, Gif-Sur-Yvette, France, [4]Laboratoires des Signaux et Systèmes, Université Paris-Saclay/CentraleSupélec/CNRS, Gif-sur-Yvette, France

Recently, the use of TOF with parallel transmission at Ultra High Field demonstrated an improvement in vessel-to-background contrast and spatial resolution. This study further investigates the in-vivo feasibility to correct for blood flow saturation effects in TOF slabs with a new double-spoke ramp pulse design optimization at 7T while mitigating in-plane TOF heterogeneities.

1320

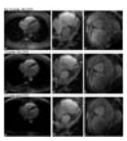

2D Outer Volume Suppression with T2-Preparation and Fat Saturation for Coronary Angiography

David Y Zeng[1], Corey A Baron[1], Adam B Kerr[1], and Dwight G Nishimura[1]

[1]Electrical Engineering, Stanford University, Stanford, CA, United States

A sequence for combined 2D outer volume suppression (OVS) with T_2-preparation and fat saturation is proposed. This sequence provides a uniform passband robust to inhomogeneities, significantly lower SAR than existing methods, and flexibility to be used as a standalone OVS sequence. Numerical simulation and phantom results verify the sequence in theory and *in vivo* results corroborate the performance in practice.

1321

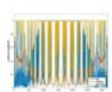

An Efficient Minimum-Time VERSE Algorithm

Graeme McKinnon[1]

[1]GE Healthcare, Waukesha, WI, United States

A computationally-efficient constrained minimum-time VERSE algorithm is presented which is sufficiently fast that it could be used for real time VERSE'ing of RF pulses during pulse sequence prescription.

1322

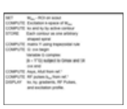

Selective excitation using Multix and Active contouR Technique

Chennagiri Rajarao Padma[1], Jayashree Ganguly[2], Hemanth Thayyullathil[2], Naveen Bajaj[2], Yogesh Kannan Mariappan [2], and Sairam Geethanath[1]

[1]Medical Imaging Research Centre, Dayananda Sagar Institutions, Bangalore, India, [2]Philips Innovation Campus, Bangalore, India

Selective excitation using Multix and Active contouR Technique (SMART) proposed here, is an optimization framework for the joint design of k-space trajectories and radio frequency pulses. The combination of active contour and the multix has been done for the first time which allows the use of arbitrary k-space trajectories. SMART has been prospectively implemented on two channel 3T Philips Ingenia system for different geometric shapes and organs to demonstrate arbitrary volume selective excitation and has shown improved excitation profile. Current and future work involves implementation on in-vivo studies.

1323

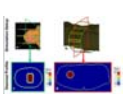

The Effect of RF Exposure Duration in RF Pulse Design Using Temperature Constraints

Cem M Deniz[1,2], Giuseppe Carluccio[1], and Christopher M Collins[1,2]

[1]Department of Radiology, Center for Advanced Imaging Innovation and Research (CAI2R) and Bernard and Irene Schwartz Center for Biomedical Imaging, New York University School of Medicine, New York, NY, United States, [2]The Sackler Institute of Graduate Biomedical Sciences, New York University School of Medicine, New York, NY, United States

There is an increasing interest in using temperature to ensure safety in MRI. We designed parallel transmission RF pulses using either SAR or temperature constraints and compared to each other and unconstrained RF pulse design in terms of excitation fidelity and safety for four different RF exposure durations (from 6 mins to 24 mins). We found that the benefit of using temperature correlation matrices on RF pulse design diminishes as RF exposure duration increases. However, safety of the subject is always guaranteed (the maximum temperature was equal to 39° C). This trend was observed in both head and hip regions, where the perfusion rates are very different.

1324 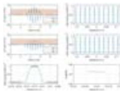

RF pulse design by optimal control with physical constraints

Armin Rund[1,2], Christoph Stefan Aigner[3], Karl Kunisch[1], and Rudolf Stollberger[2,3]

[1]Institute for Mathematics and Scientific Computing, University of Graz, Graz, Austria, [2]BioTechMed Graz, Graz, Austria, [3]Institute of Medical Engineering, Graz University of Technology, Graz, Austria

The design of customized RF pulse and slice selective gradient shapes gives rise to an optimal control problem for the Bloch equation with different inequality constraints. A state-of-the-art method of optimal control is designed especially for this problem class. The optimization model and method is applied to recent test examples. The results are validated on a 3T scanner with phantom and in vivo measurements.

1325 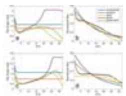

Combined flip angle and echo scaling modulation for optimal fast spin echo

Li Zhao[1] and David Alsop[1]

[1]Radiology, Beth Israel Deaconess Medical Center and Harvard Medical School, Boston, MA, United States

Fast spin echo acquisition plays an essential role in a worthy of MRI applications. But the flip angles of refocus pulses are conventionally designed intuitively. In this work, we proposed a global scheme that can provide a comprehensive framework for flip angled design and proposed the requirement with a well-proposed optimization problem. The performance of the proposed method was demonstrated on the correction of T2 blurring with numerical simulation.

1326 

Local SAR minimization of Turbo Spin-Echo sequences by Dynamic RF Shimming

Alessandro Sbrizzi[1], Arian Beqiri[2], Hans Hoogduin[1], Joseph Hajnal[2], and Shaihan J Malik[2]

[1]UMC Utrecht, Utrecht, Netherlands, [2]King's College London

Turbo Spin-Echo sequences (TSE) are frequently characterized by high local specific absorption rate (SAR), a limiting factor for their application. Here we show that the direct signal control (DSC) framework can drastically reduce the local SAR response of a TSE sequence by expanding the search-space for the amplitude and phase RF weights. A solution is found which enforces optimal contrast behavior and local SAR limits across different shim settings. A cardiac exam at 3 Tesla MRI is used as simulated test case.

1327 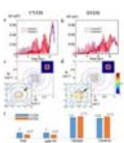

Squeezed Variable Density Spiral Trajectory for SAR Reduction in Parallel Transmission 2D RF Design

Qing Li[1], Congyu Liao[1], Huihui Ye[1], Ying Chen[1], Hongjian He[1], Qiuping Ding[1], and Jianhui Zhong[1]

[1]Center for Brain Imaging Science and Technology, Department of Biomedical Engineering, Zhejiang University, Hangzhou, Zhejiang, People's Republic of China

A squeezed variable density spiral (SVDS) trajectory was proposed to reduce SAR and peak RF power in 2D RF pulse design using parallel transmission (pTX). SVDS was generated by applying a pointwise squeezing factor to conventional variable density spiral (CVDS) trajectory. Compared to CVDS, SVDS can reduce peak RF and SAR by close to 40%, with minimal increase in the normalized root mean square error (NRMSE) of the excitation profile and pulse duration.

1328 

New method to characterize and correct with sub-μs precision gradient delays in bipolar multi-spoke RF pulses

Vincent Gras[1], Alexandre Vignaud[1], Alexis Amadon[1], Franck Mauconduit[2], Denis Le Bihan[1], and Nicolas Boulant[1]

[1]UNIRS, CEA/DRF/I2BM/Neurospin, Gif-sur-Yvette, France, [2]Siemens Healthcare, Saint Denis, France

Small gradient delays with respect to radiofrequency (RF) pulses can have disastrous effects on the performance of bipolar spokes RF pulses employed in parallel transmission (pTx) to mitigate RF field inhomogeneity problems. This work reports a new method to characterize this delay with a precision of ~20 ns, shown to appear necessary for high performance pTx. By the same token, the same physics principles underlying the method suggest a way to correct for it by simply phase-shifting every second spoke RF pulse. The technique is validated with measurements on a water phantom and on an adult volunteer at 7T.

1329 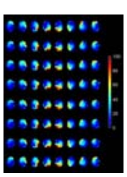

Validation of the universal pulse concept at 7 Tesla on the Nova 8Tx/32Rx head coil with parallel transmit kT-point RF pulses

Vincent Gras[1], Franck Mauconduit[2], Alexandre Vignaud[1], Alexis Amadon[1], Markus Boland[3], Tony Stöcker[3], and Nicolas Boulant[1]

[1]UNIRS, CEA/DRF/I2BM/Neurospin, Gif-sur-Yvette, France, [2]Siemens Healthcare, Saint Denis, France, [3]DZNE, Bonn, Germany

At ultra-high field, the use of parallel transmit (pTx) kT-point RF pulses can greatly improve the excitation uniformity of non-selective radiofrequency pulses but this approach generally requires additional pre-scans to map subject-specific transmit field sensitivities and compute optimal waveforms thereupon. Alternatively, quasi-optimal RF pulses can be obtained by replacing subject-specific field maps by a so-called field database resulting from the accumulation of field maps acquired in a small cohort. This concept is validated here at 7 Tesla on the Nova 8Tx/32Rx head coil with the implementation of a MP-RAGE protocol integrating universal kT-point pTx pulses.

1330 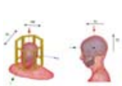

Probabilistic analysis of the SAR intersubject variability safety factor in parallel transmission MRI

Morgane Le Garrec[1], Vincent Gras[1], Marie-France Hang[1], Guillaume Ferrand[2], Michel Luong[2], and Nicolas Boulant[1]

[1]DRF/I2BM/NeuroSpin, CEA, Gif sur Yvette, France, [2]DRF/Irfu/SACM, CEA, Gif sur Yvette, France

Electromagnetic simulations remain to date the preferred method to assess the Specific Absorption Rate (SAR). Within that framework, taking into account the SAR intersubject variability by using a multiplicative safety factor on generic model results remains attractive due to its computational simplicity. Here we report a probabilistic analysis based on the unscented transform sampling scheme followed by the reconstruction of a polynomial approximation of the SAR with respect to head geometrical and position variables. Probabilities of exceeding a given SAR value in the population are returned and safety factors can be deduced based on risk over benefit ratio assessments.

1331 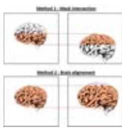

B1+ maps intersubject variability study for universal pulses applications in parallel transmission MRI

Morgane Le Garrec[1], Vincent Gras[1], Michel Luong[2], and Nicolas Boulant[1]

[1]DRF/I2BM/NeuroSpin, CEA, Gif sur Yvette, France, [2]DRF/Irfu/SACM, CEA, Gif sur Yvette, France

Despite its power to mitigate B1+-inhomogeneity, subject-specific tailored parallel transmission (pTx) suffers from a cumbersome workflow involving measurement of field maps as well as online pulse design. Recently however, it was shown that RF inhomogeneity-mitigating (universal) pulses could be found offline to work robustly over a given B1+ maps-database, thus potentially sparing the user the time-consuming calibration. To gain further performance with improved database matching for universal pulses, in this work we investigate with electromagnetic simulations the intersubject B1+ map variability by systematically varying position (in Z and Y), head length and head breadth of a reference head model.

Traditional Poster

Multimodal & Multiparametric

Exhibition Hall 1332-1366 Monday 8:15 - 10:15

1332 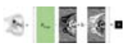

Water and Fat Based Partial Volume Correction for PET/MRI

Hyungseok Jang[1,2] and Alan B McMillan[3]

[1]Radiology, University of Wisconsin, MADISON, WI, United States, [2]Electrical Engineering, University of Wisconsin, MADISON, WI, United States, [3]University of Wisconsin, MADISON, WI, United States

In this study we propose to develop methods that improve the resolution of PET images by utilizing water and fat-based partial volume correction. These methods are expected to be particularly useful in simultaneous breast PET/MR imaging as white adipose tissue is known to be minimally FDG avid.

1333 

Simultaneous Estimation of ADC, T2-relaxation, Perfusion and 11C-acetate PET Uptake in Prostate Cancer

Mikael Skorpil[1,2], Patrik Brynolfsson[1], Axel Hartwig[3], and Mathias Engström[4]

[1]Department of Radiation Sciences, Umeå University, Umeå, Sweden, [2]Department of Radiology, Uppsala, Sweden, [3]Healthcare Systems, GE Healthcare, Stockholm, Sweden, [4]Applied Science Laboratory, GE Healthcare, Uppsala, Sweden

Multiparametric MRI is the standard to evaluate suspected prostate cancer. T2-weighted and DWI are essential, while DCE is less crucial. We here demonstrate that simultaneous quantification of ADC, T2-relaxation and perfusion fraction f, which was calculated from non-IVIM low b-value data, is feasible in combination with 11C-acetate PET/MR imaging. ADC and T2-values differed significantly between healthy tissue and cancer, while f was more inconsistent. An important benefit of simultaneous acquisition is the lack of image mismatch between T2-maps and DWI. This enables more objective tumor grading, decreased inter-rater variability and using mathematical/statistical approaches or computer-aided detection to estimate cancer probability.

1334

Zero-echo-time PET/MRI attenuation correction shows good correlation between 15O-water PET and simultaneously acquired ASL in standard regional flow territories

Markus Fahlström[1], Karolina Lindskog[2], Lieuwe Appel[1], Mathias Engström[3], Johan Wikström[1], Gunnar Antoni[4], Eva Kumlien[5], Elna-Marie Larsson[1], and Mark Lubberink[1]

[1]Surgical Sciences, Uppsala University, Uppsala, Sweden, [2]Biomedical Technology, Medical Physics and IT, Uppsala University Hospital, Uppsala University Hospital, Uppsala, Sweden, [3]Applied Science Laboratory, GE Healthcare, Uppsala, Sweden, [4]Medicinal Chemistry, Uppsala University, Uppsala, Sweden, [5]Neuroscience, Uppsala University, Uppsala, Sweden

Zero-Echo-Time (ZTE) MRI for attenuation correction (AC) in hybrid PET/MRI-systems is a promising method. This study aims to examine reproducibility between 15O-water PET and simultaneously acquired Arterial Spin Labelling (ASL) using ZTE-MRI AC and the reproducibility between to subsequent ASL measurements. Measurements were performed on six subjects on an integrated 3.0 T PET/MRI-system. Regional cerebral blood flow (CBF) values from standard flow territories were compared. ASL showed good correlation with 15O-water PET, presenting another advantage of ZTE-MRI AC. A significant decrease between ASL measurements was detected, which may be important to consider when designing PET/MRI-studies.

1335

Hybrid ZTE/Dixon MR-based Attenuation Correction for Knee PET/MR Sodium Fluoride Studies

Andrew Palmera Leynes[1], Valentina Pedoia[1], Florian Wiesinger[2], Anand Venkatachari[3], Sharmila Majumdar[1], and Peder Larson[1]

[1]Radiology and Biomedical Imaging, University of California San Francisco, San Francisco, CA, United States, [2]GE Global Research, Munich, Germany, [3]GE Healthcare, Waukesha, WI, United States

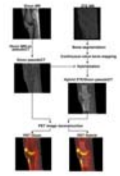

This study introduces a new hybrid ZTE/Dixon MR-based attenuation correction (MRAC) method including bone density estimation for PET/MRI and quantifies the effect of bone attenuation on sodium fluoride uptake in the knee.

1336 

Impact of new attenuation correction methods on whole-body PET/MR

Mark Oehmigen[1], Marcel Gratz[1,2], Verena Ruhlmann[3], Lale Umutlu[4], Matthias Fenchel[5], Jan Ole Blumhagen[5], and Harald H. Quick[1,2]

[1]High Field and Hybrid MR Imaging, University Hospital Essen, Essen, Germany, [2]Erwin L. Hahn Institute for MR Imaging, University Duisburg-Essen, [3]Department of Nuclear Medicine, University Hospital Essen, [4]Department of Diagnostic and Interventional Radiology and Neuroradiology, University Hospital Essen, [5]Siemens Heathineers, Siemens AG, Erlangen, Germany

Recent developments in MR-based whole-body PET/MR attenuation correction allow for adding bone information and for eliminating truncation artefacts along the patients' arms using the HUGE technique. 43 patients underwent a PET/MR whole-body examination. The PET SUV_{max} of 57 active lesions were measured for PET data reconstructed with four different µmaps: standard, standard+bone, standard+HUGE, and standard+bone+HUGE. Compared to the standard-µmap, the mean SUV_{max} of all 57 lesions increases by 14%±12% when adding bone, by 17% ±12% when adding HUGE, and by 24%±19% when adding bone+HUGE. These results are an important step towards improved MR-based attenuation correction in whole-body PET/MR hybrid imaging.

1337 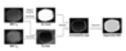

Comparison of UTE-based Attenuation Correction Methods for Simultaneous PET/MR Imaging of the Children's Brain

Chang Gao[1], Junshen Xu[1], Bowen Fan[1], Jiajin Liu[2], and Kui Ying[1,3]

[1]Department of Engineering Physics, Tsinghua University, Beijing, People's Republic of China, [2]Department of Nuclear Medicine, Chinese PLA General Hospital, People's Republic of China, [3]Key Laboratory of Particle and Radiation Imaging, Ministry of Education, Medical Physics and Engineering Institute, Tsinghua University, Beijing, People's Republic of China

In simultaneous PET/MR imaging, PET attenuation correction is based on MRI, unlike PET/CT systems, which directly use CT measurements. Various approaches have been developed based on templates, atlas information, direct segmentation of T1-weighted MR images. In the present study, we introduced two approaches of UTE-based attenuation correction for simultaneous PET/MR imaging focusing on children's brain, including segmentation-based method and Support Vector Machine (SVM) regression method. The results have been compared with Gaussian Mixture Regression (GMR) model method.

1338 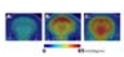

A Non-invasive Method for Quantifying Cerebral Blood Flow by Hybrid PET/MR

Tracy Ssali[1,2], Udunna Anazodo[1,2], Jonathan Thiessen[1,2], Frank Prato[1,2], and Keith St Lawrence[1,2]

[1]Lawson Health Research Institute, London, ON, Canada, [2]Medical Biophysics, Western University, London, ON, Canada

While PET with $[^{15}O]H_2O$ is the gold standard for imaging CBF, quantification requires measuring the arterial input function (AIF), which is an invasive and noisy procedure. ASL is an attractive alternative, however, its accuracy is limited by low SNR. Considering these limitations, we propose a hybrid PET/MRI approach using global CBF measurements from phase contrast MRI to convert $[^{15}O]H_2O$ PET data into CBF maps. To test this method, using a large animal model, CBF was measured by this hybrid approach and by PET only, where the AIF was measured. Good agreement was found over a CBF range (20-100 ml/100g/min).

1339 

Effects of B1 Correction on the Accuracy of T1, T2 and ADC Values Measured with a Diffusion-Weighted Dual-Echo Steady-State (DW-DESS) Sequence

Rachel W Chan[1], Aaron Boyes[1], and Masoom A Haider[1,2]

[1]Medical Imaging, Sunnybrook Health Sciences Centre, Toronto, ON, Canada, [2]Medical Imaging, University of Toronto, Toronto, ON, Canada

Diffusion-weighted dual-echo steady-state (DW-DESS) imaging allows multiple MR parameters to be quantified without image distortion. In this work, we investigate the effects of B1 correction on the accuracy of T1, T2 and ADC parameters estimated from DW-DESS. We extend the quantification to species with ADC and T2 values that are similar human cancers by using a novel phantom mixture. The accuracy of parameter estimates measured with DW-DESS is improved after B1 correction, with correlation coefficients of 0.912, 0.997 and 0.778 without B1 correction to 0.993, 0.998 and 0.947 after B1 correction (for T1, T2 and ADC, respectively).

1340 

Improved clinical workflow for simultaneous whole-body PET/MRI using high-resolution CAIPIRINHA-accelerated MR-based attenuation correction

Martin T. Freitag[1], Matthias Fenchel[2], Philipp Bäumer[1], Thorsten Heußer[3], Christopher M. Rank[3], Marc Kachelrieß[3], Klaus Kopka[4], Antonia Dimitrakopoulou-Strauss[5], Frederik Giesel[6], Uwe Haberkorn[6], Klaus H. Maier-Hein[7], Ralf Floca[7], Mark E. Ladd[3], Heinz-Peter Schlemmer[1], and Florian Maier[3]

[1]Department of Radiology, German Cancer Research Center (DKFZ), Heidelberg, Germany, [2]Siemens Healthineers, Erlangen, Germany, [3]Medical Physics in Radiology, German Cancer Research Center (DKFZ), Heidelberg, Germany, [4]Divison of Radiopharmaceutical Chemistry, German Cancer Research Center (DKFZ), Germany, [5]Clinical Cooperation Unit Nuclear Medicine, German Cancer Research Center (DKFZ), Heidelberg, Germany, [6]Nuclear Medicine, University Hospital Heidelberg, Heidelberg, Germany, [7]Junior Group Medical Image Computing, German Cancer Research Center (DKFZ), Heidelberg, Germany

The present study assesses the value and reproducibility of a novel CAIPIRINHA-accelerated T1-weighted Dixon-based prototype for whole-body PET/MRI in comparison to the clinical standard. This prototype allows the aquisition of an MR-based attenuation correction and a high-resolution T1w DIXON stack that may be used for diagnostic correlation of PET findings in one single step. Voxel-wise intra-individual differences, intermethod-agreement using regression and bland-altman plot analysis, inter-reader agreement for image quality and a repeated measurement experiment in a healthy volunteer without tracer injection were pefomed. The novel prototype demonstrated a high reproducibility of standardized uptake value quantification compared to the standard and excellent image quality for all body regions. Smaller breathing artifacts in the lungs may transfer on the PET µmap and thus influence the attenuation correction. Therefore, physicians and the technicians need to assess the µmap to veriy artifact-free acquisition. The novel protoype is useful for clinical PET/MRI studies towards time-efficient protocols as a separate T1w-sequence may be omitted.

1341

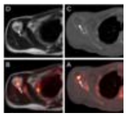

Preliminary Clinical Experience with FDG-PET/MRI in Plasma Cell Dyscrasias

Tyler J Fraum[1], Daniel R Ludwig[1], Ephraim E Parent[1], Farrokh Dehdashti[1], Michelle Miller-Thomas[1], Monica Shokeen[1], Keith Stockerl-Goldstein[1], Ravi Vij[1], and Kathryn J Fowler [1]

[1]Mallinckrodt Institute of Radiology, Washington University School of Medicine, St Louis, MO, United States

Multiple myeloma (MM) is an attractive target for FDG-PET/MRI, given the inherent limitations of both MRI and FDG-PET/CT when obtained separately. We performed FDG-PET/MR in a total of 36 patients with clinical diagnoses of a plasma cell dyscrasia (PCD), including a subset that underwent PET/CT and PET/MRI on the same day as part of a research protocol. FDG-PET/MRI was feasible for both the initial staging and subsequent treatment response assessment of PCDs and provided additional useful information compared with PET/CT. Sagittal T1-weighted images of the spine should be incorporated into standard protocols to improve spinal lesion detection.

1342

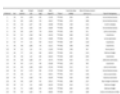

Application of MR-based truncation correction (HUGE) in whole-body PET/MR hybrid imaging

Maike E. Lindemann[1], Mark Oehmigen[1], Jan Ole Blumhagen[2], and Harald H. Quick[1,3]

[1]University Hospital Essen, Essen, Germany, [2]Siemens Healthcare GmbH, [3]Erwin L. Hahn Institute for Magnetic Resonance Imaging

In quantitative PET-imaging, it is essential to correct for the attenuation of photons in tissue. In combined PET/MR-imaging the attenuation correction (AC) is based on MR-data and subsequent tissue class segmentation. The MR-FOV is limited due to B0-inhomogeneities and gradient nonlinearities. Therefore, the AC-map is truncated and reconstructed PET-data are biased. HUGE (B0-Homogenization using gradient enhancement), which determines an optimal readout gradient to compensate gradient nonlinearities, was applied in whole-body PET/MR examinations of 24 oncologic patients. The extension of the MR-FOV for MR-based AC showed an improvement of PET-quantification in integrated PET/MR-imaging by reducing the truncated areas of the AC-map.

1343

3D Printed Phantom for PETMR Attenuation Correction

Derrick Gillan[1], Thomas Hope[1], and Peder Larson[1]

[1]Radiology and Biomedical Imaging, UCSF Medical Center, San Francisco, CA, United States

This experiment sought to explore PET/MRI attenuation correction with a 3D printed skull phantom used to mimic bone attenuation and MR characteristics.

1344

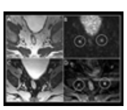

Optimal MRI sequences for 68Ga-PSMA-11 PET/MRI in evaluation of biochemically recurrent prostate cancer

Spencer T. Lake[1], Kirsten L. Greene[2], Antonio C. Westphalen[1], Spencer C. Behr[1], Ronald Zagoria[1], Eric J. Small[3], Peter R. Carroll[2], and Thomas A. Hope[1]

[1]Radiology and Biomedical Imaging, UCSF, San Francisco, CA, United States, [2]Urology, UCSF, San Francisco, CA, United States, [3]Medicine, Division of Hematology and Oncology, UCSF, San Francisco, CA, United States

On ^{68}Ga-PSMA-11 PET/MRI for biochemically recurrent prostate cancer, small PSMA-positive lesions are detected on some, but not all MRI sequences. To determine the most effective sequences to obtain for a ^{68}Ga-PSMA-11 PET/MRI protocol, the sensitivities of small FOV T2, T1 post-contrast, and diffusion-weighted sequences for identification of small abdominopelvic nodes were evaluated. In addition, multiphasic contrast-enhanced Differential Subsampling with Cartesian Ordering (DISCO) images were evaluated for detection of prostate bed recurrence. Examination of 48 consecutive patients indicates that small FOV T2 images are most sensitive for small abdominopelvic nodes and DISCO images are most sensitive for prostate bed recurrence.

1345

T1 and T2 mapping using highly accelerated radial data acquisition and alternating direction method of multipliers

Zhiyang Fu[1], Zhitao Li[1], Mahesh Bharath Keerthivasan[1], Diego R Martin[2], Maria I Altbach[2], and Ali Bilgin[1,2,3]

[1]Electrical and Computer Engineering, University of Arizona, Tucson, AZ, United States, [2]Department of Medical Imaging, University of Arizona, Tucson, AZ, United States, [3]Biomedical Engineering, University of Arizona, Tucson, AZ, United States

Quantitative MRI requires accurate parameter estimation but long acquisition time limits the use of conventional techniques in the clinic. Recently, several T1 and T2 mapping methods based on highly accelerated radial trajectories have been proposed. The reconstruction problems in these works are formulated as unconstrained optimizations and solved using the non-linear conjugate gradient method. We propose an alternative formulation based on the alternating direction method of multipliers which reduces reconstruction time without compromising reconstruction quality.

1346

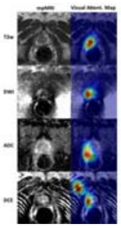

Eye Tracking System for Prostate Cancer Diagnosis Using Multi-Parametric MRI

Haydar Celik[1,2,3], Baris Ismail Turkbey[4], Peter Choyke[4], Ruida Cheng[5], Evan McCreedy[5], Matthew McAuliffe[5], Naji Khosravan[6], Ulas Bagci[6], and Bradford J Wood[1]

[1]Clinical Center, National Institutes of Health, Bethesda, MD, United States, [2]SZI, Children's National Health System, Washington, DC, United States, [3]Pediatrics, George Washington University, Washington, DC, United States, [4]NCI, National Institutes of Health, Bethesda, MD, United States, [5]CIT, National Institutes of Health, Bethesda, MD, United States, [6]Center for Research in Computer Vision, University of Central Florida, Orlando, FL, United States

Medical images have been studied using eye tracker systems from visual search and perception perspectives since 1960's. However number of studies for the multi slice imaging is very limited due to the technical challenges. We developed a software to overcome the difficulties, and enable visual search/perception studies using multi-parametric MRI of prostate cancer. Multiparametric MR images (T2w, DWI, ADC map, and DCE) were synchronized with the eye tracker system and visual-attention maps were successfully created for each image types using gaze information. This is the first multiparametric MR study using an eye tracker system.

1347

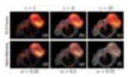

A Constrained Least Squares Approach to MR Image Fusion

Nicholas Dwork[1], John M. Pauly[1], and Jorge Balbas[2]

[1]Electrical Engineering, Stanford University, Stanford, CA, United States, [2]Mathematics, California State University in Northridge, Northridge, CA, United States

Fusing a lower resolution color image with a higher resolution monochrome image is a common practice in medical imaging. By incorporating spatial context and/or improving the Signal-to-Noise ratio, the fused image provides clinicians with a single frame of the most complete diagnostic information. In this paper, image fusion is formulated as a convex optimization problem which avoids image decomposition and permits operations at the pixel level. This results in a highly efficient and embarrassingly parallelizable algorithm based on widely available robust and simple numerical methods that realizes the fused image as the global minimizer of the convex optimization problem.

1348

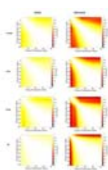

A Comparison of Optimised Single-Shot MR Fingerprinting Pulse Sequence Designs.

Jack Allen[1], James Kennedy[2], and Peter Jezzard[1]

[1]FMRIB, Nuffield Department of Clinical Neuroscience, University of Oxford, Oxford, United Kingdom, [2]Radcliffe Department of Medicine, University of Oxford, Oxford, United Kingdom

The parameter mapping accuracy of MR Fingerprinting (MRF) relies on specific signal patterns for each set of parameters. Choice of sequence design and acquisition parameters are two aspects that affect this. We optimised the TR and Flip Angle (FA) of a selection of simulated single-shot MRF designs, based on Inversion-Recovery Gradient Echo (IR-GRE), GRE, Spin Echo (SE) and IR-SE sequences. We compared the parameter assignment accuracy of each optimised design. Our results suggest that GRE-based sequences should be used for single-shot MRF.

1349

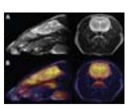

First results from an MRI compatible small animal PET insert operating in a clinical 3T PET/MRI

Matthew S. Fox[1,2], Vanessa L. Palmer[3], Graham Schellenberg[3], Jarod Matwiy[4], Scott B. King[4], Andrew L. Goertzen[5,6,7], and Jonathan D. Thiessen[1,2]

[1]Imaging Program, Lawson Health Research Institute, London, ON, Canada, [2]Department of Medical Biophysics, University of Western Ontario, London, ON, Canada, [3]Cubresa, Winnipeg, MB, Canada, [4]National Research Council of Canada, Winnipeg, MB, Canada, [5]Department of Radiology, University of Manitoba, Winnipeg, MB, Canada, [6]Department of Physics and Astronomy, University of Manitoba, [7]PET/CT Imaging Program, Section of Nuclear Medicine, Health Sciences Centre, Winnipeg, MB, Canada

Reaching sub-millimeter limits in spatial resolution and improved temporal resolution, simultaneous PET/MRI using a pre-clinical MR compatible PET insert enables new discoveries in science and medicine. We recently evaluated a versatile MR compatible small animal PET insert in collaboration with Cubresa. Presented here are the first simultaneous images obtained using both imaging modes within our clinical 3T MRI.

1350

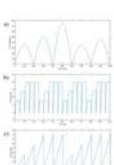

Quality Factors for Efficient and Precise MRF Imaging

Danielle Kara[1], Mingdong Fan[1], Jesse I. Hamilton[2], Nicole Seiberlich[2,3], Mark Griswold[2,3], and Robert Brown[1]

[1]Physics, Case Western Reserve University, Cleveland, OH, United States, [2]Biomedical Engineering, Case Western Reserve University, Cleveland, OH, United States, [3]Radiology, University Hospitals Case Medical Center, Cleveland, OH, United States

With the invention of MRF imaging, there is considerable freedom in input parameter selection, but it is difficult to determine how each choice affects the resulting parameter maps. Quality factors are introduced as a means of comparing MRF sequences with various input parameters (FA, TR, TE, N) on their abilities to precisely quantify T1 and T2. Simulations, fully sampled, and undersampled experiments verified that sequences with higher quality factors result in lower standard deviations in R1 and R2. With quality factor analysis, researchers and clinicians can readily determine the appropriate MRF input parameters to image more efficiently and precisely.

1351

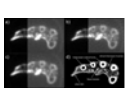

Cross-Modality MR Image Reconstruction: CT-Constrained Anisotropic Diffusion to Preserve Edge Information in MRI of an Ancient Mummified Hand

Johannes Fischer[1], Ali Caglar Özen[1], Dmitry Kurzhunov[1], Marco Reisert[1], Agazi Tesfai[1], Frank Rühli[2], Ute Ludwing[1], and Michael Bock[1]

[1]Dept. of Radiology, Medical Physics, Medical Center – University of Freiburg, Freiburg, Germany, [2]Institute of Evolutionary Medicine, Medical Faculty, University of Zürich, Zürich, Switzerland

Constrained reconstruction is making use of additional image information to improve the precision in the reconstruction of undersampled MR data. Here we use co-registered CT-data as an anisotropic diffusion constraint to improve sharpness in short T_2* images reconstructed from undersampled 3D UTE data of a mummified human hand. The results are compared to other established reconstruction methods.

1352 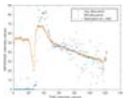

Contrast matching of ultra-high resolution minimum deformation averaged MRI models to facilitate computation of a multi-modal model of the human brain

Julie Broni Munk[1,2], Nina Jacobsen[1,2], Maciej Plocharski[2], Lasse Riis Østergaard[2], Markus Barth[1], Andrew L. Janke[1], and Steffen Bollmann[1]

[1]Centre for Advanced Imaging, University of Queensland, Brisbane, Australia, [2]Department of Health Science and Technology, Aalborg University, Aalborg, Denmark

A contrast matching algorithm was developed to enable non-linear coregistration of multi-modal minimum deformation averaged MRI models using cross correlation. The registration results show that the contrast conversion enables non-linear multi-modal coregistration.

1353 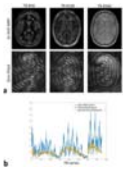

Fast Analytical Solution for Extreme Unaliasing of MR Fingerprinting Image Series

Eric Y. Pierre[1], Mark A. Griswold[2,3], and Alan Connelly[1]

[1]Imaging Division, The Florey Institute of Neuroscience and Mental Health, Melbourne, Australia, [2]Biomedical Engineering, Case Western Reserve University, Cleveland, OH, United States, [3]Radiology, Case Western Reserve University & University Hospitals, Cleveland, OH, United States

A non-iterative analytical solution to the MRF image reconstruction problem is presented. The method performs a direct interpolation of the acquired k-space points based on a singular-vector basis of fingerprints from a first-pass MRF estimate. The method is shown to drastically reduce spatio-temporal aliasing, allowing accurate T1 and T2 measurements for a single slice with a 7.6s acquisition, without need for auto-calibration data, and with computational overhead an order of magnitude faster than previously reported iterative image-based methods.

1354 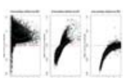

Removing the estimation bias due to the noise floor in multi-parameter maps

Karsten Tabelow[1], Chiara D'Alonzo[1], Lars Ruthotto[2], Martina F. Callaghan[3], Nikolaus Weiskopf[4], Joerg Polzehl[1], and Siawoosh Mohammadi[5]

[1]WIAS, Berlin, Germany, [2]Emory University, Atlanta, USA, [3]Wellcome Trust Centre for Neuroimaging, UCL Institute of Neurology, University College London, London, United Kingdom, [4]Department of Neurophysics, Max Planck Institute for Human Cognitive and Brain Sciences, Leipzig, Germany, Leipzig, Germany, [5]Department of Systems Neuroscience, Medical Center Hamburg-Eppendorf, Hamburg, Germany

We demonstrate the bias effect due to the low signal-to-noise ratio of ultra-high resolution (0.5µm isotropic) Multi-Parameter Mapping acquisitions of quantitative R1, R2* and PD maps and develop a method for improved parameter estimation.

1355 

Analyzing the Bayesian Approach to Partial Volume in Magnetic Resonance Fingerprinting

Debra McGivney[1], Anagha Deshmane[2], Yun Jiang[2], and Mark Griswold[1,2]

[1]Radiology, Case Western Reserve University, Cleveland, OH, United States, [2]Biomedical Engineering, Case Western Reserve University, Cleveland, OH, United States

We present work to optimize the parameters used in the Bayesian approach to partial volume in MRF. Care needs to be taken when choosing parameter values to balance effects from noise and over regularization of the solution. MRF brain data from a normal volunteer is analyzed to determine the optimal parameters in separating white matter from gray matter and gray matter from CSF. Parameter choices are confirmed by examining the results from our algorithm in regions of pure white matter.

1356 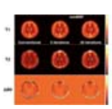

Accelerated Magnetic Resonance Fingerprinting Reconstruction using Majorization-Minimization

Yang Li[1], SHUAI Wang[1], Edward S. Hui[2,3], Di Cui[2], Hing-Chiu Chang[2], and Yik-Chung Wu[1]

[1]Department of Electrical and Electronic Engineering, The University of Hong Kong, Pokfulam, Hong Kong, [2]Department of Diagnostic Radiology, The University of Hong Kong, Pokfulam, Hong Kong, [3]The State Key Laboratory of Brain and Cognitive Sciences, The University of Hong Kong, Pokfulam, Hong Kong

Magnetic resonance fingerprinting (MRF) is a novel and efficient method for the estimation of MR parameters, such as off-resonance (DB0), proton density (PD), T1 and T2. Because of the highly undersampled readout that is conventionally used, large number of dynamics (e.g. <1000) are often acquired for maintaining the fidelity of MR parameter estimations (a.k.a. dictionary matching). In this study, we propose a new algorithm, MRF reconstruction using majorization-minimization (mmMRF), such that fidelity of dictionary matching can remain similar even when significantly less number of dynamics are available.

1357 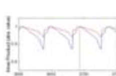

Toward an Optimized Dictionary for Pattern Matching in Magnetic Resonance Fingerprinting

Kun Yang[1], Yun Jiang[1,2], Mark Griswold[1,2], Vikas Gulani[1,2], and Debra McGivney[2]

[1]Dept. of Biomedical Engineering, Case Western Reserve University, Cleveland, OH, United States, [2]Dept. of Radiology, University Hospitals of Cleveland, Cleveland, OH, United States

An important issue in magnetic resonance fingerprinting (MRF) is the precision of pattern matching. The sensitivity of inner product between the signal and dictionary can be corrupted by closely spaced dictionary entries. In order to make MRF more sensitive and precise, four modifications of the MRF dictionary are proposed. The performance of each method is tested and compared over 30 repetitions in a phantom scan. Some of the methods demonstrate a significant reduction in the error over the original MRF dictionary.

1358

Proton Density Mapping and Receiver Bias Correction for Absolute Quantification with MR Fingerprinting

Anagha Deshmane[1], Debra McGivney[2], Yun Jiang[1], Dan Ma[2], and Mark Griswold[2]

[1]Biomedical Engineering, Case Western Reserve University, Cleveland, OH, United States, [2]Radiology, Case Western Reserve University, Cleveland, OH, United States

MR Fingerprinting (MRF) can simultaneously map multiple parameters and can be used to compute estimates of tissue fractions. However, MRF-derived M_0 maps contain information about both proton density (PD) and the receiver sensitivity profile (RP). Here we estimate relative PD and RP from MRF M_0 and T_1 maps. Relative PD and tissue fractions are combined for absolute quantity mapping of CSF, gray matter, and white matter as a fraction of the voxel equilibrium magnetization.

1359

In vivo MR blood oximetry based on $$$T_2$$$-prepared bSSFP

Michael C Langham[1], Ana E Rodríguez-Soto[1], Hyunyeol Lee[1], Nadav Schwartz[2], and Felix W Wehrli[1]

[1]Radiology, University of Pennsylvania, Philadelphia, PA, United States, [2]Obstetrics and Gynecology, University of Pennsylvania, Philadelphia, PA, United States

To develop in vivo MR oximetry based on T2-prepared bSSFP constant refocusing-pulse interval ($$$\tau_{180}$$$) T_2-preparation, three-parameter signal fitting for T_2 extraction and magnetization reset for shortened pulse sequence cycle were implemented and evaluated against a multi-spin echo sequence using static and flowing $MnCl_2$ solutions with known T_2 values. The whole-blood T_2 was also quantified to investigate the effect of varying . The phantom results support three-parameter fitting, and <5% error incurred in T_2 quantification with shortened T_2-preparation cycle and presence of constant flow. Approximately 10% longer whole-blood T_2 was observed with constant relative to varying .

1360

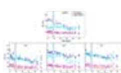

Comparison of Renal R2* Analysis Methods

Inge Manuela Kalis[1], Axel Joachim Krafft[2], and Michael Bock[2]

[1]Dept. of Radiology, Medical Physics, Medical Center - University of Freiburg, Germany, Freiburg, Germany, [2]Medical Center - University of Freiburg, Germany

BOLD MRI can be applied as an indirect measure of the oxygenation level changes in the kidneys while performing an experiment with a functional renal challenge. These changes are detected by the relaxation rate R2* in the renal cortex and medulla. For R2* analysis different methods are proposed, such as the conventional manual ROI method and a compartmental method. Here, these methods and two further compartmental methods are compared to each other by analyzing full time-resolved renal BOLD MR experiments in healthy volunteers.

1361

Development of contrast agents for simultaneous PET/MRI of murine tumor models

Samuel C. Gilmore[1], Abbie Shepard[2], Christine Howison[3], Joshua M. Goldenberg[2], Julio Cárdenas-Rodríguez[3], and Mark D. Pagel[3]

[1]University of Arizona, Tucson, AZ, United States, [2]Pharmaceutical Sciences, University of Arizona, Tucson, AZ, United States, [3]Medical Imaging, University of Arizona, Tucson, AZ, United States

PET/MRI contrast agents represent a new field of molecular imaging that provide an outstanding opportunity to employ simultaneous PET/MRI instrumentation for quantitative imaging. Over 90 responsive MRI contrast agents have been reported that change their contrast based on a biomarker and agent concentration, limiting their utility *in vivo* because a change in signal could arise from the presence of the biomarker and/or a change in the concentration of the agent. We propose to use PET to quantify the agent concentration, and a comparison of PET and MRI contrast can quantitatively evaluate the biomarker in a concentration-independent manner. Herein we describe the synthesis and characterization of ^{18}F-radiolabeled responsive MRI contrast agents that are designed to measure pH and redox state using simultaneous PET/MRI for small animal studies.

1362

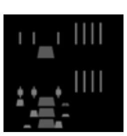

STEAM-CPMG: A method for localized Pulsed-Field-Gradient-Stimulated-Echo CPMG acquisitions

Ericky Caldas de Almeida Araujo[1,2,3] and Olivier Scheidegger[1,3,4]

[1]Institute of Myologie, La Pitié-Salpêtrière University Hospital, Paris, France, [2]CEA/DRF/I2BM/MIRCen, Fontenay aux Roses, France, [3]Institute for Diagnostic and Interventional Neuroradiology, Inselspital, Bern University Hospital, University of Bern, Bern, Switzerland, [4]Department of Neurology, Inselspital, Bern University Hospital, University of Bern, Bern, Switzerland

The CPMG method has been long applied for multi-component T2 studies which have been shown to reveal the micro-anatomical compartmentation of water in biological tissue. A new method for localized CPMG acquisitions that makes use of the Stimulated Echo Acquisition Mode technique is presented. Besides offering localized T2-relaxation data within less than 10 s, the method is suited for performing Diffusion-Relaxation-Correlation-Spectroscopy studies. Such studies allow evaluating the translational diffusion of the different T2-compartments observed in vivo and shall offer new insights on diffusion and relaxation processes in biological tissues. The method has been validated in vitro.

1363

Early changes of irradiated parotid glands evaluated by T1rho-weighted imaging: a pilot study

Zhengyang Zhou[1], Jian He[2], and Weibo Chen[3]

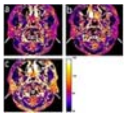

[1]Department of Radiology, Drum Tower Hospital, School of Medicine, Nanjing University, Nanjing, People's Republic of China, [2]Department of Radiology, Drum Tower Hospital, School of Medicine, Nanjing University, [3]Philips Healthcare, Shanghai, People's Republic of China

Twenty-six NPC patients underwent serial T1rho-weighted imaging to evaluate the dynamic changes of parotid glands in patients undergoing intensity-modulated radiation therapy. Parotid volumes, T1rho values, mean radiation doses, and xerostomia degrees were recorded. Change rates of T1rho values were correlated with atrophy rates, mean radiation doses and xerostomia degrees. During RT, parotid volume decreased and parotid T1rho values increased significantly. The change rate of T1rho value correlated with the atrophy rate significantly at post-RT. Intra- and interobserver reproducibility of T1rho measurements were excellent. Dynamic changes of radiation-induced parotid damage in NPC patients underwent IMRT could be evaluated by T1rho-weighted imaging.

1364

A short protocol for determining apparent kurtosis validated in a hybrid MR-PET clinical environment

Ricardo Loucao*[1,2], Ana-Maria Oros-Peusquens*[1], Karl-Josef Langen[1], Hugo Ferreira[2], and Nadim Jon Shah[1]

[1]INM-4, Research Centre Jülich, Jülich, Germany, [2]Instituto de Biofísica e Engenharia Biomédica, Sciences Faculty, University of Lisbon, Lisbon, Portugal

Mean kurtosis (MK) obtained from the kurtosis tensor is often associated with acquisition protocols that may be long for clinical demands. Apparent kurtosis (Kapp), obtained from the direct fit of the signal to an exponential decay, is faster to acquire and may provide with similar information. Directional averaging is required to preserve spherical invariance; however, in clinical applications the trace of diffusion tensor measured with 3 directions is often used as tissue marker with good results. In this study we investigate Kapp derived from trace data in forty brain tumour patients and compare it to mean kurtosis. Kapp was found to be underestimated but the two metrics show a significantly high degree of correlation.

1365

68Ga-PSMA dose reduction for imaging the pelvic region with simultaneous PET/MR

Edwin E.G.W. ter Voert[1,2], Hannes W. Nagel[1], Gaspar Delso[3], and Irene A. Burger[1]

[1]Nuclear Medicine, University Hospital Zurich, Zurich, Switzerland, [2]University of Zurich, Zurich, Switzerland, [3]GE Healthcare, Waukesha, WI, United States

When performing simultaneous single station PET and MR scans in the pelvic region, the PET acquisition time could be increased to match the usually more extensive MR protocol acquisition time. The gain in detected coincidences could be applied to decrease the PET tracer dose and thus the patient's radiation burden, while maintaining the same image quality. In this study we investigate the minimal ^{68}Ga-PSMA dose for a 15-minute single station PET(/MR) scan to match image quality of the standard 2 minutes scan at full dose.

1366

Comparison of Myelin Water Fractions from Multi-Echo Spin-Echo and Multi-Gradient Echo Techniques

Eva Alonso Ortiz[1], Ives R. Levesque[1,2], and G. Bruce Pike[3]

[1]McGill University, Montreal, QC, Canada, [2]Research Institute, McGill University Health Centre, Montreal, QC, Canada, [3]University of Calgary, Calgary, AB, Canada

Myelin Water Fraction (MWF) imaging is typically achieved using a Multi-Echo Spin-Echo (MESE) sequence that has a long acquisition time. The Multi-Gradient Recalled Echo (MGRE) sequence on the other hand, is fast, has multi-slice and 3D imaging capabilities, high temporal sampling of the signal decay curve, and low SAR. In this study, we imaged 11 healthy volunteers using MESE and MGRE sequences to perform a method-comparison study for the MWF. Our results suggest that the MGRE approach to MWF imaging is highly promising.

Traditional Poster

Elastography

Exhibition Hall 1367-1386 Monday 8:15 - 10:15

1367

High Resolution 3D GRE Brain MR Elastography is Feasible with a High Performance Compact 3T Scanner

Arvin Arani[1], Roger C Grimm[1], Joshua D Trzasko[1], Paul T Weavers[1], Brandon J Nelson[1], Richard Ehman[1], Clifford R Jack[1], Matthew A Bernstein[1], and John Huston III[1]

[1]Radiology, Mayo Clinic, Rochester, MN, United States

Several groups have investigated the role of magnetic resonance elastography (MRE) for the diagnosis of neurological diseases, which has primarily been done using 2D imaging acquisitions. The objective of this study is to determine if 3D FGRE MRE can localize small regions of elevated stiffness for brain MRE applications on a high performance compact 3T head only scanner. This study demonstrated that a compact 3T scanner has sufficient gradient performance to successfully acquire high resolution 3D FGRE MRE exams, and localize inclusions as small as 1.75cm in diameter, which is not possible on a conventional 3T scanner.

1368

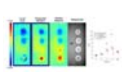

Robust MR elastography stiffness quantification using a localized divergence free finite element reconstruction

Daniel Fovargue[1], Ralph Sinkus[1], and David Nordsletten[1]

[1]Division of Imaging Sciences and Biomedical Engineering, King's College London, London, United Kingdom

The increasing use of MR elastography demands that fast, robust, and out-of-the-box reconstruction methods are available. A new local direct method is presented here to fit these needs. The method utilizes the finite element method, assumes that stiffness is locally homogeneous, and includes additional advancements that improve quality and robustness. Efficacy of the proposed method is demonstrated across phantoms and volunteer data in the brain and breast. The method is contrasted with other standard techniques, showing similar or improved accuracy and robustness, improved computational cost and an independence from regularization parameters.

1369

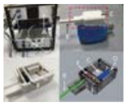

A novel MR Elastography transducer concept based on a rotational eccentric mass: the gravitational transducer

Jurgen Henk Runge[1,2], Stefan Heinz Hoelzl[1], Jelizaveta Sudakova[1], Ayse Sila Dokumaci[1], Jules Laurent Nelissen[3,4], Jack Lee[1], Jaap Stoker[2], Aart Johannes Nederveen[2], David Nordsletten[1], and Ralph Sinkus[1]

[1]Division of Imaging Sciences and Biomedical Engineering, King's College London, London, United Kingdom, [2]Radiology, Academic Medical Center, Amsterdam, Netherlands, [3]Biomedical NMR, Eindhoven University of Technology, Eindhoven, Netherlands, [4]Preclinical and Translational MRI, Academic Medical Center, Amsterdam, Netherlands

Several transducer designs are in use for MR Elastography, based mainly on either pneumatic (or compressed) air or on electromagnetic engine-coils fixed to a lamella. These technologies have enabled significant development within the MR Elastography community and shaped its clinical application. In this abstract, we build on these concepts to introduce a novel transducer that limits image artefacts, limits resonant frequencies and vibrational impurities, and importantly preserves transducer amplitude with frequency; effectively improving the quality of the wave data that can be encoded with MR.

1370

Fast Magnetic Resonance Elastography using a DENSE approach with Multi Phase Offset Readout

Johannes Strasser[1], Lukas Pirpamer[1], Franz Fazekas[1], and Stefan Ropele[1]

[1]Department of Neurology, Medical University of Graz, Graz, Austria

In MRE, motion encoded phase images are acquired to calculate mechanical tissue parameters based on shear wave propagation. We here propose a fast multi readout MRE imaging concept based on the displacement encoding via stimulated echo acquisition (DENSE). In this proof of concept study, phantom experiments yielded excellent clear wave images. The results indicate that the proposed technique could be used to acquire images using short echo times and accelerate the total acquisition time of MRE examinations.

1371

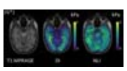

Reproducibility Study of Direct and Non-Linear Inversion High-Resolution Magnetic Resonance Elastography (MRE) of the Hippocampus

Lucy V Hiscox[1,2], Mike Perrins[2], Curtis L Johnson[3], Matt DJ McGarry[4,5], Eric Barnhill[6], John Huston III[7], Ingolf Sack[6], Jürgen Braun[6], Edwin JR van Beek[2], John M Starr[1], and Neil Roberts[2]

[1]Alzheimer Scotland Dementia Research Centre, University of Edinburgh, Edinburgh, United Kingdom, [2]Clinical Research Imaging Centre, University of Edinburgh, Edinburgh, United Kingdom, [3]Department of Biomedical Engineering, University of Delaware, [4]Thayer School of Engineering, Dartmouth College, [5]Department of Biomedical Engineering, Columbia University, [6]Institute for Medical Informatics, Charité Universitätsmedizin Berlin, [7]Department of Radiology, Mayo Clinic

Certain neurological disorders may not be detected with current clinical imaging modalities. Magnetic Resonance Elastography (MRE) combines acoustics with MRI to provide maps of tissue mechanical properties and may be sensitive to subtle tissue pathologies. Two published approaches for performing high-resolution MRE (so-called Direct Inversion and Non-Linear inversion) were applied to enable comparison of test-retest reproducibility of the hippocampus. Intraclass correlation coefficient found DI and NLI to display fair (0.42) and excellent (0.95) reproducibility, respectively, for measuring the magnitude of the complex shear modulus $|G^*|$. Future work will assess the relative magnitude of technical and biological variance including both sex and ageing effects.

1372

Anisotropic shear modulus estimation in ex vivo white matter of the brain using magnetic resonance elastography and finite element modeling

John L Schmidt[1], Dennis J Tweten[1], Ruth J Okamoto[1], Andrew A Badachhape[2], Joel R Garbow[3], and Philip V Bayly[1,2]

[1]Mechanical Engineering and Materials Science, Washington University in St. Louis, St. Louis, MO, United States, [2]Biomedical Engineering, Washington University in St. Louis, St. Louis, MO, United States, [3]Radiology, Washington University in St. Louis, St. Louis, MO, United States

White matter in the brain is thought to be mechanically anisotropic and vulnerable to mechanical strain. By studying mechanical shear wave propagation in *ex vivo* brain tissue using magnetic resonance elastography (MRE), and comparing to results from computer models, shear moduli and shear anisotropy were estimated. This method allows the relaxation of assumptions of isotropy and homogeneity in traditional MRE inversions. The ratio of shear moduli governing shear parallel and perpendicular to fiber direction was approximately 1.25, indicating mild anisotropy in shear. This quantitative characterization of shear anisotropy in white matter has important implications for traumatic brain injury modeling.

1373

Utilization of MR Elastography for selective boost to dominant intraprostatic lesions

Lumeng Cui[1,2], Paul Babyn[3], Francis Bui[4], and Niranjan Venugopal[1]

[1]Medical Physics Department, Saskatoon Cancer Centre, Saskatchewan Cancer Agency, Saskatoon, SK, Canada, [2]Division of Biomedical Engineering, University of Saskatchewan, Saskatoon, SK, Canada, [3]Department of Medical Imaging, University of Saskatchewan and Saskatoon Health Region, Saskatoon, SK, Canada, [4]Department of Electrical & Computer Engineering, University of Saskatchewan, Saskatoon, SK, Canada

MRE has the ability to distinguish between elastic properties of the tissue. Furthermore, it is maturing as a technique to differentiate normal and cancerous tissue. In this work we present a strategy to establish high quality MRE data, and present a method to incorporate this information into a radiation treatment planning framework. This new information is used to evaluate the efficacy of dose escalation to dominant intraprostatic lesions using a volumetric modulated arc therapy technique.

1374 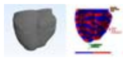

Waveguide Effects in Cardiac Magnetic Resonance Elastography: A Finite Element Study

Armando Manduca[1], Timothy L Rossman[2], David S Lake[1], Kevin J Glaser[3], Arvin Arani[3], Shivaram P Arunachalam[3], Phillip J Rossman[3], Joshua D Trzasko[3], Dan Dragomir-Daescu[2], Richard L Ehman[3], and Philip A Araoz[3]

[1]Physiology and Biomedical Engineering, Mayo Clinic, Rochester, MN, United States, [2]Division of Engineering, Mayo Clinic, Rochester, MN, United States, [3]Radiology, Mayo Clinic, Rochester, MN, United States

MR elastography is increasingly being applied to thin or small structures in which wave propagation is dominated by waveguide effects, which can bias stiffness results with common processing approaches. Finite element simulations of a realistic cardiac geometry were used to investigate the importance of waveguide effects, and to study the ability of the curl operator to remove these effects. The results establish that waveguide effects in a cardiac geometry can strongly bias stiffness results, but can be correctly handled by application of the curl operator to the measured displacement field, followed by true 3D inversion.

1375 

In vivo cerebral MR elastography in a mouse model of Alzheimer's disease: preliminary results

Shreyan Majumdar[1] and Dieter Klatt[1]

[1]Richard and Loan Hill Department of Bioengineering, University of Illinois at Chicago, Chicago, IL, United States

In vivo magnetic resonance elastography (MRE) experiments on Alzheimer's disease (AD) mouse model were conducted. The AD and Control mice were in the age group of 3-4 months (n = 4 for both). Median stiffness values for the overall mouse brain (central axial slices) and for the hippocampus region were calculated. No differences were observed between the two groups for the overall brain. For the hippocampus region, a trend of cerebral stiffness decrease in AD was measured. The small sample size did not allow for statistically significant conclusions. Further experiments are underway.

1376 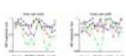

Introduction of IVPD-MRE: Quantitative Assessment of Shear Stiffness without Spatial Derivative Operators

Shreyan Majumdar[1], Pakhi Chaturvedi[1], and Dieter Klatt[1]

[1]Richard and Loan Hill Department of Bioengineering, University of Illinois at Chicago, Chicago, IL, United States

Intravoxel phase dispersion (IVPD) in MRE describes signal loss of the MR magnitude due to spin dephasing imposed by voxel deformation. The extensity of IVPD is, among other parameters, dependent on the tissue stiffness. Therefore, tissue stiffness can be quantified by analyzing IVPD-imposed signal loss within a single voxel. The new approach does not rely on the use of spatial derivative operators as in conventional MR Elastography. In the present work, we examine in simulations the extensity of IVPD for varying experimental conditions and present stiffness maps of an inhomogeneous phantom, which were calculated by numerically fitting the IVPD equation.

1377 

Comparison of mechanical properties of porcine brain tissue in vivo and ex vivo using MR elastography

Charlotte A Guertler[1], Ruth J Okamoto[1], John L Schmidt[1], Andrew A Badachhape[2], Curtis L Johnson[3], and Philip V Bayly[1,2]

[1]Mechanical Engineering, Washington University in St. Louis, St. Louis, MO, United States, [2]Biomedical Engineering, Washington University in St. Louis, St. Louis, MO, United States, [3]Biomedical Engineering, University of Delaware, Newark, DE, United States

Computational models of traumatic brain injury (TBI) require accurate estimates of brain tissue mechanical properties, however properties of brain tissue *ex vivo* may differ from corresponding properties *in vivo*. To characterize possible differences, we performed MR elastography (MRE) on four Yucatan mini-pigs *in vivo*. Brain tissue samples from the same animals were later tested using *ex vivo* MRE. Shear moduli of both *in vivo* and *ex vivo* brain tissue were estimated using local direct inversion. Our results suggest that *in vivo* tissue is stiffer than *ex vivo* tissue at the same frequency, which has important implications for TBI model development.

1378 

Hadamard Encoding for Magnetic Resonance Elastography

Christian Guenthner[1], Jurgen H Runge[2,3], Ralph Sinkus[2], and Sebastian Kozerke[1]

[1]Institute for Biomedical Engineering, University and ETH Zurich, Zurich, Switzerland, [2]Division of Imaging Sciences and Biomedical Engineering, King's College London, London, United Kingdom, [3]Department of Radiology, Academic Medical Center, Amsterdam, Netherlands

We propose the use of Hadamard encoding for Magnetic Resonance Elastography (MRE) of the full displacement vector field (4D-MRE). To this end, motion is encoded along the four diagonals of the regular cube spanned by the main gradient axes. This allows for a factor four higher phase accumulation compared to classical, unbalanced four-point encoding within the same acquisition time. In this abstract, we demonstrate the increase in phase-to-noise ratio for a gel phantom and show the direct benefit of using Hadamard encoding in-vivo to capture high-quality wave displacement maps in the brain.

1379 

Development and validation of spin-echo planar imaging (SE-EPI) based MR Elastography on 3T: A phantom and volunteer study

Hui Wang[1], Suraj D. Serai[2], Tom Cull[3], Jonathan R. Dillman[2], Charles Dumoulin[2], and Andrew Trout[2]

[1]Philips, Cincinnati, OH, United States, [2]Radiology, Cincinnati Children's Hospital Medical Center, Cincinnati, OH, United States, [3]Philips, Cleveland, OH, United States

While MRE based on 2D gradient recalled echo (GRE) MRI is FDA approved at 1.5T, the utility of 2D GRE MRE in the liver at 3T is limited by susceptibility effects and relatively long echo times that results in less SNR. MRE performance, particularly at 3T, can be improved by developing a faster technique that is less sensitive to liver T2* effects. In this work, we describe the development of SE-EPI MRE and its validation with respect to 2D GRE MRE in phantoms and healthy volunteers.

1380

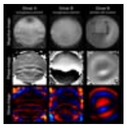

Two novel low-cost 3D-printed mechanical actuators for MR elastography using exact end-to-end motion and centripetal force

Wiebke Neumann[1], Lothar R. Schad[1], and Frank G. Zöllner[1]

[1]Computer Assisted Clinical Medicine, Medical Faculty Mannheim, Heidelberg University, Mannheim, Germany

For reliable quantification of the shear modulus of soft tissues, MR elastography (MRE) needs consistent methods of low-frequency wave induction to the region of interest in the human body. This work proposes two novel designs of 3D-printed mechanical actuators powered by compressed air. Driver A offers constant and specific actuation amplitude independent of the chosen frequency of wave induction. Driver B employs centripetal force for wave induction. Contrary to conventionally used air cushions, the amplitude increases at higher frequencies, thus, making it suitable for high frequency MRE and multi-source wave induction.

1381

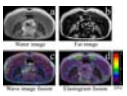

Integration of MR Elastography and Fat/Water Separation Imaging

Tomokazu Numano[1,2], Daiki Ito[1,2], Takaaki Onishi[1], Kazuyuki Mizuhara[3], Koichi Takamoto[4], Hisao Nishijyo[5], Masaki Misawa[2], and Naotaka Nitta[2]

[1]Radiological Science, Tokyo Metropolitan University, Tokyo, Japan, [2]National Institute of Advanced Industrial Science and Technology, Tsukuba, Japan, [3]Mechanical Engineering, TOKYO DENKI UNIVERSITY, Tokyo, Japan, [4]Judo Neurophysiotherapy, University of Toyama, Toyama, Japan, [5]System Emotional Science, University of Toyama, Toyama, Japan

In the present study, we developed a method to combine a simple MRE technique with a fat/water separation method (Dixon method) based on a conventional gradient-echo type multi-echo MR sequence (GRE-MultiEcho-MRE). Because the proposed method used the GRE-multiecho MRE, it is possible to select shortest in-/opposed-phase TE in the 1st TE. Thus, the proposed method allows to increase signal-to-noise ratio of fat/water images.

1382

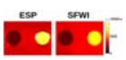

Stacked Frequency Wave Inversion (SFWI): Heterogeneous And Edge-Preserving Direct Inversion For Magnetic Resonance Elastography (MRE)

Eric Barnhill[1], Monika Bahl[2], Florian Dittmann[1], Sebastian Hirsch[1], Jürgen Braun[3], and Ingolf Sack[1]

[1]Radiological Science, Charité Universitätsmedizin Berlin, Berlin, Germany, [2]Physics, Indian Institute of Technology Delhi, New Delhi, India, [3]Medical Informatics, Charité Universitätsmedizin Berlin, Berlin, Germany

A new reconstruction method for MR elastography exploits a recent finding of mathematical uniqueness to develop a heterogeneity-accommodating and edge-preserving direct inversion method that uses first order derivatives. We investigate this new method on FEM models and a cohort of in vivo brain acquisitions by comparing it with a previously published method known as ESP. In models the method removes artefacts from use of second derivatives and homogeneity assumptions. In brain images appear better conditioned, but shows values differing from ESP in more anisotropic brain regionss.

1383

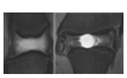

Validation of MRE measurements of shear modulus in both annulus fibrosus and nucleus pulposus within in two animal species

Delphine Perie[1,2], Lauriane Jugé[3], Alexandra Mlodzinski[1], and Lynne Bilston[3]

[1]Mechanical Engineering, Polytechnique Montreal, Montreal, QC, Canada, [2]Research Center, Sainte-Justine Hospital, Montreal, QC, Canada, [3]NeuRA, Sydney, Australia

Magnetic resonance elastography (MRE) is an effective method to measure the shear modulus of the nucleus pulposus, and its changes with degenerescence. However, MRE was not used for the annulus fibrosus. This study validated the use of MRE for the measurements of the shear modulus variations within the intervertebral discs between regions (annulus fibrosus versus nucleus pulposus) and animal species (bovine versus kangaroo). Shear dynamic mechanical tests and MRE showed equivalent tissue differences. This study also highlighted that the loading history of the intervertebral disc has to be considered when choosing an animal model.

1384

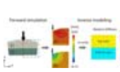

Magnetic Resonance Elastography based on Finite Deformation Imaging and Topology Optimization

Luyao Cai[1], Claus Pedersen[2], and Corey Neu[1,3]

[1]Biomedical Engineering, Purdue University, West Lafayette, IN, United States, [2]Dassault Systèmes, Germany, [3]Mechanical Engineering, University of Colorado Boulder, CO, United States

We developed an inverse modeling approach for magnetic resonance elastography of tissues undergoing finite (large) deformations at physiologically-relevant loading rates. Inverse modeling was designed to directly incorporate displacement-encoded MRI with topology optimization to reveal stiffness distributions. The approach was validated using forward simulations with known material properties and boundary conditions, and sensitivity analyses. Inverse modeling may enable noninvasive characterization of material stiffness for complex tissues like articular cartilage in disease and repair.

1385

Optimal spatial resolution for accuracy and precision in simulated and experimental micro-MRE at 11.7 T

Felicia Julea[1], Jin Long Yue[1], Tanguy Boucneau[1], Marion Tardieu[2], Benoit Larrat[3], Claire Pellot-Barakat[4], and Xavier Maître[1]

[1]Imagerie par Résonance Magnétique Médicale et Multi-Modalités, IR4M, CNRS, Univ. Paris-Sud, Université Paris-Saclay, Orsay, France, [2]Centre de Recherche sur l'Inflammation, CRI, Inserm, CNRS, Univ. Pierre et Marie Curie, Paris, France, [3]Unité d'Imagerie par Résonance Magnétique et Spectroscopie, NeuroSpin, I2BM, DRF, CEA, Gif Sur Yvette, France, [4]Imagerie Moléculaire In Vivo, IMIV, Inserm, CEA, CNRS, Univ. Paris-Sud, Université Paris-Saclay, Orsay, France

MRE outcomes depend on various factors, which include SNR, spatial resolution, mechanical frequency, induced shear wave amplitude, and reconstruction method. It was formerly shown in a simulation study that 7 to 10 voxels were needed to properly resolve the shear wavelength, λ_{ref}, and both accurately and precisely quantify the mechanical properties of the targeted tissue by inversion of the equation of motion. The purpose here is to experimentally reproduce the conditions defined by the simulation to determine the actual influence of the acquisition voxel size, ***a***, on MRE acquisitions and validate the predicted λ_{ref}/a conditions for optimal MRE reconstruction.

1386

Alteration of mechanical tissue parameters during progressive formalin fixation measured by broadband Magnetic Resonance Elastography using a compact and portable tabletop scanner

Jürgen Braun[1], Heiko Tzschätzsch[2], Clara Körting[3], Marika Jenderka[3], Angela Ariza de Schellenberger[2], Toni Drießle[4], Michael Ledwig[4], and Ingolf Sack[2]

[1]Department of Medical Informatics, Charité - Universitätsmedizin Berlin, Berlin, Germany, [2]Department of Radiology, Charité - Universitätsmedizin Berlin, Berlin, Germany, [3]Beuth Hochschule für Technik Berlin, Berlin, Germany, [4]Pure Devices GmbH, Würzburg, Germany

A compact tabletop MR elastography (MRE) device was employed for rheological tests of soft tissue samples to measure the change of viscoelastic powerlaw constants in liver and brain tissue during progressive fixation. Shear-modulus dispersion functions were acquired from 300 to 5700Hz in animal tissues at different states of formaldehyde fixation and fitted by the rheological springpot-powerlaw model. Formalin fixation reduced viscosity and increased elasticity of liver tissue faster and to a higher degree than in brain tissue similar to the alteration of mechanical properties observed by in vivo elastography of hepatic fibrogenesis.

Traditional Poster

Artifacts

Exhibition Hall 1387-1406 Monday 8:15 - 10:15

1387

Robust k-space trajectory mapping with data readout concatenation and automated phase unwrapping reference point identification

E. Brian Welch[1,2,3], Ryan K. Robison[4], and Kevin D. Harkins[2,3]

[1]Radiology and Radiological Sciences, Vanderbilt University Medical Center, Nashville, TN, United States, [2]Vanderbilt University Institute of Imaging Science, Vanderbilt University Medical Center, Nashville, TN, United States, [3]Biomedical Engineering, Vanderbilt University, Nashville, TN, United States, [4]Neuroimaging Research, Barrow Neurological Institute, Phoenix, AZ, United States

A fundamental challenge when mapping k-space trajectories that require unwrapping of phase proportional to position in k-space is the accrual of phase during gradient prewinders and phase encodes, which are not sampled. To overcome this challenge, we present a simple method using data readout concatenation and automated phase unwrapping reference point identification to robustly map a broad range of trajectories. This approach works for any k-space trajectory for which data readouts can be connected to provide a path crossing near the center of k-space from which 1D phase unwrapping can be performed.

1388

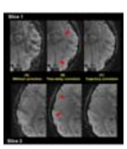

Characterization of k-space trajectory error using time delay correction for EPI

Yi-Cheng Hsu[1,2], Ying-Hua Chu[1,2], Maxim Zaitsev[2], and Fa-Hsuan Lin[1,3]

[1]Institute of Biomedical Engineering, National Taiwan University, Taipei, Taiwan, [2]Medical Physics, Department of Radiology, University Medical Center Freiburg, Freiburg, Germany, [3]Department of Neuroscience and Biomedical Engineering, Aalto University, Espoo, Finland

The ghosting artifacts in echo-planar imaging can be greatly reduced by aligning the k-space coordinates between odd and even lines based on their relative time delay. However, we found this approach is limited in artifact reduction. Specifically, we found that the image still has prominent artifacts and high spatial frequency k-space coordinates for even and odd lines still differ from each other significantly after time delay correction. This result suggested the origin of the ghosting artifact is beyond the time delays between neighboring readouts. The image artifact, however, can be greatly reduced using trajectory correction.

1389

Susceptibility-induced local ΔB0 variations are essential for predicting EPI distortions in the breast

Michael J van Rijssel[1], Frank Zijlstra[1], Peter R Seevinck[1], Peter R Luijten[1], Dennis W J Klomp[1], and Josien P W Pluim[1,2]

[1]Center for Image Sciences, UMC Utrecht, Utrecht, Netherlands, [2]Department of Biomedical Engineering, Eindhoven University of Technology, Eindhoven, Netherlands

Applications involving EPI readouts, such as diffusion weighted imaging and functional imaging, are hampered by geometrical distortions caused by static field inhomogeneities (ΔB_0). Pixel shift maps can be inferred from ΔB_0 maps. Though it is common practice to smooth these maps before calculating pixel shifts, doing so reduces susceptibility-induced local ΔB_0 variations. This study investigates the importance of local ΔB_0 changes in correctly predicting EPI distortions. Preliminary data obtained from the human breast *in-vivo* shows that susceptibility-induced changes in ΔB_0 are essential in accurately predicting EPI distortions.

1390

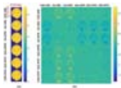

Performance assessment of EPI-distortion correction of brain images; which plane and phase encoding direction should be chosen?

Hengameh Mirzaalian[1], Benoit Scherrer[1], Onur Afacan[1], Ali Gholipour[1], and Simon K. Warfield[1]

[1]*Radiology, Harvard Medical School, Boston, MA, United States*

Echo-Planar-Imaging (EPI) is often used in DW-MRI to acquire a full volume in a short period of time. These images, however, show substantial local geometric and intensity distortions due to the susceptibility artefact. A popular method to correct for these distortions is to acquire a pair of images with opposite phase-encoding-directions (PED) but same slice-encoding-direction (SED) from which the distortion field can be estimated. While the choice of SED and PED likely impacts the correction effectiveness, it has never been rigorously quantitatively evaluated. In this work, we acquired scans with all combinations of SEDs and PEDs and evaluated the correction quality of three different distortion correction implementations.

1391

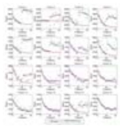

Characterising and correcting for MR signal drift in dynamic SPGR oxygen-enhanced MRI acquisitions

Adam K Featherstone[1,2], James P B O'Connor[2,3,4], Geoff J M Parker[1,2,5], and Julian C Matthews[1,2]

[1]*Division of Informatics, Imaging and Data Sciences, The University of Manchester, Manchester, United Kingdom,* [2]*CRUK & EPSRC Cancer Imaging Centre in Cambridge and Manchester, Cambridge and Manchester, United Kingdom,* [3]*Division of Molecular and Clinical Cancer Studies, The University of Manchester, Manchester, United Kingdom,* [4]*Department of Radiology, The Christie NHS Foundation Trust, Manchester, United Kingdom,* [5]*Bioxydyn Ltd., Manchester, United Kingdom*

Dynamic oxygen-enhanced (OE)-MRI, in combination with dynamic contrast-enhanced (DCE)-MRI, shows use in identifying hypoxic regions in tumours, but relies on an accurate knowledge of baseline (pre contrast-agent administration) tissue characteristics. We present a method of characterising baseline signal drift in an oxygen-enhanced MRI study of preclinical tumour xenografts, where the drift would otherwise impede quantitative analyses. We then demonstrate the utility and necessity of our methods through a comparison of calculated ΔR_1 values (reflecting tissue oxygen delivery) with and without our baseline drift correction.

1392

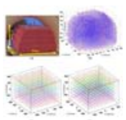

Comprehensive analysis of MR geometric distortion of multiple pulses sequence for radiotherapy applications

Max W.K. Law[1], Jing Yuan[1], Oilei O.L. Wong[1], and Ben Yu[1]

[1]*Hong Kong Sanatorium & Hospital, Hong Kong, Hong Kong, Hong Kong*

This study evaluated three-dimensional geometric distortion of six selected potential MR sequences for radiotherapy applications, acquired from a 1.5T 700mm-wide bore MR-simulator. Every sequence was investigated in three acquisition-orientations and multiple receiver-bandwidths, under various diameter-sphere-volume (DSVs). A large geometric accuracy phantom was constructed to quantify the distortion within the largest field-of-view allowed. Detailed distortion statistics, evaluation based on distortion requirements of different radiotherapy applications and comparison among sequences were reported. Results showed that sequence-types and acquisition-orientations were more influential to distortion than receiver-bandwidths. The distortion statistics are also a valuable guideline for sequence selection and optimization for radiotherapy.

1393

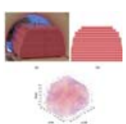

Longitudinal Monitoring of MR Image Distortion of a dedicated MR-Simulator for Radiotherapy over a 6-month Period

Max W.K. Law[1], Jing Yuan[1], Oilei O.L. Wong[1], and Ben Yu[1]

[1]*Medical Physics and Research Department, Hong Kong Sanatorium & Hospital, Hong Kong, Hong Kong*

This study investigated the variation of three-dimensional geometric distortion of geometric distortion caused by B0 inhomogeneity and gradient nonlinearity throughout a 6-month period of a 1.5T 700mm-wide bore MR-simulator. A large customized geometric accuracy phantom was constructed and a program was developed for distortion quantification. Experiment results showed that the distortion varied throughout the testing period. Regular validation of geometric accuracy might be needed if prior distortion information is used for distortion correction. Nonetheless, the variation of distortion had minimal effects on the sequences when considering radiotherapy distortion requirements.

1394

Robust On- and Off-Resonance constant amplitude spin-lock at the presence of B1 RF and B0 field inhomogeneity

Weitian Chen[1]

[1]*Imaging and Interventional Radiology, The Chinese University of Hong Kong, New Territory, Hong Kong*

T1rho is often measured by constant amplitude spin-lock, which can be played out either on-resonance or off-resonance. A major challenge to T1rho imaging with constant amplitude spin-lock is its susceptibility to B1 RF and B0 field inhomogeneity. A method to improve the robustness of on- and off-resonance constant amplitude spin-lock is presented in this work. The experimental results indicated that the proposed method can achieve superior image quality and improved quantification accuracy compared to the conventional approach in the presence of system imperfections.

1395

Correct Shaking Artifact in Diffusion Spectrum Imaging Using Estimated Maximum Likelihood

Chang-Le Chen[1], Yu-Jen Chen[2], Yung-Chin Hsu[2], and Wen-Yih Isaac Tseng[1,2,3]

[1]*Graduate Institute of Brain and Mind Sciences, National Taiwan University College of Medicine, Taipei, Taiwan,* [2]*Institute of Medical Device and Image, National Taiwan University College of Medicine, Taipei, Taiwan,* [3]*Molecular Imaging Center, National Taiwan University College of Medicine, Taipei, Taiwan*

Unexpected phase errors occurred in the k-space of the diffusion spectrum EPI sequence would lead to abrupt shifts in the phase-encoding direction across different diffusion gradient directions which cause shaking artifact of the image. The shaking artifact can lead to errors in image registration and diffusion index calculation. Here, we developed an estimated maximum likelihood method to detect and correct image shifts. After correcting the shaking artifact, the performance of registration and the diffusion index calculation were significantly improved comparing to the images without correction.

1396

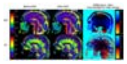

Improving Apparent Diffusion Coefficient Accuracy on a Compact 3T MRI Scanner using Gradient Non-linearity Correction

Ashley T Tao[1], Yunhong Shu[1], Ek T Tan[2], Joshua D Trzasko[1], Shengzhen Tao[1], Paul Weavers[1], John III Huston[1], and Matt A Bernstein[1]

[1]Radiology, Mayo Clinic, Rochester, MN, United States, [2]GE Global Research, Niskayuna, NY, United States

Errors are introduced into apparent diffusion coefficient quantification of diffusion weighted imaging (DWI) due to imperfect gradient linearity. A post-processing gradient non-linearity (GNL) correction algorithm can alleviate this problem on a conventional whole-body MR scanner equipped with a symmetrical gradient system. A compact 3T (C3T) scanner with a high-performance gradient was recently developed and exhibits more complex GNL than conventional whole-body gradients due to its asymmetric design. Here, we test the robustness of this GNL correction on the C3T using phantom and in-vivo experiments, and demonstrated improved accuracy of quantitative maps for DWI on the C3T using this algorithm.

1397

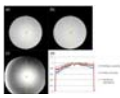

Compensation for Distribution of Receiving Sensitivity in Body Coil

Shinji Kurokawa[1], Yasuhiro Kamada[1], Masahiro Takizawa[1], and Yoshitaka Bito[1]

[1]Healthcare Business Unit, Hitachi, Ltd., Tokyo, Japan

We propose a new method to compensate for distribution of receiving sensitivity in a body coil. It corrects a shading artifact that remains after compensation based on sensitivity ratio of surface and body coils. The method utilizes body coil sensitivity taken in advance with an uniform phantom. The body coil sensitivity is transformed by referring the ratio of intensity between channels. The method is intrinsically insensitive to tissue contrast because it is cancelled by taking ratio. The method is useful when the reference image has strong tissue contrast. The effect of proposed method is examined by phantom and volunteer study.

1398

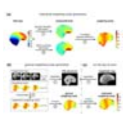

Shimming for BOLD sensitivity in the brain

Yuhang Shi[1], Signe Johanna Vannesjo[1], Karla Loreen Miller[1], and Stuart Clare[1]

[1]Oxford Centre for Functional MRI of the Brain, University of Oxford, Oxford, United Kingdom

Whole brain resting state fMRI benefits greatly from shimming due to increases in BOLD sensitivity. This work presents a rapid shim calculation method using prior knowledge of nonlinear optimization results on a large database of field maps, which can significantly reduce the time spent on shim determination for BOLD sensitivity optimization, whilst delivering shim quality that is closer to the results of nonlinear optimization.

1399

Single-Scan GRE Myelin Water Imaging with Macroscopic Field Inhomogeneity Compensation

Doohee Lee[1], Jingu Lee[1], Jongho Lee[1], and Yoonho Nam[2]

[1]Department of Electrical and Computer Engineering, Seoul National University, Seoul, Korea, Republic of, [2]Department of Radiology, Seoul St. Mary's Hospital, College of Medicine, The Catholic University of Korea, Seoul, Korea, Republic of

In this study, we propose a single-scan GRE-MWI method that corrects for the effects of macroscopic field inhomogeneity using a modified z-shimming. In addition, a new three-component magnitude model corresponding to the modified sequence is proposed. Compared to the conventional method, the results showed an improved MWF estimation, particularly in frontal lobe regions.

1400

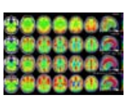

Partial Volume Correction and Transit Time correction effect in absolute perfusion quantification with 3D Pseudo-Continuous Arterial Spin Labelling.

Juan Antonio Hernandez-Tamames[1], Eva Manzanedo[2], Virginia Mato[3], Pablo Garcia-Polo[4], and Marion Smits[1]

[1]Radiology and Nuclear Medicine, Erasmus MC, Rotterdam, Netherlands, [2]Rey Juan Carlos University, [3]A Coruña University, [4]GE Healthcare

This work studies partial volume correction and transit time correction in CBF assessment with 3DPCASL sequence. It is shown how important are these corrections depending on brain regions and the amount of gray matter inside the voxel.

1401

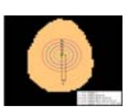

Validation of an ASL processing pipeline accounting for low SNR and the presence of an EPI artifact, using simulated and real data.

Maria-Eleni Dounavi[1,2], Aneurin J. Kennerley[2,3], Esben Thade Petersen[4,5], and Iain D. Wilkinson[1,2]

[1]Academic Unit of Radiology, University of Sheffield, Sheffield, United Kingdom, [2]Neuroimaging in Cardiovascular Disease (NICAD) Network, University of Sheffield, Sheffield, United Kingdom, [3]Department of Psychology, University of Sheffield, Sheffield, United Kingdom, [4]Danish Research Centre for Magnetic Resonance, Centre for Functional and Diagnostic Imaging and Research, Copenhagen University Hospital, Hvidovre, Denmark, [5]Center for Magnetic Resonance, DTU Elektro, Technical University of Denmark, Lyngby, Denmark

This study aimed to optimize a processing pipeline for QUASAR ASL. We have focused on 3 aspects: the assignment of AIFs in voxels; dealing with voxels having excessive values potentially due to an EPI artifact; and minimization of partial volume effects. Simulations showed that GM CBF values closer to the ground truth are obtained by using AIFs in a distance double than the nearest-neighbor AIF to every voxel. In terms of an EPI artifact present in the analysis, we have shown that identification and exclusion of influenced voxels with a developed algorithm, results in values closer to the expected ones.

1402

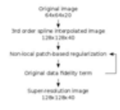

Patch-based super-resolution for arterial spin labeling MRI

Cédric Meurée[1,2,3,4,5], Pierre Maurel[2,3,4,5], Elise Bannier[2,3,4,5,6], and Christian Barillot[2,3,4,5]

[1]Siemens Healthineers, Saint-Denis, France, [2]Univ Rennes 1, F - 35043, Rennes, France, [3]INRIA, F - 35042, Rennes, France, [4]INSERM, U746, F - 35042, Rennes, France, [5]CNRS, U 6074, F - 35042, Rennes, France, [6]CHU Rennes, F - 35033, Rennes, France

Partial volume effects (PVE) are an important limitation of arterial spin labeling (ASL) acquisitions, impacting the validity of quantitative cerebral blood flow (CBF) estimations. This abstract presents a super-resolution algorithm, which includes information of high resolution (HR) structural images to reconstruct HR CBF maps from low resolution ASL series, without increasing the acquisition time. Compared with nearest neighbor, trilinear and 3rd order spline interpolations, the proposed algorithm is found to generate a CBF image closer to the one obtained with a reference HR ASL acquisition. CBF calculations can therefore be improved by using this algorithm, which reduces the PVE.

1403

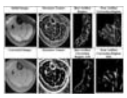

Automated segmentation of Intramuscular Connective Tissue (IMCT) from skeletal muscle in presence of artifacts: Application to Changes in IMCT in an Unilateral Limb Suspension Induced Acute Atrophy Model in the Plantarflexors

Vincent Ugarte[1], Usha Sinha[1], Vadim Malis[2], and Shantanu Sinha[3]

[1]Physics, San Diego State University, San Diego, CA, United States, [2]Physics, UC San Diego, San Diego, CA, United States, [3]Radiology, UC San Diego, San Diego, CA, United States

Chronic muscle atrophy can be induced by limb suspension and is characterized by a loss of muscle mass and force. However, there could also be changes to the connective tissue volume that may contribute to the loss of muscle function. We studied the changes in connective tissue volume in a model of chronic atrophy induced by Unilateral limb suspension (ULLS) using ultralow TE sequences. We integrated an artifact correction algorithm to a 3D fuzzy segmentation algorithm to automatically segment the connective tissue from dual echo UTEs images corrupted by artifacts. Percent connective tissue increased post-ULLS but not the absolute values.

1404

Contrast and Resolution Mixing for Magnetic Resonance Fingerprinting

Gregor Körzdörfer[1,2], Mark Griswold[3,4], Dan Ma[3], Yun Jiang[3], Josef Pfeuffer[1], Thorsten Feiweier[1], Thomas Kluge[1], and Mathias Nittka[1]

[1]Application Development, Siemens Healthcare, Erlangen, Germany, [2]Friedrich-Alexander Universität Erlangen-Nürnberg, Erlangen, Germany, [3]Department of Biomedical Engineering, Case Western Reserve University, OH, United States, [4]Dept. of Radiology, Case Western Reserve University and University Hospitals of Cleveland, OH, United States

Quantitative parameter maps obtained from Magnetic Resonance Fingerprinting (MRF) are sensitive to B1+ inhomogeneities. Extending a dictionary by an additional B1+ dimension is a promising approach to account for this. In order to improve the differentiation of data in the B1+ dimension, we implemented a novel B1+ sensitive encoding. This approach employs the extension of the conventional FISP encoding by RF spoiled parts. Since high undersampling factors prevent a direct implementation of this technique, the undersampling pattern is varied during the acquisition. We use a spiral acquisition scheme which samples most of the FISP encoded parts of the fingerprint with high resolution. RF spoiled parts as well as a small fraction of the FISP encoded parts are being sampled with low resolution.

1405

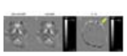

Background Field Removal Technique using Non-regularized Variable Kernels Sophisticated Harmonic Artifact Reduction for Phase Data for Quantitative Susceptibility Mapping

Hirohito Kan[1], Nobuyuki Arai[1], Masahiro Takizawa[2], Kazuyoshi Omori[2], Harumasa Kasai[1], Yasujiro Hirose[1], and Yuta Shibamoto[1]

[1]Department of Radiology, Nagoya City University Hospital, Nagoya, Japan, [2]Unit of Healthcare Business, Hitachi, Ltd.

QSM is relatively new biochemical and quantitative reconstruction method which directly estimates the iron distribution. It needs a precision of separation of local field from background field for measurement of accurate susceptibility value. We introduced a novel method using non-regularized variable kernels sophisticated harmonic artifact reduction for phase data (NR-VSHARP). The proposed method utilized multiple kernel sizes and minimization of norm only inside mask without any regularization parameter. NR-VSHARP enabled to estimate high accurate local field, compared with VSHARP. NR-VSHARP method provides high accurate local field map with saving cortical information.

1406

Noise and Artifact Reduction in 3D Abdominal and Thoracic Imaging using CAIPIRINHA

Timothy J Colgan[1,2], Karl K Vigen[1], Curtis N Wiens[1], and Scott B Reeder[1,2,3,4,5]

[1]Radiology, University of Wisconsin, Madison, WI, United States, [2]Medical Physics, University of Wisconsin, Madison, WI, United States, [3]Biomedical Engineering, University of Wisconsin, Madison, WI, United States, [4]Medicine, University of Wisconsin, Madison, United States, [5]Emergency Medicine, University of Wisconsin, Madison, WI, United States

This study investigated Controlled Aliasing In Parallel Imaging Results IN Higher Acceleration (CAIPIRINHA) in combination with Rotated Slab Excitation (ROSE) to reduce parallel imaging artifacts and residual aliasing artifacts using a coronal reconstruction and sagittal excitation. Images acquired using the CAIPIRINHA sampling pattern had fewer parallel imaging artifacts than using a conventional sampling pattern. G-factor analysis also demonstrated improved SNR performance using the CAIPIRINHA sampling pattern. The CAIPIRIHNA sampling pattern when combined with ROSE reduced residual aliasing artifacts and parallel imaging artifacts. This enables higher acceleration factors for shorter scan times, without sacrificing image quality.

Traditional Poster

Sparse & Low-Rank Reconstruction

Exhibition Hall 1407-1429 Monday 8:15 - 10:15

1407

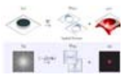

Continuous domain compressed sensing (CD-CS): application to accelerated dynamic MRI

Arvind Balachandrasekaran[1], Greg Ongie[2], and Mathews Jacob[1]

[1]Electrical and Computer Engineering, University of Iowa, Iowa City, IA, United States, [2]EECS, University of Michigan, MI, United States

We introduce a novel continuous domain compressed sensing (CD-CS) framework for the recovery of MRI data. We formulate the recovery of the high-resolution continuous domain Fourier coefficients of the image from few of its samples as a structured low-rank matrix completion problem. We also introduce novel algorithms to solve this matrix completion problem in run-times that are comparable with discrete CS formulations. The application of this algorithm to (2D+time) dynamic MRI problems is observed to yield significantly improved reconstructions compared to state of the art CS methods.

1408

Novel annihilation filter framework for accelerated parameter mapping

Arvind Balachandrasekaran[1] and Mathews Jacob[1]

[1]Electrical and Computer Engineering, University of Iowa, Iowa City, IA, United States

Quantitative parameter maps offer valuable information about various tissue attributes, which are early markers for many neurological disorders. However the long acquisition time of the associated image time series puts a restriction on the achievable spatial resolution. In this work, we introduce a novel framework, which exploits the exponential nature of the time profiles at every pixel and spatial smoothness of the exponential parameters to recover the images from highly under-sampled measurements. Our preliminary results clearly demonstrate the potential of the proposed algorithm.

1409

Task-based Optimization of Regularization in Highly Accelerated Speech RT-MRI

Jieshen Chen[1], Sajan Goud Lingala[1], Yongwan Lim[1], Asterios Toutios[1], Shrikanth Narayanan[1], and Krishna Nayak[1]

[1]Electrical Engineering, University of Southern California, Los Angeles, CA, United States

Speech RT-MRI has recently experienced significant improvements in spatio-temporal resolution, through the use of sparse sampling and constrained reconstruction. The regularization parameters used for balancing data consistency and object model consistency were often chosen by visual assessment of image quality. Here, we perform task-based optimization of regularization in highly accelerated speech RT-MRI, focusing on the production of consonants and vowels, and analyzing the articulatory features, using both qualitative and quantitative methods. Results drawn from different methods help determine proper regularization parameters for the reconstruction of specific speaking tasks.

1410

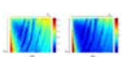

Study on regularization paremeter tuning in compressed sensing using no-reference image quality assessment

Kihun Bang[1], Jinseong Jang[1], and Dosik Hwang[1]

[1]School of Electrical and Electronic Engineering, Yonsei University, Seoul, Korea, Republic of

In Magnetic Resonance Imaging system, acquiring fewer measurements is required to reduce scan time, but it leads the aliasing artifact. Compressed Sensing is exploited to reconstruct image from undersampled data without artifacts by solving the optimization problem. However, It has some difficulites in selecting regularization parameters and this abstract propose the way to select regularization parameters by evaluating image quality. The quality of reconstructed image from proposed method is much better than the image from manual parameters. This study also has potential to be helpful in fast MR imaging.

1411

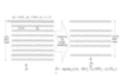

Compressed Sensing MRI Using Bunched Phase Encoding

Jingxin Zhang[1,2], Kazi Rafiqul Islam[1], and Kai Zhu[1]

[1]School of Software and Electrical Eng, Swinburne University of Technology, Melbourne, Australia, [2]Dept of Electrical and Computer Systems Eng, Monash University, Melbourne, Australia

This abstract presents a novel method for compressed sensing (CS) MRI. This method combines the variable density random undersampling and iterative image reconstruction in CS-MRI with the regularly reduced bunched phase encoding (BPE) and linear equation based image reconstruction of BPE-MRI to further reduce data acquisition time and improve image quality of CS-MRI. Simulation results demonstrate the effectiveness and advantage of the presented method.

1412 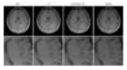

A Novel Hybrid Total Variation Minimization Method to MRI Reconstruction from Highly Undersampled Data

Hongyu Li[1], Yong Wang[2], Dong Liang[3], and Leslie Ying[1]

[1]Department of Biomedical Engineering, Department of Electrical Engineering, The State University of New York at Buffalo, Buffalo, NY, United States, [2]School of Electronic Engineering, Xidian University, Xi'an, People's Republic of China, [3]Institute of Biomedical and Health Engineering, Shenzhen Institutes of Advanced Technology, Shenzhen, People's Republic of China

This abstract presents a novel hybrid total variation minimization algorithm to reconstruct MR images from reduced measurements. The method combines the benefits of both L1 and homotopic L0 minimization algorithms for sparse signal reconstruction in the sense that substantially fewer measurements are needed for exact reconstruction. The algorithm minimizes the conventional total variation when the gradient is small, and minimizes the L0 of gradient when the gradient is large. An auto-adaptive threshold determines the transition between L1 and L0 of the gradients. The experimental results show the proposed algorithm outperforms either L1 or homotopic L0 minimization when the same reduction factor is used.

1413 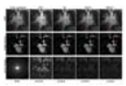

High resolution 3D MRI reconstruction using 3DMDTV regularization

Yue Hu[1], Xin Lu[1], Kuangshi Zhao[2], and Mathews Jacob[3]

[1]Harbin Institute of Technology, Harbin, People's Republic of China, [2]CSIC 703 Institute, [3]University of Iowa, Iowa City, IA, United States

Three-dimensional (3D) MRI plays an important role in many clinical applications due to its ability to provide the full geometry of the targeted region of the body. However, speed limitation remains the key challenge to 3D MRI. Here, we present a compressed sensing reconstruction scheme using the 3DMDTV regularization. The experiments demonstrate that for high acceleration factors, the proposed method has better performance than other schemes by providing more accurately recovered images with more subtle details preserved.

1414 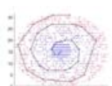

Accelerated 3D Arterial Spin Labeling using Cartesian Acquisition with Spiral Reordering and Compressed Sensing

Huajun She[1], Joshua S. Greer[1,2], Xinzeng Wang[1], Elena Vinogradov[1,3], and Ananth Madhuranthakam[1,3]

[1]Radiology, UT Southwestern Medical Center, Dallas, TX, United States, [2]Bioengineering, UT Dallas, Dallas, TX, United States, [3]Advanced Imaging Research Center, UT Southwestern Medical Center, Dallas, TX, United States

Arterial spin labeling (ASL) is a non-contrast perfusion imaging method for MRI. However, 2D ASL suffers from low signal to noise ratio. 3D ASL is favorable to overcome the limitation of 2D ASL, but 3D acquisition is time-consuming, so acceleration of 3D ASL is highly desired. The new compressed sensing (CS) theory allows perfect reconstruction far below Nyquist rate. We implemented a novel 3D TSE acquisition using Cartesian Acquisition with SPiral Reordering (CASPR), which can be undersampled and combined with CS. Preliminary results show improved image quality using 3D Sparse-BLIP reconstruction that is comparable to fully sampled acquisition.

1415 

Accelerated MR Diffusion Tensor Imaging Using Partial Fourier Compressed Sensing

Chia-Chu Chou[1], Frank Q Ye[2], Cecil Chern-Chyi Yen[3], Behtash Babadi[1], Rao P Gullapalli[4], David A Leopold[2], and JiaChen Zhuo[4]

[1]ECE, University of Maryland College Park, College Park, MD, United States, [2]Neurophysiology Imaging Facility, National Institute of Mental Health, National Institute of Neurological Disorders and Stroke, and National Eye Institute, National Institutes of Health, Bethesda, MD, United States, [3]NINDS/LFMI/CMS, National Institutes of Health, Bethesda, MD, United States, [4]Diagnostic Radiology and Nuclear Medicine, UM School of Medicine, Baltimore, MD, United States

3D-DTI are often used in ex vivo imaging to achieve superior spatial resolution and to map fine white matter structure. However, image acquisition time is long especially when many diffusion directions are used to better define orientation profiles and resolve crossing fibers. In this study we apply a new imaging acceleration technique – Partial Fourier Compressed Sensing (PFCS) on DTI acceleration. We demonstrated PFCS provide satisfactory reconstruction with only half of the raw data while retaining fine anatomical details on DTI parameter maps.

1416 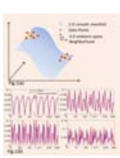

Beyond Low-Rank and Sparsity: A Manifold driven Framework for Highly Accelerated Dynamic Magnetic Resonance Imaging

Ukash Nakarmi[1], Konstantinos Slavakis[1], Jingyuan Lyu[1], Chaoyi Zhang[1], and Leslie Ying[1,2]

[1]Electrical Engineering, University at Buffalo, State University of New York, Buffalo, NY, United States, [2]Biomedical Engineering, University at Buffalo, State University of New York, Buffalo, NY, United States

The state-of-the-art methods in accelerating dynamic Magnetic Resonance (dMR) Imaging rely on sparse and/or low-rank priors. We propose a novel manifold driven framework that exploits the manifold smoothness priors to highly accelerate data acquisition in dMR. We postulate that images in dMR lie on or close to a smooth manifold and learn the manifold geometry from the navigator signals. Capitalizing on the learned manifold, we develop two regularization loss functions and subsequently build a framework to reconstruct dMR images from highly undersampled k-space data. The proposed method is shown to be superior than competitive methods in different data sets.

1417 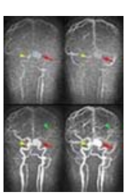

Application of Iterative Reconstruction for MR Digital Subtraction Angiography: Toward Better Visualization of Small Vessels and Reduction of Gadolinium-Based Contrast Media.

Yasutaka Fushimi[1], Tomohisa Okada[2], Akira Yamamoto[1], Tsutomu Okada[1], Aurelien Stalder[3], Christoph Forman[3], Michaela Schmidt[3], and Kaori Togashi[1]

[1]Department of Diagnostic Imaging and Nuclear Medicine, Kyoto University Graduate School of Medicine, Kyoto, Japan, [2]Human Brain Research Center, Kyoto University Graduate School of Medicine, Kyoto, Japan, [3]Siemens Healthcare GmbH, Erlangen, Germany

Improved signal and temporal footprint for dynamic MRA due to the retrospective iterative reconstruction may better visualize small peripheral vessels with reduced GBCA dose. CE-MRA-TWIST images were reconstructed twice from the same raw data, with the standard product reconstruction and with iterative reconstruction (IT) by using L1 wavelet regularization in space and time. CE-MRA-IT-TWIST nicely visualized hemodynamics in the brain even with 20% GBCA dose administration compared with CE-MRA-TWIST, especially in the arterial phase. Enhancement slope of CE-MRA-IT-TWIST was statistically higher than that of CE-MRA-TWIST.

1418

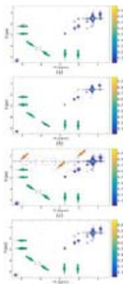

A low rank Hankel matrix reconstruction approach to recover hybrid time and frequency data in non-uniformly sampled magnetic resonance spectroscopy

Hengfa Lu[1], Xinlin Zhang[1], Tianyu Qiu[1], Jian Yang[1], Di Guo[2], Zhong Chen[1], and Xiaobo Qu[1]

[1]Department of Electronic Science, Xiamen University, Xiamen, People's Republic of China, [2]School of Computer and Information Engineering, Xiamen University of Technology, Xiamen, People's Republic of China

Magnetic resonance spectroscopy has many important applications in bio-engineering while the acquisition of high dimensional spectroscopy is usually time consuming. Non-uniformly sampling can speed up the data acquisition but the missing data points have to be restored with proper signal models. In this work, a specific two dimensional magnetic resonance signal, of which the first dimension lies in time domain while the second dimension lies in frequency domain, is reconstructed with a proposed low rank enhanced Hankel matrix method. Results on realistic magnetic resonance spectroscopy shows that proposed method outperform the state-of-art compressed sensing method on recovering low intensities spectral peaks.

1419

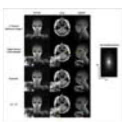

Accelerating 3D Head-and-Neck MR Imaging Using Compressed Sensing with Structure-Guided Total Variation for MR-Guided Multi-Fractional Radiotherapy

Yihang Zhou[1], Jing Yuan[1], Oi Lei Wong[1], Winky Wing Ki Fung[2], George Chiu[2], Kin Yin Cheung[1], and Siu Ki Yu[1]

[1]Medical Physics and Research Department, Hong Kong Sanatorium & Hospital, Happy Valley, Hong Kong, [2]Department of Radiotherapy, Hong Kong Sanatorium & Hospital, Happy Valley, Hong Kong

MR image-guided radiotherapy (IGRT) holds potentials on outcome improvement in the head-and-neck (HN) radiotherapy. Patients receiving MR-guided multi-fractional HN IGRT are immobilized in each treatment fraction and set up to the exact position as of the treatment planning scan. Inter-fractional MR images are supposed to show highly correlated anatomy structure and edge information which can be incorporated into compressed sensing (CS) based MR reconstruction to shorten the scan time while preserve image quality in multiple fractions. In this study, we investigated the feasibility of accelerating high spatial resolution 3D MRI using CS with structure-guided total variation for multi-fractional HN radiotherapy.

1420

Accelerate multi-dimensional magnetic resonance spectroscopy with low rank tensor and Hankel structures

Jiaxi Ying[1], Hengfa Lu[1], Qingtao Wei[2], Jiang-Feng Cai[3], Di Guo[4], Jihui Wu[2], Zhong Chen[1], and Xiaobo Qu[1]

[1]Department of Electronic Science, Xiamen University, Xiamen, People's Republic of China, [2]School of Life Sciences, University of Science and Technology of China, Hefei, People's Republic of China, [3]Department of Mathematics, Hong Kong University of Science and Technology, People's Republic of China, [4]School of Computer and Information Engineering, Xiamen University of Technology, Xiamen, People's Republic of China

Non-uniformly sampling is an effective way to accelerate high-dimensional magnetic resonance spectroscopy (MRS). The spectrum is usually reconstructed with proper prior knowledge. In this work, we exploit the intrinsic *N*-D exponential signals of multi-dimensional MRS to reconstruct the spectrum. A low rank tensor representation of multi-dimensional MRS and the exponential structure of the associated factors are simultaneously explored. Results on 3-D MRS data shows that the proposed method can faithfully reconstruct the spectrum from a small amount of measurements, allowing a significant reduction of acquiring time in real applications.

1421

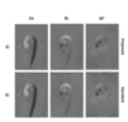

A novel compressed sensing inspired approach for flow reconstruction

Felipe Cortés[1,2], Carlos Sing-Long[2,3], and Sergio Uribe[2,4]

[1]Department of Electrical Engineering, Pontificia Universidad Católica de Chile, Santiago, Chile, [2]Biomedical Imaging Center, Pontificia Universidad Católica de Chile, Santiago, Chile, [3]Institute for Biological and Medical Engineering, Schools of Engineering, Medicine and Biological Sciences, Pontificia Universidad Católica de Chile, Santiago, Chile, [4]Department of Radiology, School of Medicine, Pontificia Universidad Católica de Chile, Santiago, Chile

High scan times are one of the most important drawbacks in 4D flow scans and multiple solutions have been proposed to solve this issue. We propose a novel method for undersampled flow reconstruction inspired on the ideas of compressed sensing. By considering the magnitude and complex phase as separate variables, we were able to impose independent properties on each, such as having a constant magnitude over all flow enconding acquisitions and enforcing low phase values on low magnitude areas, thus directly reducing the resulting images' noise. Our method was able to successfully reconstruct flow data with negligible error from undersampled data.

1422

Quantitative Susceptibility Map Reconstruction from MR Phase Data Using Morphology-Adaptive Total Variation

Li Guo[1], Yihao Guo[1], Yingjie Mei[1,2], Jijing Guan[1], Wufan Chen[1], and Yanqiu Feng[1]

[1]Guangdong Provincial Key Laboratory of Medical Image Processing, School of Biomedical Engineering, Southern Medical University, Guangzhou, People's Republic of China, [2]Philips Healthcare, Guangzhou, People's Republic of China

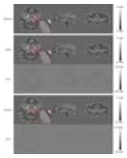

MEDI reduces streaking artifacts in QSMs by minimizing total variation in smooth regions in the susceptibility map. However, MEDI still contains artifacts near image edges because this method does not impose any constraint on voxels near edges. We aim to improve the reconstruction of quantitative susceptibility map from MR phase data by introducing morphology-adaptive TV regularization which imposes the TV constraint on the whole susceptibility map but with different weights in smooth and non-smooth regions. The performance of the proposed method is demonstrated in both simulation and in vivo data sets.

1423 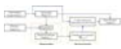

Multi-contrast image guided graph representation and its application in compressed sensing MRI reconstruction

Zongying Lai[1], Xiaobo Qu[2], Jiaxi Ying[2], Hengfa Lu[2], Zhifang Zhan[2], Di Guo[3], and Zhong Chen[2]

[1]Dept. of Communication Engineering, Fujian Provincial Key Laboratory of Plasma and Magnetic Resonance, Xiamen University, Xiamen 361005, China, xiamen, People's Republic of China, [2]Dept. of Electronic Science, Fujian Provincial Key Laboratory of Plasma and Magnetic Resonance, Xiamen University, Xiamen 361005, China, People's Republic of China, [3]Dept. of Computer Science, Xiamen University of Technology, Xiamen 361024, China, People's Republic of China

Under-sampling the k-space data and reconstructing images with sparsity constraint is one efficient way to accelerate magnetic resonance imaging However, achieving high acceleration factor is challenging since image structures may be lost or blurred when the sampled information is not sufficient. In this work, we propose a new approach to reconstruct magnetic resonance images by learning the prior knowledge from multi-contrast images with graph-based sparsifying transform. To incorporate extra information from multi-contrast image, registration is included in a bi-level optimization frame as well as the sparse reconstruction. Experiment results demonstrate that the proposed method outperforms the state-of-art with high accelerating factor.

1424 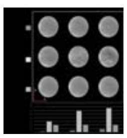

Image quality impact of randomized sampling trajectories: implications for compressed sensing

Melissa Jones[1], Richard Frayne[1,2,3], and Robert Marc Lebel[1,2,3,4]

[1]Biomedical Engineering, University of Calgary, Calgary, AB, Canada, [2]Seaman Family MR Centre, Foothills Medical Centre, Calgary, AB, Canada, [3]Radiology, University of Calgary, Calgary, AB, Canada, [4]GE Healthcare, Calgary, AB, Canada

Compressed sensing (CS) has the potential to drastically reduce MR acquisition times, however image quality of prospectively implemented CS is not as good as predicted by retrospectively under-sampled data. This may be due to the sensitivity of appropriate (randomized) CS k-space sampling to eddy currents. We show the existence of these detrimental interactions in full but randomly-sampled k-space, and quantify these interactions in under-sampled CS image reconstruction. We demonstrate how sorting the acquisition order to minimize the total k-space trajectory length mitigates this issue and improves image quality.

1425 

Optimization of Reconstruction Parameters of Compressed Sensing STIR SEMAC for Metal Artifact Reduction MRI of Hip, Knee and Ankle Arthroplasty Implants: How many Iterations and how much Regularization is needed?

Gaurav Kumar Thawait[1], Dharmdev H Joshi[1], Esther Raithel[2], Mathias Nittka[2], Wesley D Gilson[3], and Jan Fritz[1]

[1]Johns Hopkins University, Baltimore, MD, United States, [2]Siemens Healthcare GmbH, [3]Siemens Healthcare USA

Compressed sensing-(CS)-based Slice Encoding for Metal Artifact Correction (SEMAC) turbo spin echo (TSE) pulse sequences achieve high –quality metal artifact reduction MRI around arthroplasty implants. Compressed sensing-based undersampling of k-space permits the time-neutral use of SEMAC, but requires iterative reconstruction algorithms, which are time consuming. We determined minimum number of iterations and regularization required for diagnostic image quality of STIR CS-SEMAC data sets of hip, knee and ankle arthroplasty implants. Our results show that 15-17 iterations and 0.0035 regularization results in optimal image quality of STIR CS-SEMAC images, which currently requires 4-5 minutes of reconstruction time.

1426 

Flexible Prospective Compressed Sensing Acceleration of Prostate DCE-MRI with Quantized CIRCUS

James A Rioux[1,2,3], Nathan J Murtha[1,3], Allister Mason[3], Chris V Bowen[1,2,3,4], Sharon Clarke[1,2,3], and Steven D Beyea[1,2,3,4]

[1]Biomedical Translational Imaging Centre (BIOTIC), Nova Scotia Health Authority, Halifax, NS, Canada, [2]Diagnostic Radiology, Dalhousie University, Halifax, NS, Canada, [3]Physics and Atmospheric Science, Dalhousie University, Halifax, NS, Canada, [4]Biomedical Engineering, Dalhousie University, Halifax, NS, Canada

Improving the temporal resolution of dynamic contrast-enhanced (DCE) MRI sequences often requires a reduction in image spatial resolution or quality. We propose an acquisition and reconstruction strategy, Quantized CIRCUS, which allows reconstruction of prospectively accelerated DCE-MRI data with desired spatial and temporal resolution, similar to golden-angle radial acquisition schemes but using Cartesian sampling. We demonstrate that this approach allows improved temporal resolution compared to standard clinical methods, without significant degradation of image quality or resolution, which may provide more accurate information for diagnosis of diseases like prostate cancer.

1427 

Flexible convex optimization with non-smooth regularizations for accelerated MRI reconstructions

Renjie He[1], Ruobing He[2], Guobing Li[1], Nan Liu[1], Renkuan Zhai[1], Ding Yu[1], Qi Liu[1], Jian Xu[1], and Weiguo Zhang[1]

[1]United-Imaging Healthcare America, Houston, TX, United States, [2]Indiana University School of Medicine, Fort Wayne, IN, United States

Convex optimization with non-smooth regularizers has recently gained increased interest as it has shown excellent performance and the ability to facilitate most of reconstruction problems in MR convincible. While there are many approaches towards its fulfillment, a flexible yet easy and comprehensive to realize method is always beneficial. One of the algorithms is proposed in this abstract. and we demonstrate that this algorithm can be easily adapted to many reconstruction problems in MRI with accelerated performance.

1428  Quantitative Evaluation of Temporal Sparse Regularizers for Compressed Sensing Breast DCE-MRI

Dong Wang[1], Lori R Arlinghaus[2], Thomas E Yankeelov[3], and David S Smith[2]

[1]School of Science, Nanjing University of Science and Technology, Nanjing, Jiangsu, People's Republic of China, [2]Institute of Imaging Science, Vanderbilt University Medical Center, Nashville, TN 37232, [3]Institute for Computational and Engineering Sciences, and the Departments of Biomedical Engineering and Internal Medicine, The University of Texas at Austin, Austin, Texas, USA

We quantitatively evaluate temporal sparse regularizers for breast DCE-MRI data under standard compressed sensing schemes. We consider five temporal regularizers on 4.5x retrospectively undersampled Cartesian in vivo breast DCE-MRI data, namely Fourier transform (FT), Haar wavelet transform (WT), total variation (TV), second order total generalized variation (TGV$_{\alpha}^{2}$) and nuclear norm (NN). Both signal-to-error ratio and concordance correlation coefficients of the derived pharmacokinetic parameters K^{trans} (volume transfer constant) and v_e (extravascular extracellular volume fraction) are estimated. Results show that NN produces the lowest image error while TV/TGV$_{\alpha}^{2}$ produce the most accurate pharmacokinetic parameters.

1429 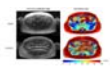 Assessing a radial multi-spin-echo sequence for robustness to motion artefacts in quantitative NMR imaging

Bertrand Coppa[1,2], Benjamin Marty[1,2], Pierre-Yves Baudin[3], Noura Azzabou[1,2], and Pierre G Carlier[1,2]

[1]NMR Laboratory, Institute of Myology, Paris, France, [2]CEA, DRF, I²BM, MIRCen, Paris, France, [3]Consultants for Research in Imaging and Spectroscopy, Tournai, Belgium

Fast parametric NMR imaging such as T2 and fat fraction mapping can be performed with a multi-spin-echo (MSE) sequence and an EPG-based model. Here, we compared a radial MSE encoding scheme to a standard Cartesian acquisition to monitor these two parameters in area subject to respiratory motion artifacts. Results show that the radial sequence was less affected from motion than the cartesian one and then improved the confidence of parameters estimation at these locations.

Traditional Poster

Post-Processing & Analysis

Exhibition Hall 1430-1476 Monday 8:15 - 10:15

1430 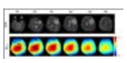 Evaluating effect of B1 field Inhomogeneity on DCE-MRI Data Analysis of Brain Tumor Patients at 3T

ANIRBAN SENGUPTA[1], RAKSHIT DADARWAL [1], RAKESH KUMAR GUPTA[2], and ANUP SINGH[1,3]

[1]Centre for Biomedical Engineering, Indian Institute of Technology Delhi, New Delhi, India, [2]Department of Radiology, Fortis Memorial Research Institute, GURGAON, [3]Biomedical Engineering, All India Institute Of Medical Science, New Delhi, India

In the current study, transmit B1 field inhomogeneity(B1FI) distribution and propagation of flip-angle(FA) related errors to Dynamic-contrast-enhanced(DCE) MRI data analysis in brain tumors of human subjects at 3T MRI were studied. Experimental and simulation studies were performed to evaluate the propagation of these errors to DCE-MRI data analysis and its correction were performed during signal intensity(S(t)) to concentration-time-curve(C(t)) conversion. This study show that B1FI introduced substantial errors in DCE-MRI data analysis(tracer-kinetic and hemodynamic parameters) and these errors were mitigated by correcting FA using B1 map. B1FI related error also showed dependence on concentration of contrast agent and length of concentration-time-curve.

1431 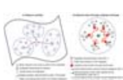 Brain Network Atlas Estimation using Centered Graph Shrinkage with Application to Developing and Aging Brains

Islem Rekik[1], Gang Li[1], Minjeong Kim[1], Weili Lin[1], and Dinggang Shen[1,2]

[1]Department of Radiology and BRIC, University of North Carolina, Chapel Hill, NC, United States, [2]Department of Brain and Cognitive Engineering, Korea University, Seoul, Republic of Korea

Learning how to average brain networks (i.e., build a *brain network atlas*) constitutes a key step in creating a reliable ‘mean’ representation of a set of normal brains, which can be used to spot deviations from the normal network atlas (i.e., abnormal cases). However, this topic remains largely unexplored in neuroimaging field. In this work, we propose a network atlas estimation framework through a non-linear diffusion along the local neighbors of each node (network) in a graph. Our evaluation on both developing and aging datasets showed a better ‘centeredness’ of our atlas in comparison with the state-of-the-art network fusion method.

1432  Robust and fast phase unwrapping strategy to improve SWI quality

Yongquan Ye[1], Jinguang Zong[2], and Weiguo Zhang[2]

[1]United Imaging of Healthcare America, Houston, TX, United States, [2]Shanghai United Imaging of Healthcare, Shanghai, People's Republic of China

A robust and fast phase unwrapping strategy was developed for multi-echo SWI, to improve image quality where classic SWI fails, such as cavity vicinity regions, as well as to provide pristine field map for subsequent QSM applications. A smoothing and a seed prioritizing method were proposed, which was demonstrated to provide very robust unwrapping on phase difference map between neighboring echoes. And with a high quality unwrapped phase difference map, the phase of all echoes can be robustly unwrapped in seconds.

1433 A Fast Adaptive Multispectral Nonlocal Denoising Filter

Michael C. Maring[1], Mustapha Bouhrara[1], and Richard G. Spencer[1]

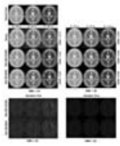

[1]*Laboratory of Clinical Investigation, National Institute on Aging, NIH, Baltimore, MD, United States*

We introduce a new high-performance nonlocal filter, NESMA, for noise reduction in multispectral (MS) MR imaging. Through extensive analysis, we show that the NESMA filter demonstrates a high degree of overall image denoising while preserving edges and small structures. We compared the performance of the NESMA filter to the multispectral nonlocal maximum likelihood (MS-NLML) filter. Although the MS-NLML filter is highly efficient, it requires extensive computational time. NESMA markedly decreases computation time while maintaining comparable levels of noise reduction and feature preservation. Finally, we show that adaptive selection of similar voxels further improves filtering quality.

1434 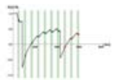

Inversion quality independent robust $$$T_1$$$-quantification of MOLLI sequence data

Thomas Kampf[1], Theresa Reiter[2], and Wolfgang Rudolf Bauer[3]

[1]*Experimental Physics V, Universität Wuerzburg, Wuerzburg, Germany,* [2]*University Hospital Wuerzburg,* [3]*University Hosptial Wuerzburg*

Quantitative mapping of the longitudinal relaxation time has gained increasing interest as it allows monitoring of important structural and functional information of the myocardium. The MOLLI sequence commonly used in clinical research requires a high quality of the inversion pulses for unbiased quantification which is non-trivial especially at high fields. In this work we present a simple modification of the MOLLI sequence which in combination with the recently introduced IGF post processing solves the problem of insufficient inversion quality as demonstrated in phantom experiments.

1435 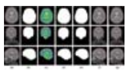

Improved Infant MRI Brain Extraction utilizing Clustering and Morphological Approaches

Yao Wu[1], Sonia Dahdouh, Marine Bouyssi-Kobar, Manoj Kumar, Josepheen Cruz, Wonsang You, and Catherine Limperopoulos

[1]*The Developing Brain Research Laboratory, Children's National Health System, Washington, DC, United States*

Accurate brain extraction is a key procedure in neuroimage analyses. This paper aims to solve the intracranial cavity overestimation issue inherent to existing brain extraction methods when applied to infant brains. We applied *k*-means clustering method and morphological approaches to improve the accuracy of previously published brain extraction techniques. Evaluation of our proposed method on 28 preterm MR images showed more robust and effective infant brain extraction compared to previous methods.

1436 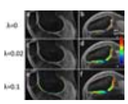

SNR-Weighted Regularization of ADC Estimates using Double-Echo in Steady-State

Bragi Sveinsson[1], Garry Gold[1], Brian Hargreaves[1], and Daehyun Yoon[1]

[1]*Radiology, Stanford University, Stanford, CA, United States*

Double-echo in steady-state (DESS) is a 3D sequence which offers both morphological images and quantitative parameter maps (SNR-efficient 3D maps of T2 and apparent diffusion coefficient (ADC)) in various applications, such as breast imaging or knee cartilage imaging. The sequence has less sensitivity to ADC than to T2, sometimes leading to noisy ADC maps. Here, we investigate the effects of using regularized fitting of the signals, with a penalty in ADC variability, to produce less noisy ADC maps. The method is designed to apply less regularization to regions with high SNR. The approach makes use of a recent analytical expression for a ratio between DESS signals.

1437 

Optimal contrast enhancement of blockface images for MRI guided reconstruction of mouse brain volumes

Christoffer Gothgen[1], Catharina Maria Holland[1], Christos Zoupis Schoinas[1], Karine Mardon[2], Maciej Plocharski[1], Lasse Riis Østergaard[1], and Andrew Janke[2]

[1]*Department of Health Science and Technology, Aalborg University, Aalborg, Denmark,* [2]*Centre for Advanced Imaging, University of Queensland, Brisbane, Australia*

Blockface imaging can improve atlases of the rodent brain by supplying high resolution images. This study compares three different contrast stretching methods for enhancing the information in blockface images together with a registration to a 16.4 T atlas of the mouse brain. Contrast enhancement technique used was histogram equalization, adjusting the image intensity values by stretching them between the bottom 1% and the top 1% and CLAHE with a clip limit of 0.01 and a uniform histogram. Registrations was rigid, affine and SyN. By using CLAHE as contrast stretching method a high similarity to the MRI was found.

1438 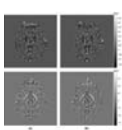

B0 Field Inhomogeneity Corrected Quantitative Susceptibility Mapping

Young-joong Yang[1], Jong-Hyun Yoon[1], Hyeon-Man Baek[2], and Chang-Beom Ahn[1]

[1]*Electrical engineering, Kwangwoon University, Seoul, Korea, Republic of,* [2]*Korea Basic Science Institute, Ochang, Korea, Republic of*

QSM is a method that generates internal susceptibility distribution of subject using material's intrinsic magnetic susceptibility property. Bo inhomogeneity affects magnitude and phase images. In this study, QSM with B0 field inhomogeneity correction is proposed. Using numerical simulation and in-vivo experiment, proposed method is verified. In simulation, improved susceptibility map is obtained with less root mean square error. In in-vivo experiment, signal loss and non-uniformity at frontal lobe are reduced. As field inhomogeneity increases according to the increase of main field strength, this method would be a more important element for QSM.

1439 

Real-time large-scale anatomical landmark detection with limited medical images

Jun Zhang[1], Mingxia Liu[1], and Dinggang Shen[1]

[1]Radiology and BRIC, UNC at Chapel Hill, Chapel hill, NC, United States

Landmark detection based on deep neural networks has achieved state-of-the-art performance in natural image analysis. However, it is challenging to detect anatomical landmarks from medical images, due to limited data. Here, we propose a *real-time large-scale* landmark detection method with *limited* training data. We train our model with image patches and test it with the entire image, inspired by fully convolutional networks. Also, we develop a weighted loss function in our model to increase the correlations between image patches and their nearby landmarks. The experimental results of detecting 1741 landmarks from brain MR images demonstrate the effectiveness of our method.

1440 

A fully automatic prostate segmentation method for both DWI and T2WI

Yi Zhu[1], Rong Wei[1], Ge Gao[2], Yajing Zhang[3], Xiaoying Wang[1,2], Jue Zhang[1,4], and Jing Fang[1,4]

[1]Academy for Interdisciplinary Studies, Peking University, Beijing, People's Republic of China, [2]Department of Radiology, Peking University First Hosp

Automatic prostate segmentation in MR images is a meaningful work, not only can be used in the first step of the Prostate Imaging Reporting and Data System,

---

1441 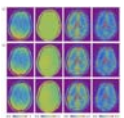

Fast fitting method for simultaneously quantifying multiple MR parameters using local optimization method with predetermined initial values

Suguru Yokosawa[1], Yo Taniguchi[1], Tomoki Amemiya[1], Toru Shirai[1], Ryota Sato[1], Yoshihisa Soutome[1], and Hisaaki Ochi[1]

[1]Research & Development Group, Hitachi, Ltd., Tokyo, Japan

A fast fitting method for quantifying multiple MR parameters using local optimization method with predetermined initial values is proposed. In the proposed method, an optimal neighborhood solution is extracted as predetermined initial values. A difference in MR parameters between the proposed method and the conventional method was less than 5 %. On the other hand, a computing time of the proposed method was approximately 15 times faster compared with the conventional method. We concluded that the proposed method can provide fast fitting process while maintaining calculation accuracy.

1442 

Improved image texture features by Gaussian mixture models of grey-level co-occurrence matrices

Tommy Löfstedt[1], Patrik Brynolfsson[1], Tufve Nyholm[1,2], and Anders Garpebring[1]

[1]Department of Radiation Sciences, Umeå University, Umeå, Sweden, [2]Akademiska Hospital, Uppsala, Sweden

Image texture features based on gray-level co-occurence matrices (GLCMs) are useful in *e.g.* the analysis of MR images of tumours. However, the features can be quite sensitive to the number of grey-levels in the analysed image, in particular if the region of interest is small. In this work we propose a new method for computing the GLCM, based on Gaussian mixture models. The results show that the new method improves the estimation of the GLCM and at the same time eliminates the difficult task of selecting the number of grey-levels.

1443 

Optimization of 2D registration using minctracc on myelin stained brain slices

Max Prihoda[1,2], Simon Hametner[3], Andreas Deistung[4], Verena Endmayr[3], Andrew Janke[5], Claude Lepage[6], Thomas Haider[7], Simon Daniel Robinson[8], Xiang Feng[4], Hans Lassmann[3], Jürgen Reichenbach[4], Evelin Haimburger[1], Christian Menard[9], Hannes Traxler[10], Siegfried Trattnig[8], and Günther Grabner[1,2,8]

[1]Department of Radiologic Technology, Carinthia University of Applied Sciences, Klagenfurt, Austria, [2]Institute for Applied Research on Ageing, Carinthia University of Applied Sciences, Klagenfurt, Austria, [3]Center for Brain Research, Medical University of Vienna, Vienna, Austria, [4]Medical Physics Group, Institute for Diagnostic and Interventional Radiology, Jena University Hospital – Friedrich Schiller-University, Jena, Germany, [5]Centre for Advanced Imaging, University of Queensland, Brisbane, Australia, [6]Montreal Neurological Institute, McGill University, Montreal, Canada, [7]University Clinic for Trauma Surgery, Medical University Vienna, Vienna, Austria, [8]High Field Magnetic Resonance Centre, Department of Biomedical Imaging and Image-guided Therapy, Medical University of Vienna, Vienna, Austria, [9]Department of Medical Engineering, Carinthia University of Applied Sciences, Klagenfurt, Austria, [10]Center of Anatomy and Cell Biology, Medical University Vienna, Vienna, Austria

Histological analyses are important for a wide spectrum of in vivo and in vitro imaging projects. But unlike MRI or CT, histological analyses are typically performed in two dimensions. Nonlinear tissue deformation and ruptures of brain tissue are often common, making analysis in slice direction more difficult. In this work, we optimized a hierarchical, nonlinear fitting pipeline on the basis of two high resolution, myelin stained brain sections using mintracc.

1444 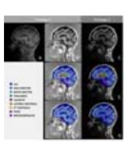

Comparison of MP2RAGE-based morphometry methods for anorexia nervosa

Bénédicte Maréchal[1,2,3], José Baiao Boto[4], Gkinis Georgios[5], Nadia Ortiz[5], Karl-Olof Lövblad[4], François Lazeyras[6], Maria Isabel Vargas[4], Alexis Roche[1,2,3], and Tobias Kober[1,2,3]

[1]Advanced Clinical Imaging Technology, Siemens Healthcare HC CEMEA SUI DI PI, Lausanne, Switzerland, [2]Department of Radiology, CHUV, Lausanne, Switzerland, [3]LTS5, EPFL, Lausanne, Switzerland, [4]Department of Neuroradiology, Geneva University Hospital, Geneva, Switzerland, [5]Department of Psychiatry, Geneva University Hospital, Geneva, Switzerland, [6]Department of Radiology and Medical Informatics, University of Geneva, Geneva, Switzerland

We explore the sensitivity of a morphometry tool to detect anorexia-related brain atrophy in MP2RAGE images. We compare volumetry resulting from two previously reported morphometry strategies on 16 patients with clinical suspicion of anorexia and identify both similarities and differences in brain atrophy evaluation.

1445 Bias and SNR of $$$T_1$$$ estimates derived from joint fitting of actual flip-angle and FLASH imaging data with variable flip angles

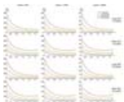

M. Dylan Tisdall[1]

[1]Radiology, Perelman School of Medicine, University of Pennsylvania, Philadelphia, PA, United States

Previous work has suggested fitting joint AFI/FLASH data for T1 and B1+ by minimizing the 2-norm of the difference between the signal model and measurements will produce unbiased estimates of T1. We demonstrate that, contrary to previous results, the estimator has a substantial bias that varies with both the true T1 and B1+, and the receive channel count. We also demonstrate that the correct ML estimator removes the effect of channel count, and that the choice of AFI protocol has a larger impact of the quality of estimates than the addition of an extra FLASH scan.

1446

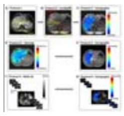

Quantification of iron liver with clinical MRI protocols

Redouane Ternifi[1], Philippe Pouletaut[1], Magalie Sasso[2], Véronique Miette[2], Fabrice Charleux[3], and Sabine F. Bensamoun[1]

[1]Sorbonne University, Université de technologie de Compiègne CNRS UMR 7338 Biomechanics and Bioengineering, Compiègne, France, [2]Echosens, R&D Department, France, [3]Radiology, ACRIM, Polyclinique Saint Côme de Compiègne, France

Iron quantification has been assessed through the development of magnetic resonance sequences. The purpose is to improve the existing MRI iron protocols to better diagnose the degree of hemochromatosis. Five volunteers with healthy livers underwent four protocols for the quantification of iron overloads concentration (IOC). The results have demonstrated that existing clinical protocols could be improved to provide spatial distribution of iron within one slice and all over the entire liver volume. IDEAL-IQ® could be the best protocol to have IOC volume representation with a short time of acquisition and standard deviation values associated to mean IOC data.

1447

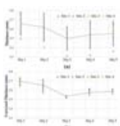

Harmonization for cortical thickness across sites in multi-center MRI study

Lin Zhao[1], Tuo Zhang[1], Xianjun Li[2], Chao Jin[2], Miaomiao Wang[2], Xiaocheng Wei[3], Hong Yin[4], Zengjun Zhang[5], Xiaoqun Yao[6], Xiaoling Zhang[7], and Jian Yang[2]

[1]Brain Decoding Research Center, Northwestern Polytechnical University, Xi'an, People's Republic of China, [2]Department of Diagnostic Radiology, the First Affiliated Hospital of Xi'an Jiaotong University, Xi'an, People's Republic of China, [3]MR Research China, GE Healthcare, Beijing, People's Republic of China, [4]Department of Radiology, Xijing Hospital, the Fourth Military University, Xi'an, People's Republic of China, [5]Department of Diagnostic Radiology, Xi'an Children Hospital, Xi'an, People's Republic of China, [6]Department of Radiology, Xi'an Gaoxin Hospital, Xi'an, People's Republic of China, [7]CT MR Department, the People's Hospital of Shaanxi Province, Xi'an, People's Republic of China

Cerebral cortex encodes crucial information of brain development, cytoarchitecture and function. However, varying data acquisition conditions at different centers could hamper group-wisely statistical analysis. This study aims to test the consistency of cortical thickness in the human brain across four sites and harmonize the deviations. Our results showed that variation of cortical thickness across sites were regionally independent, and deviation across centers could be reduced by linear regression method at a global scale, while the variations across subjects were well preserved. Those results suggest that our method has the promise in harmonizing cortical thickness measures in multi-center study.

1448

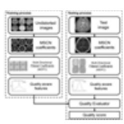

QEMDIM : Quality Evaluation using Multi-DIrectional Filter for no-reference MR image

Jinseong Jang[1], Kihun Bang[1], Hanbyeol Jang[1], and Dosik Hwang[1]

[1]School of Electrical and Electronic Engineering, Yonsei University, Seoul, Korea, Republic of

This paper proposes a new image quality assessment (IQA) for no-reference MRI, Quality Evaluation using Multi-DIrectional filters for MRI (QEMDIM), that is obtained from difference of statistical features between test images and numerous pre-scanned images in Mean Subtracted Contrast Normalization (MSCN) coefficient and Multi-Directional Filtered Coefficients (MDFC). the proposed method is capable of detecting various types of artifact and can be applied to clinical applications as well as being used to evaluate the performance of MRI hardware and software

---

1449

Diagnostic performance of texture analysis on MRI in differentiated degree of head and neck carcinoma

Yu Chen[1], Yuan Li, Yuanli Zhu, Huadan Xue, Zhuhua Zhang, Hailong Zhou, and Zhengyu Jin

[1]Peking Union Medical College Hospital, Beijing, People's Republic of China

The aim of this study was to determine the diagnostic accuracy of pathological differentiated degree of head and neck squamous cell carcinoma (HNSCC) using MRI texture analysis. The following texture analysis parameters were derived from the T1WI, T2WI , T2fs and Post-Gad T1WI based on different scale: entropy , mean pixel intensity, standard deviation(SD), skewness, and kurtosis. ROC curves and AUC of each parameter was determined, respectively. We conclude that the entropy at fine texture scale on Post-Gad T1WI had the best ability .

1450

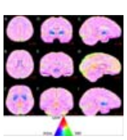

Regional variations in cerebral venous contrast using susceptibility-based MRI

Phillip G. D. Ward[1,2], Nicholas J. Ferris[1,3], Parnesh Raniga[1,4], Amanda C. L. Ng[5], David L. Dowe[2], David G. Barnes[2,6], and Gary F. Egan[1,7]

[1]Monash Biomedical Imaging, Monash University, Clayton, Australia, [2]Faculty of Information Technology, Monash University, Clayton, Australia, [3]Monash Imaging, Monash Health, Clayton, Australia, [4]The Australian eHealth Research Centre, CSIRO Health and Biosecurity, Australia, [5]Department of Anatomy and Neuroscience, The University of Melbourne, Melbourne, Australia, [6]Monash Immersive Visualisation Platform, Monash University, Clayton, Australia, [7]ARC Centre of Excellence for Integrative Brain Function, Melbourne, Australia

In this study we compared the image contrast properties of susceptibility-weighted imaging (SWI) and quantitative susceptibility mapping (QSM) for cerebral venous identification and visualisation. SWI and QSM are minimally invasive techniques to image cerebral veins with distinct contrast properties. We hypothesised that these techniques would provide complementary vein contrast in different brain regions. Contrast was measured using 1072 manually traced vein images from ten volunteers. We found regional variations in the predictive power of vein contrast and computed maps of contrast profiles that may inform which technique is best for a given application.

1451

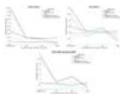

Quantitative and qualitative evaluation of bias field correction methods

Falk Luesebrink[1], Hendrik Mattern[1], Alessandro Sciarra[1], and Oliver Speck[1,2,3,4]

[1]Biomedical Magnetic Resonance, Otto-von-Guericke University, Magdeburg, Germany, [2]Center for Behavioral Brain Sciences, Magdeburg, Germany, [3]Leibniz Institute for Neurobiology, Magdeburg, Germany, [4]German Center for Neurodegenerative Disease (DZNE), Magdeburg, Germany

Bias field correction is an essential prerequisite for image analysis, especially at high field strength. In this study multiple correction methods, based on acquisition of a reference image and computational approaches with varied input parameters, are compared. The results indicate that acquisition of a conventional MPRAGE corrected by SPM yields quantitatively and qualitatively comparable results to acquiring a reference image (e.g. MP2RAGE), however, scan time is up to halfed.

1452

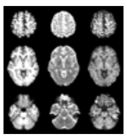

Rapid registration of EPI to high-resolution structural images

David Neil Manners[1], Claudia Testa[1], Stefania Evangelisti[1], Stefano Zanigni[1], Caterina Tonon[1], and Raffaele Lodi[1]

[1]Department of Biomedical and NeuroMotor Sciences, University of Bologna and Functional MR Unit, Policlinico S. Orsola - Malpighi, University of Bologna, Bologna, Italy

Post-processing methods that can non-linearly register diffusion-weighted EPI data to high-resolution images are useful in the context of clinical protocols. The current research attempts to apply currently available registration methods to rapidly perform such registration. Investigations on healthy subjects show that an appropriately generated target image allows good quality registration to be performed even with freely available software. This is useful for example to provide cortical seeds for diffusion tractography.

1453

A graphical programming environment for creating and executing adaptive MRI protocols

Refaat E Gabr[1], Getaneh B Tefera[1], William J Allen[2], Amol S Pednekar[3], and Ponnada A Narayana[1]

[1]Diagnostic and Interventional Imaging, University of Texas Health Science Center at Houston, Houston, TX, United States, [2]Texas Advanced Computing Center, University of Texas at Austin, Austin, TX, United States, [3]Philips Healthcare, Cleveland, OH, United States

Inline processing of magnetic resonance images allows fast feedback of analysis and immediate access to quantitative information. It further allows the development of adaptive MRI protocols. Here, we present GRAPE, a development platform for graphical programming to facilitate the development of adaptive magnetic resonance imaging (MRI) protocols. This platform provides tools to enable graphical creation, execution, and debugging of image analysis algorithms integrated with the MRI scanner, all within a graphical environment. GRAPE is demonstrated with the implementation of patient-specific optimization of the scan parameters of 3D fluid-attenuated inversion recovery (FLAIR) protocol to enhance the contrast of brain lesions in multiple sclerosis, performed on a 3.0 Tesla MRI scanner.

1454

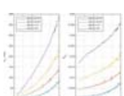

Validation of CSF based calibration for accurate and robust quantification of water content.

Zaheer Abbas[1,2], Dominik Ridder[1], Krzysztof Dzieciol[1], and Nadim Jon Shah[1,2]

[1]Medical Imaging Physics, Institute of Neuroscience and Medicine, Juelich, Germany, [2]Faculty of Medicine, RWTH Aachen, JARA, Aachen, Germany

Estimating tissue water content is challenging. Reliable quantification of the water content requires significant number of corrections and calibration to a reference. In this work, we proposed to use a region in cerebrospinal fluid for robust calibration; this is further validated in a cohort of healthy volunteers and compared to existing methods.

1455

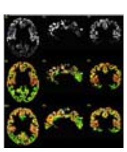

Automatic nonlinear transformation of 7T MRI brain image to Talairach stereotaxic space

Mingyi Li[1], Jian Lin[1], Katherine Koenig[1], and Mark Lowe[1]

[1]Cleveland Clinic, Cleveland, OH, United States

Transforming MRI brain images into Talairach space will greatly facilitate the comparison of neuroimaging research results across subjects and applications of atlas to research subjects and clinical patients. We developed an automatic processing pipeline based on nonlinear registration to transform 7T MRI brain images to Talairach space. The pipeline utilized matching scores derived from brain parcellation for quality assurance (QA). The pipeline was tested on subjects including five controls, three MS patients and three ALS patients. The results showed that the method generated better results than the automatic Talairach transformation provided by AFNI. The QA scores were also comparable to those computed from 3T MRI brain images in our previous study.

1456

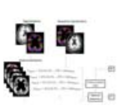

Epilepsy Surgery Followup: Resected Tissue Analysis and Classification

Fabrício Henrique Simozo[1], Tonicarlo Rodrigues Velasco[2], and Luiz Otávio Murta Jr.[1]

[1]Department of Physics, University of São Paulo, Ribeirão Preto, Brazil, [2]Clinical Hospital of the Faculty of Medicine, University of São Paulo, Ribeirão Preto, Brazil

Focal cortical dysplasia (FCD) is one of the main causes of refractory epilepsy. There is no self-sufficient method in order to evidence the presence and location of FCD, making complete diagnosis very difficult. Although some studies have addressed FCD identification, image texture is poorly explored. This study evaluated pre and post-surgical magnetic resonance images (MRI) of epilepsy patients in order to test Machine Learning classifiers and their ability to identify dysplasia using texture features and cortical thickness. Precision and recall scores suggest the capabilities of the proposed methodology in responding to the presence of FCD tissue.

1457

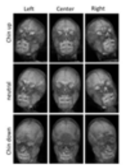

Optimization of multiple orientation QSM for building a clinically feasible protocol

Harshan Ravi[1], Wen-Tung Wang[1], Dzung Pham[1], and John Butman[1]

[1]Center for Neuroscience and Regenerative Medicine, National Institute of Helath, Bethesda, MD, United States

Quantitative Susceptibility Mapping (QSM) offers unique, quantitative information about tissue magnetic susceptibility. A multi-orientation method, calculation of susceptibility through multi-orientation sampling (COSMOS), enables the dipole inversion by acquiring data at multiple orientations. In practical imaging settings, however, it is a challenge to image the subject multiple orientations. Although small angle COSMOS has been shown to generate reasonable QSM images, the selection of orientations within a practical acquisition protocol remains an open question. In this work, we investigated the influence of the number and direction of orientations on the outcome of small angle COSMOS for in vivo imaging.

1458

Differences in parameter sensitivities of GESFIDE MR signals generated on realistic angiograms and on idealized cylinders

Philippe Pouliot[1], Louis Gagnon[2], David A Boas[2], and Frederic Lesage[1]

[1]Electrical engineering, Ecole Polytechnique Montreal, Montreal, QC, Canada, [2]Radiology, Harvard Medical School, Massachusetts General Hospital, MA, United States

Idealized models of cylinders for the vasculature are used in several quantitative MRI techniques such as for perfusion, CBV, vessel size and vascular MR fingerprinting. While limitations of these models are recognized, a direct comparison of the predicted MR signal between different cylinder models and those using a real vasculature as substrate has not been done to our knowledge. Here we compare the sensitivity of the MR signal for the GESFIDE sequence for 4 sets of , models of cylinders and 6 realistic angiograms from mouse somatosensory cortex. In general, simulation results are all different between the different angiograms and the different models of cylinders. This suggests that much care should be used in interpreting literature results based on models of cylinders, or as well with models on angiograms, to account for the possibility of biases in the absolute results. Correlations and differences in absolute values, for some parameters, may perhaps be less subject to bias.

1459

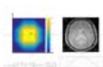

Adaptive Magnetic Resonance Image signal enhancement using squared eigenfunctions of the Schrodinger operator

Abderrazak Chahid[1], Hacene Serrai[2], Eric Achten[2], and Taous-Meriem Laleg-Kirati[1]

[1]Computer, Electrical and Mathematical Science and Engineering (CEMSE) division, King Abdullah University of Sciences and Engineering (KAUST), Thuwal, Saudi Arabia, [2]Department of Radiology, University of Gent, Gent, Belgium

The main of challenge of Magnetic Resonance Imaging (MRI) is dealing with high levels of noise which may corrupt the image especially since the noise is almost correlated with the image details. In this regard, we propose a new MRI enhancement method to overcome this limitation. The proposed MRI enhancement method relies on square sub-images enhancement depending on the noise level in each position using spatial adaptation of the Semi-Classical Signal Analysis (SCSA) method, where an enhancement parameter ***h*** is subject to a Gaussian distribution. The results show significant improvement in noise removal and preserving small details in the image.

1460

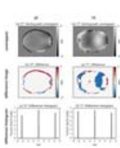

Obtaining accurate and fast unwrapped phase images

Riccardo Metere[1] and Harald E. Möller[1]

[1]NMR Unit, Max Planck Institute for Human Cognitive and Brain Sciences, Leipzig, Germany

The unwrapping of phase data is a common problem in MRI. However, its solution is non-trivial for 2D or 3D images, and there has been some general research in this direction, notably in the field of optics. The two most pupular algorithms for MRI applications are: (i) a Laplacian-based method that is fast but inaccurate; (ii) a region-merging optimization method that is accurate but very slow. Here, we propose the adoption of a recently developed and freely available unwrap algorithm that significantly outperforms the other considered methods, allowing for both fast and accurate calculation of unwrapped phase images.

1461

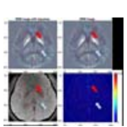

Spatial resolution properties of QSM images using MEDI algorithm

Se Young Chun[1]

[1]Electrical and Computer Engineering, UNIST, Ulsan, Korea, Republic of

We investigated the spatial resolution of the MEDI reconstructed QSM images by deriving an analytical expression of the estimator in terms of the true QSM image. The implication of this expression is that no regularization will be applied to some part of the QSM images if the corresponding magnitude image area contains strong edges and relatively strong regularization will be applied to some part of the QSM images if the corresponding magnitude image area contains low magnitude values. Our simulations with a phantom and a in-vivo QSM image confirm this analysis; Impulse perturbations were suppressed on the area where the magnitude image has low contrasts and impulses were preserved on the area where the magnitude image has high contrast or edges.

1462 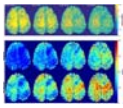

AWESOME-Based De-Noising of Complex-Valued fMRI Time Series

Henrik Marschner[1], Laurentius Huber[2], André Pampel[1], and Harald E. Möller[1]

[1]NMR, Max Planck Institute for Human Cognitive and Brain Sciences, Leipzig, Germany, [2]Section on Functional Imaging Methods, National Institute of Mental Health, Bethesda, MD, United States

In this study we investigate possible benefits of an application of 'AWESOME' de-noising on fMRI. The application in a high-SNR finger tapping experiment showed a reduction of the already low thermal noise contribution and therefore improvement of tSNR and reduction of false positives; no adverse effects in the form of smoothing or suppression of 'true' activation was observed. A second investigation of the scalability of tSNR improvement on a resting state experiment with variable slice thickness / SNR showed that thermal noise can be reliably reduced and the tSNR proportionally improved without visible reduction of detail sharpness / resolution.

1463 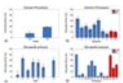

Assessment of interplatform reproducibility of T1 quantification methods used for DCE-MRI: results from a multicenter phantom study

Octavia Bane[1], Stefanie Hectors[1], Mathilde Wagner[1,2], Lori R Arlinghaus[3], Madhava Aryal[4], Michael Boss[5], Yue Cao[4], Thomas L Chenevert[6], Fiona Fennessy[7], Wei Huang[8], Nola Hylton[9], Jayashree Kalpathy-Cramer[10], Kathryn E Keenan[5], Dariya Malyarenko[6], Robert Mulkern[7], David Newitt[9], Karl F Stupic[5], Lisa Wilmes[9], Thomas Yankeelov[11], Yi-Fen Yen[10], Stephen E Russek[5], and Bachir Taouli[1]

[1]Translational and Molecular Imaging Institute, Icahn School of Medicine at Mount Sinai, New York, NY, United States, [2]Radiology, Groupe Hospitalier Pitié Salpêtrière, Paris, France, [3]Institute of Imaging Science, Vanderbilt University Medical Center, Nashville, TN, United States, [4]Radiation Oncology, University of Michigan, Ann Arbor, MI, United States, [5]Physical Measurement Laboratory, National Institute of Standards and Technology (NIST), Boulder, CO, United States, [6]Radiology, University of Michigan, Ann Arbor, MI, United States, [7]Radiology, Brigham and Women's Hospital, Boston, MA, United States, [8]Advanced Imaging Research Center, Oregon Health & Science University, Portland, OR, United States, [9]Radiology, University of California San Francisco Mount Zion Hospital, San Francisco, CA, United States, [10]Martinos Center for Biomedical Imaging, Massachusetts General Hospital, Charlestown, MA, United States, [11]Biomedical Engineering, University of Texas at Austin, Austin, TX, United States

Our multicenter study examined variability in T_1 quantification by testing common inversion-recovery spin echo and variable flip angle (VFA) protocols, as well as T_1 mapping methods used by participating sites, using a phantom with known T_1 values. We found field strength dependence of the accuracy, and platform dependence of the repeatability of T_1 measurements with the common VFA protocol. Accuracy for site-specific protocols was influenced by site, while repeatability, by type of protocol. Our findings suggest modified IR methods and VFA protocols with multiple flip angles and B_1 correction as good methods for repeatable T_1 measurement.

1464 

Bio-inspired optimization of technical fiber-reinforced ramifications using high-resolution MRI of Dracaena marginata branchings as concept generators

Linnea Hesse[1,2], Tom Masselter[1,3,4], Nils Spengler[5], Jan Gerrit Korvink[5], Jochen Leupold[6], and Thomas Speck[1,2,4]

[1]Botanical Garden, University Freiburg, Plant Biomechanics Group, Freiburg, Germany, [2]Freiburg Centre for Interactive Materials and Bioinspired Technologies (FIT), Freiburg, Germany, [3]Freiburg Centre for Interactive Materials and Bioinspired Technologies (FIT), Freiburg, [4]Competence Network Biomimetics, Germany, [5]Karlsruhe Institute of Technology, Institute of Microstructure Technology, Eggenstein-Leopoldshafen, Germany, [6]Department of Radiology University Medical Center Freiburg, Medical Physics, Freiburg, Germany

MRT is still a little-known and highly underestimated imaging method within the field of functional morphology and biomechanics of plants and biomimetics. Its non-invasive and non-destructive character in combination with a large variety of applicable imaging sequences, gives this method a strong potential to shed light to various unanswered scientific questions concerning both the plant structure and function as well as on physiology. Using a Bruker Biospec 94/20 9.4T and a 3D FLASH sequence we could gain new insights into the biomechanics and development of dragon tree ramifications as a source of inspiration for the optimization of technical fiber-reinforced ramifications.

1465 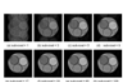

Fast Bloch-Torrey simulation of 3D RF spoiled gradient echo sequences using a number of subvoxels and molecular diffusion effect

Ryoichi Kose[1] and Katsumi Kose[2]

[1]MRTechnolocy, Inc., Tsukuba, Japan, [2]University of Tsukuba, Tsukuba, Japan

RF spoiled gradient echo sequences were studied both with experiments and Bloch-Torrey simulation. The Bloch simulation of the 256×256×32 voxel images clarified that adequate number of subvoxels were required for artifact-free images. The Bloch-Torrey simulation for one voxel magnetization clarified that adequate number of subvoxels were required for image intensity reproduction by diffusion effect. In conclusion, molecular diffusion effects are indispensable to reproduce the image contrast in SPGR.

1466 

Analysis of error in Fat-Water Quantifications Originated from Models

Xiaoqi Wang[1], Xiaoguang Cheng[2], Li Xu[2], and Li Baoqing[3]

[1]Clinical Science, Philips Healthcare, Beijing, People's Republic of China, [2]Department of Radiology, Beijing Jishuitan Hospital, [3]Department of Radiology, Beijing Shijingshan Hospital

Fat-water separation imaging methods with multi-echo acquisition require specific fat spectrum model. The optimal spectrum model to be applied relies on the fat chemical properties as well as the acquisition scheme regarding to, for example, TR and TE. Herein we exam the consequence if inaccurate fat spectrum is used in the fat quantification processing, and analyze the related errors.

1467 

Liver Biopsy Analysis to Determine Fat Droplet Distribution

Benjamin Andrew Ratliff[1,2], Diego Hernando[2,3], Curtis Wiens[2], Changqing Wang[2,4,5], Rao Watson[6], Rashmi Agni[6], Claude B Sirlin[7], and Scott B Reeder[1,2,3,8,9]

[1]Biomedical Engineering, University of Wisconsin, Madison, Madison, WI, United States, [2]Radiology, University of Wisconsin, Madison, Madison, WI, United States, [3]Medical Physics, University of Wisconsin, Madison, Madison, United States, [4]School of Automation Engineering, University of Electronic Science and Technology of China, Chengdu, People's Republic of China, [5]School of Biomedical Engineering and Guangdong Provincial Key Laboratory of Medical Image Processing, Southern Medical University, Guangzhou, People's Republic of China, [6]Pathology, University of Wisconsin, Madison, Madison, United States, [7]Radiology, University of California, San Diego, San Diego, United States, [8]Medicine, University of Wisconsin, Madison, Madison, United States, [9]Emergency Medicine, University of Wisconsin, Madison, Madison, United States

The purpose of this work was to quantify the size and clustering of fat droplets using liver biopsy, as part of a long-term effort to characterize the relationship between tissue microstructure and quantitative MRI signals in fat-containing tissue. Three H&E stained liver core biopsies with varying fat-fractions were analyzed using segmentation software in order to generate probability density functions for fat droplet size and location. This work demonstrates that fat droplet distribution in the liver can be modeled statistically to determine the size and location distribution of fat droplets, potentially enabling characterization of the MR signal observed from fatty liver.

1468 

Diffusion effects on T2 relaxometry with triple echo steady-state free precession sequence

Yangzi Qiao[1], Chao Zou[1], Xin Liu[1], and Hairong Zheng[1]

[1]Shenzhen Institutes of Advanced Technology, Chinese Academy of Sciences, Shenzhen, People's Republic of China

In this study, the underestimation of T_2 by TESS was revealed through simulation and phantom study. The bias becomes significant in high resolution TESS imaging with larger unbalanced gradient moment, as the diffusion effect can not be neglected. A possible correction scheme was also proposed, the results validated the diffusion effect on T_2 estimation. However, the correction method relies on T_1/T_2/D as priori to calculate the signal change ratio through EPG algorithm. A possible solution might be simultaneous estimation on apparent diffusion coefficient and T_2.

1469 

Brain activity alteration during the training period of the Hybrid Assistive Limb® (HAL) for chronic spinal cord injuries: a task-based fMRI case report

Kousaku Saotome[1,2], Akira Matsushita[3,4], Aiki Marushima[3], Hiroaki Kawamoto[1,5], Hideo Tsurushima[1,3], Tomohiko Masumoto[6], Masashi Yamazaki[7], Akira Matsumura[3], and Yoshiyuki Sankai[1,5]

[1]Center for Cybernics Reseach, University of Tsukuba, Tsukuba, Japan, [2]Graduate School of Comprehensive Human Science Majors of Medical Sciences, University of Tsukuba, Tsukuba, Japan, [3]Department of Neurosurgery, Faculty of Medicine, University of Tsukuba, Tsukuba, Japan, [4]Department of Neurosurgery, Ibaraki Prefectural University of Health Sciences, Inashiki, Japan, [5]Faculty of Engineering, Information and Systems, University of Tsukuba, Tsukuba, Japan, [6]Department of Radiology, Faculty of Medicine, University of Tsukuba, Tsukuba, Japan, [7]Department of Orthopaedic Surgery, Faculty of Medicine, University of Tsukuba, Tsukuba, Japan

We previously developed the novel brain phantom showing image contrast and construction similar to those of in vivo MRI. This phantom has the potential to quantitatively assess the capability of the motion-corrected PROPELLER technique, which has been never approached. In the current study, we investigated the rotational frequency dependencies of the different two motion-corrected PROPELLER techniques by using our brain phantom. Our findings allow to quantitatively assess the capability of the Motion-Correction in PROPELLER.

1470 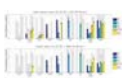

Determining the Time Efficiency of Quantitative MRI Methods using Bloch Simulations

Willem van Valenberg[1,2], Frans M. Vos[1,3], Stefan Klein[2], Lucas J. van Vliet[1], and Dirk H.J. Poot[1,2]

[1]Quantitative Imaging, Delft University of Technology, Delft, Netherlands, [2]Biomedical Imaging Group, Erasmus Medical Center, Rotterdam, Netherlands, [3]Radiology, Academic Medical Center, Amsterdam

When measuring T_1, T_2, T_2^*, PD, or B_1^+, we prefer the MRI sequence that provides the best precision in the allowed scan time (i.e. having optimal time efficiency). However, experimentally determining the time efficiency is impractical when comparing many sequences, each possibly with varying settings, and multiple tissue types of interest. Here, we derive time efficiency through Bloch simulations which is applicable to any MRI sequence and tissue type. A specific strength of our framework is that it does not require an explicit fitting procedure which may not yet exist when designing novel MR sequences.

1471 

Quantitative DCE-MRI Accuracy Evaluation Using Dynamic Physical vs. Digital Phantom: a Cross-Validation

Yuan Le[1], Yuxiang Zhou[2], Eric Stinson[3], Stephen J. Riederer[3], and Joel P. Felmlee[3]

[1]Radiology, Mayo Clinic Arizona, Scottsdale, AZ, United States, [2]Radiology, Mayo Clinic Arizona, Phoenix, AZ, United States, [3]Radiology-Diagnostic, Mayo Clinic, Rochester, MN, United States

To study the image accuracy of quantitative DCE-MRI a digital phantom and computer simulation were usually used. To validate the digital phantom method, we conducted a cross-validation study comparing the image accuracy estimation from simulation with that from a dynamic physical phantom with contrast infusion. Results showed that the estimated errors were usually higher with the physical phantom, likely due to the difference in reproducibility. Consistency was found in the measurement error comparison between imaging techniques when the temporal resolution was high.

1472

Early enhancement in breast DCE-MRI is sparse and can be imaged with a reduced FOV to increase temporal resolution

Federico Pineda[1], Ty O Easley[1], and Gregory Karczmar[1]

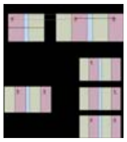

[1]Radiology, University of Chicago, Chicago, IL, United States

Early enhancement in breast DCE-MRI is very sparse, if the FOV is reduced in these images and aliasing occurs, the likelihood that two significantly enhancing voxels overlap is low. We present a method for ‘unfolding’ of aliased DCE-MRI acquisitions that closely approximates fully-sampled acquisitions. This method could be used to increase the temporal resolution of DCE-MRI at very early times when enhancement is rapidly changing, allowing for the accurate measurement of early lesion kinetics.

1473 

Simulation of Sound Pressure Level of MRI Scan Considering Eddy Currents

Yukari Yamamoto[1], Yo Taniguchi[1], Hisaaki Ochi[1], and Yoshihisa Soutome[1]

[1]Medical Systems Research Department, Research & Development Group, Hitachi, Ltd., Tokyo, Japan

Since optimal waveforms should be chosen for each gradient pulse in order to reduce sound pressure levels (SPLs) in MRI scans, the simulation accuracy of the SPL must be improved. Assuming that the eddy current component is a cause of the disagreement between the measured and the simulated SPLs, we compared the simulation results with and without the eddy current component in this study. By including the eddy current component in the simulation, the magnitude of the SPL decreased, which reflects the decrease in the peak amplitude of the frequency component of the gradient waveform. However, the eddy current component did not affect the change trends of the SPLs depending on the change of waveforms. On the other hand, a slight change in the peak position of the frequency response functions appears to cause a significant change in the SPL, and the error of the FRF was also thought to cause disagreement between the measured and simulated SPLs.

1474 

The effect of MR noise and resolution on textural features in simulated and real textures: implications for clinical practice.

Joshua Shur[1], Matthew Orton[2], Simon Doran[2], James D'Arcy[2], David Collins[2], Maria Bali[1], Martin Leach[2], and Dow-Mu Koh[1]

[1]The Royal Marsden NHS Foundation Trust, London, United Kingdom, [2]Institute of Cancer Research, United Kingdom

Sensitivity of textural features to acquisition parameters has important clinical implications. The aim of this study is to investigate the effect of noise and resolution on textural features.

We compared textural features from a uniform and simulated texture, varied with noise, with experiment in a uniform phantom and organic texture.

Our data demonstrate that a uniform texture behaves as if it has inherent texture, due to presence of artefact, and this in turn will influence textural features as noise and acquisition parameters are varied.

We note that certain textural features used in clinical practice vary widely with image noise, whereas others appear to be robust.

1475 

Quantification of contrast agent-induced enhancement of brain lesions in multiple sclerosis

Jung-Jiin Hsu[1], William A. Stern[1], Jung-Yu C. Hsu[2], and Roland G. Henry[1]

[1]Department of Neurology, University of California San Francisco, San Francisco, CA, United States, [2]Department of Cell Biology and Anatomy, National Cheng Kung University, Tainan, Taiwan

Contrast agents are routinely used in MRI to detect and evaluate tissue lesions. Conventional clinical protocols use T_1-weighted sequences to visualize Gd contrast agent enhancement. Because T_1-weighted MRI does not produce quantitative measurements, it is difficult to describe the lesion enhancement in quantitative terms and to infer the degree of the underlining disease activities of the lesions. A fast, whole-brain high-resolution T_1 mapping method was developed to address this problem and applied to multiple sclerosis.

1476 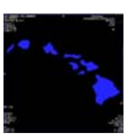

LEI-ALOHA – Magnetic Resonance Imaging in the Tropical Island Setting

Christopher John Wiggins[1] and Benedikt A Poser[2]

[1]Scannexus BV, Maastricht, Netherlands, [2]Faculty of Psychology and Neuroscience, Maastricht University, Maastricht, Netherlands

While there are exceptions, most major MRI research centers are located in urban areas where a sizeable population is served by a large medical infrastructure and/or university. For researchers and technical staff alike, this often precludes the possibility of combining their research program with a remote, island-based lifestyle. Here we propose a set of theoretical techniques that form a framework for a purely philosophical research program.

Traditional Poster

Pulse Sequences

Exhibition Hall 1477-1511 Monday 8:15 - 10:15

1477 

Respiratory Self-Gating using Principal Component Analysis in 2D Golden Angle Radial Free Breathing Cine Imaging

Alexander Fyrdahl[1,2], Karen Holst[1,2], Martin Ugander[1,2], and Andreas Sigfridsson[1,2]

[1]Department of Molecular Medicine and Surgery, Karolinska Institutet, Stockholm, Sweden, [2]Department of Clinical Physiology, Karolinska University Hospital, Stockholm, Sweden

Due to respiratory motion, cardiac imaging is performed during breath holding. Breath holding can be strenuous, or even impossible, for patients with heart disease. We suggest a method for respiratory self-gating using a Golden Angle radial k-space trajectory and principal component analysis. Radial trajectories sample the middle of k-space, which corresponds to the large structure content of the image, each repetition time. The respiratory motion can be detected from the raw k-space data and the motion signal can be used to perform retrospective respiratory gating.

1478

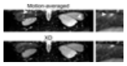

Free-Breathing T2-Weighted Abdominal Examination Using Radial 3D Fast Spin-Echo Imaging

Thomas Benkert[1,2], John P Mugler III[3], Bjorn Stemkens[2,4,5], Daniel K Sodickson[1,2], Hersh Chandarana[1,2], and Kai Tobias Block[1,2]

[1]Center for Advanced Imaging Innovation and Research (CAI2R), Department of Radiology, New York University School of Medicine, New York, NY, United States, [2]Bernard and Irene Schwartz Center for Biomedical Imaging, Department of Radiology, New York University School of Medicine, New York, NY, United States, [3]Department of Radiology and Medical Imaging, University of Virginia, Charlottesville, VA, United States, [4]Department of Radiotherapy, University Medical Center Utrecht, Utrecht, Netherlands, [5]Center of Advanced Imaging Innovation and Research (CAI2R), Department of Radiology, New York University School of Medicine, New York, NY, United States

A 3D fast spin-echo (FSE) sequence design for free-breathing T_2-weighted abdominal examination is described. Due to use of radial stack-of-stars sampling, the sequence provides pure T_2 contrast and achieves high robustness to motion, enabling that patients can be scanned during shallow breathing. Using an integrated FID navigator, the sequence can additionally be combined with the self-navigated XD-GRASP reconstruction principle for patients who perform deep breathing. Furthermore, the navigator can be used for bulk-motion detection. Initial results in a free-breathing adult volunteer are shown.

1479

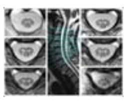

Rapid Spinal Cord Imaging

Matthias Weigel[1,2] and Oliver Bieri[1,2]

[1]Radiology, Radiological Physics, University Hospital Basel, Basel, Switzerland, [2]Dept. of Biomedical Engineering, University of Basel, Basel, Switzerland

For rapid spinal cord imaging, an inversion recovery prepared balanced steady state free precession (bSSFP) sequence with time-limited cine sampling was developed. It simultaneously acquires eight consecutive images of remarkable different tissue contrasts at 0.67mm in-plane resolution within a single measurement of only 51s per slice. The acquired images can be further combined to considerably improve the contrast to noise ratios (CNR) of the spinal cord tissues such as gray matter and white matter. Representative examples for images measured at different cervical spinal cord locations, various image combinations, and CNR gains are shown.

1480

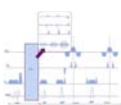

Synthetic MRI of the spine using outer volume suppression and virtual coil concepts to further increase scan productivity

Suchandrima Banerjee[1], Ken-pin Hwang[2], Peng Lai[1], Marcel Warntjes[3], and Ajit Shankaranarayanan[1]

[1]Global MR Applications & Workflow, GE Healthcare, Menlo Park, CA, United States, [2]Department of Imaging Physics, University of Texas M.D. Anderson Cancer Center, Houston, TX, United States, [3]SyntheticMR AB, Linköping, Sweden

Several methods for rapid simultaneous quantification of proton density, T1 and T2 maps from a single acquisition have emerged recently, allowing for retrospective synthesis of MR images with any desired contrast weighting from these maps. This work adapts a 2D fast spin echo based mapping method to spine MRI where scans are typically long and prone to artifacts. Outer volume suppression was incorporated to be able to save time by encoding only the anatomy of interest without aliasing concerns. Interleaved k-t sampling and virtual coil methods were explored to overcome limited coil acceleration capability and to further increase scan productivity.

1481

Three-dimensional T1-weighted spiral imaging of the spine

Ryan K Robison[1], Dinghui Wang[1], Melvyn Ooi[2], and James G Pipe[1]

[1]Imaging Research, Barrow Neurological Institute, Phoenix, AZ, United States, [2]Philips Healthcare, United States

Spine imaging requires lengthy examination times to yield sufficient SNR and to account for patient motion. Spiral MRI is a promising method for yielding high SNR acquisitions with reduced scan times and is more robust to patient motion. This work investigates the feasibility of applying spiral MRI to T1w imaging of the spine. Initial results indicate that spiral is well suited for anatomical spine imaging.

1482

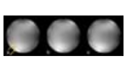

Intra-Scan Center Frequency Drift Correction for 3D Spiral Exams

Ashley G Anderson III[1], Ryan K Robison[1], Dinghui Wang[1], Melvyn B Ooi[2], and James G Pipe[1]

[1]Magnetic Resonance Technology Design Group, Barrow Neurological Institute, Phoenix, AZ, United States, [2]Philips Healthcare, Cleveland, OH, United States

High gradient demand and heating results in a changing main magnetic field and center frequency drift during minutes-long acquisitions. Center frequency drifts on the order of tens of Hz may produce visible artifacts in images acquired with long-readout spiral acquisitions. We propose a method for removing such artifacts in spiral acquisitions by demodulating individual spiral arms using a linear interpolation of center frequency measured before and after a scan.

1483

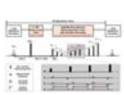

Slice-Accelerated Single-Shot Variable-Flip-Angle Fast Spin Echo with Very Long Echo Trains

Eun Ji Lim[1,2], Suhyung Park[1], Seong-Gi Kim[1,2], and Jaeseok Park[1]

[1]Department of Biomedical Engineering, Sungkyunkwan Univiersity, Suwon, Korea, Republic of, [2]Center for Neuroscience Imaging Research, Institute for Basic Science (IBS), Suwon, Korea, Republic of

A Fast spin echo (FSE) pulse sequence has been a main workhorse for clinical imaging due to its flexible contrast. Simultaneous multi-slice (SMS) FSE in [1] was shown to be efficient for slice acceleration without much loss of signals. Nevertheless, the previous SMS FSE methods, which employ high-flip-angle, spatially-selective multi-band RF pulses for both excitation and refocusing, still remain sub-optimal due to either high energy deposition or elongated echo spacing (ESP) and thereby limited echo train length (ETL). The purpose of this work is to develop a novel, slice-accelerated single-shot variable-flip-angle (VFA) FSE with very long echo trains, in which multi-band RF pulses are used only for excitation while short hard pulses with VFA are utilized along the refocusing pulse train, enabling very short ESP and very long ETL and thus enhancing imaging efficiency. It is shown that the proposed method makes it possible to complete whole brain imaging within 30 sec without apparent artifacts and noise.

1484 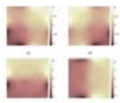

SPAMM Based Dual Current Injection to Accelerate Data Acquisition in Magnetic Resonance Electrical Impedance Tomography

Nashwan Naji[1], Kemal Sümser[1], and B. Murat Eyüboğlu[1]

[1]Electrical and Electronics Engineering, Middle East Technical University, Ankara, Turkey

Reducing acquisition time in magnetic resonance electrical impedance tomography (MREIT) improves signal to noise ratio and temporal resolution of measured conductivity data. On the other hand, the reconstruction accuracy of MREIT can be improved by acquiring multiple data using different current injection patterns, which in turn increases the total scan time. In this study, a novel pulse sequence is proposed to reduce the scan time in MREIT by injecting two current patterns in a single acquisition. This method is experimentally realized using a physical phantom, and its feasibility is evaluated.

1485 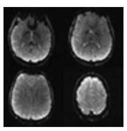

Full-FOV, whole-brain, half-millimetre in-plane readout-segmented EPIK for high-resolution fMRI studies

Seong Dae Yun[1] and N. Jon Shah[1,2]

[1]Institute of Neuroscience and Medicine, Medical Imaging Physics (INM-4), Forschungszentrum Juelich, Juelich, Germany, [2]Faculty of Medicine, Department of Neurology, JARA, RWTH Aachen University, Aachen, Germany

Since the advent of EPI, numerous approaches have been suggested to enhance its resolution for high-resolution fMRI. Recently, several methods were demonstrated for fMRI with a sub-millimetre resolution. However, none of them can achieve such resolution with a full-FOV and, at the same time, with whole-brain coverage. This work aims to develop a novel imaging method based on EPIK in combination with readout-segmentation to achieve half-millimetre resolution with a full FOV. Here, under a typical fMRI constraint (TR of 3 s), the method was shown to provide 93 slices when further combined with the multi-band technique.

1486 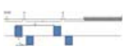

Diffusion-weighted Echo Planar Spectroscopic Imaging in human brain at 3T

Manoj K Sarma[1], Zohaib Iqbal[1], Andres Saucedo[1], Paul M Macey[2], and M. Albert Thomas[1]

[1]Radiological Sciences, UCLA School of Medicine, Los Angeles, CA, United States, [2]School of Nursing, UCLA School of Medicine, Los Angeles, CA, United States

There have been only few attempts to obtain maps of the diffusion properties of brain metabolites with diffusion weighted spectroscopic imaging. In this study we developed an echo planar based diffusion weighted spectroscopic imaging (DW-EPSI) method which uses a pairs of bipolar diffusion gradient to measure the apparent diffusion coefficient (ADC) of metabolites across an entire slice. The sequence was tested and validated on phantom and five healthy volunteers. The ADC values from DW-EPSI are in agreement with previous studies. The novel technique will enable a better understanding of the intracellular metabolism and water diffusivity correlates in pathologies.

1487 

Inversion Recovery with SMS PROPELLER

Ola Norbeck[1,2], Enrico Avventi[1,2], Henric Rydén [1], and Stefan Skare[1,2]

[1]Neuroradiology, Karolinska University Hospital, Stockholm, Sweden, [2]Clinical Neuroscience, Karolinska Institutet, Stockholm, Sweden

We show that simultaneous multi-slice (SMS) PROPELLER can be used with inversion recovery. This is accomplished by using an adiabatic multi-band RF pulse (PINS-DANTE), an in-house developed PROPELLER sequence and a reconstruction that calibrates both in-plane-GRAPPA and slice-GRAPPA weights for all PROPELLER blade angles on a single fully sampled PROPELLER blade volume.

1488

Spectral-Model Based Undersampling of Multi-Phase MSI: Application to Diffusion-Weighted Imaging Near Metal

Kevin Koch[1] and S Sivaram Kaushik[2]

[1]Radiology, Medical College of Wisconsin, Milwaukee, WI, United States, [2]Applications and Workflow, GE Healthcare, Milwaukee, WI

Diffusion weighted imaging around metal implants is a difficult task that requires a combination of multi-spectral MRI approaches with non-CPMG spin-echo refocusing techniques. Current implementations of this approach have shown promising initial clinical results. Further work on improving the acquisition efficiency of these techniques are required to achieve robust clinical viability. Here, we present an approach that utilizes the MSI spectral domain to enable spectral undersampling of diffusion-weighted acquisitions. The approach is also easily extendable to other multi-phase implementations of MSI, such as thermometry or relaxometry, where multiple volumes of data need to be acquired for quantitative computations.

1489

MR Imaging of Magnetic Ink Patterns via Off-Resonance Sensitivity

Stephanie L Perkins[1,2], Xinwei Shi[1,3], Hans Weber[1], Bruce L Daniel[1], and Brian A Hargreaves[1]

[1]Radiology, Stanford University, Stanford, CA, United States, [2]Bioengineering, Stanford University, Stanford, CA, United States, [3]Electrical Engineering, Stanford University, Stanford, United States

Printed magnetic ink creates predictable B0 field perturbations based on printed shape and magnetic susceptibility. This can be exploited for contrast in MR imaging techniques that are sensitized to off-resonance, such as fat-suppressed imaging with spectral presaturation. Magnetic ink therefore has the potential to be used in temporary tattoos for creating MR-visible skin markings of arbitrary shape and size, with applications in surgical planning, radiation therapy, tracking of joint movement, or other image registration scenarios. Here we characterize the susceptibility variations of magnetic ink and demonstrate application for MR-visible skin markings.

1490

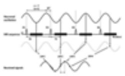

Multiple−TR neuronal resonance-MRI (NR-MRI) for detection of weak oscillating magnetic field

Ki Hwan Kim[1,2], Hyo-Im Heo[1], and Sung-Hong Park[1,2]

[1]Department of Bio and Brain Engineering, Korea Advanced Institute of Science and Technology (KAIST), Daejeon, Korea, Republic of, [2]Graduate School of Medical Science and Engineering, Korea Advanced Institute of Science and Technology (KAIST), Daejeon, Korea, Republic of

We propose a new approach termed neuronal resonance MRI (NR-MRI) with multiple TRs for detection of weak oscillating magnetic field. NR MRI could detect signals from oscillating magnetic fields with random frequency, phase, and on/off intervals, without synchronization between MR acquisition and neuronal oscillation. The detected signals showed higher SNR with increasing number of dynamic scans, demonstrating that temporal averaging is possible with NR-MRI. Two−TR approach showed multiple frequency components in an absolute frequency spectrum with no *a priori* target frequency information while suppressing the systematic noises, which warrants further investigation.

1491

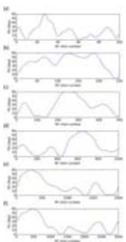

Determination of the Optimum Pattern Length of MRF Sequences

Karsten Sommer[1], Thomas Amthor[1], Peter Koken[1], Jakob Meineke[1], and Mariya Doneva[1]

[1]Philips Research Europe, Hamburg, Germany

An important open question in magnetic resonance fingerprinting (MRF) is the optimal choice of sequence parameters, i.e. the ideal length and shape of the pattern that defines the variation of the acquisition parameters. Here we apply a Monte Carlo based measure of sequence performance to find the optimal flip angle pattern for different pattern lengths. Afterwards, the most efficient pattern is found by evaluating these optimized sequences' actual performance in phantom experiments using various acceleration factors.

1492

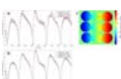

On the Influence of Intra-Voxel Dephasing in FISP-MRF with Variable Repetition Time

Sebastian Flassbeck[1], Simon Schmidt[1], Mathies Breithaupt[1,2], Peter Bachert[1], Mark E. Ladd[1], and Sebastian Schmitter[1,3]

[1]Medical Physics in Radiology, German Cancer Research Center (DKFZ), Heidelberg, Germany, [2]Institute for Forensic Medicine and Traffic Medicine, [3]Physikalisch-Technische Bundesanstalt (PTB), Braunschweig and Berlin, Germany

In this work we investigate the impact of intra-voxel dephasing on standard FISP-MRF measurements and propose the use of a constant TR to improve the robustness against spatially changing magnetic fields. The results have shown that FISP MRF measurements with a variable TR are susceptible to intra-voxel dephasing, which may generate temporal signal modulations that are likely to cause quantification errors in relaxation parameters. This can be alleviated by fixing TR without loss of encoding capability.

1493

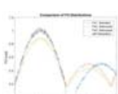

An algorithm for refocusing of T2* effects in bSSFP-MRF with relaxation corrections

Mingdong Fan[1], Danielle Kara[1], Jesse I. Hamilton[2], Nicole Seiberlich[2,3], Mark Griswold[2,3], and Robert Brown[1]

[1]Physics, Case Western Reserve University, Cleveland, OH, United States, [2]Biomedical Engineering, Case Western Reserve University, Cleveland, OH, United States, [3]Radiology, University Hospitals Case Medical Center, Cleveland, OH, United States

It is found that bSSFP-MRF is in general subject to T2* not T2 relaxation. Like traditional bSSFP, dephasing effects of intra-voxel inhomogeneities can be refocused in bSSFP-MRF with appropriate choices in TR, TE, and FA so that parameter maps are reflective of T2 rather than T2*. An algorithm is introduced and verified in simulation for refocusing intra-voxel dephasing at TE for bSSFP-MRF with corrections to previous work for relaxation effects previously assumed as negligible. These corrections are relevant for bSSFP-MRF in which T2 is not much larger than TR to ensure that T2 maps do not contain T2* effects.

1494

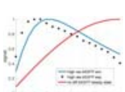

Ingredients for balanced SSFP Microimaging

Sebastien Bär[1], Thomas Oerther[2], Angelina Müller[3], Matthias Weigel[4], Matthias Wapler [3], and Jochen Leupold[1]

[1]Dept. of Radiology, Medical Physics, University Medical Center Freiburg, Freiburg, Germany, [2]Bruker Biospin GmbH, Ettlingen, Germany, [3]Department of Microsystems Engineering IMTEK, University of Freiburg, Freiburg, Germany, [4]Clinics of Radiology and Nuclear Medicine, Radiological Physics, University Hospital Basel, Basel, Switzerland

In this work, balanced SSFP microimaging was succesfully performed in 3D (voxel size 40µm x 40µm x 94µm) and 2D (in-plane resolution 16µm x 16µm) on a 7T small animal system and a small-bore 7T spectrometer with maximally used gradient amplitude of 1.03 T/m. Key for optimzed image quality was the choice of susceptibility matched phantom materials and the proper choice of bSSFP flip angle under consideration of diffusion attenuation due to imaging gradients.

1495 

Rapid background magnetic field inhomogeneity correction in MR-based oxygen imaging

Yasheng Chen[1], Xiaodong Zhang[2], Cihat Eldeniz[3], Dustin Ragan[1], Liam Comiskey[1], Melanie Fields[4], Kristin Guilliams[1], Jin-Moo Lee[1], Andria Ford[1], and Hongyu An[3]

[1]Neurology, Washington Univ. in St. Louis, St. Louis, MO, United States, [2]Radiology, Peking University Hospital, Beijing, People's Republic of China, [3]Radiology, Washington Univ. in St. Louis, St. Louis, MO, United States, [4]Pediatrics, Washington Univ. in St. Louis, St. Louis, MO, United States

Quantitative blood oxygenation level dependent (qBOLD) technique provides an invaluable and noninvasive means for mapping brain oxygen extraction fraction (OEF) and R2’ in various neurological disorders. However, background magnetic field inhomogeneity causes errors in the measurement. In this work, we propose a triple echo asymmetric spin echo sequence with imbedded Z-shimming table to measure and correct the adversary effect of the field inhomogeneity. With both simulation and 16 patient image sets, we have demonstrated the effectiveness of the proposed technique.

1496 

Improving Arterial Spin Labeling Acquisition to Reduce the Effect of Delayed Arrival Time

Andre Monteiro Paschoal[1], Renata Ferranti Leoni[1], Antonio Carlos dos Santos[2], Bernd Uwe Foerster, and Fernando Fernandes Paiva[3]

[1]Physics Department, University of Sao Paulo, Ribeirao Preto, Brazil, [2]Internal medicine, Medical School of Ribeirao Preto, Ribeirao Preto, Brazil, [3]Physics Institute of Sao Carlos, University of Sao Paulo, Sao Carlos, Brazil

Arterial Spin Labeling (ASL) is a powerful technique to evaluate cerebral blood flow. To analyze hemodynamics effects with ASL, multiples acquisitions over the time are realized, which is called multiphase ASL. In conventional multiphase ASL methods, the later phases has low contrast to noise ratio, so it becomes difficult to analyze it. This study purposes a solution to this problem, through a modulation in the acquisition flip angle. With this technique, the flip angle of all phases follows a modulation equation, so that the ASL signal over the phases becomes nearly constant.

1497 

Territorial Arterial Spin Labeling by Using Asymmetrically RF-shimmed Labeling Pulse with 4-channel RF Transmit at 3T

Kosuke Ito[1], Atsushi Kuratani[1], Nobuyuki Yoshizawa[1], and Masahiro Takizawa[1]

[1]Healthcare Business Unit, Hitachi, Ltd., Tokyo, Japan

Territorial ASL (tASL) using asymmetrically RF-shimmed labeling pulse was proposed. By using 4-channel RF transmit coil, spatially asymmetric transmission was applied to pCASL pulse. Proposed method does not require longer duration of RF pulse. Also, by using knowledge of B_1 map, appropriate scaling was applied to the tASL image, and labeling efficiency was consistent between nonselective ASL and tASL. Proposed method was implemented to a 3T MRI system, and demonstrated tASL in-vivo by a volunteer study. tASL of RICA, LICA, and VBA was imaged.

1498 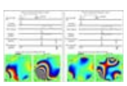

Phase Encoding with Bloch-Siegert effect using Parallel Transmit

Yuqing Wan[1], Maolin Qiu[1], Gigi Galiana[1], and R. Todd Constable[1,2]

[1]Radiology & Biomedical Imaging, Yale School of Medicine, New Haven, CT, United States, [2]Neurosurgery, Yale School of Medicine, New Haven, United States

A gradient-free, Bloch-Siegert effect based nonlinear spatial encoding scheme was introduced for silent scanning and to eliminate gradient-induced eddy currents in conventional MRI. We implemented a phase encoding scheme with a parallel transmit system on a 7T scanner to demonstrate feasibility. As a proof of concept, we demonstrated that B-S RF pulses can easilty produce nonlinear spatial encoding for MR imaging. The SAR limitations at 7T limit the efficiency of the encoding, but suggest the feasibility of this approach at lower fields.

1499 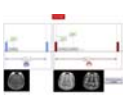

Tri-Fast Spin Echo: A Minimalistic Cross-Platform Multi-Spectral qMRI Pulse Sequence for Routine Clinical Use

Ning Hua[1], Mitchell Horn[2], Stephan Anderson[3], and Hernan Jara[1]

[1]Boston University, Boston, MA, United States, [2]Boston University, MA, United States, [3]Boston University

Purpose: To develop a simple and cross-platform pulse sequence that meets the following criteria: 1) all directly acquired images are clinically useful, 2) achieves minimalistic scan times, and 3) leads to excellent image quality as well as accurate MS-qMRI mapping. Methods: Tri-FSE consists of a single-echo-FSE sequence that is run in temporal concatenation with a dual-echo FSE sequence that all together generate T1-, T2, and PD-weighted directly acquired images. Results: Tri-FSE was implemented at medium and high spatial resolution at 1.5T and 3.0T. Conclusion: Tri-FSE is a dual purpose simple pulse sequence that is useful for clinical and scientific purposes.

1500 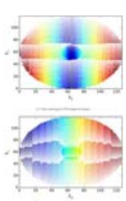

Accelerated 3D GRASE for T2 and PD Weighted High Resolution Images

Alexandra Cristobal-Huerta[1], Dirk Poot[1], Mika Vogel[2], and Juan Antonio Hernandez-Tamames[1]

[1]Department of Radiology and Nuclear Medicine, Erasmus MC, Rotterdam, Netherlands, [2]GE Healthcare B.V., Hoevelaken, Netherlands

Parallel Imaging techniques have not been introduced for Gradient and Spin Echo sequences being a limiting factor for clinical use. Enabling PI for GRASE requires new view-ordering schemes that acquire an autocalibration region while simultaneously mitigating artifacts and obtaining the desired contrast. The purpose of this work is to present new 2D PI accelerated Cartesian view-ordering schemes with either T2 or PD contrast in multi-shot VFA 3D-GRASE, for relevant SAR and scan time reduction compared to 3D-FSE/TSE.

1501  A new ultrafast 3D gradient-echo-based imaging method: RASE-II

JaeKyun Ryu[1,2], WonBeom Jung[1,2], Sun Young Chae[1,3], Geun-Ho Im[4,5], Jung Hee Lee[1,3,4], Seong-gi Kim[1,2], and Jang-Yeon Park[1,2]

[1]Center for Neuroscience Imaging Research, Institute for Basic Science (IBS), Suwon, Korea, Republic of, [2]Department of Biomedical Engineering Sungkyunkwan University (SKKU), Suwon, Korea, Republic of, [3]Department of Health Sciences and Technology, SAIHST, Sungkyunkwan University, Seoul, Korea, Republic of, [4]Center for Molecular and Cellular Imaging, Samsung Biomedical Research Institute, Seoul, Korea, Republic of, [5]Department of Radiology, Samsung Medical Center, Sungkyunkwan University, Seoul, Korea, Republic of

One version of a new ultrafast *gradient-echo-based* 3D imaging technique using spatiotemporal encoding (RASE-II) is proposed which provides constant TE across all spins. RASE-II maintains most of appealing features of other *spin-echo-based* SPEN imaging methods such as no Nyquist ghosting and high tolerance to field inhomogeneities. RASE-II also has less sensitivity not only to SAR and B_1-inhomogeneity effects because of low flip angles, but also to T_2^* signal modulation due to constant TE. As a promising tool for fMRI, RASE-II shows significant improvement of tSNR over GE-EPI. Its performance is demonstrated by lemon and in-vivo rat brain imaging at 9.4T.

1502 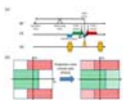 Dual Echo Trajectory : Comparison to Partial Fourier Acquisition and Sequence Optimization

Jeehun Kim[1] and Jongho Lee[1]

[1]Department of Electrical and Computer Engineering, Seoul National University, Seoul, Korea, Republic of

In this study, we compared two acceleration methods in spin echo imaging; previously proposed Dual Echo Trajectory (DuET) and partial Fourier acquisition. Also, we further improved DuET with interleaved multislice acquisition and echo timing correction.

1503  Blood saturation modeling in multiband multislab Time-of-Flight brain MRI

Alexis Amadon[1], Gaël Saïb[1], Nicolas Boulant[1], and Alexandre Vignaud[1]

[1]DRF / I2BM / NeuroSpin / UNIRS, CEA-Saclay, Gif-sur-Yvette, France

Multiband multislab Time-of-Flight angiography has recently been proposed for reduced acquisition time and improved sensitivity in the human brain at 3T and 7T. However, in these previous studies, blood saturation has not been taken into account as blood traverses several slabs acquired simultaneously. Here a simple modeling of blood magnetization history is provided to take this saturation into account, which appears essential to avoid strong losses of blood to background signal ratio. Slab-dependent multiband-added VUSE pulses are simulated to counteract these losses both at 3T and 7T, from which a methodology is derived to optimize multiband TOF sequence parameters.

1504 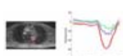 Simultaneous Multi-Volume 4D Phase Contrast Flow MRI

David Feinberg[1,2] and Liyong Chen[1,2]

[1]Advanced MRI Technologies, LLC, Berkeley, CA, United States, [2]Helen Wills Neuroscience Institute, Univ of California, Berkeley, Berkeley, CA, United States

A new technique of simultaneous 4D flow imaging acquired with simultaneous multiple 3D volumes (SMV) is presented. The velocity measurements are compared to conventional 4D flow imaging and have very good correspondence.

1505 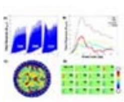 Spatial Mapping Using Radio Frequencies: A Non-Linear Approach to Silent MRI

Robert Nikolov[1], Simona Nikolova[1], Clara Eng[2], and Pierre Baldi[1]

[1]University of California Irvine, Irvine, CA, United States, [2]University of California Berkeley, Berkeley, CA, United States

Recent advances for silent MRI have shown that spatial encoding can be achieved using RF rather than linearly varying static magnetic field gradients. This has been demonstrated using homogeneous transmit (B_1) fields with linearly varying phase gradients. Similar results can be achieved with linear B_1 amplitude gradients with homogeneous phase. The efficacy of either method is limited by a maximum B_1 gradient strength (phase or magnitude) per specific absorption rate. Here we demonstrate a novel approach to relieve this restriction where highly nonlinear B_1 gradients can be used for combined amplitude and phase modulation with reconstruction using state-of-the-art machine learning models.

1506 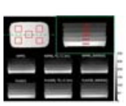 SNR Efficiency of Combined Bipolar Gradient Echoes: Theoretical Expressions and Experimental Verification

Jean-David Jutras[1], Keith Wachowicz[1,2], and Nicola De Zanche[1,2]

[1]Oncology, University of Alberta, Edmonton, AB, Canada, [2]Medical Physics, Cross Cancer Institute, Edmonton, AB, Canada

Multi-echo bipolar pulse sequences are becoming increasingly popular in structural brain imaging applications that require high SNR efficiency and minimal geometrical distortions or water-fat shifts. However, various discrepant expressions for the SNR as a function of T_2^* and the sampling bandwidth were previously reported, making it unclear as to how multiple bipolar echoes should be combined to maximize SNR. In this study, we compare some traditional single-echo (low-bandwidth) FLASH and MPRAGE sequences with their multi-echo bipolar (high bandwidth) counterparts and validate the SNR theory via phantom measurements. Bipolar MPRAGE/FLASH yield SNR gains of ~1.3/1.6-fold, in good agreement with the theory.

1507  Signal Coding for SNR Multiplying Effect and Scan Acceleration Flexibility

Yudong Zhu[1]

[1]Zhu Consulting, Scarsdale, NY, United States

In a way that augments existing encoding, signal coding promotes a multiplying effect of SNR and flexibility of scan acceleration. Its essence is to push for noise decimation by acquiring sums of marked signals from all components where the marking can be achieved by RF, gradient or other means. Its application to multi-slice MRI opens up a regime that enjoys both a √N SNR enhancement, as analogous to that of volumetric MRI, and flexibility with scan time budget, as equal or superior to that of existing multi-slice MRI.

1508

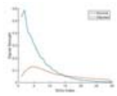

Sequence Design by Signal Inversion Using Extended Phase Graphs

Nicholas Dwork[1] and John Pauly[1]

[1]Electrical Engineering, Stanford University, Stanford, CA, United States

In this work, we show that MR signal progression can be represented as an autonomous discrete linear dynamical system when the small angle approximation is made. This formalism can be used to determine an optimal set of flip angles to yield a desired magnetic state. We present an an example of maintaining a constant signal strength with a Fast Spin Echo sequence.

1509

GPU optimized fast Bloch simulator for arbitrary MRI pulse sequences

Ryoichi Kose[1] and Katsumi Kose[2]

[1]MRTechnology, Inc., Tsukuba, Japan, [2]University of Tsukuba, Tsukuba, Japan

A GPU optimized fast Bloch simulator was developed for arbitrary pulse sequence inputs. The simulator was applied to multi-slice imaging using 256×256×512 calculation matrix. As a result, we found that the number of short pulses used to approximate the selective excitation pulse and the number of subvoxels used for imaging in the cross-sectional plane were essential to simulation speed.

1510

MRI Pulse Sequence Development Using Graphical User Interface Modules

Saulius Archipovas[1], Thorsten Honroth[1], Cristoffer Cordes[1,2], Matthias Günther[1,2], and David Porter[1]

[1]Fraunhofer MEVIS, Bremen, Germany, [2]University of Bremen, Bremen, Germany

We present a preliminary study on developing MRI pulse sequences using graphical user interface elements. We introduce a prototype where a sequence developer can specify a sequence structure and parameter dependencies just using the GUI. As a result, a sequence developer can concentrate on the MRI sequence design, rather than on software engineering issues. The GUI-based development framework is decoupled from the manufacturer's development environments and promises to promote the development of basic sequence designs that are independent of the scanner platforms used.

1511

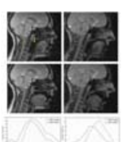

Assessing intrinsic velum height in vowels using time-resolved MRI

Martin Krämer[1], Melanie Weirich[2], Karl-Heinz Herrmann[1], Adrian P Simpson[2], and Jürgen R Reichenbach[1,3,4,5]

[1]Medical Physics Group, Institute of Diagnostic and Interventional Radiology, Jena University Hospital - Friedrich Schiller University Jena, Jena, Germany, [2]Institut für Germanistische Sprachwissenschaft, Friedrich Schiller University Jena, Jena, Germany, [3]Michael Stifel Center for Data-driven and Simulation Science Jena, Friedrich Schiller University Jena, Jena, Germany, [4]Abbe School of Photonics, Friedrich Schiller University Jena, Jena, Germany, [5]Center of Medical Optics and Photonics, Friedrich Schiller University Jena, Jena, Germany

Real-time MRI and synchronised audio were used to examine intrinsic velum height in German vowels. Two adult female subjects produced five repetitions of a set of sentences containing, among other target material, the point vowels /i: a: u:/ in the same phonologically non-nasalised context. Even in this small sample, the subjects exhibit variation in velum height across vowel categories, and show considerable interindividual variation in velum height during the production of the same vowel category. Collection of further data from normal subjects will be used to create a robust baseline for the assessment of abnormal velum activity.

Traditional Poster

Reconstruction

Exhibition Hall 1512-1531 Monday 8:15 - 10:15

1512

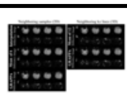

Strategies for Compensating for Missing k-space Data in a Novel Half-Fourier Reconstruction

Seul Lee[1] and Gary Glover[2]

[1]Electrical Engineering, Stanford University, Stanford, CA, United States, [2]Radiology, Stanford University, Stanford, CA, United States

Functional MRI (fMRI) is sensitive to off-resonance from air-tissue susceptibility interfaces. Existing half-Fourier reconstruction is vulnerable to off-resonance since it may lose most of the image energy (near k=0) with a large amount of off-resonance. In a previous study, we suggested a new half Fourier (even/odd (E/O)) reconstruction and showed it was more robust to off-resonance compared to Homodyne reconstruction. E/O reconstruction acquires every other line in k-space. Therefore, neighboring data can be used to compensate for the missing data. In this study, we suggest several strategies for compensating for missing k-space data in kx-ky as well as kz direction.

1513

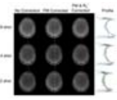

Reducing acquisition time while maintaining spatial resolution with extended readouts and R2* modeling

Alex Cerjanic[1,2], Giang Chau Ngo[1,2], and Bradley P Sutton[1,2]

[1]Bioengineering, University of Illinois at Urbana-Champaign, Urbana, IL, United States, [2]Beckman Institute, University of Illinois at Urbana-Champaign, Urbana, IL, United States

Single shot readouts are limited in length by field inhomogeneity and R2* relaxation. With the inclusion of a complex field map, existing field corrected reconstruction algorithms can compensate for both field inhomogeneity and R2* relaxation during extended readouts. Results for spiral acquisitions of up to 56ms in length are demonstrated on a human volunteer.

1514

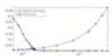

Accelerated Regularized Image Reconstruction in Spatiotemporal MRI

Alexander Gutierrez[1], Di Xiao[1], Jarvis Haupt[1], Albert Jang[2], Steen Moeller[2], and Michael Garwood[2]

[1]University of Minnesota, Minneapolis, MN, United States, [2]Center for Magnetic Resonance Research, University of Minnesota

Interest in spatiotemporally-encoded MRI methods has increased over the last decade due mainly to their high tolerance to magnetic field inhomogeneities. However, the data acquired in spatiotemporal MRI can lead to challenging image reconstruction problems. In this abstract we propose a new framework for reconstructing images that leverages compressible structure in recent spatiotemporal encoding techniques to enable an iterative approximate inversion of the Bloch-equations for imaging. In particular, we can often obtain a visually indistinguishable reconstruction up to an order of magnitude faster than using the full inversion.

1515

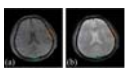

Fast Multi-contrast MRI Super-resolution with Similar Anatomical Structure

Hong Zheng[1], Zhengjian Bai[2], Yunsong Liu[1], Di Guo[3], Jiyang Dong[1], Zhong Chen[1], and Xiaobo Qu[1]

[1]Dept. of Electronic Science, Fujian Provincial Key Laboratory of Plasma and Magnetic Resonance, Xiamen University, Xiamen 361005, China, Xiamen, People's Republic of China, [2]School of Mathematical Sciences, Xiamen University, Xiamen 361005, China, People's Republic of China, [3]Dept. of Computer Science, Xiamen University of Technology, Xiamen 361024, China, People's Republic of China

Since magnetic resonance imaging (MRI) can offer images of an object with different contrasts, e.g., T1-weighted or T2-weighted, the shared information between inter-contrast images can be used to benefit super-resolution. Regarding the image as a locally stationary Gaussian process and using the least square method, we found weights of a local window are to be nearly invariant to image contrasts, which can be further used to transfer the shared information from one contrast to another. We analyze this property with comprehensive mathematics and numeric experiments. The reconstructed edges are more consistent to the original high-resolution image, indicated with higher PSNR and SSIM than the compared methods.

1516

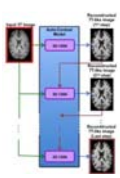

7T-like MR Images Synthesis from 3T MRI using Auto-Context Convolutional Neural Network

khosro bahrami[1], Islem Rekik[1], Feng Shi[1], and Dinggang Shen[1,2]

[1]University of North Carolina at Chapel Hill, Chapel Hill, NC, United States, [2]Department of Brain and Cognitive Engineering, Korea University, Seoul, Korea, Republic of

We propose a novel multi-step Convolutional Neural Network (CNN) architecture to cascade multiple CNNs, along with an Auto-Context Model (ACM), called Auto-Context CNN, to reconstruct 7T-like MR images from 3T MR images. Basically, we non-linearly map the input 3T MR images to their corresponding 7T MR images. To do so, in the training stage, we first partition the training 3T and 7T MR images into overlapping 3D patches, then we train the Auto-Context CNN to map each 3T patch to the center voxel in the corresponding 7T patch. In the testing step, we apply the trained Auto-Context CNN to generate the 7T-like MRI patch from each input 3T patch.

1517

Evaluation of convex programming for super-resolution MRI reconstruction using shifted slice acquisitions

Onur Afacan[1], Ali Gholipour[1], Benoit Scherrer[1], and Simon K. Warfield[1]

[1]Radiology, Boston Children's Hospital and Harvard Medical School, Boston, MA, United States

Super-resolution methods have recently became popular due to their ability to generate isotropic high resolution images from multiple low resolution acquisitions. In this work, we developed and evaluated a convex programming solution to the super-resolution reconstruction and applied it to combine shifted thick slice T2 images into images with isotropic resolution. With this formulation, using phantom and volunteer experiments, we show that, it is possible to generate high resolution images with better resolution and accuracy compared to the previously developed methods.

1518

The use of SPIRIT to reject and replace motion-corrupted data

Mark Bydder[1], Stanislas Rapacchi[1], Olivier Girard[1], Wafaa Zaaraoui[1], and Jean-Philippe Ranjeva[1]

[1]Aix-Marseille Université, Marseille, France

The SPIRIT parallel imaging algorithm was evaluated for use in a data rejection and replacement scheme to reduce motion artefacts.

1519 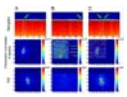

A method for identifying and fixing faulty navigator corrections in system-reconstructed multi-shot 3D diffusion weighted images

Bruce Langford[1], Thomas Neuberger[2,3], and Paul Bartell[1,4]

[1]Department of Animal Science, The Pennsylvania State University, University Park, PA, United States, [2]Department of Biomedical Engineering, The Pennsylvania State University, University Park, PA, United States, [3]Huck Institutes of the Life Sciences, The Pennsylvania State University, [4]Interdepartmental Graduate Program in Neuroscience, The Pennsylvania State University

Unusual artifacts appear in some reconstructed images of a multi-segment 3D EPI-DTI sequence with navigator correction on a 7T Bruker Biospec system running Paravision 6.1. Navigator helps to compensate for subject movement within the scanner. However, by examining the k-space of the system processed volumes and the raw navigator data, the artifacts were attributed to navigator overcompensation, which resulted in the over representation of a few lines in k-space. After zeroing the affected lines, image quality was on par with other volumes with no artifacts, eliminating the need to rescan subjects.

1520 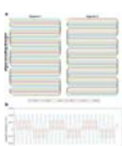

Iterative reconstruction of highly undersampled multi-echo EPI – a novel dynamic contrast approach to tackle distortions

Tim Sprenger[1,2], Jonathan I. Sperl[2], Marion I. Menzel[2], and Anne Menini[2]

[1]TUM, Munich, Germany, [2]GE Global Research, Munich, Germany

We propose a highly undersampled multi echo EPI sequence combined with a selfcalibrating reconstruction pipeline to adress offresonance artifacts. Ideas from the areas fieldmap, RPG and temporal subspace transform are combined yielding distortion free dynamic contrast images.

1521 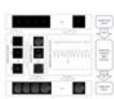

k-t Rank Separation Reconstruction for non-Cartesian parallel fMRI

Fei Wang[1], Juergen Hennig[1], and Pierre LeVan[1]

[1]Department of Radiology, Medical Physics, Medical Center - University of Freiburg, Freiburg, Germany

Low-rank sparse (L-S)-reconstruction has been successfully applied to k-t-accelerated applications like cardiac cine imaging. We propose a novel way of k-t rank separation for the reconstruction of non-Cartesian parallel fMRI. Instead of reconstructing the fMRI images separately, the proposed method reconstructs images jointly. This method extracts temporal signal variation information from k-t space directly, thus exactly preserving dynamic information. The results show a higher dynamic signal recovery rate and shorter reconstruction time.

1522 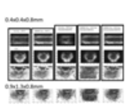

SQUASHER: Slice quadratic phase with HSn encoding and reconstruction

Steen Moeller[1], Xiaoping Wu[2], Noam Harel[2], Mike Garwood[2], and Mehmet Akcakaya[1]

[1]Center for Magnetic Resonance Research, Minneapolis, MN, United States, [2]University of Minnesota, Minneapolis, MN, United States

For 3D imaging, frequency-swept excitation can be used to obtain broad bandwidth and sharp slab profiles. The quadratic phase from such RF excitation imparts spatiotemporal encoding and can be leveraged for added encoding. Here we show that, by sliding the quadratic phase across the slice-encoding direction, synergy can be achieved when combining frequency-swept excitation with Fourier encoding, which has inherent optimal noise-properties.

1523 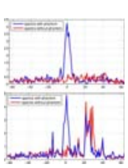

Extraction of NMR Signal from a Portable Single-Sided Magnet System in a Noisy Environment

W. Scott Hoge[1,2], Mirko Hrovat[3], Alan Hrovat[3], Mikayel Dabaghyan[3], Iga Muradyan[1,2], James Butler[1,2], and Samuel Patz[1,2]

[1]Radiology, Brigham and Women's Hospital, Boston, MA, United States, [2]Harvard Medical School, Boston, MA, United States, [3]Mirtech, Inc, Brockton, MA, United States

MR is a useful method for monitoring patients with pulmonary edema. To prevent difficult and costly transportation of patients to an MR imaging location, a portable magnet system was recently developed.The system necessarily operates in a noisy electro-magnetic environment,thus signal processing methods are needed to extract the NMR signal from a measurement system that is flooded with signal from external sources. This work compares a traditional adaptive filter theory approach against a sub-space projection approach. We demonstrate with phantom data measurements that these methods can improve detection of the NMR signal in anoisy environment.

1524 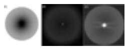

Pseudo-inverse constrained (PICO) reconstruction reduces colored noise of PROPELLER and improves the gray-white matter differentiation

Jyh-Miin Lin[1,2], Shang-Yueh Tsai[3], Hing-Chiu Chang[4], Hsiao-Wen Chung[5], Hsin Chia Chen[6,7], Yen-Heng Lin[8], Chung-Wei Lee[7], Ya-Fang Chen[7], Daniel Scoffings[9], Tilak Das[9], Jonathan H. Gillard[2], Andrew J. Patterson[10], and Martin J. Graves[10]

[1]Graduate Institute of Biomedical Electronics and Bioinformatics, National Taiwan University, Taipei, Taiwan, [2]Department of Radiology, University of Cambridge, Cambridge, United Kingdom, [3]Department of Applied Physics, National Chengchi University, Taipei, Taiwan, [4]Department of Diagnostic Radiology, Li Ka Shing Faculty of Medicine, The University of Hong Kong, Hong Kong, Hong Kong, [5]Department of Electrical Engineering, National Taiwan University, Taipei, Taiwan, [6]Department of Medical Imaging, Madou Sinlau Hospital, Tainan, Taiwan, [7]Department of Medical Imaging, National Taiwan University Hospital, Taipei, Taiwan, [8]Department of Medical Imaging, National Taiwan University Hospital Yun-Lin Branch, Taipei, Taiwan, [9]Department of Radiology, Cambridge University Hospitals NHS Foundation Trust, Cambridge, United Kingdom, [10]MRIS unit, Cambridge University Hospitals NHS Foundation Trust, Cambridge, United Kingdom

The image quality of Periodically Rotated Overlapping ParallEL Lines with Enhanced Reconstruction (PROPELLER) MRI is degraded by the “colored noise” or “blue noise”. Total variation (TV) denoising is expected to reduce colored noise and improve the overall image quality. However, no study has compared different TV algorithms for reducing colored noise. This study explores two TV denoising methods: (1) image domain denoising (IDD), and (2) Pseudo-Inverse COnstrained (PICO) reconstruction. Comparing these two TV denoising methods, PICO significantly reduces the noise level of PROPELLER and improves the gray-white matter differentiation.

1525 

Distortion Correction in Readout-Segmented EPI using View Angle Tilting Combined with Phase Modulated RF Pulse

Wei Liu[1], Kun Zhou[1], and Fang Dong[1]

[1]Siemens Shenzhen Magnetic Resonance Ltd, Shenzhen, People's Republic of China

The VAT technique has been applied in ss-EPI to eliminate the distortion along the phase encoding direction. However the long echo spacing in ss-EPI will lead to more phase errors introduced by B0 inhomogeneity and require more VAT gradient, which results an increasing image blurring and limits the spatial resolution. The rs-EPI features much shorter echo spacing compared with ss-EPI, which could be much suitable for VAT. In this study, the VAT technique is integrated into a rs-EPI sequence to further improve the distortion. In addition, phase modulated pulse is used to reduce the image blurring caused by VAT.

1526 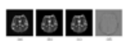

An improved image-based method for field inhomogeneity map in distorted brain EPI image

Seiji Kumazawa[1], Takashi Yoshiura[2], Akihiro Kikuchi[1], Go Okuyama[1], and Masataka Kitama[1]

[1]Department of Radiological Technology, Faculty of Health Sciences, Hokkaido University of Science, Sapporo, Japan, [2]Department of Radiology, Graduate School of Medical and Dental Sciences, Kagoshima University, Kagoshima, Japan

To correct the distortion in EPI due to field inhomogeneity, an image-based method for estimating the field map from the distorted EPI image has been proposed. However, this method suffers from long computation times. Our purpose was to improve an image-based method in terms of the computation time. Whereas the previous method synthesized EPI image in k-space requiring a lot of execution of FFT, our method synthesized EPI image in the image-domain. Our method reduced the computation time in the almost same NRMSE in previous method. Our results suggest that our improved method was able to perform a reasonable estimation of the field map.

1527 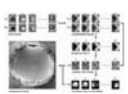

Selective Channel Combination of 3D Phase Offset Corrected 7T MRI Phase Images

Shaeez Usman Abdulla[1], David C Reutens[1], Kieran O'Brien[2], and Viktor Vegh[1]

[1]Centre for Advanced Imaging, University of Queensland, Brisbane, Australia, [2]Siemens Healthcare Australia Pty. Ltd., Australia

A number of MRI applications rely on accurate phase images. At ultra-high field, the limitations of various processing techniques and the absence of a volume reference coil make the combination of multi-channel signal phase challenging. We propose a method which combines phase offset corrected signal phase data across a selection of channels. We evaluated method performance at two different gradient recalled echo MRI echo times. We qualitatively and quantitatively studied the combined phase quality in distinct brain regions. We found that using a subset of channels leads to improved phase images than when all channels are used in the combination.

1528 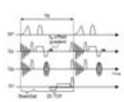

Acceleration and Artifact Suppression in Selective TOF MRA with Sampling Reduction

Takashi Nishihara[1], Kuniharu Oka[1], Masahiro Takizawa[1], and Hiroyuki Itagaki[1]

[1]Healthcare Business Unit, Hitachi, Ltd., Tokyo, Japan

We confirmed that 2D beam excitation presaturation-pulse (hereafter BeamSat pulse) can saturate the vessels selectively in brain. Although BeamSat can visualize hemodynamics, the scan time is long (about 5 minutes) because the based sequence is 3D TOF. The single thick slice 2D TOF was used for based sequence to reduce the scan time and the k_s offset was added to saturate background brain signal. We showed that this method can accelerate the scan time to 0.6-0.8 seconds without the notable loss of vessel visualization.

1529 

SPARKLING: Novel Non-Cartesian Sampling Schemes for Accelerated 2D Anatomical Imaging at 7T Using Compressed Sensing

Carole Lazarus[1], Pierre Weiss[2], Nicolas Chauffert[1], Franck Mauconduit[3], Michel Bottlaender[4], Alexandre Vignaud[4], and Philippe Ciuciu[1]

[1]CEA/NeuroSpin, INRIA/Parietal, Gif-sur-Yvette Cedex, France, [2]CNRS/ITAV, Toulouse, France, [3]Siemens Healthineers, Saint-Denis, France, [4]CEA/NeuroSpin, Gif-sur-Yvette Cedex, France

We present for the first time the implementation of novel non-Cartesian trajectories on a 7T scanner for 2D anatomical imaging. The proposed SPARKLING curves (Segmented Projection Algorithm for Random K-space sampLING) are a new type of non-Cartesian segmented sampling trajectories which allow fast and efficient coverage of the k-space according to a chosen variable density [1]. To demonstrate their potential, a high-resolution (0.4x0.4x3.0mm^3) T2*-weighted image was acquired with an 8-fold undersampled SPARKLING trajectory. Images were reconstructed using non-linear iterative reconstructions derived from the Compressed Sensing theory.

1530

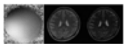

A Blind Deconvolution Approach to Fast MR T2 Mapping

Jingyuan Lyu[1], Dong Liang[2], Chaoyi Zhang[1], Ukash Nakarmi[1], and Leslie Ying[1,3]

[1]Electrical Engineering, State University of New York at Buffalo, Buffalo, NY, United States, [2]Shenzhen Institutes of Advanced Technologies, Shenzhen, People's Republic of China, [3]Biomedical Engineering, State University of New York at Buffalo, Buffalo, NY, United States

MR parameter mapping has shown great potential but is still limited in clinical application due to the lengthy acquisition time. To accelerate the acquisition speed using multi-channel coils, we propose a novel blind deconvolution based approach to parameter mapping. The proposed method reconstructs the series of T2-weighted images, coil sensitivities of all channels, and the T2 maps simultaneously through a highly efficient, k-space based blind deconvolution approach. The experimental results show the potential of highly accelerated T2 mapping by the proposed method.

1531

Alternating Direction Method of Multipliers for Diffusion Basis Functions (DBF)

Odin Eufracio[1], Mariano Rivera[1], and Johan Van Horebeek[1]

[1]Centro de Investigacion en Matematicas AC, Guanajuato, Mexico

We propose a new framework to solve the Diffusion Basis Functions model based on the alternating direction method of multipliers. We present an iterative, simple and efficient algorithm with closed-form updates. The proposal introduces a new regularization term to promote sparsity in the number of estimated fibers. Our experimental result shows that diffusion dictionary approaches benefit from our proposal.

Traditional Poster

Young Investigator Awards

Exhibition Hall 31-36 Monday 13:45 - 15:45

31

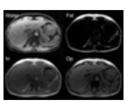

Free-breathing volumetric fat/water separation by combining radial sampling, compressed sensing, and parallel imaging

Thomas Benkert[1,2], Li Feng[1,2], Daniel K. Sodickson[1,2], Hersh Chandarana[1,2], and Kai Tobias Block[1,2]

[1]Radiology, NYU School of Medicine, New York, NY, United States, [2]Bernard and Irene Schwartz Center for Biomedical Imaging, Department of Radiology, NYU School of Medicine, New York, NY, United States

Fat-suppressed T1-weighted gradient-echo imaging is commonly used for abdominal MR examination. However, image quality can be compromised by inhomogeneous fat suppression and imperfect breath-holding. To overcome both limitations, we describe a novel technique for free-breathing fat/water separation (Dixon-RAVE).

Motion-robust acquisition is achieved by using radial sampling. A model-based reconstruction, which incorporates compressed sensing, parallel imaging, and fat deblurring, is used to obtain fat and water maps. Two extensions are described that enable motion-resolved fat/water separation (XD-Dixon-RAVE) and dynamic contrast-enhanced fat/water separation (DCE-Dixon-RAVE). The technique is demonstrated for various clinical applications, including free-breathing liver and breast exams in volunteers and patients.

32

Direct Quantitative ^{13}C-Filtered ^{1}H Magnetic Resonance Imaging of PEGylated Biomacromolecules In Vivo

Rohan D. A. Alvares[1], Justin Y. Lau[2,3], Peter M. Macdonald[1], Charles H. Cunningham[2,3], and R. Scott Prosser[1,4]

[1]Department of Chemistry, University of Toronto, Toronto, ON, Canada, [2]Department of Medical Biophysics, University of Toronto, Toronto, ON, Canada, [3]Sunnybrook Research Institute, Toronto, ON, Canada, [4]Department of Biochemistry, University of Toronto, Toronto, ON, Canada

We demonstrate a new platform technology in which macromolecular constituents, such as proteins and drug delivery systems, are observed directly and quantitatively in vivo using 1H MRI of 13C-labeled polyethylene glycol (13C-PEG) tags. The 28 kDa 13C-PEG tags are non-immunogenic, and each bears approximately 2500 spectroscopically equivalent 1H nuclei appearing at a single resonance position. By filtering the 1H PEG signal through the directly coupled 13C nuclei, background water and fat signals are largely eliminated. We demonstrate the approach by monitoring in real-time the distribution of 13C-PEG and 13C-pegylated albumin injected into the hind leg of a mouse.

33

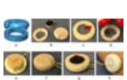

Hybrid MRI-ultrasound acquisitions, and scannerless real-time imaging

Frank Preiswerk[1], Matthew Toews[2], Cheng-Chieh Cheng[1], Jr-yuan George Chiou[1], Chang-Sheng Mei[3], Lena F. Schaefer[1], W. Scott Hoge[1], Benjamin M. Schwartz[4], Lawrence P. Panych[1], and Bruno Madore[1]

[1]Department of Radiology, Brigham and Women's Hospital, Harvard Medical School, Boston, MA, United States, [2]The Laboratory for Imagery, Vision and Artificial Intelligence, École de Technologie Supérieure, Montréal, QC, Canada, [3]Department of Physics, Soochow University, Taipei, Taiwan, [4]Google Inc, New York, NY, United States

The goal of this project was to combine MRI, ultrasound (US) and computer science methodologies toward generating MRI at high frame rates, inside and even outside the bore. A small US transducer, fixed to the abdomen, collected signals during MRI. Based on these signals and correlations with MRI, a machine-learning algorithm created synthetic MR images at up to 100 frames per second. In one particular implementation volunteers were taken out of the MRI bore with US sensor still in place, and MR images were generated on the basis of ultrasound signal and learned correlations alone, in a 'scannerless' manner.

34

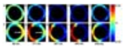

Imaging Left-ventricular Mechanical Activation in Heart Failure Patients using Cine DENSE MRI: Validation and Implications for Cardiac Resynchronization Therapy

Daniel Auger[1], Kenneth C. Bilchick[2], Jorge A. Gonzalez[2], Sophia X. Cui[1], Jeffrey W. Holmes[1,2], Christopher M. Kramer[2,3], Michael Salerno[1,2], and Frederick H. Epstein[1,3]

[1]Department of Biomedical Engineering, University of Virginia Health System, Charlottesville, VA, United States, [2]Medicine/Cardiology/Electrophysiology, University of Virginia Health System, Charlottesville, VA, United States, [3]Radiology/Medical Imaging, University of Virginia Health System, Charlottesville, VA, United States

This study developed methods for imaging left-ventricular (LV) mechanical activation, with application to identifying optimal LV pacing sites for cardiac resynchronization therapy (CRT). Cine displacement encoding with stimulated echoes (DENSE) was used for strain imaging, and mechanical activation time was defined as the time of onset of circumferential shortening (TOS). Active contours were applied to strain data to automatically compute TOS. Results showed a strong correlation between TOS and electrical activation time, heterogeneity of the location of latest activation, and a significant association between TOS at the LV pacing site and CRT response. These methods may enable improved CRT implementation.

35

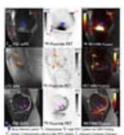

PET/MR Imaging of Metabolic Bone Activity in Osteoarthritis

Feliks Kogan[1], Audrey Fan[1], Emily McWalter[2], Uchechukwuka Monu[1], Edwin Oei[3], Andrew Quon[1], and Garry Gold[1,4,5]

[1]Radiology, Stanford University, Stanford, CA, United States, [2]2Department of Mechanical Engineering, University of Saskatchewan, Saskatoon, SK, Canada, [3]Department of Radiology & Nuclear Medicine, Erasmus MC, University Medical Center, Rotterdam, Netherlands, [4]Department of Bioengineering, Stanford University, Stanford, CA, United States, [5]Department of Orthopaedic Surgery, Stanford University, San Francisco, CA, United States

Osteoarthritis (OA) is a leading cause of disability, resulting in reduced quality of life, at tremendous societal cost. New hybrid PET/MR systems allow for simultaneous, sensitive, and quantitative assessments of early bone activity in OA with PET, which can be correlated with high-resolution quantitative MR methods of soft tissues to study the pathogenesis of OA. We demonstrate promising initial results of simultaneous PET/MR hybrid imaging of knee OA. Results suggest that PET/MR may detect metabolic abnormalities in subchondral bone, which appear normal on MRI. These advancements will allow us to detect and track early and reversible changes in OA.

36

Quantifying the Influence of Respiration and Cardiac Pulsations on the Cerebrospinal Fluid Dynamics using Real-Time Phase-Contrast MRI

Selda Yildiz[1], Suraj Thyagaraj[2], Ning Jin[3], Xiadong Zhong[4], Soroush Heidari Pahlavian[2], Bryn Martin[5], Francis Loth[2], John Oshinski[6], and Karim G. Sabra[1]

[1]Woodruff School of Mechanical Engineering, Georgia Institute of Technology, Atlanta, GA, United States, [2]Department of Mechanical Engineering, Conquer Chiari Research Center, The University of Akron, Akron, OH, United States, [3]MR R&D Collaborations, Siemens Healthcare, Columbus, OH, United States, [4]MR R&D Collaborations, Siemens Healthcare, Atlanta, GA, United States, [5]Department of Biological Engineering, The University of Idaho, Moscow, ID, United States, [6]Department of Radiology & Imaging Sciences and Biomedical Engineering, Emory University, Atlanta, GA, United States

Cerebrospinal fluid (CSF) flow undergoes periodic pulsatile motion driven by cardiac and the respiratory forces. Invasive studies using spinal taps as well as non-invasive studies using phase contrast MRI (PCMRI) sequences have well documented the cardiac-driven CSF flow. PCMRI, however, often uses a conventional cine-phase contrast technique gated to the cardiac cycle, and thus cannot measure the effects of respiration or other non-cardiac transient events such as coughing. Examining these effects requires the ability to perform real-time MRI measurements of continuous CSF flow along the spine and cranial cavity, and determine accurate instantaneous CSF flow velocity values.

Traditional Poster

Cartilage, Meniscus, Tendon, Ligaments

Exhibition Hall 1532-1562 Monday 16:15 - 18:15

1532

Six-month follow-up of the patients with the low-grade femoral cartilage lesions using T2 mapping at 3 and 7 Tesla

Vladimir Juras[1,2], Markus Schreiner[1], Rahel Heule[3], Pavol Szomolanyi[1,2], Stefan Zbyn[1,4], Vladimir Mlynarik[1], Stefan Marlovits[5], Didier Laurent[6], Celeste Scotti[6], Joerg Goldhahn[6], Kubiak Ewa[6], Haber Harry[6], Ivan Frollo[2], Oliver Bieri[3], and Siegfried Trattnig[1,7]

[1]Department of Biomedical Imaging and Image-Guided Therapy, Medical University of Vienna, Vienna, Austria, [2]Department of Imaging Methods, Slovak Academy of Sciences, Institute of Measurement Scinece, Bratislava 4, Slovakia, [3]Division of Radiological Physics, University of Basel Hospital, Basel, Switzerland, [4]Research Unit of Medical Imaging, Physics and Technology, University of Oulu, Oulu, Finland, [5]University Clinic for Trauma Surgery, Medical University of Vienna, Vienna, Austria, [6]Novartis Institutes for Biomedical Research, Basel, [7]CD Laboratory for Clinical Molecular MR Imaging

Transverse relaxation time (T2) maps were assessed as a potential marker for the long-term follow-up of the patients with cartilage lesions ICRS Grade I-II in four time points (baseline, 8 days, 3 and 6 months). T2 mapping was based on a 3D triple echo steady state imaging sequence delivering high quality high-resolved T2 maps at ultra-high field MRI. The results showed opposite trends of T2 values at 3T (a decrease) and 7T (an increase) over time. The statistically significant difference was found in case of deep zone of the cartilage lesion at 3T. T2 mapping could be used in the future as a good alternative to cartilage biopsies in clinical trials on new therapies aimed at cartilage regeneration.

1533

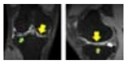

Automated Segmentation of Knee Cartilage from MR Images using Sequential Multi-atlas Registration and Shape-constrained Locally-weighted Voting for Quantitative Knee Joint Assessment

Han Sang Lee[1], Helen Hong[2], Young Cheol Yoon[3], and Junmo Kim[1]

[1]School of Electrical Engineering, KAIST, Daejeon, Korea, Republic of, [2]Dept. of Software Convergence, Seoul Women's University, Seoul, Korea, Republic of, [3]Department of Radiology, Samsung Medical Center, Seoul, Korea, Republic of

We propose a multi-atlas segmentation method for the knee cartilage in T2 PD MR images using sequential multi-atlas registrations and locally-weighted voting (LWV). To select training atlases similar to the test image, a 2D projection image-based atlas selection method is proposed. Then, to extract a bone model to be used as registration target in cartilage segmentation, the bone is segmented by sequential multi-atlas registrations and LWV. Finally, to segment a cartilage without leakage into low-contrast surroundings, the cartilage is segmented by bone-mask-based cartilage registration and shape-constrained LWV with distance and structure similarity weights, as well as atlas similarity weight.

1534

MR Microscopy of early changes in osteoarthritis – Ex-vivo study of the osteochondral degenerative process at 7T

Benedikt Hager[1,2], Sonja Walzer[3], Vladimir Juras[1,4], Martin Zalaudek[1], Xeni Deligianni[5], Oliver Bieri[5], Andreas Berg[6], Joachim Friske[1], Reinhard Windhager[3], and Siegfried Trattnig[1,2]

[1]High Field MR Centre, Department of Biomedical Imgaing and Image-guided Therapy, Medical University of Vienna, Vienna, Austria, [2]Christian Doppler Laboratory for Clinical Molecular MR Imaging, Vienna, Austria, [3]Department of Orthopaedic Surgery, Medical University of Vienna, Vienna, Austria, [4]Department of Imaging Methods, Institute of Measurement Science, Slovak Academy of Sciences, Bratislava, Slovakia, [5]Department of Radiology, Division of Radiological Physics, University of Basel Hospital, Basel, Switzerland, [6]Center for Medical Physics and Biomedical Engineering, Medical University of Vienna, Vienna, Austria

Visualizing the early changes in osteoarthritis is still challenging the musculoskeletal imaging community. Especially structures of the osteochondral junction cannot be depicted by conventional MRI due to their thinness and short T2/T2* relaxation times. A variable echo time sequence in combination with high field 7T and a MR microscopy setup, allows microscopic resolution and echo times in the sub-millisecond range and can be used for visualizing short T2/T2* structures of the cartilage-bone interface such as calcified cartilage. In this study we focused on imaging early changes in osteoarthritis as approach for bringing biological information closer to clinic related applications.

1535

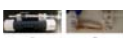

The effect of loading on T2* and MT ratio in tendons: A feasibility study

Saeed Jerban[1], Amin Nazaran[1], Michael Carl[2], Xin Cheng[1], Eric Y Chang[1,3], and Jiang Du[1]

[1]Radiology, University of California, San Diego, San Diego, CA, United States, [2]GE Healthcare, San Diego, CA, United States, [3]Radiology Service, VA San Diego Healthcare System, San Diego, CA, United States

UTE_MRI is assumed to be a great non-invasive technique to assess tendons as a unique viscoelastic tissue, with a very short T2. Early stage of tendon diseases, is hypothesized to affect the mechanical properties of tendon sooner and quicker than its morphology. This study, focused on the UTE-based T2* and MTR variations of the tendon samples under mechanical loading. Stretching the tendon samples with different loads using an MRI-compatible device resulted in significant reductions of T2* and increases in MTR. The MTR regional variations and shifts, obtainable by presented approach will help for assessing tendon quality and health level.

1536

The effect of loading on ultrashort echo time magnetization transfer (UTE-MT) imaging and modelling parameters in human articular cartilage: a feasibility study

Saeed Jerban[1], Ma Yajun[1], Michael Carl[2], Xin Cheng[1], Eric Y Chang[1,3], and Jiang Du[1]

[1]Radiology, University of California, San Diego, San Diego, CA, United States, [2]GE Healthcare, San Diego, CA, United States, [3]Radiology Service, VA San Diego Healthcare System, San Diego, CA, United States

UTE_MRI is assumed to be a great non-invasive technique to assess articular cartilage (AC) as a unique viscoelastic tissue, with a very short T2. Early stage of cartilage osteoarthrosis, is hypothesized to affect the mechanical properties of AC, sooner and quicker than its morphology. This study, focused on the application of the UTE_MT modelling and MT ratio variations in femorotibial AC in loaded knee. Compressing the cadaveric human intact knee with different loads, using an MRI-compatible device, resulted in significant increases macromolecule fraction. The local MTR maxima in the AC were interestingly shifted towards the contact point after loading.

1537

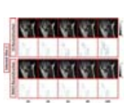

Accelerated Musculoskeletal MRI using Region of Interest Compressed Sensing

Amaresha Shridhar Konar[1,2], Nithin N Vajuvalli[1], Shivaprasad Chikop[1], and Sairam Geethanath[1]

[1]Medical Imaging Research Center, Dayananda Sagar Institutions, Bangalore, India, [2]Healthcare, Wipro GE Healthcare, Bangalore, India

MusculoSkeletal (MSK) MRI is used for analyzing injuries, and the knee injury is one of the common injuries reported in sports. Current work uses Compressed Sensing (CS) based reconstruction technique called Region Of Interest Compressed Sensing (ROICS). The proposed method has been demonstrated on five datasets at chosen acceleration factors. The reconstructed images are compared with the reference images using line intensity profile and NRMSE graph to demonstrate the utility of the proposed ROICS method on MSK MRI. The qualitative and quantitative result shows that ROICS performs better than CS. Current and future work involves the prospective implementation of ROICS on MSK MRI.

1538

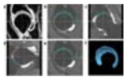

Algorithm for Semi-Automatic Segmentation of Hip Acetabular Cartilage Applied to Patients with Femoroacetabular Impingement

Casey P. Johnson[1], Joost Mulders[2], Douglas Martin[3], Patrick M. Morgan[4], and Jutta M. Ellermann[3]

[1]Center for Magnetic Resonance Research, University of Minnesota, Minneapolis, MN, United States, [2]Consultant, Costa Mesa, CA, United States, [3]Radiology, University of Minnesota, Minneapolis, MN, United States, [4]Orthopaedic Surgery, University of Minnesota, Minneapolis, MN, United States

A new algorithm to segment the acetabular cartilage based on a single 3D DESS data set is presented. This development was motivated by a need to simplify visualization of 3D quantitative maps of acetabular cartilage damage for surgical planning and arthroscopic correlation. A rapid segmentation algorithm is an important element of this framework, which will be used to guide reparative arthroscopic surgery of patients with femoroacetabular impingement.

1539

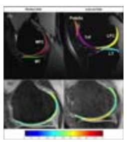

Comparison of T1ρ quantification, SNR, and reproducibility in 3D Magnetization-Prepared Angle-Modulated Partitioned k-space Spoiled Gradient Echo Snapshots (3D MAPSS) and 3D Fast Spin Echo (CubeQuant) techniques.

Matthew Tanaka[1], Valentina Pedoia[1], Dharshan Chandramohan[1], Weitian Chen[1], and Xiaojuan Li[1]

[1]University of California, San Francisco, San Francisco, CA, United States

Though T2 cartilage mapping has been shown to be sequence dependent, few studies have looked at the inter-sequence variation of cartilage T1ρ quantification. This study compares T1ρ quantification, SNR, and reproducibility of the MAPSS and CubeQuant T1ρ sequences. Four healthy controls received unilateral knee scans. Each patient was scanned twice and was removed from the scanner between scans. Significant differences were found in T1ρ quantification with comparable SNR and reproducibility. This study highlights the importance of using same sequences for quantitative cartilage imaging in multicenter studies.

1540

Comparative T2 and T1ρ Mapping of Patellofemoral Cartilage under in situ Mechanical Loading with Prospective Motion Correction

Thomas Lange[1], Benjamin R. Knowles[1], Michael Herbst[1,2], Kaywan Izadpanah[3], and Maxim Zaitsev[1]

[1]Department of Radiology, Medical Physics, Medical Center - University of Freiburg, Freiburg, Germany, [2]John A. Burns School of Medicine, University of Hawaii, Honolulu, HI, United States, [3]Department of Orthopedic and Trauma Surgery, Medical Center - University of Freiburg, Freiburg, Germany

Robust comparative T_2 and $T_{1\rho}$ mapping of patellofemoral cartilage under in situ loading is demonstrated with prospective motion correction and T_2 and $T_{1\rho}$ changes in response to loading are evaluated quantitatively, focusing on the load-bearing lateral patellar facet. T_2 and $T_{1\rho}$ mapping were performed with equal spatial resolution and field of view for different loading conditions (0/20/40 kg). While no significant T_2 differences for the three loading conditions were observed, $T_{1\rho}$ in superficial patellar cartilage was significantly reduced under loading. The quantitative findings suggest that $T_{1\rho}$ is a more reliable and sensitive marker for load-induced changes than T_2.

1541

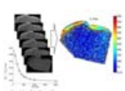

Correlation time mapping of articular cartilage degeneration in equine model

Abdul Wahed Kajabi[1,2], Mikko J. Nissi[3,4], Juuso Ketola[2], Jaakko K. Sarin[3], Victor Casula[1,2], Juha Töyräs[3,4], René Van Weeren[5], Harold Brommer[5], Jos Malda[5,6], Irina A.D. Mancini[5], Matti Hanni[1,2,7], and Miika T. Nieminen[1,2,7]

[1]Medical Research Center, University of Oulu and Oulu University Hospital, Oulu, Finland, [2]Research Unit of Medical Imaging, Physics and Technology, University of Oulu, Oulu, Finland, [3]Department of Applied Physics, University of Eastern Finland, Kuopio, Finland, [4]Diagnostic Imaging Center, Kuopio University Hospital, Kuopio, Finland, [5]Department of Equine Sciences, Utrecht University, Netherlands, [6]Department of Orthopaedics, University Medical Center Utrecht, Netherlands, [7]Department of Diagnostic Radiology, Oulu University Hospital, Oulu, Finland

Correlation time mapping was utilized to study structural alterations in articular cartilage of the femoral trochlea harvested from skeletally mature equines. Samples originated from a study in which surgically created lesions in the lateral trochlear ridge of the femur were filled with different materials and were left to heal for 12 months. Correlation time maps of the cartilage or repaired tissues were obtained from fitting $T_{1\rho}$ relaxation dispersion data. The correlation times of the repair tissue from the lesion site and tissue next to the lesion site were significantly shorter than the correlation times in a location distant from the lesion, indicating gradual degenerative changes observed in early osteoarthritis.

1542

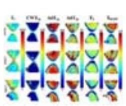

Multiparametric MRI assessment reveals early cartilage degeneration at 2 and 8 weeks after anterior cruciate ligament transection in a rabbit model

Victor C. Casula[1,2], Abdul Wahed Kajabi[1,2], Simo Ojanen[1,3], Mikko Finnilä[1,3], Rami Korhonen[3,4], Walter Herzog[5], Simo Saarakkala[1,2], Mikko J. Nissi[3,4], and Miika T. Nieminen[1,2,6]

[1]Research Unit of Medical Imaging, Physics and Technology, University of Oulu, Oulu, Finland, [2]Medical Research Center, University of Oulu and Oulu University Hospital, Oulu, Finland, [3]Department of Applied Physics, University of Eastern Finland, Kuopio, Finland, [4]Diagnostic Imaging Center, Kuopio University Hospital, Kuopio, Finland, [5]Human Performance Laboratory, Faculty of Kinesiology, University of Calgary, Calgary, AB, Canada, [6]Department of Diagnostic Radiology, Oulu University Hospital, Oulu, Finland

The sensitivity of several quantitative MRI parameters to early degenerative changes in articular cartilage was investigated in an experimentally induced anterior cruciate ligament transection (ACLT) rabbit model. Namely T_1, continuous wave $T_{1\rho}$ ($CWT_{1\rho}$), adiabatic $T_{1\rho}$ ($AdT_{1\rho}$) and $T_{2\rho}$ ($AdT_{2\rho}$), T_2 and T_{RAFF} (relaxation along a fictitious field) were measured at 9.4 T. All parameters showed significant elongation within two weeks of ACLT, except T_{RAFF}. Rotating frame parameters showed some evidence of superior sensitivity to cartilage alterations. A multiparametric approach may enhance the discrimination power of quantitative MRI for early cartilage degeneration.

1543

T2-mapping evaluation of talar cartilage for chronic lateral ankle instability (LAI) with isolated anterior talofibular ligament (ATFL) tear, and combined ATFL and calcaneofibular ligament (CFL) tear

Hongyue Tao[1], Yang Qiao[1], Yiwen Hu[1], Xu Yan[2], Kui Ma[3], Yinghui Hua[3], and Shuang Chen[1]

[1]Department of Radiology, Fudan University Affiliated Huashan Hospital, Shanghai, People's Republic of China, [2]MR Collaboration NE Asia, Siemens Healthcare, Shanghai, People's Republic of China, [3]Department of Sports Medicine, Fudan University Affiliated Huashan Hospital, Shanghai, People's Republic of China

The study aimed to use T2-mapping to quantitatively evaluate talus cartilage for chronic lateral ankle instability (LAI) with isolated anterior talofibular ligament (ATFL) tear, and combined ATFL and calcaneofibular ligament (CFL) tear. Seventeen patients with ATFL tear, 10 with ATFL+CFL tear, and 21 healthy subjects were recruited. All participants underwent T2-mapping scan, and patients completed American-Orthopedic-Foot-and-Ankle-Society (AOFAS) scoring. The results indicated that chronic LAI with ATFL+ CFL tear may result in much larger and more severe cartilage degeneration than isolated ATFL tear, and medial anterior of talus could be the main cartilage compartment affecting patients' clinical symptom and prognosis.

1544

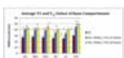

T1ρ acquired at higher Spin Lock Frequency and Composite R2 - R1ρ are better predictors of Patient-Reported Outcome in Osteoarthritis

Taylor Jan Leong[1], Valentina Pedoia[1], Colin Russell[1], and Sharmila Majumdar[1]

[1]Radiology and Biomedical Imaging, UCSF, San Francisco, CA, United States

Synopsis: The agreement and associations of T1ρ values with different spin lock frequencies were evaluated for the detection of radiographic knee OA and association with patient-reported outcomes. Analyses were performed in vivo at 3T MRI. Significant differences were identified between FSL 500 Hz, 3 TSL and T2 in all knee compartments and between FSL 700 Hz, 3 TSL and FSL 500 Hz, 3 TSL. While similar behavior was observed in distinguishing radiographic OA, T1ρ computed at higher FLS (700 Hz) and R2-R1ρ 700Hz demonstrated a better association with patient-reported outcomes.

1545

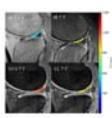

Knee dGEMRIC at 7 T: Validation against 1.5 T and comparison of T1 mapping methods

Pernilla Peterson[1], Emma Olsson[1], Lars E. Olsson[1], Carl Johan Tiderius[2], and Jonas Svensson[3]

[1]Dept. of Translational Medicine, Lund University, Malmö, Sweden, [2]Dept. of Orthopedics, Skåne University Hospital, Lund, Sweden, [3]Dept. of Medical Imaging and Physiology, Skåne University Hospital, Lund, Sweden

dGEMRIC (delayed Gadolinium Enhanced Magnetic Resonance Imaging of Cartilage) is a well-established technique for cartilage quality assessment in osteoarthritis at 1.5 T. The aim of this study was to establish dGEMRIC at 7 T by validation against 1.5 T and comparison of three T1 mapping methods: inversion recovery, variable flip angle and look locker. Both healthy volunteers and patients with early signs of osteoarthritis were scanned at both field strengths postcontrast. We conclude that dGEMRIC is feasible at 7 T and that inversion recovery is the preferred T1 mapping approach at 7 T.

1546

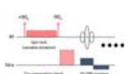

T1ρ assessment of cartilage in a large animal model of traumatic joint injury

Daniel Thedens[1], David Heckelsmiller[2], Barbara Laughlin[2], Mothana Saad Eldine[2], Douglas Pedersen[2], Douglas Fredericks[2], and Jessica Goetz[2]

[1]Radiology, University of Iowa, Iowa City, IA, United States, [2]Orthopedics & Rehabilitation, University of Iowa, Iowa City, IA, United States

MRI offers the opportunity for early characterization of cartilage in injured joints with emerging contrast mechanisms such as T1ρ. The purpose of this work was to investigate the ability of T1ρ to detect early cartilage changes in a large animal (goat) model of PTOA. T1ρ imaging of injured joints showed increased relaxation times six months after injury compared to uninjured contralateral joints in five animals. T1ρ may help better elucidate the time course and mechanisms of cartilage degeneration in PTOA.

1547

Biomechanical T2-mapping in osteoarthritis with 3D-TESS at 7T MRI

Sebastian Roehrich[1], Pavol Szomolanyi[1], Markus Schreiner[2], Vladimir Juras[1], Rahel Heule[3], Oliver Bieri[3], and Siegfried Trattnig[1,4]

[1]Department of Biomedical Imaging and Image-guided Therapy, High Field MR Centre, Medical University of Vienna, Vienna, Austria, [2]Department of Orthopedic Surgery, Medical University of Vienna, Vienna, Austria, [3]Department of Radiology, Division of Radiological Physics, University of Basel Hospital, Basel, Switzerland, [4]Christian Doppler Laboratory for Clinical Molecular MR Imaging, Vienna, Austria

Biochemical MRI of hyaline cartilage shows promising results for the evaluation of OA. In this study we implemented in-vivo compression and a fast 3D-TESS sequence at 7T for cartilage transversal relaxation time (T2)-mapping of healthy volunteers and patients with risk factors for the development of early osteoarthritis of the knee (OA). Results show a location-dependent and differing behavior of T2-values under compression between the two groups, further increasing the value of T2-values as possible biomarker for OA.

1548

T2 -mapping and dGEMRIC of the patellar cartilage - long term follow-up after patellar stabilizing surgery in childhood

Eva Bengtsson Moström[1], Eveliina Lammentausta[2], Thröstur Finnbogason[3], Lars Weidenhielm[4,5], Per-Mats Janarv[1,5], and Carl Johan Tiderius[6]

[1]Department of Women´s and Children´s Health, Karolinska Institutet, Stockholm, Sweden, [2]Department of Diagnostic Radiology, Oulu University Hospital, Finland, [3]Department of Paediatric Radiology, Karolinska University Hospital, Sweden, [4]Department of Molecular Medicine and Surgery, Karolinska Institutet, Sweden, [5]Stockholm Sports Trauma Research Center, Karolinska Institutet, Sweden, [6]Department of Orthopedics, Lund University, Sweden

Recurrent patellar dislocation in childhood often require surgical stabilization, but the effects on cartilage quality after surgery is unknown. 17 patients were examined with T2 and dGEMRIC ≥5 years after surgery. dGEMRIC was shorter centrally, whereas T2 was longer most medially in the patellar cartilage of the operated patella ($p<0.05$). The short dGEMRIC indicates loss of glycosaminoglycans in the patella of the operated knee. Longer T2 may be an early sign of joint pathology. These findings may indicate an imbalance in the synthesis of matrix molecules, a sign of early cartilage degeneration.

1549

Cartilage T2 Relaxation Times in Both Knees of Healthy Individuals

James Yoder[1,2], Uchechukwuka Monu[2,3], and Garry E Gold[2,4]

[1]Human Biology, Stanford University, Stanford, CA, United States, [2]Radiology, Stanford University, Stanford, CA, United States, [3]Electrical Engineering, Stanford University, Stanford, CA, United States, [4]Bioengineering, Stanford University, Stanford, CA, United States

The ACL-injured population is predisposed to developing radiographic Osteoarthritis post injury. Quantitative biomarkers such as T2 relaxation times evaluate the macromolecular composition of the cartilage matrix. Assessing the variation in this quantitative measure between knees of healthy individuals can help us identify degenerative difference brought on by injury. Using projection maps and pre-defined compartments, we measured the T2 relaxation times and quantified intrinsic differences between the knees of a group of healthy volunteers using coefficient of variation. This study demonstrates that there are similar T2 relaxation times for the left and right knees of healthy individuals.

1550

A prospective natural history study on cartilage composition changes in patients with low-grade cartilage injury

Didier Laurent[1], Vladimir Juras[2], Vladimir Mlynarik[2], Markus Schreiner[2], Pavol Szomolanyi[2], Stefan Zbyn[2,3], Celeste Scotti[1], Joerg Goldhahn[4], Harry Haber[1], Ewa Kubiak[1], Ronenn Roubenoff[1], Stefan Marlovits[5], and Siegfried Trattnig[2]

[1]Translational Medicine, Novartis Institutes for Biomedical Research, Basel, Switzerland, [2]Biomedical Imaging and Image-guided therapy, Medical University of Vienna, Vienna, Austria, [3]Research Unit of Medical Imaging, Physics and Technology, University of Oulu, Oulu, Finland, [4]Institutes for Biomechanics, ETH, Zurich, Switzerland, [5]Traumatology, Medical University of Vienna, Vienna, Austria

Changes in the macromolecular structure of articular cartilage were monitored in patients with a low-grade cartilage defect by using a comprehensive, compositional MRI approach over a period of 6 months. Preliminary results showed that, while no large change in glycosaminoglycan contents was observed, the bi-layer structure bound to the collagen fiber organization may have been further deteriorated over time.

1551

The Effect of Fat Saturation on Calculated T2 and T2* Relaxation Times in Articular Cartilage

Mary E Hall[1], Feliks Kogan[2], and Garry Gold[2]

[1]Mechanical Engineering, Stanford University, Stanford, CA, United States, [2]Radiology, Stanford University, CA, United States

This study aimed at identifying differences in T2 and T2* relaxation times in knee cartilage with and without the use of fat suppression. Four volunteers were scanned with 3D cones, 2D multi-echo FSE, and qDESS sequences with and without fat sat. For cones and qDESS, T2* and T2 values increased with use of fat sat. For 2D FSE, values did not change. The results show that use of fat sat can have an effect on quantitative MRI parameters.

1552

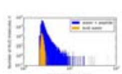

Simulated reorientational correlation times of collagen-associated water

Jouni Karjalainen[1], Matti Hanni[1,2,3], Mikko J. Nissi[4,5], and Miika T. Nieminen[1,2,3]

[1]Research Unit of Medical Imaging, Physics and Technology, University of Oulu, Oulu, Finland, [2]Medical Research Center, University of Oulu and Oulu University Hospital, Oulu, Finland, [3]Department of Diagnostic Radiology, Oulu University Hospital, Oulu, Finland, [4]Department of Applied Physics, University of Eastern Finland, Kuopio, Finland, [5]Diagnostic Imaging Center, Kuopio University Hospital, Kuopio, Finland

Correlation times of molecular motions are fundamentally related to magnetic relaxation. We use molecular dynamics simulations to compute the reorientational correlation times of water molecules associated with a model collagen molecule. Our aim is to provide a reference independent of measurements of correlation times of water in articular cartilage. The results suggest that although the reorientation slows down close to the protein surface, the diffusion between the different water pools appears to render the average correlation times short as compared to a water molecule trapped close to the macromolecule.

1553

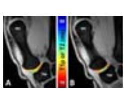

T1ρ and T2 of Articular Cartilage in the Thumb Carpometacarpal Joint

Matthew F. Koff[1], Parina H. Shah[1], Ryan E. Breighner[1], Darryl B. Sneag[1], Ogonna Nwawka[1], and Hollis G. Potter[1]

[1]Department of Radiology and Imaging, Hospital for Special Surgery, New York, NY, United States

Radiography is commonly used to evaluate osteoarthritis at the thumb carpometacarpal (CMC) joint, but newer quantitative magnetic resonance imaging (MRI) techniques provide additional information regarding biochemical composition of trapezial (TM) and 1st metacarpal (MC) articular cartilage. Morphologic MRI and quantitative T1ρ and T2 mapping of the thumb CMC joint was performed. T1ρ and T2 values of the TM and MC were similar, and full ligamentous tears were not found. This pilot study showed that quantitative T1ρ and T2 mapping is feasible at the human thumb CMC joint.

1554

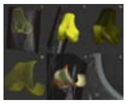

3D modeling of cartilage surfaces at the knee using clinical magnetic resonance imaging data

James MacKay[1], Josh Kaggie[1], Tom Turmezei[2,3], Graham Treece[3], Martin Graves[1], Andrew McCaskie[4], and Fiona Gilbert[1]

[1]Radiology, University of Cambridge, Cambridge, United Kingdom, [2]Radiology, Royal National Orthopaedic Hospital, Stanmore, United Kingdom, [3]Engineering, University of Cambridge, Cambridge, United Kingdom, [4]Division of Trauma & Orthopaedic Surgery, University of Cambridge, Cambridge, United Kingdom

We present a surface-based method for analyzing articular cartilage at the knee using clinical MRI data. This method offers several advantages over existing approaches, including the ability to visualize the spatial distribution of cartilage thickness and compositional parameters, and perform surface-based comparisons between individuals and within individuals over time using statistical parametric mapping. We outline the steps involved in the analysis pipeline and describe initial results in 5 human cadavers and 2 human subjects in vivo, demonstrating the promise of this technique.

1555

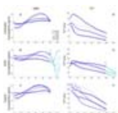

Quantitative susceptibility mapping of articular cartilage at different orientations to investigate susceptibility anisotropy

Olli Juhani Nykänen[1], Juha Töyräs[1,2], Ville Kolehmainen[1], Lassi Rieppo[3], Simo Saarakkala[3], Karin Shmueli[4], and Mikko Johannes Nissi[1,2]

[1]Department of Applied Physics, University of Eastern Finland, Kuopio, Finland, [2]Diagnostic Imaging Center, Kuopio University Hospital, Kuopio, Finland, [3]Research Unit of Medical Imaging, Physics and Technology, University of Oulu, [4]Department of Medical Physics & Biomedical Engineering, University College London

In this study we examined ex-vivo bovine articular cartilage using quantitative susceptibility mapping (QSM). Our purpose was to find a reliable QSM measurement and estimation protocol and then study how different enzymatic and chemical degradations affect the susceptibility of articular cartilage, in order to establish the feasibility of QSM for the assessment of articular cartilage. Treatments by trypsin (to degrade proteoglycans) and EDTA (to remove calcifications) were found to have minimal effects on the susceptibility. However, a significant depth-wise anisotropy of susceptibility in cartilage was observed. Further studies are warranted to investigate the susceptibility changes in cartilage.

1556

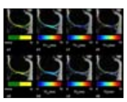

In Vivo Multicomponent T1ρ and T2 Relaxation Mapping of Human Knee Cartilage

Azadeh Sharafi[1], Ding Xia[1], Gregory Chang [1], and Ravinder Regatte[1]

[1]Radiology, New York University, School of Medicine, New York, NY, United States

In this study, we demonstrated the feasibility of in-vivo biexponential T1ρ and T2 relaxation measurement of knee articular cartilage using 3T MRI in clinically feasible scan times in eight healthy volunteers. Our preliminary results demonstrate that the biexponential model better represents the relaxation behavior in articular cartilage and can be used to distinguish different water compartments associated with macromolecules (tightly bound and loosely bound water) in the cartilage.

1557

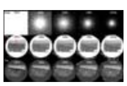

Compressed Sensing Microscopic MRI in Articular Cartilage at 7T: Quantitative Determination of GAG Concentration using dGEMRIC Method

Nian Wang[1], Farid Badar[2], and Yang Xia[2]

[1]Center for In Vivo Microscopy, Department of Radiology, Duke University, Durham, NC, United States, [2]Physics and Center for Biomedical Research, Oakland University, Rochester, MI, United States

To evaluate the compressed sensing feasibility of quantification GAG concentration using dGEMRIC method, high resolution T1 mapping of articular cartilage was accelerated using various acceleration factors. It demonstrates that using CS doesn't introduce major deviations in quantification of GAG concentration even with acceleration factor of 16, which holds great promise in making quantitative imaging techniques more accessible for clinical applications.

1558

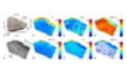

Quantitative multiparametric relaxation time mapping of experimental model of osteoarthritis in the equine

Mikko Johannes Nissi[1,2], Abdul Wahed Kajabi[3], Juuso Ketola[3], Jaakko K Sarin[1], Victor Casula[3,4], Irina A. D. Mancini[5], Harold Brommer[5], René P van Weeren[5], Jos Malda[5,6], Juha Töyräs[1], and Miika T Nieminen[3,4,7]

[1]Department of Applied Physics, University of Eastern Finland, Kuopio, Finland, [2]Department of Diagnostic Radiology, Kuopio University Hospital, Kuopio, Finland, [3]Research Unit of Medical Imaging, Physics and Technology, University of Oulu, Oulu, Finland, [4]Medical Research Center Oulu, Oulu University Hospital and University of Oulu, Oulu, Finland, [5]Department of Equine Sciences, Faculty of Veterinary Medicine, Utrecht University, Utrecht, Netherlands, [6]Department of Orthopaedics, University Medical Center Utrecht, Utrecht, Netherlands, [7]Department of Diagnostic Radiology, Oulu University Hospital, Oulu, Finland

In this study, sensitivity of several quantitative MRI (qMRI) parameters, namely T_1, T_2, continuous wave (CW) $T_{1\rho}$, adiabatic $T_{1\rho}$, adiabatic $T_{2\rho}$ and T_{RAFF} were investigated for their sensitivity to secondary degenerative changes in equine articular cartilage specimens (n=13+6 lesions and controls, respectively) due to presence of surgically induced lesions in the adjacent tissue. Significant differences in relaxation times between ROIs in the secondary affected, lesion repair tissue and adjacent controls area or control animals were detected. The findings suggest that properties of cartilage are altered due to the presence of a lesion in adjacent tissue.

1559

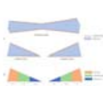

Zonal differences of T1rho and T2 relaxation times of the meniscus: comparison study between normal and osteoarthritis knees

Shigeo Hagiwara[1], Shoichiro Takao[1], Hon Yu[1], Yasuhito Kaneko[1], Taiki Nozaki[1], Ran Schwarzkopf[2], and Hiroshi Yoshioka[1]

[1]Radiological Sciences, University of California Irvine, Orange, CA, United States, [2]Orthopaedic Surgery, University of California Irvine, Orange, CA, United States

We compared the zonal differences of T1rho and T2 relaxation times of the meniscus in normal and osteoarthritis knees. Our study indicates that T1rho and T2 relaxation times in degenerative meniscus decrease and demonstrate more homogenous values throughout the meniscus.

1560

A Comparison of T2 Measurement Changes on MRI and Clinical Correlation in a Pilot Randomised Controlled Trial Comparing Meniscal Allograft Transplantation to Physiotherapy

Nick Smith[1], Charles Edward Hutchinson[2], Victoria Sherwood[3], David Wright[4], Peter Thompson[5], Andy Metcalfe[6], Matthew Costa[7], and Tim Spalding[5]

[1]Orthopaedics, University Hospital Coventry and Warwickshire, Coventry, United Kingdom, [2]Health Sciences, University of Warwick, Coventry, United Kingdom, [3]Medical Physics, University Hospital Coventry and Warwickshire, [4]University Hospital Coventry and Warwickshire, [5]Orthopaedics, University Hospital Coventry and Warwickshire, [6]Health Sciences, University of Warwick, [7]Orthopaedics, University of Oxford

This pilot study shows the T2 changes that occur within cartilage in patients with meniscal transplantation. A full trial to prove whether meniscal allograph translation is justied

---

1561

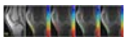

Regionally Dependent T2* Values of the Patellar Tendon in Collegiate Basketball Players

Erin C. Argentieri[1], Parina H. Shah[1], Ogonna K. Nwawka[1], and Matthew F. Koff[1]

[1]Deparment of Radiology and Imaging - MRI, Hospital for Special Surgery, New York, NY, United States

Patellar tendinosis is a significant debilitation in collegiate and professional athletes that frequently leads to reduced performance. The quantitative magnetic resonance imaging (MRI) technique of T2* mapping is well suited to evaluate patellar tendinosis. This study evaluated regional differences of T2* values in collegiate basketball players pre-season. Short and long T2* values were both prolonged proximally, and no correlations were found with corresponding morphologic imaging. Continued longitudinal imaging will permit the evaluation of the development of tendinosis or micro-tears.

1562

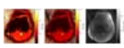

Spiral Fingerprinting of Articular Knee Cartilage and Bone

Joshua Kaggie[1], Guido Buonincontri[2], Michela Tosetti[2], James MacKay[3], Rolf F Schulte[4], Ferdia A Gallagher[3], and Martin J Graves[3]

[1]Radiology, University of Cambridge, Cambridge, United Kingdom, [2]IMAGO7 Research Center and IRCCS Stella Maris, Pisa, Italy, [3]Radiology, University of Cambridge, [4]GE Global Research, Munich, Germany

Magnetic resonance fingerprinting (MRF) seeks to acquire MRI parameter maps at shorter overall scan duration than achievable through separate image acquisitions. This work demonstrates multi-slice MRF at 3T for T1, T2, and proton-density mapping of a healthy human knee at a high in-plane spatial resolution (0.7x0.7mm^{2}) with an eight-channel transmit/receive coil at 3T. The spiral trajectories enabled quantification of tissues with ultrashort echo-times, such as trabecular bone.

Traditional Poster

Muscle & Bone

Exhibition Hall 1563-1596 Monday 16:15 - 18:15

1563

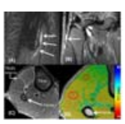

Quantitative Evaluation of T2 Signal Intensity for the Assessment of Muscle Denervation

Parina H. Shah[1], Erin C. Argentieri[1], Matthew F. Koff[1], and Darryl B. Sneag[1]

[1]Radiology and Imaging, Hospital for Special Surgery, New York, NY, United States

Presence and severity of muscle denervation due to peripheral neuropathy are conventionally evaluated using needle electromyography (EMG); the results of which are critical in the diagnosis of nerve injury and prognosticating nerve recovery. Routine MRI can confirm the presence of denervation but is unable to quantify severity and relies on qualitative detection of diffuse T2-weighted signal hyperintensity of the muscle and fatty infiltration (if chronic). This pilot study explores the role of T2 mapping in the diagnosis denervation and for quantification of severity. T2 mapping may be an important complement to EMG results, particularly given the drawbacks associated with EMG.

1564

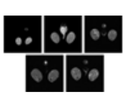

Noninvasive MRI Biomarkers for Muscular Dystrophy Progression in Young Muscle

Joshua S Park[1], Ravneet Vohra[1], Thomas Klussmann[1,2], Niclas Bengtsson[3,4], Jeffrey Chamberlain[2,3,4,5], and Donghoon Lee[1]

[1]Radiology, University of Washington, Seattle, WA, United States, [2]Biochemistry, University of Washington, Seattle, WA, United States, [3]Neurology, University of Washington, Seattle, WA, United States, [4]Senator Paul D. Wellstone Muscular Dystrophy Cooperative Research Center, University of Washington, Seattle, WA, United States, [5]Medicine, University of Washington, Seattle, WA, United States

Muscular dystrophy is a family of inherited diseases characterized by progressive muscle weakness that leads to muscle damage and wasting, and in the case of Duchenne muscular dystrophy (DMD), is fatal. Clinical measures of muscular dystrophy rely on surgical biopsy, which is invasive and provides a limited overview of the disease's progression. Magnetic resonance imaging (MRI) may provide valuable information pertaining to tissue characteristics of this disease. We performed multi-parametric MRI to assess the changes in young dystrophic mice. The changes observed in skeletal muscles demonstrate MRI parameters may be used to track disease progression and future treatment options.

1565 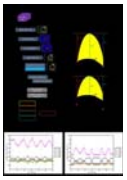

Semi-automated analysis of diaphragmatic motion with cine MRI in controls and non-ambulant Duchenne Muscular Dystrophy (DMD) patients

Courtney Bishop[1], Rexford Newbould[1], Valeria Ricotti[2], Christopher Sinclair[3], Jordan Butler[3], RB Matt Evans[3], Jasper Morrow[3], Mike Hanna[3], Paul M Matthews[4], Tarek Yousry[3], John Thornton[3], Francesco Muntoni[3], and Robert Janiczek[5]

[1]Imanova, London, United Kingdom, [2]UCL, Institute of Child Health, London, United Kingdom, [3]University College London, [4]Imperial College London, United Kingdom, [5]GlaxoSmithKline, Brentford, United Kingdom

This study presents both an analysis pipeline for measuring diaphragmatic motion from cine MRI data, and the application of this image processing technique to investigate exploratory MRI endpoints of respiratory function in both healthy controls and non-ambulant DMD boys. Cine-derived metrics of diaphragm motility and contractility correlated with sitting spirometry-derived forced vital capacity, and showed relationships with disease progression surrogates of age and months non-ambulatory, as well as a longitudinal change over 12 months. Longitudinal changes were not seen in spirometry measures.

1566 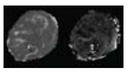

Potential of Stimulated Echo Diffusion-weighted Imaging as Disease Marker in Duchenne Muscular Dystrophy

Bauke Kogelman[1], Maaike van Putten[2], Matt Hall[3], Chris Clark[3], Andrew Blamire[4], Paola Porcari[4], and Louise van der Weerd[1,2]

[1]Radiology, LUMC, Leiden, Netherlands, [2]Human Genetics, LUMC, Leiden, Netherlands, [3]Institute of Child Health, University College London, London, United Kingdom, [4]Newcastle Magnetic Resonance Centre, Newcastle University, Newcastle, United Kingdom

We used stimulated echo diffusion weighted imaging (STE-DWI) in a mouse model of Duchenne muscular dystrophy (*mdx*). From the data in *mdx* or wild type animals we observe that although muscle fibre size is smaller in the mdx mouse, the diffusion data show increased diffusibility – opposite to the hypothesised effect if fibre size is the main determinant of restricted water diffusion. Muscle fibre permeability is significantly greater in the mdx mouse, suggesting that the overall system permeability has a countering effect on diffusion restriction. Additional modelling is required to capture these two opposing effects.

1567 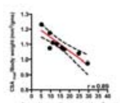

Magnetic resonance biomarkers for cachexia in a mouse model of pancreatic ductal adenocarcinoma.

Ravneet S Vohra[1], Matthew Campbell[1], Joshua Park[1], Kayla Gravelle[2], Stella wHang[2], Yak-Nam Wang[2], Joo-Ha Hwang[3], David Marcinek[1], and Donghoon Lee[1]

[1]Department of Radiology, University of Washington, Seattle, WA, United States, [2]Center for Industrial and Medical Ultrasound Applied Physics Laboratory, University of Washington, Seattle, WA, United States, [3]Department of Medicine, University of Washington, Seattle, WA, United States

Cancer induced cachexia is prevalent with many cancers and is characterized by loss of muscle and fat mass. In pancreatic cancer the syndrome affects approximately 80% of patients. Non-invasive multi-parametric MRI was used to monitor the progression of cachexia in a genetically engineered mouse model of pancreatic ductal adenocarcinoma (PDAC). Using pixel-by-pixel comparison, we demonstrate a significant decrease in skeletal muscle T_2 and increase in magnetization transfer ratio (MTR). Additionally, we found significant difference in diffusion parameters.

1568 

Fast delineation of calf muscles for quantitative MRI applications

Pierre-Yves Baudin[1], Morin Beyeler[2], Pierre G Carlier[3,4], and Olivier Scheidegger[2,3]

[1]Consultants for Research in Imaging and Spectroscopy, Tournai, Belgium, [2]Support Center for Advanced Neuroimaging, Institute for Diagnostic and Interventional Neuroradiology, Inselspital, Bern University Hospital, University of Bern, Switzerland, [3]NMR Laboratory, Institute of Myology, Paris, France, [4]CEA, DRF, I²BM, MIRCen, NMR Laboratory, Paris, France

One typical obstacle in quantitative MRI lies in the delineation of the regions of interest. When not absolutely necessary, per-muscle analyses are often abandoned, resulting in the loss of a wealth information. A software dedicated to accelerated segmentation of muscle images was recently introduced. It was tested here on the calf muscles of healthy volunteers and Duchenne patients. Results showed an important gain in average speed and were close to the manual segmentation used as reference. Thus, the tested software proved to be a valuable tool for quantitative analysis of skeletal muscle NMR images.

1569 

Influence of muscle fiber tension on 31P MRS recovery parameter after intense exercise

Kevin Moll[1], Alexander Gussew[1], and Jürgen R. Reichenbach[1]

[1]Medical Physics Group, Institute of Diagnostic and Interventional Radiology, Jena University Hospital - Friedrich Schiller University Jena, Jena, Germany

When performing exercise induced 31P MRS motion and activities from the everyday life and the positioning of the investigated extremities within the MR scanner should be considered, since this could induce partial ischemia effects like muscular cramps. The aim of this study was to prove the effect of muscle tension on metabolic parameter measured by 31P MRS after an intense exercise. PCr recovery as well as pH kinetic was significantly slowed by a partial ischemia preventing a quantitative evaluation.

1570 

Multi-parametric characterization of highly fat infiltrated muscular dystrophy patients: results of a multi-variate analysis.

Alberto De Luca[1,2], Alessandra Bertoldo[1], Denis Peruzzo[2], Maria Grazia D'Angelo[3], Martijn Froeling[4], and Filippo Arrigoni[2]

[1]Department of Information Engineering, University of Padova, Padova, Italy, [2]Neuroimaging Lab, Scientific Institute IRCCS Eugenio Medea, Bosisio Parini (LC), Italy, [3]Functional Rehabilitation Unit, Neuromuscular Disorders, Scientific Institute IRCCS Eugenio Medea, Bosisio Parini (LC), Italy, [4]Radiology Department, University Medical Center Utrecht, Utrecht, Netherlands

Limb Girdle Muscular Dystrophies (LGMD) are a family of myopathies characterized by progressive degeneration and fat infiltration of muscular tissue. In the context of a study that includes Dixon, T_2 quantification and diffusion MRI (dMRI), we investigated a multi-variate analysis to remove the effect of fat from concurrent measures and correlate them with clinical indexes of strength. In our dataset of highly infiltrated patients, T_2 and dMRI metrics were strongly biased by fat. Our results show that it is possible to mitigate the bias by multi-variate modeling of the FF effect while retaining disease specific effects.

1571 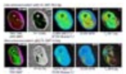

Changes in muscle morphometry, composition and performance in patients with sporadic inclusion body myositis

Didier Laurent[1], Jonathan Riek[2], Christopher DJ Sinclair[3], John S. Thornton[3], Ronenn Roubenoff[1], Dimitris A. Papanicolaou[4], Parul Houston[5], Tarek Yousry[3], Pedro M. Machado[3], and Michael G. Hanna[3]

[1]Novartis Institutes for Biomedical Research, Basel, Switzerland, [2]VirtualScopics, LLC, Rochester, NY, United States, [3]MRC Centre for Neuromuscular Diseases, UCL Institute of Neurology, London, United Kingdom, [4]Novartis Pharmaceuticals Corporation, East Hanover, NJ, United States, [5]Novartis Pharma AG, Basel, Switzerland

A comprehensive MRI approach was used to characterize changes in muscle structure and composition in patients with sporadic inclusion body myositis (sIBM) over 1-year. Results showed progressive deterioration in muscle quality, e.g. increased connective tissue volume in the most affected muscles, and this appeared to be associated with a functional impact.

1572 

Correlating MRI and Histological Parameters in GRMD Muscles: A Comparison Between 3T and 4.7T Acquisitions

Aydin Eresen[1], Stephen McConnell[1], Sharla Birch[2], Wade Friedeck[3], Jay Griffin[4], Joe Kornegay[5], and Jim Ji[1]

[1]Department of Electrical and Computer Engineering, Texas A&M University, College Station, TX, United States, [2]Department of Veterinary Pathobiology, Texas A&M University, College Station, TX, United States, [3]Small Animal Imaging and Radiology, Texas A&M University, College Station, TX, United States, [4]Department of Large Animal Clinical Sciences, Texas A&M University, College Station, TX, United States, [5]Department of Veterinary Integrative Biosciences, Texas A&M University, College Station, TX, United States

The relationship between localized histological truth and various MRI quantitative measures were investigated using canine models. In this study, GRMD pectineus muscle samples were imaged on a 3T clinical scanner and a 4.7T small-bore scanner. Trichrome stained histology slice was registered to the 3D MRI volume. Localized quantitative MRI parameters are correlated with histology analysis (muscle, fibrosis and interstitial tissue percentage). Parameters derived from the 4.7T MRI data show consistent correlations, while those from 3T MRI data do not show consistent correlation.

1573 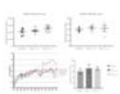

Targeted modulation of retinoid signaling using polymeric nanoparticles in a mouse model of Amyotrophic Lateral Sclerosis

David Medina[1], Eugene Chung[1], Ricki Ceton[1], Robert Bowser[1], Rachael Sirianni[1], and Gregory Turner[2]

[1]Neurobiology, Barrow Neurological Institute, Phoenix, AZ, United States, [2]Research Imaging, Barrow Neurological Institute, Phoenix, AZ, United States

Retinoid signaling activity in the CNS, mediated by RARβ, directly influences ALS pathology development and progression in vivo and CNS targeted delivery of RARβ agonists can reduce ALS pathology in vivo when delivered systemically via polymeric nanoparticles. In this study the therapeutic affect of adapalene, a RARβ agonist, loaded nanoparticles were examined by measuring quadriceps volume in a SOD1^{G93A} mouse model of ALS.

1574 

Multicomponent 3D-T1ρ and T2 Relaxation Mapping of Skeletal Muscle: In-vivo Feasibility

Azadeh Sharafi[1], Gregory Chang [1], and Ravinder Regatte[1]

[1]Radiology, New York University, School of Medicine, New York, NY, United States

In this study, we investigated the in-vivo feasibility of multicomponent 3D-T1ρ and T2 relaxation mapping in calf muscle using 3T MRI in clinically feasible scan times on eight healthy volunteers. Our preliminary results demonstrate that the biexponential model better characterized the relaxation behavior in calf muscle and can be used to differentiate between different water compartments associated with macromolecules (collagen and contractile proteins) and extracellular/vascular water in calf muscle.

1575 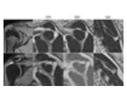

Fat fraction and muscular volume of entire supraspinatus muscle with/without tendon tear using IDEAL-IQ sequence

Taiki Nozaki[1], Yasuyo Teramura[1], Takeshi Hara[2], Saya Horiuchi[1], Atsushi Tasaki[3], Yasuyuki Kurihara[1], and Hiroshi Yoshioka[4]

[1]Radiology, St.Luke's International Hospital, Tokyo, Japan, [2]Department of Intelligent Image Information, Gifu University, [3]St.Luke's International Hospital, [4]Radiology, University of California, Irvine

Muscular atrophy and fatty degeneration of the supraspinatus muscle occurs after rotator cuff tear. It is often necessary to evaluate for these muscle abnormalities following tears to determine surgical candidacy. We usually evaluate this on a single slice. However, it is not well known whether this slice is representative of fatty degeneration and muscular atrophy overall. Furthermore, it is also not known how fatty degeneration and muscular atrophy will progress after tear. The purpose of this study was to make a standardized fat fraction and muscular volume model in patients with or without supraspinatus tendon tear using IDEAL-IQ sequence.

1576 

Perturbed muscle mitochondrial function in Sarcopenia

Jamie XM Ho[1], Stacey KH Tay[2], Subhasis Banerji [3], and Mary C Stephenson[4]

[1]A*STAR-NUS Clinical Imaging Research Centre, Singapore, Singapore, [2]Division of Paediatric Genetics and Metabolism, National University Hospital, [3]National University of Singapore, [4]A*STAR-NUS Clinical Imaging Research Centre

In this study we use 31P MRS in combination with Near Infra-red Spectroscopy to assess muscle mitochondrial function and changes in oxygenation in patients with Sarcopenia as to date, the etiology and molecular mechanisms of sarcopenia remain poorly understood. 10 males diagnosed with sarcopenia and 10 healthy controls were scanned where 31P MRS: A fully relaxed 31P MR spectrum data and exercise paradigm were acquired. MVC were significantly different between the sarcopenic and healthy groups (p=0.0044). Despite this, there was a tendency for increased ATP turnover in patients compared with healthy controls (44% and 66% MVC (ATP turnover p= 0.5642 44%MVC, p= 0.6128 66%MVC). Patients with sarcopenia showed significantly higher oxidative ATP synthesis ATP at 66%MVC where p= 0.0477. These results indicate that at least some of this increased requirement can be met oxidatively, with no contribution from breakdown of PCr at the end of exercise.

1577

Disease progression in skeletal muscles of Myotonic Dystrophy Type 1 evaluated using quantitative MRI

Linda Heskamp[1], Marlies van Nimwegen[2], Guillaume Bassez[3], Marieke Ploegmakers[1], Jean-Francois Deux[3], Baziel van Engelen[2], and Arend Heerschap[1]

[1]Radiology and Nuclear Medicine, Radboud university medical center, Nijmegen, Netherlands, [2]Neurology, Radboud university medical center, Nijmegen, Netherlands, [3]Neuromuscular Reference Center, Henri Mondor university hospital, Paris, France

We studied the occurrence and progression of fatty infiltration, atrophy and edema-like processes in calf and thigh muscles of Myotonic Dystrophy Type 1 (DM1) patients. Fat fraction (FF) and muscle volume (MV) were obtained by a DIXON-sequence and T2 of muscle water ($T2_{water}$) was calculated by a bi-component extended-phase-graph model. Calf and thigh muscles show fatty infiltration and increased $T2_{water}$ in non-fat infiltrated and fat infiltrated muscles. Atrophy is observed in four calf muscles and one thigh muscles. FF significantly increases in 10 months in fat infiltrated and non-fat infiltrated muscles, but MV only decreases in fat infiltrated thigh muscles.

1578

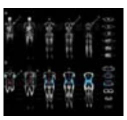

Body Composition Analysis Combined with Individual Muscle Measurements using Dixon-MRI

Janne West[1,2,3], Thobias Romu[2,3,4], Sofia Thorell[1,3,5], Hanna Lindblom[5], Emilia Berin[5], Anna-Clara Spetz Holm[5], Lotta Lindh Åstrand[5], Magnus Borga[2,3,4], Mats Hammar[5], and Olof Dahlqvist Leinhard[1,2,3]

[1]Department of Medical and Health Sciences, Linköping University, Linköping, Sweden, [2]Advanced MR Analytics AB, Linköping, Sweden, [3]Center for Medical Image Science and Visualization (CMIV), Linköping University, Linköping, Sweden, [4]Department of Biomedical Engineering, Linköping University, Linköping, Sweden, [5]Obstetrics and Gynecology, Linköping University, Linköping, Sweden

Body composition analysis is increasingly important for diagnosis and follow-up in many patient groups and medical conditions. The combined fat and muscle quantification on global and regional level is not commonly reported. In this study a Dixon-MRI based acquisition and body composition analysis was extended to quantify individual muscles. Test-retest reliability was established in a clinically relevant group of 36 postmenopausal women. This method enables advanced phenotyping combined with measurements of specific muscles to target clinical questions.

1579

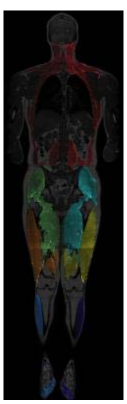

A Potential Pathophysiological Link Between Generalized and Localized Muscle Fat Infiltration in Chronic Whiplash Patients

Anette Karlsson[1,2], Anneli Peolsson[3], James Elliott[4], Thobias Romu[1,2], Helena Ljunggren[3], and Olof Dahlqvist Leinhard[2,5]

[1]Department of Biomedical Engineering, Linköping University, Linköping, Sweden, [2]Center for Medical Image Science and Visualization, Linköping University, Linköping, Sweden, [3]Department of Medical and Health Sciences, Physiotherapy, Linköping University, Linköping, Sweden, [4]Department of Physical Therapy and Human Movement Sciences, Feinberg School of Medicine, Northwestern University, Chicago, IL, United States, [5]Department of Medical and Health Sciences, Linköping University, Linköping, Sweden

Muscle fat infiltration (MFI) in the cervical multifidi muscles and whole-body skeletal muscle tissue was measured in participants with chronic whiplash associated disorders (WAD) using whole-body fat-water separated MRI to investigate potential interaction between deep neck muscle and generalized MFI. Thirty participants with chronic WAD and 30 matched controls were included. MFI in multifidi was strongly associated to whole-body MFI as well as to severity of WAD. The strong association between Multifidi MFI and whole-body MFI indicates that both generalized factors and localized effects related to the trauma may be important for understanding the pathophysiology of chronic WAD.

1580

Whole-body MRI in facioscapulohumeral muscular dystrophy: Preliminary results

Doris G. Leung[1,2], Li Pan[3], John A. Carrino[4], Kathryn R. Wagner[1,2], and Michael A. Jacobs[5,6]

[1]Center for Genetic Muscle Disorders, Kennedy Krieger Institute, Baltimore, MD, United States, [2]Neurology, The Johns Hopkins University School of Medicine, Baltimore, MD, United States, [3]Siemens Healthcare, Baltimore, MD, United States, [4]Radiology and Imaging, Hospital for Special Surgery, New York, NY, United States, [5]Radiology and Radiological Science, The Johns Hopkins University School of Medicine, Baltimore, MD, United States, [6]Sidney Kimmel Comprehensive Cancer Center, The Johns Hopkins University School of Medicine, Baltimore, MD, United States

Facioscapulohumeral muscular dystrophy (FSHD) is a hereditary disorder that causes progressive muscle wasting. Whole-body MRI (WBMRI) was used to scan 24 adults with genetically-confirmed type 1 FSHD. Muscles were scored for fat infiltration and edema-like changes. Fat infiltration scores were compared to muscle strength and function measurements. Our analysis reveals a distinctive pattern of muscle involvement and sparing in FSHD. Averaged fat infiltration scores for muscle groups in the legs were statistically significantly associated with quantitative muscle strength and 10-meter walk time. We conclude that WBMRI offers a promising disease biomarker in FSHD and other muscular dystrophies.

1581 

DTI imaging application of vastus medialis oblique muscle in recurrent patellar dislocation

Lisi Liu[1], Zhuozhao Zheng[2], Huishu Yuan[1], and Lizhi Xie[3]

[1]Radiology Department of Peking University Third Hospital, Beijing, People's Republic of China, [2]Radiology Department of Tsinghua Changgung Hospital, Beijing, People's Republic of China, [3]GE Healthcare, MR Research China, Beijing, People's Republic of China

The osseous-related factors that influence patellofemoral joint instability have been well-studied in plenty of the previous reported literatures. However, the muscle-related factors that affect patellofemoral joint instability have not been fully revealed. MRI is a noninvasive imaging method, including conventional MRI scans and diffusion tensor imaging (DTI) sequence, which can respectively reflect the macroscopic and microscopic structures of the muscle fibers.[1,2] In the current study, the cross-sectional area were measure with DTI parameters of FA, ADC, and λ1, λ2, λ3 of vastus medialis oblique (VMO). Thereafter, these parameters were compared between the recurrent patellar dislocation patients and the healthy volunteers.

1582 

Diffusion Tensor imaging in the Injuries of the Levator Ani Muscle in Female Pelvic Floor Dysfunction

Huici Zhu[1], Jianyu Liu[1], Yan Zhou[1], and Lizhi Xie[2]

[1]Radiology Department of Peking University Third Hospital, Beijing, People's Republic of China, [2]GE Healthcare, MR Research China, BeiJing, People's Republic of China

To find the most vulnerable component of levator muscle, this research compared the levator ani muscle which contains pubovisceral, puborectal and iliococcygeal muscles between the control group and the patient group by using DTI. 49 female PFD (pelvic floor dysfunction) patients and 51 female healthy subjects underwent DTI imaging on a 3.0T MR system. A significant difference was found in the FA value of the right pubovisceral muscle between the two groups, and therefore, this part are more likely to be damaged comparing with other compartments of levator ani muscle. DTI with fiber tractography permits the evaluation of the injuries of levator ani muscle, which has a certain effect in revealing the pathogenesis of the female pelvic floor dysfunction.

1583 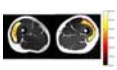

Analysis of T2 Relaxation Times in Vastus Lateralis Muscle after Anterior Cruciate Ligament Injury

Richard Dylan Lawless[1], Peter A. Hardy[2,3], Anders Andersen[3,4], and Brian Noehren[5]

[1]College of Engineering, Department of Biomedical Engineering, Lexington, KY, United States, [2]Department of Radiology, College of Medicine, Lexington, KY, United States, [3]Magnetic Resonance Imaging and Spectroscopy Center, Lexington, KY, United States, [4]Department of Neuroscience, College of Medicine, [5]Department of Rehabilitation, College of Health Sciences, Lexington, KY, United States

Anterior cruciate ligament (ACL) injuries are associated with a persistent decrease in quadriceps muscle strength despite rehabilitation. Previous studies have shown that ACL injury results in muscle disorganization, which could account for the loss in strength. We sought to use dual-spin echo and multi-spin echo sequences to estimate T2 of the vastus lateralis in injured and uninjured limbs of twenty-two ACL injured subjects. T2 of the injured limb was significantly longer than the uninjured limb for both pulse sequences. Our results suggest that T2 relaxation may provide clinicians a means to quantitatively monitor muscle recovery after ACL injury.

1584 

Optimal excitation location for magnetic resonance elastography of the supraspinatus muscle

Daiki Ito[1,2], Tomokazu Numano[1,2], Kazuyuki Mizuhara[2,3], Koichi Takamoto[4], Takaaki Onishi[1], and Hisao Nishijo[5]

[1]Department of Radiological Science, Graduate School of Human Health Science, Tokyo Metropolitan Unversity, Arakawa, Japan, [2]Health Research Institute, National Institute of Advanced Industrial Science and Technology, Tsukuba, Japan, [3]Department of Mechanical Engineering, Tokyo Denki University, Adachi, Japan, [4]Department of Judo Neurophysiotherapy, Graduate School of Medicine and Pharmaceutical Sciences, University of Toyama, Toyama, Japan, [5]Department of System Emotional Science, Graduate School of Medicine and Pharmaceutical Sciences, University of Toyama, Toyama, Japan

It is difficult to palpate the supraspinatus muscle since it is difficult to determine their anatomic location superficially. Magnetic resonance elastography (MRE) can measure tissue stiffness quantitatively only if vibrations reach these tissues. To vibrate the tissues efficiently, it is necessary to determine the best excitation location. We investigated the excitation location suitable for MRE of the supraspinatus muscle. When the excitation location was placed on the trapezius muscle, the wave images represented clear wave propagation compared with those on the head of humerus. Therefore, optimal excitation location may be the trapezius muscle in the MRE of the supraspinatus muscle.

1585 

Simultaneous measurement of muscle transverse relaxation rates of R2, R2' and R2*: application in unilateral femoral artery embolization

Chengyan Wang[1], Rui Zhang[2], Bihui Zhang[3], Haochen Wang[3], Xiaodong Zhang[4], Min Yang[3], Jue Zhang[1,2], Xiaoying Wang[1,4], and Jing Fang[1,2]

[1]Academy for Advanced Interdisciplinary Studies, Peking University, Beijing, People's Republic of China, [2]College of Engineering, Peking University, Beijing, People's Republic of China, [3]interventional radiology and vascular surgery, Peking University First Hospital, Beijing, People's Republic of China, [4]Department of Radiology, Peking University First Hospital, Beijing, People's Republic of China

Diagnosis of the ischemic lesion is challenging and often requires the use of pharmaco-mechanical methods. This study demonstrates the feasibility of using a susceptibility-based MRI technique with the multi-echo gradient and spin echo (MEGSE) sequence to assess the skeletal muscle oxygenation alternations in animal model of unilateral femoral artery embolization. The results shown that the skeletal muscle R2 decreases obviously from after femoral artery embolization, while R2' increases correspondingly. MEGSE seems to be an appropriate method for the evaluation of skeletal muscle ischemia after embolization.

1586

Feasibility of Quantifying Bone Metabolism in the Femoral Neck in Human Subjects using Multi-Modality Imaging

Christian Tyler McHugh[1], William Raynor[1], Tom Werner[1], Abass Alavi[1], and Chamith S Rajapakse[1]

[1]*University of Pennsylvania, Philadelphia, PA, United States*

18F-sodium fluoride (NaF) is a readily available radiotracer that has shown great potential to study bone metabolism associated with osseous diseases such as osteoporosis. We analyzed PET/CT and MRI data to study the effects of bone volume fraction and marrow distribution on the uptake of NaF in the proximal femur. Our data showed that the mean standardized uptake (SUV_{mean}) decreased with age and became more significant when local adjustments for bone and bone marrow were taken into account. We foresee the importance of high-resolution microstructural bone MRI for the partial volume correction of PET data for accurate quantification bone metabolism.

1587

Segmentation of CMF Bones from MRI with A Cascade Deep Learning Framework

Dong Nie[1], Li Wang[1], Jianfu Li[2], Daeseung Kim[2], James J. Xia[2], and Dinggang Shen[1]

[1]*Department of Radiology and BRIC, UNC-Chapel Hill, USA, Chapel Hill, NC, United States,* [2]*Houston Methodist Hospital, Houston, TX, USA*

Accurate segmentation of CMF bones from MRI is one of the most important fundamental steps in clinical applications, and it can also be used in other areas, such as character animation and assistive robotics. In this paper, we propose a cascade framework based on the recently well-received and prominent deep learning methods. Specifically, we first propose a 3D fully convolutional network architecture for a coarse segmentation of the bone tissue. Further, we propose to utilize CNN for fine-grained level segmentation around the predicted bone tissue area. The conducted experiments show that our proposed 3D deep learning model could achieve good performance in terms of segmentation accuracy.

1588

Robust Pore Water Suppression in Cortical Bone with Multiple Adiabatic Inversion Recovery

Kevin D Harkins[1], Sasidhar Uppuganti[1], Jeffry S Nyman[1], and Mark D Does[1]

[1]*Vanderbilt University, Nashville, TN, United States*

Measurement of bound water concentration in cortical bone with MRI is a promising method for evaluating bone fracture risk. One approach to measure bound water involves suppression of pore water signal with an adiabatic inversion-recovery pulse sequence. However, this approach requires a priori knowledge of pore water T_1 which itself is expected to vary with bone porosity. We propose to minimize the effect of subject-dependent pore water T_1 variation by in bound water imaging using a multiple adiabatic inversion recovery preparation optimized to suppress pore water over a broad T_1 domain.

1589

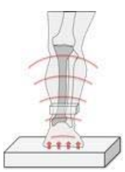

MRI Assessment of the Effect of Low-Magnitude Mechanical Stimulation on Postmenopausal Bone Loss

Chamith S Rajapakse[1], Wenli Sun[1], Christian Tyler McHugh[1], Ben Newman[1], Mona M Al Mukaddam[1], Peter J Snyder[1], and Felix W Wehrli[1]

[1]*University of Pennsylvania, Philadelphia, PA, United States*

Low-magnitude mechanical stimulation (LMMS) has shown great potential as a non-pharmacological intervention for improving bone quality in animal models. However, human trials have yielded less compelling evidence, possibly related to difficulties in maintaining adherence and use of conventional imaging techniques not being able to detect subtle longitudinal changes. Here we investigated the use of high-resolution structural bone MRI in monitoring treatment efficacy of LMMS in postmenopausal women. The data show that baseline bone volume fraction at the distal tibia is associated with the changes observed over one year of active LMMS or placebo treatment.

1590

Potential of High Resolution Isotropic Microstructural MRI of the Proximal Femur

Austin G. Alecxih[1], Elizabeth A. Kobe[2], Alyssa J. Johncola[2], Marissa L. Evans[2], Shivali Patel[2], Sun M. Kim[2], Benjamin T. Newman[2], Gregory Chang[3], Christian McHugh[2], and Chamith S. Rajapakse[2]

[1]*University of Pennsylvania, Philadelphia, PA, United States,* [2]*University of Pennsylvania,* [3]*New York University*

Microstructural MRI based finite element modelling is an area of current research in regards to the role that this technology can play as an efficient and affordable metric for quantifying bone integrity and for identifying fracture risk. This study was conducted in an attempt to unveil the extent to which MRI resolution impacts the quantitative output generated by finite element models pertaining to the parameter of bone stiffness of the proximal femur in vitro. Conclusions reveal a statistically significant variance relative to the values generated for two differing MRI resolution classes.

1591

Simplified approach to quantification for hand synovitis in rheumatoid arthritis using dynamic contrast enhanced MRI: pixel-by-pixel time intensity curve shape analysis

Yuto Kobayashi[1], Tamotsu Kamishima[2], Taro Sakashita[3], Hiroyuki Sugimori[2], Shota Ichikawa[1], Atsushi Noguchi[4], Michihito Kono[4], Toshitake Iiyama[5], and Tatsuya Atsumi[4]

[1]Graduate School of Health Sciences, Hokkaido University, Sapporo, Japan, [2]Faculty of Health Sciences, Hokkaido University, Sapporo, Japan, [3]National Sale Division, CT Sales Department, Application Group, Toshiba Medical Systems Corporation, Tochigi, Japan, [4]Internal Medicine 2, Hokkaido University Hospital, Sapporo, Japan, [5]Yaesu Clinic, Tokyo, Japan

Quantification for synovitis using time intensity curve (TIC) shape analysis of rheumatoid arthritis has been believed to require long acquisition time up to 6-7 minutes to observe washout phase. In this study, we found that wash out phase does not contribute to accurate depiction of synovitis in the hand and simplified TIC shape analysis could significantly decrease acquisition time from about 6 minutes to 3 minutes.

1592

A novel approach to measure tibial component migration by low field markerless magnetic resonance imaging

Femke F. Schroder[1,2], Frank F. J. Simonis[2], Dean F.M. Pakvis[1], Rianne Huis in't Veld[1], and Bennie ten Haken[2]

[1]Centre for Orthopaedic Surgery OCON., Hengelo, Netherlands, [2]University of Twente, Faculty of Science and technology, Enschede, Netherlands

This study evaluated if low field MRI is a practical alternative for Roentgen stereophotogrammetric-analysis (RSA) to measure prosthetic migration. This also included determining the optimal registration method for this purpose. The detection of migration on low field MRI was sufficient for clinical use in two of the translation directions and all three rotational directions. Manual registration proved to be the most accurate method for markerless MRI (MMRI) estimation of the migration.

1593

Quantitative Mapping of the Ischemic Femoral Head in a Piglet Model of Legg-Calve-Perthes Disease

Casey P. Johnson[1], Luning Wang[1], Ferenc Toth[2], Cathy S. Carlson[2], Harry K. W. Kim[3,4], and Jutta M. Ellermann[5]

[1]Center for Magnetic Resonance Research, University of Minnesota, Minneapolis, MN, United States, [2]Veterinary Population Medicine, University of Minnesota, St. Paul, MN, United States, [3]Texas Scottish Rite Hospital, Dallas, TX, United States, [4]Orthopaedic Surgery, UT Southwestern, Dallas, TX, United States, [5]Radiology, University of Minnesota, Minneapolis, MN, United States

This study investigated the sensitivities of T1, T2, continuous-wave T1ρ, adiabatic T1ρ, and RAFF relaxation times to ischemia-induced necrosis and subsequent repair of the developing femoral head in a piglet model of Legg-Calve-Perthes disease (LCPD), a disabling childhood hip disorder. Quantitative maps of ischemic and control femoral heads acquired ex vivo at 9.4T MRI were compared numerically and validated with histology. Our findings reveal that the relaxation times provide complementary information on the status of the pathological hip, which can potentially address a clinical need for diagnostic imaging tools to assess the early stages of LCPD.

1594

Age estimation using MR imaging of the third molar teeth and the medial clavicular epiphysis: Validation of a multifactorial approach

Thomas Widek[1,2], Pia Baumann[3], Heiko Merkens[1], Thomas Ehammer[1], Andreas Petrovic[2,4], Isabella Klasinc[1,5], Martin Urschler[1,2,6], and Eva Scheurer[7]

[1]Ludwig Boltzmann Institute Clinical Forensic Imaging, Graz, Austria, [2]BioTechMed, Graz, Austria, [3]University Center of Legal Medicine Lausanne-Geneva, University Hospital of Lausanne, Switzerland, [4]Institute of Medical Engineering, Graz University of Technology, Austria, [5]Institute of Forensic Medicine, Medical University of Graz, Austria, [6]Institute for Computer Graphics and Vision, Graz University of Technology, Austria, [7]Institute of Forensic Medicine, University of Basel - Health Department Basel, Switzerland

High migration rates in the last years put forensic age estimation of living people at the forefront of forensic research. The established standard for age estimation uses images acquired with ionizing radiation, therefore radiation-free alternatives such as MRI are currently of high interest. In this study a CT based multifactorial approach that combines wisdom teeth and clavicles was validated with MRI data. The sensitivity to estimate subjects under 18 years of age as minors with MRI lies above 93%. Our results showed that MR could replace the CT based multifactorial Approach.

1595

Three-dimensional fracture visualization with Zero Echo Time MRI

Gaspar Delso[1], Geoffrey Warnock[2], Caroline Zellweger[2], Felipe de Galiza[2], Irene Burger[2], Martin Huellner[2], and Patrick Veit-Haibach[2]

[1]GE Healthcare, Cambridge, United Kingdom, [2]University Hospital of Zurich, Zurich, Switzerland

The present study is aimed at assessing the performance of proton density-weighted zero-echo time (ZTE) acquisition for the visualization of bone fractures.

1596

An Efficacy Analysis of Whole-Body Magnetic Resonance Imaging in the Diagnosis and Follow-Up of Polymyositis and Dermatomyositis

Zhen-guo Huang[1], Min-xing Yang[1], Bao-xiang Gao[1], Xiao-liang Chen[1], He Chen[1], and Kai-ning Shi[2]

[1]China-Japan Friendship Hospital, Beijing, People's Republic of China, [2]Philips Healthcare (China)

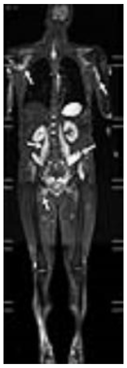

To evaluate the value of whole-body magnetic resonance imaging (WBMRI) in diagnosing muscular and extramuscular lesions in patients with polymyositis (PM) and dermatomyositis (DM). A retrospective analysis of WBMRI data was performed on PM / DM patients who met the Bohan and Peter diagnostic criteria. WBMRI comprehensively displays the muscular involvement in PM / DM patients, and has the ability to diagnose other associated extramuscular diseases, such as ILD and systemic malignancy. WBMRI can also help screen for multifocal steroid-induced osteonecrosis.

Traditional Poster

Miscellaneous MSK

Exhibition Hall 1597-1622 Monday 16:15 - 18:15

1597

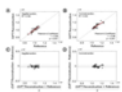

Deformable Registration of In Vivo Human Spine Magnetic Resonance Imaging Using Scale Invariant Feature Transform (SIFT) Algorithm

Dong-Hoon Lee[1,2], Do-Wan Lee[3,4,5], Yong Hyun Chung[2], and Bong-Soo Han[2]

[1]Brain and Mind Centre, University of Sydney, Sydney, Australia, [2]Department of Radiological Science, Yonsei University, Wonju, Korea, Republic of, [3]Ewha Brain Institute, Ewha Womans University, Seoul, Korea, Republic of, [4]Department of Biomedical Engineering, The Catholic University of Korea College of Medicine, Seoul, Korea, Republic of, [5]Research Institute of Biomedical Engineering, The Catholic University of Korea, Seoul, Korea, Republic of

Deformable registration process for in vivo human spine MR images can provide the crucial information to investigate the diagnostic performance and treatment effects of pathologies. Here, based on the scale invariant feature transform (SIFT) algorithm, we attempted to evaluate the deformable registration process for spine images, and compared with commercially mounted algorithm in MRI system. The results qualitatively and quantitatively showed fine results, and clearly showed the reproducibility of the use of SIFT algorithm compared with commercially mounted stitching algorithm on MRI system. Our approach can be helpful for the extension of other medical imaging modalities for image deformable registration.

1598

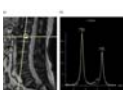

Perfusion and Fat Content of Lumbar Vertebral Body: Global and Regional Analysis

Hou-Ting Yang[1,2], Yi-Jui Liu[3], Hing-Chiu Chang[4], Xiang-Wei Xie[5], Ming-Fun Lin[5], and Wing P. Chan[5,6]

[1]Department of Nuclear Medicine, Chang Gung Memorial Hospital, Taoyuan, Taiwan, [2]Program of Electrical and Communications Engineering, Feng Chia University, Taichung, Taiwan, [3]Department of Automatic Control Engineering, Feng Chia University, Taichung, Taiwan, [4]Department of Diagnostic Radiology, The University of Hong Kong, Hong Kong, [5]Department of Radiology, Wan Fang Hospital, Taipei Medical University, Taipei, Taiwan, [6]Department of Radiology, School of Medicine, College of Medicine, Taipei Medical University, Taiwan

Vertebral blood perfusion has been reported that there was a decrease trend in normal aging people and post-menopause women and those with arteriosclerosis, fat marrow increased and osteoporosis. Although DCE-MRI and MRS have shown potential probing bone marrow content and blood perfusion characteristics of vertebra body in previous studies, all of these were ROI analysis only and lack regional information for bone marrow content and blood perfusion. Therefore, The purposes of this study were to investigate the regional perfusion and bone marrow content in vertebra body with use of DCE-MRI and six-point Dixon IDEAL technique by pixel-by-pixel analysis.

1599

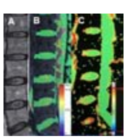

Non-Gaussian water diffusion kurtosis imaging and T2* mapping of Intervertebral Disc Degeneration at 3T MR

Feifei Zeng[1], Yun fei Zha[1], Dong Xing[1], Liang Li[1], and Hui Lin[2]

[1]Radiology, Renmin Hospital of Wuhan University, Wuhan, People's Republic of China, [2]GE healthcare China

To assess the feasibility of detecting early biochemical changes of nucleus pulposus (NP) in intervertebral disk degeneration (IVDD) by diffusion kurtosis imaging (DKI), and compare mean kurtosis (MK) and T2* mapping in IVDD according to Pfirrmann grades. Twenty individuals underwent lumbar sagittal T2-weighted image, DKI and T2* mapping. DKI related parameters—mean kurtosis (MK) and T2* values were measured. The differences between MK and T2* value in NP were highly significant. Pfirrmann grades were inversely significantly correlated with T2* values in the NP, and positively correlated with MK values, especially between Pfirrmann grade II ,III and Ⅳ.

1600

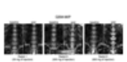

Bone marrow iron assessment using quantitative susceptibility mapping in iron overload rabbit model

Yoonho Nam[1], Eo-Jin Hwang[1], and Joon-Yong Jung[1]

[1]Department of Radiology, Seoul St.Mary's Hospital, College of Medicine, The Catholic University of Korea, Seoul, Korea, Republic of

The aim of our study was to assess the feasibility of quantitative susceptibility mapping (QSM) as a tool to quantify bone marrow iron level non-invasively. Nine rabbits were scanned before and after iron accumulations, and bone marrow susceptibility values of these rabbits were evaluated from the reconstructed QSM images. The results showed a linear correlation between the measured susceptibility changes and the injected iron doses.

1601 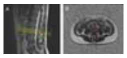

Quantitative study of longitudinal distribution of fat fraction in the lumbar spine

Huiying Chen[1], Huishu Yuan[1], Lizhi Xie[2], and Ning Lang[1]

[1]Peking University Third Hospital, Beijing, People's Republic of China, [2]GE Healthcare, MR Research China, People's Republic of China

The aim of this study was to explore the fat fraction(FF) variation of inter and intra vertebral bodies in the lumbar spine, by using water-fat imaging. In lumbar spine, L1 and L2 vertebras demonstrated lower FF level but with more common 'margin higher' FF distribution pattern comparing to other vertebras, which might be related to stress and activities of the vertebra. We suggested that FF distribution pattern indicate certain skeletal remodeling that affects bone strength, which may be a promising indicator in assessing prevalent fracture besides the increased average FF of the whole vertebral body.

1602 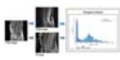

Intervertebral disc heterogeneity decoded with MRI histogram analysis

Christian Waldenberg[1,2], Hanna Hebelka[2,3], Helena Brisby[2,4], and Kerstin Magdalena Lagerstrand[1,2]

[1]Dept. of Medical Physics and Techniques, Sahlgrenska University Hospital, Gothenburg, Sweden, Sahlgrenska University Hospital, Gothenburg, Sweden, [2]Institute of Clinical Sciences, Sahlgrenska Academy, University of Gothenburg, Gothenburg, Sweden, [3]Dept of Radiology, Sahlgrenska University Hospital, Gothenburg, Sweden, [4]Dept of Orthopaedics, Sahlgrenska University Hospital, Gothenburg, Sweden

Low back pain has major consequences for both the individual as well as for the society which often results in sick leave from work. Unfortunately, health care today lacks diagnostic techniques and procedures necessary to select and treat patients who would most benefit from treatment. Histogram analysis based on MRI imaging has the potential to display disc heterogeneity and possibly depict painful discs. A total of 98 histograms of 49 intervertebral discs were generated based on three mid-sagittal slices of high quality T2W MRI images and T2-maps. Using MATLAB, a two component Gaussian mixture distribution model was fitted to the histogram data in order to retrieve disc heterogeneity measures. Mann-Whitney U-test displayed a significant difference in disc heterogeneity measures with increased Pfirrmann grade.

1603 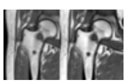

Synthetic contrast optimization of bone metastases

Catharina Petersen[1] and Marcel Warntjes[1,2]

[1]SyntheticMR, Linköping, Sweden, [2]Center for Medical Image Science and Visualization (CMIV), Linköping University Hospital, Linköping, Sweden

To achieve optimal contrast when imaging bone metastases, the patient would have to imaged multiple times at various contrast settings. This is not possible in practice, resulting in the use of standard contrasts that are often sub-optimal due to patient-specific variations in both healthy and metastatic tissue.

Using synthetic MRI, it is possible to synthesize a multitude of contrasts from a single scan. This makes it possible to determine optimal contrast weighing post-scan. Studying bone metastases, synthetic images where used to develop a mathematical model of perceived contrast, taking both tissue properties and the human visual system into account.

1604 

The presence of newly defined classical features of intraneural perineurioma may obviate the need for fascicular biopsy and pathologic diagnosis

Thomas J Wilson[1], Shelby A Stewart[2], B. Matthew Howe[3], Robert J Spinner[4], and Kimberly K Amrami[5]

[1]Neurosurgery, Mayo Clinic, Rochester, MN, United States, [2]Radiology, Mayo Clinic, Rochester, MN, United States, [3]Radiology, Mayo Clinic, [4]Neurosurgery, Mayo Clinic, Rochester, MN, [5]Radiology, Mayo Clinic, Rochester, MN

Intraneural perineurioma is typically diagnosed by targeted fascicular biopsy and histopathologic analysis. Through review of clinical history and magnetic resonance imaging of consecutive patients undergoing fascicular biopsy, we define the classical features of intraneural perineurioma as no cancer history, unifocal disease, moderate-severe T2 hyperintensity, moderate-severe contrast enhancement, homogeneous contrast enhancement, fusiform shape, and enlargement of involved nerves. This combination of features has a high specificity and moderate sensitivity for the diagnosis of perineurioma. When the classical features of perineurioma defined in this study are present, the high specificity of this combination of features may obviate the need for fascicular biopsy.

1605 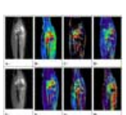

The value of dynamic contrast-enhanced MRI quantitative parameters in evaluating the efficacy of neoadjuvant chemotherapy for osteosarcoma

ma huan[1], li kun[2], and cao peng[3]

[1]Department of Radiology, The Third Affiliated Hospital of Kunming Medical University, KunMing, Yunnan Province, People's Republic of China, [2]The Third Affiliated Hospital of Kunming Medical University, [3]GE healthcare, china, KunMing, Yunnan Province, People's Republic of China

Osteosarcoma is the most common bone sarcoma in children and adolescents 1. Response of osteosarcoma to NAC should be assessed preoperatively, but conventional imaging has limit, and histopathological examination cannot dynamically observe the response of tumor to treatment. DCE-MRI can reflect the pathophysiology of tumor at microvascular and cellular level. Currently, researchers have used DCE-MRI qualitative and semi-quantitative method to analyze the response of osteosarcoma to NAC, but studies on DCE-MRI quantitative analysis are rarely reported. Therefore, we analyzed the quantitative parameter change of DCE-MRI in 17 patients of osteosarcoma before and after NAC, and compared good response and poor response to chemotherapy in order to explore the value of DCE-MRI quantitative parameters in assessing the response of osteosarcoma to NAC.

1606 

Fat Fraction Histogram Analysis: Insights into the Biology of Lipomatous Tumors

Mikael Skorpil[1,2], Henric Rydén[3], Elisabet Lidbrink[4], Otte Brosjö[5], and Johan Berglund[6,7]

[1]Department of Radiation Sciences, Umeå University, Umeå, Sweden, [2]Department of Radiology, Uppsala, Sweden, [3]Department of Neuroradiology, Karolinska University Hospital, Stockholm, Sweden, [4]Department of Oncology and Pathology, Karolinska Institute and Karolinska University Hospital, Solna, Sweden, [5]Department of Orthopaedic Surgery, Karolinska University Hospital, Solna, Sweden, [6]Department of Medical Radiation Physics, Karolinska University Hospital, Stockholm, Sweden, [7]Department of Clinical Science, Intervention and Technology, Karolinska Institute, Stockholm, Sweden

Fat content evaluation in soft-tissue tumors is based on visual grading of T1-weighted images with uncertain accuracy and inter-rater variability. We used a multi-point Dixon technique to quantitatively measure the distribution of proton density fat fraction in different lipomatous tumors. The effect of radiotherapy on fat content in a myxoid liposarcoma was also assessed, with histograms revealing a distinct alteration. Our data give supporting evidence that maturation of tumor cells is the cause for the lipoma-like areas seen after radiotherapy of myxoid liposarcomas. On a voxel level (2×2×2 mm^3) various lipomatous tumors exhibited different fat fraction histograms.

1607 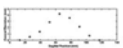

Characterization of Through-Plane and In-Plane Artifacts using a 3D-Printed Grid Phantom with an Embedded Metal Hip Implant

Gregory Hong[1,2], Matthew G Teeter[1,3], Jaques S Milner[1], Steven I Pollmann[1], Maria Drangova[1,2], and David W Holdsworth[1,2,3]

[1]Robarts Research Institute, London, ON, Canada, [2]Department of Medical Biophysics, University of Western Ontario, London, ON, Canada, [3]Department of Surgery, University of Western Ontario, London, ON, Canada

Metal Artifact Reduction (MAR) is required for orthopedic imaging near implants. Novel MAR techniques have been developed in the past decade, creating a need for quantitative evaluation of the effectiveness of geometric distortion correction. We have developed a 3D-printed modular conformal grid phantom, consisting of a grid of regularly spaced spherical markers. This phantom provides a measure of inherent field inhomogeneity, and contains a conformal cavity in which a metal object can be embedded. This approach provides a means to characterize through-plane and in-plane artifacts across a 3D volume, facilitating testing and validation of novel MAR techniques during development.

1608 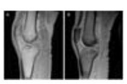

Cartesian UTE with echo time below 0.5 millisecond

Franciszek Hennel[1], Markus Weiger[1], Manuela Rösler[1], Roger Luechinger[1], Bertram Wilm[1], and Klaas P Pruessmann[1]

[1]Institute for Biomedical Engineering, ETH, Zurich, Switzerland

MRI with sub-millisecond TE typically uses non-Cartesian sampling strategies such as radial UTE leading to increased sensitivity to eddy currents and a high computational burden. We report that TE values in the range so far reserved for radial UTE can be reached with Cartesian sampling using a gradient coil dedicated for muscoskeletal applications in humans.

1609 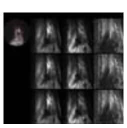

Iterative Denoising of Undersampled PROPELLER Diffusion-Weighted Imaging near Metal Implants

Sampada Bhave[1], S. Shivram Kaushik[2], and Kevin M Koch[1]

[1]Medical College Wisconsin, Milwaukee, WI, United States, [2]GE Healthcare

Diffusion weighted imaging is widely used in musculoskeletal MR imaging. Current implementations of diffusion-weighted imaging include the use of PROPELLER DUO imaging sequence and multi-spectral MRI imaging techniques. However, these implementations are restricted by long acquisition times. In this work we propose to an approach to undersample the blades in a uniform fashion and denoise the reconstructed image using total variation based denoising approach. This approach provides acceptable results up to an acceleration factor of 3 and reduces the scan time. This reduction in scan time can be used to acquire multiple slices within clinically feasible scan times.

1610 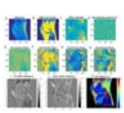

Ultrashort Echo Time Chemical Shift Quantitative Susceptibility Mapping (UTE-CS-QSM) for Hemosiderin Assessment in Hemophilic Arthropathy

Xing Lu[1,2], Annette von Drygalski[3], Alexey Dimov[4], Lena Volland[3], Zhe Liu[4], Yi Wang[4], Jiang Du[1], and Eric Y Chang[1,5]

[1]Department of Radiology, University of California, San Diego, CA, United States, [2]Institute of Electrical Engineering, Chinese Academy of Science, Beijing, People's Republic of China, [3]Department of Medicine, Division of Hematology/Oncology, University of California, San Diego, CA, United States, [4]Department of Radiology, Weill Cornell Medical College, New York, NY, United States, [5]Radiology Service, VA San Diego Healthcare System, San Diego, CA, United States

Hemosiderin deposition in hypertrophic synovium is a hallmark of progressive hemophilic arthropathy and accumulates with joint bleeding. . Conventional quantification of hemosiderin uses semi-quantitative MRI scores, assigning grades of small, moderate, or large to assess the burden of hemosiderin. To date, there is no known method to assess or quantify hemosiderin concentration within synovium due to the extremely short T2 values of this tissue. In this pilot study, we demonstrated that the clinically compatible IDEAL UTE-CS-QSM technique can be used to quantify hemosiderin depositions. We have shown that synovium in joints with hemophilic arthropathy demonstrates various susceptibility values, likely corresponding to different concentrations of hemosiderin.

1611

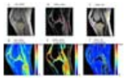

Chemical Shift T1 Quantification with Three-dimensional Ultrashort Echo Time Cones Imaging and IDEAL (3D UTE-Cones-IDEAL) Processing

Xing Lu[1,2], Michael Carl[3], Yajun Ma[1], Yanchun Zhu[1], Yinghua Zhao[1], Wenhui Yang[2], Eric Y Chang[1,4], and Jiang Du[1]

[1]Department of Radiology, University of California, San Diego, CA, United States, [2]Institute of Electrical Engineering, Chinese Academy of Science, Beijing, People's Republic of China, [3]GE Healthcare, San Diego, CA, United States, [4]Radiology Service, VA San Diego Healthcare System, San Diego, CA, United States

Conventional T1 measurements are subject to errors due to fat contamination and invisibility of the short T2 components. In this study, we aimed to develop 3D UTE with Cones sampling and IDEAL processing (3D UTE-Cones-IDEAL) with variable TRs for robust fat/water separation and more accurate T1 estimation of joint tissues ex vivo and in vivo. The results show that this technique can robustly separate water and fat signal and lead to longer T1s for water-rich tissues (such as muscle, tendon and peripheral nerve), and shorter T1s for fat-rich tissues.

1612

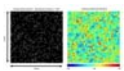

On the Source of MRI Off-Resonance Observables in Arthroplasty-Induced Metallosis

Kevin Koch[1], Matthew Koff[2], Thomas Bauer[3], and Hollis Potter[2]

[1]Radiology, Medical College of Wisconsin, Milwaukee, WI, United States, [2]MRI Division, Hospital for Special Surgery, New York, NY, United States, [3]Anatomic Pathology and Orthopaedic Surgery, Cleveland Clinic, Cleveland, OH, United States

The deposition of metal particles near total joint replacements has substantial impact on patient morbidity. Current standards of clinical management of patients with symptomatic total hip replacements are highly leveraged on the presence of wear debris in periprosthetic tissues. Our group has recently developed methods to perform off-resonance based identification of metal particle deposits. Here, we provide analysis on the source of tissue-based metal particle Larmor frequency offsets. The results of this analysis provide new insight on the role of off-resonance observables in the progression of symptomatic failed total hip replacements.

1613

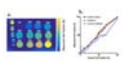

Fat Fraction and R2* as Measures of Bone Marrow Composition and Structure: Validation in Fat-Water-Bone Phantoms

Timothy JP Bray[1,2], Alan Bainbridge[3], Shonit Punwani[1], Yiannis Ioannou[2], and Margaret A Hall-Craggs[1]

[1]Centre for Medical Imaging, University College London, London, United Kingdom, [2]Centre for Adolescent Rheumatology, University College London, London, United Kingdom, [3]Medical Physics, University College London Hospitals

MRI is becoming central to clinical decision-making in diseases involving the bone marrow, including spondyloarthritis and multiple myeloma. Both diseases cause alterations in marrow composition and structure, but there is currently no reliable method for quantifying these changes. Here, we describe a series of fat-water-bone phantoms enabling validation of proton density fat-fraction (PDFF) and R2* as measures of marrow composition and trabecular bone mineral density (BMD) respectively. Our data suggest that PDFF measurements can be achieved with excellent accuracy. Furthermore, there was a strong relationship between R2* and BMD, suggesting that R2* could be used to monitor BMD in vivo.

1614

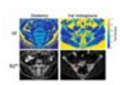

Simultaneous Quantification of Fat Fraction and R2* as measures of Bone Oedema/Adiposity and Structure in Spondyloarthritis

Timothy JP Bray[1], Alan Bainbridge[2], Corinne Fisher[3], Shonit Punwani[1], Yiannis Ioannou[3], and Margaret A Hall-Craggs[1]

[1]Centre for Medical Imaging, University College London, London, United Kingdom, [2]Medical Physics, University College London Hospitals, [3]Centre for Adolescent Rheumatology, University College London

Treatment decisions in patients with spondyloarthritis increasingly involve the use of MRI to assess the extent, severity and type of inflammation surrounding the joints. However, conventional spin echo imaging requires subjective interpretation and gives little information about trabecular structure, despite the fact that new bone formation and bone destruction may both occur in spondylorthritis. Here, we describe the use of chemical shift-encoded MRI as a quantitative method for assessing inflammation of the sacroiliac joints. Specifically, we demonstrate the use of proton-density fat fraction and R2* as measures of bone marrow composition and structure, respectively, in both active and chronic inflammation.

1615

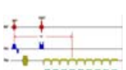

Application of lower extremity oxygenation imaging in animal model of microsphere-induced femoral artery embolization

Chengyan Wang[1], Haochen Wang[2], Bihui Zhang[2], Rui Zhang[3], Xiaodong Zhang[4], Min Yang[2], Jue Zhang[1,3], Xiaoying Wang[1,4], and Jing Fang[1,3]

[1]Academy for Advanced Interdisciplinary Studies, Peking University, Beijing, People's Republic of China, [2]interventional radiology and vascular surgery, Peking University First Hospital, Beijing, People's Republic of China, [3]College of Engineering, Peking University, Beijing, People's Republic of China, [4]Department of Radiology, Peking University First Hospital, Beijing, People's Republic of China

Embolization following percutaneous intervention is a universal problem occurring in all vascular beds, especially in lower extremities. This study assesses the performance of a noninvasive MRI based oxygenation imaging, in characterizing muscle oxygen extraction fraction (OEF) level after microsphere-induced lower extremity embolization in animal models. By comparison of the calculated muscle OEFs and R2' before and after surgery, significantly increase could be found. The results show promise in the evaluation of early muscle ischemia in many clinical diseases such as acute lower limb embolism or peripheral artery disease.

1616

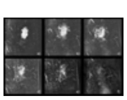

Age estimation of soft tissue hematomas using 3.0 T MRI: A feasible approach

Kathrin Ogris[1], Thomas Widek[2], Eva Hassler[3], Andreas Petrovic[4], Thorsten Schwark[1,2], Peter Grabuschnigg[1], and Eva Scheurer[5]

[1]Institute of Forensic Medicine, Medical University of Graz, Graz, Austria, [2]Ludwig Boltzmann Institute Clinical Forensic Imaging, Graz, Austria, [3]Division of Neuroradiology, Vascular and Interventional Radiology, Department of Radiology, Medical University of Graz, Graz, Austria, [4]Institute of Medical Engineering, Graz University of Technology, Graz, Austria, [5]Institute of Forensic Medicine, University of Basel - Health Department Basel, Basel, Switzerland

Forensic imaging requires reliable analysis of hematomas and their resolution as they can have significant medico-legal consequences. In 30 healthy volunteers autologous blood was injected into the subcutaneous fatty tissue of the thigh and repetitive MRI scans of the artificial hematoma were performed on a 3T scanner. Due to the contrast behavior three relevant age ranges were defined and validated. The generated approach correctly classified all tested hematomas with an age less or equal 24 hours. The development of a reliable and objective MR-based age estimation method of hematomas is in the interest of justice.

1617

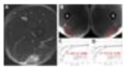

Assessment of the Myotendinous Junction After Injury in Elite Athletes Using 3D Ultrashort Echo Time Magnetization Transfer (UTE-MT) Imaging and Modeling

Yajun Ma[1], Heinz R Hoenecke[2], Douglas G Chang[3], Jiang Du[1], and Eric Y Chang[1,4]

[1]University of California, San Diego, San Diego, CA, United States, [2]Orthopedic Surgery, Scripps Clinic, San Diego, California, USA, [3]Orthopedic Surgery, University of California, San Diego, United States, [4]Radiology Service, VA San Diego Healthcare System, San Diego, United States

Myotendinous injuries are very common in sports, most often affecting the lower extremities. Both clinical examination and MRI have been widely used for the diagnosis and prognosis of acute myotendinous injuries. However, current paradigms remain insufficient as re-injury rates are as high as 34%. For elite athletes, the balance between rehabilitation time and risk of re-injury after return to play can be extremely challenging. Using conventional MRI techniques, clinical interpretation focuses on the evaluation of edema, fluid, and hemorrhage rather than the assessment of the injured/healing components of the myotendinous junction. Furthermore, immature and mature fibrous scar tissue as well as native tendon have very short T2 values and are “invisible” with clinical MRI, thus precluding their distinction and assessment. A technique to quantitatively characterize macromolecules in injured/healing myotendinous junctions could be particularly useful in recovering athletes.

1618

2D Adiabatic UTE T1rho Imaging: Reduced Sensitivity to the Magic Angle Effect

Yajun Ma[1], Yanchun Zhun[1], Jiang Du[1], and Eric Y Chang[1,2]

[1]Radiology, University of California, San Diego, San Diego, CA, United States, [2]Radiology Service, VA San Diego Healthcare System, San Diego, United States

Spin lattice relaxation in the rotating frame (T1rho) has been proposed as a biomarker to probe biochemical changes in cartilage. It reflects the slow interactions between motion-restricted water molecules and their local macromolecular environment, and provides unique biochemical information in the low frequency region ranging from a few hundred hertz to a few kilohertz. Changes to the extracellular matrix (ECM), such as proteoglycan (PG) loss, may be reflected in measurements of T1rho and T1rho dispersion. However, T1rho based on conventional continuous wave (CW) spin-locking preparation pulses demonstrate strong magic angle effects. Studies have shown an increase of over 100% in measured T1rho when the fibers were oriented from parallel to 54° relative to the B0 field. Adiabatic T1rho has been proposed to reduce the magic angle effect. However, many joint tissues such as the deep layers of articular cartilage, menisci, ligaments and tendons have short T2 relaxation and cannot be reliably imaged and quantified using the adiabatic T1rho sequence. In this study we aimed to develop a novel 2D adiabatic ultrashort echo time (UTE) T1rho sequence for magic angle insensitive imaging of both short and long T2 tissues in the joint.

1619

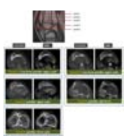

Efficacy of double inversion recovery MR imaging in evaluation of the synovium without contrast enhancement

Wook Jin[1], YeNa Son[1], Geon-Ho Jahng[1], Jang Gyu Cha[2], Seong Jong Yun[1], and Kyung Nam Ryu[3]

[1]Radiology, Kyung Hee University Hospital at Gangdong, Seoul, Korea, Republic of, [2]Radiology, Soonchunhyang University Bucheon Hospital, Buchoen, Korea, Republic of, [3]Radiology, Kyung Hee University Medical Center, Seoul, Korea, Republic of

A double-inversion recovery (DIR) sequence simultaneously voids two sources of signals from two different tissues by applying two 180 degree inversion pulses before a signal acquisition. To investigate the efficacy of the DIR image in visualization of the knee synovium without contrast enhancement, contrast-enhanced T1-weighted fat suppressed images (CET1FS) were compared with DIR images in knee MR. Our results showed DIR images were well correlated with CET1FS images.

1620

The use of quantitative perfusion metrics in evaluating the relationship between perfusion level and intervertebral disc degeneration

jiao wang[1], yun fei zha[1], dong xing[1], bing wu[2], and hui lin[2]

[1]Department of Radiology,Renmin Hospital of Wuhan University, wu han, People's Republic of China, [2]GE healthcare China

To explore the relationship between perfusion level and intervertebral disc degeneration.18 individuals underwent MRI exams including DCE-MRI, T2*mapping as well as conventional lumbar imaging. The cranial and caudal VSB and CEP perfusion parameters (Ktrans, Kep, Ve) as well as T2* values of discs were measured. it was found that T2* showed a negative correlation with the Pfirrmann grades, while showed no correlation with the perfusion parameters.

1621

A Prospective, Longitudinal Assessment of Adverse Local Tissue Reactions in Resurfacing Hip Arthroplasty Versus Primary Total Hip Arthroplasty

Matthew F. Koff[1], Owen G. Drinkwater[1], Danyal G. Nawabi[2], Edwin Su[3], Douglas Padgett[4], and Hollis G. Potter[1]

[1]Department of Radiology and Imaging, Hospital for Special Surgery, New York, NY, United States, [2]Department of Orthopedic Surgery - Hip Preservation Service, Hospital for Special Surgery, New York, NY, United States, [3]Department of Orthopedic Surgery - Adult Reconstruction and Joint Replacement Service, Hospital for Special Surgery, New York, NY, United States, [4]Department of Orthopedic Surgery - Adult Reconstruction and Joint Replacement Service - Adult Reconstruction and Joint Replacement Service, Hospital for Special Surgery, New York, NY, United States

Total hip arthroplasty devices are successful achieving pain reduction, but adverse local tissue reactions (ALTRs) frequently occur for metal-on-metal hip resurfacing arthroplasty (HRA) patients. This longitudinal study evaluated if HRA patients have a greater prevalence of ALTRs as compared to ceramic-on-poly (COP) patients. Images were acquired at 2 time points, with a 1 year interval, and evaluated for synovitis and ALTR. ALTR prevalence and synovial thickness was greater in HRA than COP subjects at both time points, with significant increases at the second time point. This study will permit a better understanding of the natural history in the development of ALTR near arthroplasty.

1622

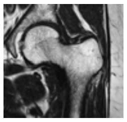

In vivo assessment of trabecular bone in the proximal femur

Maria Kalimeri[1], Christiani Jeyakumar Henry[2], Su Xiao Di[3], Marlena C Kruger[4], and John James Totman[5]

*[1]A*STAR-NUS Clinical Imaging Research Centre, Singapore, Singapore, [2]Clinical Nutrition Research Centre, Singapore, Singapore, [3]Institute of Materials Research and Engineering, Singapore, Singapore, [4]School of Food and Nutrition, Massey Institute of Food Science and Nutrition, Massey University, New Zealand, [5]Diagnostic Radiology, A-STAR-NUS Clinical Imaging Research Centre, Singapore, Singapore*

Osteoporosis is a bone disease that predominately affects postmenopausal women. Routine screening of osteoporosis is performed by means of Dual X-ray Absorptiometry (DXA) which is limited by its inability to differentiate between cortical and trabecular bone, reduced accuracy due to overlying tissue and the use of ionising radiation. In this abstract, we investigate the use of MRI as an alternative, in a cohort of 95 Chinese-Singaporean postmenopausal women. Strong correlations with DXA measurements were observed, in addition to significant differences between the normal and osteopenic, normal and osteoporotic groups.

Traditional Poster

fMRI Acquisition & Analysis

Exhibition Hall 1623-1656 — Tuesday 8:15 - 10:15

1623

Isotropic High Spatial Resolution fMRI Using Accelerated Variable Density Spiral and SLIDER

Xuesong Li[1], Xiaodong Ma[1], Lyu Li[1,2], Yan Tong[3], Sen Song[4], and Hua Guo[1]

[1]Center for Biomedical Imaging Research, Department of Biomedical Engineering, School of Medicine, Tsinghua University, Beijing, People's Republic of China, [2]Philips Healthcare, Shanghai, People's Republic of China, [3]FMRIB Centre, Nuffield Department of Clinical Neurosciences, John Radcliffe Hospital, Oxford, United Kingdom, [4]Department of Biomedical Engineering, School of Medicine, Tsinghua University, People's Republic of China

fMRI with high spatial resolution is beneficial for studies in psychology and neuroscience, but is limited by various factors such as prolonged imaging time and low signal-to-noise ratio. In this work, we combined Dual-TRACER method with SLIDER technique to obtain up to 1mm isotropic fMRI image, while maintaining temporal resolution comparable with conventional acquisition. Using the proposed method, finger somatotopy maps were successfully located on a 3T scanner.

1624

Dual-Echo Cardiac Gating Spiral Sequence for Cervical Spine fMRI

Christine Law[1] and Gary Glover[1]

[1]Stanford University, Stanford, CA, United States

We optimized a spiral sequence for dual-echo cardiac gating applied to cervical spine fMRI. Dual-echo obviates dependency on variable initial longitudinal magnetization that would, otherwise, require T1 correction. Spiral acquisition allows short echo time and readout duration which maximizes SNR and BOLD contrast. Our technique improves tSNR and fMRI activation when compared with ungated sequence.

1625

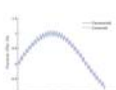

Frequency offset correction for accelerated 3D-EPI with segmented reference data

Martina F Callaghan[1], Nadège Corbin[1], Marina Papoutsi[2], Nikolaus Weiskopf[1,3], and Oliver Josephs[1]

[1]Wellcome Trust Centre for Neuroimaging, UCL Institute of Neurology, London, United Kingdom, [2]Huntington's Disease Research Centre, Institute of Neurology, UCL, London, United Kingdom, [3]Department of Neurophysics, Max Planck Institute for Human Cognitive and Brain Sciences, Leipzig, Germany

3D-EPI is beneficial for real-time fMRI applications because the acquisition can be accelerated in both the in-plane and through-plane phase-encoded directions significantly increasing temporal resolution. Fully-sampled reference data are required in order to map coil sensitivities and unfold the aliased images that result. Acquiring these data with a segmented EPI readout matches the EPI-related distortions and dropouts between the un-accelerated reference data and the accelerated fMRI data. However, systematic differences in eddy-current-related phase between the segments can introduce errors during frequency offset correction (employed to correct for slow frequency drifts) unless accounted for. Here we present a simple correction scheme that greatly improves the tSNR of the time series.

1626

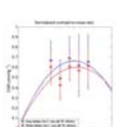

Echo-time optimization in Spin Echo EPI fMRI using BOLD-sensitivity models and hypercapnic manipulation at 3T

Don Marcial Ragot[1,2] and Jean Chen[1,2]

[1]Dept. of Medical Biophysics, University of Toronto, Toronto, ON, Canada, [2]Rotman Research Institute, Toronto, ON, Canada

The preferred echo-time (TE) used in most spin-echo EPI (SE-EPI) fMRI studies is approximately the tissue T2 value (65–100ms at 3 T). In this study, we use a hypercapnia paradigm with SE-EPI and three metrics of BOLD-sensitivity to model the TE that maximizes BOLD detection at 3 T. We concluded that while the maximal absolute BOLD contrast occurs near tissue T2 (~75ms), a TE of 55ms both maximizes tissue CNR and minimizes BOLD effects from non-neuronal sources.

1627

Local B0 temporal instability detected using a modified Multi-Echo GRE-EPI sequence with Flipped-Blips (MEPI-FB): application to fMRI with visual presentation of faces

Catarina Rua[1,2], Mark R. Symms[3], Brice Fernandez[4], Ana Beatriz Solana[5], Mauro Costagli[2], Alberto Del Guerra[1], and Michela Tosetti[2,6]

[1]Department of Physics, University of Pisa, Pisa, Italy, [2]Imago7 Research Center, Pisa, Italy, [3]GE Healthcare, Pisa, Italy, [4]GE Healthcare, Orsay, France, [5]GE Global Research, Munich, Germany, [6]IRCCS Stella Maris, Pisa, Italy

Field-mapping techniques using a reference scan allow accurate distortion correction of EPI data. However, due to the strong B_0 dependency with head motion and other physiological artefacts in fMRI acquisitions, the reference field-map does not adequately correct for dynamic non-linear changes in image intensity. In this work we show the feasibility of a method to map temporal variations of the B_0-field at 7 Tesla, using a high-resolution Multi-echo EPI sequence, acquiring three echo-modules with reverse phase-encoding direction on the second echo. The robustness of the method was tested during an fMRI acquisition with visual presentation of faces.

1628

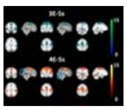

Less may be better: comparison of Multi-Echo-ICA de-noising for three and four echo EPI acquisitions in studies of seed-based functional connectivity

Jed Wingrove[1], Owen O'Daly[1], and Fernando Zelaya[1]

[1]Centre for Neuroimaging Sciences, IoPPN, King's College London, London, United Kingdom

This work is a formal comparison between different echo acquisitions (3 and 4 echo) for the use with multi-echo independent component analysis de-noising of resting-state functional MRI data. We look to evaluate and determine the optimal acquisition required for de-noising of resting state data which is often plagued with artifacts and noise.

1629

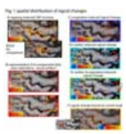

Cortical Depth-Dependent Physiological Noise Cleaning in High-Resolution VASO Imaging

Andrew Hall[1], Laurentius Huber[2], Daniel A Handwerker[3], Javier Gonzales-Castillo[3], Natasha Topolski[3], and Peter A Bandettini[3]

[1]Section on Functional Imaging Methods, NIH/NIMH, Bethesda, MD, United States, [2]section on functional imaging methods, NIH/NIMH, [3]NIH/NIMH

As functional analyses move toward finer detail and higher resolution, sources of noise that were nuisances are now becoming more significant. While noise removal is well studied in lower-resolution, gradient echo BOLD-weighted imaging, it is not as well understood in high resolution VASO. We examine the efficacy of physiological noise cleaning methods that are commonly used in many fMRI studies.

1630

Validation of Motion Correction with Multiband SLOMOCO using Multiband SimPACE

Xiaopeng Zhou[1], Wanyong Shin[1], Erik Beall[1], and Mark Lowe[1]

[1]The Cleveland Clinic, Cleveland, OH, United States

A Multiband version of the SimPACE sequence was developed to validate multiband SLOMOCO motion correction method. With the increasing use of simultaneous multi-slice acquisition techniques to acquire fMRI data more efficiently, the traditional motion correction methods need to be modified or improved to better correct subject motion in fMRI. This preliminary study showed that multiband SLOMOCO can detect the outermost slice motion better than single-slice SLOMOCO. Multiband SimPACE is a promising sequence to further facilitate the improvement of motion correction methods including multiband SLOMOCO.

1631

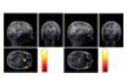

Impact of prospective motion correction in 7T fMRI studies

Arturo Cardenas-Blanco[1,2], David Berron[2], Yi Chen[2], Hendrik Mattern[3], Renat Yakupov[3], Alessandro Sciarra[3], Oliver Speck[1,3,4,5], and Emrah Düzel[1,2]

[1]DZNE, Magdeburg, Germany, [2]Institute of cognitive neurology and dementia research (IKND), Magdeburg, Germany, [3]Department of Biomedical Magnetic Resonance, Institute of Experimental Physics, Otto-von-Guericke-University, Magdeburg, Germany, [4]Center for Behavioral Brain Sciences, Magdeburg, Germany, [5]Leibniz Institute for Neurobiology, Magdeburg, Germany

Recently, more fMRI studies are aiming to assess the role of small anatomical regions of the brain in cognitive processes which requires sub-millimiter voxel resolution. At high resolution rigid body motion during the acquisition plays a significant role. The aim of this study is to assess the potential benefits of correcting for subject motion introduced distortions and image degradation prospectively in fMRI studies. This study demonstrates that prospective motion correction increases tSNR and therefore increases sensitivity. These results increment the potential applications of fMRI to unveil, more accurately, the role of smaller parts of the brain in different cognitive processes.

1632

Phase-offset Multiplanar Echo-planar Imaging (POMP-EPI) to Accelerate fMRI Acquisition without Parallel Imaging

Patricia Lan[1], Haisam Islam[1], and Gary Glover[1]

[1]Stanford University, Stanford, CA, United States

Simultaneous-multislice (SMS) has significantly improved fMRI acquisition due to its increase in SNR efficiency. However, SMS requires parallel-imaging in the slice-direction, which may be inapplicable due to the scarcity of receiver-coils with adequate sensitivity in the slice-direction. Hence, we propose the POMP-EPI method, which accelerates fMRI acquisition without using parallel-imaging. POMP-EPI works by using Gz-gradient blips in an EPI sequence to shift each of the simultaneously excited slices into different regions of an extended FOV, such that no aliasing occurs, resulting in simple reconstruction of images, shorter TRs, and increased SNR efficiency.

1633

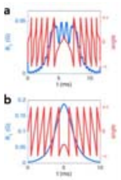

High-resolution semi-adiabatic spin-echo fMRI at 7T.

Haisam Islam[1], Christine Law[2], Gary Glover[3], and Priti Balchandani[4]

[1]Bioengineering, Stanford University, Stanford, CA, United States, [2]Stanford University, Stanford, CA, United States, [3]Radiology, Stanford University, Stanford, CA, United States, [4]Radiology, Neuroscience, Mount Sinai, NY, United States

Spin-echo fMRI provides greater functional specificity than gradient-echo fMRI, but suffers from lower sensitivity. At higher field strengths, the spin-echo signal contribution from smaller capillaries, closer to the site of neural activity, increases. A major challenge of MRI at high field strengths, however, is increased B1 inhomogeneity, which can impact the performance of RF pulses, in particular refocusing pulses. Here, we use an adiabatic refocusing pulse and a matched-phase excitation pulse to perform high-resolution spin-echo fMRI at 7T. We compare the results to a similar gradient-echo acquisition, and show sharper activation better localized to gray matter in the spin-echo results.

1634

Simultaneous brain and spinal cord fMRI using slice-based dynamic shimming

Haisam Islam[1], Christine Law[2], and Gary Glover[2]

[1]Bioengineering, Stanford University, Stanford, CA, United States, [2]Stanford University, Stanford, CA, United States

Simultaneous brain and spinal cord fMRI would be beneficial for studying the nervous system, but is challenging due to the poor B0 homogeneity and small size of the spinal cord. Here, we used dynamic shimming and reduced FOV imaging to address these issues. We obtained improved T2*-weighted images of brain and spinal cord with high clarity. We validated the method for fMRI applications using an fMRI experiment with a fist-clenching task, in which we obtained activation in all regions expected to be involved in the task, including the motor cortices, cerebellum, and C6-C8 spinal cord region.

1635

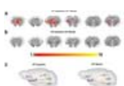

Mu opioid receptor activation signatures on brain activity and connectivity by fMRI in mice

Md Taufiq Nasseef[1], Emmanuel Darcq[1], Praveen Kulkarni[2], and Brigitte L. Kieffer[1]

[1]Department of Psychiatry, Douglas Mental Health University Institute, Montreal, QC, Canada, [2]Center for Translational Neuro-Imaging, Northeastern University, Boston, MA, United States

Mu opioid receptors (MORs) mediate the strong analgesic and rewarding effects of morphine. We used non-invasive imaging fMRI in wild-type and MOR knockout mice to assess MOR-dependent effects at the scale of the whole brain. Here, we present striatum seed-based signatures identified by BOLD activation map, functional connectivity and directionality. We identified MOR-specific activation of the striatum between 2 and 7 minutes after morphine administration. Furthermore, during this time interval, the brain connectivity was altered by morphine in wild type but not mutant mice. This is the first reported on-target morphine activation signature in the striatum of live animals.

1636

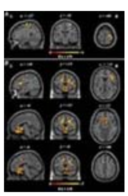

Altered Spontaneous Brain Activity in Children with type 1 Gaucher disease: a Resting-state fMRI Study

Di Hu[1], Shengpei Wang[2], Huiying Kang[1], Xiaolu Tang[1], Hong Zhang[1], Huiguang He[2], and Yun Peng[1]

[1]Beijing children's hospital, Beijing, People's Republic of China, [2]Research Center for Brain-inspired Intelligence, Institute of Automation, Chinese Academy of Sciences, Beijing, People's Republic of China

This is the first study to examine differences in spontaneous neural activity between GD patients and healthy controls. Our results indicate that decreased of neural activity in motor area; increased neural activity in the olfaction-, vision- and algesthesia -related structures; dysfunction of neural activity in emotion- , recognition- and speech- related structures and cerebellum. These results promote a further understanding of underlying neurophysiological mechanisms in the intrinsic brain of GD type I, which will aid in the development of treatment plans for GD type I patients that address both physical and psychological concern and preventing neurological disease in early stage.

1637

Resting-state network patterns in extremely preterm born young adults

Michael Hütel[1], Andrew Melbourne[1], Joanne Beckmann[2], Jonathan Rohrer[1], Neil Marlow[2], and Sebastien Ourselin[1]

[1]UCL, London, United Kingdom, [2]Institute for Women's Health, University College Hospital

Rates of extreme-prematurity are increasing worldwide. Neuroimaging studies allow us to investigate the underlying tissue substrate of the broader neuropsychological differences observed in preterm cohorts; but the long-term neuroimaging phenotype of extremely-preterm adolescents is relatively unknown. Here we investigate resting-state functional MRI to establish if there is a variability in the pattern of functional networks in extremely-preterm born 19 year-olds relative to a group of their term-born peers.

1638

Comparison of fMRI analysis methods for heterogeneous BOLD responses in block design studies

Jia Liu[1], Ben A Duffy[1], David Bernal-Casas[1], Zhongnan Fang[1], and Jin Hyung Lee[1]

[1]Stanford University, Palo Alto, CA, United States

Improper selection of analysis methods can lead to significant errors when analyzing fMRI data with heterogeneous BOLD responses. Here, we used rodent optogenetic fMRI data and simulations to investigate different analysis methods' detection and characterization performance. Our results show that, in the presence of heterogeneous BOLD responses, conventionally used GLM with a canonical basis set leads to considerable errors, while the gamma, finite impulse response, B-spline, and Fourier basis sets show robust performance.

1639

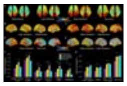

Differential Reduction of Repertoire of Functional Patterns in Sensory and Cognitive Neuronal Systems in Propofol Anesthesia

Xiaolin Liu[1], Kathryn K Lauer[2], B. Douglas Ward[3], Christopher Roberts[2], Gollapudy Suneeta[2], Suyan Liu[2], William Gross[2], Shi-Jiang Li[3], Jeffrey Binder[4], and Anthony G Hudetz[5]

[1]Radiology, Medical College of Wisconsin, Milwaukee, WI, United States, [2]Anesthesiology, Medical College of Wisconsin, Milwaukee, WI, United States, [3]Biophysics, Medical College of Wisconsin, Milwaukee, WI, United States, [4]Neurology, Medical College of Wisconsin, Milwaukee, WI, United States, [5]Anesthesiology, University of Michigan, Ann Aobor, MI, United States

We propose that the diversity of distinct functional patterns of the brain can be quantified by the variance explained by the first few principal components of regional voxel functional imaging signals. We report that propofol sedation is associated with a global reduction of repertoire of functional patterns. While sensory-processing-related and high-order cognitive-processing-related brain regions both showed a reduction during propofol sedation, it was the changes in the sensory-processing-related regions that correlated the loss and return of consciousness. The findings provided important insights into anesthetic modulation of different neuronal systems and the neural correlates of consciousness at the systems level.

1640

Control study of arterial spin labeling and multi-phase enhancement technique in evaluation of renal blood flow in different age population

Yimin Wang[1], Ailian Liu, Jinghong Liu, Meiyu Sun, Qingwei Song, Ye Li, Anliang Chen, Shifeng Tian, and Hanpei Zhang

[1]The First Affiliated Hospital of Chengdu Medical College, Chengdu, People's Republic of China

This study is aim to assess ability of arterial spin labeling technique(ASL) and multi-phase enhanced magnetic resonance (MCE-MR) of evaluate renal perfusion in different ages population with normal renal function by 1.5T MRI. Meanwhile, to evaluate difference between ASL and MCE-MR of renal perfusion.

1641

Predicting Diffusion Tensors from Resting-State Functional MRI

Lichi Zhang[1], Han Zhang[1], Qian Wang[2], Pew-Thian Yap[1], Xiaobo Chen[1], and Dinggang Shen[1]

[1]Department of Radiology and BRIC, University of North Carolina at Chapel Hill, Chapel Hill, NC, United States, [2]Med-X Research Institute, School of Biomedical Engineering, Shanghai Jiao Tong University, Shanghai, People's Republic of China

It has been recently reported that the spatio-temporal correlation of white matter BOLD signals in resting-state functional MRI (rs-fMRI) can be captured using functional correlation tensors (FCTs). FCTs exhibit anisotropy information similar to diffusion tensor imaging (DTI). In this work, we employ a patch-based strategy to improve the noise-robustness of FCTs. Then, we adopt regression forest to learn a mapping from FCTs to DTs. Testing using unseen images, the predicted DTs show high similarity with the actual DTs. This validates the fact that FCTs carries information that is highly correlated with DTs.

1642

Group differences in default mode network connectivity not just anti-correlation depend on choice of nuisance regressor model

William J Cottam[1,2,3] and Dorothee P Auer[1,2,3]

[1]Radiological Sciences, Division of Clinical Neuroscience, University of Nottingham, Nottingham, United Kingdom, [2]Arthritis Research UK Pain Centre, University of Nottingham, Nottingham, United Kingdom, [3]Sir Peter Mansfield Imaging Centre, University of Nottingham, Nottingham, United Kingdom

Resting state fMRI is prone to a large range of factors affecting the acquired data and processing pipelines available, which can impact on the outcome of a study. This study assessed the similarity of time series taken from aCompCor outputs to global signal to assess the inclusion of a 'proxy' global signal and its effect on group-wise tests of default-mode connectivity. The first components of both white matter and CSF were highly correlated with global signal and regressing either global signal or aCompCor outputs altered group-comparisons of functional connectivity. Future studies should scrutinise and report their postprocessing pipelines clearly.

1643

Reduction of Scanner's Noise in Recorded Voice Responses Using an Inline Reference Scanner's Noise for Automated Measurement of Voice Response Time in Overt Speech fMRI

Kwan-Jin Jung[1] and Jacquie Kurland[2]

[1]Institute of Applied Life Sciences, Human MR Center, University of Massachusetts Amherst, Amherst, MA, United States, [2]Department of Communication Disorders, University of Massachusetts Amherst, Amherst, MA, United States

The overt voice response in fMRI is critical to aphasia neuroimaging studies. A commercially available active noise cancelling microphone makes this application possible. However, an automated measurement of the voice response time is not reliable due to remaining scanner noises. The incomplete noise cancellation is due to uneven slice time intervals in the EPI sequence. The remaining noise was reduced using a post-processing approach based on a previously published method that used a template of a reference noise. The response time was measured from the noise-reduced voice signal using an amplitude and duration threshold after an envelope filtering.

1644

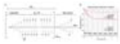

Distortion-free fMRI using multi-slice 2D-bSSFP at 7 tesla

Olivier Reynaud[1], Ileana Ozana Jelescu[1], and Rolf Gruetter[1]

[1]*CIBM, EPFL, Lausanne, Switzerland*

Balanced Stead-State Free Precession (bSSFP) techniques have been proposed as an alternative to GE-EPI to address the problem of co-registration between functional/structural scans at high field. However, 3D imaging is suboptimal for localized fMRI applications, and result in distortions, blurring, and increased sensitivity to motion/physiological noise. Here, we propose to use 2D-bSSFP and cartesian readouts and demonstrate that (i) bSSFP signal characteristics are preserved in a new steady-state, (ii) resting-state fMRI (RS-fMRI) can be performed with 2D-bSSFP, (iii) the 2D-bSSFP temporal SNR levels with that of 3D-bSSFP, resulting in - at least - equal fMRI performances at high field.

1645

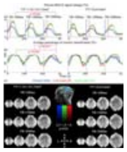

7T-fMRI: Faster temporal resolution increases BOLD sensitivity and fMRI-based decoding performance specifically at high-spatial resolution

Peter E Yoo[1], Sam E John[2], Shawna Farquharson[1,3], Thomas J Oxley[4], Sonal Josan[5], Roger J Ordidge[1], Jon O Cleary[1], and Bradford A Moffat[1]

[1]*Anatomy and Neuroscience, The University of Melbourne, Melbourne, Australia,* [2]*Department of Electrical & Electronic Engineering, The University of Melbourne, Australia,* [3]*Imaging Division, Florey Institute of Neuroscience and Mental Health, Melbourne, Australia,* [4]*Department of medicine and Neurology, The University of Melbourne, Australia,* [5]*Siemens Healthcare, Melbourne, Australia*

The benefits of ultra-high fMRI are maximized at high spatial resolutions with less physiological noise contribution. However, increasing the temporal resolution is often avoided at such high spatial resolutions due to limitations in the temporal signal-to-noise-ratio (tSNR). We investigated the effects of varying spatial and temporal resolutions on fMRI sensitivity measures at 7T, and their implications on an fMRI application, Brain-Computer-Interface (BCI). We demonstrate overall BOLD sensitivity increased with temporal resolution despite the tSNR decrease specifically at high-spatial resolution 7T-fMRI. We further demonstrate that this sensitivity increase also improved the accuracy of linear classifiers commonly used in BCIs.

1646

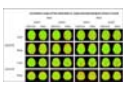

Automatic physiological noise estimator with PESTICA in HCP resting state fMRI data

Wanyong Shin[1], Erik Beall[1], and Mark J Lowe[1]

[1]*Radiology, Cleveland Clinic, Cleveland, OH, United States*

Recent work with accelerated HCP rs-fMRI data shows strong correlation with non-neuronal noise sources, and their noise patterns appears to be linked across simultaneously excited slices (SMS)[1,2]. To correct for these noise sources, a measurement of physiologic cycles is needed, which can be supplied by monitoring, but not always available or accurate, or PESTICA which estimates physiological signal fluctuation from EPI data itself[3]. If the noise is dependent on SMS location, PESTICA could more efficiently detect physiologic signal fluctuation in HCP fMRI. In this study, we modified PESTICA for the SMS acuisition and evaluated performance compared with monitored physiological signals

---

1647

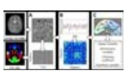

Investigating Altered Brain Functional Network in Alzheimer's Disease Using a Joint Framework of Graph Theoretical Analysis and Machine Learning

Chen-Pei Lin[1], Shih-Yen Lin[1,2], Chia-Wen Chiang[1], Kuan-Hung Cho[1], Chien-Yuan Lin[3,4], and Li-Wei Kuo[1,5]

[1]*Institute of Biomedical Engineering and Nanomedicine, National Health Research Institutes, Miaoli, Taiwan,* [2]*Department of Computer Science, National Chiao Tung University, Hsinchu, Taiwan,* [3]*GE Healthcare, Taiwan,* [4]*GE Healthcare MR Research China, Beijing, People's Republic of China,* [5]*Institute of Medical Device and Imaging, National Taiwan University College of Medicine, Taiwan*

The progressive decline in cognitive abilities occurred in the early stage of Alzheimer's disease (AD) is often difficult to be distinguished from the symptoms of mild cognitive impairment (MCI). This study incorporated graph theoretical analysis and machine learning approach to investigate the alterations of brain functional network in AD. Statistical approach demonstrated regions with significantly altered network characteristics, which were also reported to be linked to AD in previous studies. Machine learning approach using TensorFlow also showcases the significant discriminative power of the brain network measures. Future work includes incorporation of other type of network measures, behavior and biochemical assessments, and more complex deep learning models.

1648

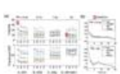

Modeling serial correlations in fMRI time series collected by faster TRs

Jingyuan Chen[1] and Gary Glover[2]

[1]*Electrical Engineering & Radiology, Stanford University, Stanford, CA, United States,* [2]*Electrical Engineering & Radiology, Stanford University, CA, United States*

Serial correlations of fMRI time series are altered at faster TRs (<1s) due to reduced signal to noise ratio per time frame. Thus, caution is advised when utilizing serial correlation models describing long TR (2~3s) conditions with fast acquisitions. Here, we show that statistical models alternative to the commonly used first order auto-regressive (AR) model – AR2 and AR1moving-average(MA)1 model —can achieve reasonable fitting for short TR data and improve the accuracy of activation estimates. Potential model bias can be further reduced by low-pass filtering.

1649

Measurement of high frequency band signals by ultra-high temporal resolution imaging in task-based fMRI

Yul-Wan Sung[1], Daehun Kang[1,2], and Seiji Ogawa[1]

[1]*Kansei Fukushi Research Institute, Tohoku Fukushi University, Sendai, Japan,* [2]*GSIS and RIEC, Tohoku University, Sendai, Japan*

Recent advances in MRI technique such as the multiband sequence have made fast sampling available up to 100-200 ms TR for whole brain acquisition. However, its usefulness is limited because there is not found any significant functional changes needed to be sampled with that short TR. In this study, we challenged to detect task-induced fast signals with the ultra-high temporal resolution imaging with 100 Hz sampling rates.

1650

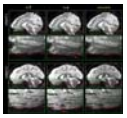

Correction of EPI geometric distortion in slice direction using reversed slice-select gradients and topup

Anna I. Blazejewska[1], Thomas Witzel[1], Lawrence L. Wald[1,2], and Jonathan R. Polimeni[1]

[1]A.A. Martinos Center for Biomedical Imaging, MGH/Harvard, Charlestown, MA, United States, [2]Division of Health Sciences and Technology, Harvard-MIT, Cambridge, MA, United States

Conventional single-shot Echo Planar Imaging (EPI) protocols used by fMRI studies suffer from geometric distortion occurring in the phase-encoding direction. Ultrahigh field (>3T), high-resolution fMRI using thin slices requires decrease of the slice-encoding bandwidth, which may lead to the additional geometric distortions and “slice bending” in the slice-encoding direction. Here we use gradient-echo (GRE) EPI sequence that allows the polarity of the slice-select gradient to be flipped between positive and negative values to demonstrate this effect and to enable the application of FSL’s topup to perform distortion correction. This correction will further improve geometric alignment of the EPI data with anatomical reference data used in fMRI studies.

1651

Improved specificity of high-resolution fMRI with surface-based cortical ribbon smoothing

Anna I Blazejewska[1], Oliver Hinds[2], and Jonathan R. Polimeni[1,3]

[1]Martinos Imgaing Center, MGH/Harvard, Charlestown, MA, United States, [2]Orchard Scientific, Somerville, MA, United States, [3]Division of Health Sciences and Technology, Harvard-MIT, Cambridge, MA, United States

High-resolution fMRI data enables strategies to improve spatial specificity of the measured fMRI activations through anatomically-informed sampling. Here we demonstrate that cortical surface-based smoothing of high-resolution data can improve the specificity of fMRI activations by simultaneously canceling thermal noise through spatial averaging while avoiding physiological noise contamination from superficial CSF and signal dilution from subjacent white matter. By combining both tangential and radial smoothing using our surface-based analysis framework, specificity of responses to a breathold challenge can be similar in high-resolution data natively sampled at 1.1 mm iso. and unsmoothed data at a conventional resolution of 3.0 mm iso.

1652

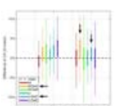

Optimal resolution for searchlight classification of BOLD fMRI data.

Hendrik Mandelkow[1], Jacco A de Zwart[1], Catie Chang[1], and Jeff H Duyn[1]

[1]Advanced MRI section, LFMI, NINDS, National Institutes of Health, Bethesda, MD, United States

Information-theoretic approaches to BOLD fMRI analysis, like the Searchlight method for multivariate pattern analysis (MVPA), suggest that distinctive local patterns of BOLD signal on a spatial scale of millimeters carry information that allows the classification or decoding of perceptual stimuli. In this study high-resolution (1.2mm) BOLD fMRI experiments at 7T combined with naturalistic movie stimuli reveal that Searchlight decoding primarily relies on a neurogenic BOLD signal that is spatially smooth, unlike the accompanying physiological artifacts. As a result the optimal fMRI resolution peaks between 2 and 4mm, a voxel size well above the technical limits of fMRI.

1653

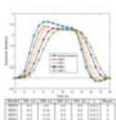

Optimization of white matter fMRI analysis using physiologically derived hemodynamic response functions

Matthew J Courtemanche[1], Carolyn J Sparrey[2], Xiaowei Song[3], Alexander MacKay[4,5], and Ryan CN D'Arcy[3,6,7]

[1]School of Mechatronic Systems Engineering, Simon Fraser University, Surrey, BC, Canada, [2]School of Mechatronic Systems Engineering, Simon Fraser University, [3]Fraser Health Authority, Surrey, BC, Canada, [4]Department of Physics, The University of British Columbia, Vancouver, BC, Canada, [5]Department of Radiology, The University of British Columbia, Vancouver, BC, Canada, [6]School of Computing Science, Simon Fraser University, Burnaby, BC, Canada, [7]School of Engineering Science, Simon Fraser University, Burnaby, BC, Canada

White matter functional MRI has been successfully demonstrated in studies using high-field scanners and customized sequences. In the current study, we demonstrated that conventional GRE EPI using 3T MRI replicated white matter activation in the corpus callosum at both the group and individual levels (61.5% of individuals). Importantly, hemodynamic response functions (HRF) using delayed-onset improved sensitivity to white matter activation over the canonical HRF developed from gray matter activity. The results suggest that white matter fMRI studies, which are increasingly reported in the literature, benefit significantly from optimization in acquisition and analysis methods.

1654

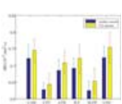

Characterization of structural and functional connectivity in epilepsy by integrating diffusion and functional tensor imaging

Jing Hu[1], Baxter P. Rogers[2,3], Xi Wu[1], Bennett Landman[2,4], Adam W. Anderson[2,5], Bassel Abou-Khalil[6], Victoria L. Morgan[2,3], and Zhaohua Ding[2,4]

[1]Department of Computer Science, Chengdu University of Information Technology, Chengdu, People's Republic of China, [2]Institute of Imaging Science, Vanderbilt University, Nashville, TN, United States, [3]Department of Radiology and Radiological Sciences, Vanderbilt University, Nashville, TN, United States, [4]Department of Electrical Engineering and Computer Science, Vanderbilt University, Nashville, TN, United States, [5]Department of Biomedical Engineering, Vanderbilt University, Nashville, TN, United States, [6]Department of Neurology, Vanderbilt University, Nashville, TN, United States

Although previous studies have tried to combine diffusion tensor imaging (DTI) and resting-state functional magnetic resonance imaging (rs-fMRI) in clinic studies, they only use rs-fMRI for gray matter and DTI for white matter pathways. In this study, DTI and rs-fMRI were leveraged for conjoint analysis of structural and functional connectivity in white matter. The results showed that in temporal lobe epilepsy patients, there was an increased functional fractional anisotropy in contralateral fiber bundles, which were accompanied by increases in mean diffusivity in ipsilateral bundles. This reflects complex interactions between disease evolution and compensatory adaption.

1655

On the relation between Global Signal Normalization, Global Signal Subtraction, and Global Signal Regression in Resting-State fMRI

Alican Nalci[1] and Thomas T. Liu[1]

[1]UCSD Center for Functional MRI, La Jolla, CA, United States

In resting-state fMRI, global signal regression (GSR), global signal subtraction (GSS) and global signal normalization (GSN) are widely used nuisance removal methods. So far these techniques have been treated as distinct operations and the relation between them has not been clearly described. In this paper, we mathematically and empirically show that GSS and GSN are nearly identical processes in resting-state fMRI. We further show that in terms of resting-state functional connectivity maps, GSS and hence GSN are similar processes to GSR when considering seed time courses that have a good fit to the global signal time course.

1656 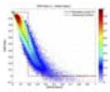

Global Signal Regression acts as a Temporal Downweighting Process in Resting-State fMRI

Alican Nalci[1] and Thomas T. Liu[1]

[1]UCSD Center for Functional MRI, La Jolla, CA, United States

Global signal regression (GSR) is a controversial preprocessing method in resting-state fMRI. It has been claimed that the process can introduce artifactual anti-correlations in resting-state connectivity maps. However, a consensus regarding its use has been lacking, due in part to the difficulty in understanding its effects. We show that GSR can be well approximated by a temporal downweighting of the voxel time series, where the weighting factor is a function of the global signal magnitude and is uniform across space. This helps address the concerns about GSR and provides a novel framework for understanding its effects on resting-state data.

Traditional Poster

fMRI: Mechanisms & Physiology

Exhibition Hall 1657-1680 Tuesday 8:15 - 10:15

1657 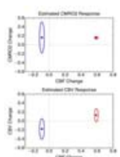

Quantifying the dynamics of cerebral blood flow, oxygen metabolism, and deoxygenated blood volume with a combined normoxia/hyperoxia method

Eulanca Y. Liu[1,2,3], Frank Haist[4,5], David J. Dubowitz[3,6], and Richard B. Buxton[3,6]

[1]Neurosciences Graduate Program, University of California, San Diego, La Jolla, CA, United States, [2]Medical Scientist Training Program, University of California, San Diego, La Jolla, CA, United States, [3]Center for Functional MRI, University of California, San Diego, La Jolla, CA, United States, [4]Psychiatry, University of California, San Diego, [5]Center for Human Development, University of California, San Diego, [6]Radiology, University of California, San Diego

To better understand the dynamics of the BOLD response in terms of CBF, $CMRO_2$, and deoxygenated blood volume, we used a combined normoxia/hyperoxia approach to untangle their relative contributions. This method was applied to both the positive activation response and the post-stimulus undershoot, the origins of which are still debated. A simple model of the BOLD response based on flow, metabolism, and volume, modified to include the effects of hyperoxia, was applied. For the origin of the undershoot, these data provide strong evidence for a CBF undershoot, moderate evidence for elevated $CMRO_2$, and no evidence for elevated CBV (Balloon Model).

1658 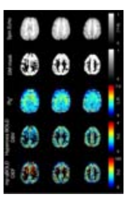

Improving qBOLD based measures of brain oxygenation using hyperoxia BOLD derived measures of blood volume

Alan J Stone[1] and Nicholas P Blockley[1]

[1]FMRIB, Nuffield Department of Clinical Neurosciences, University of Oxford, Oxford, United Kingdom

Measurements of deoxygenated blood volume (DBV) via the streamlined-qBOLD technique are larger than typically reported in the literature, resulting in underestimation of oxygen extraction fraction (OEF). In this study we address this limitation by acquiring a separate measurement of DBV using the BOLD response to the administration of oxygen, which has been shown to be specifically sensitive to venous blood volume. By combining measurements of the reversible transverse relaxation rate, R_2', and DBV to measure OEF, we were able to show better agreement with whole brain OEF from the TRUST method than OEF measured with streamlined-qBOLD.

1659 

Measurement of cerebral venous blood oxygen saturation via T2* fitting with velocity encoded phase imaging

Alberto Merola[1], Michael A Germuska[1], Kevin Murphy[1], and Richard G Wise[1]

[1]CUBRIC, Cardiff University, Cardiff, United Kingdom

Measurements of cerebral venous O_2 saturation with MRI would enable use to estimate brain O_2 consumption, a marker of brain activity. Here we propose a new method with this aim, that exploits a Fourier velocity encoding scheme combined with multi-echo acquisitions for estimating T_2* and then, through calibration curves, O_2 saturation. Synthetic data are analysed and pilot data from resting state and visual stimulus acquisitions (two subjects) are reported. The new method is shown to supply plausible estimates of baseline levels and changes in O_2 saturation in the sagittal sinus following stimulation.

1660 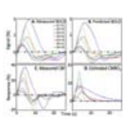

Estimation of cerebral metabolic rate of oxygen from measured hemodynamic response function and cerebral blood flow using arterial spin labeling

Jung Hwan Kim[1], Amanda Taylor[1], and David Ress[1]

[1]Neuroscience, Baylor College of Medicine, Houston, TX, United States

In the brain, brief neural activity creates changes in local blood flow (CBF) and oxygen uptake ($CMRO_2$). Functional magnetic resonance imaging (fMRI) can measure these changes as a blood oxygenation level dependent (BOLD) signal. The BOLD response to brief stimulations is often termed the hemodynamic response function (HRF). We recently proposed the Arterial Impulse model for the HRF based on a combination of underdamped CBF and $CMRO_2$ responses. Here, we used arterial spin-labeling (ASL) to measure both the BOLD HRF and CBF, and then used our model to obtain estimates of the $CMRO_2$ time course.

1661

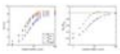

Correcting for imperfect spin echo refocusing in gas-free fMRI calibration

Avery JL Berman[1,2], Erin L Mazerolle[2], M Ethan MacDonald[2], Nicholas P Blockley[3], Wen-Ming Luh[4], and G Bruce Pike[1,2]

[1]Montreal Neurological Institute, McGill University, Montreal, QC, Canada, [2]Radiology and Hotchkiss Brain Institute, University of Calgary, Calgary, AB, Canada, [3]FMRIB Centre, Nuffield Department of Clinical Neurosciences, University of Oxford, Oxford, United Kingdom, [4]Cornell MRI Facility, Cornell University, Ithaca, NY, United States

Gas-free calibration is an appealing new alternative for calibrated fMRI. Using simulations, we determined that estimates of the calibration parameter, M, obtained directly by estimating R_2' with asymmetric spin echo imaging, are negatively biased. This is due to imperfect spin echo refocusing of spins diffusing in the extravascular space. When we modelled the spin echo attenuation as a quadratic-exponential decay, the imperfect refocusing effects were accurately accounted for over intermediate to large vessel sizes. When tested in vivo, increases in M were observed when using the quadratic model, however, additional sources of decay also contributed to M.

1662

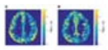

Dual-calibrated fMRI measurement of resting capillary and venous blood volumes

Michael Germuska[1], Alberto Merola[1], and Richard G Wise[1]

[1]CUBRIC, Cardiff University, Cardiff, United Kingdom

The potential for dual-calibrated fMRI to provide quantitative estimates of physiological parameters has been increasingly investigated. We present a novel analysis methodology to estimate capillary (CBV_{cap}) and venous (CBV_v) blood volumes. These parameter estimates are made in addition to standard physiological parameters (cerebral blood flow (CBF), oxygen extraction fraction (OEF), and cerebral metabolic rate of oxygen ($CMRO_2$)). Maps of CBV_{cap} demonstrate a marked reduction in the appearance of large vessels (compared to CBV_v data) and show significant correlations with CBF and $CMRO_2$. These findings suggest an important role for CBV_{cap} for assessing cerebral metabolic function and neurovascular coupling.

1663

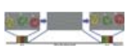

Measurements of the flow component of the hemodynamic response function in human cerebral cortex

David Ress[1] and JungHwan Kim[1]

[1]Neuroscience, Baylor College of Medicine, Houston, TX, United States

Brief cortical neural activity creates changes in local blood flow and oxygen uptake. Functional magnetic resonance imaging can measure this neurovascular coupling as a blood oxygen level dependent (BOLD) signal. The BOLD response to brief stimulation is termed the hemodynamic response function (HRF). We developed a computational model for the BOLD HRF, which predicts that the flow component of the HRF is a simple underdamped sinusoid. To test this prediction, we used arterial spin labeling to measure both CBF and BOLD responses in human cortex with high spatial and temporal resolution. Results confirm a significant flow undershoot in five subjects.

1664

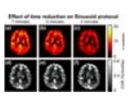

Rapid cerebrovascular reactivity mapping: Comparison of a sinusoid protocol with the conventional block protocol

Nicholas P Blockley[1], James W Harkin[2], and Daniel P Bulte[3]

[1]FMRIB Centre, Nuffield Department of Clinical Neurosciences, University of Oxford, Oxford, United Kingdom, [2]Department of Physics, University of Oxford, Oxford, United Kingdom, [3]Institute of Biomedical Engineering, University of Oxford, Oxford, United Kingdom

Cerebrovascular reactivity (CVR) mapping is a useful technique for *stress testing* the brain. However, clinical adoption of CVR mapping has so far been hindered by relatively long scan durations of 7-12mins. In this study we show that by using a sinusoidal carbon dioxide stimulus in place of a conventional block protocol, equivalent CVR maps can be produced in a much shorter scan duration of 3-5mins.

1665

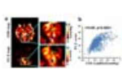

Towards self-calibrated functional connectivity mapping

Peiying Liu[1], Marco Pinho[2], Yang Li[1], Li Pan[3], Babu G Welch[2,4], and Hanzhang Lu[1]

[1]Radiology, Johns Hopkins University School of Medicine, Baltimore, MD, United States, [2]Radiology, University of Texas Southwestern Medical Center, Dallas, TX, United States, [3]Siemens Healthcare, Baltimore, MD, United States, [4]Neurological Surgery, University of Texas Southwestern Medical Center, Dallas, TX, United States

The BOLD signal in functional connectivity MRI(fcMRI) may be affected by non-neural factors, such as vascular function. In this study, we utilized a multiparametric mapping method to measure functional connectivity(FC) maps and cerebrovascular reactivity(CVR) concomitantly, and examined the relationship between these two indices in both healthy volunteers and patients with cerebrovascular disease. Significant correlations were found between FC and CVR across brain regions, suggesting that cerebrovascular function should be accounted for when using BOLD fcMRI to assess brain functions. Concomitant acquisition of neural and vascular MRI may allow calibration/normalization of FC signal and more accurate estimation of brain functional connectivity.

1666

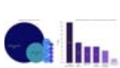

Clinical mapping of cerebrovascular reactivity using MRI: a framework for reaching consensus

Molly G Bright[1], Erin L Mazerolle[2], Olivia Sobczyk[3], Audrey P Fan[4], Matthias JP van Osch[5], Clarisse I Mark[6], Laurentius Huber[7], Avery JL Berman[2,8], Daniel P Bulte[9], Bruce G Pike[2], Claudine J Gauthier[10], and Nicholas P Blockley[11]

[1]Sir Peter Mansfield Imaging Centre, School of Medicine, University of Nottingham, Nottingham, United Kingdom, [2]Hotchkiss Brain Institute, Department of Radiology, University of Calgary, Canada, [3]Institute of Medical Science, University of Toronto, Canada, [4]Radiological Sciences Laboratory, Stanford University, United States, [5]C.J. Gorter Center for High Field MRI, Radiology, Leiden University Medical Center, Netherlands, [6]Centre for Neuroscience Studies, Queen's University, Canada, [7]Section on Funtional Imaging Methods, National Institute for Mental Health, United States, [8]Montreal Neurological Institute, McGill University, Canada, [9]Institute of Biomedical Engineering, University of Oxford, United Kingdom, [10]PERFORM Centre, Concordia University, Canada, [11]FMRIB Centre, Nuffield Department of Clinical Neurosciences, University of Oxford, United Kingdom

There is increasing clinical interest in mapping cerebrovascular reactivity (CVR), the response of cerebral blood vessels to a carbon dioxide stimulus. However, the application of CVR mapping varies greatly across sites due to a lack of methodological standardisation. We established an international network of over 100 researchers and administered a survey to establish current practice. Guided by QIBA and UPICT protocols, we developed a framework for reaching consensus, and identified areas where agreement already exists. Immediate achievable targets and long-term aims for the CVR community are defined, with the ultimate goal of establishing CVR as a robust clinical imaging marker.

1667

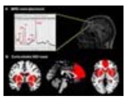

Corticolimbic Hyperresponse to Emotion and Glutamatergic Function in People with High Schizotypy: A Multimodal fMRI-MRS Study

Gemma Modinos[1], Anna McLaughlin[1], Alice Egerton[1], Katrina McMullen[2], Veena Kumari[1], Gareth J Barker[1], Christian Keysers[3,4], and Steven CR Williams[1]

[1]Institute of Psychiatry, Psychology & Neuroscience, King's College London, London, United Kingdom, [2]Centre for Brain Health, University of British Columbia, BC, Canada, [3]Social Brain Lab, Netherlands Institute for Neuroscience, an institute of the Netherlands Academy for Arts and Sciences KNAW, Amsterdam, Netherlands, [4]Psychology, University of Amsterdam, Amsterdam, Netherlands

Our recent functional magnetic resonance (fMRI) studies reported that elevated neural responses to emotional stimuli are present in the early stages of psychotic disorders and in individuals at clinical high risk for psychosis. Our present study combined fMRI with proton magnetic resonance spectroscopy (^{1}H-MRS) at 3T and shows that corticolimbic hyperresponsivity to emotion is directly related to glutamate concentrations in healthy people with subclinical psychotic-like experiences. These data not only support preclinical animal models of psychosis by demonstrating an important link between corticolimbic neurophysiology and neurotransmission, but also suggest a scientific basis for future development of novel interventions focused on emotional regulation to prevent or delay progression from the vulnerability to the psychotic state

---

1668

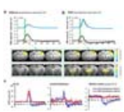

A novel role of intrinsic astrocytic calcium spikes to mediate brain states through central/dorsal thalamic nuclei

Maosen Wang[1,2], Yi He[1,2], and Xin Yu[1]

[1]Max Planck Institute for Biological Cybernetics, Tuebingen, Germany, [2]Graduate Training Centre of Neuroscience, International Max Planck Research School, University of Tuebingen, Tuebingen, Germany

The astrocytic Ca^{2+} signal could be simultaneously acquired with either BOLD-fMRI or LFP signal in the rat cortex under anesthesia. Intrinsic astrocytic Ca^{2+} bursts spikes were detected in the cortex with suppressed spontaneous LFP and negative BOLD fMRI signal. These astrocytic Ca^{2+} spike events were different from the normal activity-evoked Ca^{2+} signal and also differentiate themselves from the lesion/stimulation-induced large-scale depolarization or spreading depression given the instantaneous whole-brain pattern and correlation with the thalamic LFP. The intrinsic astrocytic Ca^{2+} spike may mediate the brain states through the arousal thalamic pathway.

1669

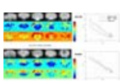

Defining the challenges in awake rat fMRI

Wen-Ju Pan[1], Rui Tang[1], Jacob Billings[1], Maysam Nezafati[1], and Shella Keilholz[1]

[1]Emory University/Georgia Institute of Technology, Atlanta, GA, United States

Awake rat fMRI has been growing in popularity in recent years because it eliminates confounds associated with the use of anesthesia. However, issues arising from animal restriction have not been completely identified or recognized by the research community. We conducted a pilot study on immobilization training for awake rat fMRI studies and provide some relevant experiences that highlight potential issues to be resolved.

1670

magna cum laude

Neural and Physiological Responses to Vagus Nerve Stimulation in rats

Jiayue Cao[1], Kun-Han Lu[2], Matthew Ward[1], Terry Powley[1,3], and Zhongming Liu[1,2]

[1]Biomedical Engineering, Purdue University, West Lafayette, IN, United States, [2]Electrical and Computer Engineering, Purdue University, West Lafayette, IN, United States, [3]Psychological Sciences, Purdue University, West Lafayette, IN, United States

Vagus nerve stimulation (VNS) is an electroceutical treatment for both brain and visceral organs disorders. To better understand its function in autonomic brain-body interaction, we applied electrical stimulation to the vagus nerve to perturb brain activity and visceral organ physiology. By simultaneously measuring the VNS-induced brain and physiological responses, we separated the afferent neuronal and efferent physiological effects of VNS on the blood oxygen level dependent functional magnetic resonance imaging responses and mapped part of the brain's autonomic control networks modulated by VNS. This work offers a unique way to characterize the brain-activation profile of VNS with variable parameters.

1671

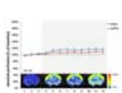

Is sevoflurane a viable alternative anaesthetic for functional MRI in mice?

Rebecca Klee[1], Thomas Mueggler[1], Andreas Bruns[1], Markus von Kienlin[1], and Basil Künnecke[1]

[1]Pharma Research and Early Development, Roche Innovation Center Basel, F. Hoffmann-La Roche Ltd, Basel, Switzerland

In preclinical fMRI, the volatile anaesthetic isoflurane is valued for its ease of use and controllability, and is frequently applied to prevent anxiety and subject motion. Yet, isoflurane increases cerebral blood flow and particularly in mice it limits cerebrovascular response to neural activity, thus curtailing fMRI. Sevoflurane, a close relative to isoflurane, has been reported to be less vasodilatory. Hence, we evaluated whether sevoflurane could serve as an improved anaesthesia modality for fMRI in mice. Perfusion MRI however revealed high basal cerebral perfusion and restricted cerebrovascular reserve capacity in an acetazolamide-induced hypercapnic challenge akin to those previously reported for isoflurane.

1672

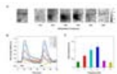

Frequency-dependent hemodynamic response to somatosensory stimulation in ketamine-anesthetized mice

Hyun-Ji Shim[1,2], Joonsung Lee[1], Jungryun Lee[1], Jeong Pyo Son[1,2], Won Beom Jung[1,3], Sangwoo Kim[1], and Seong-Gi Kim[1,2,3]

[1]Center for Neuroscience Imaging Research, Institute for Basic Science (IBS), Suwon, Korea, Republic of, [2]Health Sciences and Technology, Samsung Advanced Institute for Health Sciences and Technology (SAIHST), Sungkyunkwan Universiy, Suwon, Korea, Republic of, [3]Biomedical Engineering, Sungkyunkwan University, Suwon, Korea, Republic of

Optimizing parameters of electrical forepaw stimulation is necessary to investigate biophysical and molecular properties of fMRI signals. However stimulation parameters and anesthesia in mice are not well-defined. Here we introduced ketamine anesthesia in mice. Initially, forepaw stimulation frequency was refined with for CBV-weighted OIS experiments. To translate electrical stimulation parameters from OIS into BOLD fMRI, we tested two stimulation frequencies. Application of our sensory stimulus parameters evoked well-localized and robust BOLD fMRI signals in ketamine anesthetized mice.

1673

Non-invasive evaluation of functional and structural connectome changes in the mouse brain related to drug-induced neuro-modulation

Thomas Bienert[1], Neele Hübner[1], Anna Mechling[1], Tanzil Mahmud Arefin[1,2,3], Marco Reisert[4], Máté Döbrössy[5], Philipp Janz[6], Carola Haas[6], Laura Adela Harsan[1,7,8], Jürgen Hennig[4], Dominik von Elverfeldt[1], and Karl Egger[9]

[1]Advanced Molecular Imaging Research (AMIR), Medical Physics, Department of Radiology, University Medical Center Freiburg, Freiburg, Germany, [2]Faculty of Biology, University of Freiburg, Freiburg, Germany, [3]Department of Translational Medicine and Neurogenetics, Institute of Genetics and Molecular and Cellular Biology (IGBMC), Illkirch-Graffenstaden, Strasbourg, France, [4]Medical Physics, Department of Radiology, University Medical Center Freiburg, Freiburg, Germany, [5]Division of Stereotactic and Functional Neurosurgery, Department of Neurosurgery, University Medical Center Freiburg, Freiburg, Germany, [6]Experimental Epilepsy Research, Department of Neurosurgery, University Medical Center Freiburg, Freiburg, Germany, [7]Department of Biophysics and Nuclear Medicine, University Hospital Strasbourg, Strasbourg, France, [8]Laboratory of Engineering, Informatics and Imaging, University of Strasbourg, Strasbourg, France, [9]Department of Neuroradiology, University Medical Center Freiburg, Freiburg, Germany

Analysis of neuro-functional connectivity derived from rs-fMRI and neuro-structural connectivity derived from DTI/Fiber Tracking might enable researchers to monitor and characterize physiological or drug induced neuro-modulation in the mouse brain. In our study we present a framework for the analysis on healthy mice with erythropoietin (EPO) treatment. Brain regions with pronounced neuro-modulation in histology also showed changes in neuro-functional and neuro-structural data.

1674

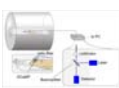

Hemodynamic and neuronal response in rat under Isoflurane-supplemented Medetomidine sedation assessed by simultaneous BOLD fMRI and Ca2+ recordings

Timo van Alst[1], Lydia Wachsmuth[1], Franziska Albers[1], Florian Schmid[1], and Cornelius Faber[1]

[1]Department of Clinical Radiology, University of Muenster, Muenster, Germany

fMRI in rodents has become a widely used technique with various applications in preclinical research. In this context, most studies are performed with anesthetized animals. Medetomidine evolves as a frequently used sedative but long term stability is limited -prolonged stability can be achieved by addition of Isoflurane. Several recent fMRI studies have used this combination. We evaluated the effects of this combination of anesthetics using a multimodal setup of BOLD fMRI and Ca^{2+} recordings. Even small addition of Isoflurane resulted in a significant decrease of neural (Ca^{2+}) and hemodynamic (BOLD) responses to a distinct electrical stimulus.

1675

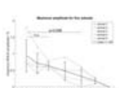

Anesthesia-dependent effects on BOLD onset and amplitude assessed by line scanning fMRI with 50 ms temporal resolution

Franziska Albers[1], Timo van Alst[1], Lydia Wachsmuth[1], Florian Schmid[1], and Cornelius Faber[1]

[1]Department of Clinical Radiology, University of Muenster, Muenster, Germany

Medetomidine sedation is a common anesthetic regimen for rodent fMRI studies. However, depth and duration of the sedation may prove insufficient for MR imaging. Adding isoflurane is an efficient way to increase depth and duration of sedation. In rats we varied the concentration of additional isoflurane (0 - 1.5 %) and performed 1D line scanning upon electric forepaw stimulation to characterize the effect of increasing isoflurane on amplitude and onset of the BOLD response. While low concentrations did not significantly alter amplitudes or onsets, we found severely reduced amplitudes and delayed onsets for higher concentrations (> 0.7 %) of isoflurane.

1676

Effect of alfaxalone anesthesia on brain functional connectivity in rhesus monkeys

Chun-Xia Li[1], Doty Kempt[1], Leonard Howell[1,2], and Xiaodong Zhang[1,2]

[1]Yerkes Imaging Center, Yerkes National Primate Research Center, Emory University, Atlanta, GA, United States, [2]Division of Neuropharmacology and Neurologic Diseases, Yerkes National Primate Research Center, Emory University

Alfaxalone is suggested to be an optimal anesthetic to examine brain injuries in experimental animals. However, little is known about its impact on neural activity in anesthetized subjects. In the present study, adult rhesus monkeys were used to examine its impact on functional connectivity. The results demonstrate that alfaxalone induces significantly reduced functional connectivity in the dominant default-mode network (DMN), inter-hemisphere connectivity in primary somatosensory cortex and caudate compared to isoflurane. The findings reveal that alfaxalone suppress neural activity more dramatically than light isoflurane anesthesia in monkeys, suggesting it is ideal for investigating anatomical and microstructural changes in animal models but not good for evaluating neuronal activity with fMRI.

1677

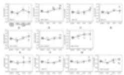

Dose-dependent effects of prolonged isoflurane administration on resting cerebral blood flow and functional connectivity: a preliminary study in rhesus monkeys

Chun-Xia Li[1] and Xiaodong Zhang[1,2]

[1]Yerkes Imaging Center, Yerkes National Primate Research Center, Emory University, Atlanta, GA, United States, [2]Division of Neuropharmacology and Neurologic Diseases, Yerkes National Primate, Emory University

Isoflurane is widely used in biomedical research with the prolonged duration of administration up to several hours. However, the manner in which neurophysiology and functional connectivity are affected by the length of anesthesia remains poorly understood. In the present study, cerebral blood flow (CBF) and default model network (DMN) were examined using arterial spin-labeling perfusion and resting state functional MRI techniques. The functional connectivity in the dominant DMN decreased substantially during 4-hour administration of isoflurane at any given dosage. CBF in most brain regions decreased at the low dose (0.89 %), but did not change markedly when higher doses of isoflurane (1.05 %, 1.19 %) were administrated. The study revealed dose-dependent effects of isoflurane on brain functionality and regional CBF during prolonged anesthesia administration of isoflurane, suggesting those effects should be considered in the experimental design or the interpretation of the outcome of related neuroimaging studies using anesthetized animals or humans.

1678

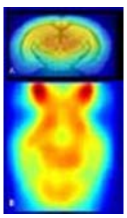

Differential effects of anesthetics on mouse brain connectivity and function as probed by resting-state fMRI and [18]FDG-PET

Meltem Karatas[1,2,3,4], Laetitia Degiorgis[1], Marion Sourty[1], Daniel Roquet[1], Lionel Thomas[5], Patrice Marchand[5], Thomas Bienert[3], Lee Hsu-Lei[3], Julien Lamy[1], Chrystelle Po[1], Frédéric Boisson[5], David Brasse[5], Dominik von Elverfeldt[3], Izzie Jacques Namer[1,6], Jean-Paul Armspach[1], Ipek Yalcin[2], and Laura-Adela Harsan[1,3,6,7]

[1]ICube, CNRS, University of Strasbourg, Strasbourg, France, [2]INCI, CNRS, University of Strasbourg, Strasbourg, France, [3]Department of Radiology, Medical Physics, University Medical Center Freiburg, Freiburg, Germany, [4]Faculty of Biology, University of Freiburg, Freiburg, Germany, [5]IPHC, CNRS, University of Strasbourg, Strasbourg, France, [6]Engineering Science, Computer Science, and Imaging Laboratory, Integrative Multimodal Imaging in Healthcare, CNRS, University of Strasbourg, Strasbourg, France, Strasbourg, France, [7]Department of Biophysics and Nuclear Medicine, University Hospital Strasbourg, Strasbourg, France

Mice resting state functional connectivity (FC) studies are highly attractive given the large number of existing murine models of neuropsychiatric disorders. Currently, most of mouse rs-fMRI studies are carried out under anesthesia, to limit motion and animal distress. Yet, anesthetics affect brain FC. Currently, no reliable awake mouse brain FC reference is available. We compared mouse brain rs-fMRI patterns under medetomidine or isoflurane anesthesia and paralleled the experiments with static ^{18}FDG-PET exams, where the tracer biodistributions occurred under isoflurane, medetomidine anesthesia or in conscious state, reflecting the brain glucose metabolism, as indirect measures of neuronal activity.

1679

Functional and Metabolic Connectivity of the Awake and Anesthetized Brain

Alan B McMillan[1], Abigail Z Rajala[2], Bethany J Stieve[2], Rick L Jenison[3], Rasmus M Birn[4], and Luis C Populin[2]

[1]Radiology, University of Wisconsin, MADISON, WI, United States, [2]Neuroscience, University of Wisconsin, MADISON, WI, United States, [3]Psychology, University of Wisconsin, MADISON, WI, United States, [4]Psychiatry, University of Wisconsin, MADISON, WI, United States

This study evaluated the effect of anesthesia on functional and metabolic brain connectivity, measured with simultaneous PET/MR using an awake monkey model. Results show a profound disruption of functional connectivity, effective connectivity, and novel approaches to metabolic connectivity following the administration of IV ketamine.

1680

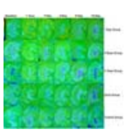

Effect of Repeated Injection of Iodixanol on Rrenal Function in Healthy Wistar Rats by Using Functional MRI

Yongfang Wang[1], Ke Ren[1], Lizhi Xie[2], Wenge Sun[1], Yi Liu[1], Songbai Li[1], Ke Xu[1], Xin Zhang[1], and Yuli Zheng[1]

[1]Department of Radiology, First Affiliated Hospital of China Medical University, Liaoning, People's Republic of China, [2]GE Healthcare, MR Research China, Beijing, Beijing, People's Republic of China

In clinical practice, for complex, recurrent disease, the same patient may need to use contrast agents repeatedly. However, the administration of multiple use of contrast-medium within a short period of time may put patients at risk1 .So, the aim of this work is to examine differences in rats' potential kidney injury provoked by iodixanol with respect to different intervals and different times. By using fMRI we observed whether repeated intravenous injection of iodixanol at different time intervals could lead to aggravate kidney damage and then find the shortest time interval. Simultaneously, monitoring kidney damage by sNGAL and detecting the cause of renal injury by immunohistochemistry were also performed.

Traditional Poster

fMRI: Neuroscience Applications

Exhibition Hall 1681-1729 Tuesday 8:15 - 10:15

1681 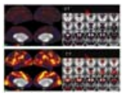

Tradeoffs in pushing the spatial resolution of fMRI for the 7 T Human Connectome Project

An Thanh Vu[1], Keith Jamison[2], Matthew F Glasser[3], Steve M Smith[4], Timothy Coalson[3], Steen Moeller[2], Edward J Auerbach[2], Kamil Ugurbil[2], and Essa Yacoub[2]

[1]Center for Imaging of Neurodegenerative Diseases, Veteran Affairs Health Care System, San Francisco, CA, United States, [2]Center for Magnetic Resonance Imaging, University of Minnesota, [3]Washington University, [4]Oxford Centre for Functional MRI of the Brain, Oxford University

Here we describe subsequent work by the Human Connectome Project (HCP), taking the initial advancements obtained at 3 T and pushing spatial resolution even further at ultrahigh field strengths. To assess the impact of spatial resolution on the resultant detectability of resting state networks throughout the brain, we compare 7 T data acquired at various isotropic spatial resolutions (2 mm, 1.6 mm, 1.5 mm, 1.25 mm, and 0.9 mm) using the 2 mm 3 T HCP rfMRI data as baseline. 7 T functional networks show enhanced BOLD CNR, resulting in sharper, stronger, and more well defined spatial detail even at the group level.

1682 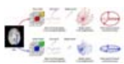

Spatial Registration of fMRI Data Using Functional Correlation Tensors

Yujia Zhou[1,2], Pew-Thian Yap[2], Han Zhang[2], Lichi Zhang[2], Qianjin Feng[1], and Dinggang Shen[2]

[1]Guangdong Provincial Key Laboratory of Medical Image Processing, School of Biomedical Engineering, Southern Medical University, Guangzhou, People's Republic of China, [2]Department of Radiology and BRIC, University of North Carolina, Chapel Hill, NC, United States

Inter-subject registration of functional MRI (fMRI) data is a key step for group analysis. Here, we propose a novel registration strategy that considers functional information from both gray matter (GM) and white matter (WM). This is achieved using functional correlation tensors (FCTs), which capture the local correlation of the BOLD signals. Features extracted from both GM and WM functional correlation tensors are utilized in a multi-channel Large Deformation Diffeomorphic Metric Mapping (LDDMM) registration framework for fMRI registration. Experimental results indicate that our method can achieve better functional registration compared with state-of-the-art methods.

1683 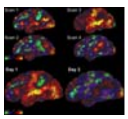

Is resting-state fMRI guided brain target localization for TMS reliable and reproducible?

Lipeng Ning[1], Joan A Camprodon[2], Nikos Makris[2], and Yogesh Rathi[1]

[1]Brigham and Women's Hospital, Boston, MA, United States, [2]Massachusetts General Hospital, Boston, MA, United States

Transcranial magnetic stimulation (TMS) is a noninvasive treatment approach for major depressive disorder (MDD). A recently proposed method[1] is to stimulate a sub-region in the left dorsolateral prefrontal cortex (DLPFC) that is most anti-correlated with the subgenual cingulate (SGC) as obtained from resting-state functional MRI (rsfMRI). To test the reliability of this approach, we examined 100 data sets from the Human Connectome Project (HCP)[5] with each subject scanned 4 times on two different days. We found large variability in the inter-scan rsfMRI-guided target for each subject, which can significantly reduce the efficacy of TMS therapy in MDD.

1684 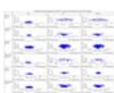

The impact of geometric distortion correction on multisite rs-fMRI data

Nicolas Hehn[1,2], Ana Beatriz Solana Sánchez[1], Dirk Bequé[1], Nikolaos Koutsouleris[3], Axel Haase[2], Bjoern Menze[4], and Carlos Cabral[3]

[1]GE Global Research, Munich, Germany, [2]Department of Medical Engineering, Technische Universität München, Munich, Germany, [3]Department of Psychiatry and Psychotherapy, Ludwig-Maximilians-Universität, Munich, Germany, [4]Department of Informatics, Technische Universität München, Munich, Germany

This study addresses the goal of reducing site-variance in the correlation values of multisite rs-fMRI data by correcting for site-specific EPI-related geometric distortions. Three geometric distortion correction methods (B0 fieldmap and image-based unwarping) were applied separately to a calibration dataset consisting of six subjects traveling to three sites. The change of the correlation values and their site-homogeneity was evaluated in dependency of the quantified geometric distortion correction values for six networks and all subjects. It could be shown that the distortion correction had no significant impact on the correlation values and no correlation between the two parameters was found.

1685 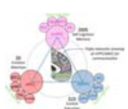

Growing Apart or Growing Together: a Novel “Developing Triple Network” Hypothesis for Baby Connectome Study

Han Zhang[1], Weiyan Yin[2], Weili Lin[1], and Dinggang Shen[1,3]

[1]Department of Radiology and BRIC, University of North Carolina at Chapel Hill, Chapel Hill, NC, United States, [2]Department of Biomedical Engineering and BRIC, University of North Carolina at Chapel Hill, Chapel Hill, NC, United States, [3]Department of Brain and Cognitive Engineering, Korea University, Seoul, Korea, Republic of

For baby connectome study, we propose a “developing triple network” model based on our findings from precious longitudinal infant resting-state fMRI data, which extends previous “triple network model” to 0-2 years old, a pivotal period which we have little knowledge on. Our developmental model provides future study with key information on early functional connectivity. We found medial prefrontal area is growing apart and its long-range FC is growing together at different speeds in the first 2 years. We, for the first time, found a novel early developmental pattern with both local and long-range FC increases at 6-9 months but decreases afterwards, indicating pivotal neural pruning mechanism from system neuroscience view point.

1686 

Radiation-induced Brain Abnormalities: Plasticity, Progression and Outcome Prediction

Han Zhang[1] and Dinggang Shen[1,2]

[1]Department of Radiology and BRIC, University of North Carolina at Chapel Hill, Chapel Hill, NC, United States, [2]Department of Brain and Cognitive Engineering, Korea University, Seoul, Korea, Republic of

Brain plasticity is fascinating and important to our life. Radiation therapy can cause brain injury which may cover or progress, posing an ideal case to study brain plasticity. We used a rare and unique cohort of nasopharyngeal carcinoma patients with normal-appearing brains to study irradiation injury in its preclinical stage in context of brain functional and structural plasticity. We found an acute increase in local brain activity, followed by its extensive reduction; and significant functional connectivity loss in the default mode network. Such radiosensitive functional alterations were intriguingly found to be plastic. By contrast, a progressive late disrupted integrity of the related white matter was starting to be significant after one year at the far end. Early increased local brain functional activity was able to predict severe later brain necrosis through a bridge of brain connectome. These findings highlight the importance of brain connectomics in translational clinical study.

1687

Pediatric Brain Functional Parcellation from Birth to 2-Years-Old

Weiyan Yin[1] and Weili Lin[2]

[1]Department of Biomedical Engineering and Biomedical Research Imaging Center, University of North Carolina at Chapel Hill, Chapel Hill, NC, United States, [2]Department of Radiology and Biomedical Research Imaging Center, University of North Carolina at Chapel Hill, Chapel Hill, NC, United States

Brain functional parcellation has been shown to discern brain functional atlases in adults. In this study, multigraph K-way clustering[1] was employed to reveal temporal evaluation of brain funcitonal atlases in 71 healthy children longitudinally scanned at 1/3/6/9/12/18/24 months of age. Results revealed temporal evolution of brain functional networks during the first two years of life.

1688

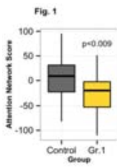

Connectome Based Predictive Modeling: Relating Social Measures to Functional Brain Organization

Evelyn MR Lake[1], Emily S Finn[2], Monica D Rosenberg[3], Xilin Shen[4,5], Dustin Scheinost[4,5], Marvin M Chun[2,3,6], and R Todd Constable[1,2,7]

[1]Radiology and Biomedical Imaging, Yale University, Cambridge, MA, United States, [2]Interdepartmental Neuroscience Program, Yale University, [3]Department of Psychology, Yale University, [4]Department of Diagnostic Radiology, Yale School of Medicine, [5]Radiology and Biomedical Imaging, Yale University, [6]Department of Neurobiology, Yale University, [7]Department of Neurosurgery, Yale School of Medicine

We examine the relationship between functional brain networks and behaviour in individuals with autism from the Autism-Brain-Imaging-Data-Exchange. We find a difference in attention network strength between groups (autism vs. control) using an a priori defined network for high-attention [1]. In addition, connectome based predictive modeling (CPM) successfully predicted inattention and communication scores. Finally, on a test group of autistic patients (not used in the CPM), we found network strengths to be more similar to individuals used the CPM with autism than controls. Together, these results indicate that connectivity may prove to be a valuable tool in the diagnosis and treatment of autistic individuals.

1689

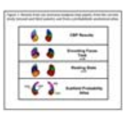

Neurofunctional topography of the human hippocampus: Converging data from a series of studies

Jennifer Lene Robinson[1], Jessica Busler[2], Meredith Reid, Nouha Salibi[3], Xinyu Zhao, and Gopikrishna Deshpande[4]

[1]Psychology, Auburn University, Auburn, AL, United States, [2]Psychology, Auburn University, [3]Siemens Healthcare, [4]Electrical and Computer Engineering, Auburn University

The hippocampus, one of the most phylogenetically preserved structures in the human brain, has been a topic of interest to evolution theorists and cognitive neuroscientists alike. Malfunctions in the hippocampus are hallmark features in a number of psychiatric and neurological conditions, further amplifying interest. Little advancement has been made regarding the neurofunctional topography of the structure. We used high-field, high-resolution neuroimaging techniques to demonstrate convergent evidence on a new theory of hippocampal organization. Data from this project are expected to catalyze efforts in neuroscience and medicine to better understand hippocampal functioning and promote the identification of healthy and aberrant signaling.

1690

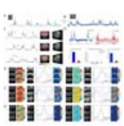

Spatio-temporal extent of spontaneous and sensory evoked neural network activity.

Miriam Schwalm[1], Felipe Aedo-Jury[1], Florian Schmid[2], Lydia Wachsmuth[2], Andrea Kronfeld[1], Hendrik Backhaus[1], Cornelius Faber[2], and Albrecht Stroh[1]

[1]Institute for Microscopic Anatomy and Neurobiology, Johannes Gutenberg-University Mainz, Mainz, Germany, [2]Department of Clinical Radiology, University of Münster, Nordrhein-Westfalen, Germany

Preclinical functional Magnetic Resonance Imaging in rodents has become a vital research tool for observing functional network connectivity at rest or during sensory stimulation. There is an ongoing debate about the differential effects of anesthesia on cortical connectivity, since functional connectivity networks fluctuate depending on global brain state. We analyzed the spontaneous and sensory evoked BOLD signal in rats during different network states induced by Isoflurane and Medetomidine anesthesia, finding them to lead to fundamentally different cortical connectivity. These results are crucial for interpreting rodent studies in the framework of translational resting state research including awake human data.

1691

Connectivity of the Default Mode Network – Prior and post an oddball paradigm

Irene Neuner[1,2,3,4], Ravichandran Rajkumar[1,2,3,4], Shukti Ramkiran[1], Tracy Warbrick[1], Jorge Arrubla[1], and N Jon Shah[1,3,4,5,6]

[1]Institute of Neuroscience and Medicine 4 (INM4), Forschungszentrum Juelich GmbH, Juelich, Germany, [2]Department of Psychiatry, Psychotherapy and Psychosomatics, RWTH Aachen University, Aachen, Germany, [3]JARA – BRAIN – Translational Medicine, Juelich, Germany, [4]TRIMAGE-consortium, Juelich, Germany, [5]Department of Neurology, RWTH Aachen University, Aachen, Germany, [6]Department of Electrical and Computer Systems Engineering, and Monash Biomedical Imaging, School of Psychological Sciences, Monash University, Melbourne, Australia

The DMN is shown to be highly active during resting state and is rapidly deactivated during externally directed tasks. However, it is unclear how demanding the task needs to be to switch the DMN out of the resting state mode. Aiming to answer this question we chose a visual oddball paradigm and assessed the functional connectivity of the DMN during resting state in a rest-task-rest design. The oddball paradigm demands very little cognitive resources and therefore we hypothesize that the DMN will not be altered in its connectivity pattern during post task resting state.

1692

Resting-state Functional Network Connectivity Pattern as a Cognitive Marker for Task Performance

Hua Xie[1], Javier Gonzalez-Castillo[2], Eswar Damaraju[3,4], Peter Bandettini[2,5], Vince Calhoun[3,4], and Sunanda Mitra[1]

[1]Department of Electrical and Computer Engineering, Texas Tech University, Lubbock, TX, United States, [2]Section on Functional Imaging Methods, National Institute of Mental Health, National Institutes of Health, Bethesda, MD, United States, [3]The Mind Research Network, Albuquerque, NM, United States, [4]Department of Electrical and Computer Engineering, University of New Mexico, Albuquerque, NM, United States, [5]Functional MRI Facility, National Institute of Mental Health, National Institutes of Health, Bethesda, MD, United States

Attentional lapses have been shown to be associated with an altered connectivity and activation pattern of the default-mode network. To further our understanding of the relationship between resting-state connectivity pattern and task performance, we analyzed a multitask dataset including four mental tasks (rest, memory, video, and math). We computed whole-brain connectivity patterns using all volumes during rest (rs-FNC), and the dynamic functional network connectivity (dFNC) patterns during tasks with a sliding window method. We compared similarity between the rs-FNC pattern and dFNCs, which was correlated to the task performance and thus might be used as a cognitive biomarker.

1693

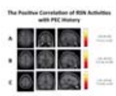

Dependency of the Activations Detected in Resting State Networks on the History of Physical Exercise Activities in Community Dwelling Older Adults

Mika Ueno[1], Sachiko Kiyama[2,3], Ayuko Tanaka[3,4], and Toshiharu Nakai[1,5]

[1]NeuroImaging & Informatics, NCGG, Ohbu, Japan, [2]College of Liberal Arts and Sciences, Mie University, Tsu, Japan, [3]NeuroImaging & Informatics, National Center for Geriatrics & Gerontology, Ohbu, Japan, [4]Faculty of Human Sciences, Kobe Shoin Women's University, Kobe, Japan, [5]Department of Radiological Science, Nagoya University Graduate School of Medicine, Nagoya, Japan

In order to explore biomarkers to reflect the effects of long-term physical exercise (PE) on the activities in RSNs, the relationship among the history of participation in PE clubs, the activations in RSNs and the physical activity (PA) was investigated. The activation in the ACG was decreased depending on longer history of PE as well as higher PA indicated by IPAQ scales. These findings may reflect less demand for cognitive integration. It was suggested that both recovery and sedation of the activity in the RSNs against the age-related changes in brain activation may be the biomarker in healthy older adults.

1694

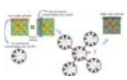

Hybrid high-order resting-state functional connectivity networks for mild cognitive impairment diagnosis

Yu Zhang[1], Han Zhang[1], Xiaobo Chen[1], and Dinggang Shen[1]

[1]Biomedical Research Imaging Center, University of North Carolina at Chapel Hill, Chapel Hill, NC, United States

This study proposes a novel approach named “hybrid high-order FC networks” to explore the higher-level interactions among brain regions for improving the diagnosis performance of early mild cognitive impairment. We first construct the low-order network and the topographical similarity-based high-order network. With the two-level FC networks, we propose to construct a new “associated high-order network”, which is formed by estimating the higher-level interactions between the high-order sub-networks and low-order sub-networks. We further devise a multi-kernel learning strategy to integrate the dynamic networks of the three different levels. A high diagnosis accuracy of 91.5 % demonstrates effectiveness of our proposed approach.

1695

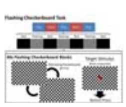

Functional Bold and Functional T1rho Decoupled in Bipolar Disorder

Joseph J Shaffer[1], Casey P Johnson[1], Jeffrey D Long[2], Jess G Fiedorowicz[3], Gary E Christensen[4], John A Wemmie[3], and Vincent A Magnotta[1]

[1]Radiology, University of Iowa, Iowa City, IA, United States, [2]Biostatistics, University of Iowa, Iowa City, IA, United States, [3]Psychiatry, University of Iowa, Iowa City, IA, United States, [4]Electrical and Computer Engineering, University of Iowa, Iowa City, IA, United States

Functional T1 relaxation in the rotating frame (fT1ρ) is a new method of functional imaging that is thought to reflect changes in brain metabolism due to pH. FT1ρ may provide a more direct measurement of neuronal activity than the blood-oxygen level dependent (BOLD) contrast that is typically used for functional imaging. Here we applied both methods in order to study brain activation during a flashing checkerboard paradigm in participants with bipolar disorder as compared to controls. Linear mixed effect regression modeling revealed decoupling between the two imaging modalities in bipolar disorder in several brain regions.

1696

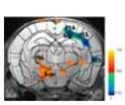

Low-dose radiation disrupts functional brain connectivity during nociceptive heat stimulation in a mouse model

Silke Kreitz[1,2], Sandra Strobelt[1], Michael Uder[2], and Andreas Hess[1]

[1]Institute for Pharmacology and Toxicology, Friedrich-Alexander Universität Erlangen-Nuremburg, Erlangen, Germany, [2]Department for Radiology, University Hospital der FAU Erlangen-Nuremberg, Erlangen, Germany

Due to improved medical techniques such as CT and radiotherapy todays children are more exposed to low-dose radiation than previous generations. However, little is known about the influence of low-dose radiation on the brain’s development. We hypothesize that altered functional connectivity of activated areas during pain processing can serve as a marker for disturbed brain development. In a mouse model we showed that functional connectivity during nociceptive stimulation after P10 irradiation is disrupted in cortical areas that mature postnatal. We could demonstrate that pain processing is influenced by low-dose irradiation which is in concordance with the brain’s developmental state.

1697 

Greater Connectivity Between Cerebellar Vermis and Insular Attention Resting Network in HIV Patients

Steffan Soosman[1], Thomas Ernst[1], and Linda Chang[1]

[1]*John A Burns School of Medicine, University of Hawaii at Manoa, Honolulu, HI, United States*

Individuals infected with HIV frequently have HIV-associated neurocognitive disorders (HAND), despite effective plasma viral suppression. Various resting state networks studied with fMRI have been shown to be attenuated in HIV compared to seronegative controls. This study shows an increased connectivity in HIV subjects between the cerebellar vermis and bilateral insulae. Using clinical correlates, we conclude that this increased connectivity may be due to decreased efficiency in functional connectivity in the HIV-infected brain.

1698 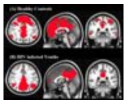

Resting State Brain Networks in Perinatally HIV-infected Adult Youths

Manoj K Sarma[1], Bharat Biswal[2], Margaret A Keller[3], Tamara Welikson[4], Irwin Walot[5], David E Michalik[6], Karin Nielsen-Saines[7], Jaime Deville[7], Andrea Kovacs[8], Eva Operskalski[8], Joseph Ventura[9], and M. Albert Thomas[1]

[1]*Radiological Sciences, UCLA School of Medicine, Los Angeles, CA, United States,* [2]*Biomedical Engineering, New Jersey Institute of Technology, Newark, NJ, United States,* [3]*Pediatrics, Harbor-UCLA Medical Center, Torrance, CA, United States,* [4]*Semel Institute for Neuroscience and Human Behavior, UCLA School of Medicine, Los Angeles, CA, United States,* [5]*Radiology, Harbor-UCLA Medical Center, Torrance, CA, United States,* [6]*Infectious disease-Pediatrics, Miller Children's Hospital, Long Beach, CA, United States,* [7]*Pediatrics, UCLA School of Medicine, Los Angeles, CA, United States,* [8]*Pediatrics, Keck School of Medicine of USC, Los Angeles, CA, United States,* [9]*Psychiatry and Biobehavioral Sciences, UCLA School of Medicine, Los Angeles, CA, United States*

Youths with perinatally infected HIV survive longer with combination antiretroviral therapy, but remain at risk for poor cognitive outcomes. Since changes in cognitive function may be preceded by subtle changes in brain function, resting-state functional magnetic resonance imaging (rs-fMRI) may become useful in evaluating functional connectivity in these youths. We evaluated alterations in brain functional connectivity in eight perinatally HIV-infected youths and eleven healthy controls. Results from this study demonstrate that, compared to normal subjects, the strength of the several networks connectivity including DMN, Dorsal Attention, Lateral Visual, were significantly decreased in several regions among perinatally HIV-infected youth. The detailed mechanisms, implications of these brain activities and networks exhibiting changes will require further investigation.

1699 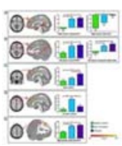

Impaired interactions of large-scale networks predict relapse behavior in heroin-dependent individuals

Qiang Li [1], Jiajie Chen[1], Jierong Liu[1], Wei Li[1], and Wei Wang[1]

[1]*Tangdu Hospital, Fourth Military Medical University, Xi'an, People's Republic of China*

Coupling of large-scale brain networks may underlie cognitive dysfunction in psychiatric disorders including addiction. However, whether the deficit of interactions among large-scale brain networks is associated with relapse behavior of heroin addiction remains unknown. This is the first neuroimaging study to assess coupling of large-scale networks that predict relapse in heroin addiction. In this study, we utilized a resting-state functional connectivity method of functional magnetic resonance imaging and found that abnormally higher functional connectivity between the SN and DMN, and lower functional connectivity between the left ECN and DMN were associated with the relapse behavior in treated heroin-dependent patients.

1700 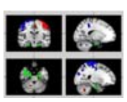

Localization of the epileptogenic neural network by the resting state fMRI in patients with the temporal lobe epilepsy

Oleksii Omelchenko[1], Mykola Makarchuk[1], and Volodymyr Rogozhyn[2]

[1]*Human and Animal Physiology, Taras Shevchenko National University of Kyiv, Kyiv, Ukraine,* [2]*Radiology Department, Shupyk National Medical Academy of Postgraduate Education, Kyiv, Ukraine*

Precise localization of the epileptogenic zone and its delineation from eloquent cortex, are crucial for successful surgery. We propose analysis of macroscopic brain neural networks connectivity in the resting state and during the movement execution in patients with TLE for the possible epileptogenic macroscopic neural network localisation and motor cortex mapping. Our results show the concordant topography of the resting state network and the EEG epileptiform activity. Resting state fMRI could potentially depict the epileptogenic neural network in TLE which includes regions of temporal lobe and hippocampus. Motor network was shown to remain unaffected in TLE during interictal period.

1701 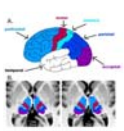

Higher Thalamocortical Connectivity May Reduce Efficacy of Temporal Resection

Bryson B Reynolds[1], Jasmine S Sondhi[1], Monica Giraldo-Chica[2], Baxter P Rogers[1], Bennett A Landman[3], Bassel Abou-Khalil[4], Adam W Anderson[5], and Victoria L Morgan[1]

[1]*Radiology and Radiological Sciences, Vanderbilt University Medical Center, Nashville, TN, United States,* [2]*Psychiatry, Vanderbilt University Medical Center, Nashville, TN, United States,* [3]*Electrical Engineering and Computer Science, Vanderbilt University, Nashville, TN, United States,* [4]*Neurology, Vanderbilt University Medical Center, Nashville, TN, United States,* [5]*Biomedical Engineering, Vanderbilt University, Nashville, TN, United States*

Functional connectivity of the thalamus could inform the potential efficacy of temporal resection in temporal lobe epilepsy. Diffusion and functional MRI was collected from 22 patients who underwent surgical treatment for temporal lobe epilepsy. The thalamus was segmented into six subregions based on diffusion tractography to six regions encompassing the entire cortex. Functional connectivity was calculated between each thalamic subregion and cortical region for each patient. Higher functional connectivity between the contralateral temporal-thalamic subregion and the cortex was associated with seizure recurrence after surgery.

1702

Disrupted Cortical Modulation of Hypothalamus Functioning for Visceral Homeostasis in Patients with Irritable Bowel Syndrome

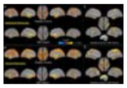

Xiaolin Liu[1], Shi-Jiang Li[2], Reza Shaker[3], Alan Silverman[4], Mark Kern[3], B. Douglas Ward[2], Gisela Chelimsky[4], and Manu R Sood[4]

[1]Radiology, Medical College of Wisconsin, Milwaukee, WI, United States, [2]Biophysics, Medical College of Wisconsin, Milwaukee, WI, United States, [3]Gastroenterology, Medical College of Wisconsin, Milwaukee, WI, United States, [4]Pediatric Gastroenterology, Medical College of Wisconsin, Milwaukee, WI, United States

The hypothalamus plays a critical role in maintaining visceral homeostasis. We evaluated, using functional imaging, hypothalamus functional connectivity in adolescent IBS patients and controls who received rectal distension stimulations. More extensive hypothalamus connectivity was observed in liminal than subliminal condition in controls, but not in IBS patients. Compared with controls, IBS patients showed significantly reduced hypothalamus connectivity in the bilateral prefrontal cortices, supplementary motor and premotor areas, bilateral sensorimotor cortex, and limbic subareas, which are specifically involved in homeostatic regulation. The findings support that reduced cortical and limbic modulations of hypothalamus functioning underlies disrupted visceral homeostasis in IBS patients.

1703

Patterns of the whole brain default mode network for alcohol addiction among the alcohol preferring rats

Yue Liu[1], Ning Zheng[2], Taotao Liu[3], Binbin Nie[4], Jie Wang[2], and Fuqiang Xu[2]

[1]Wuhan National Laboratory for Optoelectronics, Huazhong University of Science and Technology, Wuhan, People's Republic of China, [2]Wuhan Institute of Physics and Mathematics, Chinese Academy of Sciences, Wuan, People's Republic of China, [3]Department of Anesthesiology, Peking University Third Hospital, Beijing, People's Republic of China, [4]Insititute of High Energy Physics, Chinese Academy of Sciences, Beijing, People's Republic of China

Alcohol preferring and non-preferring rats were trained with two-bottle choice methods. The whole brain default mode network was acquired during different period of addiction training and after alcohol injection. The correlation coefficients among 28 regions were calculated by mean-value of Pearson correlation. The changes of brain connections after alcohol consumption in different stage of alcohol addiction is significant different. Furthermore, some addiction or reward associated regions and new possible areas (NAc, Tu, VTA, IC, Hypo, SNC, Au, DB, Hipp, VLPO, etc.) showed difference during the training. Our findings could provide preliminary functional connection support of neurobiological circuits change.

1704

Cocaine applied in a “binge paradigm” induces a region-specific and persistent brain circuitry modulation.

Elisabeth Jonckers[1], Michael Belloy[1], Dany Dsouza[2], Marleen Verhoye[1], Thomas Mueggler[2], and Annemie Van der Linden[1]

[1]Bio-Imaging Lab, University of Antwerp, Wilrijk, Belgium, [2]Roche Pharma Research and Early Development, Roche Innovation Center Basel, Basel, Switzerland

Our pre-clinical rodent study showed an increased Functional Connectivity at the level of the striatum and the cingulate cortex induced by cocaine injection. The effect was detectable 4 hours after administering cocaine and sustained for 24h.

1705

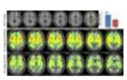

Resting state fMRI in Patients Infected with Hepatitis C Virus

Santosh Kumar Yadav[1], Ajay Vardaan[2], Rakesh Kumar Gupta[3], Pradeep Kumar Gupta[3], Samir Mohindra[4], Deepak Kaura[5], Francesco Marincola[1], Ena Wang[1], and Mohammad Haris[1]

[1]Research Department, Sidra Medical and Research Center, Doha, Qatar, [2]Department of Medicine, King George Medical University, Lucknow, India, [3]Department of Radiology and Imaging, Fortis Memorial Research Institute, India, [4]Department of Gastroenterology, Sanjay Gandhi Post graduate Institute of Medical Science, India, [5]Department of Radiology, Sidra Medical and Research Center, Doha, Qatar

Current study measured the amplitude of low-frequency fluctuations (ALFF) and insular functional connectivity (FC) in Hepatitis C virus patients and compared with age and gender matched control using RESTplus software. HCV patients showed significantly reduced ALFF in the right insula. The right insular FC strength was lower in patients than control. Neuropsychological test scores were significantly lower in HCV patients. Changes in ALFF and FC provide new evidences of altered neuronal activity in HCV patients.

1706

Resting state fMRI in Migraine

Kenneth M Jackson[1], Steven C Liu[1], Maryam Falahpour[1], Christy Jackson[2], Frank Haist[3], Richard B Buxton[1], and David J Dubowitz[1]

[1]Radiology, University of California San Diego, La Jolla, CA, United States, [2]Neurology, Scripps Clinic, La Jolla, CA, United States, [3]Psychiatry, University of California San Diego, La Jolla, CA, United States

We used resting state fMRI to evaluate changes in functional connectivity during migraine episodes, and the response to treatment. The results provide preliminary evidence for a change in functional connectivity in the DMN during migraine, and for the ability of serotonin agonists to restore resting state connectivity. We also identified key brain regions impacted by migraine and then normalized following sumatriptan.

1707

Real-time fMRI functional connectivity self-regulation and motor performance

Patricia Vargas[1,2,3,4], Ranganatha Sitaram[1,2,3,5,6], Pradyumna Sepúlveda[3,4], Cristian Montalba[4], Mohit Rana[1,2,3], Cristian Tejos[4,7], and Sergio Ruiz[1,2,3,5]

[1]Department of Psychiatry, Faculty of Medicine. Pontificia Universidad Católica de Chile, Santiago, Chile, [2]Interdisciplinary Center for Neuroscience, Pontificia Universidad Católica de Chile, Santiago, Chile, [3]Laboratory for Brain Machine Interfaces and Neuromodulation, Pontificia Universidad Católica de Chile, Santiago, Chile, [4]Biomedical Imaging Center, Pontificia Universidad Católica de Chile, Santiago, Chile, [5]Institute of Medical Psychology and Behavioral Neurobiology, University of Tübingen, Tübingen, Germany, [6]Institute for Biological and Medical Engineering, Pontificia Universidad Católica de Chile, Santiago, Chile, [7]Department of Electrical Engineering, Pontificia Universidad Católica de Chile, Santiago, Chile

Brain-Computer interfaces have been used for the rehabilitation of motor and cognitive functions. They can be used to train voluntary neural activity, leading to behavioral effects depending on the targeted brain areas.

The aim of this study was to test the feasibility of achieving volitional control of M1-cerebellum functional connectivity with a real-time fMRI (Rt-fMRI) system and evaluates its influence in motor performance.

Nine healthy subjects were trained in a protocol with visual feedback and motor imagery.

The results indicate that voluntary self-regulation of cerebellum-M1 connectivity is feasible with Rt-fMRI, but the effects on motor performance need to be further studied.

1708  Altered Functional Connectivity in Essential Tremor Patients immediately following Thalamotomy using MRI guided Focused Ultrasound

Li Jiang[1], Jiachen Zhuo[1], Prashant Raghavan[2], Dheeraj Gandhi[2], Elias R. Melhem[2], and Rao Gullapalli[1]

[1]Center for Metabolic Imaging & Therapeutics, Department of Diagnostic Radiology & Nuclear Medicine, University of Maryland Baltimore School of Medicine, Baltimore, MD, United States, [2]Department of Diagnostic Radiology & Nuclear Medicine, University of Maryland Baltimore School of Medicine, Baltimore, MD, United States

Essential tremor (ET) is a common neurological disorder. It is often characterized by progressive tremor of the arms or hands during voluntary movements. Ablation of the ventralis intermedius nucleus (VIM) of thalamus appears to be an effective treatment for ET. However, little is known regarding changes in the brain networks among ET patients and even less regarding the network changes following the thalamotomy. This study used resting state fMRI to investigate the changes in functional connectivity (FC) in brain networks immediately after the thalamotomy and reveals reduced FC between the ablated VIM and the motor cortex and cerebellum.

1709 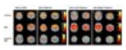 Disruption of Functional Connectivity in Neonates with Hypoxic Ischemic Encephalopathy at Term

Li Jiang[1], Jiachen Zhuo[1], Dina Metwally[2], Rao Gullapalli[1], and Prashant Raghavan[1]

[1]Center for Metabolic Imaging & Therapeutics, Department of Diagnostic Radiology & Nuclear Medicine, University of Maryland Baltimore School of Medicine, Baltimore, MD, United States, [2]Pediatrics, University of Maryland Baltimore School of Medicine, Baltimore, MD, United States

Perinatal hypoxic-ischemic encephalopathy (HIE) is one of the most common causes of severe, long-term neurologic deficits in children. Up to 40% of infants with HIE who present minimal to no abnormality on structure MRI may still have manifest neurological deficits in later life. In this study, we hypothesize that functional connectivity (FC) of the brain in infants with HIE at term may be altered and that resting-state functional MRI (rs-fMRI) may provide deeper insights into the altered nature of the brain networks, especially the motor network and the thalamocortical network in infants with HIE.

1710  Towards specific biomarkers of chronic pain: Modelling behavior readouts of developing pain to resting-state functional connectivity using a developmental trajectory in a mouse model of chronic pain from bone cancer

David Buehlmann[1,2], Giovanna Diletta Ielacqua[1], Joanes Grandjean[3], Jael Xandry[4], and Markus Rudin[1,4]

[1]Inst. for Biomedical Engineering, ETH & University of Zurich, Zurich, Switzerland, [2]Neuroscience Center Zurich, Zurich, Switzerland, [3]Singapore Bioimaging Consortium, Singapore, Singapore, [4]Inst. for Pharmacology & Toxicology, University of Zurich, Zurich, Switzerland

We performed longitudinal behavioral readouts of pain and resting-state fMRI in a mouse model of chronic pain from breast cancer derived tibial bone metastases. The developmental trajectory of behavioral readouts was used to model the fMRI response to extract pain-specific functional connectivity changes during development of a chronic pain state. The specificity of these functional readouts was supported through inhibition of osteolytic activity, reducing the nociceptive input. Thereby, characteristic functional changes could be reduced and in some regions prevented. These results emphasize the specificity of the functional readouts for developing chronic pain and could be used to evaluate novel treatments.

1711  Altered Variability in Functional Connectivity of the Anterior Cingulate Cortex in Patients with Refractory and Nonrefractory Major Depressive Disorders

Bochao Cheng[1,2], Gang Ning[1], Yong He[3], and Qiyong Gong[2]

[1]Radiology Department, West China Second University Hospital of Sichuan University, Chengdu, People's Republic of China, [2]Huaxi MR Research Center, HMRRC, West China Hospital, Sichuan University, Chengdu, People's Republic of China, [3]State Key Laboratory of Cognitive Neuroscience and Learning, Beijing Normal University, Beijing, People's Republic of China

Although substantial efforts have been made to elucidate the neuronal basis of both refractory MDD (rMDD) and nonrefractory MDD (nrMDD), the results are inconsistant. We apply the resting-state dynamic functional connectivity (D-RSFC) to explore the divergence of neuroal basis between rMDD and nrMDD. Our results demonstrated that the D-RSFC method can well reveal the dysfunctional brain networks in the MDD. The prefrontal-limbic circuit is the most stable dysfunctional brain network in both MDD subtypes. Additionally, we speculate that the OFC-sgACC circuit, especially the frontal part of the left OFC-sgACC circuit, might be the biomarker for evaluating treatment response in MDD.

1712 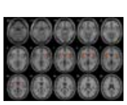 Increased inter-hemispheric functional connectivity in restless legs syndrome using voxel-mirrored homotopic connectivity

Yong Zhang[1], Kang-An Li[2], Yun-Cheng Wu[3], Zhenyu Zhou[4], and Gui-Xiang Zhang[2]

[1]MR Research China, GE Healthcare, Shanghai, People's Republic of China, [2]Radiology, Shanghai First People's Hospital, Shanghai, People's Republic of China, [3]Neurology, Shanghai First People's Hospital, Shanghai, [4]MR Research China, GE Healthcare, Beijing, People's Republic of China

This preliminary study used voxel- mirrored homotopic connectivity (VMHC), a novel resting-state fMRI parameter to investigate inter-hemispheric functional activity changes in restless legs syndrome (RLS). Ten RLS patients and ten age- and gender-matched healthy controls were recruited for comparison. The RLS group showed increased VMHC in the amygdala, putamen and insula, as compared to normal controls. Increased VMHC in the insular cortex and putamen might reflect their functions in perception and motor control. Increased VMHC in the amygdalae could be relevant to the disturbed sleep at night, considering its primary role in the processing of memory and emotion.

1713

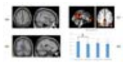

Effects of Lithium on resting-state fMRI in HIV-associated neurocognitive disorder

Yuchuan Zhuang[1], Madalina Tivarus[2], Eric H. Decloedt[3,4], John A. Joska[5], Jianhui Zhong[2], and Giovanni Schifitto[6]

[1]Department of Electrical and Computer Engineering, University of Rochester, Rochester, NY, United States, [2]Department of Imaging Sciences, University of Rochester Medical Center, Rochester, NY, United States, [3]Department of Medicine, Stellenbosch University, South Africa, [4]Department of Medicine, University of Cape Town, South Africa, [5]Department of Psychiatry and Mental Health, University of Cape Town, South Africa, [6]Department of Neurology, University of Rochester Medical Center, Rochester, NY, United States

This study firstly tested adjunctive lithium therapy in HIV patients with HAND. We examined the lithium effect using resting-state fMRI, and functional connectivity, amplitude of low-frequency fluctuation(ALFF) and fractional ALFF were calculated. We found significantly decrease of low-frequency oscillation and functional connectivity in lithium-treated group compared to placebo group, while neurocognitive performance was not different between the two groups.

1714

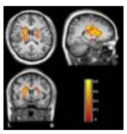

Altered gray matter cerebral blood flow and its connectivity indicate a potential cognitive dysfunction of chronic subcortical stroke patients

Caihong Wang[1], Peifang Miao[1], Peng Li[1], Jingchun Liu[2], Lin Jiang[3], Hao Liu[1], Dandan Zheng[4], Zhenyu Zhou[4], and Jingliang Cheng[1]

[1]Department of MRI, The First Affiliated Hospital of Zhengzhou University, Zhengzhou, People's Republic of China, [2]Department of Radiology, Tianjin Key Laboratory of Functional Imaging, Tianjin Medical University General Hospital, Tianjin, People's Republic of China, [3]School of Medical Imaging, Tianjin Medical University, Tianjin, People's Republic of China, [4]GE Healthcare MR Research China, Beijing

In order to investigate gray matter cerebral blood flow (CBF) and CBF connectivity alterations in chronic stroke patients, 60 patients and 60 controls were recruited to undergo 3D ASL technique. The patients exhibited increased CBFs in contralesional SFG, thalamus and ITG, and decreased CBF in ipsilesional Post_CG. Further analysis showed decreased CBF connectivity in patients in ipsilesional Pre_CG, MFG and Msfg. Importantly, the patients exhibited disconnections between the SFG and MFG, mSFG, Pre_CG. Current results suggest that stroke-induced cognitive dysfunction may be a connectivity disorder from the perspective of CBF connectivity.

1715

fMRI and spectroscopic characterization of sensory and pain processing in “pain-free” mice

Giovanna Diletta Ielacqua[1], Aileen Schroeter[1], Aline Seuwen[1], David Buehlmann[1,2], Jael Xandry[3], John N. Wood[4], and Markus Rudin[1,3]

[1]Institute for Biomedical Engineering, ETH and University of Zurich, Zurich, Switzerland, [2]Neuroscience Center Zurich, Zurich, Switzerland, [3]Institute of Pharmacology and Toxicology, University of Zurich, Zurich, Switzerland, [4]Molecular Nociception Group, Wolfson Institute for Biomedical Research, University College London, London, United Kingdom

FMRI has been widely used to assess changes in brain activity evoked by innocuous and noxious stimuli. However, stimulus-evoked fMRI (se-fMRI) measurements in mice have turned out challenging, and it is still under investigation whether and under which conditions se-fMRI applications in mice can lead to reliable readouts. Generally, se-fMRI could be a useful tool to characterize genetically modified mouse strains, such as mice exhibiting altered nociception. In this study, NaV1.7fl/fl:AdvCre mice were characterized with respect to neural processing of different types of peripheral stimuli and compared to a wildtype control group. Results of behavioral tests are compared to outcomes of fMRI and spectroscopic measurements.

1716

Phenotyping assay of neuropathic pain models using resting state functional connectivity MRI and Graph theoretical analysis

Yuji Komaki[1,2], Fumiko Seki[1,2,3], Keigo Hikishima[4], Masaya Nakamura[2], and Hideyuki Okano[2]

[1]Laboratory Animal Research Department, Central Institute for Experimental Animals, Kawasaki, Japan, [2]Keio University, Tokyo, Japan, [3]Brain Science Institute, RIKEN, Saitama, Japan, [4]Okinawa Institute of Science and Technology Graduate University (OIST), Japan

Resting state functional connectivity MRI was performed with neuropathic pain model mice.The functional network was constructed by temporal correlation analysis at the whole brain level based on the Allen brain atlas. Graph theoretical analysis was conducted to evaluate the feature of constructed networks. Compared with the intact model, degree and eigenvector centrality of neuropathic pain model showed a significant reduction in the primary somatosensory area. The clustering coefficient and local efficiency were significantly increased in the ACA. Significantly higher betweenness centrality was observed in the VPL. These results indicate that amount of information about connection to S1 was decreased. Neuropathic pain disrupt the pain matrix and the pain matrix that includes ACA and VPL may construct the complicated network. Integration of resting state functional connectivity MRI and graph theoretical analysis can evaluate the interactive complex networks of each region, not only existence or non-existence of activation region.

1717

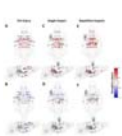

Reorganization of Rodent Resting-state Functional Networks after mild Traumatic Brain Injury

Chia-Feng Lu[1,2,3], Yu-Chieh Jill Kao[1,2], Huai-Lu Chen[1,4], Fei-Ting Hsu[1,5], Ping-Huei Tsai[1,2,5], Hua-Shan Liu[1,6], Li-Chun Hsieh[1,5], Gilbert Aaron Lee[1,4], and Cheng-Yu Chen[1,2,5]

[1]Translational Imaging Research Center, College of Medicine, Taipei Medical University, Taipei, Taiwan, [2]Department of Radiology, School of Medicine, College of Medicine, Taipei Medical University, Taipei, Taiwan, [3]Department of Biomedical Imaging and Radiological Sciences, National Yang-Ming University, Taipei, Taiwan, [4]Department of Medical Research, Taipei Medical University Hospital, Taipei, Taiwan, [5]Department of Medical Imaging, Taipei Medical University Hospital, Taipei, Taiwan, [6]School of Biomedical Engineering, College of Biomedical Engineering, Taipei Medical University, Taipei, Taiwan

Complex network analysis unraveled the mTBI-related functional reorganization with the disruption of long-distance connections of thalamocortical interactions and enhanced local connectivity segregation in the regions of neocortex and thalamic nuclei.

1718

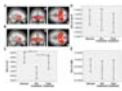

Enhanced striatum connectivity is irrelevant to baseline perfusion in major depressive disorder following sertraline treatment

Changwei W. Wu[1,2], Zi-Xuan Chang[3], I-Ling Chung[4], Chien-Yuan Lin[5], Ching-Po Lin[6], Chi-Bin Yeh[7], and Hong-Wen Kao[4]

[1]Graduate Institute of Humanities in Medicine, Taipei Medical University, Taipei, Taiwan, [2]Brain and Consciousness Research Center, Taipei Medical University, Taipei, Taiwan, [3]Department of Biomedical Sciences and Engineering, National Central University, Taoyuan, Taiwan, [4]Department of Radiology, Tri-Service General Hospital, National Defense Medical Center, Taipei, Taiwan, [5]GE Healthcare, Taipei, Taiwan, [6]Institute of Neuroscience, National Yang-Ming University, Taipei, Taiwan, [7]Department of Psychiatry, Tri-Service General Hospital, National Defense Medical Center, Taipei, Taiwan

We revisited the sertraline treatment effect on RSFC in drug-naïve MDD patients and evaluated the association between RSFC, ALFF and baseline CBF level. Twenty-four unmedicated MDD subjects were recruited and treated with sertraline for 6 weeks. Results showed negative correlation between HAM-D scores and striatum-MPFC RSFC. However, the therapeutic effect on RSFC was irrelevant to the CBF or ALFF levels, implying better temporal synchronizations from the neural basis.

1719

Learning Subnetwork Biomarkers via Hypergraph for Classification of Autism Disease

Chen Zu[1], Yue Gao[2], Brent Munsell[3], Minjeong Kim[1], Ziwen Peng[4], Yingying Zhu[1], Wei Gao[5], Daoqiang Zhang[6], Dinggang Shen[1], and Guorong Wu[1]

[1]University of North Carolina at Chapel Hill, Chapel Hill, NC, United States, [2]School of Software, Tsinghua University, Beijing, China, [3]Department of Computer Science, College of Charleston, Charleston, SC, USA, [4]Centre for Studies of Psychological Application, School of Psychology, South China Normal University, Guangzhou, China, [5]Biomedical Imaging Research Institute (BIRI), Department of Biomedical Sciences and Imaging, Cedars-Sinai Medical Center, Los Angeles, CA, USA, [6]Department of Computer Science and Technology, Nanjing University of Aeronautics and As-tronautics, Nanjing, China

Most brain network connectivity models consider correlations between discrete-time series signals that only connect two brain regions. Here we propose a method to explore subnetwork biomarkers that are significantly distinguishable between two clinical cohorts. We construct a hypergraph by exhaustively inspecting all possible subnetworks for all subjects. The objective function of hypergraph learning is to jointly optimize the weights for all hyperedges. We deploy our method to find high order childhood autism biomarkers from rs-fMRI images. Promising results have been obtained from comprehensive evaluation on the discriminative power in diagnosis of Autism.

1720

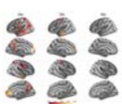

Relationship between static and dynamic brain functional connectivity in autism spectrum disorders

Adam Liska[1,2], Hongyuan You[3], and Payel Das[4]

[1]CIMeC, Center for Mind/Brain Sciences, University of Trento, Rovereto, Italy, [2]Functional Neuroimaging Laboratory, Center for Neuroscience and Cognitive Systems @ UniTn, Istituto Italiano di Tecnologia, Rovereto, Italy, [3]Department of Computer Science, University of California, Santa Barbara, Santa Barbara, CA, United States, [4]IBM Thomas J. Watson Research Center, Yorktown Heights, NY, United States

There is an increased interest in the dynamics of brain functional connectivity, as measured via temporal covariance in resting-state fMRI BOLD signal, and its aberrations in brain disorders. We studied and compared two measures of regional dynamic behaviour, flexibility and variability, across two datasets and show that patients diagnosed with autism spectrum disorder show increased dynamic connectional variability in several brain regions. Furthermore, we establish an interesting association between static and dynamic functional connectivity measures.

1721

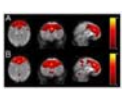

Modulation of Saslience Network Activation after 4 Weeks Verbal Training in Older Adults

Toshiharu Nakai[1,2], Ayuko Tanaka[3,4], Mika Ueno[1], Atsunobu Suzuki[5], and Sachiko Kiyama[4,6]

[1]NeuroImaging & Informatics, NCGG, Ohbu, Japan, [2]Department of Radiological Science, Nagoya University Graduate School of Medicine, Nagoya, Japan, [3]Faculty of Human Sciences, Kobe Shoin Women's University, Kobe, Japan, [4]NeuroImaging & Informatics, National Center for Geriatrics & Gerontology, Ohbu, Japan, [5]Department of Social and Human Environment, Graduate School of Environmental Studies, Nagoya, Japan, [6]College of Liberal Arts and Sciences, Mie University, Tsu, Japan

The potential of RSN to detect the early change of neuronal networks induced by short-term cognitive intervention was investigated by using a verbal training task to read short sentences aloud everyday for 4 weeks. Twenty community dwelling older adults participated in this study. Activation in the anterior SN was decreased after the training, suggesting optimization of salience processing to integrate visual information and language production. The SN may be potentially a biomarker to firstly reflect the change in response to cognitive interventions in older adults and this finding may be applied to optimize training protocols for each individual.

1722

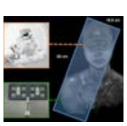

Functional Connection Between Brain and Right Upper-arm: A rs-fMRI Study

Chia-Wei Li[1,2], Min-Ling Lin[2], Jyh-Horng Chen[2,3], and Wing P. Chan[1,4]

[1]Department of radiology, Wan Fang Hospital, Taipei Medical University, Taipei, Taiwan, [2]Department of Electrical Engineering, National Taiwan University, Taipei, Taiwan, [3]Neurobiology and Cognitive Science Center, National Taiwan University, Taipei, Taiwan, [4]Department of Radiology, School of Medicine, College of Medicine, Taipei Medical University, Taipei, Taiwan

This study aimed to explore the functional coupling between the central nervous system and the peripheral nervous system of upper limb. We established a novel imaging-platform to collect the functional images from human brain and upper limb simultaneously. This study disclosed the functional coupling between the peripheral nervous system of upper limb and the brain cortex and demonstrated that peripheral nervous system also involved in the regulation of brain cognitive function and related network changes.

1723

Network Analysis Revealed Two Distinct Neuronal Circuits Involved in Nociceptive Processing within the Rat Brain after Ablation of TRPV1-Expressing Peripheral Neurons

Isabel Wank[1], Lisa Kutsche[1], Silke Kreitz[1], and Andreas Hess[1]

[1]Institute of Pharmacology and Toxicology, University of Erlangen-Nuremberg, Erlangen, Germany

Pain is a vital danger signal, as it prevents the body from suffering burns by hot items. Using BOLD-fMRI, we evaluated the rat's brain response to increasing thermal stimuli to detect which brain structures are involved especially in the processing of nociceptive heat. Therefore, we eradicated selectively the nociceptive-specific TRPV1-expressing neurons via Resiniferatoxin-induced excitotoxicity. This missing nociceptive input from the periphery resulted in a widespread suppression of brain activity in most brain structures except some parts of the brainstem. Graphtheoretical network analysis revealed two distinct circuits of brain structures involved in the processing of noxious temperatures above 48° C.

1724

Interrogating neurotransmitter systems using resting-state fMRI

Joanes Grandjean[1], Michaela Bürge[2], David Bühlmann[3], Hannes Sigrist[2], Erich Seifritz[2], Franz X. Vollenweider[2], Christopher R. Pryce[2], and Markus Rudin[3,4]

[1]Singapore BioImaging Consortium, Agency for Science, Research and Technology, Singapore, Singapore, [2]Psychiatric Hospital, University of Zurich, Switzerland, [3]Institue for Biomedical Engineering, University and ETH Zürich, Switzerland, [4]Institute of Pharmacology and Toxicology, University of Zurich, Switzerland

We assessed functional connectivity (FC) in the mouse brain following psilocybin administration. Conventional analysis using dual regression and reference spatial maps derived from independent component decomposition identified a decrease in FC within the ventral striatum network in animals administered with psilocybin relative to vehicle. Dopamine D1 and serotonin 5HT2a receptor gene expression as well as projection maps from the ventral tegmental area and dorsal raphe nuclei obtained from the Allen Brain Institute database were used as spatial references in a secondary dual regression analysis to disentangle the contribution of dopamine and serotonin systems to whole-brain functional connectivity changes.

1725

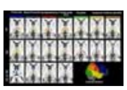

Thalamocortical neural responses to whole body heat exposure: A resting-State Functional MRI study

Shaowen Qian[1], Qingjun Jiang[1], Kai Liu[1], Bo Li[1], Jianxun Qu[2], and Gang Sun[1]

[1]Jinan Military General Hospital, Jinan, People's Republic of China, [2]GE Healthcare China

In this study, we replicated previous findings about spatially distinct thalamic correlations with cortical regions of interest. Using bi-directional functional analysis, we firstly clarified cortical-subcortical activity during hyperthermic condition by thalamocortical functional connectivity. Specifically, we found weakening connectivity of cortical fronto-polar/anterior cingulate cortex and prefrontal areas with the corresponding thalamic nuclei. On the contrary, the motor/premotor and somatosensory cortical subdivisions showed increased connectivity with thalamic nuclei. The thalamic pulvinar showed reduced connectivity with bilateral superior and middle temporal pole, but increased connectivity with bilateral middle and inferior temporal gyrus.

1726

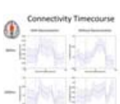

Use of Simultaneous Multi-Slice Imaging to Assess Dynamic Connectivity During a Self-Paced Finger Tap Task

Eleanor Barratt[1], Matthew Brookes[1], and Susan Francis[1]

[1]School of Physics, University of Nottingham, Nottingham, United Kingdom

Previous fMRI studies have demonstrated a number of functional networks in the brain. The introduction of simultaneous multi-slice (SMS) -imaging has allowed a larger volume coverage of the brain to be acquired with a shorter repetition time (TR), increasing temporal resolution so that dynamic connectivity (DC) measures are more achievable. Here, we use sub-second SMS-imaging to assess DC in sensorimotor networks during a self-paced finger tap experiment, and demonstrate changes in DC during individual button presses.

1727

Relationship between GABA and glutamate and inter- and intra-regional intrinsic connectivity as measured by resting-state fMRI

Sarina J Iwabuchi[1,2], Felix Raschke[3], Lena Palaniyappan[4,5], and Dorothee P Auer[1,2]

[1]Radiological Sciences, Division of Clinical Neuroscience, University of Nottingham, Nottingham, United Kingdom, [2]Sir Peter Mansfield Imaging Centre, University of Nottingham, Nottingham, United Kingdom, [3]Department of Radiotherapy and Radiation Oncology, OncoRay National Center for Radiation Research in Oncology, Dresden, Germany, [4]Departments of Psychiatry and Medical Biophysics & Robarts Research Institute, Western University, London, ON, Canada, [5]Lawson Health Research Institute, London, ON

Associations between GABAergic and glutamatergic systems and measures of brain connectivity have been reported previously. However, there is currently no evidence for associations between these systems and local connectivity measures, limiting our understanding of inhibitory/excitatory balance and connectivity across differing spatial ranges. We demonstrated that only regional connectivity and spontaneous activity, but not long-range connectivity, were associated with GABA and GABA/Glx ratio in the ACC. We suggest that this correlation between measures of intra-regional connectivity and GABA in the ACC may be driven by interneuron activity. Further, associations between neurotransmitter pools and inter-regional connectivity may be region/network and context-specific.

1728 

The intrinsic functional mechanism for olfactory-visual association in the human brain as quantified by fMRI

Brittany Martinez[1], Prasanna Karunanayaka[1], Jianli Wang[1], Xin Zhang[2], Bing Zhang[2], and Qing X. Yang[1]

[1]Radiology, Penn State University, Hershey, PA, United States, [2]Radiology, Nanjing University Medical School, Nanjing, People's Republic of China

The purpose of this study was to elucidate the reciprocal effect of olfactory-visual associations on olfactory and visual processing in the human brain using fMRI. Young, cognitively healthy participants underwent 3 separate olfactory-visual association paradigms, including either neutral, semantically congruent, or semantically incongruent visual cues. The data revealed significant olfactory activation in the POC and visual areas in response to visual cues, regardless of semantic meaning (neutral, congruent, or incongruent). This reciprocally increased activation in the POC and visual cortex during olfactory-visual cue pairing and subsequent visual cue presentations may suggest an intrinsic functional mechanism for multisensory associative learning.

1729 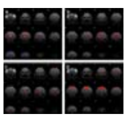

Functional magnetic resonance imaging shows network activation from a non-visual light stimulus of deep brain photoreceptors in songbirds

Bruce Langford[1], Thomas Neuberger[2,3], Nanyin Zhang[2,4], and Paul Bartell[1,5]

[1]Department of Animal Science, The Pennsylvania State University, University Park, PA, United States, [2]Department of Biomedical Engineering, The Pennsylvania State University, University Park, PA, United States, [3]Huck Institutes of the Life Sciences, The Pennsylvania State University, [4]The Neuroscience Program, The Huck Institutes of Life Sciences, [5]Interdepartmental Graduate Program in Neuroscience

Many avian species go through circannual changes in reproductive organs. Seasonal changes are triggered by non-visual photostimulation, made possible by the existence of nuclei with containing opsin channels. Photoactivation occurs when photosensitive neurons are stimulated, resulting in a cascade of activity in the brain, which initiates gonadal growth. Photorefraction is on a time-scale much longer than an experiment. We used echo planar imaging fMRI with a laser for stimulation and performed independent component analysis on each phase (before, during, and after stimulation). Network activation patterns differ in each phase.

Traditional Poster

Diffusion: Biophysical Modeling & Microstructure

Exhibition Hall 1730-1776 Tuesday 13:45 - 15:45

1730 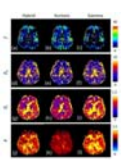

Hybrid Modeling for Perfusion Quantification Using Intravoxel Incoherent Motion MRI

Yen-Peng Liao[1], Shin-ichi Urayama[2], Hidenao Fukuyama[2], and Denis Le Bihan[3]

[1]Human Brain Research Center, Kyoto University Graduate School of Medicine, Kyoto, Japan, [2]Training Program of Leaders for Integrated Medical System, Kyoto University, Kyoto, Japan, [3]Neurospin, Gif-sur-Yvette, France

IVIM-MRI has been used to estimate perfusion-relative parameters. To increase signal fitting robustness in case of limited SNR, an asymptotic method was recommended. Hence, with the asymptotic method, a threshold b-value should be determined above which flow contamination is deemed negligible. Various diffusion models and a wide range of values for this threshold can be found in the literature. These two effects on quantification were investigated using both computer simulations and human brain data. The results showed that the choice of the model and the threshold critically influenced the quantitative parameters. We proposed a hybrid-modeling method to minimize systematic errors.

1731 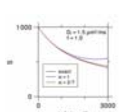

Optimizing the Signal Model for Diffusional Kurtosis Imaging

Jens H Jensen[1,2], Vaibhav Mohanty[1,2], Emilie T McKinnon[1,2,3], and Joseph A Helpern[1,2,3,4]

[1]Department of Radiology and Radiological Science, Medical University of South Carolina, Charleston, SC, United States, [2]Center for Biomedical Imaging, Medical University of South Carolina, Charleston, SC, United States, [3]Department of Neurology, Medical University of South Carolina, Charleston, SC, United States, [4]Department of Neuroscience, Medical University of South Carolina, Charleston, SC, United States

A generalized signal model for diffusional kurtosis imaging (DKI) is proposed containing an adjustable parameter that can be optimized to reduced systematic errors in kurtosis estimates. This is illustrated by applying an established tissue model for diffusion in brain to fix the parameter, and numerical simulations are employed to demonstrate the improvement in accuracy relative to kurtosis estimates obtained with the standard DKI signal model. Finally, in vivo brain data is used to compare mean kurtosis estimates obtained with the standard and optimized DKI signal models.

1732

Diffusion-weighted MR imaging of kidney after administration of 2 types of iodinated contrast medium: a time course study in CIN animal model

Kai Zhao[1], Xueqing Sui[1], Rui Wang[1], Zhiyong Lin[1], Xiaodong Zhang[1], Jian Luo[1], and Xiaoying Wang[1]

[1]Department of Radiology, Peking University First Hospital, Beijing, People's Republic of China

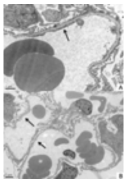

DWI is a preeminent noninvasive method to quantify renal function, which may be helpful to understand the pathogenesis of CIN. Our time course study indicates that the iodinated contrast medium can induce some affect to the different zone of kidney. And some differences do exist on the renal transport function after the two kinds of iodinated CM administration.

1733

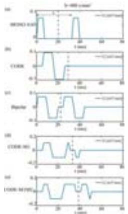

Monte-Carlo Analysis of Quantitative Diffusion Measurements Using Motion-Compensated Diffusion Weighting Waveforms

Yuxin Zhang[1,2], Óscar Peña-Nogales[3], James H. Holmes[2], and Diego Hernando[1,2]

[1]Medical Physics, University of Wisconsin, Madison, Madison, WI, United States, [2]Radiology, University of Wisconsin, Madison, Madison, WI, United States, [3]Laboratorio de Procesado de Imagen, Universidad de Valladolid, Valladolid, Spain

Advanced diffusion MRI acquisition strategies based on motion-compensated diffusion-encoding waveforms have been proposed to reduce the signal voids caused by tissue motion. However, quantitative diffusion measurements obtained from these motion-compensated waveforms may be biased relative to standard monopolar gradient waveforms. This study evaluated the effect of different diffusion encoding gradient waveforms on the signal decay and diffusion measurements, using Monte-Carlo simulations with different microstructures and several reconstruction signal models. The results show substantial bias in observed signal decay and quantitative diffusion measurements in the same microstructure across different gradient waveforms, in the presence of restricted diffusion.

1734

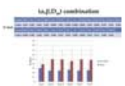

White Matter Structural Differences among Subjects with Obstructive Sleep Apnea after Persistent CPAP-Treatment: A Non-Gaussian Diffusion MR Study with TBSS

Jiaxuan Zhang[1,2], Terri E. Weaver[3], Zheng Zhong[1,4], Robyn A. Nisi[3], Kelly R. Martin[3], M. Muge Karaman[1], and Xiaohong Joe Zhou[1,5]

[1]Center for MR Research, University of Illinois at Chicago, Chicago, IL, United States, [2]Department of Radiology, Tongji Hospital, Huazhong University of Science and Technology, Wuhan, People's Republic of China, [3]College of Nursing, University of Illinois at Chicago, Chicago, IL, United States, [4]Department of Bioengineering, University of Illinois at Chicago, Chicago, IL, United States, [5]Departments of Radiology, Neurosurgery, and Bioengineering, University of Illinois at Chicago, Chicago, IL, United States

Obstructive sleep apnea (OSA) can result in brain white matter (WM) injuries due to the hypoxic exposure. Continuous positive airway pressure (CPAP) is a common method for treating OSA patients. However, it is unclear why some patients respond to the treatment whereas others do not. In this study, we employ a non-Gaussian diffusion MRI method using a continuous-time random-walk (CTRW) model with TBSS analysis to investigate the WM microstructural variations among OSA patients who responded differently to identical CPAP-treatment. Our results have shown that CTRW-related parameters in some WM tracts exhibited significant difference between the responders and non-responders.

1735

A modified tri-exponential model for multi-b-value diffusion-weighted imaging to detect the strictly diffusion-limited compartment and its initial application in grading and differential diagnosis of gliomas

Qiang Zeng[1], Biao Jiang[2], Jianmin Zhang[1], Feina Shi[3], Fei Dong[2], and Chenhan Ling[1]

[1]Department of Neurosurgery, Second Affiliated Hospital of Zhejiang University College of Medicine, Hangzhou, People's Republic of China, [2]Department of Radiology, Second Affiliated Hospital of Zhejiang University College of Medicine, Hangzhou, People's Republic of China, [3]Department of Neurology, Second Affiliated Hospital of Zhejiang University College of Medicine, Hangzhou, People's Republic of China

In this study, we focused on the strictly diffusion-limited compartment with extremely low ADC. Because of the negligible signal attenuation of this compartment, the ADC of this compartment was set as zero. By adding this compartment to the two-compartment model, we presented a modified tri-exponential model. The AICcs of this model were found to be lower than the bi-exponential model and the conventional tri-exponential model, indicating this model is the best. Additionally, the parameters derived from this model, especially the fraction of the strictly diffusion-limited compartment (f_0), showed potential clinical value in distinguishing the grade of malignancy of tumors.

1736

A Fractional Motion Diffusion Model for a Twice-Refocused Spin Echo Pulse Sequence: Analytical Expression and in vivo Demonstration

Muge Karaman[1] and Xiaohong Joe Zhou[1,2]

[1]Center for MR Research, University of Illinois at Chicago, Chicago, IL, United States, [2]Departments of Radiology, Neurosurgery, and Bioengineering, University of Illinois at Chicago, Chicago, IL, United States

The anomalous diffusion behavior of biological tissue has been investigated by several studies using non-Gaussian diffusion models. Among these, the fractional motion (FM) model has attracted an intense interest by the biophysics community and was recently been introduced to the MR community. The current diffusion signal formulism based on the FM model is limited to a simple Stejskal-Tanner gradient despite the widespread use of the eddy-current-resistant gradient waveform with the twice-refocused spin echo (TRSE) technique. In this study, we theoretically derive a formulism based on the FM diffusion model to characterize anomalous diffusion using a TRSE sequence, and experimentally validate it on healthy human brain *in vivo*.

1737

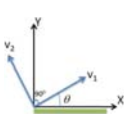

Substantial Error in MD Estimation Introduced by Trace Imaging

Mohammad Alipoor[1], Göran Starck[2], and Stephan E Maier[1,3]

[1]Radiology, University of Gothenburg, Goteborg, Sweden, [2]Radiation Physics, University of Gothenburg, Sweden, [3]Radiology, Brigham and Women's Hospital, Harvard Medical School, Boston, MA, United States

Since the single compartment diffusion tensor model does not reflect all contributions in diffusion signal, subsequent implications also may not hold in practice. One of the implications proven wrong here, is that mean diffusivity (MD) maps, which result from diffusion measurements along three orthogonal directions (trace imaging), are independent of the direction of the applied orthogonal gradient triplet. Simulation results with anisotropic multi-compartment diffusion models and human nerve fiber data confirm that the MD measured by trace imaging, which is typically used for rapid stroke delineation, is substantially dependent on the direction of the applied orthogonal gradient triplet and b-value.

1738

Translocation of Water Molecules in Tissue

Gregory J Wilson[1], Charles S Springer[2], and Jeffrey H Maki[1]

[1]Radiology, University of Washington, Seattle, WA, United States, [2]Advanced Imaging Research Center, Oregon Health and Science University, Portland, OR, United States

Numerical simulations of water molecule translocation are presented. The molecules execute random walks in a 3D ensemble of digital cells with density and size pertinent for biological tissue. The mean net displacements reflect “hindered” or “restricted” translocations for both extra- and intracellular water, characterized by an infinite number of exponentials. The hindrance is very sensitive to the cell membrane permeability, in the range for tissue – and controlled by active cell metabolism.

1739

The Maastricht Diffusion Toolbox (MDT): Modular, GPU accelerated, dMRI microstructure modeling

Robbert Leonard Harms[1,2] and Alard Roebroeck[1]

[1]Maastricht University, Maastricht, Netherlands, [2]Brain Innovation, Maastricht, Netherlands

MDT's object oriented modular design allows arbitrary user specification and combinations of dMRI compartment models, diffusion microstructure models, likelihood functions and optimization algorithms. Many diffusion microstructure models are included, and new models can be added simply by adding Python script files. GPU based computations allow for ~60x faster model fitting; e.g. the 81 volume example NODDI dataset can be fitted whole brain in about 40 seconds, which makes MDT ideal for population studies. MDT can be extended to other modalities and models such as quantitative MRI. The software is open source and freely available at https://github.com/cbclab.

1740

Simulating measurements of diffusion across the cell membrane with DEXSY and FEXSY

James Olav Breen-Norris[1,2], Bernard Siow[1,2,3], Ben Hipwell[1], Ioana Oprea[2], Thomas A. Roberts [1], Mark F. Lythgoe[1], Andrada Ianus[2], Daniel C. Alexander[2], and Simon Walker-Samuel[1]

[1]Centre for Advanced Biomedical Imaging, Division of Medicine, UCL, London, United Kingdom, [2]Microstructure Imaging Group, Centre for Medical Image Computing, UCL, London, United Kingdom, [3]Sir Francis CRICK Institute

Here, we use numerical simulations to demonstrate the feasibility of measuring diffusion exchange across the cell membrane using DEXSY (Diffusion Exchange spectroscopy) and compare it with FEXSY (Filter Exchange Spectroscopy). Simulations were carried out using the CAMINO platform, for a range of permeabilities, in a substrate chosen to model nerve tissue. The results of these simulations suggest that both DEXSY and FEXSY are capable of measuring diffusion exchange, over a physiologically meaningful range of permeabilities, and an extended range of permeabilities (0.365 to 2.008 µm/s). These results demonstrate the potential for these techniques to be used to differentiate pathology from normal tissue.

1741

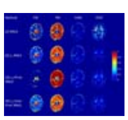

Deconvolution based approaches for the simultaneous quantification of IVIM, Free Water and non-Gaussian behavior in Diffusion MRI.

Alberto De Luca[1,2], Filippo Arrigoni[2], Alessandra Bertoldo[1], and Martijn Froeling[3]

[1]Department of Information Engineering, University of Padova, Padova, Italy, [2]Neuroimaging Lab, Scientific Institute IRCCS Eugenio Medea, Bosisio Parini (LC), Italy, [3]Radiology Department, University Medical Center Utrecht, Utrecht, Netherlands

The in-vivo Diffusion MRI (dMRI) signal does not generally arise from a single diffusion process but from the sum of multiples. In this study we investigated a deconvolution approach to simultaneously estimate non-Gaussian diffusion, free water (FW), IVIM and tissue fractions. We analyzed the brain data of a subject acquired with 60 different b-values with four deconvolution based approaches, and compared their results in terms of identified components. The four approaches provided consistent results, with the IVIM compartment being the most similar component across the four methods. Reliable quantification of multiple compartments, including membrane restrictions, is feasible with regularized approaches.

1742

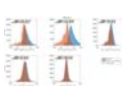

White matter biomarkers from fast protocols using axially symmetric diffusion kurtosis imaging

Brian Hansen[1], Ahmad Raza Khan[1], Noam Shemesh[2], Torben Ellegaard Lund[1], Ryan Sangill[1], Leif Østergaard[1], and Sune Nørhøj Jespersen[1,3]

[1]CFIN/MINDLab at the Department of Clinical Medicine, Aarhus University, Aarhus, Denmark, [2]Champalimaud Neuroscience Programme, Champalimaud Centre for the Unknown, Lisbon, Portugal, [3]Department of Physics and Astronomy, Aarhus University, Aarhus, Denmark

White matter tract integrity (WMTI) can be used to characterize tissue microstructure in areas with strongly aligned fiber bundles. Several WMTI biomarkers have now been validated against microscopy and provided promising results in studies of brain development, aging, and brain disorders. In clinical settings, however, the diffusion kurtosis imaging (DKI) protocol utilized as part of WMTI imaging may be prohibitively long. Consequently, the diagnostic value of the WMTI parameters is mostly explored in dedicated animal studies and clinical studies of slowly progressing diseases. Here, we evaluate WMTI based on recently introduced axisymmetric DKI which has lower data demand than conventional DKI.

1743 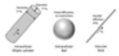

Inferring cell morphology in the heart with a compartment model of diffusion MRI

Darryl McClymont[1], Irvin Teh[1], Hannah Whittington[1], Craig Lygate[1], and Jürgen Schneider[1]

[1]*Cardiovascular Medicine, University of Oxford, Oxford, United Kingdom*

We propose a three-compartment model to perform cytometry in cardiac diffusion MRI. Our approach adapts the VERDICT model to account for the anisotropic geometry of cardiomyocytes. The model was fit to data from ex-vivo mouse heart imaged with multiple diffusion times, diffusion directions, and q-shells. The model yields realistic volume fractions (intracellular/extracellular/vascular = 68/16/16%) and cell radii (7-9.5 µm). The parameters derived could aid quantitative characterisation of cardiomyopathies including hypertrophy and fibrosis.

1744 

A novel diffusion compartment imaging (DCI) model that captures the asymmetry of WM microstructure heterogeneity

Benoit Scherrer[1], Maxime Taquet[1,2], Etienne Saint-Onge[1], Gaetan Rensonnet[2], and Simon K Warfield[3]

[1]*Department of Radiology, Boston Children's Hospital, Harvard Medical School, Boston, MA, United States,* [2]*ICTEAM, Universite catholique de Louvain, Louvain-La-Neuve, Belgium,* [3]*Boston Children's Hospital, Harvard Medical School, Boston, MA, United States*

The DIAMOND diffusion compartment imaging (DCI) model has been recently proposed to model the 3-D diffusivity of each compartment with a statistical distribution of diffusion tensors. This enabled the assessment of compartment-specific diffusion characteristics while also capturing the intra-compartment heterogeneity. The approach, however, could only describe symmetric heterogeneity, while tissue heterogeneity likely differs along and perpendicular to the fascicles' orientation. In this work we propose a new statistical distribution model able to capture the asymmetric nature of tissue heterogeneity. We demonstrate that it captures different axial and radial heterogeneities in presence of dispersion and investigate results with in vivo data.

1745 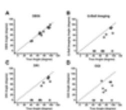

The Impact of Edema and Crossing Fibers on Diffusion MRI: ODF vs. DBSI

Ze-Zhong Ye[1], Sam Gary[2], Sourajit Mitra Mustafi[3], G. Russell Glenn[4,5,6], Fang-Cheng Yeh[7], Chunyu Song[8], Peng Sun[9], Yu-Chien Wu[3], Jens H. Jensen[4,5], and Sheng-Kwei Song[8,9,10]

[1]*Chemistry, Washington University, St. Louis, MO, United States,* [2]*Biology, Juniata College, Huntingdon, PA, United States,* [3]*Center for Neuroimaging, Indiana University, Indianapolis, IN, United States,* [4]*Center for Biomedical Imaging, Medical University of South Carolina, Charleston, SC, United States,* [5]*Radiology and Radiological Science, Medical University of South Carolina, Charleston, SC, United States,* [6]*Neurosciences, Medical University of South Carolina, Charleston, SC, United States,* [7]*Biomedical Engineering, Carnegie Mellon University, Pittsburgh, PA, United States,* [8]*Biomedical Engineering, Washington University, St. Louis, MO, United States,* [9]*Radiology, Washington University, St. Louis, MO, United States,* [10]*Hope Center for Neurological Disorder, Washington University, St. Louis, MO, United States*

We quantitatively examined the effect of fiber crossing and edema on DTI metrics employing phantoms made of mouse trigeminal nerves and agarose gel. Edema mimicked by gel coating significantly impaired the accuracy of estimated crossing angles using the diffusion orientation distribution function. Diffusion basis spectrum imaging (DBSI) was able to estimate crossing angles in the presence of edema and recover individual nerve baseline diffusivity.

1746 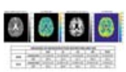

Empirical reproducibility of clinically feasible ensemble average propagator imaging

Kurt Schilling[1], Vishwesh Nath[2], Justin Blaber[2], Prasanna Parvathaneni[2], Adam W Anderson[1], and Bennett A Landman[2]

[1]*Biomedical Engineering, Vanderbilt University, Nashville, TN, United States,* [2]*Computer Science, Vanderbilt University*

In this study, we measure the reproducibility of metrics derived from the ensemble averaged propagator (EAP) estimated using the 3D-SHORE technique using a clinically feasible high angular resolution diffusion dataset repeated 11 times on a single subject. We find very low reproducibility in measures of microstructural restriction (including the mean-squared displacement and return to origin probability) as well as measures of the orientation distribution function (including peaks of the ODF). This study highlights the limitations of using advanced models with empirical data, particularly in the low-SNR regime.

1747 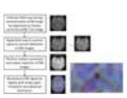

Reconstruction of fetal diffusion MRI using a spherical harmonic model

Maria Kuklisova Murgasova[1], Alessandro Daducci[2], Georgia Lockwood-Estrin[3], Daan Christiaens[1], Mary Rutherford[1], J Donald Tournier[1], Joseph V Hajnal[1], and Meritxell Bach Cuadra[2]

[1]*Division of Imaging Sciences & Biomedical Engineering, King's College London, London, United Kingdom,* [2]*École Polytechnique Fédérale de Lausanne, Lausanne, Switzerland,* [3]*Health Services & Population Research, King's College London, London, United Kingdom*

We present a novel method for reconstruction of fetal dMRI based on spherical harmonic model that includes motion correction, distortion correction and super-resolution reconstruction. We show that all these steps are important for producing good quality results. Our method will facilitate investigations into brain white-matter development in utero.

1748 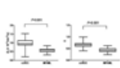

Monoexponential, Biexponential, and Stretched exponential Diffusion-weighted Imaging Models: Quantitative Biomarkers for Differentiating Renal Clear Cell Carcinoma and Minimal Fat Angiomyolipoma

Haojie Li[1], Yao Hu[1], Daoyu Hu[1], and Zhen Li[1]

[1]*Radiology, Tongji Hospital, Tongji Medical College, Huazhong University of Science and Technology, Wu Han, People's Republic of China*

Compared to monoexponential DWI model, biexponential and stretched exponential DWI models are feasible and useful in the noninvasive tissue characterization of renal tumors. Water molecular diffusion heterogeneity index (α) and Dt may provide additional information and could lead to improved differentiation with better sensitivity and specificity in differencing MFAML from ccRCC compared with mean ADC, Dp, fp, and DDC values in clinical setting.

1749 

Preliminary Investigation on NODDI for Studying Spinal Cord Microstructure of Postoperative CSM Patients

Xiaodong Ma[1], Xiao Han[2], Wen Jiang[3], Zhe Zhang[1], Erpeng Dai[1], Yishi Wang[1], Xiaoguang Cheng[3], and Hua Guo[1]

[1]Center for Biomedical Imaging Research, Department of Biomedical Engineering, School of Medicine, Tsinghua University, Beijing, China, Beijing, People's Republic of China, [2]Department of Surgery, Beijing Jishuitan Hospital, Beijing, China, Beijing, People's Republic of China, [3]Department of Radiology, Beijing Jishuitan Hospital, Beijing, China

In this study, the neurite orientation dispersion and density imaging (NODDI) was used to investigate the spinal cord microstructure for postoperative CSM patients. MRI data were acquired on eleven patients with a long time after surgery. The value of the calculated parameters (OD, Viso and Vic) were preliminarily evaluated. Statistical results show that OD of grey matter is lower at the stenotic level than the normal level, and Viso in both grey and white matter is higher. To the best of our knowledge, this is the first time that the application of NODDI in the spinal cord disease was reported.

1750 

Exploring ex vivo brainstem complex pathways with diffusion microstructure at 11.7T

Sophie Bernadette Sébille[1,2], Anne-Sophie Rolland[2], Carine Karachi[2,3], Marie-Laure Welter[2,4], Eric Bardinet[1,2], and Mathieu David Santin[1,2]

[1]Center of NeuroImaging Research - CENIR, Paris, France, [2]Inserm U 1127, CNRS UMR 7225, Sorbonne Universités, UPMC Univ Paris 06 UMR S 1127, Institut du Cerveau et de la Moelle épinière, ICM, Paris, France, [3]AP-HP, Hôpital de la Pitié-Salpêtrière, Department of Neurosurgery, Paris, France, [4]AP-HP, Hôpital de la Pitié-Salpêtrière, Department of Neurology, Paris, France

We performed multi-shell 3D segmented EPI on a post mortem macaque brain at 11.7T (resolution 200 µm iso, 120 directions) and evaluated NODDI as a tool to accurately extract brainstem pathways. We showed that the orientation dispersion map can help in segmenting ROIs used for tractography. Microstructure information opens promising perspectives for the exploration of the brainstem complex organization ex vivo in human and non-human primate.

1751 

Introducing axonal myelination in connectomics: a preliminary analysis of g-ratio distribution in healthy subjects

Matteo Mancini[1,2], Giovanni Giulietti[2], Nick Dowell[3], Barbara Spanò[2], Neil Harrison[3], Marco Bozzali[2], and Mara Cercignani[2,3]

[1]University of Rome "Roma Tre", Rome, Italy, [2]Neuroimaging Laboratory, Santa Lucia Foundation, Rome, Italy, [3]Clinical Imaging Sciences Centre, University of Sussex, Brighton, United Kingdom

We estimated the g-ratio (i.e., the ratio of the inner and the outer diameters of myelinated axons) in-vivo in two different datasets of healthy subjects using diffusion and magnetization data. We used this measure to characterize the organization of the structural connectome and compared it to the information obtained by the streamlines reconstructed using tractography. The g-ratio significantly differentiated hub-related aspects of the connections and subcortico-cortical organization. These preliminary results showed that this measure could provide complementary information to the connectome structure.

1752 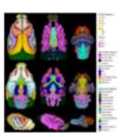

Population averaged ferret brain templates for in-vivo and ex-vivo anatomical and diffusion tensor MRI

Elizabeth B Hutchinson[1,2,3], Susan Schwerin[3,4], Kryslaine Radomski[4], Neda Sadeghi[1,2], Michal Komlosh[2,3], Jeffrey Jenkins[1,2,3], Okan Irfanoglu[1,2,3], Sharon Juliano[4], and Carlo Pierpaoli[1,2]

[1]Quantitative Medical Imaging Section, NIBIB, NIH, Bethesda, MD, United States, [2]SQITS/NICHD, NIH, Bethesda, MD, United States, [3]Henry M. Jackson Foundation, Bethesda, MD, United States, [4]APG, Uniformed Services University of the Health Sciences, Bethesda, MD, United States

In-vivo and Ex-vivo anatomical MRI and DTI templates were generated for the ferret brain along with region of interest segmentation masks based on known ferret neuroanatomy. Templates were built from multiple ferret brain images for each modality using advanced template building tools including symmetric normalization transformation for structural templates and Diffeomorphic Registration for Tensor Accurate AlignMent of Anatomical Structures (DRTAMAS) for DTI templates. The resulting templates are made available on an interactive web site (mriferretatlas.nichd.nih.gov).

1753 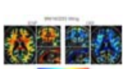

magna cum laude

In-vivo whole-brain Neurite Orientation Dispersion and Density Imaging at sub-millimeter scale using gSlider-SMS

Elda Fischi-Gomez[1,2], Susie Y. Huang[1,2], Hui Zhang[3], and Kawin Setsompop[1,2]

[1]Athinoula A. Martinos Center for Biomedical Imaging, Massachusetts General Hospital. Department of Radiology, Charlestown, MA, United States, [2]Harvard Medical School, Boston, MA, United States, [3]Department of Computer Science & Centre for Medical Image Computing, University College London, United Kingdom

We demonstrate the feasibility of applying microstructural models of diffusion to sub-millimeter isotropic resolution whole brain images in-vivo. The NODDI model was successfully fitted to a 700µm DWI dataset acquired using the generalized SLIce Dithered Enhanced Resolution Simultaneous MultiSlice (gSlider-SMS) acquisition[1]. We demonstrate the ability to map finer-scale structures using this high-resolution data when compared to traditional multi-shell 2 mm isotropic acquisition.

1754

Cerebellar connectivity influences brain network topology

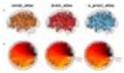

Fulvia Palesi[1,2], Giovanni Savini[2,3], Letizia Casiraghi[2,4], Gloria Castellazzi[2,5], Paolo Vitali[6,7], Giancarlo Germani[6,7], Egidio D'Angelo[2,4], and Claudia AM Gandini Wheeler-Kingshott[4,6,8]

[1]Department of Physics, University of Pavia, Pavia, Italy, [2]Brain Connectivity Center, C. Mondino National Neurological Institute, Pavia, Italy, [3]Department of Physics, University of Milan, Milan, Italy, [4]Department of Brain and Behavioral Sciences, University of Pavia, Pavia, Italy, [5]Department of Electrical, Computer and Biomedical Engineering, University of Pavia, Pavia, Italy, [6]Brain MRI 3T Mondino Research Center, C. Mondino National Neurological Institute, Pavia, Italy, [7]Neuroradiology Unit, C. Mondino National Neurological Institute, Pavia, Italy, [8]Queen Square MS Centre, Department of Neuroinflammation, UCL Institute of Neurology, London, United Kingdom

Graph theory based approaches applied to diffusion weighted MRI data have been used for understanding cerebral processing at whole-brain scale. Nevertheless, a few studies have considered including the connectivity with the cerebellum. In this work, the cerebellar role in the whole-brain connectomic was investigated by combining automatic tools and *a priori* information about cerebellar connections. We assert that it is important to incorporate the knowledge that cerebro-cerebellar connections are all contralateral. Moreover, our findings demonstrate that network topology is highly influenced by the presence or the absence of the cerebellum suggesting that it plays a key role in brain processing.

1755

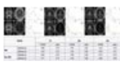

Comparison of between-subject and single-subject between-session variability in in vivo DKI brain studies

Nino Kobala[1], Farida Grinberg[1,2], Ezequiel Farrher[1], Ketevan Kotetishvili[3], and Jon N Shah[1,2]

[1]Forschungszentrum Jülich GmbH, Institute of Neuroscience and Medicine - 4, Juelich, Germany, [2]JARA, RWTH Aachen University, Department of Neurology, Faculty of Medicine, Aachen, Germany, [3]Georgian Technical University, Department of Physics, Tbilisi, Georgia

The knowledge of intra- and inter-subject variability of diffusion kurtosis imaging metrics plays an important role for interpretation of the results of the clinical trials. The purpose of this work is to investigate and compare between-session variability of a single subject with between-subject variability diffusion kurtosis parameters in different anatomical regions. Variability is quantified in terms of the coefficient of variation, which can provide the baseline for interpretation of clinical trials and single-subject longitudinal examinations.

1756

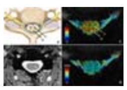

MR imaging of the cervical spinal cord in patients with spinal muscular atrophy and healthy controls

Wieke Haakma[1,2], Marloes Stam[3], Martijn Froeling[1], Marielle E.P. Philippens[4], Clemens Bos[1], Alexander Leemans[5], Ludo van der Pol[3], and Jeroen Hendrikse[1]

[1]Department of Radiology, University Medical Center Utrecht, Utrecht, Netherlands, [2]Department of Forensic Medicine and Comparative Medicine Lab, Aarhus University, Aarhus, Denmark, [3]Department of Neurology, University Medical Center Utrecht, Utrecht, Netherlands, [4]Department of Radiotherapy, Cancer Center, University Medical Center Utrecht, Utrecht, Netherlands, [5]Image Sciences Institute, University Medical Center Utrecht, Utrecht, Netherlands

We studied the architecture and diffusion characteristics in the cervical spine and nerves in spinal muscular atrophic (SMA) patients and healthy controls. We showed the asymmetrical architectural configuration of the cervical nerves in SMA patients. We computed diffusion values of which the mean, axial, and radial diffusivity were lower in the SMA patients than in healthy controls which are in accordance with the clinical symptoms of these patients. Diffusion values of the cervical spine (grey, white and the whole myelum) showed no differences.

1757

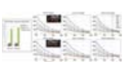

T2 relaxation rates of the fast and slow bi-exponential diffusion components in the in vivo corpus callosum

Qiuyun Fan[1], Susie Y. Huang[1], Aapo Nummenmaa[1], Thomas Witzel[1], and Lawrence L. Wald[1,2]

[1]Massachusetts General Hospital, Charlestown, MA, United States, [2]Harvard-MIT Division of Health Sciences and Technology, MIT, Cambridge, MA, United States

Bi-exponential diffusion model is widely used to fit for non-Gaussian diffusion. T2 relaxation rates differ between structural compartments, which may bias the results of fits to microstructure models. We incorporate T2 relaxation into the bi-exponential model and leveraged the Gmax = 300mT/m gradient strength of the Connectome scanner to study the apparent T2 times of the two diffusion components. A longer T2 was found for the fast diffusion component when the model allows for different T2 times, but both multiple T2s and single T2 models seem to fit to the data fairly well. The added T2 parameter affects volume fraction more than diffusivity estimates.

1758

Determining how varying the number of gradients measurements affects fitted surface to volume ratios in tube samples using oscillating spin echo gradients

Morgan Mercredi[1], Sheryl Herrera[1], Richard Buist[2], and Melanie Martin[1,3]

[1]Physics and Astronomy, University of Manitoba, Winnipeg, MB, Canada, [2]Radiology, University of Manitoba, [3]Physics, University of Winnipeg, Winnipeg, MB, Canada

There is an increasing drive to use diffusion spectroscopy to infer the sizes of structures in samples. Here, we use apodised cosine gradient spin echo sequences (OGSE) to infer the surface to volume ratio of a collection of packed capillary tubes. Aiming to reduce imaging times, this study examines how the number of gradients affects the accuracy and precision of the fitted parameters. We found that collecting OGSE data with two b-values may be sufficient to infer information about small structures, especially if higher gradients strengths are used.

1759

Determining surface to volume ratios in capillary tube samples using oscillating gradient spin echo sequences

Morgan Mercredi[1], Sheryl Herrera[1], Richard Buist[2], and Melanie Martin[1,3]

[1]Physics and Astronomy, University of Manitoba, Winnipeg, MB, Canada, [2]Radiology, University of Manitoba, [3]Physics, University of Winnipeg, Winnipeg, MB, Canada

There is an increasing drive to use diffusion spectroscopy to infer the sizes of structures in samples. Most methods use pulsed gradient spin echo sequences which cannot provide short enough diffusion times to probe very small structures. Instead, we use oscillating gradient spin echo sequences (OGSE) to probe the short-time regime allowing for small structures to be measured. Here we use the apodised cosine OGSE to infer the surface to volume ratio of a collection of packed capillary tubes, and use it approximate the tube diameters.

1760 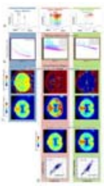

Translating AxCaliber on a clinical system : 600mT/m versus optimized 80mT/m protocol

Tanguy Duval[1], Tom Mingasson[1,2], Eric Klawiter[3], Nikola Stikov[1,4], and Julien Cohen-Adad[1,5]

[1]Polytechnique Montreal, Montreal, QC, Canada, [2]Ecole Centrale de Nantes, Nantes, France, [3]A.A. Martinos Center for Biomedical Imaging, Massachusetts General Hospital, Harvard Medical School, Boston, MA, United States, [4]Montreal Heart Institute, Montreal, QC, Canada, [5]Functional Neuroimaging Unit, CRIUGM, Universite de Montreal, Montreal, QC, Canada

Most model-based diffusion metrics (AxCaliber metrics) have been shown to be less stable and more biased on clinical systems due to the limited gradient strength (40-80mT/m versus >300mT/m on preclinical scanners). In this work we wanted to (i) find the best AxCaliber protocol at 80mT/m and (ii) quantify the bias in the estimated metrics. For these aims, we first optimized an 80mT/m AxCaliber protocol using simulations, then compared experimentally (on an ex vivo cat spinal cord) a 600mT/m protocol versus the optimized 80mT/m protocol. Using the 600mT/m maps as a ground truth, our results show that even though axon diameter cannot be estimated robustly, the fraction of restricted water can be measured accurately (<3% error) and precisely (r^2 >0.76) on clinical systems. The short duration of the optimized protocol opens the way to the use of reliable model-based diffusion MRI metrics on a clinical system, metrics that would be particularly useful to measure the degree of myelination through the fiber g-ratio.

1761 

Multi-Spherical Diffusion MRI: An in-vivo Test-Retest Study of Time-Dependent q-space Indices

Rutger Fick[1], Alexandra Petiet[2], Mathieu Santin[2], Anne-Charlotte Philippe[2], Stephane Lehericy[2], Rachid Deriche[1], and Demian Wassermann[1]

[1]Universite Cote d'Azur, Inria, France, Sophia Antipolis, France, [2]CENIR, Institut du Cerveau et de la Moelle epineere, Paris, France

Effective representation of the diffusion signal's dependence on diffusion time is a sought-after challenge in diffusion MRI (dMRI). As a solution, we recently proposed Multi-Spherical Diffusion MRI (MS-dMRI) to represent the dMRI signal in this four-dimensional space - varying over gradient strength, direction and diffusion time. Our representation allows for the estimation of time-dependent q-space features, providing unique insights on the tissue microstructure. In the study, we assess test-retest reproducibility of these indices in three C57Bl6 wild-type mice. We find that due to our effective regularization methodology during signal fitting, these time-dependent features can be estimated reliably without overfitting the data.

1762 

Value of MR DWI with different mathmatical models in the differential diagnosis liver neoplasms

Qu Zhaohui[1], Gao Xuemei, Cheng Jingliang, and Wang Shaoyu

[1]The First Affiliated Hospital of Zhengzhou University, Zhengzhou, People's Republic of China

To investigate the utility value of monoexponential model,biexponential model and diffusion kurtosis model diffusion weighted imaging in diagnosis

---

1763 

Accelerated Diffusion-weighted ^{129}Xe MRI Morphometry of Emphysema in COPD and Alpha-1 Antitrypsin Deficiency Patients

Alexei Ouriadov[1], Eric Lessard[1], Fumin Guo[1], Heather M Young[1], Anurag Bhalla[1], David G McCormack[2], and Grace Parraga[1]

[1]Robarts Research Institute, London, ON, Canada, [2]Division of Respirology, University of Western Ontario, London, ON, Canada

In this proof-of-concept evaluation, we evaluated ^{129}Xe MRI ADC/morphometry estimates using two different acceleration factors (AF) in a small group of never-smokers, COPD ex-smokers with emphysema and Alpha-1 Antitrypsin Deficiency patients. Such estimates were obtained for three different cases: fully sampled k-space; 50% under-sampling in the phase-encoding direction, AF=2; and 66% undersampling, AF=3. The results of this study showed that the difference in ADC/morphometry estimates from fully sampled and under-sampled k-space were similar to that observed with accelerated ^{3}He multi-b diffusion-weighted MRI in healthy subjects. These differences increase however, with increasing emphysema severity, which requires further investigation.

1764 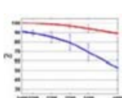

Can fast diffusion kurtosis imaging be quantitative in the brain?

Yen-Shu Kuo[1,2], Shun-Chung Yang[3], Ya-Fang Chen[3], and Wen-Chau Wu[3,4,5]

[1]Graduate Institute of Biomedical Electronics and Bioinformatics, National Taiwan University, Taipei, Taiwan, [2]Radiology, Cathay General Hospital, Taipei, Taiwan, [3]Medical Imaging, National Taiwan University Hospital, Taipei, Taiwan, [4]Graduate Institute of Oncology, National Taiwan University, Taipei, Taiwan, [5]Graduate Institute of Clinical Medicine, National Taiwan University, Taipei, Taiwan

This study was aimed to investigate the applicability of fast DK imaging for both cerebral gray matter and white matter as a quantitative method. Our experimental data reveal that the dependence of *D* and *K* on b-values predominantly exists in areas containing a noticeable amount of cerebrospinal fluid. *D* is more sensitive to b-value choice than *K*. With b-values carefully chosen to account for signal-to-noise ratio and model fidelity, fast DK imaging-derived indexes can be quantitative with negligible dependence on b-values in most gray matter and white matter.

1765

Can we trust structural connectivity?

Silvia Obertino[1], Flora Danti[1], Mauro Zucchelli[1], Francesca Benedetta Pizzini[2], and Gloria Menegaz[1]

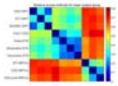

[1]Computer Science, University of Verona, Verona, Italy, [2]Neuroradiology, University Hospital Verona, Verona, Italy

Structural connectivity models result from a complex processing chain involving many different steps, each having an impact on the reliability of the final measures. One of the hottest questions in the state-of-the-art is thus “To which extent can we trust the structural connectome?”. In this work, we tackled this issue by focusing on the typical processing pipeline and investigating the impact of the main involved steps. MRTrix CSD-based probabilistic tractography provided the highest stability across subjects and MRTrix reached the largest distance with respect to other softwares in both individual subject and group analysis.

1766 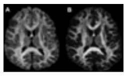

Diffusion Imaging Reveals White Matter Damage in Ice Hockey Players for Up To Two Months Post-Concussion

Alexander Mark Weber[1], Michael Jarrett[2], Enedino Hernandez-Torres[2], Shiroy Dadachanji[1], David K. B. Li[1], Jack Taunton[1], and Alexander Rauscher[2]

[1]University of British Columbia, Vancouver, BC, Canada, [2]Pediatrics, University of British Columbia, Vancouver, BC, Canada

Traumatic brain injury (TBI) is a leading cause of disability in adults. More sophisticated methods are required in order to understand its underlying pathophysiology and disease progression. Recent interest in an assumption-free DTI analysis, diffusion entropy (DE), has produced some promising results for investigating white matter (WM) and grey matter (GM) microstructure. We set out to test DE against the much more common fractional anisotropy (FA) analysis, in both WM and GM, in 45 hockey players over one season. 11 players sustained a concussion and were scanned at 72 hours, 2 weeks, and 2 months post-injury.

1767 

Fast Linear Fitting of Bi-Exponential Intra-Voxel Incoherent Motion (IVIM) Models

Eric Thomas Peterson[1], Natalie May Zahr[2,3], Edith Vioni Sullivan[2], and Adolf Pfefferbaum[1]

[1]Biosciences, SRI International, Menlo Park, CA, United States, [2]Psychiatry and Behavioral Sciences, Stanford University, Stanford, CA, United States, [3]Bioscience, SRI International, Menlo Park, CA, United States

This work introduces an extremely fast (whole image in ~5s) IVIM fitting procedure based on two sequential linear fits and demonstrates that it is comparable to the more traditional but much slower non-linear fitting. This method is valuable because current fitting methods typically take a significant amount of time, typically from minutes to hours, due to their iterative and non-linear nature. Therefore, this technique can be used as a fitting method alone and also as a way to seed more advanced techniques with accurate starting values.

1768 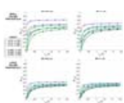

Sensitivity of STEAM diffusion MRI to permeability in white matter tissue: a simulation study

Ioana Diana Oprea[1], Andrada Ianus[2], Olga Ciccarelli[3], and Ivana Drobnjak[4]

[1]Medical Physics, University College London, London, United Kingdom, [2]Computer Science, University College London, [3]Institute of Neurology, University College London, [4]University College London

This study investigates the sensitivity of the Stimulated-Echo Acquisition Mode (STEAM) diffusion-weighted signal to permeability quantified with water exchange time τ_{ex}. In order to do this, Monte Carlo simulations were generated for a range of histologically-plausible τ_{ex} and practical scanner acquisition parameters. The results suggest that on the standard clinical scanner (G=70mT/m), STEAM estimates short exchange times (<0.9s), which are characteristic in tissue with myelin damage, while tissue with longer exchange times (>1.5s) is practically indistinguishable from impermeable tissue. The Connectome scanner (G=300mT/m) estimates a much wider range, however needs careful optimisation since the resolution limit is highly dependent on the sequence parameters and SNR’s.

1769 

Diffusion kurtosis metrics as sensitive biomarkers of ageing

Farida Grinberg[1,2], Nino Kobalia[1], Ezequiel Farrher[1], and N. Jon Shah[1,2,3]

[1]Institute of Neuroscience and Medicine 4, Research Centre Jülich, Jülich, Germany, [2]Department of Neurology, Faculty of Medicine, RWTH Aachen University, Aachen, Germany, [3]JARA - BRAIN - Translational Medicine, RWTH Aachen University, Germany

Diffusion tensor imaging is an established tool for the examination of WM connectivity and microstructural changes across the lifespan. More recently, advanced diffusion MRI techniques, such as diffusion kurtosis imaging (DKI), have been shown to provide richer information on tissue microstructure. Thus far, only a few works have been published related to DKI in healthy ageing. In this work, we examined, in a large cohort of subjects, the potential of DKI metrics to unravel microstructural changes due to ageing in different brain regions.

1770 

Stability of co-electrospun brain-mimicking fibers for diffusion MRI

Fenglei Zhou[1,2], Matthew Grech-Sollars[3], Adam Waldman[3,4], Geoffrey J. M. Parker[1,5], and Penny L. Hubbard Cristinacce[6]

[1]Division of Informatics, Imaging & Data Sciences, School of Health Sciences, The University of Manchester, Manchester, United Kingdom, [2]The School of Materials, The University of Manchester, Manchester, United Kingdom, [3]Division of Brain Sciences, Imperial College London, London, United Kingdom, [4]Centre for Clinical Brain Sciences, The University of Edinburgh, Edinburgh, United Kingdom, [5]Bioxydyn Limited, Manchester, United Kingdom, [6]Division of Neuroscience & Experimental Psychology, The University of Manchester, United Kingdom

This work investigates the stability and reproducibility of brain-mimicking microfiber phantoms. These microfibers were produced by co-electrospinning (co-ES) and characterized by scanning electron microscopy (SEM). Grey matter (GM) and white matter (WM) phantoms were constructed from random and aligned microfibers, respectively. MR data were acquired from these phantoms over a period of 17 months. SEM images reveal that there were some changes in the pore size and porosity of co-ES fibers over a period of 30 months. MR measurements showed variations within the limits expected for intra-scanner variability, thereby confirming the phantom stability over 17 months.

1771

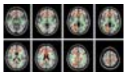

Abnormal white matter integrity in parkinson's disease patients with cognitive impairment revealed by tract-based spatial statistics

Hui Yu[1] and Mingming Huang[1]

[1]*Department of Radiology, Affiliated Hospital of Guizhou Medical University, Guiyang, China, Guiyang, People's Republic of China*

Results from recent neuroimaging studies suggest that PD patients with cognitive impairment(PDCI) is associated with abnormal white matter integrity. In this study, we used tract-based spatial statistics (TBSS) method combined with diffusion tensor imaging (DTI) to investigate the microstructural integrity of the white matter in PDCI. Results from TBSS demonstrated that PDCI patients had significantly lower FA than healthy controls in anterior thalamic radiation(atr), corticospinal tract (cst), cingulated gyrus(cg), forceps minor(fi), the right inferior fronto-occipital fasciculus(ifo), inferior longitudinal fasciculus(ilf), superior longitudinal fasciculus(slf) and uncinate fasciculus(uf). There were no white matter integrity changes in PD patients without cognitive dysfunction, And also significantly correlation was found between FA in the right ifo and MoCA scores.

1772

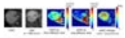

Changes of non-Gaussian diffusion MRI parameters at different diffusion times in a human breast carcinoma xenograft model

Mami Iima[1,2], Tomomi Nobashi[3], Hirohiko Imai[4], Sho Koyasu[5], Akira Yamamoto[1], Masako Kataoka[1], Yuji Nakamoto[1], Tetsuya Matsuda[6], and Kaori Togashi[1]

[1]*Department of Diagnostic Imaging and Nuclear Medicine, Graduate School of Medicine, Kyoto University, Kyoto, Japan,* [2]*Hakubi Center for Advaned Research, Kyoto University, Kyoto, Japan,* [3]*Graduate Schoolof Medicine, Kyoto University, Kyoto, Japan,* [4]*Research and Educational Unit of Leaders for Integrated Medical System, Center for the Promotion of Interdisciplinary Education and Research, Kyoto University, Kyoto, Japan,* [5]*Radiation Biology Center, Kyoto University, Kyoto, Japan,* [6]*Department of Systems Sciece, Graduate School of Informatics, Kyoto University, Kyoto, Japan*

The relationship between diffusion time and diffusion parameters obtained from 7.0T MRI using a human breast carcinoma xenograft model was investigated. There was an increase in K values and decrease in ADCo as well as sADC values in 27.6ms compared to 9.6 ms. Some tumor showed heterogeneous sADC change derived from two different diffusion times.

1773

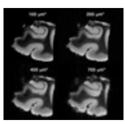

Gray matter cellular volume fraction imaging and Alzheimer's disease

Farshid Sepehrband[1], Nyoman D Kurniawan, and Kristi A Clark

[1]*Laboratory of Neuro Imaging, USC Mark and Mary Stevens Neuroimaging and Informatics Institute, Keck School of Medicine of USC, University of Southern California, Los Angeles, CA, United States*

Neuronal loss is one of the major outcomes of neurodegenerative diseases such as Alzheimer's disease (AD) [1,2]. Given the microscopic level of changes associated with neurodegeneration, it is challenging to image with conventional MRI techniques. Microstructural diffusion-weighted MRI is a powerful tool, which has been shown to be sensitive to microscopic brain tissue characteristics [3,4]. However, a relative lack of specificity has impeded its transition to clinic.

Here we focus primarily on deriving cell content information in gray matter and apply it to AD. We acquired multi-shell dMRI of two postmortem samples of human hippocampal tissue (one AD and one control) at the same time, with isotropic resolution of 200 mm, using a 16.4T scanner. We modeled signal attenuation based on the observed evidence of faster signal decay of the cellular compartment. Then, we derived the cell volume fraction by fitting the model to the data and compared it within and between our tissues.

1774

Clinically Feasible Optic Nerve Diffusion Basis Spectrum Imaging at 3T

Joo-won Kim[1,2,3], Peng Sun[4], Sheng-Kwei Song[4], Samantha Lancia[5], Courtney Dula[5], Robert T Naismith[5], and Junqian Xu[1,2,3,6]

[1]*Translational and Molecular Imaging Institute, Icahn School of Medicine at Mount Sinai, New York, NY, United States,* [2]*Department of Radiology, Icahn School of Medicine at Mount Sinai, New York, NY, United States,* [3]*Graduate School of Biomedical Sciences, Icahn School of Medicine at Mount Sinai, New York, NY, United States,* [4]*Department of Radiology, Washington University, Saint Louis, MO, United States,* [5]*Department of Neurology, Washington University, Saint Louis, MO, United States,* [6]*Department of Neuroscience, Icahn School of Medicine at Mount Sinai, New York, United States*

Optic nerve MRI is susceptible to eyeball movement. The relatively long acquisition time of advanced diffusion MRI (dMRI) methods exacerbates the motion sensitivity in optic nerve dMRI and limits the clinical implementation of these methods. In this work, we evaluate a short (less than 2.5 min per eye) single slice coronal optic nerve dMRI acquisition protocol at 3T and propose a 2D optic nerve center searching algorithm customized for such dMRI data. We demonstrate improved optic nerve center contrast after image alignment and the expected benefits of reduced partial volume effects from diffusion basis spectrum imaging (DBSI) analysis.

1775

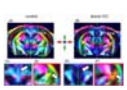

Detection of abnormal brain neural circuits in draxin knockout mice using DTI-MRI

Yuri Kitamoto[1], Tatsuya Higuma[1], Makoto Hirakane[1], Mitsuhiro Takeda[1], Sosuke Yoshinaga[1], Rikita Araki[2], Hideaki Tanaka[1], Yohei Shinmyo[3], and Hiroaki Terasawa[1]

[1]*Faculty of Life Sciences, Kumamoto University, Kumamoto, Japan,* [2]*Bruker BioSpin K.K., Yokohama, Japan,* [3]*Graduate School of Medical Sciences, Kanazawa University, Ishikawa, Japan*

The aim of this study is to clarify the role of the axon guidance molecule Draxin in the construction of brain neural circuits by DTI-MRI. MRI was performed on draxin knockout, dra(–), and normal mice both *in vivo* and *ex vivo*. The *in vivo* study of dra(–) revealed that the nerve fibers in the corpus callosum did not intersect with the midline. The *ex vivo* study of dra(–) demonstrated that the thalamocortical nerve fibers did not extend toward the cerebral neocortex through the internal capsule. We successfully evaluated the influences caused by the Draxin loss with DTI-MRI.

1776 

Characteristic analysis of in vivo and ex vivo rat brains by 7.0 T DTI MR

Chunhua Wang[1], Li Song, Ruzhi Zhang, and Fabao Gao

[1]Department of Radiology, West China Hospital, Chengdu, People's Republic of China

Ex vivo diffusion tensor imaging (DTI) are widely used in experimental studies for excellent images. The comparison between in vivo and ex vivo DTI has been conducted without the same scan parameters. We aimed to compare the living and fixed white and gray matters under the same condition and explore the effects of coil and signal average. Diffusivities were significant different between living and fixed brains. Coil and signal average significantly affected the signal-to-noise ratio of ex vivo white and gray matters. The results indicate that fixation and MR conditions should be considered in clinical and experimental DTI studies.

Traditional Poster

Diffusion: Processing, Analysis, & Visualization

Exhibition Hall 1777-1814 Tuesday 13:45 - 15:45

1777 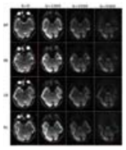

Evaluation of the Quality of Eddy-Currents and EPI Distortion Correction for Diffusion MRI: A Dataset for Benchmarking

Mustafa Okan Irfanoglu[1,2,3], Amritha Nayak[1,2,3], Joelle Sarlls[4], and Carlo Pierpaoli[1,2]

[1]Quantitative Medical Imaging Section, NIBIB/NIH, Bethesda, MD, United States, [2]SQUITS/NICHD/NIH, Bethesda, MD, United States, [3]Henry Jackson Foundation, Bethesda, MD, United States, [4]NIH MRI Research Facility, National Institute of Neurological Disorders and Stroke, National Institutes of Health, Bethesda, MD, United States

In recent years, numerous methodologies have been proposed for the correction of motion, eddy-currents and echo planar imaging (EPI) distortions for diffusion MRI data. The typical strategy to assess the quality of these corrections is to compare them to an undistorted image, such as a T1-weighted or T2-weighted structural image, with different quality measures such as outlines, similarity metrics or segmentation overlaps. Even though several of these measures are quantitative, the use of wide range of validation strategies in combination with data with significantly different distortion properties complicates a direct comparison of these techniques. In this work, we propose a quantitative, unbiased and robust strategy to evaluate the performances of these correction techniques and provide a publicly available benchmarking dataset.

1778 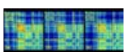

Compressed Sensing to Accelerate Connectomic Histology in the Mouse Brain

Nian Wang[1], Gary Cofer[1], Robert J. Anderson[1], Russell Dibb[1], Yi Qi[1], Alexandra Badea[1], and G. Allan Johnson[1]

[1]Center for In Vivo Microscopy, Department of Radiology, Duke University, Durham, NC, United States

We evaluated the utility of compressed sensing (CS) for diffusion tensor (connectomic) histology in the mouse brain at high field (9.4T). We explored the effect of b values, compression factors, and k-space sampling strategies. We were able to achieve compression factors of 4X through judicious choice of k-space sampling patterns. Comparison to a comprehensively acquired data set (full sampling at 43 µm with 120 angles) allowed us to reduce the acquisition time by nearly 30X with minimal loss in the resulting connectome.

1779 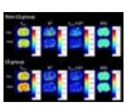

Prediction of outcome in bilateral common carotid artery occlusion (BCCAO) rats by intravoxel incoherent motion (IVIM) analysis at 11.7 Tesla

Shunrou Fujiwara[1,2], Yuki Mori[2,3], Daniela Martinez de la Mora[2,3], Kuniaki Ogasawara[1], and Yoshichika Yoshioka[2,3]

[1]Department of Neurosurgery, Iwate Medical University, Morioka, Japan, [2]WPI Immunology Frontier Research Center, Osaka University, Suita, Japan, [3]Center for Information and Neural Networks (CiNet), NICT and Osaka University, Suita, Japan

Rats with the bilateral carotid artery occlusion (BCCAO) was often used for assessment of the brain damage caused by chronic cerebral hypoperfusion as a longitudinal ischemic animal model; however, the mortality is high and it has remained unclear what kinds of initial cerebral hemodynamic changes occurred in the brain in the hyperacute phase after BCCAO and whether the changes related with the mortality in rats or not. Intravoxel incoherent motion (IVIM), which is the basic concept of diffusion-weighted imaging (DWI), can non-invasively demonstrate various hemodynamic situations at one time DWI scan with multiple b values. Here, we investigated whether the outcome of BCCAO rats associated with cerebral hemodynamic changes assessed using IVIM- DWI.

1780 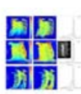

Correction of nonuniform diffusion weighting in DWI using vendor-provided gradient characteristics

Dariya I Malyarenko[1], Yuxi Pang[1], Lisa J Wilmes[2], Ek Tsoon Tan[3], John E Kirsch[4], Julien Sénégas[5], Michael A Jacobs[6], David C Newitt[2], and Thomas L Chenevert[1]

[1]Radiology, University of Michigan, Ann Arbor, MI, United States, [2]Radiology and Biomedical Imaging, University of California San Francisco, San Francisco, CA, United States, [3]GE Global Research, Niskayuna, NY, United States, [4]Siemens Healthcare, Malvern, PA, United States, [5]Philips Research Laboratories, Hamburg, Germany, [6]Radiology and Radiological Science, John Hopkins University School of Medicine, Baltimore, MD, United States

System-specific gradient nonlinearity (GNL) causes spatially nonuniform weighting in diffusion weighted imaging (DWI). This leads to systematic bias and variability in derived apparent diffusion coefficient (ADC) maps, diminishing their quantitative utility for multi-site, multi-platform clinical trials. An ADC error correction methodology for three-direction DWI acquisition was developed previously using an empiric system GNL approximation. Here we demonstrate implementation of correction for three clinical scanners using the system-specific gradient-channel fields derived from vendor-provided spherical harmonic tables. Implemented correction substantially improves precision and removes ADC bias for ice-water phantoms. Comparable accuracy and performance is achieved across all gradient platforms.

1781 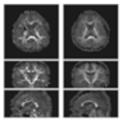

Toward Analytic Computation of Fiber-Radial Diffusional Kurtosis by Q-space Data Representation with Radial Basis Functions

Yoshitaka Masutani[1] and Koh Sasaki[1,2]

[1]*Graduate School of Information Sciences, Hiroshima City University, Hiroshima, Japan,* [2]*Hiroshima Heiwa Clinic, Hiroshima, Japan*

To enhance the robustness of the fiber-radial diffusional kurtosis computation, the signal decay in the Q-space can be averaged among the fiber-radial orientations. By using the radial basis functions with Gaussian basis, it is shown that the fiber-radial signal decay can be represented in a pseudo-analytic form with the Bessel function. By using in-vivo diffusion MRI data, the computation results were presented in comparison with those by diffusion kurtosis tensor of 4th order to prove the effectiveness of the proposed method.

1782 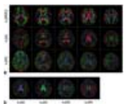

Directional sensitivity of anomalous diffusion assessed using a tensorial fractional motion model

Boyan Xu[1], Gaolang Gong[2], Yaoyu Zhang[1], Yang Fan[3], Bing Wu[3], and Jia-Hong Gao[1]

[1]*Center for MRI Research, Peking University, Beijing, People's Republic of China,* [2]*State Key Laboratory of Cognitive Neuroscience and Learning, Beijing Normal University, Beijing, People's Republic of China,* [3]*MR Research China, GE Healthcare, Beijing, People's Republic of China*

Anisotropic diffusion in the nervous system is most commonly modeled by the apparent diffusion tensor, which is based on normal diffusion theory. However, the departure of the diffusion-induced signal attenuation from the mono-exponential form indicates the existence of anomalous diffusion. The fractional motion (FM) model, which is considered as the appropriate anomalous diffusion theory for biological tissues, has been applied to diffusion MRI. However, the directional sensitivity of the FM model in biological tissues remains elusive. In this study, this issue was addressed via tensor analysis in analogy with the diffusion tensor.

1783 

Solving the free water elimination estimation problem by incorporating T2 relaxation properties

Quinten Collier[1], Jelle Veraart[1,2], Arnold J. den Dekker[1,3], Floris Vanhevel[4], Paul M. Parizel[4], and Jan Sijbers[1]

[1]*Vision Lab, University of Antwerp, Antwerp, Belgium,* [2]*Center for Biomedical Imaging, Department of Radiology, New York University School of Medicine, New York, NY, United States,* [3]*Delft Center for Systems and Control, Delft University of Technology, Delft, Netherlands,* [4]*Department of Radiology, Antwerp University Hospital, Antwerp, Belgium*

The free water elimination (FWE) model fitting problem is inherently ill-conditioned, leading to the need for solutions that can avoid or deal with these kinds of fitting problems. In this work, we evaluate a model extension to the FWE model that exploits the T2-relaxation properties and subsequently leads to a well-posed fitting problem that can be easily solved using standard estimation techniques.

1784 

Investigating the Effects of Concurrent Magnetic Field Monitoring on High Angular Resolution Diffusion Imaging: Application to Cortical Parcellation

Yoojin Lee[1,2], Bertram Wilm[1], Tara Ganepola[3,4], Alexander Leemans[5], Martin I. Sereno[6], Daniel C. Alexander[4], Klaas Pruessmann[1], and Zoltan Nagy[2]

[1]*Institute for Biomedical Engineering, ETH Zürich, Zürich, Switzerland,* [2]*Laboratory for Social and Neural Systems Research, University of Zürich, Zürich, Switzerland,* [3]*Department of Cognitive, Perceptual and Brain Sciences, University College London, London, United Kingdom,* [4]*Centre for Medical Image Computing, University College London, London, United Kingdom,* [5]*Image Sciences Institute, University Medical Center Utrecht, Utrecht, Netherlands,* [6]*Psychology Department and Neuroimaging Center, San Diego State University, CA, United States*

The concurrent field monitoring has been proposed to eliminate image artifacts in diffusion imaging introduced by the long lasting eddy currents from the diffusion-encoding gradients. In this work we investigated the effects of field monitoring system on HARDI and applied the improved HARDI data to cortical parcellation. We showed that the field monitoring improved the HARDI data quality especially in anterior/posterior poles of the brain and air-tissue interfaces. This regional improvement was also clear in the cortical classification results, where the field monitoring improved the accuracy of the V1/V2 by 3%, compared to ~0.5% in the motor strip.

1785 

Predicting patient survival in hepatocellular carcinoma (HCC) from diffusion weighted magnetic resonance imaging (DW-MRI) data using neural networks

Florian Ettlinger[1], Patrick Christ[1], Georgios Kaissis[2], Freba Ahmaddy[2], Felix Grün[1], Sebastian Schlecht[1], Alexander Valentinitsch[2], Seyed-Ahmad Ahmadi[3], Bjoern Menze[1], and Rickmer Braren[2]

[1]*Image-Based Biomedical Modeling Group, Technical University of Munich, Munich, Germany,* [2]*Institute of Radiology, Technical University of Munich, Munich, Germany,* [3]*Department of Neurology, Ludwig Maximilian University of Munich*

In this work we present a method to predict patient survival in hepatocellular carcinoma (HCC). We automatically segment HCC from DW-MRI images using fully convolutional neural networks. In a second step we predict patient survival rates by calculating different features from ADC maps. We calculate Histogram features, Haralick features and propose new features trained by a 3D Convolutional Neural Network (SurvivalNet). Applied to 31 HCC cases, SurvivalNet accomplishes a classification accuracy of 65% at a precision and sensitivity of 64% and 65% when trained using our automatic tumor segmentation in a fully automatic fashion.

1786 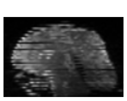

Automatic detection of volumes affected by subvolume movement

Kerstin Pannek[1], Jurgen Fripp[1], Joanne George[2], Roslyn Boyd[2], Paul Colditz[2], and Stephen Rose[1]

[1]*The Australian E-Health Research Centre, CSIRO, Brisbane, Australia,* [2]*The University of Queensland, Brisbane, Australia*

Diffusion-weighted MRI is prone to a number of artefacts, including movement between subvolumes in an interleaved acquisition. Affected volumes need to be identified and dealt with before further processing. We use a registration based approach to identify volumes affected by subvolume motion, and demonstrate that a single metric, calculated from all subjects acquired using the same acquisition protocol, is sufficient to reliably identify such volumes. Importantly, the detection threshold is determined from the data itself, and can be applied to multi-shell data.

1787

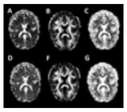

Exploring the potentials and limitations of improved free-water elimination DTI techniques

Rafael Neto Henriques[1], Ørjan Bergmann[2], Ariel Rokem[3], Ofer Pasternak[4], and Marta Morgado Correia[1]

[1]Cognition and Brain Sciences Unit, MRC, Cambridge, United Kingdom, [2]Haukeland University Hospital, Bergen, Norway, [3]eScience Institute, The University of Washington, Seattle, WA, United States, [4]Departments of Psychiatry and Radiology, Brigham and Women's Hospital, Harvard Medical School, Boston, MA, United States

Free-water diffusion tensor imaging (fwDTI) was previously proposed to remove CSF partial volume effects of measures based on the diffusion tensor. Nevertheless, this diffusion-weighted technique is still subject to several pitfalls. In this study, an improved algorithm to fit the fwDTI to data acquired with two or more diffusion-weighting gradients is proposed. This algorithm is then used to explore the advantages and limitations of suppressing free-water in synthetic and in vivo diffusion-weighted data.

1788

Impact of Prior Distribution and Central Tendency Measure on Bayesian IVIM Model Fitting

Oscar Gustafsson[1], Mikael Montelius[1], Göran Starck[1], and Maria Ljungberg[1]

[1]Department of Radiation Physics, University of Gothenburg, Gothenburg, Sweden

Bayesian model fitting has been shown to yield robust estimates of the IVIM parameters. However, various methodological choices have differed between studies, which may have substantial effect on the results. This study investigates the effect that the prior distributions and central tendency measures may have, using both in vivo data and simulations. The results show that the prior distribution can play a significant role at commonly seen signal-to-noise levels. The choice of central tendency measure has less effect on the estimates. However, it may be chosen to emphasize either accuracy or precision.

1789

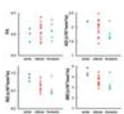

Characterization of the ulnar nerve using multislice DTI using a multiband factor of 1, 2, and 3

Tina Jeon[1], Ek Tsoon Tan[2], Maggie Mei Kei Fung[3], and Darryl B Sneag[1]

[1]Radiology and Imaging, Hospital for Special Surgery, New York, NY, United States, [2]GE Global Research, Niskayuna, NY, United States, [3]Apps & Workflow, GE Healthcare, New York, NY, United States

Multiband (MB) echo planar MR imaging (EPI) excites and refocuses multiple slice locations simultaneously using MB radiofrequency excitation and refocusing pulses that are subsequently un-aliased by exploiting differences in coil sensitivities. In this study, we investigated the feasibility of using MB diffusion tensor (DT) EPI with a multiband factor of 1, 2, and 3 to interrogate the ulnar nerve at different locations in the arm.

1790

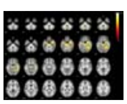

Fractional anisotropy spatial covariance analysis in Parkinson’s disease suggests a disease related degeneration pattern

Xingfeng Li[1,2], Yue Xing[1,2], Antonio Martin Bastida[3], Stefan Schwarz[1,2], Piccini Paola[3], Dorothee P. Auer[1,2], and Xingfeng Li and Yue Xing[4]

[1]Radiological Sciences, Division of Clinical Neuroscience, School of Medicine, University of Nottingham, Nottingham, United Kingdom, [2]Sir Peter Mansfield Imaging Centre, School of Medicine, University of Nottingham, [3]Centre for Neurodegeneration and Neuroinflammation, Imperial College London, London, United Kingdom, [4]Both authors contributed equally.

Parkinson’s disease (PD) is characterised by disrupted functional and structural brain networks. Structural network changes are thought to better reflect progression of the neurodegeneration. To study the pattern of neurodegeneration in Parkinson’s disease (PD), we investigated the correlation pattern of fractional anisotropy (FA) with substantia nigra (SN) using a structural covariance analysis method. We also correlated FA maps with the unified Parkinson's disease rating scale (UPDRS); we found a disruption of SN covariance FA maps in PD compared to controls. Moreover, disease severity was significantly correlated with FA in cerebellar and anterior cingulate cortex (ACC).

1791

Novel application of the reversed gradient method in Diffusion Weighted-MRI for tumor response assessment in head and neck squamous cell carcinoma patient undergoing radiation therapy.

David Aramburu Nuñez[1,2,3], Jose Luis del Olmo Claudio[3], Silvia Reigosa Montes[3], Antonio López Medina[3], Moises Mera Iglesias[4], Francisco Salvador Gómez [3], Íñigo Nieto[5], Alfonso Calzado[2], Amita Shukla-Dave[6], and Victor M Muñoz[5]

[1]Medical Physics, Memorial Sloan-Kettering Cancer Center, NEW YORK, NY, United States, [2]Department of Radiology, Complutense University, MADRID, Spain, [3]Department of Medical Physics and Radiological protection, Galaria - Hospital do Meixoeiro – Complexo Hospitalario Universitario de Vigo, VIGO, Spain, [4]Medical Physics, Oncoserv, Santiago de los Caballeros – Dominican Republic, Dominican Republic, [5]Department of Radiation Oncology, Galaria - Hospital do Meixoeiro – Complexo Hospitalario Universitario de Vigo, Spain, [6]Departments of Medical Physics & Radiology, Memorial Sloan-Kettering Cancer Center, NY, United States

Reversed gradient method can reduce geometric distortion leading to accurate measurement of ADC. We designed a new phantom for distortion assessment and tested the reversed gradient method in both phantom and head and neck cancer patients, obtaining a relevant increase in mutual information values (phantom: 13% – 35%; patients: 6% - 100%). The voxel-wise analysis of the tumor showing variation of ADC with treatment exhibits significant difference ($p<0.01$) in calculated ADC between corrected and raw images. In future studies, the reverse gradient method may be included as part of clinical DW-MRI that focus on tumor response assessment.

1792 

Age-related effect on white matter changes and lexical retrieval

Natalie Yu-Hsien Wang[1], Fan-pei Gloria Yang[1], Yiyang Chen[2], Toshiharu Nakai[3], and Makoto Miyakoshi[4]

[1]Center for Cognition and Mind Sciences, National Tsing Hua University, Hsinchu, Taiwan, [2]Department of Biomedical Engineering, Mingchuan University, Taiwan, [3]Department of Gerontechnology, National Center for Geriatrics and Gerontology, Obu, Japan, [4]Swartz Center for Computational Neuroscience, University of California San Diego, San Diego, United States

Identifying age-related white matter change is vital to understanding neurodegeneration. With studies focusing mainly on memory, little is known of age-related change in language function. This current study bridges the gap by investigating the relationship between changes of WM integrity and task-based language performance. The behavioural evidence revealed significant different between young and healthy elderly people in phonemic as well as semantic retrieval. Also, TBSS analysis suggest significant difference in white matter volume between the two groups. However, correlation between white matter indices, FA and MD, was not found, indicating that degeneration of language function cannot be account for solely on white matter changes or particular task type.

1793 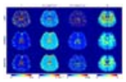

Robust mapping of diffusion parameters of the combined IVIM-Kurtosis-model using artificial neural networks in the human brain

Marco Bertleff[1], Sebastian Domsch[1], and Lothar Schad[1]

[1]Computer Assisted Clinical Medicine, Heidelberg University, Mannheim, Germany

In this work we present an artificial neural network (ANN) approach for the evaluation of the combined IVIM-Kurtosis model and robust mapping of the diffusion parameters in the human brain. Measuring seven healthy subjects the parameter map quality could be improved compared to an ordinary least squares regression by significantly reducing outliers and decreasing the variance while preserving the tissue contrast. An ROI-based analysis additionally showed a better agreement of the mean parameter values with the literature along with a better distinction between white and grey matter for the ANN approach.

1794 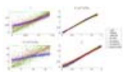

Simulation study for the evaluation of DWI data with the IVIM-Kurtosis model based on artificial neural networks

Marco Bertleff[1], Sebastian Domsch[1], and Lothar Schad[1]

[1]Computer Assisted Clinical Medicine, Heidelberg University, Mannheim, Germany

In this work we present an evaluation approach based on artificial neural networks (ANN) for fitting the IVIM-Kurtosis model parameters on the basis of simulated DWI data. The ANN approach is compared to an ordinary bounded least squares regression (LSR) in terms of correlation between estimates and ground truth, systematic, statistical and total estimation error. While for D and K high correlations and low errors were found for both LSR and ANN, a significant improvement was observed for f and D^* regarding correlation coefficients, precision and the total estimation error when using ANN.

1795 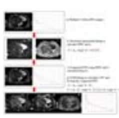

New approach to improve the reliability of IVIM parameters using computed DWI based on stretched exponential model

Eunju Kim[1,2], Jinwoo Hwang[1], Jae-Hun Kim[3], and Marc Van Cauteren[4]

[1]Philips Healthcare, Seoul, Korea, Republic of, [2]Hanyang University, Seoul, Korea, Republic of, [3]Samsung Medical Center, Seoul, Korea, Republic of, [4]Philips Healthcare, Tokyo, Japan

We propose a new approach to IVIM analysis using computed DWI (cDWI) based on stretched exponential model. IVIM analysis is widely studied clinically to evaluate tissue perfusion and diffusivity using a range of low and high b values. However, signal attenuation curves of different b values are heterogeneous because of biological effects from multiple components and patient's motion during the acquisition. So we generated cDWI first using stretched exponential model which can better fit for signal attenuation curve and analyse IVIM parametric maps using cDWI. The proposed approach can fit more robustly the IVIM model parameters.

1796 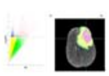

Longitudinal tissue changes in tumefactive demyelinating lesion associated with the administration of disease modifying drugs: a free water diffusion MRI study.

Salvatore Andrea Lacava[1], Ofer Pasternak[2], Maurizia Chiusole[3], Giorgio Rossi[4], John Dewitt Port[5], and Nivedita Agarwal[6]

[1]Trento University, Department of Cognitive Science, Trento, Italy, [2]Brigham and Women's Hospital, Harvard Medical School, [3]Section of Neurology, Hospital of Rovereto, [4]Section of Neurology, Hospital of Rovereto, APSS, [5]Section of Neuroradiology, Mayo Clinic, [6]Neuroradiologist, U.O. Radiology

It is challenging to diagnostically distinguish tumefactive demyelinating lesions (TDLs) from tumors surrounded by massive edema and mid-line shift such as high grade gliomas. We demonstrate free water diffusion MRI analysis to identify water diffusivity compartments in the lesion, and to monitor effects of medical treatment over time. We believe that free water diffusion analysis can be important adjunct to conventional MR, and adds value by improving our understanding of the histologic components of a lesion, which can help clinical diagnosis and potentially avoid biopsy.

1797

Multi-Tensor Filtering based on Expectation-Maximization Framework

Etienne St-Onge[1,2], Benoit Scherrer[2], Maxime Taquet[2,3], and Simon Warfield[2]

[1]Computer Science, Université de Sherbrooke, Sherbrooke, QC, Canada, [2]Computational Radiology, Harvard Medical School, Boston, MA, United States, [3]ICTEAM, Université catholique de Louvain, Louvain-La-Neuve, Belgium

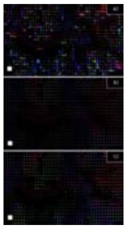

In this abstract, we introduce a new multi-tensor regularization and denoising technique based on Expectation-Maximization framework. To reduce filtering blurring effect and preserve sharp edges, we incorporated anisotropic regularization weight to the framework. We also utilize a tensor similarity metric, made from a quaternion representation, to improve the regularization and preserve tensor characteristics. Finally, we evaluate and compare filtering methods using a diffusion MRI synthetic phantom and in-vivo acquisition.

1798

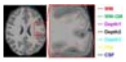

Cortical Diffusion Analysis of Human Connectome Project Data Identifies Granular Cortices

Qiyuan Tian[1,2], Christoph W.U. Leuze[2], Hua Wu[3], Grant Yang[1,2], Jingyuan Chen[1,2], Jonathan R. Polimeni[4,5], and Jennifer A. McNab[2]

[1]Department of Electrical Engineering, Stanford University, Stanford, CA, United States, [2]Department of Radiology, Stanford University, Stanford, CA, United States, [3]The Center for Cognitive and Neurobiological Imaging, Stanford University, Stanford, CA, United States, [4]Athinoula A. Martinos Center for Biomedical Imaging, Massachusetts General Hospital, Boston, MA, United States, [5]Department of Radiology, Harvard Medical School, Boston, MA, United States

We performed whole-brain cortical surface-based analysis of diffusion orientations on 100 subjects from the Human Connectome Project. Correlations between diffusion angles (angles between primary diffusion orientations and cortical surface normals) and cortical thickness and curvature were removed using rank-based linear regression. The resulting diffusion angle maps show radial diffusion orientations in all regions except for a few granular cortices which have predominantly tangential diffusion orientations. Identification of the granular cortices is greatly enhanced in the group-averaged map compared to a single-subject dataset.

1799

A Bayesian approach for diffusional kurtosis imaging

Eizou Umezawa[1], Daichi Ishihara[2], Yasunari kono[3], Toshiaki Nakai[4], and Ryoichi Kato[1]

[1]School of Health Sciences, Fujita Health University, Aichi, Japan, [2]Department of Radiology, Nagoya City University Hospital, [3]Washimi Orthopedic Surgery, [4]Department of Radiology, Fujita Health University Hospital

We propose a Bayesian approach for improving the accuracy of diffusional kurtosis imaging in a small number of data acquisitions. Gaussian-approximated prior distributions are made from primary maximum-likelihood estimation (MLE). The approach was tested using a healthy volunteer data in which a part of signals was replaced with simulated glioma signals. Although the approach does not yield further improvement when MLE has a certain degree of accuracy, the approach has effect to reduce large misestimations and did not cause false shrinkage of dispersions that the sample parameters inherently have. The approach reduces the burden of data acquisition.

1800

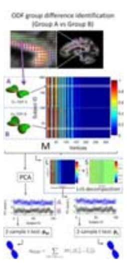

Low Rank plus Sparse Decomposition of ODF Distributions: Whole brain Statistical Analysis of Higher Order Diffusion Datasets

Steven H. Baete[1,2], Ying-Chia Lin[1,2], Ricardo Otazo[1,2], and Fernando E. Boada[1,2]

[1]Center for Advanced Imaging Innovation and Research (CAI2R), NYU School Of Medicine, New York, NY, United States, [2]Center for Biomedical Imaging, Dept of Radiology, NYU School Of Medicine, New York, NY, United States

Recent advances in data acquisition make it possible to use high quality diffusion data for routine in vivo study of white matter architecture. The dimensionality of these data sets requires a more robust methodology for their statistical analyses than currently available. Here we propose a apply Low-Rank plus Sparse (L+S) matrix decomposition to reliably detect voxelwise group differences in the Orientation Distribution Function that are robust against the effects of noise and outliers. We demonstrate the performance of this approach to replicate the established negative association between global white matter integrity and physical obesity in the Human Connectome dataset.

1801

Robust identification of rich-club organization in weighted and dense structural connectomes

Xiaoyun Liang[1], Chun-Hung Yeh[1], Robert Elton Smith[1], Alan Connelly[1], and Fernando Calamante[1]

[1]Florey Institute of Neuroscience and Mental Health, Melbourne, Australia

Rich-club organizations, characterizing the higher-level topology of the brain network, has been commonly identified from structural connectomes constructed using DTI based on network degrees. This analysis can however be compromised by the following issues: (i) DTI limitations in resolving crossing-fibers; and (ii) the original degree-metric based approach is unsuitable for highly-connected connectomes, because it leads to nodes with indistinguishably high degrees. Importantly, increasing evidence suggests that brain connectomes could be very dense. To address these issues, we propose a robust framework by: (i) applying advanced-tractography to construct connectomes; and (ii) developing a h-degree based method, RICHER, to identify rich-club organization.

1802

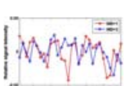

Assessment of Inherent Variation in Diffusion Tensor Measurements with Multi-band EPI in Rhesus Monkeys

Yuguang Meng[1] and Xiaodong Zhang[1,2]

[1]Yerkes Imaging Center, Yerkes National Primate Research Center, Emory University, Atlanta, GA, United States, [2]Division of Neuropharmacology and Neurologic Diseases, Yerkes National Primate Research Center, Emory University, Atlanta, GA, United States

Multi-band EPI technique is becoming prevalent in diffusion MRI because it can reduce the scanning time substantially by simultaneously exciting multiple slices and then decoding signal by parallel MR imaging reconstruction algorithms. However, little is known about its influence on the inherent variations of diffusion measurements with or without multi-band parallel acquisitions. This study compared the variations of the *in-vivo* diffusion MRI measurement results by multi-band and conventional parallel acquisitions. The results showed that the inherent variations of diffusion MRI measurements can be reduced by multi-band parallel acquisition compared to conventional parallel MRI acquisition.

1803

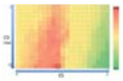

Individualized prediction of mild cognitive impairment based on patterns of altered tract integrity over the whole brain using diffusion spectrum imaging

Yu-Jen Chen[1], Yun-Chin Hsu[1], Yu-Ling Chang[2], Ming-Jang Chiu[3], and Wen-Yih Isaac Tseng[1,4]

[1]Institute of Medical Device and Imaging, National Taiwan University College of Medicine, Taipei, Taiwan, [2]Department of Psychology, National Taiwan University, Taipei, Taiwan, [3]Department of Neurology, National Taiwan University Hospital, Taipei, Taiwan, [4]Molecular Imaging Center, National Taiwan University, Taipei, Taiwan

In this study, we tested the capability of individualized prediction for mild cognitive impairment (MCI) by using the information of whole brain tract integrity produced by tract-based automatic analysis method. The information was trained to search the tract segments that could most accurately separate the MCI patients and healthy participants. The optimal tract segments were searched with the area under receiver operating characteristic curve of 0.76. These specific segments of white matter tracts could potentially serve as imaging biomarker for predicting patients with MCI.

1804

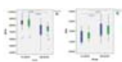

Histogram Analysis of Intravoxel Incoherent Motion MR Imaging–Related Parameters in Brain Glioma Grading: A Comparison Between 2D and 3D methods

Chunhong Wang[1], Yihao Guo[2], Maodong Chen[2], Yingjie Mei[2,3], Xiaodong Zhang[4], Jing Zhang[1], Xiang xiao[1], Yanqiu Feng[2], and Yikai Xu[1]

[1]Department of Medical Imaging Center, Nanfang Hospital, Southern Medical University, Guangzhou, People's Republic of China, [2]Guangdong Provincial Key Laboratory of Medical Image Processing, School of Biomedical Engineering, Southern Medical University, Guangzhou, People's Republic of China, [3]Philips Healthcare, Guangzhou, China., [4]Department of Medical Imaging Center, The Third Affiliated Hospital, Southern Medical University, Guangzhou, People's Republic of China

Gliomas are the most common primary neoplasms of the brain, World Health Organization (WHO) clarify it from low grade(LGGs; grade II) to high grade(HGGs; grades III, IV). The objective of this study was to explore which method is the best method with little time consuming and good grading of glioma.

1805

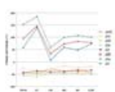

Preliminary analysis of micro-structural changes in different locations of brain tissue affected by acute ischemic stroke using diffusional kurtosis imaging

Liuhong Zhu[1], Zhongping Zhang[2], Qihua Cheng[1], Funan Wang[1], and Gang Guo[1]

[1]Radiology, Xiamen No.2 Hospital, Xiamen, People's Republic of China, [2]MR Research China, GE Healthcare, People's Republic of China

The performance of diffusion kurtosis imaging (DKI) in the analysis of micro-structural changes of brain tissue affected by acute ischemic stroke was explored. 199 lesions in common affected locations were divided into six groups. The value of DKI-derived indices and their changed percentage relative to normal contralateral ROI were calculated. Multiple comparisons among groups indicated that kurtosis indices (especially MK and Ka) showed better performance compared to diffusion indices (ADC, MD, Da and Dr) in detecting structure changes of brain tissues affected by acute ischemic stroke.

1806

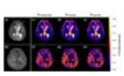

Rapid Measurement of Perfusion Fraction in Clinical Neuroimaging

Emma M Meeus[1,2,3], Jan Novak[2,3], Hamid Dehghani[1,4], and Andrew C Peet[2,3]

[1]Physical Sciences of Imaging in Biomedical Sciences (PSIBS), University of Birmingham, Birmingham, United Kingdom, [2]Institute of Cancer and Genomic Sciences, University of Birmingham, Birmingham, United Kingdom, [3]Department of Oncology, Birmingham Children's Hospital, Birmingham, United Kingdom, [4]School of Computer Science, University of Birmingham, Birmingham, United Kingdom

This study investigated the reliability of using a rapid three *b*-value diffusion-weighted imaging to determine intravoxel incoherent motion (IVIM) parameters. Grey matter simulations were conducted to assess the bias and reproducibility of the parameters with *b*-value distributions: $b_{0,300,500,1000}$, $b_{0,500,1000}$ and $b_{0,300,1000}$. The same *b*-value distributions were assessed with a volunteer cohort. The results showed that the use of two high *b*-values provided a good estimate of the perfusion fraction, which was further improved by an increase in the SNR level. In conclusion, the measurement of IVIM-*f* was achievable using a three *b*-value protocol.

1807

Minimizing the error in finding peak orientations of fiber ODF in diffusion MRI using Nelder-Mead simplex method

Kuan-Hung Cho[1], Chun-Hung Yeh[2], Yi-Ping Chao[3,4], Ching-Po Lin[5], and Li-Wei Kuo[1,6]

[1]Institute of Biomedical Engineering and Nanomedicine, National Health Research Institutes, Miaoli, Taiwan, [2]The Florey Institute of Neuroscience and Mental Health, Melbourne, Australia, [3]Department of Computer Science and Information Engineering, Chang Gung University, Taoyuan, Taiwan, [4]Department of Neurology, Chang Gung Memorial Hospital at Linkou, Taoyuan, Taiwan, [5]Institute of neuroscience, National Yang-Ming University, Taipei, Taiwan, [6]Institute of Medical Device and Imaging, National Taiwan University College of Medicine, Taipei, Taiwan

Discrete mesh search method is commonly used to determine fiber orientations by searching orientations corresponding local maxima of orientation distribution function (ODF). However, this method may produce extra errors relating to the number of sampling points of ODF in fiber orientation estimate. We address this problem and minimize the error of fiber orientation estimate by using Nelder-Mead simplex method. The results from computer simulation and phantom experiment show that Nelder-Mead simplex method gives accurate fiber orientation estimation better than discrete mesh search method with ODF sampling points less than 163,842.

1808

Application of Weighted Diffusion Subtraction (WDS) to Synovial Sarcomas: Possibility of Visualising Tumor Cellularity

Manabu Arai[1], Shigeo Okuda[2], Sota Oguro[2], Kuniaki Ohori[2], and Koichi Oshio[2]

[1]Department of Radiology, Nippon Kokan Hospital, Kawasaki, Japan, [2]Department of Diagnostic Radiology, Keio University School of Medicine, Tokyo, Japan

DWI and ADC values are widely used for tissue characterization. However, the relationship between the ADC values and the histological findings is still controversial. Weighted diffusion subtraction (WDS) was originally developed to eliminate T2 shine-through ambiguity in diffusion MRI evaluations. In this study, we applied WDS technique to diffusion weighted images of synovial sarcomas to evaluate the complex and heterogeneous tissue. Correspondence was found between WDS and histological findings on visual inspection. WDS seems to be a valuable visualization tool.

1809

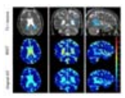

Quantifying Reconstruction Uncertainty with Image Quality Transfer

Ryutaro Tanno[1,2], Aurobrata Ghosh[1], Francesco Grussu[3], Enrico Kaden[1], Antonio Criminisi[2], and Daniel C Alexander[1]

[1]Computer Science, University College London, London, United Kingdom, [2]Microsoft Research Cambridge, [3]Institute of Neurology, University College London

Image quality transfer employs machine learning techniques to enhance quality of images by transferring information from rare high-quality datasets. Despite its successful applications in super-resolution and parameter map estimation of diffusion MR images, it still remains unclear how to assess the veracity of the predicted image in practice, especially in the presence of pathology or features not observed in the training data. Here we show that one can derive a measure of uncertainty from the IQT framework and demonstrate its values as a surrogate measure of reconstruction accuracy (e.g. root mean square error).

1810

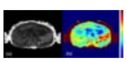

Analyses of Diffusion kurtosis imaging for spleen with liver disease

Yuhki Hamada[1], Daisuke Yoshimaru[1], Yuhichi Suzuki[2], Nozomi Mogi[3], and Ayumu Funaki[1]

[1]Tokyo Women's Medical University Yachiyo Medical Center, Yachiyo, Japan, [2]The University of Tokyo Hospital, [3]Tokyo women's Medical University Medical Center East

We evaluated the relationship between the mean kurtosis values (MK) and spleen size for the prediction of liver disease. As a result, there was no difference between the regular spleen and spleen with liver disease in the MK. Therefore, we consider that the splenic cell density and inner pressure remain unchanged even if patients have the enlarged spleen with liver diseases.

1811

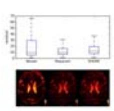

Compact representation of the diffusion signal for multi-shell HARDI

Daan Christiaens[1,2], J-Donald Tournier[1,2], Maria Kuklisova-Murgasova[1,2], and Joseph V Hajnal[1,2]

[1]Centre for the Developing Brain, King's College London, London, United Kingdom, [2]Division of Imaging Sciences & Biomedical Engineering, King's College London, London, United Kingdom

With the advent of multi-shell acquisition, there is an increasing need for compact linear orthonormal representations of the DWI signal that extend over the radial as well as angular domain. In this work, we evaluate and compare 3 candidate basis function sets: spherical Bessel functions with and without reparametrization and the SHORE basis. Results show that the reparametrized Bessel functions and SHORE basis can faithfully represent the DWI signal with low numbers of parameters, and can be tuned to the properties of the signal independently of acquisition parameters.

1812

Characterizing diffusion weighted images using Clustering Analysis of Spherical Harmonics (CASH)

Manish Amin[1], Guita Banan[1], Matthew Hey[2], Luis Colon-Perez[3], Haiqing Huang[4], Mingzhou Ding[4], Catherine Price[5], and Thomas Mareci[1,6]

[1]Physics, University of Florida, Gainesville, FL, United States, [2]Applied Physiology and Kinesiology, University of Florida, Gainesville, FL, United States, [3]Psychiatry, University of Florida, Gainesville, FL, United States, [4]Biomedical Engineering, University of Florida, Gainesville, FL, United States, [5]Clinical and Health Psychology, University of Florida, Gainesville, FL, United States, [6]Biochemistry and Molecular Biology, University of Florida, Gainesville, FL, United States

Diffusion weighted imaging has become an important tool for understanding how pathology affects brain structure. However, the standard method of diffusion tensor imaging (DTI) is inadequate in complex fiber regions. Other more complex diffusion models calculate the diffusion displacement probability function (DPF) 1, but current methods to extract the information from the DPF are limited. To this end, we introduce a data-driven method combining spherical harmonic representations of the DPF with the clustering analysis of spherical harmonic (CASH) coefficients, to provide an enhanced diffusion data characterization that includes information about the number of unique fiber orientations present in each voxel.

1813  Characterization of Spinal Cord DTI Metrics in Clinically Asymptomatic Pediatric Subjects with Incidental Congenital Lesions

Sona Saksena[1], Mahdi Alizadeh[2], Devon M Middleton[3], Laura Krisa[4], MJ Mulcahey[4], Feroze B Mohamed[1], and Scott H Faro[3]

[1]Radiology, Thomas Jefferson University, Philadelphia, PA, United States, [2]Bioengineering, Temple University, Philadelphia, PA, United States, [3]Radiology, Temple University, Philadelphia, PA, United States, [4]Occupational Therapy, Thomas Jefferson University, Philadelphia, PA, United States

Synopsis: Hydromyelia and syringomyelia are essentially cystic abnormalities of the spinal cord (SC). The prevalence of these abnormalities in the clinically normal pediatric population is uncommon to rare. Out of 26 healthy typically developing (TD) pediatric subjects scanned in this study, 4 subjects had incidental findings of hydromyelia (n=3) and syringomyelia (n=1) lesions within the thoracic SC. These subjects were healthy and clinically normal. DTI parameters were calculated by using ROIs drawn on the whole cord along the entire SC. DTI parameters were significantly different in the cord above the subject with syringomyelia lesion compared to the TD subjects. However, no significant difference in DTI parameters was found in the cord above the subjects with hydromyelia lesions. This study demonstrates that DTI has the potential to be used as an imaging biomarker to evaluate the SC above and below the congenital lesions in asymptomatic subjects and one should use caution while including them into a normative data population.

1814  Can DTI Predict the MRI Level of Injury in Pediatric Spinal Cord Injury Subjects?

Sona Saksena[1], John Gaughan[2], Devon M Middleton[3], Laura Krisa[4], MJ Mulcahey[4], Chris Conklin[1], Mahdi Alizadeh[5], Scott H Faro[3], and Feroze B Mohamed[1]

[1]Radiology, Thomas Jefferson University, Philadelphia, PA, United States, [2]Biostatistics Consulting Cente, Temple University School of Medicine, Philadelphia, PA, United States, [3]Radiology, Temple University, Philadelphia, PA, United States, [4]Occupational Therapy, Thomas Jefferson University, Philadelphia, PA, United States, [5]Bioengineering, Temple University, Philadelphia, PA, United States

The purpose of this study was to determine whether DTI parameters can be used to predict the level of injury as observed on conventional MRI data in pediatric spinal cord injury (SCI) subjects and to estimate the cut points for the DTI parameters which best discriminates the abnormal MRI from normal appearing MRI regions. Ten subjects with chronic SCI underwent repeat axial DTI scans based on inner field of view sequence. FA, MD, AD and RD were calculated by using ROIs drawn on the whole cord along the entire spinal cord for both scans. FA, MD, RD were significant predictors of the MRI level of injury. The cut points for FA, MD, AD and RD discriminated the abnormal MRI from normal appearing MRI regions in these subjects. DTI has the potential to serve as a surrogate for an abnormal MRI level corresponding to a region of SCI in instances where the MRI scans are unavailable, unreliable or there is an equivocal clinical exam.

Traditional Poster

Other

Exhibition Hall 1815-1876 | Tuesday 13:45 - 15:45

1815  Towards interpretation of 3-tissue constrained spherical deconvolution results in pathology

Thijs Dhollander[1], David Raffelt[1], and Alan Connelly[1,2]

[1]The Florey Institute of Neuroscience and Mental Health, Melbourne, Australia, [2]The Florey Department of Neuroscience, University of Melbourne, Melbourne, Australia

Multi-shell multi-tissue constrained spherical deconvolution (**MSMT-CSD**) and single-shell 3-tissue CSD (**SS3T-CSD**) resolve WM fibre orientation distributions and GM and CSF tissue compartments by deconvolving WM, GM and CSF response functions from the diffusion MRI data. We aim for more general interpretation of the “WM/GM/CSF” compartments obtained from 3-tissue CSD methods, specifically in the presence of pathology. We demonstrate their potential in this context and provide a simple framework that aids interpretation, with healthy tissues as a frame of reference. “CSF-like” partial volume is related to interstitial fluid, while “GM-like” partial volume may indicate gliosis, given an appropriate context.

1816 Evaluation of Motion-Compensated Spatially-Constrained IVIM (MC-SCIM) Model of Diffusion-weighted MRI for Assessment of Fibrosis in Crohn’s Disease using Surgical Histopathology Scores

Sila Kurugol[1], Moti Freiman[1], Jeffrey Goldsmith[2], Ryne Didier[1], Onur Afacan[1], Jeanette M Perez-Rossello[1], Michael J Callahan[1], Athos Bousvaros[3], and Simon K Warfield[1]

[1]Radiology, Boston Children's Hospital and Harvard Medical School, Boston, MA, United States, [2]Pathology, Boston Children's Hospital and Harvard Medical School, Boston, MA, United States, [3]Pediatrics, Boston Children's Hospital and Harvard Medical School, Boston, MA, United States

Distinguishing bowel regions with fibrosis and regions with active inflammation would be clinically useful in Crohn’s disease to determine best therapy. Commonly used ADC model of DW-MRI, which encapsulates multiple diffusion components into a single parameter, may not suffice to fully describe tissue microenvironments. IVIM model, which describes fast and slow diffusion components, is not commonly used in clinic because of challenges of reliably estimating its parameters due to noise and physiological motion. We recently introduced a motion-compensated spatially-constrained incoherent motion model (MC-SCIM) for reliable parameter estimation. Here we compared MC-SCIM parameters to scores of inflammation and fibrosis from histopathology.

1817 Potential value of turbo-spin echo diffusion-weighted imaging in nasopharynx: primary study for differential diagnosis between recurrent nasopharyngeal carcinoma and post-chemoradiation fibrosis

Shui xing Zhang[1]

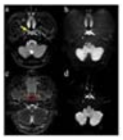

[1]Radiology, Guangdong General hospital, Guangzhou, People's Republic of China

In our study, we found significantly higher image quality, lesion conspicuity and less distortion of TSE-DWI based on Alsop method compared with SS-EPI according to image quality scores. Frustratingly, the SNR for TSE-DWI was lower than for SS-EPI and the result was consistent with other non EPI-DWI sequences in previous studies. Clinically, the low SNR of TSE-DWI remains a major concern. May be it is contributed to the long reception time and higher actual resolution of TSE images compared with SS-EPI and the more efficient k-space coverage of SS-EPI. The CNR of nasopharynx lesions on DW images was significantly better for TSE-DWI imaging than for SS-EPI imaging, which enables a better visual discrimination of nasopharynx lesions with TSE-DWI imaging. In conclusion, TSE-DWI with fewer artifacts and much higher resolutions, which was near impossible before, will make up for the slightly poorer SNR. The ADC values of the brainstem, which was less affected by the susceptibility artifacts and ghosts, showed no significant differences between the two DWI techniques. However, the ADC values of the lesions on TSE were significantly different than those on SS-EPI. This result is obtained coincide with the previous result.These differences may be primarily attributed to susceptibility artifacts and ghost that also resulted in inhomogeneous ADC maps because nasopharyngeal DWI is vulnerable to these artifacts. Therefore, the ADC measurements from TSE-DWI might be more accurate than those from SS-EPI.

1818

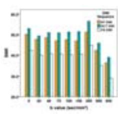

Intravoxel Incoherent Motion Diffusion-weighted MR Imaging of the Liver: Influence of Combined Respiratory-cardiac Triggering Method on Signal-to-noise Ratio and Repeatability of Quantitative Parameters

Jinning Li[1], Caiyuan Zhang[2], Yanfen Cui[2], Huanhuan Liu[2], Weibo Chen[3], and Dengbin Wang[2]

[1]Radiology, Xinhua Hospital, Shanghai Jiao Tong University School of Medicine, Shanghai, People's Republic of China, [2]Radiology, Xinhua Hospital, Shanghai Jiao Tong University School of Medicine, [3]Philips Healthcare

As extremely susceptible to various kinds of motions, diffusion-weighted magnetic resonance imaging always leads to insufficient image quality and poor reproducibility of quantitative measurements, especially for the liver. However, the use of combined respiratory-cardiac triggering, sychronizing data acquisitions with respiratory and cardiac cycles, could effective improve the signal-to-noise ratio and the repeatability of apparent diffusion coefficient and intravoxel incoherent motion parameters in the liver compared with respiratory triggering and free breathing without triggering method.

1819

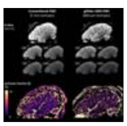

High-Resolution Intravoxel Incoherent Motion (IVIM) with Generalized SLIce Dithered Enhanced Resolution Simultaneous MultiSlice (gSlider-SMS): Effect on CSF Partial Volume Contamination

John Conklin[1], Thomas Witzel[2], and Kawin Setsompop[2]

[1]Department of Medical Imaging, University of Toronto, Toronto, ON, Canada, [2]Athinoula A. Martinos Center for Biomedical Imaging, Massachusetts General Hospital, Charlestown, MA, United States

In this work, we introduce a high-resolution acquisition strategy for IVIM brain imaging using generalized Slider Simultaneous MultiSlice (gSlider-SMS) diffusion MRI. An SNR efficient multi b-value 10 simultaneous slice acquisition was used to obtain IVIM parameter maps with submillimeter isotropic resolution. Compared to a conventional acquisition (2 mm isotropic), high resolution IVIM provided improved delineation of the cortex and reduced partial volume contamination with CSF. Cortical perfusion measurements using the standard acquisition were falsely elevated by approximately 40% compared to gSlider-SMS IVIM. High resolution IVIM may provide more reliable perfusion information for evaluation of cortically based pathology.

1820

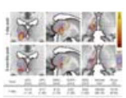

Diffusion weighted imaging of the cerebello-thalamic pathway after MR guided high intensity focused ultrasound (HIFU) thalamotomy

José A. Pineda-Pardo[1], Raul Martínez-Fernández[2,3], Rafael Rodríguez-Rojas[1], Marta Del-Alamo[1], Frida Hernández[1], Lydia Vela[1], and José A. Obeso[1]

[1]Centro Integral de Neurociencias AC (CINAC), HM Puerta del Sur, Hospitales de Madrid, Móstoles, Spain, [2]Centro Integral de Neurociencias AC (CINAC), HM Puerta del Sur, Hospitales de Madrid, Móstoles, [3]CEU San Pablo University, Madrid, Spain

In here we aimed at characterizing the impact of the HIFU thalamotomy over the cerebello-thalamic pathway. We used probabilistic tractography to map the subject-specific anatomy of this pathway, we defined a set of regions along a group average pathway, and we extracted DTI based average values in these regions. We found local and distant alterations along the pathway 3-months post-treatment. These changes were strongly correlated with the clinical improvement of the patients. These findings serve to strengthen DWI, as a tool to aid in the targeting of HIFU in the treatment of essential tremor.

1821

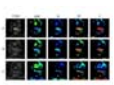

Value of the Intravoxel Incoherent Motion MRI in Pretreatment Predicting and Monitoring the Early Response to Chemoradiotherapy in Esophageal Squamous Cell Carcinoma

fei ping li[1], zhongping zhang[2], and Xiaoping Yu[1]

[1]Hunan Cancer Hospital, Changsha, People's Republic of China, [2]MR Research China, GE Healthcare, Beijing, People's Republic of China

Chemoradiotherapy (CRT) was considered to be a very effective treatment regimen for locally advanced or unresectable esophageal cancer (EC). Usually the therapy-induced early changes of tumor microenvironment were prior to morphological changes, which cannot be detected by traditional imaging techniques. This study used intravoxel incoherent motion diffusion-weighted imaging (IVIM-DWI) to investigate the early response to CRT in esophageal squamous cell carcinoma (ESCC). It was found that the IVIM-DWI parameters (ADC and D) might be valuable in pretreatment predicting and monitoring the early treatment response to CRT in ESCC.

1822

Rectal Adenocarcinoma: Diagnostic Accuracy of Diffusion Kurtosis Imaging (DKI) and its Correlation with Prognostic Factors

Lan Zhu[1], Xu Yan[2], Cai xia Fu[3], Huan Zhang[1], Zilai Pan[1], and Fuhua Yan[1]

[1]Radiology, Ruijin Hosptial, Jiaotong University, Shanghai, People's Republic of China, [2]MR Collaboration NE Asia, Siemens Healthcare, Shanghai, People's Republic of China, [3]APPL, Siemens Shenzhen Magnetic Resonance Ltd, Shenzhen, People's Republic of China

The high resolution MRI and conventional DWI suffers from unsatisfying accuracy in assessment of some prognostic factors of rectal adenocarcinoma. We employed DKI, a protocol mainly for evaluating the complexity of biologic tissues, to explore its diagnostic accuracy and correlation with prognostic factors. The kurtosis of DKI exhibited highest correlation with histologic grades especially the new grading criterion and higher potential in differentiation of high- and low grade tumors, and also in predicting nodal status, with higher specificity than or equivalent sensitivity to diffusivity and ADC. In conclusion, DKI could be a promising tool in predicting prognosis of rectal adenocarcinoma.

1823

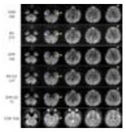

A Comparison of Readout Segmented EPI and Interleaved EPI in High Resolution Diffusion Weighted Imaging

Yishi Wang[1], Xiaodong Ma[1], Zhe Zhang[1], Erpeng Dai[1], Ha-Kyu Jeong[2], Bin Xie[3], Chun Yuan[1,4], and Hua Guo[1]

[1]Center for Biomedical Imaging Research, Department of Biomedical Engineering, School of Medicine, Tsinghua University, Beijing, People's Republic of China, [2]BIU Clinical Science MR, Philips Korea, Seoul, Korea, Republic of, [3]Healthcare Department, Philips Research China, Shanghai, People's Republic of China, [4]Vascular Imaging Laboratory, Department of Radiology, University of Washington, Seattle, WA, United States

Multi-shot interleaved EPI (iEPI) and readout segmented EPI (RS-EPI) are two alternative strategies for high resolution diffusion imaging. This study made a comparison of the two methods in different aspects. Our comparison showed that the iEPI had the advantage of largely reducing the geometric distortion. Both RS-EPI and iEPI could achieve high resolution diffusion tensor imaging.

1824

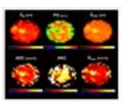

Evaluation of diffusion weighted imaging (DWI), kurtosis imaging (DKI) and q-space imaging (QSI) for profiling whole human breast tumour tissue microstructure

Nicholas Senn[1], Yazan Masannat[2,3], Ehab Husain[3,4], Bernard Siow[5], Steven D Heys[2,3], and Jiabao He[1]

[1]Aberdeen Biomedical Imaging Centre, University of Aberdeen, Aberdeen, United Kingdom, [2]Breast Unit, Aberdeen Royal Infirmary, Aberdeen, United Kingdom, [3]School of Medicine, University of Aberdeen, Aberdeen, United Kingdom, [4]Pathology Department, Aberdeen Royal Infirmary, Aberdeen, United Kingdom, [5]MRI Unit, The Francis Crick Institute, London, United Kingdom

We investigated a clinically viable QSI protocol in whole breast tumours excised from patients on a clinical scanner within a clinically feasible time frame. QSI has been largely limited to the preclinical setting, requiring strong gradients and a long acquisition time. We compared QSI against conventional DWI and DKI and found that diffusion indices across these techniques were consistent. Previous studies have shown that QSI provides a comprehensive characterisation of tissue microstructure, particularly in the presence of restricted diffusion. These results provide pivotal foundation for the clinical translation of QSI in breast cancer diagnosis and prognosis.

1825

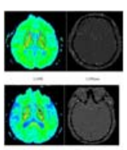

Effect of hyperglycemia on deep nucleus microstructure and iron deposition in people with type 2 diabetes: a DKI and SWI study

Junyi Dong[1], Chengcheng Zheng[1], Qingwei Song[1], Qiang Wei[1], Weiwei Wang[1], Yanwei Miao[1], and Bing Wu[2]

[1]Department of Radiology,First Affiliated Hospital of Dalian Medical University, Dalian 116011, People's Republic of China, [2]GE healthcare China, Beijing

In this paper,the experimental group and the control group were respectively used as the people with type 2 diabetes and the health people ,the effect of high blood glucose on the microstructure and iron deposition in patients with type 2 diabetes mellitus was studied used DKI and SWI study,and it is concluded that the high blood glucose level may have certain damage to the microstructure of the deep core.Furthermore,iron deposition may exacerbate the damage of microstructure.In conclusion,DKI and SWI study can evaluate secondary brain microstructure changes from hyperglycemia in T2DM patients.

1826

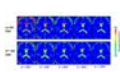

Optimal strategy for measuring intraventricular temperature using second-order motion compensation DWI

Shuhei Shibukawa[1,2], Tetsu Niwa[3], Naoki Ohno[2], Toshiaki Miyati[2], Tomohiko Horie[1], Susumu Takano[1], Nao Kajihara[1], Toshiki Saito[1], Tetsuo Ogino[4], and Yutaka Imai[3]

[1]Department of Radiology, Tokai university hospital, Isehara, Japan, [2]Division of Health Sciences, Graduate School of Medical Sciences, Kanazawa University, Kanazawa, Japan, [3]Radiology, Tokai University School of Medicine, Isehara, Japan, [4]Healthcare department, Philips Electronics Japan, LTD, Japan

A method for monitoring the intraventricular cerebrospinal fluid (CSF) temperature calculated from the DWI is affected by the CSF pulsation. Moreover, DWI should be obtained by optimal b value according to the diffusion coefficient of the measuring tissues. We investigated the second-order motion compensation DWI (2nd-MC DWI) to the determination of the intraventricular temperature to improve that accuracy with optimal b value. In the case of using the optimal b value based on the literature (ie., approximately 400 s/mm^2), the intraventricular temperature can be more accurately estimated with 2nd-MC DWI than conventional no-motion compensation DWI.

1827

Estimation of a novel set of intra and extracellular diffusivity parameters from modern DW-MRI

Mario Ocampo-Pineda[1], Alessandro Daducci[2,3,4], and Alonso Ramirez-Manzanares[1]

[1]Computer Science, Centro de Investigacion en Matematicas, Guanajuato, Mexico, [2]Computer Science Department, University of Verona, Italy, [3]University Hospital Center (CHUV) and University of Lausanne (UNIL), Switzerland, [4]Signal Processing Lab (LTS5), École Polytechnique Fédérale de Lausanne, Switzerland

We present a novel framework to estimate on in-vivo data a) independent intra and extracellular axial-diffusivities, b) extracellular radial-diffusivity, c) non-parametric bundle dispersion, d) axonal diameter indexes, and e) intracellular volume fractions. Our methodology does not fix a priori the value of any of these parameters or uses tortuosity models on the extracellular radial diffusivity. The proposal is an extension of the ED^3 method, which provided the best solution on the signal prediction on the White Matter Modelling Challenge 2015. We perform a comprehensive set of synthetic experiments under realistic conditions to validate the capabilities of the proposal.

1828 

Prediction of Radiotherapy Response in Nasopharyngeal Carcinoma Patients Using Diffusion-Kurtosis Imaging

Weiyuan Huang[1], Jiianjun Li[2], Feng Chen[3], Yingman Zhao[4], and Xiaolei Zhu[5]

[1]Department of Radiology, Hainan General Hospital, Haikou, People's Republic of China, [2]Department of Radiology, Hainan General Hospital, People's Republic of China, [3]Department of Radiology, Hainan General Hospital, Haikou, China, People's Republic of China, [4]department of Radiology, Hainan General Hospital, People's Republic of China, [5]MR scientific marketing NE Asia, Siemens Healthcare

The first row: A 62-year-old man with NPC who was a nonresponder. The lesions located at the left nasopharyngeal wall and cavum. Manual draw an ROI within the boundaries of the NPC on Kmean map. The tumor’s maximum diameter was 3.5 before radiotherapy. Residual tumor was detected after radiotherapy. Mean Dmean and Kmean values were 1.48 10-3 mm2/s and 0.72 before treatment. The second row: A 63–year-old man with NPC who was a responder. The lesion affect the bilateral mucous membrane of the nasopharynx. The tumor’s maximum diameter was 3.09 before radiotherapy. No residual tumor was detected after radiotherapy. Mean Dmean and Kmean values were 1.22 10-3 mm2/s and 0.83 before treatment. NRG: non response group RG: reponse group

---

1829 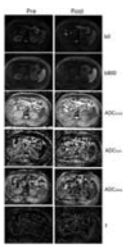

Effect of gadolinium contrast agent on IVIM derived parameters of abdominal organs

Yukun Chen[1], Chao Ma[1], Aiguo Jin[1], Li Wang[1], Minjie Wang[1], Luguang Chen[1], Caixia Fu[2], Xu Yan[2], and Jianping Lu[1]

[1]Radiology, Changhai Hospital of Shanghai, Shanghai, People's Republic of China, [2]MR Collaboration NE Asia, Siemens Healthcare, Shanghai, People's Republic of China

This study investigated potential effects of gadolinium contrast agent on the IVIM derived parameters such as Dfast (blood microcirculation), Dslow (pure extravascular water diffusion), f (perfusion fraction) and the commonly used DWI-derived ADC of abdominal organs. The result shows that gadolinium administration does not make statistically significant differences in Dslow, Dfast, f or ADC of the liver, spleen, or pancreas. In the kidney, however, ADC values are significantly lower with post-contrast than pre-contrast.

1830 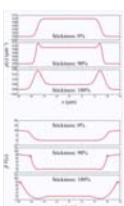

Imaging energy landscapes

Evren Özarslan[1], Kadir Şimşek[2], Cem Yolcu[1], and Carl-Fredrik Westin[1,3]

[1]Department of Biomedical Engineering, Linköping University, Linköping, Sweden, [2]Department of Physics, Bogazici University, Istanbul, Turkey, [3]Department of Radiology, Brigham and Women's Hospital, Harvard Medical School, Boston, MA, United States

We discuss the usage of a recently-proposed diffusion-sensitising gradient waveform for the purpose of imaging the potential energy landscape in which water molecules diffuse. The energy landscape encodes information about bulk heterogeneities of the medium as well as effects such as adsorption at the boundaries.

1831 

IVIM-derived parameters in evaluating the pathological features and hypoxia of nasopharyngeal carcinoma xenografts

Youping Xiao[1], Yunbin Chen[1], Xiang Zheng[1], Ying Chen[1], Li Peng[1], Jianji Pan[2], and Weibo Chen[3]

[1]Radiology, Fujian Medical University Cancer Hospital, Fuzhou, People's Republic of China, [2]Radiation Oncology, Fujian Medical University Cancer Hospital, Fuzhou, People's Republic of China, [3]Philips Healthcare, Shanghai, People's Republic of China

Intravoxel incoherent motion diffusion weighted imaging was conducted on different radio-sensitive human NPC xenografts (CNE-1 and CNE-2) in order to investigate its application value in assessing the pathological features and tumor’s hypoxia of xenografts. CNE-2 xenografts of higher radio-sensitivity behaved greater changes on IVIM-parameters than CNE-1 xenografts of lower radio-sensitivity after fractional radiations. D and f values correlated significantly with the pathological features and tumor’s hypoxia of xenografts. Thus, IVIM-parameters is potentially valuable in evaluating the effect of radiotherapy in NPC.

1832 

High-resolution diffusion imaging of post-mortem monkey brain: comparison of 3D Spin Echo and 3D segmented EPI sequence at 11.7T

Sophie Bernadette Sébille[1,2], Anne-Sophie Rolland[2], Carine Karachi[2,3], Marie-Laure Welter[2,4], Eric Bardinet[1,2], and Mathieu David Santin[1,2]

[1]Center of NeuroImaging Research - CENIR, Paris, France, [2]Inserm U 1127, CNRS UMR 7225, Sorbonne Universités, UPMC Univ Paris 06 UMR S 1127, Institut du Cerveau et de la Moelle épinière, ICM, Paris, France, [3]AP-HP, Hôpital de la Pitié-Salpêtrière, Department of Neurosurgery, Paris, France, [4]AP-HP, Hôpital de la Pitié-Salpêtrière, Department of Neurology, Paris, France

Diffusion-weighted spin echo (SE) acquisition is the golden-standard of diffusion imaging, yet it is limited by a very long acquisition time. This work present the optimization of a 3D segmented Echo Planar Imaging (EPI) sequence with the goal of reducing acquisition time and be able to perform tractography and to promote further analysis such as microstructure or histology correlation.

1833

Comparaison of in vivo and ex vivo high resolution imaging of the mouse brain at 11.7T

Sophie Bernadette Sébille[1,2], Isaac Adanyeguh[1,2], Elise Marsan[2], Sirenia Lizbeth Mondragon-Gonzalez[2,3], Fatma Gargouri[1,2], and Mathieu David Santin[1,2]

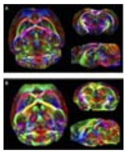

[1]Center of NeuroImaging Research - CENIR, Paris, France, [2]Inserm U 1127, CNRS UMR 7225, Sorbonne Universités, UPMC Univ Paris 06 UMR S 1127, Institut du Cerveau et de la Moelle épinière, ICM, Paris, France, [3]Behavior, Emotion and Basal Ganglia (BEBG), Brain and Spine Institute, Paris, France

This study compares high resolution in vivo and ex vivo diffusion imaging of mouse brain at 11.7T. The study shows that even with the advancement in image sequences and equipment, ex vivo imaging remains superior to in vivo imaging in terms of resolution with clear delineation of brain structures. However, fractional anisotropy values obtained from ex vivo imaging may not be a true representation of the in vivo condition. Nonetheless, the resolution obtained from in vivo imaging should allow for longitudinal studies.

1834

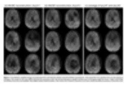

Comparison of MUSSELS vs MUSE for Multi-Shot Diffusion Imaging

Merry Mani[1], Mathews Jacob[2], Baolian Yang[3], and Vincent Magnotta[1]

[1]Department of Radiology, University of Iowa, Iowa City, IA, United States, [2]Department of Electrical and Computer Engineering, University of Iowa, Iowa City, IA, United States, [3]GE Healthcare

Multi-shot diffusion weighted (MS-DW) imaging can offer reduced echo-time (TE) and improved SNR to enable high spatial resolution applications. However, the reconstruction of the high resolution diffusion weighted images (DWI) from the multiple shots is challenging because of the presence of motion-induced phase variations between shots. Recently, two methods were proposed to reconstruct the phase-compensated DWIs. In this work, we compare the performance of the methods, MUSE and MUSSELS, to reconstruct the DWIs from a MS-DW acquisition.

1835

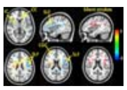

Fiber connection density differences detected in patients with sickle cell disease

Julie Coloigner[1], Jacob Antony[1], Roza Vlosova[2], Adam Bush[3], Soyoung Choi[4], Maxime Descoteaux[5], Jean-Christophe Houde[5], Thomas Coates[6], Natasha Lepore[2], and John Wood[7]

[1]Radiology, Children's hospital Los Angeles, Los Angeles, CA, United States, [2]Radiology, Children's hospital, Los Angeles, CA, United States, [3]Biomedical Engineering, University of Southern California, Los Angeles, CA, United States, [4]Neuroscience Graduate Program, University of Southern California, Los Angeles, CA, United States, [5]Sherbrooke Connectivity Imaging Lab (SCIL), Computer Science Department, University of Sherbrooke, Sherbrooke, QC J1K 0A5, Canada, [6]Hematology, Children's hospital, Los Angeles, CA, United States, [7]Cardiology, Children's hospital, Los Angeles, CA, United States

Sickle cell disease (SCD) is a chronic disorder characterize by progressive cerebrovascular damage. We hypothesized that subtle cerebral injury might be visible with diffusion imaging data in these patients. Tractography based on the fiber orientation distribution function (ODF) was applied in order to investigate the character and severity of white matter injury in patients with SCD. We found both decreased and increased fiber density in patients, compared to control subjects that co-localized with silent cerebral infarctions. These data suggest progressive white matter injury and compensatory mechanisms in SCD patients.

1836

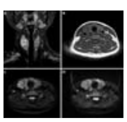

Diffusion weighted imaging in thyroid nodule: comparison of readout-segmented EPI and single-shot EPI Techniques

Luguang Chen[1], Peipei Sun[1], Bin Xu[1], Qiang Hao[1], Caixia Fu[2], Minjie Wang[1], and Jianping Lu[1]

[1]Radiology, Changhai Hospital of Shanghai, Shanghai, People's Republic of China, [2]Application development, Siemens Shenzhen Magnetic Resonace Ltd, Shenzhen, People's Republic of China

Diffusion weighted imaging showed the potential to evaluate thyroid disease. This study aimed to evaluate whether readout-segmented EPI (RS-EPI) can provide better image quality in imaging thyroid gland in comparison with single-shot EPI (SS-EPI), and to compare ADC values, acquired from RS-EPI with those of SS-EPI. Sixteen patients were examined using both techniques. There were significant differences in susceptibility, motion artifacts, except for detectability of thyroid nodules and ADC measurements between RS-EPI and SS-EPI. The present study found that the RS-EPI technique provides significant image quality improvement compared with SS-EPI in imaging thyroid gland at 3 Tesla.

1837

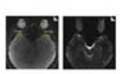

Towards a practical protocol for accurate and reliable MR-derived diffusion changes of the optic nerve in optic neuritis

Weiling Lee[1], Soo Lee Lim[1], Ling Ling Chan[1], Winston Eng Hoe Lim[1], and Helmut Rumpel[1]

[1]Diagnostic Radiology, Singapore General Hospital, Singapore, Singapore

Optic neuritis is a demyelinating inflammation of the optic nerve that often occurs in association with multiple sclerosis and neuromyelitis optica. Magnetic resonance imaging (MRI), especially diffusion-tensor imaging (DTI) is highly sensitive for inflammatory changes in the optic nerves. We propose a DTI protocol which balances susceptibility artefacts, scan time, and resolution for better image quality and clinical practicality. It allows a 1 mm in-plane resolution in order to avoid partial volume averaging with cerebrospinal fluid (CSF) surrounding the optic nerve in examining fractional anisotropy (FA) values and apparent diffusion coefficient (ADC) for severity of optic neuritis.

1838

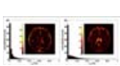

Joint estimation of free water and perfusion fraction in human brain

Anna Scherman Rydhög[1], André Ahlgren[1], Filip Szczepankiewicz[1], Ronnie Wirestam[1], Carl-Fredrik Westin[2], Linda Knutsson[1,3], and Ofer Pasternak[2]

[1]Department of Medical Radiation Physics, Lund University, Lund, Sweden, [2]Brigham and Women's Hospital, Harvard Medical School, Boston, MA, United States, [3]Department of Radiology (Adjunct), Johns Hopkins School of Medicine, Baltimore, MD, United States

The perfusion of blood affects the estimation of diffusivities, especially fast components such as free water. Here, we acquired human data to demonstrate the applicability of a three-compartment model for the joint estimation of tissue diffusivities, free water, and the perfusion fraction. We evaluated the feasibility of the model by comparing a multiple b-value approach with a shorter, clinically feasible approach. The conclusion is that the two-compartment free-water estimation is affected by both water and blood. The three-compartment model disentangles these effects, useful in distinguishing between changes originating from capillary blood from those originating from the extracellular space.

1839

Fractional motion related diffusion MRI in the detection of acute ischemic stroke

Yang Fan[1], Boyan Xu[2], Lu Su[3], Bing Wu[1], Zhenyu Zhou[1], Peiyi Gao[3], and Jia-Hong Gao[2]

[1]MR Research China, GE Healthcare, Beijing, People's Republic of China, [2]Center for MR Research, Peking University, Beijing, People's Republic of China, [3]Department of Radiology, Beijing Tiantan Hospital, Beijing, People's Republic of China

The use of FM model has been demonstrated in distinguishing low- and high-grade pediatric brain tumors. However, its feasibility in detecting acute stroke has not yet been investigated. In this work, FM model was applied in patients with acute ischemic stroke and compared with traditional ADC to investigate its clinical potential.

1840

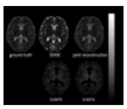

Model-Based Joint Reconstruction for Multi b-Value Diffusion-Weighted Imaging

Zhongbiao Xu[1], Li Guo[1], Wenxing Fang[2], Chenguang Zhao[2], Yingjie Mei[1,3], Zhifeng Chen[4], Wufan Chen[1], Ed X. Wu[5,6], Feng Huang[7], and Yanqiu Feng[1]

[1]School of Biomedical Engineering, Guangdong Provincial Key Laborary of Medical Image Processing, Southern Medical University, Guangzhou, People's Republic of China, [2]Philips Healthcare (Suzhou), Suzhou, People's Republic of China, [3]Philips Healthcare, Guangzhou, People's Republic of China, [4]Department of Biomedical Engineering, Zhejiang University, Hangzhou, People's Republic of China, [5]laboratory of Biomedical Imaging and Signal Processing, The University of Hong Kong, Hong Kong SAR, People's Republic of China, [6]Department of Electrical and Electronic Engineering,The University of Hong Kong, Hong Kong SAR, People's Republic of China, [7]Neusoft Medical System, Shanghai, People's Republic of China

In current multi b-value DWI, each b-value image is usually reconstructed independently by using parallel MRI techniques. In this work, we propose a model-based joint reconstruction method for the reconstruction of under-sampled multi b-value DWI data. The proposed method can directly estimate quantitative parameters form k-space data, and exploit inter-image constraint to improve the quality of reconstructed image.

1841

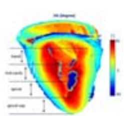

High Resolution Cardiac DTI - Fiber Tractography Statistics of the ex Vivo pig Heart

David Lohr[1], Maxim Terekhov[1], Andreas Max Weng[2], Anja Schroeder[3,4], Heike Walles[3,4], and Laura Maria Schreiber[1]

[1]Comprehensive Heart Failure Center, University Hospital Wuerzburg, Wuerzburg, Germany, [2]Department of Diagnostic and Interventional Radiology, University Hospital of Wuerzburg, Wuerzburg, Germany, [3]Department Tissue Engineering and Regenerative Medicine, University Hospital Wuerzburg, Wuerzburg, Germany, [4]Translational Center Wuerzburg 'Regenerative therapies', Wuerzburg branch of the Fraunhofer IGB, Wuerzburg, Germany

A whole heart, high resolution diffusion tensor data set with 1.3 mm isotropic voxels was acquired in 15 ex vivo pig hearts using a Stejskal-Tanner sequence at 3T. ADC, FA and HA values were calculated and analyzed for the whole heart. Purpose was to create a reliable statistical reference of diffusion parameters. Sharp modes for median and interquartile range of the ADC and median and mean values of the helix angle indicate similar distributions of those values for the individual hearts. This provides a statistically compelling reference for future cardiac DTI pig studies in vivo and at higher field strengths.

1842

In Vivo 3D Single-Shot Echo-Planar DWI at 7T for Mapping Tissue Microstructure using Mean Apparent Propagator (MAP) MRI

Alexandru Korotcov[1,2], Asamoah Bosomtwi[1,2], Elizabeth Hutchinson[1,3], Michal Komlosh[1,3], Carlo Pierpaoli[3], Peter J Basser[3], Andrew Hoy[2,4], and Bernard Dardzinski[2,4]

[1]Center for Neuroscience and Regenerative Medicine, Henry M. Jackson Foundation, Bethesda, MD, United States, [2]Radiology and Radiological Sciences, Uniformed Services University of the Health Sciences, Bethesda, MD, United States, [3]Eunice Kennedy Shriver National Institute of Child Health and Human Development, National Institutes of Health, Bethesda, MD, United States, [4]Center for Neuroscience and Regenerative Medicine, Uniformed Services University of the Health Sciences, Bethesda, MD, United States

A number of advanced diffusion models have demonstrated great promise for mapping tissue microstructure in *ex vivo* studies with high resolution and fidelity using a wide range of diffusion weightings, but the increased acquisition time (days) is not feasible *in vivo*. In this study we have addressed some basic DWI acquisition pitfalls by using 3D single-shot EPI on a high-field (7 Tesla) pre-clinical MRI system, and adapted one of the most promising diffusion modeling techniques, mean apparent propagator (MAP) MRI *in vivo* to derive information about rat brain microstructure within a reasonable time frame.

1843

Intravoxel Incoherent Motion (IVIM) in Evaluation of Orbital Masses

Ya-wen AO[1], Jun Chen [1], Liang Zhang[1], Fei Sang[1], Hong-yan Nie[1], Dong-jie Huang[1], Hui Lin[2], and Bing Wu[2]

[1]Department of Radiology, Renmin Hospital of Wuhan University, Wuhan, People's Republic of China, [2]GE Healthcare China, Shanghai, People's Republic of China

Diffusion-weighted imaging (DWI) has been proven that malignant orbital masses demonstrate significantly and visually appreciable lower apparent diffusion coefficient (ADC) than benign orbital masses[1-2]. Nevertheless, ADC cannot separate the pure molecular diffusion from the motion of water molecules in the capillary network; thus, perfusion contamination would increase the ADC value. According to the IVIM DWI model[3], both microscopic perfusion and diffusivity can be separated using a biexponential decay function, providing additional parameters for tissue characterization. From the result we can see that it is feasible that quantitative parameters of orbital masses can be derived from IVIM DWI.

1844 

Harmonization for DTI measurements mapping across sites in multi-center MRI study

Chuanzhu Sun[1], Lijun Bai[1], Hao Yan[2,3], Shan Wang[1], Xiaocui Wang[1], Xianjun Li[1,4], Chao Jin[5], Xiaocheng Wei[6], Hong Yin[7,8], Zengjun Zhang[9], Xiaoqun Yao[10], Xiaoling Zhang[11], Jian Yang[5], Jian Yang[5], and Jian Yang[5]

[1]Department of Biomedical Engineering, the Key Laboratory of Biomedical Information Engineering of the Ministry of Education, Xi'an Jiaotong University, Xi'an, People's Republic of China, [2]Xidian University, Xidian University, People's Republic of China, [3]Center for Language and Brain, Shenzhen Institute of Neuroscience, Shenzhen University, shenzhen, People's Republic of China, [4]Department of Radiology, the First Affiliated Hospital, Xi'an Jiaotong University, xi'an, People's Republic of China, [5]Department of Radiology, the First Affiliated Hospital, Xi'an Jiaotong University, Xi'an, People's Republic of China, [6]MR Research China, GE Healthcare, Beijing, People's Republic of China, [7]Department of Radiology, Xijing Hospital, Fourth Military Medical University, Xi'an, People's Republic of China, [8]Department of Radiology, Xijing Hospital, Fourth Military Medical University, xi'an, People's Republic of China, [9]Department of Diagnostic Radiology, Xi'an Children Hospital, Xi'an, People's Republic of China, [10]Department of Radiology, Xi'an Gao Xin Hospital, Xi'an, People's Republic of China, [11]Department of MRI Diagnosis, Shannxi Provincial People's Hospital, Xi'an, People's Republic of China

Despite the fact that multi-site diffusion imaging studies are increasingly used to study brain disorders, but it is noteworthy that there are large differences among diffusion measurements from different sites. The current study aimed to confirm the variability and to harmonize data across sites. Our results indicated that not only DTI metrics in human brain within inter-site but also within inter-site changed obviously. Furthermore, a brain voxel-based model was developed to harmonize the DTI metrics and to reduce the deviation compared with reference site data and thus improve the reliability of group analysis in multi-center study.

1845

Benefits of flow, eddy current and concomitant field compensation in diffusion weighted MRI

Lars Mueller[1], Andreas Wetscherek[1,2], Tristan Anselm Kuder[1], and Frederik Bernd Laun[1,3]

[1]Medical Physics in Radiology, German Cancer Research Center, Heidelberg, Germany, [2]Joint Department of Physics, The Institute of Cancer Research and The Royal Marsden NHS Foundation Trust, London, United Kingdom, [3]Institute of Radiology, University Hospital Erlangen

Diffusion-weighted MRI suffers from artifacts due to flow, concomitant fields and eddy currents. Different combinations of compensation for these effects were examined in phantom measurements as well as in vivo in the brain and in the prostate. The signal variations in the phantom measurements indicate that it could be advantageous to simultaneously compensate of all three effects over only flow and concomitant field compensation. This could not be seen in the in vivo results, where flow and concomitant field compensation proved to be as good as the full compensation.

1846 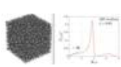

Diffusion Diffraction Inside Out

Valerij G Kiselev[1], Alexander Ruh[1], and Bibek Dhital[1]

[1]Dpt of Radiology, Medical Physics, University Medical Center Freiburg, Freiburg, Germany

Diffusion diffraction, a famous result on NMR in porous media founds little application to in-vivo MRI. Beyond the high technical requirements, the reason can be seen in the principal limitations of this technique. It probes the shape of identical closed pores, which are not typical in-vivo. In this work, we generalize diffusion diffraction for an infinite connected compartment outside impermeable inclusions such as space external to biological cells with low membrane permeability. The signal at high diffusion weighting is expressed in terms of the inclusions' correlation function. The developed theory is supported by experiments in aqueous suspension of polystyrene microbeads.

1847 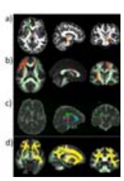

Investigation of Diffusion Tensor Indices by ROI analysis and TBSS of Patients with Depressive Symptoms in the Elderly with Dementia

Tsung-Yuan Li[1,2], Ni-Jung Chang[1], Clayton Chi-Chang Chen[1,3], and Jyh-Wen Chai[1,3,4]

[1]Department of Radiology, Taichung Veterans General Hospital, Taichung, Taiwan, Taichung, Taiwan, [2]Department of Medical Imaging and Radiological Sciences, Chung Shan Medical University, Taichung, Taiwan, Taichung, Taiwan, [3]Department of Biomedical Engineering, HungKuang University, Taichung, Taiwan, Taichung, Taiwan, [4]College of Medicine, China Medical University, Taichung, Taiwan, Taichung, Taiwan

The differences of indices in diffusion tensor images (DTI) of patients with dementia are well-discussed in recent years. However, the comorbidity of dementia and depression was observed. In this study, we focused on the white matter changes associated with depressive symptoms in dementia and the relationship between DTI indices and cognitive functions in depressed and non-depressed patients. By an ROI-based analysis of the indices and TBSS analysis in DTI, we investigated the differences between patients of dementia with depression and without depression. Furthermore, we correlate the differences with the score of some clinical cognitive test to figure out the subtle differences.

1848 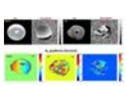

Myocardium Tissue DTI with Stimulated Echo at Large Susceptibility Induced B0 gradients: Examination of the Shimming Strategies Efficiency and Errors.

Maxim Terekhov[1], David Lohr[1], and Laura Maria Schreiber[1]

[1]Comprehensive Heart Failure Center, University Hospital Wuerzburg, Wuerzburg, Germany

In this paper, we investigated experimentally and statistically the effect of distortions of myocardium DTI with STEAM-EPI due to susceptibility induced gradients varied in a range of factor 10 to 20 to the reference. The special focus was given to examining the effect of prolonged EPI-readout, B_0-shimming effect and motion-induced shimming errors relevant for high-resolution DTI in-vivo. Fresh ex-vivo pig hearts were used for DTI measurements with an in-house developed STEAM-EPI sequence. The distribution of diffusion directions components was found well preserved for prolonged readout even at high internal gradient.

1849

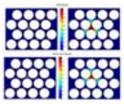

Validating Particle Dynamics in Monte Carlo Diffusion Simulation using the Finite Element Method

Jonathan Rafael-Patiño[1], Alonso Ramirez-Manzanares[1], Joaquin Peña[1], and Hui Zhang[2]

[1]Computer Science, Centro de Investigacion en Matematicas, Guanajuato, Mexico, [2]Department of Computer Science and Centre for Medical Image Computing, University College London, London, United Kingdom

Monte-Carlo Diffusion Simulation (MCDS) is commonly used to develop and validate analytical models for quantifying tissue microstructure using diffusion MRI. However, the validation of the tools implementing MCDS has been limited, especially for complex domains, such as the extra-cellular space of brain tissue. To address this challenge, we propose a novel framework using the Finite Element Method (FEM), an established method for solving the diffusion equation with complex domains, to provide the ground-truth to assess MCDS. We demonstrate the framework by assessing how the accuracy of MCDS is influenced by the number of particles and the number of diffusion steps.

1850

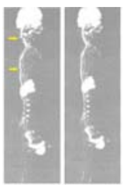

Distortion free whole-body diffusion weighted imaging using a self-adaptive post deformation algorithm

Lizhi Xie[1], Bo Hou[2], and Zhenyu Zhou[1]

[1]GE HealthCare, MR Research China, Beijing, People's Republic of China, [2]Department of Radiology, Peking Union Medical College Hospital, People's Republic of China

Conventional Whole-Body DWI that consists of several sequential stations often troubled geometric distortions and signal drops in areas with strong susceptibility, such as the neck and lumbar vertebra. The aim of this study was to propose a new WBDWI protocol and post process deformation algorithm to get distortion free whole body images. Consistently good results were received and in helps to diagnose several cases of tumors that were previously unclear to the volunteers and patients.

1851

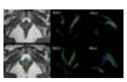

A longitudinal follow-up study of levator ani muscle injury during vaginal delivery using diffusion tensor imaging

yujiao zhao[1], zhizheng zhuo[2], and wen shen [1]

[1]Tianjin First Center Hospital, tianjin, People's Republic of China, [2]Philips Healthcare, Beijing, China, beijing, People's Republic of China

Levator ani muscle (LAM) injury has been known to be highly associated with vaginal delivery, the natural recovery course of injured LAM is unclear recurrently. Diffusion tensor imaging (DTI) with fiber tracking is a useful noninvasive MRI technique, which can be used to assess pelvic floor muscles injury and recovery quantitatively, and the fiber tract can display the direction and thickness of LAM fibers. In this study, we tried to apply DTI imaging to explore the natural recovery course of LAM injury during vaginal delivery. And the results showed that the injured LAM during vaginal delivery has some degree of repair as time goes on.

1852

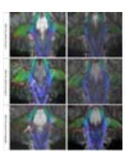

Shortening acquisition time and increasing resolution to (1 mm)³ isotropic in 7T diffusion MRI (dMRI) still allows resolving fiber orientations and fiber crossings: a step towards clinical applications?

Ralf Lützkendorf[1], Robin M Heidemann[2], Sebastian Baecke[1], Michael Luchtmann[3], Jörg Stadler[4], Thorsten Feiweier[2], Jörn Kaufmann[5], and Johannes Bernarding[1]

[1]Biometry and Medical Informatics, University of Magdeburg, Magdeburg, Germany, [2]Siemens Healthcare GmbH, Erlangen, Germany, [3]Neurosurgery, University of Magdeburg, Magdeburg, Germany, [4]Leibniz Institute for Neurobiology, Magdeburg, Germany, [5]Neurology, University of Magdeburg, Magdeburg, Germany

Prior results in single-shot diffusion weighted EPI indicated that voxel sizes below (1.4mm)3 prohibit reliable resolution of fiber orientations and fiber crossings. Here we compare zoomed single-shot EPI with (1mm)³ isotropic resolution with readout-segmented EPI with (1.4mm)³ and (1.0mm)³ isotropic at ultra-high field strength of 7 Tesla. In all cases, fiber density orientation maps could be determined reliably thus enabling a resolution of main fiber directions and crossings even at (1mm)³ resolution.

1853

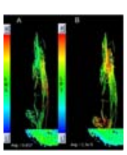

Applied Research of Diffusion Tensor Imaging in traumatic tibial nerve injury

Xiaojuan Wang[1,2], Chen Zhao[2], Kening Xu[1], and Lizhi Xie[3]

[1]Radiology Department of the 251 st Hospital of PLA, Zhangjiakou, People's Republic of China, [2]HeBei North University, Zhangjiakou, People's Republic of China, [3]GE Healthcare, MR Research China, BeiJing, People's Republic of China

DTI plays an important role in detecting nerve injury. It offers a great opportunity for imaging the tibial nerve injury follow trauma.In this work, we demonstrated DTI combined with DTT can clearly review the morphological transformation of Nerve fiber after tibial nerve injured; quantitatively analyze the damage degree,which can provide detailed information for clinical treatment.

1854

Scan time reduction in DWI of the pancreas using simultaneous multislice technique with different acceleration factors: how fast can we go?

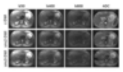
Jana Taron[1], Petros Martirosian[2], Thomas Kuestner[3], Mike Notohamiprodjo[1], Jakob Weiss[1], Ahmed Othman[1], Konstantin Nikolaou[1], and Christina Schraml[1]

[1]Department of of Diagnostic and Interventional Radiology, University Hospital of Tuebingen, Tuebingen, Germany, [2]Section on Experimental Radiology, Department of Diagnostic and Interventional Radiology, University Hospital of Tuebingen, Tuebingen, Germany, [3]Institute of Signal Processing and System Theory, University of Stuttgart, Stuttgart, Germany

We investigated the feasibility of simultaneous multislice-accelerated diffusion-weighted imaging of the pancreas using an acceleration factor of 2 and 3 (sms2/sms3-DWI) and its influence on image quality, acquisition time and apparent diffusion coefficients in comparison to conventional sequences (c-DWI) in ten healthy volunteers and 20 patients at 1.5 T. Images recorded with sms2-DWI offered high quality with a scan time reduction to one third; sms3-DWI showed significantly poorer overall image quality. In conclusion, sms2-DWI is feasible in clinical routine providing high image quality and a substantial reduction of acquisition time, whereas the use of higher acceleration factors is currently not recommended.

1855

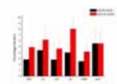

Robustness of kurtosis acquisition via simultaneous multi-slice EPI: a test-retest in children

Antonio Napolitano[1], Chiara Carducci[2], Laura Filograna[2], Vittorio Cannatà[3], and Giovanna Stefania Colafati[2]

[1]Medical Physics department, Bambino Gesù children's hospital, Rome, Italy, [2]Imaging Department, Bambino Gesù children's hospital, Rome, Italy, [3]Medical Physics department, Bambino Gesù children's hospital, ROME, Italy

Diffusion kurtosis imaging is an emerging technique based on non-gaussian diffusion of water in biologic systems and provides complementary information to the traditional diffusion. Although the method is very promising in identifying new biomarkers, it suffers from long time acquisition, which is very challenging in . However, a recent technique, named simultaneous multi-slice (SMS) acquisition, allows multiple slices acquisition thus drastically reducing the acquisition time. The purpose of this work is then to study the robustness of diffusion kurtosis in children when acquired via sms method.

1856

Mental training effects on adolescent brain networks

Olga Tymofiyeva[1], Eva Henje Blom[2,3,4], Justin Yuan[1], Colm G Connolly[2], Tiffany C Ho[2,5], Lisa Baldini[6], Trevor Flynn[1], Matthew D Sacchet[5], Kaja Z LeWinn[2], Rebecca Dumont Walter[1], Tony T Yang[2], and Duan Xu[1]

[1]Radiology & Biomedical Imaging, University of California, San Francisco, San Francisco, CA, United States, [2]Psychiatry, University of California, San Francisco, San Francisco, CA, United States, [3]Clinical Neuroscience, Karolinska Institutet, Stockholm, Sweden, [4]Clinical Sciences, Umeå Universitet, Umeå, Sweden, [5]Psychology and Neurosciences Program, Stanford University, Stanford, CA, United States, [6]PGSP-Stanford PsyD Consortium

In this study we used diffusion MRI network analyses to examine the effects of a 12-week training of attention and emotion regulation. Our preliminary results in 24 healthy adolescents demonstrate an improvement of executive attention and an increase of the node strength of the left anterior cingulate cortex.

1857

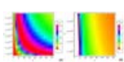

Analytical Solutions of Bloch NMR Flow Equations: Emerging and Future Diffusion Magnetic Resonance Imaging

Bamidele Omotayo Awojoyogbe[1] and Michael Oluwaseun Dada[1]

[1]Physics, Federal University of Technology, Minna, Nigeria, Minna, Niger State, Nigeria

Diffusion imaging has proved to be very important in clinical diagnosis and its exclusive application to numerous medical problems is currently plagued with some limitations which is most pronounced in heterogeneous voxels. In order to address this problem, we have presented an analytical method with which diffusion MR signals can be evaluated from point to point within a voxel of interest. The proposed method is shown to be useful in brain tumor diagnosis and general computational tissue imaging. The interesting part of this method is that only few data are required for image reconstruction.

1858

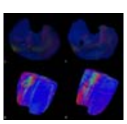

Diffusion Tensor Imaging of human muscle at ultra-high-field (7T) MR.

Chiara Giraudo[1], Stanislav Motyka[1], Christoph Resinger[2], Thorsten Feiweier[3], Siegfried Trattnig[1], and Wolfgang Bogner[1]

[1]Department of Biomedical Imaging and Image-guided Therapy- MR Centre of Excellence, Medical University of Vienna, Vienna, Austria, [2]Orthopedic Department, Evangelisches Krankenhaus Wien, Vienna, Austria, [3]Siemens Healthcare GmbH, Erlangen, Germany

Ultra-high-field (7T) imaging already demonstrated to provide more robust DTI measurements in comparison to 1.5 and 3T in the brain but, to the best of our knowledge, it was not applied for DTI measurements on human muscles. Our results showed higher SNR as well as an overall improvement in DTI metrics for the entire calf muscle at 7T than at 3T. Single muscle analyses (gastrocnemii, tibialis anterior) demonstrated more heterogeneous results. Future studies including a larger population and considering technical challenges (e.g.,RF inhomogeneity, gradient performance) are necessary to assess if 7T may provide higher benefits in specific muscles.

1859

Effect of Velocity-compensated Diffusion Preparation for Spinal Cord Diffusion Imaging

Zhe Zhang[1], Xiaodong Ma[1], Chun Yuan[1,2], and Hua Guo[1]

[1]Center for Biomedical Imaging Research, Department of Biomedical Engineering, School of Medicine, Tsinghua University, Beijing, People's Republic of China, [2]Vascular Imaging Laboratory, Department of Radiology, University of Washington, Seattle, WA, United States

The spinal cord and surrounding cerebrospinal fluid undergo significant cardiac pulsations, which can influence the microscopic motion-sensitive diffusion preparation and cause signal void in the diffusion images. In this work, velocity-compensated diffusion-encoding gradient waveform was implemented in spinal cord diffusion imaging and the images are compared with traditional monopolar preparation and cardiac gating approaches. Results show that with velocity-compensated diffusion preparation, the spinal cord diffusion imaging shows fewer signal voids compared to the traditional monopolar diffusion preparation. Using velocity-compensated diffusion preparation without cardiac triggering can provide a new approach for spinal cord diffusion imaging.

1860

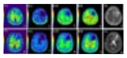

The diffusion kurtosis imaging findings of preoperative glioma-related epilepsy

Ankang GAO[1], Jingliang Cheng[2], Jie Bai[2], Yong Zhang[2], Shujian Li[2], Zanxia Zhang[2], Yijie Zhang[2], Xiao Cheng[2], and Shaoyu Wang[3]

[1]The First Affiliated Hospital of Zhengzhou University, Zheng Zhou, People's Republic of China, [2]The First Affiliated Hospital of Zhengzhou University, [3]MR Scientific Marketing Specialist, Siemens Healthcare Ltd.,Shanghai,201318, China

MK not only reflects the microstructure of the glioma， but also may reflect neurotransmitter metabolism microenvironment.

1861

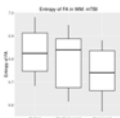

Diffusion Entropy of Fractional Anisotropy Values in White Matter in Mild Traumatic Brain Injury

Alexander Mark Weber[1], Michael Jarrett[1], Shiroy Dadachanji[2], David K. B. Li[3], Jack Taunton[4], and Alexander Rauscher[1]

[1]Pediatrics, University of British Columbia, Vancouver, BC, Canada, [2]University of British Columbia, Vancouver, BC, Canada, [3]Radiology, University of British Columbia, Vancouver, BC, Canada, [4]Division of Sports Medicine, University of British Columbia, Vancouver, BC, Canada

A paper in Radiology by Delic et al. in 2016 looked at the Shannon entropy of fractional anisotropy values in white matter in the brains of people with mTBI and controls, and found significant differences between the two. We attempted to replicate their findings with retrospective mTBI data of our own. We did not find any significant differences with controls, and ice hockey athletes concussed after two weeks. We also did not find any changes in concussed athletes comparing data before injury with data after 3 days, 2 weeks, and 2 months.

1862

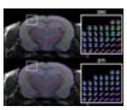

Exploring Cortical Fiber Crossings in Mice using Diffusional Kurtosis Imaging

Emilie T McKinnon[1,2,3], Jens H Jensen[1,2], G Russell Glenn[2,4], Andy Y Shih[2,4], and Joseph A Helpern[1,2,3,4]

[1]Department of Radiology and Radiological Science, Medical University of South Carolina, Charleston, SC, United States, [2]Center for Biomedical Imaging, Medical University of South Carolina, Charleston, SC, United States, [3]Department of Neurology, Medical University of South Carolina, Charleston, SC, United States, [4]Department of Neuroscience, Medical University of South Carolina, Charleston, SC, United States

The ability of diffusional kurtosis imaging (DKI) to detect multiple intravoxel fiber directions in vivo is demonstrated for mouse cortex, with two or more directions being detected in the majority of voxels. The distribution of angular differences between the different fiber directions for individual voxels peaked at near 90º, suggestive of a grid-like pattern of neurites. Our findings support the feasibility of DKI-based tractography in mouse cortex.

1863

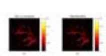

A Study on Total-Variation Regularization for Model-Based Reconstruction in DTI

Kazem Hashemizadeh[1], Samer Merchant[2], Dong Liang[3], Rong-Rong Chen[1], Edward Dibella[1,2,4], Edward Hsu[2], and Leslie Ying[5]

[1]Dept. of Electrical and Computer Engineering, University of Utah, SALT LAKE CITY, UT, United States, [2]Department of Biomedical Engineering, University of Utah, SALT LAKE CITY, UT, United States, [3]Biomedical and Health Engineering, Shenzhen Institutes of Advanced Technology, Shenzhen, People's Republic of China, [4]Department of Radiology and Imaging Sciences, University of Utah, SALT LAKE CITY, UT, United States, [5]Department of Biomedical Engineering, The State University of New York (SUNY) at Buffalo, NY, United States

In this work, we study total-variation (TV) regularization for model-based reconstruction from undersampled DTI data. Various TV regularization methods are examined. Using ex-vivo brain DTI data, we show that imposing TV constraints on DWI provide more reliable quantitative estimates of diffusion than those imposing TV constraints directly on the tensor. A gradient descent algorithm with line backtracking is used for better convergence to optimal solution. For highly undersampled data of 12 diffusion encoding directions and a reduction factor of R=4, we show that good estimates of primary eigen-vector, fractional anisotropy, and mean diffusivity can still be obtained using TV-based regularization.

1864

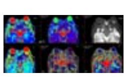

Repeatability of apparent diffusion coefficient and intravoxel incoherent motion parameters at 3.0 Tesla in orbital masses.

Augustin Lecler[1], Julien Savatovsky[1], and Laure Fournier[2]

[1]Radiology, Fondation Ophtalmologique Adolphe de Rothschild, Paris, France, [2]Radiology, Hôpital Européen Georges Pompidou, Paris, France

- IVIM technique is feasible in the orbit with a good to acceptable repeatability of ADC and D. (coefficient of variation range 12%-25%)
- Interobserver repeatability agreement is excellent for all the IVIM parameters in the orbit. (intraclass correlation coefficient range 90-95%)
- The use of PF or D* as biomarkers should be cautious because of high test-retest and interobserver variabilities.

1865

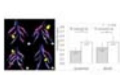

Functional Assessment of Lumbar Nerve Roots Using Direct Coronal Single-Shot Turbo Spin-Echo Diffusion Tensor Imaging - Application to Patients with Bilateral Spinal Canal Stenosis Showing Unilateral Neurological Symptom -

Takayuki Sakai[1], Masami Yoneyama[2], Yasuchika Aoki[3], Toshiaki Miyati[4], and Noriyuki Yanagawa[1]

[1]Radiology, Eastern Chiba Medical Center, Chiba, Japan, [2]Philips Electronics Japan, Tokyo, Japan, [3]Orthopaedic Surgery, Eastern Chiba Medical Center, Chiba, Japan, [4]Kanazawa University, Ishikawa, Japan

Clinically, there are some patients with spinal canal stenosis who have unilateral neurological symptom despite the existence of bilateral nerve compression on the conventional MRI images. The purpose of this study was to investigate the availability of TSE-DTI for patients with bilateral spinal canal stenosis who have unilateral neurological symptom. At the level responsible for symptom, the average FA values of symptomatic side were significantly lower than those of asymptomatic side. FA values of TSE-DTI might be helpful in identification of responsible lumbar nerves roots for patients with bilateral spinal canal stenosis who have unilateral neurological symptom.

1866 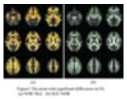

Investigation of Diffusion Tensor Indices by TBSS analysis and of Patients with symptoms of neuropsychiatric systemic lupus erythematosus

YUNG CHIEH CHANG[1], YA PING CHEN, NI JUNG CHANG, KAO LUN WANG, CLAYTON CHI CHANG CHEN, and JYH WEN CHAI

[1]Department of Radiology, Taichung Veterans General Hospital, Taichung city, Taiwan

In this project, we attempted to study the NPSLE subjects without abnormal lesion in conventional MR imaging in order to investigate the effective imaging biomarkers in early detection of neurological degeneration. Brain diffusion-tensor imaging with TBSS analysis was performed for studying the micro-structural alternations in NPSLE patients. The preliminary results illustrated statistically significant differences of FA and MD in some important nerve tracts between NPSLE patients and normal volunteers. There also existed a significant difference between NPSLE patients with and without depression.

1867 

Age Related Diffusion and Tractography Changes in Typically Developing Pediatric Cervical and Thoracic Spinal Cord

Mahdi Alizadeh[1], Yusra Sultan[2], Sona Saksena[3], Chris J Conklin[3], Devon M Middleton[1], Joshua M Fisher[3], Laura Krisa[4], Scott H Faro[5], MJ Mulcahey[4], and Feroze B Mohamed[3]

[1]Temple University, Philadelphia, PA, United States, [2]Drexel University, Philadelphia, PA, United States, [3]Radiology, Thomas Jefferson Hospital University, Philadelphia, PA, United States, [4]Occupational Therapy, Thomas Jefferson Hospital University, Philadelphia, PA, United States, [5]Radiology, Temple University, Philadelphia, PA, United States

This study investigates age related changes in diffusion tensor imaging and tractography parameters in pediatric spinal cord. This will help to understand maturation process in pediatric population and consequently will help for detection of diseased or injured spinal cord.

1868 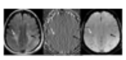

Observing the evolution of MS plaques using SWI and DCS-PWI

Liang Han[1], Lemei Tang[1], Weiwei Wang[1], Qingwei Song[1], Ailian Liu[1], Yanwei Miao[1], and Bing Wu[2]

[1]Department of Radiology,First Affiliated Hospital of Dalian Medical University, Dalian 116011, People's Republic of China, [2]GE healthcare China, Beijing

In this study，we aim to study the morphologic and micro-hemodynamic changes of MS plaques using SWI and DSC-PWI. We selected twenty-one MS patients diagnosed by the McDonald criteria (Revised Edition 2010) underwent MR scans including SWI and dynamical susceptibility contrasted MR perfusion weighted imaging (DSC-PWI) at baseline. Then Results were obtained by follow-up and scan. The MS plaques shows decreased phase value and blood perfusion. The characteristic of MS plaque is hypointense foci with small veins and only “abnormal vessels” region predict early changes.

1869 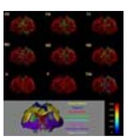

The influence of rat strain on multi-parametric white matter metrics – a Tractometry study

Daniel Barazany[1], Debbie Anaby[1], and Derek K Jones[1]

[1]CUBRIC, Cardiff University, Cardiff, United Kingdom

White matter macrostructural organization and its microstructural composition are two complementary features that may help understand intact brain development, function and brain impairment. The Tractometry framework, which aims to characterise white matter by multi parametric MR metrics, was applied on 3 rat strains (Wistar, SD and Lewis). In this study we examined the impact of rat strain on microstructural features of white matter in the brain, which is suspected to origin from their genetics background.

1870 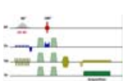

Targeted-FOV DWI can better depict the microemboli-induced renal lesions comparing to conventional full-FOV DWI

Chengyan Wang[1], Li Jiang[2], Hanjing Kong[1], Fei Gao[3], Wenjian Huang[1], Rui Wang[4], Lian Ding[1], Yan Jia[5], Hui Xu[5], He Wang[6], Xiaodong Zhang[4], Li Yang[5], Jue Zhang[1,3], Xiaoying Wang[1,4], and Jing Fang[1,3]

[1]Academy for Advanced Interdisciplinary Studies, Peking University, Beijing, People's Republic of China, [2]Philips Healthcare, Suzhou, People's Republic of China, [3]College of Engineering, Peking University, Beijing, People's Republic of China, [4]Department of Radiology, Peking University First Hospital, Beijing, People's Republic of China, [5]Renal Division, Peking University First Hospital, Beijing, People's Republic of China, [6]Institute of Science and Technology for Brain-Inspired Intelligence, Fudan University, Shanghai, People's Republic of China

DWI suffers from problems of severe geometric distortion and artifacts due to the susceptibility gradients and long echo train length (ETL), and the spatial resolution is quite limited due to the single-shot EPI acquisition scheme. This study investigates the utility of a targeted-FOV (TFOV) DWI technique in characterizing acute renal injure caused by microemboli injection in animal models. Compared with full-FOV DWI, the TFOV DW images show apparently higher image quality and better depiction of renal lesions. The advantage of TFOV DWI technique in characterizing microemboli-induced acute renal injure in is quite obvious.

1871 

Diffusion MRI and magnetic resonance spectroscopy reveal microstructural and functional alteration in chronic mild stress exposed rat brains: A CMS recovery study

Ahmad Raza Khan[1], Brian Hansen[1], Ove Wiborg[2], Christopher D Kroenke[3], and Sune N Jespersen[1,4]

[1]Clinical Medicine, Center of Functionally Integrative Neuroscience, Aarhus, Denmark, [2]Clinical Medicine, Translational Neuropsychiatry Unit, Risskov, Denmark, [3]Advanced Imaging Research Center, Portland, OR, United States, [4]Department of Physics and Astronomy, Aarhus, Denmark

Chronic mild stress (CMS) exposure leads to depression and other psychiatric disorder. Temporal changes post CMS exposure is still unclear. Present study employed CMS exposure on rats and utilised in-vivo longitudinal diffusion MRI and magnetic resonance spectroscopy (MRS) to reveal microstructural and functional alterations up to eight weeks post CMS exposure. Advanced diffusion kurtosis metrics have revealed significant alteration in stress sensitive regions, such as amygdala, hippocampus, prefrontal cortex and caudate putamen. MRS also showed significant metabolic alteration in ventral hippocampus, particularly on week1 post CMS exposure. Present finding could be useful in treatment of depression or similar disorders.

1872

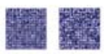

Diffusion-weighted images super resolution via external and internal patch-based regularization

ying fu[1], xi wu[1], yangzhi peng[2], and jiliu zhou[1]

[1]School of Computer Science, Chengdu University of Information Technology, chengdu, People's Republic of China, [2]College of Electronic Engineering, Chengdu University of Information Technology, chengdu, People's Republic of China

Super-resolution (SR) of diffusion weighted imaging (DWI) data is an ill-posed problem, which can be regularized by exploiting diverse priors learned from image patches. In this work, based on patch-based strategy of SR, we propose a new regularization method to reconstruct DW images, which integrates the sparse representation prior with dictionary learned from external image patches and non-local self-similarity prior learned from internal image patches. Meanwhile, in dictionary learning part, nonparametric Bayesian method is adopted to infer dictionary learning variables such as the size of the dictionary from data automatically. Experimental results demonstrate that the proposed method outperforms current methods in DWI reconstruction.

1873

Intravoxel incoherent motion (IVIM) diffusion-weighted imaging for response evaluation of hepatocellular carcinoma after resin- and glass-based radioembolization

Claus Christian Pieper[1], Alois Martin Sprinkart[1], Carsten Meyer[1], Hans Heinz Schild[1], Guido Matthias Kukuk[1], and Petra Mürtz[1]

[1]Radiology, University Hospital Bonn, Bonn, Germany

Intravoxel incoherent motion (IVIM) model-based analysis of diffusion-weighted imaging (DWI) is increasingly employed in oncologic imaging. Although first experiences with IVIM DWI for response analysis of hepatocellular carcinoma (HCC) after embolization therapies in general have recently been reported, response characteristics of specific treatment options are so far unknown. We describe differences in treatment response parameters of HCCs obtained by IVIM DWI in resin-radioembolization and glass-radioembolization.

1874

Changes of intravoxel incoherent motion (IVIM) diffusion-weighted imaging based parameters in patients undergoing transjugular intrahepatic portosystemic shunt (TIPS) creation – An initial analysis

Claus Christian Pieper[1], Alois Martin Sprinkart[1], Daniel Thomas[1], Carsten Meyer[1], Wolfgang Block[1], Hans Heinz Schild[1], Guido Matthias Kukuk[1], and Petra Mürtz[1]

[1]Radiology, University Hospital Bonn, Bonn, Germany

The creation of a transjugular intrahepatic portosystemic shunt (TIPS) influences hepatic blood flow dynamics. TIPS-related changes of diffusion-weighted imaging based intravoxel incoherent motion (IVIM) parameters at 1.5 T were investigated in liver parenchyma of cirrhotic patients. An increase of the IVIM perfusion fraction was found, indicating improved microvascular flow within the liver tissue after decompression of the portal vein. Diffusion parameters were not significantly influenced by TIPS-creation.

1875

White matter abnormalities of brain and cervical spinal cord in Hepatic Myelopathy patients: a diffusion tensor imaging study

Liu-Xian Wang[1], Lin Liu[2], Kang Liu[3], Ning-Bo Fei[4], Long-Biao Cui[3], Yi-Bin Xi[3], Ting-Ting Liu[3], Wei Qin[2], and Hong Yin[3]

[1]Department of Radiology, Xijing Hospital, The Fourth Military Medical University, shaanxi, xi'an, People's Republic of China, [2]School of Life Sciences and Technology, Xidian University, People's Republic of China, [3]the fourth military medical university, People's Republic of China, [4]School of Life Sciences and Technology, Xidian University, xi'an, People's Republic of China

The prominent syndrome of HM such as spastic paraparesis is usually considered resulting from abnormal function of thoracic segments, nevertheless, the involvement of intracranial fibers and cervical spinal cord is not clear. In this study, we found a widespread and robust white matter tract abnormality in brain of HM and non-HM patients, without significant difference with cervical spinal cord. Our finding may help shedding light on the underlying pathological mechanism of HM.

1876

Signal behavior of Ultra-High-b radial DWI (UHb-rDWI) signal in different tract of the cervical spinal cord

Bijaya Thapa[1,2], Nabraj Sapkota[1,2], YouJung Lee[1], EunJu Kim[1], John Rose[3], Lubdha M. Shah[4], and Eun-Kee Jeong[1,4]

[1]Utah Center for Advanced Imaging Research, University of Utah, Salt Lake City, UT, United States, [2]Department of Physics and Astronomy, University of Utah, Salt Lake City, UT, United States, [3]Department of Neurology, University of Utah, Salt Lake City, UT, United States, [4]Department of Radiology and Imaging Sciences, University of Utah, Salt Lake City, UT, United States

The ultrahigh-b radial DWI (UHb-rDWI) technique is used to study the white matter disease in the spinal cord. The diffusion signal from the extra axonal (EA) space drops to noise level while that from the intra axonal (IA) space is almost constant at UHb region for the myelinated axons where the myelin layers prohibit the exchange of water molecules between IA and EA spaces. However for partially or unmyelinated axons, the diffusion signal from IA space is no longer constant. The signal behavior at UHb region could be used as a biomarker for the demyelination and axonal loss.

Traditional Poster

Arterial Spin Labeling Applications

Exhibition Hall 1877-1898 Tuesday 16:15 - 18:15

1877

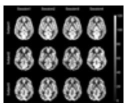

Reliability of Single- and Multi-TI ASL measurements with a clinical product sequence

Antonio Ricciardi[1,2], Marco Castellaro[3], Alberto Miglioranza[3], Giancarlo Germani[4,5], Paolo Vitali[4,5], Giuseppe Micieli[6], Egidio D'Angelo[7,8], Fulvia Palesi[7,9], Gloria Castellazzi[7,10], Claudia AM Gandini Wheeler-Kingshott[1,7,8], Enrico De Vita[11,12], and Alessandra Bertoldo[3]

[1]Institute of Neurology, University College London, London, United Kingdom, [2]Department of Medical Physics and Biomedical Engineering, University College London, London, United Kingdom, [3]Department of Information Engineering, University of Padova, Padova, Italy, [4]Brain MRI 3T Mondino Research Center, C. Mondino National Neurological Institute, Pavia, Italy, [5]Neuroradiology Unit, C. Mondino National Neurological Institute, Pavia, Italy, [6]Department of Emergency Neurology, C. Mondino National Neurological Institute, Pavia, Italy, [7]Brain Connectivity Center, C. Mondino National Neurological Institute, Pavia, Italy, [8]Department of Brain and Behavioral Sciences, University of Pavia, Pavia, Italy, [9]Department of Physics, University of Pavia, Pavia, Italy, [10]Department of Electrical, Computer and Biomedical Engineering, University of Pavia, Pavia, Italy, [11]Neuroradiological Academic Unit, Department of Brain Repair and Rehabilitation, Institute of Neurology, University College London, London, United Kingdom, [12]Lysholm Department of Neuroradiology, National Hospital for Neurology and Neurosurgery, UCL Hospitals Foundation Trust, University College London, London, United Kingdom

Single-TI Arterial Spin Labeling (ASL) is sensitive to delayed arterial arrival time (AAT) of blood in the tissues. Multi-TI was introduced to overcome this limitation. Moreover, it allows estimating AAT that, therefore, can shed some light in the characterization of the brain haemodynamic processes. In this study, we compare the reliability of the multi-TI approach to the single-TI in a test-retest protocol. The sequence tested was the Siemens product sequence FAIR PASL with 3D-GRASE readout. Results show an overall good level of reliability both in single- and multi-TI, but also a possible sensitivity to the macro-vascular component in multi-TI data.

1878

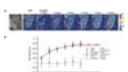

Physiologically synchronized multi-module pulsed arterial spin labeled (SymPASL) MRI

Hung Phi Do[1] and Krishna S Nayak[2]

[1]Physics and Astronomy, University of Southern California, Los Angeles, CA, United States, [2]Electrical Engineering, University of Southern California, Los Angeles, CA, United States

Physiologically synchronized multi-module pulsed arterial spin labeling (**SymPASL**) involves pulsed labeling that is applied several times prior to pulsations in the arterial blood supply. Simulations and *in vivo* measurements in human kidneys demonstrate that SymPASL provides superior SNR and SNR efficiency compared to conventional flow-sensitive alternating inversion recovery (**FAIR**) ASL with a single labeling pulse. Simulations suggest that SymPASL provides comparable SNR and SNR efficiency to pseudo-continuous ASL (**PCASL**), with lower specific absorption rate (**SAR**).

1879

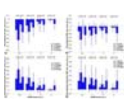

Hadamard-encoded Multi-delay PCASL: Should the Bolus Durations be T1-adjusted?

Jia Guo[1], Marc R. Lebel[2], Samantha Holdsworth[1], and Greg Zaharchuk[1]

[1]Radiology, Stanford University, Stanford, CA, United States, [2]GE Healthcare, Calgary, Canada

It has been hypothesized that in multi-delay arterial spin labeling (ASL), employing T_1-adjusted labeling durations (LDs) should provide a more balanced signal-to-noise (SNR) across ASL signals, therefore improving the accuracy of the transit delay (TD) and perfusion estimation. However, this claim has not been thoroughly tested. In this study, we evaluated the effects on the TD and perfusion estimation using LDs both with and without T_1-adjusted weighting, using the Hadamard-encoded multi-delay ASL sequence. Using Monte Carlo simulations and *in vivo* experiments, T1-adjusted weighting was more prone to noise and was likely to underestimate the TD and perfusion measurements compared to that without.

1880

Cerebral Blood Flow and Bolus Arriving Time Changes in Patients with Diabetes Detected by Multi-TI ASL

Yelong Shen[1], Bin Zhao[1], Lirong Yan[2], Kay Jann[2], Guangbin Wang[1], Junli Wang[1], Bao Wang[1], Josef Pfeuffer[3], Tianyi Qian[4], and Danny JJ Wang[2]

[1]Shandong Medical Imaging Research Institute, School of Medicine, Shandong University, Jinan, People's Republic of China, [2]Laboratory of FMRI Technology (LOFT)，Mark & Mary Stevens Neuroimaging and Informatics Institute，Keck School of Medicine，University of Southern California (USC), LA, CA, United States, [3]Siemens Healthcare, Erlangen, Germany, [4]Siemens Healthcare, MR Collaborations NE Asia, Beijing, People's Republic of China

This study aimed to simultaneously measure cerebral blood flow (CBF) and bolus arriving time (BAT) in a cohort of subjects with type II diabetes, and compared the results with those of matched control subjects using a multi-TI 3D GRASE pulsed-ASL (PASL) sequence. The voxel-based analysis showed that the CBF and BAT values in patients with diabetes presented significant differences compared to healthy subjects, especially in some particular areas of the brain. These differences may be related to functional changes in patients with diabetes, which may have occurred before the onset of the symptoms.

1881

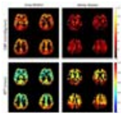

Estimation of Cerebral Blood Flow and Arterial Transit Time Using Partial Volume Corrected Multi-TI Arterial Spin Labeling Imaging

Youngkyoo Jung[1,2,3], Megan E Johnston[2], and Christopher T Whitlow[1,2,3]

[1]Radiology, Wake Forest School of Medicine, Winston-Salem, NC, United States, [2]Biomedical Engineering, Wake Forest School of Medicine, Winston-Salem, NC, United States, [3]Clinical and Translational Sciences Institute, Wake Forest School of Medicine, Winston-Salem, NC, United States

A novel PVC algorithm using Multi-TI ASL, acquiring ASL images at multiple PLDs, has been proposed to estimate CBF and ATT in GM and WM separately. A 3D kernel was used to reduce noise sensitivity and improve the estimation power. The proposed method successfully estimated four perfusion parameters (GM CBF, GM ATT, WM CBF, and WM ATT) simultaneously, and may allow region- or voxel-based perfusion analyses in WM, as well as GM.

1882

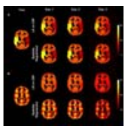

Investigating the Sensitivity to Partial Volume Estimates of Partial Volume Correction for Single Postlabeling Delay Pseudo-continuous ASL

Moss Y Zhao[1], Egill Rostrup[2,3], Otto M Henriksen[3], Yingyi Xiao[4], and Michael A Chappell[1]

[1]Institute of Biomedical Engineering, University of Oxford, Oxford, United Kingdom, [2]Functional Imaging Unit, Department of Clinical Physiology, Nuclear Medicine and PET, Copenhagen University Hospital Rigshospitalet Glostrup, Copenhagen, Denmark, [3]Department of Clinical Physiology, Nuclear Medicine and PET, Copenhagen University Hospital Rigshospitalet Blegdamsvej, Copenhagen, Denmark, [4]St Hilda's College, University of Oxford, Oxford, United Kingdom

This work investigates the sensitivity of partial volume correction methods to partial volume estimates using single-PLD PCASL. Random and biased errors were applied to partial volume estimates to simulate the variabilities in tissue segmentation. The results have indicated that current partial volume correction methods trade off accuracy in spatial variations in CBF against sensitivity to noise and errors in the partial volume estimates.

1883

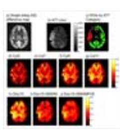

Regional Heterogeneity in Moyamoya Disease: Discovering Local Arterial Transit Time Information from Single-Delay Arterial Spin Labeling

Wendy W Ni[1] and Greg Zaharchuk[1]

[1]Radiology, Stanford University, Stanford, CA, United States

Arterial transit information provides valuable diagnostic information in steno-occlusive pathologies. We propose deriving transit information from the regional spatial heterogeneity (ReHet) of standard single-delay pseudo-continuous arterial spin labeling difference images. With image processing and machine learning, we demonstrate the potential of this technique in identifying regions with slow arterial flow in pre-operative Moyamoya disease patients. We investigate a selection of 7 different ReHet metrics, and identify trends that will inform better design of ReHet metrics and machine learning models.

1884

White matter cerebral blood flow in a large healthy cohort from the CARDIA study

Sudipto Dolui[1,2], Guray Erus[1], David R. Jacobs, Jr.[3], R. Nick Bryan[1], and John A. Detre[1,2]

[1]Department of Radiology, University of Pennsylvania, Philadelphia, PA, United States, [2]Department of Neurology, University of Pennsylvania, Philadelphia, PA, United States, [3]Division of Epidemiology and Community Health, University of Minnesota, Minneapolis, MN, United States

By analyzing cerebral blood flow (CBF) maps generated from arterial spin labeling (ASL) data averaged across 436 cognitively healthy middle-aged subjects from the CARDIA study, we characterized the CBF distribution in white matter. CBF is specifically decreased in periventricular regions in a pattern not reflective of partial volume effects as estimated from the structural MRI segmentation. White matter lesion frequency mapping based on Fluid Attenuated Inversion Recovery (FLAIR) images from the same cohort demonstrates that lesions tend to occur in regions where group averaged CBF is lowest.

1885

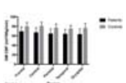

Arterial spin labelling measurements of cortical perfusion in multiple sclerosis show widespread reduced cortical metabolism

Ruth Oliver[1], Heidi Beadnall[1], Chenyu Wang[1], Matthew Kiernan[1], Todd Hardy[1,2], and Michael Barnett[1]

[1]Brain and Mind Centre, University of Sydney, Sydney, Australia, [2]Neuroimmunology Clinic, Concord Hospital

Multiple sclerosis (MS) is primarily an inflammatory demyelinating disease of the central nervous system. However, there is also growing evidence that cortical dysfunction may also be associated with disability in MS. Few studies have investigated cortical cerebral perfusion in MS, and even fewer have utilised arterial spin labelling (ASL) MRI, which offers noninvasive quantitative assessment of cerebral function using endogenous contrast. ASL is an inherently low resolution imaging modality known to be affected by the partial volume (PV) effect, leading to an underestimation of grey matter (GM) perfusion. Decreases in GM perfusion could reflect neuronal loss or metabolic dysfunction; PV correction techniques allow decoupling of structure and function. It is hypothesized that reduced regional GM perfusion after PV correction reflects a genuine decreased tissue metabolism, rather than atrophy.

1886

Pseudo-continuous arterial spin labeling considerations in patients with sickle cell anemia

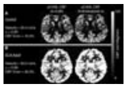

Meher R Juttukonda[1], Lori C Jordan[2], Melissa C Gindville[2], Larry T Davis[1], Jennifer M Watchmaker[3], Sumit Pruthi[1], and Manus J Donahue[1]

[1]Radiology and Radiological Sciences, Vanderbilt University Medical Center, Nashville, TN, United States, [2]Pediatrics - Division of Pediatric Neurology, Vanderbilt University Medical Center, Nashville, TN, United States, [3]Medical Scientist Training Program, Vanderbilt University, Nashville, TN, United States

Pseudo-continuous arterial spin labeling (pCASL) MRI involves labeling of flowing arterial blood water; therefore, the flow velocity of the blood water affects the efficiency of pCASL labeling. This effect has been quantified in healthy subjects but has not been examined in adults with sickle cell anemia (SCA). In this study, we illustrate that cervical flow velocities are elevated in adults with SCA, resulting in a reduced pCASL labeling efficiency of 0.72, and errors associated with this phenomenon are more than twice as large as those associated with bolus arrival time variability when long post-labeling delays times are used.

1887 

Improved reproducibility of longitudinal renal ASL perfusion measurements in children with chronic kidney disease using retrospective motion correction

Fabio Nery[1], Enrico De Vita[2,3], Chris A. Clark[1], Isky Gordon[1], and David L. Thomas[3]

[1]UCL Great Ormond Street Institute of Child Health, Developmental Imaging and Biophysics Section, London, United Kingdom, [2]National Hospital for Neurology and Neurosurgery, Lysholm Department of Neuroradiology;, [3]UCL Institute of Neurology, Department of Brain Repair and Rehabilitation

Arterial spin labelling (ASL) is a unique MR approach for quantifying tissue perfusion non-invasively. However, it is prone to motion-related artefacts which limit its application in the clinical domain, especially outside the brain. In this work, we combine a motion-insensitive ASL acquisition scheme with a specifically tailored retrospective motion correction pipeline. This enabled repeatable renal perfusion measurements to be obtained in the first ASL study in paediatric patients with moderate/severe chronic kidney disease.

1888 

Simultaneous Multi-Slice Cardiac ASL

Terrence Jao[1] and Krishna Nayak[2]

[1]Biomedical Engineering, University of Southern California, Los Angeles, CA, United States, [2]Electrical Engineering, University of Southern California, Los Angeles, CA, United States

Cardiac arterial spin labeling (ASL) is a promising technique for the quantification of myocardial blood flow (MBF) and has been shown to detect clinically relevant changes in myocardial perfusion under vasodilator stress. However, current cardiac ASL techniques have limited spatial coverage because they cannot be repeated for multiple slices due to limited duration of pharmacologically induced peak stress (~3 min). In this work, we demonstrate the feasibility of using blipped CAIPI bSSFP for cardiac FAIR ASL.

1889 

Measurement of lung perfusion using optimized pseudo-continuous arterial spin labeling of pulmonary arteries and fast True-FISP imaging at 3 Tesla

Petros Martirosian[1], Rolf Pohmann[2], Martin Schwartz[1,3], Thomas Küstner[3,4], Wolfhard Binder[5], Christina Schraml[4], Ferdinand Seith[4], Nina Schwenzer[4], Klaus Scheffler[2,6], Konstantin Nikolaou[4], and Fritz Schick[1]

[1]Section on Experimental Radiology, University of Tübingen, Tübingen, Germany, [2]Max Planck Institute for Biological Cybernetics, Tübingen, Germany, [3]Institute of Signal Processing and System Theory, University of Stuttgart, Stuttgart, Germany, [4]Department of Diagnostic and Interventional Radiology, University of Tübingen, Tübingen, Germany, [5]Department of Paediatric Cardiology, University of Tübingen, Tübingen, Germany, [6]Department of Biomedical Magnetic Resonance, University of Tübingen, Tübingen, Germany

Pseudo-continuous-arterial-spin-labeling (pCASL) has been successfully applied in the brain and kidney providing high signal-to-noise-ratio. The aim of this study was to optimize pCASL for measurement of lung perfusion by optimized labeling of pulmonary arteries and fast signal acquisition. Effective labeling of pulmonary arteries was possible by ECG triggering and an appropriate orientation of the labeling plane. Sufficient signal from lung parenchyma was acquired by True-FISP imaging with TE=1ms. The presented method provides high quality perfusion images of the lung without applying intravenous contrast agents and offers diagnostic imaging of lung diseases such as pulmonary embolism and bronchial carcinoma.

1890 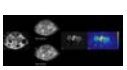

Quantification of mouse renal perfusion using arterial spin labeled MRI at 1 Tesla

Quyen N. Do[1], Ananth J. Madhuranthakam[1,2], Peter Bendel[3], and Robert E. Lenkinski[1,2]

[1]Radiology, University of Texas Southwestern Medical Center, Dallas, TX, United States, [2]Advanced Imaging Research Center, University of Texas Southwestern Medical Center, Dallas, TX, United States, [3]Aspect Imaging, Shoham, Israel

The current work demonstrates the use of a 1 Tesla desktop MR system to study mouse kidney perfusion through arterial spin labeling (ASL) technique. The validity of the implementation was tested by (1) comparing obtained perfusion results with literature values for normal mice and (2) challenging the technique with mice treated with a blood vessel vasoconstrictor drug. Potential applications include easy assessments of disease state, metabolism, and tissue perfusion using a compact MR system.

1891 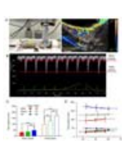

Validation of quantitative pre-clinical pseudo-continuous ASL in rat brain

Manon A. Simard[1], James R. Larkin[1], Alexandre A. Khrapitchev[1], James A. Meakin[2], Thomas W. Okell[2], Peter Jezzard[2], Michael A. Chappell[3], and Nicola R. Sibson[1]

[1]CRUK and MRC Oxford Institute for Radiation Oncology, Department of Oncology, University of Oxford, Oxford, United Kingdom, [2]FMRIB Centre, Nuffield Department of Clinical Neurosciences, University of Oxford, Oxford, United Kingdom, [3]Institute of Biomedical Engineering, Department of Engineering, University of Oxford, Oxford, United Kingdom

Guidelines for pre-clinical ASL are lacking. We propose MRI parameters for the use of pseudo-continuous ASL in rats. Carotid artery velocity was determined in three rat strains. Bloch simulations for ASL with this information and with parameters for pre-clinical scanners were used to determine the optimal width of the tagging plane required for blood inversion in this smaller species. The use of multiple post-label delays (PLD) in ASL-MRI generated blood arrival maps indicating that a PLD of 550ms was sufficient. Validation of CBF maps generated from ASL was performed using autoradiography, the current gold-standard technique for pre-clinical perfusion measurement.

1892

Combined 3D perfusion and diffusion MRI to phenotype the mouse brain: evaluation and application to a model of schizophrenia

Ivy Uszynski[1,2], Lydiane Hirschler[1,3], Jan M. Warnking[1,2], Cyril Poupon[4], Jean-Christophe Deloulme[1,2], and Emmanuel L. Barbier[1,2]

[1]Grenoble Institut des Neurosciences, Université Grenoble Alpes, Grenoble, France, [2]INSERM U1216, Grenoble, France, [3]Bruker Biospin, Ettlingen, Germany, [4]NeuroSpin, CEA Saclay, Gif-sur-Yvette, France

Perfusion and diffusion imaging both represent powerful tools in order to phenotype mouse models of brain diseases. Indeed, imaging cerebral blood flow (CBF) may be seen as a surrogate marker of brain metabolism while diffusion imaging provides the structural aspects of brain wiring. To evaluate the potential of combined CBF/Diffusion phenotyping, we evaluated the effect of knocking-out (KO) the microtubule-associated protein 6 (MAP6), which plays a critical role during the development of cerebral axonal tracts. Experiments were performed on homogeneous C57Bl6/129Sv mice using 3D pseudo-continuous Arterial Spin Labeling (pCASL) and 3D diffusion tensor imaging (DTI) at 9.4T.

1893

Multiphase pseudo-continuous ASL to image cerebral blood flow in mice at 9.4T

Jessica Buck[1], James Larkin[1], Alexandr Khrapichev[1], Manon Simard[1], Kevin Ray[1], Michael Chappell[2], and Nicola Sibson[1]

[1]Oxford Institute for Radiation Oncology, Department of Oncology, University of Oxford, Oxford, United Kingdom, [2]Institute of Biomedical Engineering, Department of Engineering Science, University of Oxford, Oxford, United Kingdom

Pseudo-continuous arterial spin labelling is regarded as the gold standard for clinical ASL, and can be improved in humans using multiphase sequences, but has not previously been implemented in mice. A multiphase pseudo-continuous ASL sequence to measure cerebral blood flow in mice was successfully implemented using respiratory triggering and optimisation of imaging readout, tag placement, labelling bolus duration, and post-label delay. Multiphase pseudo-continuous ASL is sensitive to changes in perfusion in an intracerebral glioma model.

1894

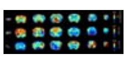

3-Dimensional cerebral blood flow and transit time mouse brain mapping using Dynamic Arterial Spin Labeling (DASL)

Lydiane Hirschler[1,2,3], Ivy Uszynski[1,2], Jan M Warnking[1,2], and Emmanuel L Barbier[1,2]

[1]Grenoble Institut des Neurosciences, Université Grenoble Alpes, Grenoble, France, [2]Inserm U1216, Grenoble, France, [3]Bruker Biospin, Ettlingen, Germany

Measuring the arterial transit time (ATT) helps for the optimization and quantification of arterial spin labeling experiments. Moreover, ATT may provide information on potential underlying vascular pathologies. In preclinical perfusion studies, multiple 2D-slices are commonly acquired to measure perfusion. However, this readout limits the number of slices for which ATT can be measured accurately in rodents. In this study, we implemented and optimized a dynamic ASL labeling scheme with a 3D echo planar imaging (EPI) readout to simultaneously map cerebral blood flow, arterial transit time and tissue T1 in the mouse brain at 9.4T.

1895

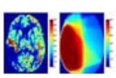

Perfusion decrease during radiochemotherapy is not fully explained by volumetric gray matter changes

Jan Petr[1], Henri JMM Mutsaerts[2,3], Frank Hofheinz[1], Iris Asllani[4], Matthias JP van Osch[5], Ivan Platzek[6], Annekatrin Seidlitz[7,8,9,10], Mechthild Krause[7,8,9,10,11], and Jörg van den Hoff[1,12]

[1]PET center, Institute of Radiopharmaceutical Cancer Research, Helmholtz-Zentrum Dresden-Rossendorf, Dresden, Germany, [2]Brain Sciences Research Program, Sunnybrook Research Institute, Toronto, Canada, [3]Department of Radiology, Academic Medical Center, Amsterdam, Netherlands, [4]Rochester Institute of Technology, Rochester, NY, United States, [5]Department of Radiology, Leiden University Medical Center, Leiden, Netherlands, [6]Department of Radiology, University Hospital Carl Gustav Carus, Technical University Dresden, Dresden, Germany, [7]Department of Radiation Oncology, Faculty of Medicine and University Hospital Carl Gustav Carus, Technical University Dresden, Dresden, Germany, [8]OncoRay – National Center for Radiation Research in Oncology, Faculty of Medicine and University Hospital Carl Gustav Carus, Dresden, Germany, [9]German Cancer Consortium (DKTK), Dresden, Germany, [10]German Cancer Research Center (DKFZ), Heidelberg, Germany, [11]Institute of Radiooncology, Helmholtz-Zentrum Dresden-Rossendorf, Dresden, Germany, [12]Department of Nuclear Medicine, University Hospital Carl Gustav Carus, Technical University Dresden, Dresden, Germany

Radiochemotherapy in brain-tumor patients was shown to cause gray matter (GM) volume and cerebral blood flow (CBF) changes. The interaction of these two effects, however, remains unclear. Here, we investigated GM volume and ASL CBF changes and their interaction in the healthy hemisphere of 38 glioblastoma patients undergoing radiochemotherapy with Temozolomide. We found a statistically significant CBF decrease with dependence on the RT-dose. PV-corrected results indicated that, while to a certain extent the apparent CBF decrease measured by ASL is caused by GM atrophy, there still remain significant CBF changes that cannot be explained by structural changes alone.

1896

Feasibility and value of VTE-ASL in quantitative evaluation of unilateral renal embolism in rabbits

Hanjing Kong[1], Fei Gao[2], Chengyan Wang[1], Yan Jia[3], Hui Xu[3], Xiaodong Zhang[4], Li Yang[3], Jue Zhang[1,2], Xiaoying Wang[1,4], and Jing Fang[1,2]

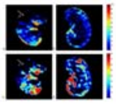

[1]Academy for Advanced Interdisciplinary Studies, Peking University, Beijing, People's Republic of China, [2]College of Engineering, Peking University, Beijing, People's Republic of China, [3]Renal Division, Peking University First Hospital, Beijing, People's Republic of China, [4]Department of Radiology, Peking University First Hospital, Beijing, People's Republic of China

Arterial spin labeling with variable echo time (VTE-ASL) is a perfusion imaging technique capable of noninvasive estimating of GFR. But the application of VTE-ASL in renal disease is still lagging behind. The goal of this study was to investigate the feasibility of GFR and RBF using VTE-ASL in evaluation of unilateral renal embolism in rabbits. Compared with normal kidney, embolism area has large decrease in GFR and RBF, and was confirmed by histological findings.

1897 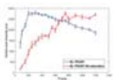

Spatially localised measurements of oxygen extraction fraction using modified T2-relaxation-under-spin-tagging (SL-TRUST)

Caitlin O'Brien[1], Thomas Okell[1], and Peter Jezzard[1]

[1]FMRIB, Nuffield Department of Clinical Neurosciences, University of Oxford, Oxford, United Kingdom

An existing MR sequence, TRUST (T2-relaxation-under-spin-tagging), is adapted in order to obtain spatially localised T2 measurements for venous blood. T2-encoding, and hence determination of venous oxygenation, is achieved via localised encoding of the longitudinal magnetisation, that is then decoded in the sagittal sinus. Saturation pulses enable spatial localisation by removing signal from unwanted brain regions. Thus, hemispheric and global T2 measurements are acquired and compared. The delay between labelling and arrival of tagged venous blood in the sagittal sinus is evaluated and shown to increase in the presence of saturation pulses.

1898 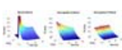

Can We Trust TRUST Venous Oximetry in Sickle Cell Disease?

Adam Michael Bush[1], Thomas Coates[2], Herbert Meiselman[3], and John Wood[4]

[1]Biomedical Engineering/ Cardiology, University of Southern California/ Children's Hospital Los Angeles, Los Angeles, CA, United States, [2]Hematology, Children's Hospital Los Angeles, Los Angeles, CA, United States, [3]Physiology and Biophysics, University of Southern California, Los Angeles, CA, United States, [4]Cardiology, University of Southern California/ Children's Hospital Los Angeles, Los Angeles, CA, United States

In this work we derive a de novo T_{2b} oximetry calibration curve for hemaglobin S containing red blood cells. We then compare predictions made by this calibration and existing T_{2b} calibrations in 84 subjects in vivo using TRUST MRI. We found that predictions for venous oxygenation saturation and cerebral metabolic rate are widely different depending on the T_{2b} calibration used for oximetry conversion.

Traditional Poster

DSC & DCE

Exhibition Hall 1899-1923 Tuesday 16:15 - 18:15

1899 

Optimization of Echo Times for CBV Measurements in the Arterial Input Function, Brain, and High-Grade Tumor Tissue using Error Analysis for DSC-MRI

Laura C. Bell[1], Mark D. Does[2], Ashley M. Stokes[1], Leslie C. Baxter[1], Kathleen M. Schmainda[3], and C. Chad Quarles[1]

[1]Barrow Neurological Institute, Phoenix, AZ, United States, [2]Vanderbilt University Institute of Imaging Science, Nashville, TN, United States, [3]Medical College of Wisconsin, Milwaukee, WI, United States

This abstract demonstrates that the optimal TE for a single-echo DSC-MRI acquisition is 30-35 ms (without a preload) and 23-30 ms (with a standard full-dose preload) for a high-grade glioma population. Optimal TEs were calculated using error analysis on T2* values quantified during the first-pass of contrast agent using dual-echo DSC, and were shown to be the weighted-average of these values. Furthermore, we demonstrate that the optimal TE depends on tissue type (tumor/healthy tissue/AIF) and preload.

1900 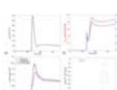

Improving Simultaneous T1 and T2* Measurements for Dynamic Susceptibility Contrast MRI using a 3D Distributed Spirals Sequence

Laura C. Bell[1], Dallas C. Turley[2], Natenael B. Semmineh[1], James G. Pipe[2], and C. Chad Quarles[1]

[1]Translational Bioimaging Group, Barrow Neurological Institute, Phoenix, AZ, United States, [2]MR Technology Design Group, Barrow Neurological Institute, Phoenix, AZ, United States

Multi-echo (ME) DSC-MRI enables the simultaneous assessment of contrast-agent induced T_1 and T_2* changes, but its sensitivity to and the quantification of these T_1 changes could be confounded by long TR and TE. Using simulations, we demonstrate that conventional 2D ME scans underestimate contrast agent concentration and DCE-MRI kinetic parameters. To solve this problem, we propose a 3D ME spiral acquisition that enables lower TRs and minimal TEs for improved T_1 quantification and a range of echo times to main T_2* sensitivity.

1901 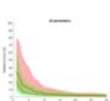

Joint DCE- and DSC-MRI processing using the Gradient correction model

Ondřej Macíček[1], Radovan Jiřík[1], and Zenon Starčuk jr.[1]

[1]Magnetic Resonance and Cryogenics, Institute of Scientific Instruments of the CAS, v. v. i., Brno, Czech Republic

The contribution presents a method for simultaneous processing of the DCE- and DSC-MRI perfusion data acquired using a multi-echo sequence. It is an extension of the sequential application of the so-called gradient correction model. In the sequential approach, relaxivity parameters are estimated from the DSC signal based on perfusion parameters calculated from the DCE signal. Here the perfusion and relaxivity parameters are estimated using an iterative alternating optimization strategy. The impact on accuracy and precision is tested on synthetic data. The results show that the suggested approach can yield a remarkable improvement, especially for noisy data.

1902

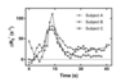

Correction of R2* Effects in Arterial Input Function of Fast Dynamic Contrast-Enhanced MRI for Accurate Cerebral Blood Flow Measurement

Benoit Bourassa-Moreau[1], Réjean Lebel[1], Guillaume Gilbert[2], and Martin Lepage[1]

[1]Département de médecine nucléaire et radiobiologie, Centre d'imagerie moléculaire de Sherbrooke, Sherbrooke, QC, Canada, [2]MR Clinical Science, Philips Healthcare Canada, Markham, ON, Canada

Signal loss resulting from R_2^* effects is usually neglected in fast dynamic contrast-enhanced perfusion imaging. A new flow-compensated 3D RF-spoiled dual gradient echo sequence was designed to quantify the R_2^* variation during a bolus injection of contrast agent and its effect on cerebral blood flow measurement. Moderate R_2^* effects are found to be amplified by the non-linear relationship between signal ratio and concentration. This is shown to lead to substantial changes in peak arterial input function and measured cerebral blood flow.

1903

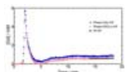

Improved Arterial Input Function Measurements Using Phase-versus-Time and Modified Look-Locker Inversion Recovery: Phantom Validation Study

Nicholas Majtenyi[1], Gregory O. Cron[2,3,4], Hanif Gabrani-Juma[5], Andreas Greiser[6], Robert A. deKemp[7], Ran Klein[5], Thanh B. Nguyen[8], and Ian G. Cameron[1,2,4]

[1]Carleton University, Ottawa, ON, Canada, [2]Medical Imaging, The Ottawa Hospital, [3]The Ottawa Hospital Research Institute, [4]Radiology, The University of Ottawa, [5]Division of Nuclear Medicine, The Ottawa Hospital, [6]Siemens Healthcare, Erlangen, Germany, [7]Cardiac PET Centre, University of Ottawa Heart Institute, [8]Radiology, The Ottawa Hospital

Dynamic contrast-enhanced (DCE)-MRI is used to quantify organ perfusion abnormalities in many diseases, but is prone to errors. This study investigated the accuracy of a new method for measuring the arterial input function (AIF) in a flowing-water phantom using phase-versus-time measurements with pre- and post-DCE Modified Look-Locker Inversion Recovery (MOLLI) T_1 measurements (Phase+MOLLI). The Phase+MOLLI technique provides an important improvement over previous methods since it avoids signal saturation and gives correct [Gd] values for the washout of the AIF. The Phase+MOLLI method was validated to be accurate, reproducible, and flow-insensitive so that it may be used for clinical DCE-MRI.

1904

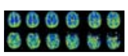

Dynamic Susceptibility Contrast MRI at 7T: Tail Scaling Analysis and Inferences About Field Strength Dependence

Linda Knutsson[1,2], Xiang Xu[3,4], Freddy Ståhlberg[1,5], Peter B. Barker[3], Pia Sundgren[5], Peter C.M. van Zijl[3,4], and Ronnie Wirestam[1]

[1]Department of Medical Radiation Physics, Lund University, Lund, Sweden, [2]Department of Radiology (Adjunct), Johns Hopkins School of Medicine, Baltimore, MD, United States, [3]Russell H. Morgan Department of Radiology and Radiological Sciences, Johns Hopkins University School of Medicine, Baltimore, MD, United States, [4]F.M. Kirby Research Center for Functional Brain Imaging, Kennedy Krieger Institute, Baltimore, MD, United States, [5]Department of Diagnostic Radiology, Lund University, Lund, Sweden

In this study, a dynamic susceptibility contrast MRI (DSC-MRI) protocol for cerebral perfusion imaging at 7T was designed. With reduced contrast agent dose, the obtained perfusion maps showed the same visual appearance as seen at lower field strengths. In addition, a correction method was applied to obtain quantitative estimates of CBF and CBV in order to assess whether previous predictions of a field-strength dependence of the in vivo transverse relaxivity, leading to overestimated perfusion estimates, were supported. We concluded that assumptions of a field-strength dependence were plausible, based on observations of further elevated CBF and CBV estimates at 7T.

1905

Impact of Reference Time Curve Determination on the Correction of Contrast Agent Extravasation in Dynamic Susceptibility Contrast MRI

Mu-Lan Jen[1], Ping Hou[1], Jason M Johnson[2], Donald F Schomer[2], and Ho-Ling Liu[1]

[1]Department of Imaging Physics, The University of Texas M. D. Anderson Cancer Center, Houston, TX, United States, [2]Department of Diagnostic Radiology, The University of Texas M. D. Anderson Cancer Center, Houston, TX, United States

This study investigated the influence of reference time curve determination on DSC leakage correction. Our findings suggested that the reference time curve obtained with inclusion of leaky tissue could lead a significantly different in K_2, which supported that the probable error in lesion blood volume quantification with inaccurate automated segmentation process.

1906

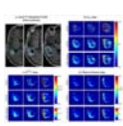

Robust reference-region DCE-MRI analysis with a vascular component and two-fit analysis

Zaki Ahmed[1] and Ives Levesque[1,2]

[1]Medical Physics Unit, McGill University, Montreal, QC, Canada, [2]Research Institute of the McGill University Health Centre, QC, Canada

The Extended Reference Region Model (ERRM) can quantify tumour perfusion without needing an arterial input function and includes a vascular term to account for the plasma volume. The addition of the vascular term also leads to larger variability in the estimated parameters. This study notes that one of the ERRM fitting parameters should be the same for all voxels. A two-fit approach is proposed that takes advantage of this constraint to reduce the number of fitting parameters from four to three. Evaluation in simulation and in-vivo found that the proposed two-fit approach resulted in a substantial decrease in variability for K^{Trans} and k_{ep} estimates.

1907

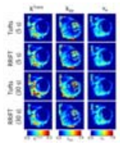

Quantitative DCE-MRI Analysis using a Reference Tissue and AIF Tail

Zaki Ahmed[1] and Ives Levesque[1,2]

[1]Medical Physics Unit, McGill University, Montreal, QC, Canada, [2]Research Institute of the McGill University Health Centre, QC, Canada

The reference region model can quantify tumour perfusion without needing an arterial input function (AIF) and provides relative estimates, i.e. $K^{Trans}/K^{Trans,RR}$ and $v_e/v_{e,RR}$ which are usually converted to absolute K^{Trans} and v_e by using literature-based values for $K^{Trans,RR}$ and $v_{e,RR}$. However, this approach fails to account for inter-patient variability. This study proposes a method that uses the Reference Region and AIF Tail (RRIFT) to estimate patient-specific $K^{Trans,RR}$ and $v_{e,RR}$. The AIF tail is the post-peak part of the AIF and is easier to measure than the complete AIF. Evaluation in simulation and in-vivo showed that RRIFT provides comparable results to Tofts model, and even outperforms the Tofts model at slower temporal resolutions.

1908

Feasibility and value of View-shared Compressed Sensing combined fast DCE-MRI in quantitative evaluation of unilateral renal embolism in rabbits

Hanjing Kong[1], Bin Chen[2,3], Hao Li[1,4], Bihui Zhang[5], Haochen Wang[5], Xiaodong Zhang[6], Min Yang[5], Jue Zhang[1,2], Xiaoying Wang[1,6], and Jing Fang[1,2]

[1]Academy for Advanced Interdisciplinary Studies, Peking University, Beijing, People's Republic of China, [2]College of Engineering, Peking University, Beijing, People's Republic of China, [3]Department of technical research and development, Instrumentation Technology and Economy Institute, Beijing, People's Republic of China, [4]Department of Radiology, University of Cambridge, United Kingdom, [5]Interventional radiology and vascular surgery, Peking University First Hospital, Beijing, People's Republic of China, [6]Department of Radiology, Peking University First Hospital, Beijing, People's Republic of China

Dynamic-contrast enhanced MR imaging is widely employed as a clinical tool in kidney imaging and renal function measurements. Some novel works have been made in improve temporal resolution. In this work, we adopt a 3D Cartesian MRI with compresses sensing and variable view sharing sequence to explore its evaluation in renal embolism assessment. GFR was calculated and renal embolism was confirmed by histological results. Fast DCE-MRI is a promising method for renal embolism diagnose.

1909

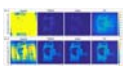

Comparison of (k,t) sampling schemes for DCE MRI pharmacokinetic parameter estimation

Yannick Bliesener[1], Sajan G. Lingala[1], Justin P. Haldar[1], and Krishna S. Nayak[1]

[1]Department of Electrical Engineering, University of Southern California, Los Angeles, CA, United States

We demonstrate an approach to evaluate and compare (k,t) sampling patterns for DCE-MRI. We compute Cramér-Rao lower bounds on the variance of pharmacokinetic (PK) parameter estimates, using pathologically- and anatomically-realistic digital reference objects. The framework allows for the optimization of sampling patterns independent of any specific estimator. We apply this framework to a 2D reference object for four sampling patterns: keyhole, TRICKS, lattice, and golden angle sampling. It is shown that TRICKS, lattice, and golden angle sampling enable low variance estimation for low undersampling factors. Out of these, lattice sampling keeps variances lowest with increasing undersampling factors.

1910

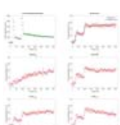

Influence of parameter initial values on DCE parameter estimates in pharmacokinetic modeling: a simulation study

Charlotte Debus[1,2,3,4], Ralf Floca[5], Amir Abdollahi[1,2,3,4], and Michael Ingrisch[6]

[1]German Cancer Consortium (DKTK), Heidelberg, Germany, [2]Translational Radiation Oncology, Heidelberg Institute of Radiation Oncology (HIRO), German Cancer Research Center (DKFZ), Heidelberg, Germany, [3]Department of Radiation Oncology, Heidelberg Ion-Beam Therapy Center (HIT), Heidelberg University Hospital, Heidelberg, Germany, [4]National Center for Tumor Diseases (NCT), Heidelberg, Germany, [5]Software development for Integrated Diagnostics and Therapy, German Cancer Research Center DKFZ, [6]Institute for Clinical Radiology, Ludwig-Maximilians-University Hospital Munich

In pharmacokinetic analysis of DCE-MRI data, the choice of initial parameter values for fitting has been reported to have a significant impact on the outcome of the optimization and hence, on parameter estimates. In this study, we investigated the influence of initial values by fitting simulated concentration time curves with varying combinations of initial parameters, using the two compartment exchange model. The resulting parameter estimates were visualized and compared to the true values, used for simulation, by means of relative errors. Results showed that the choice of initial values has little influence on the precision of the pharmacokinetic analysis.

1911

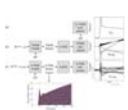

Nested tracer-kinetic model-based DCE-MRI reconstruction from under-sampled data

Sajan Goud Lingala[1], Yi Guo[1], Naren Nallapareddy[2], Yannick Bliesener[1], R Marc Lebel[3], and Krishna S Nayak[1]

[1]Electrical Engineering, University of Southern California, Los Angeles, CA, United States, [2]Biomedical Engineering, Case Western Reserve University, Cleveland, OH, United States, [3]GE Healthcare, Calgary, Canada

We propose a novel nested tracer-kinetic (TK) model based constrained reconstruction method for DCE-MRI reconstruction from under-sampled data. This approach models the concentration time profiles as a sparse linear combination of temporal bases constructed from TK models of varying complexity. Subspaces from the models of plasma volume, Patlak, and the extended-Tofts are constructed. A spatial mask determining the TK model complexity at every pixel location is derived. Reconstruction involves iteration between data consistency and pixel wise projection of the concentration profiles on one of the three subspaces. We demonstrate its utility in retrospective under-sampled reconstruction of brain tumor DCE-MRI datasets.

1912

Measurement of Murine Single-Kidney Glomerular Filtration Rate using Dynamic Contrast Enhanced MRI

Kai Jiang[1], Hui Tang[1], Prassana K. Mishra[2], Slobodan I. Macura[2], and Lilach O. Lerman[1]

[1]Division of Nephrology and Hypertension, Mayo Clinic, Rochester, MN, United States, [2]Division of Biochemistry and Molecular Biology, Mayo Clinic, Rochester, MN, United States

A method for noninvasive assessment of mouse glomerular filtration rate (GFR) using dynamic contrast enhanced MRI (DCE-MRI) was developed and validated. The kinetics of gadolinium in the abdominal aorta and two kidneys were measured using a snapshot fast low angle shot based T_1 mapping method with a temporal resolution of 1 s. A modified bi-compartmental model was used for quantification of GFR by a least-squares fitting. As a reference standard, GFR was also measured using FITC-inulin clearance. Single-kidney GFR measured from both methods showed a good agreement, suggesting the proposed DCE-MRI method provides an accurate measurement of murine single-kidney GFR.

1913

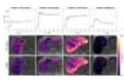

Patlak analysis of dynamic gadoxetic acid-enhanced MR imaging is an effective and simpler alternative to compartmental pharmacokinetic modelling for assessing liver function

Matthew R Orton[1], Mihaela Rata[1], Dow-Mu Koh[1,2], Maria Bali[1,2], Robert Grimm[3], David J Collins[1], James A d'Arcy[1], and Martin O Leach[1]

[1]CRUK Cancer Imaging Centre, Division of Radiotherapy and Imaging, Institute of Cancer Research, Sutton, United Kingdom, [2]Depertent of Radiology, Royal Marsden NHS Foundation Trust, Sutton, United Kingdom, [3]Siemens Healthcare, Erlangen, Germany

Liver perfusion and function can be assessed using gadoxetic acid combined with DCE-MRI imaging and pharmacokinetic (PK) modelling. Whilst compartmental PK models give a good account of the contrast changes over the first five minutes of enhancement, the Patlak graphical approach is a simpler alternative that is more easily implemented. Patlak evaluation requires the specification of a delay time after which the initial transients in the uptake curves have decayed, so the purpose of this abstract is to present a preliminary evaluation of the sensitivity of liver uptake rate estimates to the Patlak delay time.

1914

Vastly accelerated linear least squares fitting with numerical optimization for dual delay compensated quantitative liver perfusion mapping

Ramin Jafari[1], Yi Wang[1], Martin R. Prince[2], and Pascal Spincemaille[2]

[1]Cornell University, Ithaca, NY, United States, [2]Weill Cornell Medicine, New York, NY, United States

Accurate liver perfusion quantification requires correction for dual arterial and portal venous input delays, but such dual delay correction in current nonlinear perfusion methods is computationally too expensive to apply in perfusion mapping. We realize that the kinetic equation is a linear differential equation that would allow fast linear processing. Accordingly, we propose to use linear least squares (LLS) fitting to this kinetic equation with fast conjugate gradient search for processing dynamic contrast enhanced MRI data. Our proposed LLS vastly (~300 times) accelerate computation in perfusion quantification, enabling for the first time accurate liver perfusion mapping with dual delay corrections.

1915

Absolute Quantification of Brain Perfusion using Golden Angle Compressed Sensing DCE-MRI

Radovan Jiřík[1], Marie Daňková[2], Pavel Rajmic[2], Lucie Krátká[1], Lenka Dvořáková[1], Eva Dražanová[1], and Zenon Starčuk, jr.[1]

[1]Institute of Scientific Instruments of the CAS, Brno, Czech Republic, [2]Department of Telecommunications, Brno University of Technology, Brno, Czech Republic

A DCE-MRI method for absolute quantification of cerebral blood flow (CBF) and volume (CBV) and vessel permeability surface area product is presented. It is based on L+S compressed sensing, the two-compartment exchange model (2CXM) and blind deconvolution estimation of the arterial input function. The method is evaluated on data from a healthy rat.

1916

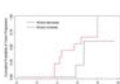

Parameters From Dynamic Contrast-Enhanced Magnetic Resonance Imaging Are Biomarkers Predicting Response after Radiation to Brain Metastases

Zhuo Shi[1], Lizhi Xie[2], Peng Wang[1], Xinming Zhao[1], and Han Ouyang[1]

[1]National Cancer Center/Cancer Hospital, Chinese Academy of Medical Sciences and Peking Union Medical College, Beijing, People's Republic of China, [2]GE HealthCare, MR Research China, Beijing, People's Republic of China

Dynamic contrast-enhanced (DCE) MRI provides additional information regarding blood-brain barrier integrity, and K^{trans} is directly proportional to the level of permeability of the blood-brain barrier. In our study, we found demonstrates that SRS of cerebral metastasis is associated with a reduction of K^{trans} values in the early post-treatment period. DCE-MRI derived parameters of K^{trans} may be a promising imaging biomarker of tumor aggressiveness.

1917

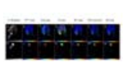

Quantification of tracer kinetic and hemodynamic parameters of human breast tumor and fibro-glandular tissue using DCE-MRI data

Snekha Sehrawat[1], Pradeep Kumar Gupta [2], Meenakshi Singhal[2], Rakesh Kumar Gupta[2], and Anup Singh[1,3]

[1]Centre for Biomedical Engineering, Indian Institute of Technology Delhi, Delhi, India, [2]Fortis Memorial Research Institute, Gurgaon, India, Delhi, India, [3]Department for Biomedical Engineering, AIIMS Delhi, New Delhi, India.

Objective of current study was to develop a framework for computing tracer kinetic parameters using GTKM model and hemodynamic parameters using first pass analysis of human breast tissue for characterizing of breast lesion; and also differentiation of the histological grade II and III of breast cancer. A significant difference between benign, malignant and fibroglandular tissues; and also between grade II and III of breast cancer were observed.

1918

The Vanishing Shutter-Speed Limit

Ruiliang Bai[1], Charles S. Springer, Jr.[2], and Peter J. Basser[1]

[1]Section on Quantitative Imaging and Tissue Sciences, DIBGI, NICHD, National Institutes of Health, Bethesda, MD, United States, [2]Advanced Imaging Research Center, Oregon Health & Science University, Portland, OR, United States

Dynamic-contrast-enhanced MRI (DCE-MRI) has been widely used to characterize microvasculature permeability. Recently, it was shown to reveal metabolic activity using the shutter-speed pharmacokinetic paradigm (SSP), in which steady-state intra/extracellular water exchange kinetics was incorporated into DCE-MRI data analysis. Interesting insights into DCE-MRI signals come from modeling the extravascular tissue MR signal. The questions addressed here are, “When can extravascular ^1H_2O longitudinal magnetization recovery from inversion/saturation still be described by a single-exponential process, and when can the intra/extracellular water exchange kinetics be accurately determined?”

1919

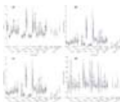

Whole Brain Dynamic Contrast-Enhanced MRI Study of Blood-Brain Barrier Disruption in Systemic Lupus Erythematosus Patients: Implications on the Choice of Tracer Kinetic Model

Dennis Lai-Hong Cheong[1], Mary C Stephenson[1], and Sen Hee Tay[2]

[1]Clinical Imaging Research Centre, Singapore, Singapore, [2]Division of Rheumatology, National University Hospital, Singapore

Current evidence suggests that blood-brain barrier (BBB) integrity is one of the potential biomarkers to diagnose neuropsychiatric systemic lupus erythematosus patients. We use DCE MRI and performed tracer kinetic analysis using both a distributed parameter (DP) model and the modified Tofts (MT) model. More Leaky BBB in SLE patients with anti-NR2 in their sera than the controls was detected by the permeability related parameters from both models. However, Ktrans of MT model, which is commonly used in DCE MRI of cancer studies, might be less reliable than DP model permeability parameters in this study.

1920

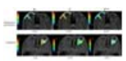

Feasibility and Value of Quantitative Dynamic Contrast Enhancement MR imaging in the Evaluation of Lymphoma and Inflammatory Pseudotumor in the Orbit

Liyuan Song[1], Lizhi Xie[2], and Junfang Xian[1]

[1]Department of Radiology, Beijing Tong Ren Hospital,Capital Medical University, Beijing, People's Republic of China, [2]GE Healthcare, MR Research China, Beijing, People's Republic of China

This work assessed the feasibility of quantitative parameters derived from dynamic contrast enhanced MR imaging (DCE-MRI) and evaluated the value of quantitative dynamic contrast enhanced MR imaging in the differential diagnosis between lymphoma and inflammatory pseudotumor in the orbit.

From the results we can see that it is feasible that quantitative parameters of DCE-MRI can be applied in the differential diagnosis between lymphoma and inflammatory pseudotumor in the orbit. Thus, it can probably be used as imaging biomarkers to predict prognosis and aggressiveness of orbital lymphoma.

1921

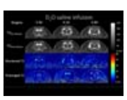

Assessment of hydrodynamics and T2 alterations in spontaneously hypertensive rat under short-term hyperhydration

Kun-I Chao[1], Cheng-He Li[1], Sheng-Min Huang[1], Pei-Lun Yu[1], Kung-Chu Ho[2], Shang-Yueh Tsai[3], Ping-Huei Tsai[4], and Fu-Nien Wang[1]

[1]Biomedical Engineering and Environmental Science, National Tsing Hua Unerversity, Hsinchu, Taiwan, [2]Nuclear Medicine, Chang Gung Memorial Hospital, Taoyuan, Taiwan, [3]Graduate Institute of Applied Physics, National Chengchi University, Taipei, Taiwan, [4]Department of Radiology, Taipei Medical University Hospital, Taipei, Taiwan

With a fluid infusion of 2% of body weight in the D_2O perfusion imaging experiment, the tissues are expected in a hyperhydration state. In this study, we conduct both D_2O and H_2O infusion experiments on spontaneously hypertension rat (SHR). Fast and slow flow of brain were analyzed by a two-compartmental parallel model. Pre- and post-infusion T2 maps were acquired. The slow flow matched the T2 prolonged regions, which could be due to the CSF production and flow.

1922

Feasibility study of a Dialyzer as a multi-compartment Perfusion Phantom for microvascular tracer kinetic Modelling

Tanja Gaa[1], Lothar R. Schad[1], and Frank G. Zöllner[1]

[1]Computer Assisted Clinical Medicine, Medical Faculty Mannheim, Heidelberg University, Mannheim, Germany

Dynamic contrast enhanced MRI combined with tracer kinetic modelling allows for the determination of quantitative perfusion parameters. To achieve standardized examinations and data analysis, phantoms are employed to investigate the reproducibility of perfusion parameters by imitating tissue on capillary level. In this study we used a dialysis filter with a semipermeable membrane of the fibers which enables the simulation of two compartment kinetics and can thus serve as imitation of capillaries and interstitium which might be closer to the anatomical conditions.

1923

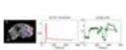

Feasibility of using Active Contrast Encoding (ACE)-MRI for Assessment of Tumor Treatment Response

Jin Zhang[1], Willis Chen[1], Kerryanne Winters[1], and Sungheon Gene Kim[1]

[1]Center for Advanced Imaging Innovation and Research (CAI2R), Dept. Radiology, NYU School of Medicine, New York, NY, United States

Active Contrast Encoding MRI (ACE-MRI) is a recently proposed method to conduct DCE-MRI experiment without the need to perform separate T_1 and B_1 measurement. The purpose of this study is to further investigate the feasibility of using the ACE-MRI method for evaluation of tumor treatment response in a mouse model of breast cancer. The results of the ACE-MRI method were compared with conventional DCE-MRI data analysis with separately measured T_1 maps. Our preliminary results demonstrate that the ACE-MRI method can be used to evaluate tumor treatment response reliably.

Traditional Poster

Relaxation: Mechanisms & Applications

Exhibition Hall 1924-1943 Tuesday 16:15 - 18:15

1924 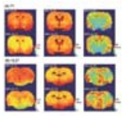

Accurate Tissue Oxygen Level-dependent MRI with true T1-weighted signal

SoHyun Han[1], HyungJoon Cho[2], and Seong-Gi Kim[1,3]

[1]*Center for Neuroscience Imaging Research, Institute for Basic Science (IBS), Suwon, Korea, Republic of,* [2]*Department of Biomedical Engineering, Ulsan National Institute of Science and Technology, Ulsan, Korea, Republic of,* [3]*Department of Biomedical Engineering, Sungkyunkwan University, Suwon, Korea, Republic of*

Tissue oxygen level dependent (TOLD) MRI utilizes that T_1 is directly related with tissue pO_2. TOLD MRI is acquired by gradient echo based with a minimized TE. However, T_2^* contribution may not fully be suppressed. Here, we investigated the modulations of longitudinal and transverse relaxation times with oxygen challenge (OC) and compared TOLD signals from FLASH, UTE, and TSE at 7 T and 15.2 T. At both magnetic fields, T_2 did not change with tissue pO_2 while T_1 did. Spin echo and UTE appear to reflect true pO_2 levels due to invariability in T_2 during OC and minimized T_2^* with ultrashort TE, respectively.

1925 

Direct Assessment of Magnetization Transfer Effects with T1 qMRI

Mitchell Horn[1], Ning Hua[1], Stephan Anderson[1], and Hernan Jara[1]

[1]*Boston University, Boston, MA, United States*

Purpose: To measure inaccuracies on T1 qMRI caused by magnetization transfer effects that are inherent to MRI pulse sequences. Methods: The mixed-TSE pulse sequence was used at several RF power levels to image a series of agarose gels, sucrose solutions, and Gd solutions. Results: Measured T1s are increasingly underestimated as a function of increasing semisolid pool size and RF power level. Conclusion: Uncorrected magnetization transfer effects can cause large underestimation of T1 measurements in tissue imaged with RF intensive pulse sequences. This work could have implications for the design of more accurate qT1 mapping algorithms.

1926 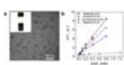

MR Contrast Effects of Intrinsically Gd-chelated Melanin Nanoparticles at 1.5 and 11.7 Tesla

Soojeong Cho[1], Weiguo Li[1], Andrew C Larson[1], and Dong-Hyun Kim[1]

[1]*Radiology, Northwestern University, Chicago, IL, United States*

The development of polymeric contrast agents exhibiting a high MR relaxivity has been achieved using bio-inspired metal chelating melanin nanoparticle (Mel NP) synthesized with dopamine or L-3,4-dihydroxyphenylalanine (L-DOPA). In here, we described our simple one-pot synthesis to prepare new Gd chelated Mel NP and their specific features of efficient MR T1 imaging along with their high intrinsic Gd chelation efficiency.

1927 

Effect of vendor specific formalin composition and concentration on post-mortem MRI of human brain tissue

Christoph Birkl[1], Martin Soellradl[1], Anna Maria Toeglhofer[2], Johannes Haybaeck[2,3], Lukas Pirpamer[1], Franz Fazekas[1], Stefan Ropele[1], and Christian Langkammer[1]

[1]*Department of Neurology, Medical University of Graz, Graz, Austria,* [2]*Department of Neuropathology, Institute of Pathology, Medical University of Graz, Graz, Austria,* [3]*Department of Pathology, Medical Faculty, Otto-von-Guericke-University, Magdeburg, Germany*

Formalin fixation is common procedure to prevent tissue autolysis by crosslinking proteins. Not unexpectedly this affects the relaxation properties of the tissue. In addition, quantitative relaxation time constants of formalin fixed brain tissue show a broad variation across different studies. To investigate the contribution of the formulation of formalin to this variability we investigated MR relaxation times of pure formalin solutions from different vendors and the effect of formalin concentration on MR relaxation times of fixed brain tissue. Our results showed a strong variation of relaxation times depending on the concentration used and more importantly on the vendor specific composition of the formalin solutions.

1928 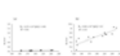

Relaxation time shortening by oxygen molecules: Strong enhancement in a viscous solution with cellular viscosity

Masayuki Taguchi[1] and Toru Yamamoto[2]

[1]*Graduate School of Health Sciences, Hokkaido University, sapporo, Japan,* [2]*Faculty of Health Sciences, Hokkaido University, sapporo, Japan*

Since oxygen molecules are paramagnetic, they shorten the relaxation time as well as gadolinium contrast medium. The effect of relaxation time shortening by the paramagnetic substance is enhanced with an increase in viscosity of the solution as in the cell. We investigated the longitudinal and transverse relaxivities of oxygen in viscous solution with cellular viscosity and clarified that the relaxation time shortening by oxygen molecules strongly increases with an increase in viscosity. This effect of oxygen in the cell may be visible by using pulse sequences that enhance the signal from the cellular proton.

1929 

Characterization of the Four Pool Model in formalin-fixed sheep's brain using NMR spectroscopy

Alan P. Manning[1], Alex L. MacKay[1,2], and Carl A. Michal[1]

[1]Physics and Astronomy, University of British Columbia, Vancouver, BC, Canada, [2]Radiology, University of British Columbia, Vancouver, BC, Canada

Despite its importance, T_1 relaxation in brain and spinal cord is not well understood. The Four Pool Model gives a fundamental framework for its understanding in white and grey matter tissue. In this work, we characterize the Four Pool Model for the first time in formalin-fixed sheep's brain using NMR spectroscopy. We find this is a suitable system, and our results are consistent with previous studies: T_1 is multi-exponential and the values measured result from a convolution of pure relaxation and exchange processes.

1930 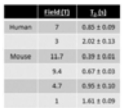

	Field (T)	T_2 (s)
Human	7	0.85 ± 0.09
	3	2.02 ± 0.13
Mouse	11.7	0.39 ± 0.01
	9.4	0.67 ± 0.03
	4.7	0.95 ± 0.10
	1	1.61 ± 0.09

Transverse relaxation of cerebrospinal fluid depends on glucose concentration

Alexia Daoust[1], Steven Dodd[1], Govind Nair[1], Nadia Bouraoud[1], Stephen Jacobson[1], Stuart Walbridge[1], Daniel S Reich[1], and Alan Koretsky[1]

[1]National Institute of Neurological Disorders and Stroke, National Institutes of Health, Bethesda, MD, United States

Brain relaxometric properties are widely used by the NMR community. While brain tissue relaxivities are well established, much less work has been done on CSF relaxivities. To clarify this point, we characterized the CSF relaxometric properties at various field strengths *in vivo* and *in vitro*. Our results suggest that low field is more optimal to quantify CSF T_2 due to smaller residual gradients. There is a significant difference between *in vitro* CSF T_2 vs saline T_2 that is mostly explained by the glucose relaxivity. This finding was confirmed *in vivo*, opening the possibility of studying glucose regulation of CSF at the resolution of MRI.

1931 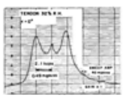

Origin of Dipolar Effects - Achilles Tendon at 3T and 11.7T.

Nikolaus M. Szeverenyi[1], Jiang Du[1], and Graeme M. Bydder[1]

[1]Radiology, Univ. of California, San Diego, San Diego, CA, United States

We examined the MR image appearance of human Achilles tendon as a function of orientation to the B0 field at 3 T and 11.7 T. Images were registered and displayed a remarkable similarity in the fine discernable structural features at both field strengths. Residual dipolar effects are responsible for the contrast on these images, rather than frequency changes that scale with magnetic field.

1932 

Effect of T1 on Multi-echo Gradient Echo based Myelin Water Fraction

Hongpyo Lee[1], Yoonho Nam[2], Dong-Hyun Kim[1], and Hongpyo Lee[1]

[1]Yonsei University, Seoul, Korea, Republic of, [2]Seoul St. Mary's Hospital, College of Medicine, The Catholic University of Korea, Seoul, Korea, Republic of

Myelin Water Fraction uses the property that myelin water has shorter T2* relaxation time compared to axonal/extra-cellular water. Previous studies found that not only the T2/T2* relaxation time but also the T1 relaxation time is difference between these compartments. The T1 relaxation time of myelin water is known to be affected by the cross-relaxation therefore the term “apparent T1” is considered more accurate. In this study, we analyze the effect of this ‘apparent’ T1 in mGRE based MWF. Our results show that the MWF estimation is dependent on the differential T1 of different compartments. T1 effect on the MWF can makes overestimation error. Using the low flip angle could reduce the this error, but it gives rise to insufficient SNR on MWF. Also, increasing TR could be another choice for reducing estimated error, but it leads to inefficient scan time. Thus, GRE-MWF is needed to compensated T1 effect for accurate quantification.

1933 

Development and Systematic Analysis of 2D and 3D GRE Myelin Water Imaging

Hyeonggeol Shin[1], Se-Hong Oh[2], and Jongho Lee[1]

[1]Electrical and Computer Engineering, Seoul National University, Seoul, Korea, Republic of, [2]Biomedical Engineering, Hankuk University of Foreign Studies, Seoul, Korea, Republic of

In this study, we developed high quality GRE-MWI methods for 2D and 3D acquisitions and performed systematic analysis on TR and flip angle. The myelin water images showed that image quality was higher in 2D than in 3D. Over a range of TR (56 ms to 1630 ms), the myelin water fraction was uniform when Ernst angles (assume T1 of 800 ms) were used. The fractions were overestimated when larger flip angles were used.

1934 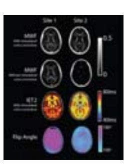

Making Myelin Water Imaging Mainstream: Multi-site and Multi-vendor Reproducibility

Emil Ljungberg[1], Julien Cohen-Adad[2], Lisa Eunyoung Lee[1], Alexander Rauscher[3], David Li[1,4], Anthony Traboulsee[1], Alex MacKay[4,5], Chase Figley[6], Jongho Lee[7], and Shannon Kolind[1,4]

[1]Medicine, Neurology, University of British Columbia, Vancouver, BC, Canada, [2]Electrical Engineering, Polytechnique Montréal, Montreal, QC, Canada, [3]Pediatrics, University of British Columbia, Vancouver, BC, Canada, [4]Radiology, University of British Columbia, Vancouver, BC, Canada, [5]Physics and Astronomy, University of British Columbia, Vancouver, BC, Canada, [6]Radiology, University of Manitoba, Winnipeg, MB, Canada, [7]Electrical and Computer Engineering, Seoul National University, Seoul, Korea, Republic of

Myelin water imaging (MWI) is a quantitative T_2 relaxation-based MRI technique, measuring the amount of myelin in the central nervous system. We investigated the reproducibility of MWI using GRASE with 3T MR scanners from two different vendors at two sites. Using stimulated echo correction, differences in the refocusing flip angle profile between the two sites were effectively corrected for and myelin estimates between the two sites were found to be highly correlated (slope=1.12, R^2=0.96). This is the first multi-vendor and multi-site reproducibility study of MWI using GRASE, encouraging future multicenter MWI studies.

1935

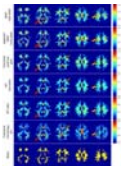

Spatial distribution of myelin concentration in healthy volunteers measured in GRE myelin water imaging, ViSTa myelin water imaging, quantitative MT and DTI

Dongmyung Shin[1], Sehong Oh[2], and Jongho Lee[1]

[1]Department of Electrical and Computer Engineering, Seoul National University, Seoul, Korea, Republic of, [2]Department of Biomedical Engineering, Hankuk University of Foreign Studies, Yongin, Korea, Republic of

This study investigated the spatial distribution of several myelin imaging methods. Myelin water fraction in GRE-MWI, apparent MWF in ViSTa-MWI, fractional pool size (F) in qMT, MT saturation, MT ratio, and FA in DTI were compared for their spatial distribution in white matter. Strong correlations were measured particularly between GRE-MWI and ViSTa-MWI and also among MT contrasts. FA showed least correlations with the other parameters.

1936

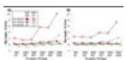

Measurement of T1, T2, and flip angle with double-angle inversion-recovery balanced steady state free precession with application to imaging the eye

Eric R. Muir[1] and Shengwen Deng[2,3]

[1]Research Imaging Institute and Ophthalmology, University of Texas Health Science Center, San Antonio, TX, United States, [2]Research Imaging Institute, University of Texas Health Science Center, San Antonio, TX, United States, [3]Biomedical Engineering, University of Texas at San Antonio, San Antonio, TX, United States

Fast measurement of T1 and T2 can be made with high signal to noise using inversion-recovery Look-Locker (LL) bSSFP. However, the LL-bSSFP signal is dependent on the flip angle, which must be known for accurate T_1 and T_2 calculation. In this study we investigated methods to additionally map and correct for the flip angle with the acquisition of two LL-bSSFP scans with two different flip angles, avoiding the need for a separate flip angle mapping protocol. Simulations and scans of the eye showed that T_1, T_2, and the flip angle could be measured with the double-angle LL-bSSFP method.

1937

Quantitative relaxation time mapping of axillary lymph nodes and recommended parameters for 3T lymphatic node substructure imaging

Rachelle Crescenzi[1], Paula M.C. Donahue[2,3], Vaughn G Braxton[1], Allison O Scott[1], and Manus J Donahue[1,4,5,6]

[1]Radiology and Radiological Sciences, Vanderbilt University Medical Center, Nashville, TN, United States, [2]Physical Medicine and Rehabilitation, Vanderbilt University Medical Center, Nashville, TN, United States, [3]Vanderbilt Dayani Center for Health and Wellness, Nashville, TN, United States, [4]Neurology, Vanderbilt University Medical Center, Nashville, TN, United States, [5]Psychiatry, Vanderbilt University Medical Center, Nashville, TN, United States, [6]Physics and Astronomy, Vanderbilt University, Nashville, TN, United States

A lack of MRI methods exist that are designed with sensitivity to the lymphatics, even though components of the lymphatic system have been discovered in every major organ system of the body and likely play an understudied role in disease. In this work we performed quantitative relaxation time mapping in axillary lymph node substructures, the cortex and hilum, for the first time at 3 Tesla and used these values to optimize structural imaging parameters for the lymphatics. Knowledge of fundamental MR parameters in the lymphatics is the first step to developing novel imaging sequences that exploit lymphatic tissue in vivo.

1938

Relaxation Times and Magnetic Susceptibility of Human Umbilical Cord Blood at 3 Tesla

Sharon Portnoy[1], Natasha Milligan[2], Mike Seed[3,4], John G. Sled[1,5], and Christopher K. Macgowan[1,6]

[1]Department of Medical Biophysics, University of Toronto, Toronto, ON, Canada, [2]Department of Obstetrics and Gynecology, Mount Sinai Hospital, Toronto, ON, Canada, [3]Department of Pediatrics and Diagnostic Imaging, University of Toronto, Toronto, ON, Canada, [4]Division of Cardiology, The Hospital for Sick Children, Toronto, ON, Canada, [5]Mouse Imaging Centre, The Hospital for Sick Children, Toronto, ON, Canada, [6]Department of Physiology and Experimental Medicine, The Hospital for Sick Children, Toronto, ON, Canada

With an increasing proportion of fetal cardiovascular MRI scans being performed at 3 Tesla, there is growing need for an accurate calibration, which characterizes relationships between MRI properties (T_1, T_2, susceptibility) and blood properties (oxygen-saturation, sO_2 and hematocrit, Hct) at 3T. Accordingly, relaxometry measurements were performed at 3T on cord blood specimens (N=89) with a broad range of hematocrits ($0.09<Hct<0.82$) and oxygen-saturations ($7\%<sO_2<100\%$). We also measured fetal blood susceptibility, which, to our knowledge, has never been reported. The data were effectively described by a simple, two-compartment model for blood.

1939

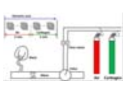

Hemodynamic response to respiratory challenge evaluated by dynamic R2’ imaging: application for acute renal ischemia caused by microsphere-induced renal artery embolism

Chengyan Wang[1], Bihui Zhang[2], Haochen Wang[2], Hanjing Kong[1], Fei Gao[3], Li Jiang[4], He Wang[5], Xiaodong Zhang[6], Min Yang[2], Jue Zhang[1,3], Xiaoying Wang[1,6], and Jing Fang[1,3]

[1]Academy for Advanced Interdisciplinary Studies, Peking University, Beijing, People's Republic of China, [2]interventional radiology and vascular surgery, Peking University First Hospital, Beijing, People's Republic of China, [3]College of Engineering, Peking University, Beijing, People's Republic of China, [4]Philips Healthcare, Suzhou, People's Republic of China, [5]Institute of Science and Technology for Brain-Inspired Intelligence, Fudan University, Shanghai, People's Republic of China, [6]Department of Radiology, Peking University First Hospital, Beijing, People's Republic of China

The clinical use of iodinated or gadolinium contrast agents for renal hemodynamic imaging is limited in the presence of renal dysfunction due to its increased risks of exacerbating renal damage. Therefore, we performed a modified HRI technique with a specific-designed magnetic-susceptible sequence that could separate R2’ from the BOLD signals in a unilateral microemboli-induced AKI model. The results show that R2’ in normal or less affected regions reduced after carbogen challenge, while the R2’ in the most affected lesions increased significantly. The dR2’ map could indicate the most affected areas accurately confirmed with the final anatomic T2w image.

1940 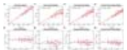

Determination of Oxygenation Extraction Fraction for People with Sickle Cell Anemia using Calibration Model Specific to SCA Blood

Wenbo Li[1,2], Xiang Xu[1,2], Peiying Liu[1], John Strouse[3,4], Hanzhang Lu[1], Peter van Zijl[1,2], and Qin Qin[1,2]

[1]Department of Radiology, Johns Hopkins University School of Medicine, Baltimore, MD, United States, [2]F.M. Kirby Research Center for Functional Brain Imaging, Kennedy Krieger Institute, Baltimore, MD, United States, [3]Division of Pediatric Hematology, Johns Hopkins University School of Medicine, Baltimore, MD, United States, [4]Division of Hematology, Duke University, Durham, NC, United States

For the blood T_2-based MRI oximetry methods, the calibration model to convert blood T_2 to blood oxygenation (Y) is critical to calculate the brain oxygen extraction fraction (OEF). Here, we established a calibration model specific to people with sickle cell anemia (SCA) using in vitro blood T_2 measurements on SCA blood samples under various conditions. The results show that the use of calibration models based on normal blood underestimate Y, and thus overestimate OEF, for individuals with SCA. Using a fast T_2 protocol to measure oxygenation in the internal jugular vein (IJV), the whole-brain OEF values of individuals with SCA were determined and compared with healthy volunteers.

1941 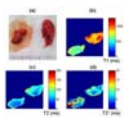

Cause of death or caused by death: Differentiation of thromboemboli and post-mortem clots using quantitative MRI

Bridgette Webb[1,2], Martin Urschler[1,2], Marlene Leoni[3], Bernhard Neumayer[1,2], Thomas Widek[1,2], Sylvia Scheicher[1,2], Rudolf Stollberger[2,4], and Thorsten Schwark[1,5]

[1]Ludwig Boltzmann Institute for Clinical Forensic Imaging, Graz, Austria, [2]BioTechMed, Graz, Austria, [3]Institute of Pathology, Medical University Graz, Graz, Austria, [4]Institute of Medical Engineering, Graz University of Technology, Graz, Austria, [5]Institute of Forensic Medicine, Medical University Graz, Graz, Austria

MRI is increasingly being used in post-mortem examinations to assist in determining cause of death. Post-mortem changes, such as the formation of post-mortem clots (PMC), present a specific challenge in forensic imaging where differentiation between these alterations and pathological findings (e.g. thromboemboli) is essential. This work imaged thromboemboli and PMC samples collected during autopsy at 3T. K-means clustering was applied to analyse voxel-grouping in the resulting quantitative data. Clusters specific to a single clot type were identified in 3 of the 4 samples. Preliminary findings indicated the existence of at least one common differentiating cluster specific to PMC.

1942 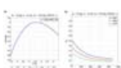

An optimised 2D MPRAGE sequence for T1 contrast in the fetal brain: application to slice to volume reconstruction and multiband acceleration

Giulio Ferrazzi[1], Anthony N. Price[1], Rui Pedro AG Teixeira[1], Francesco Padormo[2], Lucilio Cordero-Grande[1], Emer Hughes[1], Laura McCabe[1], Mary Rutherford[1], Maria Kuklisova Murgasova[1], and Joseph V. Hajnal[1]

[1]Division of Imaging Sciences & Biomedical Engineering, King's College London, London, United Kingdom, [2]Translational and Molecular Imaging Institute, Icahn School of Medicine at Mount Sinai, New York, United States

Ultrafast single-shot T_2 weighted images are common practise in fetal MR exams. However, there is limited experience with fetal T_1 acquisitions.

In this study, a 2D gradient echo sequence with an adiabatic inversion was optimized to be robust to fetal motion and to preserve contrast. We also explore slice to volume registration and super resolution reconstruction methods to enhance the resolution, and we show pilot data from a multiband accelerated version of the above-mentioned sequence.

1943 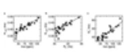

Combination of MT and R_2^* measurements to distinguish between contributions of semisolids and iron to R_1

Xu Jiang[1], Erika Raven[1,2], Peter van Gelderen[1], and Jeff H. Duyn[1]

[1]Advanced MRI Section, LFMI, NINDS, National Institutes of Health, Bethesda, MD, United States, [2]Center for Functional and Molecular Imaging, Georgetown University Medical Center, Washington, DC, United States

In human brain, the apparent longitudinal relaxation rate (R_1) primarily originates from magnetization transfer (MT) effects associated with the macromolecular ^{1}H-proton fraction (***f***), although in some regions the iron concentration may contribute as well (Rooney, 2007). To quantify their relative contributions at 7 T, we measured ***f*** and R_1 of water protons ($R_{1,WP}$) corrected for MT effects using a pulsed, transient MT approach (van Gelderen, 2016). The iron concentration was taken from literature and correlated with R_2^*. The results indicate that the combination of R_2^* and MT measurements may provide a sensitive means to quantify $R_{1,WP}$, ***f*** and iron concentration.

Traditional Poster

Electric Property Imaging & Susceptibility Imaging

Exhibition Hall 1944-1968 Tuesday 16:15 - 18:15

1944 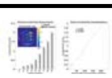

On the feasibility of synthetic sodium MRI based on tissue conductivity

Nazim Lechea[1], Yu Peng Liao[2], and N. Jon Shah[1,2]

[1]INM4, JARA-Faculty of Medicine, RWTH Aachen University, Aachen, Germany, Juelich, Germany, [2]Institute of Neuroscience and Medicine-4, Forschungszentrum Juelich, Juelich, Germany

The recently proposed magnetic resonance electrical property tomography opens new opportunities for sodium ion characterisation. In this study, a model was built by measuring electrical conductivity and sodium MRI in different saline solutions. We exploit this interdependence with additional temperature correction to build a synthetic sodium brain map based on in vivo electrical conductivity. The results were compared to sodium MRI measurements. A statistically significant Pearson correlation (p<0.001; r=0.43) was observed between the two modalities while Bland-Altman analysis revealed discrepancies between them with a mean difference ~4mMol/L in whole brain. The proposed approach facilitates tissue sodium extraction.

1945 

Advanced 3D simultaneous conductivity and susceptibility imaging with mitigation of nonlinear phase evolution effect.

Kang-Hyun Ryu[1], Jaewook Shin[1], Hongpyo Lee[1], and Dong-Hyun Kim[1]

[1]Electrical &Electronic Engineering, Yonsei University, Seoul, Korea, Republic of

Simultaneous Quantitative conductivity and susceptibility mapping (QCSM) can acquire both 3D conductivity and 3D susceptibility map with a single scan 3D multi-echo GRE sequence. However, error occurs due to nonlinear phase evolution in some regions producing false values especially for conductivity. In this study, we analyzed this effect and propose a way to mitigate this effect.

1946 

Evaluation of dual-echo EPI for in-vivo current mapping in individual subjects during transcranial Direct Current Stimulation

Mayank S Jog[1], Lirong Yan[2], Kay Jann[2], Lucas Parra[3], Marom Bikson[3], and Danny JJ Wang[2]

[1]Biomedical Engineering, University of California Los Angeles, Los Angeles, CA, United States, [2]University of Southern California, CA, United States, [3]Biomedical Engineering, City College of New York, NY, United States

Transcranial Direct Current Stimulation (tDCS) is a neuromodulation technique that uses milliampere currents to modulate cortical excitability. Although tDCS has been shown to treat clinical symptoms and improve cognition, the distribution of tDCS currents in the brain remains unknown. Here we show a MRI technique that measures a component of the magnetic field induced by tDCS currents in-vivo. Experimental data acquired using this technique is compared to model-based simulations. Our results demonstrate that mapping the tDCS current-induced magnetic fields in individual subjects is feasible; opening an avenue to map electric currents directly and track target engagement in individual subjects.

1947 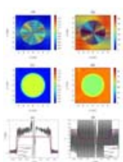

A stabilized convection-reaction magnetic resonance electrical property tomography (crMREPT) using viscosity-type regularization

Changyou Li[1], Wenwei Yu[2], and Shao Ying Huang[1,3]

[1]Singapore University of Technology and Design, Singapore, Singapore, [2]Center for Frontier Medical Engineering, Chiba University, Japan, [3]Department of Surgery, National University of Singapore, Singapore

Convection-reaction MREPT (crMREPT) method is a more general approach to reconstruct an electrical property map based on B_1-maps from a magnetic resonance imaging (MRI) scanner compared to other existing methods in the literature, such as electrical property tomography (EPT) and local Maxwell tomography (LMT). However, crMREPT shows global spurious oscillations in the reconstructed maps and persistent artifacts in the region when $$$\small\triangledown|B_1|$$$ is small. We propose a solution to effectively mitigate the artifacts by applying a viscosity-type regularization. This abstract shows that the proposed method significantly increases the accuracy of the reconstructed electrical property maps and reduces the sensitivity to noise comparing to crMREPT.

1948 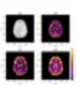

Three-Dimensional Model-Based Conductivity Mapping with Regularization and a Non-Negativity Constraint

Kathleen M Ropella[1] and Douglas C. Noll[1]

[1]Biomedical Engineering, University of Michigan, Ann Arbor, MI, United States

We present a three-dimensional model-based approach to calculating conductivity using MRI. Our proposed method is formulated as an inverse problem based on the phase-based conductivity equation. The algorithm includes an edge-preserving regularization term and we explore the utility of non-negativity constraints. Structural information is also used to inform regions over which to regularize. We present results for simulation, phantom, and human brain data.

1949 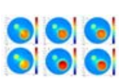

Use of Padding to Eliminate Low Convective Field Artifact in Conductivity Maps Obtained by cr-MREPT

Gulsah Yildiz[1], Gokhan Ariturk[1], and Yusuf Ziya Ider[1]

[1]Electrical and Electronics Engineering, Bilkent University, Ankara, Turkey

Convection-reaction equation based Magnetic Resonance Electrical Properties Tomography (cr-MREPT) has been developed by Hafalir et.al; however Low Convective Field causes artifacts. This study investigates how padding can be used in practice to eliminate the LCF artifact in conductivity reconstructions. Simulation and experimental results are given to demonstrate that conductivity images are improved by padding.

1950 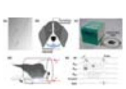

In Vivo Current Density Distribution of Brain during Electrical Stimulation

Nitish Katoch[1], Bup Kyung Choi[1], Saurav ZK Sajib[1], Jin Woong Kim[2], Hyung Joong Kim[1], Oh In Kwon[3], and Eung Je Woo[1]

[1]Kyung Hee University, Seoul, Korea, Republic of, [2]Radiology, Chonnam National University Medical School, Gwangju, Korea, Republic of, [3]Konkuk University, Seoul, Korea, Republic of

In deep brain stimulation, *in vivo* mapping of brain response is indispensable to secure its clinical applications. Estimation of current density distribution by stimulating currents can provide alternative way for understanding the therapeutic effects in electrical stimulation. MREIT method enables high-resolved mapping of electromagnetic tissue properties such as current density and conductivity of living tissues. In this study, we experimentally imaged current density distribution of *in vivo* canine brains by applying MREIT to electrical stimulation. The resulting current pathway and volume activation may provide useful information for adjusting the surgical planning and proving the therapeutic effects of DBS.

1951

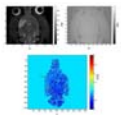

Conductivity Measurements at 21.1 T using MR Electrical Property Tomography

Ghoncheh Amouzandeh[1,2], Jens T. Rosenberg[1], and Samuel Colles Grant[1,3]

[1]Center for Interdiscplinary Magnetic Resonance, Florida State University, Tallahassee, FL, United States, [2]Physics, Florida State University, Tallahassee, FL, United States, [3]Chemical & Biomedical Engineering, Florida State University, Tallahassee, FL, United States

This study explores the opportunity of using ultra-high field (21.1 T) for producing electrical conductivity maps. Phantoms with known NaCl concentrations were used to compare conductivity maps generated by phase-based MREPT with actual values measured at 900 MHz with a dielectric probe. Phase-based MREPT also was evaluated for *in vivo* ischemic brain using an MCAO rat model. Increased conductivity values were noted in the stroked region of the rat brain.

1952

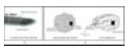

Current density imaging using novel carbon electrodes proposed for Deep Brain Stimulation (DBS)

Munish Chauhan[1], Neeta Ashok Kumar[1], Fanrui Fu[1], and Rosalind J Sadleir[1]

[1]School of Biological and Health Systems Engineering, Arizona State University, TEMPE, AZ, United States

Deep Brain Stimulation (DBS) is popular in the treatment of movement disorders. Conventional metal DBS electrodes present MR safety and susceptibility problems. We implemented novel carbon fiber electrodes that produced low susceptibility artifacts for imaging DBS current densities at 7 T. We used Magnetic Resonance Electrical Impedance Tomography (MREIT) to measure the z-component of the magnetic flux density (B_z) resulting from DBS-like pulses and reconstructed projected current density maps (J^P) in two objects (agarose-gelatin phantom and ex-vivo piglet brain). We did not observe susceptibility artifact, and reconstructed projected current density maps agreed with simulation in the electrode neighborhood.

1953

Quantitative Susceptibility Mapping of Paramagnetic and Diamagnetic Substances at 3T-MR, 1.5T-MR and CT.

Yasutaka Fushimi[1], Kyoko Takakura[1], Tomohisa Okada[2], Takuya Hinoda[1], Aki Kido[1], and Kaori Togashi[1]

[1]Department of Diagnostic Imaging and Nuclear Medicine, Kyoto University Graduate School of Medicine, Kyoto, Japan, [2]Human Brain Research Center, Kyoto University Graduate School of Medicine, Kyoto, Japan

We compared QSM value of paramagnetic and diamagnetic substances at 3T-MR, 1.5T-MR, and CT in this study. Phantoms with different concentration gadoterate meglumine (Gd) and calciumcarbonate ($CaCO_3$) were created. QSM at 3T and 1.5T and CT imaging were performed for these phantoms. QSM of Gd phantom showed positive susceptibility and QSM of $CaCO_3$ showed negative susceptibility. QSM demonstrated consistent results in paramagnetic and diamagnetic substances at 3T and 1.5T. QSM and CT values were correlated well.

1954

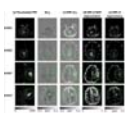

Susceptibility Mapping Reveals Inter-Hemispheric Differences in Venous Density in Patients with Brain Arteriovenous Malformations

Emma Biondetti[1], Alvaro Rojas Villabona[2], Anita Karsa[1], Rolf Jäger[2], David L Thomas[3], and Karin Shmueli[1]

[1]Medical Physics and Biomedical Engineering, University College London, London, United Kingdom, [2]Brain Repair and Rehabilitation, Institute of Neurology, University College London, London, United Kingdom, [3]Leonard Wolfson Experimental Neurology Centre, Institute of Neurology, University College London, London, United Kingdom

Brain arteriovenous malformations (AVMs) are vascular abnormalities characterised by arteriovenous shunting with the lack of a capillary bed. Recent studies have shown that it is possible to create diagrams of the cerebral vein network (venograms) from images of magnetic susceptibility ($$$\chi$$$). Here, we used $$$\chi$$$-based venograms to calculate the hemispheric percentage of venous voxels (venous density) in each hemisphere in AVM patients and healthy subjects. We found larger venous densities in the AVM-containing hemispheres than in the contralateral hemispheres, and more variable venous density in AVM patients than in healthy subjects.

1955

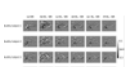

Evaluating The Accuracy of Susceptibility Maps Calculated from Single-Echo versus Multi-Echo Gradient-Echo Acquisitions

Emma Biondetti[1], Anita Karsa[1], David L Thomas[2], and Karin Shmueli[1]

[1]Medical Physics and Biomedical Engineering, University College London, London, United Kingdom, [2]Leonard Wolfson Experimental Neurology Centre, Institute of Neurology, University College London, London, United Kingdom

For Susceptibility Mapping (SM), Laplacian-based methods (LBMs) can be used on single- or multi-echo gradient echo phase data. Previous studies have shown the advantage of using multi-echo versus single-echo data for noise reduction in susceptibility-weighted images and simulated data. Here, using simulated and acquired images, we compared the performance of two SM pipelines that used multi- or single-echo phase data and LBMs. We showed that the pipeline that fits the multi-echo data over time first and then applies LBMs gives more accurate local fields and $$$\chi$$$ maps than the pipelines that apply LBMs to single-echo phase data.

1956

A Robust 3D Phase Unwrapping Method with Application to Quantitative Susceptibility Mapping

Junying Cheng[1,2], Biaoshui Liu[2], Yingjie Mei[2,3], Yihao Guo[2], Maodong Chen[2], Xiaoyun Liu[1], Wufan Chen[1,2], and Yanqiu Feng[2]

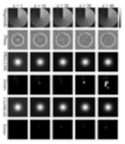

[1]School of Automation Engineering, University of Electronic Science and Technology of China, Chengdu, People's Republic of China, [2]Guangdong Provincial Key Laboratory of Medical Image Processing, School of Biomedical Engineering, Southern Medical University, Guangzhou, People's Republic of China, [3]Philips Healthcare, Guangzhou, People's Republic of China

In susceptibility-weighted imaging and quantitative susceptibility mapping, phase unwrapping methods are generally needed to restore the underlying true phase from the principal period (-π, π]. However, current phase unwrapping algorithms are challenged by noise, rapid phase changes and open-end cutlines. In this paper, a 2D phase unwrapping method based on pixel clustering and local surface fitting (CLOSE) was extended to 3D. The simulation and in vivo data is used to test the performance of the proposed method, with a comparison to a region growing method and PRELUDE, which are widely used for human brain phase-related imaging. The proposed method is demonstrated that can accurately unwrap 3D phase data even in the presence of severe noise, rapid phase changes, and open-end cutlines, and will benefit phase-related 3D MRI applications.

1957

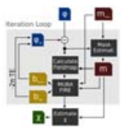

Iterative Background Phase Correction: Recovering Data for QSM

Johannes Lindemeyer[1] and N. Jon Shah[1,2]

[1]Institute of Neuroscience and Medicine - 4, Medical Imaging Physics, Forschungszentrum Jülich, Jülich, Germany, [2]Department of Neurology, Faculty of Medicine, JARA, RWTH Aachen University, Aachen, Germany

We present a technique to improve the preparation process of phase data for QSM. In order to compensate for data loss caused by strong local phase gradients near the surface of the brain support, harmonic and dipole-based fitting are used to determine the responsible background fields within an extended brain mask. In an iterative approach, phase data are corrected regarding such contributions prior to further QSM processing steps. This allows for the acquisition of more reliable field maps and larger evaluation masks, which finally leads to more robust susceptibility maps.

1958

Incorporating macroscale susceptibility in QSM reconstruction with 3D spiral acquisition.

Giang-Chau Ngo[1,2], Berkin Bilgic[3,4], Borjan Gagoski[4,5], and Bradley P. Sutton[1,2]

[1]Bioengineering, University of Illinois at Urbana-Champaign, Urbana, IL, United States, [2]Beckman Institute, University of Illinois at Urbana-Champaign, Urbana, IL, United States, [3]Martinos Center for Biomedical Imaging, Department of Radiology, Massachusetts General Hospital, Charlestown, MA, United States, [4]Harvard Medical School, Boston, MA, United States, [5]Boston Children's Hospital, Boston, MA, United States

Macroscale magnetic susceptibility creates large variations in the phase images preventing the direct analysis of local tissue-dependent phase in quantitative susceptibility mapping. Unwrapping and background field removal are important steps for calculating tissue phases and susceptibility maps. In this work, a 3D spiral acquisition is combined with an image reconstruction pipeline modelling the macroscale magnetic susceptibility to provide more accurate tissue phases and susceptibility maps, by reducing image distortions and facilitating unwrapping and background phase removal.

1959

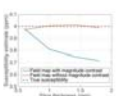

Effects of Spatial Resolution on Quantitative Susceptibility Mapping

Timothy J Colgan[1,2], Samir D Sharma[1], Diego Hernando[1,2], and Scott B Reeder[1,2,3,4,5]

[1]Radiology, University of Wisconsin, Madison, WI, United States, [2]Medical Physics, University of Wisconsin, Madison, WI, United States, [3]Biomedical Engineering, University of Wisconsin, Madison, WI, United States, [4]Medicine, University of Wisconsin, Madison, United States, [5]Emergency Medicine, University of Wisconsin, Madison, WI, United States

The purpose of this study was to investigate the effects of spatial resolution on the performance of quantitative susceptibility mapping (QSM). The combination of magnitude contrast in spoiled gradient echo images and the voxel sensitivity function can create significant errors in the estimated B_0 field map. This work evaluated the use of proton density weighted imaging and joint R_2* and field map estimation to reduce the impact of imaging resolution on QSM. Our results indicate that reducing magnitude contrast in the complex-valued echo images will reduce errors in the field map estimates and, thus, the susceptibility estimates in QSM.

1960

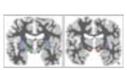

Evaluation of Quantitative Susceptibility Mapping for the visualization of the Globus Pallidus Internus and Subthalamic Nucleus at 3T and 7T

Fei Cong[1,2], Zhangyan Yang[1,2], Xiaohong Joe Zhou[3], Bo Wang[1], Yan Zhuo[1], and Lirong Yan[4]

[1]State Key Laboratory of Brain and Cognitive Science, Beijing MRI Center for Brain Research, Institute of Biophysics, Chinese Academy of Sciences, Beijing, People's Republic of China, [2]Graduate University, Chinese Academy of Sciences, Beijing, People's Republic of China, [3]Center for Magnetic Resonance Research, University of Illinois at Chicago, Chicago, IL, United States, [4]Stevens Neuroimaging and Informatics Institute, University of Southern California, Los Angeles, CA, United States

The globus pallidus internus (GPi) and subthalamic nucleus (STN) (Figure 1) were the commonly used nuclei in deep brain stimulation (DBS) for the treatment of the Parkinson disease. In this study, we evaluated the QSM, T2* weighted and SWI methods for the visualization the GPi and STN on both 3T and 7T scanners. Our results showed the QSM at 7T displayed an excellent delineation of the GPi and STN, compared with T2* and SWI images.

1961

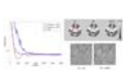

Primal-Dual Implementation for Quantitative Susceptibility Mapping (QSM)

Youngwook Kee[1], Kofi Deh[1], Alexey Dimov[1,2], Pascal Spincemaille[1], and Yi Wang[1,2]

[1]Weill Cornell Medical College, New York, NY, United States, [2]Cornell University, Ithaca, NY, United States

We investigate the computational aspects of the prior term in the field-to-susceptibility inversion problem for QSM. Providing a spatially continuous formulation of the problem, we analyze 1) its Euler-Lagrange equation that appears degeneracy and 2) the Gauss-Newton conjugate gradient (GNCG) algorithm that employs numerical conditioning. We propose a primal-dual (PD) formulation that avoids such degeneracy and use the Chambolle-Pock algorithm to solve this alternative formulation; thus numerical conditioning is not required. The two methods were tested and validated on numerical/gadolinium phantoms and *ex-vivo*/*in-vivo* MRI data. The PD formulation with the Chambolle-Pock algorithm was faster and more accurate than GNCG.

1962

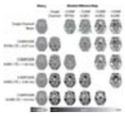

The challenge of phase offset correction for quantitative susceptibility mapping at ultra-high field

Steffen Bollmann[1], Simon Robinson[2], Kieran O'Brien[1,3], Viktor Vegh [1], Andrew Janke[1], Lars Marstaller[4], David Reutens[1], and Markus Barth[1]

[1]Centre for Advanced Imaging, University of Queensland, Brisbane, Australia, [2]High Field Magnetic Resonance Centre, Department of Biomedical Imaging and Image-Guided Therapy, Medical University of Vienna, Vienna, Austria, [3]Siemens Healthcare Pty Ltd, Brisbane, Australia, [4]Cardiff University, School of Psychology, Cardiff, United Kingdom

One challenge in quantitative susceptibility mapping (QSM) at ultra-high field (> 3 T) is the combination of phase data from phased array receive coils. We assessed the performance of COMPOSER (COMbining Phase data using a Short Echo-time Reference scan) with separate reference scans and with an intrinsic reference scan, as well as a reference-free single-channel method. Our results show that reference scans can bias QSM results at ultra-high field. We conclude that ultra-short echo-time reference scans reduce quantitation bias and remove the transmit field phase when using COMPOSER to combine phase data at ultra-high field.

1963

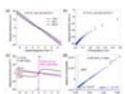

Accuracy of magnetic resonance based susceptibility measurements

Hannah E Erdevig[1,2], Stephen E Russek[1], Slavka Carnicka[1], Karl F Stupic[1], and Kathryn E Keenan[1]

[1]Precision Measurement Laboratory, NIST, Boulder, CO, United States, [2]Department of Physics, University of Colorado Boulder, Boulder, CO, United States

We examined the accuracy of MR-based susceptibility quantification relative to conventional measurements in preparation of making a standard susceptibility phantom. SQUID magnetometry of tissue mimics provides absolute accuracy of approximately 100 ppb while MR-based techniques give relative accuracy of 10 ppb.

1964

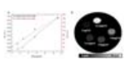

Quantification of Dendronized Superparamagnetic Iron Oxide Nanoparticles in Rat Liver Using Quantitative Susceptibility Mapping

Jeam Haroldo Oliveira Barbosa[1], Imen Miladi[2], Patrick Poulet[2], Kofi Mawuli Deh[3], Yi Wang[3], and Carlos Ernesto Garrido Salmon[1]

[1]InBrain Lab, Department of Physics, Faculty of Philosophy, Sciences and Letters of Ribeirão Preto, University of Sao Paulo, Ribeirão Preto, SP, Brazil, Brazil, [2]Laboratoire des sciences de l'ingénieur, de l'informatique et de l'imagerie (ICube), UMR 7357, Fédération de Médecine Translationnelle de Strasbourg, Université de Strasbourg/CNRS, Illkirch, France, [3]Department of Physiology, Biophysics and Systems Biology, Weill Cornell Medicine, Cornell University, New York, United States

Quantitative Susceptibility Mapping was environment independent to quantify iron of SPIONs compared with R2*.

1965

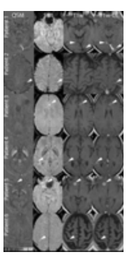

Assessment of melanin content and its influence on susceptibility contrast in melanoma metastases

Sina Straub[1], Frederik B. Laun[1,2], Martin T. Freitag[3], Christian Kölsche[4,5], Heinz-Peter Schlemmer[3], Mark E. Ladd[1], and Till Schneider[3,6]

[1]Department of Medical Physics in Radiology, German Cancer Research Center (DKFZ), Heidelberg, Germany, [2]Institute of Radiology, University Hospital Erlangen, Erlangen, Germany, [3]Department of Radiology, German Cancer Research Center (DKFZ), Heidelberg, Germany, [4]Department of Neuropathology, Institute of Pathology, University of Heidelberg, Heidelberg, Germany, [5]German Cancer Consortium (DKTK), CCU Neuropathology, German Cancer Research Center (DKFZ), Heidelberg, Germany, [6]Department of Neuroradiology, University of Heidelberg, Heidelberg, Germany

Melanoma metastases can be classified as melanotic or amelanotic based on their T1-weighted magnetic resonance signal. However, the underlying contrast mechanisms have remained unclear and have been attributed to melanin and/or blood products. In this study, non-hemorrhagic cerebral melanoma metastases were investigated using quantitative susceptibility mapping. Susceptibility values for metastases with no, small or high melanin content were very similar (−0.023±0.046 ppm / -0.006±0.02 ppm / -0.018±0.017 ppm). Non-hemorrhagic melanoma metastases show weakly diamagnetic susceptibility values and melanin is not a source of strong susceptibility.

1966

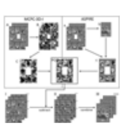

A Simple Phase Imaging REconstruction method (ASPIRE)

Korbinian Eckstein[1], Siegfried Trattnig[1], and Simon Daniel Robinson[1]

[1]High Field Magnetic Resonance Centre, Department of Biomedical Imaging and Image-Guided Therapy, Medical University of Vienna, Vienna, Austria

Combining phase data from multi-channel coils at high field is challenging. Many approaches involve optimization or iterative steps which require offline reconstruction. We present a simple method that avoids the need for unwrapping or other fragile or time consuming steps by using echo times that satisfy $T_{E,2}=2\,\cdot\,T_{E,1}$. ASPIRE is compared with the Roemer method, MCPC-3D-I and the Hermitian inner product. ASPIRE achieves similar phase matching quality to Roemer but has the advantage that the combined phase values correspond to the B0 field. It is less computationally demanding than MCPC-3D-I and has higher CNR than the Hermitian inner product.

1967

Enhancing Quantitative Susceptibility Mapping by Using Gradient L2 Regularization with Morphological Priors

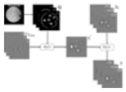

Yihao Guo[1], Li Guo[1], Yingjie Mei[1,2], and Yanqiu Feng[1]

[1]Guangdong Provincial Key Laboratory of Medical Image Processing,School of Biomedical Engineering,Southern Medical University, Guangzhou, People's Republic of China, [2]Philips Healthcare, Guangzhou, China.

TKD, LSQR and CSC methods have been proposed to reconstruct QSM from field map. However, these three methods result in inconsistent in the magic angle and can be further improved. This work introduces efficient gradient L2 regularization with morphological information from magnitude images for enhancing the QSM reconstructed by TKD, LSQR and CSC methods.

1968

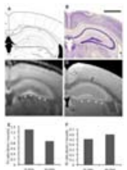

Functional and structural ex vivo “MRI staining” using manganese-enhanced MRI (MEMRI), Gd-DTPA and Mn-Gd mixture

Chika Sato[1], Kazuhiko Sawada[2], David Wright[3,4], Tatsuya Higashi[1], and Ichio Aoki[1]

[1]Molecular Imaging and Theranostics, National Institute of Radiological Sciences, QST, Chiba, Japan, [2]Department of Nutrition, Faculty of Medical and Health Sciences, Tsukuba International University, [3]Anatomy and Neuroscience, The University of Melbourne, [4]The Florey Institute of Neuroscience and Mental health

To reveal brain 3D microstructures noninvasively and microscopically using MRI, we developed “ex vivo MEMRI” and Mn-Gd double-contrast methods, and then compared them with conventional ex vivo Gd-DTPA-doped contrast. Because MEMRI sample loses contrast after perfusion fixation, we examined the stability of Mn^{2+} accumulation in ex vivo tissue samples. In addition, we tried to improve the contrast of MEMRI in combination with Gd-DTPA. The Mn-Gd double-contrast showed novel contrast and improved visibility. The functional “MRI staining” methods we developed in this study will be useful for visualizing whole brain 3D microstructures with a higher throughput compared to histological staining.

Traditional Poster

All Things CEST/MT

Exhibition Hall 1969-1989 Tuesday 16:15 - 18:15

1969

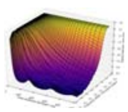

A singular value decomposition approach to quantitative magnetization transfer

Riccardo Metere[1], Samuel A. Hurley[2], André Pampel[1], Karla Loreen Miller[2], and Harald E. Möller[1]

[1]NMR Unit, Max Planck Institute for Human Cognitive and Brain Sciences, Leipzig, Germany, [2]FMRIB Centre, Nuffield Department of Clinical Neurosciences, University of Oxford, Oxford, United Kingdom

Quantitative magnetization transfer experiments require extensive sampling of the off-resonance spectrum to obtain information of the relaxation properties of non-water protons. To reduce the acquisition times, the off-resonance sampling has been optimized in previous works based on the stability of approximate biophysical model fits. Here, we use a singular value decomposition approach for the analysis of the principal components. In particular we propose a data-driven optimization method for the acquisition scheme and we discuss the potential impact of applying this analysis for parameter estimations, including potential extensions of the classical biophysical models.

1970

Highly Accelerated Chemical Exchange Saturation Transfer (CEST) Imaging by Combining Parallel Imaging and Compressed Sensing at 3T

Kyungmin Nam[1,2], Namgyun Lee[1,3], Ha-Kyu Jeong[1,4], Seth A. Smith[5,6,7], and Chulhyun Lee[1,2]

[1]Bio-Imaging Research Team, Korea Basic Science Institute, Cheongju, Korea, Republic of, [2]Bio-Analysis Science, University of Science and Technology, Daejeon, Korea, Republic of, [3]University of Southern California, Los Angeles, CA, United States, [4]Philips Healthcare Korea, Seoul, Korea, Republic of, [5]Biomedical Engineering, Vanderbilt University, Nashville, TN, United States, [6]Radiology and Radiological Sciences, Vanderbilt University, Nashville, United States, [7]Opthamology, Vanderbilt University, Nashville, TN, United States

Chemical Exchange Saturation Transfer (CEST) imaging is an emerging molecular MRI method. It has been difficult for CEST imaging to adopt into clinical routine since CEST imaging is required relatively long scan time due to multiple saturation offsets. Here, we propose a novel, highly accelerated 3D CEST reconstruction technique by combining parallel imaging and compressed sensing.

1971

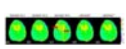

Fast, Reliable 3D Amide Proton Transfer Imaging of Brain Tumors at 3T with Variably-accelerated Sensitivity Encoding (vSENSE)

Yi Zhang[1], Hye-Young Heo[1], Shanshan Jiang[1], Paul A. Bottomley[1], and Jinyuan Zhou[1,2]

[1]Division of MR Research, Department of Radiology, Johns Hopkins University, Baltimore, MD, United States, [2]F. M. Kirby Research Center for Functional Brain Imaging, Kennedy Krieger Institute, Baltimore, MD, United States

The clinical use of amide proton transfer (APT) imaging is hindered by long scan times. Accuracy generally limits the use of conventional sensitivity encoding (SENSE) methods in APT, to an acceleration factor of 2. A novel variably-accelerated sensitivity encoding (vSENSE) method can provide more accurate results and therefore substantially higher overall acceleration factors than conventional SENSE. Here, vSENSE is further developed to eliminate the requirement that one fully-sampled APT frame be acquired, and extended to three dimensions (3D). Furthermore, we combine vSENSE with parallel transmit saturation, and apply it proactively to three normal volunteers and eleven patients with brain tumors.

1972

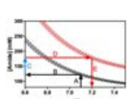

isoAPTR* - a novel method to measure tumour pHi using CEST MRI

Kevin J Ray[1], James R Larkin[1], Michael A Chappell[2], and Nicola R Sibson[1]

[1]Oxford Institute for Radiation Oncology, Department of Oncology, University of Oxford, Oxford, United Kingdom, [2]Institute of Biomedical Engineering, Department of Engineering Science, University of Oxford

Quantitative CEST MRI studies have so far been hindered by the fact that variations in multiple factors produce identical CEST effect changes. This remains the case when CEST MRI data are analysed using metrics that control for the contaminating effects of T_1 and T_2, such as APTR*. In this work we introduce isoAPTR*, a novel methodology which, in combination with independent measurement of labile proton concentration, can estimate the change in intracellular pH between two APTR* measurements. We demonstrate the utility of this method by applying it to measure the intracellular pH of U87 glioma in rats.

1973

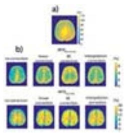

The comparison of different strategies for transmit field inhomogeneity correction of Amide-CEST and NOE effects at 7T

Vitaliy Khlebnikov[1], Johannes Windschuh[2], Jeroen CW Siero[1,3], Moritz Zaiss[4], Peter R Luijten[1], Dennis WJ Klomp[1], and Hans Hoogduin[1]

[1]Department of Radology, University Medical Center Utrecht, Utrecht, Netherlands, [2]Division of Medical Physics in Radiology, Deutsches Krebsforschungszentrum (DKFZ) [German Cancer Research Center], Heidelberg, Germany, [3]Spinoza Center for Neuroimaging, Amsterdam, Netherlands, [4]Scheffler, Max Planck Institute for Biological Cybernetics, Tübingen, Germany

We compared three methods for B1 correction of relaxation-compensated Amide-CEST and Nuclear Overhauser Enhancement (NOE) effects at 7T: (1) a linear model; (2) the eight-point interpolation method; and (3) Bloch-McConnell equations (BE) correction algorithm. In the low B1 regime of 0.10 - 0.50 µT, a simple linear model is sufficient to mitigate B1 inhomogeneity of Amide-CEST and NOE effects at 7T.

1974

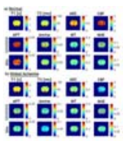

Quantification of Multi-pool Contribution to Endogeneous CEST Effects in Global Ischemia

Iris Yuwen Zhou[1], Jerry S Cheung[1], Enfeng Wang[1,2], Xiaoan Zhang[2], and Phillip Zhe Sun[1]

[1]Massachusetts General Hospital and Harvard Medical School, Charlestown, MA, United States, [2]Department of Radiology, 3rd Affiliated Hospital, Zhengzhou University, Henan, People's Republic of China

CEST MRI has been used for quantitative assessment of dilute metabolites and/or pH in ischemic tissue and in tumors. However, conventional asymmetry analysis (MTRasym) may be confounded by concomitant effects such as RF spillover, semisolid macromolecular MT and NOE effects. Therefore, decoupling multiple contributions is essential for elucidating the origins of in vivo CEST contrast for improved quantification. Here we used an Image Downsampling Expedited Adaptive Least-squares (IDEAL) fitting algorithm which is not strongly constrained by image SNR and initial values for fitting. It provides a closer estimation of MTRasym that calculated from acquired data than voxel-wise multi-pool Lorentzian fitting and unravels the major contributors to CEST contrasts between white and gray matters as well as to the CEST changes after global ischemia.

1975

Lorentzian Probabilistic Sum based Z-Spectrum fitting approach for computing CEST and NOE contrast and its Comparison with Lorentzian Sum and Asymmetry Analysis

Ayan Debnath[1] and Anup Singh[1,2]

[1]Centre for Bio-Medical Engineering, Indian Institute of Technology Delhi (IIT Delhi), New Delhi, India, [2]Department of Biomedical Engineering, All India Institute of Medical Sciences Delhi, India, New Delhi, India

In this study, we proposed a Z-spectrum fitting method based upon Lorentzian Probabilistic Sum (LPS) for computing CEST and NOE contrast. Proposed fitting method was tested on multi-pool Z-spectra data acquired using simulations and from *in-vivo* human brain data at 7T. Proposed fitting results were compared with asymmetry analysis and another fitting method based on Linear Sum (LS) of Lorentzian functions. Results of this study show that both LPS and LS nicely fit z-spectra; however, LPS provide more accurate estimation of NOE and CEST contrast. Therefore, proposed LPS model can be used for improved estimation of separate CEST and NOE components.

1976

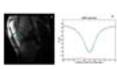

3D gagCEST of articular cartilage in the knee at 7 T correlates with clinical findings

Sander Brinkhof[1], Razmara Nizak[2], Vitaliy Khlebnikov[3], Dennis Klomp[3], Bennie ten Haken[4], Jeanine J Prompers[3], and Daniel Saris[2,5]

[1]University Medical Center Utrecht, Utrecht, Netherlands, [2]Orthopaedics, University Medical Center Utrecht, Utrecht, [3]Radiology, University Medical Center Utrecht, Utrecht, Netherlands, [4]Faculty of Science and Technology, University of Twente, Enschede, Netherlands, [5]MIRA Institute for Biomedical Technology and Technical Medicine, University of Twente, Enschede, Netherlands

The purpose of this study was to assess the sensitivity of 3D gagCEST at 7T in cartilage repair patients with respect to healthy volunteers. Six healthy volunteers were scanned for stability assessments and five patients with cartilage defects were included to assess clinical applicability of the gagCEST sequence. The mean GAG effect size in healthy controls is 10.2 %, which is three times higher than the coefficient of variation in the stability assessments. The results of this study demonstrate the stability of 3D gagCEST at 7T and the results from patients with cartilage defects indicate a correlation with clinical findings.

1977

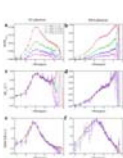

Quantitatively Evaluate the Chemical Exchange Effect in Off-resonance Spin Lock Using Perturbation of Longitudinal Relaxation Rate in Rotating Frame (PLRF) Analysis

Yi Wang[1], Yang Fan[2], and Jia-Hong Gao[1]

[1]Center for MRI Research, Peking University, Beijing, People's Republic of China, [2]MR Research Group, GE Healthcare China, Beijing, People's Republic of China

Chemical exchange effect can be evaluated by off-resonance spin-lock sequence (CESL), but it remains unclear whether the effect is accurately reflected. In this study, with the help of perturbation of longitudinal relaxation rate in rotating frame (PLRF) analysis, we quantitatively compared signal from CESL and chemical exchange saturation transfer (CEST) sequences and tested the condition for acquiring high-quality signal from CESL sequence which can accurately reflect chemical exchange effect.

1978 

Chemical exchange rotation transfer (CERT) using adiabatic hyperbolic secant pulses

Eugene C. Lin[1], Zhongliang Zu[1], Elizabeth A. Louie[1], Xiaoyu Jiang[1], and Daniel F. Gochberg[1]

[1]*Vanderbilt University Institute of Imaging Science, Nashville, TN, United States*

Chemical exchange rotation transfer (CERT) is an emerging approach for imaging solutes and solute exchange that avoids some of the contributions from the asymmetric background in biological tissues that confound chemical exchange saturation transfer (CEST). To further improve the robustness of CERT methods when there is field inhomogeneity, we examined adiabatic hyperbolic secant pulses for solute saturation. In addition to addressing field homogeneity issues, this new method reveals a new mechanism to generate contrast based on the delay time between pulse.

1979 

Elegant method to quantify chemical exchange processes for pH CEST imaging

Steffen Goerke[1], Johannes Windschuh[1], Moritz Zaiss[1,2], Jan-Eric Meissner[1], Mark E Ladd[1], and Peter Bachert[1]

[1]*Division of Medical Physics in Radiology, German Cancer Research Center (DKFZ), Heidelberg, Germany,* [2]*Department of High-field Magnetic Resonance, Max-Planck-Institute for Biological Cybernetics, Tübingen, Germany*

A novel concentration-independent approach is presented to determine the pH-dependence of exchange rates employing a single CEST image of a set of model solutions at different pH. Not only the comparatively short acquisition time, but also the robustness against variations in relaxation parameters makes this modality an elegant way to determine exchange rates *in vitro*. The calibrated functions are required for accurate pH mapping *in vivo* using CEST, as well as for design of exogenous CEST contrast agents.

1980 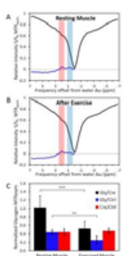

Muscular glycogen detection with CEST imaging in living rat at 14.1T

Elise Vinckenbosch[1], Hongxia Lei[2], Nicolas Kunz[1], Masoumeh Dehghani[1], and Rolf Gruetter[1,2]

[1]*Laboratory for functional and metabolic imaging, Ecole Polytechnique Fédérale de Lausanne, Lausanne, Switzerland,* [2]*Center for Biomedical Imaging (CIBM-AIT), Ecole Polytechnique Fédérale de Lausanne, Lausanne, Switzerland*

Glycogen is the principle intracellular storage for energetic needs in muscle and information about its spatial distribution would be a great additional tool for traumatology and sport sciences. In this study, we aimed to map *in vivo* muscular glycogen using CEST imaging in rodent. We have shown that optimal B_1 saturation power allowed CEST imaging glycogen distinguishable from the neighboring creatine at 14.1 Tesla. We applied our optimized protocol on muscle after exercise session, resulting in 50% reduction of MTR_{asym} comparing to muscle at resting state. This is supporting the specificity of our method and is consistent with literature.

1981

Rapid 3D CEST using volumetric reduced field of view imaging

Jianbo Shao[1], Bing Wu[2], and Hui Lin[3]

[1]*Wuhan Children Hospital, Wuhan, People's Republic of China,* [2]*GE healthcare MR Research China, Beijing, People's Republic of China,* [3]*GE healthcare MR Research China*

A reduced field of view CUBE acquisition was proposed for CEST imaging. It is advantageous in situations where the imaging volume may be constrained to a region of the whole volume. Clinical feasible acquisition (10s per volume) was achieved at 2mm isotropic resolution.

1982 

The origins of CEST contrast in ischemic tissue: effects of hypotonic stress on the nervous system of Aplysia californica

Tangi Roussel[1], Pavel Svehla[1], Denis Le Bihan[1], and Luisa Ciobanu[1]

[1]*NeuroSpin, Commisariat à l'Energie Atomique et aux Energies Alternatives, Gif-sur-Yvette, France*

Recent CEST MRI methods such as Amide Proton Transfer (APT) imaging allow the detection of brain tumors and stroke by generating novel image contrasts which depend on the chemical exchange. In this paper, we are studying the effects of ischemia on the CEST signal at a tissue level using the nervous system of Aplysia californica, a widespread model in neuroscience. A significant change in the Z spectrum was observed at 2.5 ppm after hypotonic shock in the abdominal ganglion and was quantified as a +2.88% MTR increase. Cell swelling, which is a known phenomenon in ischemic tissue, could potentially cause such effect.

1983 

Simultaneous Acquisition of Multiple Z-spectra using Sinc-Modulated RF Pulse Trains in Gradient Encoded CEST MRI

Hirohiko Imai[1], Kiyotaka Miyake[2], and Tetsuya Matsuda[2]

[1]*Center for the Promotion of Interdisciplinary Education and Research, Kyoto University, Kyoto, Japan,* [2]*Department of Systems Science, Graduate School of Informatics, Kyoto University, Kyoto, Japan*

We propose a use of sinc-modulated RF pulse train instead of the conventional continuous wave RF irradiation under the presence of constant gradient as a saturation scheme in chemical exchange saturation transfer (CEST) MRI aiming at a simultaneous acquisition of multiple Z-spectra. The proposed method was applied for a glutamic acid solution in water. The multiple Z-spectra could be observed along the gradient encoding direction by repetitive application of the saturation scheme. Thus, the present study shows the potential of the proposed methodology for accelerating the CEST MRI.

1984 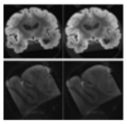

Investigation of magnitude and phase CEST effects in fixed whole brains and tissue samples: a combined 3T and 9.4T study

Ana-Maria Oros-Peusquens[1], Nuno Andre da Silva[1], and N. Jon Shah[1]

[1]Research Centre Juelich, Juelich, Germany

Saturation transfer effects were investigated in fixed tissue at 3T and 9.4T and a range of saturation powers. Z-spectra on magnitude as well as phase data were studied with high spatial and spectral resolution, also due to the excellent performance of a PCA-based denoising algorithm. The preliminary findings do not support the presence of an APT effect in fixed tissue; however, saturation transfer effects could be enhanced in pathological tissue, similar to in vivo findings in e.g. tumour or stroke. This study opens the way to a systematic investigation of saturation transfer effects in healthy and pathological fixed tissue.

1985 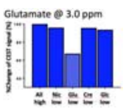

An assessment of interdependent chemical exchange saturation transfer (CEST) signals from metabolites with overlapping chemical shift frequencies and proton exchange rates

Masaya Takahashi[1], Keisuke Ishimatsu[1], Shanrong Zhang[1], Kazufumi Kikuchi[1], and A. Dean Sherry[1]

[1]Advanced Imaging Researh Center, UT Southwestern Medical Center, Dallas, TX, United States

The objectives are to investigate how the chemical exchange saturation transfer (CEST) signal measured at a given frequency is independent of the neighboring CEST signals. We measured the CEST signals from combinations of four metabolites at 3.5, 3, 2 and 1 ppm with 5 different powers and 3 different durations of presaturation pulse to investigate the parameter-dependence and interdependency of each CEST signal in phantoms. The CEST signal of glutamate was less impacted by concentration changes in other exchanging species by subtracting CEST signals at two different power levels.

1986 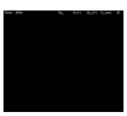

Modeling the increased inhomogeneous magnetization transfer (ihMT) signal from high amplitude, low duty cycle irradiation

Gopal Varma[1], Aaron K Grant[1], Olivier M Girard[2], Valentin H Prevost[2], Guillaume Duhamel[2], and David C Alsop[1]

[1]Radiology, Division of MR Research, Beth Israel Deaconess Medical Center, Harvard Medical School, Boston, MA, United States, [2]Aix Marseille Univ, CNRS, CRMBM, Marseille, France

Pulsed implementations of RF saturation for MT and ihMT are dependent on the duty cycle of the MT pulse relative to its repetition period. The ihMT signal increases following preparation with high B_1, low duty cycle MT pulses. A model was developed to fit ihMT data acquired at different duty cycles, along with the more standard variations in power and offset frequency. Output parameters from the fit were reasonable. The model allowed simulation of the ihMT signal as a function of experimental parameters related to the saturation preparation, and can be used to guide future experiments and/or optimize ihMT.

1987 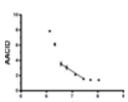

Improved Measurement Precision for AACID CEST MRI of Brain pH using the 2 ppm Amine Resonance

Mohammed Albatany[1,2] and Robert Bartha[1,2]

[1]Department of Medical Biophysics, University of Western Ontario, London, ON, Canada, [2]The Centre for Functional and Metabolic Mapping, Robarts Research Institute, University of Western Ontario, London, ON, Canada

The chemical exchange saturation transfer (CEST) method called Amine and Amide Concentration Independent Detection (AACID) can produce image contrast that is dependent on tissue pH.   The AACID value is calculated by taking the ratio of the 3.5 ppm amide CEST effect to the 2.75 ppm amine CEST effect and varies linearly with pH in the physiological range. In the current study, we compare the range of the AACID values obtained in 24 mice with brain tumors and normal tissue using the 2 ppm and 2.75 ppm amine resonances. Using the 2 ppm amine resonance increased the AACID range by 39% compared to the 2.75 ppm resonance and led to reduced measurement variability across the brain suggesting that using the 2 ppm amine resonance could improve AACID based pH measurement in-vivo.

1988 

Towards Eliminating Magnetization Transfer (MT) Effect on CEST Quantification Using MR Fingerprinting: Simulations

Pei Han[1,2], Zhengwei Zhou[3,4], Kui Ying[1,2], and Debiao Li[3,4,5]

[1]Department of Engineering Physics, Tsinghua University, Beijing, People's Republic of China, [2]Key Laboratory of Particle and Radiation Imaging, Ministry of Education, Beijing, People's Republic of China, [3]Biomedical Imaging Research Institute, Cedars-Sinai Medical Center, Los Angeles, CA, United States, [4]Department of Bioengineering, University of California Los Angeles, Los Angeles, CA, United States, [5]Department of Imaging, Cedars-Sinai Medical Center, Los Angeles, CA, United States

In this work, a new quantitative chemical exchange saturation transfer (q-CEST) method based on MR fingerprinting is developed to eliminate the influence of MT effect. Signal evolutions are generated by using a series of hard saturation pulses with different amplitudes and durations. The dictionary is constructed using the 2-pool model. Simulation experiments based on the 3-pool model were performed, and simulation results show that good mapping accuracy was achieved even in the presence of the MT effect.

Towards an Early Detection of Prostate Cancer using Zinc-Sensitive iCEST MRI

1989

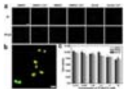

Yue Yuan[1], Xiaolei Song[1], and Jeff Bulte[1]

[1]*The Russell H. Morgan Department of Radiology and Radiological Science, The Johns Hopkins University, Baltimore, MD, United States*

As compared to normal prostate tissue, prostate cancer cells exhibit a dramatic reduction in zinc content. We have used ^{19}F-based ion-CEST (iCEST) MRI to sense differential Zn^{2+} levels between normal and malignant prostate cell lines. We were able to observe clear differences in zinc-induced iCEST signal between normal cells and cancer cells, which was validated by microscopy using a zinc-sensitive fluorescent dye. Hence, iCEST MRI may have potential as a new means to non-invasively detect early prostate malignant transformation.

Traditional Poster

Hepatopancreaticobiliary

Exhibition Hall 1990-2030 Wednesday 8:15 - 10:15

1990

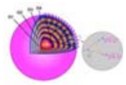

A biodegradable macromolecular MRI contrast agent for enhanced liver metastasis

Xiaoxuan Zhou[1], Hongjie Hu[1], Yue Qian[1], Yuxin Han[2], Mingzhou Ye[2], Jianbin Tang[2], Peipei Pang[3], and Jun Yang[3]

[1]*Radiology, Sir Run Run Shaw Hospital, Zhejiang, People's Republic of China,* [2]*Chemical and Biological Engineering, Zhejiang University, Zhejiang, People's Republic of China,* [3]*Life Science, GE healthcare, Shanghai, People's Republic of China*

Tumor metastasis accounts for the related mortality, and precise diagnostic imaging of distant metastasis plays a significant role in clinical administration and treatment plan. Enhanced MRI with small-molecule contrast agent (CA) is a favorite imaging modality. However, small-molecule CA has some unsatisfied flaws such as short blood circulation time, low relaxivity and non-specificity. In this study, we synthesized a macromolecular CA with high relaxivity and long blood circulation time, and assessed early liver metastasis with enhanced MRI using this macromolecular CA.

1991

3D contrast enhanced high definition, free-breathing Dixon imaging using radial stack of stars and respiratory gating and tracking: Clinical comparison to state of the art breath hold Dixon imaging

Gabriele Beck[1], Michael Wyss[2,3], Rene Patzwahl[3], Joachim Hohmann[3], Christoph Andreas Binkert[3], Lars van Loon[1], and Hans Peeters[1]

[1]*Philips Healthcare, Best, Netherlands,* [2]*Philips Healthcare, Switzerland,* [3]*Institute for Radiology and Nuclearmedicine, Kantonsspital Winterthur, Switzerland*

We investigated a motion immune Dixon TFE approach incorporating a 3D radial stack-of-stars acquisition module interleaved with a spiral excitation navigator to gate and track the acquisition. Image quality, sharpness and streaking artifact level and its variability over different patient breathing patterns is efficiently improved to an extent where it is preferred over the state-of-the art breath hold (BH) Dixon scans. Next to that, it allowed scan time reductions of 30% in average. This technique provides motion-free, high resolution hepatic imaging with the benefits of Dixon providing consistent good fat suppression over a large FOV with water, fat, IP and OP diagnostic information all-in-one scan.

1992

Quantification of Hepatic Fat Fraction and Liver/Spleen R2* in a Healthy Cohort at 3 Tesla

Rosalind Gerson[1], Chris Bowen[2,3], Manjari Murthy[2], and Sharon Clarke[2,3]

[1]*School of Medicine, Dalhousie University, Halifax, NS, Canada,* [2]*Biomedical Translational Imaging Centre, QEII Health Sciences Centre, Halifax, NS, Canada,* [3]*Department of Diagnostic Radiology, Dalhousie University, Halifax, NS, Canada*

Non-invasive quantification of hepatic fat and iron with MRI has generated increasing clinical interest, particularly given the prevalence of chronic liver disease. Elevated R2* is a biomarker of iron deposition in the liver and spleen. The normative distribution of R2* in these organs at 3T is not well described, but is necessary for confident diagnosis of mild to moderate levels of iron deposition. Based on measurements in 97 adults selected from the general population, we confirm that ~20% have fatty liver and suggest that a hepatic R2* > 89 s^{-1} and splenic R2* > 69 s^{-1} can be considered abnormal.

1993

Spectroscopy-Based R2 Relaxometry for Liver Iron Quantification at 1.5T and 3.0T

Diego Hernando[1,2], Changqing Wang[1,3,4], Ryan J. Mattison[5], Takeshi Yokoo[6,7], and Scott B. Reeder[1,2,8,9,10]

[1]*Radiology, University of Wisconsin-Madison, Madison, WI, United States,* [2]*Medical Physics, University of Wisconsin-Madison, Madison, WI, United States,* [3]*School of Automation Engineering, University of Electronic Science and Technology of China, Chengdu, People's Republic of China,* [4]*School of Biomedical Engineering and Guangdong Provincial Key Laboratory of Medical Image Processing, Southern Medical University, Guangzhou, People's Republic of China,* [5]*Medicine, University of Wisconsin School of Medicine and Public Health, WI, United States,* [6]*Radiology, University of Texas-Southwestern, Dallas, TX, United States,* [7]*Advanced Imaging Research Center, University of Texas-Southwestern, Dallas, TX, United States,* [8]*Biomedical Engineering, University of Wisconsin-Madison, Madison, WI, United States,* [9]*Medicine, University of Wisconsin-Madison, Madison, WI, United States,* [10]*Emergency Medicine, University of Wisconsin-Madison, Madison, WI, United States*

R2-based techniques for liver iron quantification using Spin-Echo (SE) imaging require long acquisitions. In contrast, single-voxel Stimulated-Echo Acquisition Mode (STEAM)-MR spectroscopy enables liver R2 measurements in a single breath-hold. However, the accuracy and field strength dependence of STEAM-MRS R2 quantification are unknown. This study evaluated the accuracy and field strength dependence of STEAM-MRS for R2 quantification in healthy controls and patients with liver iron overload. At 1.5T, STEAM-MRS R2 was in close agreement with SE-MRI-based R2. Further, STEAM-MRS R2 measurements were highly correlated across field strengths. Finally, STEAM-MRS R2 measurements at 1.5T and 3.0T were calibrated to liver iron concentration.

1994

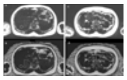

Correlation between incidental fat deposition in the liver and pancreas in asymptomatic patients

Mounes Aliyari Ghasabeh[1], Manijeh Zarghampour[2], Li pan[3], Pegah Khoshpouri[2], Farnaz Najmi Varzaneh[2], Nannan Shao[2], Ankur Pandy[2], Pallavi Pandy[2], Danial Fouladi[2], and Ihab R Kamel[2]

[1]The Russell H. Morgan Department of Radiology and Radiological Sciences, Johns Hopkins Hospital, Baltimore, MD, United States, [2]The Russell H. Morgan Department of Radiology and Radiological Sciences, Johns Hopkins Hospital, [3]Siemens Healthcare, Baltimore, MD, USA

Liver steatosis is the most common parenchymal liver disease in Western Countries and it may progress to steatohepatis, fibrosis and cirrhosis. Also, fat deposition in liver and pancreas can cause diabetes by increasing resistance to insulin. Magnetic Resonance Spectroscopy (MRS) has been shown to strongly correlate with histology in liver fat quantification. However, MRS has some limitations such as breathing artifact and difficulties in avoiding vessels or bile ducts within the voxel. So, it is desirable to utilize a novel and robust imaging technique that can screen for the presence of fat in the liver and pancreas.

1995

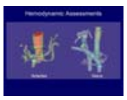

Hemodynamic Assessments of Hepatic Vasculatures using 4D-PCA and MRFD

Takeshi Yoshikawa[1], Yoshiharu Ohno[1], Katsusuke Kyotani[2], Kouya Nishiyama[2], Shinichiro Seki[1], and Yuji Kishida[3]

[1]Advanced Biomedical Imaging Research Center, Kobe University Graduate School of Medicine, Kobe, Japan, [2]Center of Radiology and Radiation Oncology, Kobe University Hospital, Kobe, Japan, [3]Radiology, Kobe University Graduate School of Medicine, Kobe, Japan

We introduced new assessment method of liver hemodynamics using 4D-PCA and new flow analytic technique including wall shear stresses. We found 4D-PCA and MRFD enables detailed hemodynamic assessment and has the potential to be used for liver disease assessments.

1996

MRI of Liver Cysts in Autosomal Dominant Polycystic Kidney Disease: Effect of Genotype

Zerwa Farooq[1], Ashkan Heshmatzadeh Behzadi[1], Jon Blumenfeld[2], and Martin R Prince[1,3]

[1]Radiology, Weill Cornell Medicine, New York, NY, United States, [2]Nephrology, Weill Cornell Medicine, New York, NY, United States, [3]Radiology, Columbia University, New York, NY, United States

ADPKD patients (n=25) undergoing abdominal MRI were analyzed 2 times each by 2 separate reviewers using a) thresholding; b) region growing c) cyst diameter d) semi-manual segmentation to determine liver cyst volume. Using the most reproducible technique, 75 additional ADPKD patients were studied correlating their liver parameters with genotype, gender and age. Semi-manual segmentation was the best technique for measuring cyst volume with intraclass correlation coefficient of 0.99. PKD1 mutation was found to be associated with higher total liver volume and liver cyst volume across different age groups and gender compared to PKD2 mutation, suggesting greater hepatic involvement with PKD1.

1997

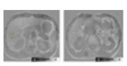

Feasibility and grading performance of Quantitative Susceptibility Mapping for Hepatic Iron quantification

Huimin Lin[1], Hongjiang Wei[2], Xu Yan[3], Caixia Fu[4], Stephan Kannengiesse[5], Chunlei Liu[2,6], and Fuhua Yan[1]

[1]Department of Radiology, Ruijin Hospital, Shanghai Jiaotong University School of Medicine, Shanghai, People's Republic of China, [2]Department of Electrical Engineering and Computer Sciences, University of California, Berkeley, CA, United States, [3]MR Collaboration NE Asia, Siemens Healthcare, Shanghai, People's Republic of China, [4]Siemens Shenzhen Magnetic Resonance Ltd, Shenzhen, People's Republic of China, [5]MR Applications Predevelopment, Siemens Healthcare, Erlangen, Germany, [6]The Helen Wills Neuroscience Institute, University of California, Berkeley, CA, United States

This study aimed to evaluate the performance of Quantitative Susceptibility Mapping (QSM) on estimating and grading the liver iron concentration (LIC), using Ferriscan-R2 values as reference. Thirty-three patients suspected of hepatic iron overload were included in this study. The results showed a significant positive correlation between QSM and Ferriscan-based LIC (r=0.924). ROC analysis revealed that QSM could accurately grade LIC for low and moderate iron overload patients, indicating that high-quality QSM maps may allow to reliably estimate and grade iron deposition in the liver.

1998

Characterization of Primary Liver Cancers with DWI Histogram Analysis

Sara Lewis[1], Steven Peti[2], Stefanie Hectors[1], Michael King[2], Juan Putra[3], Swan Thung[3], and Bachir Taouli[1]

[1]Translational and Molecular Imaging Institute, Icahn School of Medicine at Mount Sinai, New York, NY, United States, [2]Department of Radiology, Icahn School of Medicine at Mount Sinai, New York, NY, [3]Department of Pathology, Icahn School of Medicine at Mount Sinai, New York, NY, United States

ADC measurement using DWI have shown promise for characterizing focal liver lesions. In this study, we assessed the ability of advanced ADC histogram parameters to distinguish the histological diagnosis and the grade of primary malignant liver cancers. We found that both ADC mean and ADC percentiles could distinguish between tumor types; ADC percentiles were also predictive of tumor grade for HCC and ICC. Advanced ADC histogram analysis may be useful for accurate tumor diagnosis and prediction of tumor grade.

1999

Simultaneous liver and spleen 2D MRE and 3D MRE acquisitions: Preliminary results

Paul Kennedy [1], Kevin J. Glaser[2], Curtis L. Johnson[3], Bradley Bolster Jr. [4], Jalpan Jani[1], Kashif Khokhar[1], Richard L. Ehman[2], and Bachir Taouli[1,5]

[1]Translational and Molecular Imaging Institute, Icahn School of Medicine at Mount Sinai, New York, NY, United States, [2]Department of Radiology, Mayo Clinic, Rochester, MN, United States, [3]Department of Biomedical Engineering, University of Delaware, DE, United States, [4]Siemens Healthcare, Salt Lake City, UT, United States, [5]Department of Radiology, Icahn School of Medicine at Mount Sinai, New York, NY, United States

We present initial results of 2D MR elastography (MRE) and 3D MRE acquired in liver and spleen using a dual driver configuration in 13 subjects, 5 healthy and 8 with liver disease. 2D MRE showed a trend to higher stiffness in healthy subjects however in cirrhotic subjects liver stiffness was generally higher with 3D MRE. 3D MRE showed significantly higher liver stiffness in cirrhotic subjects compared to healthy subjects, with spleen stiffness also increased but not reaching significance. Coefficient of variation with single and dual drivers was 5% for liver and spleen in 2D and 3D MRE.

2000

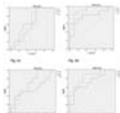

Liver quantification with dynamic contrast-enhanced MRI for evaluation in hepatic function and staging of post-hepatitic liver cirrhosis

Zhang Lan[1]

[1]MRI, The 1st affiliated hospital of Henan University of TCM, ZhengZhou, People's Republic of China

To evaluate the value of DCE-MR for hepatic reserve function assessment and staging in post-hepatitic liver cirrhosis (PHLC). 10 patients with compensatory PHLC, 10 with decompensatory PHLC and 10 healthy volunteers were performed DCE-MRI scanning. All data were calculated by Extended Tofts model fitting with pharmacokinetic curve and the permeability and perfusion parameters were measured in quantification. The new method validated the feasibility of using quantitative parameters of DCE-MRI with pharmacokinetic model to assess liver cirrhosis. In conclusion, DCE-MRI quantitative parameters can be used for diagnosing and staging liver cirrhosis.

2001

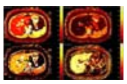

Assessment of the Hepatocyte Fraction for Estimation of Liver Function Based on a Simple Pharmacokinetic Model

Ruo-kun Li[1], Fu-hua Yan[2], Jin-wei Qiang[3], Hui-min Lin[2], Weibo Chen, Tomoyuki Okuaki, and Eunju Kim

[1]Radiology, Ruijin hospital of Shanghai Jiaotong University, Shanghai, People's Republic of China, [2]Ruijin hospital of Shanghai Jiaotong University, [3]Jinshan hospital of Fudan Univeristy

There were 16 consecutive patients (12 men, 5 women; mean age, 45.7 years; range, 33–65 years). Imaging was performed on clinical 3T scanner (Philips Ingenia) using 32ch body/cardiac coil. A hepatocyte fraction (HF) map and K map were derived. The HF and K values for Gd-EOB-DTPA were correlated with Child-Pugh scores. Patients with Child-Pugh class B disease showed significantly lower liver FA value and K value. HF value and K value were positively correlated with the Child–Pugh scores ($r=0.752$ to 0.855, $p<0.05$). HF value and K value had the largest AUC of 0.975 and 0.78 for distinguishing the Child–Pugh class A of cirrhosis from class B. K value had the most area under receiver operating characteristic curve (AUC) of 0.99 for identifying the presence of liver cirrhosis.The study suggested that hepatocyte fraction and hepatic uptake derived from Gd-EOB-DTPA-enhanced MRI can quantify liver function.

2002

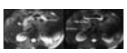

Quantitative T1 and T2 measurements of pancreas at 7 Tesla using a multi-transmit system

Mariska Damen[1], Quincy van Houtum[2], Maarten van Leeuwen[3], Peter Luijten[2], Andrew Webb[1], Dennis Klomp[2], and Catalina Arteaga de Castro[2]

[1]Radiology, Leiden University Medical Center, Leiden, Netherlands, [2]Imaging Division, University Medical Center Utrecht, Utrecht, Netherlands, [3]Radiology, University Medical Center Utrecht, Utrecht, Netherlands

Inversion recovery and echo time series were obtained at 7T with a multi-transmit system to determine the T1 and T2 relaxation times of the healthy pancreas. These parameters are crucial when optimizing MR protocols. The T1 and T2 values found were in average 921+/-98 ms and 57+/-12 ms respectively. Excellent T2 contrast is obtained for the pancreas at TE/TR=80ms/17s.

2003

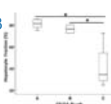

Quantitative Assessment of Hepatic function with Hepatocyte Fraction

Mengqi He[1], Yingjie Mei[2,3], Jing Zhang[1], Zeyu Zheng[1], Hongxiang Li[1], Tomoyuki Okuaki[4], Eunju Kim[5], and Yikai Xu[1]

[1]Department of Medical Imaging Center, Nanfang Hospital, Southern Medical University, Guangzhou, People's Republic of China, [2]Guangdong Provincial Key L
[4]MR Clinical Science, Philips Healthtech, Tokyo, Japan, [5]MR Clinical Science, Philips Healthcare, Seoul, Korea

Gadoxetic acid has been shown to evaluate liver function as it is known to be actively taken up by hepatocytes via organic anion transporters (OATPs). The me
Pugh classification method which is still the most commonly applied method for evaluating liver function in clinical. The hepatocyte fractions were significantly di
–Pugh scores between A and C, B and C. The hepatocyte fraction could be considered as a promising method for the quantitative assessment of liver function.

2004

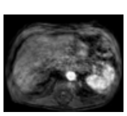

Assessment of interrater agreement and reliability for characterization of respiratory motion related artifacts at gadoxetate disodium-enhanced liver MRI

Kristina Imeen Ringe[1], Julian Luetkens[2], Rolf Fimmers[3], Renate Hammerstingl[4], Guenter Layer[5], Martin Maurer[6], Claas Naehle[7], Sabine Michalik[8], Peter Reimer[9], Christina Schraml[10], Andreas Schreyer[11], Patrick Stumpp[12], Thomas Vogl[4], Frank Wacker[1], Winfried Willinek[13], and Guido Kukuk[2]

[1]Department of Diagnostic and Interventional Radiology, Hannover Medical School, Hannover, Germany, [2]Department of Diagnostic and Interventional Radiology, University Hospital of Bonn, Bonn, Germany, [3]Department of Medical Biometry, Informatics and Epidemiology, University Hospital of Bonn, Bonn, Germany, [4]Department of Diagnostic and Interventional Radiology, Clinic of the Goethe University, Frankfurt, [5]Department of Diagnostic and Interventional Radiology, Klinikum der Stadt Ludwigshafen, Ludwigshafen, Germany, [6]Department of Radiology, University Hospital of Bern, Bern, Switzerland, [7]Division of Radiology and Nuclear Medicine, Kantonspital St. Gallen, St. Gallen, Switzerland, [8]Department of Radiology, Asklepios Klinik Altona, Hamburg, Germany, [9]Instiute of Diagostic and Interventional Radiology, Städtisches Klinukum Karlsruhe, Karlsruhe, Germany, [10]Department of Diagnostic and Interventional Radiology, University Hospital of Tuebingen, Tuebingen, Germany, [11]Department of Radiology, University Hospital Regensburg, Regensburg, Germany, [12]Department of Diagnostic and Interventional Radiology, University Hospital Leipzig, Leipzig, Germany, [13]Department of Radiology, Neuroradiology, Ultrasounnd and Nuclear Medicine, Krankenhaus der Barmherzigen Brueder, Trier, Germany

In this prospective multicenter study, interrater agreement and reliability for characterization and grading of respiratory motion artifacts related to the injection of gadoxetate disodium were evaluated. Interrater agreement and reliability for scoring of motion artifacts in the arterial phase was excellent among experienced abdominal radiologists from different European tertiary referral centers with an intraclass correlation coefficient of 0.983 and 0.985, respectively. Characterization and grading of respiratory motion artifacts can thus be performed with a high level of confidence, which is a prerequisite for assessing the incidence of this phenomenon in larger multicenter studies.

2005 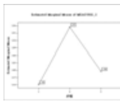

The predictive value of diffusion-weighted imaging on radiation-induced liver injury of hepatic malignancies

Xiaohong Ma[1], Shuang Wang[1], Yongjian Zhu[1], Han Ouyang[1], Chunwu Zhou[1], and Xinming Zhao[1]

[1]Diagnostic Radiology, Cancer Hospital, Chinese Academy of Medical Sciences, Peking Union Medical College, Beijing, People's Republic of China

Radiation-induced liver injury (RILI) is one of the most dreaded complications of radiation therapy (RT)，which prevents radiation dose escalation and limits the effectiveness of the treatment . Therefore, it was important to predict and evaluate the RILI on hepatic malignancy using the RT in the early term. In this study, the ADCmid-RT value was significantly highest, and had negative correlation with the radiation dose. As the ADCmid-RT value was less than 1.29 x10-3mm2/s, the RILI could possibly occur. Therefore, the ADCmid-RT value may serve as a biomarker for predicting RILI in patients with hepatic malignancies treated with RT.

2006 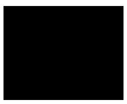

Inter- and intra-reviewer agreement of region-of-interest-based quantification of liver R2* in patients with iron overload

Camilo A Campo[1], Diego Hernando[1,2], Tilman Schubert[1], Andrew Van Pay[1], and Scott B Reeder[1,2,3,4,5]

[1]Radiology, University of Wisconsin-Madison, Madison, WI, United States, [2]Medical Physics, University of Wisconsin-Madison, Madison, WI, United States, [3]Biomedical Engineering, University of Wisconsin-Madison, Madison, WI, United States, [4]Medicine, University of Wisconsin-Madison, Madison, WI, United States, [5]Emergency Medicine, University of Wisconsin-Madison, Madison, WI, United States

This study evaluated the inter- and intra-reviewer agreement of different region-of-interest (ROI) sampling methods for the quantification of liver R2* (1/T2*) in patients with iron overload. 37 MRI datasets from patients suspected of having liver iron overload were retrospectively analyzed using ROI sampling methods that have been previously reported. Our results demonstrate that the inter- and intra-reviewer agreement of liver R2* quantification improve when using ROIs that are large in size and number. We conclude that researchers and clinicians should strive to sample as much area of the liver by using multiple large ROIs.

2007

Hepatocellular Carcinoma with Capsule Appearance in Gadoxetic Acid-enhanced MR Images : Correlation with Dynamic CT and Pathologic Fibrous Capsule

Jei Hee Lee[1], Bohyun Kim[1], and Young Bae Kim[2]

[1]Radiology, Ajou University School of Medicine, Suwon, Korea, Republic of, [2]Pathology, Ajou University School of Medicine, Suwon, Korea, Republic of

For visualization of capsule appearance on HCC, GaMR is comparable with dynamic CT. And pathologic fibrous capsule can be seen as hypointense rim in HBP. Lower visualization of capsule appearance in TP on GaMR seem to be parenchymal enhancement during the transitional phases. Hyperintensity rim in T2 weighted images with hopointense rim on HBP shows disruption of fibrous capsule with extension of tumor cells across the fibrous capsule in pathology. Hypointense rim on the HBP in the 2014 version of LI-RADS should not be considered as capsule appearance, and further study is also needed.

2008 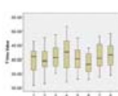

Liver T1rho Distribution across Eight Functionally Independent Segments

Weibo Chen[1], Xin Chen[2], Li Yang[3], Shanshan Wang[2], Queenie Chan[4], and Guangbin Wang[2]

[1]Philips Healthcare, Shanghai, People's Republic of China, [2]Shandong Medical Imaging Research Institute Affiliated to Shandong University, Shandong University, Ji Nan, People's Republic of China, [3]Department of Radiology, Shanghai Institute of Medical Imaging, Zhongshan Hospital, Fudan University, Shanghai, People's Republic of China, [4]Philips Healthcare, Hong Kong, People's Republic of China

ROI-based analysis may suffer from sampling errors due to the user-defined placement of the ROI and the choice of slice location. The aim of our study was to find an approach that allow the detection and measurement of the T1rho values of the hepatic segments.

2009 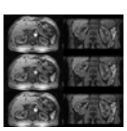

GRASP with Motion Compensation for DCE-MRI of the Abdomen

Koji Fujimoto[1], Li Feng[1], Rocardo Otazo[1], Kai Tobias Block[1], Henry Rusinek[1], Nicole Wake[1], and Hersh Chandarana[1]

[1]Center for Advanced Imaging Innovation and Research (CAI2R) and Bernard and Irene Schwartz Center for Biomedical Imaging, Department of Radiology, New York University School of Medicine, New York, NY, United States

A method to combine information of respiratory states with a non-rigid motion model is proposed to reconstruct motion-compensated 4D images of dynamic-contrast enhanced MRI with high temporal resolution. Abdominal DCE-GRASP MRI was reconstructed by grouping 4 consecutive spokes as one dynamic frame (0.6sec/frame). Respiratory motion was obtained from central k-space data (as in XD-GRASP). A temporal TV constraint was applied separately for each respiratory state. By using an optical-flow algorithm, four sets of motion vectors were obtained. Motion-compensated GRASP reconstruction was performed by including the motion vectors and showed improved image quality and reduced motion blurring.

2010

HCC detection in pre-transplant patients: A comparative retrospective study between multiphasic CT, gadoxetic acid-enhanced MRI and extracellular gadolinium based contrast-enhanced MRI

Sahar Semaan[1], Christopher Song[1], Sara Lewis[1], Manjil Chatterji[1], M. Isabel Fiel[2], Cecilia Besa[3], and Bachir Taouli[3]

[1]Radiology, Icahn School of Medicine at Mount Sinai, New York, NY, United States, [2]Department of Pathology, Icahn School of Medicine at Mount Sinai, New York, NY, United States, [3]Translational and Molecular Imaging Institute, Icahn School of Medicine at Mount Sinai, New York, NY, United States

In this study, we present preliminary data comparing the diagnostic performance of multiphasic contrast-enhanced CT with contrast enhanced MRI using a liver specific gadolinium based contrast agent (GBCA), gadoxetic acid (Gd-EOB-DTPA) and extracellular (EC) GBCAs, using explant pathologic data as the reference. We also assessed the added value of delayed hepatobiliary phase (HBP) imaging and DWI in HCC detection. Our data suggests that CT and MRI have similar overall sensitivities for HCC detection and that the addition of DWI and HBP improved HCC detection when using Gd-EOB-DTPA.

2011

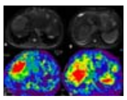

The value of magnetic resonance elastography in differential diagnosis of hepatocellular carcinoma and intrahepatic cholangiocarcinoma

kan liu[1], qi zhang[2], hong mei zhang[2], han ouyang[2], and xinming zhao[2]

[1]Imaging Diagnosis, National Cancer Center/Cancer Hospital, Chinese Academy of Medical Science and Peking Union Medical College, beijing, People's Republic of China, [2]National Cancer Center/Cancer Hospital, Chinese Academy of Medical Science and Peking Union Medical College

To determine the value of MRE in the differential diagnosis of hepatocellular carcinoma and intrahepatic cholangiocarcinoma with 3.0-T MR scanner . The MRE were performed in 36 patients(26 hepatocellular carcinomas and 11 intrahepatic cholangiocarcinomas) by using 60-Hz mechanical waves and Spin echo echo planar sequence.Intrahepatic cholangiocarcinomas had significantly greater mean shear stiffness than hepatocellular carcinoma (9.08 ±2.13kPa vs 6.54 ±1.84kPa). They have statistically significant differences(p<0.01).MRE can help the differentiation of hepatocellular carcinoma and intrahepatic cholangiocarcinoma.

2012

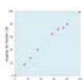

Hepatic fat quantification using automated six-point Dixon methods: comparison with conventional chemical shift based gradient-echo sequences and computed tomography.

Tomohiro Namimoto[1], Masataka Nakagawa[1], Kie Shimizu[1], Takeshi Nakaura[1], Kosuke Morita[1], and Yasuyuki Yamashita[1]

[1]Diagnostic Radiology, Kumamoto University, Kumamoto, Japan

To compare automated six-point-Dixon(6-p-Dixon) with dual-echo GRE chemical shift imaging(CSI) for quantification of hepatic fat fraction(FF) with CT. In a phantom study, various FF vials were performed to validate the accuracy. In clinical study, fifty-nine patients were examined both 3.0T MRI and CT. Quantitative measurements were calculated SI-index of CSI and imaging-FF of 3D-6-p-Dixon. In phantom study, linear regression between FF and imaging-FF/SI-index showed good agreement(imaging-FF R^2=0.992:0-100%FF;SI-index R^2=0.978:0-34.7%FF). In clinical study, linear regression between imaging-FF and SI-index showed good agreement(R^2=0.890). CT attenuation value was strongly correlated with imaging-FF(R^2=0.852) and SI-index(R^2=0.812). Imaging-FF of 6-p-Dixon has potential for automated hepatic fat quantification.

2013

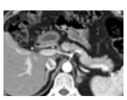

Value of Noncontrast MR Imaging with Diffusion-weighted Imaging for Detection of Primary Small (≤ 20mm) Solid Pancreatic Tumors and Prediction of Pancreas Ductal Adenocarcinoma

Hyun Jeong Park[1] and Kyung Mi Jang[2]

[1]Radiology, Chung-Ang Universitiy Hospital, Seoul, Korea, Republic of, [2]Samsung medical center

With recent advances of MRI in abdominal imaging, improved performances on T2-weighted image and diffusion- weighted imaging (DWI) are achieved for pancreatic tumors. We hypothesized that diagnostic performance for detection of primary solid tumors of pancreas on noncontrast MRI with DWI could be sufficiently high and noncontrast MRI with DWI would be useful for pancreas screening. We conducted this study to determine the diagnostic performance of noncontrast MRI with DWI for detection of primary small (≤20mm) pancreatic solid tumors and prediction of ductal adenocarcinoma in comparison with pancreas CT and pancreas MRI with MR cholangiopancreatography.

2014

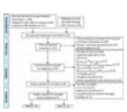

Gadoxetic acid disodium-enhanced magnetic resonance imaging for staging of liver fibrosis: a meta-analysis

Yuelang Zhang[1], Xiang Li[2], Haitian Liu[1], Chenxia Li[2], and Jian Yang [2]

[1]The First Hospital of Medical School, Xi'an Jiaotong University, Xi'an, People's Republic of China, [2]The First Hospital of Medical School, Xi'an Jiaoto, Xi'an, People's Republic of China

To collect and summarize parameters used by gadoxetic acid-enhanced MR imaging (GD-EOB-DTPA-enhanced MRI) for staging of liver fibrosis (LF) and evaluate diagnostic performance. A systematic literature search was performed in PubMed, Web of science, Embase and Medline database. Studies used frequently-used parameter were included. Pooled weighted mean difference (WMD) was applied to determine the clinical significance. Pooled sensitivity, specificity, and summary receiver operating characteristics (SROC) curve were calculated to evaluate diagnostic performance. Finally, 5 studies were included, and contrast enhancement index (CEI) was the most frequently-used parameter, which was considered to be an efficient biomarker in the staging of LF.

2015

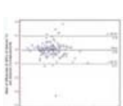

Apparent Diffusion Coefficient of Hepatocellular Carcinomas on Diffusion-Weighted Imaging: Correlation with Histopathologic Tumor Grade versus Arterial Vascularity during the Dynamic MRI

In Kyung Park[1], Jeong-Sik Yu[1], Eun-Suk Cho, Joo Hee Kim, and Jae Joon Chung

[1]Department of Radiology, Yonsei University Gangnam Severance Hospital, Seoul, Korea, Republic of

Depending on the difference of cellular densities related to the histopathologic grades of HCCs, some investigators have recently suggested apparent diffusion coefficient (ADC) on diffusion-weighted imaging (DWI) as an effective biomarker for the prediction of the patients' prognosis before the treatment of HCC. In the present study, ADCs of well- or poorly differentiated HCCs were lower than moderately differentiated HCCs; meanwhile the degree of arterial phase enhancement during the dynamic imaging rather well stratified the ADCs of the lesions. We concluded that ADC could not be independently used to estimate the histopathologic grades of HCCs.

2016

Quantification of liver fat after Gd-EOB-DTPA injection: a IDEAL-IQ feasibility study

Yuan Tian[1], Pengfei Liu[1], and Lizhi Xie[2]

[1]Department of MR, The First Affiliated Hospital of Harbin Medical University, Harbin, People's Republic of China, [2]GE HealthCare, MR Research China, Beijing, People's Republic of China

This article is to explore the feasibility of liver fat quantification via dynamic liver enhancement scanning after injection of Gd-EOB-DTPA. IDEAL-IQ was used to quantify liver fat in 65 patients who were injected with contrast. IDEAL-IQ was performed four times to determine the fat fraction (FF) and R2*. One-way repeated-measures analysis was conducted to evaluate the difference between the four time points of the FF. The assessment of FF at four time points in liver, spleen and spine showed no significant differences. However, after injection of contrast agent, R2* was increased, and the IDEAL-IQ result was relatively stable.

2017

A Preliminary Study of the Clinical Value of FM Model in Malignant Tumor of Liver

huang can[1]

[1]Department of Radiology, Beijing Chaoyang Hospital, Beijing, People's Republic of China

Several models have been proposed to explain the anomalous diffusion in biological tissues. Among them, the fractional motion (FM) model was considered more appropriate. In this study, the FM model was applied to assess its feasibility for diagnosing malignant tumors of liver. It was found that the FM model could improve the diagnostic accuracy in differentiation normal liver tissue and tumor lesion, indicating the potential of the FM model to facilitate future studies of pathological changes in clinical populations.

2018

Liver Iron Concentration determined with Gradient Echo MRI by Signal Intensity Ratio: Effects of Patient Characteristics

Arthur Peter Wunderlich[1,2], Holger Cario[3], Isabelle Tomczak[1], Meinrad Beer[1], and Stefan Andreas Schmidt[1]

[1]Diagnostic and Interventional Radiology, Ulm University, Medical Center, Ulm, Germany, [2]Section for Experimental Radiology, Ulm University, Medical Center, Ulm, Germany, [3]Department of Pediatrics and Adolescent Medicine, Ulm University, Medical Center, Ulm, Germany

To investigate the relation between signal intensity ratios gained from gradient echo (GRE) MRI and liver iron concentration (LIC), we studied the influence of patient characteristics. 168 patients (71 f, 97 m; 49 with Thalassemia major, 101 without Thalassemia) suspected for liver iron overload were scanned according to Ferriscan® with spin echo MRI to obtain reference LIC values, and GRE protocols suitable for LIC determination. GRE analysis by manually drawn liver and muscle ROIs yielded liver-to-muscle signal intensity ratios (SIR). Correlation analysis of ln (SIR) to reference LIC revealed differences between patient subgroups concerning disease, gender and age.

2019

Liver Iron Concentration determined by Gradient Echo MRI using Signal Intensity Ratios: Impact of Acquisition Parameters and Image Quality

Arthur Peter Wunderlich[1,2], Holger Cario[3], Isabelle Tomczak[1], Meinrad Beer[1], and Stefan Andreas Schmidt[1]

[1]Diagnostic and Interventional Radiology, Ulm University, Medical Center, Ulm, Germany, [2]Section for Experimental Radiology, Ulm University, Medical Center, Ulm, Germany, [3]Department of Pediatrics and Adolescent Medicine, Ulm University, Medical Center, Ulm, Germany

Tissue signal intensity ratio (SIR) has been used for a long time to determine liver iron concentration (LIC) based on gradient echo MRI. We studied the influence of acquisition parameters FA, RF spoiling and saturation regions, as well as image quality score, on the correlation of natural logarithm of SIR values to reference LIC obtained with spin echo. In our cohort of 85 patients, no significant influence on the slope of linear regression line was found, neither of acquisition protocol settings nor image quality, whereas the intercept was dependent on parameters influencing T_1 sensitivity, namely FA and RF spoiling.

2020

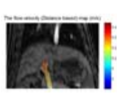

Vascular Input Function Correction with Inflow Relative Enhancement Quantification in Liver DCE-MRI

Jia Ning[1], Tilman Schubert[2,3], Huijun Chen[1], Chun Yuan[1,4], and Scott B Reeder[3,5,6,7,8]

[1]Center for Biomedical Imaging Research, Department of Biomedical Engineering, School of Medicine, Tsinghua University, Beijing, People's Republic of China, [2]Clinic for Radiology and Nuclear Medicine, Basel University Hospital, Basel, Switzerland, [3]Department of Radiology, University of Wisconsin-Madison, Madison, WI, United States, [4]Department of Radiology, University of Washington, Seattle, WA, United States, [5]Department of Medical Physics, University of Wisconsin-Madison, Madison, WI, United States, [6]Department of Biomedical Engineering, University of Wisconsin-Madison, Madison, WI, United States, [7]Department of Medicine, University of Wisconsin-Madison, Madison, WI, United States, [8]Department of Emergency Medicine, University of Wisconsin-Madison, Madison, WI, United States

Dynamic contrast enhanced magnetic resonance imaging (DCE-MRI) with pharmacokinetic modeling can help to quantify the perfusion and function of liver. The accurate pharmacokinetic modeling relies on the accurately and reliably captured vascular input function (VIF)s. However, due to the fast blood velocity, the blood in the large vessels including abdominal aorta and the main branch of the portal vein experiences only a limited number of excitations and hasn't reached a steady state. This introduces bias in the VIFs, and consecutively bias in pharmacokinetic parameters. In this study, we sought to correct the inflow effect on VIF acquisition in liver DCE-MRI.

2021 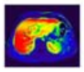

Gadoxetate disodium (Gd-EOB-DTPA) DCE-MRI of the Liver for the Assessment of Parenchymal Alterations in Primary Sclerosing Cholangitis

Sarah Keller[1], Jan Sedlacik[2], Fabian Kording[1], Gerhard Adam[1], Christoph Schramm[3], and Jin Yamamura[1]

[1]Diagnostic and Interventional Radiology and Nuclear Medicine, University Medical Center Hamburg Eppendorf, Hamburg, Germany, [2]Neuroradiology, University Medical Center Hamburg Eppendorf, Hamburg, Germany, [3]Internal Medicine, University Medical Center Hamburg Eppendorf, Hamburg

This study evaluates the feasibility of dynamic contrast-enhanced magnetic resonance imaging (DCE-MRI) with Gd-EOB-DTPA for detection of hepatic inflammation/fibrosis in comparison to Ultrasound elastography in primary sclerosing cholangitis (PSC).

2022 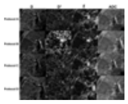

Evaluation of Intravoxel Incoherent Motion with Different b Values in Patients with Hepatocellular Carcinoma

Li Yang[1], Mengsu Zeng[2], Xuhao Song[2], Caixia Fu[3], and Xu Yan[3]

[1]Department of Radiology, Shanghai Institute of Medical Imaging, Zhongshan Hospital, Fudan University, Shanghai, People's Republic of China, [2]Department of Radiology, Zhongshan Hospital, Fudan University, [3]Siemens Healthcare, Shanghai, P.R. China

Intravoxel incoherent motion (IVIM) model provides both pure water motion and microcirculation by using multiple b values. IVIM imaging has been shown to be useful for assessment of liver diseases, including liver fibrosis and hepatocellular carcinoma. However, the clinical implementation of IVIM imaging is limited by long acquisition time. We compared IVIM imaging with different b-values to determine the combination of b-values in IVIM imaging that allows the relatively short acquisition time to obtain reproducible values of the IVIM parameters in patients with hepatocellular carcinoma. Our results showed at least 10b-values should be used in IVIM imaging for the assessment of hepatocellular carcinoma, and 5b-values IVIM imaging might increase errors in the perfusion-related f and D* values.

2023 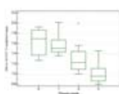

Pancreatic MRI associated with pancreatic fibrosis and postoperative fistula: comparison between pancreatic cancer and non-pancreatic cancer tissues

Yoshifumi Noda[1], Satoshi Goshima[1], Natsuko Suzui[2], Tatsuhiko Miyazaki[2], Kimihiro Kajita[1], Hiroshi Kawada[1], Nobuyuki Kawai[1], Hiromi Koyasu[1], and Masayuki Matsuo[1]

[1]Department of Radiology, Gifu University, Gifu, Japan, [2]Department of Pathology, Gifu University, Gifu, Japan

Pancreatic cancer (PC) occurs a histopathologically stronger pancreatic fibrosis compared to other non-PC. The risk factors of postoperative pancreatic fistula (POPF) were reported as soft or normal pancreatic parenchyma, and ampullary or duodenal disease. In this study, in patients with non-PC, frequency of POPF was greater due to lower grade of pancreatic fibrosis, and our results suggest that T1 signal and ADC value of the pancreas may link to the POPF. The T1 signal and ADC value of the pancreas may be a potentially useful imaging biomarker for the assessment of pancreatic fibrosis and POPF.

2024 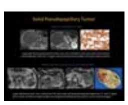

Magnetic Resonance Imaging: Solid Pseudopapillary Neoplasm of the Pancreas, Mimics and Histopathological Correlation

Nikhar Kinger[1], Peter Harri[1], Lauren F Alexander[1], Courtney Coursey Moreno[1], and Pardeep K Mittal[1]

[1]Department of Radiology and Imaging Sciences, Emory University School of Medicine, Atlanta, GA, United States

SPN is a rare epithelial neoplasm of low grade malignant potential for local and metastatic spread, occurring predominantly in young females. Differential diagnosis of SPN includes a wide spectrum of cystic and solid entities in the pancreas including pancreatic neuroendocrine, serous or mucinous cystadenoma or carcinoma, intrapancreatic splenules etc. Contrast enhanced MRI plays a key role in characterization of SPN and its mimics , helps to reach a specific diagnosis and narrows the differential, which is complimentary to EUS and biopsy when findings are equivocal to reach an accurate diagnosis which is of utmost importance for management and treatment planning

---

2025

Pancreatic changes in patients with liver cirrhosis and diabetes: a 3-T MRI evaluation

Tomohiro Sato[1], Katsuyoshi Ito[1], Tsutomu Tamada [1], Akira Yamamoto[1], and Akihiko Kanki[1]

[1]Radiology, Kawasaki Medical School, Kurashiki city, Japan

The liver plays a pivotal role in glucose metabolism, so 60-80% of patients with cirrhosis experience impaired glucose tolerance and hyperinsulinemia, and 10-50% develop diabetes. This study was intended to clarify the extent to which pancreatic MRI findings are affected by the presence of diabetes mellitus in patients with liver cirrhosis. On 3-T MRI, size of the pancreas was significantly increased, the grade of pancreatic lobulation was significantly reduced, and pancreatic SIRs on T2WI with fat suppression were significantly increased in cirrhotic patients complicated with diabetes as compared to cirrhotic patients without diabetes.

2026 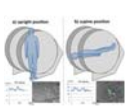

Evaluation of gravity effect on portal venous flow using multi-posture MRI

Yoshisuke Kadoya[1], Tosiaki Miyati[2], Naoki Ohno[2], Satoshi Kobayashi[2], and Toshifumi Gabata[1]

[1]Radiology, Kanazawa University Graduate School of Medicine, Kanazawa, Japan, [2]Division of Health Sciences, Kanazawa University Graduate School of Medical Sciences, Kanazawa, Japan

Portal venous flow (PVF) seems to be affected by gravity, ie., it depends on the body posture. We validated the effect of gravity on PVF in supine and upright positions using an original multi-posture MRI. We compared maximum PVF, PVF velocity, PVF volume, and cross-sectional area of portal vein between supine and upright positions. The mean PVF velocity, PVF volume, maximum PVF, and cross-sectional area in the upright position were significantly lower than those in the supine position. Gravity reduces PVF velocity and volume, and these differences between postures potentially provide new diagnostic information.

2027 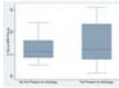 Pre-operative MRI quantification of hepatic fat and its correlation with histology, BMI and length of peri-operative stay following resection of liver metastases

Davinia Ryan[1], Alessandra Borgheresi[1], Simone Krebs[1], Sarah Eskreis-Winkler[1], and Lorenzo Mannelli[1]

[1]Department of Radiology, Memorial Sloan Kettering Cancer Center, New York, NY, United States

We correlate pre-operative quantification of hepatic fat on MRI in patients with colorectal cancer metastatic to the liver with the presence of fat on histology of the resected specimen, patient BMI and hospital length of stay.

2028  The effects of a 2 week hyperenergetic high carbohydrate or high fat diet on subcutaneous, visceral fat and metabolism

Mehri kaviani [1], Carolyn Chee[2], Caroline Hoad[1], Stephen Bawden[1,3], Peter Mansell[2], Sally Cordon[2], Aithal Guruprasad[3], Ian Macdonald[2], and Penny Gowland[1]

[1]Sir Peter Mansfield Imaging Centre,Physics and Astronomy, Nottingham University, Nottingham, United Kingdom, [2]School of Life Sciences, Nottingham University, Nottingham, United Kingdom, [3]NIHR Nottingham Digestive Diseases Biomedical Research Unit, Nottingham University Hospitals NHS Trust and University of Nottingham

With the rise in obesity globally, there is great interest in quantifying body composition and in particular metabolically active visceral adipose tissue (VAT). Increased accumulation of VAT has been linked with an increase in risk factors for cerebrovascular disease and Type 2 Diabetes (T2DM) . We investigated the degree to which weight, subcutaneous fat visceral fat, liver and lipid markers are affected by 2 weeks of overfeeding at 25% excess energy given as either carbohydrate or fat. 2 weeks of 25% excess energy overfeeding of either carbohydrate of fat does not alter subcutaneous or visceral abdominal fat in line with no changes in weight. MRI measurements of SAT and VAT can be used in longitudinal studies of diet to ascertain any changes in abdominal body fat deposition.

2029  Liver T1rho detects liver fibrosis without impact of fatty liver in patients with chronic hepatitis B: a prospective study

shuangshuang xie[1], qing li[1], zhizheng zhuo[2], yu zhang[2], yue cheng[1], and wen shen[1]

[1]Tianjin First Center Hospital, Tianjin, People's Republic of China, [2]Philips healthcare, Beijing, People's Republic of China

This study investigated the merit of liver T1rho values for detecting fibrosis in patients with chronic hepatitis B and the potential impact of fatty liver on T1rho measurements. Eighteen healthy control subjects, eighteen patients with clinically diagnosed simple fatty and eighteen with liver fibrosis were underwent T1rho MRI and mDIXON-Quant. Mean T1rho values and fat fraction (FF) were compared among the three groups. Receiver operating characteristic (ROC) curve analysis was performed to evaluate the merit of T1rho values for detecting liver fibrosis. T1rho values were correlated with FF and clinical data. Our results showed significant differences in T1rho values among the three groups and T1rho had moderate diagnostic efficacy to detect fibrosis. T1rho values were not correlated with FF, subject age, or body mass index. We conclude liver T1rho values can be used as a MR biomarker for liver fibrosis and are not influenced by fatty liver severity.

2030  Diffusion-Weighted Imaging and Variable Flip Angle T1 Mapping in Progression Assessment of Liver Fibrosis Caused by Hepatitis B Virus Infection: A longitudinal study

Peng Hu[1], Jihong Sun, Fangfang Lv, Borui Pi, Fangping Xu, Guocan Han, Xi Hu, Yue Wang, Ning Huang, Xia Wu, Yong Zhang, Jun Yang, Peipei Pang, and Xiaoming Yang

[1]Department of Radiology, Sir Run Run Shaw Hospital, Zhejiang University School of Medicine, Hangzhou, People's Republic of China

Liver fibrosis caused by Hepatitis B virus (HBV) is a worldwide health problem. However, liver biopsy as the gold standard of diagnosing and evaluating therapy of liver fibrosis is an invasive examination with possible errors from sampling and intra- and inter-observer interpretation (1, 2). The non-invasive MRI may be a promising modality to evaluate the liver fibrosis. We used diffusion-weighted imaging (DWI) and variable flip angle (VFA) T1 mapping to explore the progression of liver fibrosis caused by HBV infection in a longitudinal study.

Traditional Poster

Body Imaging Novel Techniques & Indications

Exhibition Hall 2031-2063 Wednesday 8:15 - 10:15

2031  Effect of fitting model on the accuracy of T2 and T2* magnetic resonance based liver iron concentration

Tiffany Lin[1], Shirong Zhang[1], Michael Liu[1], and Sachin Jambawalikar[1]

[1]Radiology, Columbia University, New York, NY, United States

Literature has suggested mixed results regarding agreement between T2 relaxivity based liver iron concentration (LIC) and T2* relaxivity based LIC The purpose of the following study is to determine whether or not choice of relaxivity fitting models will impact the agreement of the results.

2032 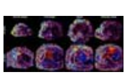 Comparison of 2D and 3D Magnetic Resonance Elastography (MRE) Wave-Image Quality Across a Range of Body Mass Indices

Yesenia Covarrubias[1], Jonathan C Hooker[1], Ethan Z Sy[1], Saya Igarashi[1], Jennifer Cui[1], Cheng William Hong[1], Nikolaus Szeverenyi[1], Jeffrey B Schwimmer[2,3], Rohit Loomba[4], Scott B Reeder[5,6,7,8,9], Kevin Glaser[10], Meng Ying[10], Richard Ehman[10], and Claude B Sirlin[1]

[1]Radiology, Liver Imaging Group, University of California, San Diego, San Diego, CA, San Diego, CA, United States, [2]Division of Gastroenterology, Hepatology, and Nutrition, Department of Pediatrics, University of California, San Diego, San Diego, CA, [3]Gastroenterology, Rady Children's Hospital San Diego, San Diego, CA, [4]NAFLD Translational Research Unit, Division of Gastroenterology, University of California, San Diego, La Jolla, CA, [5]Radiology, University of Wisconsin - Madison, Madison, WI, [6]Medical Physics, University of Wisconsin - Madison, Madison, WI, [7]Biomedical Engineering, University of Wisconsin - Madison, Madison, WI, [8]Medicine, University of Wisconsin - Madison, Madison, WI, [9]Emergency Medicine, University of Wisconsin - Madison, Madison, WI, [10]Radiology, Mayo Clinic, Rochester, MN

This analysis of 129 adults compared the wave-image quality of two-dimensional (2D) and three-dimensional (3D) magnetic resonance elastography (MRE) across a range of body mass indices (BMIs). Wave-image quality of each scan was measured quantitatively by region of interest (ROI) areas. We found that 3D MRE provides higher wave-image quality compared to 2D MRE and that wave-image quality was not statistically associated with BMI (p=0.3422). Further research with larger BMI cohorts is needed to confirm our findings.

2033

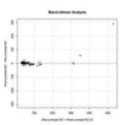

Gadolinium-enhanced high-flip-angle R2* mapping enables estimation of a greater range of R2* values

Jonathan Hooker[1], Yesenia Covarrubias[1], Cheng William Hong[1], Soudabeh Fazeli Dehkordy[1], Adrija Mamidipalli[1], Ethan Z Sy[1], Gavin Hamilton[1], and Claude B Sirlin[1]

[1]Liver Imaging Group, Department of Radiology, University of California, San Diego School of Medicine, San Diego, CA, United States

The range of R2* values estimated from MR sequences using low flip angles (FA) is limited by the background signal decay. The administration of contrast allows the use of higher FAs and increases the signal to noise ratio (SNR), allowing the estimation of a greater range of R2* values. We compared pre- and post-contrast R2* values in 158 patients and observed large discrepancies at R2* values greater than 300s^{-1}. Our findings suggest that in patients with severe iron overload, post-contrast high-FA R2* mapping may be the preferred sequence for iron quantification.

2034

Comprehensive dynamic contrast-enhanced 3D MR imaging of the breast with fat/water separation and high spatiotemporal resolution using Dixon Radial Volumetric Encoding (Dixon-RAVE)

Thomas Benkert[1,2], Kai Tobias Block[1,2], Samantha Heller[1,2], Melanie Moccaldi[1,2], Daniel K Sodickson[1,2], Sungheon Gene Kim[1,2], and Linda Moy[2]

[1]Center for Advanced Imaging Innovation and Research (CAI2R), Department of Radiology, New York University School of Medicine, New York, NY, United States, [2]Bernard and Irene Schwartz Center for Biomedical Imaging, Department of Radiology, New York University School of Medicine, New York, NY, United States

Conventional clinical breast MRI consists of several separate T_1-weighted scans, including both pre-contrast fat-suppressed and non-fat-suppressed acquisitions as well as the acquisition of dynamic contrast-enhanced phases.

Here, we show how this entire exam can be replaced by a single comprehensive scan, therefore reducing overall scan time and simplifying the clinical workflow. This is achieved by using radial stack-of-stars sampling in combination with a model-based fat/water separation technique, which takes into account the off-resonant blurring of fat and integrates both compressed sensing and parallel imaging. The approach is validated in 24 patients and results were evaluated by two radiologists.

2035

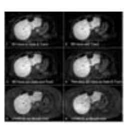

Free-Breathing Hepatobiliary Phase Imaging: Comparison of Five Free-Breathing Scans with Conventional Breath Hold Scan

Kimihiro Kajita[1], Satoshi Goshima[1], Yoshifumi Noda[1], Hiroshi Kawada[1], Tomoyuki Okuaki[2], Masatoshi Honda[3], Nobuyuki Kawai[1], Hiromi Koyasu[1], and Masayuki Matsuo[1]

[1]Radiology, Gifu University Hospital, Gifu City, Japan, [2]Philips Healthcare, Tokyo, Japan, [3]Philips Electronics Japan, Tokyo, Japan

We applied five free-breathing scan sequences to gadoxetic acid-enhanced hepatobiliary phase imaging. Breath hold eTHRIVE demonstrated the highest SNR on the liver, although it is also revealed the disadvantage for the patients with unstable breath hold. On the other hand, free-breathing 3D VANE with gate and track demonstrated the highest image quality with equivalent SNR to breath hold eTHRIVE. It is notable that free-breathing 3D VANE produced steady and effective image quality for all patients regardless of breath hold ability.

2036

BOLD MRI of Activated Human Pancreas

Bozhu Chen[1], Jian He, and Zhengyang Zhou

[1]Radiology, Drum Tower Hospital, the Affiliated Hospital of Nanjing University Medical School, Nanjing, People's Republic of China

Glucose ingestion activates the pancreatic functions and increases the oxygen consumption, we hypothesized that BOLD MRI could detect the alterations during the glucose challenge. BOLD MRI was performed in 12 volunteers before and after glucose ingestion. A transient but significant decrease in pancreatic T2* values was observed after glucose ingestion. BOLD MRI may serve as a non-invasive tool to detect the activation of human pancreas.

2037

Intravoxel incoherent motion (IVIM) and diffusion kurtosis imaging (DKI) for differential diagnosing hepatocellular carcinoma (HCC) from hepatic hemangioma (HHA).

Ye Ju[1], Ailian Liu[1], Qingwei Song[1], Meiyu Sun[1], Lihua Chen[1], and Lizhi Xie[2]

[1]The First Affiliated Hospital of Dalian Medical University, Dalian, People's Republic of China, [2]MR Research, GE Healthcare, Beijing, People's Republic of China

Intravoxel incoherent motion (IVIM) imaging is an extension of diffusion weighted imaging (DWI) that can be used to investigate both diffusion and perfusion changes in tissues. DKI adapts a kurtosis based model to depict the non-Gaussian diffusion process, which could be caused by the presence of different barriers in cellular complex structures (e.g. cell membranes and organelle compartments).Initial application of DKI focused on neuroimaging, Recently, it has also been reported that DKI may help to assess response to treatment in HCC. Comparing the IVIM and DKI parameters between carcinoma (HCC) and hepatic hemangioma(HHA) we found that IVIM and DKI can supply many meritorious parameters, combining with the IVIM and DKI may help in increasing the sensitivity and specificity of antidiastole.

2038

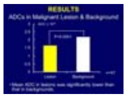

Abstract Fast Advanced Spin Echo Diffusion-Weighted Imaging

Takeshi Yoshikawa[1], Katsusuke Kyotani[2], Yoshimori Kassai[3], Kouya Nishiyama[2], Shinichiro Seki[1], Yuji Kishida[4], and Yoshiharu Ohno[1]

[1]Advanced Biomedical Imaging Research Center, Kobe University Graduate School of Medicine, Kobe, Japan, [2]Center of Radiology and Radiation Oncology, Kobe University Hospital, Kobe, Japan, [3]Toshiba Medical Systems Corporation, Otawara, Japan, [4]Radiology, Kobe University Graduate School of Medicine, Kobe, Japan

To reduce distortion on abdominal EPI-DWI, we developed Fast Advanced Spin Echo (FASE)-DWI for abdominal 3T imaging. FASE-DWI improved distortion and showed equivalent diagnostic performance and be used as an alternative to EPI-DWI.

2039

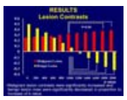

Computed Diffusion-Weighted Image for Abdominal MRI

Takeshi Yoshikawa[1], Katsusuke Kyotani[2], Yoshimori Kassai[3], Kouya Nishiyama[2], Shinichiro Seki[1], Yuji Kishida[4], and Yoshiharu Ohno[1]

[1]Advanced Biomedical Imaging Research Center, Kobe University Graduate School of Medicine, Kobe, Japan, [2]Center of Radiology and Radiation Oncology, Kobe University Hospital, Kobe, Japan, [3]Toshiba Medical Systems Corporation, Otawara, Japan, [4]Radiology, Kobe University Graduate School of Medicine, Kobe, Japan

The purpose of this study was to assess capability of computed DWI in evaluation of various abdominal diseases. We found cDWI can improve image quality and malignant lesion contrast, conspicuity, and detection. cDWI is a useful post-processing tool for abdominal MRI.

2040

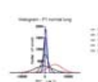

Optimisation for Pulmonary R2* Quantification and Repeatability Evaluation

Alex Weller[1], Matthew Orton[1], David Collins[1], James D'Arcy[1], and Nandita de-Souza[1]

[1]Radiotherapy and Imaging, The Institute of Cancer Research, Surrey, United Kingdom

In 5 patients with lung cancer, UTE-MRI was used to derive pulmonary R2* in lung and establish its repeatability. Plausible R2* values were obtained only when using TEs of 0.08 and 0.2 ms: higher TEs produced implausible mean negative R2* within individual patients and a cohort R2* not significantly different from zero, due to lack of signal decay beyond TE=0.2ms. Pulmonary R2* values derived using TEs of 0.08 and 0.2ms were higher than prior reports where longer echo-times were employed. Test-retest limits-of-agreement were +90.5%to -47.5% indicating that a 90% increase in R2*is required post-radiotherapy to reliably demonstrate radiation-induced change.

2041

Initial Experience of MR Elastography Using Spatially Selective Excitation for the Pancreas.

Yohei Itoh[1], Yasuo Takehara[2], Naoki Ooishi[3], Masataka Sugiyama[1], Ikumi Igarashi[1], Maho Hayashi[1], Satoshi Usami[1], Takasuke Ushio[1], Yuki Hirai[1], Nobuko Yoshizawa[1], Shuhei Yamashita[1], Hatsuko Nasu[1], Tetsuya Wakayama[4], Atsushi Nozaki[4], Hiroyuki Kabasawa[4], and Harumi Sakahara[1]

[1]Diagnostic Radiology & Nuclear Medicine, Hamamatsu University school of Medicine, Shizuoka, Japan, [2]Fundamental Development for Advanced Low Invasive Diagnostic Imaging, Nagoya University Graduate School of Medicine, Nagoya, Japan, [3]Radiology, Hamamatsu University Hospital, Shizuoka, Japan, [4]GE Healthcare Japan, Tokyo, Japan

We tried reduced-FOV MR elastography using a local excitation technique called FOCUS for the pancreas. Comparing conventional-MRE with FOCUS-MRE, there was no significant differences of the measurable are of pancreas. In both methods, the higher the body mass index was, the smaller the measurable area of the pancreas.

2042

Test-Retest Repeatability of MR Elastography (MRE) Stiffness Measurements of Liver Phantoms

Jun Chen[1], Phillip J Rossman[1], Kevin J Glaser[1], and Richard L Ehman[1]

[1]Radiology, Mayo Clinic, Rochester, MN, United States

All the previous test-retest human liver MRE studies could involve physiological stiffness change . In this study, our goal was to evaluate MRE test-retest repeatability with liver phantoms to avoid the possible influence of physiological changes in humans. We hypothesized that the variations of test-retest MRE stiffness measurements of phantoms were smaller than that of human livers.

2043

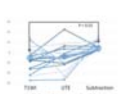

The assessment of gallstones using three dimensional ultra-short echo time in vivo

Mamoru Takahashi[1], Yasuo Takehara[2], Norihiro Tooyama[1], Katsutoshi Ichijo[1], Tomoyasu Amano[3], Takuya Matsumoto[3], Tomoyuki Okuaki[4], Yukiko Fukuma[4], and Harumi Sakahara[5]

[1]Radiology, Seirei Mikatahara General Hospital, Hamamatsu, Japan, [2]Fundamental Development for Advanced Low Invasive Diagnostic Imaging, Nagoya University, Graduate School of Medicine, [3]Seirei Mikatahara General Hospital, Hamamatsu, Japan, [4]Philips Electronics Japan, Ltd., Tokyo, Japan, [5]Radiology, Hamamatsu University School of Medicine, Hamamatsu, Japan

First clinical study using 3D dual echo UTE sequence for suspected gall stone patients was performed. All gallstones were able to be detected as positive signal in-vivo. Our study may indicate that UTE has an added value of depicting impacted stones or hepatolithiasis as positive signal.

2044 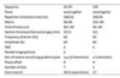

Magnetic resonance elastography for uterine fibroids

Yoshie Omiya[1], Shintaro Ichikawa[1], Utaroh Motosugi[1], and Hiroshi Onishi[1]

[1]*University of Yamanashi, Chuo, Japan*

We evaluated the feasibility of magnetic resonance elastography (MRE) for uterine fibroids and the effect of imaging sequences (i.e., spin-echo echo-planar imaging [SE-EPI] and gradient-echo [GRE]) on stiffness measurements. All MRE were performed in two cross-sectional planes (i.e., axial and sagittal). SE-EPI-MRE showed lower fibroid stiffness values than GRE-MRE. Each MRE method is a valid and reliable technique for measuring the stiffness of uterine fibroids.

2045 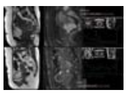

MRI to evaluate the response of the locally advanced cervical cancer to CCRT: MRS(magnetic resonance spectroscopy), DWI(diffusion weighted image), and T2WI

Byung Chul Kang[1] and Hye Ran Hyun[2]

[1]*Radiology, Mokdong Hsopital, EWUMC, Seoul, Korea, Republic of,* [2]*Radiology, Mokdong Hospital, EWUMC, Seoul, Korea, Republic of*

MRS(MR Spectroscopy) as well as T2Wi, and diffusion weighted images may be used to evaluate the response of LACC to CCRT.

2046

Comparative analysis of image in changing breath hold method of B1 calibration at 3.0T abdomen MRI

Cho Ja Ryong[1], Park Jong Bin[2], and Cho Seoung Bong [2]

[1]*Radiology, Seoul National University Bundang hospital, Gyeonggi-do, Korea, Republic of,* [2]*Radiology, Seoul National University Bundang Hospital, Seongnam, Korea, Republic of*

Evaluation of image analysis according to changing breath hold methods of B1 calibration .

2047 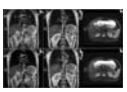

Using 2D-PACE to trigger scan and supervise motion on Breath-Hold imaging

Qiong Zhang[1] and Yuanyuan Kang[1]

[1]*Siemens Shenzhen Magnetic Resonance Ltd, Shen Zhen, People's Republic of China*

A simple 2D pace module was implemented in a Breath-Hold imaging work flow to trigger the normal scan and supervise the motion. Our preliminary experiments show that within the newly added module, images are more immune to respiratory motion artifacts and the detail of small structures are clearer.

2048 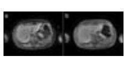

Quiet Motion-Robust Technique for 4D T1-Weighted Fat-Suppressed Abdominal Imaging

Ty A. Cashen[1], Naoyuki Takei[2], Kang Wang[1], Tao Zhang[3], Lloyd D. Estkowski[4], and Ersin Bayram[3]

[1]*Global MR Applications and Workflow, GE Healthcare, Madison, WI, United States,* [2]*Global MR Applications and Workflow, GE Healthcare, Hino, Japan,* [3]*Global MR Applications and Workflow, GE Healthcare, Houston, TX, United States,* [4]*Global MR Applications and Workflow, GE Healthcare, Menlo Park, CA, United States*

Acoustic noise generated by MR systems represents one of the major barriers to patient comfort, particularly for the pediatric population. Reducing the slew rate of the gradient field is one way to effectively decrease acoustic noise; however, this comes at the expense of scan time. For breath-hold abdominal imaging, longer scan times mean a more stressful breath-hold for the patient, reduce temporal resolution for multi-phase imaging, and may allow for more motion artifact due to suboptimal breath-holding. This work describes an accelerated 3D multi-phase technique compatible with fat saturation for both quiet and motion-robust abdominal imaging.

2049 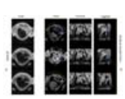

High-resolution 3D lung 1H-MRI in rodents at 9.4T with an optimized multi-echo gradient echo sequence

Dhaval B Shah[1], Nicola Bertolino[1], Marilena Preda[2], Robert Zivadinov[1,2], and Ferdinand Schweser[1,2]

[1]*Buffalo Neuroimaging Analysis Center, Department of Neurology, Jacobs School of Medicine and Biomedical Sciences, University at Buffalo, The State University of New York, Buffalo, NY, United States,* [2]*MRI Clinical and Translational Research Center, Jacobs School of Medicine and Biomedical Sciences, University at Buffalo, The State University of New York, Buffalo, NY, United States*

Preclinical MR lung imaging has been challenging due to lower tissue density compared to other organs. Current practice has been 2D spin-echo or gradient echo with relatively lower resolution. In this work we present an optimized high resolution 3D Multi Gradient Echo and demonstrate the results by comparing it with state of the art 2D Gradient echo.

2050 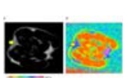

Receiver operating characteristic analysis of fat-fraction is effective in differentiating identifying an optimal threshold to differentiate between brown and white adipose tissue ex vivo and in situ in rats using 3-point IDEAL MRI

Terence Jones[1,2], Narendra Reddy[3], Sarah Wayte[4], Thomas Barber[2,3], and Charles Edward Hutchinson[1,2]

[1]Department of Radiology, University Hospitals Coventry & Warwickshire NHS Trust, Birmingham, United Kingdom, [2]Warwick Medical School, University of Warwick, Coventry, United Kingdom, [3]Department of Endocrinology, University Hospitals Coventry & Warwickshire NHS Trust, Birmingham, United Kingdom, [4]Medical Physics, University Hospitals Coventry & Warwickshire NHS Trust, Coventry, United Kingdom*

Brown adipose tissue (BAT) has lower fat content than white adipose tissue (WAT), which has been exploited using Dixon-based MRI to identify BAT. We sought to identify the optimal threshold to differentiate between BAT and WAT in rats on the basis of fat fraction.

Fat fraction within BAT was significantly lower than WAT in rodents. Receiver operating characteristic analysis showed that differentiating BAT and WAT on the basis of fat fraction had excellent accuracy in both *ex vivo* and *in situ*. The optimal cut-off to separate BAT and WAT was significantly lower in rats exposed to cold, likely secondary to lipolysis.

2051

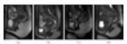

Cyclic Changes of the Boundary Sharpness of Uterine Zonal Structures Visualized by High-resolution T2-weighted Images in Young and Middle-aged Females during the Menstrual Cycle

Yong-Lan He[1], Ning Ding[1], Ya-Fei Qi[1], Tianyi Qian[2], Yuan Li[3], Huadan Xue[1], and Zhengyu Jin[1]

[1]Radiology, Peking Union Medical College Hospital, Beijing, People's Republic of China, [2]2. MR Collaboration NE Asia, Siemens Healthcare, Beijing, People's Republic of China, [3]OB&GYN, Peking Union Medical College Hospital, Beijing, People's Republic of China

This study aimed to demonstrate the cyclic changes of the boundary sharpness of uterine three zonal structures of young and middle-aged women on 3T using a 3D T2-weighted SPACE sequence during the menstrual cycle. Peri-ovulatory phase exhibited the clearest boundary sharpness of corpus zonal structures following by FP, LP and MP, while that of the cervix were almost well-defined during the menstrual cycle.

2052

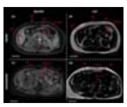

Resistance and susceptibility to diabetes - characterising the ‘Thin on the Outside Fat on the Inside’ (TOFI) profile using magnetic resonance imaging: a pilot study in Asian and Caucasian women

Ivana R Sequeira[1], Wilson Yip[1], Louise WW Lu[1], Reza Nemati[2], Dech Dokpuang[2], Jun Lu[2], and Sally D Poppitt[1]

[1]Human Nutrition Unit, School of Biological Sciences, University of Auckland, Auckland, New Zealand, [2]Faculty of Health and Environmental Sciences, Auckland University of Technology, Auckland, New Zealand

Prediction of risk for dysglycaemia and adverse metabolic health is difficult, with some outwardly lean individuals having greater susceptibility to type 2 diabetes (T2D) than obese resilient individuals. Using 3T MR Imaging and spectroscopy we showed, in 10 Asian Chinese and 6 European Caucasian healthy or prediabetic women (18 – 70 years and BMI 25 – 50 kg/m^2), that greater storage of fat within riskier ectopic sites, i.e. pancreas and liver, may in part explain the reported increased risk of T2D in Asian Chinese populations compared to their Caucasian counterparts at the same BMI and younger age.

2053

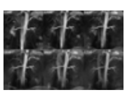

Parameter Optimization for Non-contrast-enhanced Renal MR Angiography and Its Age-dependent Preliminary Study

Wansha Wu[1], Ke Ren[1], Jiannan Shang[1], Wenge Sun[1], Yi Liu[1], Songbai Li[1], and Ke Xu[1]

[1]the First Hospital of China Medical University, Shenyang, People's Republic of China

Our purpose was to investigate the feasibility of NCE-MRA using Time-SLIP technique on healthy volunteers by determining the optimized TI value and its preliminary relationship with age as well. 61 healthy volunteers were recruited and divided into two age groups. The acquired data using six differernt TIs sequences were measured and analyzed to get three parameters including VKR, grade of renal artery branches and grade of imaging quality. In conclusion, the Time-SLIP technique is able to obtain renal MR angiography with optimized TI value 1500ms. Moreover, the age of individual subjects can affect the optimized TI value.

2054

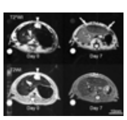

A new technique of SPIO-enhanced MRI: delayed recovery of T2*-weighted signal intensity as a novel diagnostic marker for visualization of irradiated liver parenchyma.

Toshihiro Furuta[1,2], Masayuki Yamaguchi[1], Manabu Minami[3], Osamu Abe[2], and Hirofumi Fujii[1]

[1]Division of Functional Imaging, Exploratory Oncology Research & Clinical Trial Center, National Cancer Center, Kashiwa, Japan, [2]Department of Radiology, Graduate School of Medicine, University of Tokyo, Tokyo, Japan, [3]Department of Radiology, Graduate School of Comprehensive Human Sciences, University of Tsukuba, Tsukuba, Japan

Visualization of irradiated liver parenchyma may assist safety margin assessment in radiotherapy. We demonstrate that an MR imaging technique has the ability to visualize irradiated liver parenchyma after 30-Gy irradiation in a tumor-bearing rat model. In this technique, superparamagnetic iron oxide (SPIO) is administered to label Kupffer cells (KCs) before, rather than after irradiation. A dose of 30-Gy is a lower, more clinically relevant dose than that used in the previous studies. Our results suggest that 30-Gy irradiation delays the recovery of hepatic T2*-weighted signal after SPIO administration. Presumably, irradiation delays degradation process of SPIO in the KCs.

2055

Changes in fat distribution and composition during ketogenic diet investigated by MRI and MRS.

Martin Buechert[1], Thomas Lange[1], Peter Deibert[2], and Paul Urbain[3]

[1]Medical Physics, Department of Radiology, Medical Center – University of Freiburg, Freiburg, Germany, [2]Medical Center – University of Freiburg, Freiburg, Germany, [3]Department of Medicine I, Section of Clinical Nutrition and Dietetics, Medical Center – University of Freiburg, Freiburg, Germany

Changes in fat distribution and composition during ketonic diet were investigated in a sub group of twelve volunteers of a larger study. Liver fat concentrations in the examined cohort turned out to be surprisingly low compared to patient cohorts with similar BMI measured in other studies. The hypotheses that intra-hepatic fat may be reduced during a ketogenic diet could not be confirmed. However the composition of the sub group may have biased the outcome. While the MRI protocol and analysis worked well, MRS analysis of data acquired with the given protocol in subjects with low hepatic fat reaches its limitations.

2056

Ethnic variation in body composition of men with type 2 diabetes from automated analysis of Dixon MRI

Haris Shuaib[1], Brandon Whitcher[2], Kevin Keraudren[2], David Greer[2], Geoff Charles-Edwards[1,3], and Louise M Goff[4]

[1]Guy's & St. Thomas NHS Foundation Trust, London, United Kingdom, [2]Klarismo Ltd, [3]Division of Imaging Sciences and Biomedical Engineering, King's College London, London, United Kingdom, [4]Diabetes & Nutritional Sciences Division, King's College London, London, United Kingdom

This work explores the role of body composition and its relationship with the development of type 2 diabetes in White European and Black African men. An investigation of differences in body composition between these two groups was performed via automated image segmentation and analysis of Dixon MR images. Our initial results suggest visceral adipose tissue may not be a principal determinant in the development of type 2 diabetes in Black African men as it is with White European men.

2057

Quantitative MRI parameters for adipose tissue characterization in obese patients

Nikita Garnov[1,2], Stefanie Lehmann[2], Ulf Retschlag[2], Nicolas Linder[1,2], Alexander Schaudinn[1,2], Arne Dietrich[2,3], Andreas Oberbach[2], Thomas Kahn[1], and Harald Busse[1]

[1]Diagnostic and Interventional Radiology, Leipzig University Hospital, Leipzig, Germany, [2]Integrated Research and Treatment Center (IFB) AdiposityDiseases, Leipzig University Medical Center, Leipzig, Germany, [3]Department of Visceral, Transplantation, Thoracic and Vascular Surgery, Division of Bariatric Surgery, Leipzig University Hospital, Leipzig, Germany

In obesity research and clinical practice, disease progress or response to therapy is typically evaluated by the reduction of body weight, adipose tissue (AT) volume or comorbidity remission rates. However, little is currently known about therapy-induced changes in subcutaneous and visceral AT composition and how to quantify them. Lean control subjects had recently been shown to have significantly higher T1 relaxation times in both SAT (301 ms) and VAT (360 ms) than severely obese patients (275 and 294 ms, respectively). Aims of this study were to characterize AT by quantitative MRI and evaluate the intra-individual changes at two time points.

2058

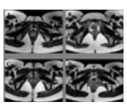

The investigation of the relationship between obstetrical risk factors and pelvic floor injuries: a MRI-based study

Limei Guo[1], Yujiao Zhao[1], Zhizheng Zhuo[1], and Wen Shen[1]

[1]Tianjin First Center Clinical College, Tianjin, People's Republic of China

Vaginal childbirth is an important cause to pelvic floor injuries. In this study, we aim to identify various forms of the injuries and the association with obstetrical risk factors in primiparous women. The results showed that there were significant differences about the proportions of various patterns of the pelvic floor injuries and the severity of LAM injuries between the groups with and without obstetrical risk factors.

2059

Phosphorus MRSI reveals subtle changes in metabolic profile of hepatic tissue in insulin resistant population.

Lorenz Pfleger[1,2], Peter Wolf[1], Martin Gajdošík[1,2], Sabina Smajiš[1], Marek Chmelík[3], Anton Luger[1], Siegfried Trattnig[2], Michael Krebs[1], and Martin Krššák[1,2]

[1]Endocrinology & Metabolism, Internal Medicine III, Medical University of Vienna, Wien, Austria, [2]High-field MR Centre, Department of Biomedical Imaging and Image-guided Therapy, Medical University of Vienna, Wien, Austria, [3]Clinical Molecular Imaging, Karl Landsteiner Institute, Wien, Austria

This study employed ultra-high field (7T) ^{1}H and ^{31}P MRS for the characterization of subtle hepatic tissue changes in insulin sensitive and insulin resistant group of healthy volunteers. Hepatic lipids, the forward rate of ATP synthesis and profile of metabolites containing ^{31}P were assessed. Decreased inorganic phosphate was found in the subgroup of volunteers with increased hepatic fat accumulation and increased phosphocholine was found in the insulin sensitive subgroup. Concentration of ^{31}P containing metabolites found here are well within the range of previous publications and subtle differences point towards their role in pathophysiology of metabolic syndrome and/or hepatic steatosis.

2060

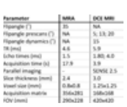

Renal perfusion is decreased in kidneys with multiple renal arteries as demonstrated by renal DCE MRI

Anneloes de Boer[1], Margreet F. Sanders[2], Nico van den Berg[1], Peter J. Blankestijn[2], and Tim Leiner[3]

[1]Center for Image Sciences, University Medical Center Utrecht, Utrecht, Netherlands, [2]Nephrology, University Medical Center Utrecht, Utrecht, Netherlands, [3]Radiology, University Medical Center Utrecht, Utrecht, Netherlands

The presence of multiple renal arteries per kidney is associated with hypertension. The smaller vessel diameter is thought to lead to decreased renal perfusion, which activates the renin-angiotensin-aldosterone system (RAAS), resulting in increased systemic blood pressure. We measured renal blood flow (RBF) using dynamic contrast enhanced (DCE) MRI to investigate the relation between number of renal arteries, RAAS activity and RBF. The number of renal arteries was associated with reduced RBF and increased RAAS activity. In all patients, we observed that reduced RBF was associated with increased RAAS activity.

2061

Development of a lesion-wise metric for evaluation of predictive models of prostate cancer on multiparametric MRI

Ethan Leng[1], Jin Jin[2], Lin Zhang[2], Joseph S. Koopmeiners[2], and Gregory J. Metzger[1]

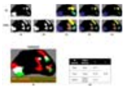

[1]Center for Magnetic Resonance Research, University of Minnesota, Minneapolis, MN, United States, [2]Division of Biostatistics, School of Public Health, University of Minnesota, Minneapolis, MN

A novel lesion-wise metric was developed to evaluate the quality of predictive models of prostate cancer that use quantitative multiparametric MR data to perform prediction on a voxel-wise basis. The metric is based on the Jaccard similarity coefficient and emphasizes overlap and co-localization of ground truth and predicted lesions. Experiments to characterize the metric demonstrated that it qualitatively reflected the goodness of predictions and was more accurate and informative than voxel-wise measures of sensitivity and specificity. We propose that the metric may be customized to select the best predictive models for specific clinical applications such as performing targeted prostate biopsies.

2062

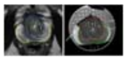

Why is the Peripheral Zone of the Normal Human Prostate High in ADC Value and T2-Weighted Signal Intensity?

Edward William Johnston[1], Colleen Bailey[2], Elisenda Bonet-Carne[2], Hayley Pye[3], Susan Heavey[3], Dominic Patel[4], Ashwin Sridhar[5], Bernard Siow[6], Thomy Mertzanidou[2], William Devine[1], Jagadish Kalasthry[1], Joey Clemente[1], David Hawkes[2], Hayley Whitaker[3], Manuel Rodriguez-Justo[4], Greg Shaw[5], Daniel Alexander[2], Alexander Freeman[4], Roger Bourne[7], Eleftheria Panagiotaki[2], and Shonit Punwani[1]

[1]Centre for Medical Imaging, University College London, London, United Kingdom, [2]Centre for Medical Image Computing, University College London, London, United Kingdom, [3]Research Department for Tissue & Energy, University College London, London, United Kingdom, [4]Department of Pathology, University College London Hospital, University Street, United Kingdom, [5]Department of Urology, University College London Hospital, London, United Kingdom, [6]Francis Crick Institute, University College London, London, United Kingdom, [7]Discipline of Medical Radiation Sciences, University of Sydney, Sydney, Australia

The biophysical basis of MRI signal in the normal human prostate is uncertain, whereby the normal peripheral zone has high ADC values and returns high signal on T2-weighted imaging. In this study, we use MRI in combination with quantitative digital histopathology to offer an explanation. Paired scans were performed at 3T on a human prostate, prior to and following prostatectomy and changes in zonal morphology and MRI characteristics were measured. The peripheral zone collapsed and reduced in T2 signal intensity and ADC value ex-vivo. Digital histopathological analysis suggested the peripheral zone stores more ejaculatory fluid than the transition zone.

2063

Coronal View Renal Perfusion FAIR-ASL Measurements in Mice

Fabian Tobias Gutjahr[1], Thomas Kampf[1], Stephan Michael Günster[1], Patrick Winter[1], Volker Herold[1], Wolfgang Rudolf Bauer[2], and Peter Michael Jakob[1]

[1]Department of Physics, University of Würzburg, Würzburg, Germany, [2]Department of Internal Medicine I, Division of Cardiology, University Hospital Würzburg

Renal perfusion measurements in coronal view using FAIR-ASL can be problematic in small animals as the selective inversion slice can label a large fraction of the inflowing blood. In this work, an alternative orientation for the selective inversion slice is shown to increase the sensitivity of the measurement.

Traditional Poster

Body: Cancer

Exhibition Hall 2064-2103 Wednesday 8:15 - 10:15

2064

Diagnostic accuracy of 3-T magnetic resonance imaging with Star VIBE: versus computer tomography in pulmonary nodules

Nan Yu[1], Chuangbo Yang, Qi Yang, Shaoyu Wang, Yong Yu, and Taiping He

[1]The first affiliated hosptial of Shaanxi traditional chinese medical university, Xian Yang, People's Republic of China

Star VIBE (MRI) sequence in obtaining scan under free breathing can provide high-resolution imaging. Therefore, we assessed the accuracy of magnetic resonance imaging (MRI) for detecting pulmonary nodules by comparing the detection rate of high-resolution Star vibe sequence with the MSCT results.   We concluded that pulmonary nodules with the maximum diameter more than 3mm can be detected by star-vibe (MRI) sequence with a satisfactory accuracy. Although pulmonary nodules with the max diameter less than 3mm had relatively low sensitivity, the accurate treatment decisions may also be made.

2065

Histogram analysis of pharmacokinetic parameters of DCE-MRI: differentiating malignant from benign solitary pulmonary nodules

Feng Feng[1], Ganlin Xia[2], and Peng Cao[3]

[1]Nantong Tumor Hospital, Nantong, People's Republic of China, [2]Nantong Tumor Hospital, [3]Shanghai East Hospital

A histogram analysis approach has been shown to be a premising tool in discriminating malignant and benign SPNs in terms of their heterogeneity. The purpose of our study was thus to primarily assess the diagnostic performance of DCE-MRI for stratifying the malignant and benign using histogram analysis. The results showed that the mean value of K^{trans} and K_{ep}, Kurtosis and skewness assessments from V_e of DCE-MRI histograms may be useful for differentiating malignant from benign SPNs.

2066

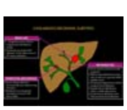

A case-based approach to MR imaging patterns of cholangiocarcinoma and post-intervention features

Peter Aaron Harri[1], Juan Camacho[2], Lauren Alexander[1], and Pardeep Mittal[1]

[1]Radiology and Imagining Sciences, Emory University School of Medicine, Atlanta, GA, United States, [2]Radiology, Medical Univeristy of South Carolina

Cholangiocarcinoma may demonstrate typical imaging manifestations and common patterns of organ involvement, guiding diagnosis, and facilitating imaging follow up after therapy. Adequate knowledge of tumoral biology in cholangiocarcinoma and current image-guided therapeutic approaches, along with imaging appearance of cholangiocarcinoma before and after image-guided interventions is crucial for adequate diagnosis and surveillance .MR imaging plays a key role for patient management, assessing therapy response and patient surveillance.

2067

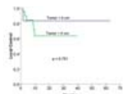

Treatment Response of Target Tumors and Its Impact on Local Control in Patients with Hepatocellular Carcinoma after Stereotactic Ablative Radiotherapy: Serial Changes of MRI Measurements

Li Ya-Hui[1], Chen Ran-Chou, Huang Wen-Yen, Chang Wei-Chou, and Tang Zun-Cheng

[1]Tri-Service general hospital, Taipei, Taiwan

Functional imaging techniques have a potential role in evaluation of treatment response in patients with HCC after SABR. After SABR, the increase of ADC value > 10% had marginally improved local control. A further large-scale study to identify the predictive value of parameters in functional MRI in validated.

2068

Diagnostic Value of Calculated High B Value DWI for Prostate Cancer Detection

Mathilde Wagner[1], Idoia Corcuera[1], Sara Lewis[1], Martin Kang[1], Stefanie Hectors[1], Ardeshir Rastinehad[2], Yasmina Chaibi[3], and Bachir Taouli[1]

[1]Translational and Molecular Imaging Institute, Icahn School of Medicine at Mount Sinai, New York, NY, United States, [2]Department of Urology, Icahn School of Medicine at Mount Sinai, New York, NY, United States, [3]Olea Medical

We compared image quality, lesion conspicuity and diagnostic performance of calculated and acquired b1600 DW images for prostate cancer (PCa) detection and assessed the added value of calculated b2000 images for PCa detection. We showed that calculated b1600 had equivalent image quality and diagnostic performance for PCa detection compared to acquired b1600 images with improved tumor-to-PZ contrast ratio, which suggests that calculated b1600 could be an alternative to acquired b1600 to decrease acquisition time. We also showed that calculated b2000 had better tumor conspicuity than b1600.

2069

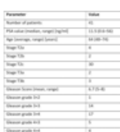

Impact of an additional endorectal imaging coil on MR image quality and cancer detection in the prostate

Josephin Gawlitza[1], Martin Reiss-Zimmermann[1], Gregor Thörmer[1], Alexander Schaudinn[1], Nikita Garnov[1], Lars-Christian Horn[2], Minh Do[3], Roman Ganzer[3], Jens-Uwe Stolzenburg[3], Thomas Kahn[1], Michael Moche[1], and Harald Busse[1]

[1]Diagnostic and Interventional Radiology, Leipzig University Hospital, Leipzig, Germany, [2]Institute of Pathology, University of Leipzig, Leipzig, Germany, [3]Urology Department, Leipzig University Hospital, Leipzig, Germany

Multiparametric MRI has been shown to improve detection, localization and characterization of patients with suspected prostate cancer (PCa). The current PIRADS guideline (v2, 2015) states that the additional use of an endorectal imaging coil (ERC) increases SNR at any magnetic field strength which may be particularly useful for staging and inherently lower SNR sequences (DWI or DCE). On the other hand, phased array coils with 16 or more elements may also provide adequate SNR. This work assesses the potential benefit of an ERC for the detection of prostate cancer– within the same patients.

2070

An mpMRI derived Logistic Regression Model for Gleason 4 Pattern Prediction in Peripheral Zone Prostate Cancer

Michela Antonelli[1], Edward W Johnston[2], Manuel Jorge Cardoso[1], Sebastien Ourselin*[1,3], and Shonit Punwani*[4]

[1]Translational Imaging Group, CMIC, University College London, London, UK, London, United Kingdom, [2]Centre for Medical Imaging, University College London, London, UK, London, United Kingdom, [3]Dementia Research Centre, Department of Neurodegenerative Disease, UCL Institute of Neurology, London, UK, [4]Academic Radiology, University College London Centre for Medical Imaging, London, UK

Gleason grade is the most important determinant of prognosis and survival in prostate cancer, and is determined using prostate biopsy. Here we investigate whether multi-parametric MRI can be used to classify Gleason grade non-invasively with logistic regression (LR) models, classifying tumours into 3+3 and those containing a 4 component. A selection of clinical and quantitative MRI metrics were used. The LR model was trained in ninety-nine patients and tested following a Leave-One-Out (LOO) analysis on a temporal separated cohort of nineteen patients. LR models were shown to predict the presence of Gleason 4 component in cancer lesions both before and after LOO analysis.

2071

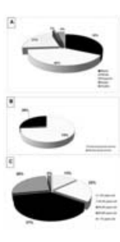

Evaluation of T1/T2 ratios in a pilot study as a potential biomarker of biopsy - proven benign and malignant breast lesions in correlation with histopathological disease stage.

Marina Alexandra Malikova[1], Jaroslaw N Tkacz[2], Priscilla J Slanetz[3], Adam Aakil[2], Chao-Yu Guo[4], and Hernan Jara[2]

[1]Surgery, Boston University, Boston, MA, United States, [2]Radiology, Boston Medical Center, Boston, MA, United States, [3]Radiology, Beth Israel Deaconess Medical Center, Harvard Medical School, Boston, MA, United States, [4]Biostatistics, Boston University, Boston, MA, United States

The T1/T2 ratios obtained by qMRI provide measures that strongly correlate with histopathological findings. This quantitative information of tissue properties can provide basis for improving the specificity of diagnostic breast imaging and serve as a tool to assess response to treatment and contralateral breast involvement.

2072 Using preoperative MRI to prevent unnecessary lymphadenectomies in patients with grade 1 endometrial cancer decreases operating room times and post-operative complications.

Elizabeth Maddox[1], Ashley Cahoon[2], Jessica Robbins[2], Krupa Patel-Lippmann, David Kushner[3], Ahmed Al-Niaimi[3], and Elizabeth Sadowski[2]

[1]Radiology, University of Wisconsin, madison, WI, United States, [2]Radiology, University of Wisconsin, WI, [3]OBGYN, University of Wisconsin, WI

MRI can exclude myometrial invasion (MI) and cervical invasion (CI) with high accuracy in endometrial carcinoma. Women with small tumors, no MI, no CI and no evidence of extra-uterine spread have a very low risk of lymph node metastasis, and lymphadenectomy can be avoided. The goal of our study was to demonstrate how using preoperative MRI to prevent unnecessary lymphadenectomy can affect operating room time (OR) and post-operative complications. We performed an IRB approved retrospective study evaluating MRI results, lymphadenectomy status, operative times, and post-operative complications. This demonstrated a statistically significant decrease in OR times and post-operative complications.

2073 

Assessment of intravoxel incoherent motion diffusion-weighted MR imaging in solitary pulmonary nodules : comparison and correlation with dynamic contrast-enhanced MR imaging.

Shuchang Zhou[1] and Liming Xia[2]

[1]Radiology, Tongji Hospital, Huazhong University of Science and Technology, Wuhan, People's Republic of China, [2]Radiology, Tongji Hospital of Huazhong University of Science and Technology, Wuhan, People's Republic of China

The study aim to compare the intravoxel incoherent motion (IVIM) and DCE-MRI for distinguishing benign pulmonary nodules and lung cancer and evaluate the diagnostic performance of two methods. We found ADCtotal,D,D*from IVIM and Tmax,SLE from DCE-MRI valuable for differential diagnosis ,with D and Tmax have better sensitivity and accuracy.But parameters between the two methods show poor correlation.Combination of IVIM and DCE-MRI can get excellent diagnostic performance.

2074 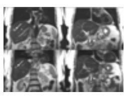

Variable Refocusing Flip Angle Single-Shot Fast Spin Echo Imaging of Liver Lesions: Improved Lesion Contrast and Speed

Robert M Hicks[1], Andreas M Loening[2], Shreyas S Vasanawala[2], Michael A Ohliger[1], and Thomas A Hope[1]

[1]Radiology, University of California, San Francisco, San Francisco, CA, United States, [2]Radiology, Stanford University School of Medicine, Stanford, CA, United States

Variable refocusing flip angle single-shot fast spin echo (vrfSSFSE) decreases T2-decay related blurring, allows increased K-space coverage while maintaining clinically relevant echo times, and reduces specific absorption rate. We evaluated clinical image quality and acquisition time of vrfSSFSE for imaging liver lesions in comparison with conventional SSFSE in patients undergoing 68Ga-DOTA-TOC PET on a 3T time-of-flight PET/MRI. Quantitative analysis of 53 lesions in 27 patients demonstrated higher mean CNR with vrfSSFSE (9.9 vs. 6.7, $p<0.001$) and 1.7-fold increase in speed compared to SSFSE. vrfSSFSE improves liver lesion contrast with shorter scan times acquired using a single 20 second breath hold.

2075 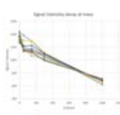

Reduction of the variation in parameter estimation from atypical signal intensity decay or its variation near tumor in low b factors using a ROI-based analysis method in IVIM model for prostate diffusion imaging

In Chan Song[1], Sang Youn Kim[1], Jeong Yeon Cho[1], and Seung Hyup Kim[1]

[1]Radiology, Seoul National University Hospital, Seoul, Korea, Republic of

In an IVIM technique, atypical signal intensity decay in low b factors or its variation at neighboring pixels at tumor lesion may be caused by tumor heterogeneity or spatial mismatch due to image distortion in EPI sequence, which can make estimated IVIM parameters be unreliable in conventional pixel-by-pixel method. Thus, to obtain more reliable IVIM outputs for prostate IVIM MR imaging, we suggest a new and simple ROI-based analysis method using all data of surrounding pixels in estimation and our study demonstrates a ROI-based analysis method decreased variation in IVIM parameters and can provide more reliable IVIM map images.

2076 

Prediction of low-risk breast cancer using quantitative DCE-MRI and its pathological basis

Tingting Xu[1] and Guangyu Tang[1]

[1]Department of Radiology, Tenth People's Hospital,TongjiUniversity School of medicine, Shanghai, Shanghai, People's Republic of China

Purpose: This study aimed to evaluate the difference in dynamic contrast enhanced magnetic resonance imaging characteristics between low-risk and non-low-risk breast cancers and to explore the possible pathological basis.

Materials and methods: Approval from the institutional review board and informed consent were acquired for this study. The MR images of 104 lesions with pathologically proven breast cancer were retrospectively analyzed.

Result: Low-risk tumors showed significantly lower K^{trans} and K_{ep} values and higher ADC value than non-low-risk breast cancers.

Conclusion: The prediction parameter using K^{trans}, K_{ep}, and ADC obtained on DCE-MRI and diffusion-weighted imaging could facilitate the identification of low-risk breast cancers.

2077 Using ngram-based features to explore the correlation of prostate MR findings and PI-RADS classification

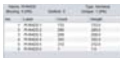

Shuai Ma[1], Yi Liu[1], Ge Gao[1], Rui Wang[1], Yahui Shi[2], Zuofeng Li[2], Juan Wei[2], and Xiaoying Wang[1]

[1]Peking University First Hospital, Beijing, People's Republic of China, [2]Philips Research China, Shanghai, People's Republic of China

The decision tree trained on MR descriptions by natural language processing (NLP) method represents a desirable performance in identifying low-risk PI-RADS 2-3 classes with high precision and high-risk PI-RADS 5 class with high recall. From the decision path, several specific features are adopted to make decision and the identification of key indicator contributes to distinguish PI-RADS 2 class from PI-RADS 3 class.

2078

"Push-button" PET/MRI using a continuous scan 3D quantitative T2 MRI sequence

Isabel Dregely[1], Claudia Prieto[1], Radhouene Neji[2], Camila Munoz[1], Rene Botnar[1], Andrew Mallia[3], Gary Cook[3], and Vicky Goh[3]

[1]Biomedical Engineering, King's College London, London, United Kingdom, [2]Siemens Healthcare Limited, Frimley, United Kingdom, [3]Cancer Imaging, King's College London, London, United Kingdom

To avoid overtreatment and repeated use of invasive biopsies, there is a need for improved diagnostic tools for prostate cancer risk stratification. Simultaneous Positron Emission Tomography / Magnetic Resonance Imaging (PET/MRI) systems are promising, however, fundamental differences in PET and MR imaging methodology currently limit full integration and thus the true potential of simultaneous PET/MR: While PET is a rather straightforward, single 3D scan, the MRI exam is complex and current clinical practice consists of several 2D sequences with different image contrast weightings and spatial coverage, performed in a serial fashion. Here, we propose a single, 3D, quantitative T2-MRI sequence that parallels the continuous scan workflow of PET data acquisition.

2079

Prostate Cancer: Differentiation of Transition Zone Cancer from Benign Prostatic Hyperplasia by Using Diffusion Kurtosis imaging, Intravoxel Incoherent motion and ultra-high b-value apparent diffusion coefficient techniques

Yan Zhong[1], Lu Ma[2], Yanguang Shen, Yingwei Wang[3], Jingjing Pan, Haiyi Wang, and Huiyi Ye

[1]Chinese PLA General Hospital, Beijing, People's Republic of China, [2]Chinese PLA General Hospital, People's Republic of China, [3]Chinese PLA General Hospital

To evaluate the value of the (kurtosis, perfusion and diffusion) parameters in the differentiation of TZ cancer from benign GH.30 patients underwent preoperative 3-T magnetic resonance (MR) imaging. Each parameter in TZ carcinomas and GH were compared using Student's t test, receiver operating characteristics (ROC) analysis. All parameters except for D* in TZ carcinoma and GH were significantly different, and showed the same sensitivity for differentiating TZ carcinoma from GH (92.3%), and K and ADCs with equal specificity (96.7%).The monoexponential ultra-high b value ADC calculation is more practical to discriminate TZ carcinoma from GH.

2080

Differential Diagnosis of Ovarian Tumor and Degenerated Subserous Leiomyoma Using Diffusion-tensor Imaging

Xijia Deng[1], Ailian Liu[1], Jinghong Liu[1], Meiyu Sun[1], Bing Wu[2], Lihua Chen[1], Anliang Chen[1], and Jiaojiao Zhu[1]

[1]Department of Radiology, the First Affiliated Hospital of Dalian Medical University, Dalian, People's Republic of China, [2]GE healthcare China, Beijing, People's Republic of China

Ovarian cancer is one of the most common malignant tumor of female reproductive organs, which is the first cause of death in gynecological malignancies. A mixed cystic and solid appearance of an ovarian mass is usually difficult to differentiate from degenerated subserous leiomyoma. In this study, DTI MR measurements were performed to investigate the difference of the ADC and FA values in ROIs of the soild component region between ovarian tumors and uterine fibroids.

2081

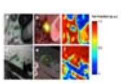

Improved lymph node staging using MRI mDixon fat fraction measurements in patients with intermediate and high-risk prostate cancer

James O'Callaghan[1], Edward Johnston[1], Arash Latifoltojar[1], Harbir Sidhu[1], Magdalena Sokolska[2], Jamshed Bomanji[3], Alan Bainbridge[2], and Shonit Punwani[1]

[1]UCL Centre for Medical Imaging, London, United Kingdom, [2]Medical Physics, University College London Hospital, London, United Kingdom, [3]Institute of Nuclear Medicine, University College London Hospital, London, United Kingdom

The staging of lymph nodes in prostate cancer is important for the planning and monitoring of treatments. However, there is currently a paucity of techniques that can accurately identify the presence of metastases in small nodes.

In this study, we investigate the usefulness of signal fat fraction from MRI mDixon acquisitions in discriminating between benign and metastatic nodes using ^{18}F-Choline PET as a reference standard.

We present data suggesting that in comparison to commonly used diameter measurements, mDixon fat fraction may be better at discriminating benign from involved lymph nodes that are <10mm in short axis diameter.

2082

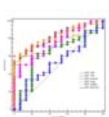

The Histogram analysis of quantitative Dynamic enhanced and Diffusion-weighted Intravoxel Incoherent Motion MRI for pathologic Gleason grading of prostate cancer

Ru wen[1], Junkang Shen[2], Wenlu Zhao[3], Peng Cao[4], and Jiangfen Wu[4]

[1]Department of imaging, The second affiliated hospital of Soochow university, Soochow, People's Republic of China, [2]The second affiliated hospital of Soochow university, soochow, People's Republic of China, [3]The second affilicated hospital of Soochow university, People's Republic of China, [4]GE healthcare China

There are different treatments for low-risk and high-risk prostate cancer patients in clinical, NCCN guidelines recommend proactive monitoring management as the preferred treatment for patients with low risk PCa (GS ≤6) ,and active measures for intermediate/high-risk patients. Our research found that both DCE and IVIM quantitative parameters Histogram analysis results can successfully distinguish LG from HG PCa ,and their diagnostic performance was not statistically significant. Considering the method we used to acquire quantitative parameters of DCE-MRI , IVIM may provide us a new way for those who cannot bear the invasive intravenous injection of contrast agent .

2083

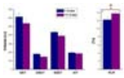

Association of breastfeeding duration with abdominal fat distribution and adipose tissue hydration at 4.5 years

Suresh Anand Sadananthan[1], Wei Wei Pang[2], Navin Michael[1], Mya Thway Tint[2], Kuan Jin Lee[3], Lynette Pei-Chi Shek[4], Yap Kok Peng Fabian[5,6], Keith M Godfrey[7], Melvin Khee-Shing Leow[8,9], Yung Seng Lee[1,4], Peter D Gluckman[1,10], Christiani Jeyakumar Henry[8], Marielle Valerie Fortier[11], Yap Seng Chong[1,2], and S. Sendhil Velan[3]

*[1]Singapore Institute for Clinical Sciences, A*STAR, Singapore, [2]Department of Obstetrics & Gynaecology, Yong Loo Lin School of Medicine, National University of Singapore, Singapore, [3]Singapore BioImaging Consortium, A*STAR, Singapore, [4]Department of Paediatrics, Yong Loo Lin School of Medicine, National University of Singapore, Singapore, [5]Department of Paediatric Endocrinology, KK Women's and Children's Hospital, Singapore, [6]Lee Kong Chian School of Medicine, Nanyang Technological University, Singapore, [7]MRC Lifecourse Epidemiology Unit & NIHR Southampton Biomedical Research Centre, University of Southampton & University Hospital Southampton NHS Foundation Trust, Southampton, United Kingdom, [8]Clinical Nutrition Research Centre, Singapore Institute for Clinical Sciences, A*STAR, Singapore, [9]Department of Endocrinology, Tan Tock Seng Hospital, Singapore, [10]Liggins Institute, University of Auckland, Auckland, New Zealand, [11]Department of Diagnostic and Interventional Imaging, KK Women's and Children's Hospital, Singapore*

The association of the duration of breastfeeding with childhood obesity is equivocal. The first year of life is a period of hypertrophic expansion of adipocytes with little increase in adipocyte number. Hence, over-nutrition during this period could potentially result in persistent changes in adipocyte size that may last until adulthood. In this study, we have investigated the association of breastfeeding duration with abdominal fat distribution and adipose tissue cellularity at 4.5 years. Our results indicate a weak protective effect of longer breastfeeding duration on abdominal subcutaneous adipose tissue volumes and subcutaneous adipose tissue morphology.

2084

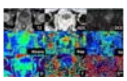

Noninvasive Quantification of Prostate Cancer Using IVIM：evaluation of IVIM perfusion-related parameters by comparing to quantitative DCE-MRI

Yu Guo[1], Penghui Wang[1], Chao Chai[1], Zhizheng Zhuo[2], Yu Zhang[2], and Wen Shen[1]

[1]Tianjin First Center Hospital, tianjin, People's Republic of China, [2]Philips Healthcare, Beijing, People's Republic of China

The purpose of the study was to evaluate the clinical usefulness of IVIM technique for the PCa and furtherly investigate the diffusion and perfusion characteristics among PCa, normal peripheral zone (PZ) and central gland (CG) comparing to pharmacokinetic parameters based on quantitative DCE-MRI. The IVIM was performed at 11 b values of 0, 10, 20, 30, 50, 75, 100, 250, 500, 750 and 1000s/mm^2. The D value in prostate cancer were significantly lower than those in the PZ and CG. The perfusion fractions in PCa were significantly higher than those in the PZ. There were no significant differences in the PCa, PZ and CG for the D*, which had large SDs. D showed significant negative correlations with Ktrans and Kep respectively, while f showed a significantly positive correlations with Ktrans and Kep. IVIM can provide more detailed information on perfusion and diffusion of prostate cancer noninvasively without intravenous contrast agent administration.

2085

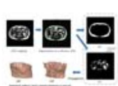

Quantification of abdominal subcutaneous and visceral fat by magnetic resonance imaging of the proton at 3T: application to an overfeeding protocol.

Angeline Nemeth[1], Hélène Ratiney[1], Benjamin Leporq[1], Kevin Seyssel[2], Bérénice Segrestin[3], Pierre-Jean Valette[4], Martine Laville[3], and Olivier Beuf[1]

[1]Univ. Lyon, INSA‐Lyon, Université Claude Bernard Lyon 1, UJM-Saint Etienne, CNRS, Inserm, CREATIS UMR 5220, U1206, F69621, Lyon, France, [2]Department of Physiology, Faculty of Biology and Medicine, University of Lausanne, Lausanne, Switzerland, [3]Centre de Recherche en Nutrition Humaine Rhône-Alpes (CRNH-RA), Centre Hospitalier Lyon Sud, Pierre-Bénite, Lyon, France, [4]Hospices Civils de Lyon, Département d'imagerie digestive, CHU Edouard Herriot, Lyon, France

Overweight and obesity are a major worldwide health problem increasing the risk to develop pathologies such as diabetes and cardiovascular disease. The metabolic risk is modulated by the adiposity distribution and the fatty acid composition. Quantitative MRI to assess the fat volumes and composition is still little used. This study shows, using a single 3D multiple gradient echo sequence, that overfeeding has a significant effect on fat storage in the body with an increase of visceral and subcutaneous abdominal adipose tissues volumes, fat storage in the liver and seems to have an effect on stored fat composition.

2086

Magnetic Resonance Imaging Studies of a Testosterone and Estrogen-supplemented Experimental Mouse Model of Lower Urinary Tract Symptoms

Devkumar Mustafi[1], Erin McAuley[2], Rebecca Valek[1], Erica Markiewicz[1], Marta Zamora[1], Aytekin Oto[1], Donald VanderGriend[2], and Gregory S Karczmar[1]

[1]Radiology, The University of Chicago, Chicago, IL, United States, [2]Surgery, The University of Chicago, Chicago, IL, United States

Lower urinary tract symptoms (LUTS) affect many elderly men and cause urinary obstruction and prostatic enlargement. The aim of this study was to use functional/anatomic MRI for serial imaging of LUTS development in a testosterone/estrogen-supplemented experimental mouse model. These mice exhibited a greater increase in prostate volume and decrease in urethra volume than control mice, and changes in urethral and prostatic volume were strongly inversely correlated. Results suggest that serial MRI could improve understanding of initiation and development of LUTS as well as the origin of clinical symptoms of benign prostatic hyperplasia, and evaluate effects of therapy in mouse models.

2087

Region-adaptive Deformable Registration for MRI/CT Pelvic Images via Bi-directional Image Synthesis

Xiaohuan Cao[1,2], Jianhua Yang[1], Yaozong Gao[2], Guorong Wu[2], and Dinggang Shen[2]

[1]School of Automation, Northwestern Polytechnical University, Xi'an, People's Republic of China, [2]Department of Radiology and BRIC, University of North Carolina at Chapel Hill, Chapel Hill, NC, United States

Registering pelvic CT and MRI can help propagate accurate delineation of pelvic organs (prostate, bladder and rectum) from MRI to CT, since it is difficult to directly obtain accurate organ labels from CT due to its low soft-tissue contrast. We propose to use image synthesis to first eliminate the appearance gap between modalities by performing image synthesis in bi-directions in order to provide more anatomical information for guiding the registration. Then, a hierarchical region-adaptive registration framework is proposed to utilize the significant anatomical information from each modality to guide accurate MRI/CT deformable registration.

2088

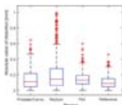

On the influence of susceptibility-related field inhomogeneities caused by intestinal gases on the distortion in prostate and cervix

Julian Emmerich[1], Rebecca Schilling[2], Sina Straub[1], Asja Pfaffenberger[3], and Frederik Bernd Laun[1,4]

[1]Medical Physics in Radiology, German Cancer Research Center (DKFZ), Heidelberg, Germany, [2]Medical Faculty, University Hospital Ulm, Ulm, Germany, [3]Medical Physics in Radiation Oncology, German Cancer Research Center (DKFZ), Heidelberg, Germany, [4]Institute of Radiology, University Hospital Erlangen, Erlangen, Germany

Due to field inhomogeneities, MR-images suffer from image distortions in frequency-encoding direction. Using MRI as a tool for dose planning in MR-guided radiation therapy, image distortions play an important role in defining safety margins and the planning target volume (PTV). To investigate the influence of susceptibility-related field inhomogeneities on the distortion in prostate and cervix, distortions maps based on phase images were calculated for data acquired in a MR-guidance study. It was found that maximum distortions in prostate and rectum can be as large as 0.6 mm or 1.0 mm respectively, which should be considered when defining PTVs.

2089

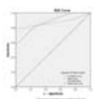

The Value of Apparent Diffusion Coefficient Map based on PI-RADS v2 in Predicting Clinically Significant Prostate cancer

Wang Huihui[1] and Wang Xiaoying[1]

[1]Peking University First Hospital, Beijing, People's Republic of China

To determine the value of ADC map in identifying clinically significant prostate cancer, the ADC PI-RADS scores and mean ADC values of index lesion based on PI-RADS v2 were measured. ADC PI-RADS score may be good as overall PI-RADS v2 score in predicting clinically significant PCa. The clinically significant cancers had higher ADC scores and lower ADC values. An ADC value of 619-889×10-6 mm2/s may be useful in the identification of clinically significant cancers.

2090

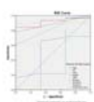

The predictive value of preoperative examination in differenciating high and low Gleason score of radical prostatectomy specimens

Wang Huihui[1] and Wang Xiaoying[1]

[1]Peking University First Hospital, Beijing, People's Republic of China

To evaluate the value of different preoperative examniations in differenciating high/low Gleason score, prostate volumev(PV), PSA, PSA density (PSAD), DRE, multiparametric MRI (mpMRI) and transrectal ultrasound guided biopsy were analyzed. The area under curve (AUC) of PSAD was 0.911 with the cut-off level of 0.25, which was even better than biopsy(AUC=0.887). MpMRI performed good diagnostic accuracy according to PI-RADS v2 by Reader 1(AUC=0.831) and 2(AUC=0.933).

2091

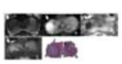

Evaluation of Prostate Imaging Reporting and Data System version 2 (PI-RADS v2) in predicting clinically significant prostate cancer: a whole-mount step-section analysis

Wang Huihui[1] and Wang Xiaoying[1]

[1]Peking University First Hospital, Beijing, People's Republic of China

The diagnostic accuracy of PI-RADS v2 for clinically significant cancer was evaluated by using whole-mount step-section slides as standard of reference. All significant cancers could be identified and the accuracy of PI-RADS 3 to 5 for predicting significant cancer was 91.7%, with high sensitivity (100%) and negative predictive value (100%).

2092

3D T2-weighted fast spin echo (FSE) with outer volume suppression versus 2D FSE in the prostate: Comparison of lesion detection in the transition zone and image quality

Paul Benjamin Stoddard[1], Valentina Taviani[2], Suchandrima Banerjee[2], Bruce L. Daniel[1], Anshul Haldipur[1], Brian A. Hargreaves[3], Shreyas S. Vasanawala[1], and Andreas M. Loening[1]

[1]Radiology, Stanford University, Stanford, CA, United States, [2]Global MR Applications and Workflow, GE Healthcare, [3]Electrical Engineering and Radiology, Stanford University, Stanford, CA, United States

3D T2-weighted imaging (T2WI) of the prostate for prostate cancer (PCa) is often hampered by motion artifacts and signal starvation. However, incorporating reduced phase field of view capability using outer volume suppression (OVS) into 3D fast spin echo (FSE) can overcome these obstacles. In the prostatic transition zone (TZ), superior contrast and diminished blur were found over standard 2D FSE, with preserved SNR and anatomic detail. Diagnostic confidence was greater with 3D, whether used alone or in combination with 2D. Furthermore, less equivocal diagnoses resulted with the combination of 2D and 3D.

2093

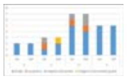

Test-Retest Reliability of in bore MRI Guided Prostate Biopsy: a pilot study to optimize the current repeated biopsy paradigm in patients on Active Surveillance?

Kareem K Elfatairy[1], Christopher P Filson[2], Adeboye O Osunkoya[3], Rachel L Geller[3], and Sherif G Nour[1]

[1]Radiology, Emory University-School of Medicine, Atlanta, GA, United States, [2]Urology, Emory University-School of Medicine, Atlanta, GA, United States, [3]Pathology, Emory University-School of Medicine, Atlanta, GA, United States

Consistent results throughout repeated biopsy sessions is an essential requirement for any tool used for active surveillance. TRUS biopsy showed inconsistent results in repeated biopsy sessions. Regarding MRI guided biopsy, the reliability of repeated biopsies needs to be established. 5 patients with 17 lesions which were repeatedly biopsied under direct MRI guidance were included. Kappa statistics showed moderate agreement. Negative predictive value for 2nd biopsy was 93% and for 3rd biopsy was 90%. Consistent biopsy results may obviate the need for the current paradigm of obtaining annual prostate biopsies in patients undergoing active surveillance

---

2094

Computer-Aided Diagnosis of Prostate Cancer on Multiparametric MRI: the Application for Cancer Localization

Ge Gao[1], Chengyan Wang, Xiaoying Wang, Jue Zhang, Yajing Zhang, and Yajing Zhang[2]

[1]Peking University First Hospital, Beijing, People's Republic of China, [2]Philips Healthcare, Suzhou, People's Republic of China

Multiparametric MRI (mpMRI), including T2WI, DWI/ADC and DCE, is becoming a promising noninvasive tool for prostate cancer (PCa) detection, localization and stage. Although PI-RADS has provides recommendations for image reading and reporting, the interpretation of mpMRI is still challenging for clinical work, for poor interobserver agreement and strong experience dependence. We therefore developed a machine learning model that combines features derived from mpMRI for PCa detection and localization. The model predicted the transition zone (TZ) and peripheral zones (PZ) separately and compared with whole-mount step-section slide. The computer-aided diagnosis (CAD) achieved excellent performance both in PZ and TZ.

2095

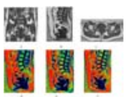

Can MR quantitative fat fraction technique evaluates bone marrow toxicity during radiotherapy and chemotherapy?

Jingling Li[1], Xiaocheng Wei[2], Shun Qi[1], Hong Yin[1], and Haitao Zhao[1]

[1]Xijing Hospital, Xi 'an, People's Republic of China, [2]GE Research China, GE Healthcare, People's Republic of China

Bone marrow toxicity is very common side effect during radio-chemotherapy treatment of pelvic tumors. In this study, six patients with cervical cancer were included. The Bone marrow fat faction of the subjects were evaluated using quantitative fat fraction MR technique before each week's treatment and at the end of whole five weeks' therapy. The results indicated that MRI was sensitive to marrow composition changes and can evaluate the real time bone marrow toxicity during radio-chemotherapy. This could potentially benefit patient with a more optimized treatment plan.

2096

Whole-Tumor Quantitative Apparent Diffusion Coefficient Histogram Analysis in Differentiating intrahepatic mass-forming cholangiocarcinoma from poorly differentiated hepatocellular carcinoma

Xianlun Zou[1], Yaqi Shen[1], Yao Hu[1], Zhen Li[1], and Daoyu Hu[1]

[1]Department of Radiology, Tongji Hospital, Tongji Medical College, Huazhong University of Science and Technology, Wu han, People's Republic of China

Differentiating intrahepatic mass-forming cholangiocarcinoma (IMCC) and poorly differentiated hepatocellular carcinoma(pHCC) is often difficult for radiologists, but it is important for providing appropriate treatments. In our study, we use noncontrast MRI with diffusion-weighted imaging in combination with whole-tumor quantitative apparent diffusion coefficient (ADC) histogram analysis to differentiate IMCC from pHCC. The result reveals that ADC histogram analysis based on the whole-tumor can be considered a useful and noninvasive method to help differentiate IMCC from pHCC. Especially $ADC_{25\%}$ of histogram analysis allows differentiation of IMCC from pHCC with higher accuracy.

2097

Preoperative MRI of Uterine Malignant Mixed Mullerian Tumors versus Endometrial Carcinomas with Emphasis on Dynamic Enhancement Characteristics

Sandra Alheli Garza[1], Tara Sagebiel[2], Wei Wei[3], Jingfei Ma[4], and Priya Bhosale[2]

[1]Department of Diagnostic and Interventional Imaging, University of Texas Health Science Center at Houston, Houston, TX, United States, [2]Diagnostic Radiology Department, MD Anderson Cancer Center, Houston, TX, United States, [3]Biostatistics Department, MD Anderson Cancer Center, Houston, TX, United States, [4]Department of Imaging Physics, MD Anderson Cancer Center, Houston, TX, United States

Distinguishing uterine malignant mixed mullerian tumors (MMMTs) from endometrial carcinomas preoperatively by pelvic MRI may help with surgical and treatment planning of this highly aggressive tumor. Our study found that prolapse of tumor through the external cervical os, delayed iso- or hyper-enhancement, high mean tumor: myometrium positive enhancement integral (PEI) ratio and low tumor signal enhancement ratio (SER) are more commonly seen in patients with MMMT and may alert the radiologist to the possibility of this diagnosis.

2098

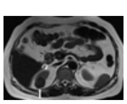

Differentiation of Fat-Poor Renal Angiomyolipoma from Other Renal Tumors with Low Signal Intensities on T2-weighted MR Image

Deuk Jae Sung[1], Ki Choon Sim, Na Yeon Han, Beom Jin Park, Min Ju Kim, and Sung Bum Cho

[1]Radiology, Anam Hospital, Korea University College of Medicine, Seoul, Korea, Republic of

A low T2 signal intensity is a well-known feature of fat-poor angiomyolipoma and papillary renal cell carcinoma. However, many other renal tumors showing low T2 signal intensity are encountered in daily practice. So, a low T2 signal intensity is not a pathognomonic finding for fat-poor angiomyolipoma and papillary RCC. Even though renal mass biopsy might be considered to establish a diagnosis for tumors without typical imaging features of renal cell carcinoma, the decision to biopsy or not sometimes seems to be difficult in small renal tumors. Accurate MR imaging characterization of renal masses is essential for ensuring appropriate management and avoiding unnecessary surgical procedure.

2099

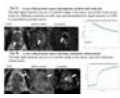

Usefulness of Subtracted Images from 4 Minutes to 1 Minute in Dynamic Contrast-enhanced (DCE) Magnetic Resonance (MR) Imaging for Prostate Cancer; Pilot Study

Sung Kyoung Moon[1], Hyug-Gi Kim[2], Kyung Mi Lee[1], and Joo Won Lim[1]

[1]Radiology, Kyung Hee University Hospital, College of Medicine, Kyung Hee University, Seoul, Korea, Republic of, [2]Department of Biomedical Engineering, College of Electronic Information Engineering, Kyung Hee University, Korea, Republic of

The purpose of our study is to assess the usefulness of subtracted images from 4-1 min in DCE MR imaging for the prostate cancer diagnosis. Subtracted images from 4-1 min were assessed for the visual washout scores of prostate cancer and normal PZ, and compared with the time-contrast media curve patterns in each patient. A subtraction image set of DCE MRI 4-1 min mirrored time - concentration curve patterns of DCE MR imaging in prostate cancer and normal PZ. This subtraction image set can be a more simple method to display the DCE characteristics without any additional post-processing.

2100

Dynamic contrast-enhanced MRI for uterine cervical cancer: correlations with clinical staging and pathologic types

Xiaoduo Yu[1], Meng Lin[1], Lizhi Xie[2], Han Ouyang[1], and Chunwu Zhou[1]

[1]Cancer Hospital, Chinese Academy of Medical Sciences, Beijing, People's Republic of China, [2]GE Healthcare, MR Research China, Beijing

Tumor blood supply is closely related to the tumor occurrence, development, metastasis and prognosis. MRI is the optimal imaging method for investigating uterine cervical carcinoma, which provides excellent morphological information using conventional series. Additionally, the tumor perfusion information can be quantitatively assessed by dynamic contrast-enhanced MRI (DCE-MRI). DCE derived parameters include MaxSlop, CER, IAUGC, K^{trans}, K_{ep} and V_e. Our results showed mild negative correlation to clinical FIGO stage based on mean and maximum of K^{trans} and K_{ep}, increased minimum MaxSlop, and increased max- and mini-mum K^{trans} in squamous cell carcinoma than those of adenocarcinoma. DCE-MRI is a significant supplement to provide valuable morphological information that contributes to clinical decision-making and prognosis prediction.

2101

Value of DWI and dynamic contrast-enhanced MRI in differentially diagnosing stage- Ⅰ a endometrial carcinomas and endometrial polyps

Yuan Chen[1] and Jingliang Cheng[1]

[1]MRI Division, the First Affiliated Hospital of Zhengzhou University, Zhengzhou, People's Republic of China

Yuan Chen,female,graduated from Zhengzhou University,Master's degree in reading at the First Affiliated Hospital of Zhengzhou University.

2102

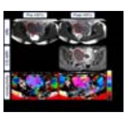

Conductivity imaging for assessing the treatment outcome of MR-HIFU ablation of uterine fibroids

Sin-Yuin Yeo[1], Ulrich Katscher[2], Young-Sun Kim[3], and Holger Gruell[1]

[1]University Hospital Cologne, Cologne, Germany, [2]Philips Research Europe, Hamburg, Germany, [3]Samsung Medical Center, Seoul, Korea, Republic of

MR-HIFU is a non-invasive thermal therapy used to treat symptomatic uterine fibroids. During therapies, clinicians utilize information provided by MRI for treatment planning and to ensure ablation of fibroids using non-invasive temperature monitoring via PRFS thermometry. Thereafter, the therapeutic outcome is determined by measuring the non-perfused volume (NPV) following contrast agent administration. We present a case study using Electric Properties Tomography (EPT) for assessment of treatment outcome by correlating the change in conductivity to the NPV. An increase in conductivity of up to 20% was observed. Thus, EPT is a promising approach for assessment of treatment outcome.

2103

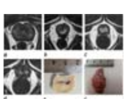

Benign prostatic hyperplasia after prostatic arterial embolization in a canine model: a 3T multi-parametric MR imaging and whole-mount step-section pathology correlated longitudinal study

Basen Li[1] and Liang Wang [2]

[1]Department of Radiology, Tongji Hospital, Tongji Medical College, Huazhong University of Science and Technology, Wuhan, People's Republic of China, [2]Department of Radiology, Tongji Hospital, Tongji Medical College, Huazhong University of Science and Technology

Prostatic arterial embolization (PAE) is a minimally invasive procedure developed in the recent years. Recent studies reported clinical applications of PAE in the treatment of BPH, and its safety and efficacy was confirmed. For the basic theory research, some scholars have made preliminary animal experiments in beagle dogs and pigs.To the best of our knowledge, there is no longitudinal study regarding BPH morphological and functional characteristics of BPH in different periods after PAE with multi-parametric magnetic resonance imaging (mp-MRI).

Traditional Poster

Breast Cancer

2104

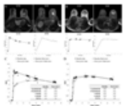

Estimating breast tumor blood flow during neoadjuvant chemotherapy using interleaved high temporal and high spatial resolution MRI

Leonidas Georgiou[1], Nisha Sharma[2], David Broadbent[1,3], Daniel Wilson[3], Barbara J Dall[2], Anmol Gangi[1,4], and David L Buckley[1]

[1]Division of Biomedical Imaging, University of Leeds, Leeds, United Kingdom, [2]Department of Radiology, Leeds Teaching Hospital NHS Trust, [3]Department of Medical Physics and Engineering, Leeds Teaching Hospital NHS Trust, [4]Department of Western General Hospital, NHS Lothian

An ideal breast MRI protocol might include high spatial and high temporal resolution images acquired following a single contrast agent injection. Here we present an acquisition strategy to acquire both for clinical reporting and tracer kinetic analysis. The approach was evaluated using simulations and tested through application in patients undergoing neoadjuvant chemotherapy. Radiologists could adapt similar protocol strategies to examine the physiological characteristics of tumors and their associated changes during treatment without significantly compromising the data used for clinical reporting.

2105

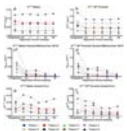

Reducing computation time for registration in Breast DCE-MRI: Effects of percent sampling on kinetic analysis model parameters, uncertainties, and goodness of Fit

Matthew Mouawad[1], Heather Biernaski[2], Muriel Brackstone[3,4], Michael Lock[4,5], Anat Kornecki[6,7], Olga Shmuilovich[6,7], Ilanit Ben Nachum[6,7], Frank S Prato[1,2,6], R. Terry Thompson[1,2,6], Stewart Gaede[1,2,8], and Neil Gelman[1,2,6]

[1]Medical Biophysics, Western University, London, ON, Canada, [2]Lawson Imaging, Lawson Health Research Institute, London, ON, Canada, [3]Surgical Oncology, London Regional Cancer Program, London, ON, Canada, [4]Oncology, Western University, London, ON, Canada, [5]Radiation Oncology, London Regional Cancer Program, London, ON, Canada, [6]Medical Imaging, Western University, London, ON, Canada, [7]Diagnostic Imaging, St. Joseph's Health Center, London, ON, Canada, [8]Physics and Engineering, London Regional Cancer Program, London, ON, Canada

Patient movement during dynamic contrast enhanced breast MRI acquisition can degrade signal enhancement curves. Non-rigid image registration can improve enhancement curves, but computation time can be long, especially if all voxels are sampled for cost function estimation. This work investigates the influence of the percentage of voxels sampled (PS) on goodness-of-fit, kinetic model parameter values and uncertainties. The spatial distribution of parameter values was more strongly influenced by registration and PS compared to global tumor measures. Registration with very low PS values increased parameter uncertainties compared to unregistered. 5 PS provided similar performance to 100 PS with reduced computation time.

2106

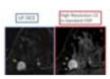

Detection and Morphology of Breast Lesions with Very Early Phase of Ultrafast Dynamic Contrast Enhanced MRI using Compressed Sensing Reconstruction

MASAKO KATAOKA[1], Natsuko Onishi[2], Shotaro Kanao[2], Hajime Sagawa[3], Mami Iima[1], Makiko Kawai[2], Akane Ohashi[2], Rena Sakaguchi[2], Ayami Ohno Kishimoto[2], Marcel Dominik Nickel[4], Masakazu Toi[5], and Kaori Togashi[2]

[1]Diagnostic Imaging and Nuclear Medicine, Kyoto University Graduate School of Medicine, Kyoto, Japan, [2]Kyoto University Graduate School of Medicine, Kyoto, Japan, [3]Division of Clinical Radiology Service, Kyoto University Hospital, Kyoto, Japan, [4]MR Application Predevelopment, Siemens Healthcare GmbH, Erlangen, Germany, [5]Breast Surgery, Kyoto University, Kyoto, Japan

Using ultrafast DCE MRI (UF-DCE)with compressed sensing reconstruction, detection rate and morphology of breast lesions on very early phase images within 1 minutes post contrast injection were compared to those on full diagnostic protocol (FDP). Almost all (95%) of the lesions reported on FDP were identified on UF-DCE. Size of the lesions were slightly smaller on UF-DCE but within-2mm difference in 96% of masses. Considering that wash-in kinetic information can be obtained by UF-DCE, the current data of equivalent lesion detection, size and morphology evaluation on UF-DCE support its application to abbreviated breast MRI protocol.

2107

10 Second Temporal Resolution of Early Enhancement Visualization: Framework for Fast Breast MRI Screening

Jorge E Jimenez[1], Roberta M Strigel[1,2,3], Kevin M Johnson[1], Leah C Henze Bancroft[1], Scott B Reeder[1,2,4,5,6], and Walter F Block[1,2,4]

[1]Department of Medical Physics, University of Wisconsin-Madison, Madison, WI, United States, [2]Department of Radiology, University of Wisconsin School of Medicine and Public Health, Madison, WI, United States, [3]Carbone Cancer Center, University of Wisconsin-Madison, Madison, WI, United States, [4]Department of Biomedical Engineering, University of Wisconsin-Madison, Madison, WI, United States, [5]Department of Medicine, University of Wisconsin School of Medicine and Public Health, Madison, WI, United States, [6]Department of Emergency Medicine, University of Wisconsin School of Medicine and Public Health, Madison, WI, United States

In this work, we present a new methodology for an abbreviated dynamic contrast enhanced (DCE) MRI breast screening protocol. The methodology relays on a novel dynamic reconstruction scheme, local low-rank, applied to breast MR imaging for the first time. Our work provides the framework for a high resolution (0.83 mm isotropic), ultra-fast (10 second volumetric frame rate) imaging technology to deliver detailed information of the early enhancement phase of breast lesions, preserving diagnostic accuracy while shortening exam times. We demonstrate the feasibility of the proposed approach.

2108

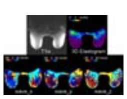

3D Volumetric Noncompressive Breast MR Elastography

Jun Chen[1], Roger Grimm[1], Anshuman Panda[2], Bhavika Patel[2], Judy James[2], Kevin J Glaser[1], Jennifer Kugel[1], Yuan Le[2], Alvin Silva[2], and Richard L Ehman[1]

[1]Radiology, Mayo Clinic, Rochester, MN, United States, [2]Radiology, Mayo Clinic, Scottsdale, AZ, United States

Sternum drivers for breast MRE can produce shear waves in breasts without breast compression effect, which can result in increased breast stiffness due to tissue nonlinearity. A recent 5-slice 2D GREMRE sequence study found sternum driver MRE was a very reproducible method. In our current study, we were able to use 40-slice 3D GREMRE volumetric MRE sequence to compute volumetric breast elastograms in patients.

2109

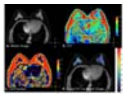

T2* Mapping for Breast Tumor categorizing

Xiaoqi Wang[1] and Lan Liu[2]

[1]Clinical Science, Philips Healthcare, Beijing, People's Republic of China, [2]Department of Radiology, Jiangxi Cancer Hospital

Utilizing the state of art water-fat separation method with multi-echo acquisition in mDIXON quant to explore the relationship between magnetic resonance transverse relaxation time (T2*) and the pathological type of breast tumors.

2110

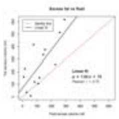

MRI can assess breast cancer related lymphoedema tissue composition and guide management strategy

Marco Borri[1], Kristiana D. Gordon[2,3], Julie C. Hughes[1], Erica D. Scurr[1], Dow-Mu Koh[1], Martin O. Leach[1], Peter S. Mortimer[2,3], and Maria A. Schmidt[1]

[1]CR-UK Cancer Imaging Centre, Royal Marsden NHS Foundation Trust and Institute of Cancer Research, London, United Kingdom, [2]Cardiac and Vascular Sciences, St. George's University of London, London, United Kingdom, [3]Skin Unit, Royal Marsden NHS Foundation Trust and Institute of Cancer Research, London, United Kingdom

Here we present an MRI-based approach to assess breast cancer related lymphoedema tissue composition (fluid, fat, and muscle volumes) and we evaluate a cohort of 13 patients. Our measurements indicate that fat, which cannot be eliminated by first line treatment, was the predominant component of the swelling. Furthermore, changes in tissue composition were not uniform along the arm. Quantification of the volume and spatial distribution of different tissue components could greatly improve treatment delivery and patient selection for optimal treatment. With a 6 minute MRI scan and automated post-processing, this methodology shows potential for implementation in clinical practice.

2111

Accuracy of Multi-Expert algorithm for segmenting the breast

Artem Mikheev[1], Laura Heacock[1], Jean Logan[1], and Henry Rusinek[1]

[1]Radiology Dept., NYU School of Medicine, New York, NY, United States

Breast density, defined as fraction of fibroglandular tissue (FGT), and post-contrast FGT enhancement (background parenchymal enhancement) are considered cancer risk factors. These MRI measures are recommended for radiologic reports and are promising cancer biomarkers. There is a general agreement that isolating the breasts from the chest wall (CW) is the most difficult to automate step in the FGT segmentation pipeline. Various methods for this task have been reported, but all show significant limitations. We have previously developed a semi-automated FGT segmentation tool that required approximately 7 min per case. We are reporting a new algorithm based on six overlapping Experts that significantly improves segmentation speed and accuracy.

2112

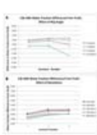

Quantifying Fibroglandular Tissue Volume using Chemical-Shift Encoded MRI: Validation in a Phantom

Leah C Henze Bancroft[1], Diego Hernando[1,2], Xiaoke Wang[1], Scott B Reeder[1,2,3,4,5], and Roberta M Strigel[1,2,6]

[1]Department of Medical Physics, University of Wisconsin-Madison, Madison, WI, United States, [2]Department of Radiology, University of Wisconsin-Madison, Madison, WI, United States, [3]Department of Biomedical Engineering, University of Wisconsin-Madison, Madison, WI, United States, [4]Department of Emergency Medicine, University of Wisconsin-Madison, Madison, WI, United States, [5]Department of Medicine, University of Wisconsin-Madison, Madison, WI, United States, [6]Carbone Cancer Center, University of Wisconsin-Madison, Madison, WI, United States

Increased breast density is a known risk factor for the development of breast cancer. Quantitative MRI methods have the potential to provide accurate, volumetric measures of breast tissue volume and density. A novel, confounder-corrected chemical shift encoded (CSE) MRI technique designed to provide accurate fibroglandular tissue volume and density quantification is validated using a fat and water phantom. The CSE MRI technique provided accurate quantification of water and volumes and was robust to changes in spatial resolution and complexity of fat/water interfaces, indicating this method is expected to produce accurate and robust quantification of fibroglandular and adipose tissue in-vivo.

2113

T2 Relaxation Times of Breast Fibroglandular Tissue Measured From High Resolution, Non-Fat Saturated MR Imaging

Meredith Sadinski[1], Dana Haddad[1], Michelle Zhang[1], Elizabeth A Morris[1], and Elizabeth J Sutton[1]

[1]Radiology, Memorial Sloan Kettering Cancer Center, New York, NY, United States

Reported T2 values in breast tissue are sparse and often disagree. In this study we estimate the T2 relaxation time of fibroglandular breast tissue including fatty compartments intermixed within the fibroglandular matrix. T2 mapping was performed at high spatial resolution for 15 patients at 3T with 4 TEs from 12 to 160 ms and intra- and inter-patient T2 heterogeneity were evaluated. T2 within the finroglandular environment is on the order of 100 ms with a mean standard deviation per patient of 29.6 ms. We hypothesize that this heterogeneity may reflect differences in the fibroglandular microenvironment related to breast cancer risk.

2114

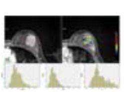

Application of Whole-lesion Histogram Analysis of Pharmacokinetic Parameters in Dynamic Contrast-Enhanced MR Imaging of Breast lesions with CAIPIRINHA-Dixon-TWIST-VIBE Technique

Yiqi Hu[1], Tao Ai[1], Xu Yan[2], Dominik Nickel[3], and Liming Xia[1]

[1]Radiology, Tongji Hospital, Wuhan, People's Republic of China, [2]MR Collaboration NE Asia, Siemens Healthcare, [3]MR Collaboration, Siemens Healthcare

As the use of neoadjuvant chemotherapy is gradually increased in the treatment of breast cancer, evaluating its therapeutic effect is gaining importance. However, tumors are markedly heterogeneous in cells, micro-environmental factors and vasculature structures, which manifests as radiologic heterogeneity. A few studies have been trying to extract heterogeneity metrics from regions of interest (ROIs) such as by means of histogram analysis. Thus, the aim of our study is to investigate the feasibility of whole-lesion histogram analysis of pharmacokinetic parameters in breast T1-weighted dynamic contrast-enhanced MR imaging (DCE-MRI) for differentiating the malignant from benign breast lesions.

2115

Comparison of methods for high spatial-resolution breast diffusion imaging

Jessica Ann McKay[1], Sudhir Ramanna[2], Steen Moeller[2], Edward J Auerbach[2], Gregory J Metzger[2], Michael T Nelson[2], Kamil Ugurbil[2], Essa Yacoub[2], and Patrick J Bolan[2]

[1]Department of Biomedical Engineering, University of Minnesota, Minneapolis, MN, United States, [2]Department of Radiology, University of Minnesota, Minneapolis, MN, United States

Diffusion weighted imaging (DWI) has applications in the screening, diagnosis, and treatment monitoring of breast cancer, but its clinical value in is limited by the low resolution and artifacts of standard methods. In this work we compared a standard method with two high-resolution techniques: read-out segmented EPI (RS-EPI) and single-shot simultaneous multi-slice EPI with in-plane slice encoding (SMS-IPSE). Both the SMS-IPSE and RS-EPI methods can produce high-resolution, accurate diffusion-weighted images at the cost of decreased SNR within a clinically practical 5-minute time window, enabling the detection of smaller lesions.

2116

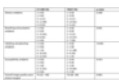

Advanced Ultrafast Dynamic Contrast Enhanced Breast MRI with Compressed Sensing VIBE

Suzan Vreemann[1], Alejandro Rodriguez-Ruiz[1], Dominik Nickel[2], Marnix Maas[1], Nico Karssemeijer[1], Elisabeth Weiland[2], Berthold Kiefer[2], and Ritse Mann[1]

[1]Radiology and Nuclear Medicine, Radboud University Medical Centre, Nijmegen, Netherlands, [2]MR-Application Predevelopment, Siemens Healthcare GmbH, Erlangen, Germany

Previous work showed that ultrafast breast DCE-MRI enables assessment of the contrast inflow curve while providing images at diagnostic spatial resolution. However, the slice thickness (~2.5mm) prevented multiplanar reconstructions and therefore did not yield the same morphological information as obtained with conventional T1-weighted series. We evaluate a compressed sensing VIBE sequence (CS-VIBE) for ultrafast breast MRI that enables high spatio-temporal resolution for both dynamic inflow analysis and morphological evaluation. Two reader-studies were conducted to evaluate image quality and lesion morphology assessment. Our results show that CS-VIBE combines the advantages of both high-spatial and high-temporal resolution of clinically available sequences.

2117

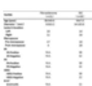

Dynamic contrast-enhanced magnetic resonance imaging in discriminating invasive ductal carcinoma and fibroadenoma: 2D maximum diameter versus 3D whole-tumor

Ting Liang[1], Hongwen Du[1], Gang Niu[1], Peng Cao[1], Chenxia Li[1], Heng Liu[1], Miaomiao Wang[1], and Jian Yang[1]

[1]Department of Diagnostic Radiology, the First Affiliated Hospital of Xi'an Jiaotong University, Xi'an, Shaanxi, People's Republic of China

DCE quantitative measurement plays an important role in the identification of breast tumors. However, different ROI placement can directly affect the inspection results. However, there is no clear standard protocol for clinical routine use. This study aims to evaluate the effect of 2-dimensional maximum diameter (2DMD) and 3-dimensional whole-tumor (3DWT) on quantitative DCE-MRI in differentiating invasive ductal carcinoma (IDC) and breast fibroadenoma which are confirmed by surgical pathology, and determined the more efficient approach for ROI measurement. Our results suggested that 2DMD mean value has more diagnostic performance than 3DWT assessment in distinguishing IDC from fibroadenoma.

2118

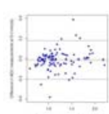

Comparison of whole tumor and single slice ROIs for measuring ADC in breast cancer

Jessica Gibbs[1], Ella Jones[1], Lisa Wilmes[1], David C Newitt[1], John Kornak[1], Melanie Regan[1], and Nola Hylton[1]

[1]University of California, San Francisco, CA, United States

Diffusion weighted imaging is a promising technique to monitor treatment response in patients undergoing pre-surgical chemotherapy, but manually drawn whole tumor measurements are time-consuming and subject to inter-user variability. In this study of 60 patients with sequential DWI exams during treatment, we measured apparent diffusion coefficient (ADC) from whole tumor ROIs and from a single central slice of the tumor. We found strong agreement in ADC between the two methods, suggesting that a slice from the center of the tumor may accurately represent the ADC of the entire tumor.

2119

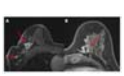

Abbreviated Breast Magnetic Resonance Imaging (MRI) for Extent of Disease Evaluation in Newly Diagnosed Breast Cancer

Stephanie Lee-Felker[1], Lindsey Storer[2], Bo Li[2], Anne Hoyt[2], and Melissa Joines[2]

[1]Radiology, UCLA, Los Angeles, CA, United States, [2]UCLA

In this retrospective study, an abbreviated protocol consisting of pre-contrast T1 and first post-contrast T1 sequences with fat saturation had near perfect detection of index and secondary cancers, as well as suspicious axillary and internal mammary lymph nodes, in women with newly diagnosed breast cancer. In conjunction with clinical histories and prior imaging examinations, an abbreviated breast MRI protocol is adequate for ipsilateral extent of disease and contralateral breast screening in newly diagnosed breast cancer.

2120

Dynamic Contrast-Enhanced Breast MRI using A Chemically Fat-Suppressed View-Sharing Technique

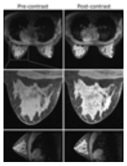

Kang Wang[1], Naoyuki Takei[2], Courtney Morrison[3], Leah Henze Bancroft[3], Ping Ni Wang[3], James H Holmes[4], Ersin Bayram[5], Roberta M Strigel[3,4,6], Frederick Kelcz [4], and Frank R Korosec[3,4]

[1]Global MR Applications & Workflow, GE Healthcare, Madison, WI, United States, [2]Global MR Applications & Workflow, GE Healthcare, Hino, Japan, [3]Medical Physics, University of Wisconsin-Madison, Madison, WI, United States, [4]Radiology, University of Wisconsin-Madison, Madison, WI, United States, [5]Global MR Applications & Workflow, GE Healthcare, Houston, TX, United States, [6]Carbone Cancer Center, University of Wisconsin-Madison, Madison, WI, United States

In clinical breast MRI, the dynamic contrast-enhanced (DCE) T1-weighted fat-suppressed scan plays an essential role for lesion detection and characterization. In order to improve temporal resolution of the dynamic scan, view-sharing techniques are typically used along with Dixon-based water-fat separation methods. However, there are several limitations and drawbacks of using Dixon-based techniques. In this work, we proposed to use chemical fat suppression with view-sharing to improve the temporal resolution of DCE breast MRI.

2121

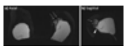

Image quality of silicone-specific STIR Cube-FLEX MRI for breast implant imaging

Kanae K. Miyake[1,2], Debra M. Ikeda[1], Jafi A. Lipson[1], Jeong Seon Park[1], Lloyd Estkowski[3], and Bruce L. Daniel[1]

[1]Radiology, Stanford University School of Medicine, Stanford, CA, United States, [2]Radiology, Rakuwakai Otowa Hospital, Kyoto, Japan, [3]GE Medical Systems

3D Fast-Spin-Echo MRI with Short Tau inversion recovery fat suppression and 2-point Dixon decomposition of water and silicone signal (STIR Cube-FLEX or “Si-Cube”) is a recently developed silicone-specific sequence providing isotropic, high-resolution 3D datasets that are easily reformatted into any plane. We performed a reader study to evaluate the image quality of Si-Cube in 39 females, and found Si-Cube is robust to artifacts and has equivalent image quality to conventional 2D silicone-specific sequences (C-2D). The ability to reformat Si-Cube images in any plane potentially obviates the need to obtain C-2D sequences in other planes, streamlining the overall implant imaging protocol.

2122

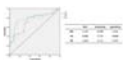

Comparing the diagnosis efficiency of different parameters of diffusion kurtosis imaging model in benign and malignant breast lesions

Ying-ying Wang[1], Yan Zhang[1], Jingliang Cheng [1], Baohong Wen[1], and Dandan Zheng[2]

[1]The First Affiliated Hospital of Zhengzhou University, zheng zhou, People's Republic of China, [2]GE Healthcare,MR Research China, People's Republic of China

In order to comparethe diagnosis efficiency of different parameters derived from diffusion kurtosis imaging model in benign and malignant breast lesions, eighty patients were analyzed in this study . DKI data with six b-values and 15 directions were acquired using single-shot SE-EPI sequence. The values of mean kurtosis (MK), axial kurtosis (AK) and radial kurtosis (RK) in malignant lesions group were significantly higher than those in benign lesions groups. The diagnosis efficiency of these parameters were also analyzed. The results showed that DKI-derived parameters can be used to distinguish the malignant lesions and benign lesions, especially AK and MK

2123

Ductal carcinoma in situ of the breast: Investigation of quantitative MRI features of lesion and normal tissue to predict recurrence after treatment

Averi Kitsch[1,2], Brian Johnston[1,2], Savannah Partridge[1,2], and Habib Rahbar[1,2]

[1]Radiology, University of Washington, Seattle, WA, United States, [2]Breast Imaging, Seattle Cancer Care Alliance, Seattle, WA, United States

Ductal carcinoma in situ (DCIS) is a pre-invasive breast cancer that may be overtreated due to lack of reliable clinical and pathological prognostic features. Kinetics parameters on dynamic contrast-enhanced MRI have shown promise as breast cancer risk biomarkers. We compared imaging parameters of lesions and normal breast tissue between patients with DCIS recurrence and matched controls and found that patients with larger lesions with higher signal enhancement ratio (SER) and higher background parenchymal enhancement (BPE) on preoperative MRI were more likely to recur. These MRI biomarkers show promise for decreasing DCIS overtreatment and warrant further study in larger cohorts.

2124

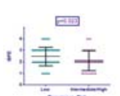

Breast Background Parenchymal Enhancement as a Marker of Breast Cancer Recurrence Risk

Dania Daye[1], Dorothy A Sippo[1], Elkan F Halpern[1], Vishala Mishra[1], Constance D Lehman[1], and Aditya Bardia[2]

[1]Department of Radiology, Massachusetts General Hospital, Boston, MA, United States, [2]Department of Medicine, Massachusetts General Hospital, Boston, MA, United States

Emerging studies suggest that imaging features could complement standard pathologic variables in cancer prognostic assessment. Studies on the association of background parenchymal enhancement (BPE) with breast cancer prognosis remain limited. The goal of this study was to investigate the complementary value of breast BPE as a prognostic marker for breast cancer recurrence risk assessment. DCE-MRI images were retrospectively analyzed from 100 women with breast cancer. Oncotype DX score was used as a surrogate for cancer recurrence. Our results suggest that BPE could complement histopathologic factors in predicting breast cancer recurrence risk and could potentially improve breast cancer prognostication.

2125

Perfusion Parameters at Dynamic Contrast-enhanced Breast MR Imaging are Associated with Disease-Specific Survival in Patients with Triple-Negative Breast Cancer

Vivian Youngjean Park[1], Eun-Kyung Kim[1], Min Jung Kim[1], Jung Hyun Yoon[1], and Hee Jung Moon[1]

[1]Radiology, Yonsei University College of Medicine, Seoul, Korea, Republic of

We investigated the association between perfusion parameters in pretreatment MR imaging and survival outcome. This retrospective study included 61 consecutive patients (median age, 50 years; range, 27-77 years) diagnosed with TNBC who underwent pretreatment DCE breast MR imaging and definitive surgery. The median follow-up time was 46.1 months. Among pretreatment variables, a higher ve value and higher peak enhancement at pretreatment MR imaging were significantly associated with worse disease-specific survival in patients with TNBC. With further validation, these perfusion parameters have the potential to aid in the pretreatment risk stratification of patients with TNBC and in evidence-based clinical decision support.

2126 

Quantitative Breast MRI Background Parenchymal Enhancement for Predicting Response to Chemotherapy

Vignesh Arasu[1], Paul Kim[2], Roy Harnish[2], Cody McHargue[2], Wen Li[2], David C Newitt[2], Ella Jones[2], Laura J Esserman[2], Bonnie N Joe[2], and Nola M Hylton[2]

[1]University of California, San Francisco, San Francisco, CA, United States, [2]University of California, San Francisco

The purpose of this study was to investigate how background parenchymal enhancement (BPE) may additively improve an MR tumor model for prediction of non-pathologic complete response (non-PCR) patients in the neoadjuvant setting. BPE identified 24-36% of non-PCR patients independent of tumor factors while maintaining a low misclassification of PCR patients. In conjunction with a tumor model using tumor and treatment factors, addition of BPE may improve residual cancer prediction of up to 60% of patients, but results were not statistically significant.

2127 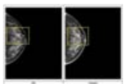

The Significance of Joint Clinical Application of Digital Mammary Gland 3D Tomosynthesis with Magnetic Resonance Imaging for Diagnosis of Breast Cancer

Wenwen Fan[1], Han Ouyang[1], Chunwu Zhou[1], Xinming Zhao[1], and Lizhi Xie[2]

[1]National Cancer Center/Cancer Hospital, Chinese Academy of Medical Sciences and Peking Union Medical College, Beijing, People's Republic of China, [2]GE HealthCare, MR Research China, Beijing, People's Republic of China

Synopsis In recent years, the incidence rate of breast cancer in China has been rising rapidly, which highlights the importance of early diagnosis. Therefore, how to improve the detection rate and reduce the recall rate become significant for the breast cancer prevention and treatment. Considering the tissue overlapping effect from conventional digital mammary gland photography technology may lead to false positive and negative results.

2128 

Multicenter study of intravoxel incoherent motion (IVIM) metrics in breast cancer with software comparison.

Gene Young Cho[1,2,3], Elizabeth J Sutton[2], Linda Moy[1,3], Lucas Gennaro[2], Artem Mikheev[1,3], Henry Rusinek[1,3], James S Babb[1,3], Daniel K Sodickson[1,3], Elizabeth A Morris[2], Sunitha B Thakur[2], and Eric E Sigmund[1,3]

[1]Radiology, Bernard and Irene Schwartz Center for Biomedical Imaging, New York University School of Medicine, New York, NY, United States, [2]Radiology, Memorial Sloan Kettering Cancer Center, New York, NY, United States, [3]Radiology, Center for Advanced Imaging Innovation and Research (CAI2R), New York University Langone Medical Center, New York, NY, United States

This study compares data collected from different MR vendor systems using different software packages to better understand the robustness and reproducibility of IVIM metrics. Patient data from 2 sites (Site 1 & 2) from 1.5/3T systems (GE/Siemens) were analyzed with 2 software packages to derive IVIM biomarkers and their intersite/software variability. Results show that metrics of IVIM average and histogram analysis are robust quantitative imaging biomarkers for breast cancer.

2129 

Using Natural Language Processing to Explore the Correlation of Breast MR Findings and BI-RADS classification

Yuan Jiang[1], Yi Liu[1], Yahui Shi[2], Zuofeng Li[2], Juan Wei[2], and Xiaoying Wang[1]

[1]Radiology, Peking University First Hospital, Beijing, People's Republic of China, [2]Philips Research China, Shanghai, People's Republic of China

The decision tree trained on MR descriptions by natural language processing (NLP) method shows desirable capability in identifying the high-risk BI-RADS 5-6 class.From the decision path, we identify the key indicators to distinguish BI-RADS 5-6 from the relatively low-risk classes. And the inner heterogeneity of BI-RADS 4 cases makes it difficult to build a general model for this class.

2130 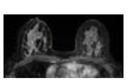

Quantitative analysis of background parenchymal enhancement in whole breast on MRI: influence of menstrual cycle and comparison with qualitative analysis

Tae Hee Kim[1], Doo Kyoung Kang[1], Sun Young Park[1], and Joo Sung Sun[1]

[1]Radiology, Ajou University Hospital, Suwon, Korea, Republic of

We quantitatively analyzed the background parenchymal enhancement of whole breast on MRI using in-house software with MATLAB.

The mean values of BPE were well correlated with qualitative grades of BPE.

The mean and ninety percentile values of BPE were lowest in 2nd week of menstrual cycle and highest in 4th week with statistical significance (p=0.005 for mean values and p=0.003 for nienty percentile, respectively).

2131 

Gradient tracing for segmentation of low resolution, low T1-weighted breast MR images

Jacob Johnson[1], Leah Henze Bancroft[1], Ryan Zea[2], Diego Hernando[1,3], Scott Reeder[1,3,4,5,6], and Roberta Strigel[1,3,7]

[1]Radiology, UW- Madison, Madison, WI, United States, [2]Biostatistics and Medical Informatics, UW- Madison, WI, United States, [3]Medical Physics, UW- Madison, Madison, WI, United States, [4]Medicine, UW- Madison, Madison, WI, United States, [5]Biomedical Engineering, UW-Madison, Madison, WI, United States, [6]Emergency Medicine, UW- Madison, Madison, WI, United States, [7]Carbone Cancer Center, UW-Madison, Madison, WI, United States

Segmentation of breast MR images remains a challenge and a necessity for a variety of quantitative applications. We present a semi-automatic methodology for segmentation of breast tissue for the special case of low resolution, low flip angle chemical shift encoded MRI (CSE-MRI) with water-fat separation. User interaction is required to set the bounds of the segmentation, while the chest wall and skin are segmented automatically. The results differed with corrections by an experienced radiologist by 4.2% average error per case. The method exhibits comparable accuracy to published methods and high agreement between non-expert reviewers.

2132

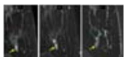

Sub-millimeter bSSFP isotropic T2 weighted breast imaging - results of a prospective clinical study to determine if specificity of breast MRI can be improved.

Frederick Kelcz[1], Leah Henze Bancroft[2], Jorge E. Jimenez[2], and Walter F. Block[2]

[1]Radiology, University of Wisconsin, Madison, WI, United States, [2]Medical Physics, University of Wisconsin, WI, United States

Although DCE-MRI is the mainstay of breast MRI diagnosis, specificity is limited due to multiple enhancing benign lesions. Specificity can by improved by viewing T2 information, but conventional T2 imaging is limited by spatial resolution. We performed a prospective clinical study of a novel T2-like imaging sequence with sub-mm spatial resolution to determine if a breast radiologist could improve his assessment of benignity. Results show that excellent spatial resolution was achieved, but at the cost of increased noise and loss of T2 contrast. Ultimately, the radiologist felt less confident in more cases than he felt more confident regarding benign lesions.

2133

Association of Preoperative MR Imaging Features with Positive Resection Margins in Breast Conservation Surgery

Min Sun Bae[1], Luca A. Carbonaro[1], Elizabeth J. Sutton[1], and Elizabeth A. Morris[1]

[1]Department of Radiology, Memorial Sloan Kettering Cancer Center, New York, NY, United States

Breast conservation surgery (BCS) is a standard treatment for early-stage breast cancer, and includes a complete removal of the tumor with a margin of tumor-free breast tissue. If margins of the resected tissue are involved at final surgical pathology, patients undergo additional surgery. Although MR imaging is the most sensitive modality for breast cancer, the effect of preoperative MR imaging on the improvement of surgical outcomes is controversial. There are only a few studies evaluating association between preoperative MR imaging features and positive resection margins (RMs) in patients with invasive breast cancer.

2134

Quantitative assessement of MRI Background Parenchymal Enhancement in comparison with qualitative assessment – Can it predict breast cancer?

Barbara Bennani-Baiti[1] and Pascal Andreas Baltzer[1]

[1]Department of Biomedical Imaging and Image-guided Therapy, Medical University of Vienna, Vienna, Austria

While breast density is a recognized risk factor for breast cancer, the role of background parenchymal enhancement (BPE) is still controversially discussed. Since BPE reflects hormonally active breast tissue, it may serve as a biomarker for malignancy. Current assessment of BPE, however, is hampered by the subjective nature of its assessment. We therefore tested an automated approach that quantified the percentage of enhancing breast tissue of the entire contralateral breast. This pilot study finds the amount of quantitatively assessed enhanced breast parenchyma as a percentage of the entire breast to inversely correlate with breast cancer risk, while visually estimated BPE did not correlate with breast cancer.

2135

Is ADC heterogeneity helpful in characterizing ductal carcinoma in situ (DCIS) at 3.0T breast MRI

Oi Lei Wong[1], Gladys Goh Lo[2], Jing Yuan[1], Helen Hei Lun Chan[2], Ting Ting Wong[3], and Polly Suk Yee Cheung[3]

[1]Medical Physics and Research Department, Hong Kong Sanatorium & Hosptial, Hong Kong, Hong Kong, [2]Department of Diagnostic & Interventional Radiology, Hong Kong Sanatorium & Hosptial, Hong Kong, Hong Kong, [3]Breast Care Center, Hong Kong Sanatorium & Hosptial, Hong Kong, Hong Kong

In this study, we intended to investigate the relationship between ADC heterogeneity of DCIS lesions and DCIS lesioxn morphology, histological grade and BIRADS classification using 3T DW breast MRI. Increasing heterogeneity was observed with increasing DCIS histological grade and increasing BIRADS, but not reaching significance level, was observed based on our results. This study was mainly limited in the small numbers of DCIS lesions, so statistical power has to be further strengthened in future studies with larger sample size.

Traditional Poster

Lung

Exhibition Hall 2136-2164 Wednesday 8:15 - 10:15

2136

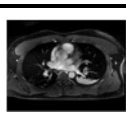

Utility of MRI for the Evaluation of Acute Pulmonary Embolism

Anthony Jedd[1], James Costello[1], Shannon Urbina[1], Bobby Kalb[1], and Diego Martin[1]

[1]Medical Imaging, Banner University Medical Center, Tucson, AZ, United States

CT-PA is the gold standard for diagnosis of pulmonary embolism, but requires use of radiation and iodinated contrast. There is an overall low incidence of positive studies (5%) in the patient population 18-45. Our study evaluates the negative predictive value of MRI as the primary imaging modality for exclusion of suspected PE in patients <40 y/o and/or relative contraindication to iodinated contrast. We found a negative predictive value of 99% in our patient population. These results suggest that MRI is an effective first-line imaging modality to exclude PE, while reducing exposure to ionizing radiation and iodinated contrast.

2137 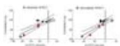

Evaluation of ventilation changes in lung transplant recipients with hyperpolarized helium-3 MR imaging: Comparison with pulmonary function tests

Lucia Flors[1], Talissa A Altes[2], John P Mugler III[1], G Wilson Miller[1], Jaime F Mata[1], Sarah K Kilbourne[3], Hannah C Mannem[3], Max M Weder[3], and Yun M Shim[3]

[1]Radiology and Medical Imaging, University of Virginia, Charlottesville, VA, United States, [2]Department of Radiology, University of Missouri, [3]Pulmonary and Critical Care Medicine, University of Virginia

Purpose: To determine if the changes in lung ventilation using HP 3He-MRI can provide in vivo pulmonary physiology highly relevant in defining CLAD phenotypes among lung transplant patients, phenotypes which otherwise are undetectable by the usual PFT parameters such as FEV1. Methods: Thirteen lung transplant recipients underwent ventilation HP 3He MR lung imaging and spirometry; the latter was compared to baseline spirometry. Time from transplant was 2.5 ±2.5 yrs. Results/ Conclusion: Declined lung function after lung transplant correlated well with decreased ventilated lung volume in the transplanted lung found with HP 3He MRI.

2138 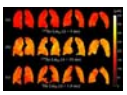

3D Mapping of Whole Lung Morphometry with 129Xe Diffusion-Weighted MRI and Compressed Sensing: Comparison with 3He

Ho-Fung Chan[1], Neil J Stewart[1], Juan Parra-Robles[1,2], Guilhem J Collier[1], and Jim M Wild[1]

[1]Academic Unit of Radiology, University of Sheffield, Sheffield, United Kingdom, [2]Department of Bioengeering, Universidad Carlos III de Madrid, Madrid, Spain

3D whole lung morphometry maps were acquired with ^{129}Xe DW-MRI and compressed sensing. Prospective three-fold undersampled 3D ^{129}Xe lung morphometry (Lm_D) maps were derived using the stretched exponential model (SEM) and compared with equivalent ^{3}He datasets. Five healthy volunteers were imaged using a range of ^{129}Xe diffusion times and the most agreeable ^{129}Xe and ^{3}He Lm_D results were obtained with a ^{129}Xe diffusion time of 8.5 ms. These results indicate that the Lm_D values derived from the SEM are dependent on diffusion time and that ^{129}Xe could present a clinically-viable alternative to ^{3}He for whole lung morphometry mapping.

2139 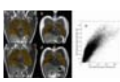

Rapid acquisition of co-registered 3D xenon-129 and proton images of the human lung in a single breath-hold using compressed sensing

Guilhem Jean Collier[1], Paul J Hughes[1], Felix C Horn[1], Ho-Fung Chan[1], Graham Norquay[1], Neil J Stewart[1], and Jim M Wild[1]

[1]Academic Unit of Radiology, University of sheffield, Sheffield, United Kingdom

The feasibility and suitability of using compressed sensing to accelerate the acquisition of 3D lung ventilation images with hyperpolarized ^{129}Xe and to enable same-breath anatomical ^{1}H imaging was investigated. Fully sampled and prospective data were acquired from one healthy smoker. Retrospective simulations showed a good agreement between fully sampled and reconstructed images using different error metrics. The method was further validated by comparing quantitative imaging metrics; percentage ventilated volume, distribution of signal intensity and maps of coefficient of variation in prospectively acquired data. The results indicate that the method can be implemented for clinical evaluation in patients with lung diseases.

2140 

Large-scale production of highly-polarized 129Xe

Graham Norquay[1], Guilhem J Collier[1], Madhwesha Rao[1], Adam Maunder[1], Oliver I Rodgers[1], Neil J Stewart[1], and Jim M Wild[1]

[1]Academic Unit of Radiology, University of Sheffield, Sheffield, United Kingdom

Rapid production of large volumes of highly polarized ^{129}Xe with continuous-flow spin-exchange optical pumping (SEOP) ^{129}Xe polarizers is vital for high-throughput hyperpolarized (HP) ^{129}Xe lung imaging and emergent clinical applications with dissolved ^{129}Xe, e.g. brain perfusion. However, the production rate is limited by cell volume, previously between 300-1500 cm^3. Here we present a custom-built ^{129}Xe polarizer designed with a SEOP cell volume of 3500 cm^3 which can produce ^{129}Xe polarized to 35% at a Xe production rate of 1200 mL/hour, enabling high-SNR ^{129}Xe lung imaging of naturally abundant Xe and high-SNR ^{129}Xe brain imaging with isotopically-enriched Xe.

2141 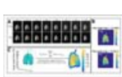

Double tracer gas single breath washout (SBW) lung imaging with hyperpolarized Xe-129 and He-3

Felix C Horn [1], Guilhem J Collier[1], Ho-Fung Chan[1], Neil J Stewart[1], Laurie Smith[1], and Jim M Wild[1,2]

[1]Academic Radiology, University of Sheffield, Sheffield, United Kingdom, [2]Insigneo Institute, University of Sheffield, Sheffield, United Kingdom

Single breath washout (SBW) is an emerging pulmonary function test due to its relative simplicity and speed. Most significant outcome parameter, phase III ‘alveolar’ slope (tracer gas decay during mid-exhalation) is sensitive to ventilation heterogeneity. In this work, a method is presented for SBW-imaging with two tracer gases with inherently different physical properties: hyperpolarized ^{129}Xe and ^{3}He. Findings in our study are in agreement with trends seen in SBW from pulmonary function lab: the heavier, less diffusive gas (^{129}Xe) has a steeper phase III slope. This indicates increased regional ventilation heterogeneity due to a lesser degree of diffusional mixing.

2142

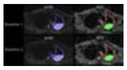

Assessment of Repeatability of Disease Burden and ADC estimates in Malignant Pleural Mesothelioma using Diffusion Weighted Imaging

Lin Cheng[1], Matthew D. Blackledge[1], David J. Collins[1], Nina Tunariu[1,2], Matthew R. Orton[1], Martin O. Leach[1], and Dow-Mu Koh[1,2]

[1]Division of Radiotherapy and Imaging, Cancer Research UK Cancer Imaging Centre, Institute of Cancer Research, London, United Kingdom, [2]Radiology, Royal Marsden Hospital, London, United Kingdom

We demonstrate the repeatability of tumour volume and apparent diffusion coefficient (ADC) estimates; obtained by combining 3D semi-automatic segmentation with a global ADC threshold using DW-MRI in malignant pleural mesothelioma. The results of our classification of solid tumour show excellent repeatability of mean and median ADC estimates and tumour volume. Our methodology provides a clinical tool for radiologists to evaluate tumour burden of MPM in a fast and highly repeatable way.

2143

Dissolved phase Hyperpolarized Xenon-129 pulmonary imaging in the presence of gaseous Xenon signal

Jeff Kammerman[1], Andrew Hahn[1], Scott Haile Robertson[2], Bastiaan Driehuys[2], and Sean B Fain[1]

[1]Department of Medical Physics, University of Wisconsin at Madison, Madison, WI, United States, [2]Center for In Vivo Microscopy, Department of Radiology, Duke University Medical Center, Durham, NC, United States

Dissolved-phase hyperpolarized Xenon-129 imaging shows promise as a means to evaluate gas transfer from the airspaces of the lungs to parenchymal tissue and the blood stream. This typically requires selective excitation of dissolved-phase 129Xe, but its short T_2^* requires the use of short RF pulses. This reduces the achievable spectral selectivity and often leads to unwanted excitation of gas-phase Xenon. In this work, we present a method to selectively remove gas-phase contamination from dissolved-phase images. Our method is developed and validated with guidance from simulated data using a digital phantom and shown to be feasible in human subject scans.

2144

Optimizing data efficiency in SENCEFUL-based lung perfusion studies

Andreas Max Weng[1], Tobias Wech[1], Lenon Mendes Pereira[1], Simon Veldhoen[1], Andreas Steven Kunz[1], Thorsten Alexander Bley[1], and Herbert Köstler[1]

[1]Department of Diagnostic and Interventional Radiology, University Hospital of Würzburg, Würzburg, Germany

SElf-gated Non-Contrast-Enhanced FUnctional Lung imaging (SENCEFUL) allows assessment of lung ventilation and perfusion without the use of contrast agent or ionizing radiation. The original implementation, however, is rather inefficient in terms of data usage when reconstructing perfusion weighted datasets, as it analyzes data from a single breathing state only. In this study we present an approach that uses data from all breathing states, aiming at an improved quality of the resulting perfusion maps. A registration algorithm was applied for this purpose.

2145

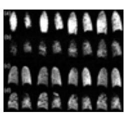

Assessment of lung inflation state on the repeatability of hyperpolarized gas ventilation MRI

Paul John Clifford Hughes[1], Laurie Smith[1,2], Felix C. Horn[1], Alberto Biancardi[1], Neil J. Stewart[1], Graham Norquay[1], Guilhem J. Collier[1], and Jim Wild[1,3]

[1]POLARIS, Academic Unit of Radiology, University of Sheffield, Sheffield, United Kingdom, [2]Sheffield Childrens Hospital, Sheffield, United Kingdom, [3]Insigneo Institute for in silico Medicine, Sheffield, United Kingdom

Repeatability of inflation levels, and the imaging metrics derived from them, is important in hyperpolarized gas MRI, particularly when attempting to measure a response from interventions. This work presents same-session repeatability of 5 different inflation levels and their accuracy in comparison to plethysmography measures. Further the effect of inflation level on percent ventilated lung volume and coefficient of variation was investigated. The most repeatable lung volumes were total lung capacity, functional residual capacity plus 1 liter and residual volume. Percent ventilated lung volume was repeatable to within a maximum of 2% error.

2146

Optimization of free breathing radial DCE-MRI protocol for quantitative clinical evaluation of pleural malignancies

Thomas S.C. Ng[1], Ravi T. Seethamraju[2], and Ritu R. Gill[1]

[1]Radiology, Brigham and Women's Hospital, Boston, MA, United States, [2]Siemens Healthcare USA

Clinical diagnosis of pleural malignancies and evaluation of their treatment response to novel anti-angiogenic agents would benefit from quantitative clinical DCE-MRI. Implementation of robust DCE-MRI of the thorax is challenging given the presence of significant respiratory motion. We optimized a clinical DCE-MRI protocol based upon the Radial Stack of Stars acquisition scheme to obtain 3-dimensional motion insensitive DCE-MRI of pleural malignancies. When compared to other commonly used DCE-MRI protocols with cartisian acquisitions, our free breathing protocol demonstrated good SNR, minimal motion down to a spatial resolution of 2mm3.

2147

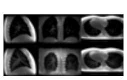

3D UTE Cones for high resolution MR lung imaging and lung density visualisation

Konstantinos G. Zeimpekis[1,2], Klaas Prüssmann[2], Florian Wiesinger[3], Patrick Veit-Haibach[1], and Gaspar Delso[4]

[1]Nuclear Medicine, University Hospital Zurich, Zurich, Switzerland, [2]Information Technology and Electrical Engineering, ETH, Zürich, Switzerland, [3]GE Global Research, Munich, Germany, [4]GE Healthcare, Waukesha, WI, United States

The primary objective of this study is to test 3D UTE Cones clinically for MR lung imaging. The purpose of the investigation is twofold. Primary goal is to test whether or not Cones can be used for high resolution lung anatomical imaging that might be useful for imaging vessels or pulmonary nodules. We test also the possibility for detecting and visualising the lung density that can also be used for imaging parenchyma diseases and more importantly can lead to more accurate extraction of lung attenuation maps for PET/MR attenuation correction.

2148 

Reproducibility and Methodological Considerations for Dissolved-Phase 129Xe Spectroscopy in Patients with Idiopathic Pulmonary Fibrosis.

Neil J Stewart[1], Nicholas D Weatherley[1], Ho-Fung Chan[1], Laura C Saunders[1], Madhwesha Rao[1], Guilhem J Collier[1], Laurie Smith[1], Matthew Austin[2], Graham Norquay[1], Stephen A Renshaw[3], Stephen M Bianchi[2], and Jim M Wild[1]

[1]Academic Unit of Radiology, University of Sheffield, Sheffield, United Kingdom, [2]Academic Directorate of Respiratory Medicine, Sheffield Teaching Hospitals, Sheffield, United Kingdom, [3]Infection, Immunity and Cardiovascular Disease, University of Sheffield, Sheffield, United Kingdom

The reproducibility of quantitative parameters of pulmonary gas-exchange function derived from ^{129}Xe chemical shift saturation recovery (CSSR) and high-resolution spectroscopy (HRS) was evaluated in patients with idiopathic pulmonary fibrosis. Of the CSSR-derived parameters, surface-area-to-volume ratio was found to be most reproducible (intraclass correlation κ=0.756). Furthermore, the ratio of ^{129}Xe signal in pulmonary red blood cells (RBC) to tissue/plasma (TP) from HRS exhibited good reproducibility (κ=0.760). The clinical interpretation of these results is discussed along with methodological considerations and their bearing on the future clinical potential of these techniques.

2149 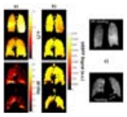

Implications of B0 and B1 inhomogeneity for bSSFP imaging of hyperpolarized media

Neil James Stewart[1] and Jim Michael Wild[1]

[1]University of Sheffield, Sheffield, United Kingdom

The effect of B_0 and B_1 transmit inhomogeneity on 3D bSSFP lung imaging with hyperpolarized ^{129}Xe was simulated using flip angle and off-resonance frequency maps in combination with the matrix product operator approach to predict ^{129}Xe magnetization dynamics and associated bSSFP signal distributions. B_1-related signal drop-off was predicted in posterior and some anterior regions, whilst central regions were generally robust to flip angle variations. Regions of high off-resonance frequency near the diaphragm resulted in low simulated bSSFP signal, corresponding spatially to banding artifact locations. When combined, the two factors led to mean bSSFP image intensity variations ~15-20%.

2150 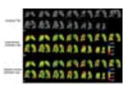

Comparison of quantitative algorithms for calculating VDP from hyperpolarized 129Xe MRI – testing reproducibility of a biomarker of airway obstruction

Wei Zha[1], Mu He[2], Bastiaan Driehuys[3,4,5,6], and Sean B Fain[1,7,8]

[1]Department of Medical Physics, University of Wisconsin-Madison, Madison, WI, United States, [2]Department of Electrical and Computer Engineering, Duke University, NC, United States, [3]Department of Biomedical Engineering, Duke University, NC, United States, [4]Department of Medical Physics, Duke University, NC, United States, [5]Department of Radiology, Duke University, NC, United States, [6]Center for In Vivo Microscopy, Duke University, NC, United States, [7]Department of Biomedical Engineering, University of Wisconsin-Madison, Madison, WI, United States, [8]Department of Radiology, University of Wisconsin-Madison, Madison, WI, United States

There is a need to establish robust quantification pipelines to analyze ^{129}Xe ventilation MRI for multi-center studies. Moreover, there is increasing interest in quantifying not only ventilation defect percent, but also regions of low and high ventilation. To this end, we sought to determine inter-method agreement between two different semi-automated quantitative mapping approaches — linear binning and adaptive *K*-means. The results suggest that once bias field corrections are applied consistently, both ventilation analysis methods agree well when classifying ventilation into 4 bins. Thus, with key steps outlined here, either method can be readily deployed in multi-center studies.

2151 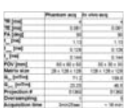

Density-adapted UTE for SF6 visualisation in small animal lung imaging

Marta Tibiletti[1], Armin M. Nagel[2,3], and Volker Rasche[4]

[1]Core Facility Small Animal MRI, Ulm University, Ulm, Germany, [2]Department of Diagnostic and Interventional Radiology, University Medical Center Ulm, Ulm, Germany, [3]Institute of Radiology, University Hospital Erlangen, Erlangen, Germany, [4]Internal Medicine II, University Hospital of Ulm, Ulm, Germany

Fluorinated gases as hexafluorane (SF6) may be used to visualize ventilations in lungs clinical and preclinical acquisitions. SF6 is characterized by T1 ~ T2* ~ 1 ms, therefore is best visualized with sequences allowing for short TR and TE, such as 3D UTE. SNR is generally limited by low spin density and low thermal polarization. In this work, we applied a density-adapted sampling scheme, previously developed for 23Na imaging, to the visualization of SF6 in phantom and in-vivo lung mice acquisitions. We verified that it increases image SNR and sharpness with respect to regular sampling without significant drawbacks.

2152 

Quantifying Changes in Time-Resolved Hyperpolarized ^{129}Xe Spectroscopy among Healthy and IPF Subjects

Elianna A Bier[1,2], Scott H Robertson[1,2], Rohan S Virgincar[1,3], Mu He[1,4], Ziyi Wang[1,3], Geoff M Schrank[1], Rose Marie Smigla[5], Craig Rackley[6], H. Page McAdams[6], and Bastiaan Driehuys[1,2,3,6]

[1]Center for In Vivo Microscopy, Duke University Medical Center, Durham, NC, United States, [2]Medical Physics Graduate Program, Duke University, Durham, NC, United States, [3]Department of Biomedical Engineering, Duke University, Durham, NC, United States, [4]Department of Electrical and Computer Engineering, Duke University, Durham, United States, [5]Division of Pulmonary, Allergy and Critical Care, Department of Medicine, Duke University Medical Center, Durham, NC, United States, [6]Department of Radiology, Duke University Medical Center, Durham, NC, United States

The spectral parameters of ^{129}Xe in airspaces, interstitium and red blood cells (RBCs) are sensitive to disease. We sought to test how these parameters change during inhalation, breath-hold, and exhalation, and identify dynamic signatures that distinguish healthy subjects from patients with idiopathic pulmonary fibrosis (IPF). We find in all subjects that the RBC amplitude oscillates at the cardiac pulsation frequency. However, in IPF patients, this oscillation is also prominent in the chemical shift and phase of the RBC resonance. These dynamic metrics are potentially useful biomarkers for disease progression, as well as discriminating between different pathologies that impact gas exchange.

2153

Continuous Cryogen-Free Up-Concentration of Hyperpolarized $^{129}$Xe Gas

Wolfgang Kilian[1], Lorenz Mitschang[1], Sergey Korchak[1], and Jan Wind[2]

[1]Physikalisch-Technische Bundesanstalt (PTB), Berlin, Germany, [2]Helmholtz-Zentrum Geesthacht, Geesthacht, Germany

A semipermeable membrane was utilized to separate the process gas helium from a continuous gas stream containing hyperpolarized $^{129}$Xe. By this the xenon partial pressure was increased by a factor of ten and the gross amount of helium was removed from the gas stream which was fed from the polarizer to a liquid probe within an NMR spectrometer. Using a sample of dissolved cryptophane-A cage allowed to separate the effects of up-concentration and polarization loss. The increase in xenon partial pressure was still a twofold higher than the polarization loss we have seen and improvements are obvious from the analysis.

2154

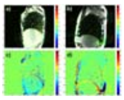

Diaphragm displacement during ABC controlled breath holding: is there an optimal inspiratory threshold?

Evangelia Kaza[1,2], David John Collins[2], Matthew Orton[2], and Martin Osmund Leach[2]

[1]University Hospitals of Leicester NHS Trust, Leicester, United Kingdom, [2]CRUK Cancer Imaging Centre, Institute of Cancer Research and Royal Marsden Hospital, London, United Kingdom

Diaphragm motion range during controlled breath-holding at three different inspiratory levels was assessed during dynamic MRI employing an Active Breathing Coordinator (ABC). Colour intensity projections displayed diaphragm position with time. Diaphragm displacements were calculated from difference images between the end and beginning of breath-holds. Overall, diaphragm volume displacements were smaller for the 75% deep inhalational volume (DIV) threshold typically applied in lung and breast radiotherapy, than for the shallower inspiratory levels of 50% and 25% DIV. The clinical standard 75% DIV threshold not only expands the lungs more but also decreases diaphragm motion range.

2155

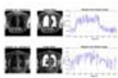

Evaluation of the impact of blood inflow on free-breathing 2D dynamic oxygen-enhanced MRI

Jose L Ulloa[1,2], Alexandra R Morgan[1], Tony Lacey[1], and Geoff JM Parker[1,2]

[1]Bioxydyn Ltd, Manchester, United Kingdom, [2]School of Health Sciences, The University of Manchester, Manchester, United Kingdom

Technical validation of dynamic oxygen–enhanced MRI (OE-MRI) techniques is required for them to become accepted and useful imaging biomarkers. In this work we quantify the impact of using different scanner platforms and protocols on the parameterisation of dynamic single-slice OE-MRI of the lung. Results show that blood in-flow effects consistently provided lower estimates of baseline T_1 and higher estimates of maximum change in partial pressure of oxygen, but it does not influence the wash in time estimation. This suggests that sensitivity to variation in ventilation is approximately equivalent using both protocols.

2156

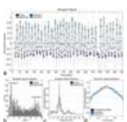

Point-resolved spectroscopy with self-navigation for precise reversible transverse relaxation quantification in pulmonary tissue robust to breathing state variation at 1.5 and 3 Tesla

Jascha Zapp[1], Sebastian Domsch[1], Sebastian Weingärtner[1,2,3], and Lothar R Schad[1]

[1]Computer Assisted Clinical Medicine, Heidelberg University, Mannheim, Germany, [2]Electrical and Computer Engineering, University of Minnesota, Minneapolis, MN, United States, [3]Center for Magnetic Resonance Research, University of Minnesota, Minneapolis, MN, United States

The reversible transverse relaxation time is currently under investigation as a promising biomarker for diagnosis of lung diseases. We propose an enhanced point-resolved spectroscopy sequence for precise relaxation quantification with self-navigation robust to breathing state variation. The obtained relaxation times show evidence for sensitivity to tissue structure alteration during normal breathing. This approach potentially enables a precise assessment of tissue structure in pulmonary diseases such as fibrosis and COPD.

2157

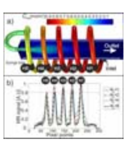

Fast Dynamic Lung Ventilation MRI of Hyperpolarized 129-Xenon using Spiral k-space Sampling

Ozkan Doganay[1,2], Tahreema N. Matin[2], Brian Burns[1,2], Rolf F. Schulte[3], Fergus V. Gleeson[1,2], and Daniel Bulte[1,2]

[1]Department of Oncology, University Of Oxford, OXFORD, United Kingdom, [2]Department of Radiology, The Churchill Hospital, OXFORD, United Kingdom, [3]General Electric Global Research, Munich, Germany

We implemented a spiral k-space sampling approach for Dynamic hyperpolarized ^{129}Xe Ventilation Imaging (DXeVI) of human lungs. The gas-inflow effect, susceptibility artifacts, spatial and temporal resolutions for capturing Gas Flow Patterns (GFPs) were quantified in the gas-flow phantom and compared to corresponding simulated GFPs. DXeVI of GFPs are shown to be sensitive to small gas flow changes between the anterior and posterior lung regions in healthy three subject. This technique can potentially be used to detect and quantify ventilation defects associated with early stage COPD or asthma to assess disease severity, response to treatments and to identify disease progression.

2158

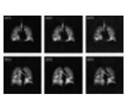

k-space based Restoration of Hyperpolarized Xenon-129 MRI

He Deng[1], Junshuai Xie[1], Huiting Zhang[1], Xianping Sun[1], and Xin Zhou[1]

[1]Key Laboratory of Magnetic Resonance in Biological Systems, State Key Laboratory of Magnetic Resonance and Atomic and Molecular Physics, National Center for Magnetic Resonance in Wuhan, Wuhan Institute of Physics and Mathematics, Chinese Academy of Sciences, Wuhan, People's Republic of China

The magnetization of hyperpolarized media (such as Xenon-129, Helium-3 and Carbon-13) is nonrenewable, which makes it difficult to achieve both high signal-to-noise ratio and good spatial resolution in reconstructed MR images. Consequently, a *k*-space based restoration method is proposed to improve the quality of hyperpolarized MR images in this study, aiming to improve the visual quality of such images. Moreover, a new descriptor is proposed to measure the visual quality of hyperpolarized MR images. Experimental results demonstrated the proposed method is beneficial in visualizing detailed structures in pulmonary images, such as ventilation fine defects.

2159

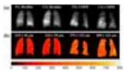

Human Lung Morphometry using Hyperpolarized 129Xe Multi-b Diffusion MRI with Compressed Sensing

Huiting Zhang[1,2], Junshuai Xie[2], Sa Xiao[2], Xian Chen[2], Xiuchao Zhao[2], Ke Wang[3], Guangyao Wu[3], Chaohui Ye[1,2], and Xin Zhou[2]

[1]School of Physics, Huazhong University of Science and Technology, Wuhan, People's Republic of China, [2]Key Laboratory of Magnetic Resonance in Biological Systems, State Key Laboratory of Magnetic Resonance and Atomic and Molecular Physics, National Center for Magnetic Resonance in Wuhan, Wuhan Institute of Physics and Mathematics, Chinese Academy of Sciences, Wuhan, People's Republic of China, [3]Department of Magnetic Resonance Imaging, Zhongnan Hospital of Wuhan University, Wuhan, People's Republic of China

This work is to investigate the feasibility of compressed sensing (CS) on the morphologic measurement of lung microstructure using hyperpolarized ^{129}Xe diffusion magnetic resonance imaging (MRI). The fully sampled (FS) and prospective CS multi-b diffusion MRI data were obtained from five healthy subjects and one COPD patient, respectively. The maps and global average values of mean linear intercept length (L_m) were calculated using cylinder model. The results were compared between FS and CS method for all subjects. The difference between FS and CS ranged from -2.3% to 7.2%. A highly Person's correlation (R=0.988) between FS and CS was presented.

2160

MRI Characterization of Lung Lesions from Pulmonary Tuberculosis

Liya Wang[1,2], Zhou Liu[1], Tianran Li[1], Sulan Wei[1], Xien Bai[3], Yuzhong Zhang[4], and Hui Mao[2]

[1]Radiology, Cancer Hospital of Chinese Academy of Medical Sciences at Shenzhen, China, Shenzhen, People's Republic of China, [2]Radiology and Imaging Sciences, Emory University School of Medicine, Atlanta, GA, United States, [3]MR Technical Services, Siemens Healthcare Ltd., People's Republic of China, [4]Radiology, Longhua People's Hospital of Shenzhen, People's Republic of China

This work demonstrated that lung MRI can be applied to imaging and characterize the abnormalities and lesions in patients with history of pulmonary tuberculosis (TB) with the validation of clinical CT. Results and examples show that MRI not only offers a non-radiation imaging alternative to CT for the lung examination, but also can provide additional information on lung soft tissue properties.

2161

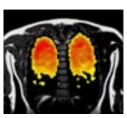

Determination of RF and acquisition properties for optimal scan performance in 19F-MRI of inhaled perfluoropropane

Mary Neal[1], Prosenjit Dutta[1], John Simpson[2], Andrew Blamire[1], and Pete Thelwall[1]

[1]Newcastle Magnetic Resonance Centre, Newcastle University, Newcastle upon Tyne, United Kingdom, [2]Institute of Cellular Medicine, Newcastle University, Newcastle upon Tyne, United Kingdom

^{19}F-MRI of inhaled perfluoropropane gas allows assessment of lung ventilation properties with a thermally polarised tracer gas. Due to the scarcity of signal from the non-hyperpolarised gas-phase imaging agent, optimal scan protocol design plays a critical role in image quality. Acquisition variables and coil power performance were modelled to determine the optimal image acquisition parameters for a spoiled gradient echo pulse sequence for human ^{19}F birdcage and chest surface coils. Application of optimised scan protocols to human studies shows acceptable image quality for assessment of lung function.

2162

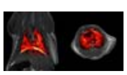

1H MAGNETIC RESONANCE IMAGING OF THE LUNGS USING PROPANE AS AN INHALATION AGENT

Ashlyn Kopanski[1], Francis Hane[2], Tao Li[1], and Mitchell Albert[3]

[1]Lakehead University, Thunder Bay, ON, Canada, [2]Lakehead University, MURILLO, ON, Canada, [3]Thunder Bay, ON, Canada

We used 80% propane/20% oxygen mixture as an imaging agent and conventional 1H MRI to image the lungs of a living rat. We believe that this is the first time propane gas has been used in vivo for imaging of the lungs. We obtained an SNR approaching 50 from the propane in the lungs. Our results demonstrate that propane has a possibility of being used as a lung imaging modality for detection of various pulmonary diseases.

2163

A Portable Constant-Volume Ventilator for Rodent Hyperpolarized Gas MRI

Rohan S Virgincar[1,2], Jerry Dahlke[2], Scott H Robertson[2,3], Bastiaan Driehuys[1,2,3,4], and John Nouls[2,4]

[1]Biomedical Engineering, Duke University, Durham, NC, United States, [2]Center for In Vivo Microscopy, Duke University Medical Center, Durham, NC, United States, [3]Medical Physics Graduate Program, Duke University, Durham, NC, United States, [4]Radiology, Duke University Medical Center, Durham, NC, United States

Hyperpolarized ^{129}Xe MRI is a powerful probe of lung ventilation, perfusion and gas-exchange. It can be used in both clinical and preclinical settings, where the latter enables rapid discovery of new applications and early testing of therapies in animal models. However, preclinical hyperpolarized gas MRI has been limited to a few expert sites, owing to the challenge of reliably delivering hyperpolarized gas to small animals. Here, we present a constant-volume ventilator that allows for high-resolution hyperpolarized gas imaging and spectroscopy during precisely controlled multi-breath acquisitions. The ventilator is compact, portable, and easy to duplicate and disseminate.

2164

2D-Turbo Spin-Echo Sequence with Incremental Trigger Delay Time for Monitoring Vascular Signal Suppression in Peripheral Pulse Gated Black-blood Lung MR Imaging

Ryotaro Kamei[1], Yuji Watanabe[2], Sungtak Hong[3], Koji Sagiyama[1], Ryo Murayama[1], Satoshi Kawanami[2], and Hiroshi Honda[1]

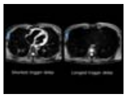

[1]Department of Clinical Radiology, Kyushu University Graduate School of Medical Sciences, Fukuoka, Japan, [2]Department of Molecular Imaging and Diagnosis, Kyushu University Graduate School of Medical Sciences, Fukuoka, Japan, [3]Philips Electronics Japan, Ltd, Tokyo, Japan

Breath-hold black-blood magnetic resonance imaging of the lung provides promising results in focal lesion detection. Using peripheral pulse gating, we intended to monitor the degree of vascular suppression and the changes in tissue contrast more closely than in the previously reported methods. Black-blood fat-saturated T2-weighted images were acquired for healthy volunteers with incremental delay time points throughout the pulse cycle. The relative ratios of the specific tissue to the muscle were quantified. The systolic phase provided superior black-blood effects and was considered optimal for signal acquisition.

Traditional Poster

Neuro: Animal Studies

Exhibition Hall 2165-2197 Wednesday 13:45 - 15:45

2165

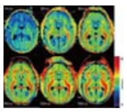

Developmental assay with Magnetization Transfer Ratio in non-human primate

Marin Nishio[1,2], Yuji Komaki[2,3], Fumiko Seki[2,3,4], Junichi Hata[2,3,4], Akiko Uematsu[2,3,4], Ryutaro Yano[2,3], Ryosuke Ishihara[2,3], Erika Sasaki[2,3], Hideyuki Okano[3], and Akira Furukawa[1]

[1]Tokyo Metropolitan University, Tokyo, Japan, [2]Central Institute for Experimental Animals (CIEA), Kawasaki, Japan, [3]School of Medicine Keio University, [4]Brain Science Institute, RIKEN

MTR reflects the protein content such as myelin of brain. We examined the age-related MTR for common marmosets (1-18 months). Almost all regions of the brain have increased as T1 relaxation similar curve and the rate change of the MTR in each region was different. In voxel-wise analysis, MTR increase shows back-to-front maturation patterns in white matter. This pattern has observed in human studies. MTR can be a good marker to evaluate the normal brain development of common marmoset, and eventually a suitable parameter to assess brain developmental disorders for study, diagnosis, and treatments.

2166

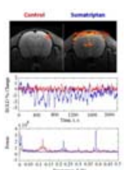

The Pain of Pre-Clinical fMRI

Aneurin James Kennerley[1], Devashish Das[2], Fiona Boissonade[3], and Milena De-Felice[3]

[1]Psychology, University of Sheffield, Sheffield, United Kingdom, [2]Biological Services, University of Sheffield, Sheffield, United Kingdom, [3]School of Clinical Dentistry, University of Sheffield, Sheffield, United Kingdom

This study uses multi-parametric MRI measures to further our understanding on the pathophysiology of migraine in a novel preclinical model of medication overuse headache. Rats undergo sustained triptan exposure inducing cutaneous allodynia. Following drug exposure, we perform ASL, NMR, connectivity and evoked response BOLD fMRI to investigate sustained neuronal adaptations/changes. We investigate how drug overuse leads to latent sensitization to migraine triggers 20 days after exposure. We find significantly altered CBF levels in triptan treated animals. NMR reveals changes in GABA & Tau metabolite levels. fMRI shows changes in functional connectivity and activation of brain regions associated with pain pathways.

2167

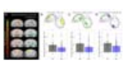

Loss of lateral asymmetry in the brain of mouse models of autism

Jacob Ellegood[1], Benjamin C Darwin[1], Matthijs C Van Eede[1], Mark Henkelman[1,2], and Jason P Lerch[1,2]

[1]Hospital for Sick Children, Toronto, ON, Canada, [2]Department of Medical Biophysics, University of Toronto, Toronto, ON, Canada

Examination of lateral asymmetry differences in mouse models related to Autism. Using 42 different mouselines as a representative sample of an autistic population, we show a loss of asymmetry in the mutant mice compared to wild-type that may be indicative of functional and/or behavioural variations.

2168

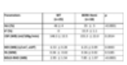

Cerebral metabolic and physiological evidence supporting a shift toward glycolysis in a mouse model with congenital anemia.

Min Hui Cui[1], Sandra Suzuka[2], Mary E Fabry[2], Seetharama A Acharya[3,4], Henny H Billett[2], and Craig A Branch[1,4]

[1]Radiology, Albert Einstein College of Medicine, Bronx, NY, United States, [2]Medicine/Hematology, Albert Einstein College of Medicine, Bronx, NY, United States, [3]Albert Einstein College of Medicine, Bronx, NY, United States, [4]Physiology & Biophysics, Albert Einstein College of Medicine, Bronx, NY, United States

The effect of congenital anemic hypoxia on brain energy metabolism was studied on BERK-Hemi mouse exhibiting poor oxygen delivery secondary to reduced hemoglobin oxygen affinity. Regionally increased CBF in BERK-Hemi mouse was correlated with decreased mean diffusivity and tissue T1. Additionally, BERK-Hemi mouse exhibited elevated concentrations in N-acetylaspartate, glutamate, total choline and glucose in thalamus, but a lower concentration of glutamine. Together, the results suggest BERK-Hemi mice develop a compensatory mechanism which leads to increased glycolysis to combat hypoxia and increased reactive oxygen stress.

2169

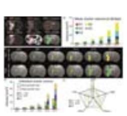

Monitoring glioma heterogeneity during tumor growth using clustering analysis of multiparametric MRI data

Benjamin Lemasson[1,2], Nora Collomb[1,2], Alexis Arnaud[3,4], Florence Forbes[3,4], and Emmanuel Luc Barbier[1,2]

[1]U836, Inserm, Grenoble, France, [2]Université Grenoble Alpes, Grenoble Institut des Neurosciences, Grenoble, France, [3]INRIA, Grenoble, France, [4]LJK, Université Grenoble Alpes, Grenoble, France

Brain tumor heterogeneity plays a major role during gliomas growth and for the tumors resistance to therapies. The goal of this study was to demonstrate the ability of clustering analysis applied to multiparametric MRI (mpMRI) data to summarize and quantify intralesional heterogeneity during tumor growth. A mpMRI dataset of rats bearing glioma was acquired during the tumor growth (5 maps, 8 animals and 6 time points). After co-registration of every MR data over time, a clustering analysis was performed using a Gaussian mixture distribution model. Although preliminary, our results show that clustering analysis of mpMRI has a great potential to monitor quantitatively intralesional heterogeneity during the growth of tumors.

2170

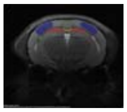

Characterization of a Murine High Altitude Exposure Model

Alexandru Korotcov[1,2], Asamoah Bosomtwi[1,2], Andrew Hoy[1,2], Daniel P. Perl[1,3], Nathan Cramer[1,4], Xiufen Xu[4], Clarke Tankersley[4], Zygmunt Galdzicki[1,4], and Bernard J. Dardzinski[1,2]

[1]Center for Neuroscience and Regenerative Medicine, Uniformed Services University of the Health Sciences, Bethesda, MD, United States, [2]Radiology and Radiological Sciences, Uniformed Services University of the Health Sciences, Bethesda, MD, United States, [3]Pathology, Uniformed Services University of the Health Sciences, Bethesda, MD, United States, [4]Anatomy, Physiology and Genetics, Uniformed Services University of the Health Sciences, Bethesda, MD, United States

MRI is a useful technology for longitudinal assessments, which are critical for understanding vascular changes in the brain. Exposure to high-altitude (HA), hypoxic conditions, e.g. by military personnel, can result in physiological changes and ultimately degradation of neurobehavioral performance. We utilized in vivo MR imaging in mice to examine changes in brain vasculature, myelination and structure and to provide longitudinal insights into pathological changes caused by long-term exposure to HA. We observed changes in T2 that reflect edema/inflammation, fractional anisotropy changes that suggest changes in white matter myelination, and rCBF and VDi imaging indicating adaptations to HA conditions.

2171

Modulation of structural and functional networks in the ischemic mouse brain by stem cell therapy

Claudia Green[1], Anuka Minassian[1], Andreas Beyrau[1], Stefanie Vogel[1], Michael Diedenhofen[1], Melanie Nelles[1], Dirk Wiedermann[1], and Mathias Hoehn[1,2]

[1]In-vivo NMR, MPI for Metabolism Research, Cologne, Germany, [2]Dept. Radiology, Leiden University Medical Center, Leiden, Netherlands

In this study we combined rs-fMRI and diffusion MRI to assess the therapeutic capacity of cortically injected human neural stem cells in the mouse brain after stroke during 3 months. Seed-based analysis of diffusion anisotropy maps and functional connectivity were conducted interrelated with the main focus on the effect of stroke and treatment on the contralesional hemisphere. A delayed breakdown in functional network strength for the therapeutically treated group compared to a sham treated group is observed. However, diffusion anisotropy parameters stay stable with an increasing trend for the thalamus.

2172

Using intravoxel incoherent motion method to evaluate the effect of butylphthalide in middle cerebral artery occlusion rat model

Dandan Zheng[1], Baohong Wen[2], Baoqiong Zhao[2], and Jingliang Cheng[2]

[1]MR Research China, GE Healthcare, Beijing, People's Republic of China, [2]Department of MRI, The First Affiliated Hospital of Zhengzhou University, Zhengzhou, People's Republic of China

Stroke is the third leading cause of death in industrialized countries and the most frequent cause of acquired adult. Butylphthalide has been shown to have protective effects against ischemic stroke. This study would like to observe the temporal evolution of parameters calculated by IVIM model in an experimental middle cerebral artery occlusion (MCAO) rat model, and how the butylphthalide effect the physiological changes.

2173

In vivo Magnetic Resonance Imaging of the Marmoset Spinal Cord at 7T

Jennifer A. Lefeuvre[1,2], Wen-Yang Chiang[3], Nicholas J. Luciano[1], Cecil C. Yen[3], Mathieu D. Santin[2], Stéphane Lehéricy[2], Steve Jacobson[4], Afonso C. Silva[3], Daniel S. Reich[1], and Pascal Sati[1]

[1]TNS/NIB/NINDS, National Institutes of Health, Bethesda, MD, United States, [2]CENIR, UPMC-Inserm U1127, CNRS 7225, Institut Cerveau Moelle, Paris, France, [3]CMS/LFMI/NINDS, National Institutes of Health, Bethesda, MD, United States, [4]VIS/NIB/NINDS, National Institutes of Health, Bethesda, MD, United States

When induced to have experimental autoimmune encephalomyelitis (EAE), marmosets can suffer from motor and sensory deficits highly suggestive of lesions located in the spinal cord. In this study, we developed an in vivo spinal cord imaging protocol at 7T for marmosets, and were able to visualize gray and white matter as well as focal EAE lesions. Future work will focus on characterizing the spatiotemporal evolution of spinal cord EAE lesions over the disease course.

2174

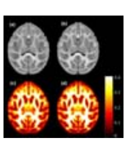

The effects of breastfeeding versus formula-feeding on cerebral cortex maturation in infant rhesus macaques

Zheng Liu[1,2], Martha D. Neuringer[1,3], John W. Erdman Jr.[4,5], Matthew J Kuchan[6], Laurie Renner[1], Emily E. Johnson [1], and Christopher D. Kroenke[1,2]

[1]Neuroscience, Oregon National Primate Research Center, Beaverton, OR, United States, [2]Advanced Imaging Research Center, Oregon Health and Science University, Portland, OR, United States, [3]Casey Eye Institute, Oregon Health and Science University, Portland, OR, United States, [4]Food Science and Human Nutrition, University of Illinois at Urbana-Champaign, Urbana, IL, United States, [5]Nutritional Sciences, University of Illinois at Urbana-Champaign, Urbana, IL, United States, [6]Abbott Nutrition, Columbus, OH, United States

Infant rhesus macaques were studies to test the effects of breastfeeding versus formula-feeding on cerebral cortex maturation. Through analysis of structural and diffusion MR images, brain volume over the first 6 months of life was not significantly altered by formula-feeding versus breastfeeding, or by formula lutein supplementation. However, cellular maturation within cerebral cortical gray matter differed between formula-fed and breastfed animals. Lower gray matter FA of breastfed infants is interpreted to reflect greater neuronal arborization. This difference may be related to the different social experience as well as the nutrient composition of breast milk.

2175

Behavioral and Image Evidence for Mild Traumatic Brain Injury in Rats with the Skull Helmet

Yu-Chieh Jill Kao[1,2], Chia-Feng Lu[1,2,3], Huai-Lu Chen[1,4], Ping-Huei Tsai[1,2,5], Fei-Ting Hsu[1,5], Hua-Shan Liu[1,6], Gilbert Aaron Lee[1,4], Paul Blakeley[1,4], Li-Chun Hsieh[1,5], Bao-Yu Hsieh[7], and Cheng-Yu Chen[1,2,5]

[1]Translational Imaging Research Center, College of Medicine, Taipei Medical University, Taipei, Taiwan, [2]Department of Radiology, School of Medicine, Taipei Medical University, Taipei, Taiwan, [3]Department of Biomedical Imaging and Radiological Sciences, National Yang-Ming University, Taipei, Taiwan, [4]Department of Medical Research, Taipei Medical University Hospital, Taipei, Taiwan, [5]Department of Medical Imaging, Taipei Medical University Hospital, Taipei, Taiwan, [6]School of Biomedical Engineering, College of Biomedical Engineering, Taipei Medical University, Taipei, Taiwan, [7]Department of Biomedica, China Medical University, Taichung, Taiwan

An experimental model of mild traumatic brain injury (mTBI) mimicking the pathological outcomes in mTBI patients found in motorcycle accident was developed. The longitudinal behavioral and imaging assessment showed the functional deficit but intact brain structure in our model, which could be further used to explore early fluid and image biomarkers for mTBI

2176

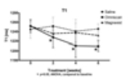

Post-contrast Signal Enhancement in Dentate Nucleus on Unenhanced T1 Weighted MRI in Rodents

Kurt Hermann Bockhorst[1], Juan Herrera[1], Shakuntala Kondraganti[1], Jarek Wosik, and Ponnada Narayana[1]

[1]Department for Diagnostic and Interventional Imaging, UT Health Science Center At Houston, Houston, TX, United States

Some of the gadolinium based contrast agents are shown to produce enhancements on T1-weighted images long after their administration in certain brain structures in humans, raising questions about the safety of these agents. The enhancement is thought to be due to dechelation of the contrast agents. Understanding the pathophysiological effects requires systematic pre-clinical studies. As a first step towards this goal we conducted longitudinal in vivo studies in rodents administered Magnevist and Omniscan for ten days to quantify the temporal profile of enhancement using relaxometry and investigate if this enhancement has an effect on the tissue microstructure. Our results show that Ominiscan lowers both T1 and T2 starting from week 2 post contrast administration. However, such changes were not observed in Magnevist and saline treated animals. The contrast agents do not appear to have significant effect on any of the DTI measures.

2177

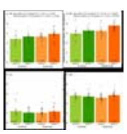

Altered Cerebral Blood Flow and Cerebrovascular Function after Voluntary Exercise in Adult Mice

Lindsay S Cahill[1], Jonathan Bishop[1], Lisa M Gazdzinski[1], Adrienne Dorr[2], Bojana Stefanovic[2,3], and John G Sled[1,3]

[1]Mouse Imaging Centre, The Hospital for Sick Children, Toronto, ON, Canada, [2]Sunnybrook Research Institute, Toronto, ON, Canada, [3]Department of Medical Biophysics, University of Toronto, Toronto, ON, Canada

A longitudinal study employing continuous arterial spin labelling MRI with a hypercapnic challenge was used to examine changes in cerebral blood flow with physical exercise in healthy, adult mice. We found that exercise resulted in increases in the normocapnic and hypercapnic blood flow in the hippocampus and that these changes were positively correlated to the volume of the hippocampus following exercise. Interestingly, hypercapnic hippocampal blood flow prior to exercise was predictive of the distance subsequently run and exposure to this voluntary exercise regime was found to reduce these pre-existing blood flow differences.

2178

Altered nigrostriatal system in the MPTP Squirrel Monkey model revealed by diffusion MRI at 11.7T.

Alexandra Petiet[1,2], Mathieu Santin[1,2], Elodie Laffrat[2], Romain Valabrègue[1,2], Thomas Samoyeau[2], Stéphane Hunot[2], and Stéphane Lehéricy[1,2]

[1]Center for Neuroimaging Research, Brain and Spine Institute, Paris, France, [2]CNRS UMR 7225/INSERM 1127/UPMC UM75, Brain and Spine Institute, Paris, France

Parkinson’s disease (PD) is characterized by neurodegeneration of the dopaminergic neurons in the substantia nigra pars compacta (SNc). The 1-methyl-4-phenyl-1,2,3,6-tetrahydropyridine (MPTP) neurotoxin can induce Parkinson syndrome in primate models. We evaluated the nigrostriatal (NS) pathway degeneration in MPTP Squirrel monkeys using diffusion MRI. The results showed significantly increased fractional anisotropy in all NS regions of the MPTP group (SN, caudate and putamen regions). Axial diffusivity also significantly increased in the SN and caudate regions, while radial diffusivities did not show any differences, except a significantly decreased λ3 in the putamen. Those results should help develop preclinical evaluation of PD therapeutics.

2179

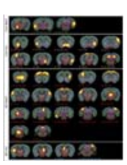

Allosteric activation of mGluR4 receptor reversing social behavior deficits modifies the reward-related resting state networks in mu opioid receptor knock-out mice

Anna E. Mechling[1,2], Kirsten Kleim[1], Tanzil Arefin[1,2], Hsu-Lei Lee[1], Thomas Bienert[1], Jürgen Hennig[1], Dominik von Elverfeldt[1], Brigitte Lina Kieffer[3], and Laura-Adela Harsan[1,4,5]

[1]Medical Physics, University Medical Center Freiburg, Freiburg, Germany, [2]Faculty of Biology, Albert-Ludwig-University Freiburg, Freiburg, Germany, [3]Department of Psychiatry, Douglas Hospital Research Center, School of Medicine, McGill University, Montreal, QC, Canada, [4]Engineering Science, Computer Science, and Imaging Laboratory, Integrative Multimodal Imaging in Healthcare, University of Strasbourg, Strasbourg, France, [5]Department of Biophysics and Nuclear Medicine, University Hospital Strasbourg, Strasbourg, France

Mu opioid receptor (MOR) knock-out *Oprm*1$^{-/-}$ mice exhibit deficits in social behavior and repetitive behavior, which are phenotypes related with autism spectrum disorders (ASD). Thus, MOR deficient mice were recently proposed as monogenic models of ASD. Moreover, a decrease in metabotropic glutamate receptor 4 (mGluR4) levels was found in these mice. A treatment with VU0155041, an allosteric modulator of mGluR4, reversed behavioral deficits in *Oprm*1$^{-/-}$ mice. Here, we investigated the remodeling on brain connectivity level in *Oprm*1$^{-/-}$ mice under VU0155041-treatment and found enhancement of positive correlation towards frontal brain areas involved in reward-processing due to the compound.

2180

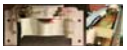

Measuring of Whole Brain Perfusion in the Awake Marmoset Using Continuous Arterial Spin Labeling

Cecil Chern-Chyi Yen[1], Wen-Yang Chiang[1,2], and Afonso C. Silva[1]

[1]Cerebral Microcirculation Section, National Institute of Neurological Disorders and Stroke, National Institutes of Health, Bethesda, MD, United States, [2]Biomedical Engineering, Texas A&M University, College Station, TX, United States

The common marmoset, a small New World primate, is a popular non-human primate for transgenic lines of brain disease models and 3D printed helmets to immobilize the head for awake MRI. However, cerebral blood flow (CBF), a crucial component to normal brain functions, has not been measured to date in awake marmosets. In this study, we demonstrate the feasibility of measuring whole brain CBF in the awake marmoset using a continuous arterial spin labeling MRI sequence and dedicated hardware, comprising of a spin-labeling coil and a novel 10-channel phased array in a 7T animal MRI system.

2181

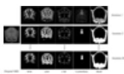

Learning-based Segmentation for Monkey Brain MRI

Cuijin Lao[1,2], Jiawei Chen[2], Li Wang[2], Gang Li[2], and Dinggang Shen[2]

[1]Department of Information Engineering, Liuzhou City Vocational College, Liuzhou, People's Republic of China, [2]Department of Radiology and BRIC, University of North Carolina at Chapel Hill, Chapel Hill, NC, United States

Accurate segmentation of monkey brain MRI is of great importance in studying the brain development, pathogenesis and progression of neurological diseases. However, it is challenging for automatic segmentation due to noise, low contrast and partial volume effect. Existing tools fine-tuned to human brain MRI are ineffective for monkey brain MRI due to their difference from human brain MRI. In this study, we propose a machine learning-based framework for the segmentation of monkey brain MRI into skull, cerebellum, white matter (WM), gray matter (GM), and cerebrospinal fluid (CSF) of the cerebrum. The experiment results demonstrate that our proposed method outperforms than previous methods.

2182

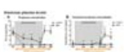

In vivo Diffusion tensor imaging to unravel the contribution of thyroid hormones in seasonal neuroplasticity in European Starlings (Sturnus vulgaris)

Jasmien Orije[1], Geert De Groof[1], Elisabeth Jonckers[1], Sander Raymaekers[2], Marleen Verhoye[1], Veerle Darras[2], and Annemie Van der Linden[1]

[1]Bio-Imaging Lab, University of Antwerp, Wilrijk, Belgium, [2]Laboratory of Comparative Endocrinology, KU Leuven, Leuven, Belgium

The effect of thyroid hormones on seasonal neuroplasticity in adult songbirds was never investigated before. To study this we treated photorefractory starlings with methimazole, which resulted in a depletion of thyroid hormones plasma levels. Using repeated measures of in vivo DTI and song recordings, neuroplasticity and song behaviour were monitored over different photoperiods. We found indications that thyroid hormones can modulate the seasonal neuroplasticity both directly at the level of the song control system, as suggested by direct changes in song behaviour after methimazole-treatment, and indirectly via the hypothalamus-pituitary-gonad axis, as methimazole-treatment inhibited the testosterone increase upon photostimulation.

2183

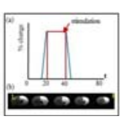

Enhanced neuroplasticity by physical exercise for hypoxic ischemic injured rat brain monitored by BOLD-fMRI

Sun Young Chae[1,2], Geun Ho Im[3,4], Moon-Sun Jang[3,4], Won-Beom Jung[1,5], and Jung Hee Lee[1,2,3,5]

[1]Center for Neuroscience Imaging Research, Institute for Basic Science (IBS), Suwon, Korea, Republic of, [2]Department of Health Sciences and Technology, SAIHST, Sungkyunkwan University, Seoul, Korea, Republic of, [3]Department of Radiology, Samsung Medical Center, Sungkyunkwan University School of Medicine, Seoul, Korea, Republic of, [4]Center for Molecular and Cellular Imaging, Samsung Biomedical Research Institute, Seoul, Korea, Republic of, [5]Department of Global Biomedical Engineering, Sungkyunkwan University, Suwon, Korea, Republic of

Physical exercise is known to boost the spontaneous recovery, but the exact mechanism for exercise induced recovery after brain injury is not clearly known. In this study, we show enhanced neuroplasticity with physical exercise on the intact side as well as the damaged side for the HI injured rat brain by calculating the brain activation maps from BOLD-fMRI: Increased inter-hemispheric transfer and intra-hemispheric extension of activated areas were observed with physical exercise covering the widespread sensory-motor related areas in the contralesional hemisphere.

2184

Quantification of vascular water transport using time-resolved pulsed arterial spin labelling MRI at 9.4 T

Adnan Bibic[1,2], Thea Sordia[1], Erik Henningsson[3], Linda Knutsson[1,4], Freddy Ståhlberg[2], and Ronnie Wirestam[1]

[1]Medical Radiation Physics, Lund University, Lund, Sweden, [2]Lund University Bioimaging Centre, Lund University, Lund, Sweden, [3]Centre for Mathematical Sciences, Lund University, Lund, Sweden, [4]Department of Radiology (Adjunct), Johns Hopkins School of Medicine, Baltimore, MD, United States

In this study, an improved quantification approach for measuring ASL transit-time parameters is proposed. The concept is based on multi-TI ASL measurements, where the dynamics of the inverted spins are described by the Fokker-Planck equation. The random forces in this equation are assumed to occur due to pseudo-diffusion in the capillaries and subsequent filtration through the blood brain barrier (BBB). The obtained time for the intravascular water to distribute from arteries through the capillary bed and into the parenchyma can, for example, be related to the capillary function as well as to the integrity of the BBB.

2185 

Phenotyping of transgenic Huntington's disease minipigs by MR spectroscopy

Nina Nagelmann[1], Frauke Freisfeld[2], Robin Schubert [2], Sarah Schramke[2], Verena Schuldenzucker [2], Lorena Rieke[2], Tamara Matheis[2], Harald Kugel[1], Ralf Reilmann[1,2], and Cornelius Faber[1]

[1]Department of Clinical Radiology, University Hospital Muenster, Muenster, Germany, [2]George-Huntington-Institute, Muenster, Germany

Huntington's Disease (HD) is a fatal neurodegenerative disorder, caused by a single genetic mutation, and characterized by deficits in motor coordination, behavior and cognition. A transgenic minipig model of HD has been established. Here, we employ single voxel MRS at 3 T to acquire metabolic profiles from the brain of this model over four years. We show that seven metabolite combinations can be quantified in adolescent and adult minipigs. Pathologic alterations in the phenotype were not observed at the age studied.

2186 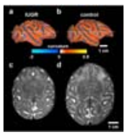

Perturbed development of rhesus macaque fetal cerebral cortex and white matter in an IUGR pregnancy, secondary to placental insufficiency, characterized by in utero diffusion MRI

Xiaojie Wang[1], Jamie O Lo[2], Colin Studholme[3], Zheng Liu[1], and Christopher D Kroenke[1]

[1]Advanced Imaging Research Center, OHSU, Portland, OR, United States, [2]Department of Obstetrics and Gynecology, OHSU, [3]Pediatrics, Bioengineering, and Radiology, University of Washington, Seattle, WA

In utero diffusion and anatomical MRI measurements were performed on a naturally occurring intrauterine growth restriction (IUGR) and 3 control pregnant rhesus monkeys. Water diffusion anisotropy (FA) within fetal cerebral cortex as well as white matter was used to characterize abnormal development in the IUGR fetal brain. Markedly higher cortical FA, indicating aberrent morphogenesis of cortical neurons, was observed in the IUGR fetal brain compared to controls. In addition, significantly reduced FA in a number of white matter tracts was also found in the IUGR fetal brain, reflecting perturbed white matter development.

2187 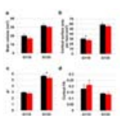

Effects of first-trimester alcohol exposure on fetal brain development characterized by in utero diffusion MR

Xiaojie Wang[1], Colin Studholme[2], Natali Newman[3], Matthew M Ford[3], Kathleen A Grant[3], and Christopher D Kroenke[1]

[1]Advanced Imaging Research Center, OHSU, Portland, OR, United States, [2]Pediatrics, Bioengineering, and Radiology, University of Washington, [3]Division of Neuroscience, Oregon National Primate Research Center

To assess the impact of first-trimester ethanol consumption on rhesus macaque fetal brain development, we employed anatomical and diffusion MRI to characterize macroscopic as well as cellular-level changes in ethanol exposed fetuses relative to controls at gestation days (G) 110 and G135. At both time points, perturbed brain maturation indicated by decreased brain volume, cortical surface area, and folding was seen in the ethanol exposed group. In addition, a trend for higher cortical water diffusion anisotropy seen in ethanol exposed group at G110 indicates abnormal dendritic differentiation.

2188 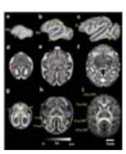

Anatomical and diffusion MRI fetal brain templates for the rhesus macaque at gestation days 85, 110, and 135

Xiaojie Wang[1], Zheng Liu[1], Colin Studholme[2], and Christopher D Kroenke[1]

[1]Advanced Imaging Research Center, OHSU, Portland, OR, United States, [2]Pediatrics, Bioengineering, and Radiology, University of Washington

In utero T2-weighted (T2W) and diffusion MR images were acquired from control rhesus macaque fetuses at gestation days 85, 110, and 135. High-resolution T2W volumes and diffusion MR volumes were reconstructed using retrospective motion-correction techniques. Population-averaged T2W templates and fractional anisotropy (FA) templates were generated for each time point. Development of fetal tissue zones and gyrification of cerebral cortex were assessed using the T2W templates. In addition, morphogenesis of cortical neurons and maturation of white matter tracts were also characterized using the FA templates.

2189 

USPIO-enhanced magnetic resonance imaging of N-ethyl-N-nitrosourea- induced endogenous rat gliomas: contribution of USPIO-related iron-loaded microglia to signal changes

Ryuta ITO[1], Atsuko YAMAMOTO[2], Shigehiro MORIKAWA[3], and Kiyoshi MURATA[1]

[1]Radiology, Shiga University of Medical Science, Otsu, Japan, [2]Radiology, Kohka public hospital, Kohka, Japan, [3]Shiga University of Medical Science, Otsu, Japan

We assessed whether ultrasmall superparamagnetic iron oxide (USPIO) phagocytosed by microglia contribute to tumor enhancement in MR imaging of N-ethyl-N-nitrosourea (ENU)-induced endogenous rat brain gliomas by comparing MR images with the corresponding histological sections. USPIO-enhanced MR imaging may provide pure vascular bed images in the early phase within 6 hours after intravenous administration of USPIO agent because it was histologically proved that the administrated agent remained within intravascular space. In the late phase at 63-66 hours after the administration, USPIO-enhanced Gradient-Recalled-Echo T2-weighted images may depict the distribution of microglia that were magnetically labeled by USPIO agent.

2190

Optical control of blood flow in naive animals

Ravi L Rungta[1], Bruno-Félix Osmanski[1], Davide Boido[1], Mickael Tanter[2], and Serge Charpak[1]

[1]U1128, INSERM, Paris, France, [2]U979, INSERM, Paris, France

Optogenetics is increasingly used to map brain activation using techniques that rely upon functional hyperemia, for example opto-fMRI. Here we demonstrate that light stimulation protocols similar to those commonly used in opto-fMRI increase blood flow in mice that do not express light sensitive proteins. These results impose careful consideration on the use of photo-activation in studies involving blood flow regulation and suggest light could be used as a technical or therapeutic tool to locally increase blood flow in a controlled fashion.

2191

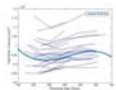

Longitudinal Analysis of Rhesus Monkey Brain Development Using Tensor-Based Structural Morphometry

Jeongchul Kim[1,2], Richard Bacus[1,2], Youngkyoo Jung[1,2,3], and Christopher Whitlow[1,2,3,4]

[1]Radiology Informatics and Image Processing Laboratory, Wake Forest School of Medicine, Winston Salem, NC, United States, [2]Department of Radiology, Wake Forest School of Medicine, Winston Salem, NC, United States, [3]Department of Biomedical Engineering, Wake Forest School of Medicine, Winston Salem, NC, United States, [4]Clinical and Translational Sciences Institute, Wake Forest School of Medicine, Winston Salem, NC, United States

Translational research models using brain MRI to study non-human primates (NHPs) can provide insight into normal/abnormal human neurodevelopment. In particular, voxel-wise longitudinal imaging designs can characterize the trajectory of change in brain structure among individual subjects. This study analyzes morphometric changes among a cohort of rhesus monkeys during late infancy, revealing total brain volume decreases driven by local volumetric contraction in frontal, parietal and temporal lobes. Characterizing NHP neurodevelopment may facilitate our understanding of complex normal and delayed human brain development, and provide a model to evaluate the influence of postnatal experiences on brain structure, cognitive ability and social behaviors.

2192

Developmental morphometry of the marmoset brain from infancy to adulthood

Stephen J Sawiak[1,2], Y Shiba[3], L Oikonomidis[3], C P Windle[4], G Cockcroft[4], E T Bullmore[1,5], and A C Roberts[3]

[1]Behavioural and Clinical Neuroscience Institute, University of Cambridge, Cambridge, United Kingdom, [2]Wolfson Brain Imaging Centre, University of Cambridge, Cambridge, United Kingdom, [3]Dept of Physiology, Development and Neuroscience, University of Cambridge, [4]Dept of Psychology, University of Cambridge, [5]Dept of Psychiatry, University of Cambridge

Understanding the development of brain circuits through infancy to adulthood is crucial in determining the causes of mental health disorders, half of which are established before early adulthood. We use MRI to track the development of> 200 discrete brain regions in a longitudinal primate brain study of 41 marmosets. Tensor-based morphometry indicated key regions of myelination from 3-6 months of age, and clustering of growth trajectories fitted with cubic splines allowed parcellation of regions based on growth patterns. We present maps of development showing differing patterns and rates of growth not only across lobes but between primary and associative areas.

2193

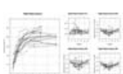

Dynamic Longitudinal DTI Metric Changes of Hippocampus in Developing Non-Human Primate

Akiko Uematsu[1,2,3], Junichi Hata[1,3], Yuji Komaki[3], Fumiko Seki[1,2,3], Chihoko Yamada[3], Erika Sasaki[1,2,3], and Hideyuki Okano[1,2]

[1]Keio University School of Medicine, Tokyo, Japan, [2]Riken, Wako, Japan, [3]Central Institute for Experimental Animals, Kawasaki, Japan

We investigated typical hippocampal development of a non-human primate model, common marmoset, using longitudinal DTI metrics data. Our findings showed dynamical non-linear developmental changes of hippocampal volume, MD and RD especially in its anterior part and suggested its neural turning point would be at puberty. These findings would give insights of disorder and disease of onset specific to developmental period.

2194

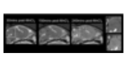

Dynamic uptake of manganese in the developing mouse brain

Holly E Holmes[1], Orlando Aristizabal[1], Oghale Obaro-Best[1,2], Estefania Gallego[1], Hari Rallapalli[1], and Daniel H Turnbull[1]

[1]Skirball Institute of Biomolecular Medicine, NYU School of Medicine, New York, NY, United States, [2]Department of Chemistry, SUNY Plattsburgh, Plattsburgh, NY, United States

Manganese-enhanced MRI (MEMRI) is a powerful technique for imaging rodent neuroanatomy. We investigated differences in the uptake of paramagnetic manganese ions (Mn^{2+}) in the mouse brain at two postnatal days: P7 and P21. We observed higher uptake of Mn^{2+} in all neuroanatomical regions-of-interest (ROIs) at P7; this increased uptake was reflected in the shorter T1 times at P7 relative to P21. We also observed faster clearance of Mn^{2+} within the ventricles at P21. Our findings highlight the spatiotemporal differences in Mn^{2+} uptake and may be useful when planning MEMRI studies in the developing mouse brain.

2195

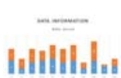

Morphological growth patterns in common marmoset developing brain

Fumiko Seki[1,2,3], Yuji Komaki[1,2], Junichi Hata[1,2,3], Akiko Uematsu[1,2,3], Erika Sasaki[1,2], Keigo Hikishima[4], and Hideyuki Okano[1,3]

[1]Department of Physiology, Keio University, Tokyo, Japan, [2]Central Institute of Experimental Animals, [3]Laboratory for Marmoset Neural Architecture, RIKEN BSI, [4]Okinawa Institute of Science and Technology Graduate University

The postnatal brain development at the macroscale in common marmoset has been studied based on the volume measurement, as is not well-studied despite its importance. Maximizing the feature that it takes only 2 years to reach adulthood, the longitudinal MRI was conducted for 23 subjects. The volume of gray matter was inverted U curve trajectories, while increase of white matter became stable around 12 months old. Developmental patterns of regions in cerebral cortex were similar to gray matter but different in developmental timing. The study can demonstrate overall growth patterns were similar to patterns previously reported in humans and other monkeys.

2196 

Voxel Based Alterations in White Matter Volume following Lipophilic Iron Treatment

Douglas G Peters[1], Carson J Purnell[2], Michael D. Tobia[3], Qing X Yang[3], James R Connor[2], and Mark D Meadowcroft[2,3]

[1]Neural and Behavioral Sciences, The Pennsylvania State University - College of Medicine, Hershey, PA, United States, [2]Neurosurgery, The Pennsylvania State University - College of Medicine, Hershey, PA, United States, [3]Radiology, The Pennsylvania State University - College of Medicine, Hershey, PA, United States

We show that there are observable VBM changes in white matter and grey matter fractions of an aging mouse and these changes are attenuated with a lipophilic high iron diet. This data support the hypothesis that regressive white matter degeneration may be prevented with increased access to CNS iron. Animals that do not have brain iron overloading show longitudinal white matter changes not observed in the iron loaded animals. Furthermore, our data supports the white matter retrogenesis model observed in the aging human brain.

2197 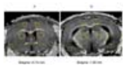

Fast macromolecular proton fraction mapping validated in the murine model of cuprizone induced demyelination

Marina Khodanovich[1], Irina Sorokina[2], Valentina Glazacheva[1], Andrey Akulov[3], Alexandr Romashchenko[3], Tatyana Tolstikova[4], Lilia Mustafina[5], and Vasily Yarnykh[6]

[1]Laboratory of Neurobiology, Tomsk State University, Tomsk, Russian Federation, [2]N.N.Vorozhtsov Novosibirsk Institute of Organic Chemistry, Russian Federation, [3]Institute of Cytology and Genetics, Novosibirsk, Russian Federation, [4]N.N.Vorozhtsov Novosibirsk Institute of Organic Chemistry, Novosibirsk, Russian Federation, [5]Siberian State Medical University, Tomsk, Russian Federation, [6]Department of Radiology, University of Washington, Seattle, WA, United States

A recently developed quantitative MRI method, fast macromolecular proton fraction mapping (MPF) has shown a promise as a biomarker of myelin in human and animal studies with a particular advantage of sensitivity to grey matter (GM) demyelination. This study aimed to histologically validate the capability of MPF mapping using the cuprizone demyelination model. MPF strongly correlated with quantitative histology in all animals (r=0.95, p<0.001) as well as in treatment and control groups taken separately (r=0.97, p=0.001 and r=0.95, p=0.003, respectively). Close agreement between MPF and histology suggests that fast MPF mapping enables robust and accurate quantitative non-invasive assessment of demyelination.

Traditional Poster

Brain Tumor Imaging

Exhibition Hall 2198-2229 — Wednesday 13:45 - 15:45

2198 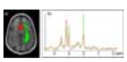

Changes of metabolite levels with low SNR in brain tumours measured by hybrid FET PET and 3D MRSI

Jörg Mauler[1], Karl-Josef Langen[1,2], Andrew A. Maudsley[3], Omid Nikoubashman[4], Christian Filss[1,2], Gabriele Stoffels[1], and N. Jon Shah[1,5]

[1]Institute of Neuroscience and Medicine, Medical Imaging Physics (INM-4), Forschungszentrum Jülich, Jülich, Germany, [2]Department of Nuclear Medicine, Faculty of Medicine, RWTH Aachen University, Aachen, Germany, [3]Miller School of Medicine, University of Miami, Miami, FL, United States, [4]Department of Neuroradiology, Faculty of Medicine, RWTH Aachen University, Aachen, Germany, [5]Department of Neurology, Faculty of Medicine, JARA, RWTH Aachen University, Aachen, Germany

The specificity of MR based diagnosis of gliomas may be improved by O-(2-[18F]fluoroethyl)-L-tyrosine (FET) uptake measured with PET and metabolite changes obtained from simultaneously acquired volumetric MR spectroscopic imaging. In order to cope with low SNR of the metabolites, the MR spectra of 25 patients were subject-specifically averaged within the tumour borders transferred from FET PET and compared to non-affected white matter of the contra lateral side. Strongest signal drops were found for GLU (0.58±0.43, WHO II) and NAA (0.33±0.13, WHO II-IV), strongest increase for CHO/NAA (3.9±2.4). The metabolite changes showed no dependency on tumour grade.

2199 

Proton MR spectroscopy detection of high lipid levels without central necrosis and high intensity on DWI is characteristics of germinoma

Fumiyuki Yamasaki[1], Yasuyuki Kinoshita[1], Satoshi Usui[1], Takeshi Takayasu[1], Ryo Nosaka[1], Manish Kolakshyapati[1], Taiichi Saito[1], Kazuhiko Sugiyama[2], and Kaoru Kurisu[1]

[1]Neurosurgery, Hiroshima University, Hiroshima, Japan, [2]Clinical Oncology & Neuro-oncology Program, Hiroshima University Hospital, Hiroshima

MRS and DWI of germinoma

2200 

Parameter Estimation in a Mathematical Model of Murine Glioma from MR Imaging

Eric J Kostelich[1], Erica M Rutter[2], Tracy L Stepien[3], Barrett J Anderies[1], Jonathan D Plasencia[4], Eric C Woolf[5], Adrienne C Scheck[5], Gregory H Turner[6], Qingwei Liu[6], David Frakes[4], Vikram Kodibagkar[4], Yang Kuang[1], and Mark C Preul[7]

[1]Mathematical & Statistical Sciences, Arizona State University, Tempe, AZ, United States, [2]Mathematics, North Carolina State University, Raleigh, NC, United States, [3]Mathematics, University of Arizona, Tucson, AZ, United States, [4]Biological and Health Systems Engineering, Arizona State University, Tempe, AZ, [5]Neuro-Oncology Research, Barrow Neurological Institute, Phoenix, AZ, United States, [6]BNI-ASU Center for Preclinical Imaging, Barrow Neurological Institute, Phoenix, AZ, United States, [7]Neurosurgery Research, Barrow Neurological Institute, Phoenix, AZ, United States

This study assesses the feasibility of estimating and quantifying the uncertainty in growth parameters for a mathematical model of glioma growth from MR imaging. Five immunocompetent albino mice were inoculated intracranially with syngeneic GL261 tumor cells and followed by serial imaging for 25 days. We simulated the growth of the tumor from the known initial conditions using a popular two-parameter reaction-diffusion model and compared the results with the imaging. Our simulations show that the growth and diffusion rates in the model cannot be identified from imaging data alone. Uncertainty quantification in model predictions of the tumor is problematic.

2201 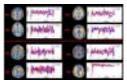

Anticorrelated networks dysfunction in patients with brain tumor in frontal lobe

Chen Niu[1], Xiao Ling[1], Pan Lin[2], Kun Zhang[3], Xin Liu[4], Hao Song[2], Liping Guo[1], Wenfei Li[1], Maode Wang[5], and Ming Zhang[1]

[1]Department of Medical Imaging, The First Affiliated Hospital of Xi'An Jiaotong University, Xi'An, People's Republic of China, [2]Key Laboratory of Biomedical Information Engineering of Education Ministry, Institute of Biomedical Engineering, Xi'an Jiaotong University, [3]Department of Electronics Engineering, Northwestern Polytechnical University, [4]Technical University Munich, [5]Department of neurosurgery, The First Affiliated Hospital of Xi'An Jiaotong University, Xi'An, People's Republic of China

The aim of this study is to evaluate whether the lesion in frontal lobe would cause the change of brain positive and negative network interaction, thereby affecting cognitive function. We employed a MSIT to compare the task-positive and DMN changes of brain tumor patients and the healthy controls. Our results indicated the interaction relationship between the task-positive and DMN in patients with brain tumor in the frontal lobe was significantly decreased. We suggest that reduced anti-correlation between DMN and task-positive networks in patients with brain tumor may be caused by dysfunctional DMN, thus affecting the cognitive function of patient.

2202 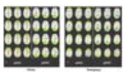

Default Mode Sub-network in Brain Tumor: A Resting State fMRI Study

Xiao Ling[1], Chen Niu[1], Pan Lin[2], Kun Zhang[3], Xin Liu[4], Wenfei Li[1], Liping Guo[1], and Ming Zhang*[1]

[1]Department of Medical Imaging, the First Affiliated Hospital of Xi'an Jiaotong University, Xi'an, People's Republic of China, [2]Key Laboratory of Biomedical Information Engineering of Education Ministry, Institute of Biomedical Engineering, Xi'an Jiaotong University, Xi'an, People's Republic of China, [3]Department of Electronics Engineering, Northwestern Polytechnical University, Xi'an, People's Republic of China, [4]Technical University Munich

The aim of the study was to observe the activation of DMN in patients with different types and location brain tumors, and as so to investigate whether the type and location of tumor would affect DMN spatial distribution. In our study, we compared the spatial distribution of DMN both glioma and meningioma. Finally, our findings show that DMN integrity is impaired as a result of tumor, and the DMN spatial distribution could be affected by the location of the brain tumor.

2203 

In Vivo 3D Metabolic Correlation Mapping using 1H Echo Planar Spectroscopic Imaging in IDH-mutant Gliomas at 3T

Zhongxu An[1], Vivek Tiwari[1], Sandeep Ganji[1], Marco C. Pinho[1], Bruce Mickey[1], Edward Pan[1], Elizabeth Maher[1], and Changho Choi[1]

[1]Advanced Imaging Research Center, University of Texas Southwestern Medical Center, Dallas, TX, United States

We present a 3D high resolution 2HG and other metoblites imaging in gliomas with metoblic correlation mapping technique to differentiate areas with different metabolic activities.

2204 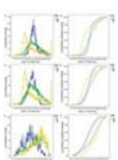

Texture analysis of diffusion weighted imaging for the evaluation of tumor heterogeneity based on different regions of interest

Shan Wang[1] and Jiangfen Wu[2]

[1]The affiliated hospital of xuzhou medical university, Xuzhou, People's Republic of China, [2]GE healthcare china

Texture analysis of DWI based on different ROI can provide various significant parameters to evaluate tumor heterogeneity, which were correlated with tumor grade. Particularly, the inhomogeneity value derived from whole tumor ROI provided high diagnostic value in differentiating HGGs from LGGs and predicting the status of tumor proliferation.

2205 

Reproducibility of 3D short TE MRSI in patients with high-grade glioma

Yan Li[1], Stojan Maleschlijski[1], and Sarah J Nelson[1]

[1]Department of Radiology and Biomedical Imaging, University of California San Francisco, San Francisco, CA, United States

The study evaluated the reproducibility of metabolite profiles within the normal appearing white matter that were acquired using automatic prescription of short echo time magnetic resonance spectroscopic imaging for ten patients with high grade glioma.

2206 

Whole tumor volume based histogram analysis of ADC for differentitating between WHO grade II and III glioma

Yingqiu Liuyang[1], Jin Shang[1], Yanwei Miao[1], Bing Wu[2], and Yan Guo[3]

[1]First Affiliated Hospital of Dalian Medical University, Dalian, People's Republic of China, [2]GE Healthcare,China,Beijing, [3]GE Healthcare,Lifescience,China

In this study, the differential diagnostic value of histogram analysis of ADC signal value based on entire region of grade II and III tumor is investigated, and further aimed at revealing the microscopic changes of glioma in the evolution of low grade to high grade.Conclusion that,histogram analysis of ADC signal value based on entire tumor could provide more information in differentiation of grade II and III glioma. Several parameter showed superior diagnostic value.

2207 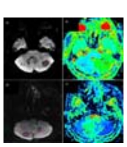

Quantitative analysis of MR diffusion-weighted imaging for differential diagnosis of cerebral alveolar echinococcosis and brain metastases

Jian Wang[1], Ling Wu[1], Juan Ma[1], Chunhui Jiang[1], Sailike Duishanbai[2], Geng Dangmurenjiapu[2], and Chen Liu[2]

[1]MRI Room，First Affiliated Hospital，Xinjiang Medical University, Urumqi 830011, China, Urumchi, People's Republic of China, [2]Department of Neurosurgery，First Affiliated Hospital，Xinjiang Medical University, Urumqi 830011, China

Synopsis：This study aims to probe the role of the quantitative analysis of MR diffusion-weighted imaging in differentiating Cerebral Alveolar Echinococcosis (CAE) with Brain metastases (BM).There was significant difference of the mean ADC values and eADC values (P<0.05) of the solid region between CAE and BM. There was no significant difference of the mean ADC values (P＞0.05) between CAE and BM，but there was significant difference that of the eADC values (P<0.05). MR-DWI was valuable for making diagnosis and differential diagnosis of patients with CAE and BM. EADC values is better than the ADC values.

2208

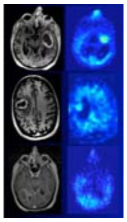

Do gadolinium-based contrast agents alter 23Na T1 relaxivity in glioma?

Frank Riemer[1], Mary A McLean[2], Fulvio Zaccagna[1], James T Grist[1], Rolf F Schulte[3], Joshua Kaggie[1], Colin Watts[4], Stephen J Price[4], Martin J Graves[1], and Ferdia A Gallagher[1]

[1]Department of Radiology, University of Cambridge, Cambridge, United Kingdom, [2]Cancer Research UK Cambridge Institute, University of Cambridge, Cambridge, United Kingdom, [3]GE Global Research, Munich, Germany, [4]Neurosurgery Division, Dept. of Clinical Neurosciences, University of Cambridge, Cambridge, United Kingdom

Incomplete fluid suppression on fluid-attenuated inversion-recovery ^{23}Na-MRI (IR-^{23}Na-MRI) was observed in three patients undergoing IR-^{23}Na-MRI after gadolinium contrast injection, as part of a brain tumour imaging study. To evaluate this, ^{23}Na-MRI T_1 maps were acquired before and after injection of a gadolinium-based contrast agent on a grade IV glioma (GBM) patient, which showed a statistically significant change of ^{23}Na-MRI T_1 within the peritumoral oedema (p=0.0095). Gadolinium contrast-enhanced ^{23}Na-MRI could potentially add further applications for sodium imaging and probe tumour tissue structure in new ways to investigate proliferation and treatment response.

2209

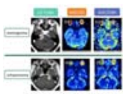

Can q-space imaging differentiate meningioma from cranial nerve schwannoma?

Hitomi Nagano[1], Koji Sakai[1], Jun Tazoe[1], Masashi Yasuike[1], Hajime Yokota[2], Kentaro Akazawa[3], Naoya Hashimoto[4], and Kei Yamada[1]

[1]Radiology, Kyoto Prefectural University of Medicine, Kyoto, Japan, [2]Radiological Sciences, David Geffen School of Medicine at UCLA, [3]Radiology, Johns Hopkins University, [4]Neurosurgery, Kyoto Prefectural University of Medicine, Kyoto, Japan

Q-space imaging (QSI) is an extended version of diffusion weighted image technique which can be utilized for observing microstructure of brain in micrometer order. In order to assess whether QSI can differentiate between the two most common extra-axial brain tumors of the posterior fossa, we performed histogram analyses as well as ROC analyses on the q-space data of meningioma and cranial nerve schwannoma (CNSch). We also assessed the apparent diffusion coefficient (ADC) for comparison. As a result, we have shown that mean displacement derived from QSI as well as ADC are able to differentiate meningioma from CNSch.

2210

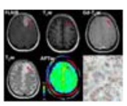

Identifying Isocitrate Dehydrogenase Genotype in Low-grade Glioma Non-invasively using Amide Proton Transfer-Weighted (APTW) Imaging

Shanshan Jiang[1,2], Charles Eberhart[3], Maria Adelita Vizcaino Villalobos[3], Xianlong Wang[2], Yu Wang[4], Hao Yu[2], Tianyu Zou[2], Yongxing Du[2], Hye-Young Heo[2], Yi Zhang[1], Peter Van Zijl[1], Jinyuan Zhou[1], and Zhibo Wen[2]

[1]Department of Radiology, Johns Hopkins University School of Medicine, Baltimore, MD, United States, [2]Department of Radiology, Southern Medical University, Zhujiang Hospital, Guangzhou, People's Republic of China, [3]Department of Pathology, Johns Hopkins University School of Medicine, Baltimore, MD, United States, [4]Department of Pathology, Southern Medical University, Zhujiang Hospital, Guangzhou, People's Republic of China

We explored the radiographic features of isocitrate dehydrogenase (IDH) wildtype and mutated tumors in glioma patients preoperatively using APTW imaging at 3 Tesla. 26 patients with newly suspected low-grade gliomas were recruited, surgical specimens were obtained for pathological analysis, and corresponding APTW signal intensities were recorded. Results showed that the IDH1 wild-type tumors had significantly higher APTW signal intensity than the IDH1 mutant tumors. The area under the ROC curve (AUC) for APTW to differentiate IDH1 wild-type from IDH1 mutant was 0.750. APT imaging has the potential for discriminating IDH genotypes in WHO grade-II gliomas.

2211

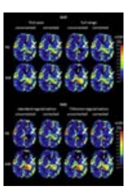

Influence of leakage correction on DSC-based CBV values acquired without and with prebolus in human high-grade glioma

Dennis M. Hedderich[1], Anne Kluge[1], Thomas Pyka[2], Claus Zimmer[1], Jan S. Kirschke[1], Benedikt Wiestler[1], and Christine Preibisch[1]

[1]Department of Neuroradiology, Klinikum rechts der Isar, Technische Universität München, Munich, Germany, [2]Department of Nuclear Medicine, Klinikum rechts der Isar, Technische Universität München, Munich, Germany

Aim of this study was to investigate the influence of leakage correction methods on dynamic susceptibility contrast (DSC)-based measures of cerebral blood volume (CBV), using patient data acquired with and without pre-bolus. Two post-processing techniques were compared with respect to normalized CBV (nCBV) in contrast enhancing tumor tissue. Generally, CBV increased or decreased after leakage correction for data acquired without or with prebolus, respectively. The best agreement between corrected nCBV values, obtained in the same patients without and with prebolus, respectively, was obtained for a reference curve-based correction approach.

2212

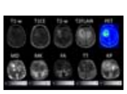

Multimodal study of treated brain tumours combining non-Gaussian diffusion MRI and 18F-FET-PET

Farida Grinberg[1,2], Ganna Blazhenets[1,3], Francesco D'Amore[1], Ezequiel Farrher[1], Christian Filβ[1], Karl-Josef Langen[1], and N. Jon Shah[1,2,4]

[1]Institute of Neuroscience and Medicine 4, Research Centre Jülich, Jülich, Germany, [2]Department of Neurology, Faculty of Medicine, JARA, RWTH Aachen University, Aachen, Germany, [3]Institute of Nuclear Physics, Faculty of Mathematics and Natural Sciences, University of Cologne, Cologne, Germany, [4]JARA - BRAIN - Translational Medicine, RWTH Aachen University, Germany

PET using O-(2-18F-fluoroethyl)-L-tyrosine (18F-FET) provides important diagnostic information in brain tumours. In this work, we report a novel combined application of PET imaging and MRI with advanced non-Gaussian diffusion MRI methods including diffusion kurtosis imaging and gamma-distribution function imaging. This is the first multimodal study combining metabolic information from FET-PET and microstructural information gained from non-Gaussian diffusion models. The main goal was to investigate the advantages of such a combined application in tumour assessment and to compare the sensitivity of various non-Gaussian diffusion metrics to the underlying microstructural tissue properties.

2213

Relating the Evolution of RT-Induced Vascular Injury to surrounding white matter microstructure in Adult Glioma Patients

Melanie A Morrison[1], Andrew Leynes[1], Angela Jakary[1], Prasanna Parvathaneni[1], Peder Larson[1], and Janine Lupo[1]

[1]Radiology and Biomedical Imaging, University of California San Francisco, San Francisco, CA, United States

In the treatment of gliomas, radiation therapy (RT) is associated with long-term effects including vascular injury in the form of cerebral microbleeds (CMBs), and changes in the white matter and thickness of cortex. Ultra high-field MRI techniques were used to characterize RT-induced changes across serial scans in support of ongoing investigations of the role of anti-angiogenic therapies in minimizing treatment effects. Steady increases in the number of CMBs was observed decades post-RT. CMB foci were characterized by increased isotropic diffusion when compared to surrounding white matter, which showed signs of degradation in as few as two months between serial scans.

2214

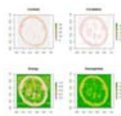

Differentiation of glioblastoma and primary central nervous system lymphoma by using MR image-based texture features

Akira Kunimatsu[1], Kouhei Kamiya[2], Yasushi Watanabe[2], Yuichi Suzuki[2], Natsuko Kunimatsu[3], Harushi Mori[1], and Osamu Abe[1]

[1]Department of Radiology, The University of Tokyo, Tokyo, Japan, [2]Department of Radiology, The University of Tokyo Hospital, Tokyo, Japan, [3]Department of Radiology, International University of Health and Welfare Mita Hospital, Tokyo, Japan

We evaluated the feasibility of machine learning-based differentiation between glioblastoma and primary central nervous system lymphoma by using texture features of post-contrast MR images. Cross validation showed that more than 80% of teacher data were correctly assigned. Trial data comprised of atypical image variants were correctly assigned in up to 78.6% by the best classifiers.

2215

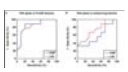

Effect of Lesion-related Signal Variation in Proton Density Reference Image on Blood Flow Quantification with Arterial Spin Labeling MRI for Differentiating Pseudo-progression from True Progression in Gliomas

Jason M Johnson[1], Mu-Lan Jen[2], David D Shin[3], Ping Hou[2], Caroline Chung[4], Donald F Schomer[1], and Ho-Ling Liu[2]

[1]Department of Diagnostic Radiology, The University of Texas MD Anderson Cancer Center, Houston, TX, United States, [2]Department of Imaging Physics, The University of Texas MD Anderson Cancer Center, Houston, TX, United States, [3]Department of Radiology, University of California, San Diego, La Jolla, CA, United States, [4]Department of Radiation Oncology, The University of Texas MD Anderson Cancer Center, Houston, TX, United States

CBF quantification using ASL is an important MR technique for the evaluation of suspicious enhancing lesions for patients' status post chemotherapy treatment. The quantification requires an estimate of equilibrium magnetization of blood which is often obtained using a set of proton density (PD) reference images; however, this approach can lead to errors in CBF based on tissue variation in PD which could then lead to inaccurate assessment of pseudo-progression (PsP) versus true progression (TP). Our work showed that PD variation led to a reduced diagnostic performance of CBF particularly in the region of enhancing lesions with pathologic proven TP.

2216

Effect of Lesion Contaminated Nuisance Regressors on Resting-state fMRI Connectivity in Patients with Brain Tumors

Ai-Ling Hsu[1,2], Ping Hou[1], Sujit S Prabhu[3], Rivka R Colen[4], Ashok J Kumar[4], Jason Michael Johnson[4], Donald F Schomer[4], Jyh-Horng Chen[2], and Ho-Ling Liu[1]

[1]Department of Imaging Physics, The University of Texas MD Anderson Cancer Center, Houston, TX, United States, [2]Institute of Biomedical Electronics and Bioinformatics, National Taiwan University, Taipei, Taiwan, [3]Department of Neurosurgery, The University of Texas MD Anderson Cancer Center, [4]Departments of Diagnostic Radiology, The University of Texas MD Anderson Cancer Center

Resting-state fMRI has been shown its potential for pre-surgical mapping. The potential confounds are commonly removed by regressing out the averaged fluctuation over masks of white matter and cerebrospinal fluid. However, for the patients with brain lesions, these masks may be contaminated by lesions. In current study, we generated masks by segmentation and template approaches. Although these masks were contaminated by lesion in most of our patients, no significant difference in FC was found due to this effect, which might be related to small samples. Comparing to segmentation approach, more variable results were observed when masks obtained by template approach.

2217

Exploring the distribution of inflow and outflow bloodstream type in pituitary adenoma by dynamic contrast-enhanced MRI

Miaomiao Wang[1], Rihua Jiao[2], Yanan Li[1], Congcong Liu[1], Jianxin Guo[1], Chao Jin[1], and Jian Yang[1]

[1]Department of Diagnostic Radiology, the First Affiliated Hospital of Xi'an Jiaotong University, Xi'an, People's Republic of China, [2]ISN Lab, Xidian University

In this study, a new approach for assessing distribution of bloodstream inflow and outflow type based on the three-time point (3TP) method was used to semi-quantitative analysis of the microcirculation characteristics in whole pituitary adenoma by dynamic contrast-enhanced MRI (DCE-MRI). The volume percentage of persistently enhancing type of time-intensity curve (TIC) in adenoma was higher than normal region. Meanwhile, adenomas with hyperprolactinemia were shown a significant decrease of volume percentage in speed up the downhill type when compared with the adenoma without hyperprolactinemia. This method could identify the different distribution of vascularity between normal pituitary and subtype of adenoma.

2218 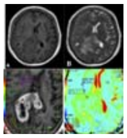

Application of High B-value Diffusion-Weighted Imaging in Defining High-grade Glioma Infiltration Regions

Chunhui Jiang[1], Jian Wang[2], Juan Ma[2], Abudureheman Yibanu[2], and Chen Liu[3]

[1]*MRI Room，Department of Imaging Center, The First Affiliated Hospital of Xinjiang Medical University, Urumqi, People's Republic of China,* [2]*MRI Room，Department of Imaging Center, The First Affiliated Hospital of Xinjiang Medical University,* [3]*Department of Neurosurgery, The First Affiliated Hospital of Xinjiang Medical University*

Objective To evaluate the role of the ADC value in patients with high-grade glioma (WHO III-IV) using high B-value diffusion weighted imaging (DWI), as a potential noninvasive quantitative index in defining the boundary of glioma. Methods 25 cases of surgical pathologically confirmed glioma underwent the DWI scan with b=1000 and 3000s/mm² respectively in a 3T MR scanner. The ADC values of the glioma substantial zone, cerebral parenchyma within 0-10/10-20mm radium and the cerebral parenchyma of the opposite sphere are statistically analyzed by SPSS17.0. Results When b=1000 and 3000 s/mm², the difference in the ADC values of the tumor and the 0-10mm region had no statistical significance (P>0.05). When b-value = 1000 s/mm², there is statistically valid difference among ADC values of 10-20mm area, lesions and comparing group (P<0.05); When b-value =3000 s/mm², there is no statistically valid difference among ADC values of 10-20mm area and lesions（P>0.05）. The ADC value of 10-20mm area is validly lower than the lesions. Conclusion The ADC value in high B value DWI scan indicating that the ADC value is more sensitive in quantitatively analyzing the infiltration zone of glioma relative to the low B value DWI scan.

2219

The value of vessel size imaging in grading oligodendroglioma

Hong Guo[1]

[1]*Daping Hospital & Research Institute of Surgery, Chongqing, People's Republic of China*

Applying vessel size imaging(VSI) and dynamic susceptibility contrast MR (DSC-MR) to explore difference of the microvessel between grade Ⅱ and Ⅲ oligodendroglioma. We discovered both VSI and DSC-MR could identify different grades of oligodendroglioma, but the power of VSI was better than DSC-MR.

2220 

Radiographic Atlas of Tumor Growth Pattern in Glioblastoma

Morteza Esmaeili[1], Anne Line Stensjøen[1], Erik Magnus Berntsen[1], Ole Solheim[1,2,3], and Ingerid Reinertsen[3,4]

[1]*Department of Circulation and Medical Imaging, Norwegian University of Science and Technology, NTNU, Trondheim, Norway,* [2]*Department of Neurosurgery, St. Olav's University Hospital, Trondheim, Norway,* [3]*Norwegian National Advisory unit for Ultrasound and Image Guided Therapy, St. Olav's University Hospital, Trondheim, Norway,* [4]*Department of Medical Technology, SINTEF, Trondheim, Norway*

In this study we assess the growth pattern of one of the most aggressive brain tumor in adults. Surgery is a standard of care for these patients, and understanding the prominent growth direction of tumor lesions can eventually benefit surgical planning. Contrast-enhanced MR data at two time-points of diagnosis and pre-operation were analyzed to derive mean 3D vector field demonstrating the growth directions. A DTI white matter (WM) atlas was used to investigate the degree of agreement and alignment of the generated vector field towards white matter fibers.

2221 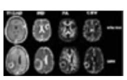

Differentiation of Brain Infections from Necrotic Glioblastomas using Diffusion Tensor Imaging and Perfusion Weighted Imaging

Sumei Wang[1], SANJEEV CHAWLA[1], Mohamed Metkees[1,2], Seyed Ali Nabavizadeh[1], Gaurav Verma[1], Arastoo Vossough[1], Suyash Mohan[1], and Harish Poptani[1,3]

[1]*Radiology, UNIVERSITY OF PENNSYLVANIA, PHILADELPHIA, PA, United States,* [2]*Biological Anthropology, National Research Centre, Cairo, Egypt,* [3]*Cellular and Molecular Physiology, University of Liverpool, Liverpool, United Kingdom*

To determine whether combined use of diffusion and perfusion MRI can help in differentiating brain infections from glioblastomas (GBMs), 13 patients with infections and 20 patients with GBMs underwent DTI and DSC-PWI. Significantly lower median values of mean diffusivity (MD) and higher fractional anisotropy (FA) were observed in central core of infective lesions than in GBMs. Additionally, significantly decreased median and maximum values of relative cerebral blood volume (rCBV) from enhancing region were observed in patients with infections compared with those of GBMs. The best classification model consisted of MD from central core and $rCBV_{max}$ from enhancing region.

2222 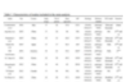

The diagnostic performance of DCE-MRI in differentiating high-from low-grade gliomas: A systematic review and meta-analysis

Zhe Liu[1], Xiang Li[1], Ting Liang[1], Tong Yi Bian[1], Miao Miao Wang[1], Li Qin Sun[1], Gang Niu[1], and Jian Yang[1]

[1]*Department of Diagnostic Radiology, the first affiliated hospital of XI'AN jiaotong universityDepartment of Diagnostic Radiology, XI'AN, People's Republic of China*

Dynamic contrast-enhanced magnetic resonance imaging (DCE-MRI) has been provided for noninvasive assessment of different grade of gliomas. But the diagnostic performance of this new approach was variant among the recent reports. This study included 10 DCE-MRI studies regarding to differentiating high grade gliomas (HGGs) from low grade gliomas (LGGs). The meta-analysis results demonstrated that parameters of DCE-MRI have high diagnostic performanc (Ktrans and Ve) in distinguishing HGGs from LGGs. DCE-MRI can be used as an important tool for the assessment of neovascular permeability and for the pre-operative grading of glioma.

2223 

Imaging Characteristics According to the IDH Mutation and 1p19q Codeletion Status of Lower Grade Gliomas

Yae Won Park[1], Sung Soo Ahn[1], and Seung-Koo Lee[1]

[1]*Yonsei University College of Medicine, Seoul, Korea, Republic of*

Preoperative prediction of genotypic classification with MRI is useful because IDH mutation and 1p/19q codeletion status are important prognostic and predictive factors in lower-grade gliomas (WHO grade II and III). In this study we found that various preoperative imaging features including lobar/nonlobar or central location, enhancement characteristics, tumor margin, diffusion characteristics, ependymal/cortical involvement were different between IDH-wildtype and IDH-mutant group. Therefore preoperative MRI may be helpful to predict IDH mutation status in lower-grade gliomas.

2224

Development and validation of a MRI-based radiomics prognostic classifier in patients with primary glioblastoma multiforme

Xin Chen[1], Zaiyi Liu[2], Xinqing Jiang[1], Xinhua Wei[1], and Zhongping Zhang[3]

[1]Department of radiology, Guangzhou First People's Hospital, Guangzhou, People's Republic of China, [2]Department of radiology, Guangdong General Hospital, Guangdong Academy of Medical Sciences, Guangzhou, People's Republic of China, [3]GE Healthcare China, Guangzhou, People's Republic of China

Glioblastoma multiforme (GBM) is the most frequent and deadly type of primary malignant tumor in the central nervous system with a median survival range of only 9-15 months. We developed and validated a MRI-based radiomics classifier to predict overall survival(OS) in patients with newly diagnosed GBM. The results showed that a 7-radiomics classifier allows prediction of survival and stratification of patients with newly diagnosed GBM into a low- or high-risk group for OS.

2225

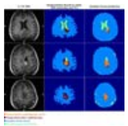

Tumor progression prediction in high grade glioma using multimodal image analysis and random forest machine learning

Charlotte Debus[1,2,3,4], Maximilian Knoll[1,2,3,4], Sebastian Adeberg[3,4], Stefan Rieken[3,4], Jürgen Debus[1,2,3,4], and Amir Abdollahi[1,2,3,4]

[1]German Cancer Consortium (DKTK), Heidelberg, Germany, [2]Translational Radiation Oncology, National Center for Tumor Diseases (NCT), German Cancer Research Center (DKFZ), Heidelberg, Germany, [3]Heidelberg Institute of Radiation Oncology (HIRO), National Center for Radiation Research in Oncology (NCRO), Heidelberg, Germany, [4]Heidelberg Ion-Beam Therapy Center (HIT), Department of Radiation Oncology, Heidelberg University Hospital, Heidelberg, Germany

Tumor delineation in radiotherapy planning of high grade glioma is challenging due to infiltrative growth patterns and physiological tumor heterogeneity. We used random forest machine learning to classify tissue types and predict tumor progression based on parameters derived from multi-modal functional and metabolic imaging. In an integrative approach, eight patients with recurrent high grade glioma were investigated retrospectively, and the resulting predicted tumor volumes were compared to standard T_1 weighted contrast-enhanced MRI based segmentations. Predictions of tumor tissue could identify original tumor volumes well and yielded promising results with respect to tumor progression in terms of sensitivity and specificity.

2226

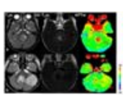

Molecular imaging of pediatric cerebellar tumors using endogenous protein-based amide proton transfer MR imaging at 3 Tesla

Hong Zhang[1], Yi Zhang[2], Xiaolu Tang[1], Huiying Kang[1], Di Hu[1], Jinyuan Zhou[2], and Yun Peng[1]

[1]Department of Radiology, Beijing Children’s Hospital, Capital Medical University, Beijing, People's Republic of China, [2]Department of Radiology, Johns Hopkins University, MD, United States

Amide proton transfer (APT)-MRI is a chemical exchange saturation transfer (CEST) based approach in which the amide protons of endogenous proteins and peptides are irradiated to accomplish detection using the water signal. In this study, the APT approach was incorporated with standard brain MRI sequences and applied to children with cerebellar tumors at 3T. The initial results show that APT imaging can enhance the noninvasive identification of tissue heterogeneity and may be a biomarker of tumor grade in pediatric cerebellar tumors.

2227

Comparison of native longitudinal relaxation rate, apparent diffusion coefficient, and extravascular extracellular volume fraction in vestibular schwannoma in type 2 neurofibromatosis before and after antiangiogenic therapy

Ka-Loh Li[1], Ibrahim Djoukhadar[1], Sha Zhao[1], Natale Quartuccio[1], Amy Watkins[1], Xiaoping Zhu[1], and Alan Jackson[1]

[1]Division of Informatics, Imaging and Data Sciences, The University of Manchester, Manchester, United Kingdom

The relationship between three functional parameters related to cell density, ADC, $R1_N$, and v_e, were examined in 12 patients with vestibular schwannomas pre- and post- anti-angiogenic therapy. 3D maps of $R1_N$ obtained with variable flip angle images, and v_e derived from DCE-MRI were compared to 3D maps of ADC. The tumor mean values of ADC, $R1_N$ and v_e showed correlation to each other before bevacizumab treatment. This correlation was lost after three-months of treatment. Both $R1_N$ and ADC displayed power in prediction of treatment. $R1_N$ showed more sensitive to anti-angiogenic therapy induced changes in VS than ADC or ve.

2228

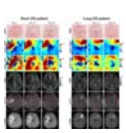

Metabolic and functional MR imaging probe early response in glioblastoma patients treated with combination antiangiogenic-chemoradiation therapy

Ovidiu C Andronesi[1], Morteza Esmaeili, Ronald Borra, Kyrre Emblem, Elizabeth Gerstner, Marco Pinho, Scott Plotkin, Andrew Chi, April Eichler, Jorg Dietrich, Percy Ivy, Patrick Wen, Dan Duda, Rakesh Jain, Bruce Rosen, Gregory Sorensen, and Tracy Batchelor

[1]Radiology, Massachusetts General Hospital, Boston, MA, United States

Precise assessment of treatment response in glioblastoma during combined antiangiogenic and chemoradiation remains a challenge. In particular, early detection of treatment response by standard anatomical imaging is confounded by pseudo-response or pseudo-progression. Metabolic changes probed by MRSI are more specific for tumor physiology and less confounded by changes in blood-brain barrier permeability.

2229

Assessment of therapeutic response in glioma with spillover-, MT- and T1-corrected amide proton transfer MR imaging

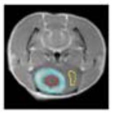

Jing Zhao[1], Yiying Zhao[2], Yinsheng Chen[2], Zhongping Chen[2], and Yin Wu[1]

[1]Paul C. Lauterbur Research Centre for Biomedical Imaging, Shenzhen Institutes of Advanced Technology, Chinese Academy of Sciences, Shenzhen, People's Republic of China, [2]Department of Neurosurgery, Cancer Center, Sun Yat-Sen University, Guangzhou, People's Republic of China

Amide proton transfer (APT) MR imaging has proved to be capable of detecting/grading brain tumors as well as assessing treatment response. Routinely used magnetization transfer (MT) asymmetry is contaminated with MT, nuclear overhauser effect (NOE) and T_1 relaxation time of water. In this study, the dominant contributors of direct water saturation and MT to Z-spectrum were estimated from a sum of two Lorentzian functions, and APT was corrected with T_1 scale and inverse Z-spectrum analysis. Results showed that the corrected APT can reliably depict glioma heterogeneity post-treatment, in accordance with H & E histological observations.

Traditional Poster

Psychiatric Neuroimaging

Exhibition Hall 2230-2258 Wednesday 13:45 - 15:45

2230

Longitudinal opto-pharmaco-fMRI of Selective Serotonin Reuptake Inhibition

Horea-Ioan Ioanas[1,2], Bechara John Saab[2], and Markus Rudin[1]

[1]Institute for Biomedical Engineering, ETH and University of Zurich, Zürich, Switzerland, [2]Preclinical Laboratory for Translational Research into Affective Disorders, DPPP, Psychiatric Hospital, University of Zurich, Zürich, Switzerland

The serotonergic system is a high-centrality node in the brain network implicated in affective disorders and their treatment. We use optogenetics, fMRI, and pharmacology to image serotonergic effects of antidepressant treatment in mice at the whole-brain level. We stimulate the ascending serotonergic system and perform functional imaging at multiple time points over the course of antidepressant (fluoxetine) treatment. We establish the feasibility of this paradigm, and report two trends in serotonergic kinetics: (a) increased serotonergic system signal transmission upon acute, but not chronic fluoxetine administration, (b) decreased serotonergic system excitability during the first phase of chronic fluoxetine administration.

2231

Graph-based network analysis of multi-echo resting-state fMRI data in people with high schizotypy

Kurtis Stewart[1], Owen O'Daly[1], Gareth J Barker[1], Katrina McMullen[2], Veena Kumari[1], Steven CR Williams[1], and Gemma Modinos[1]

[1]Institute of Psychiatry, Psychology & Neuroscience, King's College London, London, United Kingdom, [2]Centre for Brain Health, University of British Columbia, BC, Canada

We applied graph theoretical network analysis on multi-echo resting-state fMRI data to examine whether healthy people with subclinical psychotic-like experiences (schizotypy) show abnormal functional brain topology compared to similar subjects without such experiences. While we did not observe significant between-group differences in any connectivity measure (Local and global efficiency, Modularity, and Small-worldness), within the schizotypy group we found that modularity and small-worldness were directly related to the severity of subclinical psychotic-like experiences. This demonstrates the feasibility of applying graph theory on multi-echo rs-fMRI in individuals with vulnerability for psychotic disorders and encourages the application of these methods in psychosis research.

2232

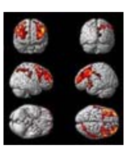

Cerebral blood flow measurements in patients with depression and comorbid hypertension in depression using 3D arterial spin labeling

Ying Liu[1], Huishu Yuan[1], Xiangzhu Zeng[1], Zheng Wang[1], and Lizhi Xie[2]

[1]Radiology, Peking University Third Hospital, Beijing, People's Republic of China, [2]GE Healthcare, MR Research China, Beijing, People's Republic of China

The aim of this study is to explore the potential differences of the quantitative CBF values among patients with depression, patients with hypertension and patients with comorbid hypertension in depression by using whole brain 3D PCASL and to investigate the correlation between CBF values and degrees of depression. The results indicate that CBF values decrease in frontal and parietal lobes in patients with comorbid hypertension in depression, whereas not in patients with depression or patients with hypertension, hypertension may play a synergistic action in the progress of depression.

2233

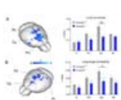

Homozygous loss of autism-risk gene CNTNAP2 results in reduced local and long-range prefrontal connectivity

Adam Liska[1,2], Ryszard Gomolka[2], Mara Sabbioni[3], Alberto Galbusera[2], Stefano Panzeri[4], Maria Luisa Scattoni[3], and Alessandro Gozzi[2]

[1]CIMeC, Center for Mind/Brain Sciences, University of Trento, Rovereto, Italy, [2]Functional Neuroimaging Laboratory, Center for Neuroscience and Cognitive Systems @ UniTn, Istituto Italiano di Tecnologia, Rovereto, Italy, [3]Neurotoxicology and Neuroendocrinology Section, Department of Cell Biology and Neurosciences, Istituto Superiore di Sanità, Rome, Italy, [4]Neural Computation Laboratory, Center for Neuroscience and Cognitive Systems @ UniTn, Istituto Italiano di Tecnologia, Rovereto, Italy

Functional connectivity aberrancies as measured with resting-state fMRI (rsfMRI) have been consistently observed in the brains of autism spectrum disorders (ASD) patients. However, genetic and neurobiological underpinnings of these findings remain unclear. Here we used rsfMRI to show that homozygous mice lacking the strongly ASD-associated gene CNTNAP2 exhibit default-mode network connectivity alterations associated with reduced social investigation, a core “autism trait” in mice. These findings reveal a causal link between an ASD-associated mutation and functional connectivity aberrancies and suggest that homozygous loss-of-function mutations in CNTNAP2 may predispose to ASD through a selective dysregulation of functional coupling between integrative cortical areas.

2234

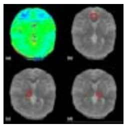

A preliminary study on amide proton transfer-weighted MR imaging in patients with obsessive-compulsive disorder

Yan Li[1], Naying He[1], Hongmin Xu[1], Chencheng Zhang[2], Weibo Chen[3], Yansong Zhao[4], Yi Zhang[5], Jinyuan Zhou[5], Haiyan Jin[6], and Fuhua Yan[1]

[1]Department of Radiology, Ruijin Hospital,Shanghai Jiao Tong University School of Medicine, Shanghai, People's Republic of China, [2]Department of Functional Neurosurgery, Ruijin Hospital,Shanghai Jiao Tong University School of Medicine, Shanghai, People's Republic of China, [3]Philips Healthcare, Shanghai, People's Republic of China, [4]Philips Healthcare, Cleveland, OH, United States, [5]Department of Radiology, Johns Hopkins University School of Medicine, Baltimore, MD, United States, [6]Department of Psychiatry, Ruijin Hospital,Shanghai Jiao Tong University School of Medicine, Shanghai, People's Republic of China

The aim of this study is to evaluate the feasibility of amide proton transfer-weighted (APTW) MR imaging to detect cerebral abnormalities in patients with obsessive-compulsive disorder (OCD) and to explore its clinical utility. Five OCD patients and 9 normal healthy controls (NC) underwent APTW MR imaging. The magnetic resonance ratio asymmetry (MTR_{asym}) values at 3.5ppm of anterior cingulate cortex (ACC) and thalamus were measured on axial APTW images. We found a trend of increased MTR_{asym}(3.5ppm) or APTW within ACC in OCD patients compared with controls. No significant difference was found between groups in the MTR_{asym}(3.5ppm) within bilateral thalamus. Our results suggest that APTW imaging maybe a promising approach to investigate pathological changes underlying OCD and may provide insights into clinical diagnosis of OCD.

2235

Pharmacological Inhibition of ERK Pathway Rescues Morpho-Anatomical Aberrancies Associated with 16p11.2 Chromosomal Deletion

Marco Pagani[1,2], Joanna Pucilowska[3], Camilla Robol[1], Joseph Vithayathil[3], Caitlin Kelly[3], Colleen Karlo[3], Riccardo Brambilla[4], Gary E. Landreth[3], and Alessandro Gozzi[1]

[1]Functional Neuroimaging Laboratory, Center for Neuroscience and Cognitive Systems, Istituto Italiano di Tecnologia, Rovereto, Italy, [2]CIMeC, Center for Mind/Brain Sciences, University of Trento, Rovereto, Italy, [3]Department of Neurosciences, Case Western Reserve University, Cleveland, OH, [4]School of Biosciences, Cardiff University, Cardiff, United Kingdom

16p11.2 microdeletion is the most common copy number variation in autism. Recent studies revealed that mice harboring this microdeletion exhibit a paradoxical elevation of ERK activity, macroscale gray matter abnormalities and autistic-like behavioral deficits. By using high-resolution morpho-anatomical MRI, we show that prenatal treatment with an ERK pathway inhibitor rescues hippocampal and septal anatomical deficits in 16p11.2del mutants. The effect was associated with amelioration of anxiety behaviors. These results provide the first example of the rescue of developmental gray matter abnormalities in this mouse model, and support the translational use of structural MRI to assess putative therapeutic effects in autism.

2236

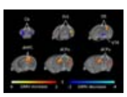

Aberrant striatal anatomy and gray matter connectivity networks in mice lacking autism-associated gene CNTNAP2.

Marco Pagani[1,2], Alberto Galbusera[1], and Alessandro Gozzi[1]

[1]Functional Neuroimaging Laboratory, Center for Neuroscience and Cognitive Systems, Istituto Italiano di Tecnologia, Rovereto, Italy, [2]CIMeC, Center for Mind/Brain Sciences, University of Trento, Rovereto, Italy

Mice lacking CNTNAP2 exhibit robust autism-like behavioral traits, including stereotyped behaviors and excessive self-grooming. By using high resolution morpho-anatomical imaging in CNTNAP2 mutant mice, we identified marked volumetric alterations subcortical substrates implicated in ASD motor stereotypy, with a prominent involvement of the dorsal striatum. Importantly, we also show that in mutant mice, striatal but not cortical regions, exhibit dramatically expanded gray matter network extension, encompassing aberrant trophic interaction between limbic, subcortical and prefrontal regions. The observed striatal volumetric and gray matter network abnormalities serve as a plausible morpho-anatomical substrate for some of the stereotypy exhibited by CNTNAP2 mutant mice.

2237

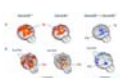

Altered default mode network organization and functional connectivity in mice lacking autism-associated gene Shank3

Marco Pagani[1,2], Camilla Robol[1], Richard Gomolka[1], Adam Liska[1,2], Alberto Galbusera[1], Anna Aksiuto[1], and Alessandro Gozzi[1]

[1]Functional Neuroimaging Laboratory, Center for Neuroscience and Cognitive Systems, Istituto Italiano di Tecnologia, Rovereto, Italy, [2]CIMeC, Center for Mind/Brain Sciences, University of Trento, Rovereto, Italy

Mutations in autism-associated gene Shank3 have been associated to alterations in striatal function and core autistic behaviors. However, the neocortical substrates affected by Shank3 mutations remain undetermined. By using structural and functional MRI in Shank3B mutant mice, we identified key alterations in prefrontal and associative regions of the mouse default mode network (DMN). Specifically, we show that prefrontal and antero-posterior areas of the DMN present decreased gray matter volume, an effect associated with reduced local and long-range prefrontal functional connectivity. Our findings suggest that Shank3 mutations may predispose to autism via a selective trophic and functional downregulation of prefrontal areas.

2238

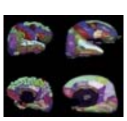

Different patterns of cortical matter changes in first episode bipolar manic adolescents: a surface-based structural MRI study with cluster analysis

Wenjing Zhang[1], Wade Weber[2], Huaiqiang Sun[1], Min Wu[1], Qiyong Gong[1], Melissa DelBello[2], and Su Lui[1]

[1]Huaxi MR Research Center (HMRRC), Department of Radiology, West China Hospital of Sichuan University, Chengdu, People's Republic of China, [2]Department of Psychiatry and Behavioral Neuroscience, University of Cincinnati College of Medicine, Cincinnati, OH, United States

With an objective neuroimaging data-driven method using agglomerative hierarchical clustering analysis, two patterns of cortical matter changes among 58 first episode bipolar manic adolescents has been identified. And the clinical feature especially the intelligence quotient was corresponding to the subtyping among these patients. While the effect of medication and illness duration have been minimized, our findings provided new evidence indicating the existence of two neurobiologically distinct subgroups of patients with first episode bipolar mania, which may reflect qualitatively distinct genetic influences or neurodevelopmental alterations.

2239 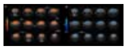 Muscarinic receptor agonism prevents the functional connectivity aberrancies produced by the psychotogenic drug phencyclidine (PCP)

Carola Canella[1,2], Adam Liska[1,2], Valentina Piretti[1], Alberto Galbusera[1], Adam Schwarz[3,4], and Alessandro Gozzi[1]

[1]Functional Neuroimaging Laboratory, Center for Neuroscience and Cognitive Systems @ Unitn, Istituto Italiano di Tecnologia, Rovereto, Italy, [2]CIMeC, Center for Mind/Brain Sciences, University of Trento, Rovereto, Italy, [3]Psychological and Brain Sciences, Indiana University, Bloomington, IN, United States, [4]Radiology and Imaging Sciences, Indiana University, Indianapolis, IN, United States

NMDA receptor antagonists like ketamine or phencyclidine (PCP) induce robust schizophrenia-like symptoms in rodents via glutamatergic disinhibition of cortico-limbo-thalamic substrates. We show that acute administration of PCP in the mouse elicits aberrant fronto-hippocampal and thalamo-cortical functional connectivity, an effect that can be prevented by pharmacological activation of M1/M4 muscarinic receptors. These changes highlight a previously unreported permissive contribution of muscarinic receptors on the aberrant connectional signatures produced by NMDAr antagonism which bear relevance for human connectivity mapping in hyperglutamatergic states and schizophrenia.

2240  Machine-learning classification of ADHD with biomarkers of cerebral cortical thickness: parcellation schemes, gender effects and feature selection

Hsin-Yu Chen[1], Chia-Min Chen[1], Teng-Yi Huang[1], and Tzu-Chao Chuang[2]

[1]National Taiwan University of Science and Technology, Taipei, Taiwan, [2]National Sun Yat-sen University, Kaohsiung, Taiwan

In this study, we attempt to use machine-learning algorithms for ADHD classification with cerebral cortical thickness. We compared three cortical parcellation schemes and three different sets of features. The results supported the usage of Aparc and A2009s of FreeSurfer and suggested that recursive feature elimination effectively increased the predication accuracies. In addition, gender is an influential feature for the classification.

2241  Compulsivity as a Transdiagnostic Trait in Humans and Animal Models

Muriel M. K. Bruchhage[1], Ilse van Ooijen–van de Vondervoort[2], Erwin L. A. Blezer[3], Katarzyna Kapusta[2], Houshang Amiri[2], David J. Lythgoe[1], Marcel P. Zwiers[4], Rick M. Dijkhuizen[5], Jeffrey C. Glennon[2], Sarah Durston[5], Daniel Brandeis[6], Jan Buitelaar[4], Steven C. R. Williams[1], and Flavio Dell'Acqua[7]

[1]Centre for Neuroimaging Sciences, Institute of Psychiatry, Psychology and Neuroscience, King's College London, London, United Kingdom, [2]Department of Cognitive Neurscience, Radboud University Medical Center, Nijmegen, Netherlands, [3]Center for Image Sciences, University Medical Center Utrecht, Utrecht, Netherlands, [4]Department of Cognitive Neuroscience, Donders Institute for Brain, Cognition and Behaviour, Radboud University Medical Center, Nijmegen, Netherlands, [5]Brain Center Rudolf Magnus, University Medical Center Utrecht, Utrecht, Netherlands, [6]Department of Child and Adolescent Psychiatry and Psychotherapy, Central Institute of Mental Health Mannheim, Mannheim, Germany, [7]NatBrainLab, Department of Forensics and Neurodevelopmental Sciences, Sackler Institute of Translational Neuroimaging, King's College London, London, United Kingdom

Obsessive-compulsive disorder (OCD) and diabetes mellitus type 2 (DM2) show compulsive behaviour1 and share genetic vulnerability2. Using Diffusion Tensor Imaging as a translational approach, we investigated differences in corpus callosum (CC) body white matter microstructure in a paediatric human OCD cohort and juvenile animal models for OCD and DM2. In all three groups, fractional anisotropy increased in the CC body compared to controls, which correlated with increasing compulsive behaviour. This was coupled with a decrease in CC mean diffusivity in the animal models. Our results underline the importance of compulsive behaviour as a possible trans-diagnostic trait across OCD and DM2.

2242  Remitted and non-remitted patients with schizophrenia show distinct patterns of white matter tract alterations

Jing-Ying Huang[1], Chih-Min Liu[2,3], Tzung-Jeng Hwang[2,3], Yu-Jen Chen[1], Yung-Chin Hsu[1], Hai-Gwo Hwu[2,3], and Wen-Yih Isaac Tseng[1,3,4,5]

[1]Institute of Medical Device and Imaging, National Taiwan University College of Medicine, Taipei, Taiwan, [2]Department of Psychiatry, National Taiwan University Hospital, Taipei, Taiwan, [3]Graduate Institute of Brain and Mind Sciences, National Taiwan University College of Medicine, Taipei, Taiwan, [4]Department of Medical Imaging, National Taiwan University Hospital, Taipei, Taiwan, [5]Molecular Imaging Center, National Taiwan University, Taipei, Taiwan

To investigate the relations between white matter tracts and treatment outcome, we performed diffusion spectrum imaging (DSI) and whole brain tract-based automatic analysis (TBAA) comparisons of the tract integrity over the whole brain. As compared with health controls, non-remitted patients showed reduced integrity in 7 fiber tract bundles, whereas remitted patients only showed 4 fiber tract bundles. When comparing with remitted patients, non-remitted patients showed reduced integrity in the same 7 fiber tract bundles as those found in comparison with healthy controls. Our results support that remitted and non-remitted patients had distinctly different severity of tract alterations.

2243 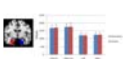 Altered amygdala function in nicotine-dependent individuals

Zhujing Shen[1], Peiyu Huang[1], Chao Wang[1], Wei Qian[1], and Minming Zhang[1]

[1]Radiology, The 2nd Affiliated Hospital of Zhejiang University School of Medicine, Hangzhou, People's Republic of China

To investigate the role of amygdala in nicotine dependence, we examined its structural and functional changes in smokers. Volume, amplitude of low frequency fluctuations (ALFF) and seed-based functional connectivity (FC) was used to detect differences. Results showed that although there was no significant volume change, right amygdala activity increased in smokers compared with nonsmokers. Furthermore, FC between the left amygdale and left orbit frontal cortex (OFC) increased while the right amygdale and bilateral OFC decreased in smokers. These results suggest that abnormal amygdala function may underlie the occurrence of nicotine dependence.

2244 Microstructure Alterations of Earthquake Survivors: A Longitudinal MR Diffusion Study

Linghui Meng[1], Kaiming Li, and Jing Jiang

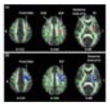

[1]Huaxi MR Research Center (HMRRC), Department of Radiology, West China Hospital of Sichuan University, Chengdu, People's Republic of China

To reveal how traumatic events affect the integrity of brain microstructure in trauma-exposed non-PTSD people, we performed a longitudinal tract-based spatial statistics (TBSS) analysis in earthquake survivors using diffusion tensor imaging (DTI) data collected 25 days (TimePoint 1) and 2 years (TimePoint 2) after the Wenchuan earthquake. Our results showed that fractional anisotropy (FA) in several brain regions at TimePoint 2 were significantly increased compared with those at TimePoint 1. The increased FA in these regions may serve as the underlying neural substrates as brain recovered from the trauma.

2245

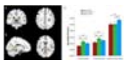

A Diffusion Tensor Imaging Study of White Matter Microstructure Concerning Suicidal Ideation in Major Depressive Disorder

Huawei Zhang[1], Xiaoqi Huang[1], and Zhiyun Jia[2]

[1]Radiology, Huaxi MR Research Center(HMRRC), Chengdu, People's Republic of China, [2]Huaxi MR Research Center(HMRRC), Chengdu, People's Republic of China

Suicide is a serious public health problem, but little is known of microstructural abnormalities of white matter regarding suicidal ideation (SI). Sixteen depressive patients with SI, 16 depressive patients without SI and 32 age- and gender-matched healthy controls received MRI scans on a 3T magnet. Whole-brain voxel-based analysis was used to compare fractional anisotropy (FA) across the three groups with threshold at $p<0.005$(uncorrected) at voxel level and 50 for cluster size with SPM8. The three groups had significant differences of FA in the left centrum semiovale (peak Z=4.64 at -30, -38, 34), right centrum semiovale (peak Z=3.54 at 32, -34, 32) and right splenium of corpus callosum (peak Z=4.64 at 4, -34, 12). The alterations of white matter tract indicate that white matter integrity, especially a “frontal-related WM disconnection” may underlie the pathophysiology of suicidal ideation in depression.

2246

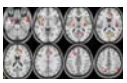

Gray matter reduction is associated with poor treatment response in patients with schizophrenia: A voxel-based morphometry study with a strict control of multiple clinical variables

Jing-Ying Huang[1], Chih-Min Liu[2,3], Tzung-Jeng Hwang[2,3], Yu-Jen Chen[1], Yung-Chin Hsu[1], Hai-Gwo Hwu[2,3], and Wen-Yih Isaac Tseng[1,3,4,5]

[1]Institute of Medical Device and Imaging, National Taiwan University College of Medicine, Taipei, Taiwan, [2]Department of Psychiatry, National Taiwan University Hospital, Taipei, Taiwan, [3]Graduate Institute of Brain and Mind Sciences, National Taiwan University College of Medicine, Taipei, Taiwan, [4]Department of Medical Imaging, National Taiwan University Hospital, Taipei, Taiwan, [5]Molecular Imaging Center, National Taiwan University, Taipei, Taiwan

To investigate whether remitted and non-remitted patients with schizophrenia had distinctly different gray matter volumes, we used voxel-based morphometry (VBM) to analyze group difference by controlling all possible clinical variables. As compared with remitted patients, the non-remitted patients showed 10 brain areas with significantly decreased gray matter volume. Our results imply that remitted and non-remitted patients might have distinct patterns of gray matter reduction, and the characteristics of gray matter change might represent the structural correlate of treatment response in patients with schizophrenia.

2247

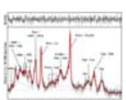

Repeated Binge Alcohol Intoxication Leads to Lower Choline-Containing Compound Signals in Rat Brain: An In Vivo Marker of Alcohol-Induced Neurobiological Abnormalities

Dong-Hoon Lee[1,2], Do-Wan Lee[3,4,5], Ji-Yeon Park[6], Hae-Jin Park[7], Kyu-Ho Song[4,5], Yong Hyun Chung[2], Dong-Cheol Woo[8], and Bo-Young Choe[4,5]

[1]Brain and Mind Centre, University of Sydney, Sydney, Australia, [2]Department of Radiological Science, Yonsei University, Wonju, Korea, Republic of, [3]Ewha Brain Institute, Ewha Womans University, Seoul, Korea, Republic of, [4]Department of Biomedical Engineering, The Catholic University of Korea College of Medicine, Seoul, Korea, Republic of, [5]Research Institute of Biomedical Engineering, The Catholic University of Korea, Seoul, Korea, Republic of, [6]Department of Radiation Oncology, University of Florida, Gainesville, FL, United States, [7]Department of Radiation Oncology, Ajou University School of Medicine, Suwon, Korea, Republic of, [8]MR Core Laboratory, Asan Institute for Life Sciences, Asan Medical Center, Seoul, Korea, Republic of

Alcohol is the most commonly abused intoxicating substance among young and middle-aged adults, and ranks highly as a cause of disability and mortality. A pattern of heavy consumption, called binge drinking, leads to various psychiatric disorders. We used in vivo proton magnetic resonance spectroscopy (^{1}H MRS) to quantitatively assess neurochemical responses in hippocampus in a rat model of repeated-binge alcohol (RBA) intoxication. We determined that choline-containing compound, gamma-aminobutyric acid, and total N-acetyl-aspartate (tNAA: N-acetyl-aspartate + N-acetyl-aspartyl-glutamate) signals were highly sensitive to binge alcohol intoxication, which provides insights into neurochemical alterations associated with alcohol abuse.

2248

Eigenvector centrality mapping evaluating disease progression in Parkinson disease ：a longitudinal study

qiaoling zeng[1], xiaojun guan[1], min xuan[1], quanquan gu[1], xiaojun xu[1], and minming zhang[1]

[1]2nd Affiliated Hospital, Zhejiang University School of Medicine, hangzhou, People's Republic of China

Studied longitudinally 21 PD patients using Eigenvector centrality mapping,discovered significantly decreased EC values in right postcentral gyrus, and increased EC values in right cerebellum, right supplementary motor area (right SMA) as compared to B group. right postcentral gyrus in F group is negativelycorrelatedwithhoehn and yahr staging(HY) stage (r =-0.48, $p < 0.05$). Variation of EC values (F group-B group) in right cerebellum is positively correlated with changeofUPDRS-III scores. The current study demonstrated that deterioration and compensation exists through different circuit along with PD progression.

2249

Cerebral perfusion in Schizophrenia: an Arterial Spin Labeling study

Icaro Agenor Ferreira Oliveira[1], Tiago Guimaraes[2], Roberto Souza[2], Antonio Santos[3], Jaime Hallak[2], and Renata Ferranti Leoni[1]

[1]Physics Department, University of Sao Paulo, Ribeirao Preto, Brazil, [2]Department of Neuroscience and Behavioral Sciences, University of Sao Paulo, [3]Department of Medical Clinic, University of Sao Paulo

Schizophrenia is a mental disorder with structural and functional alterations that are not completely comprehended. We used a pseudo-continuous ASL protocol to investigate changes in resting CBF in schizophrenic patients. In addition, quantitative T1 and Gray Matter Volume (GMV) were assessed. Decreased CBF, GMV, and T1 values were observed in schizophrenic patients compared with healthy controls in several brain regions consistent with patients' symptoms, such as deficits in planning solving and organizing thoughts. Therefore, motor, sensorial and cognitive impairments observed in schizophrenia may be related to CBF deficits and structural alterations in localized brain regions.

2250

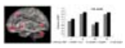

Distortions in Dynamic Functional Connectivity in Autism Spectrum Disorders

Rajesh K Kana[1], Haley M Bednarz[1], D Rangaprakash[2,3], and Gopikrishna Deshpande[2,4,5]

[1]Department of Psychology, University of Alabama at Birmingham, Birmingham, AL, United States, [2]AU MRI Research Center, Department of Electrical and Computer Engineering, Auburn University, Auburn, AL, United States, [3]Department of Psychiatry and Biobehavioral Sciences, University of California Los Angeles, Los Angeles, CA, United States, [4]Department of Psychology, Auburn University, Auburn, AL, United States, [5]Alabama Advanced Imaging Consortium, Auburn University and University of Alabama Birmingham, Birmingham, AL, United States

Autism spectrum disorders (ASD) are neurodevelopmental disorders that have been associated with disruptions in brain connectivity. Using resting-state fMRI, we assessed the variability of whole-brain connectivity in individuals with ASD. Using a variable, sliding-window technique to calculate the variance of dynamic functional connectivity (vDFC), we show increased vDFC in ASD as compared to typically developing controls among prefrontal regions and within the salience network. Measures of vDFC were significantly correlated with measures of social functioning among all subjects. This work is significant as it suggests increased neural noise and disorganization in ASD.

2251

Characteristics of Cortical and Subcortical Abnormalities in Pediatric Attention Deficit Hyperactivity Disorder patients

Lu Lu[1], Lianqing Zhang[1], Xuan Bu[1], Hailong Li[1], Xiaoxiao Hu[1], Ying Chen[1], Xinyu Hu[1], Lanting Guo[2], Qiyong Gong [1], and Xiaoqi Huang[1]

[1]Huaxi MR Research Center (HMRRC), Department of Radiology, West China Hospital of Sichuan University, Chengdu, People's Republic of China, [2]Department of Psychiatry, West China Hospital of Sichuan University

The current study combine the analysis of the cortical measures and subcortical structures' volume to evaluate the cerebral structure alterations in a relative large drug-naive ADHD sample. In addition, we also invest the anatomical–age correlation between two groups. Our findings (i) highlighted the crucial role of the frontostriatal circuits in the pathophysiology of ADHD, (ii) indicated the abnormality in neural development trajectory in ADHD.

2252

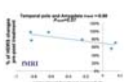

Pretreatment PET and MRI imaging markers of lithium treatment response/nonresponse in patients with bipolar depression

Chuan Huang[1,2,3], Karl Spuhler[3], Mala Ananth[4], Elizabeth Bartlett[3], Jie Ding[3], Xiang He[2], Christine DeLorenzo[1,3], and Ramin Parsey[1]

[1]Psychiatry, Stony Brook Medicine, Stony Brook, NY, United States, [2]Radiology, Stony Brook Medicine, Stony Brook, NY, United States, [3]Biomedical Engineering, Stony Brook University, Stony Brook, NY, United States, [4]Neurobiology & Behavior, Stony Brook University, Stony Brook, NY, United States

Bipolar disorder is one of the most prevalent psychiatric diseases in developed countries, and virtually all major psychiatric associations recommend lithium as the first line therapy for bipolar patients in the depressive phase of the illness, despite relatively low response rate for the drug and relatively high likelihood of side effects. However, no predictive criteria which indicate an individual patient's responsiveness to lithium are employed clinically. In this work, we present preliminary findings demonstrating an association between baseline, multimodal neuroimaging measurements and lithium treatment outcome.

2253

Association between Major Depressive Disorder and the Functional Val158Met Polymorphism in Catechol-O-Methyltransferase as Assessed by Diffusion MRI

Chuan Huang[1,2,3], Karl Spuhler[3], Christine DeLorenzo[1,3], and Ramin Parsey[1]

[1]Psychiatry, Stony Brook Medicine, Stony Brook, NY, United States, [2]Radiology, Stony Brook Medicine, Stony Brook, NY, United States, [3]Biomedical Engineering, Stony Brook University, Stony Brook, NY, United States

Major Depressive Disorder is a debilitating illness that impacts 1 in 6 people in the United States during their lifetime. Particularly when monoamine levels are low, depression is associated with reduced volume in the front-limbic-striatum emotional processing network. Catechol-O-Methyltransferase (COMT) is responsible for most dopamine degradation in the frontal cortex. Guided by past literature, we examined the effect of COMT genotype on white matter integrity in the amygdala, hippocampus and parahippocampus in depressed patients along with healthy controls. Our results suggest the existence of sex-genotype interaction which is clinically relevant for women suffering from depression.

2254

Structural alterations in major depressive disorder and bipolar disorder-I: A meta-analysis of voxel-based morphometry study

Qiang Luo[1], Ziqi Chen[1], Xinyu Hu[1], Xiaoqi Huang[1], and Qiyong Gong[1]

[1]Huaxi MR Research Center (HMRRC), Chengdu, People's Republic of China

We used the SDM software to detect the similarities and differences of gray matter (GM) volume between MDD and BD, and found the significant decreases of GM in the bilateral insula and left inferior frontal gyrus (LIFG) characterized both MDD and BD-I, which may be related with the clinical symptoms including using few words and exhibiting poor choices of conversation topics during depressive state in both two affective disorders. AND the MDD patients had significantly lower GM volumes in the right superior temporal gyrus and right amygdala in comparison with BD-I patients, which indicated that reduced GM volume in the right angular gyrus specifically characterizes BD-I which may contribute to the manic symptom.

2255

It's all about the money: fMRI Reward Anticipation in Prodromal Psychotic Disorder.

Stijn Michielse[1], Jim van Os[1,2], and Machteld Marcelis[1,3]

[1]Psychiatrie & Psychologie, Maastricht University, Maastricht, Netherlands, [2]Department of Psychosis Studies, King's College London, King's Health Partners, London, United Kingdom, [3]Institute for Mental Health Care, Eindhoven, Netherlands

N/A

2256

Relationship Between DTI of the Brainstem Auditory Pathway and Latency of the Auditory M100 Response is Altered in Autism Spectrum Disorder

Jeffrey I Berman[1,2], J Christopher Edgar[1,2], Lisa Blaskey[1], Emily S Kuschner[1], and Timothy PL Roberts[1,2]

[1]Radiology, Children's Hospital of Philadelphia, Philadelphia, PA, United States, [2]Radiology, University of Pennsylvania, Philadelphia, PA, United States

Alterations to the auditory system's structure and function may underlie the auditory processing and language disorders prevalent in autism spectrum disorder (ASD). This multimodal study compared DTI of the brainstem auditory pathway to magnetoencephalography (MEG) measures of auditory conduction velocity (M100 latency). The M100 latency measures the time between auditory stimulus and auditory cortex response. DTI and MEG were acquired from 29 children with ASD and 31 controls. Increased brainstem auditory pathway FA was predictive of faster signal conduction in controls (shorter M100 latency) ($p<0.01$), but not ASD. These results indicate ASD impacts the structure-function relationships throughout the auditory system.

2257

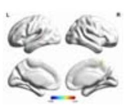

A study on the alteration of gray matter structure and the abnormality of iron metabolism in the post traumatic stress disorder

Tao Hai Li[1] and ming zhao[1]

[1]radiology department, the Southwest Hospital of Third Military Medical University, chongqing, People's Republic of China

By using the VBM method，We found Neuronal damage may occurred in the early stage of the PTSD patients and dysfunction in orbitofrontal cortex, insula cortex which involving in the limbic system, and the precuneus involving in the DMN might play a critical role in pathophysiology of PTSD. By using the SPS rat model to mimic the PTSD disease, we also found iron accumulation in the prefrontal cortex, striatum, hippocampus in the SPS rat model. This study indicated that iron may be involved in the pathology of PTSD, and could be nominated as a novel molecule involved in the pathology of PTSD and provide a potential target for therapeutic intervention of PTSD.

2258

Gulf War Illness Patients Exhibit Impaired Connectivity in Multiple Brain Function Networks Consistent with Chronic Multi-Symptom Illness: A Resting State fMRI Study

Kaundinya Gopinath[1], Binod Thapa-Chetry[2], Lou Ouyang[2], Lisa Krishnamurthy[2], Venkatagiri Krishnamurthy[1], Aman Goyal[2], Parina Gandhi[2], Yan Fang[2], Unal Sakoglu[3], and Robert Haley[2]

[1]Department of Radiology & Imaging Sciences, Emory University, Atlanta, GA, United States, [2]University of Texas Southwestern Medical Center, Dallas, TX, United States, [3]University of Houston Clear-Lake, Houston, TX, United States

Around 200,000 veterans (up to 32% of those deployed) of the 1991 Gulf War (GW) suffer from GW illness (GWI), which is characterized by multiple deficits in cognitive, emotion, somatosensory and pain domains. In this study we examined 22 GWI patients and 30 age-matched controls with resting state fMRI (rsFMRI) in order to map impairments in brain function networks in GWI with graph theory based advanced network analysis methods. Results show widespread impairments in functional connectivity of cognition, affective, somatosensory and pain processing brain function networks in GWI consistent with multi-symptom nature of the illness.

Traditional Poster

Visual System

Exhibition Hall 2259-2278 | Wednesday 13:45 - 15:45

2259

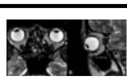

Quantitative analysis of shape of eyes with high myopia by high-resolution three-dimensional magnetic resonance imaging

Baohong Wen[1], Dandan Zheng[2], Ge Yang[3], Tianyong Xu[2], and Jingliang Cheng[1]

[1]Department of MRI, The First Affiliated Hospital of Zhengzhou University, Zhengzhou, People's Republic of China, [2]MR Research China, GE Healthcare, Beijing, People's Republic of China, [3]Department of Ophthalmology, The First Affiliated Hospital of Zhengzhou University, Zhengzhou, People's Republic of China

Myopia is a major cause of blindness worldwide. 134 patients with high myopia and 120 emmetropic volunteers were examined. All of the participants were scanned by high resolution 3D T2-weighted CUBE MRI sequence. This study is to evaluate the preoperative localization and postoperative assessment value of high-resolution 3D MRI for high myopia. It is shown that the axial length, horizontal length, vertical length and volume of the high myopia were significantly longer than those of the emmetropia. And high resolution 3D MRI could clearly demonstrate the position of staphylomas, superior rectus, inferior rectus, medial rectus, lateral rectus and optic nerve.

2260

High spatial resolution MRI-based three dimensional pathologic myopia eyes: a first step towards image-guided posterior sclera reinforcement

Baohong Wen[1], Ge Yang[2], Dandan Zheng[3], Tianyong Xu[3], and Jingliang Cheng[1]

[1]Department of MRI, The First Affiliated Hospital of Zhengzhou University, Zhengzhou, People's Republic of China, [2]Department of Ophthalmology, The First Affiliated Hospital of Zhengzhou University, Zhengzhou, People's Republic of China, [3]MR Research China, GE Healthcare, Beijing, People's Republic of China

Eyes of 66 high myopia patients who were to undergo posterior scleral reinforcement surgery (PSR) were examined by high-resolution three dimension cube magnetic resonance imaging. It is demonstrated that 3D MRI technique is helpful to PSR preoperative localization by comparing the precision rate of buckling strips position in groups with and without 3D MRI-guided. The present study demonstrates that it is possible to not only check the eyeball shape of the pathologic myopia patients accurately, but also assistant the PSR surgery by using 3D MRI technique.

2261

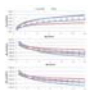

Characterizing the Effect of Age on Measures of White Matter Integrity in the Optic Radiations of Children with and without Neurofibromatosis Type 1

Peter M K de Blank[1], Michael J Fisher[2], Marisa Prelack[3], Amy Waldman[3], and Jeffrey I Berman[4]

[1]Pediatrics, University Hospitals Rainbow Babies & Children, Cleveland, OH, United States, [2]Pediatrics, The Children's Hospital of Philadelphia, [3]Pediatric Neurology, The Children's Hospital of Philadelphia, [4]Radiology, The Children's Hospital of Philadelphia

DTI measures in the optic radiations are a promising biomarker of vision in children with optic pathway gliomas, but normal values for fractional anisotropy (FA), radial diffusivity (RD), and mean diffusivity (MD) in young children have not been defined. In 40 children with neurofibromatosis type I (NF1) and 55 healthy control children between 0-14 years of age, we measured FA, RD and MD in the optic radiations. This study represents the first investigation of normal DTI measures in the optic radiations in young children and demonstrates an altered developmental trajectory in the optic radiations of children with NF1.

2262

Multi-parametric magnetic resonance imaging for differentiating benign from malignant orbital lymphoproliferative disorders

Xiao-Quan Xu[1] and Fei-Yun Wu[1]

[1]Radiology, The First Aaffiliated Hospitla of Nanjing Medical University, Nanjing, People's Republic of China

We applied multi-parametric magnetic resonance (MR) imaging techniques, including conventional MR, diffusion weighted imaging (DWI) and dynamic contrast enhance MR imaging (DCE-MRI) in the evaluation of orbital lymphoproliferative disorders (OLPDs).These three imaging techniques evaluated the morphologic, diffusion and perfusion characteristic,respectively. We aim to determine the optimal combination of parameters derived from 3T multi-parametric MR imaging for differentiating malignant from benign OLPDs.

2263

Improved 2D navigated multishot DTI of the optic nerve with triggered eye fixation.

Saikat Sengupta[1,2], Alex Smith[2,3], Samantha By[2,3], Ha-Kyu Jeong[4], and Seth Smith[1,2]

[1]Department of Radiology, Vanderbilt University Medical Center, Nashville, TN, United States, [2]Vanderbilt University Institute of Imaging Science, [3]Department of Biomedical Engineering, Vanderbilt University, Nashville, TN, United States, [4]Philips Electronics, Korea, Republic of

Optic Nerve DTI is of high interest in pathologies of the anterior visual pathway but high quality high-resolution diffusion MRI in the optic nerve is challenging because of involuntary eye motion. Vulnerability to motion induced phase errors is increased when multishot EPI (mshEPI) is used for achieving high imaging resolutions. In this abstract we present a triggered diffusion MRI approach with eye fixation that can significantly improve quality of optic nerve DTI, especially with mshEPI.

2264

magna cum laude

Role of visual cortex during after and before critical developmental period in early blind and late blind: An fMRI study

A Ankeeta[1], Senthil Kumaran[1], and Rohit Saxena[2]

[1]Department of NMR and MRI Facility, All India Institute of Medical Sciences, New Delhi, India, [2]Dr. RP Centre for Ophthalmic Sciences, All India Institute of Medical Sciences, New Delhi, India

Visual cortex is preserved and is performing during non-visual stimuli showing development of specific compensatory mechanisms associated with visual area in blind subjects. Blind people process auditory language stimuli faster than sighted people. Some language functions suggest cortical reorganization in the blind subjects.

2265

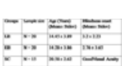

A tract-based diffusion analysis in early and late blind subjects in the optic nerve and optic radiation

A Ankeeta[1], Senthil Kumaran[1], and Rohit Saxena[2]

[1]Department of NMR and MRI Facility, All India Institute of Medical Sciences, New Delhi, India, [2]Dr. RP Centre for Ophthalmic Sciences, All India Institute of Medical Sciences, New Delhi, India

Tractography Based Spatial statistics was carried out on the DTI and T1 data acquired in 20 late blind, 20 early blind and 15 healthy controls at 3 T. Early blind showed more white matter impairments as compared to the late blind suggesting plasticity in the early blind than in the late blind. The cross modal plastic changes in the late blind were not as significant as those in the early blind subjects, supporting the conception of prospective plasticity of brain may decrease with onset of age of blindness.

2266

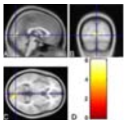

Morphometric Analyses of Visual Cortex in Patients with Retinitis Pigmentosa

Yanqiu Zhang[1], Dapeng Shi[1], Xirang Guo[2], Meiyun Wang[1], Xiaona Xu[1], Cuihua Zhao[1], and Dandan Zheng[3]

[1]Radiology, Zhengzhou University People's Hospital (Henan Provincial People's Hospital), Zhengzhou, People's Republic of China, [2]Ophthalmology, Zhengzhou University People's Hospital (Henan Provincial People's Hospital), Zhengzhou, People's Republic of China, [3]GE Healthcare MR Research China, People's Republic of China

Possible effects on the structures of visual cortex using high-resolution anatomical MRI have not been established so far. The aim of this study was to investigate volumetric alterations in visual cortex of RP patients using voxel based morphometry (VBM). Our results demonstrated that RP is associated with degeneration of structures in the visual cortex, and prevention of visual cortical degeneration may need to become a new therapeutic goal for RP patients, which may have significant meaning for clinical to guide RP patients' treatment in a more reasonable way in future.

2267

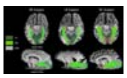

How does blindness onset impact on the structure of the optic radiation?

Chiara Maffei[1], Isabella Giachetti[1], Stefania Mattioni[1,2], Ceren Battal[1], Mohamed Rezk[1,2], Olivier Collignon[1,2], and Jorge Jovicich[1]

[1]CIMeC Center for Mind/Brain Sciences, Trento University, Trento, Italy, [2]Institute of Psychology (IPSY) and of Neurosciences (IoNS); University of Louvain-la-Neuve; Belgium

The human brain is capable of massive reorganization in case of sensory deprivation. Blind studies show white and gray matter changes depending on blindness onset. However, the anatomical reorganization of the optical tract in blind is largely unknown. We investigated the changes in the optic radiation tract using diffusion-based tractography techniques in early and late blind subjects compared to age- and gender-matched healthy sighted controls. We found activity-dependent alterations of the optical radiation, demonstrating the importance of visual experience for the integrity of the tract. The characterization of such reorganization processes may have clinical value when assessing sight restoration possibilities.

2268

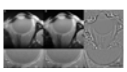

Ultra-high spatial resolution imaging in vivo of human retina at 3T

Yongsheng Chen[1,2], Yang Song[3], Jiani Hu[2], Yongquan Ye[2], Yu Wang[3], Ying Wang[4], Bruce A. Berkowitz[5,6], Yan kang[1], Guang Yang[3], and E. Mark Haacke[1,2,3,4,7]

[1]Sino-Dutch Biomedical and Information Engineering School, Northeastern University, Shenyang, People's Republic of China, [2]Department of Radiology, Wayne State University, Detroit, MI, United States, [3]Shanghai Key Laboratory of Magnetic Resonance, East China Normal University, Shanghai, People's Republic of China, [4]Department of Biomedical Engineering, Wayne State University, Detroit, MI, United States, [5]Department of Anatomy and Cell Biology, Wayne State University, Detroit, MI, United States, [6]Department of Ophthalmology, Wayne State University, Detroit, MI, United States, [7]The MRI Institute for Biomedical Research, Detroit, United States

Imaging in vivo human retina remains a considerable challenge due to the thinness of the retina and eye motion. Here we provide proof-of-concept data supporting the use of an asymmetric gradient echo scan with TE to 5 ms and an effective resolution of 37 μm in the readout direction after partial Fourier reconstruction. To reduce motion, we employed a cued-blinking strategy and collected the data multiple times and averaged data that after co-registration. Preliminary results showed retina/choroid layer clearly with sufficient SNR to obtain a transretinal T1 map from vitreous body to sclera.

2269

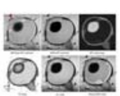

Age-related MRI changes in the connective tissues of the eye

Yolandi van der Merwe[1,2], John S. Gnalian[3], Ning-Jiun Jan[1,2], Ian A. Sigal[1,2], and Kevin C. Chan[1,2,3]

[1]Department of Ophthalmology, University of Pittsburgh, Pittsburgh, PA, United States, [2]Department of Bioengineering, University of Pittsburgh, Pittsburgh, PA, United States, [3]Neuroimaging Laboratory, University of Pittsburgh, Pittsburgh, PA, United States

The structural organization and compositions of the corneoscleral shell determine the biomechanical behavior of the eye, and are important in aging and diseases such as glaucoma and myopia. However, characterizing the structure and composition of the eye and their changes with age or intraocular pressure remains a challenge. In this study, we showed that T2 mapping, magnetization transfer MRI and diffusion tensor MRI can be used to detect and differentiate age- and intraocular pressure-related changes in the porcine eyes. Multi-modal MRI may be useful for evaluating the biomechanical and (patho-)physiological mechanisms in the corneoscleral shell non-invasively and quantitatively.

2270

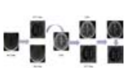

Permeability of the Blood-brain Barrier may Differentiate Neuromyelitis Optica Spectrum Disorder from Multiple Sclerosis

Xiaoxiao Ma[1], Jinhao Lyu[1], Bing Wu[2], Jun Yang[3], Deihui Huang[4], Lin Ma[1], and Xin Lou[1]

[1]Department of Radiology, Chinese PLA General Hospital, Beijing, People's Republic of China, [2]GE healthcare China, Beijing, Beijing, People's Republic of China, [3]GE healthcare China, Shanghai, Shanghai, People's Republic of China, [4]Department of Neurology, Chinese PLA General Hospital, Beijing, People's Republic of China

The aim of our study was to characterize blood-brain barrier (BBB) permeability in neuromyelitis optica spectrum disorder (NMOSD) and multiple sclerosis (MS) using dynamic contrast-enhanced MRI (DCE-MRI). Twenty-two NMOSD patients and twenty-three MS patients were enrolled. Significantly higher BBB permeability were found in lesions and normal appearing grey matter in MS group when compared with NMOSD but no differences were observed in corpus callosum. Hence BBB permeability, measured by DCE-MRI may be used for differential diagnosis between NMOSD and MS and may provide novel insights into the underlying pathological differences.

2271

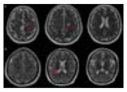

Radiomics Features Extracted from MRI as Biomarkers for Neuromyelitis Optica Spectrum Disorder and Multiple Sclerosis Differentiation

Xiaoxiao Ma[1], Mengjie Fang[2], Jun Yang[3], Jinhao Lyu[1], Xin Li[3], Deihui Huang[4], Di Dong[2], Lin Ma[1], and Xin Lou[1]

[1]Department of Radiology, Chinese PLA General Hospital, Beijing, People's Republic of China, [2]Chinese Academy of Sciences, Beijing, People's Republic of China, [3]GE healthcare, Shanghai, People's Republic of China, [4]Department of Neurology, Chinese PLA General Hospital, Beijing, People's Republic of China

The aim of our study was to ultilize combined radiomcis features extracted from T2-weighted MRI images as quantitative imaging biomarkers to differentiate neuromyelitis optica spectrum disorder (NMOSD) and multiple sclerosis (MS). Twenty-nine NMOSD patients and forty-five MS patients were enrolled. Our study showed 61 radiomics features and 8-feature-based radiomics signature were significantly different between NMOSD and MS. Therefore, radiomics may be an newly useful method which provides a promising non-invasive way of differentiating NMOSD and MS.

2272

The Role of the Human Visual Cortex in Assessment of the Long-term Durability of Retinal Gene Therapy in Follow-on RPE65 Clinical Trial Patients

Manzar Ashtari[1,2,3], Elena Nikonova[4], Kathleen A. Marshall[5], Gloria J. Young[1], Puya Aravand[1], Wei Pan[6], Gui-shuang Ying[6], Aimee E. Willett[1], Mani Mahmoudian[1], Albert M. Maguire[1,2,5], and Jean Bennett[1,2,5]

[1]Center for Advanced Retinal and Ocular Therapeutics (CAROT), University of Pennsylvania, Philadelphia, PA, United States, [2]F.M. Kirby Center for Molecular Ophthalmology, Scheie Eye Institute, University of Pennsylvania, Philadelphia, PA, United States, [3]Department of Radiology, University of Pennsylvania, Philadelphia, PA, United States, [4]University of Pittsburgh, Pittsburgh, PA, United States, [5]Center for Cellular and Molecular Therapeutics, The Children's Hospital of Philadelphia, Philadelphia, PA, United States, [6]Westat Biostatistics and Data Management Core, University of Pennsylvania, Philadelphia, PA, United States

Leber's congenital amaurosis (LCA) is a rare blinding disease with no cure. Recently, patients with LCA underwent retinal gene therapy and regained their vision to a great extent. We followed this group of LCA patients before and up to three years on an annual basis after gene therapy using fMRI to assess the feasibility and durability of retinal gene therapy over time and the role fMRI could play as an outcome measure for other future retinal interventions.

2273

The fate of auditory-visual cross modal plasticity after vision restoration through retinal gene therapy: Does auditory activity leave the visual cortex once vision returns?

Aimee E. Willett[1], Mani Mahmoudian [1], Gloria J. Young[1], Albert M. Maguire[2,3], Jean Bennett[1,2,3], and Manzar Ashtari[1,2,4]

[1]Center for Advanced Retinal and Ocular Therapeutics (CAROT), University of Pennsylvania, Philadelphia, PA, United States, [2]F.M. Kirby Center for Molecular Ophthalmology, University of Pennsylvania, Philadelphia, PA, United States, [3]Center for Cellular and Molecular Therapeutics, The Children's Hospital of Philadelphia, Philadelphia, PA, United States, [4]Department of Radiology, University of Pennsylvania, Philadelphia, PA, United States

Visual deprivation causes auditory-driven activity of occipital areas due to a process named auditory-visual cross modal plasticity. The present study explores the impact of visual restoration on this cross modal phenomenon and employs functional magnetic resonance imaging (fMRI) to describe changes in auditory task stimulation of the visual cortex after visual ability improvement in a population of eight Leber's Congenital Amaurosis (LCA) patients. Results show the persistence of auditory-visual cross modal connectivity up to three years after gene therapy administration and reveal strong positive trends between visual ability after treatment and cross modal maintenance.

2274

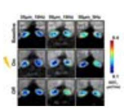

Diffusion fMRI of mouse optic nerve with antidromic electrical stimulation

Tsen-Hsuan (Abby) Lin[1], Willaim M Spees[1,2], Michael Wallendorf[3], Yen-Yu Ian Shih[4], Anne H Cross[2,5], and Sheng-Kwei Song[1,2,6]

[1]Radiology, Washington University School of Medicine, St. Louis, MO, United States, [2]The Hope Center for Neurological Disorders, Washington University School of Medicine, St. Louis, MO, United States, [3]Biostatistics, Washington University School of Medicine, St. Louis, MO, United States, [4]Neurology, The University of North Carolina in Chapel Hill, NC, United States, [5]Neurology, Washington University School of Medicine, St. Louis, MO, United States, [6]Biomedical Engineering, Washington University in St. Louis, St. Louis, MO, United States

Previously, we have successfully employed diffusion fMRI (dfMRI) to assess impaired axonal function in experimental autoimmune encephalomyelitis (EAE) mice undergoing visual stimulation. However, the prior dfMRI experiments cannot resolve contributions from retinal dysfunction to the decreased dfMRI changes observed in EAE mice. To address this shortcoming, we implanted an MR-compatible tungsten electrode at lateral geniculate nucleus (LGN) to perform antidromic stimulation of optic nerves. We demonstrated perpendicular apparent diffusion coefficient decreased with antidromic electrical stimulation at LGN bypassing visual input through retina.

2275

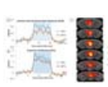

fMRI of Visual Stimuli in a Tau Model of Alzheimer's Disease

Payam Nahavandi[1], Arun Niranjan[1], Yolanda Ohene[1], Ian F Harrison[1], Ozama Ismail[1], Tracey K Murray[2], Ross A Johnson[3], Michael J O'neill[2], Emily C Collins[3], Jack A Wells[1], and Mark F Lythgoe[1]

[1]University College London, London, United Kingdom, [2]Eli Lilly and Company, Windlesham, United Kingdom, [3]Eli Lilly and Company, Indianapolis, IN, United States

There is a need for non-invasive biomarkers that enable accurate tracking of early, pre-symptomatic phases of Alzheimer's disease (AD). Previous fMRI studies have differentiated AD patients from healthy controls. However, it is unknown whether the accumulation of tau or amyloid pathology is driving the fMRI irregularity. This is the first study to investigate whether tau pathology alone can modulate task-based BOLD fMRI. We observed stronger BOLD responses to visual stimulation in lateral geniculate nucleus and superior colliculus in the tau cohort, mirroring observations in mild AD and MCI patients.

2276

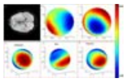

Functionally Informed Fiber Tracking Using Combination of Diffusion and Functional MRI

Zhipeng Yang[1,2], Jiliu Zhou[1], John C. Gore[2,3,4], Zhaohua Ding[2,3,5], and Xi Wu[1,2]

[1]Department of Computer Science, Chengdu University of Information Technology, Chengdu, People's Republic of China, [2]Vanderbilt University Institute of Imaging Science, Nashville, TN, United States, [3]Biomedical Engineering, Vanderbilt University, Nashville, TN, United States, [4]Radiology and Radiological Sciences, Vanderbilt University, Nashville, TN, United States, [5]Electrical Engineering and Computer Science, Vanderbilt University, Nashville, TN, United States

While fiber tractography using diffusion weighted MRI is a primary method that has achieved great success during the past decade, it however suffers from a number of inherent limitations. On the basis of the concept of a spatio-temporal correlation tensor we have introduced previously as a descriptor of the functional architecture in white matter, we propose in this study a novel algorithm for tractography by combing diffusion and functional MRI. Our experimental results show clear improvement of tractography accuracy for fiber tracts in the visual circuit, which demonstrates a great potential for reconstructing functional structure in brain whiter matter.

2277

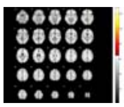

Study of functional connectivity of default mode network and frontoparietal network in neuromyelitis optica

Han Yongliang[1], Li Yongmei[1], LUO Qi[1], ZENG Chun[1], WANG Jingjie[1], DU Silin[1], ZHANG Xiaohui[1], and GUO Youyou[1]

[1]Department of Radiology, the First Affiliated Hospital of Chongqing Medical University, Chongqing, People's Republic of China

Neuromyelitis optica (NMO) is an inflammatory, demyelinating syndrome of the central nervous system characterized by severe attacks of optic neuritis and myelitis, but investigators in several studies observed abnormalities in deep gray matter. Functional MRI (fMRI) has the potential to further understanding of the neuropathologic mechanisms of NMO. In the present study, our aim was to investigate patients with NMO-related alterations of brain functional connectivity(FC) in resting state in default mode network (DMN) and frontoparietal network(FPN) using independent component analysis(ICA) and their correlations with clinical features.

2278

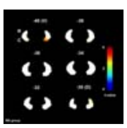

Reorganisation of cerebellar and dentate nucleus activity in multiple sclerosis subjects performing a complex visuomotor task: An event-related fMRI study

Adnan A.S. Alahmadi[1,2], Rebecca S. Samson[1], Matteo Pardini[1,3], Egidio D'Angelo[4,5], Karl J. Friston[6], Ahmed T. Toosy[1], and Claudia AM Gandini Wheeler-Kingshott[1,4,7]

[1]UCL Institute of Neurology, Queen Square MS Centre, University College London, London, United Kingdom, [2]Department of Diagnostic Radiology, Faculty of Applied Medical Science, KAU, Jeddah, Saudi Arabia, [3]Department of Neurosciences, Rehabilitation, Ophthalmology, Genetics and Maternal and Child Health, University of Genoa, Genoa, Italy, [4]Department of Brain and Behavioural Sciences, University of Pavia, Pavia, Italy, [5]Brain Connectivity Centre, C. Mondino National Neurological Institute, Pavia, Italy, [6]Wellcome Centre for Imaging Neuroscience, University College London, London, United Kingdom, [7]Brain MRI 3T Mondino Research Center, C. Mondino National Neurological Institute, Pavia, Italy

This study investigates the response to different grip force levels in the cerebellum and its dentate nucleus in MS. We found that cerebellar responses were functionally parcellated; with linear effects in the anterior cerebellum and complex nonlinear responses in the posterior cerebellum. This behaviour is consistent with healthy subjects (nonlinear responses in bilateral lobules V-VI and ipsilateral VIII), although MS subjects additionally show a strong linear response in lobule I-IV and nonlinear responses primarily localised in lobules V-VI. In the dentate nucleus, the motor portion in MS was silent as compared to the healthy subjects.

Traditional Poster

Fetal & Pediatric Neuroimaging

Exhibition Hall 2279-2309 Wednesday 13:45 - 15:45

2279

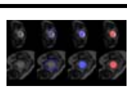

Fast and Robust Detection of Fetal Brain in MRI using Transfer Learning based FCN

DEFENG WANG[1,2], Jinpeng Li[2], YISHAN LUO[2,3], DANTONG MIAO[4], XIN ZHANG[4], Queenie Chan[5], Winnie CW CHU[2], LIN SHI[6,7,8], and BING ZHANG[4]

[1]Shenzhen Research Institute, The Chinese University of Hong Kong, Shenzhen, People's Republic of China, [2]Department of Imaging and Interventional Radiology, The Chinese University of Hong Kong, Hong Kong, Hong Kong, [3]Shenzhen Research Institute,The Chinese University of Hong Kong, Shenzhen, People's Republic of China, [4]Department of Radiology, Nanjing Drum Tower Hospital,The Affiliated Hospital of Nanjing University Medical School, Nanjing, People's Republic of China, [5]Philips Healthcare, Hong Kong, [6]Chow Yuk Ho Technology Center for Innovative Medicine, Hong Kong, [7]Therese Pei Fong Chow Research Centre for Prevention of Dementia, [8]Department of Medicine and Therapeutics, The Chinese University of Hong Kong, Hong Kong

In this work, we proposed a transfer learning based FCN method which can automatically detect the fetal brain in MRI. We used the off-the-shelf model weights trained on nature images to initialize a fully connected network (FCN), and then fine-tuned the model on the fetal MRIs. We tested our method on two datasets with different MRI sequences, and the results demonstrated that the proposed method is automatic, fast and robust for detection of fetal brain in MRI.

2280

Prenatal Maternal Depression and Anxiety Alter Hippocampal Development in Fetuses

Yao Wu[1], Diane Lanham, Samantha Bauer, Gilbert Vezina, and Catherine Limperopoulos

[1]The Developing Brain Research Laboratory, Children's National Health System, Washington, DC, United States

The hippocampus plays an important role in stress regulation. This study aims to investigate the relationship between prenatal maternal stress and fetal hippocampal volumetric growth using magnetic resonance imaging (MRI). Results suggest that maternal depression and anxiety are associated with smaller left hippocampal volumes in female fetuses in the third trimester of pregnancy.

2281

A pilot study of lateral ventricle volume from in utero foetal brain magnetic resonance imaging (MRI)

Dadi Zhao[1,2], Dantong Miao[3,4], Rui Shen[2], Feng Wang[5], Bing Zhu[4], Yu Sun[5,6], and Bing Zhang[4]

[1]State Key Laboratory of Bioelectronics, Southeast University, Nanjing, People's Republic of China, [2]School of Biological Science and Medical Engineering, Southeast University, Nanjing, People's Republic of China, [3]The First School of Clinical Medicine, Nanjing Medical University, Nanjing, People's Republic of China, [4]Department of Radiology, Drum Tower Hospital of Nanjing University Medical School, Nanjing, People's Republic of China, [5]Southeast University - Jiangsu Institute of Biomaterials and Medical Devices, Nanjing, People's Republic of China, [6]Institute of Cancer and Genomic Science, University of Birmingham, United Kingdom

Neuroimaging for foetus brain is a challenging problem in which there are several issues to be solved. We proposed a general solution and finally reconstruct the lateral ventricle volume that is of great significance for clinical study. Firstly, slices were realigned to correct for the motion between acquisition of individual slices including transposition and rotation. Secondly, slices with motion artefacts were excluded and inconsistencies in intensity patterns resulting from the motion were estimated and corrected for. Thirdly, the structure of lateral ventricle was segmented via adaptive segmentation. Finally, the volume was reconstructed from irregularly sampled data.

2282

Correlation of fetal MRI with neurodevelopmental outcome in fetuses with ventriculomegaly

Xin Mu[1], Hosung Kim[1], Duan Xu[1], and Orit Glenn[1]

[1]Department of Radiology and Biomedical Imaging, University of California San Francisco, SAN FRANCISCO, CA, United States

Ventriculomegaly (VM) is the most common referred abnormality for fetal MRI and may be isolated or associated with additional abnormalities. We performed MR exams in 46 fetus diagnosed with isolated VM on ultrasound (US) and assessed neurodevelopmental outcome at 12 and 30 months with Bayley-III. Ventricle size (VS) measured by US and MRI and Bayley-III scores were analyzed using linear models. VS measured at older gestational age and longitudinal VS changes on MRI predicted outcome better than at younger age and on US. The presence of additional brain findings on fetal MRI significantly correlated with outcome and improved outcome predictability.

2283

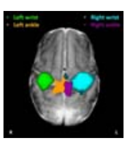

Precise mapping of the developing somatosensory homunculus in the preterm human brain with fMRI and robotic tools

Sofia Dall'Orso[1], Johannes Steinweg[2], Alessandro G Allievi [1], David A Edwards[1,2], Etienne Burdet[1], and Tomoki Arichi[1,2]

[1]Bioengineering, Imperial College London, London, United Kingdom, [2]Centre for the Developing Brain, Kings College London, London, United Kingdom

The mature somatosensory cortex is known to be somatotopically organized, but it is not known when this functional organization emerges in human life. We aimed to map functional responses across the somatosensory cortex of preterm infants using fMRI and automated robotic tools. A preterm "homunculus" topology was identified with a spatially distinct distribution of functional responses following somatosensory stimulation delivered to the mouth, wrists and ankles. The results suggest that as seen in animal studies, the human preterm period is likely to be critical for the development of the somatosensory system.

2284

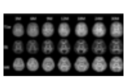

Heterogeneous increases of cortical mean kurtosis across brain regions during infancy

Huiying Kang[1,2,3], Qinmu Peng[2,3], Minhui Ouyang[2], Xiaolu Tang[1], Di Hu[1], Hong Zhang[1], Yun Peng[1], and Hao Huang[2,3]

[1]Department of Radiology, Beijing Children's Hospital, Capital Medical University, Beijing, People's Republic of China, [2]Department of Radiology, Children's Hospital of Philadelphia, Philadelphia, PA, United States, [3]Department of Radiology, Perelman School of Medicine, University of Pennsylvania, Philadelphia, PA, United States

Brain development in the first few years of life is dramatic. The microstructural changes of infant grey matter measured by mean kurtosis, a non-Gaussian diffusion metric more sensitive to cortical microstructure than traditional diffusion metric, is not known. This study recruited 16 typical developing 3-32-months-old infants to investigate microstructural changes of the cerebral cortex by using Diffusion Kurtosis Imaging (DKI). Our results showed positive correlation between the mean kurtosis (MK) value and age. Differentiated age-dependent MK increases among different cortical regions suggest spatiotemporally heterogeneous pattern in cortical development.

2285

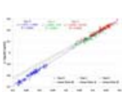

Relationship between Surface Area, Cortical Thickness and Folding in Infants

Gang Li[1], Li Wang[1], Weili Lin[1], John H Gilmore[2], and Dinggang Shen[1]

[1]Department of Radiology and BRIC, University of North Carolina at Chapel Hill, Chapel Hill, NC, United States, [2]Department of Psychiatry, University of North Carolina at Chapel Hill, Chapel Hill, NC, United States

An intrinsic relationship between surface area, cortical thickness and folding was found in adult mammalian brains across species, which was thought to relate to the mechanism of cortical folding. However, this relationship remains unclear in the dynamic developing human infant brains. To fill this gap, we jointly analyze surface area, cortical thickness and folding at birth, 1, and 2 years of age, using 219 longitudinal MRI scans from 73 infants. We reveal that the relationship between these cortical properties is gender-independent, but age-specific, with a substantial change in the first year and a subtle change in the second year.

2286

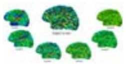

Spherical Wavelets based Study of Multi-scale Cortical Folding in Infants

Dingna Duan[1,2], Islem Rekik[1], Shunren Xia[2], Weili Lin[1], John H Gilmore[3], Dinggang Shen[1], and Gang Li[1]

[1]Department of Radiology and BRIC, University of North Carolina at Chapel Hill, Chapel Hill, NC, United States, [2]College of Biomedical Engineering & Instrument Science, Zhejiang University, Hangzhou, People's Republic of China, [3]Department of Psychiatry, University of North Carolina at Chapel Hill, Chapel Hill, NC, United States

Examining cortical folding development at various scales may help better understand brain cognition and motor functions. We propose a curvature-based multi-scale method using spherical wavelets to study the longitudinal changes of cortical folding during infancy. We applied our method on 219 longitudinal MR images from 73 healthy infants at 0, 1, and 2 years of age. We reveal scale-specific and region-specific developmental patterns of infant cortical folding. Specifically, at coarser levels, many primary folds flatten out; while at finer levels, the majority of the minor folds become more convoluted, providing new insights into early brain development.

2287

Lipid fractions as a marker for myelin maturation in the developing brain

Benyamin Deldar[1], Emer Hughes[1], Nora Tusor[1], Serena Counsell[1], A. David Edwards[1], and J-Donald Tournier[1]

[1]Centre for the Developing Brain, Division of Imaging Sciences and Biomedical Engineering, King's College London, London, United Kingdom

Myelination is an important aspect of brain development, but current myelin mapping techniques require extensive acquisition times and are therefore difficult to use routinely in neonates. In this study, we present results from a large cohort of neonates born preterm spanning a wide age range (26 to 125 weeks' post-menstrual age) obtained using a recently proposed method that relies on existing routine data. Our results show good agreement with the expected spatial and temporal pattern of myelin formation over the age range studied, and may form the basis for future studies assessing myelin in the developing brain.

2288

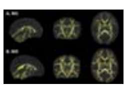

Assessing white matter tract development in formula fed versus breastfed infants at 1 month and 3 months

Giang-Chau Ngo[1,2], Clarisa Carruthers[3], Catherine Vu[3], Alex Cerjanic[1,2], Monica Muthaiya[1], Marie Drottar[3], Jonathan Litt[4], Ivan Frantz[4], Ryan Larsen[2], Borjan Gagoski[3], P. Ellen Grant[3], and Bradley P. Sutton[1,2]

[1]Bioengineering, University of Illinois at Urbana-Champaign, Urbana, IL, United States, [2]Beckman Institute, University of Illinois at Urbana-Champaign, Urbana, IL, United States, [3]Boston Children's Hospital, Boston, MA, United States, [4]Beth Israel Deaconness, Boston, MA, United States

Diffusion Tensor Imaging and Tract-Based Spatial Statistic on FA, RD and AD were applied to investigate white matter development in formula fed infants and breast fed infants. Thirty-six infants (thirty breast fed and six formula fed) were scanned at 1 month and twenty-two (twelve breast fed and ten formula fed) at 3 months. Increased FA and decreased RD values were observed in breast fed infants at 1 month with differences becoming insignificant at 3 months.

2289

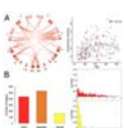

Non-negative matrix factorisation reveals developmental trajectories of structural subnetworks

Gareth Ball[1], Richard Beare[1], and Marc L Seal[1,2]

[1]Developmental Imaging, Murdoch Children's Research Institute, Melbourne, Australia, [2]Department of Paediatrics, University of Melbourne, Melbourne, Australia

We model the structural network architecture of the brain as a set of superposed subnetworks, or network components. We use non-negative matrix factorisation, an unsupervised and data-driven approach, to reliably identify separable subnetworks and track their development over the human lifespan. In the NKI-Rockland lifespan sample (n=196), we find evidence for an increased reliance on local communication between neighbouring regions, rather than through heavily-connected network hubs in older age. This method shows good potential for further exploration of the human structural connectome.

2290

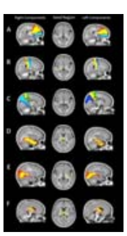

Structural thalamocortical connectivity in the developing infant brain

Rali Dimitrova[1,2], Jonathan O'Muircheartaigh[1,2], Judit Ciarrusta[1,2], Dafnis Batalle[1], Emer Hughes[1], Johannes Steinweg[1], Emily Perry[2], Johanna Kangas[2], Ines Pote[2], Serena Counsell[1], Jo Hajnal[1], Declan Murphy[2], David Edwards[1], and Grainne McAlonan[2]

[1]Centre for the Developing Brain, King's College London, London, United Kingdom, [2]Institute of Psychiatry, Psychology and Neuroscience, King's College London, London, United Kingdom

Thalamocortical development in early life is crucial for normal brain functioning and abnormalities to these networks are thought to underpin atypical neurodevelopment. However, to date examination of this system in the infant has been hampered by the lack of age-appropriate population atlases. In this study we circumvent this problem by applying independent component analysis to parcellate the thalamocortical projections and their underlying thalamic seed in 6-months-old infants using diffusion MRI.

2291

A Longitudinal Diffusion-Weighted Infant Brain Atlas with Spatio-Temporal Consistency

Jaeil Kim[1], Geng Chen[1], Pew-Thian Yap[1], Weili Lin[1], and Dinggang Shen[1]

[1]Department of Radiology and BRIC, University of North Carolina at Chapel Hill, Chapel Hill, NC, United States

In this abstract, we introduce a longitudinal diffusion-weighted infant brain atlas. For construction of this longitudinal atlas, we collected the diffusion-weighted images of 36 subjects, scanned at 5 time points (at neonate, 3, 6, 9 and 12 months of age). Our method builds the atlas from the diffusion-weighted images without the need for any diffusion models. Also, our method, based on patch-based sparse representation, preserves more structural details with spatial-temporal consistency in the longitudinal atlas. Thus, when applied to quantitative analysis of infant brain images, more accuracy can be achieved.

2292

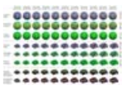

Longitudinally consistent infant cortical surface atlases and parcellations from birth to 6 years of age

Zhengwang Wu[1], Gang Li[1], Yu Meng[1], Li Wang[1], Weili Lin[1], and Dinggang Shen[1]

[1]BRIC, UNC-Chapel Hill, Chapel Hill, NC, United States

For the first time, a longitudinally consistent infant cortical surface atlas with densely-sampled 11 time points (at 1, 3, 6, 9, 12, 18, 24, 36, 48, 60, and 72 months of age) is built for better exploring the dynamic and critical early brain development, based on 339 serial MRI scans from 50 healthy infants. The longitudinal consistency and unbiasedness are ensured by an advanced two-stage group-wise surface registration during the atlas construction. To equip parcellations for our atlases, both the FreeSurfer parcellation (for coarse parcellation) and HCP MMP parcellation (for fine-grained parcellation) are mapped onto our infant atlases.

2293

Multi-parametric brain morphometry using a big data approach

Farshid Sepehrband[1], Clio Gonzalez-Zacarias[2], Lu Zhao[2], Arthur W Toga[2], and Kristi A Clark[2]

[1]Laboratory of Neuro Imaging, Keck School of Medicine of USC, Los Angeles, CA, United States, [2]Laboratory of Neuro Imaging

Many studies have explored the relationship between neuroanatomical measures (such as cortical thickness or surface area) and cognition or health. Conventionally, generalized linear models are used to identify between-group differences within single measurements (e.g., regional cortical thickness), which ignores the possible interaction between neuroanatomical features. Incorporating a large number of regressors is not recommended in regression analyses, mainly due to the curse of dimensionality [1]. Multi-parametric classification approaches can be used to ameliorate the latter issue and to capture brain complexity [2]. The down side is that these approaches have less interpretability compared to regression techniques –because these techniques primarily focus on prediction accuracy rather than building an interpretable model. Here we present an approach that enables multi-parametric regression analysis by employing big data routine.

2294

Comparison of postnatal trajectory of neonatal white matter development between preterm and term neonates during the neonatal stage

Chao Jin[1], Yanyan Li[1], Xianjun Li[1,2], Miaomiao Wang[1], Congcong Liu[1], Jie Gao[1], Qinli Sun[1], Xiaocheng Wei[3], and Jian Yang[1,2]

[1]Department of Diagnostic Radiology, the first Affiliated Hospital of Xi'an Jiaotong University, Xi'an, People's Republic of China, [2]Department of Biomedical Engineering, School of Life Science and Technology, Xi'an Jiaotong University, Xi'an, People's Republic of China, [3]MR Research China, GE Healthcare, Beijing, People's Republic of China

Due to exposure to extrauterine environment, neonatal brain development is in totally different ways after birth, compared with the 'protected' gestation. However, little is known about the postnatal trajectory of neonatal brain development, especially for the differences between preterm and term neonates. This study aims to investigate the postnatal maturation of brain white matter (WM) during the neonatal stage and further provide comparison between preterm and term neonates. Our results suggest that during the neonatal stage, preterm neonates show weaker development capacity than term in optical and somatosensory functions, while present catching up maturation in motor function.

2295

Constrained spherical deconvolution has the potential to better characterize neuronal structure in Cerebral Palsy before and after therapy.

Adam Scott Bernstein[1], Amber L. Pokorney[2], Harry Hu[2], Jeffrey H. Miller[2], Burris Duncan[3], and Theodore Trouard[1]

[1]Biomedical Engineering, University of Arizona, Tucson, AZ, United States, [2]Phoenix Children's Hospital, Phoenix, AZ, United States, [3]Pediatrics, University of Arizona, Tucson, AZ, United States

Cerebral Palsy is a nonprogressive condition that results in very heterogenous motor and other deficits that usually arises during the peripartum period. Many studies have tried to characterize changes in the brain of patients with cerebral palsy using fractional anisotropy and tractography based on diffusion tensor imaging, but few have utilized any of the more recent techniques, such as constrained spherical deconvolution, to more adequately account for complex fiber structures. These more recent techniques also offer more descriptive scalar measures of microstructure, such as apparent fiber density, that can be used to better characterize changes in neural structure.

2296

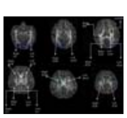

White Matter Abnormalities in Congenital Heart Disease Assessed Using Advanced Diffusion Imaging

Sarina Karmacharya[1], Borjan Gagoski[2], Lipeng Ning[1], Martha E. Shenton[1,3], Ellen Grant[2], and Yogesh Rathi[1]

[1]Brigham and Women's Hospital, Harvard Medical School, Boston, MA, United States, [2]Boston Children's Hospital, Harvard Medical School, Boston, MA, United States, [3]VA Healthcare, Boston, MA, United States

The study examined white matter (WM) abnormalities in neonates with Congenital Heart Disease (CHD) (19 CHD and 16 typically developing (TD) neonates). Gaussian mixture model showed that neonates with CHD have lower cellular volume and density in UF, SFOF, left IFOF, and CC. Fractional Anisotropy was lower in neonates with CHD in bilateral UF, CC, and left SLF. NODDI results indicated lower intracellular volume in the bilateral SFOF, and higher fiber orientation dispersion in the left CC and SLF in CHD. Our results demonstrate that significant WM abnormalities related to language areas are seen in neonates with CHD.

2297

BOLD MR Imaging of Placenta in Congenital Heart Disease

Vincent Kyu Lee[1,2], Alexander M. El-Ali[3], Alexandria Zahner[2], Kavita Vani[4], Vidya Rajagopalan[5], Michelle Gruss[2], Jennifer Adibi[6], Vincent J. Schmithorst[1,2], and Ashok Panigrahy[1,2]

[1]Radiology, University of Pittsburgh, Pittsburgh, PA, United States, [2]Radiology, Children's Hospital of Pittsburgh UPMC, Pittsburgh, PA, United States, [3]Radiology, University of Pittsburgh Medical Center, Pittsburgh, PA, United States, [4]Obstetrics, Gynecology and Reproductive Sciences, University of Pittsburgh Medical Center, Pittsburgh, PA, United States, [5]Radiology, Children's Hospital of Los Angeles, Los Angeles, CA, United States, [6]Epidemiology, University of Pittsburgh, Pittsburgh, PA, United States

We examined whether features of placental BOLD MRI in underlying setting of fetal congenital heart disease (CHD) differ from those of healthy controls, and the imaging data correlated with first trimester maternal serum markers (PAPP-A, β-hCG) known to influence vasculogenesis/angiogenesis. We explored correlation between fetal brain resting stat networks and imaging and hormonal biomarkers of the placenta. We used temporal, spatial, and spatio-temporal to analyze the squared-root-mean variance and distribution differences in BOLD signal between CHD and controls. Difference in spatial and temporal BOLD signal variance is present in CHD pregnancies compared to healthy controls were observed.

2298

Multi-shell Multi-band Diffusion Imaging (MSMBDI) is more predictive of executive deficits in Preadolescents with Complex Congenital Heart Disease (CHD) compared to standard diffusion tensor imaging (DTI)

Vincent Kyu Lee[1,2], Mark Greenhalgh[1,2], William T. Reynolds[1,2], Timothy D. Verstynen[3], Fang-Cheng Yeh[4], Cecilia W. Lo[5], Vincent J. Schmithorst[1,2], and Ashok Panigrahy[1,2]

[1]Radiology, University of Pittsburgh, Pittsburgh, PA, United States, [2]Radiology, Children's Hospital of Pittsburgh UPMC, Pittsburgh, PA, United States, [3]Psychology, Carnegie Mellon University, Pittsburgh, PA, United States, [4]Neurological Surgery, University of Pittsburgh, Pittsburgh, PA, United States, [5]Developmental Biology, University of Pittsburgh, Pittsburgh, PA, United States

We tested whether Multi-shell Multi-band Diffusion Imaging (MSMBDI) would be superior to standard DTI at delineating microstructural cortical association fiber abnormalities and predicting executive function preadolescents with complex congenital heart disease (CHD). Using both a hypothesis-driven approach (manual tractography) and a data-driven approach (q-space diffeomorphic reconstruction) we examined white matter tracts in correlation with NIH Toolbox and complementary battery of neuropsychological test. We show that MSMBDI – when compared to standard DTI – showed greater sensitivity towards white matter structure differences, superior at detecting microstructural differences in cortical association tracts in CHD compared to controls, and more predictive of executive deficits.

2299

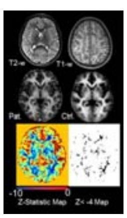

Myelin-Water-Imaging in Hypomyelinating Leukodystrophies

Steffi F. Dreha-Kulaczewski[1,2], Hagen H. Kitzler[3], Hannes Wahl[3], Peter Dechent[4], Jutta Gärtner[5], Sean Deoni[6,7], and Robert Steinfeld[5]

[1]Department of Pediatric and Adolescent Medicine, Department of Pediatric and Adolescent Medicine, University Medical Center Goettingen, Goettingen, Germany, [2]Department of Neuroradiology, University Medical Center Goettingen, Goettingen, Germany, [3]Department of Neuroadiology, University Hospital Carl Gustav Carus, Technische Universität Dresden, Dresden, Germany, [4]Department of Cognitive Neurology, University Medical Center Goettingen, Goettingen, Germany, [5]Department of Pediatrics and Adolescent Medicine, University Medical Center Goettingen, Goettingen, Germany, [6]Advanced Baby Imaging Lab, Brown University School of Engineering, Providence, Providence, RI, United States, [7]Department of Radiology, University of Colorado Denver, Denver, CO, United States

Emerging clinical research in hypomyelinating leukodystrophies (HLD) necessitates definition of surrogate markers as endpoints in possible clinical trials. Standardized assessment of myelination using myelin sensitive MRI is therefore highly desirable. Proposed protocols comprise DTI, MT-imaging and myelin water imaging employing the mcDESPOT sequence. We report first experiences applying mcDEPSOT in patients with cerebral folate deficiency. Myelin water fraction (MWF) allowed assessment of subtle gradual and regional changes with sufficient spatial resolution. The extent of the myelin deficit in diffuse hypomyelination can more reliably be evaluated using the MWF parameter. McDESPOT seems a feasible, system independent method to study pediatric HLD.

2300

Divergent trajectory of age-related cerebellar volume change in children with ataxia telangiectasia

Rob A. Dineen[1], Stefan Pszczolkowski[1], Felix Raschke[2], Hannah McGlashan[1], Manish Prasad[3], Gabriel Chow[3], William Whitehouse[4], and Dorothee P. Auer[1]

[1]Radiological Sciences, University of Nottingham, Nottingham, United Kingdom, [2]Radiotherapy and Radiation Oncology, University Hospital Carl Gustav Carus of the Technische Universität Dresden, Dresden, Germany, [3]Paediatric Neurology, Nottingham University Hospitals NHS Trust, Nottingham, United Kingdom, [4]Division of Child Health, University of Nottingham, Nottingham, United Kingdom

Cerebellar atrophy occurs in the inherited neurodegenerative syndrome Ataxia Telangiectasia (A-T) but the trajectory of cerebellar atrophy across childhood and its relationship to clinical status is unknown. We report cerebellar and fourth ventricular volumes (normalized to intracranial volume) from 24 children with A-T and 24 matched controls. Cerebellar volume declined linearly with increasing age in the A-T group with a divergent trajectory of age-related cerebellar volume change compared to normally-developing children. Fourth ventricular volume increased with age in children with A-T and correlated with clinical status, and may provide an imaging marker of neurological status in childhood A-T.

2301

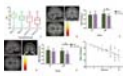

The effect of the dopamine D4 receptor −616 C/G polymorphism on gray matter volume and functional connectivity in pediatric primary nocturnal enuresis patients

Bing Yu[1], Mingzhu Huang[2], Xu Zhang, Kaining Shi[3], and Qiyong Guo[1]

[1]Shengjing Hospital of China Medical University, Shenyang, People's Republic of China, [2]Shengjing Hospital of China Medical University, [3]Philips healthcare

The study assessed the effects of (DRD4) -616 (rs747302) gene variation on gray matter volume (GMV) and arousal from sleep (AS) scores in children that suffered from primary nocturnal enuresis (PNE) and normal controls and found that The −616 C/G SNP in the DRD4 promoter may affect the AS scores and GMV in the thalamus and pregenual ACC in PNE children.

2302

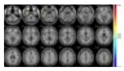

Altered regional brain activities in children with nonsyndromic cleft lip and/or palate (CL/P): a resting-state functional MRI study

Hua CHENG[1], YingZi GAO[1], Yang FAN[2], WenJing ZHANG[3], and Yun PENG[1]

[1]Imaging Center, Beijing Children's Hospital, Capital Medical University, Beijing, People's Republic of China, [2]MR Research China,GE Healthcare, [3]Beijing Stomatological Hospital, Capital Medical University

Resting state-fMRI has been widely used as an effective method to evaluate the of brain functional changes in physiological and pathological process. Altered regional brain activities, especially in verbal and cognitive areas were found in children with nonsyndromic CL/P using resting-state fMRI. It helps to understand the abnormality of functional architecture of CL/P which implies different structures and cognitive patterns in CL/P compared with normal development children.

2303

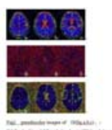

Study on the brains of perinatally HIV infected asymptomatic adolescents by intravoxel incoherent motion diffusion weighted imaging

Jing Zhang[1], Yunfei Zha[2], Guangyao Wu[3], and GE healthcare China[4]

[1]Department of Radiology, Remin Hospital of Wuhan University, Wuhan, People's Republic of China, [2]Remin Hospital of Wuhan University, wuhan, People's Republic of China, [3]Zhongnan Hospital of Wuhan University, People's Republic of China, [4]GE healthcare China, Beijing, People's Republic of China

IVIM diffusion is applied to detect the changes in the brain of perinatally HIV-infected adolescents in our work. 18 children with HIV positive and 17 HIV negative children underwent MRI scan on a 3.0T whole body scanner including multi-b diffusion imaging. The IVIM parameters (D, D*and f) were obtained by fitting using MITK software. Correlation of IVIM parameters and CD4+T cell counts, CD4/CD8 ratio were analyzed. D* value of caudate nucleus and frontal white matter decreased significantly in HIV positive children and the changes of D* were positively correlated with CD4+T cell counts and CD4/CD8 ratio. However，D and f were not statistically significant. IVIM improves on the detection brain damage in HIV infected asymptomatic adolescents as compared to conventional DWI.

2304

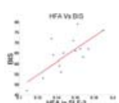

Microstructural heterogeneity of Superior longitudinal fasciculus (SLF-II) predicts impulsivity in healthy young girls

Yogesh Rathi[1], Julia Cohen-Gilbert[1], Michael Rohan[1], Elizabeth Olson[1], Benjamin Reid[2], Sarina Karmacharya[2], Martha E Shenton[1], Sion Harris[1], and Marisa M Silveri[1]

[1]Harvard Medical School, Boston, MA, United States, [2]Brigham and Women's Hospital, Boston, MA, United States

Diffusion MRI (dMRI) is sensitive to microstructural arrangement of cells and axons in the brain. In this abstract, we analyzed dMRI data from 30 healthy children (14 girls, 13.9 ± 0.8 yrs, 16 boys, 13.4 ± 0.9 yrs). Advanced multi-tensor tractography was used to trace the SLF-II and heterogeneity in fractional anisotropy (HFA)4 (the standard deviation in FA) was computed in all subjects. Subjects were separated into two groups (males, females) and correlation between HFA and total Barratt Impulsivity Scores (BIS) was computed for each group. A statistically significant correlation was found between HFA in left SLF-II and BIS in girls but not in boys. The SLF-II has been known to be involved in spatial attention and executive control and higher heterogeneity in white matter integrity in SLF-II seems to be involved in impulsive/attentional network in young girls but not boys.

2305

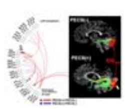

DTI-based Connectome Analysis to Predict Outcome of Picture Exchange Communication System (PECS) in Young Children with Autistic Spectrum Disorders

Jeong-Won Jeong[1,2]

[1]Pediatrics, Wayne State University, Detroit, MI, United States, [2]Translational Imaging Lab, Children's Hospital of Michigan, Detroit, MI, United States

The aim of this study is to apply DTI-based connectome analysis to investigate the neural substrate and mechanism of picture exchange communication system (PECS) in young children with ASD. Seventeen non-verbal children with ASD who underwent PECS and 3T DTI (age: 3.05±0.82 years, 10 boys) were retrospectively selected for whole brain connectome analysis . Compared with 5 children who failed PECS (non-verbal after PECS), 12 children who succeeded PECS (verbal after PECS) showed significantly increased betweeness, local efficiency and nodal strength in anterior inferior occipital gyrus (p <0.01). Such increases may be an effective imaging marker to detect ASD children who will become verbal after PECS.

2306

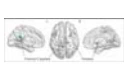

Disrupted Brain Network Topology in Pediatric Tourette Syndrome: A Resting-State fMRI Study

Yi Liao[1], Haibo Qu[1], Xijian Chen[1], Chuan Fu[1], Yuexin Jiang[1], and Gang Ning[1]

[1]Department of Radiology, West China Second University Hospital, Sichuan University, Chengdu, People's Republic of China

Tourette syndrome is a neurobehavioral disorder characterized by motor and vocal tics beginning in childhood. Previous neuroimaging investigations suggested impaired cortico-striato-thalamo-cortical activity during motor control. We hypothesized that the small-world properties of functional connectomes would be abnormal in pediatric Tourette Syndrome patients. Compared with control subjects, the Tourette Syndrome patients showed altered quantitative values in the global properties, characterized by higher path length, higher normalized characteristic path length and lower global efficiency, implying a shift toward regular networks. The Tourette Syndrome group showed decreased nodal efficiency in the posterior part of left cingulum and right putamen comparing to the controls.

2307 

Correlation Between Cerebral Blood Flow And Whole Brain Perfusion In Children Undergoing Deep Sedation.

Malek I MAKKI[1,2], Ruth O'Gorman[3], Olivier Baledent[2], Philip Buhler[4], Markus Weiss[4], Christian Kellenberger[5], Ianina Scheer[5], and Achim Schmitz[4]

[1]MRI Research, University Children Hospital, Zurcih, Switzerland, [2]BioFlow, University Picardie Jules Verne, Amiens, France, [3]MRI Research, University Children Hospital, Zurich, Switzerland, [4]Anesthesia, University Children Hospital, Zurich, Switzerland, [5]Radiology, University Children Hospital, Zurich, Switzerland

Anaesthetics such as those used for sedation in paediatric MRI affect cerebral blood flow and hemodynamics to varying degrees. This study examines the link between brain perfusion measured by arterial-spin-labelling and cerebral blood flow measured by phase-contrast MRI in 2 cohorts of children undergoing sedation either with propofol or a combination of propofol and ketamine. Significant correlations were observed between these 2 variables for both groups.

2308 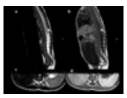

MRI characteristics predicts clinical outcomes in severe hand, foot, and mouth disease：analysis of 412 children in China

Zhouyang Lian[1], Shuixing Zhang[2], Kannie W.Y. Chan, and Guanshu Liu

[1]Guangdong Academy of Medical Sciences/Guangdong General Hospital, Guangzhou, People's Republic of China, [2]Guangdong Academy of Medical Sciences/Guangdong General Hospital, People's Republic of China

Most severe hand, foot, and mouth disease(HFMD) are caused by EV71 infections, which can result in central nervous system complications. So magnetic resonance imaging (MRI) acquisition is important for the patients with EV71 infection to reveal the location of lesions and select the potential severe cases with poor prognosis. We aim to reviewed MRI characteristics of the severe HFMD, using a multivariate approach to compare the prognosis of different lesion sites based on a large cohort with follow-up. Our findings suggested lesions located in medulla oblongata (P<0.015)and spinal cord(P<0.001) on MRI associated with poor prognosis.

2309 

Altered microstructural integrity of white matter tracts in children with aromatic L-amino acid decarboxylase deficiency

Chih-Hsien Tseng[1,2], Wuh-Liang Hwu[3,4], Yu-Jen Chen[1], Yun-Chin Hsu[1], and Wen-Yih Isaac Tseng[1,2,5,6]

[1]Institute of Medical Device and Imaging, National Taiwan University College of Medicine, Taipei, Taiwan, [2]Institute of Biomedical Engineering, National Taiwan University College of Medicine, Taipei, Taiwan, [3]Department of Medical Genetics, National Taiwan University Hospital and National Taiwan University College of Medicine, Taipei, Taiwan, [4]Department of Pediatrics, National Taiwan University Hospital and National Taiwan University College of Medicine, Taipei, Taiwan, [5]Graduate Institute of Brain and Mind Sciences, National Taiwan University College of Medicine, Taipei, Taiwan, [6]Molecular Imaging Center, National Taiwan University, Taipei, Taiwan

Aromatic L-amino acid decarboxylase (AADC) deficiency is an inherited disorder that impairs synthesis of dopamine and serotonin. To investigate whether the white matter tracts are impaired in children with AADC deficiency, diffusion tensor imaging data were obtained from 7 children with AADC deficiency and 7 matched controls. Fractional anisotropy (FA) of 76 white matter tracts was measured and compared between the two groups. Fiber tracts of dopaminergic and serotonergic systems, and those connecting regions responsible for executive functions or regulating motor functions showed lower FA in patients. Our findings are consistent with clinical manifestations and pathophysiology of AADC deficiency.

Traditional Poster

Neurologic Disease: From A to Z

Exhibition Hall 2310-2337 Wednesday 13:45 - 15:45

2310 

Understanding white matter pathology in ALS using a multimodal approach

Matt C Gabel[1], Rebecca Broad[1], Daniel C Alexander[2], Gary H Zhang[2], Nigel Leigh[3], and Mara Cercignani[1]

[1]Clinical Imaging Sciences Centre, Brighton and Sussex Medical School, Brighton, United Kingdom, [2]Centre for Medical Image Computing and Computer Science, University College London, London, United Kingdom, [3]Trafford Centre for Medical Research, Brighton and Sussex Medical School, Brighton, United Kingdom

Multimodal diffusion MRI and quantitative MT techniques were used to examine the nature of abnormalities in the corticospinal tracts (CSTs) of amyotrophic lateral sclerosis (ALS) patients. Our data show reductions in axonal volume fraction (AVF) located superiorly to reductions in myelin volume fraction (MVF). We also find extensive decreases in fiber volume fraction (FVF) throughout the entire CST, supporting the hypothesis of axonal loss as the primary pathological mechanism in ALS.

2311

DTI of the Sciatic Nerve in Patients with Charcot-Marie-Tooth Diseases

Cristah E Artrip[1], Michael D. Pridemore[1], Jun Li[2], and Richard D. Dortch[1,3]

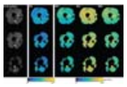

[1]Vanderbilt Institute of Imaging Science, Vanderbilt University, Nashville, TN, United States, [2]Neurology, Vanderbilt University, Nashville, TN, United States, [3]Radiology and Radiological Sciences, Vanderbilt University, Nashville, TN, United States

This study examines the sensitivity of DTI metrics to proximal sciatic nerve pathology in a cohort of patients with Charcot-Marie-Tooth (CMT) diseases and matched controls, with the longer-term goal of developing objective biomarker of disease progression and treatment response. Prior studies have shown that DTI metrics can relate to disability in other neuropathies. Here we demonstrate that robust DTI can be performed in the proximal sciatic nerve of patients with CMT, and the resulting metrics are sensitive to myelin and/or axonal pathologies. Future studies will test if DTI measures predict disability in patients with CMT.

2312

Graph-based analysis of brain structural MRI data in Multiple System Atrophy

Claudia Testa[1,2], Riccardo Gubellini[1], Stefano Zanigni[1], Lia Talozzi[1], Giulia Giannini[3], Giovanna Calandra-Buonaura[3], Pietro Cortelli[3], Daniel Remondini[2,4], Gastone Castellani[2,4], Paola Fantazzini[4,5], Claudio Bianchini[1], Stefania Evangelisti[1], Caterina Tonon[1], David Neil Manners[1], and Raffaele Lodi[1]

[1]Department of Biomedical and NeuroMotor Sciences, University of Bologna and Functional MR Unit, Policlinico S. Orsola - Malpighi, Bologna, Italy, Bologna, Italy, [2]INFN-Bologna, Bologna, Italy, [3]Department of Biomedical and NeuroMotor Sciences, University of Bologna and IRCCS Istituto delle Scienze Neurologiche di Bologna, Bologna, Italy, [4]Department of Physics and Astronomy, Bologna, Italy, [5]Centro Enrico Fermi, Roma, Italy

We investigated the differences in global and regional topological properties and the modular organization of brain networks derived from anatomical covariance of structural MRI between Multiple System Atrophy patients (subdivided in the variants MSA-C, MSA-P) and healthy controls (HC). No differences were found in global, local and small-worldness measures between MSA and HC or between MSA-C and MSA-P. The investigation of modular organization, which reflects differences in properties that underlie the functionality of the brain, has shown a segregation in a cortical-subcortical motor network in patient groups, which may underpin both the typical parkinsonian and cerebellar features of the disorder.

2313

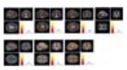

Detection of subtle white matter alterations in migraine using diffusion kurtosis imaging

Yu-Shiuan Liang[1], Ming-Ting Wu[2], Ching-Sen Shih[3], and Ming-Chung Chou[1,4]

[1]Department of Medical Imaging and Radiological Sciences, Kaohsiung Medical University, Kaohsiung, Taiwan, [2]Department of Radiology, Kaohsiung Veterans General Hospital, Kaohsiung, Taiwan, [3]Department of Neurology, Kaohsiung Veterans General Hospital, Kaohsiung, Taiwan, [4]Department of Healthcare Administration and Medical Informatics, Kaohsiung Medical University, Kaohsiung, Taiwan

Migraine subjects were demonstrated to exhibit white matter alterations detected by diffusion tensor imaging (DTI). Due to the Gaussian assumption of water distribution employed in DTI technique, the measured diffusivity may not be accurate and may hinder the detection of white matter alterations. Diffusion kurtosis imaging (DKI) was demonstrated to better characterize white matter alterations without Gaussian assumption and has not been utilized to detect white matter alterations in migraine subjects. This study performed DKI to detect microstructural white matter alterations and demonstrated that diffusion kurtosis parameters were more sensitive to subtle white matter alterations than diffusion tensor parameters.

2314

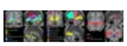

Comprehensive assessment of white matter alterations in Tourette syndrome using automatic whole-brain tract-specific analysis

Chih-Hsien Jerry Tseng[1,2], Wang-Tso Lee[3,4], Shinn-Forng Peng[5], Chien-Feng Huang[1], Yu-Jen Chen[1], Yun-Chin Hsu[1], and Wen-Yih Isaac Tseng[1,2,4,6]

[1]Institute of Medical Device and Imaging, National Taiwan University College of Medicine, Taipei, Taiwan, [2]Institute of Biomedical Engineering, National Taiwan University College of Medicine, Taipei, Taiwan, [3]Department of Pediatrics, National Taiwan University College of Medicine, Taipei, Taiwan, [4]Graduate Institute of Brain and Mind Sciences, National Taiwan University College of Medicine, Taipei, Taiwan, [5]Department of Medical Imaging, National Taiwan University Hospital, Taipei, Taiwan, [6]Molecular Imaging Center, National Taiwan University, Taipei, Taiwan

To identify microstructural alteration of white matter tracts in patients with Tourette syndrome (TS), diffusion spectrum imaging data were obtained from 14 patients and 14 matched controls. Whole-brain tract-based automatic analysis was employed to investigate the differences in white matter microstructures between the two groups. As compared with the controls, patients with TS showed altered tract integrity in callosal fibers, cingulum, thalamic radiations and corticospinal tracts. The altered white matter tracts account for clinical hallmarks and pathophysiology of TS, and might serve as structural correlates of TS.

2315

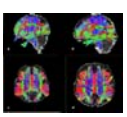

White matter microstructural changes in Rett syndrome: a whole brain tract-specific analysis

Tz-Yun Jan[1], Wang-Tso Lee[2], Shinn-Forng Peng[3], and Isaac Wen-Yih Tseng[4]

[1]National Taiwan University, Taipei, Taiwan, [2]National Taiwan University, Taiwan, [3]National Taiwan University Hospital, [4]National Taiwan University

Rett syndrome (RTT) is characterized by trajectory changes in cognition and motor functions. To understand the disease-specific pathologic changes of each tract bundle in white matter in stable stage of RTT, we applied tract-specific analysis of the whole brain to investigate the alteration of 76 major tracts by diffusion spectrum image. In conclusion, the altered microstructural integrity in RTT were covered in whole brain, however, in systematically view, most of them were located in associative and commissure tract bundles. Surprisingly, the GFA value of anterior commissure in RTT was higher than controls, which might explain the well-preserved visual perception clinically.

2316

Quantitative evaluation of brain volume change after phthalate esters exposure using voxel-based morphometry

Ju-Chien Wu[1], Jun-Cheng Weng[1,2], Jeng-Dau Tasi[3], Chao-Yu Shen[1,2,4], and Shu-Li Wang[5]

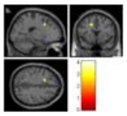

[1]Department of Medical Imaging and Radiological Sciences, Chung Shan Medical University, Taichung, Taiwan, [2]Department of Medical Imaging, Chung Shan Medical University Hospital, Taichung, Taiwan, [3]School of Medicine and Department of Pediatrics, Chung Shan Medical University and Hospital, Taichung, Taiwan, [4]Institute of Medicine, Chung Shan Medical University, Taichung, Taiwan, [5]National Institute of Environmental Health Sciences, National Health Research Institutes, Miaoli, Taiwan

The products made by phthalate esters could be found everywhere. But there were only a few studies mentioned about the influence of phthalate esters exposure on brain volume. We used the voxel-based morphometry analysis to observe the correlation between the concentrations of maternal urine phthalate esters (MBP, MBzP, DEHP, MEHP, MEOHP) and children's brain volume of gray and white matter. We found the negative correlation between the concentrations and the volume of frontal gyrus and cingulate gyrus.

2317

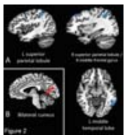

Network-dependent changes in functional connectivity at 7 tesla in young adults with Down syndrome

Katherine A Koenig[1], Se-Hong Oh[1], Melissa R Stasko[2], Emma Lissemore[2], Elizabeth Roth[2], Anne Birnbaum[2], Thomas Scheidemantel[3], Hudson Taylor[2], Nancy Roizen[3], Stephen Ruedrich[3], Mark Lowe[1], and Alberto Costa[2]

[1]Imaging Institute, The Cleveland Clinic, Cleveland, OH, United States, [2]Case Western Reserve University, Cleveland, OH, United States, [3]University Hospitals, Cleveland, OH, United States

This works uses 7 tesla MRI to assess resting state functional connectivity (rs-fMRI) in young adults with Down syndrome (DS). As compared to matched controls, individuals with DS show increased rs-fMRI in the default mode network, but decreased rs-fMRI in a network related to executive function.

2318

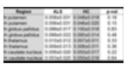

No Evidence of Increased Iron Accumulation in the Deep Gray Matter of Patients with Amyotrophic Lateral Sclerosis (ALS)

Florian Borsodi[1], Valeriu Culea[1], Christian Langkammer[1], Michael Khalil[1], Lukas Pirpamer[1], Stefan Quasthoff[1], Christian Enzinger[1,2], Franz Fazekas[1], and Stefan Ropele[1]

[1]Department of Neurology, Medical University of Graz, Graz, Austria, [2]Division of Neuroradiology, Vascular and Interventional Radiology, Department of Radiology, Medical University of Graz, Graz, Austria

Iron accumulation in deep gray matter occurs during normal aging, but has also been observed in several neurodegenerative diseases. To investigate if this still holds true for ALS, we aimed at assessing the iron content in deep gray matter structures of 24 ALS patients with quantitative susceptibility mapping and its relation to 28 controls. We did not find any significant differences in iron levels between ALS patients and controls. This may indicate that iron accumulation in deep gray matter is a specific feature that is not associated with neurodegenerative diseases in general, but rather reflects more specific degenerative processes.

2319

Brain structural MRI and perfusion signature of ALS patients with different levels of cognitive deficits

Bo Hou[1], Dong-chao Shen[2], Pan Peng[2], Bo Cui[2], Xiao-lu Li[1], Hui You[1], Li-zhi Xie[3], Li-ying Cui[2], and Feng Feng[1]

[1]Radiology, Peking Union Medical College Hospital, Beijing, People's Republic of China, [2]Neurology, Peking Union Medical College Hospital, Beijing, People's Republic of China, [3]Ge Healthcare, MR Research China, Beijing, People's Republic of China

This study was done to explore potential brain changes in ALS patients with different levels of cognitive deficits with voxel-based analysis of CBF generated by pCASL and VBM. Significant GM loss and CBF decrease were demonstrated in the severe frontotemporal dementia group. No difference of GM or CBF was found between ALS-Cn and ALS-Ci. Differences between ALS-Ci and ALS-FTD overlapped with those found between ALS-Cn and ALS-FTD, and the changes were more widespread in the latter contrast.

2320

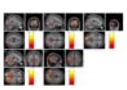

Mapping brain functional alterations in chemotherapy-treated breast cancer women using resting-state fMRI

Xuan-Ru Zhang[1], Vincent Chin-Hung Chen[2,3], Dah-Cherng Yeh[4], Chao-Yu Shen[1,5,6], and Jun-Cheng Weng[1,6]

[1]Department of Medical Imaging and Radiological Sciences, Chung Shan Medical University, Taichung, Taiwan, [2]School of Medicine, Chang Gung University, Taoyuan, Taiwan, [3]Department of Psychiatry, Chang Gung Memorial Hospital, Chiayi, Taiwan, [4]Breast Center, Taichung Tzu Chi Hospital, Taichung, Taiwan, [5]Institute of Medicine, Chung Shan Medical University, Taichung, Taiwan, [6]Department of Medical Imaging, Chung Shan Medical University Hospital, Taichung, Taiwan

Breast cancer (BC) is one of the common public health problems, and chemotherapy was the major treatment for breast cancer. The previous study showed abnormal brain function was associated with the late effects of chemotherapy (5 to 10 years). The purpose of our study was to evaluate the early effects of post-chemotherapy BC patients (in 6 months). We investigated the resting-state functional differences between post-chemotherapy BC patients and healthy control. Our results provided the evidence of brain functional changes in women with breast cancer and highlight the importance of the breast cancer-related chemotherapy.

2321

brain iron accumulation in amyotrophic lateral sclerosis - a quantitative susceptibility mapping study

Qiuli Zhang[1], Haining Li[1], Yuchen Zhang[1], Dandan Zheng[2], Lijun Bai[3], and Ming Zhang[1]

[1]Radiology, the First Affilicated Hospital of Xi'an Jiaotong University, Xi'an, Shaanxi, People's Republic of China, [2]GE Healthcare, MR Research China, Beijing, People's Republic of China, [3]School of Life Science and Technology, Xi'an Jiaontong University, the Key Laboratory of Biomedical Information Engeering, Ministry of Education, Xi'an, Shaanxi, People's Republic of China

Iron accumulation can induce a wide range of neuron disorders in central nerve system. Increased serum ferritin has been found to predict poor clinical outcome in ALS. We used quantitative susceptibility mapping to explore brain iron accumulation and theri clinical relevance. Increased iron level has been found in both cortical and subcortical motor related regions. The iron concentration in the primary motor cortex is responsible for deteriorated clinical syndrome, suggested its potential role for disease management. While increased iron concentration in the bilteral caudate contributed to impaired executive function, indicated network-based dysfunction for cognition decline in ALS.

2322

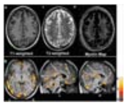

Regional Brain Myelin Changes in Patients with Heart Failure

Bhaswati Roy[1], Mary Woo[1], Gregg Fonarow[2], Ronald M Harper[3,4], and Rajesh Kumar[4,5,6]

[1]UCLA School of Nursing, University of California at Los Angeles, Los Angeles, CA, United States, [2]Division of Cardiology, University of California at Los Angeles, Los Angeles, CA, United States, [3]Neurobiology, University of California at Los Angeles, Los Angeles, CA, United States, [4]Brain Research Institute, University of California at Los Angeles, Los Angeles, CA, United States, [5]Anesthesiology, University of California at Los Angeles, Los Angeles, CA, United States, [6]Radiological Sciences, University of California at Los Angeles, Los Angeles, CA, United States

Heart Failure (HF) patients show gray matter injury in multiple brain areas, based on various MRI techniques; such injury can accompany loss of subcortical and white matter myelin integrity. However, the extent of regional myelin changes in HF is unclear. We examined regional myelin integrity in HF patients, and found decreased values, likely resulting from hypoxic/ischemic processes, in critical autonomic, cognitive, respiratory, and mood control sites. These functions are deficient in the condition. Myelin mapping, based on simple-to-calculate ratios of T1- and T2-weighted images, is useful for evaluating regional myelin changes.

2323

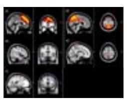

Investigation of neuroinflammation and cognitive dysfunction following a major burn injury and critical care admission using advanced MR imaging

Mary Elizabeth Finnegan[1,2], Matthew Grech-Sollars[1,3], Lesley Honeyfield[1,3], Philip Benjamin[1], Rebecca Quest[1,3], Edward JR Watson[4,5], Naz Nordin[4,5], Olivia Clancy[4,5], Ahmed Al-Hindawi[4,5], Agnes Nilsen[6], Ashley Mehmet[6], Klara Nenadlova[6], Lisa Williams[4], Trudi Edginton[6], Sara De Simoni[3], Marcela Vizcaychipi[4,5], and Adam Waldman[3,7]

[1]Department of Imaging, Imperial College Healthcare NHS Trust, London, United Kingdom, [2]Department of Bioengineering, Imperial College London, London, United Kingdom, [3]Department of Medicine, Imperial College London, London, United Kingdom, [4]Magill Department of Anaesthesia, Chelsea and Westminster Hospital NHS Foundation Trust, London, United Kingdom, [5]Department of Academic Anaesthesia, Imperial College London, London, United Kingdom, [6]Department of Psychology, Westminster University, London, United Kingdom, [7]Centre for Clinical Brain Sciences, University of Edinburgh, Edinburgh, United Kingdom

We used advanced MR imaging methods to investigate neurophysiological changes following major burns injury in a cohort of patients with reduced cognitive function compared to age and sex-matched controls. In this preliminary study, small regions of increased connectivity were observed in patients in two brain networks extracted from resting-state fMRI data using ICA. However, the significance of these results is unclear given the broad range of neurological functions implicated by the cognitive deficits. Furthermore, we found no significant difference between patients and controls for TBSS, volumetric analysis and MR spectroscopy. SWI indicated large areas of microbleeds in one patient.

2324

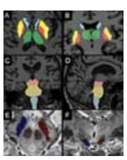

Region-specific damage in Progressive Supranuclear Palsy studied using multimodal quantitative MRI

Nadya Pyatigorskaya[1,2,3], Rahul Gaurav[3], Claire Ewenczyk[4], Cecile Gallea[3], Romain Valabregue[3], Fatma Gargouri[3], Eric Bardinet[3], Isabelle Arnulf[2,5], Cyril Poupon[6], Marie Vidailhet[2,4], and Stephane Lehericy[1,2,3]

[1]Neuroradiology department, APHP, Pitié Salpêtrière, Paris, France, [2]UPMC Univ Paris 06, UMR S 1127, CNRS UMR 7225, ICM, F-75013, Sorbonne Universités, Paris, France, [3]Centre de NeuroImagerie de Recherche – CENIR, ICM, Paris, France, [4]Clinique des mouvements anormaux, Département des Maladies du Système Nerveux, Hôpital Pitié-Salpêtrière, APHP, Paris, France, [5]Service des pathologies du Sommeil, Hôpital Pitié-Salpêtrière, APHP, Paris, France, [6]NeuroSpin, CEA, Gif-Sur-Yvette, France

We used quantitative multimodal MRI to investigate the region-specific damage in progressive supranuclear palsy (PSP) in order to generate a precise model of neurodegeneration at various levels of the central nervous system, including brainstem nuclei, basal ganglia and cortex. PSP patients showed extensive volume decrease and microstructural diffusion changes in the brainstem and the basal ganglia in agreement with previous pathological studies. These results suggest the possibility of direct noninvasive assessment of brain damage in PSP not only in the basal ganglia and the cortex, as done previously, but also in small brainstem nuclei.

2325

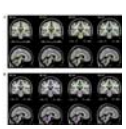

Autosomal dominant cerebellar ataxia: The search for imaging biomarkers

Isaac Mawusi Adanyeguh[1], Pierre-Gilles Henry[2], Vincent Perlbarg[1], Tra My Nguyen[1], Daisy Rinaldi[1], Celine Jauffret[1], Romain Valabregue[1,3], Uzay Emrah Emir[2], Dinesh Kumar Deelchand[2], Alexis Brice[1], Gulin Oz[2], Alexandra Durr[1], and Fanny Mochel[1]

[1]INSERM U 1127, CNRS UMR 7225, Sorbonne Universités, UPMC Univ Paris 06 UMR S 1127, Institut du Cerveau et de la Moelle épinière, ICM, F-75013, Paris, France, [2]Center for Magnetic Resonance Research, University of Minnesota, Minneapolis, MN, United States, [3]Center for NeuroImaging Research, Institut du Cerveau et de la Moelle épinière, 75013 Paris, France

Spinocerebellar ataxias (SCAs) are neurodegenerative disorders characterized by predominant atrophy of the cerebellum and pons, with the main symptom being ataxia. There is currently no treatment for this disorder due to the lack of robust biomarkers to evaluate the disease progression. This study aimed to identify robust biomarkers for this disorder using a combination of magnetic resonance spectroscopy and imaging techniques. This study confirmed neurometabolic alterations in SCAs as well as microstructural modifications resulting from the disease. This study also showed that imaging biomarkers are more sensitive to disease progression than clinical scores.

2326

Dynamic Quantitative Imaging of Sodium During Migraine Onset and Propagation at 21.1 T

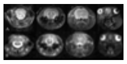

Nastaren Abad[1,2], Jens T. Rosenberg[1], Samuel Colles Grant[1,2], and Michael G. Harrington[3]

[1]Center for Interdiscplinary Magnetic Resonance, National High Magnetic Field Laboratory, Tallahassee, FL, United States, [2]Chemical & Biomedical Engineering, Florida State University, Tallahassee, FL, United States, [3]Molecular Neurology Program, Huntington Medical Research Institutes, Pasadena, CA, United States

The brain allocates >50% of its energy reserves to the regulation of sodium homeostasis, indicating the critical importance of sodium and its fluxes in normal brain and neurological disorders. The purpose of this study was to evaluate *in vivo* ^{23}Na in the brain using a rat model of migraine induced by nitroglycerin injection. The ultra-high field of 21.1 T was employed to quantify alterations in bulk sodium during and following the onset of central sensitization related to migraine. Multi-slice 2D CSI of sodium were acquired longitudinally to identify localized increases in sodium concentrations during a 3-h period following sensitization induction.

2327 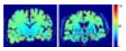

Endogenous assessment of hippocampus degeneration in end-stage renal disease with T1rho mapping and its comparison to voxel based measurement

Lin Wang[1] and Shenghong Ju[1]

[1]Radiology, Zhongda hospital, Medical school of Southeast university, Nanjing, People's Republic of China

It is reported that the brain always be an injured target organ in end-stage renal disease (ESRD) patients, a series of pathophysiologic changes easily make the iron accumulate in brain and accelerate the brain degeneration, which results in the brain cognitive function decline. T1rho relaxation time can reflect the changes of the macromolecular substance content and can be shorten by the Paramagnetic component, which makes it the ability to distinguish the healthy controls from ESRD patients. Voxel based measurement as a classical methods to verify the volume of each brain section, which can be also used to represent the structure of the brain. Combined with the results of neuropsylogical tests, T1rho mapping can better characterize the hippocampus in ESRD patients and the conclusions give a support for considering that the brain function changes earlier than structure changes.

2328 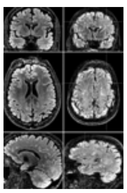

Evaluation of PROspective MOtion correction on high-resolution 3D-FLAIR acquisitions in epilepsy patients

Sjoerd B Vos[1,2], Caroline Micallef[3], Frederik Barkhof[1,3,4], Andrea Hill[2,5], John S Duncan[2,5], and Sebastien Ourselin[1,6]

[1]Translational Imaging Group, CMIC, University College London, London, United Kingdom, [2]Epilepsy Society MRI Unit, Chalfont St Peter, United Kingdom, [3]Neuroradiological Academic Unit, Department of Brain Repair and Rehabilitation, UCL Institute of Neurology, London, United Kingdom, [4]Department of Radiology and Nuclear Medicine, VU University Medical Center, Amsterdam, Netherlands, [5]Department of Clinical and Experimental Epilepsy, UCL Institute of Neurology, London, United Kingdom, [6]Dementia Research Centre, UCL Institute of Neurology, London, United Kingdom

FLAIR is the single most sensitive MRI contrast to detect lesions underlying focal epilepsies but 3D sequences used to obtain isotropic high-resolution images are susceptible to motion. PROspective MOtion correction (PROMO) was applied to 3D-FLAIR scans in epilepsy patients to evaluate clinical benefit. Two radiologists reviewed 40 scans without and 80 with PROMO assessing six criteria on a seven-point Likert scale. PROMO scans can achieve near-identical image quality as nonPROMO scans, but intensity inhomogeneity was generally poor using PROMO. The percentage of scans with bad image quality was 4-fold lower with PROMO than without on the other five criteria.

2329 

Brain iron accumulation in Wilson disease measured by QSM and MR relaxometry

Monika Dezortova[1], Vit Herynek[1], Julio Acosta-Cabronero[2], Lenka Kotackova[3], Daniela Zahorakova[4], Simon Daniel Robinson[5], Filip Jiru[1], Radan Bruha[6], Zdenek Marecek[7], Milan Hajek[1], and Petr Dusek[8]

[1]MR-Unit, Dept Diagnostic and Interventional Radiology, Institute for Clinical and Experimental Medicine, Prague, Czech Republic, [2]German Center for Neurodegenerative Diseases, Magdeburg, Germany, [3]Institute of Clinical Biochemistry and Laboratory Diagnostics, Charles University in Prague, 1st Faculty of Medicine and General University Hospital, Prague, Czech Republic, [4]Dept Pediatrics and Adolescent Medicine, Charles University in Prague, 1st Faculty of Medicine and General University Hospital, Prague, Czech Republic, [5]Dept Biomedical Imaging and Image guided Therapy, Medical University of Vienna, Vienna, Austria, [6]4th Dept Internal Medicine, Charles University in Prague, 1st Faculty of Medicine and General University Hospital, Prague, Czech Republic, [7]KlinMed, Prague, Czech Republic, [8]Dept Neurology and Center of Clinical Neuroscience, Charles University in Prague, 1st Faculty of Medicine and General University Hospital, Prague, Czech Republic

Relaxometry and quantitative susceptibility mapping were used in patients with neurologic symptoms of Wilson disease (WD) that leads to copper metabolism disturbances and its gradual accumulation in liver and brain. These quantitative MR techniques revealed decreased T2 relaxation times in the basal ganglia, higher susceptibility in the deep gray matter nuclei and no T1 changes. It indicates presence of insoluble para- or superparamagnetic compounds, presumably in a form of hemosiderin. These deposits appear to be not related to the ceruloplasmin oxidase activity nor with the severity of neurological symptoms.

2330 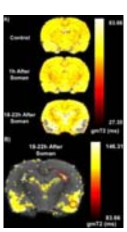

A Chemical Warfare Nerve Agent Causes Regional Changes in Brain T2—Consistent with Localized Edema

Kevin Lee[1], Sara Bohnert[2], Cory Vair[2], Ying Wu[1], John Mikler[2], and Jeff Dunn[1]

[1]Radiology, University of Calgary, Calgary, AB, Canada, [2]National Defence, Defence Research And Development Canada, Suffield, AB, Canada

Chemical Warfare Nerve Agents (NAs) are toxic compounds that have the potential to cause mass casualty scenarios. The United Nation has categorized NAs as a weapon of mass destruction. The immediate and short-term effects of NA exposure is well understood, however, our understanding of the neurological effect at a sub-lethal dose is limited. We have found localized edema that may serve as a good biomarker to test novel treatments.

2331

Enhanced visualization of lesions in focal cortical dysplasia using the fluid and white-matter suppression (FLAWS) sequence

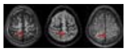

Xin Chen[1], Tianyi Qian[2], Tobias Kober[3,4,5], Nan Chen[1], and Kuncheng Li[1]

[1]Radiology, Xuanwu Hospital Capital Medical University, Beijing, People's Republic of China, [2]MR Collaborations NE Asia, Siemens Healthcare, Beijing, People's Republic of China, [3]Advanced Clinical Imaging Technology, Siemens Healthcare AG, Lausanne, Switzerland, [4]Radiology, University Hospital (CHUV), Lausanne, Switzerland, [5]LTS5, École Polytechnique Fédérale de Lausanne, Lausanne, Switzerland

High contrast in the lesion area is one of the most important prognostic factors for focal cortical dysplasia (FCD). The fluid and white-matter suppression (FLAWS) sequence provides two sets of 3D contrasts from one acquisition: one nulls the white-matter signal, the other nulls the cerebral spinal fluid signal. A new image (the FLAWS contrast) calculated from these two images may enhance the visualization of FCD lesion features, specifically the blurred grey-white matter interface and the transmantle sign. In this study, we assessed the ability of FLAWS to visualize FCD lesions. Our results demonstrate that FLAWS is sensitive to lesional tissue, especially the transmantle sign, providing additional value in MR-based FCD diagnostics.

2332 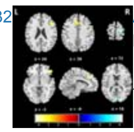

Altered whole brain connectivity related to time of drug usage in methamphetamine abusers

Ming Zhou[1], Xiaobo Zhou[2], Xinyu Hu[1], Lu Lu[1], Lianqing Zhang[1], Jing Li[2], Jiayu Sun[1], and Xiaoqi Huang[1]

[1]Department of Radiology, Huaxi MR Research Center, Chengdu, People's Republic of China, [2]Department of Psychiatry, West China Hospital, Sichuan Univers

The current study aimed to use a novel graph-
theory approach known as degree centrality to help diagnose methamphetamine abusers. Our findings identified increased degree centrality in right middle front

---

2333 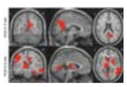

Could ASL separate MCS from VS in patients with DOC ?

Bing Wu[1], Yi Yang[2], Shuai Zhou[1], Hai Song[1], Lubin Wang[3], Jianghong He[2], Zheng Yang[3], and Xinhuai Wu[1]

[1]Radiology Dept., PLA Army General Hospital, Beijing, People's Republic of China, [2]Neurosurgery Dept., PLA Army General Hospital, Beijing, People's Republic of China, [3]Academy of Military Medical Sciences, Beijing, People's Republic of China

This study used 3D pseudo-continuous arterial spin labeling (pcASL) to compare cerebral blood flow (CBF) patterns in minimally conscious state (MCS) patients with those in vegetative state (VS) ones. The results identified different CBF patterns within specific brain regions in VS patients compared with MCS. ASL may serve as an adjunctive method to separate MCS from VS in DOC patients, and could be used in longitudinal assessments of patients with severe brain injuries.

2334 

The effect of Amantadine on Persistent Vegetative State patients: an fMRI pilot study

Cheuk Ying Tang[1], Xiao Wei Chen[2], Saiming Cheng[3], Victoria X Wang[4], Johnny C Ng[4], Edmund Wong[5], and Zhen Lan Li[6]

[1]Radiology & Psychiatry, Ichan School of Medicine at Mount Sinai, New York, NY, United States, [2]Rehabilitation medicine, The First Hospital of Jilin University, Changchun, People's Republic of China, [3]Radiology, The First Hospital of Jilin University, [4]Radiology, Icahn School of Medicine at Mount Sinai, [5]Icahn School of Medicine at Mount Sinai, [6]Rehabilitation Medicine, The First Hospital of Jilin University

Task based fMRI and resting state scans were acquired on Persistent Vegetative State Patients before and after the administration of Amandatine. Significant clusters of activation was detected post treatment.

2335 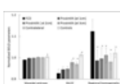

Attenuated low frequency oscillations in focal cortical dysplasia

Lalit Gupta[1], Paul A Hofman[1], René M Besseling[2], Jacobus F Jansen[1], and Walter H Backes[1]

[1]Departments of Radiology and Nuclear Medicine, Maastricht University Medical Center, Maastricht, Netherlands, [2]Department of Electrical Engineering, Eindhoven University of Technology, Eindhoven, Netherlands

The objective was to assess the time-signature of spontaneous BOLD brain fluctuations in patients with focal cortical dysplasia (FCD) and to compare these with other regions and healthy controls. Whole cerebrum resting-state functional MRI time-series were analyzed using three different BOLD measures: wavelet entropy, regional homogeneity and fractional amplitude of low frequency fluctuations. All the three BOLD measures indicated attenuated low frequency oscillations in FCD lesions compared to controls. Also abnormal BOLD activity was found in the proximal and contralateral region, which can complicate the interpretation on what regions are functionally normal, functionally connected or abnormal in patients with FCD.

2336 

Wired minds: The neural underpinning of the entrepreneurial brain

Paulo Reis Rodrigues[1], David Moreno-Dominguez[1], Marc Ramos[1], Pablo Villoslada[2], David Gallardo-Pujol[3], and Vesna Prčkovska[1]

[1]Mint Labs, Barcelona, Spain, [2]IDIBAPS, Hospital Clinic, Barcelona, Spain, [3]Department of Personality, Universitat Barcelona, Barcelona, Spain

Very little is known on how the entrepreneurial brain works. While previous work has examined only certain personality traits at a time, some of which are discussed here, this work aims to take an overall view of the traits found in an entrepreneur (determined by psychometric evaluations) and compare these to structural connectivity levels and cortical volumes in certain areas of the brain.

2337 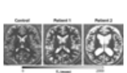

Cortical thickness in relation to m.3243A>G mutation load in MELAS syndrome

Roy Haast[1], Dimo Ivanov[1], Jacobus F.A. Jansen[2], Hubert Smeets[3], Irenaeus de Coo[4], Elia Formisano[1], and Kâmil Uludağ[1]

[1]Department of Cognitive Neuroscience, Maastricht University, Maastricht, Netherlands, [2]Department of Radiology, Maastricht University Medical Centre, Maastricht, Netherlands, [3]Department of Genetics and Cell Biology, Maastricht University, Maastricht, Netherlands, [4]Department of Neurology, Erasmus MC, Rotterdam, Netherlands

The m.3242A>G mitochondrial mutation is known to cause the MELAS syndrome. A group of MELAS patients was scanned using multi-parameter quantitative 7T MRI to assess brain changes related to mutation load and disease duration. Here, we focused on cortical thickness differences between control subjects and MELAS patients and within patients as a function of mutation load. MELAS patients were characterized by a reduced cortical thickness compared to control subjects in several regions. Within these regions, cortical thickness decreases with increasing mutation load for the fusiform and planum temporal gyri, which are involved in visual working memory and auditory processing, respectively.

Traditional Poster

Aging Brain & Dementia

Exhibition Hall 2338-2378 — Wednesday 13:45 - 15:45

2338

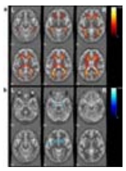

Age-related change of the whole brain T1 relaxation time: voxel-wise study with MP2RAGE

Gosuke Okubo[1], Tomohisa Okada[1], Akira Yamamoto[1], Yasutaka Fushimi[1], Tsutomu Okada[1], and Kaori Togashi[1]

[1]Department of Diagnostic Imaging and Nuclear Medicine, Kyoto University Graduate School of Medicine, Kyoto, Japan

Correlation was investigated between normal aging and T1 relaxation time in the deep gray matter with MP2RAGE sequence using voxel-based analysis (VBA) and regions-of-interest (ROIs) focusing on the deep gray matter (GM). Seventy healthy subjects were included. In VBA, linear correlation was explored, whereas second order regression was added in ROI analysis. The results showed relationship that varied among deep GM structures. Those findings will shed light on further investigation of T1 relaxation time in patient groups.

2339

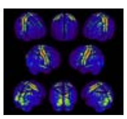

Factors influencing the detection of age-dependent variations of cortical myelin by MP2RAGE at 9.4T.

Gisela E Hagberg[1,2], Jonas Bause[2], Thomas Ethofer[1,3], Philipp Ehses[2], Thomas Dresler[1], Cornelia Herbert[4], Rolf Pohmann[2], gunamony Shajan[2], Andreas Fallgatter[1], Marina Pavlova[1], and Klaus Scheffler[1,2]

[1]Biomedical Magnetic Resonance, University Hospital Tübingen, Tübingen, Germany, [2]High Field Magnetic Resonance, Max-Planck Institute for Biological Cybernetics, Tübingen, Germany, [3]3General Psychiatry&Psychotherapy, University Hospital Tübingen, Tübingen, Germany, [4]University Ulm, Germany

Detection of subtle variation of the myeloarchitecture within the cerebral cortex may be feasibile with high-field mapping of the longitudinal relaxation time. However, besides myelin other factors like iron or variation of the grey matter volume may impact this MR parameter. In the present work we propose a model that includes and quantifies these factors. We found a regionally dependent, continuous increase from early adulthood into the middle ages that tentatively can be assigned to myelin.

2340

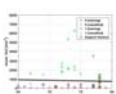

Individual Evaluation System Development Concept Research for Personalized Brain Aging Process Using Machine Learning

Kyung Mi Lee[1], Hyug-Gi Kim[1], Sung Kyoung Moon[1], Eui Jong Kim[1], and Woo Suk Choi[1]

[1]Radiology, Kyung Hee University Hospital, Seoul, Korea, Republic of

White matter hyperintensities (WMH) is one of the important characteristics of cerebral small vessel disease (cSVD). To diagnosis individual WMH evaluation method and investigate the degree of WMH form using MR image, we proposed that machine learning based on WMH group classification and individual diagnosis system.

2341

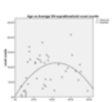

Neuromelanin-weighted MRI in revealing human development and age-related changes in locus coeruleus and substantial nigra

Yue Xing[1,2], Abdul Halim Sapuan[1], Robert Dineen[1,3], Andrew Cooper[4], and Dorothee Auer[4]

[1]1Radiological Sciences, Division of Clinical Neuroscience, University of Nottingham, Queen's Medical Centre, University of Nottingham, Nottingham, United Kingdom, [2]Sir Peter Mansfield Imaging Centre, School of Medicine, University of Nottingham, Nottingham, United Kingdom, [3]Sir Peter Mansfield Imaging Centre, School of Medicine, University of Nottingham, United Kingdom, [4]Radiological Sciences, Division of Clinical Neuroscience, University of Nottingham, Queen's Medical Centre;, University of Nottingham, Nottingham, United Kingdom

Rapid neuromelanin-weighted MR imaging sequence was performed to noninvasively inspect the physiological changes of substantial nigra and Locus ceruleus across a wide range of age in healthy subjects using neuromelanin-sensitive MRI for the first time.

2342

Characterizing brain iron deposition in patients with subcortical vascular mild cognitive impairment using quantitative susceptibility mapping: A potential biomarker

Yawen Sun[1], Yan Zhou[1], Yao Wang[1], Xu Han[1], Weina Ding[1], Yong Zhang[2], Qun Xu[3], and Jianrong Xu[1]

[1]Department of Radiology, Ren Ji Hospital, School of Medicine, Shanghai Jiao Tong University, Shanghai, People's Republic of China, [2]Ge Applied Science Laboratory, GE Healthcare, Shanghai, People's Republic of China, [3]Department of Neurology, Ren Ji Hospital, School of Medicine, Shanghai Jiao Tong University, Shanghai, People's Republic of China

The presence and pattern of iron accumulation in subcortical vascular mild cognitive impairment (svMCI) or their effects on cognition has rarely been investigated. The purposes of the present study were to investigate brain iron deposition in deep gray matter nuclei in svMCI patients using quantitative susceptibility mapping (QSM) and its correlation with the severity of cognitive impairment. Susceptibility values were found to be elevated within bilateral hippocampus and right putamen in svMCI group compared with controls, which were related to cognitive measurements. Our result suggests that brain iron deposition which relation to cognition indicates the clinical relevance of the biomarker.

2343

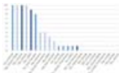

Early detection of Alzheimer's Disease using a combined index of gray matter texture

Subin Lee[1], Hyunna Lee[2], Heesoog Kim[1], and Ki Woong Kim[1,3,4]

[1]Brain & Cognitive Sciences, Seoul National University, Seoul, Korea, Republic of, [2]Asan Medical Center, Seoul, Korea, Republic of, [3]Department of Neuropsychiatry, Seoul National University Bundang Hospital, Seoul, Korea, Republic of, [4]College of Medicine, Seoul National University, Seoul, Korea, Republic of

Development of sensitive markers that can detect Alzheimer's Disease at its pre-dementia stages is of critical importance. We hypothesized that altered cytoarchitecture caused by AD pathology would lead to a subtle altered pattern of voxel intensities on MRI which could be detected by texture analysis. In a training set of 111 AD and 141 normal controls, we extracted a set of texture features from core regions affected by pathology – precuneus, posterior cingulate cortex, hippocampus – that could efficiently discriminate between the two groups (AUC=0.875, *p*<0.001) as well as predict MCI/AD conversion from the normal stage (AUC=0.716, *p*=0.031).

2344

The profile pattern of white matter hyperintensities (WMH) has a primary role on discriminating the cognitive function.

Heisoog Kim[1,2], Jiwon Han[2], Hyunna Lee[3], and Ki Woong Kim[2]

[1]brain & cognitive sciences, Seoul national university, Seoul, Korea, Republic of, [2]Psychiatry, Seoul National University Budang Hospital, Budang, Korea, Republic of, [3]Asan Medical Center, Korea, Republic of

The areas in cerebral white matter appearing hyperintense on T2-weighted and fluid-attenuated inverse recovery (FLAIR) MRI are commonly referred to as white matter lesions (WMLs). Diverse scores and rating systems have been used for evaluating WMLs. However, these visual rating scales are still qualitative and subjective, leading to low reliability and reproducibility. The purpose of this study is to investigate the relation between cognitive functions and WMLs clustered by their profiles of distance from the ventricle, establishing the quantitative and objective evaluation of WMLs.

2345

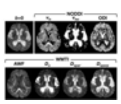

Diffusion microstructural imaging of reversible and irreversible changes within the corticospinal tract in idiopathic normal pressure hydrocephalus

Kouhei Kamiya[1], Masaaki Hori[2], Ryusuke Irie[2], Masakazu Miyajima[3], Madoka Nakajima[3], Koji Kamagata[2], Kouhei Tsuruta[2], Yuichi Suzuki[1], Asami Saito[2], Misaki Nakazawa[4], Harushi Mori[1], Akira Kunimatsu[1], Hajime Arai[3], Shigeki Aoki[2], and Osamu Abe[1]

[1]Department of Radiology, the University of Tokyo, Tokyo, Japan, [2]Department of Radiology, Juntendo University School of Medicine, Tokyo, Japan, [3]Department of Neurosurgery, Juntendo University School of Medicine, Tokyo, Japan, [4]Department of Radiological Sciences, Graduate School of Human Health Sciences, Tokyo Metropolitan University, Tokyo, Japan

Microstructural changes of the corticospinal tract (CST) in idiopathic normal pressure hydrocephalus (iNPH) before and after CSF shunt surgery were studied using NODDI and WMTI. Pathological increase of orientational coherence and its postoperative normalization were shown, indicating axon stretching and its recovery. To the contrary, decrease of axon density was present in iNPH and remained after the surgery. Simulation using undulating cylinder model demonstrated both NODDI and WMTI can separate the effects from axon density and undulation. These results suggest possibilities of diffusion MRI to distinguish between reversible and irreversible microstructural changes in iNPH, and raise expectation for prediction of treatment outcome.

2346

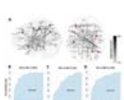

Global Change of Intrinsic Functional Networks as an Imaging biomarker of Alzheimer's disease

Chia-Feng Lu[1,2,3], Wen-Jin Hsieh[1,4], Yu-Chieh Jill Kao[1,2], Paul Blakeley[1,5], Fei-Ting Hsu[1,4], Hua-Shan Liu[1,6], Ping-Huei Tsai[1,2,4], Li-Chun Hsieh[1,4], and Cheng-Yu Chen[1,2,4]

[1]Translational Imaging Research Center, College of Medicine, Taipei Medical University, Taipei, Taiwan, [2]Department of Radiology, School of Medicine, College of Medicine, Taipei Medical University, Taipei, Taiwan, [3]Department of Biomedical Imaging and Radiological Sciences, National Yang-Ming University, Taipei, Taiwan, [4]Department of Medical Imaging, Taipei Medical University Hospital, Taipei, Taiwan, [5]Department of Medical Research, Taipei Medical University Hospital, Taipei, Taiwan, [6]School of Biomedical Engineering, College of Biomedical Engineering, Taipei Medical University, Taipei, Taiwan

The change of whole-brain connectivity during resting state can be a reliable feature in discriminating patients with Alzheimer's disease (AD) from patients with mild cognitive impairment and cognitively healthy elders. Significant correlations between resting-state functional connectivity and cognitive decline measured by Mini-Mental State Examination (MMSE) were further identified.

2347

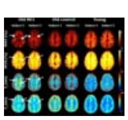

Demyelination in Mild Cognitive Impairment

Mustapha Bouhrara[1], David A. Reiter[1], Christopher M. Bergeron[1], Linda M. Zukley[1], Susan M. Resnick[1], Stephanie Studenski[1], Josephine M. Egan[1], Luigi Ferrucci[1], and Richard G. Spencer[1]

[1]National Institute on Aging (NIA), National Institutes of Health (NIH), Baltimore, MD, United States

An emerging hypothesis suggests that the underlying pathophysiology of mild cognitive impairment (MCI) involves alterations in brain myelination. These alterations may represent an important correlate of dementia. Several studies have examined this correlation; however, these earlier analyses were performed using non-myelin-specific methods such as relaxation times, magnetization transfer and diffusion. This greatly complicates the interpretation of such imaging results in terms of myelin content. Our results show direct evidence of MWF alterations and loss in MCI using a direct measure of myelin-bound water.

2348

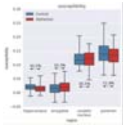

No significant increase of magnetic susceptibility found in subcortical gray matter of patients with Alzheimer's Disease

Jakob Meineke[1], Fabian Wenzel[1], Iain D Wilkinson[2], and Ulrich Katscher[1]

[1]Philips Research Europe, Hamburg, Germany, [2]University of Sheffield

Quantitative Susceptibility Mapping (QSM) and volumetry are used to study the deep gray-matter nuclei of patients with Alzheimer's Disease (AD) and healthy control subjects. QSM is performed using "Joint background-field removal and segmentation-Enhanced Dipole Inversion" (JEDI), which leverages the information from automated model-based segmentation and allows the compact single-step formulation of the ill-posed inversion problem of QSM. For comparison QSM is also performed using L1-MEDI from the MEDI-Toolbox. The tissue magnetic susceptibility shows no significant difference between the Alzheimer group compared to the healthy control group. In contrast, the normalized volume of segmented gray-matter regions is significantly reduced in AD patients.

2349

Using Calibrated Proton Density Imaging to Measure Blood-Brain Partition Coefficient in Aging and Alzheimer's Disease Mice

Scott William Thalman[1], David Powell[2,3], Andrew Shen[4], Anika M.S. Hartz[4,5], and Ai-Ling Lin[1,4,6]

[1]Biomedical Engineering, University of Kentucky, Lexington, KY, United States, [2]Biomedical Engineering, University of Kentucky, KY, United States, [3]Magnetic Resonance Imaging and Spectroscopy Center, [4]Sanders-Brown Center on Aging, University of Kentucky, KY, United States, [5]Molecular and Biomedical Pharmacology, University of Kentucky, [6]Pharmacology and Nutritional Sciences, University of Kentucky

In this study we determine the blood-brain partition coefficient (BBPC) in aging C57Bl6/N mice and the transgenic 129S6/Tg2576 mouse model of Alzheimer's disease using a calibrated proton density imaging approach. Aging mice demonstrate a 5.5% reduction in BBPC compared to young mice (0.94±0.04 mL/g vs 0.99±0.04 mL/g, $p = 0.02$), however Tg2576+ mice preliminarily demonstrate an elevated BBPC compared to wild-type controls (01.03±0.04 mL/g vs 1.00±0.05 mL/g). These high quality BBPC maps acquired much faster than previously reported could potentially be used to correct cerebral blood flow measurements derived from arterial spin labeling.

2350

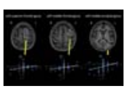

Neuroanatomical substrates that account for worsening performance in the Clock-Drawing Test in mild cognitive impairment

Satoshi Nakajima[1,2], Susumu Mori[1,3], Kaori Togashi[2], and Kenichi Oishi[1]

[1]Radiology, Johns Hopkins University School of Medicine, Baltimore, MD, United States, [2]Diagnostic Imaging and Nuclear Medicine, Kyoto University Graduate School of Medicine, Kyoto, Japan, [3]F. M. Kirby Research Center for Functional Brain Imaging, Kennedy Krieger Institute, Baltimore, MD, United States

The Clock-Drawing Test (CDT) is used to screen and select cognitively impaired individuals for further evaluation. For the clinical interpretation of the CDT, an understanding of the neuroanatomical substrates that account for a decline in the CDT score is essential. We investigated the relationships between regional volume loss and a decline in the CDT score in two years. Atrophy in the left prefrontal and middle-occipital gyri was correlated with a decline in the CDT score. The result validated the use of the CDT, combined with memory tests that evaluate parieto-temporal functions, as part of an overall cognitive screening.

2351

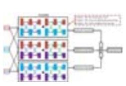

Deep Cross-Modal Feature Learning and Fusion for Early Dementia Diagnosis

Tao Zhou[1], Kim-Han Thung[1], and Dinggang Shen[1]

[1]Department of Radiology and BRIC, University of North Carolina at Chapel Hill, Chapel Hill, NC, United States

Studies have shown that neuroimaging data (e.g., MRI, PET) and genetic data (e.g., SNP) are associated with the Alzheimer's Disease (AD). However, to achieve a more accurate AD diagnosis model using these data is challenging, as these data are heterogeneous and high-dimensional. Thus, we first used region-of-interest based features and deep feature learning to reduce the dimension of the neuroimaging and SNP data, respectively. Then we proposed a deep cross-modal feature learning and fusion framework to fuse the high-level features of these data. Experimental results show that our method using MRI+PET+SNP data outperforms other comparison methods.

2352

Use of population-specific atlases for brain morphometry: benefits in Alzheimer's Disease diagnosis decision support for Chinese patients

Bénédicte Maréchal[1,2,3], Peipeng Liang[4,5,6], Lin Shi[7], Tianyi Qian[8], Defeng Wang[5,6], Tobias Kober[1,2,3], Alexis Roche[1,2,3], and Kuncheng Li[4]

[1]Advanced Clinical Imaging Technology, Siemens Healthcare HC CEMEA SUI DI PI, Lausanne, Switzerland, [2]Department of Radiology, CHUV, Lausanne, Switzerland, [3]LTS5, EPFL, Lausanne, Switzerland, [4]Department of Radiology, Xuanwu Hospital, Capital Medical University, Beijing, China, [5]Research Center for Medical Image Computing, Department of Imaging and Interventional Radiology, The Chinese University of Hong Kong, Shatin, New Territories, Hong Kong, China, [6]Shenzhen Research Institute, The Chinese University of Hong Kong, Shenzhen, China, [7]Department of Medicine and Therapeutics, The Chinese University of Hong Kong, Shatin, NT, Hong Kong, [8]MR Collaboration Northeast Asia, Siemens Healthcare, Beijing, China

We investigate the potential of a Chinese-specific brain atlas derived from a large MR database of healthy Chinese subjects to accurately support Alzheimer's Disease diagnosis using automated brain volumetry in the Chinese population. Our experiments show that disease detection sensitivity is higher than when using either a Westerner-specific atlas and normative ranges or combining a Westerner atlas with Chinese-specific normative ranges. These findings suggest that population-specific models improve the reliability of medical decision support systems based on automated brain volumetry.

2353

Prediction of early stage of AD based on functional connectivity network characteristics: an fMRI-based study

Zhizheng Zhuo[1,2], Zhuqing Long[1], Bin Jing[1], Xiangyu Ma[1], Han Liu[1], Jianxin Dong[1], Xiao Mo[1], Qi Yan[1], and Haiyun Li[1]

[1]Bio-medical Engineering, Capital Medical University, Beijing, People's Republic of China, [2]Clinical Science, Philips Healthcare, Beijing, People's Republic of China

MCI (Mild Cognitive Impairment) is a pre-stage of Alzheimer's Disease (AD). And the early detection of MCI is important for early treatment of AD patients. In this work, prediction efficiency of early stage of AD based on the functional connectivity network characteristics was evaluated by using a couple of classifiers with AAL_90 and AAL_1024 templates. The results showed that brain functional characteristics were effective in the prediction of MCI with a SVM-based classifier. And a more fine template could improve prediction accuracy.

2354

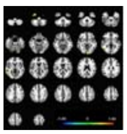

Acupoint-Specific Effect of Acupuncture in Alzheimer's Disease: A Functional MRI Study

Yi Shan[1], Yunpeng Bian[2], Zhiqun Wang[3], Zhilian Zhao[1], Mo Zhang[1], Jie Lu[1], and Kuncheng Li[1]

[1]Xuanwu hospital, Capital Medical University, Beijing, People's Republic of China, [2]University of Science and Technology of China, Hefei, China, [3]Oriental Hospital，Beijing University of Chinese Medicine, Beijing, China

Acupuncture has been a major therapeutic method in Chinese medicine for treating Alzheimer's disease (AD) with validation and safety. In this study, we use functional magnetic resonance imaging (fMRI) to investigate the acupoint-specific effect of acupuncture in treating for AD. We found acupuncture at real acupoints activated brain areas primarily in the left uvula, right superior temporal gyrus and right uncus, while acupuncture at sham acupoints only activated areas in the left insula. These results showed that acupoint-specific effect of acupuncture presented by fMRI may help to facilitate its clinical use in AD treatment.

2355

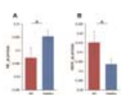

Disrupted brain connectivity networks in Alzheimer's Disease

Xiaoqing Ji[1], Haiyang Geng[2,3], Rui Li[1], Le He[1], and Chun Yuan[1,4]

[1]Center for Biomedical Imaging Research, Tsinghua University, Beijing, People's Republic of China, [2]Institute of Affective and Social Neuroscience, Shenzhen University, Shenzhen, People's Republic of China, [3]Neuroimaging Center, University Medical Center Groningen, University of Groningen, Groningen, Netherlands, [4]Department of Radiology, University of Washington, Seattle, WA, United States

In this study, we used graph theory-based approaches to explore the topological organization of whole brain network in Alzheimer's Disease. We performed resting state fMRI on 6 AD patients and 19 normal controls. Topological properties such as small-world, efficiency and nodal centrality were calculated and nonparametric permutation tests were further used for group comparisons. The results showed that high-level cognitive regions including parietal cortex, vmPFC, precuneus and emotional regions including caudate and thalamus were changed in the topological metrics, this may be a biomarker for AD classification.

2356

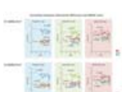

Evaluating glymphatic system by diffusion images: Alzheimer's disease cases analyzed by Diffusion Tensor Image analysis Along Perivascular Space (DTI-ALPS)

Toshiaki Taoka[1], Yoshitaka Masutani[2], Hisashi Kawai[1], Toshiki Nakane[1], Kiwamu Matsuoka[3], Fumihiko Yasuno[3], and Shinji Naganawa[1]

[1]Dept. of Radiology, Nagoya University, Nagoya, Japan, [2]Dept. of Biomedical Information Sciences, Hiroshima City University, Hiroshima, Japan, [3]Dept. of Psychiatry, Nara Medical University, Kashihara, Japan

We tried to evaluate the activity of human glymphatic system by diffusion images. Our subjects were Alzheimer's disease (AD), in which it is known that the activity of the glymphatic system is impaired in animal experiments. We evaluated the diffusivity along the perivascular spaces as well as projection fibers and association fibers, and correlated them with MMSE score. There were significant positive correlation between diffusivity along perivascular spaces and MMSE score, indicating impaired water diffusivity related to AD severity. Our result may indicate that activity of the glymphatic system can be evaluated by diffusion images.

2357

Can EPVS reflect Cerebral Blood Flow and Cognitive State in MCI and AD Patients?

Jin Shang[1], Liu Yang Yingqiu[1], Yanwei Miao[1], and weiwei wang[1]

[1]First Affiliated Hospital of Dalian Medical University, Dalian, People's Republic of China

EPVS may reflect underlying cerebral small vessel disease. We assumed the presence of EPVS were associated with cerebral blood flow (CBF) reduction ,and can accurately reflect the cognitive state.The study verifies a good coherence between EPVS and CBF in BG and CS of AD patients , and furthermore reflects of EPVS as the biomarker of cognitive status to a certain extent.

2358

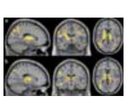

A Potential Biomarker of Alzheimer's Disease: T1sat of the Thalamus

Parshant Sehrawat[1], H. Michael Gach[2], Wenna Duan[1], Andrea Gillman[3], James T. Becker[4], Oscar L. Lopez[5], and Weiying Dai[1]

[1]Department of Computer Science, State University of New York at Binghamton, Binghamton, NY, United States, [2]Department of Radiation Oncology, Washington University, St Louis, MO, United States, [3]Center of Neuroscience, University of Pittsburgh, PA, United States, [4]Department of Psychology, University of Pittsburgh, PA, United States, [5]Department of Psychiatry and Neurology, University of Pittsburgh, PA, United States

Biomarkers for Alzheimer's disease (AD) are crucial for early diagnosis and treatment monitoring once therapies become available. In this study, the spin-lattice relaxation time in the rotating frame with (T_{1sat}) and without (T_{1nosat}) off-resonance saturation was measured at 1.5 T in the cardiovascular health study cognition study cohort. Cross-sectional and longitudinal studies of the normalized difference (ΔT_{1RF}) between T_{1sat} and T_{1nosat} revealed regions of statistical significance in the brain that are associated with dementia pathogenesis. ΔT_{1RF} changes in the thalamus were consistent for the cross-sectional and longitudinal studies, indicating that ΔT_{1RF} could be a promising imaging biomarker for AD.

2359

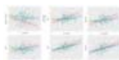

Hippocampal atrophy is correlated to cerebrospinal fluid levels of ceruloplasmin, neuroinflammation and total tau in Alzheimer's disease

Azhaar Ahmad Ashraf[1] and Dr Po-Wah So[1]

[1]Neuroimaging, Institute of Psychiatry, Psychology and Neuroscience, King's College London, London, United Kingdom

The aim of the study was to characterise the relationship between cerebrospinal fluid (CSF) iron regulatory proteins (ferritin, ceruloplasmin), neuroinflammation and MRI-derived hippocampal volume in healthy controls, mild cognitive impairment and Alzheimer's disease subjects. Ceruloplasmin positively correlated with neuroinflammation and ferritin in MCI and AD while in the latter group, it was negatively correlated with hippocampal volume. Ferritin positively correlated with neuroinflammation in HC and AD but also with tau levels in MCI. Iron dyshomeostasis, neuroinflammation and tau metabolism may increase hippocampal atrophy and aggravate AD pathogenesis.

2360

Altered Hippocampal Functional Connectivity with PCC in SCI, MCI and AD

Hui Zhang[1], Joseph Shiu-Kwong Kwan[2], Pui-Wai Chiu[1,3], Edward S. Hui[1], Queenie Chan[4], and Henry Ka-Fung Mak[1,5,6]

[1]Department of Diagnostic Radiology, The University of Hong Kong, Hong Kong, Hong Kong, [2]Department of Medicine, The University of Hong Kong, Hong Kong, Hong Kong, [3]State Key Laboratory of Brain and Cognitive Sciences, The University of Hong Kong, [4]MR Clinical Science, Philips Healthcare, Hong Kong, Hong Kong, [5]State Key Laboratory of Brain and Cognitive Sciences, The University of Hong Kong, Hong Kong, Hong Kong, [6]Alzheimer's Disease Research Network, The University of Hong Kong, Hong Kong, Hong Kong

Brain imaging research has elucidated the structural and functional changes at the clinical stages of AD and MCI, however, the characteristics of resting-state functional connectivity of SCI are largely unstudied. Hippocampus is among the first regions targeted by AD pathology. In this study, we employed resting state fMRI to study the connectivity between hippocampus and posterior cingulate cortex in SCI, MCI and AD groups. In the preliminary results, the connectivity between hippocampus and PCC in SCI was found stronger than control and other two neurodegenerative groups which may suggest that compensatory mechanisms providing preserved hippocampal pathway in SCI.

2361

Brain iron load, as measured by Quantitative Susceptibility Mapping, promotes beta-Amyloid associated functional brain change in elderly subjects but not in Super-Agers

Jiri MG van Bergen[1], Xu Li[2], Frances-Catherine Quevenco[1], Sandra Leh[1], Anton F Gietl[1], Valerie Treyer[1,3], Rafeal Meyer[1], Alfred Buck[3], Roger M Nitsch[1], Peter CM van Zijl[2], Christoph Hock[1], and Paul G Unschuld[1]

[1]Institute for Regenerative Medicine, University of Zurich, Zurich, Switzerland, [2]F.M. Kirby center for Functional Brain Imaging, Kennedy Krieger Institute and Johns Hopkins School of Medicine, MD, United States, [3]Department of Nuclear Medicine, University of Zurich, Switzerland

To investigate whether brain iron load has an impact on Aβ associated functional brain change, this study investigated a large sample of cognitively healthy adults including 44 Super-Agers (subjects over the age of 85 without cognitive impairments) using simultaneous assessment of Amyloid-PET for Aβ-plaque-density, QSM for estimation of iron load and resting-state-fMRI.

Our findings indicate that the combination of Aβ-plaque-density with other neurodegenerative change (iron), has an impact on brain functionality, reflected by significant changes of resting state functional connectivity. Additionally, Aβ-plaque-density had no significant effect on functional connectivity in Super-Agers.

2362

Demonstration of Abnormal Cortical Layers In Alzheimer's Disease Using Subtracted Tissue Attenuated Inversion Recovery (STAIR) Pulse Sequences

Shujuan Fan[1], Yajun Ma[1], Xing Lv[1], Jiang Du[1], Graeme M. Bydder[1], and Nikolaus M. Szeverenyi[1]

[1]Radioliogy, Univ. of California, San Diego, San Diego, CA, United States

The use of subtracted STIR images designed to null white and gray matter respectively is illustrated in formalin fixed brain samples at 11.7T. The images show the normal layers of the cerebral cortex with high contrast. The layers were less well seen, or not seen at all in Alzheimer's Disease samples. Use of MT pulses with the STIR sequences produces high positive and negative contrast on difference images. The STIR subtraction technique made have general application, and be used with different forms of data acquisition. It may also be useful in other clinical situations for demonstrating changes due to small differences in T1 in the presence of long T1 fluids.

2363

Motor cortex hypointensity on SWI is associated with APOE status in cognitive impaired patients

Mina Park[1], Yeonsil Moon[2], Seol-Heui Han[2], and Won-Jin Moon[1]

[1]Radiology, Konkuk University Medical Center, SEOUL, Korea, Republic of, [2]Neurology, Konkuk University Medical Center, SEOUL, Korea, Republic of

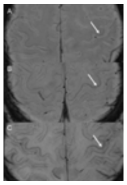

We evaluated the prevalence and its associated risk factors of motor cortex hypointensity on SWI in cognitive impaired patients. This retrospective study included 116 cognitively impaired patients (28 Alzheimer disease patients and 88 mild cognitive impaired patients). Among them, 83 patients showed positive motor cortex hypointensity on SWI and it was associated with age. Furthermore, the group with positive motor cortex hypointensity on SWI had less APOE4 allele carriers than negative group and this shows (+) APOE4 allele may act as an accelerating factor of cognitive decline even before iron accumulation starts to show changes in the motor cortex.

2364 

Racial differences in cerebral microcirculatory function and cognitive function

Junjie Wu[1], Ganesh Chand[2], Om Sharma[2], Deqiang Qiu[1], and Ihab Hajjar[2]

[1]Department of Radiology and Imaging Sciences, Emory University School of Medicine, Atlanta, GA, United States, [2]Department of Medicine, Emory University School of Medicine, Atlanta, GA, United States

We examined racial differences in cerebrovascular reactivity (CVR) to carbon dioxide and their associations with cognitive function among patients with mild cognitive impairment and hypertension. The results provide evidence for association between impaired CVR and executive dysfunction. Hypertensive African Americans have more compromised cerebral microcirculatory function compared to Caucasians.

2365 

Synergistic Effect of β-Amyloid and Microvascular Abnormality on Longitudinal Cognitive Decline in Elderly Subjects at Risk for Alzheimer's Disease (AD)

Jun Hua[1,2], M Wyss[3], J. M. G. van Bergen[4], S. J. Schreiner[4], S. C. Steininger[4], A. F. Gietl[4], A. Buck[5], R. M. Nitsch[4], K. P. Pruessmann[3], H. Lu[1,2], P. C. M. van Zijl[1,2], M. Albert[6], C. Hock[4], and P. G. Unschuld[4]

[1]Neurosection, Div. of MRI Research, Dept. of Radiology, Johns Hopkins University School of Medicine, Baltimore, MD, United States, [2]F.M. Kirby Research Center for Functional Brain Imaging, Kennedy Krieger Institute, Baltimore, MD, United States, [3]Institute for Biomedical Engineering, University of Zürich and ETH Zürich, Zürich, Switzerland, [4]Division of Psychiatry Research and Psychogeriatric Medicine, University of Zürich, Zürich, Switzerland, [5]Division of Nuclear Medicine, University of Zürich, Zürich, Switzerland, [6]Department of Neurology, Johns Hopkins University School of Medicine, Baltimore, MD, United States

Progressive impairment in multiple cognitive domains is a clinical hallmark of Alzheimer's Disease (AD), which is the most frequent cause for dementia in the elderly and is neuropathologically characterized by both cerebral β-amyloid (Aβ) accumulation and microvascular abnormalities. Here, we report significant co-localization of regions with microvascular abnormalities measured by arteriolar-cerebral-blood-volume (CBVa) MRI and Aβ accumulation measured by PiB-PET in elderly subjects at-risk for AD. Multiple regression analysis suggested that CBVa and Aβ may have a synergistic effect on longitudinal cognitive decline in these subjects . Both variables may need to be considered for secondary prevention trials in such populations.

2366 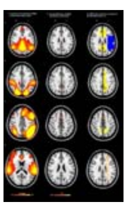

The mediating effects of functional disconnection on the association between structural disconnection and cognitive impairment in symptomatic carotid artery disease

Dewen Meng[1,2], Akram A Hosseini[1], Richard J Simpson[1,2], Robert A Dineen[1,2], and Dorothee P Auer[1,2]

[1]Radiological Sciences, Division of Clinical Neurosciences, School of Medicine, University of Nottingham, Nottingham, United Kingdom, [2]Sir Peter Mansfield Imaging Centre, School of Medicine, University of Nottingham, Nottingham, United Kingdom

This study investigated the association between functional disconnection of cognitive networks, structural disconnection indexed as microscopic damage of specific white matter tracts, and global cognitive impairment in symptomatic carotid artery disease. The findings regarding the mediating effects of functional disconnection on the association between structural disconnection and global cognitive impairment provided promising implications for future studies that develop therapies for patients with vascular cognitive disorder.

2367 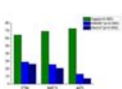

The Correlation of Olfactory Dysfunctions and Hippocampal Atrophy in Patients with Cognitive Impairment: A Potential Clinical Marker for Alzheimer's Disease

Bing Zhang[1], Bin Zhu[1], Yun Xu[2], and Qing.X Yang[3]

[1]Department of Radiology, Affiliated Drum Tower Hospital of Nanjing University Medical School, Nanjing, China, NanJing, People's Republic of China, [2]Department of Neurology, Affiliated Drum Tower Hospital of Nanjing University Medical School, Nanjing, China, NanJing, People's Republic of China, [3]Department of Radiology, Pennsylvania State College of Medicine, Hershey, PA, USA, Hershey, PA, United States

Olfactory deficits have been observed in subjects with Alzheimer's disease (AD) and its potential as a biomarker has been demonstrated by several recent studies. However, its sensitivity and specificity in detecting early AD have not been validated in the Chinese population where aging population is growing rapidly. In this study, by using a 3.0 T MR scanner, we evaluate the presence of olfactory deficits and hippocampal volume loss measured by FreeSurfer (6.0) based on local population in China, to validate the use of olfactory test battery as a clinical AD marker.

2368 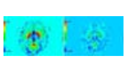

Subcortical Nuclei Iron Deposition of Alzheimer's Patients on MRI-QSM: Maybe a Diagnostic Indicator

Lei Du[1], Yijiang Zhu[1], Tianbin Song[2], Lizhi Xie[3], and Guolin Ma[1]

[1]Department of Radiology, China-Japan Friendship Hospital, Beijing, People's Republic of China, [2]Department of Nuclear Medicine, Xuanwu Hospital,Capital Medical University, Beijing, People's Republic of China, [3]GE Healthcare, Beijing, People's Republic of China

Based on gradient echo (GRE) magnetic resonance phase data, quantitative susceptibility mapping (QSM) is a novel technique which allows the non-invasive assessment of magnetic tissue susceptibility distribution in mild alzheimer’s disease (AD). In this study ,we investigated the correlation between mini-mental state examination (MMSE) and bulk tissue magnetic susceptibility in subcortical nuclei of 14 mild AD subjects and 14 cognitively healthy controls scanned at 3T . A strong linear correlation between them was found in caudate nucleus and dentate nucleus. Hence, QSM can be used for early AD diagnosis and intervention.

2369

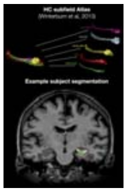

Hippocampal T1-weighted and FLAIR contrast is associated with CSF biomarkers in asymptomatic individuals with parental history of Alzheimer’s disease

Christine L Tardif[1], Robert S C Amaral[1], Gabriel A Devenyi[1], Pedro Rosa-Neto[2], Judes Poirier[2], John Breitner[2], M Mallar Chakravarty[1], and The PREVENT-AD Research Group[2]

[1]Cerebral Imaging Centre, Douglas Mental Health Institute, Montreal, QC, Canada, [2]Douglas Mental Health Institute, Montreal, QC, Canada

Cerebrospinal fluid (CSF) β-amyloid and phosphorylated-tau are consistently used as biomarkers related to the pathophysiology and clinical severity of individuals in the earliest phases of Alzheimer’s disease (AD). This study shows that T1-weighted and FLAIR signal intensity in the hippocampal subfields, normalized using the fimbria, are associated with ApoE4 status and CSF biomarkers. The FLAIR results suggest that presence of inflammation in the subiculum of ApoE4 carriers and in the CA1 and molecular layers of the hippocampus in subjects with low CSF β-amyloid burden as tau pathology increases.

2370

Modulated the Physiological Response Delay to Prevent Overestimating the Disruption of Default Mode Network in Alzheimer’s Disease

Yi-Tien Li[1,2], Chun-Yuan Chang[1], Yi-Cheng Hsu[1], Jong-Ling Fuh[3], and Fa-Hsuan Lin[1,4]

[1]Institute of Biomedical Engineering, National Taiwan University, Taipei, Taiwan, [2]Department of Medical Imaging, Taipei Medical University-Shuang Ho Hospital, New Taipei City, Taiwan, [3]Neurological Institute, Taipei Veterans General Hospital, Taipei, Taiwan, Taipei, Taiwan, [4]Department of Neuroscience and Biomedical Engineering, Aalto University, Espoo, Finland

This study quantified the impact of physiological noise correction in characterizing the resting-state fMRI in Alzheimer’s disease (AD) patients with age- and gender-matched 17 healthy subjects and 15 AD patients. Using a seed-based correlation method with seeds at posterior cingular cortex and medial prefrontal cortex, we found that the difference in the functional connectivity between AD patients and healthy controls was significantly reduced when physiological noise was suppressed.

2371

summa cum laude

Association between whole brain functional connectivity and cortical thickness throughout healthy aging

Bruno Hebling Vieira[1] and Carlos Ernesto Garrido Salmon[1]

[1]InBrain Lab, Department of Physics, Faculty of Philosophy, Sciences and Letters of Ribeirão Preto, University of São Paulo, Ribeirão Preto, Brazil

The aging process entails morphological and functional alterations in the human brain. Using magnetic resonance imaging data of 130 subjects aged between 18 and 81 years from a publicly available dataset we obtained whole brain cortical thickness estimates and resting state connectivity to study how healthy aging affects these. Additionally, we studied the relationship between cortical thickness and functional connectivity. A heterogeneous thinning profile was observed and also a dominance in increases in connectivity, with few decreases. Connectivity correlates with thickness with temporal and occipital seed ROIs. These results might help to understand how connectivity and thickness relate in neuropathologies.

2372

Exaggeration of Tau Pathology by Amyloid-β production in PS2APPxTauP301L Transgenic Mouse Model of Alzheimer’s Disease

Vineela D Gandham[1], William J Meilandt[2], Kai H Barck[1], Maj Hedehus[1], Kimberly Malesky[1], Claire Le Pichon[2], Oded Foreman[3], Gai Ayalon[2], Kimberly Scearce-Levie[2], and Richard AD Carano[1]

[1]Biomedical Imaging, Genentech, South San Francisco, CA, United States, [2]Neuroscience, Genentech, South San Francisco, CA, United States, [3]Pathology, Genentech, South San Francisco, CA, United States

The PS2APP, PS2APPxTau$_{P301L}^{Het}$, Tau$_{P301L}^{Homo}$, Tau$_{P301L}^{Het}$ transgenic mouse models of AD were characterized using MRI, and various regional brain atrophies were detected using a completely automated analysis by SPM-8. Furthermore, through MRI (both ROI and voxel based morphometry) and histology we showed that the presence of PS2APP mutation in PS2APPxTau$_{P301L}^{Het}$ triple transgenic mouse model exaggerates the Tau pathology. The presented results will enable MRI as a great tool to non-invasively assess the disease progression over time in preclinical therapeutic studies targeting Aβ and Tau pathology.

2373

The relationship between brain white matter hyperintensities burden and age-related neuropathologies is location dependent

Chantal Sopacua[1], Arnold M. Evia[1], Aikaterini Kotrotsou[1], Sue E. Leurgans[2,3], David A. Bennett[2,3], Julie A. Schneider[2,3,4], and Konstantinos Arfanakis[1,2,5]

[1]Department of Biomedical Engineering, Illinois Institute of Technology, Chicago, IL, United States, [2]Rush Alzheimer's Disease Center, Rush University Medical Center, Chicago, IL, United States, [3]Department of Neurological Sciences, Rush University Medical Center, Chicago, IL, United States, [4]Department of Pathology, Rush University Medical Center, Chicago, IL, United States, [5]Department of Diagnostic Radiology, Rush University Medical Center, Chicago, IL, United States

White matter hyperintensities (WMH) are white matter lesions appearing hyperintense in T2-weighted MRI. WMH are common in older adults and have been associated with increased risk of cognitive decline and dementia. Previous efforts have attempted to identify the neuropathologies associated with whole brain WMH burden. However, it is yet to be determined if the relationship between regional WMH burden and age-related neuropathologies is the same, or varies, in different parts of the brain. Therefore, the purpose of this research was to investigate the association between regional WMH burden and neuropathologies in a community cohort of older adults.

2374

MRI of longterm changes in vascularization and functional connectivity in a mouse model of vascular cognitive impairment

Philipp Boehm-Sturm[1,2], Joseph Kuchling[3], Susanne Mueller[1,2], Marco Foddis[1], Carsten Finke[3], Celeste Sassi[1], Christoph Harms[1], Stefan Paul Koch[1], Ulrich Dirnagl[1], and Tracy Deanne Farr[1,4]

[1]Department of Experimental Neurology, Center for Stroke Research Berlin, and NeuroCure, Charité University Medicine Berlin, Berlin, Germany, [2]Charité Core Facility 7T experimental MRIs, Charité University Medicine Berlin, Berlin, Germany, [3]Department of Neurology, Berlin Center for Advanced Neuroimaging, NeuroCure Clinical Research Center Neuroimmunology, and Berlin School of Mind and Brain, Charité University Medicine Berlin and Humboldt University Berlin, Berlin, Germany, [4]School of Life Sciences, University of Nottingham, Nottingham, United Kingdom

Chronic mouse brain hypoperfusion produces white matter damage; a feature of vascular cognitive impairment. Despite growing interest in this model, we have struggled to observe a strong phenotype. The present study aimed to improve the phenotype through extended hypoperfusion (6m). We examined the effect on various MR biomarkers including functional connectivity and vascular remodeling. We found massive structural changes including arterial neovessels, small subcortical strokes, and microbleeds. Animals showed behavioral deficits accompanied by changes in resting state MRI signals of the cingulate cortex, which is functionally connected to regions related to behavior (hippocampus) and emotion (amygdala).

2375

White matter hyperintensity burden assessed ante-mortem and post-mortem on the same older adults

Arman Kulkarni[1], Arnold M. Evia[1], Julie A. Schneider[2,3,4], David A. Bennett[2,3], and Konstantinos Arfanakis[1,2,5]

[1]Department of Biomedical Engineering, Illinois Institute of Technology, Chicago, IL, United States, [2]Rush Alzheimer's Disease Center, Rush University Medical Center, Chicago, IL, United States, [3]Department of Neurological Sciences, Rush University Medical Center, Chicago, IL, United States, [4]Department of Pathology, Rush University Medical Center, Chicago, IL, United States, [5]Department of Diagnostic Radiology, Rush University Medical Center, Chicago, IL, United States

White matter hyperintensities (WMH) are commonly observed in brain MR images of older adults. Recently, more and more research studies assess WMH burden using ex-vivo MRI, aiming at directly linking WMH to the underlying neuropathologies detected at autopsy. The purpose of this work was twofold: 1) to investigate the relationship between WMH burden assessed in-vivo and ex-vivo on the same older adults, and 2) to test the hypothesis that WMH burden assessed ex-vivo is higher than that assessed in-vivo for longer ante-mortem intervals (AMI) (i.e. from in-vivo MRI to death).

2376

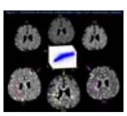

Fast multivariate relaxometry can differentiate neurodegenerative disease processes and phenotypes

Gabriel Mangeat[1,2], Benjamin De Leener[1], Virginija Danylaité Karrenbauer[3,4], Marcel Warntjes[5,6], Nikola Stikov[1,7], Caterina Mainero[2,8], Julien Cohen-Adad[1,9], and Tobias Granberg[2,8,10,11]

[1]NeuroPoly Lab, Institute of Biomedical Engineering, Polytechnique Montréal, Montreal, QC, Canada, [2]Athinoula A. Martinos Center for Biomedical Imaging, MGH, Charlestown, MA, United States, [3]Department of Clinical Neuroscience, Karolinska Institutet, Stockholm, Sweden, [4]Department of Neurology, Karolinska University Hospital, Stockholm, Sweden, [5]Center for Medical Imaging Science and Visualization, CMIV, Linköping, Sweden, [6]SyntheticMR, Linköping, Sweden, [7]Montreal Health Institute, Montreal, QC, Canada, [8]Harvard Medical School, Boston, MA, United States, [9]Functional Neuroimaging Unit, CRIUGM, Université de Montréal, Montréal, QC, Canada, [10]Department of Clinical Science, Intervention and Technology, Karolinska Institutet, Stockholm, Sweden, [11]Department of Radiology, Karolinska University Hospital, Stockholm, Sweden

Hereditary diffuse leukoencephalopathy with spheroids (HDLS) and multiple sclerosis (MS) are demyelinating and neurodegenerative disorders that can be hard to distinguish clinically and radiologically. Here, we present a framework to extract independent physiological sources of signal from time-efficient multiple quantitative relaxometry (T1, T2 and PD maps) to characterize varying degrees and mechanisms of tissue disruption. The method can aid in the differentiation of HDLS and MS (p=0.007), as well as identify MS subtypes (p=0.0007), which would be helpful in ensuring a correct diagnosis and treatment of these disorders.

2377

What Happens to the Hippocampus 12-months After Training? A Longitudinal Linear Mixed Effects Model Analysis of Mild Cognitive Impairment in the SMART Trial

Kathryn Mary Broadhouse[1], Chao Suo[1,2,3,4], Maria Fiatarone Singh[5,6], Nicola Gates[1,3,4], Wei Wen[4,7], Perminder Sachdev[4,7], Henry Brodaty[4,8], Nidhi Saigal[9], Nalin Singh[9], Guy Wilson[9], Jacinda Meiklejohn[9], Bernhard Baune[10], Michael Baker[5,11], Nasmin Foroughi[12], Yi Wang[9,13], Yorgi Marvos[11], and Michael J Valenzuela[1,14]

[1]Regenerative Neuroscience Group, Brain and Mind Centre, Sydney, Australia, [2]Brain and Mental Health Laboratory, Monash Institute of Cognitive and Clinical Neuroscience, Monash University, Sydney, Australia, [3]School of Psychiatry, University of New South Wales, Sydney, [4]Centre for Healthy Brain Ageing, School of Psychiatry, University of New South Wales, Sydney, [5]Exercise Health and Performance Faculty Research Group, Faculty of Health Sciences and Sydney Medical School, The University of Sydney, [6]Hebrew SeniorLife and Jean Mayer USDA Human Nutrition Research Center on Aging at Tufts University, Boston, [7]Neuropsychiatric Institute, Prince of Wales Hospital, Sydney, NSW, Australia, [8]Dementia Collaborative Research Centre, University of New South Wales, Sydney, NSW, Australia, [9]Exercise Health and Performance Faculty Research Group, Faculty of Health Sciences, The University of Sydney, Lidcombe, NSW, Australia., [10]Department of Psychiatry, School of Medicine, University of Adelaide, Adelaide, SA, Australia, [11]School of Exercise Science, Australian Catholic University, Strathfield, NSW, Australia., [12]Clinical and Rehabilitation Research Group, Faculty of Health Sciences, The University of Sydney, Lidcombe, NSW, Australia., [13]Department of Medicine and the Diabetes Center, University of California, San Francisco, San Francisco, CA, USA, [14]School of Medical Sciences, Sydney Medical School, University of Sydney, Sydney, NSW, Australia.

Mild cognitive impairment (MCI) increases future risk of dementia, however, several studies have shown that mental and physical exercise reduce this risk. From the Study of Mental Activity and Resistance Training (SMART) we have previously shown significantly improved global cognitive function immediately after 6 months of progressive resistance training in MCI. In this analysis, we compare longitudinal hippocampal volume change in MCI using linear mixed effects models over an 18-month period comprised of a 6-month training phase and a 12-month post training follow-up. Our results show both isolated cognitive and progressive resistance training significantly diminished the rate of left hippocampal atrophy compared to a double sham intervention across training and an extended follow-up period.

2378

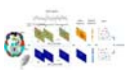

Extraction of Both Dynamic Functional and Structural Connectivity from Resting-state fMRI for MCI Classification

Xiaobo Chen[1], Han Zhang[1], Lichi Zhang[1], and Dinggang Shen[1]

[1]Department of Radiology and BRIC, University of North Carolina at Chapel Hill, CHAPEL HILL, NC, United States

In this abstract, we show that the diagnosis accuracy of mild cognitive impairment (MCI) can be significantly improved by integrating dynamic information contained in the traditional functional connectivity (FC) from grey matter (GM) regions and the functional correlation tensors (FCT) from white matter (WM) regions, both computed from resting-state fMRI (RS-fMRI). The advantages of our method include: 1) dynamic FC is exploited to reveal rich time-varying information in FC, and 2) the anatomical structure information within WM can be well incorporated in RS-fMRI.

Traditional Poster

TBI & SCI

Exhibition Hall 2379-2399 Wednesday 13:45 - 15:45

2379

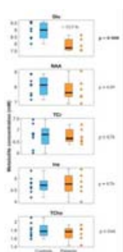

Magnetic resonance spectroscopy demonstrates decreased glutamate in the anterior cingulate cortex in individuals with spinal cord injury

Carina Graf[1,2], Erin L. MacMillan[3], John K. Kramer[2,4], and Cornelia Laule[1,2,5]

[1]Department of Radiology, University of British Columbia, Vancouver, BC, Canada, [2]International Collaboration on Repair Discoveries (ICORD), Vancouver, BC, Canada, [3]Faculty of Medicine (Division of Neurology), University of British Columbia, Vancouver, BC, Canada, [4]Faculty of Education (School of Kinesiology), University of British Columbia, Vancouver, BC, Canada, [5]Department of Pathology & Laboratory Medicine, University of British Columbia

We investigated metabolites in the anterior cingulate cortex using magnetic resonance spectroscopy in individuals with spinal cord injury (SCI). Short-TE PRESS at 3T provided reliable fits for glutamate (Glu), N-Acetyl-aspartate (NAA), total creatine (tCr), myo-Inositol and total choline. SCI patients had 11.3 % less Glu. Given the role of Glu in synaptic transmission between neurons and also between neurons and oligodendrocytes, reduced Glu in SCI may reflect decreased synaptic density and activity due to a loss of sensory input in the anterior cingulate cortex. Further research investigating the effect of sensory input loss on metabolite concentrations in SCI is warranted.

2380

Neurodegeneration and its interaction with motor impairment in sub-acute SCI revealed by quantitative MRI

Maryam Seif[1], Patrick Grabher[1], Alan Thompson[2], Armin Curt[1], and Patrick Freund[1,2,3,4]

[1]Spinal Cord Injury Center Balgrist, University of Zurich, Zurich, Switzerland, [2]Department of Brain Repair and Rehabilitation, UCL Institute of Neurology, London, United Kingdom, [3]Wellcome Trust Centre for Neuroimaging, UCL Institute of Neurology, London, United Kingdom, [4]Department of Neurophysics, Max Planck Institute for Human Cognitive and Brain Sciences, Leipzig, Germany

Spinal cord injury (SCI) leads to immediate sensorimotor and autonomic dysfunction and SCI patients generally show little clinical recovery within the first year after injury. Early structural changes at the spinal and brain level and their interactions with recovery rate are not well understood. The aim of our study was to reveal trauma-induced neurodegeneration and its interaction to impairment within early stage after injury employing quantitative neuroimaging technique. Our finding showed that significant atrophy and microstructural changes initiated in neural sensorimotor system within already early stage after SCI and quantitative neuroimaging methods hold potential to disclosing these neurodegeneration mechanisms.

2381

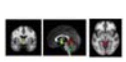

Progressive ventricles enlargement and CSF volume increases as a marker of neurodegeneration in SCI patients: A longitudinal MRI study

Maryam Seif[1], Gabriel Ziegler [2,3], and Patrick Freund[1,4,5,6]

[1]Spinal Cord Injury Center Balgrist, University of Zurich, Zurich, Switzerland, [2]Institute of Cognitive Neurology and Dementia Research, Otto-von-Guericke-University Magdeburg, Magdeburg, Germany, [3]German Center for Neurodegenerative Diseases (DZNE), Magdeburg, Germany, [4]Department of Brain Repair and Rehabilitation, UCL Institute of Neurology, London, United Kingdom, [5]Wellcome Trust Centre for Neuroimaging, UCL Institute of Neurology, London, United Kingdom, [6]Department of Neurophysics, Max Planck Institute for Human Cognitive and Brain Sciences, Leipzig, Germany

Following Spinal Cord Injury the sensorimotor and limbic system immediately undergo progressive neurodegeneration (atrophy). Next to the focal grey and white matter atrophy, localized CSF and ventricular volume changes may provide additional biomarkers for brain atrophy. We therefore aimed to track brain atrophy by means of CSF volume changes and ventricular enlargements over two years following SCI. Our finding showed an increase of local CSF volume as well as ventricles enlargement in patients over time. The CSF volume which is normally used as a biomarker of general atrophy, showed also sensitivity to local degenerative changes in SCI.

2382

Brain metabolism and temperature assessment in traumatic brain injury subjects using 3D Echo-planar Spectroscopic Imaging

Bhanu Prakash KN[1], Sanjay K Verma[1], Andrew A Maudsley[2], and Sendhil Velan S[1]

[1]Laboratory of Molecular Imaging, Singapore Bioimaging Consortium, Singapore, Singapore, [2]Miller School of Medicine, University of Miami, Miami, FL, United States

Traumatic brain injury (TBI) results in a broad spectrum of symptoms and disabilities and has a high rate of mortality and morbidity. TBI is associated with elevated brain temperature due to inflammation. TBI has heterogeneous consequences of pathophysiology, changed intracranial dynamics and cerebral metabolism. In some cases there is an increase in ICP and cerebral perfusion which makes the management of the injury difficult . Therapeutic hypothermia is recommended as one of the acute management techniques as it increases neuroprotection, decreases cerebral metabolism and ICP. To induce hypothermia and monitor the brain temperature a noninvasive and accurate assessment of cerebral temperature is essential. MR based temperature measurement based on the water resonance frequency, relaxation times (T1, T2), spectroscopy, proton density, diffusion etc. have been widely used. Echo-planar spectroscopic imaging (EPSI) method has the advantage of simultaneous acquisition of water and spectrum in a single TR, by which we can acquire the whole brain spectrum in a short time . In this study we have explored changes in brain temperature due to cerebral metabolic changes in control, mild and moderate TBI subjects.

2383

Thalamic Atrophy following mTBI is Associated with Persistent Post-Concussive Symptoms and Cognitive Fatigue

Jiachen Zhuo[1], Li Jiang[1], Chandler Sours[1], Prashant Raghavan[1], Jerry L Prince[2], and Rao P Gullapalli[1]

[1]Diagnostic Radiology and Nuclear Medicine, University of Maryland School of Medicine, Baltimore, MD, United States, [2]Electrical and Computer Engineering, Johns Hopkins University

Even mild TBI patients with negative CT and MRI may experience persistent post-concussive symptoms (PCS) and declined cognition more than 3 months post injury. In this prospective study of regional brain volume changes in mTBI patients, we found progressive thalamic atrophy from acute to chronic stages post injury, especially within the patient group that showed persistent PCS at 6 months. Thalamic volume atrophy also correlated with cognitive fatigue and processing speed within the same symptomatic mTBI group. Further studies on vulnerability of the thalamus may provide more insights into TBI recovery and lead to potential Therapies.

2384

Effects of cumulative non-concussive head impact exposure associated with youth football on MRI measures of gray matter structure

Lynn Della Grotta[1], Jillian E Urban[2], Megan Johnston[2], Elizabeth M Davenport[3], Mark A Espeland[4], Youngkoo Jung[5], Daryl A Rosenbaum[6], Alex K Powers[7], Joel D Stitzel[2], Joseph A Maldjian[3], and Christopher T Whitlow[8]

[1]Radiology, Wake Forest School of Medicine, Winston Salem, NC, United States, [2]Biomedical Engineering, Wake Forest School of Medicine, [3]Radiology, University of Texas Southwestern Medical Center, [4]Biostatistical Sciences, Wake Forest School of Medicine, [5]Radiology & Biomedical Engineering, Wake Forest School of Medicine, [6]Family and Community Medicine, Wake Forest School of Medicine, [7]Neurosurgery, Wake Forest School of Medicine, [8]Radiology, Biomedical Engineering, and Clinical and Translational Sciences Institute, Wake Forest School of Medicine

Millions of children play American football, however, youth players are largely absent from studies addressing the public health questions about safety and concussion. Furthermore, many studies investigating effects of sports-related head impact exposure on brain structure have focused on white matter, with few evaluating the effects on gray matter (GM) structure. In this study, we combined measures of head impact biomechanics and brain MRI to investigate the effects of repetitive non-concussive exposure on gray matter volume and microstructural integrity. We demonstrate statistically significant relationships between exposure metrics and MRI measures of GM diffusion characteristics after one season of youth football.

2385

Repetitive Head Impact Exposure and Later-Life Neurochemistry: A Magnetic Resonance Spectroscopy Investigation in Symptomatic Former NFL Players

Michael Alosco[1], Benjamin Rowland[2], Yorghos Tripodis[3], Hujun Liao[2], Alicia Chua [3], Brett Martin[4], Ofer Pasternak[5], Sarina Karmacharya[5], Johnny Jarnagin[6], Christine Chaisson[4], Robert C Cantu[7,8], Martha E Shenton[5], Richard Greenwald[9,10], Michael McClean[11], Neil W Kowall[12,13], Ann C McKee[12,14,15], Robert A Stern[16], and Alexander P Lin[2]

[1]Neurology, Boston University School of Medicine, Boston, MA, United States, [2]Radiology, Center for Clinical Spectroscopy, Brigham and Women's Hospital, Harvard Medical School, MA, [3]Biostatistics, Boston University School of Public Health, [4]Data Coordinating Center, Boston University School of Public Health, MA, [5]Psychiatry, Psychiatry Neuroimaging Laboratory, Radiology, Brigham and Women's Hospital, Harvard Medical School, MA, [6]Neurology, Boston University School of Medicine, MA, [7]Neurology, Neurosurgery, Boston University School of Medicine, MA, [8]Concussion Legacy Foundation, [9]Simbex, [10]Thayer School of Engineering, Dartmouth College, [11]Environmental Health, Boston University School of Public Health, MA, [12]Neurology, Pathology and Laboratory Medicine, Boston University School of Medicine, [13]Neurology Service, VA Boston Healthcare System, [14]VA Boston Healthcare System, [15]Department of Veterans Affairs Medical Center, Bedford, [16]Neurology, Neurosurgery, Anatomy & Neurobiology, Boston University Alzheimer's Disease and CTE Center, Boston University School of Medicine, MA

This study examined magnetic resonance spectroscopy (MRS) as a potential biomarker for chronic traumatic encephalopathy (CTE). 79 former National Football League players and 23 same-age controls completed MRS. Cumulative head impact index (CHII) estimated repetitive head impact (RHI) exposure. Principal component analysis derived clinical composites. Former NFL players had lower parietal white matter (PWM) NAA ($p=0.048$). Higher CHII predicted lower PWM creatine ($p=0.028$). Anterior cingulate gyrus (ACG) metabolites correlated with visual memory ($p=0.008$-0.044). ACG glutamate ($p=0.032$) and glutamate/glutamine ($p=0.012$) predicted psychomotor/executive function. Posterior cingulate gyrus myo-inositol predicted verbal memory ($p=0.048$). MRS may facilitate detection of RHI-related neurological conditions, including CTE.

2386

White matter microstructure in adolescent female soccer athletes: diffusion MRI relations with years of high-school experience, concussion history, and cognitive measurements.

Yukai Zou[1,2], Xianglun Mao[3], Ikbeom Jang[3], Nicole L. Vike[2], Thomas S. Redick[4], Thomas M. Talavage[1,3], and Joseph V. Rispoli[1]

[1]Weldon School of Biomedical Engineering, Purdue University, West Lafayette, IN, United States, [2]College of Veterinary Medicine, Purdue University, West Lafayette, IN, United States, [3]School of Electrical and Computer Engineering, Purdue University, West Lafayette, IN, United States, [4]Department of Psychological Sciences, Purdue University, West Lafayette, IN, United States

Understanding how contact sports activities potentially affect the brains and cognitive abilities of adolescent athletes in both short and long-term scales is critical. Using 3 Tesla diffusion-weighted imaging (DWI) and tract-based spatial statistics, this study investigated the white matter microstructure of 13 high-school female soccer athletes over one competition season. No significant difference of DWI metrics across the season was observed. However, regression analyses showed significant effects of years of high-school experience and concussion history on the DWI metrics within corticothalamic and limbic pathways, and the abnormal changes of DWI metrics may relate to cognitive impairments.

2387

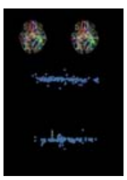

Quality control for human brain advanced diffusion imaging for assessment of concussion

Joong Hee Kim[1], Laurena Holleran[1], Pashtun Shahim[1], and David Brody[1]

[1]Neurology, Washington University School of Medicine in St. Louis, St. Louis, MO, United States

Most concussive brain injury is not readily detected in conventional MRI or standard DTI, requiring advanced imaging methodology. However, reliability of any newly developed imaging technology should be tested prior to starting full scale studies. Here we present a protocol which will enable inter-lab comparison of any advanced diffusion imaging technology with objective quantitative analysis. High spatial resolution diffusion imaging with optimized multiband pulse sequence performed on subjects twice at 1.25 mm isotropic voxel size. Post image processing including outlier exclusion and distortion correction was optimized. Brain parcellation based quantitative analyses was used to provide objective measures of reproducibility.

2388

MRI based early monitoring and quantitative assessment of macrophages infiltration after experimental traumatic brain injury in mice

Sushanta Kumar Mishra[1,2], Subash Khushu[1], and Gurudutta Gangenahalli[2]

[1]NMR Research Centre, Institute of Nuclear Medicine and Allied Sciences, Delhi, India, Delhi, India, [2]Division of Stem Cell and Gene Therapy Research, Institute of Nuclear Medicine and Allied Sciences, Delhi, India, Delhi, India

The inflammatory response following traumatic brain injury (TBI) is regulated by phagocytic cells, comprising resident microglia and infiltrating macrophages. The present study was to monitor the early effect of monocytes/phagocytic accumulation and further to explore its kinetics in TBI mice. Localized macrophage population was monitored using USPIO nanoparticles enhanced in vivo serial magnetic resonance imaging (MRI). Flow cytometry based gating study was performed to discriminate between resident microglia (Ly6G¯CD11b+CD45low) and infiltrating macrophages (Ly6G˜CD11b+CD45high). Imaging and flow cytometric analysis revealed that maximum macrophage infiltration occurs between 66-72 h post injury (42-48 h post administration of USPIO) at the site of inflammation.

2389

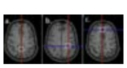

Proton Magnetic Resonance Spectroscopy of Mild Traumatic Brain Injury in the Military

Lasya Sreepada[1], Joshua Ladner[1], Huijun Liao[1], Benjamin Rowland[1], Kristin Heaton[2], and Alexander Lin[1]

[1]Center for Clinical Spectroscopy, Brigham and Women's Hospital & Harvard Medical School, Boston, MA, United States, [2]U.S. Army Research Institute of Environmental Medicine, Natick, MA, United States

The objective of this ^{1}H MRS study was to determine the neurochemical profiles of military members with mild Traumatic Brain Injury (mTBI) and compare with age-matched, healthy military controls. Analysis of metabolite concentrations in three brain regions revealed a significant global decrease in total creatine (tCr) in mTBI subjects, as well as elevated GSH in the posterior cingulate and increased Glx in both posterior white matter and anterior cingulate regions, when compared to controls. These results could identify key biomarkers of mTBI and indicate neuroinflammatory changes and impaired brain function or integrity in mTBI.

2390

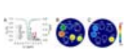

Simultaneous detection of glucose and glutamate by CEST MRI: a preliminary study for experimental brain injury

Tsang-Wei Tu[1], Georgios Z Papadakis[2], Zsofia Kovacs[2], William Reid[2], Dima Hammoud [2], and Joseph Frank[2]

[1]Radiology and Imaging Sciences, National Institutes of Health, Bethesda, MD, United States, [2]Radiology and Imaging Sciences, National Institutes of Health

The current study investigated the CEST sensitivity and specificity for simultaneous glucose (glucoCEST) and glutamate (gluCEST) detection on a phantom and a rodent brain injury. Using a median saturation power (2μT) and short saturation duration (2s), the MTRasym at 1.2, 2.1 and 2.9ppm could detect the glucose content, while the MTRasym at 3ppm could measure the glutamate in vivo. The glucoCEST results were compared in parallel to the ^{18}F-FDG PET detecting the tissue uptake of glucose, while the gluCEST data were shown comparable to ^{18}F-DPA PET radio-ligands binding to translocator protein (TSPO) for imaging microglial activation in the injured brain.

2391

Longitudinal changes of cerebral perfusion in patients with moderate traumatic brain injury

Suk-tak Chan[1], Jonathan Welt[2], Emad Ahmadi[3], Eva Ratai[1], Jacqueline Namati[2], Michael Lev[3], Jarone Lee[4], Anastasia Yendiki[1], Benjamin Vakoc[2], Blair A Parry[4], Cora Ordway[5], and Rajiv Gupta[3]

[1]Athinoula A. Martinos Center for Biomedical Imaging, Department of Radiology, Massachusetts General Hospital, Charlestown, MA, United States, [2]Department of Dermatology, Massachusetts General Hospital, Boston, MA, United States, [3]Division of Neuroradiology, Department of Radiology, Massachusetts General Hospital, Boston, MA, United States, [4]Department of Emergency Medicine, Massachusetts General Hospital, Boston, MA, United States, [5]Department of Cognitive, Linguistic and Psychological Sciences, Brown University, Providence, RI, United States

There is increasing evidence that neurovascular dysregulation contributes to the persistent symptoms in patients with traumatic brain injury (TBI). Damaged microvasculature may disrupt the neurovascular coupling, where the local cerebral blood flow (CBF) no longer matches the metabolic requirements of the tissue. In the present study, we found that there was a diffuse hypoperfusion at thalamus, posterior cingulate gyrus, precuneus and white matter in 2-week follow-up scan relative to the 48-hour initial and 3-month follow-up scans. Low perfusion was sustained in both frontal and parietal cortices in 3-month follow-up scan. Our perfusion findings in these brain regions suggest that hypoperfusion may play a role in the post-traumatic symptoms of moderate TBI.

2392

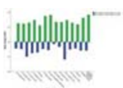

Longitudinal changes of neurovascular responses to breathhold challenge in patients with moderate traumatic brain injury

Suk-tak Chan[1], Jonathan Welt[2], Emad Ahmadi[3], Jacqueline Namati[2], Michael Lev[3], Jarone Lee[4], Benjamin Vakoc[2], Eva Ratai[1], Anastasia Yendiki[1], Blair A Parry[4], Cora Ordway[5], and Rajiv Gupta[3]

[1]Athinoula A. Martinos Center for Biomedical Imaging, Department of Radiology, Massachusetts General Hospital, Charlestown, MA, United States, [2]Department of Dermatology, Massachusetts General Hospital, Boston, MA, United States, [3]Division of Neuroradiology, Department of Radiology, Massachusetts General Hospital, Boston, MA, United States, [4]Department of Emergency Medicine, Massachusetts General Hospital, Boston, MA, United States, [5]Department of Cognitive, Linguistic and Psychological Sciences, Brown University, Providence, RI, United States

There is an increasing evidence that neurovascular dysregulation contributes to the persistent symptoms in patients with traumatic brain injury (TBI). Damaged microvasculature may disrupt the neurovascular coupling, especially under physiological stress, where the local cerebral blood flow (CBF) no longer matches the metabolic requirements of the tissue. Our findings of negative or abnormally delayed blood oxygenation level dependent (BOLD) signal changes in response to breathhold challenge can potentially be used as an imaging marker to localize subtle abnormal vascular function in individual patients with moderate TBI. The restoration of abnormally delayed BOLD responses at chronic stage suggest that such an imaging marker may be used to follow up the patients.

2393

A Repetitive Traumatic Brain Injury Model Characterized with Diffusion Tensor and Diffusion Kurtosis Imaging with Neuropathological Correlation

Fengshan Yu[1,2], Dinesh K. Shukla[3], Christina M. Marion[2], Kryslaine L. Radomski[1,2], Reed G. Selwyn[4], Regina C. Armstrong[1,2], and Bernard J. Dardzinski[1,5]

[1]Center for Neuroscience and Regenerative Medicine, Uniformed Services University of the Health Sciences, Bethesda, MD, United States, [2]Anatomy, Physiology and Genetics, Uniformed Services University of the Health Sciences, Bethesda, MD, United States, [3]Department of Psychiatry, University of Maryland School of Medicine at Baltimore, Baltimore, MD, [4]Radiology, University of New Mexico, Albuquerque, NM, United States, [5]Radiology and Radiological Sciences, Uniformed Services University of the Health Sciences, Bethesda, MD

Mild traumatic brain injury (mTBI) often involves single (s-mTBI) or repetitive (r-mTBI) head injury, which may differ in the potential for long term symptoms and chronic neurodegeneration. Non-invasive approaches that can detect damage and predict outcome are a high priority for clinical care of mTBI patients. Magnetic resonance (MR) diffusion tensor imaging (DTI) and diffusion kurtosis imaging (DKI) techniques can identify microstructural changes associated with Gaussian (DTI) and non-Gaussian (DKI) water diffusion properties. Mouse models of s-mTBI and r-mTBI targeting anterior brain regions (impact site at bregma) were developed for longitudinal MRI studies with corresponding neuropathology.

2394

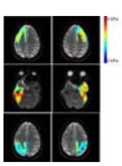

Neuroimaging in Concussion: A Magnetic Resonance Elastography Pilot Study

Alvin C Silva[1], Yuan Le[1], Yuxiang Zhou[1], Anshuman Panda[1], Catherine Chong[2], Arvin Forghanian-Arani[3], Kevin Glaser [3], Jun Chen[3], Annelise Silva[4], Kent Nelson[1], and Richard Ehman[3]

[1]Radiology, Mayo Clinic Arizona, Phoenix, AZ, United States, [2]Neurology, Mayo Clinic Arizona, Phoenix, AZ, United States, [3]Mayo Clinic Rochester, Rochester, MN, United States, [4]Research, Mayo Clinic Arizona, Phoenix, AZ, United States

As concussion, even when symptomatic, can be occult on routine imaging, there is clinical need for a more accurate diagnostic assessment. The objective of this study was to assess the utility of brain magnetic resonance elastography (MRE), a non-invasive neuroimaging technique, to detect changes in brain stiffness in concussed patients relative to healthy controls.

2395

Quantitative Susceptibility Mapping in Mild Traumatic Brain Injury

Hui-Hsien Lin[1,2], Hua-Shan Liu[2,3], Ping-Huei Tsai[1,2,4], Fei-Ting Hsu[1,2], Chia-Feng Lu[2,4,5], Yu-Chieh Jill Kao[2,4], Wen-Jin Hsieh[1,2], Ho-Fang Huang[2,6], Huai-Lu Chen[2,6], Paul Blakeley[2,6], Gilbert Aaron Lee[2,6], and Cheng-Yu Chen[1,2,4,6]

[1]Department of Medical Imaging, Taipei Medical University Hospital, Taipei Medical University, Taipei, Taiwan, [2]Translational Imaging Research Center, College of Medicine, Taipei Medical University, Taipei, Taiwan, [3]School of Biomedical Engineering, College of Biomedical Engineering, Taipei Medical University, Taipei, Taiwan, [4]Department of Radiology, School of Medicine, College of Medicine, Taipei Medical University, Taipei, Taiwan, [5]Department of Biomedical Imaging and Radiological Sciences, National Yang-Ming University, Taipei, Taiwan, [6]Department of Medical Research, Taipei Medical University Hospital, Taipei Medical University, Taipei, Taiwan

The present study investigated whether quantitative susceptibility mapping is able to identify particular characteristics of alterations in white matter and other brain regions in patients with mild traumatic brain injury (mTBI). Our study suggests that quantitative susceptibility mapping is capable of indicating iron and myelin disturbances in white matter and thalamus for patients with mTBI.

2396

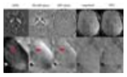

Imaging of thalamic calcium deposits due to sports-related concussion using Quantitative Susceptibility Mapping (QSM)

Ferdinand Schweser[1,2], Deepa P Ramasamy[1], Jesper Hagemeier[1], Barry Willer[3], Nicola Bertolino[1], Dhaval Shah[1], David J Poulsen[4], John Leddy[5], and Robert Zivadinov[1,2]

[1]Buffalo Neuroimaging Analysis Center, Department of Neurology, Jacobs School of Medicine and Biomedical Sciences, University at Buffalo, The State University of New York, Buffalo, NY, United States, [2]MRI Clinical and Translational Research Center, Jacobs School of Medicine and Biomedical Sciences, University at Buffalo, The State University of New York, Buffalo, NY, United States, [3]Department of Psychiatry, Jacobs School of Medicine and Biomedical Sciences, University at Buffalo, The State University of New York, Buffalo, NY, United States, [4]Department of Neurosurgery, Jacobs School of Medicine and Biomedical Sciences, University at Buffalo, The State University of New York, Buffalo, NY, United States, [5]Department of Orthopaedics, Jacobs School of Medicine and Biomedical Sciences, University at Buffalo, The State University of New York, Buffalo, NY, United States

This work explored the hypothesis that the activation of N-methyl-D-aspartate (NMDA)-receptors in the thalamus results in persistent calcium deposits after a sports-related concussion that can be visualized clinically with Quantitative Susceptibility Mapping at 3 Tesla. The study involved 22 retired professional contact-sports athletes and 45 controls. We found a significantly higher incidence of thalamic micro-calcifications in contact-sports athletes compared to controls, in particular in ice hockey players.

2397

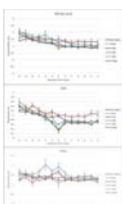

Diffusion Tensor imaging assessment for the spinal cord injury using 9.4 Tesla

Abdullah Ali Asiri[1,2], Mohammed Alnasser[3], Saied Alamri[4], Chantelle Reid[5], Marc Ruitenberg[5], and Nyoman Kurniawan[1]

[1]Centre for Advanced Imaging, The University of Queensland, Brisbane, Australia, [2]Radiology department, College of applied medical sciences, Najran University, Najran, Saudi Arabia, [3]Radiology Department, King Fahad Medical City, Ministry of health, Riyadh, Saudi Arabia, [4]Radiology Department, King Saud for Chest and Respiratory diseases, Ministry of health, Riyadh, Saudi Arabia, [5]Laboratory for Neural Injury and Repair, School of Biomedical Science, University of QLD, Brisbane, Australia

Spinal cord injury (SCI) is a devastating damage that can result in permanent disabilities. MRI provides precise details of spinal cord post traumatic compression, which are useful for the diagnosis of the injury, surgical planning, post-surgical measurements and estimation long-term outcomes (Kramer, Freund,& Curt, 2014). In this study, 4 SCI mice were scanned at the 9.4T to acquire high-resolution images and diffusion tensor imaging at two b-values. The area of both white and gray matter were measured in several slices and compared to the pre-injury imaging. Spinal cord white and gray matters were also examined using DTI.

2398

Traumatic Spinal Cord Injury Induces Cortical Diffusion MRI Changes

Peng Sun[1], Rory KJ Murphy[2], Paul Gamble[3], Ajit George[1], Wilson Z. Ray[2], and Sheng-Kwei Song[1]

[1]Radiology, Washington University in Saint Louis, Saint Louis, MO, United States, [2]Neurological Surgery, Washington University in Saint Louis, Saint Louis, MO, United States, [3]Washington University in Saint Louis, Saint Louis, MO, United States

Spinal cord injury (SCI) is a significant public health problem. A major shortcoming limiting efforts to improve the treatment of SCI is the lack of quantifiable metrics on which to base clinical decisions. In current study, we have utilized diffusion basis spectrum imaging (DBSI) to more accurately differentiate and quantify axonal injury, demyelination, inflammation and edema/tissue loss. DBSI results suggest chronic SCI does result in axonal injury and edema/tissue loss at the level of the cerebral peduncle. These results demonstrated axons may be preserved rostral to the site of injury, and may provide some insight as to why some patients respond to more recent epidural stimulation even years out from injury.

2399

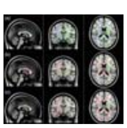

Assessing Functional and Structural Connectivity in ex-Professional Athletes

Mitchell W. Doughty[1], Michael D. Noseworthy[1,2], Rober Boshra[1], Kyle I. Ruiter[3], and John F. Connolly[1,3]

[1]School of Biomedical Engineering, McMaster University, Hamilton, ON, Canada, [2]Department of Electrical and Computer Engineering, McMaster University, [3]Department of Linguistics and Languages, McMaster University

Recently there has been considerable attention directed towards the increased risk for head injuries that athletes face while participating in high impact sports. Furthermore, there is also heightened interest in asymptomatic sub-concussive blows that possibly lead to long term neurological deficits. The goal of this study was to investigate retired professional athletes, who played at least 4 seasons of Canadian football, using functional connectivity mapping and DTI techniques. When compared to an age matched control population, differences were observed both in functional and structural connectivity, suggesting that even years after retiring the brain still exhibits signs of damage.

Traditional Poster

Neuro: Techniques

Exhibition Hall 2400-2421 Wednesday 13:45 - 15:45

2400

Neonatal MRI rotational motion correction using a wireless accelerometer (WiMoCo)

Martyn Paley[1], Steven Reynolds[1], Nurul Ismail[1], Mari Herigstad[1], Deborah Jarvis[1], and Paul Griffiths[1]

[1]Academic Radiology, University of Sheffield, Sheffield, United Kingdom

A wireless accelerometer has been used to measure rotation angles on a dedicated neonatal MRI system. The measured angles have been used to help correct the k-space data to reduce ghosting artifacts. No interference between the accelerometer and the MR system was observed. Some limited improvement in ghosting was found but further work is required on the reconstruction algorithm. The device offers fast temporal resolution (10ms) and no sequence acquisition time overhead as it is a totally independent measurement system.

2401

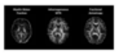

Comparison of inhomogeneous magnetization transfer imaging with myelin water imaging (MWI) and diffusion tensor imaging (DTI)

Ece Ercan[1], Gopal Varma[2], Burkhard Maedler[3], Ivan E Dimitrov[4,5], Marco Pinho[1,4], Ben Wagner[1], Elizabeth Davenport[1], Joseph Maldjian[1], Robert E Lenkinski[1,4], and Elena Vinogradov[1,4]

[1]Radiology, University of Texas Southwestern Medical Center, Dallas, TX, United States, [2]Radiology, Division of MR Research, Beth Israel Deaconess Medical Center, Harvard Medical School, Boston, MA, United States, [3]Philips Healthcare, Germany, [4]Advanced Imaging Research Center, University of Texas Southwestern Medical Center, Dallas, TX, United States, [5]Philips Healthcare, Gainesville, FL, United States

Inhomogeneous magnetization transfer (ihMT) imaging is an enhanced magnetization transfer technique, which has been shown to produce a higher white/gray matter contrast compared to conventional MT methods. This contrast is thought to be originating from dipolar order effects in myelinated tissues. In this study we compare ihMT with myelin water imaging and diffusion tensor imaging.

2402

In-vivo 3D T1rho mapping of the whole Brain: Multi-component Analysis

Rajiv G Menon[1], Azadeh Sharafi[1], and Ravinder R Regatte[1]

[1]Bernard and Irene Schwartz Center for Biomedical Imaging, Department of Radiology, New York University Langone Medical Center, New York, NY, United States

In this study, we demonstrate the in vivo feasibility of multicomponent 3D-T1rho relaxation mapping of whole brain using 3T MRI in five healthy subjects. Our preliminary results suggest that the bi-exponential model better represents the relaxation behavior in white matter and has potential to differentiate between different water compartments associated with myelin bound water (short component) and intra-extracellular water (long component).

2403

BrainVis: A cloud-connected 3D exploration and visualization tool for multi-modal neuroimaging data

Vesna Prčkovska[1], Tim Peeters[1], David Moreno-Dominguez[1], and Paulo Rodrigues[1]

[1]Mint Labs, Barcelona, Spain

Diffusion MRI tractography is central to the study of complex brain circuitry since it is the only non-invasive technique capable of measuring the brain’s wiring. Data visualization gets increasingly complex as tractography is combined with morphometric results in structural connectomes, and even more so when coupled with functional information from fMRI techniques. Such complex imagery, aggregating multi-modal information, 3D meshes, and statistical maps is often visualized using research tools with complicated user interfaces (UIs) and cluttered visualizations.

BrainVis is a sophisticated, free 3D neuroimaging visualization tool with a simple UI aimed for effective exploration of neuroimaging data towards demonstrating neurobiological findings.

2404

Distributed rCBF changes caused by high frequency rTMS on lateral prefrontal cortex

Jun Xie[1], Wei Peng[1], Jian Zhang[1], Da Chang[1], and Ze Wang[1]

[1]Hangzhou Normal University, Hangzhou, People's Republic of China

The repetitive application of transcranial magnetic stimulation (rTMS) on left dorsolateral prefrontal cortex (DLPFC) have been consistently shown to be beneficial for treating various neuropsychiatrical or neuropsychological disorders, however its neural mechanisms still remain unclear. In this study, we measured the effects of high-frequency left DLPFC rTMS using cerebral blood flow (CBF). The results showed the rTMS induced CBF redistribution in the default mode network, including increased rCBF in temporal cortex which was correlated with increased behavior performance, but reduced rCBF in precuneus and cerebellum.

2405

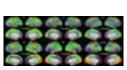

Exploring complementarity in multi-modal imaging of cortex microstructure: a diffusion and relaxometry study

Jean-François Cabana[1], Guillaume Gilbert[2], Nikola Stikov[3,4], Julien Cohen-Adad[3], Laurent Létourneau-Guillon[5,6,7], and Dang Nguyen[6,8,9]

[1]CRCHUM, Université de Montréal, Montreal, QC, Canada, [2]MR Clinical Science, Philips Healthcare Canada, Markham, ON, Canada, [3]NeuroPoly Lab, Ecole Polytechnique, Montreal, QC, Canada, [4]Montreal Heart Institute, University of Montreal, Montreal, QC, Canada, [5]CHUM Notre-Dame, Montreal, QC, Canada, [6]CRCHUM, Montreal, QC, Canada, [7]Université de Montréal, Montreal, QC, Canada, [8]Division of Neurology, CHUM Notre-Dame, Montreal, QC, Canada, [9]Department of Neuroscience, Université de Montréal, Montreal, QC, Canada

We explored the utility and complementarity of different diffusion and relaxometry metrics for cortical imaging. The following metrics were assessed for correlation: mean kurtosis (MK) from diffusion kurtosis imaging, intra-cellular volume fraction (ICVF), from the NODDI model, intra-neurite volume fraction (VINT), from the multi-compartment microscopic diffusion imaging (MCMICRO) model, R1 (=1/T1), R2* (=1/T2*) and the ratio of T1w/T2w images. Some global similarities can be seen between most cortical maps, while some features that suggest complementarity between diffusion and relaxometry maps were also observed. This study emphasizes the importance of better understanding and characterising the relationship between different MRI-derived metrics.

2406

Inductively coupled coils enable dental MRI with 350 um isotropic resolution in 2 min

Ute Ludwig[1,2], Anne-Kathrin Eisenbeiss[1,2], Philipp Amrein[1,2,3], Tabea Flügge[2,3], Johannes Maier[2,3], Katja Nelson[2,3], and Jan-Bernd Hövener[1,2,4]

[1]Department of Radiology, Medical Physics, Medical Center - University of Freiburg, Freiburg, Germany, [2]Faculty of Medicine, University of Freiburg, Freiburg, Germany, [3]Division of Oral and Maxillofacial Surgery, Medical Center - University of Freiburg, Freiburg, Germany, [4]Partner Site Freiburg, German Consortium for Cancer Research (DKTK), Heidelberg, Germany

High-resolution MRI of the lower jaw with an isotropic voxel size of 350 µm was performed at 3T using a 4-cm loop coil (LC) with and without an inductively coupled volume coil (ICC) enclosing the target region. Within this region, a much higher SNR was obtained and the resolution of anatomical details was strongly enhanced with the ICC. A new, custom-made holder for the LC improved the overall handling. Compared to earlier results, the scan time was reduced by 50%, now 2 minutes, to provide very high resolution MRI of 2-3 teeth.

2407

Quantitative Measurement of Cerebral Blood Volume Across 173 Brain Regions In Anethesia and Response to CO2

Liam Timms[1], Codi Gharagouzloo[2], Ju Qiao[3], Zihang Fang[1], Praveen Kulkarni[4], Anne van De Ven[1], and Craig Ferris[5]

[1]Physics, Northeastern University, Boston, MA, United States, [2]Gordon Center for Medical Imaging, Massachusetts General Hospital, Harvard Medical School, Boston, MA, [3]Bioengineering, Northeastern University, Boston, MA, United States, [4]Psychology, Northeastern University, Boston, MA, United States, [5]Physics, Bioengineering, Northeastern University, Boston, MA, United States

We use a technique based on positive contrast quantitative imaging of super paramagnetic iron oxide nanoparticles with optimized parameters which we have previously introduced called QUTE-CE to measure CBV across a detailed rat brain atlas. This is done for an anesthetized state and then changes in an awake hypercapnic state are additionally quantified. The former provides a baseline for future work and reflects evolutionary and developmental forces. The latter demonstrates the potential of the technique for measuring changes in CBV and provides a measure of perfusion reserve.

2408

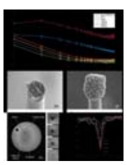

Carbon fiber electrodes for single-unit recording combined with artifact-free MRI

Miguel Roberto Chuapoco[1], Ben Andrew Duffy[2], Hyun Joo Lee[2], ManKin Choy[2], and Jin Hyung Lee[2,3]

[1]Department of Chemical Engineering, Stanford University, Stanford, CA, United States, [2]Department of Neurology and Neurological Sciences, Stanford University, [3]Departments of Bioengineering, Neurosurgery, Electrical Engineering, Stanford University, Stanford University

Combining unit recording and fMRI is a powerful method that allows for interrogation of the brain at the cellular and network level. However, implanted metal recording electrodes produce susceptibility artifacts that distort MR images. Here, we fabricate single carbon-fiber electrodes and implant them into rat hippocampus and use an agarose phantom to quantify its MR distortion. These carbon-fiber electrodes record from a single unit in CA1 and distort a significantly lower volume of voxels compared to metal electrodes. These results lay the groundwork for an electrode design that can be used for single-unit recording and fMRI in same subjects.

2409

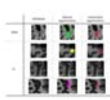

AUTOMATED DETECTION OF WHITE-MATTER AND CORTICAL LESIONS IN MP2RAGE AT ULTRA-HIGH FIELD USING A SINGLE SCAN

Mário João Fartaria [1,2,3], Alexis Roche[1,2,3], Alexandra Şorega[4], Kieran O'Brien[5,6], Gunnar Krueger[7], Bénédicte Maréchal[1,2,3], Pascal Sati[8], Daniel S. Reich[8], Tobias Kober[1,2,3], Meritxell Bach Cuadra[2,3,9], and Cristina Granziera[10,11]

[1]Advanced Clinical Imaging Technology, Siemens Healthcare AG, Lausanne, Switzerland, [2]Department of Radiology, Centre Hospitalier Universitaire Vaudois (CHUV) and University of Lausanne (UNIL), Lausanne, Switzerland, [3]Signal Processing Laboratory (LTS 5), Ecole Polytechnique Fédérale de Lausanne (EPFL), Lausanne, Switzerland, [4]Department of Radiology, Valais Hospital, Sion, Switzerland, [5]Centre for Advanced Imaging, University of Queensland, Brisbane, Queensland, QC, Australia, [6]6. Siemens Healthcare Pty Ltd., Brisbane, Queensland, Australia, [7]Siemens Medical Solutions USA, Boston, MA, United States, [8]Translational Neuroradiology Section, Institute of Neurological Disorders and Stroke, National Institutes of Health (NIH), Bethesda, MD, United States, [9]Medical Image Analysis Laboratory (MIAL), Centre d'Imagerie BioMédicale (CIBM), Lausanne, Switzerland, [10]Martinos Center for Biomedical Imaging, Massachusetts General Hospital and Harvard Medical School, Boston, MA, United States, [11]Department of Clinical Neurosciences, Centre Hospitalier Universitaire Vaudois (CHUV) and University of Lausanne (UNIL), Lausanne, Switzerland

Ultra-high-field Magnetic Resonance Imaging (7T MRI) has been shown to be a valuable tool to assess focal and diffuse pathology in multiple sclerosis (MS) patients, both in grey- and in white-matter. In this work, we developed and evaluated a method to automatically assess MS lesion load using magnetization-prepared two inversion-contrast rapid gradient-echo (MP2RAGE) MRI at 7T. The validation was conducted in a cohort of twenty MS patients from two research centers through a ground truth based on manual segmentations performed by a radiologist. Our single-sequence segmentation accurately detects visible white-matter and cortical lesions.

2410

Harmonization for fractional anisotropy measurement at 3T in healthy subjects

Miaomiao Wang[1], Xianjun Li[1,2], Chao Jin[1], Congcong Liu[1], Jianxin Guo[1], Hui Hao[1], and Jian Yang[1]

[1]Department of Diagnostic Radiology, the First Affiliated Hospital of Xi'an Jiaotong University, Xi'an, People's Republic of China, [2]Department of Biomedical Engineering, School of Life Science and Technology, Xi'an Jiaotong University

In current clinical practice, the absence of standard protocol of diffusion tensor imaging (DTI) challenges the consistency of DTI data, and thus affects the accuracy of data group analysis. This study aims to assess the inconsistency of DTI-derived fractional anisotropy (FA) based on the different clinical protocols and further make them into harmonization. Results suggest the effects of slice thickness and b-value of FA are anatomy dependent, which is more stable in white matter with packed and orientation consistent fibers. Besides, a developed polynomial fitting model was used to make FA harmonization among different DTI protocols.

2411 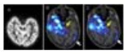

Automatic registration of MRI and transcranial ultrasound for the analysis of neurological disorders

Yiming Xiao[1,2], Dante De Nigris[3], Ian J. Gerard[4], Yuhan Ma[4], Donatella Tampieri[5], D. Louis Collins[4], and Hassan Rivaz[1,2]

[1]PERFORM Centre, Concordia University, Montreal, QC, Canada, [2]Department of Electrical and Computer Engineering, Concordia University, Montreal, QC, Canada, [3]NeuroRx Research, Montreal, QC, Canada, [4]Montreal Neurological Institute, McGill University, Montreal, QC, Canada, [5]Department of Diagnostic and Interventional Neuroradiology, Montreal Neurological Hospital, Montreal, QC, Canada

Transcranial ultrasound (TCUS) can be used to diagnose and monitor a range of neurological conditions, such as Parkinson's disease. However, reliable quantitative examination and multi-modal image analysis that involves TCUS require TCUS-MRI registration to guide the interpretation and measurement of the TCUS. We demonstrate that accurate rigid registration can be achieved through aligning gradient orientations of the 3D TCUS and an associated pseudo-TCUS constructed from the T1w MRI.

2412 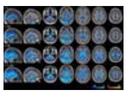

Evaluation of multispectral segmentation of gray matter based on 3D T1-, T2 and T2-weighted FLAIR images for gray matter segmentation

Kotikalapudi Raviteja[1], Pascal Martin[2], Niels K Focke[2], and Benjamin Bender[1]

[1]Diagnostic and Interventional Neuroradiology, University Hospital Tübingen, Tübingen, Germany, [2]Neurology and Epileptology, University Hospital Tübingen, Tübingen, Germany

An ideal classification of brain tissue structures as segmented gray matter (GM) has been a challenge while using standard T1-weighted image. One of the important ways of addressing this issue would be to use additional information from multispectral imaging such as T2- and T2-weighted FLAIR images. We evaluated the effect of multispectral segmentation on GM segmentation using SPM12 VBM and compared it with T1-only segmentation. We found that T1-segmentation overestimates dura, meninges and vessels as GM. This problem was successfully addressed by multispectral segmentation, which should be used as a segmentation model for future VBM studies.

2413 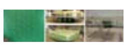

A modular RF coil platform for ex-vivo imaging of brain slices at 9.4T

Shubharthi Sengupta[1], Francisco J Fritz[1], Ron Hellenbrand[2], René Finger[2], Christopher J Wiggins[3], and Alard Roebroeck[1]

[1]Dept. of Cognitive Neuroscience, Faculty of Psychology and Neuroscience, Maastricht University, Maastricht, Netherlands, [2]Lab Engineering & Instrumentation Department, Maastricht University, Netherlands, [3]Scannexus, Maastricht, Netherlands

We present a modular 9.4T RF coil platform that can be used for imaging slabs of tissue as large as a sagittal section of a human brain (dia. 18cm), with a thickness of up to 2cm. The 23-channel receive array was designed with a layered printed circuit approach to ensure the coils' decoupling and proximity to the sample and with on-coil, low-noise preamplifier circuits. A 7 channel, phased transmit array capable of parallel transmission (pTx) makes homogeneous excitation of a large range of samples possible. The high homogeneous contrast-to-noise acquisitions enabled by the coil will allow high resolution anatomical imaging at 9.4T.

2414 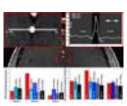

Head-to-head comparison of ferumoxytol and gadolinium-enhanced intracranial MRA at 7T vs. non-contrast TOF

Daniel Schwartz[1], Ramon F Barajas[2], John Grinstead[3], Laszlo Szidonya[4], Jenny Firkins[4], William Rooney[5], and Edward Neuwelt[6]

[1]Neurology/AIRC, OHSU, Portland, OR, United States, [2]Radiology/AIRC, OHSU, [3]Siemens Medical, [4]Neurology, OHSU, [5]AIRC, OHSU, [6]Neurology/Neurosurgery, OHSU

7T imaging of neurovasculature with TOF affords sub-millimeter resolution and can make it possible to visualize extremely small vessels such as the lenticulostriate arteries; however, TOF can be hampered by flow and pulsation artifacts. K-space reordering and the administration of a contrast agent can greatly reduce these artifacts while still allowing for small vessel conspicuity. We acquired gadolinium and ferumoxytol-based MRA alongside TOF in three patients and two radiologists rated vessel conspicuity and artifact. Artifacts were diminished with contrast, though there were no differences in artifact due to k-space reordering, and vessel conspicuity was high in all acquisitions.

2415 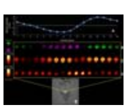

Bias in Aqueductal Cerebrospinal Fluid Flow Quantification Obtained using 2D PC-MRI

Sudarshan Ragunathan[1,2] and James G Pipe[1]

[1]Barrow Neurological Institute, Phoenix, AZ, United States, [2]School of Biological Health and Systems Engineering, Arizona State University, Tempe, AZ, United States

This focus of this work was to determine the extent of RF saturation induced bias in cerebrospinal fluid flow quantification using 2D PCMRI. The velocity distribution within a flow region inherently biases the average estimate per voxel towards faster spins in that voxel. This effect was studied through variations in flip angle. The results indicated that higher flip angles would introduce more bias in the flow estimates, which could be a possible reason for the lack of consensus concerning the use of PCMRI in determining patient responsiveness to surgical interventions in NPH studies.

Magnetic Resonance Neurography (MRN) in the abdomen: the feasibility of imaging the celiac plexus with motion-compensated 3D SHINKEI

2416

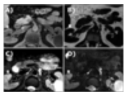

Cyril J Ferrer[1], Clemens Bos[1], Lisanne Kok[1], Masami Yoneyama[2], Makoto Obara[2], Marijn van Stralen[1], Chrit T.W Moonen[1], and Lambertus W Bartels[1]

[1]UMC Utrecht, Utrecht, Netherlands, [2]Philips Electronics Japan, Tokyo, Japan

Recently, the 3D-SHINKEI (3D nerve-SHeath signal increased with INKed rest-tissue RARE Imaging) sequence was introduced for peripheral MR neurography. This method uses an improved Motion Sensitized Driven Equilibrium (iMSDE) prepulse to suppress muscle and slow flow signal, for improved visualization of peripheral nerves. Applying this method in the abdomen would provide the potential to image the celiac plexus, which is involved in various pain mechanisms, e.g. due to pancreatic cancer and other upper gastrointestinal malignancies. In this work, we show the feasibility of MRN of the celiac plexus in volunteers by using cardiac and respiratory motion-compensated 3D SHINKEI.

2417

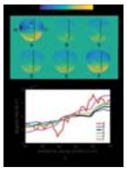

Magnetic flux density comparisons between in-vivo TACS human Magnetic Resonance Electrical Impedance Tomography measurements and MRI-derived human computational models

Aprinda Indahlastari[1], Aditya Kumar Kasinadhuni[2], Kevin Castellano[2], Christopher Saar[1], Casey Weigel[1], Bakir Mousa[1], Munish Chauhan[1], Thomas H Mareci[2], and Rosalind J Sadleir[1]

[1]Arizona State University, Tempe, AZ, United States, [2]University of Florida

actual current densities applied to the brain in neuromodulation therapies. MREIT can be used to determine actual current densities delivered to the brain by measuring Bz. Here we present Bz distributions resulting from trans-temporal current injection obtained from MREIT imaging during 10 Hz TACS in a healthy human subject. Comparisons of MREIT results to MRI-derived computational models suggested that actual contact areas between electrodes and scalp may be smaller than electrode surface areas, and in-vivo tissue conductivity values, particularly skin and skull, may be different than assumed.

2418

Altered microstructural integrity in patients with tuberous sclerosis complex revealed by whole-brain tract-specific analysis

Chien-Feng Huang[1], Chih-Hsien Tseng[1,2], Pi-Chuan Fan[3], and Wen-Yih Isaac Tseng[1,2,4]

[1]Institute of Medical Device and Imaging, National Taiwan University College of Medicine, Taipei, Taiwan, [2])Institute of Biomedical Engineering, National Taiwan University College of Medicine, Taipei, Taiwan, [3]Department of Pediatrics, National Taiwan University Hospital and National Taiwan University College of Medicine, Taipei, Taiwan, [4]Molecular Imaging Center, National Taiwan University, Taipei, Taiwan

To investigate whether the white matter tracts are altered in patients with tuberous sclerosis complex, we used whole-brain tract-specific analysis of diffusion spectrum imaging (DSI) data to measure the alteration of 76 major white matter tracts, and compared the property between 27 patients and 27 matched controls. As compared to the controls, patients showed significantly lower GFA in 13 tracts. The altered microstructural integrity of the white matter tracts in TSC supports the hypothesis of underlying microstructural changes in the brains of TSC.

2419

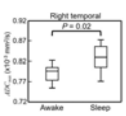

Dynamic ADC Change during Cardiac Cycle in Human Brain in Sleep State

Ryoko Yamamori[1], Tosiaki Miyati[1], Naoki Ohno[1], Yuki Hiramatsu[1], Toshiharu Kurita[2], Seika Miki[1], Akiko Sekiya[1], Yuri Hoshina[3], and Toshifumi Gabata[4]

[1]Division of Health Sciences, Graduate School of Medical Sciences, Kanazawa University, Kanazawa, Ishikawa, Japan, Kawazawa, Japan, [2]East Medic Corporation, Kanazawa, Ishikawa, Japan, Japan, [3]Department of Inspection, Japanese Red Cross Kanazawa, Japan, [4]Department of Radiology, Kanazawa University Hospital, Kanazawa, Japan

The glymphatic system is a waste clearance pathway in brain. During sleep, the increase in the interstitial influx results in faster waste removal. Apparent diffusion coefficient (ADC) in brain significantly changed during the cardiac cycle, and this change (ΔADC) shows the degree of fluctuation in water molecules. Therefore, we analyzed fluctuation of water molecules in the brain of healthy subjects in awake and sleep states. Maximum ADC and ΔADC of the white matter increased in sleep state. Fluctuation analysis facilitates the noninvasive evaluation of the dynamic state of water movement in the brain in sleep state as a glymphatic MRI.

2420

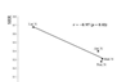

The Nulling Signal Produced by Inversion Recovery for Gray Matter is Related to Neuronal Density in the Thalamic Subnuclei: A 7T MRI Study

Nambeom Kim[1], Young-Don Son[1,2], Kyung-Jin Lee[1,2], Yeong-Bae Lee[1,3], and Chang-Ki Kang[1,4]

[1]Neuroscience Research Institute, Gachon university, Incheon, Korea, Republic of, [2]Department of Biomedical Engineering, Gachon University, [3]Department of Neurology, Gachon University Gil Medical Center, Gachon University, [4]Department of Radiological Sciences, Gachon University

The thalamus acts as a gateway to higher brain centers that are involved in cognition, sleep, arousal, as well as sensory and motor information [1–5]. Additionally, changes in the thalamic subnuclei (TS) have been implicated in a number of neuropsychiatric disorders. In a postmortem study, the neuronal number as well as the total volume of the thalamus were significantly decreased in schizophrenic subjects or elevated in major depression subjects, especially in the medial dorsal nucleus [6,7]. As a result, the ability to estimate neuronal density in the thalamic subnuclei (TS) using in-vivo imaging is highly desired.

2421

Automated T2 Relaxometry of the Hippocampus

Gavin Paul Winston[1,2], Sjoerd B Vos[2,3], Jane L Burdett[1,2], M Jorge Cardoso[3], Sebastien Ourselin[3], and John S Duncan[1,2]

[1]Department of Clinical and Experimental Epilepsy, UCL Institute of Neurology, London, United Kingdom, [2]Epilepsy Society MRI Unit, Chalfont St Peter, United Kingdom, [3]Translational Imaging Group, Centre for Medical Image Computing, UCL, London, United Kingdom

Hippocampal sclerosis (HS), the most common cause of refractory temporal lobe epilepsy, is associated with hippocampal volume loss and increased T2-signal. These can be identified on quantitative imaging with hippocampal volumetry and T2 relaxometry. Whilst hippocampal segmentation for volumetry has been automated, T2 relaxometry currently involves subjective manual delineation of regions-of-interest. In this work, we validate an automated technique for hippocampal T2 relaxometry and show in a group of healthy controls and patients with HS that a combination of hippocampal volume and T2 values can reliably distinguish the groups and that automated measurement is more reproducible than manual measurement.

Traditional Poster

Neuro: Processing & Analysis

Exhibition Hall 2422-2441 Wednesday 13:45 - 15:45

2422

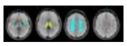

Comparison of Susceptibility Weighted Imaging MRI implementations across vendors: Implications for multi-centre studies

Maryam Abaei[1], Sjoerd B. Vos[2,3], Derek L.G. Hill[1], Robin Wolz[1,4], Marios C Yiannakas[5], Magdalena Sokolska[6], Sebastien Ourselin[2,7], John Duncan[2,8], and David Thomas[9,10]

[1]IXICO PLC, London, United Kingdom, [2]Translational Imaging Group, CMIC, University College London, London, United Kingdom, [3]Epilepsy Society MRI Unit, Chalfont St Pete, United Kingdom, [4]Department of Computing, Imperial College, London, United Kingdom, [5]UCL Institute of Neurology, University College London, London, London, United Kingdom, [6]Department of Medical Physics and Bioengineering, University College Hospital, London, United Kingdom, [7]Dementia Research Centre, University College London, London, United Kingdom, [8]Department of Clinical and Experimental Epilepsy, UCL Institute of Neurology, Chalfont St Peter, United Kingdom, [9]Brain Repair & Rehabilitation, UCL Institute of Neurology, London, United Kingdom, [10]Leonard Wolfson Experimental Neurology Centre, UCL Institute of Neurology, London, United Kingdom

Multi-centre, MRI, Susceptibility Weighted imaging, Brain, Clinical Studies

---

2423

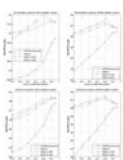

A simple partial volume correction method for magnetization transfer ratio images

Enrico De Vita[1,2], Ruth Oliver[3], Chris Sinclair[4], David L Thomas[4], Xavier Golay[4], Simon Mead[5,6], and John S Thornton[1,4]

[1]Lysholm Department of Neuroradiolgy, National Hospital for Neurology and Neurosurgery, London, United Kingdom, [2]Academic Neuroradiological Unit. Dept. of Brain Repair and Rehabilitation, University College London, United Kingdom, [3]Sydney Neuroimaging Analysis Centre, Sydney, Australia, [4]Academic Neuroradiological Unit. Dept of Brain Repair and Rehabilitation, University College London, United Kingdom, [5]National Prion Clinic, National Hospital for Neurology and Neurosurgery, United Kingdom, [6]MRC Prion Unit. Department of Neurodegenerative Diseases, UCL Institute of Neurology, United Kingdom

We here demonstrate how partial volume correction by linear regression in the style originally proposed for arterial spin labelling MRI can be used to perform a simple and effective partial volume correction for Magnetisation Transfer Ratio data.

2424

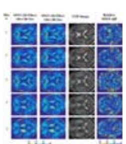

A Novel Expectation Maximization based Multi Voxel Spatial Regularization Algorithm with Stimulated Echo Contribution (MVSR-STE) for Multi Component Analysis of the Quantitative T2 Relaxometry

Dushyant Kumar[1], Hari Hariharan[1], Jens Fiehler[2], Susanne Siemonsen[2], Jan Sedlacik[2], and Ravinder Reddy[1]

[1]Radiology, University of Pennsylvania, Philadelphia, PA, United States, [2]Klinik und Poliklinik für Neuroradiologische Diagnostik und Intervention, Universitätsklinikum Hamburg-Eppendorf, Hamburg, Germany

Problem: The quantification accuracy of myelin water fraction mapping based on multi echo spin echo (MESE) T2 relaxometry is compromised due to high SNR requirement, along with the need to account for contributions from stimulated echo pathways.

Methods: A novel expectation-maximization post-processing method, with convergence guaranty, is proposed, which accounts for stimulated contributions intrinsically, while simultaneously improving noise robustness by utilizing spatial correlation from 3D local neighborhood.

Results & Conclusions: Results demonstrate improved quantifications as a result of the proposed algorithm.

2425

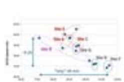

Gradient non-linearity effects on upper cervical cord area measurement from MPRAGE brain MRI acquisitions

Nico Papinutto[1], Rohit Bakshi[2], Peter A Calabresi[3], Eduardo Caverzasi[1,4], Todd Constable[5], Gina Kirkish[1], Govind Nair[6], Jiwon Oh[3,7], Daniel Pelletier[8], Dzung L Pham[9], Daniel S Reich[6], William Rooney[10], Snehashis Roy[9], Daniel Schwartz[10], Russell T Shinohara[11], Nancy L Sicotte[12], William A Stern[1], Ian Tagge[10], Shahamat Tauhid[2], Subhash Tummala[2], and Roland G Henry[1,13]

[1]Department of Neurology, University of California San Francisco, San Francisco, CA, United States, [2]Department of Neurology, Brigham and Women's Hospital, United States, [3]Department of Neurology, The Johns Hopkins University, United States, [4]Department of Brain and Behavioral Science, Univeristy of Pavia, Italy, [5]Yale University, School of Medicine, United States, [6]Translational Neuroradiology Section, National Institute of Neurological Disorders and Stroke, United States, [7]Department of Neurology, University of Toronto, Canada, [8]Department of Neurology, University of Southern California, United States, [9]Center for Neuroscience and Regenerative Medicine, Henry M. Jackson Foundation, United States, [10]Advanced Imaging Research Center, Oregon Health & Science University, United States, [11]Department of Biostatistics and Epidemiology, Perelman School of Medicine, University of Pennsylvania, United States, [12]Department of Neurology, Cedars-Sinai Medical Center, United States, [13]Department of Radiology, University of California San Francisco, United States

Upper cervical cord area (UCCA) is strongly associated with physical disability in patients with multiple sclerosis, particularly in progressive stages of disease. Standard brain high-resolution 3D T1-weighted acquisitions that include the upper cervical cord can be used to provide estimates of UCCA. Depending on subject positioning in the scanner, gradient non-linearity can introduce up to 10% variability in UCCA measurements from volumetric brain MPRAGE scans. In planning a study, use of 3D correction methods provided by the scanner vendors seems optimal. Alternatively, to retrospectively correct data, we propose methods based on a phantom acquisition or normalization with vertebral body diameters.

2426

Evaluating White Matter Changes in Amyotrophic Lateral Sclerosis from T1-weighted MRI using 3-D Texture Analysis

Abdullah Ishaque[1], Yee-Hong Yang[2], and Sanjay Kalra[3]

[1]Neuroscience and Mental Health Institute, University of Alberta, Edmonton, AB, Canada, [2]Department of Computing Science, University of Alberta, [3]Division of Neurology, University of Alberta

Amyotrophic lateral sclerosis is a fatal neurodegenerative disease of the motor system with substantial disease burden in white matter. Clinical MRI studies are used only to exclude diagnoses of symptom-mimicking neurological disorders. We propose that texture analysis performed on structural MRI can provide a surrogate marker for subtle white matter changes that are observed in ALS. This study shows significant correlations between texture features from T1-weighted imaging and diffusion measures such as fractional anisotropy and mean diffusivity. These texture features also demonstrated significant differences between ALS and controls and can potentially be used clinically for diagnosis and disease monitoring.

2427

Impact of the topology of brain microbleeds on the structural brain network

Xiaopei Xu[1], Henry KF Mak[1,2], Kui-Kai Lau[3], Pak Lun Lam[4], and Edward S Hui[1,2]

[1]Department of Diagnostic Radiology, The University of Hong Kong, HKSAR, People's Republic of China, [2]The State Key Laboratory of Brain and Cognitive Sciences, The University of Hong Kong, HKSAR, People's Republic of China, [3]Department of Medicine, The University of Hong Kong, HKSAR, People's Republic of China, [4]Li Ka Shing Faculty of Medicine, The University of Hong Kong, HKSAR, People's Republic of China

We aim to investigate the effect of the topology of brain microbleeds (BMBs), lobar (n = 32) versus deep/infratentorial (n = 31), on structural brain network in patients with TIA or first-time stroke. Our results demonstrated that the efficiency of the local and global networks of both BMB cohorts were lower compared to controls (n = 31), and that only the load of the patients with lobar BMBs was strongly associated with decrease in the efficiency of local and global networks independent of vascular risk factors. These findings suggested that lobar and deep BMBs likely have distinct pathophysiological underpinnings.

2428

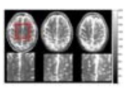

A Method for Quantification of T1 in Multiple Sclerosis Lesions

Yong Ik Jeong[1], Adil Javed[2], Nancy Arndt[2], Keigo Kawaji[2], Adam Hasse[2], and Timothy J Carroll[2]

[1]Northwestern University, Evanston, IL, United States, [2]University of Chicago

The development of multiple sclerosis lesions appear as different contrast mechanisms on the different MR imaging scans. In T1 weighted images, these evolve into hypointense lesions and representative of demyelination. In this study, we propose a method of quantifying T1 values using retrospective data of T1 weighted images, and apply this method to investigate potential trends of T1 changes in multiple sclerosis patients across time. We look at four patients imaged at three time points across 12 months, and find that an increase in T1 of lesions may be a trend.

2429

Distinct and common gray matter volume and cortical thickness abnormalities between non-comorbid medication-naive patients with major depressive disorder and social anxiety disorder

Youjin Zhao[1], Chandan Shah[1], Su Lui[1], and Qiyong Gong[1]

[1]Department of Radiology,West China Hospital of Sichuan University, Huaxi MR Research Center (HMRRC), Chengdu, People's Republic of China

An overlap of diagnosis frequently occurs between major depression disorder (MDD) and social anxiety disorder (SAD) and few studies directly compare neuroanatomical abnormalities in the two disorders. Pure MDD patients (n = 37), pure SAD patients (n = 24) and healthy controls (n = 41) underwent T1-weighted magnetic resonance imaging (MRI). Gray matter volume and cortical thickness were compared in the three groups. The main findings of this study were that (i) MDD and SAD patients shared common neural substrates in frontal-subcortical circuits; and (ii) MDD patients manifested more widespread brain structure alterations than SAD patients.

2430

Robust and automatic spinal cord detection on multiple MRI contrasts using machine learning

Charley Gros[1], Benjamin De Leener[1], Allan R. Martin[2], Michael G. Fehlings[2], Virginie Callot[3,4], Nikola Stikov[1,5], and Julien Cohen-Adad[1,6]

[1]NeuroPoly Lab, Institute of Biomedical Engineering, Polytechnique Montreal, Montréal, QC, Canada, [2]Division of Neurosurgery, Department of Surgery, University of Toronto, Toronto, ON, Canada, [3]Aix Marseille Univ, CNRS, CRMBM, Marseille, France, [4]APHM, Hôpital de la Timone, Hôpital de la Timone, Pôle d'imagerie médicale, Marseille, France, [5]Montreal Heart Institute, Montréal, QC, Canada, [6]Functional Neuroimaging Unit, CRIUGM, Université de Montréal, Montreal, QC, Canada

Detecting the spinal cord on a large variety of MRI data is challenging but essential for the automation of quantitative analysis pipelines. For the past few years, machine learning algorithms have outperformed most unsupervised image processing methods. The present study investigates the performance of two different machine learning algorithms, Convolutional Neural Networks (CNN) and Support Vector Machine (SVM), on MRI data from different vendors, with a variety of pathology, contrast, resolution and FOV. Results suggest strong performance of the CNN approach, opening the door to application in multi-center analysis pipelines.

2431

Microstructural alterations in patients after liver transplantation and treated with calcineurin inhibitors – a quantitative MRI study

Lukas Goede[1], Birte Schmitz[1], Henning Pflugrad[2], Anita Blanka Tryc[2], Hannelore Barg-Hock[3], Jürgen Klempnauer[3], Karin Weissenborn[2], Heinrich Lanfermann[1], and Xiao-Qi Ding[1]

[1]Institute for Neuroradiology, Hannover Medical School, Hannover, Germany, [2]Department of Neurology, Hannover Medical School, Hannover, Germany, [3]Clinic for Visceral and Transplant Surgery, Hannover Medical School, Hannover, Germany

With the aim to evaluate possible brain microstructural alterations associated with calcineurin inhibitor (CNI) therapy, ninety patients after liver transplantation (OLT) treated with different doses of CNI and 32 gender- and age-adjusted healthy volunteers were studied with quantitative MRI (qMRI). T1, T2, T2*, Proton density (PD) and phase changes (derived from susceptibility-weighted imaging, SWI) were measured in 18 brain regions (regions of interest, ROIs). The values were compared between the groups of patients and the controls, which showed significant differences between the groups, indicating alterations of brain microstructure in patients after OLT.

2432

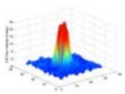

Increased Anisotropy as Possible Compensatory Plasticity of Ventral Thalamic Nuclei to Gait Disturbance in Patients with Idiopathic Normal Pressure Hydrocephalus

Ping-Huei Tsai[1,2,3], Yung-Chieh Chen[4], Shih-Wei Chiang[5,6], Hua-Shan Liu[3,7], Ming-Chung Chou[8], Fei-Ting Hsu[2,3], Yu-Chieh Kao[1,3], Chia-Feng Lu[1,3], Hsiao-Wen Chung[6], and Cheng-Yu Chen[1,2]

[1]Department of Radiology, School of Medicine, College of Medicine, Taipei Medical University, Taipei, Taiwan, [2]Department of Medical Imaging, Taipei Medical University Hospital, Taipei, Taiwan, [3]Translational Imaging Research Center, College of Medicine, Taipei Medical University, Taipei, Taiwan, [4]1Department of Biomedical Imaging and Radiological Sciences, National Yang-Ming University, Taipei, Taiwan, [5]Department of Radiology, Tri-Service General Hospital, Taipei, Taiwan, [6]Graduate Institute of Biomedical Electrics and Bioinformatics, National Taiwan University, Taipei, Taiwan, [7]School of Biomedical Engineering, College of Biomedical Engineering, Taipei Medical University, Taipei, Taiwan, [8]Department of Medical Imaging and Radiological Sciences, Kaohsiung Medical University, Kaohsiung, Taiwan

This study allows improved localization of sensorimotor-related thalamic nuclei providing non-invasive evaluation of the microstructural changes of thalamus after iNPH, which may have a potential to contribute to early diagnosis and better prognosis prediction in the patients.

2433

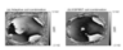

Effects of coil combination algorithms on Quantitative Susceptibility Mapping

Riccardo Metere[1], Ahmad Seif Kanaan[1,2], Berkin Bilgic[3], Torsten Schlumm[1], and Harald E. Möller[1]

[1]NMR Unit, Max Planck Institute for Human Cognitive and Brain Sciences, Leipzig, Germany, [2]Department of Psychiatry, Social Psychiatry and Psychotherapy, Hannover Medical School, Hannover, Germany, [3]A. A. Martinos Center for Biomedical Imaging and Department of Radiology, Harvard Medical School, Boston, MA, United States

Quantitative Susceptibility Mapping is an imaging technique for obtaining information of the magnetic susceptibility from phase images. If the phase information is obtained from a coil composed of multiple receive elements (coil array), the resulting images need to be combined. This step is non-trivial, and several algorithms, with different performances, have been proposed. Here we compare two different coil combination algorithms: the adaptive combine method and a recently proposed extension of ESPIRiT. For each, we compared both single subject and group-averaged QSM maps, where we observed that the results are sensitive to the method used for coil combination.

2434

IMPROVEMENT OF TOF-MRA IMAGE RECONSTRUCTION FROM UNDERSAMPLED DATA BY HEURISTIC MODIFICATION

Akira YAMAMOTO[1], Koji FUJIMOTO[1], Yasutaka FUSHIMI[1], Tomohisa OKADA[2], Kei SANO[3], Toshiyuki TANAKA[3], and Kaori TOGASHI[1]

[1]Department of Diagnostic Imaging and Nuclear Medicine, Graduate School of Medicine, Kyoto University, Kyoto, Japan, [2]Human Brain Research Center, Graduate School of Medicine, Kyoto University, Kyoto, Japan, [3]Department of Systems Science, Graduate School of Informatics, Kyoto University, Kyoto, Japan

We study a heuristic modification of the NESTA algorithm for compressed sensing reconstruction of TOF-MRA images, where at each iteration the calculated k-space data are replaced with the original (acquired) data wherever the latter are available. We compared the modified method with the original method. In qualitative visual analysis, reconstructed images from the modified method were a little noisier but with better vessel signal delineation. In quantitative analysis, the modified method as compared with the original method marked higher rVBR values in lower sampling ratio, and caused no image degradation in higher sampling ratio. The modified method therefore provides a viable option in improving reconstruction of the NESTA algorithm for TOF-MRA undersampled data.

2435

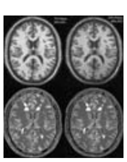

COMPARISON OF BRAIN ATROPHY MEASURES FOR CLINICAL USE IN MULTIPLE SCLEROSIS

Loredana Storelli[1], Elisabetta Pagani[1], Maria Assunta Rocca[1], Wim Van Hecke[2], Nicola De Stefano[3], Alex Rovira[4], Jaume Sastre-Garriga[5], Jacqueline Palace[6], and Massimo Filippi[1]

[1]Neuroimaging Research Unit, San Raffaele Scientific Institute, Vita-Salute San Raffaele University, Milan, Italy, [2]R&D icometrix Leuven Belgium, Leuven, Belgium, [3]Department of Medicine, Surgery and Neuroscience, University of Siena, Siena, Italy, [4]Department of Radiology, Hospital Universitari Vall d'Hebron, Barcelona, Spain, [5]Centre d'Esclerosi Múltiple de Catalunya (Cemcat), Department of Neurology/Neuroimmunology, Hospital Universitari Vall d'Hebron, Universitat Autònoma de Barcelona, Barcelona, Spain, [6]Nuffield Department of Clinical Neurosciences, University of Oxford, Oxford, United Kingdom

Aim of this study was to test two available methods (FSL-SIENAx/SIENA and Icometrix-MSmetrix) used for brain atrophy estimation on MR images of multiple sclerosis (MS) patients for a future clinical use. The accuracy and precision of these methods, as well as their main steps, were evaluated on 3D-T1 and 3DT2-FLAIR sequences of a simulated dataset, MRI of MS patients acquired at different scanners, field strengths, and on longitudinal dataset. From the comparison, SIENAx/SIENA showed a worst image registration, brain extraction and higher dependence on image acquisition quality than MSmetrix software. FSL pipelines showed better accuracy for cross-sectional and longitudinal analysis.

2436 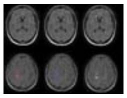

A SEMI-AUTOMATIC METHOD TO SEGMENT MULTIPLE SCLEROSIS LESIONS ON FLAIR MAGNETIC RESONANCE IMAGES

Loredana Storelli[1], Paolo Preziosa[1], Elisabetta Pagani[1], Vittorio Martinelli[2], Giancarlo Comi[2], Andrea Falini[3], Massimo Filippi[1], and Maria Assunta Rocca[1]

[1]Neuroimaging Research Unit, San Raffaele Scientific Institute, Vita-Salute San Raffaele University, Milan, Italy, [2]Department of Neurology, San Raffaele Scientific Institute, Vita-Salute San Raffaele University, Milan, Italy, [3]Department of Neuroradiology, San Raffaele Scientific Institute, Vita-Salute San Raffaele University, Milan, Italy

Aim of the study was to adapt and evaluate on FLAIR images a recently developed semi-automatic method for segmentation of hyperintense multiple sclerosis (MS) lesions on dual-echo (DE) PD/T2-weighted MRI. FLAIR MRI scans were obtained from 17 clinically isolated syndromes patients on a 1.5T scanner. The method was based on a region growing approach initialized by manual identification of lesions. The stop condition was formulated combining intensity and edge detection constraints. High similarity with the manual segmentation (the gold standard) was found, as well as a low misclassification of lesion voxels. Operator time required for lesion segmentation was importantly reduced.

2437 

Selecting parcellation schemes for regional cortical thickness estimations using a machine learning approach

Hsin-Yu Chen[1], Chia-Min Chen[1], Teng-Yi Huang[1], and Tzu-Chao Chuang[2]

[1]Department of Electrical Engineering, National Taiwan University of Science and Technology, Taipei, Taiwan, [2]Department of Electrical Engineering, National Sun Yat-sen University, Taiwan

In this study, we present a systematic approach to derive effective MR biomarkers of cerebral cortical thickness using machine learning methods and a large-scale database. Three neuroanatomical parcellation schemes for assessing region cortical thickness were compared. The results supported using the Desikan–Killiany atlas[1] of FreeSurfer produced robust results of age and gender predictions in normal subjects.

2438 

Fully automated morphometric brain volume extraction vs FreeSurfer

Shiami Luchow[1], Quadrelli Scott[2], Jameen Arm[1], Oun Al-iedani[1], Kate Skehan[1], Kristen Fisher[1], Benjamin Schmitt[3], Benedicte Marechal[4], and Saadallah Ramadan[1]

[1]University of Newcastle, Callaghan, Australia, [2]Princess Alexandra Hospital, Woolongabba, Australia, [3]Siemens Healthcare, Macquarie Park, Australia, [4]Siemens Healthcare, Lausanne, Switzerland

Brain architecture has been shown to change with different disease processes and this can be quantitatively measured using automated brain segmentation methods. FreeSurfer is a validated automated brain morphometry analysis method but requires time-consuming post-processing and is computationally complex. Fully automated prototype brain morphometry post-processing is available on our scanner, which generates brain morphology data at the end of the sequence acquisition and doesn't require manual post-processing. This study confirms that this prototype software yields brain morphology data that is highly correlated to FreeSurfer for major brain regions. Therefore, it can be used to investigate biomarkers of brain atrophy in research and clinical research arenas.

2439 

A patch-based method for lesion in-painting in the spinal cord

Ferran Prados[1,2], Manuel Jorge Cardoso[1], Marios C Yiannakas[2], Baris Kanber[1,2], Hugh Kearney[2], Claudia AM Gandini Wheeler-Kignshott[2,3,4], and Sebastien Ourselin[1]

[1]Translational Imaging Group, CMIC, Dep. of Medical Physics and Biomedical Engineering, University College London, London, United Kingdom, [2]UCL Institute of Neurology, Queen Square MS Centre, University College London, London, United Kingdom, [3]Department of Brain and Behavioural Sciences, University of Pavia, Italy, [4]Brain MRI 3T Mondino Research Center, C. Mondino National Neurological Institute, Italy

Multiple Sclerosis lesions can impair most automated image-processing pipelines. They can be present with different sizes, contrasts and shapes and at multiple locations across the central nervous system. Whilst lesion-filling is often a required pre-processing step in the analysis of brain MR images, its potential utility in spinal cord imaging remains unexplored. This study introduces a method for in-painting lesions in the spinal cord and demonstrates its efficacy for improving the results of spinal cord MR image analysis.

2440 

Patient-specific 3D Printable Anatomical Brain Models from a Web App

Ferran Prados[1], Daniil Nikitichev[1], Manuel Jorge Cardoso[1], Tom Vercauteren[1], and Sebastien Ourselin[1]

[1]Translational Imaging Group, CMIC, Dep. of Medical Physics and Biomedical Engineering, University College London, London, United Kingdom

The process for obtaining 3D printed models from patient-specific brain Magnetic Resonance Imaging (MRI) datasets remains tedious for non-computer scientists, despite the availability of various open-source image segmentation software and the current affordability of 3D printers. In this work, we present a web app that takes advantage of cloud computing technologies to propose a practical and straightforward system for anyone to upload brain MRI datasets and automatically receive corresponding patient-specific 3D printable models. Using our tool requires absolutely no specific installation or configuration.

2441 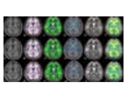

Automated Brain Tissue and Myelin Volumetry Based on Quantitative MR Imaging with Variable In-plane Resolutions

Christina Andica[1], Akifumi Hagiwara[1,2], Misaki Nakazawa[1,3], Masaaki Hori[1], and Shigeki Aoki[1]

[1]Radiology, Juntendo University, Tokyo, Japan, [2]Radiology, The University of Tokyo Graduate School of Medicine, Tokyo, Japan, [3]Radiological Sciences, Tokyo Metropolitan University Graduate School of Human Health Sciences, Tokyo, Japan

Automated brain tissue segmentation and volumetric assessment based on the quantification of the T1 relaxation time, T2 relaxation time and the proton density (PD) have demonstrated good accuracy and reproducibility. Recently, an automated myelin volume calculation based on quantitative imaging also has been introduced. This study showed that automated brain tissue and myelin volumetry based on quantitative MR imaging with lower in-plane resolutions have good repeatability and can be obtained in short acquisition times, which is beneficial for follow-up study.

Traditional Poster

Neurovascular

Exhibition Hall 2442-2468 Wednesday 13:45 - 15:45

2442

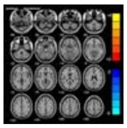

Excitatory Repetitive Transcranial Magnetic Stimulation (rTMS) Induces Contralesional Cortex-Cerebellar Pathways to Facilitate Motor Recovery after Acute Ischemic Stroke

Jing Li[1], Zhentao Zuo[2], Xuewei Zhang[1,3], Jie Lu[1], Xiali Shao[1], Rong Xue[2], Yong Fan[4], Yuzhou Guan[5], and Weihong Zhang[1]

[1]Department of Radiology, Peking Union Medical College Hospital, Peking Union Medical College & Chinese Academy of Medical Sciences, Beijing, People's Republic of China, [2]State Key Laboratory of Brain and Cognitive Science, Beijing MR Center for Brain Research, Institute of Biophysics, Chinese Academy of Sciences, Beijing, People's Republic of China, [3]Department of Interventional Radiology, China Meitan General Hospital, Beijing, People's Republic of China, [4]Department of Radiology, Department of Radiology, School of Medicine, University of Pennsylvania, Philadelphia, PA, United States, [5]Department of Neurology, Peking Union Medical College Hospital, Peking Union Medical College & Chinese Academy of Medical Sciences, Beijing, People's Republic of China

In this study we used the Diffusion Tensor Imaging method to assess motor pathway changes in acute ischemic stroke patients after high frequency repetitive transcranial magnetic stimulation (rTMS). We found that the excitatory rTMS applied to the ipsilesional primary motor cortex induced the contralesional cortex-cerebellar loop to facilitate motor recovery. The result is consistent with those of our former studies and gives us a clue to understand the therapeutic mechanism of rTMS for early stroke patients.

2443

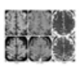

Detection of cerebral microvascular lesions using 7 T MRI in patients with neuropsychiatric systemic lupus erythematosus

yuka oikawa[1], okinori murata[2], nobuhito sasaki[2], ami matsumoto[2], akihiro ootsu[2], yutaka nakamura[2], yukari ninomiya[2], makoto sasaki[3], and kohei yamauchi[2]

[1]Division of Pulmonary Medicine,Allergy,and Rhematology,Department of internal Medicine, Iwate Medical University, morioka, Japan, [2]Pulmonary Medicine,Allergy,and Rheumatology, Iwate Medical University, Morioka, Japan, [3]Ultra-High Field MRI and Department of Radiology, Iwate Medical University, morioka, Japan

We investigated whether high-resolution images obtained using ultrahigh field MRI at 7 T can detect microcerebrovascular lesions in patients with neuropsychiatric systemic lupus erythematosus (NPSLE) that have never been detected by conventional MRI. We prospectively examined 20 patients with SLE, including five with NPSLE, using a 7 T MRI scanner. On the high-resolution T1WIs obtained at 7 T, minute punctate/linear hyperintense lesions in subcortical and/or cortical areas were found in four (80%) NPSLE patients and one (7%) non-NPSLE patient. High-resolution T1WIs obtained at 7 T can detect minute lesions, indicating intracerebral microvascular lesions in patients with NPSLE.

2444

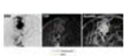

Acceleration-selective Arterial Spin Labeling (AccASL) MR Angiography of Brain Arteriovenous Malformation

Osamu Togao[1], Akio Hiwatashi[1], Makoto Obara[2], Koji Yamashita[1], Ryotaro Kamei[1], and Hiroshi Honda[1]

[1]Clinical Radiology, Graduate School of Medical Sciences, Kyushu University, Fukuoka, Japan, [2]Philips Electronics Japan, Tokyo, Japan

In the present study, we demonstrated the clinical utility of acceleration-selective arterial spin labeling (AccASL) MR angiography (MRA) in brain arteriovenous malformations (AVMs). AccASL-MRA significantly improved the visualization of AVM in comparison with time-of-flight (TOF)-MRA. AccASL-MRA could detect the nidus and draining veins in all patients. In particular, the detection of deep venous drainage by AccASL-MRA led to the accurate Spetzler-Martin grading. AccASL-MRA could serve as a noninvasive tool to evaluate brain AVMs without the use of contrast agents.

2445

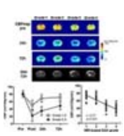

Cerebral Blood Flow of CASL Perfusion Imaging to Predict Neurobehavioral Outcome in a Murine Model of Subarachnoid Hemorrhage

Kazumasu Sasaki[1,2], Tatsushi Mutoh[2,3], Kazuhiro Nakamura[2,3], Tomoko Mutoh[3,4], Yasuko Tatewaki[3], Tomoyuki Yambe[1], Yasuyuki Taki[3], and Tatsuya Ishikawa[2]

[1]Department of Preclinical Evaluation, Institute of Development, Aging and Cancer (IDAC), Tohoku University, Sendai, Japan, [2]Research Institute for Brain and Blood Vessels-AKITA, Akita, Japan, [3]Department of Nuclear Medicine and Radiology, IDAC, Tohoku University, Sendai, Japan, [4]Graduate School of Psychology, Kobe Shoin Women's University, Kobe, Japan

Early brain injury/ischemia is a recent therapeutic target of subarachnoid hemorrhage (SAH) that contributes to triggering delayed cerebral ischemia (DCI) [1]. However, little is known about the role of cerebral blood flow (CBF) and neurobehavioral profiles at acute stage on functional outcome of the rodent model to simulate clinical severity early after SAH. The present study demonstrated the feasibility of MRI-based CBF measurements using the continuous arterial spin labeling (CASL) perfusion images for precise grading of the severity in a murine model of endovascular perforation model of SAH.

2446

Relationship between venous congestion and susceptibility of collecting veins: an in-vivo QSM study with developmental venous anomaly

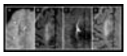

Jinhee Jang[1], Yoonho Nam[1], Song Lee[1], Hyun Seok Choi[1], So-Lyung Jung[1], Kook-Jin Ahn[1], and Bum-soo Kim[1]

[1]*Radiology, Seoul St. Mary's hospital, College of Medicine, The Catholic University of Korea, Seoul, Korea, Republic of*

A developmental venous anomaly (DVA) is a common vascular malformation, with an unusual-locating collection vein and fine venous structures draining into it. Occasionally, abnormal signal intensity is combined in draining area of DVA, which is a result of venous congestion. In this work, we explored the magnetic susceptibility of draining veins in DVAs with and without venous congestion. DVAs with venous congestion showed higher susceptibility values in collecting veins than those without venous congestion. Using 3D GRE and QSM, we could assess the oxygen metabolism of brain tissue with venous congestion.

2447

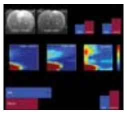

Modulation of the peri-infarct neurovascular function by Beta-Hydroxybutyrate

Paolo Bazzigaluppi[1], Evelyn Lake[2], Margaret Koletar[3], Rafal Janik[4], James Mester[5], Conner Adams[6], Peter Carlen[7], and Bojana Stefanovic[4]

[1]*Medical biophysics, Sunnybrook Research institute, Toronto, ON, Canada,* [2]*Yale University, CT, United States,* [3]*Sunnybrook Research Institute,* [4]*Sunnybrook Research Institute, ON, Canada,* [5]*Sunnybrook Research Center, ON, Canada,* [6]*ON, Canada,* [7]*Krembil Research Intitute, Toronto, ON, Canada*

In view of the failure of neurocentric treatments for ischemic stroke, this work examines a pleiotropic modulation of the neurogliovascular unit exerts beneficial effects in the treatment of brain stroke. Oxydative metabolism of glucose in the peri-ischemic tissue has potentially detrimental effects on tissue; in contrast, ketones' metabolism - in light of the reduced amount of oxygen required - provides a safer alternative. We employed functional CASL, in situ electrophysiology, and biochemical analysis to show short-term benefits of early administration of β-Hydroxybutyrate to metabolically challenged brain tissue following focal ischemia.

2448

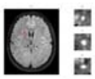

White Matter Hyperintensities Segmentation and Stereological Bias Correction On Clinical MRIs

Chau Q. Vu[1] and John C. Wood[2]

[1]*Biomedical Engineering, University of Southern California, Los Angeles, CA, United States,* [2]*Division of Cardiology and Radiology, Children's Hospital Los Angeles, Los Angeles, CA, United States*

White matter hyperintensities are lesions in the brain that exhibit high signal intensity on T2-weighted FLAIR images. In this study, we designed a seed-based segmentation method of these lesions from T2-weighted images of 1.3mm axial resolution, utilizing the local gradient field on a breadth-first search scheme as well as level thresholding and smoothing for false-positive reduction. Additionally, since clinical MRIs are at lower resolution of 1x1x5mm, we modeled the relationship between lesion cross-sectional radius and its true volume with a cubic polynomial fit to correct for stereological bias.

2449

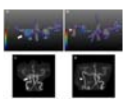

4D Flow MRI analysis of cerebral blood flow before and after EC-IC bypass surgery

Erika Orita[1], Tetsuro Sekine[1], Ryo Takagi[1], Yasuo Amano[1,2], Takahiro Andoh[1], Makoto Obara[3], Yoshio Matsumura[1], and Shin-ichiro Kumita[1]

[1]*Radiology, Nippon Medical School, Tokyo, Japan,* [2]*Radiology, Nihon University School of Medicine, Tokyo, Japan,* [3]*Healthcare, Philips Electronics Japan, Tokyo, Japan*

The purpose of this study was to demonstrate the feasibility of 4D Flow MRI to monitor the change of flow dynamics between before and after extracranial-intracranial (EC-IC) bypass surgery. We enrolled 14 patients who underwent EC-IC bypass. In all, 5 patients underwent radial artery graft (RAG) bypass and 9 patients underwent superficial temporal artery (STA) bypass. All patients underwent 4D Flow MRI preoperatively and 3 weeks after surgery. We measured blood flow volume (BFV) of bilateral internal carotid artery (ICA), basilar artery (BA), and EC-IC bypass artery using 4D flow MRI. Post/pre-operative BFV ratio of contralateral ICA was statistically higher in patients with the RAG bypass group than in those with the STA bypass group (1.28±0.26 in RAG bypass group vs 0.94±0.14 in STA bypass group, $p<0.01$). 4D Flow MRI could assess comprehensive flow dynamics of EC-IC bypass surgery. It is feasible to clarify the change of contribution from each artery.

2450

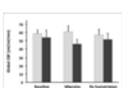

The role of serotonin in cerebral blood flow and oxygen metabolism in migraine

Kenneth M Jackson[1], Steven C Liu[1], Christy Jackson[2], Richard B Buxton[1], and David Dubowitz[1]

[1]*Radiology, University of Californai San Diego, La Jolla, CA, United States,* [2]*Neurology, Scripps Clinic, La Jolla, CA, United States*

We examined the CBF and CMRO2 changes that accompany menstrual migraine, and evaluated the response to sumatriptan to determine the role of serotonin in migraine pathophysiology. Migraine is accompanied by a decline in global CBF and CMRO2 that appears to be serotonin-mediated. There is also a decline in stimulus-dependent CBF to a visual stimulus, that appears to also involve serotonin, but acts differently from the global responses. A decline in visual stimulus-dependent CMRO2 is not serotonin mediated, and appears to follow the normal variation in stimulus-dependent CMRO2 response that changes with normal menstrual cycle.

2451

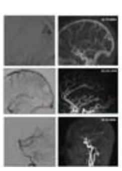

Triple Magnetic Resonance Angiography (triple-MRA) for confirmation of obliteration following Gamma Knife Radiosurgery for Arterial-Venous Malformations of the brain

Alvaro Rojas Villabona[1,2], Francesca Benedetta Pizzini[3], Thomas Solbach[4], Giuseppe Ricciardi[3], Magdalena Sokolska[5,6], Christos Lemonis[3], Enrico De Vita[6], Yuriko Suzuki[7], Matthias JP Van Osch[7], Roberto Israel Foroni[3], Stefania Montemezzi[8], David Atkinson[9], Michele Longhi[10], Elisa Ciceri[3], Neil Kitchen[2], Antonio Nicolato[10], Xavier Golay[6], and Hans Rolf Jäger[4,6]

[1]The Gamma Knife Centre at Queen Square, National Hospital for Neurology and Neurosurgery, London, United Kingdom, [2]Department of Neurosurgery, National Hospital for Neurology and Neurosurgery, London, United Kingdom, [3]Neuroradiology Unit, Department of Diagnostic and Pathology, University Hospital of Verona, Verona, Italy, [4]The Lysholm Department of Neuroradiology, National Hospital for Neurology and Neurosurgery, London, United Kingdom, [5]Medical Physics and Bioengineering, University College London Hospital, London, United Kingdom, [6]Academic Neuroradiological Unit, Department of Brain Repair and Rehabilitation, Institute of Neurology, University College London, London, United Kingdom, [7]C. J. Gorter Center for High Field MRI, Department of Radiology, Leiden University Medical Center, Leiden, Netherlands, [8]Radiology Unit, Department of Diagnostic and Pathology, University Hospital of Verona, Verona, Italy, [9]Centre for Medical Imaging, University College London, London, United Kingdom, [10]Department of Neuroscience, University Hospital of Verona, Verona, Italy

This study assesses whether a combination of three Magnetic Resonance Angiography (MRA) techniques, referred to as triple-MRA, can be used as an alternative to DSA for confirmation of AVM obliteration following GKR and to characterise residual AVMs in case of incomplete response.

The follow up DSA and triple-MRA of twenty-four patients were independently reviewed by two observers regarding the presence/absence of a residual AVM. Triple-MRA consistently agreed with DSA regarding the absence or presence of residual AVMs and proved to be highly suitable for characterisation of residual AVMs.

2452

Application of 3D SPACE MRI on intracranial aneurysm: A preliminary study

Bing Tian[1,2], Christopher Hess[1], Farshid Faraji[1], Megan K Ballweber[1], and David Saloner[1,3]

[1]Department of Radiology and Biomedical Imaging, University of California, San Francisco, San Francisco, CA, United States, [2]Department of Radiology, Changhai hospital of Shanghai, [3]Radiology Service, VA Medical Center, San Francisco

Most of the high resolution MRI(HRMRI) intracranial vessel wall studies on intracranial aneurysm are 2D or 3D non-isotropic technique with limitation of coverage and reconstruction. We applied pre- and post- 3D isotropic T1-weighted fast-spin-echo sequence (SPACE) methods on 16 patients with 21 stable intracranial aneurysms(4 patients follow up). Our studies showed that 3D T1-weighted high resolution SPACE can be used for evaluation of the vessel wall characteristics in patients with intracranial aneurysms, as well as changes in enhancement at follow up studies. Post-contrast SPACE images provide better image quality and improved diagnostic confidence.

2453

The feasibility of using whole-brain 3D high-resolution MRI to evaluate the therapeutic efficacy of medical therapy on symptomatic atherosclerotic plaques in the middle cerebral artery

Tao Wu[1], Jiayu Sun[2], and Zhaoyang Fan[3]

[1]radiology, West China Hospital, Sichuan University, Chengdu, People's Republic of China, [2]Radiology, West China Hospital, Sichuan University, Chengdu, People's Republic of China, [3]Biomedical Imaging Research Institute, Cedars-Sinai Medical Center, Los Angeles, Los Angeles, United States

The stroke is a common cause of death. The technique of high-resolution magnetic resonance imaging (HR-MRI) has been used to depict the vessel wall. Our study aimed to evaluate thetherapeutic efficiency of the symptomatic atherosclerotic plaque in middle cerebral artery by 3D High-resolution MRI. And we compared the imaging and clinical symptom before and after the therapy. The diagnosis of the imaging is consistent with the clinical symptom. 3D High-resolution MRI is a potential imaging technology to evaluate therapeutic efficiency of atherosclerotic plaque in middle cerebral artery.

2454

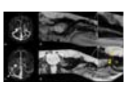

Imaging findings in patients with pulsatile tinnitus using black-blood MRI: a retrospective study

Yunduo Li[1], Le He[1], Xiangyu Cao[2], Xianling Wang[3], Shubin Chen[4], Rui Li[1], Chun Yuan[1,5], and Huijun Chen[1]

[1]Center for Biomedical Imaging Research, Department of Biomedical Engineering, School of Medicine, Tsinghua University, Beijing, People's Republic of China, [2]Neurosurgery department of the general hospital of PLA, Beijing, People's Republic of China, [3]Xuanwu Hospital, Capital Medical University, Beijing, People's Republic of China, [4]Department of Otolaryngology Head and Neck Surgery, Beijing Tongren Hospital, Capital Medical University, Beijing, People's Republic of China, [5]Department of Radiology, University of Washington, Seattle, United States

In this study, we used black-blood (BB) MRI to investigate and classify venous wall abnormalities among PT patients, and found that venous vessel wall anomalies played an important role in PT mechanism. Arachnoidal granulations overgrowth, congenital stenosis, double-lumen, arterio-venous fistula, mastoiditis and malformation were observed in this retrospective study. In conclusion, BB imaging has the potential to provide more pathological information and guide surgical treatment of PT, which is of great clinical value.

2455

Association of Atherosclerotic Plaque Characteristics between Intracranial and Extracranial Carotid Arteries in Symptomatic Patients: A 3D Multicontrast MR Vessel Wall Imaging Study

Yilan Xu[1], Chun Yuan[2,3], Zechen Zhou[4], Le He[2], Rui Li[2], Yuanyuan Cui[5], Zhuozhao Zheng[1], and Xihai Zhao[2]

[1]Department of Radiology, Beijing Tsinghua Changgung Hospital, Tsinghua University, Beijing, People's Republic of China, [2]Center for Biomedical Imaging Research, Department of Biomedical Engineering, Tsinghua University, Beijing, People's Republic of China, [3]Department of Radiology, University of Washington, Seattle, United States, [4]Philips Research China, Philips Healthcare, Beijing, People's Republic of China, [5]Department of Radiology, PLA General Hospital, Beijing, People's Republic of China

This study investigated the correlation between intracranial and extracranial carotid artery atherosclerotic disease in symptomatic patients. We found that extracranial artery disease showed larger plaque burden than intracranial artery disease. In addition, the number of extracranial plaques was found to be associated with intracranial plaque number and maximum wall thickness (MaxWT) and the extracranial carotid MaxWT was independently associated with intracraninal artery stenosis. The association of extracranial artery plaque number and MaxWT with severity of intracranial artery disease suggests that the plaque burden measurements in extracranial carotid arteries might be effective indicators for the severity of intracranial atherosclerosis.

2456

Comparison of two different measurement methods in evaluating basilar atherosclerotic plaque using high resolution MRI 3 T

Luguang Chen[1], Qi Liu[1], Qian Zhan[1], Xuefeng Zhang[1], and Jianping Lu[1]

[1]Radiology, Changhai Hospital of Shanghai, Shanghai, People's Republic of China

Evaluation of morphologic characterization of BA plaque (such as plaque area, stenosis rate and percent plaque burden) is significant and may guide treatment decisions in clinical setting. In this study, we employed the maximal lumen narrowing sites as the referenced sites to calculate morphologic parameters. This study aims to compare the Referenced and Self-referenced measurement method methods in assessing basilar atherosclerotic plaque employing dark blood HRMRI at 3 Tesla. The present study found Self-referenced method is more convenient and even better for evaluating BA plaque.

2457

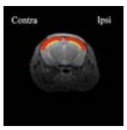

Relationship between cerebral blood flow and water diffusion in the brain of misery perfusion model mice

Takuya Urushihata[1], Hiroyuki Takuwa[1], Chie Seki[1], Yasuhiko Tachibana[1], Jeff Kershaw[1], Yuhei Takado[1], Nohuhiro Nitta[1], Ichio Aoki[1], Hiroshi Ito[2], and Takayuki Obata[1]

[1]National Institutes for Quantum and Radiological Science and Technology, Chiba, Japan, [2]Fukushima Medical University, Fukushima, Japan

We have investigated degeneration of the nerve fibers in chronic cerebral hypoperfusion model mice using DTI. Simple t-tests indicated that there are significant differences in CBF between the control and occluded sides of the brain, but there was no significant difference for MD. However, analysis of covariance showed that MD was strongly correlated with CBF, and that there were significant differences in MD between the contra- and ipsilateral sides. The result suggests degeneration of the nerve fibers due to chronic hypoperfusion. It is also suggested that CBF-related signal changes might be important for pathological diagnosis with DTI.

2458

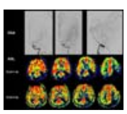

Arterial Spin Labeling Evaluation of Severity of Hypoperfusion in Symptomatic Intracranial Atherosclerotic Stenosis

Jinhao Lyu[1,2], Ning Ma[3], Bing Wu[4], Xiaoxiao Ma[1], Lin Ma[1], Zhongrong Miao[3], and Xin Lou[1]

[1]Radiology, Chinese PLA General Hospital, Beijing, People's Republic of China, [2]Jincheng General Hospital, People's Republic of China, [3]Beijing Tiantan Hospital, Capital Medical University, Beijing, People's Republic of China, [4]GE healthcare China, Beijing, People's Republic of China

Multiple post labeling delay arterial spin labeling provide dynamic perfusion information in patients with intracranial artery atherosclerotic stenosis, and is of useful to study collatera circulation. In this study, two PLD ASL was used to evaluate the severity of hypoperfusion in patients with unilateral middle cerebral artery (MCA) stenosis and we found that the severity of hypoperfusion assessed by two PLD ASL was significantly correlated with collateral circulation and associated with recurrent ischemic stroke in these patients.

2459

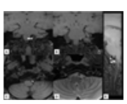

The diagnostic utility of high-resolution 3D T1-weighted SPACE imaging in patients with intracranial vertebrobasilar dissecting aneurysms.

BINBIN SUI[1], PEIYI GAO[1], YAN LIN[1], YISEN ZHANG[2], TIANYI QIAN[3], and XINJIAN YANG[2]

[1]RADIOLOGY, BEIJING TIANTAN HOSPITAL, CAPITAL MEDICAL UNIVERSITY, BEIJING NEUROSURGERY INSTITUTE, BEIJING, People's Republic of China, [2]NEUROINTERVENTION, BEIJING TIANTAN HOSPITAL, CAPITAL MEDICAL UNIVERSITY, BEIJING NEUROSURGERY INSTITUTE, BEIJING, People's Republic of China, [3]MR Collaborations NE Asia, Siemens Healthcare, BEIJING, People's Republic of China

The purpose of this study is to investigate the application value of a 3D high-resolution fat-saturated (FS) T1 SPACE sequence for the diagnosis of intracranial vertebrobasilar dissecting aneurysm (VBDA). With sub-millimetric and nearly isotropic acquisition, the 3D T1-SPACE sequence demonstrated good sensitivity and specificity for the detection of the imaging features associated with VBDAs using a large coverage area and a thin slice thickness.

2460

Reduced cortical thickness in patients with sickle cell disease and a high pain burden: baseline results from the Prevention of Morbidity in Sickle Cell Anaemia trial

Jamie M Kawadler[1], Christina Liossi[2], Chris A Clark[1], and Fenella J Kirkham[1]

[1]Developmental Neurosciences, UCL Great Ormond Street Institute of Child Health, London, United Kingdom, [2]School of Psychology, University of Southampton, Highfield, United Kingdom

Although acute vaso-occlusive pain crises are common in sickle cell disease (SCD), some patients also experience chronic daily pain. This study investigated cortical areas involved in pain processing in low-pain and high-pain groups of patients at baseline of a trial with a pain burden outcome. High-pain patients had significantly thinner cortex in the right anterior cingulate cortex, bilateral posterior cingulate cortex, bilateral precuneus and left primary motor cortex. This is the first study showing structural brain abnormalities in patients with SCD and a high pain burden; these data may provide potential biomarkers for longitudinal trials of treatment for chronic pain.

2461

White matter volume change of carbon monoxide intoxication: a 9-month follow-up study

Meng-Hsin Lee[1], Tzu-Chao Chuang[1], Hsiao-Wen Chung[2], Jie-Yuan Li[3], and Ping-Hong Lai[4]

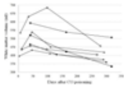

[1]Electrical Engineering, National Sun Yat-Sen University, Kaohsiung, Taiwan, [2]Electrical Engineering, National Taiwan University, [3]Neurology, E-Da Hospital, [4]Radiology, Kaohsiung Veterans General Hospital

Using automated segmentation, volume of brain tissues is assessed at around one week, one month, three months, and 9 months after CO exposure. Among all 17 patients (7 male, mean age: 42.7 yr) recruited in this prospective study, seven are diagnosed with delayed neuropsychiatric syndrome (DNS) and the other ten without. Our results indicate that the white matter volume of all DNS positive patients shows similar trends that it first increases at 1-month follow-up and then decreases, when other GM tissues remain the same. In addition, no volume change is observed in the group without DNS.

2462 

Design of a 24-channel array for imaging Intracranial vascular wall at 3T

Jo Lee[1], Xiaoqing Hu[1], Lei Zhang[1], Xiaoliang Zhang[2,3], Xin Liu[1], and Ye Li[1]

[1]Lauterbur Imaging Research Center, Shenzhen Institutes of Advanced Technology, Chinese Academy of Sciences, Shenzhen City, People's Republic of China, [2]Department of Radiology and Biomedical Imaging, University of California San Francisco, CA, United States, [3]UCSF/UC Berkeley Joint Graduate Group in Bioengineering, San Francisco, CA, United States

Atherosclerosis is a major cause of ischemic stroke. In this study we build a 24-channel head coil array with a special designed coil arrangement to detect non-stenotic atherosclerotic plaques. We compare the 24-channel head coil with Siemens 32-channel coil. For imaging test, the g-factor maps of these two coil arrays are the same, which shows that the 24-channel coil has the same capability of paralleling imaging as the 32-channel coil, and SNR maps show that at the center of the phantom which corresponds to the intracranial region of the head, the 24-channel coil is as good as 32-channel coil.

2463 

Intracranial plaque imaging using reduced field of view 3D fast spin echo

Bing Wu[1], Jianbo Shao[2], Xuehua Peng[2], Bing Wu[3], Mingmei Ge[3], Xinhuai Wu[3], Hui Lin[1], and Zhenyu Zhou[1]

[1]GE healthcare MR Research China, Beijing, People's Republic of China, [2]Wuhan Children Hospital, [3]PLA Army General Hospital

In this study, the use use of reduced FOV CUBE is studied in comparison to full FOV CUBE as well as other common techniques. It was seen that CUBE sequences provide robust and superior image details and black blood effects, due to the advantageous 3D FSE acquisition. With only 1/4 of the FOV acquired, reduced FOV CUBE may complete the scan using half of the scan time (using twice Nex) while obtaining highly consistent results as FF CUBE. Reduced FOV CUBE may also reduce the motion related artifacts that may affect the homogeneity of the lumen area.

2464 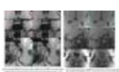

Feasibility of highly accelerated Parallel Imaging of whole brain and neck vessel wall using a high SNR 32-channel coil on 3T

Sen Jia[1], Lei Zhang[1], Xiaoqing Hu[1], Yiu-cho Chung[1], Jing Cheng[1], Xin Liu[1], Hairong Zheng[1], and Dong Liang[1]

[1]Shenzhen Institutes of Advanced Technology, Shenzhen, People's Republic of China

Three dimensional whole brain and neck vessel wall imaging of high resolution facilities the imaging of intracranial and extracranial arteries in stroke patients. However, its clinical usage is hindered by long scan time. Using a 32-channel head and neck coil system specially designed for high SNR, this work investigated the feasibility of highly accelerated parallel imaging equipped with optimally selected uniform subsampling pattern based on 3D G-factor calculated from separate calibration data and joint sparsity based denoising at acceleration factor of 6.

2465 

Assessment of cerebral perfusion autoregulation impairment – An experimental setup to quantify regional cerebral blood flow (CBF) in normal and head down tilt position

Dhaval B Shah[1], Michael G Dwyer[1], Brian Koyn[2], Nicola Bertolino[1], Cheryl Knapp[3], Barry S Willer[4], John J Leddy[5], Robert Zivadinov[1,3], and Ferdinand Schweser[1,3]

[1]Buffalo Neuroimaging Analysis Center, Department of Neurology, Jacobs School of Medicine and Biomedical Sciences, University at Buffalo, The State University of New York, Buffalo, NY, United States, [2]Health Sciences Fabrication Shop, Department of Medicine,Jacobs School of Medicine and Biomedical Sciences, University at Buffalo, The State University of New York, Buffalo, NY, United States, [3]MRI Clinical and Translational Research Center, Jacobs School of Medicine and Biomedical Sciences, University at Buffalo, The State University of New York, Buffalo, NY, United States, [4]Department of Psychiatry,Jacobs School of Medicine and Biomedical Sciences, University at Buffalo, The State University of New York, Buffalo, NY, United States, [5]Department of Orthopedics,Jacobs School of Medicine and Biomedical Sciences, University at Buffalo, The State University of New York, Buffalo, NY, United States

Previous studies using Transcranial Doppler have shown that cerebral ischemia, head trauma, and cerebral perfusion pressure are associated with an impairment of the cerebral autoregulation (CA) and alteration of perfusion. However, simulating perfusion changes and quantifying them with higher specificity repetitively has been a challenge in clinics. We propose a clinical experimental setup for an MRI-based head down tilt protocol to study the CA by quantifying perfusion. We demonstrate local perfusion change results in healthy controls and a patient.

2466 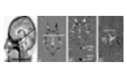

PC-MRI OF CEREBRAL BLOOD AND CSF FLOW VERSUS INTRACRANIAL PRESSURE MONITORING IN HYDROCEPHALUS PATIENTS

Armelle Lokossou[1], Olivier Baledent[1], Simon Garnotel[1], Gwenaël Pagé[1], Laurent Balardy[2], Zofia Czosnyka[3], Pierre Payoux[4], and Eric A. Schmidt[5,6]

[1]Departments of Medical Image Processing, BioFlowImage Laboratory, University Hospital of Picardie Jules Verne, AMIENS, France, [2]Department of Internal Medicine and Gerontology, Toulouse University Hospital, Toulouse, France, [3]Neurosurgical Unit, Department of Clinical Neurosciences, University of Cambridge, Cambridge, UK., [4]Department of Nuclear Medicine, CHU Toulouse, Purpan University Hospital, Toulouse, France, [5]UMR 1214 – INSERM/UPS – TONIC Toulouse Neuro-Imaging Center, Toulouse, France, [6]Departments of Neurosurgery, University Hospital of Toulouse, France

The neurosurgical guidelines recommend low invasive intracranial pressure (ICP) monitoring with infusion tests to detect CSF dynamics alteration. In this study, we investigate how PC-MRI could be helpful in intracranial flow investigations. Eighty-three patients suspected of active hydrocephalus underwent the conventional ICP investigations. All the patients had also the day before, a rapid and simple PC-MRI to assess their cerebral blood and CSF flows. We found that patients who presented altered CSF dynamics (observed by ICP monitoring) presented also the smallest cervical CSF oscillations in the population. PC-MRI brings easy, quick and non-invasive complementary information to investigate the craniospinal dynamic.

2467

Evaluating the clinical outcomes of patients with occlusion of the middle cerebral artery using susceptibility-weighted imaging

Shuang Xia[1], Chao Chai[2], Qingyuan Yang, Sile Hu, Tianyi Qian, E Mark Haacke, and Wen Shen

[1]Tianjin First Central Hospital, Tianjin, People's Republic of China, [2]Radiology Department, Tianjin First Central Hospital, Tianjin, People's Republic of China

In this study, we used the susceptibility-weighted imaging and mapping technique (SWIM) to investigate the effect of vessel susceptibility when evaluating the severity of cerebral infarction to develop an early prognosis of patients with middle cerebral artery thrombosis. By analyzing thrombus length, thrombus susceptibility, clot burden score, and the Admission and Discharge National Institute of Health Stroke Scale (NIHSS) scores between groups divided by the presence or absence of a deep medullary vein (DMVs) and between groups divided by the presence or absence of an asymmetrically prominent cortical vein (APCVs), we found that patients with a DMVs or APCVs were not affected by the burden factors of a thrombus. Compared to an APCV, a DMV suggests the presence of a larger cerebral infarction and is associated with an increased discharged NIHSS score, indicating a poor short-term prognosis.

2468

Regional impaired cerebrovascular reactivity in migraine with and without aura in the interictal state: A pilot fMRI study

Suk-tak Chan[1], Karleyton Evans[2], Allison Tian-yue Song[1], Rajiv Gupta[3], Bruce Rosen[1], Aneesh Singhal[4], and Kenneth K Kwong[1]

[1]Athinoula A. Martinos Center for Biomedical Imaging, Department of Radiology, Massachusetts General Hospital, Charlestown, MA, United States, [2]Biogen Inc., Cambridge, MA, United States, [3]Division of Neuroradiology, Department of Radiology, Massachusetts General Hospital, Boston, MA, United States, [4]Department of Neurology, Massachusetts General Hospital, Boston, MA, United States

Ischemia within the posterior circulation has been proposed as a primary mechanism for migraine. Though, in-vivo studies have yet to fully elucidate the underpinnings of this mechanism. In the current study, angiography via time of flight (ToF) MR was used to identify potential structural deficits within the posterior circulation and hypercapnic BOLD fMRI was used to detect functional vascular defects by quantifying cerebral vascular reactivity (CVR). All three MoA subjects demonstrated a negative correlation in BOLD signal within the red nuclei during CO2 challenge whereas the three MA patients demonstrated CVR within the red nuclei that was similar to that of the control subjects. ToF MR angiography images from all MoA subjects showed hypoplasia of bilateral posterior communicating arteries (PCoA) in proximity of the circle of Willis. In contrast only one out of the three MA subjects showed PCoA hypoplasia on ToF images. Our findings of hypoplasia of posterior communicating arteries combined with abnormal CVR responses within the red nuclei provide both structural and functional evidence for differential vascular defects in the migraine samples studied. We suggest that the identified vascular deficits to impose vulnerability in midbrain blood supply that may likely contribute to the migraine pathophysiology.

Traditional Poster

Neurodegenerative Movement Disorders

Exhibition Hall 2469-2504 — Wednesday 13:45 - 15:45

2469

Diffusion discriminant for mild cognitive impairment in Parkinson's disease

Aziz M. Ulug[1,2], Esin Ozturk-Isik[1], Ani Kicik[3,4], Emel Erdogdu[5], Sevim Cengiz[1], Dilek Betul Arslan[1], Seda Buker[6], Ali Bayram[3,4], Cigdem Ulasoglu-Yildiz[3,4], Elif Kurt[3,4], Zeynep Tufekcioglu[6], Basar Bilgic[6], Hasmet A. Hanagasi[6], Tamer Demiralp[3,7], and Hakan Gurvit[6]

[1]Institute of Biomedical Engineering, Bogazici University, Istanbul, Turkey, [2]CorTechs Labs, San Diego, CA, United States, [3]Hulusi Behcet Life Sciences Research Center, Istanbul University, Istanbul, Turkey, [4]Department of Neuroscience, Istanbul University, Istanbul, Turkey, [5]Institute of Psychology and Cognition Research, University of Bremen, Bremen, Germany, [6]Department of Neurology, Istanbul University, Istanbul, Turkey, [7]Department of Physiology, Istanbul University, Istanbul, Turkey

High percentage of Parkinson's disease patients develop cognitive impairment during the course of the disease progression. An imaging marker that can identify the patients who will develop cognitive impairment would be helpful in deciding the treatment strategy for these patients. We have used diffusion tensor imaging to identify brain structures which can be utilized to discriminate between Parkinson's patients with mild cognitive impairment and without cognitive deficits.

2470

Predictive markers for Parkinson's disease: A DTI based pattern classification study

Tejashree Suresh Takalkar[1], Madhura Ingalhalikar[1], Jitendra Saini[2], and Pramod Pal[2]

[1]Electronics And Telecommunication, Symbiosis Institute Of Technology, Pune, India, [2]Department Of Neurology, NIMHANS, India

This work presents a paradigm for predicting changes in pathology, supporting diagnosis and providing a potential biomarker for Parkinson's disease. This is achieved by creating a high-dimensional support vector machine (SVM) based classifier that learns the underlying pattern of pathology using numerous atlas-based regional features extracted from Diffusion Tensor Imaging (DTI) data. For the dataset of 72 controls and 73 PD patients, we achieve a 10-fold cross validation accuracy of 72.8% and a testing accuracy of 78.5%. The top discriminative features included widespread patterns of mean diffusivity changes in PD.

2471

Analysis of the Substantia Nigra from Parkinson's disease patients and control subjects using co-registered DTI and QSM data

Gerd Melkus[1,2], Santanu Chakraborty[1,2], Fahad A Essbaiheen[1,2,3], David A Grimes [4,5], and Tiago Mestre[4,5]

[1]Medical Imaging, The Ottawa Hospital, Ottawa, ON, Canada, [2]Radiology, University of Ottawa, Ottawa, ON, Canada, [3]King Saud University, Riyadh, Saudi Arabia, [4]Parkinson's Disease and Movement Disorders Center, The Ottawa Hospital Research Institute, Ottawa, ON, Canada, [5]Department of Medicine, University of Ottawa, Ottawa, ON, Canada

Different quantitative MRI techniques like Diffusion Tensor Imaging (DTI) and Quantitative Susceptibility Imaging (QSM) have been used to evaluate the substantia nigra (SN) in patients with Parkinson's disease (PD). When multimodal MRI studies are applied to acquire several quantitative parameters the analysis of each of these datasets on an individual ROI basis can time consuming. In this study we are using a co-registration approach to a standard brain template for evaluating quantitative MR data (from DTI and QSM) in the SN of PD patients and controls.

2472

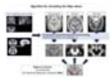

Quantifying nigral alterations in Parkinson's disease using neuromelanin and diffusion tensor imaging

hiroto takahashi[1], Yoshiyuki Watanabe[1], hisashi tanaka[1], masahito mihara[2], hideki mochizuki[2], and noriyuki tomiyama[1]

[1]Radiology, Osaka University Graduate School of Medicine, Suita, Japan, [2]Neurology, Osaka University Graduate School of Medicine, Suita, Japan

Dopaminergic neurodegeneration of the substantia nigra pars compacta (SNpc) in Parkinson's disease (PD) was evaluated quantitatively using both neuromelanin and diffusion tensor imaging. For the highly reproducible image analysis of the SNpc, an automatic region-of-interest selection method was developed with a voxel-based morphometric technique. Neuromelanin which can directly quantify dopaminergic neurodegeneration and mean diffusivity could differentiate PD patients from healthy controls and were correlated with each other. We conclude that a voxel-based evaluation using both neuromelanin and diffusion tensor imaging can reveal PD related neurodegenerative changes in the SNpc and may be a useful technique for quantitative diagnosis of PD.

2473

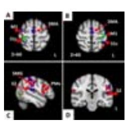

Peculiarities of brain activation during dominant hand tactile perception in lateralized Parkinson disease

Oleksii Omelchenko[1], Zinayida Rozhkova[2], and Irina Karaban[3]

[1]Human and Animal Physiology, Taras Shevchenko National University of Kyiv, Kyiv, Ukraine, [2]Radiology, Medical Clinic BORIS, Kyiv, Ukraine, [3]Department of extrapyramidal disorders, D. F. Chebotarev Institute of Herontology, Kiev, Ukraine

Parkinson's disease (PD) in mostly presented with asymmetrical motor symptoms. Disturbed sensorimotor integration and decrease of somatosensory cortex activation was previously shown. We analyzed brain activation and connectivity during the unilateral tactile stimulation in primary and non-primary hand lateralized PD patients. We have demonstrated steady contralateral S1 activation in PD. Primary hand tactile stimulation in primary hand lateralized PD patients evokes activation of primary and associative sensory, motor and executive nodes of the cortex. Mirror neuron system was activated in primary hand stimulation in PD patients. Tactile stimuli processing evokes increased connectivity of globus pallidus, premotor, prefrontal and parietal cortex.

2474

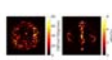

Cerebral Perfusion Correlates of MAPT and COMT Genotypes for Mild Cognitive Impairment in Parkinson's Disease at 3T

Dilek Betul Arslan[1], Ani Kıçik[2,3], Sevim Cengiz[1], Emel Erdogdu[4], Seda Buker [5], Zeynep Tufekcioglu [5], Aziz Mufit Ulug[1,6], Basar Bilgic[5], Hakan Gurvit[5], Tamer Demiralp[2,7], Erdem Tuzun[8], Hasmet Hanagasi[5], and Esin Ozturk-Isik [1]

[1]Institute of Biomedical Engineering, Bogazici University, Istanbul, Turkey, [2]Hulusi Behçet Life Sciences Research Laboratory, Istanbul University, Istanbul, Turkey, [3]Istanbul University, Institute of Experimental Medicine, Department of Neuroscience, Istanbul, Turkey, [4]Institute of Psychology and Cognition Research, University of Bremen, Bremen, Germany, [5]Department of Neurology, Istanbul Faculty of Medicine, Istanbul University, Istanbul, Turkey, [6]CorTechs Labs, San Diego, CA, USA, [7]Department of Physiology, Istanbul Faculty of Medicine, Istanbul University, Istanbul, Turkey, [8]Institute of Experimental Medicine, Istanbul University, Istanbul, Turkey

The purpose of this study is to investigate the cerebral perfusion correlates of microtubule-associated protein tau (MAPT) and catechol-O-methyl transferase (COMT) genotypes in Parkinson's Disease with mild cognitive impairment (PD-MCI) and PD with normal cognition (PD-CN) using multi inversion time pulsed arterial spin labelling magnetic resonance imaging (pASL-MRI). Cerebral blood flow (CBF) and arterial blood volume (aBV) maps of patients were calculated by using general kinetic model and compared between different genotypes of PD-MCI and PD-CN. It was found that PD-MCI with H1/H1 genotype of MAPT gene had a lower cerebral perfusion than PD-CN with H1/H2 genotype.

2475

Disrupted topological organization of brain networks in early Parkinson's disease (PD) subjects: Insights from Parkinson's Progressive Markers Initiative (PPMI) dataset

Virendra Mishra[1], Karthik Sreenivasan[1], Christopher Bird[1], Dietmar Cordes[1], and Ryan R Walsh[1]

[1]Cleveland Clinic Lou Ruvo Center for Brain Health, Las Vegas, NV, United States

In vivo imaging that reliably captures the impact of the spreading pathology of Parkinson's disease (PD), including its impact on both white and gray matter, remains elusive. In this study, we applied graph-theoretical techniques to multi-site diffusion-MRI data from a cohort of early PD-subjects in Parkinson's Progressive Markers Initiative (PPMI) database. A disrupted topological brain organization in early PD-subjects was revealed with impaired network integration, segregation, global efficiency, and local efficiency. Furthermore, there was also rearrangement of nodes in different modules between the groups. Our study opens new avenues to understanding disease progression and severity of PD from graph-theoretical approach.

2476

Decreased axial diffusivity in early Parkinson's disease subjects: Insights from Parkinson's Progressive Markers Initiative (PPMI) dataset

Virendra Mishra[1], Dietmar Cordes[1], and Ryan R Walsh[1]

[1]Cleveland Clinic Lou Ruvo Center for Brain Health, Las Vegas, NV, United States

In vivo imaging that reliably captures the impact of the spreading pathology of Parkinson's disease (PD), including its impact on both white and gray matter, remains elusive. In this study, we performed skeleton-wise analysis of multi-site DTI data from a cohort of early PD-subjects in Parkinson's Progressive Markers Initiative (PPMI) database. Tract-based-spatial-statistics analysis revealed three clusters mainly located in corticospinal tract, and superior frontal gyrus that had a lower AxD in early PD-subjects suggesting DTI measures can be used to differentiate controls and early PD, and can be further exploited to understand its role in disease progression and severity.

2477

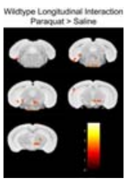

Environmental paraquat exposure and HFE genetics as factors in the development of Parkinson's disease

Mark D Meadowcroft[1,2], Carson J Purnell[1], Douglas G Peters[3], Qing X Yang[2], and James R Connor[1]

[1]Neurosurgery, The Pennsylvania State University - College of Medicine, Hershey, PA, United States, [2]Radiology, The Pennsylvania State University - College of Medicine, Hershey, PA, United States, [3]Neural and Behavioral Sciences, The Pennsylvania State University - College of Medicine, Hershey, PA, United States

This work demonstrates a decrease in R2 within the ventral-nigral region of WT-HFE mice given paraquat injections. Furthermore, the decrease in R2 relaxation rate is not observed in the H67D-HFE mutation animals. This is the first demonstration that HFE mutations may be associated with a preservation of cellular loss in the substantia nigra and ventral-midbrain of Parkinson's disease model animals.

2478

Effects of myelin changes in Parkinson's Disease on motor performance

Tobias R Baumeister[1,2], Sun Nee Tan[2,3], and Martin J McKeown[2,4]

[1]Department of Biomedical Engineering, University of British Columbia, Vancouver, BC, Canada, [2]Pacific Pakinson's Research Centre, UBC Hospital, Vancouver, BC, Canada, [3]Graduate Program in Neuroscience, University of British Columbia, [4]Faculty of Medicine, Neurology, University of British Columbia, Vancouver, BC, Canada

Parkinson's Disease is not normally associated with white matter changes in clinical MRI scans. Myelin water imaging was used to probe the white matter tissue integrity of mildly affected Parkinson's Disease patients. Partial Least Squares regression was employed to find a multivariate relation between myelin water fraction along different white matter tracts and motor performance scores. We found association between myelin water fraction and rigidity, bradykinesia and tremor scores, linking changes in white matter tissue integrity to Parkinson's Disease severity in motor scores.

2479

The Correlation Between Brain Iron Overload and Microstructure Change in Gray Matter Nucleus in Parkinson' s Disease

bingbing gao[1], bing wu[2], liang han[3], jing jing[3], and yanwei miao[3]

[1]first affiliated hospital of DaLian medical univercity, Da Lian, People's Republic of China, [2]GE healthcare, People's Republic of China, [3]first affiliated hospital of DaLian medical univercity, People's Republic of China

Enhanced Gradient Echo T2 Star Weighted Angiography (ESWAN) can sensitively shows iron overload in brain, especially gray matter; Diffusion Kurtosis Imaging (DKI) detects microstructure change of gray matter much better than Diffusion Tensor Imaging (DTI). PD patients has the iron overload in substantia nigra, and encephalatrophy on different levels--cortex, basal ganglia and midbrain. To emplore the relation between iron overload and microstructure change in extrapyramidal nuclei, we compared DKI and ESWAN parameters in PD and healthy control groups, and analysis the correlation between them. Found that there are some relations in substantia nigra, red nucleus and putamen in PD patients.

2480

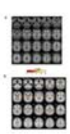

Improved detection of grey matter atrophy in Parkinson's disease in a Chinese population using the Chinese2020 template

XIUQIN JIA[1], LIN SHI[2], TIANYI QIAN[3], YING LI[1], DEFENG WANG[4,5], PEIPENG LIANG[1,4,5], and KUNCHENG LI[1]

[1]Department of Radiology, Xuanwu Hospital, Capital Medical University, Beijing, People's Republic of China, [2]Department of Medicine and Therapeutics, The Chinese University of Hong Kong, Hong Kong, Hong Kong, [3]MR Collaboration, Northeast Asia, Siemens Healthcare, Beijing, People's Republic of China, [4]Shenzhen Research Institute, The Chinese University of Hong Kong, Shenzhen, People's Republic of China, [5]Research Center for Medical Image Computing, Department of Imaging and Interventional Radiology, The Chinese University of Hong Kong, Hong Kong, Hong Kong

The human brain differs significantly between different individuals, as well as between different demographics (i.e., age, gender, and race). The aim of the present study was to investigate the effectiveness of a Chinese brain template, i.e., Chinese2020, on the detection of grey matter (GM) alteration between patients with Parkinson's disease (PD) and healthy controls (HC). The results of this study indicate that Chinese2020 was more representative of Chinese populations, which suggests that neuroimaging studies based on Chinese populations should be normalized to the Chinese brain atlas and that previous studies based on Chinese populations might need to be updated.

2481

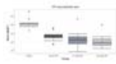

Evaluation of Neuromelanin-MRI parameters and Volumetric changes with Parkinson’s Disease Progression

Miguel A Carvalho[1,2], Sofia Reimão[3], Margherita Fabbri[4], Daisy Abreu[4], Jorge Campos[3], Joaquim F Ferreira[4,5], and Rita G Nunes[1,6]

[1]Instituto de Biofísica e Engenharia Biomédica, Faculdade de Ciências, Universidade de Lisboa, Lisbon, Portugal, [2]Physics Department, Faculdade de Ciências e Tecnologia, Universidade Nova de Lisboa, Lisbon, Portugal, [3]Neurological Imaging Department, Hospital de Santa Maria - Centro Hospitalar Lisboa Norte, Lisbon, Portugal, [4]Clinical Pharmacology Unit, Instituto de Medicina Molecular, Faculdade de Medicina, Universidade de Lisboa, Lisbon, Portugal, [5]Neurology Department, Hospital de Santa Maria - Centro Hospitalar Lisboa Norte, Lisbon, Portugal, [6]Institute for Systems and Robotics / Department of Bioengineering, Instituto Superior Técnico, Universidade de Lisboa, Lisbon, Portugal

This study aimed to characterize changes in Neuromelanin-sensitive MR images with Parkinson’s Disease (PD) progression. The area of high signal intensity in the *substantia nigra* (SN) and its contrast ratio (CR) were assessed in early and late stage PD (LSPD) patients, and in healthy individuals. The relative hippocampus and midbrain volumes were also estimated from anatomical MPRAGE scans. The SN area was found to be markedly reduced in LSPD compared to early stages of the disease and so could be a useful tool to evaluate disease progression. The decrease in relative hippocampus volume could indicate cognitive impairment, characteristic of LSPD.

2482

Robust method for detection of small variations in relaxation parameters and free water content in substantia nigra of Parkinson's disease patients.

Krzysztof Dzieciol[1], Elene Iordanishvili[1], Zaheer Abbas[1,2], Michael Winterdahl[3], Adjmal Nahimi[3], and Nadim Jon Shah[1,2]

[1]Medical Imaging Physics, Institute of Neuroscience and Medicine, Forschungszentrum Jülich, Jülich, Germany, [2]Department of Neurology, Faculty of Medicine, RWTH Aachen, JARA, Aachen, Germany, [3]Nuclear Medicine and PET Center, Aarhus University, Aarhus, Denmark

Parkinson's disease patients were investigated in order to reveal changes inside region-of-interest – substantia nigra. 31 volunteers were scanned using a well-established, quantitative free water mapping protocol. The region-of-interest is too small to obtain reliable segmentation for region-based analysis. Therefore, statistical, voxel-wise analysis of registered quantitative maps was performed. It revealed a decrease in the metrics (free water content, T1, T2* and combination of all three) in the vicinity of substantia nigra. We conclude that the reduction in total free water content could be due to a disruption of the deep grey matter integrity.

2483

Functional connectivity depending on duration of parkinsonism before diagnosis of mild cognitive impairment in Parkinson Disease: focusing on the substantia innominata.

Na-Young Shin[1], Injoong Kim[2], Yunjin Bak[1], Phil Hyu Lee[3], Seung-Koo Lee[4], and Soo Mee Lim[5]

[1]Department of Radiology, Ewha Womans University School of Medicine, Seoul, Korea, Republic of, [2]Department of Radiology, Veterans Health Service Medical Center, [3]Department of Neurology, Yonsei University College of Medicine, [4]Department of Radiology, Yonsei University College of Medicine, [5]Department of Radiology, Ewha Womans University School of Medicine

Degenerative change in the nucleus basalis of Meynert, a group of cholinergic neurons in the substantia innominata (SI) of the basal forebrain, begins in the early stages of Parkinson disease (PD) and is known to be significantly correlated with cognitive performance. We found decreased resting state functional connectivity (rsFC) in bilateral frontal areas using bilateral SI mask as a seed and significant correlation between decreased rsFC and shorter disease duration before mild cognitive impairment was diagnosed in patients with Parkinson’s disease. Therefore, our results support that cholinergic deficit plays an important role in the acceleration of cognitive decline and conversion to PD dementia.

2484

Hierarchical organization of functional networks in patients with Parkinson’s Disease

Karthik Sreenivasan[1], Virendra Mishra[1], Zhengshi Yang[1], Xiaowei Zhuang[1], Sarah Banks[1], Dietmar Cordes[1,2], Ryan R Walsh[1], and Karthik Sreenivasan[1]

[1]Cleveland Clinic Lou Ruvo Center for Brain Health, Las Vegas, NV, United States, [2]University of Colorado Boulder, Boulder, CO, United States

Earlier studies using fMRI have shown the existence of a modular structure for different brain networks. However, no information exist about hierarchical modular structure of functional connectivity networks in patients with Parkinson’s disease(PD). Using percolation analysis, we found a shift in the hierarchical modular structure of functional connectivity networks in patients with PD. A shift in the modules in caudal-rostral direction in the PD group of motorically affected patients, alongside rearrangement of connector hubs and provincial hubs in PD patients was observed. Potential application of network properties observed here, as predictors of subsequent disease progression is currently being investigated.

2485

Neuromelanin and Volumetric Evaluation in Parkinson’s Disease Patients Carrying LRRK2 or GBA Mutations

Patrícia Paulino[1,2], Sofia Reimão[3], Leonor Correia Guedes[4,5], Miguel A Carvalho[1,2], Daisy Abreu[4], Jorge Campos[3], Joaquim F Ferreira[4,5], and Rita G Nunes[1,6]

[1]Instituto de Biofísica e Engenharia Biomédica, Faculdade de Ciências, Universidade de Lisboa, Lisbon, Portugal, [2]Physics Department, Faculdade de Ciências e Tecnologia, Universidade Nova de Lisboa, Lisbon, Portugal, [3]Neurological Imaging Department, Hospital de Santa Maria - Centro Hospitalar Lisboa Norte, Lisbon, Portugal, [4]Clinical Pharmacology Unit, Instituto de Medicina Molecular, Faculdade de Medicina, Universidade de Lisboa, Lisbon, Portugal, [5]Neurology Department, Hospital de Santa Maria - Centro Hospitalar Lisboa Norte, Lisbon, Portugal, [6]Institute for Systems and Robotics / Department of Bioengineering, Instituto Superior Técnico, Universidade de Lisboa, Lisbon, Portugal

Previous studies in idiopathic Parkinson’s disease (iPD) have shown a reduction in the *substantia nigra* (SN) area hyperintense in Neuromelanin-sensitive MR images (NM-MRI). However, a few genetic mutations have been associated to PD. In this study we compared images obtained in iPD and in patients with *LRRK2* or *GBA* mutations. Images were also acquired in control subjects. The area and contrast-ratio of SN in NM-MRI and the relative midbrain volumes were evaluated. There were no significant differences in volumes, but the SN area in NM-MRI accurately differentiated *LRRK2* PD patients from controls. No differences were found between PD groups.

2486  A Behavioural and MRI Structural Study of Early Stage 6-OHDA Parkinson's Disease Rat Model

Brigida Ranieri[1,2], Ilaria Rosa[1], Davide Di Censo[1], Angelo Galante[1,2,3], Eugenio Scarnati[4], Tiziana Marilena Florio[1,2], and Marcello Alecci[1,2,3]

[1]Department of Life, Health and Environmental Sciences, University of L'Aquila, L'Aquila, Italy, [2]Laboratori Nazionali del Gran Sasso, Istituto Nazionale di Fisica Nucleare, L'Aquila, Italy, [3]SPIN-CNR Institute, CNR, L'Aquila, [4]Department of Biotechnological and Applied Clinical Sciences, University of L'Aquila, L'Aquila, Italy

We established the correlation between behaviour and functional structures in an early stage of 6-OHDA PD rat model. Behavioural data reveal that receptor sensitization develops few days after dopaminergic injury. The apomorphine-induced amplification of the motor asymmetry over time is paired to striatal shrinkage and alteration of the GM/WM area in the ipsilateral striatum, as revealed by immunohistology and ex-vivo high-resolution MRI analysis.

2487 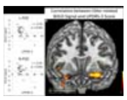 Predominance of Odor-related Functional Decline in the Primary Olfactory Cortex of Early-stage Parkinson's Disease

Jianli Wang[1], Thyagarajan Subramanian[2,3], and Qing X Yang[1,4]

[1]Radiology, Penn State College of Medicine, Hershey, PA, United States, [2]Neurology, Penn State College of Medicine, Hershey, PA, United States, [3]Neural & Behavioral Sciences, Penn State College of Medicine, Hershey, PA, United States, [4]Neurosurgery, Penn State College of Medicine, Hershey, PA, United States

The primary olfactory cortex (POC) responds to both odor-smelling and sniffing. It is not known if there are deficits in the sniffing-related or odor-related functional activities in the POC of early-stage Parkinson's disease (PD). Here we report significant PD-related deficit in the odor-related POC activation, while the sniffing-related activation was not significantly affected. These results suggest that olfactory deficits in early-stage PD are mainly due to the breakdown of the bottom-up mechanism. In addition, our finding of a negative correlation between the UPDRS-3 score and the odor-related POC activation suggests a surrogate marker for the clinical severity in early-stage PD.

2488 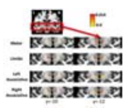 Functional network remapping of the subthalamic nucleus in Parkinson's disease

Silvina G Horovitz[1], Liang Li[1,2], Sule Tinaz[1,3], and Mark Hallett[1]

[1]HMCS, NINDS, NIH, Bethesda, MD, United States, [2]School of Biomedical Engineering, Fourth Military Medical University, Xi'an, Shaanxi, People's Republic of China, [3]Neurology Department, Yale School of Medicine, New Haven, CT, United States

We modified a parcellation method to map the motor, limbic and associative territories within the subthalamic nucleus (STN). We further evaluated whether a remapping of the STN connectivity exists in Parkinson's disease (PD) patients. Resting-state fMRI data were analyzed using independent component analysis and general linear model. In both groups, the motor area was identified in the posterior zone, while the limbic zone was more anteriorly located. The motor connections were altered in the PD patients. Our approach could be used for functional parcellations and for remapping of functional connectivity due to disease in brain areas with heterogeneous connectivity patterns.

2489  Which one is a better marker for the diagnosis of Parkinson's disease: T1 MRI or DTI

Ehsan Adeli[1], Guorong Wu[1], Min-Jeong Kim[1], and Dinggang Shen[1]

[1]Department of Radiology and Biomedical Research Imaging Center (BRIC), University of North Carolina at Chapel Hill, Chapel Hill, NC, United States

Parkinson's disease (PD) is a common neurodegenerative disorder, which progresses slowly and affects the quality of life dramatically. In this paper, we use the T1 MRI and DTI data from the PPMI study to analyze the effect of each modality through investigating the brain regions, and determine which modality can be a better marker at diagnosing the disease. For this purpose, we propose a joint feature selection and max-margin classification framework, in which we select features that best benefit the classification scheme. Our results show that the brain structural connectivity studies using DTI leads to better results.

2490 An Imaging Progression Marker for Parkinson's Disease: A 4-Year Multicenter Longitudinal Study of Substantia Nigra Free-Water

Roxana Gabriela Burciu[1], Edward Ofori[1], Derek Archer[1], Samuel Wu[2], Ofer Pasternak[3,4], Michael Okun[5,6,7], and David Vaillancourt[1,5,8]

[1]Department of Applied Physiology and Kinesiology, University of Florida, Gainesville, FL, United States, [2]Department of Biostatistics, University of Florida, Gainesville, FL, United States, [3]Department of Psychiatry, Harvard Medical School, Boston, MA, United States, [4]Department of Radiology, Harvard Medical School, Boston, MA, United States, [5]Department of Neurology, University of Florida, Gainesville, FL, United States, [6]Department of Neurosurgery, University of Florida, Gainesville, FL, United States, [7]Center for Movement Disorders and Neurorestoration, University of Florida, Gainesville, FL, United States, [8]Department of Biomedical Engineering, University of Florida, Gainesville, FL, United States

We used a bi-tensor model to calculate free-water (FW) in the substantia nigra (SN) from diffusion MRI scans obtained from the Parkinson's Progression Marker Initiative (PPMI) database with the goal of monitoring disease progression over 1 year and 4 years in Parkinson's disease (PD). Results confirm previous single-site findings by showing an increase in FW in the posterior SN over 1 year in a large multi-site study, and extend the literature by showing that FW levels in this structure continue to increase over 4 years.

2491  Altered Functional Connectivity Density in Subtypes of Parkinson's Disease: a Resting-State fMRI Study

Xiaofei Hu[1], Yuchao Jiang[2], Xiaoyue Zhou[3], Cheng Luo[2], and Jian Wang[1]

[1]Department of Radiology, Southwest Hospital, Third Military Medical University, Chongqing, 400038, P.R. China, Chongqing, People's Republic of China, [2]Key Laboratory for Neuro Information of Ministry of Education, School of Life Science and Technology, University of Electronic Science and Technology of China (UESTC), Chengdu, 610054, P.R. China, People's Republic of China, [3]Collaboration NEA, Siemens Healthcare Ltd., Shanghai, P.R. China, People's Republic of China

In the current study, combined functional connectivity density (FCD) and seed-based FC analyses were performed to fully characterize the abnormal brain networks in the two subtypes. Our findings obtained using a combination of FCD and seed-based FC analyses provide consistent evidence for that the network disorganization of the brains in the two PD subtypes were different.We also found that the FCD provided good discrimination between the AR and TD patients. These findings have important implications for understanding the neural substrates that underlie these disparate manifestations of PD.

2492

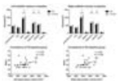

Longitudinal Volume Change of Hippocampal Subfields and Cognitive Decline in Parkinson's Disease

Xiaofei Hu[1], Xiaoyue Zhou[2], Panli Zuo[3], and Jian Wang[1]

[1]Department of Radiology, Department of Radiology, Southwest Hospital, Third Military Medical University, Chongqing, People's Republic of China, [2]Collaboration NEA, Siemens Healthcare Ltd., Shanghai, P.R. China, People's Republic of China, [3]Collaboration NEA, Siemens Healthcare Ltd., Beijing, P.R. China, People's Republic of China

We try to find out the longitudinal volume change of different hippocampal subfields in patients with PD with and without cognitive decline using magnetic resonance image (MRI). Our result shows that there is cross-sectional and longitudinal regional atrophy of specific hippocampal subfields in PD, which becomes more severe and is further extended to the bilateral CA2-3 and CA4-DG subfields in patients with cognitive decline. These results corroborate neuropathological findings and add novel information about the involvement of the hippocampus in the cognitive dysfunction of PD.

2493

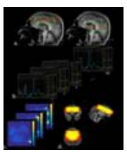

Comparison of MR spectroscopic imaging findings between different MAPT and COMT genotypes of cognitively normal or mild cognitively impaired Parkinson's disease patients at 3T

Sevim Cengiz[1], Ani Kicik[2,3], Emel Erdogdu[4], Dilek Betul Arslan[1], Seda Buker[5], Zeynep Tufekcioglu[5], Aziz Mufit Ulug[1,6], Basar Bilgic[5], Hakan Gurvit[5], Tamer Demiralp[2,7], Erdem Tuzun[8], Hasmet Hanagasi[5], and Esin Ozturk-Isik[1]

[1]Institute of Biomedical Engineering, Bogazici University, Istanbul, Turkey, [2]Hulusi Behcet Life Sciences Research Laboratory, Istanbul University, Istanbul, Turkey, [3]Istanbul University, Institute of Experimental Medicine, Department of Neuroscience, Istanbul, Turkey, [4]Institute of Psychology and Cognition Research, University of Bremen, Germany, [5]Department of Neurology, Istanbul Faculty of Medicine, Istanbul University, Istanbul, Turkey, [6]CorTechs Labs, San Diego, CA, USA, [7]Department of Physiology, Istanbul Faculty of Medicine, Istanbul University, Istanbul, Turkey, [8]Institute of Experimental Medicine, Istanbul University, Istanbul, Turkey

Microtubule-associated protein tau (MAPT) and catechol-O-methyltransferase (COMT) genotypes have been associated with cognitive impairment in Parkinson's disease (PD). The aim of this study is to compare MR spectroscopic imaging findings between cognitively normal PD (PD-CN) or mild cognitively impaired PD (PD-MCI) patients with different MAPT and COMT genotypes at 3T. We observed a higher Ins/Cr in cerebral white matter of PD-MCI with MAPT H1/H2 genotype than PD-CN with MAPT H1/H1 genotype and a higher Cho/Cr in thalamus of PD-MCI with COMT Met/Met genotype and PD-CN with COMT Val/Val or Val/Met genotype than PD-CN with COMT Met/Met genotype.

2494

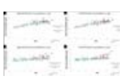

Preliminary findings of elevated iron deposition in the substantia nigra in patients with idiopathic Parkinson's disease using a high iron content evaluation of quantitative susceptibility mapping

Sean K Sethi[1], Shawn Kisch[2], Kiarash Ghassaban[1], Saifeng Liu[3], Miller Fawaz[1], Ali H. Rajput[4], Alex Rajput[4], Paul Babyn[5], Peter Szkup[5], and E. Mark Haacke[1,3,6]

[1]Research, Magnetic Resonance Innovations, Inc., Detroit, MI, United States, [2]Department of Medical Imaging, Saskatoon Health Region, [3]Research, The MRI Institute for Biomedical Research, Detroit, MI, United States, [4]Division of Neurology in the Department of Medicine, University of Saskatchewan, [5]Department of Medical Imaging, University of Saskatchewan, Saskatoon, SK, [6]Radiology, Wayne State University School of Medicine

Iron deposition in the brain has been implicated in neurodegenerative diseases like Parkinson's Disease. We used quantitative susceptibility mapping to evaluate iron content in the substantia nigra and red nucleus in 18 patients with idiopathic Parkinson's Disease (IPD). Susceptibility was calculated for whole structure and a thresholded high-iron region (RII) and compared with controls. We found that global and RII mean susceptibility higher in the substantia nigra compared with normals, and that the slope of RII susceptibility vs age is higher in IPD compared to normals which may suggest an increased rate of iron deposition at disease onset.

2495

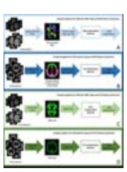

Differential Diagnosis of Parkinson's disease, Progressive Supranuclear Palsy and Corticobasal syndromes using machine learning and MRI

Marta Morgado Correia[1] and James Rowe[1,2]

[1]MRC Cognition and Brain Sciences Unit, Cambridge, United Kingdom, [2]Clinical Neurosciences, University of Cambridge, Cambridge, United Kingdom

In this study we combined machine learning with MRI for the differential diagnosis of three movement disorders: Parkinson's disease (PD), progressive supranuclear palsy (PSP) and degenerative corticobasal syndrome (CBS). We compared the performance of such approaches when using T1-weighted and diffusion MRI, as well as different methods for feature extraction. Our results suggest that such methods could be used in the future to aid the differential diagnosis of PSP, CBS and PD, in conjunction with clinical assessment, with diffusion MRI data providing the most promising results.

2496 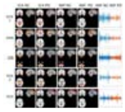

Empirical Mode Decomposition and Amplitude Characteristics of Resting-State Networks in Parkinson's Disease

Dietmar Cordes[1,2], Muhammad Kaleem[3], Xiaowei Zhuang[1], Karthik Sreenivasan[1], Zhengshi Yang[1], Virendra Mishra[1], and Ryan R Walsh[1]

[1]Cleveland Clinic Lou Ruvo Center for Brain Health, LAS VEGAS, NV, United States, [2]University of Colorado Boulder, Boulder, CO, United States, [3]University of Management & Technology, Lahore, Pakistan

In this project, amplitudes of low-frequency fluctuations in resting-state fMRI data of subjects with Parkinson's disease (PD) are studied and compared with matched normal controls. Empirical Mode Decomposition (EMD) is used to decompose the natural occurring frequency bands of major networks important in PD. The novelty of our approach lies in the data-adaptive decomposition of fMRI data using EMD, and identification of resting-state networks based on amplitude characteristics of intrinsic modes.

2497 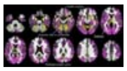

Extensive cortical involvement in patients with Huntington's Disease as measured from diffusion MRI

Jung-Sen Hsiao[1], Sung-han Lin[1], Chih-Chien Tsai[1], Chiung-Mei Chen[2], and Jiun-Jie Wang[1,3]

[1]Medical Imaging and Radiological Sciences, Chang-Gung University, Taoyuan City, Taiwan, [2]Neurology, Chang Gung Memorial Hospital, Linkou, Taoyuan City, Taiwan, [3]Neuroscience Research Center, Chang Gung Memorial Hospital, Linkou, Taoyuan City, Taiwan

Huntington's Disease (HD) is a neurodegenerative disease would result in atrophy in basal ganglia especially in caudate nucleus and putamen in the early stage of the disease. The cortical parcellation algorithm was applied to evaluate the cortical involvement in the patients with HD by using diffusion MRI and compared with voxel based morphometry. The mean diffusivity is feasible in the brain of patients with HD, which is more sensitive than the morphometric changes. Therefore mean diffusivity could be a potential image based biomarker for monitoring HD progression.

2498 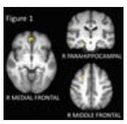

Functional connectivity disturbances in prodromal Huntington's disease predict future cognitive decline

Katherine A Koenig[1], Jian Lin[1], Mark Lowe[1], Stephen Rao[2], Mourany Lyla[2], Deborah Harrington[3,4], Jane Paulson for the PREDICT-HD investigators of HSG[5], and Sally Durgerian[6]

[1]Imaging Institute, The Cleveland Clinic, Cleveland, OH, United States, [2]Lou Ruvo Center for Brain Health, The Cleveland Clinic, Cleveland, OH, United States, [3]Department of Radiology, University of California, San Diego, La Jolla, CA, United States, [4]Research Service, VA San Diego Healthcare System, San Diego, CA, United States, [5]Carver College of Medicine, The University of Iowa, Iowa City, IA, United States, [6]BrainDataDriven, Milwaukee, WI, United States

This study investigates intrinsic functional connectivity of the dorsal caudate in prodromal Huntington's disease participants. We find that connectivity to the left caudate increases as estimated time to a manifest diagnosis decreases, and that stronger connectivity between the right middle frontal gyrus and left caudate is predictive of future cognitive decline.

2499 

Deep grey matter T2 relaxometry at 3T in Huntington's disease

Enrico De Vita[1,2], Sarah Gregory[3], Lauren Byrne[3], Filipe B Rodrigues[3], Eileanoir Johnson[3], Tarek Yousry[1,2], David Thomas[2], John S Thornton[1,2], and Edward J Wild[3]

[1]Lysholm Department of Neuroradiology, National Hospital for Neurology and Neurosurgery. UCL Hospitals NHS Foundation Trust, London, United Kingdom, [2]Academic Neuroradiological Unit. Department of Brain Repair and Rehabilitation, UCL Institute of Neurology, London, United Kingdom, [3]Huntington's Disease Centre, UCL Institute of Neurology, London, United Kingdom

Iron levels in the basal ganglia in Huntington's disease (HD) have been previously investigated at 3T with MRI using magnetic field correlation imaging, T2*, quantitative susceptibility mapping (QSM), as well as T2 relaxometry mostly at lower fields of 1.5T or less. We performed T2 mapping at 3T in a group of pre-HD (n=10) and HD patients (n=11) to investigate its association with Disease Burden Score and structural measures (caudate volume) of disease load. We found significant correlations between T2 and disease progression measures in nucleus accumbens, putamen and pallidum.

2500 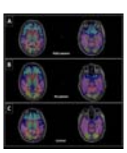

Automated Volumetry-based Morphometry in Postural Instability Gait Disorder

Eric Fang*[1], Chu Ning Ann*[1], Bénédicte Maréchal[2,3,4], Shawn Yan Zhi Tan[1], Julian Gan [5], Huihua Li[1], Eng King Tan [6], and Ling Ling Chan[1]

[1]Singapore General Hospital, Singapore, Singapore, [2]Advanced Clinical Imaging Technology, Siemens Healthcare HC CEMEA SUI DI PI, Lausanne, Switzerland, [3]Department of Radiology, University Hospital (CHUV), Lausanne, Switzerland, [4]LTS5, École Polytechnique Fédérale de Lausanne, Lausanne, Switzerland, [5]Advanced Clinical Imaging Technology, Siemens Healthcare HC CEMEA SUI DI PI, Singapore, Singapore, [6]National Neuroscience Institute, Singapore

Postural instability gait disorder (PIGD) subtype in Parkinson's disease (PD) is a major cause of morbidity. We quantified whole-brain structural changes in PIGD patients, PD patients and controls using an automated volume-based morphometry algorithm that is objective and reproducible. Compared to PD and controls, PIGD subgroup demonstrated a significant decrease in brain and globus pallidus volume, as well as grey matter content in both caudate and thalamus; but an increase in ventricular size, abnormal white matter volume and relative caudate size. MRI findings also correlate with gait imbalance severity in PIGD, suggesting a mechanism of temporal differences in segmental volume loss.

2501 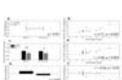

Measuring exercise-induced cerebrovascular changes in Huntington's Disease using arterial spin labelling (ASL) fMRI

Jessica J Steventon[1,2], Hannah Furby[1], James Ralph[1], Peter O'Callaghan[3], Anne Rosser[4], Monica Busse[5], and Kevin Murphy[6]

[1]CUBRIC, Cardiff University, Cardiff, United Kingdom, [2]Neuroscience and Mental Health Research Institute, Cardiff University, [3]Cardiac Services, Cardiff and Vale University Health Board, Cardiff, United Kingdom, [4]School of Medicine, Cardiff University, [5]Centre for Trials Research, Cardiff University, Cardiff, United Kingdom, [6]School of Physics and Astronomy, Cardiff University

Exercise is potentially therapeutic via vascular adaptations (angiogenesis, improved cerebral perfusion and metabolism) however the underlying dynamics are not fully understood. In Huntington´s disease (HD), where the therapeutic potential of exercise is being explored, cerebral vasculature alterations have been reported.

Here we used arterial spin labelling to examine the acute effect of aerobic exercise on the cerebrovasculature in HD patients. We show that genetic disease load is related to both baseline cerebral blood flow (CBF) and the exercise-induced change in CBF.

2502

Lessons for MRI recruitment in movement disorder: Clinical presentation is not related to motion artefacts in arterial spin labelling MRI

Jessica J Steventon[1,2], Hannah Furby[1], James Ralph[1], Anne Rosser[3], and Kevin Murphy[4]

[1]CUBRIC, Cardiff University, Cardiff, United Kingdom, [2]Neuroscience and Mental Health Research Institute, Cardiff University, [3]School of Medicine, Cardiff University, [4]School of Physics and Astronomy, Cardiff University

Motion artefacts pose significant problems for the acquisition and analysis of MRI data. In movement disorders, severe motion-related artefacts can result in data being discarded as non-usable. It is not known to what degree clinical movement symptoms can predict in-scanner motion artefacts, and thus, whether researchers can target recruitment for MRI studies based on clinical presentation.   Here we investigate whether movement severity in Huntington's disease, a neurodegenerative movement disorder, can predict in-scanner motion artefacts in arterial spin labelling data. We find that motion magnitude and variability is not more pronounced in Huntington's disease and not related to symptom severity.

2503

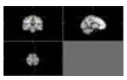

Cortical Recruitment of Motor Imagery in Timed Up and Go Task

Gina Kirkish[1], Anisha Keshavan[1], Nancy Byl[2], William Stern[1], Stacy Hatcher[1], Tracy Luks[3], and Roland Henry[1,3]

[1]Department of Neuology, University of California, San Francisco, San Fransisco, CA, United States, [2]Department of Physical Therapy and Rehabilitation Science, University of California, San Francisco, [3]Department of Radiology and Biomedical Imaging, University of California, San Francisco

A paradigm was developed to evaluate neural pathophysiology of gait and turning in individuals with Parkinson's disease (PD) using fMRI. BOLD signal change of imagined walking and turning was compared to resting state activation in PD patients and controls. Subjects performed physical examinations including the Timed Up and Go (TUG) task, ten-meter walk and a timed 360-degree turn to assess motor performance. Brain activity was compared between groups and to motor performance. This study concluded that a neural correlate of the TUG task exists in BOLD signal change in the premotor and primary motor area when imagining-turning compared to imagining-walking.

2504

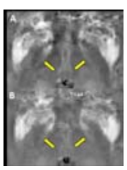

Benefits of high-resolution QSM acquisition protocol for DBS surgery planning

Alexey Dimov[1,2], Yihao Yao[3], Ilhami Kovanlikaya[4], Pascal Spincemaille[4], Jonathan Rasouli[5], Brian Kopell[5], and Yi Wang[1,2]

[1]Meing School of Biomedical Engineering, Cornell University, Ithaca, NY, United States, [2]Radiology, Weill Cornell Medical College, New York, NY, United States, [3]Department of Radiology, Tongji Hospital, Tongji Medical College, Huazhong University of Science & Technology, Wuhan, People's Republic of China, [4]Weill Cornell Medical College, New York, NY, United States, [5]Department of Neurosurgery, Mount Sinai Health System, New York, NY, United States

Deep brain stimulation is a surgical procedure routinely used in the treatment of advanced stages of Parkinson disease. DBS involves implanting of stimulating electrodes inside the patient's brain, with STN most commonly being the target brain structure. Treatment efficiency and absence of negative side effects is strongly dependent on precision of electrode placement; therefore, high requirements are imposed on preoperative patient imaging for proper identification of anatomy of interest. Histochemical studies suggest that iron (one of the major contrast contributors in QSM) is densely and heterogeneously distributed in STN. Furthermore, it is hypothesized that distribution of iron might be related to functional subdivisions in STN. Thus, DBS surgery planning might benefit from more precise calculation of susceptibility distribution, which would allow observe and characterize gradients in iron concentration in in vivo patient data potentially leading to minimization of non-motor side effects. Accordingly, we develop a high resolution QSM protocol for DBS presurgical MRI protocol.

Traditional Poster

Head, Neck, Spinal Cord

Exhibition Hall 2505-2524 Wednesday 13:45 - 15:45

2505

Improvement in Visualization of Brachial Plexus by 3D TSE MR Neurography Using Combination of STIR with SPIR at 3.0T

Hirotoshi Maruyama[1], Yasuhiro Fujiwara[2], and Tsukasa Sakemoto[1]

[1]Department of Radiology, Kumamoto Saishunso National Hospital, Kumamoto, Japan, [2]Department of Medical Imaging, Faculty of Life Sciences, Kumamoto University, Kumamoto, Japan

Magnetic resonance neurography (MRN) of the brachial plexus using a 3D turbo spin echo (TSE) sequence with short-term inversion recovery (STIR) reduces the effect of fat suppression at 3.0 T. In addition, the signal intensity of the brachial plexus is influenced by changing the effective echo time (TEeff). Therefore, we optimized the fat suppression technique and TEeff so that the 3D TSE sequence, using a combination of STIR with SPIR and an optimal TEeff (from170 ms to 293 ms), achieved better visualization of the brachial plexus without residual fat.

2506

Motion-Free MR Imaging of Brachial Plexus using the PROPELLER technique combined with Low-Refocus Flip Angle FSE

Kojiro Ono[1,2], Yasuhiro Oikawa[3], Takayuki Sakai[4], Hirofumi Watanabe[1], Akira Shirayama[1], Takumi Okubo[5], and Atsushi Senoo[2]

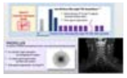

[1]Chiba Children's Hospital, Chiba, Japan, [2]Tokyo Metropolitan University, Tokyo, Japan, [3]Orthopaedic Surgery, Chiba Children's Hospital, Chiba, Japan, [4]Eastern Chiba Medical Center, Chiba, Japan, [5]Chiba Cancer Center, Chiba, Japan

The STIR Low-RFA PROPELLER method is a combination of STIR (Short-TI Inversion Recovery) suppressing fat signal homogenously and low refocus flip angle (Low-RFA) PROPELLER for flow signal reduction. Furthermore, the PROPELLER is able to reduce ghost generated by flow and motion, and to maintain high resolution by averaging of k-space. Consequently, the STIR Low-RFA PROPELLER method will be expected to produce clear brachial plexus imaging which is not affected by motion. In this study, we demonstrate that this new scheme (STIR Low-RFA PROPELLER) is superior to the conventional method (T2 weighted IDEAL) in the depiction of brachial plexus.

2507

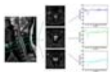

Perfusion of Spinal Cord in postoperative patient with Cervical Spondylotic Myelopathy using MR DSC technique

Chunyao Wang[1], Xiao Han[2], Wen Jiang[2], Xiaodong Ma[1], Hua Guo[1], Le He[1], and Huijun Chen[1]

[1]CBIR, School of Medicine, Tsinghua University, Beijing, People's Republic of China, [2]Jishuitan hospital, Beijing, People's Republic of China

Cervical Spondylotic Myelopathy (CSM) is a major cause of spinal cord dysfunction. However, the relationship between the degree of stenosis, tissue degeneration and sensorimotor dysfunction have not been well understood.In this study, 3 healthy volunteers and 17 CSM patients with different postoperative recovery degree were involved. We investigate the perfusion of spinal cord using MR DSC technique. The results showed a significant correlation between CBV and the postoperative severity of symptom (Japanese Orthopaedic Association score), which indicate that MR DSC perfusion of spinal cord could be an imaging biomarker to evaluate and understand CSM.

2508

An Optimal Design for 32 Channel Head-Neck Coil

Jo Lee[1], Xiaoqing Hu[1], Lei Zhang[1], Xiaoliang Zhang[2,3], Xin Liu[1], and Ye Li[1]

[1]Lauterbur Imaging Research Center, Shenzhen Institutes of Advanced Technology, Chinese Academy of Sciences, Shenzhen City, People's Republic of China, [2]Department of Radiology and Biomedical Imaging, University of California San Francisco, CA, United States, [3]UCSF/UC Berkeley Joint Graduate Group in Bioengineering, San Francisco, CA, United States

In this study, we build an optimized 32 channel head-neck coil array to improve the weak SNR of area behind cervical spine from the previous designed neck-coil array. Two of the original eight neck coils is place to the area near scruff with a new structure. Comparing the optimized 32-channel head neck coil with the previous: imaging test has improved 63% higher than the previous coil array. For g-factor measurement, optimized neck coil array is the same as the previous one. The results indicate that the optimized coil array is better for neck imaging.

2509

Toward Clinical Translation of Quantitative Spinal Cord MRI: Serial Monitoring to Identify Disease Progression in Patients with Degenerative Cervical Myelopathy

Allan R. Martin[1], Benjamin De Leener[2], Julien Cohen-Adad[2], David W. Cadotte[3], Jefferson R. Wilson[1], Lindsay Tetreault[1,4], Stefan F. Lange[1], Aria Nouri[1], Adrian Crawley[5], David J. Mikulis[5], Howard Ginsberg[1], and Michael G. Fehlings[1]

[1]Neurosurgery, University of Toronto, Toronto, ON, Canada, [2]Electrical Engineering, École Polytechnique de Montréal, [3]Neurosurgery, University of Calgary, Calgary, AB, Canada, [4]Medicine, University College Cork, Cork, Ireland, [5]Medical Imaging, University of Toronto, Toronto, ON, Canada

Degenerative cervical myelopathy (DCM) is a common cause of disability, but mild patients are often managed non-operatively and monitored for deterioration. Popular clinical assessment tools are insensitive to detect subtle disease progression. In this study, we employ multi-parametric spinal cord MRI to monitor 15 DCM patients for progression over a 1-year period, in addition to a comprehensive battery of clinical assessments. The MRI results detected progressive tissue injury in 6/7 patients with definite clinical progression and 5 additional patients (4 of which had borderline clinical progression). These MRI assessments are now being incorporated into clinical practice to inform surgical decision-making.

2510

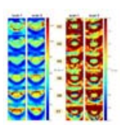

Reproducible fast T1 mapping of the human cervical spinal cord in vivo

Marco Battiston[1], Torben Schneider[2], Ferran Prados[1,3], Francesco Grussu[1], Marios C Yiannakas[1], Sebastien Ourselin[3], Claudia A M Gandini Wheeler-Kingshott[1,4,5], and Rebecca S Samson[1]

[1]UCL Institute of Neurology, Queen Square MS Centre, UCL, London, United Kingdom, [2]Philips Healthcare, Guilford, United Kingdom, [3]Translational Imaging Group, Centre for Medical Image Computing, Department of Medical Physics and Biomedical Engineering, UCL, London, United Kingdom, [4]Department of Brain and Behavioural Sciences, University of Pavia, Pavia, Italy, [5]Brain MRI 3T Mondino Research Center, C. Mondino National Neurological Institute, Pavia, Italy

The T_1 relaxation time is a fundamental quantitative Magnetic Resonance parameter widely used to characterize healthy and pathological tissue. However, quantitative T_1 mapping in the human spinal cord (SC) has been limited to date, mainly due to its small size and sensitivity to artefacts. Here we assess the reproducibility of a time efficient (<5min) SC protocol for Inversion Recovery T_1 mapping, which is considered the *gold-standard* method for T_1 estimation. Scan-rescan experiments were performed in a cohort of 4 healthy subjects. High reproducibility (whole cord intraclass correlation=0.94) of T_1 estimates was found, with whole cord intra-subject coefficient-of-variation<15% for all subjects.

2511

Optimization of Quantitative Magnetization Transfer Imaging for Accurate PSR Estimation in the Spinal Cord

Robert L Harrigan[1,2], Bennett A Landman[1,2], and Seth A Smith[2,3]

[1]Department of Electrical Engineering, Vanderbilt University, Nashville, TN, United States, [2]Vanderbilt University Institute of Imaging Science, Vanderbilt University, Nashville, TN, United States, [3]Department of Radiology and Radiological Sciences, Vanderbilt University Medical Center, Nashville, TN, United States

Quantitative magnetization transfer (qMT) sampling schemes typically attempt uniform sampling of the MT z-spectrum but this may not be optimal for PSR estimation of the human spinal cord in vivo. We utilize Monté Carlo simulations of fitting synthetic qMT data to produce an optimal sampling scheme of the MT z-spectrum. This sampling scheme is evaluated in a healthy control and compared to current best practices where we see superior PSR estimation with our optimized sampling scheme.

2512

Application of Quantitative Microstructural MR Imaging with Atlas-based Analysis for Spinal Cord in Cervical Spondylotic Myelopathy.

Masaaki Hori[1], Issei Fukunaga[1], Ryo Ueda[1,2], Kouhei Kamiya[3], Yuichi Suzuki[3], Katsutoshi Murata[4], Tomohiro Takamura [1], Nozomi Hamasaki[1], Ryusuke Irie[1], Kanako Kunishima Kumamaru[1], Michimasa Suzuki[1], and Shigeki Aoki[1]

[1]Radiology, Juntendo University School of Medicine, Tokyo, Japan, [2]Health Science, Tokyo Metropolitan University, Tokyo, Japan, [3]Radiology, The University of Tokyo Hospital, Tokyo, Japan, [4]Siemens Japan K.K., Tokyo, Japan

We investigated MR fiber g-ratio, AVF and MVF in evaluation of microstructural changes in the spinal cord in patients with cervical spondylotic myelopathy, with using atlas-based analysis by spinal cord tool box. 19 patients and 5 normal controls were included. MT-sat and NODDI data were collected at 3T MRI. The right side of fasciculus cuneatus and bilateral lateral corticospinal tracts (LSCT) of AVF were significant lower (P=0.014, 0.017, 0.014, one-way ANOVA with Scheffé's post-hoc test) and the left LSCT of MVF was significant higher (P=0.037) in the affected side spinal cord, compared with normal controls.

2513

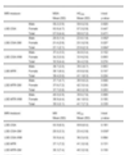

Assessing changes within the lumbosacral spinal cord in neurological disease: preliminary results of a pilot in vivo MRI study

Martina D Liechti[1,2], Marios Yiannakas[1], Nuttakarn Budtarad[1], Ahmed T Toosy[1], Xixi Yang[1,2], Ferran Prados[3], David H Miller[1], Henry H Houlden[4], Claudia AM Gandini Wheeler-Kingshott[1], and Jalesh N Panicker[2]

[1]UCL Institute of Neurology, Queen Square MS Centre, University College London, London, United Kingdom, [2]UCL Institute of Neurology, Uro-Neurology, Department of Brain Repair & Rehabilitation, University College London, London, United Kingdom, [3]Translational Imaging Group, Centre for Medical Image Computing, Department of Medical Physics and Biomedical Engineering, University College London, London, United Kingdom, [4]UCL Institute of Neurology, Department of Molecular Neuroscience, University College London, London, United Kingdom

Magnetic resonance imaging (MRI)-derived tissue-specific measures of neuronal loss and demyelination were assessed at the lumbosacral level of the spinal cord (SC) in relation to neurological dysfunction. Acquisition of grey and white matter measures for the lumbosacral SC proved feasible, and were sensitive to detect tissue-specific changes in two neurological disorders commonly associated with lumbosacral cord involvement: Multiple system atrophy and Multiple sclerosis. This preliminary study demonstrates the utility of this cutting edge MRI acquisition method to detect pathological changes in the lumbosacral SC, and is a first step towards establishing new MRI biomarkers for these patient groups.

2514

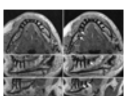

High-Resolution MRI of Dental Ceramic Implants In Vivo

Ute Ludwig[1,2], Tabea Flügge[2,3], Katja Nelson[2,3], Fabian Duttenhöfer[2,3], Ralf Kohal[2,4], Dominik von Elverfeldt[1,2], and Jan-Bernd Hövener[1,2,5]

[1]Department of Radiology, Medical Physics, Medical Center - University of Freiburg, Freiburg, Germany, [2]Faculty of Medicine, University of Freiburg, Freiburg, Germany, [3]Division of Oral and Maxillofacial Surgery, Medical Center - University of Freiburg, Freiburg, Germany, [4]Department of Prosthodontics, Medical Center - University of Freiburg, Freiburg, Germany, [5]Partner Site Freiburg, German Consortium for Cancer Research (DKTK), Heidelberg, Germany

The purpose of the study was to demonstrate the feasibility and evaluate the limitations of high-resolution MRI of ceramic implants *in vivo*. One healthy volunteer was subjected to high-resolution MRI before and after two zirconia dental implants were placed in the lower right jaw. Both implants were clearly depicted as signal voids, and no artifacts were observed using a turbo spin echo sequence. In conclusion, high-resolution *in-vivo* MRI of ceramic implants with an isotropic voxel size of (600 μm)^3 is feasible within 5 minutes scan time.

2515

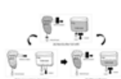

Mathematical Modeling for Evaluating Gustatory Stimulation of Parotid Gland by Proton Density MRI

Yu-Chia Cheng[1], Yi-Jui Liu[2], Yi-Hsiung Lee[3,4], Hing-Chiu Chang[5], Hui-Chu Chiu[6], Ta-Wei Chiu[7], Kang Hsu[8], Hsian-He Hsu[4,9], and Chun-Jung Juan[4,9]

[1]Master 's Program of Biomedical Informatics and Biomedical Engineering of Feng Chia University, Taichung, Taiwan, Taichung, Taiwan, [2]Department of Automatic Control Engineering, Feng Chia University, Taichung, Taiwan, Republic of China, [3]Ph.D. program in Electrical and Communication Engineering in Feng Chia University, Taichung, Taiwan, Republic of China, [4]Department of Radiology, Tri-Service General Hospital, Taipei, Taiwan, Republic of China, [5]Department of Diagnostic Radiology, The University of Hong Kong, Hong Kong, [6]Ph.D. program of Technology Management, Chung Hua University, Hsinchu, Taiwan, Republic of China, [7]Department of Medicine, Taipei Medical University, Taipei, Taiwan, Republic of China, [8]Department of Dentistry, National Defense Medical Center, Taipei, Taiwan, Republic of China, [9]Department of Radiology, National Defense Medical Center, Taipei, Taiwan, Republic of China

The parotid gland function is evaluated by gustatory stimulation using scintigraphy in clinic. Due to the saliva secretion of parotid, it is supposed to measure the water component of parotid gland using PD MRI instead of scintigraphy. Normally the drop magnitude and recover rate of signal-time curve after gustatory stimulation was used to evaluate the function of parotid gland. For more physiology and quantitative parameters of characteristics of signal-time curve, we developed a mathematical model for drainage and refill of a toilet tank to quantify the parotid gland function in this study.

2516

Residual tumour detection in post-treatment granulation tissue by using multiple diffusion models in head and neck squamous cell carcinoma patients

Noriyuki Fujima[1], Tomohiro Sakashita, Akihiro Homma, and Kohsuke Kudo

[1]Hokkaido University Hospital, Sapporo, Japan

We assessed the utility of diffusion parameters obtained by multiple fitting models for the determination of the presence of the residual tumor after the curative chemoradiation in patients with head and neck squamous cell carcinoma (HNSCC). The result of the current study revealed the center of the Gaussian distribution of diffusion coefficient (D_s) in the statistical diffusion model and diffusion heterogeneity parameter in the stretched exponential model were respectively indicated as an independent predictor for the determination of the presence of residual tumor. This result will be useful information for the daily clinical follow-up in patients with HNSCC.

2517 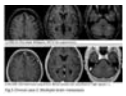

Application of a flow-sensitive black blood (FSBB) T2* sequence to cranial nerve system contrast-enhanced imaging

Keiya Hirata[1], Yuuichi Murasaki[1], Chihiro Watari[1], Tatsunori Kuroda[1], Nanako Miyamoto[1], Saeko Tomida[1], Tomokazu Oku[1], Shigeo Miyazaki[1], Masahiro Kawashima[1], Ichirou Toyota[2], Mariko Doai[2], and Hisao Tonami[2]

[1]Division of radiology, kanazawa medical university, kahokugun, Japan, [2]Department of radiology, kanazawa medical university, kahokugun, Japan

A flow-sensitive black blood (FSBB) sequence is usually used for 3D-T2*WI imaging. In an FSBB sequence, the vascular signal is suppressed by the effect of motion-probin- gradient (MPG) pulses. If this advantageous signal suppression is used, then 'contrast-enhanced volume black blood imaging' could be obtained.

2518 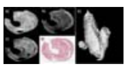

Atherosclerotic carotid plaque composition using in-vivo 3T, ex-vivo 7T MRI and histology

Rosario Lopez Gonzalez[1,2], Sin Yee Foo[2], William Holmes[3], William Stewart[4], George Welch[5], Barrie Condon[2], Keith Muir[2,6], and Kirsten Forbes[7]

[1]Clinical Physics and Bioengineering, University of Glasgow, Glasgow, United Kingdom, [2]NHS Greater Glasgow and Clyde, Glasgow, United Kingdom, [3]GEMRIC, University of Glasgow, Glasgow, United Kingdom, [4]Neuropathology, NHS Greater Glasgow and Clyde, Glasgow, United Kingdom, [5]Vascular Surgery, NHS Greater Glasgow and Clyde, Glasgow, United Kingdom, [6]Center for Stroke and Brain Imaging, University of Glasgow, Glasgow, United Kingdom, [7]Institute of Neurological Siences, NHS Greater Glasgow and Clyde, Glasgow, United Kingdom

Atherosclerotic carotid plaque morphology and plaque composition may identify unstable or vulnerable plaque that defines higher risk. The aim of this study is to evaluate the ability to identify all major carotid plaque components in in-vivo 3T, ex-vivo 7T MRI and correlation with histology.

2519 

Comparison of non-Gaussian diffusion parameters using different diffusion times in head and neck tumors

Mami Iima[1,2], Akira Yamamoto[1], Ichiro Tateya[3], Morimasa Kitamura[3], Atsushi Suehiro[3], Yo Kishimoto[3], and Kaori Togashi[1]

[1]Department of Diagnostic Imaging and Nuclear Medicine, Graduate Schoolof Medicine, Kyoto University, Kyoto, Japan, [2]Hakubi Center for Advaned Research, Kyoto University, Kyoto, Japan, [3]Department of Otolaryngology, Head and Neck Surgery., Graduate School of Medicine, Kyoto University, Kyoto, Japan

The association of diffusion parameters in patients with head and neck cancers was investigated using the different diffusion times. Although ADCo significantly decreased ($p<0.05$) and fIVIM increased ($p<0.05$) using 51ms compared to 19.1ms, there was no difference of K values. The effects of the diffusion time on IVIM and non-Gaussian diffusion parameters are not clear in head and neck cancers. Our preliminary study requires further validation with shorter diffusion time or better SNR.

2520 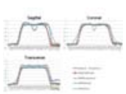

Assessment of image qualities of multi planar reformatted images depending on imaging planes of a variable refocus flip angle 3D FSE sequence (Cube) in cervical spine MRI

Yumi Koizumi[1], Masaru Sonoda[1], Tsutomu Inaoka[2], and Hideki Nagatomo[1]

[1]Division of Radiology, Seirei Sakura Citizen Hospital, Sakura, Japan, [2]Department of Radiology, Toho University Sakura Medical Center

The purpose of this study is to assess image qualities of MPR images depending on imaging planes of Cube to determine the optimal imaging plane in the cervical spine. The differences of FWHMs in frequency and phase encoding directions of the transverse, sagittal, coronal source images were compared and those encoding directions on the transverse, sagittal, coronal MPR images were compared. MRI of Volunteers image qualities were recorded by assessing sharpness of the vertebral body, spinal cord, and nerve roots on the images. To provide better image qualities in cervical spine MRI using Cube, transverse planes should be selected.

2521

Texture Analysis of MR Images in Pediatric Cervical Spinal Cord Injury

Mahdi Alizadeh[1], Chris J Conklin[2], Devon M Middleton[1], Sona Saksena[2], Laura Krisa[3], Scott H Faro[4], MJ Mulcahey[3], and Feroze B Mohamed[2]

[1]Temple University, Philadelphia, PA, United States, [2]Radiology, Thomas Jefferson Hospital University, Philadelphia, PA, United States, [3]Occupational Therapy, Thomas Jefferson Hospital University, Philadelphia, PA, United States, [4]Radiology, Temple University, Philadelphia, PA, United States

In this study we have investigated on evaluating the ability of texture analysis of routine conventional pediatric spinal cord MRI to characterize the changes of diseased or injured spinal cord.

2522 

Evaluation of cervical carotid plaque volume using 3D T1 black-blood MRI : Comparison of manual measurement and automated measurement by the software.

Shiho Isoshima[1], Masayuki Maeda[2], Katsuhiro Inoue[1], Ryohei Nakayama[3], Shinichi Takase[1], Tsunehiro Yamahata[1], and Hajime Sakuma[4]

[1]Department of Radiology, Mie University Hospital, Mie, Japan, [2]Department of Advanced Diagnostic Imaging, Mie University School of Medicine, Mie, Japan, [3]Department of Electronic and Computer Engineering, Ritsumeikan University, Shiga, Japan, [4]Department of Radiology, Mie University School of Medicine, Mie, Japan

Quantitative assessment of carotid plaque burden is required to monitor the effects of treatments for carotid atherosclerosis. Cervical carotid plaque volume in 13 patients with carotid artery stenosis was measured and evaluated using manual and automated software methods for 3D T1 black-blood MRI. Measurement reproducibility was better using the automated method than that using the manual method. The automated software developed for the measurement of carotid plaque volume was feasible and reliable and could significantly reduce the measurement time. This method appears to be of great value in clinical settings.

2523

First Application of 7T Structural, Vascular, and Diffusion Imaging to Trigeminal Neuralgia: Preliminary Results in Patients

Judy Alper[1,2], Rafael O'Halloran[3], Bradley Delman[4], Raj Shrivastava[5], and Priti Balchandani[1]

[1]Radiology, Translational and Molecular Imaging Institute, Icahn School of Medicine at Mount Sinai, New York, NY, United States, [2]Biomedical Engineering, City University of New York, New York, NY, United States, [3]Radiology, Icahn School of Medicine at Mount Sinai, New York, NY, United States, [4]Neuroradiology, Mount Sinai Medical Center, New York, NY, United States, [5]Neurosurgery and Otolaryngology, Mount Sinai Medical Center, New York, NY

Trigeminal neuralgia (TN) is a debilitating condition characterized by severe facial pain. The pathophysiology of TN is not well understood and conventional clinical imaging often fails to identify the anatomical source of pain. In this study, we perform high-resolution 7T structural, vascular and diffusion-weighted MRI to visualize the trigeminal nerve region in three TN patients and three controls. We found that 7T-MRI provided improved visualization of nerve abnormalities compared to clinical scans. We also found greater nerve asymmetry in TN patients compared to controls. Multi-modal 7T-MRI could enhance our understanding of TN etiology and provide improved clinical outcomes for TN.

2524

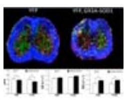

Spinal Cord MRI Water Diffusion Alterations are Linked to Early Axonal Degeneration in the YFP, G93A-SOD1 mice.

Rodolfo Gabriel Gatto[1], Weiguo Li[2], Manish Amin[3], Luis Colon-Perez[3], Jin Gao[2], Thomas H. Mareci[3], Scott T. Brady[1], Gerardo A Morfini[1], and Richard L Magin[2]

[1]Anatomy and Cell Biology, University of Illinois at Chicago, Chicago, IL, United States, [2]Biomedical Engineering, University of Illinois at Chicago, Chicago, IL, United States, [3]Biochemistry and Molecular Biology, University of Florida, Gainesville, FL, United States

Amyotrophic lateral Sclerosis (ALS) is characterized by progressive degeneration of spinal cord motor neurons. To address the role of axonal pathology in ALS, we generated a YFP,G93A-SOD1 reporter mice. Our goal in this study is to evaluate if presymptomatic alterations in MRI water diffusion in the YFP,G93A-SOD1 mice are related to alterations in axonal connectivity by histological methods. Results showed presymptomatic changes in diffusion parameters are associated to specific structural changes in axonal population. The use of this new animal model will help us to understand the structural basis of changes in water diffusion in ALS.

Traditional Poster

Multiple Sclerosis

Exhibition Hall 2525-2562 Wednesday 13:45 - 15:45

2525

Gradient and Spin Echo (GRASE) as an Alternative to Multi Echo Spin Echo (MESE) acquisition for Myelin Water Fraction Imaging

Dushyant Kumar[1], Hari Hariharan[1], Jens Fiehler[2], Susanne Siemonsen[2], Jan Sedlacik[2], and Ravinder Reddy[1]

[1]Radiology, University of Pennsylvania, Philadelphia, PA, United States, [2]Klinik und Poliklinik für Neuroradiologische Diagnostik und Intervention, Universitätsklinikum Hamburg-Eppendorf, Hamburg, Germany

Problem: The clinical utility of myelin water fraction (MWF) mapping based on multi-echo-spin-echo (MESE) T2-relaxometry is prohibitively slow (~90-120 minutes for acquisition matrix 128x128x50; TR 3s). MWF-values from T2-prep based approach and mcDESPOT (Multicomponent-driven-equilibrium-single-pulse-observation-of-T1-and-T2) matches poorly with MESE based quantification.

Methods: We compare GRASE (Gradient-and-Spin-Echo) based MWF quantifications against those from MESE and compare our algorithm against current state of the art. 3D non-selective GRASE, MESE were optimized. Implemented post-processing method utilizes spatial correlations in 3D local neighborhoods to improve noise stability, while simultaneously accounting for stimulated echo contributions.

Results & Conclusions: Results demonstrate good consistency between both sequences.

2526

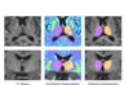

Correlation between thalamic volume and cognitive impairment in patients with MS using a high-efficiency semi-manual segmentation approach

Peter Adany[1], Douglas R. Denney[2], In-Young Choi[1,3,4], Erica B. Sherry[1], Abbey J. Hughes[2], Sharon G. Lynch[3], and Phil Lee[1,4]

[1]Hoglund Brain Imaging Center, University of Kansas Medical Center, Kansas City, KS, United States, [2]Psychology, University of Kansas, [3]Neurology, University of Kansas Medical Center, Kansas City, KS, United States, [4]Molecular & Integrative Physiology, University of Kansas Medical Center, Kansas City, KS, United States

Thalamic pathology has been linked to long-term accumulation of disability and cognitive impairment in MS. However, assessment of thalamic volume is highly challenging for automatic as well as manual segmentation techniques. The use of multiple image contrasts may improve segmentation quality. We investigated correlations of thalamic volume and cognitive performance in MS. We evaluated automatic segmentation and our new semi-manual segmentation using T1 and proton-density MRI. Results based on FreeSurfer segmentation failed to yield correlations of thalamic volume with cognitive performance in MS patients. Using semi-manual segmentation, significant correlations were found between cognitive impairment and regional thalamic atrophy in MS.

2527

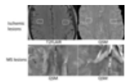

Iron is a biomarker for differentiating multiple sclerosis lesions from ischemic demyelinating lesions

Weiwei Chen[1], Yan Zhang[1], Ketao Mu[1], Susan A. Gauthier[2], Yi Wang[3,4], and Wenzhen Zhu[1]

[1]Tongji hospital, Tongji Medical College, Huazhong University of Science & Technology, Wuhan, People's Republic of China, [2]Neurology, Weill Cornell Medical College, NY, United States, [3]Radiology, Weill Cornell Medical College, NY, United States, [4]Department of Biomedical Engineering, Cornell University

Differentiation MS lesions from ischemic demyelinating lesions is important because of their totally different treatment strategies. Our results suggested that the increased susceptibility of demyelinating lesions, the presence of QSM-ring lesions and the central vein in the lesions helped to differentiate MS lesions from ischemic demyelinating lesions. Thus, QSM provided the underling iron-related pathogenesis of MS lesions, which enable to differentiate MS lesions from ischemic demyelinating lesions.

2528

Inhomogeneous Magnetization Transfer (ihMT) in normal-appearing tissue correlates with clinical EDSS score of MS patients.

Elise Van Obberghen[1], Samira Mchinda[1], Arnaud le Troter[1], Valentin H. Prevost[1], Patrick Viout[1], Elisabeth Soulier[1], Maxime Guye[1], Gopal Varma[2], David C. Alsop[2], Jean-Philippe Ranjeva[1], Jean Pelletier[3], Olivier M. Girard[1], and Guillaume Duhamel[1]

[1]Aix-Marseille Univ, CNRS, CRMBM UMR 7339, Marseille, France, [2]Radiology, Division of MR Research, Beth Israel Deaconess Medical Center, Harvard Medical School, Boston, MA, United States, [3]Aix Marseille Univ, APHM, Hôpital La Timone, Pôle de Neurosciences Cliniques, Service de Neurologie, Marseille, France

The present study was aimed at evaluating the potential of ihMT (inhomogeneous Magnetization transfer) contrast in characterizing the severity of MS disease, and investigating possible correlations between ihMT and the clinical disability score.

2529

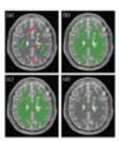

A New Iterative GPU Algorithm to Segment MS Lesions in Multi-spectral MRI Datasets

Wenzhe Xue[1], Christine M. Zwart[2], Joseph M. Hoxworth[2], Dean M. Wingerchuk[3], and J. Ross Mitchell[4]

[1]Biomedical Informatics, Arizona State University, Scottsdale, AZ, United States, [2]Radiology, Mayo Clinic, AZ, United States, [3]Neurology, Mayo Clinic, AZ, United States, [4]Research, Mayo Clinic, AZ, United States

This paper presents a new method to segment MS lesions in multi-spectral MRI exams. Our approach leverages the speed of a GPU level set algorithm and a new data term to perform multiple segmentations of brain white matter in each exam. Differences between these segmentations allow us to estimate the distribution of MS lesions. We evaluated our method on BrainWeb and MS Lesion Segmentation Challenge 2008 data. It achieved results comparable to, or better than, two top performing algorithms. The average time required by our algorithm for Challenge08 data was 20.8 seconds.

2530

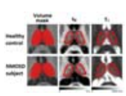

Thalamic involvement in neuromyelitis optica spectrum disorder: multicomponent relaxometry parameters and relationship with cognition

Anna J.E. Combes[1,2], Katrina McMullen[2], Irene M. Vavasour[3], Emmanuelle Lapointe[2], Robert Carruthers[2], David K.B. Li[3], Gareth J. Barker[1], Anthony Traboulsee[2], and Shannon Kolind[2,3]

[1]Neuroimaging, Institute of Psychiatry, Psychology & Neuroscience, King's College London, London, United Kingdom, [2]Neurology, University of British Columbia, Vancouver, BC, Canada, [3]Radiology, University of British Columbia, Vancouver, BC, Canada

Investigations into thalamus pathology, a known predictor of disease progression and cognitive impairment in multiple sclerosis, have yielded inconsistent results in neuromyelitis optica spectrum disorder. We found significant thalamic atrophy, but normal multicomponent relaxometry parameters in patients compared to healthy controls, providing further evidence that despite volume loss, microstructural alterations are likely subtle. Associations between MRI metrics (thalamic volume and T_1 relaxation time, linked with changes in water content) and performance on two measures of information processing speed support the hypothesis that damage to the thalamus may be involved in cognitive impairment in this population.

2531

The cytoarchitectonic anterior-posterior subdivision of BA4 reveals different resting state networks suggestive of maladaptive mechanisms in MS

Adnan A.S. Alahmadi[1,2], Rebecca S. Samson[1], Matteo Pardini[1,3], Egidio D'Angelo[4,5], Karl J. Friston[6], Ahmed T. Toosy[1], and Claudia AM Gandini Wheeler-Kingshott[1,4,7]

[1]UCL Institute of Neurology, Queen Square MS Centre, University College London, London, United Kingdom, [2]Department of Diagnostic Radiology, Faculty of Applied Medical Science, KAU, Jeddah, Saudi Arabia, [3]Department of Neurosciences, Rehabilitation, Ophthalmology, Genetics and Maternal and Child Health, University of Genoa, Genoa, Italy, [4]Department of Brain and Behavioural Sciences, University of Pavia, Pavia, Italy, [5]Brain Connectivity Centre, C. Mondino National Neurological Institute, Pavia, Italy, [6]Wellcome Centre for Imaging Neuroscience, University College London, London, United Kingdom, [7]Brain MRI 3T Mondino Research Center, C. Mondino National Neurological Institute, Pavia, Italy

This study investigates whether it is possible to characterise different resting state fMRI (rsfMRI) networks connected to the cytoarchitectonic subdivisions of Brodmann area 4 (BA4) and how these networks behave in the presence of multiple sclerosis (MS). We showed that each sub-region identifies different rsfMRI networks, with the BA4p network including more associative and higher order functional areas whereas the BA4a network includes more force-related and motor areas. In MS, functional connectivity to the right hemisphere was lost and was positively correlated with the 9-HPT, suggesting a maladaptive mechanism rather than a compensatory mechanism.

2532

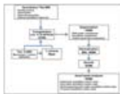

Assessment of neuronal dysfunction in benign multiple sclerosis: a sodium MRI study

Adil Maarouf[1,2,3], Soraya Gherib[1], Patrick Viout[1], Maxime Guye[1,2], Bertrand Audoin[1,3], Jean Pelletier[1,3], Jean-Philippe Ranjeva[1], and Wafaa Zaaraoui[1]

[1]Aix-Marseille Univ, CNRS, CRMBM, Marseille, France, [2]Aix-Marseille Univ, APHM, Hopital de la Timone, CEMEREM, Marseille, France, [3]Aix Marseille Univ, APHM, Hôpital de la Timone, Pôle de Neurosciences Cliniques, Service de Neurologie, Marseille, France

Assessment of neuro-degenerative process in multiple sclerosis using sodium MRI. A study in a population of 135 subjects at different disability and disease duration

---

2533

Sensitivity to pathological normal appearing white matter damage in multiples sclerosis – a comparison of DTI and DKI

Tim Sprenger[1,2], Michael Czisch[3], Brice Fernandez[4], Ines Eidner[3], Jonathan I. Sperl[5], Axel Haase[1], Frank Weber[3], Marion I. Menzel[5], and Philipp G. Sämann[3]

[1]Technische Universität München, Munich, Germany, [2]GE Global Research, Munich, Germany, [3]Max Planck Institute of Psychiatry, Munich, Germany, [4]GE Heathcare, Paris, France, [5]GE Global Research, Munich

A systematic comparison of diffusion tensor imaging (DTI) and diffusional kurtosis imaging (DKI) regarding the sensitivity to non-pathological white matter in multiple sclerosis is presented. We found first indications for a higher sensitivity of DKI compared with DTI in the normal appearing white matter compartment.

2534

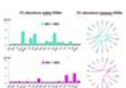

Distinct patterns of network-wise functional connectivity impairment discriminate Relapsing-Remitting Multiple Sclerosis with different disease duration

Gloria Castellazzi[1,2], Laëtitia Debernard[3,4], Tracy R Melzer[3,4], John C Dalrymple-Alford[3,5], Egidio D'angelo[2,6], David H Miller[3,4,7], Deborah F Mason[3,4,8], and Claudia AM Gandini Wheeler-Kingshott[6,7,9]

[1]Electrical, Computer and Biomedical Engineering, University of Pavia, Pavia, Italy, [2]Brain Connectivity Center, C. Mondino National Neurological Institute, Pavia, Italy, [3]New Zealand Brain Research Institute, Christchurch, New Zealand, [4]University of Otago, Christchurch, New Zealand, [5]University of Canterbury, Christchurch, New Zealand, [6]Department of Brain and Behavioral Sciences, University of Pavia, Pavia, Italy, [7]Queen Square MS Centre Department of Neuroinflammation, UCL Institute of Neurology, London, United Kingdom, [8]Department of Neurology, Christchurch Hospital, Christchurch, New Zealand, [9]Brain MRI 3T Research Center, C. Mondino National Neurological Institute, Pavia, Italy

In this work we examined functional connectivity (FC) changes *within* and *between* the resting state networks (RSNs) caused by Relapsing Remitting Multiple Sclerosis (RRMS) in two cohorts showing mild disability but different disease duration. Our results demonstrate widespread functional alterations in both *short* and *long* duration RRMS groups (MS1 and MS2). The MS1 group showed more severe FC alterations compared to the MS2 group. Overall, these results suggest that there may be pathophysiological differences in RRMS groups with different disease durations. Longitudinal studies would be needed to investigate whether FC findings are able to predict the future course.

2535

Automated evaluation of deep gray matter neuronal damage in multiple sclerosis patients

Bénédicte Maréchal[1,2,3], Alexis Roche[1,2,3], Tobias Kober[1,2,3], Wadie Ben Hassen[4], Alain Créange[5], Jérome Hodel[6], and Pierre Brugières[6]

[1]Advanced Clinical Imaging Technology, Siemens Healthcare HC CEMEA SUI DI PI, Lausanne, Switzerland, [2]Department of Radiology, CHUV, Lausanne, Switzerland, [3]LTS5, EPFL, Lausanne, Switzerland, [4]Siemens Healthcare S.A.S., Saint-Denis, France, [5]Department of Neurology, University Hospital Henri Mondor, Créteil, Switzerland, [6]Department of Neuroradiology, University Hospital Henri Mondor, Créteil, France

We investigate the potential of a technique to automatize quantification of neuronal damage from T1-weighted MR scans in multiple sclerosis patients. T1 hypointense component measures in the deep nuclei are derived from 40 MPRAGE scans (21 relapsing-remitting MS and 19 age-matched controls) through combined brain tissue classification and atlas-based segmentation algorithms. Our analysis shows that these automated measures are significantly lower in the thalamus and putamen of MS patients, which is in line with previously reported loss of structure in these regions.

2536

Changes in White Matter Integrity in MS under Fingolimod Treatment for Two Years Revealed by HARDI

Jian Lin[1], Pallab Bhattacharyya[1], Ken Sakaie[1], Robert Fox[2], and Mark Lowe[1]

[1]Radiology, Cleveland Clinic, Cleveland, OH, United States, [2]Neurology, Cleveland Clinic, Cleveland, OH, United States

In a 2 year longitudinal fingolimod study, we investigated the evolution of white matter integrity in the brain of relapsing-remitting multiple sclerosis (RRMS) patients under fingolimod treatment. Based on dMRI metrics from HARDI scans and statistical analysis, we found that MS patients experience a continued decline in white matter integrity during the first year of treatment with fingolimod with stabilization during the second year. Without a control group, it is unclear if these trends reflect on the impact of a treatment on disease progression.

2537

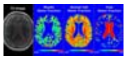

Gaining insights into Multiple Sclerosis Lesion Characteristics from Brain Tissue Microstructure Information: A multi-compartment T2 relaxometry Approach

Sudhanya Chatterjee[1], Olivier Commowick[2], Simon K. Warfield[3], and Christian Barillot[4]

[1]VisAGeS, IRISA U746, Universite de Rennes-1, Rennes, France, [2]VisAGeS Inserm U746, IRISA, Inria, Rennes, France, [3]Boston Children's Hospital, Boston, MA, United States, [4]VisAGeS, INRIA/IRISA, Inserm U746, CNRS, Rennes, France

Clinical trends and Pathogenetic ways of onset and progression of Multiple Sclerosis (MS) in patients suggest that MS is a highly heterogeneous disease. MS is predominantly a White Matter (WM) disease, which is mainly composed of myelinated axons and neuroglia type cells. Demyelination and axonal loss characterize the condition of MS in a patient. However, they follow varying trends in patients. In this work, we propose a method in which T2 relaxometry data is used to obtain a quantitative brain tissue microstructure information. This information is then studied to check its corroborations with pathogenetic understanding of MS in literature.

2538

Investigation on Optic Neuritis with DTI and Understanding Its Underlying Pathology using Monte Carlo Simulation.

You Jung Lee[1], Seoung-Eun Kim[1], John Rose[2], Eun-Ju Kim[1], Karen Salzman[3], Bradley Katz[2], and Eun-Kee Jeong[1,3]

[1]Utah Center for Advanced Imaging Research, University of Utah, Salt Lake City, UT, United States, [2]Department of Neurology, University of Utah, [3]Department of Radiology and Imaging Sciences, University of Utah, Salt Lake City, UT, United States

To understand the underlying physical and pathological meaning of optic-nerve in optic-neuritis(ON), diffusion-tensor imaging (DTI) and the corresponding Monte-Carlo Simulation (MCS) were conducted. DTI studies of four healthy subjects and seven ON patients with MS were performed and analyzed by home-built software. The measured DTI indices allowed us to monitor pathological changes such as inflammation in ON or demyelination. To investigate the clinical meanings of changes in diffusion parameters, MCS of water diffusion in optic nerve was performed.

2539

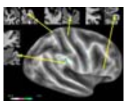

Z-Score Approach to the Detection of Cortical Lesions in Multiple Sclerosis

Richard Watts[1], Andrew Solomon[2], Kristen Koeller, and Joshua P Nickerson[1]

[1]Department of Radiology, University of Vermont, Burlington, VT, United States, [2]Department of Neurological Sciences, University of Vermont, Burlington, VT, United States

A new technique combining surface-based cortical myelin maps with Z-score methodology is developed to identify foci of cortical demyelination in patients with multiple sclerosis. The technique is found to discriminate (p=0.002) patients with MS (n=19) from patients with migraine (n=10), who often present with similar symptoms and white matter imaging findings. Regions of unusually low myelin content may correspond to lesions visible on the source T1-weighted and FLAIR images, but in other cases may be occult on either individual scan. The technique is clinically applicable, requiring only 3D T1 and FLAIR acquisitions that are already the standard of care in clinical neuroimaging.

2540

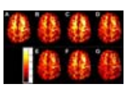

Optimization of Neurite Orientation Density and Dispersion Imaging (NODDI) for In Situ Imaging

Ken Sakaie[1], Mark Lowe[1], and Daniel Ontaneda[2]

[1]Imaging Institute, The Cleveland Clinic, Cleveland, OH, United States, [2]Mellen Center for Multiple Sclerosis, The Cleveland Clinic, Cleveland, OH, United States

In situ imaging is a valuable context for validation of imaging measures against histology. This contribution describes optimization of diffusion MRI for NODDI in in situ imaging of a multiple sclerosis patient. The results are expected to facilitate validation of advanced diffusion MRI and other tissue microstructure meausrements.

2541

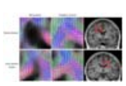

Reduced fibre density in the visual pathways of multiple sclerosis patients with optic neuritis

Sanuji Gajamange[1], David Raffelt[2], Thijs Dhollander[2], Elaine Lui[3], Annie Shelton[4], Owen White[5], Trevor Kilpatrick[1,2], Alan Connelly [2,6], Joanne Fielding [4,7], and Scott Kolbe[1]

[1]Department of Anatomy and Neuroscience, University of Melbourne, Melbourne, Australia, [2]The Florey Institute of Neuroscience and Mental Health, Melbourne, Australia, [3]Department of Radiology, Royal Melbourne Hospital, Melbourne, Australia, [4]School of Psychological Sciences and Monash Institute of Cognitive and Clinical Neurosciences, Monash University, Melbourne, Australia, [5]Department of Neurology, Royal Melbourne Hospital, Melbourne, Australia, [6]The Florey Department of Neuroscience and Mental Health, University of Melbourne, Melbourne, Australia, [7]Department of Medicine, University of Melbourne, Melbourne, Australia

Axonal degeneration is a key pathological driver of disability in multiple sclerosis (MS). Treatments aiming to reduce or reverse axonal degeneration in MS require sensitive and specific markers. Here we explore putative fibre-specific markers of axonal degeneration based on diffusion-weighted MRI metrics – fibre density and fibre bundle cross-section. MS patients with optic neuritis were compared to control subjects. We identified significant reductions to both fibre density and cross-section in the visual pathways of patients. These results indicate the pathological specificity of fibre density and cross-section measures in MS.

2542

Ultra High Field Regional Quantitative Susceptibility Mapping in Patients with Relapsing-Remitting Multiple Sclerosis: A Pilot Study

Jon Orlando Cleary[1], Amanda Ng[1], Camille Shanahan[1,2], Yasmin Blunck[1], Myrte Strik[1,2], Brad A Moffat[1], Trevor J Kilpatrick[2], Roger J Ordidge[1], and Scott C. Kolbe[1,2]

[1]Melbourne Brain Centre Imaging Unit, Department of Anatomy and Neuroscience, University of Melbourne, Parkville, Australia, [2]MS Research Group, Department of Anatomy and Neuroscience, University of Melbourne, Parkville, Australia

Multiple sclerosis (MS) is typically characterised by hyperintense T2 white matter lesions. However, the quantity and location of these may not correlate to a patient’s functional state or impending disease progression. Quantitative susceptibility mapping (QSM) is an emerging biomarker associated with tissue iron concentration and regions of demyelination in white matter. This pilot study examined both clinical and MRI parameter relationships to the QSM value over a number of brain regions in patients with mild (EDSS =or<2) relapsing and remitting MS.

2543

Pushing the limits of synthetic MRI in the evaluation of patients with Multiple Sclerosis: how much can the acquisition time be reduced?

Fernanda Cristina Rueda[1,2], Thomas Martin Doring[3], Eduardo Figueiredo[4], Soniza Alvez Leon[5], Roberto Cortes Domingues[1], Emerson Leandro Gasparetto[6], and Romeu Domingues[1]

[1]DASA, Rio de Janeiro, Brazil, [2]Universidade Federal Fluminense, Rio de Janeiro, Brazil, [3]GE Healthcare Brazil, Rio de Janeiro, Brazil, [4]GE Healthcare Brazil, [5]UFRJ, Rio de Janeiro, Brazil, [6]DASA, Sao Paulo, Brazil

In synthetic MRI, the recently developed multi delay multi–echo fast spin echo sequence (MDME) with posterior mathematical fitting provide multiple image contrasts in a single sequence acquisition and lead to potential acquisition time reductions. In this study, both, a synthetic MRI and conventional post contrast acquisition protocol for the evaluation of patients with Multiple Sclerosis were compared. Significant acquisition time reduction were achieved with synthetic MRI without neglecting lesion count capabilities

---

2544

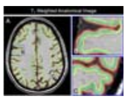

Cortical Surface Magnetization Transfer Ratio Decreases in Multiple Sclerosis are Age and Region Dependent

David A. Rudko[1], Josefina Maranzano[1], Douglas L. Arnold[1], and Sridar Narayanan[1]

[1]McConnell Brain Imaging Centre, Montreal Neurological Institute and Hospital, McGill University, Montreal, QC, Canada

Cortical pathology may be a substrate of worsening clinical symptoms in MS patients. However, the rate at which cortical pathology develops and the brain locations affected are not well known. The goal of this study was to evaluate longitudinal, age-related reductions in cortical surface magnetization transfer ratio (csMTR) of MS patients. Such reductions may be sensitive to sub-pial demyelination occurring over time.

2545

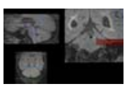

The cerebello-thalamic tract as a neural correlate for tremor in MS

Frederique Maria Christina Boonstra[1], Grace Florescu[2], Scott Kolbe[1], Chris Steward[3], Andrew Evans[2], Helmut Butzkueven[2], Peter Mitchell[3], and Anneke Van Der Walt[2]

[1]Melbourne Brain Centre, University of Melbourne, Melbourne, Australia, [2]The Royal Melbourne Hospital, Melbourne, Australia, [3]Radiology, Royal Melbourne Hospital, Melbourne, Australia

This study aims to determine the correlation between clinical tremor severity in Multiple Sclerosis (MS) and the cerebello-thalamic pathway. We found a decrease in volume of the ipsilateral Superior Cerebellar Peduncle and contralateral Thalamus. These regions of volume loss correlate with predicted neuro-anatomy indicating that the cerebello-thalamic pathway is a neural correlate of tremor severity in MS. This finding aids to a better understanding of pathogenesis and development of treatments for tremor in MS.

2546

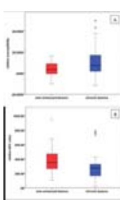

New Enhancing and Chronic Multiple Sclerosis Lesions measured on Quantitative Susceptibility Mapping and Diffusion-Weighted Imaging

Yihao Yao[1] and Yi Wang[2,3]

[1]Department of Radiology, Tongji Hospital, Tongji Medical College, Huazhong University of Science & Technology, Wuhan, People's Republic of China, [2]Department of Radiology, Weill Cornell Medical College, New York, NY, United States, [3]Biomedical Engineering, Cornell University, Ithaca, NY, United States

QSM and DWI are sensitive to changes in MS lesions at various ages. We found chronic MS lesions had higher relative susceptibilities and lower relative ADC values as compared to new enhanced lesions. Combining QSM and ADC measurements could differentiate each two subtypes in four subtypes of lesions (nodular/shell enhanced lesions, rim+/- lesions). The pattern of QSM and ADC findings suggests that shell enhanced lesions have more demyelination than nodular enhanced lesions and rim- lesions. Combining QSM and ADC measurements might be a better way to differentiate MS lesions at various ages and provide more information of micro-changes of lesion.

2547

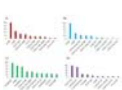

STRUCTURAL AND FUNCTIONAL MRI PREDICTORS OF DISABILITY AND COGNITIVE IMPAIRMENT ACCRUAL IN PATIENTS WITH MULTIPLE SCLEROSIS

Paola Valsasina[1], Maria Assunta Rocca[1], Fiammetta Pirro[1], Elisabetta Pagani[1], Alessandro Meani[1], Massimiliano Copetti[2], Filippo Martinelli Boneschi[3], Vittorio Martinelli[3], Giancarlo Comi[3], Andrea Falini[4], and Massimo Filippi[1]

[1]Neuroimaging Research Unit, San Raffaele Scientific Institute, Vita-Salute San Raffaele University, Milan, Italy, [2]IRCCS Casa Sollievo della Sofferenza, San Giovanni Rotondo, Italy, [3]Department of Neurology, San Raffaele Scientific Institute, Vita-Salute San Raffaele University, Milan, Italy, [4]Department of Neuroradiology, San Raffaele Scientific Institute, Vita-Salute San Raffaele University, Milan, Italy

Aim of this study was to identify the MRI predictors of medium-term disability and cognitive impairment accrual in patients with the main clinical phenotypes of multiple sclerosis (MS). Results indicated that clinical disability and cognitive impairment at follow-up were predicted by measures of structural and microstructural damage, as well as by resting state functional connectivity measures. Preserved white matter integrity predicted clinical improvement. Grey matter involvement played a critical role in MS-related clinical worsening and evolution to a more severe disease phenotype.

2548

Noise reduction with TGV, Gaussian and Wiener filtering methods in FLAIR² images

René Schranzer[1], Alexander Rauscher[2], Evelin Haimburger[1], Kristian Bredies[3], Gernot Reishofer[4], and Günther Grabner[1,5]

[1]Department of Radiologic Technology, Carinthia University of Applied Sciences, Klagenfurt, Austria, [2]UBC MRI Research Centre, University of British Columbia, Vancouver, Canada, [3]Institute for Mathematics and Scientific Computing, University of Graz, Graz, Austria, [4]Department of Radiology, Medical University of Graz, Graz, Austria, [5]Institute for Applied Research on Ageing, Carinthia University of Applied Sciences, Klagenfurt, Austria

The reduction of noise is of high value for FLAIR² images because the multiplication of FLAIR and T2 images will always result in an image with a reduced Signal-to-noise-ratio. Here different filter methods, like Gaussian, Wiener and Total Generalized Variation were used to demonstrate noise reduction. The drawback of noise reduction is a blurring effect of anatomical structures. In this study we demonstrate that TGV filtering has certain advantages compared to Wiener and Gaussian techniques in research and clinical applications.

2549

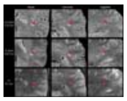

Rapid, high-resolution imaging of the central veins in multiple sclerosis at 1.5T, 3T, and 7T

Pascal Sati[1], Sunil Patil[2], Souheil I Inati[3], Govind Nair[1], Gunnar Krueger[4], and Daniel S Reich[1]

[1]Translational Neuroradiology Section, NINDS, National Institutes of Health, Bethesda, MD, United States, [2]Siemens Medical Solutions, HC NAM USA DI MR COLLAB, Bethesda, MD, United States, [3]InatiAnalytics, Potomac, MD, United States, [4]Siemens Medical Solutions, HC NAM USA DI MR COLLAB NE, Boston, MA, United States

The central vein sign (CVS) detected by magnetic resonance imaging (MRI) may aid with the diagnosis of multiple sclerosis (MS). The ability to detect central veins in the brain at any magnetic field strengths would open the pathway for future large-scale research studies, and potentially routine clinical use, of the CVS for MS diagnosis. In this study, a fast high-isotropic-resolution, whole-brain T_2^*-weighted segmented echo-planar-imaging acquisition was implemented at 1.5T, 3T and 7T. Central veins inside multiple sclerosis lesions were detected at all three different field strengths.

2550

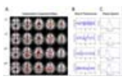

Functional MRI detects a novel cerebral venous haemodynamic signal that is disrupted in early multiple sclerosis

Scott Kolbe[1], Sanuji Gajamange[1], Jon Cleary[1], and Trevor Kilpatrick[1]

[1]Department of Anatomy and Neuroscience, University of Melbourne, Parkville, Australia

Here we report a novel haemodynamic signal using BOLD-weighted fMRI that is restricted to the internal cerebral veins and identifiable in all subjects assessed to date. This signal is oscillatory with peak power at 0.054 Hz. In early MS patients, venous power was diminished compared to controls. Venous power was inversely correlated with T2 lesion volume but not brain atrophy. These results indicate that neuroinflammation is associated with altered venous haemodynamics that could be attributable to venous structural damage previously reported in MS. This novel venous signal should also be investigated more broadly in cerebrovascular disease.

2551

Baseline DTI discriminates and predicts MS from ADEM

Parinaz Massoumzadeh[1], Wint (Arthur) Aung[2], Amber Salter[1], Safa Najmi[1], Jenny Wang[1], Tiffany Lin[1], Allysa Lui[1], Emily Egbert[1], Tammie Benzinger[1], and Soe Mar[1]

[1]Washington University in St. Louis, School of Medicine, St. Louis, MO, United States, [2]St. Louis University, School of Medicine, St. Louis, MO, United States

MS is a progressive disorder in which demyelination, axonal degeneration, and inflammation contribute to disease pathogenesis. ADEM is classically an acute, monophasic demyelinating disease in which axonal damage is present but minimal. About 20 percent of ADEM cases can have relapses and are diagnosed with MS later, posing a diagnostic dilemma at initial presentation. In this study, we investigate the role of directional diffusivity DTI as a MR biomarker to differentiate and predict Acute Disseminated Encephalomyelitis (ADEM) from Multiple Sclerosis (MS) in pediatric patients.

2552

	DWI	T1W
Resolution (mm³)	2x2x2	1x1x1
TR (ms)	24000	6.9
TE (ms)	68	3.1
TI	-	824
b-values (s mm⁻²)	0, 1200	-
no. DW directions	7, 61	-

The Role of Node Strength in Investigating Pathology

Elizabeth CA Powell[1,2], Thalis Charalambous[1], Ferran Prados[1,3], Carmen Tur[1], Daniel Altmann[1,4], Declan Chard[1,5], Sebastien Ourselin[3], Ahmed Toosy[1,5], Jonathan D Clayden[6], and Claudia AM Wheeler-Kingshott[1,7,8]

[1]Institute of Neurology, University College London, London, United Kingdom, [2]Department of Medical Physics and Biomedical Engineering, University College London, London, United Kingdom, [3]Translational Imaging Group, Centre for Medical Image Computing, Department of Medical Physics and Biomedical Imaging, University College London, London, United Kingdom, [4]Medical Statistics Department, London School of Hygiene and Tropical Medicine, London, United Kingdom, [5]National Hospital of Neurology and Neurosurgery, London, United Kingdom, [6]Institute of Child Health, University College London, London, [7]Department of Brain and Behavioural Sciences, University of Pavia, Pavia, Italy, [8]Brain MRI 3T Mondino Research Center, C. Mondino National Neurological Institute, Pavia, Italy

Graph theoretical network properties, while successful in exploring topological features of entire brain networks, have limited sensitivity to localized disease effects. This work explores the role of node strength as an objective way to characterize disease. Differences in the default mode network (DMN) between a cohort of relapsing-remitting multiple sclerosis (RRMS) patients and healthy controls (HC) have been explored using standard graph metrics (e.g. efficiency) and node strength. No differences in graph metrics were observed between the groups; however several key regions of the DMN had a significantly reduced strength in RRMS than HC (5% significance level).

2553

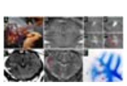

Real Time MRI-guided convection-enhanced delivery in porcine brain to model multiple sclerosis by focal demyelination

Lukasz Kalkowski[1], Izabela Malysz-Cymborska[1], Dominika Golubczyk[1], Miroslaw Janowski[2,3,4], Piotr Holak[5], Kamila Milewska[1], Zbigniew Adamiak[5], Joanna Wojtkiewicz[6], Wojciech Maksymowicz[1], Dorota Kedziorek[2,3], and Piotr Walczak[1,2,3]

[1]Department of Neurology and Neurosurgery, University of Warmia and Mazury in Olsztyn, Olsztyn, Poland, [2]Cellular Imaging Section and Vascular Biology Program, Institute for Cell Engineering, John Hopkins University, Baltimore, MD, United States, [3]Russell H. Morgan Department of Radiology and Radiological Science, John Hopkins University, Baltimore, MD, United States, [4]NeuroRepair Department, Mossakowski Medical Research Center, Polish Academy of Sciences, Warsaw, Poland, [5]Department of Surgery and Roentgenology with the Clinic, University of Warmia and Mazury in Olsztyn, Olsztyn, Poland, [6]Department of Pathophysiology, University of Warmia and Mazury in Olsztyn, Olsztyn, Poland

Modeling of multiple sclerosis is typically performed in rodents; however, due to several limitations large animal models are needed to improve clinical relevance. In this study we utilized MRI-guided convection enhanced delivery of gliotoxins (ethidium bromide and lysolecithin) to induce focal demyelination within corona radiata in pigs.

2554

Quantitative Assessment of Limbic System Damage in Multiple Sclerosis

Jie Wen[1], Dmitriy Yablonskiy[1], and Anne Cross[2]

[1]Radiology, Washington University in St. Louis, St. Louis, MO, United States, [2]Neurology, Washington University in St. Louis, St. Louis, MO, United States

The limbic system plays an important role in the emotion- and memory-related brain functions. In this study, we measured R2* and the volumes of the key elements of the limbic system and used them to detect abnormalities in the limbic system in multiple sclerosis (MS). The results showed significant differences between Secondary Progressive MS (SPMS) and healthy group. R2* of amygdala, thalamus, insula, lateral orbitofrontal and isthmus cingulate significantly correlate with clinical cognitive tests in female SPMS. Our results also showed that R2*-defined tissue alterations in the hippocampus and entorhinal cortex could identify depression behavior in MS patients.

2555

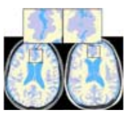

Conversion of Brain Tissue volumes by MR Images form 1.5 to 3.0 Tesla scanners for Multiple Sclerosis patients

Mehran Azimbagirad[1], Antonio Carlos dos Santos[1], and Luiz Otavio Murta Junior[1]

[1]University of Sao Paulo, Ribeirao Preto, Brazil

Brain tissue volume estimation based on MRI is crucial to several diseases such as multiple sclerosis (MS). The Images from different scanners with dissimilar magnetic fields have disparities in resolution, Signal to Noise Ratio, contrast, among others. In order to convert volume estimations from different scanners, we suggest and evaluated two methods. The dataset to validate the methods was selected from 14 years follow up study of 72 MS patients with 1.5 and 3.0 Tesla acquisitions. The quantitative study of tissue volume progress is possible using these two methods.

2556

T1 Black Hole in Multiple Sclerosis: a reassessment of the specificity at 7T

Francesca Bagnato[1], Assunta Dal-Bianco[2], Richard Dortch[1], Idan Kantor[1], Bailey Lyttle[1], Siddharama Pawate[1], Lydia Mckeithan[1], Bailey Box[1], Simon Hemetner[2], Hans Lassmann[2], Brain Welch[1], and Seth Smith[1]

[1]Vanderbilt University, Nashville, TN, United States, [2]Medical University Vienna

7T imaging and the commensurate T1-lenghtening have the potential to increase lesion sensitivity at the expense of their specificity in patients with multiple sclerosis. In our work we demonstrate that (1) T1-hypontense lesions detected on T1-w MPRAGE reflect both remyelinated and chronic demyelinated lesions as measured by histology and that (2) associations between black hole lesion load and measures of physical and cognitive disability are weak. At 7T, the increased sensitivity to lesion penalizes the T1-w MPRAGE specificity to areas with higher water content and tissue destruction seen at lower field strength.

2557

magna cum laude

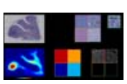

Histological Validation of Diffusion Basis Spectrum Imaging Using Autopsied Multiple Sclerosis Brain Specimens

Ajit George[1], Peng Sun[2], Anne H Cross[3], Xiaojie Wang[4], Carlos J Pérez-Torres[5], and Sheng-Kwei Song[6]

[1]Department of Radiology, Washington University, St. Louis, Saint Louis, MO, United States, [2]Department of Radiology, Washington University, St. Louis, [3]Department of Neurology, Washington University, St. Louis, MO, United States, [4]Advanced Imaging Research Center, Oregon Health & Science University, OR, United States, [5]Radiological Health Sciences, School of Health Sciences, Purdue University, West Lafayette, IN, United States, [6]Department of Radiology, Washington University, St. Louis, MO, United States

In this study, we demonstrate diffusion basis spectrum imaging (DBSI) is able to detect, differentiate and quantify different coexisting pathologies, particularly axonal loss and demyelination within autopsied multiple sclerosis human brain specimens. We correlated the DBSI derived maps with quantitative histology maps generated by means of color based segmentation. DBSI-derived fiber fraction was seen to correlate with Bielschowsky's silver stain for axonal integrity, and the DBSI-derived radial diffusivity negatively correlated with Luxol Fast Blue-Periodic Acid-Schiff (LFB-PAS) stain for myelin integrity.

2558

mcDESPOT-derived tissue parameters in the brainstem and corpus callosum of MS and NMOSD patients with cervical cord lesions

Lisa Eunyoung Lee[1], Anna J.E Combes[2], Jillian Chan[1], Robert Carruthers[1], Jacqueline Palace[3], Lucy Matthews[3], Anthony Traboulsee[1], and Shannon Kolind[1,4]

[1]Department of Medicine, University of British Columbia, Vancouver, BC, Canada, [2]Neuroimaging, Institute of Psychiatry, Psychology & Neuroscience, King's College London, London, United Kingdom, [3]Nuffield Department of Clinical Neurosciences, University of Oxford, Oxford, United Kingdom, [4]Department of Radiology, University of British Columbia, Vancouver, BC, Canada

Neuromyelitis optica spectrum disorder (NMOSD) and multiple sclerosis (MS) are demyelinating central nervous system disorders that may present with some overlapping clinical symptoms but differ pathophysiologically. We used tissue-specific quantitative measures, produced by mcDESPOT, to characterize tissue pathology in MS and NMOSD groups compared to healthy controls. We observed decreased myelin water fraction, increased T2 of intra/extracellular water, increased cerebrospinal volume fraction, and increased myelin water residence time in the brainstem and corpus callosum of MS and NMOSD subjects, compared to controls. These sensitive advanced MRI measures could provide an improved understanding of MS and NMOSD pathogenesis.

2559

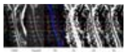

High-resolution spinal DTI imaging using RESOLVE sequence in multiple sclerosis and clinical isolated syndrome

Ningnannan Zhang[1], Zhang Zhang[1], Tianyi Qian[2], Wen Qin[1], Qiuhui Wang[1], and Chunshui Yu[1]

[1]Department of Radiology, Tianjin Key Laboratory of Functional Imaging, Tianjin Medical University General Hospital, Tianjin, People's Republic of China, [2]MR Collaborations NE Asia, Siemens Healthcare, Beijing, People's Republic of China

This study reports the preliminary application of high-resolution diffusion tensor imaging (DTI) using readout segmentation of long variable echo trains (RESOLVE) sequence for spinal cord imaging in patients with demyelinating conditions. Patients with clinical isolated syndrome (CIS) and multiple sclerosis (MS) were recruited in order to investigate image evidences in early stages and the progression of the disease. The results of DTI analyses demonstrate that MS is characterized by diffuse axonal compensation in the spinal cord.

2560

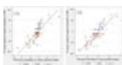

Measures of tissue coherency in T2-weighted MRI for myelin and axonal pathology: A MRI-histology correlative study in multiple sclerosis

Shrushrita Sharma[1] and Yunyan Zhang[2]

[1]Biomedical Engineering Program, University of Calgary, Calgary, AB, Canada, [2]Departments of Neurology and Clinical Neurosciences, University of Calgary, AB, Canada

Measurement of tissue coherency has been largely relying on advanced MRI. Here we presented a coherency-assessing method based on standard T2-weighted MRI. Postmortem brain samples from multiple sclerosis (MS) patients were used to validate our method. It was based on Fourier transform power spectrum, from which dominant tissue-aligning directions and angular entropy were calculated. Tissue coherency in histology was quantified using structure tensor analysis. We found that both MRI and histology coherency differentiated MS lesions from NAWM, and that MRI coherency correlated significantly with histological results. These findings suggest the potential of T2-weighted MRI in characterizing advanced tissue pathology

2561

Ultra-High B Diffusion Imaging of Cervical Spinal Cord in Multiple Sclerosis

You Jung Lee[1], Bijaya Thapa[1,2], Nabraj Sapkota[1,2], Eun-Ju Kim[1], Lubdha Shah[3], Eun-Kee Jeong[1,3], and John Rose[4]

[1]Utah Center for Advanced Imaging Research, University of Utah, salt lake city, UT, United States, [2]Department of Physics and Astronomy, University of Utah, salt lake city, UT, United States, [3]Department of Radiology and Imaging Sciences, University of Utah, salt lake city, UT, United States, [4]Department of Neurology, University of Utah

Diffusion tensor imaging (DTI) is considered as a biomarker to quantitatively evaluate the pathology in the cervical spinal cord (CSC) in MS patients. However, DTI parameters, including axial and radial diffusivities, and fractional anisotropy (FA), provides signal behavior of the water diffusion at a specific diffusion weighting. Using a ultra-high B DWI on a CSC specimen and Monte-Carlo Simulation indicate that we can learn much more insights about the CSC pathology by analyzing the signal-b curve at b > 4000 s/mm2. In this presentation, we will show unique signal behaviors of UHB-rDWI in acute and chronic legions in MS CSC.

2562

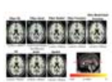

Tract Based Whole Brain White Matter Analysis using Diffusion Basis Spectrum Imaging in Multiple Sclerosis

Peng Sun[1], Ajit George[1], Robert T. Naismith[2], Sheng-Kwei Song[1], and Anne H. Cross[2]

[1]Radiology, Washington University in Saint Louis, Saint Louis, MO, United States, [2]Neurology, Washington University in Saint Louis, Saint Louis, MO, United States

Axon injury and loss, demyelination, and inflammation are the primary pathologies in multiple sclerosis (MS). However, the roles that these individual pathological processes play in MS progression are still ill defined. To investigate whole brain white matter (WM) changes, diffusion tensor imaging (DTI) and diffusion basis spectrum imaging (DBSI) were analyzed on Tract Based Spatial Statistics (TBSS) skeleton template. Both whole brain voxel-based group analysis and regional correlation analysis at the corpus callosum supported that DBSI metrics were able to quantitatively assess the white matter alterations. DBSI could be useful for quantitatively monitoring MS patient treatment and assessing neuroprotective therapies.

Traditional Poster

Neuro: Applications

Exhibition Hall 2563-2584 Wednesday 13:45 - 15:45

2563

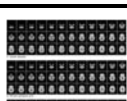

Chronic pain-related sexual dimorphism in gray matter density: A whole-brain voxel-based morphometric study on Osteoarthritis patients

Marianne M Drabek[1,2], Diane Reckziegel[1,2], Cottam J William[1,2], Xingfeng Li[2], Nadia Frowd[1], Hamza Alshuft[1,2,3], Brigitte Scammell[1], Thomas Kurien[1], and Dorothee P Auer[1,2]

[1]University of Nottingham, Arthritis Research UK Pain Centre, Nottingham NG7 2RD, England, Nottingham, United Kingdom, [2]University of Nottingham, Sir Peter Mansfield Imaging Centre, Nottingham NG7 2RD, England, Nottingham, United Kingdom, [3]Neurosurgery, Nottingham University Hospitals, Nottingham, United Kingdom

Chronic pain is a major problem for society and further studies are needed to understand pain-related developments. In particular, controversy exists over the pattern of pain-related structural changes in the brain. The current morphometric study addresses inconsistencies through a large sample of chronic osteoarthritis knee pain patients and healthy volunteers scanned at a single-site, allowing to differentiate sex effects which are usually ignored. We found significantly decreased gray matter density in pain patients in several brain regions, amongst which the left planum temporale which was driven by the female subjects and has not been mentioned in relation to pain before.

2564

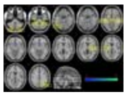

Brain Structural Alterations in Obese Adults with Impulsive Personality Traits: A Voxel-Based Morphometry Study

Baohong Wen[1], Dandan Zheng[2], Li Zheng[3], and Jingliang Cheng[1]

[1]Department of MRI, The First Affiliated Hospital of Zhengzhou University, Zhengzhou, People's Republic of China, [2]MR Research China, GE Healthcare, Beijing, People's Republic of China, [3]Peking University, Beijing, People's Republic of China

This study used voxel-based morphometry method to examine gray matter volume alterations related to impulsive personality traits in obese individuals relative to controls. 62 adolescents completed the UPPS-P Impulsive Behavior Scale were analyzed. Possible GM volume alterations were firstly analyzed at the whole brain range. The relationship of regional GM volumes with UPPS-P scores were examined in selective regions of interest. This study demonstrated that sensation seeking behavior in obese people negatively correlate with GM volumes of amygdala, OFC, hippocampus, and insula indicate high sensitivity to food cues in adult obesity that link to certain alternations of the brain structure.

2565

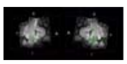

Evaluation of Whole Brain and ZOOMit T1-weighted Turbo-Spin Echo (TSE) for Visualization of Human Lenticulostriate Arteries at 3.0 T: A Preliminary Study

Samantha J. Ma[1], Jin Kyu Gahm[1], Lirong Yan[1], Yelong Shen[1], Xingfeng Shao[1], Yonggang Shi[1], and Danny JJ Wang[1]

[1]Neurology, University of Southern California, Los Angeles, CA, United States

Cerebral small vessel disease frequently affects the lenticulostriate arteries, resulting in silent strokes which contribute to progressive cognitive impairment in elderly persons. Recent studies have demonstrated the ability of MRI to non-invasively image these small arteries at 7T; however, ultrahigh magnetic field is not commonly available in clinical practice. This preliminary study evaluates the feasibility of visualizing and characterizing the lenticulostriate arteries using whole-brain and ZOOMit 3D T1-weighted turbo spin-echo at 3T.

2566

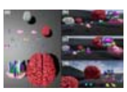

See It, Slice It, Learn It: Combined Ultra High Field MRI and High-resolution CT for an Open Source Virtual Anatomy Resource

Jon Orlando Cleary[1], Peter E Yoo[1], Brad A Moffat[1], Robert Williams[1], Susie Kerby[2], Ryan Jefferies[3], Simon Murray[2], Andrew Tan[1], Ben Loveridge[4], Amanda Ng[1], Sonal Josan[5], Leah Leighton[2], Varsha Pilbrow[2], Junhua Xiao[2], Jenny Hayes[2], and Roger J Ordidge[1]

[1]Melbourne Brain Centre Imaging Unit, Department of Anatomy and Neuroscience, University of Melbourne, Parkville, Australia, [2]Department of Anatomy and Neuroscience, University of Melbourne, Parkville, Australia, [3]Harry Brookes Allen Museum, Department of Anatomy and Neuroscience, University of Melbourne, Parkville, Australia, [4]Learning Environments, University of Melbourne, Parkville, Australia, [5]Siemens Healthcare, Melbourne, Australia

Grasping human head and neck anatomy can be challenging for students, scientists and health professionals in medical disciplines. Ultra-high field, 7T MRI can create high-resolution images with multiple contrasts, revealing structural detail not easily apparent in dissection specimens. While widely exploited in clinical and scientific studies, its use has been limited so far in creating tools for medical education. We present a multi-modal combination of ex-vivo MRI and CT to create a high-quality head and neck anatomy resource to enhance cadaveric cross-sectional anatomy teaching.

2567

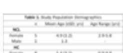

MRI Characterization of Cerebellar Atrophy in a Non-Human Primate Model of Neuronal Ceroid Lipofuscinosis

Ian Tagge[1], Lois Colgin[2], Rebecca Ducore[2], Betsy Ferguson[3], Steven Kohama[4], Jodi McBride[4], Martha Neuringer[4], Sam Peterson[4], Scott Wong[5], Robert Zweig[6], and Anne Lewis[2]

[1]Advanced Imaging Research Center, Oregon Health & Science University, Portland, OR, United States, [2]Pathology, Oregon National Primate Research Center, [3]Primate Genetics, Oregon National Primate Research Center, [4]Oregon National Primate Research Center, [5]VGTI, Oregon National Primate Research Center, [6]Clinical Medicine, Oregon National Primate Research Center

Neuronal ceroid lipofuscinosis (NCL; also known as Batten Disease) is a fatal neurodegenerative disorder that typically presents in childhood. Currently, no treatments are known that can halt or reverse the effects of NCL. A naturally occurring form of NCL analogous to late infantile-onset NCL in humans has been identified in a population of Japanese macaques (JMs). MRI examinations revealed marked cerebellar degeneration in NCL animals >4y/o (~14y/o equivalent human age) compared with controls, which is strikingly similar to human disease. This novel JM model presents a new opportunity for characterizing disease progression, identifying biomarkers, and pre-clinical therapeutic testing.

2568

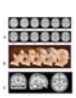

A Pseudo-Longitudinal Study of the Lifespan Neuroanatomical Changes based on a Large-scale Imaging Data

LIN SHI[1], PEIPENG LIANG[2,3,4], YISHAN LUO[3,4], KAI LIU[3], Vincent CT MOK[1], Winnie CW CHU[3], DEFENG WANG[3,4], and KUNCHENG LI[2]

[1]Department of Medicine and Therapeutics, The Chinese University of Hong Kong, Hong Kong, Hong Kong, [2]Department of Radiology, Xuanwu Hospital, Capital Medical University, Beijing, People's Republic of China, [3]Research Center for Medical Image Computing, Department of Imaging and Interventional Radiology, The Chinese University of Hong Kong, Hong Kong, Hong Kong, [4]Shenzhen Research Institute, The Chinese University of Hong Kong, Shenzhen, People's Republic of China

Understanding how brain changes over the lifetime provides the basis for new insights into neurophysiology and neuropathology. In this study, we carried out a pseudo-longitudinal study based on large-scale cross-sectional high-resolution brain MR data atlas Chinese2020 to model the brain morphological changes in Han Chinese adulthood. Our results found some novel age-related neuroanatomical changes in a standardized brain space via temporal-spatial statistical brain templates.

2569

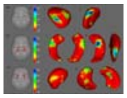

Assessment of brain volume and shape abnormalities in chemotherapy-treated breast cancer survivors using voxel-based morphometry and vertex-wise shape analysis

TzyShyuan Ng[1], Vincent Chin-Hung Chen[2,3], Dah-Cherng Yeh[4], Ren-Horng Wang[1], and Jun-Cheng Weng[1,5]

[1]Department of Medical Imaging and Radiological Sciences, Chung Shan Medical University, Taichung, Taiwan, [2]School of Medicine, Chang Gung University, Taoyuan, Taiwan, [3]Department of Psychiatry, Chang Gung Memorial Hospital, Chiayi, Taiwan, [4]Breast Center, Taichung Tzu Chi Hospital, Taichung, Taiwan, [5]Department of Medical Imaging, Chung Shan Medical University Hospital, Taichung, Taiwan

Cancer-related trauma after chemotherapy has been widely reported by breast cancer. The previous study consistently showed lower gray and white matter volume and density in patients treated with chemotherapy. The aim of this study was to find out the early effect in both brain volume and shape in the chemotherapy-treated breast cancer patients compared to healthy controls using voxel-based morphometry (VBM) and vertex-wise shape analyses, respectively. Our results showed significant changes in the brain structural volume and shape, particularly in the putamen and hippocampus.

2570

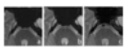

High−resolution Magnetic Resonance Imaging of Basilar Artery with Iterative Decomposition of Water and Fat with Echo Asymmetric and Least-squares Estimation(IDEAL): A Feasibility Study

Yu Zhang[1], Yun-fei ZHA[1], Liang LI[1], Lei HU[1], Hui Lin[2], and Bing Wu[2]

[1]Radiology, Renmin Hospital of Wuhan University, Wuhan, People's Republic of China, [2]GE healthcare China, People's Republic of China

To explore the potential for high-resolution MR imaging using IDEAL FSE-T2WI as compared to FSE-T2WI in the assessment of the basilar artery wall. High-resolution FSE(A/P), FSE(R/L) and IDEAL FSE(A/P) T2W images were acquired from basilar artery of 30 patients using a 3.0T MRI scanner.The threeimage sets were evaluated for overall image quality and graded using a 4-point Likert scale.IDEAL FSE-T2WI (A/P) scores is higher than FSE-T2WI (A/P) and FSE-T2WI (R/L).FSE-T2WI (A/P), FSE-T2WI (R/L) andIDEAL FSE-T2WI (A/P) difference with statistical significance,respectively.IDEAL FSE-T2WI images showed improved image quality compared to FSE-T2WI technique at 3T.

2571

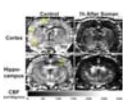

Mapping the Neurological Effect of Soman, a Chemical Warfare Nerve Agent, using 9.4T MRI

Kevin Lee[1], Sara Bohnert[2], Cory Vair[2], Ying Wu[1], John Mikler[2], and Jeff Dunn[1]

[1]Radiology, University of Calgary, Calgary, AB, Canada, [2]National Defence, Defence Research And Development Canada, Suffield, AB, Canada

Soman is a chemical warfare nerve agent that is categorized as a weapon of mass destruction. Nerve agents are potent irreversible inhibitors of acetylcholinesterase and exposure can be extremely lethal. At a sub-lethal dose, our understanding of the neurological effect is limited. To understand the soman associated physiological changes, MRI was used to quantify the cerebral blood flow after a convulsive dose of soman.

2572

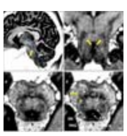

Direct Localization Human Pedunculopontine Nucleus Using 7T, Coordinate and Fiber Tracking Validation

Fei Cong[1,2], Jiawei Wang[3], Zhangyan Yang[1,2], Yan Zhuo[1], Bo Wang[1], Yuqing Zhang[3], and Lin Chen[1]

[1]State Key Laboratory of Brain and Cognitive Science, Beijing MRI Center for Brain Research, Institute of Biophysics, Chinese Academy of Sciences, Beijing, People's Republic of China, [2]Graduate University, Chinese Academy of Sciences, Beijing, People's Republic of China, [3]Department of Functional Neurosurgery, Xuanwu Hospital, Capital Medical University, Beijing, People's Republic of China

The pedunculopontine nucleus (PPN), as a potential Deep brain stimulation (DBS) target for the patients to improve gait and posture. Until now, only a few results of the location of PPN has been published. In this study, 7T ultra-high field MR system and high resolution MP2RAGE sequence were used to locate the PPN by a direct view, manually measurement and fiber tracking method were used to verify the results. The results showed a clear and accurate location of PPN.

2573

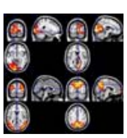

Spatial Patterns of Intersubject CBF Variability in the CARDIA study

Yunwen Shao[1], Zhengjun Li[2], Marta Vidorreta[2], Sudipto Dolui[3], Nick Bryan[3], and John Detre[4]

[1]Department of Biomedical Engineering, Tsinghua University, Beijing, People's Republic of China, [2]Department of Neurology, School of Medicine, University of Pennsylvania, [3]Department of Radiology, School of Medicine, University of Pennsylvania, [4]Departments of Neurology and Radiology, School of Medicine, University of Pennsylvania

Variability in regional relative cerebral blood flow (CBF) from resting-state arterial spin labeling (ASL) MRI data obtained in a large (N=436) cohort were examined using spatial Independent Components Analysis (ICA). Some spatial patterns of intersubject CBF variability resembled known resting-state functional networks, and were largely reproducible across split samples. Network relative CBF fluctuation across subjects was about 14%.

2574

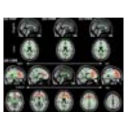

Performance of Complex Tasks of Working Memory Related to Brain Microstructure in Healthy Adults: a Diffusion Kurtosis Imaging Study

Sohae Chung[1,2], Els Fieremans[1,2], Joseph F. Rath[3], and Yvonne W. Lui[1,2]

[1]Center for Advanced Imaging Innovation and Research (CAI2R), Department of Radiology, New York University School of Medicine, New York, NY, United States, [2]Bernard and Irene Schwartz Center for Biomedical Imaging, Department of Radiology, New York University School of Medicine, New York, NY, United States, [3]Department of Rehabilitation Medicine, New York University School of Medicine, New York, NY, United States

The relationship between performance on working memory tasks of increasing difficulty and white matter (WM) microstructure assessed by diffusion kurtosis imaging (DKI) is investigated in a healthy adult population. We demonstrate that higher mean kurtosis (MK) and radial kurtosis (RK) correlate with performance on working memory tasks, particularly in frontal WM, an area responsible for executive function, suggesting better working memory performance with higher tissue complexity in frontal WM. Improving our understanding of these associations will help determine the biological underpinning of pathologies affecting cognition, as well as potentially informing and monitoring interventions such as cognitive rehabilitation.

2575

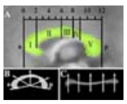

Altered Diffusion Tensor Anisotropy Rather Than Morphology in the Corpus Callosum after Lower Limb Amputation

Xuntao Yin[1], Zhichao Li[1], Guangyao Jiang[1], Xiaoyue Zhou[2], and Jian Wang[1]

[1]Radiology, Southwest Hospital, Third Military Medical University, Chongqing, People's Republic of China, [2]MR Collaboration, Siemens Healthcare Ltd, Shanghai, People's Republic of China

We examined morphological and diffusion changes of the corpus callosum (CC) in the same group of amputees for the first time. The thickness, area and diffusion tensor imaging (DTI) parameters were used to investigate the CC. Diffusion alteration in the region II of the CC was found in amputees compared with health controls. These changes suggest that fibers connecting bilateral premotor and supplementary motor areas are damaged. The alteration is only reflected in DTI parameters rather than morphological characteristics, indicating that DTI is more sensitive to detect the brain reorgnization following amputation.

2576

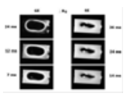

MR Imaging of tissue near aneurysm clips using short- and zero echo time MR sequences

Marco L.H. Gruwel[1], Peter Latta[2], Anna Wojna-Pelczar[2], Stefan Wolfsberger[3], and Boguslaw Tomanek[4]

[1]Biological Resources Imaging Laboratory, UNSW, Australia, Mark Wainwright Analytical Centre, Sydney, NSW, Australia, [2]Central European Institute of Technology, Masaryk University, Brno, Czech Republic, [3]Department of Neurosurgery, University of Vienna, Vienna, Austria, [4]Department of Oncology, Division of Medical Physics, University of Alberta, Edmonton, AB, Canada

Aneurysm clips are used to stop or prevent an aneurysm from bleeding. MRI is an ideal technique to diagnose aneurysms. Unfortunately, treatment assessment by MRI after surgical placement of an aneurysm clip is complicated due to the presence of the metal clip. The clip's high magnetic susceptibility causes severe, orientation dependent, variations in the local magnetic field. Often this results in pronounced MR image distortions including signal voids. The study presented here shows how ultra-short and zero echo time experiments could be used to minimize these artifacts.

2577

MRI compatible Set up for Optogenetic Stimulation of Living Brain Slices

Rita Gil[1], Daniel Nunes[1], and Noam Shemesh[1]

[1]Champalimaud Neuroscience Programme, Champalimaud Centre for the Unkown, Lisbon, Portugal

Organotypic slices are excellent controlled systems for investigating neural activity without many of the confounds introduced by in-vivo conditions. Here we describe a new setup that allows imaging of a living slice inside a MRI scanner while being stimulated with optogenetics which induces neuronal activity in pre-targeted neurons. This setup allows the survival of slices for at least three hours, without requiring new artificial CSF (aCSF) to be flushed. This property is highly advantageous for avoiding artifacts related with bubbles, motion or variation of shims during extended acquisitions.

2578

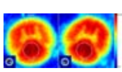

Myelin Density Measurement by ZTE in the D2O-Exchanged Spinal Cord is Unaffected by Tissue Fixation

Alan C Seifert[1,2,3], Marco Hefti[4], Mary Fowkes[4], and Junqian Xu[1,2,3,5]

[1]Translational and Molecular Imaging Institute, Icahn School of Medicine at Mount Sinai, New York, NY, United States, [2]Department of Radiology, Icahn School of Medicine at Mount Sinai, New York, NY, United States, [3]Graduate School of Biomedical Sciences, Icahn School of Medicine at Mount Sinai, New York, NY, United States, [4]Department of Pathology, Icahn School of Medicine at Mount Sinai, New York, NY, United States, [5]Department of Neuroscience, Icahn School of Medicine at Mount Sinai, New York, NY, United States

Zero echo time imaging (ZTE) of deuterium oxide (D_2O)-exchanged unfixed white matter is a proven method for measurement of myelin density. In this work, we perform D_2O-exchanged ZTE measurements on human spinal cord tissue before and after formalin fixation to assess whether fixation, which cross-links proteins, impacts the measured myelin density. A segment of human spinal cord was obtained at autopsy, subjected to D_2O-exchanged ZTE myelin density measurement, chemically fixed using formalin, and re-measured. Signal intensity was 31.36%, normalized to a reference, before fixation, and 31.44% after fixation. These similar measurements support this method's accuracy in fixed tissue.

2579

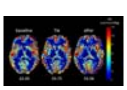

Investigating the effect of a tight necktie on arterial cerebral blood flow and venous flow velocity

Robin Lüddecke[1], Julia Forstenpointner[1], Janne Giertmühlen[1], Ralf Baron[1], Olav Jansen[2], and Thomas Lindner[2]

[1]Clinic for Neurology, University Hospital Schleswig-Holstein, Kiel, Germany, [2]Clinic for Radiology and Neuroradiology, University Hospital Schleswig-Holstein, Kiel, Germany

Wearing a necktie is mandatory in several professions. However, the constant restriction of the veins (and potentially arteries) might lead to adverse side-effects, which could already be visualized regarding intraocular pressure. In this study, the effects of a tight necktie are investigated using Arterial Spin Labeling to measure brain perfusion and venous phase-contrast angiography to show changes in venous flow velocities.

2580

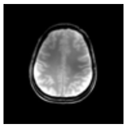

Reproducibility and Age dependence of GluCEST contrast in healthy adults

Ravi Prakash Reddy Nanga[1], David Roalf[2], Kevin D'Aquilla[1], Catherine DeBrosse[1], Puneet Bagga[1], Neill Wilson[1], Dushyant Kumar[1], Ari Borthakur[1], Mark Elliott[1], Damodar Reddy[1], Hari Hariharan[1], Neill Cynthia Epperson[2,3], and Ravinder Reddy[1]

[1]CMROI, Radiology, Perelman School of Medicine at The University of Pennsylvania, Philadelphia, PA, United States, [2]Psychiatry, Perelman School of Medicine at The University of Pennsylvania, Philadelphia, PA, United States, [3]Obstetrics and Gynecology, Perelman School of Medicine at The University of Pennsylvania, Philadelphia, PA

In this study we employed the single-slice 2D glutamateCEST (GluCEST) MRI to measure the reproducibility as well as changes in GluCEST with age in healthy human brains. GluCEST MRI appears to be a promising technique that can characterize neuronal changes in normal aging.

2581

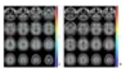

Altered brain gray matter volume and cerebral blood flow in patients with type 2 diabetes mellitus

Dong Zhang[1], Changzheng Shi[1], Rong Ma[1], Zhongping Zhang[2], and Liangping Luo[1]

[1]Medical Imaging Center, The First Affiliated Hospital of Jinan University, Guangzhou, People's Republic of China, [2]MR Research China, GE Healthcare, Beijing

Patients with type 2 diabetes mellitus (T2DM) and there relatives with high risk of diabetes both demonstrate atrophy in right temporal and left insular lobesin. Furthermore, the decrease of cerebral blood flow (CBF) was more popular in the right temporal lobe for high risk group other than T2DM patients

---

2582

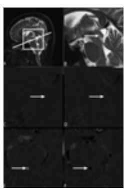

Comparison of CSF Flow Imaging Methods

Matthew Borzage[1,2,3], Skorn Ponrartana[4], Wende Gibbs[5], Hollie Lai[4], Marvin Nelson[4], Benita Tamrazi[4], Gordon McComb[6], and Stefan Blüml[7,8]

[1]Radiology, Children's Hospital Los Angeles, Los Angeles, CA, United States, [2]Rudi Schulte Research Institute, Santa Barbara, CA, United States, [3]Neonatology, Children's Hospital Los Angeles, Los Angeles, CA, United States, [4]Radiology, Children's Hospital Los Angeles, CA, United States, [5]Radiology, University of Southern California, CA, United States, [6]Neurosurgery, Children's Hospital Los Angeles, Los Angeles, CA, United States, [7]Radiology, Children's Hospital Los Angeles, CA, [8]Rudi Schule Research Institute, Santa Barbara, CA

We compared the quality of CSF flow images of ten subjects acquired with T2-weighted flow-void, phase-contrast, and tag-based MR methods. Tag-based methods included the variable image contrast TimeSLIP sequence and a newly designed method, termed TimeSTAMP, with constant contrast. Five radiologists and one neurosurgeon rated them on usefulness for identifying flow with a Likert scale: 5=highest to 1=lowest. Flow was detectable with high confidence for TimeSLIP and TimeSTAMP (4.8 ± 0.2), confidence was significantly lower ($p<0.0001$) in flow-void (2.5 ± 0.7) and phase-contrast (2.6 ± 0.5) images.

2583

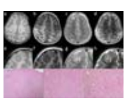

The value of 7T in the clinical evaluation of epileptic patients with tuberous sclerosis complex

Kaibao Sun[1,2], Jianfei Cui[3], Zhongwei Chen[1], Tao Jiang[4], Zhentao Zuo[1], Rong Xue[1,2], Yan Zhuo[1], Bo Wang[1], Shuli Liang[3], and Lin Chen[1,2]

[1]State Key Laboratory of Brain and Cognitive Science, Beijing MRI Center for Brain Research, Institute of Biophysics, Chinese Academy of Sciences, Beijing, People's Republic of China, [2]University of Chinese Academy of Sciences, Beijing, People's Republic of China, [3]Chinese PLA general hospital, Beijing, People's Republic of China, [4]Beijing Tian Tan Hospital, Capital Medical University, Beijing, People's Republic of China

Tuberous sclerosis complex (TSC) is an autosomal dominant genetic disease. 90% of patients with TSC suffer from epilepsy and 50% of them become medicine intractable epilepsy. Epilepsy surgery is an important treatment. However, some focal epileptogenic lesions, essential for surgery, are not well identified by current routine imaging protocols at 3T. 7T MR imaging is assessed in this study to allow better characterization of lesion details and to detect abnormalities previously unseen on 3T MRI and scalp electroencephalogram (EEG). This is the first report of clinical application of 7T MRI for pediatric patients (older than 8 years) with TSC epilepsy.

2584

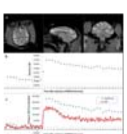

Functional neuroimaging using dynamic radial 3D UTE pulse sequences

Codi Amir Gharagouzloo[1], Chao Ma[1], Eline E. Verwer[1], Joseph B. Mandeville[2], Chuan Huang[3,4], Srinivas Sridhar[5], Georges El Fakhri[1], Dustin W. Wooten[1], and Marc D. Normandin[1]

[1]Gordon Center for Medical Imaging, Massachusetts General Hospital & Harvard Medical School, Boston, MA, United States, [2]Athinoula A. Martinos Center for Biomedical Imaging, Massachusetts General Hospital, Charlestown, MA, United States, [3]Radiology, Stony Brook University, Stony Brook, NY, United States, [4]Psychiatry, Stony Brook University, Stoney Brook, NY, United States, [5]Nanomedicine Science and Technology Center, Northeastern University, Boston, MA, United States

Functional MR neuroimaging is an essential tool for studying brain activity. Cerebral blood volume (CBV) is an important indicator of brain function, but measurements are typically qualitative or relative. Furthermore, warping and signal drift necessitate significant image pre-processing with standard EPI acquisition. In this work, we utilize a radial 3D UTE pulse sequence with optimized acquisition parameters determined from phantoms and modeling. Feasibility of dynamic UTE as a functional neuroimaging method is demonstrated in non-human primates receiving NBOH-2C-CN, a 5-HT_{2A} receptor agonist. CBV is measured dynamically throughout the whole brain and shown to agree well with an analogous EPI experiment.

Traditional Poster

Interventional

Exhibition Hall 2585-2618 Wednesday 16:15 - 18:15

2585

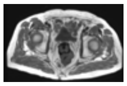

Percutaneous MRI-Guided Cryoablation of Regional Nodal Metastases in Prostate Cancer: Initial Experience

Ahmad Parvinian[1], David A Woodrum[1], Krzysztof R Gorny[1], Joel P Felmlee[1], and Lance A Mynderse[1]

[1]Mayo Clinic, Rochester, MN, United States

In this retrospective study, we examined the feasibility and safety of magnetic resonance imaging (MRI)-guided percutaneous cryoablation of regional nodal metastases in the setting of prostate cancer. The study cohort comprised eight patients with biochemically recurrent prostate cancer who had undergone prior prostatectomy and radiotherapy, thereby limiting their ability to receive further radiation to regional nodes. Technical success was achieved in all cases and there were no procedure-related complications. Our data suggest that MRI-guided cryoablation offers a feasible alternative therapy for local control of metastatic lymph nodes. Further prospective investigation is warranted to assess short- and long-term local efficacy.

2586

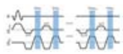

Orientation-independent z-shimmed temperature mapping near ablation probes

Megan E Poorman[1,2] and William A Grissom[1,2]

[1]Biomedical Engineering, Vanderbilt University, Nashville, TN, United States, [2]Institute of Imaging Science, Vanderbilt University, Nashville, TN, United States

MR guidance of thermal ablation is hindered by signal loss around the metallic applicators and needles used to deliver treatment. This signal loss can prevent accurate MR thermometry in the area of critical heating around the ablation probe. Here we present a multiple-echo z shimmed sequence with optimized refocusing scheme that can correct for through-plane distortion from the probe irrespective of probe and slice orientations. With the chosen refocusing scheme we achieved a signal recovery of 10 to 1 in the near-probe region when compared to a conventional gradient echo thermometry technique.

2587

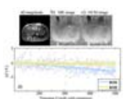

Hybrid MR-ultrasound acquisition for multi-baseline thermometry

Pei-Hsin Wu[1], Frank Preiswerk[1], Cheng-Chieh Cheng[1], and Bruno Madore[1]

[1]Radiology, Brigham and Women's Hospital, Harvard Medical School, Boston, MA, United States

MR thermometry, based on proton resonance frequency (PRF) shift, can be achieved by the phase subtraction between pretreatment baseline images and treatment images. However, breathing motion leads to phase errors that may corrupt temperature measurements. We propose the use of a hybrid MR-ultrasound imaging setup and reconstruction algorithm to provide the phase reference required for PRF thermometry in moving organs. The generated synthetic MR-ultrasound images match the acquired images in all respect except for the fact that they do not contain any heating information, and thus provide a valuable non-heated phase reference from which temperature changes can be quantified.

2588

Comparison of Temperature Mapping Methods Using Proton Resonance Frequency Shift and T1 in 3-T and 7-T MRI

Jong-Min Kim[1,2], Chulhyun Lee[3], Seong-Dae Hong[1,2], Eun-Hyuk Choi[1,2], You-Jin Jeong[1,2], Jeong-Hee Kim[4], and Chang-Hyun Oh[1,2,4]

[1]Department of Electronics and Information Engineering, Korea University, Seoul, Korea, Republic of, [2]ICT convergence technology for Health & Safety, Korea University, Sejong, Korea, Republic of, [3]Bioimaging Research Team, Korea Basic Science Institute, [4]Research Institute for Advanced Industrial Technology, Korea University, Sejong, Korea, Republic of

Although temperature imaging in 7.0 T MRI has the advantage of increased SNR compared to lower field, it is more sensitive to susceptibility causing more artifacts. Since the 7.0 T MRI is also affected more by the electrical conductivity, temperature-dependency of the electrical conductivity is also affecting the resultant images. This work compares the temperature mapping methods for RF hyperthermia in 7.0 T and 3.0 T MRI and proposes the new temperature mapping method appropriate to 7.0 T MRI under the environment of changing conductivity.

2589

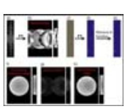

Dynamic anti-aliasing image reconstruction for localized thermal therapies

Henrik Odéen[1] and Dennis L Parker[1]

[1]Department of Radiology and Imaging Sciences, University of Utah, Salt Lake City, UT, United States

A novel image reconstruction algorithm for dynamic anti-aliasing image reconstruction (DAIR) of proton resonance frequency shift (PRFS) MR temperature maps from subsampled k-space data for localized heatings is presented. DAIR makes use of a pre-heating, fully sampled image to find and remove the aliasing artifact in a dynamic series of images. The algorithm is demonstrated using CAIPI-like sampling patterns in a 3D segmented EPI pulse sequence and focused ultrasound heatings in a tissue mimicking gelatin phantom. DAIR reconstructed PRFS temperature maps showed good agreement with fully sampled “truth” for k-space reduction factors of 2 – 4.

2590

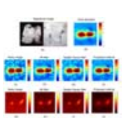

An Adaptive Non-Local Denoising Method for Real-Time MR-Thermometry

Cornel Zachiu[1], Mario Ries[1], Chrit Moonen[1], and Baudouin Denis de Senneville[1,2]

[1]University Medical Center Utrecht, Utrecht, Netherlands, [2]University of Bordeaux, Bordeuaux, France

MR-guided targeted thermal therapies often rely on temperature information provided by proton resonance frequency shift (PRFS) thermometry. However, fast MR acquisition schemes are usually employed, in order to provide temperature updates with a short latency. This may lead to noisy temperature measurements, which can have a direct impact on therapy control and monitoring. In the current study we propose a novel non-local denoising technique for real-time MR-thermometry that improves data precision, while at the same time maximizing output accuracy, feature which is not guaranteed by currently employed real-time MR-temperature denoising methods.

2591

Fast Temperature Estimation Using Golden Angle Radial from Undersampled K-Space for MR Guided Microwave Ablation

Ke Wang[1], Zijing Dong[2], Fuyixue Wang[2], Bingyao Chen[3], Jiafei Yang[3], Xing Wei[3], and Kui Ying[4]

[1]Department of Biomedical Engineering, Tsinghua University, Beijing, People's Republic of China, [2]Center for Biomedical Imaging Research, Department of Biomedical Engineering, Tsinghua University, Beijing, People's Republic of China, [3]Department of Orthopedics, First Affiliated Hospital of PLA General Hospital, Beijing, People's Republic of China, [4]Key Laboratory of Particle and Radiation Imaging, Ministry of Education, Medical Physics and Engineering Institute, Department of Engineering Physics, Tsinghua University, Beijing, People's Republic of China

Golden angle radial sampling is insensitive to motion and provides oversampled central k-space for self-navigation. This study aims to accelerate the acquisition with motion correction for MR temperature imaging by applying golden angle radial to hybrid model based on PRF method. The proposed method uses low resolution images obtained from a certain ratio of radius in k-space center to correct the period motion and magnetic field drift. Then, an iterative method is adopted to estimate the temperature by the hybrid model. Simulations and in-vivo experiments demonstrate the robustness to motion and effectiveness of the proposed method.

2592

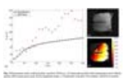

Prospective Motion Correction of MR-Thermometry using an Optical Tracking System

Urte Kaegebein[1], Enrico Pannicke[2], Thomas Hoffmann[3], Bennet Hensen[4], Frank Wacker[4], and Oliver Speck[1]

[1]Department Biomedical Magnetic Resonance, Magdeburg, Germany, [2]Chair of Electromagnetic Compatibility, Institute of Medical Engineering, 39106, Germany, [3]Institute of Neuroradiology, Magdeburg, Germany, [4]Department of Radiology, Hannover Medical School, Hannover, Germany

Accurate temperature assessment during liver ablation requires a dedicated method for motion correction. We present the first results of a prospective motion correction method for thermometry during microwave ablation using an optical Moiré Phase Tracking system. Ex-vivo studies showed a mean temperature deviation of ΔT = 0.4 °C compared to ΔT = 34.6°C without motion correction. The method can easily be integrated into the work flow if optical tracking is applied for needle placement.

2593

Accumulated Thermal Dose in MR-Guided Focused Ultrasound for the Treatment of Essential Tremor

Yuexi Huang[1], Nir Lipsman[2], Michael L. Schwartz[2], Vibhor Krishna[3], Francesco Sammartino[3], Andres Lozano[3], and Kullervo Hynynen[1,4]

[1]Sunnybrook Research Institute, Toronto, ON, Canada, [2]Division of Neurosurgery, Sunnybrook Health Sciences Centre, Toronto, ON, Canada, [3]Division of Neurosurgery, Toronto Western Hospital, Toronto, ON, Canada, [4]Department of Medical Biophysics, University of Toronto, Toronto, ON, Canada

In focused ultrasound treatment of essential tremor, MR temperature and thermal dose measurements were crucial in guiding acoustic parameters. In this study, accumulated thermal doses from repeated sonications were integrated after chemical-shift artifacts were corrected retrospectively. Accumulated thermal dose measurements showed good correlation to lesion size in followup MR imaging.

2594

Effects of ultrasound transducer ground plane configuration on SNR in MR guided focused ultrasound therapies

Emilee Minalga[1], Allison H Payne[1], Robb Merrill[1], Dennis L Parker[1], and J. Rock Hadley[1]

[1]UCAIR, University of Utah, Salt Lake City, UT, United States

The use of dedicated RF coils can increase image SNR in magnetic resonance guided focused ultrasound (MRgFUS). However, shielding and eddy current effects of the ultrasound transducer ground plane (TGP) can significantly degrade the increased SNR. Accounting for these considerations when designing the ultrasound transducer can potentially increase SNR throughout the imaging volume during MRgFUS procedures.

2595

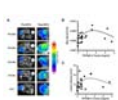

In Vivo 19F MRI for Non-invasively Investigating the Effects of Perfluorocarbon Nanoemulsion on High Intensity Focused Ultrasound Tumor Ablation

Soo Hyun Shin[1], Eun-Joo Park[2], Changki Min[1], Sun Il Choi[1], Soyeon Jeon[1], Yun-Hee Kim[1], and Daehong Kim[1]

[1]Molecular Imaging & Therapy Branch, National Cancer Center, Goyang, Korea, Republic of, [2]Dept. of Radiology, Seoul National University Hospital, Seoul, Korea, Republic of

Perfluorocarbon nanoemulsion (PFCNE) is currently studied as a precursor of microbubbles to accompany high intensity focused ultrasound (HIFU) for tumor ablation. We propose ^{19}F MRI as a valuable tool for non-invasively assessing the effects of PFCNE concentration on therapeutic efficiency of HIFU. ^{19}F MRI was used to determine the amount of PFCNE accumulated in a tumor before HIFU treatment. Tumor ablation was monitored by intra-voxel incoherent motion (IVIM) mapping, which was compared with PFCNE quantification from ^{19}F MRI for identifying the PFCNE concentration that gives optimal therapeutic efficiency.

2596

Automatic removal of water bath artifacts from MR temperature maps in focused ultrasound neurosurgery

Pooja Gaur[1,2], Beat Werner[3], and William A Grissom[1,2]

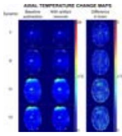

[1]Institute of Imaging Science, Vanderbilt University, Nashville, TN, United States, [2]Biomedical Engineering, Vanderbilt University, Nashville, TN, United States, [3]Center for MR-Research, University Children's Hospital, Zurich, Switzerland

During MR-guided focused ultrasound treatments in the brain, circulation of cool water around the head and ultrasound wave propagation create water motion during the signal readout, resulting in image artifacts. These artifacts vary across image dynamics, and are observable in magnitude and phase images and in temperature change maps measured during treatment. In this work, we apply a wavelet denoising algorithm to remove these artifacts from temperature maps during treatment. Results show that temperature errors can be corrected in patient data, in 0.2 s per map, suggesting that corrections could be performed during treatment.

2597

The Treatment Outcome of Magnetic Resonance guided High Intensity Focused Ultrasound Ablation of Uterine Fibroids through the Transverse and Longitudinal Scars

Bilgin Keserci[1] and Nguyen Minh DUC[2]

[1]MR Therapy, Philips Healthcare, Seoul, Korea, Republic of, [2]Department of Radiology, Pham Ngoc Thach University of Medicine, HCMC, Vietnam, Ho Chi Mihn City, Vietnam

This study investigates the technical treatment success and therapeutic efficacy of magnetic resonance guided high intensity of focused ultrasound (MR-HIFU) ablation of uterine fibroid patients with transverse and longitudinal scars. The results of the present study suggests that the scar patch could be used in MR-HIFU ablation of fibroid patients with transverse and longitudinal abdominal scars, which might no longer be regarded as an exclusion criterion.

2598

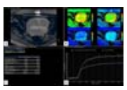

The Role of Perfusion MRI in Predicting Magnetic Resonance-guided High Intensity Focused Ultrasound Treatment Outcome in Uterine Fibroids

Bilgin Keserci[1] and Nguyen Minh DUC[2]

[1]MR Therapy, Philips Healthcare, Seoul, Korea, Republic of, [2]Department of Radiology, Pham Ngoc Thach University of Medicine, HCMC, Vietnam, Ho Chi Mihn City, Vietnam

The aim of this present work is to classify uterine fibroids by comparing the MR T1 perfusion based time-signal intensity curves of fibroid tissue with myometrium prior to HIFU ablation. Our findings in this study suggest that the newly introduced classification method could be used as the primary MRI classification parameter prior to MR-HIFU ablation not only for classifying the uterine fibroids but also predicting the treatment outcome of HIFU ablation, with the immediate NPV ratio of at least 80%.

2599

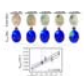

Estimation of Focused-Ultrasound Induced CNS Molecular Delivery via Dynamic Contrast-Enhanced Magnetic-Resonance Imaging

Wen Yen Chai[1,2], Po Chun Chu[3], Chih Hung Tasi[2], Chung Yin Lin[4], Hung Wei Yang[5], Hsin Yi Lai[6], and Hao Li Liu[2]

[1]Department of Diagnostic Radiology and Intervention, Chang-Gung Memorial Hospital, Taoyuan, Taiwan, [2]Department of Electrical Engineering, Chang-Gung University, Taoyuan, Taiwan, [3]Department of Research and Development, NaviFUS corp., Taipei, Taiwan, [4]Medical Imaging Research Center, Institute for Radiological Research, Chang-Gung University/Chang-Gung Memorial Hospital, Taoyuan, Taiwan, [5]Medical Science and Technology, National Sun Yat-Sen University, Kaohsiung, Taiwan, [6]Institute of Neuroscience and Technology, Zhejiang University, Zhejiang, People's Republic of China

Focused ultrasound (FUS) exposure with presence of microbubbles can transiently open the blood-brain-barrier (BBB) at targeted brain tissues. The purpose of this study is to investigate the feasibility to employ DCE-MRI to predict and estimate molecular CNS penetration under various exposure conditions and molecular sizes. Our result showed high accuracy and successful (prediction discrepancy was limited to be less than 10%) to estimate molecular penetration of FUS-induced BBB opening via imaging index (K_{trans}) from DCE-MRI. This approach may bring technology advances and facilities the clinical application of FUS-induced BBB opening to deliver therapeutic molecules for CNS disease treatment.

2600

Detection of temperature induced viscoelasticity changes using MR acoustic radiation force impulse imaging

Lorne Wyatt Hofstetter[1], Henrik Odeen[2], Joshua de Bever[3], Hailey McLean[2], Allison Payne[1], and Dennis L Parker[1]

[1]Department of Radiology and Imaging Sciences, University of Utah, Salt Lake City, UT, United States, [2]Department of Radiology and Imaging Sciences, University of Utah, [3]Department of Radiology, Stanford University

MR acoustic radiation force impulse (MR-ARFI) imaging, which measures tissue displacement caused by the concentrated force of a focused ultrasound (FUS) beam, has been used to locate and characterize the ultrasound focus. It has also been used to measure and assess changes in tissue elastic properties. We hypothesize that localized heating may denature elastic properties of tissues, and convert the elastic displacement caused by FUS to a form of viscous streaming. In this work, we propose using 3D GRE MR-ARFI with a unique timing scheme, to quickly and efficiently detect temperature induced viscoelasticity changes in a gelatin phantom during FUS heating.

2601

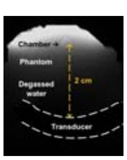

Quantification of Acoustic Radiation Force Induced Flow Velocity Changes by Phase-Contrast MRI

Che-Wei Wu[1], Chen-Hua Wu[1], Po-Hung Hsu[2], Hao-Li Liu[2], Chih-Kuang Yeh[1], and Hsu-Hsia Peng[1]

[1]Biomedical Engineering and Environment Science, National Tsing Hua University, Hsinchu, Taiwan, [2]Electrical Engineering, Chang-Gung University, Taoyuan, Taiwan

We adopted phase-contrast MRI to real-time acquire flow velocity information with transmitting focused ultrasound pulses on microbubbles in a flowing phantom. We aim to evaluate the velocity changes resulted from the formation of bubbles by secondary acoustic radiation force. We observed that temporal standard deviation of velocity and %velocity change increased with increasing MBs concentrations. It can be attributed to the formation of aggregated bubbles, which can narrow the chamber diameter and accordingly lead to higher flow velocity. In conclusion, we verified the feasibility of using phase-contrast MRI to evaluate the impact of secondary acoustic radiation force.

2602

Design of 5-channel On-coil Shimming Coil for Rat Brain MRI Guided High Intensity Focused Ultrasound: a preliminary study

Jo Lee[1], Jianhong Wen[1], Chao Zou[1], Xiaoqing Hu[1], Xiaoliang Zhang[2,3], Xin Liu[1], and Ye Li[1]

[1]Lauterbur Imaging Research Center, Shenzhen Institutes of Advanced Technology, Chinese Academy of Sciences, Shenzhen City, People's Republic of China, [2]Department of Radiology and Biomedical Imaging, University of California San Francisco, CA, United States, [3]UCSF/UC Berkeley Joint Graduate Group in Bioengineering, San Francisco, CA, United States

Signal-to-noise ratio (SNR) and homogeneity of the static magnetic field B0 are critically important in achieving accurate temperature measurement for MRI guided HIFU. In this work, a 5-channel shimming coil on the top of a 3-channel RF coil array at 3T has been fabricated to increase the B0 homogeneity and the SNR in region of interest. Phantom studies have demonstrated the the capability of the proposed shimming coil to improve B0 homogeneity and SNR of the images, which will lead to accurate temperature mapping.

2603

System for Delayed Intervention in MRI

Marc Rea[1], Noranon Dudsdeemaytha[2], and Wladyslaw Gedroyc[1]

[1]Imperial College Healthcare NHS Trust, London, United Kingdom, [2]Bioengineering, Imperial College London, London, United Kingdom

A system for Interventional MRI using Infrared tracking of a handeld needle guide was adapted for practical use in closed-bore scanners. This was achieved by mapping of the image space to a patient space with the table outside the scanner bore to permit delayed visualisation of the targeted site. This novel method enables manual intervention of complex sites to be handled with greater care than other methods, and provides a relatively low-cost option for MR-guided interventions.

2604

Radiofrequency applicator concepts for simultaneous MR imaging and hyperthermia treatment of glioblastoma multiforme: A 7.0 T (298 MHz) study

Eva Oberacker[1], Andre Kuehne[2], Helmar Waiczies[2], Jacek Nadobny[3], Sebastian Zschaeck[3], Pirus Ghadjar[3], Peter Wust[3], Thoralf Niendorf[1,2,4], and Lukas Winter[1]

[1]Berlin Ultrahigh Field Facility (B.U.F.F.), Max Delbrück Center for Molecular Medicine in the Helmholtz Association, Berlin, Germany, [2]MRI.TOOLS, Berlin, Germany, [3]Clinic for Radiation Oncology, Charité Universitätsmedizin, Berlin, Germany, [4]Experimental and Clinical Research Center (ECRC), a joint cooperation between the Charité Medical Faculty and the Max Delbrück Center for Molecular Medicine in the Helmholtz Association, Berlin, Germany

Glioblastoma multiforme is the most frequent and most aggressive malignant braintumor with de facto no long term curation by the use of current multimodal therapeutic approaches. RF heating at ultrahigh fields (B_0=7.0T, f=298MHz) has the potential of delivering sufficiently large thermal dosage for hyperthermia of relatively large tumor areas. This work focuses on EMF simulations and provides realistic applicator designs tailored for simultaneous RF heating and MR imaging. Our preliminary results suggest that RF power can be focused to both a small tumor area and a big clinical target volume based on segmented patient data.

2605

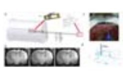

Stepwise optogenetic activation of the rat thalamic nuclei with MRI-guided robotic arm (MgRA)

Yi Chen[1,2], Patricia Pais-Roldán[1,2], Xuming Chen[1], and Xin Yu[1]

[1]Research Group of Translational Neuroimaging and Neural Control, High-Field Magnetic Resonance, Max Planck Institute for Biological Cybernetics, Tuebingen, Germany, [2]Graduate School of Neural Information Processing, University of Tuebingen, Tuebingen, Germany

An MRI-guided multiple degree-of-freedom robotic arm positioning system is developed to guide the fiber optic insertion inside a small animal MRI scanner. The fiber optic is positioned at different depth in the rat thalamus to deliver light pulses for optogenetic fMRI. The corresponding functional spatial patterns and time courses can be achieved in a stepwise manner. The MgRA positioning system provides an alternative way to study global functional projections by mapping fMRI signals driven optogenetically from different brain nuclei.

2606

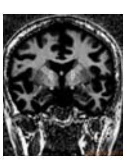

Clinical Outcome of Globus pallidus internus or subthalamic nucleus deep brain stimulation for Parkinson's disease using MRI-guided localization and verify with microelectrode

Sherman SM Lo[1], WL Poon[1], KW Tang[1], and TL Poon[2]

[1]Department of Radiology & Imaging, Queen Elizabeth Hospital, Kowloon, Hong Kong, [2]Department of Neurosurgery, Queen Elizabeth Hospital, Kowloon, Hong Kong

Globus pallidus internus (GPi) and Subthalamic nucleus (STN) are the two main target for deep brain stimulation (DBS) in treatment for patients with advanced Parkinson's disease (PD) not respond to medical therapies. MRI brain imaging is used for selection of patients for DBS and localize the target nucleus. This study confirms that GPi/STN-DBS may be placed with high accuracy by using a correct and optimal MRI-guided sequences. Correct deep brain stimulation electodes placement can provides a safe and effective treatment for severe Parkinson's disease not responsive to medical therapies.

2607

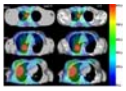

MRI-based Synthetic CT for Radiation Treatment of Lung Cancer

Hesheng Wang[1], Hersh Chandarana[2], Kai Tobias Block[2], Thomas Vahle[2,3], and Indra J Das[1]

[1]Department of Radiation Oncology, New York University School of Medicine, New York, NY, United States, [2]Bernard and Irene Schwartz Center for Biomedical Imaging, Department of Radiology, New York University School of Medicine, New York, NY, United States, [3]Siemens Healthcare GmbH, Erlangen, Germany

With emerge of MR-linear accelerator technology, the interest for MR-only radiotherapy is growing rapidly. This study evaluated the feasibility of using pseudo-CT generated from conventional Dixon-MR scans for treatment planning of lung cancer where dosimetric differences are expected to be high due to tissue inhomogeneity. A model-based method including spine was applied to generate synCT from whole-body Dixon-MR data. The plans for radiotherapy in lung cancer calculated on synCT images closely agreed with the doses computed on standard CT to within 1%. Further evaluation of the MR-based treatment planning in a large patient cohort is needed.

2608

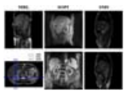

Abdominal organ tracking on a hybrid MR-Linac system using a particle filter based algorithm

Alexandra E Bourque[1,2,3], Stéphane Bedwani[1], Jean-François Carrier[1,2], Cynthia Ménard[1], Pim Borman[3], Clemens Bos[3], Bas Raaymakers[3], Nikolai Mickevicius[4], Eric Paulson[4,5], and Rob H.N. Tijssen[3]

[1]Département de radio-oncologie, Centre Hospitalier de l'Université de Montréal, Montréal, QC, Canada, [2]Département de physique, Université de Montréal, Montréal, QC, Canada, [3]Imaging division, UMC Utrecht, Utrecht, Netherlands, [4]Radiation Oncology, Medical College of Wisconsion, Milwaukee, WI, United States, [5]Radiology, Medical College of Wisconsin, Milwaukee, WI, United States

We have previously developed an autocontouring and tracking algorithm for lung tumors as an online application for MR-Linac treatments. This algorithm is now extended to abdominal organs tracking and evaluated with a range of imaging strategies on multiple systems, including single slice dynamic time-series data acquired on the 1.5T Marlin system of the MR-Linac as well as simultaneous multi-slice (SMS) and simultaneous orthogonal plane imaging (SOPI) acquired on diagnostic 1.5T Philips and 3T Siemens scanners. The wide adaptability of the algorithm on images of different contrast concludes that the method is robust and can be successfully applied in different tracking scenario.

2609

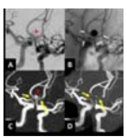

Visualization of Intracranial Aneurysms Treated with Low-profile Visualized Intraluminal Support (LVIS Jr. stent) Using Ultrashort Echo Time Magnetic Resonance Angiography

Nao Takano[1], Michimasa Suzuki[1], Ryusuke Irie[2], Munetaka Yamamoto[3], Nozomi Hamasaki[2], Haruyoshi Hoshito[2], Kanako Kunishima Kumamaru[1], Masaaki Hori[1], Hidenori Oishi[4], and Shigeki Aoki[1]

[1]Department of Radiology, Graduate School of Medicine, Juntendo University, Tokyo, Japan, [2]Department of Radiology, Juntendo University Hospital, Tokyo, Japan, [3]Department of Neurosurgery, Juntendo University School of Medicine, Tokyo, Japan, [4]Department of Neuroendovascular Therapy, Juntendo University School of Medicine, Tokyo, Japan

In this study, we evaluated the usefulness of ultrashort echo time magnetic resonance angiography (Silent MRA) for intracranial aneurysms treated with LVIS Jr. stent-assisted coil embolization by a comparison between silent MRA and three-dimensional time of flight MRA (3D TOF-MRA) because the LVIS Jr. stent had higher metal coverage than previous reported stents. In silent MRA, the score of flow in the stents was superior to that of 3D TOF-MRA ($p<0.05$). Moreover, aneurysm occlusion status was good agreement for DSA. Therefore, silent MRA might be useful for intracranial aneurysms treated with LVIS Jr. stent-assisted coil embolization.

2610

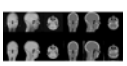

Feasibility of Zero TE MR based Radiation Therapy Planning for Head and Neck application

Cristina Cozzini[1], Mikael Bylund[2], Joakim H Jonsson[2], Josef A Lundman[2], Fredrik Illerstam[3], Tufve Nyholm[2], and Florian Wiesinger[1]

[1]GE Global Research, Munich, Germany, [2]Department of radiation sciences, Umeå University, Umeå, Sweden, [3]GE Healthcare, Danderyd, Sweden

We describe a method to convert Zero Echo Time (ZTE) MR images into synthetic CT at the resolution required for Radiation Therapy (RT). The method was tested for the head and neck application on N=8 patient data. The dose was calculated with a RT planning software and the results were compared relative to co-registered CT data.

2611

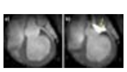

Active catheter tracking for MR-Guided Percutaneous Coronary Intervention at 3T: Initial Results in a Pig Model

Simon Reiss[1], Ali Caglar Özen[1], Thomas Lottner[1], Timo Heidt[2], Axel Joachim Krafft[1], Lisa Caroline Besch[2], Klaus Düring[3], Constantin von zur Mühlen[2], and Michael Bock[1]

[1]Department of Radiology, Medical Physics, Medical Center - University of Freiburg, Freiburg, Germany, [2]Department of Cardiology and Angiology I, University Heart Center, Freiburg, Germany, [3]MaRVis, Frechen, Germany

Compared to X-Ray fluoroscopy, cardiovascular interventions under MR-guidance do not use ionizing radiation, they provide excellent soft tissue contrast, cross-sectional imaging in arbitrary slice orientations and a variety of functional measurement techniques. MR-guided catheterization of coronary arteries has so far only been demonstrated in animal trails at 1.5T, and it remains challenging due to limited temporal and spatial resolution. Also, dedicated instruments for MR-guided coronary interventions are not yet widely available. We show that active visualization of commercial catheters for MR-guided percutaneous coronary in a pig model at 3T is feasible and enables engagement of the LCA under real-time imaging.

2612

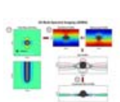

Artifact-reduced imaging of biopsy needles with 2D multi-spectral imaging

Hans Weber[1], Bruce L. Daniel[1], and Brian A. Hargreaves[1]

[1]Radiology, Stanford University, Stanford, CA, United States

MR-guidance for biopsy procedures features high intrinsic soft-tissue contrast. However, artifacts induced by the metallic needle can reduce the localization of the needle and require low susceptibility needle materials with poorer cutting performance. In this work, we explore 2D multi-spectral imaging (2DMSI) for reducing the needle artifacts for more precise needle localization and tracking or to enable the usage of conventional stainless-steel biopsy needles.

2613

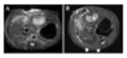

MRI of Intra-Tumoral Iron-Oxide Labeled Clostridium novyi-NT Injections During Bacteriolytic Therapy in Solid Tumors

Jingran Ji[1], Woo Ram Park[1], Yihe Yang[1], Soojeong Cho[1], Xiaoke Huang[1], Kathleen Harris[1], Weiguo Li[1], Dong-Hyun Kim[1], Zhuoli Zhang[1], and Andrew Christian Larson[1]

[1]Northwestern University, Chicago, IL, United States

Bacteriolytic therapy with Clostridium novyi-NT has shown promise as a form of cancer treatment, but concerns remain regarding route of delivery and toxicity. Our study aimed to develop a method to visualize delivery with MRI during bacteriolytic therapy. We did so by incubating bacteria with iron oxide particles. In vitro viability studies and labeling efficiency studies were then performed, followed by phantom studies. Bacteria were then directly injected into rat liver tumors as well as mouse flank tumors and imaged. We demonstrate that the labeled bacteria can be directly visualized on MRI and is a reliable indicator of successful delivery.

2614

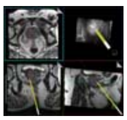

Real-time lesion targeting during MRI-guided prostate biopsy using an iPad: feasibility and initial clinical evaluation

Christiaan G. Overduin[1], Jan Heidkamp[1], Frank de Lange[1], Jelle O. Barentsz[1], and Jurgen J. Fütterer[1,2]

[1]Radiology and Nuclear Medicine, Radboud University Medical Centre, Nijmegen, Netherlands, [2]MIRA Institute for Biomedical Engineering and Technical Medicine, University of Twente, Enschede, Netherlands

Our study assessed the feasibility of a novel method for real-time lesion targeting during transrectal in-bore MRI-guided prostate biopsy using a tablet device inside the MR room. Real-time targeting was technically successful in all patients and allowed targeted biopsy of the cancer suspicious region without requiring additional needle guide adjustments in all but one patient. Prostate cancer (PCa) was found in 18 of 20 patients. Our initial clinical experience indicates a substantial decrease in biopsy and procedure time as compared to standard targeting, which could be valuable to increase clinical applicability of the technique.

2615

magna cum laude

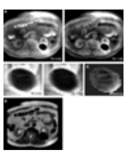

2D UTE-based MR thermometry of frozen tissue: feasibility during in vivo MRI-guided cryoablation

Christiaan G. Overduin[1], Axel J. Krafft[2], Michael Bock[2], Hans JF Langenhuijsen[3], Sjoerd F.M. Jenniskens[1], Jurgen J. Fütterer[1,4], and Tom W.J. Scheenen[1]

[1]Radiology and Nuclear Medicine, Radboud University Medical Centre, Nijmegen, Netherlands, [2]Radiology - Medical Physics, Medical Center University of Freiburg, Freiburg, Germany, [3]Urology, Radboud University Medical Centre, Nijmegen, Netherlands, [4]MIRA Institute for Biomedical Engineering and Technical Medicine, University of Twente, Enschede, Netherlands

This study assessed the feasibility of 2D UTE-based MR thermometry of frozen tissue during in vivo MRI-guided cryoablation. Axial 2D UTE images were acquired at the end of the first and second freeze cycle during an MRI-guided renal cryoablation procedure. Measurable MR signal could be obtained from frozen tissue. MR temperature maps were estimated using a relative signal level calibration performed in ex-vivo porcine muscle. Our work demonstrates the feasibility of 2D UTE-based MR thermometry of frozen tissue during in vivo MRI-guided cryoablation, which could be an important step towards clinical application of this technique.

2616

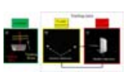

Simultaneous slice excitation for accelerated passive marker tracking via phase-only cross correlation (POCC) in MR-guided needle interventions

Andreas Reichert[1], Simon Reiss[1], Michael Bock[1], and Axel Joachim Krafft[1]

[1]Dept. of Radiology, Medical Physics, Medical Center - University of Freiburg, Freiburg, Germany

Minimally invasive interventions benefit from image guidance during instrument positioning. To ensure high image quality, MR-guided interventions are preferably performed in closed bore systems using MR markers and passive tracking sequences to localize and monitor the interventional device. In this work we accelerate a passive marker tracking sequence designed for needle-guided procedures using a simultaneous multi-slice excitation. With this technique the acquisition time is reduced by 33%, which results in a higher temporal fidelity while maintaining targeting accuracy.

2617

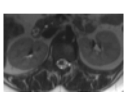

Treatment for Spontaneous Intracranial Hypotension: First Experience with MRI Guided Percutaneous Blood Patch and Fibrin Injection.

Jorge Alberto Lee Diaz[1], Gerard Deib[1], Jan Fritz[1], and Ferdinand Hui[1]

[1]Russell H. Morgan Department of Radiology and Radiological Science, Johns Hopkins University School of Medicine, Baltimore, MD, United States

MRI guided blood patch/fibrin injection (BFP) instead of CT BFP as treatment option for SIH, first case reported. Avoids radiation exposure, helpful for adolescents and women in reproductive age. Obviates CT myelography, decreasing risks, time, and making it available for patients with iodine allergy. Our case is a 26 yo female with SIH. Axial PD, Axial and Sagittal T2 HASTE were used for localization of dural ectasia. T2 HASTE MRI fluoroscopy was used for spinal needle placement at the T12-L1 epidural space and injection of 10cc autologous blood and 2 cc of fibrin. The result was improvement of symptoms.

2618

Multiparametric Comparison of Quantitative Susceptibility Mapping, R2*, and 89Zr-PET for Quantification of Targeted Magnetic Drug Therapy Biodistribution

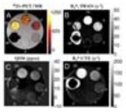

Caroline D. Jordan[1], Sravani Kondapavulur[1], Andre M. Cote[1], Misung Han[1], Kiel D. Neumann[1], Peder E. Z. Larson[1], Henry F. VanBrocklin[1], Alastair J. Martin[1], and Steven W. Hetts[1]

[1]*Radiology and Biomedical Imaging, University of California San Francisco, San Francisco, CA, United States*

Targeted magnetic drug delivery could reduce toxicity of transarterial chemoembolization when used in combination with a magnetic filtration device, and accurate quantification is necessary. We utilized ^{89}Zr-iron oxide nanoparticles (IONP) to evaluate quantitative susceptibility mapping (QSM), R_2^*, and ^{89}Zr-PET uptake. Phantom evaluations demonstrated linear correlation between QSM, R_2^*, and ^{89}Zr-PET/MR. Substantial increase in QSM and R_2^* was observed in a single hepatic lobe in a preliminary *in vivo* experiment after injection using MR only. These cross-validated techniques demonstrate a linear relationship between IONP concentration and QSM, R_2^*, and ^{89}Zr-PET *in vitro* and show promise in assessing magnetic nanoparticle tracking.

Traditional Poster

MR Safety

Exhibition Hall 2619-2653 Wednesday 16:15 - 18:15

2619

magna cum laude

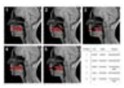

Metallic taste perception at 7 Tesla: Influences of jaw position and ionic composition of saliva

Wiebke Neumann[1], Andreas K. Bitz[2], Lothar R. Schad[1], Frank G. Zöllner[1], Mark E. Ladd[2], Armin M. Nagel[2,3], and Jonathan M. Lommen[2]

[1]*Computer Assisted Clinical Medicine, Medical Faculty Mannheim, Heidelberg University, Mannheim, Germany,* [2]*Medical Physics in Radiology, German Cancer Research Center (DKFZ), Heidelberg, Germany,* [3]*Institute of Radiology, University Hospital Erlangen, Erlagen, Germany*

Up to 40% of subjects report metallic taste sensations when exposed to strong magnetic fields. Can the perception of metallic taste during an ultra-high field (UHF) examination be lessened and thus increase patient comfort? This study experimentally examines the influence of jaw position and ionic composition of saliva (salinity and acidity) on metallic taste perception. We found that simple changes in tongue and teeth positions as well as saline in the mouth decrease the metallic taste sensation during UHF exposure. Following the current trend to UHF applications, these findings allow for further insight regarding increased patient comfort and acceptance of UHF examinations.

2620

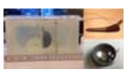

Gradient Heating of Bulk Metallic Implants

Rüdiger Brühl[1], Albrecht Ihlenfeld[1], and Bernd Ittermann[1]

[1]*Physikalisch-Technische Bundesanstalt (PTB), Braunschweig und Berlin, Germany*

The temperature increase of an excised hip prosthesis was measured under exposure to the switched gradients of a clinical 3T scanner. For the acetabular cup, insulated or embedded in gelatin gel, temperature increases of ΔT=25.8 K and 3.8 K, respectively, were observed within 10 min. From the initial temperature increase of up to 110 mK/s a gradient-induced heating power of P_G = 370 W/kg in adjacent muscle can be derived and this quantity's relation to local SAR is discussed. The results suggest that gradient-induced heating of bulk metallic implants cannot automatically be assumed to be negligible.

2621

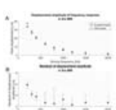

Comparison of Laser Doppler Vibrometer and Accelerometer Measurements of MRI Gradient Field Induced Vibration in Conductive Materials

Christine M. Tarapacki[1], Daniel J. Martire[1], Colin M. McCurdy[1], William Bradfield Handler[1], and Blaine A. Chronik[1]

[1]*Physics and Astronomy, Western University, London, ON, Canada*

Measuring gradient field induced vibration is essential to determine the safety of medical devices in the MR environment. This study investigated vibrations measured both inside and outside the MRI to quantitatively compare the use of accelerometers and laser Doppler vibrometers in gradient field induced vibration testing. Measures were conducted as a function of frequency over the range applicable to MRI gradient coil operation. Results indicate measurements obtained with accelerometers are comparable with laser Doppler vibrometry.

2622

3D dB/dt measuring bench design and building for safety assessment

Pauline Ferry[1], Lucien Hammen[2], Rada Alnnasouri[2], Jacques Felblinger[1,3,4], and Cédric Pasquier[1,2]

[1]*IADI, Université de Lorraine, Nancy, France,* [2]*Healtis, Nancy, France,* [3]*U947, INSERM, Nancy, France,* [4]*CIC-IT 1433, University Hospital, Nancy, France*

In this project, the goal was to build a 3D dB/dt measuring bench to map in the MR scanner gradients fields components and to detect critical positions for safety assessment. Such positions are mandatory to assess gradients induced vibrations worst cases as described in the ISO TS 10974.

2623

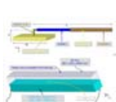

Applicability of lead electromagnetic model for an external wire with skin contact

Mikhail Kozlov[1] and Nikolaus Weiskopf[1]

[1]*Neurophysics, Max Planck Institute for Human Cognitive and Brain Sciences, Leipzig, Germany*

We calculated the electromagnetic (EM) model of an external wire with an electrode that contacts human skin at 123.2 MHz and evaluated the influence of the electrode dimension as well as the distance between the wire and the human body on the EM model using an approximation of the human body by a single tissue flat phantom. Our case study provided a strong evidence that at 123.2 MHz there is no worst-case distance between a wire and a human body that maximizes the power deposition for any wire length or electrode width.

2624

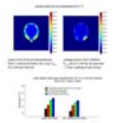

Evaluation of a thermal dose based safety concept for 7T pTx coils

Frank Seifert[1] and Bernd Ittermann[1]

[1]Physikalisch-Technische Bundesanstalt (PTB), Braunschweig und Berlin, Germany

We propose a straightforward procedure to calculate thermal dose values (CEM43) from upper limit values of tissue temperatures utilizing T-matrix formalism. The procedure is evaluated for a 7T 8-channel transmit/receive (pTx) head coil using the RF power data of a long duration neuroscience MR session and a scenario when heating of eye tissue is worst. The proposed approach, as a generalization of the thermal dose concept for body coils, is capable to determine reliably the risk of excessive tissue heating when using pTx coils.

2625

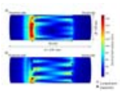

Experimental and simulated distribution of the RF electrical field inside a birdcage coil

Isabelle Saniour[1], Gwenaël Gaborit[2,3], Lionel Duvillaret[3], Anne-Laure Perrier[2], and Olivier Beuf[1]

[1]Univ. Lyon, CREATIS ; CNRS UMR 5220 ; INSERM U1206 ; INSA-Lyon ; UJM-Saint-Etienne ; Université Lyon1, Villeurbanne, France, [2]Univ. Savoie-Mont-Blanc, IMEP-LAHC, Le Bourget-du-Lac, France, [3]Kapteos, Sainte-Hélène-du-Lac, France

High-field MR systems bring additional safety issues regarding the patient. One of main concern is the heating effect caused by the high-frequency and high-power signals that can be picked up by the conductors. It is thus required to identify these regions and to quantify the electrical ***E***-field knowing that it is proportional to the square of the temperature elevation. For a direct measurement, an optical probe was used to perform a mapping of the ***E***-field distribution inside a birdcage of a preclinical MRI. Experiments and simulations were found similar with ***E***-field concentrations mainly located close to the capacitors.

2626

Quantification and impact of lead coupling on RF-induced heating in MRI.

Julie Kabil[1,2], Alexia Missoffe[1,2], Pierre-André Vuissoz[1,2], Cédric Pasquier[1,2,3], and Jacques Felblinger[1,2,4,5]

[1]Université de Lorraine, IADI, Nancy, France, [2]INSERM, U947, Nancy, France, [3]Healtis, Nancy, France, [4]CHRU Nancy, France, [5]INSERM, CIT-1433, Nancy, France

Patients carrying multiple leads like abandoned pacemaker leads are still denied MRI scans, as their situation is not currently covered by the existing safety guidelines. Therefore, to assess the impact of lead coupling regarding radiofrequency-induced heating, temperature measurements were performed on different types of simplified leads and coupling factors were introduced to quantify and evaluate the phenomenon. The lead coupling can have a significant impact on temperature and can either induce higher or lower temperatures compared to the case when the leads are alone, and thus should be considered in future MRI safety standards.

2627

An Inexpensive, Modular, DSP-based SAR Monitor for Multichannel Transmit Systems

Adam Mehina[1], Brandon Albrecht[1], Karim Damji[2], and Nicola De Zanche[3]

[1]Electrical and Computer Engineering, University of Alberta, Edmonton, AB, Canada, [2]Biomedical Engineering, University of Alberta, Edmonton, AB, Canada, [3]Oncology, University of Alberta, Edmonton, AB, Canada

We describe a modular power (SAR) monitor for multichannel systems whereby both the forward and reverse power of each channel are sampled and averaged on a dedicated board. Each board houses an inexpensive microcontroller with built-in ADCs for sampling the output of two power detectors. The microcontroller is programmed to perform time averaging, forward-reverse power subtraction and threshold detection. Multiple boards communicate simultaneously with a graphical user interface on a host computer.

2628

Test medium derivation for the safety assessment of RF-induced heating of leaded cardio implants during 1.5-T MRI

Aiping Yao[1,2], Earl Zastrow[1], and Niels Kuster[1,2]

[1]IT'IS Foundation, Zurich, Switzerland, [2]Department of Information Technology and Electrical Engineering, ETH-Zurich, Zurich, Switzerland

It is a common practice that an equivalent mathematical model of an implant is used to estimate in vivo power deposition caused by RF-implant interactions. The model is often derived under in vitro conditions. We assess the suitability of test media for RF-induced heating model derivation at 64 MHz. Based on simple generic leaded-implants, our preliminary analysis shows that the test medium specified in ASTM 2182 (ε_r = 78, σ = 0.47 S/m) may be appropriate for the safety assessment of leaded cardio implants with respect to RF-induced heating. Future analysis shall include implants with diverse topology and increased realism.

2629

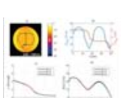

Test field diversification method for the safety assessment of RF-induced heating of AIMDs during 1.5-T MRI

Aiping Yao[1,2], Earl Zastrow[1], and Niels Kuster[1,2]

[1]IT'IS Foundation, Zurich, Switzerland, [2]Department of Information Technology and Electrical Engineering, ETH-Zurich, Zurich, Switzerland

Elongated AIMD can pick up the RF-energy during MR exposure, and locally deposit the energy in the tissue near its vicinity --- typically near the conductive electrodes. Current experimental assessment strategy is capable to achieve only a limited set of AIMD exposure conditions. In this work, we outline a method by which the exposure conditions may be diversified during experimental testing. The feasibility of the method is evaluated for three generic implants. The RF-induced deposited power of the AIMD over more than 1000 exposure conditions was evaluated and approximately 20 dB dynamic range in the deposited power was achieved.

2630

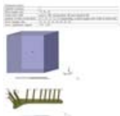

Investigation of RF-induced heating of distal radius implant system

Mikhail Kozlov[1,2] and Gregor Schaefers[1,3]

[1]MR:comp GmbH, Gelsenkirchen, Germany, [2]Max Planck Institute for Human Cognitive and Brain Sciences, Leipzig, Germany, [3]MRI-STaR GmbH, Gelsenkirchen, Germany

At 64 and 127.7 MHz RF-induced heating on or near nine distal radius implant systems was investigated. The 3-D temperature distribution after 15 minutes continuous excitation was obtained for a plane wave incident field. For one implant, random trials followed by a gradient-based investigation revealed three screw configurations that resulted in a high maximum temperature rise. Due to the smooth outcome of random trials followed by a gradient analysis, even relatively small simulation numbers allowed to reveal the configuration with the highest temperature rise for a given incident electrical field.

2631

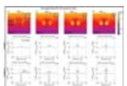

Smaller is better: Averaging mass considerations for the assessment of RF power deposition and MR safety of small implants

Eva Oberacker[1], Celal Oezerdem[1], Lukas Winter[1], and Thoralf Niendorf[1,2,3]

[1]Berlin Ultrahigh Field Facility (B.U.F.F.), Max Delbrück Center for Molecular Medicine in the Helmholtz Association, Berlin, Germany, [2]Experimental and Clinical Research Center (ECRC), a joint cooperation between the Charité Medical Faculty and the Max Delbrück Center for Molecular Medicine in the Helmholtz Association, Berlin, Germany, [3]MRI.TOOLS GmbH, Berlin, Germany

Assessment of the specific absorption rate (SAR) is a crucial tool when investigating the MR safety of implants. For RF power deposition assessments, local SAR averaged over m=10g of tissue is standard. Given the density in the human body ($\rho \approx 1g/cm^3$), this translates into a volume of $\approx 2x2x2cm^3$, which largely exceeds the size of many small implants and bears the risk of heavy underestimation of local peak SAR. Realizing these constraints together with the opportunities, we investigated discrete SAR averaging masses from m_{ave}=1g to m_{ave}=0.01g to define SAR averaging masses suitable for the safety assessment of small implants.

2632

Characterization of gradient-induced vibration: Can optical displacement sensors be replaced by miniature accelerometers?

Amin Douiri[1], Stefan Scholz[1], Wolfgang Görtz[1], Jakob Kreutner[1,2], and Gregor Schaefers[1,2]

[1]MR:comp GmbH, Gelsenkirchen, Germany, [2]MRI-STaR GmbH, Gelsenkirchen

In this study the suitability of a miniature accelerometer for vibration measurements according to ISO/TS 10974 was investigated. Gradient-induced vibration of a titanium disc was measured both with an electric accelerometer and an optical displacement sensor and the obtained datasets were compared. Taking the characteristics of the setup into account, the results indicate that the used type of accelerometer is suitable to meet the specifications given in ISO/TS 10974.

2633

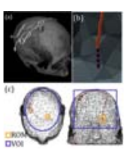

Parallel Transmission for Heating Reduction in Realistic Deep Brain Stimulation Lead Trajectories

Clare McElcheran[1], Laleh Golestanirad[2], Maria Iacono[3], Benson Yang[4], Kevan Anderson[5], Giorgio Bonmassar[2], and Simon Graham[4]

[1]University of Toronto, Toronto, ON, Canada, [2]Massachusetts General Hospital, MA, United States, [3]US Food and Drug Administration, Silver Spring, MD, United States, [4]Sunnybrook Health Sciences Centre, ON, Canada, [5]Innovere Medical, ON, Canada

Implanted devices for deep brain stimulation (DBS) create a safety concern during MRI due to heating at exposed tip of the lead. Parallel transmit (pTx) can potentially reduce heating of the lead tip when radiofrequency (RF) inputs are selected by an appropriate numerical optimization method. To date, however, this method has not considered how the trajectory of DBS leads affects heat deposition. The present work investigates the optimized pTx method for realistic DBS lead trajectories estimated from intra-operative computed tomography (CT) scans of nine patients, with simulations indicating statistically significant reduction in heating at lead tips while maintaining reasonable B_1^+-field homogeneity.

2634

Bilateral Breast Phantoms for Fusion to Human Voxel Models for Specific Absorption Rate (SAR) Simulations

Xin Li[1], Xianglun Mao[2], Thomas M Talavage[2], and Joseph V Rispoli[1]

[1]Weldon School of Biomedical Engineering, Purdue University, West Lafayette, IN, United States, [2]School of Electrical and Computer Engineering, Purdue University, West Lafayette, IN, United States

To comply with US Food and Drug Administration (FDA) guidelines of MRI safety, we propose a method to simulate Specific Absorption Rate (SAR) information with bilateral breast phantoms seamlessly integrated to a human model. This modeling method can be used with various breast phantoms. The simulation results indicate breasts with high glandular contents are more susceptible to SAR safety concerns compared to breasts with low glandular content.

2635

Attenuation of RF-induced currents within neuro-stimulation leads using a helical conductor design

Scott Kalpin[1], Norbert Kaula[2], and Ramez Shehada[3]

[1]Systems Engineering, Nuvectra Medical, Broomfield, CO, United States, [2]R&D, Nuvectra Medical, Broomfield, CO, United States, [3]R&D, Medical Technology Labs, La Mirada, CA, United States

RF currents will be induced within implanted neuro-stimulation leads when exposed to Magnetic Resonance Imaging (MRI) fields. Induced currents result in dissipative heating that manifests at the electrode/patient contact points. The ideal lead design will attenuate induced 64-MHz RF energy coming from the MRI while passing signals in the lower, intended neuro-stimulation frequency range. A Nuvectra™ SCS lead, having a helical conductor coiling design, is evaluated. Results of MRI phantom experiments demonstrate RF-induced power attenuation between -6.2 and -12.5 dB/meter when exposed to combined fields from 1.5 Tesla, 2.77 W/kg for minutes.

2636

Safety of intracranial EEG recordings at 1.5T MR: electromagnetic field simulation on a human body model

Özlem Ipek[1], Hassan Hawsawi[2], Joao Jorge[3], David W. Carmichael[4], Louis Lemieux[2], and Rolf Gruetter[3,5]

[1]Center for Biomedical Imaging (CIBM), Ecole Polytechnique Fédérale de Lausanne (EPFL), Lausanne, Switzerland, [2]Department of Clinical and Experimental Epilepsy, UCL Institute of Neurology, London, United Kingdom, [3]Laboratory of Functional and Metabolic Imaging, Ecole Polytechnique Fédérale de Laussanne (EPFL), Lausanne, Switzerland, [4]Developmental Imaging and Biophysics Section, UCL Institute of Child Health, London, United Kingdom, [5]Departments of Radiology, University of Lausanne and Geneva, Lausanne and Geneva, Switzerland

Excessive tissue heating is one of the major concerns when performing MRI in patients with icEEG due to the RF interaction between the electrodes and head tissue. No electromagnetic field simulations has been performed on in-vivo iEEG-MR setup due to the subgridding limitations of the small dimensions of these electrodes relative to those of the human body. We showed the feasibility of full body EM-field simulations based on realistic icEEG-electrode design. The proposed FDTD method for simultaneous icEEG-MRI gives results that are in broad agreement with previous experimental observations while allowing for measurements of SAR/heating along the entire implant length.

2637

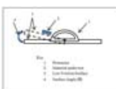

Magnetically Induced Torque Assessment per ASTM F2213 of Active Implantable Medical Device Lead Materials

Michael Childers[1] and Shiloh Sison[1]

[1]St. Jude Medical, Sylmar, CA, United States

This abstract presents magnetically induced torque measurements (per ASTM F2213) of materials commonly used in implantable leads. Implantable leads which are constructed solely from tested materials which pass the magnetically induced torque testing acceptance criteria of gravity torque, may not require magnetically induced torque testing per ASTM F2213 for MR conditionality with 3 T MR scanners.

2638

A Raspberry Pi® Based Portable Exposure Monitoring System for Magnetic Fields up to 7T.

Jens Groebner[1], Lukas M. Huber[2], Claus-Christian Glueer[2], and Rainer Herges[1]

[1]Otto Diels Institute for Organic Chemistry, Kiel University, Kiel, Germany, [2]Molecular Imaging North Competence Center, University Medical Center Schleswig-Holstein, Kiel, Germany

ICNIRP recommends reference values for movements in magnetic fringe fields of MRI systems. Several probes have been presented using custom interfaces to record data. To open this field of research to a wider public a Raspberry Pi® based magnetic field monitoring system was built. A probe consisting of both three Hall sensors and induction coils was used. All channels were converted into frequency via voltage-to-frequency-converters. Data was stored internally via python. Measurements were performed on a 7T small-animal MRI at the hand of MR-workers. Reference values were exceeded at the hand. No transient effects like vertigo or nausea were noticed.

2639

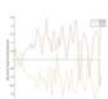

Evaluation of 50mm vs. 100mm Landmark Step Size for Pacemaker RF MRI Safety Evaluation

Lillian Boodaghians[1], Xin Huang[1], Xi Lin Chen[1], and Shiloh Sison[2]

[1]MRI Safety/Hardware Development, St. Jude Medical, Sylmar, CA, United States, [2]MRI Safety/Hardware Development, St. Jude Medical, Sunnyvale, CA, United States

Pacemakers undergo evaluation per ISO/TS 10974 to determine MRI safety. In a 64 MHz 1.5T RF coil, a quarter wavelength for RF radiation within blood is approximately 130mm, suggesting simulations performed with z-dimensional landmark step size of 100mm might not sufficiently capture RF effects on power deposition at lead electrodes and voltage levels at the generator, requiring a 50mm step size instead. Through simulations using validated transfer functions, human body models, and MRI RF coil models, it is shown that the difference in results between 50mm and 100mm simulations may be incorporated into model uncertainty and 100mm simulations are sufficient.

2640

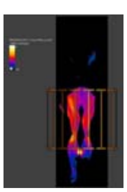

An investigation of skin/skin contact RF burns

Michael C Steckner[1] and Xin Chen[1]

[1]Toshiba Medical Research Institute, Mayfield Village, OH, United States

Third degree RF burns at skin/skin contact points have been reported. A thermal dose injury mechanism is widely assumed and thermal modeling results based on a well-documented calf burn report are presented. A hotspot ratio (Local:Whole Body SAR) of 86 results in various arbitrary CEM43 defined thresholds being exceeded after a few minutes of inadvertent skin/skin contact. The results support the hypothesis that skin/skin contact thermal injury burns are possible after several minutes of routine clinical scanning.

2641

A Method to Reduce Specific Absorption Rate for DBS Patients at 7 T MRI

Eunbi Ye[1], Youngdae Cho[1], Rupam Das[1], Hyun-Man Baek[2], and Hyoungsuk Yoo[1]

[1]University of Ulsan, Ulsan, Korea, Republic of, [2]Korea Basic Science Institute

The improtance of ultrahigh fields MRI has been rapidly increased due to its advantages in high resolution and signal-to-ratio. In this study, the SAR was analyzed in accordance with the conditions of insertion DBS and the electromagnetic field is controlled by multi-channel coil. Our reserch demonstrated the field control method using convex optimization from the fields data can be considered as a good strategy to drive the individual parameters of the RF coil for solving the inhomogeneity and SAR limitations, and it is safer for patients.

2642

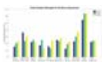

Clinically Relevant Gradient and RF Field Exposure Levels for General Neuro MRI Protocols at 3.0 T

Colin M McCurdy[1], William Bradfield Handler[1], Justin A Peterson[1], and Blaine A Chronik[1]

[1]Department of Physics and Astronomy, Western University, London, ON, Canada

Maximum fields for MRI systems pose overly restrictive guidelines for MR compatible device development. Logging of gradient strengths on a Siemens Prisma 3T MRI showed that during clinically relevant neuro scans, peak gradient strength reached 63.97 ± 0.05 mT/m, lower than the system maximum of 80 mT/m. In addition, peak slew rate during this protocol was measured to be 183.9 ± 0.2 T/m/s, compared to the system maximum of 200 T/m/s. This allows more flexibility for MR compatible device manufacturers due to the large discrepancy between the system maximum, and the practical maximums that the system reaches.

2643

Resolving Local SAR In Vitro from RF-Field Induced Heating of a 5.0 cm Long Titanium Rod at 64 MHz and 128 MHz

Krzysztof Wawrzyn[1], John Drozd[1], Jack Hendriks[1], William B. Handler[1], and Blaine A. Chronik[1]

[1]Department of Physics and Astronomy, Western University, London, ON, Canada

A methodology is developed relating the RF-induced temperature rise for an elongated conductive 5.0 cm long titanium reference rod to the local SAR produced by the incident electric field in the rods absence. Local SAR values at various spatial probing distributions in a gel filled phantom torso were systematically resolved and assessed at 64 MHz and 128 MHz using two different RF birdcage coils. A calibrated commercial E-field RMS probe and conventional standardized 10.0 cm long titanium rod were both used to validate the approach, showing good agreement. The 5.0 cm long rod shows promise as an additional approach for experimentally determining local SAR.

2644

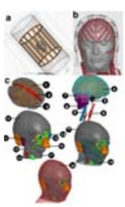

Numerical Simulation of Specific Absorption Rate (SAR) Induced in the Head as a Function of EEG Lead Conductivity during 256-channel dEEG/fMRI at 3T.

Seyed Reza Atefi[1,2], Peter Serano[3], Catherine Poulsen[4], and Giorgio Bonmassar[1,2]

[1]Harvard Medical School, Boston, MA, United States, [2]Massachusetts General Hospital, Boston, MA, United States, [3]Mechanical Engineering, University of Maryland, MD, United States, [4]Electrical Geodesics Inc., OR, United States

This study presents the numerical quantification of the relationship between the EEG lead conductivity and SAR induced in the head in EEG-fMRI at 3T and using a 256-channel dense array sensor net. SAR induced in the head normalized by the gold standard of no sensor net was an S-curve function of the EEG lead conductivity in the range 1S/m - $5.8 \cdot 10^7$ S/m, plateauing at 1 for lead conductivities below 10 S/m.

2645

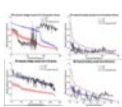

Comparison of High pass and Low pass Radio-Frequency coils in 1.5 T MRI safety assessments of Active Implantable Medical Devices

Hussain Fatakdawala[1], Xin Huang[1], and Shiloh Sison[1]

[1]St. Jude Medical, Sylmar, CA, United States

Active Implantable Medical Device (AIMD) safety assessments in MRI per ISO/TS 10974 may include computer simulations to evaluate radio-frequency (RF) induced heating of tissue and RF induced voltage at the device. It is not known if the differences in assessments between High-Pass (HP) and Low-Pass (LP) RF coils can be ignored. In this work, electric-fields and AIMD related RF induced heating and voltage results from HP and LP coils were compared. It was determined that there is a significant difference in safety assessment results between HP and LP coils (maximum symmetric mean absolute percentage error 50.21 ± 0.68%).

2646

Comparison of Pacemaker Lead Tip Heating at 1.5 T and 3T

Jessica A Martinez M[1,2], Volkan Acikel[2], Patrick Magrath[1,2], and Daniel B. Ennis[1,2]

[1]Department of Bioengineering, University of California, Los Angeles, CA, United States, [2]Department of Radiological Sciences, University of California, Los Angeles, CA, United States

Imaging patients with pacemakers at magnetic fields higher than 1.5T is widely contraindicated due to safety concerns. Since SAR increases with B_0^2 it is expected that lead tip heating (LTH) may increase substantially. Recent studies, however, provide evidence that contradicts this belief. Electromagnetic damping can occur in highly conductive materials at high field strengths and may result in lower LTH. Our objective was to compare LTH at 1.5T and 3T for five pacemakers with realistic implant configuration in the ASTM torso phantom. The results obtained showed that heating at 3T was not greater than 1.5T, which supports the argument that electromagnetic damping can result in lower LTH at higher field strengths.

2647

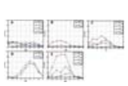

The Effect of Patient Orientation on Pacemaker Lead-Tip Heating at 1.5T

Jessica A Martinez M[1,2], Volkan Acikel[2], Patrick Magrath[1,2], and Daniel B. Ennis[1,2]

[1]Department of Bioengineering, University of California, Los Angeles, CA, United States, [2]Department of Radiological Sciences, University of California, Los Angeles, CA, United States

Patients with pacemakers or implantable cardioverter defibrillators (ICDs) may require an MRI exam of any body part. Clinical guidelines indicate that patient orientation in the scanner depends only on the body part under examination. Lead tip heating (LTH) is also a function of patient orientation. In this study our objective was to compare LTH for head-first and feet-first orientations for five pacemakers with realistic implant configuration in the ASTM torso phantom. Our results suggest that depending on the anatomical region examined, proper patient orientation in the MRI scanner can reduce LTH.

2648

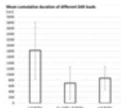

On the SAR load of typical head protocols at 7T

Oliver Kraff[1], Britta M Hüning[2], Andreas Deistung[1,3], Viktor Pfaffenrot[1], Andreas K Bitz[4], Mark E Ladd[1,4], and Harald H Quick[1,5]

[1]Erwin L. Hahn Institute for MRI, University Duisburg-Essen, Essen, Germany, [2]Clinic of Pediatrics I, Neonatology, University Hospital Essen, Essen, Germany, [3]Medical Physics Group, Institute of Diagnostic and Interventional Radiology, Friedrich Schiller University Jena, Jena, Germany, [4]Medical Physics in Radiology, German Cancer Research Center (DKFZ), Heidelberg, Germany, [5]High Field and Hybrid MR Imaging, University Hospital Essen, Essen, Germany

In this retrospective study, log files of the RF safety watchdog system were evaluated from 30 head exams performed at 7T in conjunction with the widely available 32-channel Nova Medical head coil. Head local SAR as reported by the PALI and the start/end times of each sequence were compared for eight different sequence types. This study aimed at providing insights into the expected RF exposure in UHF neurological protocols and may become useful in simulations to study realistic exposure scenarios, as well as to determine which sequences may be acceptable if a SAR reduction is required for a 7T exam.

2649

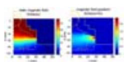

Static Magnetic Field (B0) Gradient Evaluation of a Compact 3T MR Scanner

Yunhong Shu[1], Shengzhen Tao[1], Mark Vermilyea[2], Thomas K Foo[3], Paul T Weavers[1], Joshua D Trzasko[1], John III Huston[1], and Matt A Bernstein[1]

[1]Radiology, Mayo Clinic, Rochester, MN, United States, [2]GE Global Research, Niskayuna, NY, United States, [3]GE Global Research

The strength of the static magnetic field produced by a MR system varies with the distance from the scanner. This generates a magnetic field spatial gradient (SG) which produces an attractive translational force on ferromagnetic objects that approach the system. Because the SG has bearing on patient safety related to implanted medical device, it is essential to understand the field distribution of novel magnets, since each design has its own unique SG pattern. We performed on-site evaluation of the magnetic field SG for a novel high-performance compact 3T MR scanner to ensure patient safety during the subsequent clinical trial.

2650

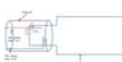

Dependence of RF-induced heating pattern during MRI of a single wire on its mode of entry in a dielectric medium

Pallab Bhattacharyya[1], Tanvir Baig[2], Bhumi Bhusal[2], Mark Lowe[1], Michael Martens[2], and Stephen Jones[1]

[1]Imaging Institute, Cleveland Clinic, Cleveland, OH, United States, [2]Physics, Case Western Reserve University, Cleveland, OH, United States

RF-induced heating of stereo encephalography (SEEG) electrodes during MRI scans could be of concern. Since the direction of entry of SEEG electrodes into brain can vary, heating of the tip of a single insulated copper wire (with bare tip) entering into a gel filled ASTM phantom axially (along the Z axis) and laterally (along the X axis) were measured as a function of the wire length. In this simple model of multi-wire multi-contact SEEG system, the resonating lengths (length with maximum heating) of the 2 configurations were same, while the lateral entry mode produced more heating.

2651

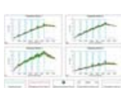

Validation of RF-induced temperature increase in a phantom: comparison of numerical simulations, MR thermometry and measurements from temperature sensors.

Shubham Gupta[1], R. Allen Waggoner[1], Keiji Tanaka[1], and Kang Cheng[1,2]

[1]Laboratory for Cognitive Brain Mapping, RIKEN Brain Science Institute, Saitama, Japan, [2]Research Resources Center, RIKEN Brain Science Institute, Saitama, Japan

In this study, we compared the temperature increase calculated by the simulations and measured by the MR-thermometry in a phantom with those measured by the optical temperature sensors, with good agreement between the methods. To ensure safety, IEC guidelines require simulations of SAR along with validation in phantoms. While it is likely impossible to simulate every possible pulse shape and phase combination in a pTx system with a large number of transmit channels, the results we present here suggest that simulations plus MR-thermometry could provide the verification currently lacking in pTx studies.

2652

The encoder as leading part of detecting torque on implants for a fully automated test method in accordance to ASTM F 2213 standard to improve MR-Safety

Karina Schuller[1], Dominik Süß[1], Manuel Stich[1], and Ralf Ringler[1]

[1]X-Ray & Molecular Imaging Lab, OTH Amberg-Weiden, Weiden, Germany

Due to magnetically induced torque, strong magnetic fields cause different effects on medical devices like implants. In accordance to that, this study should investigate by the help of a rotary encoder, if a rotary movement can be acquired to the ASTM standard. The used rotary encoder is specified with a high angular resolution, which enables detailed rotating motion detection, and its MR compatibility.

2653 

A Dedicated Measurement Probe for Quantitative Common Mode Measurements and Balun Efficiency.

Wolfgang Loew[1], Randy O Giaquinto[1], and Charles Dumoulin[1]

[1]*Imaging Research Center, Cincinnati Children's Hospital Medical Center, Cincinnati, OH, United States*

A method to measure common mode voltages and balun efficiency is described. Common mode voltages were measured with a novel common mode measurement probe and oscilloscope along a coaxial cable of a loaded loop coil which was excited with a network analyzer at 127.74MHz. The common mode measurements were performed on the loop coil without a balun and compared to the same loop coil with a balun to evaluate the common mode attenuation of the balun.

Traditional Poster

RF Coils & Systems

Exhibition Hall 2654-2674 Wednesday 16:15 - 18:15

2654 

A high density 24 channel array coil extendable to 48 channels for human cortical MRI at 7T.

Alexander JS Beckett[1], An T Vu[2], Scott Schillak[3], Lawrence L Wald[4], and David A Feinberg[1,5]

[1]*University of California, Berkeley, CA, United States,* [2]*University of California, San Francisco, CA, United States,* [3]*Virtumed, LLC, Minneapolis, MN, United States,* [4]*A. A. Martinos Center for Biomedical Imaging, Boston, MA, United States,* [5]*Advanced MRI Technologies, LLC, Sebastopol, CA, United States*

Coil arrays using smaller loop sizes allow increased signal close to the coil array. Such coil arrays with a large number of channels allow increased SNR across a large area of cortex, and accelerated imaging comparable to commercially available high-channel coils, with particularly good performance close to the coil array. These gains in SNR allow high-resolution (0.5mm isotropic) EPI

2655 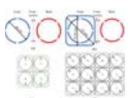

Towards a Flexible Transceiver Array for 7 T Cardiac MRI: Evaluation of Decoupling Ring Effects

Sajad Hosseinnezhadian[1,2], Roberta Frass-Kriegl[1], Sigrun Goluch[1], Michael Pichler[1], Jürgen Sieg[1], Marie Poirier-Quinot[2], Luc Darrasse[2], Ewald Moser[1], Jean-Christophe Ginefri[2], and Elmar Laistler[1]

[1]*Division MR Physics, Center for Medical Physics and Biomedical Engineering, Medical University of Vienna, Vienna, Austria,* [2]*IR4M (Imagerie par Résonance Magnétique Médicale et Multi-Modalités), Univ. Paris-Sud, CNRS, Université Paris-Saclay, Orsay, France*

In view of building a flexible 7T 2D coil array for cardiac MRI at 7 T, transmission line resonators (TLRs) with and without decoupling ring are investigated. Using 3D EM simulation and MR measurements for single elements, it could be shown that the presence of the decoupling ring does not perturb significantly the $B_1^+/\sqrt{P_{input}}$ distribution of the TLR. 3D gradient echo images for both TLRs with and without decoupling rings have been acquired. No significant degradation in the image quality due to the presence of the decoupling ring was observed.

2656 

A Sixteen-Channel Array Coil for Carbon-13 Spectroscopy of the Breast at 7T

Matthew Wilcox[1], Stephen Ogier[2], Sergey Cheshkov[3,4], Ivan Dimitrov[3,5], Craig Malloy[3,4,6], Steven M Wright[1,2], and Mary McDougall[1,2]

[1]*Biomedical Engineering, Texas A&M University, College Station, TX, United States,* [2]*Electrical and Computer Engineering, Texas A&M University, College Station, TX, United States,* [3]*Advanced Imaging Research Center, UT Southwestern Medical Center, Dallas, TX, United States,* [4]*Radiology, UT Southwestern Medical Center, Dallas, TX, United States,* [5]*Philips Medical Systems, Cleveland, OH, United States,* [6]*Internal Medicine, UT Southwestern Medical Center, Dallas, TX, United States*

Biomarkers detectable by carbon-13 NMR spectroscopy have known correlations with breast cancer characterization, but in vivo 13C spectroscopy has been limited by low SNR. To counteract this, a 16-element receive coil and isolating preamplifier box was constructed for carbon-13 spectroscopy of the breast at 7 Tesla. The array was characterized on the bench and showed good results in terms of ease of tuning, low element-to-element coupling and Q values. Scanner testing using the coil was preliminary but showed successful 1H and 13C transmission and that array elements were individually able to acquire spectra.

2657 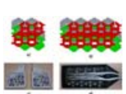

A Modular, Scaleable, and Customizable Phased Array Structure Suitable for Ultra-High Channel Phased Arrays

Wolfgang Loew[1], Christopher Ireland[1], Matthew Lanier[1], Brynne Williams[1], Matthew Batie[2], Yu Li[1], Randy O Giaquinto[1], Ron Pratt[1], and Charles Dumoulin[1]

[1]*Imaging Research Center, Cincinnati Children's Hospital Medical Center, Cincinnati, OH, United States,* [2]*Clinical Engineering, Cincinnati Children's Hospital Medical Center, Cincinnati, OH, United States*

A novel three-layer frame was developed to enable scalable phased-array coils. The geometry of the three-layer frame allows a single 12-element tile to dock with up to four identical tiles. When adjacent tiles are docked, the overlap of coils in adjacent tiles is identical to the coil overlap within a tile. Two phased-arrays setups using 12-element tiles and integrated balun coil technology were constructed. The first contained two separate tiles and the second had two interconnected tiles. The phased-array coils were evaluated with phantom imaging experiments and with multiple in-vivo experiments.

2658 

Optimal array configuration for cerebral cortex MRI at 7T: six center-fed dipoles with two loops RF coil array

Jérémie Daniel Clément[1], Rolf Gruetter[1,2,3], and Özlem Ipek[4]

[1]CIBM - LIFMET, Ecole Polytechnique Fédérale de Lausanne, Lausanne, Switzerland, [2]Department of Radiology, University of Geneva, Geneva, Switzerland, [3]Department of Radiology, University of Lausanne, Lausanne, Switzerland, [4]CIBM-AIT, Ecole Polytechnique Fédérale de Lausanne, Lausanne, Switzerland

Searching for optimal RF coil array for whole-brain MR applications, central-fed dipole was compared with fractionated dipole in a single and RF coil array configurations with combination of loop coils in measurements and electromagnetic field simulations in terms of B_1^+ transmit efficiency, field uniformity, SAR and mutual coupling in an array. High transmit field performances were shown over the cerebral cortex by using phase-only shimming with six center-fed dipoles with two loops RF coil array on experimentally measured B_1^+-maps and anatomical MR images.

2659

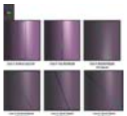

Structure Adjustment of Surface Dipole Antenna Elements for Body Imaging at 7 Tesla MRI

Suchit Kumar[1], Young-Seung Jo[2,3], Jeong-Hee Kim[4], Chulhyun Lee[3], and Chang-Hyun Oh[1,2,3,4,5]

[1]Department of Biomicrosystem Technology, Korea University, Seoul, Korea, Republic of, [2]Department of Electronics and Information Technology, Korea University, Seoul, Korea, Republic of, [3]Korea Basic Science Institute, Cheongju, Chungcheongbuk-do, Korea, Republic of, [4]Research Institute for Advanced Industrial Technology, Korea University, Sejong City, Korea, Republic of, [5]ICT Convergence Technology for Health & Safety, Korea University, Sejong City, Korea, Republic of

In ultra-high-field magnetic resonance imaging (UHF-MRI), body imaging suffers from B1 inhomogeneity due to relatively short wavelength. A range of new radio frequency (RF) coil designs has been proposed to overcome this problem. As previously reported, dipole antenna had been proposed to address this B1+ inhomogeneity problem for body imaging. In this paper, structural adjustment of dipole antenna has been tried for parallel transmission to improve overall B1+ homogeneity. Surface dipole antennas with several structures are tried and compared with our top-hat dipole antenna array reported previously. Also, static RF shimming was employed to evaluate the B1 uniformity.

2660

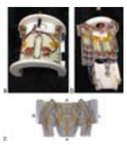

An adjustable 8-channel receive coil for population studies of marmosets

Kyle M Gilbert[1], Joseph S Gati[1], Peter Zeman[1], David J Schaeffer[1], Stefan Everling[1], and Ravi S Menon[1]

[1]Centre for Functional and Metabolic Mapping, The University of Western Ontario, London, ON, Canada

An eight-channel RF coil was developed for imaging the common marmoset at 9.4T. The coil was adjustable in width to accommodate different head sizes while maintaining high SNR, thereby facilitating the study of larger cohorts of animals. Tuning and matching of the coil did not require adjustment over the range of potential head sizes. EPI time series were acquired, showing minimal geometric distortion with a two-fold reduction factor. A two-fold reduction factor could be achieved in both the left-right and anterior-posterior directions.

2661

Fifteen-channel receive coil for high acceleration rates in UHF marmoset imaging

Kyle M Gilbert[1], Joseph S Gati[1], L Martyn Klassen[1], Stefan Everling[1], and Ravi S Menon[1]

[1]Centre for Functional and Metabolic Mapping, The University of Western Ontario, London, ON, Canada

A 15-channel receive coil, in conjunction with a 2-channel transmit coil, was developed for imaging the common marmoset at 9.4T. The high channel count produced low geometry factors while accelerating in EPI acquisitions, thereby reducing geometric distortions with minimal impact on the SNR. This demonstrates the utility and feasibility of employing higher channel counts for functional imaging of the marmoset.

2662

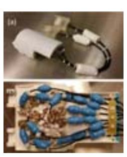

A 10-element receive-only RF coil array for imaging the brain of awake marmosets

Wen-Yang Chiang[1,2], Cecil Chern-Chyi Yen[2], Mary P. McDougall[1], and Afonso C. Silva[2]

[1]Department of Biomedical Engineering, Texas A&M University, College Station, TX, United States, [2]Cerebral Microcirculation Section, National Institute of Neurological Disorders and Stroke, National Institutes of Health, Bethesda, MD, United States

A 10-element head RF coil array was developed for imaging the brain of awake marmosets. A soccer ball design was used to improve whole brain coverage and parallel imaging acceleration when compared to our previous designs. Coil clip and PLA cement were introduced to help place the small coil elements on surfaces of irregular shape and optimize geometric decoupling. The matching network provided independent adjustments of tuning, matching, active detune and preamp decoupling, greatly simplifying the construction of coil arrays in space-limited applications. Molded-in foam padding was also introduced to provide additional comfort during awake marmoset imaging.

2663

Ladder and Overlapped Phased Array Coil Comparison for Neck Imaging at 3 Tesla

Michael J Beck[1], Dennis L Parker[1], and J Rock Hadley[1]

[1]Radiology and Imaging Sciences, University of Utah, Salt Lake City, UT, United States

A ladder and overlapped phased array coils were constructed with the same number of channels and overall dimensions to see how much of a SNR performance difference there was between the two coil construction techniques. The results show that between 2 and 12 cm within a cylindrical phantom the difference between SNR was less than 3%. With negligible performance difference the ladder array can be a viable alternative to overlapped arrays if a simpler coil construction process is desired.

2664

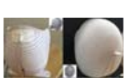

Quadrature Head Coil for Brain Imaging at 6.5 mT

Neha KOONJOO[1,2], Bryce Primavera[1,3], Jason P Stockmann[1,2], Thomas Witzel[1,2], Lawrence L Wald[1,2], and Matthew S Rosen[1,2,3]

[1]Department of Radiology, MGH/AA Martinos Center for Biomedical Imaging, Boston, MA, United States, [2]Harvard Medical School, Boston, MA, United States, [3]Department of Physics, Harvard University, Cambridge, MA, United States

Highly-resolved proton imaging is challenging in the millitesla regime. With the aim of enhancing our previous single-channel spiral head coil for operation at 276 kHz, a quadrature head coil was designed, comprised of 2 layers (inner and outer) producing orthogonal B1 fields. Images acquired with the new quadrature coil had the same signal magnitude when compared to the single-channel coil. However, the expected √2-factor signal enhancement in combined SNR was not fully realized due to a 30% higher noise floor observed in one quadrature. Improvements in gradient amplifier filtering will significantly improve the SNR.

2665

Dual-Tuned RF Coil system for Parallel Imaging of Human Lungs Using Perfluorinated Gases

Vishal Virendra Kampani[1], Randall Wayne Jones[1], Hal Cecil Charles[2], and Natalie Hussey[1]

[1]ScanMed, LLC, Omaha, NE, United States, [2]Duke University, Durham, NC, United States

To create a dual-tuned (^{1}H & ^{19}F) receive-only surface coil array for pulmonary functional imaging. This satisfies an unmet clinical need because there is currently no widely accessible 3D measure of regional lung function. As a result, the current standard of care for diagnosis and evaluation of lung disease relies nearly exclusively on global measures such as spirometry. The technical significance of this proposal is that the implementation of parallel imaging for ^{19}F MRI would provide a means to shorten breath hold times with marginal SNR impact as well as facilitate the development of real time free breathing image acquisitions.

2666

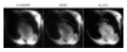

Ultra-high-field CAIPIRINHA modulated parallel transmit excitation for homogenous image reconstruction without RF shimming

Iulius Dragonu[1], Craig Buckley[1], Matthew D Robson[2], and Aaron T Hess[2]

[1]Diagnostic Imaging, MR, Siemens Healthcare Ltd, Frimley, United Kingdom, [2]Radcliffe Department of Medicine, University of Oxford, Oxford, United Kingdom

Ultra-high-field (UHF) provides higher SNR than conventional, clinically available field strengths. However, UHF suffers from heterogeneous transmit B_1^+ fields. At 7 T, the shortened transmit radio-frequency (RF) wavelengths have a similar value to the dimensions of the human head/thorax which may result in signal cancellation and local signal dropouts. In this paper, we propose a novel imaging scheme based on simultaneous excitation with all transmit channels. Controlled aliasing is used to encode each transmit channel independently which we term Tx-CAIPIRINHA.

Tx-CAIPIRINHA has been demonstrated in-vivo. The concept uses the linear superposition of B_1^+ fields via the excitation flip angle which only holds true in the low flip angle regime. When normalizing to transmit efficiency, Tx-CAIPIRINHA achieved a marginally higher SNR than B_1^+ shimming, demonstrating the constructive combination of transmit sensitives throughout the image.

2667

Towards Routine Body Imaging at 7T Using a Hybrid Dipole and Birdcage Coil Array

Jan Paska[1,2], Martijn Cloos[1,2], and Graham C Wiggins[1,2]

[1]Center for Biomedical Imaging, Department of Radiology, NYU School of Medicine, New York, NY, United States, [2]Center for Advanced Imaging Innovation and Research (CAI2R), NYU School of Medicine, New York, NY, United States

Body imaging at 7T is challenging due to wavelength effects, a low sensitivity in deep tissue1, and a large variation in body sizes across the patient population. A common approach is to use close fitting coils or dipoles2,3,4, which exhibit a high transmit and receive sensitivity and are fairly load independent, but lack the easy handling necessary for routine clinical use. We aim to construct an RF coil array for general purpose body imaging for routine use that is robust, easy, and safe to handle, while retaining adequate sensitivity in the deeper regions. Given these boundary conditions, we settled on a stand-off design5 with an RF shield. Thus, consciously sacrificing some sensitivity to improve handling and safety. After extensive optimization we converged to an optimal coil array consisting of a transceive dipole array complemented with a birdcage array for reception only. The array was completed and a sensitivity analysis with respect to body sizes was performed.

2668

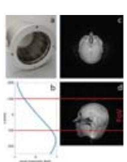

An RF birdcage coil designed for an insert gradient coil dedicated to short-T2 MRI

Manuela B. Rösler[1], Markus Weiger[1], David O. Brunner[1], Thomas Schmid[1], Romain Froidevaux[1], and Klaas P. Pruessmann[1]

[1]Institute for Biomedical Engineering, ETH Zürich and University of Zurich, Zurich, Switzerland

Two major challenges for MRI of short-T2 tissues are creating large gradient strengths and avoiding signal contamination from hardware parts, in particular the RF coils. In this work, to enable short-T2 MRI with a dedicated insert gradient coil, an RF birdcage coil was designed with a) minimized background signal and b) optimized B1 field to prevent aliasing associated with the limited monotonic range of the gradient.

2669

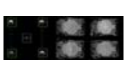

Multiple-Mouse Magnetic Resonance Imaging with CryoProbes

Aidin Arbabi[1], Dulcie A Vousden[1,2], Leigh Spencer Noakes[1], Jun Dazai[1], Shoshana Spring[1], John G Sled[1,2], Jason P Lerch[1,2], Mark Henkelman[1,2], and Brian J Nieman[1,2,3]

[1]Mouse Imaging Centre, Hospital for Sick Children, Toronto, ON, Canada, [2]Medical Biophysics, University of Toronto, Toronto, ON, Canada, [3]Ontario Institute for Cancer Research, Toronto, ON, Canada

Multiple-mouse MRI was implemented on a 7-Tesla magnet with four Cryogen (liquid helium)-cooled radio frequency probes. The high signal-to-noise ratio offered by the probes enabled spatial resolutions of 60 μm isotropic in <2 hours, a significant improvement for in vivo anatomical imaging of the mouse brain. Several 3D pulse sequences including FLASH/MP2RAGE/RARE were implemented for multiple-mouse acquisition. Manganese-enhanced T1-weighted images were obtained at two different resolutions of 60 μm and 75 μm. Results demonstrate the combined benefits of cryogen-cooled coils and multiple-mouse MRI.

2670

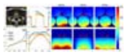

An SNR Optimized Quadrature Reception Posterior Array for Prostate Imaging at 3 Tesla

Jorge Chacon-Caldera[1], Alexander Fischer[1], Matthias Malzacher[1], and Lothar R. Schad[1]

[1]Computer Assisted Clinical Medicine, Medical Faculty Mannheim, Heidelberg University, Mannheim, Germany

Increasing signal-to-noise-ratio (SNR) in prostate MRI could facilitate the diagnosis and characterization of prostate cancers. In this work, we built a quadrature posterior surface array that aims to increase local SNR at the prostate. The coil was compared to 3 and 9 channels of the standard spine array using phantom measurements. Respectively, SNR gains of 12 and 9% were obtained using a realistic region-of-interest (ROI). Further work will be undertaken to translate the SNR gains to *in-vivo* prostate imaging at 3T.

2671

New design of flexible surface coil with variodes and remote detuning

Wenming Li[1], Shu Du[1], and Jianmin Wang[2]

[1]RF-R&D, Siemens (Shenzhen) Magnetic Resonance Ltd., Shenzhen, People's Republic of China, [2]R&D, Siemens (Shenzhen) Magnetic Resonance Ltd., Shenzhen, People's Republic of China

New design of flexible surface coil was presented. Voltage-controlled variodes instead of trimmers are used for remote coil frequency adjustment; λ/4 impedance transforming circuit are used to enable remote detune, thus detune circuits with big rigid components are moved out from the antenna part. By doing this, the antenna is covered by soft foam seamlessly which improved the flexibility significantly. Design was tested on four-element arrays. Experiments on both phantom and invivo testing show good results with this design.

2672

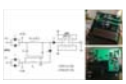

Human Brain Imaging at 7T With On-coil Transceivers

Natalia Gudino[1], Qi Duan[1,2], Jacco A de Zwart[1], Stephen J Dodd[1], Joe Murphy-Boesch[1], Peter van Gelderen[1], and Jeff H Duyn[1]

[1]Advanced MRI Section, LFMI, NINDS, National Institutes of Health, Bethesda, MD, United States, [2]Food and Drug Administration, Silver Spring, MD, United States

On-coil current-source switch-mode amplification presents high power efficiency, allows direct control of the transmit field (B1), and decoupling of elements through the amplifier output impedance. These are important advantages over conventional remote voltage-mode quasilinear amplification that should allow more efficient and safer implementation of a multi-channel transmit system. Following this approach, we present an optically controlled transceiver design that was used for initial safety assessment of the technology toward the implementation of a high channel-count pTx array for brain imaging at high-field. We acquired human brain images with this technology at 7T

2673

An adjustable field-of-view rung element for 7T transmit array coils using forced current excitation

Jiaming Cui[1], Chenhao Sun[1], Dheyaa Alkandari[1], and Steven Wright[1]

[1]Electrical& Computer Engineering, Texas A&M University, College Station, TX, United States

This abstract reports a switchable coil element which uses “forced current excitation”. The coil consists of three aligned rungs, with a total length of 37 cm. Any one or more of three rungs can be easily selected to provide a variable length or position field-of-view. The forced current approach ensures equal current on the selected rungs to give a uniform field distribution along the length of the field-of-view. Bench measurements demonstrate the expected efficiency improvement when only a single rung is selected and the uniform field pattern.

2674

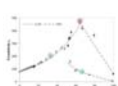

Optimization via Ultra-high Permittivity Materials of Pad Effects in Dielectric Shimming at 7 Tesla MRI

Ana Luisa Neves[1,2], Redha Abdeddaim[1], Stefan Enoch[1], Jerome Wenger[1], Johann Berthelot[1], Anne-Lise Adenot-Engelvin[3], Nicolas Mallejac[3], Franck Mauconduit[4], Lisa Leroi[5], Alexandre Vignaud[5], and Pierre Sabouroux[1]

[1]Aix Marseille Univ, CNRS, Centrale Marseille, Institut Fresnel, Marseille, France, [2]Centre Commun de Resources en Micro-ondes, Marseille, France, [3]CEA-DAM Le Ripault, Monts F-37260, France, [4]Siemens Healthineers, Saint Denis, France, [5]CEA, DRF, i2BM, NeuroSpin, UNIRS, Paris-Saclay University, Gif-sur-Yvette, France

The influence of air fraction on the permittivity of $BaTiO_3$ aqueous mixtures was assessed, with the aim of obtaining high permittivity mixtures. For extremely saturated mixtures (>50%v/v), the air fraction of the mixture plays a great role in determining ε_r, and by applying high pressure it is possible to go beyond the maximal value described in dielectric shimming literature. A $BaTiO_3$ 1cm-thick pad was manufactured (ε_r =470) and tested in a 7T MRI, as well as a conventional saturated pad (≈40%v/v, ε_r=200). Results show an overall signal improvement when using higher permittivity pads and the possibility to reduce pad-thickness.

Traditional Poster

Gradient, Shim & Magnet Technology

2675
magna cum laude

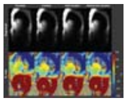

Detailing and Enhancing Respiratory Motion Induced Myocardial B0 Field Dispersion at 7.0 T: Implications for Cardiac Imaging and Spectroscopy at Ultrahigh Magnetic Field Strengths

Till Huelnhagen[1], Ariane Fillmer[2], Antje Els[1], Florian Schubert[2], Bernd Ittermann[2], and Thoralf Niendorf[1,3,4]

[1]Berlin Ultrahigh Field Facility (B.U.F.F.), Max Delbrück Center for Molecular Medicine in the Helmholtz Association(MDC), Berlin, Germany, [2]Physikalisch Technische Bundesanstalt (PTB), Berlin, Germany, [3]Experimental and Clinical Research Center, a joint cooperation between the, Charité Medical Faculty and the Max Delbrück Center for Molecular Medicine in the Helmholtz Association, Berlin, Germany, [4]DZHK (German Centre for Cardiovascular Research), partner site Berlin, Berlin, Germany

Respiratory motion induced B_0 field fluctuations, constitute a challenge for B_0 sensitive CMR like spectroscopy. Accommodating CMRS in a single breath-hold is elusive if not prohibitive. Motion corrected approaches under free breathing were demonstrated to substantially improve CMRS. Yet, B_0 field fluctuations over the respiratory cycle may compromise spectral resolution and data integrity. A compensation strategy like dynamically updated first order shims synchronized with the respiratory motion, offers the potential to enhance spectral quality and permits scan time shortening. This work details respiratory motion induced B_0 fluctuations in the interventricular septum and examines the capability of linear shimming for compensation of myocardial B_0 fluctuations.

2676

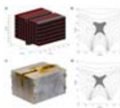

Unilateral Linear Halbach magnets for single sided magnetic resonance: generalized design framework and experimental validation

Ashvin Bashyam[1,2], Matthew Li[2,3], and Michael Cima[2,4]

[1]Electrical Engineering & Computer Science, Massachusetts Institute of Technology, Cambridge, MA, United States, [2]David H. Koch Institute For Integrative Cancer Research, Massachusetts Institute of Technology, Cambridge, MA, United States, [3]Harvard–MIT Program of Health Sciences and Technology, Massachusetts Institute of Technology, Cambridge, MA, United States, [4]Department of Materials Science and Engineering, Massachusetts Institute of Technology, Cambridge, MA, United States

Single-sided NMR has the potential for broad utility, especially as a portable diagnostic for disorders in fluid regulation. These sensors require a remote, high field, uniform magnetic field to achieve sufficient sensitivity. We demonstrate a new magnet geometry, the Unilateral Linear Halbach, that combines design principles from sweet-spot and linear Halbach magnets to achieve this goal. Sensitivity analysis using finite element analysis produces a generalized framework for Unilateral Linear Halbach design. Experimental validation through the fabrication of a magnet assembly shows close agreement with the simulated magnetic field. Unilateral Linear Halbach magnets increase the sensitivity, portability, and versatility of single sided NMR.

2677
summa cum laude

A new human-scale fast field-cycling MRI system for clinical applications

Peter J. Ross[1], Lionel M. Broche[1], Gareth R. Davies[1], and David J. Lurie[1]

[1]Aberdeen Biomedical Imaging Centre, University of Aberdeen, Aberdeen, United Kingdom

Fast-field cycling MRI is a novel technique that involves cycling the main magnetic field during image acquisition. By doing this, information on the magnetic field dependence of parameters such as the T_1 relaxation time can be investigated and exploited as a new form of endogenous image contrast. In this abstract we present progress on a new human-scale fast field-cycling MRI system with a detection field of 0.2 T.

2678

Towards ultimate air-core magnetometer sensitivity for ultra-low field MRI: A design method

Ruben Pellicer-Guridi[1], Michael Vogel[1], David Reutens[1], and Viktor Vegh[1]

[1]Centre for Advanced Imaging, UQ, Brisbane, Australia

Superconducting quantum interference devices (SQUIDs) are highly sensitive magnetometers and they have found application in ultra-low field MRI. However, they require cryogenics and their noise performance is hindered by external noise sources and the strong fields employed in pre-polarised MRI experiments. Air-core magnetometers provide an attractive alternative, as they are highly sensitive, robust and relatively cheap to manufacture. Our goal is to provide of a method to optimise the sensitivity of these devices. In this work we propose an accurate numerical model and the use of a genetic algorithm to consider previously unexplored coil configurations.

2679

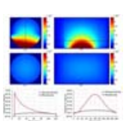

Preliminary Metamaterial Design and Fabrication for MRI at 3T

Chao Luo[1], Xiaoqing Hu[1], Xiaoliang Zhang[2,3], Xin Liu[1], and Ye Li[1]

[1]Lauterbur Research Center for Biomedical Imaging, Shenzhen Institutes of Advanced Technology, Chinese Academy of Sciences, Shenzhen, People's Republic of China, [2]Department of Radiology and Biomedical Imaging, University of California San Francisco, CA, USA, CA, United States, [3]UCSF/UC Berkeley Joint Graduate Group in Bioengineering, San Francisco, CA, USA, CA, United States

In this paper, we designed and fabricated a kind of metamaterial with 9×9 cells, which bent on phantom and inserted to a birdcage volume coil to investigate the performance for 3T MRI. The results of simulations and phantom experiments agreed with each other very well indicate that the proposed metamaterial is able to increase the B1+ fields in some region closed to the surface of phantom. This improvement of B1+ fields will benefit to 3T MRI targeted clinical applications.

2680

Dual-layered multi-channel B0 and RF coil setup for an improved shimming performance at 9.4 Tesla

Christian Mirkes[1], G. Shajan[1,2], Ali Aghaeifar[1], Irena Zivkovic[1], Kai Buckenmaier[1], and Klaus Scheffler[1,3]

[1]High-Field Magnetic Resonance Center, Max Planck Institute for Biological Cybernetics, Tübingen, Germany, [2]Institute of Neuroscience and Psychology, University of Glasgow, Glasgow, United Kingdom, [3]Biomedical Magnetic Resonance, University Hospital Tübingen, Tübingen, Germany

Multiple local shim coils can be used to improve the B_0 homogeneity at ultra-high field. In this work, a dual-layered multi-channel B_0 and RF coil setup is presented that allows a flexible design of the shim coil without influencing the RF performance. It is shown that a 16 channel B_0 coil in combination with a standard 2nd order spherical harmonics (SH) shim system can achieve a higher degree of B_0 homogeneity than a 3rd order SH shim system in the case of whole-brain shimming.

2681

An insert gradient for zero-echo-time imaging with 200 mT/m at full duty cycle

Markus Weiger[1], Johan Overweg[2], Manuela Barbara Rösler[1], Romain Froidevaux[1], Franciszek Hennel[1], Bertram Jakob Wilm[1], Alexander Penn[1], Urs Sturzenegger[3], Wout Schuth[4], Menno Mathlener[4], Martino Borgo[4], Peter Boernert[2], Christoph Leussler[2], Roger Luechinger[1], Benjamin Emanuel Dietrich[1], Jonas Reber[1], David Otto Brunner[1], Thomas Schmid[1], Laetitia Vionnet[1], and Klaas Paul Pruessmann[1]

[1]Institute for Biomedical Engineering, University and ETH Zurich, Zurich, Switzerland, [2]Philips GmbH Innovative Technologies, Hamburg, Germany, [3]Philips AG, Zurich, Switzerland, [4]Futura Composites BV, Heerhugowaard, Netherlands

Zero-echo-time (ZTE) techniques enable imaging of tissues with very short T2s, e.g. bone or myelin. Their performance directly scales with gradient strength G, which depends on the target T2 and spatial resolution. With present-day gradients the spatial resolution for T2s on the order of 100 µs is limited to several millimetres. To improve the resolution, considerably higher gradient strengths are required. As a further challenge of ZTE sequences, the strong gradients are applied with full duty cycle. The goal of this work was to develop a gradient coil that meets these challenges, offering very high amplitude at full duty cycle.

2682

Open-Source Acquisition-speed slice-by-slice controller for 32 coil B0 shimming.

Nicolas Arango[1], Jason P. Stockmann[2,3], Thomas Witzel[2,3], Lawrence L. Wald[2,3], and Jacob White[1]

[1]Electrical Engineering and Computer Science, Massachusetts Institute of Technology, Cambridge, MA, United States, [2]A. A. Martinos Center for Biomedical Imaging, Massachusetts General Hospital, Charlestown, MA, [3]Harvard Medical School, Boston, MA

Accurate B0 shimming with close-fitting coil arrays can improve brain imaging at 3T and 7T, but slice-optimizing the shimming during acquisition requires fast redistribution of dozens of multi-amp coil currents. Our open-source, low-cost ($80/channel) driver system can redistribute fifty amps to thirty-two coils in milliseconds, with milliamp accuracy. The system uses an easily reprogrammed microcontroller, optical fiber isolation, and thirty-two current-feedback coil-drivers (described previously). When used to drive sixty-four slice-specific sets of currents in a novel 32-coil shim array, stretching in an EPI brain scan was substantially reduced, without introducing driver artifacts.

2683

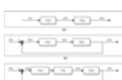

Decoupling Controller Design for Real-time Feedback of B0 Shim Systems

Paul Chang[1,2], Sahar Nassirpour[1,2], and Anke Henning[1,3]

[1]MPI for Biological Cybernetics, Tuebingen, Germany, [2]IMPRS for Cognitive and Systems Neuroscience, Eberhard University of Tuebingen, Tuebingen, Germany, [3]Institute of Physics, Ernst-Moritz-Arndt University Greifswald, Greifswald, Germany

Real-time B0 feedback has been shown to be beneficial for the controlling of B0 fluctuations. However, update rates that have been reported are slow (~100ms) and either use pre-emphasis to correct for the coupling and faster dynamics of the system or only use control the frequency

We show that for faster update rates (±1ms) pre-emphasis (i.e. dynamic decoupling) is not required and that static decoupling can perform equally well or better.

2684

Dynamic B0 Shim Controller for Digital Pre-emphasis with Sub-millisecond Update Rate

Paul Chang[1,2], Sahar Nassirpour[1,2], and Anke Henning[1,3]

[1]MPI for Biological Cybernetics, Tuebingen, Germany, [2]IMPRS for Cognitive and Systems Neuroscience, Eberhard University of Tuebingen, Tuebingen, Germany, [3]Institute of Physics, Ernst-Moritz-Arndt University Greifswald, Greifswald, Germany

High-order dynamic B0 shimming has been shown to improve the shim quality for multi-slice acquisition schemes. However, for gradient intensive sequences, eddy currents become a major problem and pre-emphasis is required. The pre-emphasis can be done flexibly with the use of digital filters as they can drive arbitrary-shaped waveforms and are scalable to a larger number of channels.

In this work, we design and implement a system to perform dynamic B0 shimming with digital pre-emphasis with a very fast update rate. The setup is then tested for performing pre-emphasis on a 9.4T scanner.

2685

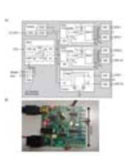

A scalable, MR compatible temperature measurement and control system

David Otto Brunner[1], Jonas Reber[2], Simon Gross[2], and Klaas Paul Pruessmann[2]

[1]Institute for Biomedical Engineering, University and ETH Zurich, Zurich, Switzerland, [2]University and ETH Zurich, Zurich, Switzerland

Tight temperature control of various devices is required to guarantee highly stable experimental conditions. E.g. B_0 field shifts induced by heating of shim irons or gain changes induced in preamplifiers can be avoided by oven controlling the critical components of the device. Furthermore, a recently presented approach of active shimming with controlled magnetic materials requires tight temperature control of a large count of devices in parallel in the bore. For such applications, we present a 14 channel, low power, MR compatible temperature measurement and control system which can be parallelized for a scalable channel count.

2686

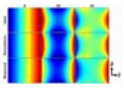

Minimum Current Ripple in the Gradient Array System by Applying Optimum-Phase Pulse-Width Modulation Pattern

Soheil Taraghinia[1], Koray Ertan[1], and Ergin Atalar[1]

[1]National Magnetic Resonance Research Center (UMRAM), Bilkent University, Ankara, Turkey

Phase-shifted Pulse Width Modulation (PWM) technique is implementable in stacked and parallel configuration of the H-bridge gradient amplifiers. However, in the gradient array systems where one stage amplifier is sufficient to drive each element, phase-shifted PWM is not feasible. In this work, similar technique is implemented by utilization of the coupling between the elements of the array and finding the optimized phases for each channel in order to have minimum current ripples. This method is tested for different gradient fields and high ripple reduction percentages achieved both in simulations and experiments.

2687

A Convertible Magnet Array and Solenoid Coil for a Portable Magnetic Resonance Imaging (MRI) System

Zhi Hua Ren[1], Wenshen Zhou[1], and Shao Ying Huang[1,2]

[1]EPD, Singapore University of Technology and Design, Singapore, Singapore, [2]Department of Surgery, National University of Singapore, Singapore, Singapore

A magnetic resonance imaging (MRI) for outdoor *in-situ* scanning is promising for biological studies. Here we propose a portable MRI system in which both the magnet array and the transceiver coil can be physically opened and closed. This is for imaging long objects in situ where cutting the object and fitting it into a bore for scanning is not an option. A convertible magnet array is designed where the force to open and to close the magnet array is minimized based on an analytical solution. Meanwhile, a convertible solenoid coil is proposed as an RF transceiver coil.

2688

An open source PXIe platform for MRI instrumentation development

Matthew Bourne[1], Robin Dykstra[1], and Sergei Obruchkov[2]

[1]School of Engineering, Victoria University of Wellington, Wellington, New Zealand, [2]School of Chemical and Physical Sciences, Victoria University of Wellington, Wellington, New Zealand

To lower the entry barrier for MRI system development, an open source PXIe platform consisting of IP for peripheral boards, an associated linux device driver and example system controller and peripheral boards were developed. The design was capable of performing system controller initiated DMA transfers in both directions with a maximum block size of 8MB. The hardware design was greatly simplified by mounting FPGA modules from Avnet onto custom PXIe compatible carrier boards. The modules from Avnet contained a System on a Chip device from Xilinx consisting of a dual core ARM processor and FPGA fabric.

2689

Distributed receivers with hardware-accelerated signal processing: Synchronous acquisition of image data and k-space trajectories

Josip Marjanovic[1], Jonas Reber[1], Lars Kasper[1], Benjamin E. Dietrich[1], David O. Brunner[1], and Klaas P. Pruessmann[1]

[1]University and ETH Zurich, Zurich, Switzerland

The demand for higher image quality led to a significant increase in the number of parallel receive coils and to the addition of sensor systems such as magnetic field monitoring probes to MR systems, boosting the demand for many high quality receive channels. Furthermore, new methods increasingly require high acquisition duty cycles and bandwidths setting new requirements on data traffic and real-time capabilities. We present a flexible, scalable receiver system addressing those issues demonstrated on an example of concurrent imaging and field monitoring with real-time processing of synchronized streams of coil and trajectory data, as required by modern reconstruction algorithms.

2690

Sensitive Imaging of Vascular Walls with an Endo-esophageal Wireless Amplified NMR Detector (WAND)

Xianchun Zeng[1,2] and Chunqi Qian[2]

[1]Radiology, Provincial People's Hospital, Guiyang, People's Republic of China, [2]Radiology, Michigan State University, East Lansing, MI, United States

To improve the detection sensitivity of MRI, a Wireless Amplified NMR Detector (WAND) is developed to image surrounding vessels from inside the esophagus. This cylindrical detector is a double frequency resonator with a single metal wire that is self-connected by a pair of varactors. It can convert wirelessly provided pumping power into amplified MR signals. When the detector is inserted inside the esophagus, vessel walls of the vertebrate artery and basal artery can be identified with greatly improved clarity. This detector will be useful to characterize subtle lesions in inflamed vessels.

2691

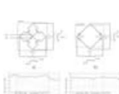

Low IF Passive Mixer Topologies for Low Power MRI Front Ends

Andreas Port[1], John Pauly[2], Fraser Robb[3], and Greig Scott[2]

[1]Institute for Biomedical Engineering, University and ETH Zurich, Zurich, Switzerland, [2]Electrical Engineering, Stanford University, Stanford, CA, United States, [3]GE Healthcare, Aurora, OH, United States

As MRI array counts expand, there is growing interest in moving more of the receive electronics onto the array, the ultimate goal being wearable, and cordless arrays. This places severe constraints on the maximum feasible power consumption per channel. We explore low power front-end topologies employing passive mixers. If combined with low-power high resolution successive approximation ADCs or continuous time sigma delta ADCs, receive arrays at only 100mW per channel may be feasible.

2692

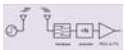

Wireless Clock Transfer for MRI Phase Correction

Jonathan Y Lu[1], Pascal Stang[2], Fraser Robb[3], John Pauly[1], and Greig Scott[1]

[1]Electrical Engineering, Stanford University, Stanford, CA, United States, [2]Procyon Engineering, Stanford, CA, United States, [3]Advanced Coils, GE Healthcare Inc, Aurora, OH, United States

One step in making wireless MRI possible is to sync the clocks at both the transmit side hardware that plays out the pulse, and the receive chain that processes the FID data. A discrepancy between the timing of the two clocks will lead to jitter that amounts to artifacts in the MRI image. In this work, we demonstrate a method to transfer a wireless clock without creating jitter artifacts in an MRI image.

2693

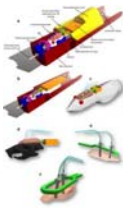

A chronic in situ coil system adapted for intracerebral stimulation during MRI in rats

Dan Madularu[1], Chathura Kumaragamage[2], Axel Mathieu[1], Praveen Kulkarni[3], M. Natasha Rajah[1], Alain Gratton[1], and Jamie Near[1]

[1]Psychiatry, McGill University, Montreal, QC, Canada, [2]Biomedical Engineering, McGill University, Montreal, QC, Canada, [3]Psychology, Northeastern University, Boston, MA, United States

We describe the fabrication and performance of a chronic in situ coil system designed to allow focal brain stimulation in awake rats while acquiring highly resolved MRI data. We developed a subcutaneously implantable receive-only surface radiofrequency coil to be fitted immediately adjacent to the rat skull surface during the cannulation procedure. SNR performance of the coil was superior to three commercially-available coils, in some instances by a factor of three. Widespread BOLD was observed in response to bicuculline and morphine microinfusions. This approach enables mapping the functional response to highly targeted stimuli such as microinfusions or optogenetics.

2694

High Power TRASE PIN Diode Control System

Eric Der[1], Vyacheslav Volotovskyy[2], Boguslaw Tomanek[3], and Jonathan C. Sharp[3]

[1]Electrical and Computer Engineering, University of Alberta, Edmonton, AB, Canada, [2]Medical Physics, Cross Cancer Institute, Edmonton, AB, Canada, [3]Oncology, University of Alberta, Edmonton, AB, Canada

TRASE is a k-space encoding method for low cost MRI that replaces conventional imaging gradients with a switchable RF transmit array. TRASE echo train sequences require rapid switching between transmit elements to cycle through up to six different phase gradient encoding fields. In vivo image resolution is currently limited because long (~500μs) refocusing pulses render the echo train sequence vulnerable to T_2 losses. Here we present a design for a high power PIN diode driver circuit capable of robust and rapid switching of short (~100μs) high power pulses for a 24cm coil. Results from 0.2T experiments are shown.

2695

The effect of Gaussian Filtering in ZTE based Attenuation Correction of PET/MR

J.M. Sousa[1], Håkan Ahlström[1], Mathias Engström[2], and Mark Lubberink[1]

[1]Department of Surgical Sciences, Uppsala University, Uppsala, Sweden, [2]GE Applied Science Laboratory, GE Healthcare, Sweden

Zero-Echo Time (ZTE) has been proposed as an alternative attenuation method for PET-MR brain imaging. However, the filtering effects on these ZTE AC maps have not been explicitly discussed, in relation to effects on reconstructed and corrected images, and that is what we aim to develop in this study.

2696

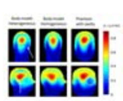

A Simple Head-sized Phantom for Realistic System Characterization at 7T

Wyger M. Brink[1], Zhiyi Wu[1], and Andrew G. Webb[1]

[1]Leiden University Medical Center, Leiden, Netherlands

A simple head-sized phantom has been developed to produce realistic B_1 and B_0 features and electrical loading conditions, as a tool for the evaluation of MR techniques and RF validation in high field MR systems.

2697

Enhancement of signal intensity using a wireless coil for FT-EPR oximetry study, implanted in an animal body

Ayano Enomoto[1], Gadisetti V.R. Chandramouli[2], Alan P Koretsky[3], Chunqi Qian[4], Murali K Cherukuri[1], and Nallathamby Devasahayam[1]

[1]Radiation Biology Branch, National Cancer Institute, Bethesda, MD, United States, [2]GenEpria Consulting Inc., Columbia, MD, [3]National Institute of Neurological Disorders and Stroke, National Institutes of Health, Bethesda, MD, United States, [4]Department of Radiology, Michigan State university, East Lansing, MI, United States

Improvement in sensitivity is required to detect the weak signals with Fourier transform Electron Paramagnetic Resonance (FT-EPR). In the proposed method, the signal from a wireless coil filled with sample was enhanced by using pumping coil in the regular EPR system. In this study, we achieved approximately 6-fold of improvement in signal intensity compared with conventional FT-EPR system under the simulated condition of animal body. We will also show the results of oximetry using the LiPc in, in vivo applications to measure tissue oxygenation.

Traditional Poster

Hybrid & Novel Technology

Exhibition Hall 2698-2718 Wednesday 16:15 - 18:15

2698

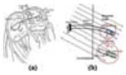

Control of an MRI-Guided Magnetically-Actuated Steerable Catheter System

Taoming Liu[1], Dominique Franson[2], Nate Lombard Poirot[3], Russell Jackson[1], Nicole Seiberlich[1,2], Mark A. Griswold[1,2,4], and Murat Cenk Cavusoglu[1,2]

[1]Electrical Engineering and Computer Science, Case Western Reserve University, Cleveland, OH, United States, [2]Biomedical Engineering, Case Western Reserve University, Cleveland, OH, United States, [3]Mechanical and Aerospace Engineering, Case Western Reserve University, Cleveland, OH, United States, [4]Radiology, University of Hospitals of Cleveland, Cleveland, United States

This paper presents a Jacobian-based inverse kinematics and open-loop control method for an MRI-guided magnetically-actuated steerable intravascular catheter system. The catheter is directly actuated by magnetic torques generated on a set of current-carrying micro-coils embedded on the catheter tip by the magnetic field of MRI scanner. The Jacobian matrix is derived from a three dimensional kinematic continuum model of the catheter deflection. The inverse kinematics are numerically computed by iteratively applying the inverse of the Jacobian matrix. Experimental evaluation compares a catheter prototype's desired trajectory to the actual trajectory.

2699

Experimental study for efficient RF-penetration through electrically-floating PET insert for MRI systems

Md Shahadat Hossain Akram[1], Craig Levin[2], Takayuki Obata[1], Genki Hirumi[3], and Taiga Yamaya[1]

[1]National Institute of Radiological Sciences, Chiba, Japan, [2]Radiology, Stanford University, CA, United States, [3]Chiba University, Chiba, Japan

PET inserts for the existing MRI systems are showing great potential for widespread and affordable low-cost simultaneous PET/MR imaging that would otherwise improve the PET sensitivity due to the proximity of detectors to the imaging region. To avoid electromagnetic interference between PET and MRI components, PET detectors are enclosed in Faraday shield cages. A electrically floating PET insert enables us to use MRI built-in body RF coil instead of using separate custom designed RF coil with the PET insert. This study experimentally evaluates different PET geometries and different design factors for efficient RF penetration through the floating-PET insert.

2700

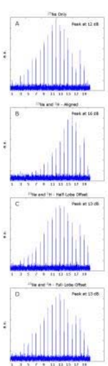

RF Power Considerations for Simultaneous Multi-Nuclear MRI/MRS

Stephen Edwin Ogier[1], Hongli Dong[1], Steve Wright[1], and John Bosshard[1]

[1]Electrical & Computer Engineering, Texas A&M University, College Station, TX, United States

There are many approaches to simultaneous multi-nuclear spectroscopy, but the simplest and potentially the most elegant involves sending all frequencies through a single broadband amplifier into a single-port, multi-tuned coil. This abstract examines a complication in this approach, that of early saturation of the amplifier due to the need to amplify two signals simultaneously. A simple solution, staggering the RF pulses a small amount to avoid the overlapping of their peaks, is shown to largely avoid the problem.

2701

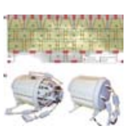

A novel head coil system with integrated transmission source for accurate attenuation correction in PET/MR scans

Lucia Navarro de lara[1], Roberta Frass-Kriegl[1], Jürgen Sieg[1], Andreas Renner[1], Michael Pichler[1], Sigrun Goluch[1], Thomas Bogner[1], Ewald Moser[1], Thomas Beyer[2], Wolfgang Birkfellner[2], Michael Figl[2], and Elmar Laistler[2]

[1]Division MR Physics - Center for Medical Physics and Biomedical Engineering, Medical Unversity of Vienna, Vienna, Austria, [2]Center for Medical Physics and Biomedical Engineering, Medical Unversity of Vienna, Vienna, Austria

A 24 channel head and neck coil for PET/MR with an integrated moving radioactive source is presented to enable transmission measurements for accurate attenuation mapping.

2702

Evaluation of a metasurface resonator for in vivo imaging at 1.5T

Shimul Chandra Saha[1], Alena V. Shchelokova[2], Ioannis Sotiriou[1], Alexey P. Slobozhanyuk[2,3], Maria Koutsoupidou[1], Elena Cellitti[1], Helena Cano-Garcia[1], Pavel A. Belov[2], Andrew Webb[4], George Palikaras[1], and Efthymios Kallos[1]

[1]MediWiSe| Medical Wireless Sensing Ltd, London, United Kingdom, [2]Department of Nanophotonics and Metamaterial, ITMO University, St. Petersburg, Russian Federation, [3]Nonlinear Physics Center, Australian National University, Canberra, Australia, [4]C.J. Gorter High Field Magnetic Resonance Center, Leiden University, Leiden, Netherlands

We present in vivo results from a metasurface structure comprising an array of brass wires embedded in a high epsilon and low loss medium. The metasurface was used to scan humans in a 1.5T MRI scanner and demonstrated enhancement of the signal-to-noise ratio up to 200% in the area-of-interest close to the metasurface.

2703 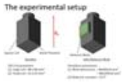

Design of Self-Resonance Modes (SRM) of monolithic ultra-high dielectric constant (uHDC) materials and RF Coils for B1 field enhancement

Sebastian Rupprecht[1], Buddhi Tilakaratne[1], Chris R Messner[1], Christopher Sica[1], Michael T Lanagan[2], Wei Chen[3], and Qing X Yang[1]

[1]*Department of Radiology, The Pennsylvania State University College of Medicine, Hershey, PA, United States,* [2]*Department of Engineering Sciences and Mechanics, The Pennsylvania State University, State College, PA, United States,* [3]*Radiology Department, Center for Magnetic Resonance Research, MN, United States*

Ultra-high dielectric constant (uHDC) materials were established as an effective B1 shimming and enhancement tool in MRI. A dielectric material operates at certain frequency range and enhances fields at an anticipated resonance frequency. We trimmed a rectangular dielectric block such that the fundamental frequency mode of the block resonated at 3 T, and compared it with a similarly sized non-resonant block. Both cases were coupled with a transmit receive surface coil resonant at 123.2 MHz. The effect of the surface coil area on the B_1 field enhancement was explored to optimize the dielectric and coil configuration.

2704 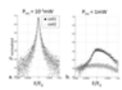

Reducing the screening during transmission using non-linear properties of high sensitivity superconductor radiofrequency coils for magnetic resonance micro imaging

Michel Geahel[1,2,3], Ludovic de Rochefort[2,4], Jean-Christophe Ginefri[2], Luc Darrasse[2], Cornelis Jacominus van der Beek[3], Javier Briatico[1], and Marie Poirier-Quinot[2]

[1]*Unité Mixte de Physique, CNRS, Thales, Univ. Paris-Sud, Université Paris-Saclay, Palaiseau, France,* [2]*Laboratoire d'Imagerie par Résonance Magnétique Médicale et Multi-Modalités (IR4M), UMR8081, CNRS, Université Paris-Sud, Université Paris Saclay, Orsay, France,* [3]*Laboratoire des Solides Irradiés, CNRS UMR 7642 & CEA/DSM/IRAMIS, Ecole Polytechnique, Palaiseau, France,* [4]*Aix-Marseille Univ, CNRS, CRMBM UMR 7339, Marseille, France*

In MRI, high-temperature superconducting (HTS) radio frequency (RF) coils have been shown to greatly improve the signal-to-noise ratio. The nonlinear behavior of superconducting materials as a function of the emitted RF power is, nowadays, one of the principal technological obstacle limiting the use of these materials on a wider scale. It could be overcome by using HTS coil in reception mode only. Here we characterize these non-linear properties and use them to decouple the HTS coil during transmit mode. This preliminary study is a promising approach to use the highly sensitive HTS coils in reception mode only.

2705 

Exploring New Possibilities in Array Design using Partially Orthogonal RF Resonators (Parti-Coils): A Numerical Simulation Study at 3 Tesla

Jorge Chacon-Caldera[1], Matthias Malzacher[1], Alexander Fischer[1], and Lothar R. Schad[1]

[1]*Computer Assisted Clinical Medicine, Medical Faculty Mannheim, Heidelberg University, Mannheim, Germany*

Partially orthogonal RF resonators (Parti-coils) is a novel concept in which RF coils are extended in an orthogonal direction. This increases overlap distance between elements. Therefore, coil density can be optimized. We show alternative geometrical coil configurations in array design using Parti-coils and compare them to an array of traditional planar coils using numerical simulations. Parti-coils enhanced the flexibility in array design, increased the overlap distance between coils by a maximum 3.2-fold, decreased next-nearest neighbor coupling by more than 6dB, showed up to 6.6% higher $|B1\text{-}|_{acc.}$ penetration depth, and a factor 1.05 increase of $|B1\text{-}|_{acc.}$ at a ROI.

2706 

Modified FCE Transmit Coil for Bilateral Breast Imaging at 7T with Array Coil Inserts

Jiaming Cui[1], Romina Del Bosque[2], Ivan Dimitrov[3], Sergey Cheshkov[3], Mary McDougall[4], Craig Malloy[3], and Steve M Wright[5]

[1]*Electrical and Computer Engineering, Texas A&M University, College Station, TX, United States,* [2]*Biomedical Engineering, Texas A&M University, Bryan, TX, United States,* [3]*Univesity of Texas Southwestern Medical Center,* [4]*Texas A&M University, TX, United States,* [5]*Texas A&M University*

This work describes a forced-current-excitation (FCE) bilateral breast coil, modified for the insertion of a 32-channel receive array for 1H imaging and spectroscopy at 7T. A previous design of the bilateral quadrature volume coil employed RF shielding which prevented the insertion of a receive array with the associated hardware and cabling. The modified bilateral coil uses twinaxial cable for the FCE-enabling quarter-wave transmission lines, allowing balanced signal transmission and eliminating the need for the shields. The results include uniform bilateral excitation, an increase in efficiency as compared to the shielded coil, and successful installation of the 32-channel receive array.

2707 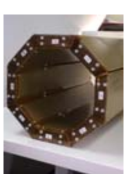

A 16 Element Bow-Tie Slot Array Coil for Parallel Transmit MRI/MRS

Dheyaa Ali Alkandari[1], Neal Hollingsworth[2], Chung-Huan Huang[2], Jiaming Cui[2], and Steven M Wright[2]

[1]*Electrical and Computer Engineering, Texas A&M University, college station, TX, United States,* [2]*Electrical and Computer Engineering, Texas A&M University*

We report a volume coil consisting of 16 bowtie slot elements arranged in eight independent modules. The slot coils provide several interesting advantages over conventional elements.   In particular they demonstrate a high degree of Intrinsic coupling between modules, making this array ideally suited for use in parallel transmit using conventional amplifiers. Additionally, all match and tune elements, baluns and feedlines are concealed between two ground planes, shielding the imaging volume from stray electric fields. Imaging results are shown at 4.7 Tesla demonstrating isolated patterns and a broad coverage in volume coil mode.

2708

In-Bore High Efficiency Current Driver

Michael Twieg[1] and Mark A Griswold[1]

[1]*Dept of Radiology, Case Western Reserve University, Cleveland, OH, United States*

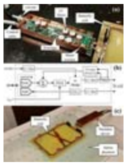

Recent work has shown the use of shim and gradient coil arrays for dynamic shimming and novel spatial encoding methods. These arrays require precise current source drivers with high power and bandwidth. Because of these demands, shim and gradient arrays are typically driven with amplifiers which are located outside the magnet bore due to constraints on power dissipation, radiofrequency interference (RFI), or magnetic materials. Here we present a highly efficient digitally-controlled switchmode current driver. We demonstrate that it is feasible to shield the RFI from the receive chain while avoiding ferrous materials and large heatsinks.

2709

A technique to compensate signal loss in an RF switch matrix system in MRI

Yun-Kyoung Ko[1], Han Lim Lee[2], Chang-Hoon Choi[1], and N. Jon Shah[1,3]

[1]Institute of Neuroscience and Medicine - 4, Forschungszentrum Juelich, Juelich, Germany, [2]School of Electrical and Electronics Engineering, Chung-Ang University, Seoul, Korea, Republic of, [3]Faculty of Medicine, Department of Neurology, JARA, RWTH Aachen University, Aachen, Germany

MRI RF channels refer to the pathways of received signals and the availability of multiple channels allows one to access multi-channel array coils. To control the use of different coils, MRI usually utilises a crossbar-type switch matrix system that interactively connects the selected coil as an input and corresponding analogue-to-digital converters as an output. However, since the RF wavelength decreases with increasing B_0, impedance in RF pathways varies in accordance with wavelength. This results in signal loss and in degraded image quality. In this study, we proposed an RF loss compensation technique for the switch matrix and verified its performance.

2710

Automated localization of 55Mn fiducial markers for coil array placement in hyperpolarized 13C MRI: dependence on number of acquired projections

Michael Ohliger[1], Cornelius von Morze[1], Jermey Gordon[1], Peder EZ Larson[1], and Daniel Vigneron[1]

[1]Radiology and Biomedical Imaging, University of California San Francisco, San Francisco, CA, United States

Accurate RF coil localization is important for hyperpolarized 13C MRI. Fiducial markers can be constructed from 55Mn and localized using projection imaging. This study examines the minimum number of projections necessary to localize the markers subject to the known distances between markers. This would potentially allow marker localization to be automated as part of prescan.

2711

Improved Decoupling for ^{13}C Coil Arrays Using Non-Conventional Matching and Preamplifier Impedance

Juan Diego Sánchez Heredia[1], Daniel Højrup Johansen[1], Rie Beck Hansen[1], Esben Søvsø Szocska Hansen[2], Christoffer Laustsen[2], Vitaliy Zhurbenko[1], and Jan Henrik Ardenkjær-Larsen[1]

[1]Department of Electrical Engineering, Technical University of Denmark, Kgs. Lyngby, Denmark, [2]Department of Clinical Medicine, Aarhus University, Aarhus, Denmark

In this study, we describe a method to obtain improved preamplifier decoupling for receive-only coils. The method relies on the better decoupling obtained when coils are matched to an impedance higher than 50 Ω. Preamplifiers with inductive imaginary impedance and low real impedance, increases the effectiveness of the decoupling. A 2-channel ^{13}C array of 50 mm loop coils show an increase of Q-factor of the coils from 247 to 365. The measured SNR, using two small phantoms, demonstrated a similar improvement.

2712

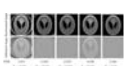

SWIFT imaging for hyperpolarized xenon in ultra-low field MRI

Takenori Oida[1], Yuki Kaga[1], Tetsuya Yamamoto[1], and Tetsuo Kobayashi[1]

[1]Dept. of Electrical Engineering, Graduate school of Engineering, Kyoto University, Kyoto, Japan

ULF-MRI is one of the recent imaging techniques. Since a polarization rate of hyperpolarized xenon is independent of B0, hyperpolarized xenon is suitable for ULF-MRI. A xenon imaging using SWIFT has been proposed by Nakamura et al. to reduce the decay caused by the xenon's diffusion. In this study, we assess the effectiveness of the SWIFT pulse sequence for hyperpolarized xenon imaging in ULF-MRI. The simulation results showed that we could obtain the hyperpolarized xenon images with the SWIFT approach in ULF-MRI and reconstructed images were improved by the oversampling in readout direction and wide bandwidth.

2713

Magnetic and RF Shielding of a Novel Compact 6MeV Linac for MRI Guided Radiation Therapy System

Shmaryu Shvartsman[1], James Dempsey[1], Tom Chmielewski[1], Gerald Fought[1], Michael Hernandez[1], Iwan Kawrakow[1], and Amit Sharma[1]

[1]ViewRay Inc, Oakwood Village, OH, United States

We report on successful testing of a novel magnetic and RF shielding technology for a 6MeV Linac for MRI guided radiation therapy system. It allows complete decoupling of the Linac and its components from the MRI system. A low field region is created where the Linac can be operated without any problems. The system is compact and allows positioning of all magnetically and RF sensitive Linac components on a rotating Gantry and treat patients from any angle.

2714

Design and characterization of an RF shield for a 400 MHz birdcage coil in a retrofitted PET camera for preclinical PET-MRI

Nicola Bertolino[1], Thy Nguyen[1], Dhaval Shah[1], Robert Zivadinov[1,2], Marcello Alecci[3,4,5], and Ferdinand Schweser[1,2]

[1]Buffalo Neuroimaging Analysis Center, Department of Neurology, Jacobs School of Medicine and Biomedical Sciences, University at Buffalo, The State University of New York, Buffalo, NY, United States, [2]MRI Clinical and Translational Research Center, Jacobs School of Medicine and Biomedical Sciences, University at Buffalo, The State University of New York, Buffalo, NY, United States, [3]Department of Life, Health and Environmental Sciences, University of L'Aquila, L'Aquila, Italy, [4]Laboratori Nazionali del Gran Sasso, Istituto Nazionale di Fisica Nucleare, Assergi, L'Aquila, Italy, [5]Dipartimento di Scienze Fisiche e Chimiche, Istituto SPIN-CNR, Coppito, LAquila, Italy

PET-MRI imaging sets the stage for truly novel imaging approaches, but preclinical hybrid systems, characterized by ultra-high static magnetic field and small bore diameter, are still in the proof-of-concept stage. In this study, we developed an optimized RF coil/shield setup for an ultra-high field compatible prototype PET ring that can be retrofitted to conventional small-animal MRI systems. In particular an original shielding solution was designed and tested with the purpose of maximizing coil efficiency, usable space inside the detector, and PET sensitivity.

2715

Wrist coil for low field MRI

Darshan Shivaramu Keelara[1], ThejasVishnu Ramesh[1], Syed Saad Siddiq[1], Padma Chennagiri[1], Samarth Singh[1], Shivaprasad Ashok Chikop[1], Shreyas Indurkar[1], and Sairam Geethanath[1]

[1]Medical Imaging Research Centre, Dayananda Sagar Institutions, Bangalore, India

Image Signal to Noise Ratio (SNR) and resolution are significant challenges in ultra-low field MRI. A single channel transmit coil and a 4-channel phased array was developed for wrist to operate at 9.5mT. The current work involves integration with the DDS module for verifying functionality. Future work is to develop phased array for head MRI.

2716

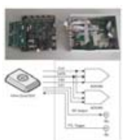

Flexible General-Purpose Embedded System for Real-time Feedback and Dynamic B0 Shimming

Paul Chang[1,2], Sahar Nassirpour[1,2], and Anke Henning[1,3]

[1]MPI for Biological Cybernetics, Tuebingen, Germany, [2]IMPRS for Cognitive and Systems Neuroscience, Eberhard University of Tuebingen, Tuebingen, Germany, [3]Institute of Physics, Ernst-Moritz-Arndt University Greifswald, Greifswald, Germany

B0 shimming methods are becoming more sophisticated. Methods such as multi-coil shimming, dynamic B0 shimming with pre-emphasis and real-time feedback all require additional hardware to drive the shim coils.

In this work, we present a novel general-purpose embedded platform for controlling any of the above mentioned shim systems. Control software can be developed on Linux, while low-level scripts are used for optimal control of hardware interfaces.

2717

Homomorphic determination of noise variance and denoising using a non-local means filter for assessing the accuracy of automated segmentation

Aziz M. Ulug[1,2], Weidong Luo[1], and Sebastian Magda[1]

[1]CorTechs Labs, San Diego, CA, United States, [2]Institute of Biomedical Engineering, Bogazici University, Istanbul, Turkey

Automated segmentation algorithms have been used more and more frequently for research and clinical purposes. There are available software packages that can determine volumes of brain structures and lesions. While signal to noise ratio in volumetric images is one of the determinants in the accuracy of such software, the effect of noise to the output results is usually not well described. We have studied effects of increased noise variance and denoising in evaluating the performance of automated segmentation tool using a synthetic phantom, one human dataset with artificially added noise, and 46 subjects scanned twice.

2718

Pushing sodium imaging into clinical use - A technical feasiblity study

Matthias Malzacher[1], Jorge Chacon-Caldera[1], Alexander Fischer[1], and Lothar R Schad[1]

[1]Computer Assisted Clinical Medicine,Medical Faculty Mannheim, Heidelberg University, Mannheim, Germany

Sodium MRI keeps becoming more interesting for multiple studies and clinical applications due to its capability to provide information on tissue viability. This information would be highly valuable in the clinical routine.We analyze technical possibilities to allow pushing sodium MRI into clinical use. In particular, we investigate approaches for transmitting and receiving sodium and proton signals using the same hardware. One main target of these approaches is to be fully compatible with standard 3T MRI systems without decreasing significantly the performance of proton imaging. We prove the feasibility for such systems. Yet, some drawbacks have to be taken into account.

Traditional Poster

Myocardial Tissue Characterization

Exhibition Hall 2719-2767 Thursday 8:15 - 10:15

2719

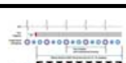

Simultaneous measurements of myocardium T1, T2 map, Cine and synthetic LGE using Inversion Recovery tiny golden angle radial balanced-SSFP within 6 second

Panki Kim[1] and Byoung Wook Choi[1]

[1]Department of Radiology, Severance Hospital, Yonsei University College of Medicine, Seoul, Korea, Republic of

In the cardiac MRI study, the quantification of T1, T2 relaxation time has become an important indication as well as the cine and the late gadolinium enhancement. In this work, we presented a novel method for simultaneous acquisition of T1, T2 map and Cine image of the myocardium based on the transient phase of inversion recovery balanced-SSFP imaging, and was proven potential both phantom and in vivo on a healthy volunteer.

2720

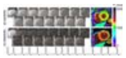

Accurate Myocardial T1-Mapping in Arrhythmia using Saturation-Recovery during Systole at 3T

Nadja M Meßner[1,2], Sebastian Weingärtner[1,3,4], Johannes Budjan[5], Dirk Loßnitzer[6], Theano Papavassiliu[2,6], Lothar R Schad[1], and Frank G Zöllner[1]

[1]Computer Assisted Clinical Medicine, Medical Faculty Mannheim, Heidelberg University, Mannheim, Germany, [2]DZHK (German Centre for Cardiovascular Research), partner site Mannheim, Mannheim, Germany, [3]Department of Electrical and Computer Engineering, University of Minnesota, Minneapolis, MN, United States, [4]Center for Magnetic Resonance Research, University of Minnesota, Minneapolis, MN, United States, [5]Institute of Clinical Radiology and Nuclear Medicine, Medical Faculty Mannheim, Heidelberg University, Mannheim, Germany, [6]1st Department of Medicine Cardiology, Medical Faculty Mannheim, Heidelberg University, Mannheim, Germany

In arrhythmic patients, ECG mis-triggering frequently leads to T_1-quantification inaccuracy.

In this study, a heart-rate independent saturation-recovery T_1-mapping method was adapted for systolic imaging at 3T by performing magnetization saturation right after the systolic imaging window and prior to R-wave detection. Estimated T_1- and ECV- values during systole were (1557±53ms/ 0.21±0.03) compared to (1585±58ms/0.21±0.03) at diastole.

Our results show that SR T_1-mapping might be an advantageous alternative to yield accurate T_1- and ECV-values in patients with arrhythmia or reduced myocardial wall-thickness.

2721

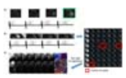

Towards High Success Rate in vivo Cardiac DTI on a Clinical 3T Scanner: Considerations on Heart Rate, Body-to-Mass Index, and Free Breathing

Christopher Nguyen[1], Sen Ma[1,2], Xiaoming Bi[3], and Debiao Li[1,2]

[1]Biomedical Imaging Research Institute, Cedars-Sinai Medical Center, Los Angeles, CA, United States, [2]Bioengineering, University of California Los Angeles, Los Angeles, CA, United States, [3]Siemens Healthcare, Los Angeles, CA, United States

Clinical translation of cardiac diffusion tensor MRI has been challenging because of the sensitivity to bulk motion and thus, low success rates of scans. Current techniques require either high gradient systems (>40 mT/m) or excess breath holding (>10 breath holds / slice) to acquire motion free cardiac DT-MRI. We propose a cardiac DT-MRI technique optimized for clinical translation and aimed at achieving high success rates in subjects with high and variable heart rate and high bold-to-mass index under free breathing conditions. Results in subjects with high BMI and variable HR yielded success rates > 90%.

2722

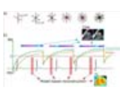

Multi-parametric cardiac MRI for T1 mapping and cine imaging using iterative model-based image reconstruction

Kirsten Miriam Becker[1], Jeanette Schulz-Menger[2,3], Tobias Schaeffter[1,4], and Christoph Kolbitsch [1,4]

[1]Physikalisch-Technische Bundesanstalt (PTB), Braunschweig and Berlin, Germany, [2]Working Group on Cardiovascular Magnetic Resonance, Experimental and Clinical Research Center (ECRC), Berlin, Germany, [3]Department of Cardiology and Nephrology, HELIOS Klinikum Berlin Buch, Berlin, Germany, [4]Division of Imaging Sciences and Biomedical Engineering, King's College London, London, United Kingdom

In cardiac MRI, different diagnostic parameters are obtained in separate scans, leading to long examination times. In this work, we present an iterative model-based reconstruction approach for continuously acquired data, which provides native T1 maps and functional cine images within a single breath hold. The continuous acquisition allows for T1 reconstruction for different cardiac phases. Evaluation in a phantom demonstrated accurate T1 values (R^2>0.99) and insensitivity to heart rates, with T1 variations of less than 5% (50 to 90 bpm). In three healthy volunteers T1 maps were assessed for diastole and systole and cine images had a consistent dark-blood contrast.

2723

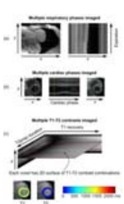

Non-ECG, Free-breathing Joint T1-T2 Mapping in the Myocardium with CMR Multitasking

Anthony G. Christodoulou[1,2], Christopher Nguyen[1], Jaime L. Shaw[1,3], Yibin Xie[1], Nan Wang[1,3], and Debiao Li[1,3]

[1]Biomedical Imaging Research Institute, Cedars-Sinai Medical Center, Los Angeles, CA, United States, [2]Cedars-Sinai Heart Institute, Cedars-Sinai Medical Center, Los Angeles, CA, United States, [3]Department of Bioengineering, University of California, Los Angeles, Los Angeles, CA, United States

Myocardial tissue characterization via quantitative T1 and T2 mapping is typically accomplished using ECG-triggering and breath-holding. Here we describe a novel method for non-ECG, free-breathing joint T1-T2 mapping using the cardiovascular low-rank tensor imaging framework for CMR multitasking. This method achieves joint T1-T2 mapping in the myocardium at multiple cardiac and respiratory phases within 1.5 min for one slice. Measurements were within the range reported in the literature, and were repeatable to 3.9% for T1 and 6.1% for T2.

2724

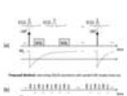

End-systolic myocardial T1 mapping using a spoiled steady-state approach: Towards reducing the confounding effect of intra-myocardial blood on native T1

Zulma Sandoval[1], Daniel Berman[2], Noel Bairey Merz[2], and Behzad Sharif[1]

[1]Biomedical Imaging Research Institute, Dept. of Biomedical Sciences, Cedars-Sinai Medical Center, Los Angeles, CA, United States, [2]Heart Institute, Cedars-Sinai Medical Center, Los Angeles, CA, United States

Recent results in myocardial tissue characterization using cardiac MRI have shown that native myocardial T1 values are confounded by intra-myocardial water content, mainly driven by intra-myocardial blood volume. We developed and tested a free-breathing T1 mapping method that, in contrast to MOLLI-based methods, avoids any magnetization preparation and therefore can achieve significantly higher temporal resolution, thereby enabling it to capture purely-systolic or purely-diastolic T1 maps. End-systolic T1 mapping using the proposed steady-state approach has the potential to generate native T1 maps with minimal confounding effect from intra-myocardial blood.

2725 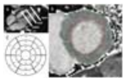

Left Ventricle Remodeling in Bicuspid Aortic Valve Evaluated by ECG, Echocardiography, and Cardiovascular Magnetic Resonance

Kenichiro Suwa[1], Amir Ali Rahsepar[1], Ahmadreza Ghasemiesfe[2], Julia Geiger[1], Alex J Barker[1], Jeremy D Collins[1], Micahel Markl[3], and James C Carr[1]

[1]Department of Radiology, Northwestern University, Chicago, IL, United States, [2]Department of Radiology, Yale New Haven Health Bridgeport Hospital, Bridgeport, CT, United States, [3]Department of Radiology and Biomedical Engineering, Northwestern University, Chicago, IL, United States

The relationship between ECG characteristics, left ventricular (LV) diastolic function by echocardiography and Gadolinium extracellular volume fraction (ECV) in bicuspid aortic valve (BAV) are unknown. We aimed to test the hypothesis that BAV has an association with LV hypertrophy, myocardial fibrosis, and diastolic dysfunction. Cardiac magnetic resonance, ECG, and echocardiography were performed in 80 patients with BAV and 34 patients with trileaflet aortic valve (TAV). ECV was significantly higher in BAV than TAV. ECV, Sokolow-Lyon voltage, Cornell product, and e' demonstrated significant relationships with LV end-diastolic volume index. ECV can be a useful predictor of LV remodeling in BAV.

2726 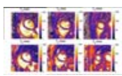

Simultaneous T1 and T2 mapping of the myocardium in normal volunteers using Cardiac MR Fingerprinting

Shivani Pahwa[1], Jesse Hamilton[2], Joseph Adedigba[3], Samuel Frankel[4], Gregory O'Connor[4], Ozden Kilinc[5], Wei-Ching Lo[2], Joshua Batesole[6], Seunghee Margevicius[7], Pingfu Fu[7], Mark A Griswold[8], Nicole Sieberlich[9], and Vikas Gulani[8]

[1]Radiology, University Hospitals Cleveland Medical Center / CWRU, Cleveland, OH, United States, [2]Biomedical Engineering, Case Western Reserve University, [3]Case Western Reserve University, [4]Case Western Reserve University School of Medicine, [5]Radiology, Case Western Reserve University, [6]Radiology, University Hospitals Cleveland Medical Center, Cleveland, OH, United States, [7]Epidemiology and Biostatistics, Case Western Reserve University School of Medicine, [8]Radiology and Biomedical Engineering, University Hospitals Cleveland Medical Center / CWRU, Cleveland, OH, United States, [9]Biomedical Engineering, University Hospitals Cleveland Medical Center / CWRU, Cleveland, OH, United States

This study reports normative cardiac T_1 and T_2 values generated in a single cardiac MRF scan in a cohort of normal volunteers. These values were compared against MOLLI (for T_1) and bSSFP (for T_2). Our results show that cardiac relaxometry values obtained with MRF at 1.5 T are comparable to values previously reported in the literature and those obtained using MOLLI and bSSFP.

2727 

Myocardial fibrosis is a predictor of adverse outcomes in thalassemia intermedia patients

Antonella Meloni[1], Nicola Giunta[2], Pietro Giuliano[2], Stefania Renne[3], Laura Pistoia[1], Vincenzo Positano[1], Calogera Gerardi[4], Vincenzo Spadola[5], Petra Keilberg[1], and Alessia Pepe[1]

[1]Fondazione G. Monasterio CNR-Regione Toscana, Pisa, Italy, [2]"ARNAS" Civico, Di Cristina Benfratelli, Palermo, Italy, [3]Presidio Ospedaliero "Giovanni Paolo II", Lamezia Terme, Italy, [4]Presidio Ospedaliero "Giovanni Paolo II" - Distretto AG2 di Sciacca, Sciacca, Italy, [5]Azienda Ospedaliera Civile - O.M.P.A. Ragusa, Ragusa, Italy

Myocardial fibrosis detected by LGE has been confirmed as an independent predictor of CV complications in thalassemia intermedia patients. Our finding is consistent with a growing evidence that LGE has a strong prognostic impact in thalassemic patients, warranting a close clinical and instrumental follow-up.

2728 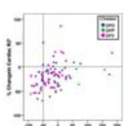

Association between cardiac iron clereance and hepatic siderosis by T2* MRI in thalassemia major patients

Antonella Meloni[1], Laura Pistoia[1], Nicolò Schicchi[2], Gennaro Restaino[3], Paolo Preziosi[4], Vincenzo Positano[1], Monica Benni[5], Maria Paola Smacchia[6], Daniele De Marchi[1], and Alessia Pepe[1]

[1]CMR Unit, Fondazione G. Monasterio CNR-Regione Toscana, Pisa, Italy, [2]Azienda Ospedaliero-Universitaria Ospedali Riuniti "Umberto I-Lancisi-Salesi", Ancona, Italy, [3]Fondazione di Ricerca e Cura "Giovanni Paolo II", Campobasso, Italy, [4]Ospedale Sandro Pertini, Roma, Italy, [5]Policlinico S. Orsola "L. e A. Seragnoli", Bologna, Italy, [6]Policlinico Umberto 1, Roma, Italy

We evaluated in thalassemia major (TM) if the cardiac efficacy of the three iron chelators (Desferrioxamine, Deferiprone, and Deferasirox) was influenced by hepatic iron levels over a follow up of 18 months. In patients treated with Deferasirox and Deferiprone percentage changes in cardiac R2* over 18 months were associated with final liver iron concentration (LIC) and percentage LIC changes. In no chelation group percentage changes in cardiac R2* were influenced by initial LIC or initial cardiac R2*.

2729 

The prognostic role of hypertrabeculation by cardiac magnetic resonance in thalassemia intermedia patients

Antonella Meloni[1], Francesca Macaione[2], Vincenzo Positano[1], Andrea Barison[1], Laura Pistoia[1], Salvatore Novo[2], Pasquale Assennato[2], and Alessia Pepe[1]

[1]Fondazione G. Monasterio CNR-Regione Toscana, Pisa, Italy, [2]Università degli Studi di Palermo, Policlinico "Paolo Giaccone", Palermo, Italy

We prospectively assessed whether the Piga's criterion for left ventricle non-compaction (LVNC) (NC/C ratio threshold of >2.5) had a prognostic role for adverse cardiovascular outcomes in thalassemia intermedia patients. We found out that patients with Piga's positive criterion had a significant higher risk of developing cardiac complications globally considered and arrhythmias.

2730

Gender-based optimization of cardiac follow up in thalassemia major patients

Antonella Meloni[1], Laura Pistoia[2], Silvia Maffei[1], Giuseppe Peritore[3], Valentina Vinci[4], Massimiliano Missere[5], Vincenzo Positano[2], Massimo Allò[6], Antonella Massa[7], and Alessia Pepe[1]

[1]Fondazione G. Monasterio CNR-Regione Toscana, Pisa, Italy, [2]CMR Unit, Fondazione G. Monasterio CNR-Regione Toscana, Pisa, Italy, [3]"ARNAS" Civico, Di Cristina Benfratelli, Palermo, Italy, [4]Azienda Ospedaliera "Garibaldi" Presidio Ospedaliero Nesima, Catania, Italy, [5]Fondazione di Ricerca e Cura "Giovanni Paolo II", Campobasso, Italy, [6]Presidio Ospedaliero ASL 5, Crotone, Italy, [7]Ospedale "Giovanni Paolo II", Olbia, Italy

Females seem to tolerate iron toxicity better, possibly as an effect of reduced sensitivity to chronic oxidative stress. Based on our data about the significantly different risk in developing cardiac complications, in females older than 20 years the FU may be performed every 24 months, thus optimizing health care costs.

2731

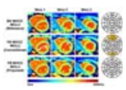

Improved Myocardial T1 mapping using a Novel Motion-Insensitive Reconstruction

Céline Smekens[1], Radhouene Neji[1,2], Reza Razavi[1], René Botnar[1], and Sébastien Roujol[1]

[1]Division of Imaging Sciences and Biomedical Engineering, King's College London, London, United Kingdom, [2]MR Research Collaborations, Siemens Healthcare Limited, Frimley, United Kingdom

Myocardial T1 mapping sequences are commonly performed under breath-hold conditions. However, motion between T1-weighted images can be observed in ~50% of acquisitions. Image registration algorithms can be used for motion correction but are not available on all scanners, can occasionally fail and remain challenging using low contrast sequences such as saturation-based T1 mapping techniques. In this study we sought to develop and evaluate a novel motion-insensitive T1 mapping reconstruction approach which automatically discards misaligned/artefact T1-weighted images.

2732

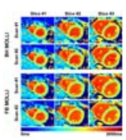

Free Breathing Myocardial MOLLI T1 Mapping using Real-time Slice Tracking and Non-Rigid Image Registration

Céline Smekens[1], Radhouene Neji[1,2], Reza Razavi[1], René Botnar[1], and Sébastien Roujol[1]

[1]Division of Imaging Sciences and Biomedical Engineering, King's College London, London, United Kingdom, [2]MR Research Collaborations, Siemens Healthcare Limited, Frimley, United Kingdom

The modified Look Locker (MOLLI) sequence is the most widely used myocardial T1 mapping approach. In this 2D sequence, several T1-weighted images are acquired within a breath hold and used to create a T1 map. However, some patients are unable to sustain stable breath-holds which generates 3D motion between the T1-weighted images. While image registration can potentially be used to correct for in-plane motion, through-plane motion cannot be corrected and may introduce bias in T1 estimates. In this study, we sought to develop and assess a free breathing MOLLI sequence with real-time slice tracking and non-rigid image registration to reduce in-plane and through-plane motion effects.

2733

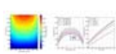

Off-resonance correction in myocardial T1-mapping using Bloch simulations of the MOLLI sequence

Nicola Martini[1], Andrea Barison[2], Maria Filomena Santarelli[3], Daniele Della Latta[1], Francesco Avogliero[1], Vincenzo Positano[2], Luigi Landini[2], and Dante Chiappino[1]

[1]Fondazione Toscana "G. Monasterio", Massa, Italy, [2]Fondazione Toscana "G. Monasterio", Pisa, Italy, [3]CNR Institute of Clinical Physiology, Pisa

Myocardial T1 mapping using MOLLI is influenced by off-resonance effects that lead to underestimation of T1. In this study a method for the correction of the off-resonance influence on T1 mapping, based on the Bloch simulations of the MOLLI sequence, is proposed. In vivo results on a healthy population (N=67) showed that the regional variation of T1 is highly correlated with the distribution of the off-resonance. The proposed method effectively reduced the artifactual T1 underestimation due to off-resonance, especially in myocardial segments that exhibited elevated B0 inhomogeneities.

2734

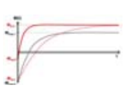

Quasi black blood T1-mapping using slice-selective TRASSI for improved visualization of the myocardium

Daniel Gensler[1,2], Tim Salinger[1,2], Georg Ertl[1,2], Peter M Jakob[3,4], and Peter Nordbeck[1,2]

[1]Department of Internal Medicine I - Cardiology, University Hospital Würzburg, Würzburg, Germany, [2]Comprehensive Heart Failure Center (CHFC), University Hospital Würzburg, Würzburg, Germany, [3]Experimental Physics 5, University of Würzburg, Germany, [4]Magnetic Resonance and X-ray Imaging MRB, Development Center X-ray Technology EZRT Fraunhofer Institute for Integrated Circuits IIS, Würzburg, Germany

Currently available T1 mapping techniques have only restricted capabilities for the visualization of the right myocardium and they have the limitation that after contrast agent application the T1-contrast between blood pool and fibrotic myocardium is partially very low.

The quasi black blood TRASSI sequence shows improved abilities for the visualization and T1-quantification of myocardial structures. So it might be suited in clinical routine for a clear visualization of the right myocardium or for the detection of slight endocardial infarctions, because it is an ultra-fast and robust cardiac T1-mapping method with a total acquisition time of less than 7s.

2735 

T1 Errors from Off-Resonance Effects for MOLLI at 3T: Experience in a Clinical Study

Justin G Grenier[1], Natasha Wiebe[2], Stephanie Thompson[2], Scott Klarenbach[2], Marcello Tonelli[3], Paolo Raggi[2], and Richard B Thompson[1]

[1]*Biomedical Engineering, University of Alberta, Edmonton, AB, Canada,* [2]*Medicine, University of Alberta, Edmonton, AB, Canada,* [3]*Medicine, University of Calgary, Calgary, AB, Canada*

The widely used MOLLI (MOdified Look-Locker Inversion recovery) T1 mapping approach underestimates T1 values as a function of several factors, including off-resonance frequency. Native T1 and matched off-resonance frequency (Δω) maps were acquired in 24 subjects as part of a study of patients with kidney disease (3T field strength). Δω within individuals had an average range 133±43Hz, and Δω was significantly correlated with underestimation of native T1, in good agreement with Bloch equation simulations. ~50% of slices had relatively large (75-150 Hz) off-resonance frequencies, for which T1 errors ranged from -25ms to -150ms.

2736 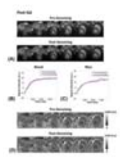

Multi-Slice GRE-MOLLI at 3T using Denoising with Low-Rank and Sparsity Constraints

Paul Kyu Han[1,2], Chao Ma[1,2], Nicolas Guehl[1,2], Nathaniel Alpert[1,2], Marc Normandin[1,2], and Georges El Fakhri[1,2]

[1]*Radiology, Massachusetts General Hospital, Boston, MA, United States,* [2]*Harvard Medical School, Boston, MA, United States*

Modified Look-Locker inversion recovery (MOLLI) uses bSSFP readout due to its high SNR, however, bSSFP is sensitive to off-resonance effects which result in banding artifacts. Recently, GRE has been proposed as an alternative readout for MOLLI, however, the low SNR efficiency of GRE-MOLLI is still a major problem. In this work, we propose to use a denoising reconstruction framework with low-rank and sparsity constraints to improve the low SNR of GRE-MOLLI. The proposed denoising method improved the low SNR of GRE-MOLLI, and multi-slice GRE-MOLLI is feasible for artifact-free T_1 mapping with wider spatial coverage at high magnetic fields ($$$\geq 3T$$$).

2737 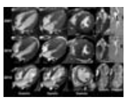

Prognostic value of cardiac MR imaging for end-stage phase of hypertrophic cardiomyopathy patients with or without adverse ventricular remodeling

Sainan Cheng[1], Chen Cui[2], Gang Yin[2], Lu Li[2], and Shihua Zhao[2]

[1]*Fuwai Hospital, Chinese Academy of Medical Sciences and Peking Union Medical College, Beijing, People's Republic of China,* [2]*Fuwai Hospital,Chinese Academy of Medical Sciences and Peking Union Medical College*

Cardiac morphology as well as LGE extent proved to be particularly heterogeneous in ES phase of HCM patients. For ES phase of HCM patients with adverse ventricular remodeling, LGE was a significant predictor of poor outcomes. But for ES phase of HCM patients without ventricular dilatation, biatrial enlargement, extremely diastolic dysfunction and higher incidences of AF may contribute more to adverse prognosis.

2738 

CMR-Derived Regional T2, T1/ECV, Myocardial Velocities, and Dyssynchrony Influenced by Donor and Recipient Characteristics after Heart Transplantation

Ryan Dolan[1], Amir Rahsepar[1], Julie Blaisdell[1], Allen Anderson[2], Kambiz Ghafourian[2], Esther Vorovich[2], Jonathan Rich[2], Jane Wilcox[2], Clyde Yancy[2], Jeremy Collins[1], Michael Markl[1], and James Carr[1]

[1]*Radiology, Northwestern University, Chicago, IL, United States,* [2]*Cardiology, Northwestern University, Chicago, IL, United States*

Cardiac MRI is increasingly being used for cardiac allograft surveillance following transplantation, so it is important to investigate which recipient and donor characteristics influence several CMR parameters: global ventricular function, myocardial velocities, dyssynchrony, T2, native T1, and ECV. Notable associations with T2 included donor age, normalized recipient-donor age difference, and recipient weight. Peak diastolic longitudinal velocity was associated with donor age and cold ischemic time.

2739 

Non-contrast T1 mapping can detect myocardial fibrosis in hypertrophic cardiomyopathy without gadolinium. Is native T1 a superior alternative to late gadolinium enhancement?

Yoshiaki Morita[1], Naoaki Yamada[1], Teruo Noguchi[2], Yoshiaki Watanabe[1], Tatsuya Nishii[1], Atsushi Kono[1], and Tetsuya Fukuda[1]

[1]*Department of Radiology, National Cerebral and Cardiovascular Center, Suita, Osaka, Japan,* [2]*Division of Cardiology, National Cerebral and Cardiovascular Center, Suita, Osaka, Japan*

Native T1 mapping is a novel cardiac magnetic resonance technique for myocardial tissue characterization without contrast administration. Native T1-mapping in hypertrophic cardiomyopathy was correlated with T1 map-based extracellular volume fraction, and native T1 of apparently late gadolinium enhancement (LGE)-negative segments were significantly longer than normal myocardium. Therefore, native T1 mapping has the potential to quantify the volume of interstitial space without gadolinium, which would be useful particularly in patients who are limited in use of gadolinium. Furthermore, native T1 would be a useful biomarker for the detection of diffuse myocardial damage difficult to evaluate using conventional LGE alone.

2740 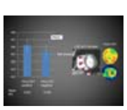

Assessment of myocardial inflammation in cardiac sarcoidosis using early gadolinium enhancement

Yoshiaki Morita[1], Naoaki Yamada[1], Teruo Noguchi[2], Yoshiaki Watanabe[1], Tatsuya Nishii[1], Atsushi Kono[1], and Tetsuya Fukuda[1]

[1]*Department of Radiology, National Cerebral and Cardiovascular Center, Suita, Osaka, Japan,* [2]*Division of Cardiology, National Cerebral and Cardiovascular Center, Suita, Osaka, Japan*

In patients with cardiac sarcoidosis, assessment of the activity of myocardial inflammation is as crucial as the choice of therapeutic strategy and monitoring of therapeutic effects. It is known that early gadolinium enhancement (at 2–5 minutes after gadolinium administration) can visualize myocardial inflammation and/or edema such as in acute myocarditis and acute myocardial infarction. In this study, images of gadolinium enhancement at 2 minutes delay were significantly associated with findings regarding active inflammation, suggesting that early gadolinium enhancement has the potential to act as a marker of inflammation activity in cardiac sarcoidosis.

2741

Simple quantification using the myocardium-to-lumen signal ratio in diffuse myocardial fibrosis of non-ischemic cardiomyopathies: Correlation with T1 mapping derived ECV

Yoshiaki Morita[1], Naoaki Yamada[1], Teruo Noguchi[2], Yoshiaki Watanabe[1], Tatsuya Nishii[1], Atsushi Kono[1], and Tetsuya Fukuda[1]

[1]Department of Radiology, National Cerebral and Cardiovascular Center, Suita, Osaka, Japan, [2]Division of Cardiology, National Cerebral and Cardiovascular Center, Suita, Osaka, Japan

Myocardial T1 mapping has recently been applied to the quantification of extracellular volume fraction (ECV) and has shown potential for the detection of myocardial fibrosis. However, for the measurement of ECV, additional scans of pre- and post-contrast T1 mapping are necessary, and the post-processing procedure is time consuming. In this study, the myocardium-to-lumen signal ratio (M/L) in conventional late gadolinium enhancement images with fixed inversion time showed acceptable levels of correlation with ECV obtained by the T1 mapping in non-ischemic cardiomyopathy, suggesting that M/L has the potential to allow for simple quantification of the fibrotic change in non-ischemic cardiomyopathies.

2742

Assessment and detection of left ventricular thrombus in patients with acute ischemic stroke using cardiac MR (ADVENT study)

Yoshiaki Morita[1], Junji Takasugi[2], Naoaki Yamada[1], Teruo Noguchi[3], Yoshiaki Watanabe[1], Tatsuya Nishii[1], Atsushi Kono[1], and Tetsuya Fukuda[1]

[1]Department of Radiology, National Cerebral and Cardiovascular Center, Suita, Osaka, Japan, [2]Division of Neurology, National Cerebral and Cardiovascular Center, Suita, Osaka, Japan, [3]Division of Cardiology, National Cerebral and Cardiovascular Center, Suita, Osaka, Japan

In patients with acute ischemic stroke (AIS), the assessment of left ventricular thrombus (LVT) is essential. In this study, we showed the utility of the early phase of gadolinium enhancement for detecting LVT in AIS patients, which conventional TTE hardly identified. CE-CMR, when using the early phase of gadolinium enhancement, should be performed on acute ischemic stroke patients, especially those with prior myocardial infarction or LV dysfunction and without definitive stroke etiologies.

2743

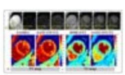

A 2D combined myocardium T1 and T2 mapping

Rui Guo[1], Zhensen Chen[1], Jianfeng zhang[1], Jianwen Luo[1], and Haiyan Ding[1]

[1]Center for Biomedical Imaging Research, Department of Biomedical Engineering, School of Medicine, Tsinghua University, Beijing, People's Republic of China

In this study, we developed a 2D combined myocardial T1 and T2 mapping sequence that uses a combination of saturation pulse and T2 preparation pulse and allows simultaneously obtaining T1 and T2 map with acceptable breath holding time (12 heartbeats). High quality multiple T1 and T2 weighted images were obtained in the other cardiac cycle between the saturation pulse and T2 preparation pulse. Phantom experiment showed that T1 and T2 measured by proposed method highly correlated with reference methods. In vivo experiment showed that the proposed sequence can yield comparable myocardium T1 and T2 values with the conventional separated T1 and T2 mapping sequences.

2744

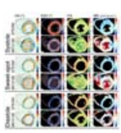

An in-vivo comparison of STEAM and 2nd order motion compensated spin-echo imaging in multi-phase cardiac DTI at 3T

Andrew David Scott[1,2], Sonia Nielles-Vallespin[1,3], Pedro Ferreira[1,2], Zohya Khalique[1], Dudley Pennell[1,2], and David Firmin[1,2]

[1]Cardiovascular Biomedical Research Unit, Royal Brompton Hospital, London, United Kingdom, [2]National Heart and Lung Institute, Imperial College London, London, United Kingdom, [3]National Heart Lung and Blood Institute, National Institutes of Health, Bethesda, MD, United States

Cardiac diffusion tensor imaging (cDTI) is a novel non-invasive method of interrogating myocardial microstructure that has seen a recent surge in interest. Many of the most interesting clinical results were obtained using stimulated echo acquisition mode (STEAM) imaging at multiple cardiac phases. Recently however, spin-echo cDTI with second order motion compensated diffusion gradients (M012-SE) was proposed. In this study we report results of a comparison of M012-SE and STEAM imaging in multiple cardiac phases at 3T in 15 healthy subjects with matched sequence parameters. While M012-SE provides comparable quality data in systole, STEAM is the more reliable technique in diastole.

2745

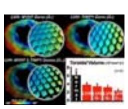

Integrated Analysis of Cardiac Genetic and Structural Alterations in Left Ventricular Hypertrophy using the Supertoroidal Model

Choukri Mekkaoui[1], Howard H Chen[1], Iris Y Chen[1], Ronglih Liao[2], William J Kostis[3], Timothy G Reese[1], Marcel P Jackowski[4], and David E Sosnovik[1]

[1]Harvard Medical School - Massachusetts General Hospital, Boston, MA, United States, [2]Brigham and Woman's Hospital, Harvard Medical School, Boston, MA, United States, [3]Rutgers Robert Wood Johnson Medical School, New Brunswick, NJ, United States, [4]University of São Paulo, São Paulo, Brazil

Response to disease occurs over many scales ranging from individual gene expression to whole organ physiology. We employed the supertoroidal model of the diffusion tensor to study the interaction between gene expression and microstructure of the heart. Left ventricular hypertrophy (LVH) was induced in C57Bl6 mice through aortic banding, and characterization of the cardiac microstructure was performed *in vivo* with DTI. The supertoroidal model was constrained by both diffusion information and gene expression data related to cardiomyocyte hypertrophy and myofiber orientation. Our model enabled further characterization of LVH by unifying information at different scales and across domains.

2746

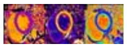

Segment and sexual variation of myocardium in T1 mapping and extracellular volume fraction with cardiovascular magnetic resonance in healthy volunteers

Yukun Cao[1], Yue Cui[1], Xiangchuang Kong[1], Shan Zhang[1], Xu Yan[2], and Heshui Shi[1]

[1]Department of Radiology, Union Hospital, Tongji Medical College, Huazhong University of Science and Technology, Wu Han, People's Republic of China, [2]MR Collaboration NE Asia, Siemens Healthcare, Shanghai, China

This study aimed to evaluate sex and segment differences of myocardium in native T1 value and ECV in healthy volunteers. We measured native T1 value of 425 segments and ECV of 424 segments. The results showed that myocardial ECV of females was higher than that of males in basal, middle and apical segments. The ECV of the apical segments was higher than in the basal and middle segments. The mean native T1 value and ECV were not associated with age, ejection function(EF), end diastolic volume(EDV), end systolic volume(ESV), and stroke volume (SV).

2747

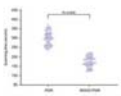

Role of free-breathing motion-corrected phase-sensitive inversion recovery (MOCO-PSIR) imaging technique for the assessment of late gadolinium enhancement

Yinyin Chen[1], Shan Yang[1], Hong Yun[1], Xiaoming Bi[2], Caixia Fu[3], Hang Jin[1], and Mengsu Zeng[1]

[1]Department of Radiology, Zhongshan Hospital, Fudan University, Department of Medical Imaging, Shanghai Medical school, Fudan University and Shanghai Institute of Medical Imaging, Shanghai, People's Republic of China, [2]MR Research and Development, Siemens Healthcare, Los Angeles, CA, United States, [3]Application development, Siemens Shenzhen Magnetic Resonance Ltd., Shenzhen, People's Republic of China

We aimed to investigate the role of motion-corrected phase-sensitive inversion recovery (MOCO-PSIR) technology for the evaluation of LGE. LGE imaging was conducted in 55 patients with MOCO-PSIR and conventional breath-hold PSIR sequences successively. Image quality was scored using a four-point scale. Compared with conventional PSIR, MOCO-PSIR showed better image quality and detected larger LGE volumes in nonischemic cardiomyopathy. Free-breathing motion-corrected PSIR method is a promising alternative to conventional PSIR sequence.

2748

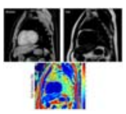

Myocardial fat quantification of normal subjects via 7-peaks mDixon model

Yu-Fen Huang[1], Feng Mao Chiu[2], Queenie Chan[3], Ya-Wen Shen[1], Chao-Jung Wei[1], and Chih-Miang Chiang[1]

[1]Executive Health Management Center, Cheng Ching Hospital, Taichung, Taiwan, [2]Philips Healthcare, Taipei, Taiwan, [3]Philips Healthcare, Hong Kong

Cardiac magnetic resonance imaging provides a lot of physiological information about myocardial pathology, and the mDixon technique also has been developed on cardiac application recently. The fat deposition in myocardium is possibly related with cardiomyopathy, so it is important to determine the fat composition of myocardium. The mDixon provides an easy way to acquire such this information within one breath hold, and it has a consistent result with magnetic resonance spectroscopy from the previous study. Also it has been reported that multipeak fat spectrum model gives more robustness, and 7-peaks model is used in this study. The aim of this study is to evaluate fat fraction of myocardium with 7-peaks model.

2749

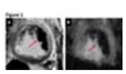

Reperfusion Hemorrhage Following Prolonged Myocardial Ischemia Leads to Fatty Degeneration of Myocardial Infarctions via Iron-Mediated, Self-Perpetuating Loop of Foam Cell and Ceroid Accumulation

Ivan Cokic[1], Avinash Kali[1], Hsin-Jung Yang[1], Richard LQ Tang[1], Joseph Francis[2], and Rohan Dharmakumar[1]

[1]Biomedical Imaging Research Institute, Cedars-Sinai Medical Center, Los Angeles, CA, United States, [2]Louisiana State University

Fatty infiltration within chronic myocardial infarctions (MI) is a common finding. It is typically observed in the peri-infarct border zone of old scars and has been linked to adverse outcomes in the chronic post-MI setting. To date, the trigger for fat deposition within old MI is unknown. Recent reports showed that iron deposits from hemorrhagic MI drive the recruitment of new monocytes/macrophages into the infarcted territory throughout the chronic phase after MI. Since iron-laden macrophages (siderophages) are prone to transforming into foam cells, we hypothesized that fatty degeneration of hemorrhagic myocardial infarctions has its origin in iron-driven foam cell formation.

2750

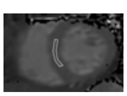

Cardiomyopathy in later-onset Fabry disease: a correlative study of T1 mapping on MR and histology

Jian-Ling Chen[1,2], Liang-Wei Chen[1,2], Sheng-Che Hung[1,2,3], Hsien-Tzu Liu[1,2], Mei-Han Wu[1,2], Fu-Pang Chang[2,4], An-Hung Yang[2,4], Ting-Rong Hsu[2,5], Dau-Ming Niu[2,5], Ming-Ting Wu[2,6], Chui-Mei Tiu[1,2], and Chien-Yuan Lin[7,8]

[1]Radiology, Taipei Veterans General Hospital, Taipei, Taiwan, [2]School of Medicine, National Yang Ming University, Taipei, Taiwan, [3]Department of Medical Imaging and Radiological Sciences, National Yang Ming University, Taipei, Taiwan, [4]Pathology, Taipei Veterans General Hospital, Taipei, Taiwan, [5]Pediatrics, Taipei Veterans General Hospital, Taipei, Taiwan, [6]Radiology, Kaohsiung Veterans Genertal Hospital, Kaohsiung, Taiwan, [7]GE Healthcare, Taipei, Taiwan, [8]GE Healthcare MR Research China, Beijing, China

Fabry disease is a rare and X-linked disorder characterized by accumulation of glycosphingolipid within lysosomes and resultant multiple organ damage including heart. Since lipid is known to shorten the MRI parameter T1, non-contrast T1 mapping has emerged as key imaging modality to assess Fabry cardiomyopathy and early detection of lipid deposition. This study provides a histologic validation of 7 male patients of untreated later-onset Fabry disease to demonstrate the negative correlation between native myocardial T1 value and severity of lipid deposition (correlation coefficient, -0.771; p, 0.042) and justifies the application of T1 mapping as a noninvasive predictor of surveillance strategy.

2751

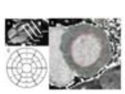

Cardiac MR Derived Extracellular Volume Measurements Using Different Contrast Agents

Amir Ali Rahsepar[1], Ahmadreza Ghasemiesfe[1], Monica J Korell[1], Jeremy D Collins[1], and James C Carr[1]

[1]Department of Radiology, Northwestern University, Chicago, IL, United States

T1 and ECV values calculated from gadoterate meglumine enhanced CMR are comparable to more routinely used gadopentetate dimeglumine and gadobutrol CMR measurements.

2752

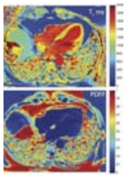

Single Breath-hold Measurement of T2 Corrected Myocardial Proton Density Fat Fraction in Humans at 3T

Ronald Ouwerkerk[1], Ranganath Muniyappa[2], Monica Skarulis[2], and Ahmed M Gharib[1]

[1]BMIB, NIDDK, Bethesda, MD, United States, [2]Metabolic Unit, NIDDK, MD, United States

Localized ^{1}H-MRS was used to determine T_2s for water and lipid signals in the human heart in a single breath hold and derive relaxation corrected proton density fat fractions.

2753

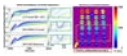

A Versatile MOLLI-based Inversion Time (TI) scout sequence for Myocardial Nulling Determination in emerging Late Gadolinium Enhanced CMR Variants: A Phantom Study

Keigo Kawaji[1], Adam Hasse[2], Amita Singh[1], Akhil Narang[1], Hui Wang[3], Timothy J Carroll[2], and Amit R Patel[1,2]

[1]Medicine, The University of Chicago, Chicago, IL, United States, [2]Radiology, The University of Chicago, Chicago, IL, United States, [3]Philips HealthTech, Cleveland, OH, United States

A Look-Locker scout is used for optimal inversion time (TI) determination of myocardial nulling in Late Gadolinium Enhancement (LGE) Cardiac Magnetic Resonance. Recently, novel LGE technique variants such as the Wideband approach have been proposed, and these approaches can lead to variability in the signal evolution between the Look-Locker TI-scout and LGE. In this study, we propose a Modified Look-Locker Inversion (MOLLI)-based TI-scout that closely matches its signal evolution to that of any LGE variant. Bloch simulation and phantom evaluation are performed to compare the null-times from the conventional LL-based and proposed MOLLI-based approaches against the LGE protocol over a range of clinically relevant T1 values observed in viability imaging.

2754

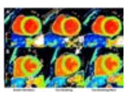

Free-breathing native cardiac T1 and T2 mapping with flexible elastic image registration: Preliminary Clinical Result

Shuo Zhang[1,2], Tomoyuki Okuaki[3], Sven Kabus[4], Bao Ru Leong[5], Yiying Han[5], Yi Hui Hung[5], Ping Wang[6], and Ru San Tan[5]

[1]Philips Healthcare, Singapore, Singapore, [2]National Heart Centre Singapore, Singapore, Singapore, [3]Philips Healthcare, Japan, [4]Philips Research, Hamburg, Germany, [5]National Heart Centre Singapore, Singapore, [6]Vanderbilt University, United States

Current myocardial T1 and T2 mapping based on inversion-recovery and single-shot readout techniques require generally at least 7 to 10 seconds breath hold. Improper and difficulties of breath hold is one of the main sources of error and reduced reproducibility. To mitigate the dependence of mapping on breath holds and also to increase patient comfort, we report free-breathing T1 and T2 mapping using different acquisition schemes using flexible elastic image registration. We demonstrate the feasibility of this approach with motion correction for increased image quality and quantification accuracy.

2755

The Correlation of Clinical and Image of Acromegaly Patients Based on 3.0T Cardiac Magnetic Resonance Quantitative Analysis of Myocardial T1 and Extracellular Volume

Jian Cao[1], Peijun Liu[1], Lu Lin[1], Xiao Li[1], Xiaopeng Guo[2], Jing An[3], Bing Xing[2], and Yining Wang[1]

[1]Radiology, PUMCH, Beijing, People's Republic of China, [2]Neurology, PUMCH, [3]MR Collaborations NE Asia, Siemens Healthcare

The aim of this study was to find out if there might be some correlation between clinical information and image measurements for acromegaly patients. And it found that for acromegaly patients, the basal slice of heart might be the most involvemented position, and its contractility had a positive correlation with GH burden, and both T1 and ECV had a negative correlation with IGF-1. And we need to enlarge the sample size and compare the changes before and after the surgery in order to give more informations to the clinicians.

2756

SMART1Map: Accuracy and Influencing Imaging Parameters For Cardiac T1 Mapping.

Malek I MAKKI[1,2], Barbara EU Burkhardt[3], and Emanuela Valsangiacomo[3]

[1]MRI Research, University Children Hospital, Zurich, Switzerland, [2]BioFlow, University Picardie Jules Verne, Amiens, France, [3]Cardiology, University Children Hospital, Zurich, Switzerland

SMART1Map sequence was performed on 6 phantoms with different T_1 values. Sixteen schemes were prescribed: 4 heart rates (60, 80, 100, 120 bpm), 2 spatial resolutions (FOV = 30 cm and FOV = 48 cm) and 2 cardiac phases (systole and diastole). The results show that SMART1Map underestimates long T_1 (native T_1 myocardium) at any scheme. We also found an increase in error with reduced FOV (all other parameters being identical), and an influence of the cardiac phases on T_1 at the levels of native and post-contrast blood and myocardium

---

2757

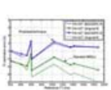

An alternative T1 estimation algorithm with a higher flip angle improves T1 mapping accuracy and precision of the MOLLI sequence

Jiaxin Shao[1], Kim-Lien Nguyen[2], and Peng Hu[1]

[1]Radiology, University of California, Los Angeles, Los Angeles, CA, United States, [2]Division of Cardiology, University of California, Los Angeles, Los Angeles, CA, United States

Good T1 estimation accuracy and precision is important for clinical application of the myocardial T1 mapping technique. Although the widely used T1 mapping technique, modified Look-Locker inversion-recovery (MOLLI), has good precision and reproducibility, it is not accurate. Several T1 estimation algorithms have been proposed to improve the accuracy for MOLLI. These algorithms however, often have reduced T1 estimation precision. We developed an improved MOLLI technique to achieve better accuracy and precision than the standard MOLLI sequence. Based on phantom and volunteer studies, a higher flip angle MOLLI with Bloch equation simulation and slice profile correction (BLESSPC) is used for T1 estimation.

2758

Coronary artery disease is not related to pathologic epicardial fat volumes, left ventricular strain or T1-relaxation times in hypertensive patients

Rami Homsi[1], Michael Meier-Schroers[1], Alois Sprinkart[1], Juergen Gieseke[2], Daniel Kuetting[1], Stefan Fischer[1], Darius Dabir[1], Julian Luetkens[1], Christian Marx[1], Hans Schild[1], and Daniel Thomas[1]

[1]Radiology, University Hospital Bonn, Bonn, Germany, [2]Philips Healthcare, Hamburg, Germany

Hypertension is related to increased amounts of epicardial fat, to myocardial fibrosis and to left-ventricular contractility disturbances despite a normal systolic left-ventricular ejection fraction. However, the presence of stable coronary atherosclerotic disease in general - and with no cardiac damage due to prior coronary pathologies - does not additionally affect these parameters.

2759

3D High Frequency Cardiac Magnetic Resonance Elastography Quantitatively Differentiates Myocardial Stiffness in Patients with HFPEF and Healthy Volunteers

Shivaram Poigai Arunachalam[1], Arvin Arani[1], Ian Chang[2], Yi Sui[1], Phillip Rossman[1], Kevin Glaser[1], Joshua Trzasko[1], Kiaran McGee[1], Armando Manduca[3], Barry Borlaug[2], Richard Ehman[1], and Philip Araoz[1]

[1]Radiology, Mayo Clinic, Rochester, MN, United States, [2]Cardiovascular Diseases, Mayo Clinic, [3]Biomedical Engineering and Physiology, Mayo Clinic

Increased myocardial stiffness in patients with heart failure with preserved ejection fraction (HFpEF) is known to affect diastolic filling. The purpose of this work was to determine if 3D high frequency cardiac MR elastography (MRE) can quantitatively differentiate increased myocardial stiffness in HFpEF patients compared to healthy volunteers. Two patients with clinical diagnosis for HFpEF and 47 healthy volunteers were studied. The myocardial stiffness of HFpEF patients (mean: 10.57 kPa) was found to be significantly stiffer ($p < 0.05$) than healthy controls (mean: 7.79 kPa). Recruitment of more HFpEF patients is underway for further validation of this finding.

2760

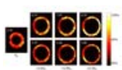

Reconstructing Inherent Stiffness in a Deforming Heart Phantom using MR Elastography

Myrianthi Hadjicharalambous[1], Adela Capilnasiu[1], Daniel Fovargue[1], Ayse Sila Dokumaci[1], Stefan Heinz Hoelzl[1], Jack Lee[1], Ralph Sinkus[1], and David Nordsletten[1]

[1]Division of Imaging Sciences and Biomedical Engineering, King's College London, London, United Kingdom

Cardiac MR-Elastography has significant potential to provide a non-invasive measure of myocardial tissue health. A core challenge in its application is the substantial motion of the heart over the cardiac cycle, which introduces a bias in the quantified *apparent* stiffness. In this work we apply a reconstruction technique for MRE designed to correct changes in apparent stiffness due to deformation. The reconstruction method is tested on anatomically accurate homogeneous and heterogeneous heart phantoms that are inflated to mimic diastolic function. The results demonstrate the ability of the reconstruction technique to retrieve intrinsic stiffness values, even under substantial inflation.

2761

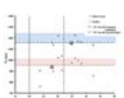

Comparison of SASHA and MOLLI sequences for Iron Quantification in the Myocardium.

Sarah McElroy[1,2], Torben Schneider[3], Daniel M Sado[4], Tarique Hussain[5,6], Amedeo Chiribiri[5], and Sarah Peel[1,2]

[1]Medical Physics Department, Guy's and St Thomas' Hospital, London, United Kingdom, [2]Department of Medical Physics and Bioengineering, Division of Imaging Sciences and Biomedical Engineering, King's College London, London, United Kingdom, [3]Philips Healthcare, Surrey, United Kingdom, [4]Cardiology Department, King's College Hospital, United Kingdom, [5]Division of Imaging Sciences & Biomedical Engineering, King's College London, London, United Kingdom, [6]Department of Pediatric Cardiology, University of Texas Southwestern, TX, United States

Development of T1 mapping in the myocardium in recent years has demonstrated that the technique can add information to inform the diagnosis or management of patients in a number of pathologies. Sequences have been developed to enable T1 mapping of the myocardium within a single breath-hold and the limitations of these sequences have been well characterized. Recent studies have investigated myocardial T1 mapping in iron overload patients using variants of the MOLLI sequence. These studies have concluded that T1 mapping could be more sensitive and reproducible than T2* mapping for the measurement of iron overload in the myocardium. The current study aims to determine the optimal T1 mapping sequence for iron overload. Simulations, phantom studies and in-vivo studies were carried out to investigate MOLLI and SASHA sequences used for T1 mapping of low T1 and T2 tissues (comparable to iron overload in the myocardium).

2762

Optimization of MOLLI reconstruction for free-breathing myocardial T1 imaging

Yun-Wen Wang[1], Yi-Fu Tsai[1], and Teng-Yi Huang[1]

[1]Department of Electrical Engineering, National Taiwan University of Science and Technology, Taipei, Taiwan

The free-breathing MOLLI (FB-MOLLI) presented in our previous study allowed T1 mapping in vivo without breath-hold. In this study, we attempted to implement unsupervised reconstruction for FB-MOLLI data sets and used a deformable method for image registration to improve the reliability of free-breathing T1 mapping. The results supported that the method improved the image alignments of the FB-MOLLI data sets and thus increased the quality of the T1 map. The variations of the repeated T1 measurements were significantly reduced in the anterolateral of the LV walls.

2763

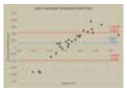

Derivation and Validation of Synthetic Hematocrit Calculation from Blood Pool T1 values at multiple different cardiac blood pools, in both high and low flow states on 3T MRI

Ozair Rahman[1], Kelvin Chow[2], James Carr[3], and Jeremy Collins[1]

[1]Radiology, Northwestern University, Chicago, IL, United States, [2]Siemens Medical Solutions, [3]Northwestern University

Comparison of the relationship between blood R1 and venous derived hematocrit in the left ventricle, left atrium, descending thoracic aorta, and short axis (apex, mid, and base) blood pools.

2764

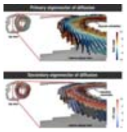

Dual identity of the interventricular septum with in vivo diffusion tensor imaging

Pedro Ferreira[1], Sonia Nielles-Vallespin[2], Andrew Scott[1], Zohya Khalique[1], Dudley Pennell[1], and David Firmin[1]

[1]Cardiovascular BRU, Royal Brompton Hospital, London, United Kingdom, [2]NHLBI, National Institutes of Health, MD, United States

Heart muscle has a complex cellular helical arrangement, where bundles of myocytes, known as sheetlets interleave with collagen-lined shear layers. The right and left ventricle form separately in early stages of cardiogenesis, resulting in a dual inter-ventricular septum. In this work we compare the myocyte and sheetlet microstructure in the septum and LV free-wall in healthy and HCM hearts with in vivo diffusion tensor imaging. Results show that the right-side of the interventricular-septum has myocyte orientations not seen in the free-wall, and also lower sheetlet angles, which may indicate an RV identity in this region.

2765

A Cost-effective 3D Printed Cardiac MR Phantom

Shivaprasad Ashok Chikop[1], Amaresh Shridhar Konar[2], Nimitha S L Reddy[3], Nithin Vajuvalli[1], Darshan Shivaramu Keelara[1], Ashwini Kumnoor[1], Ramesh Venkatesan[2], and Sairam Geethanath[1]

[1]Medical Imaging Research Centre, Dayananda Sagar Institutions, Bangalore, India, [2]Wipro-GE, Bangalore, India, [3]Embedded Systems, Dayananda Sagar University, Bangalore

Cardiac phantoms have been employed as testing and validating tools for newly developed techniques focused on sampling and reconstruction strategies. In this work, a 3D printed cardiac phantom was built to mimic the human heart. This was achieved through the integration of a peristaltic pump. Results depict the structural and functional behavior of the cardiac phantom, based on MR imaging on 1.5T scanners from 2 vendors. Ongoing work involves implementing the post-processing pipeline to correlate UI parameters with those derived from images. Future work focuses on employing PVA for preparing the heart model employing the 3D printing heart mold.

2766

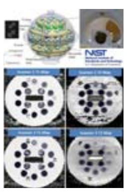

Inter-Scanner T1 and T2 Measurement Variability Evaluation on Two 3T Scanners with Identical Hardware and Software Configuration

Anshuman Panda[1], Clinton E Jokerst[1], Kristopher W Cummings[1], and Prasad M Panse[1]

[1]Radiology, Mayo Clinic, Scottsdale, AZ, United States

Inter-scanner T1 and T2 measurement variability was evaluated on two 3T scanners with identical hardware and software configuration to identify the most robust combination of sequence, parameters and post-processing that produces accurate measurement and to establish confidence intervals for T1 and T2 measurements for in-vivo studies by incorporating “native” inter-scanner variability.

2767

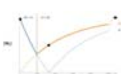

Cardiac T1 Mapping Using True Hybrid Inversion and Saturation Recovery

Glenn S. Slavin[1], Anne Menini[2], Haonan Wang[3], and Anja C.S. Brau[4]

[1]GE Healthcare, Bethesda, MD, United States, [2]GE Global Research, Munich, Germany, [3]GE Healthcare, Waukesha, WI, United States, [4]GE Healthcare, Menlo Park, CA, United States

Despite limited accuracy, MOLLI remains popular for T1 mapping due to high precision and visual quality of the maps. This is due primarily to the large dynamic range afforded by the inversion-recovery (IR) acquisition. Methods using saturation-recovery (SR) have better T1 accuracy but have relatively poor precision compared with MOLLI. This work presents a true hybrid IR/SR acquisition that targets the optimal regions of both the IR and SR relaxation curves, employs a novel method for maximizing dynamic range, and uses an improved sampling strategy. The proposed hybrid method combines the accuracy of single-point SR with the precision of IR.

Traditional Poster

Atherosclerosis Imaging

Exhibition Hall 2768-2791 Thursday 8:15 - 10:15

2768

Identification of Intrapalque Hemorrhage in Carotid Artery by Simultaneous Non-contrast Angiography and intraPlaque hemorrhage (SNAP) Imaging: A Comparison Study with MP-RAGE

Xihai Zhao[1], Dongye Li[2], Huilin Zhao[3], Xiaoyi Chen[2], Huiyu Qiao[1], Le He[1], Rui Li[1], Jianrong Xu[3], and Chun Yuan[1,4]

[1]Center for Biomedical Imaging Research, Department of Biomedical Engineering, Tsinghua University, Beijing, People's Republic of China, [2]Beijing Institute for Brain Disorders, Beijing, People's Republic of China, [3]Department of Radiology, Renji Hospital, School of Medicine, Shanghai Jiao Tong University, Shanghai, People's Republic of China, [4]Department of Radiology, University of Washington, Seattle, WA, United States

It is important to accurately identify carotid artery intraplaque hemorrhage (IPH) due to its significant association with ischemic stroke. MP-RAGE sequence has been demonstrated to be the best approach to detect carotid IPH. Recently, investigators proposed SNAP imaging technique which allows non-contrast MR angiography and identifying IPH simultaneously. This study sought to investigate the performance of SNAP imaging in detecting carotid IPH by comparing with MP-RAGE. We found that SNAP imaging detected more IPHs and showed larger IPH size than MP-RAGE, suggesting SNAP imaging might be a sensitive imaging tool to detect IPH.

2769

Predicting Procedure Successful Rate after Endovascular Recanalization for Chronic Carotid Artery Occlusion by 3D Vessel Wall Imaging

Huilin Zhao[1], Jianrong Xu[1], Xiaosheng Liu[1], Beibei Sun[1], Jieqing Wan[2], Weibo Chen[3], Xihai Zhao[4], and Chun Yuan[5]

[1]Radiology, Renji Hospital, Shanghai Jiao Tong University School of Medicine, Shanghai, People's Republic of China, [2]Neurosurgery, Renji Hospital, Shanghai Jiao Tong University School of Medicine, Shanghai, People's Republic of China, [3]MR Clinical Science, Philips Healthcare, Greater China, People's Republic of China, [4]Center for Biomedical Imaging Research,Department of Biomedical Engineering, Tsinghua University, Beijing, People's Republic of China, [5]University of Washington, WA, United States

Endovascular recanalization in patients with carotid chronic total occlusion (CTO) has been reported to be technically challenging. In this study, we retrospectively analyzed the 3D vessel wall imaging in patients with carotid CTO and its relationship to technical success rates. A total of 15 consecutive carotid CTO recanalization attempts were performed with overall technical success rate 60.0%. Compared with failure group, patients with an occlusion length <50mm, distal true lumen visibility in C1 segment on MR vessel wall images had a higher rate of successful recanalization. 3D vessel wall MR imaging may play a role in patient selection of endovascular recanalization in patients with carotid CTOs.

2770

Distribution and burden of atherosclerosis in patients with anterior circulation cerebral ischemic events: Characterization using combined extracranial and intracranial vessel wall MRI

Haifeng Gao[1,2], Jie Sun[1], Niranjan Balu[1], Dongxiang Xu[1], Daniel S Hippe[1], Chun Yuan[1], and Thomas S Hatsukami[1]

[1]University of Washington, Seattle, WA, United States, [2]Tangshan Gongren Hospital, Tangshan, People's Republic of China

Both extracranial and intracranial atherosclerosis may be implicated in large-artery atherothrombotic stroke. This proof-of-concept study characterized the distribution and burden of atherosclerosis in thirteen patients with anterior circulation cerebral ischemic events using combined extracranial and intracranial vessel wall MRI. We found that atherosclerotic plaques were highly prevalent in both extracranial and intracranial carotid arteries. Larger plaque burden measured as plaque index on black-blood vessel wall MRI, rather than luminal stenosis on time-of-flight MRA, was significantly associated with clinical symptoms. Black-blood vessel wall MRI may be useful in identifying the culprit plaque in patients with suspected large-artery atherothrombotic stroke.

2771

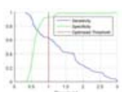

Reproducibility of Semi-automatic Carotid Intraplaque Hemorrhage Quantification using SNAP MRI

Jin Liu[1], Jie Sun[1], Thomas S. Hatsukami[1], Marina S. Ferguson[1], Niranjan Balu[1], William S. Kerwin, Daniel S. Hippe[1], Amy Wang, and Chun Yuan[1]

[1]University of Washington, Seattle, WA, United States

Intraplaque hemorrhage (IPH), a characteristic feature of high-risk atherosclerosis, can be identified as hyperintensity areas on T1-weighted MRI. Simultaneous Non-contrast Angiography and intraPlaque hemorrhage (SNAP) MRI has been shown to provide comparable IPH detection as MPRAGE with additional benefit of lumen assessment in the same scan. In this study, we developed a semi-automatic method to detect and quantify IPH on SNAP MRI with histology confirmation. An objective IPH detection threshold was identified and high scan-rescan reproducibility was obtained for semi-automatic IPH volume measurement and maximum IPH intensity.

2772

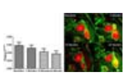

MR Imaging of Vasa Vasorum During Lipid-Lowering Therapy to Carotid Unstable Plaque: A Prospective Study in Chinese Patients

Cui Bao[1], Cui Jinguo[1], and Cai Jianming[2]

[1]Bethune international peace hospital, Shi jiazhuang, People's Republic of China, [2]Chinese PLA general hospital

Carotid plaque vasa vasorum angiogenesis from adventitia may be influenced by inflammation, could promote intraplaque hemorrhage and decrease the thickness of fibrous cap, finally, the cap is prone to rupture. Drug therapy and assessment to the vulnerable plaque, in vivo, would be of major clinical interest. To investigate whether lipid therapy leads to changes in vasa vasorum characteristics of carotid unstable plaque in chinese patients, as measured by using dynamic contrast-enhanced (DCE) MRI. Focus on inflammation to monitor the early beneficial therapy using vasa vasorum MR imaging, biomarker in vivo.

2773

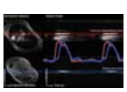

Assessment of aortic pulse wave velocity in patients with peripheral artery disease

Erin K Englund[1], Michael C Langham[1], Emile R Mohler[2], Thomas F Floyd[3], and Felix W Wehrli[1]

[1]Department of Radiology, University of Pennsylvania, Philadelphia, PA, United States, [2]Department of Medicine, University of Pennsylvania, Philadelphia, PA, United States, [3]Department of Anesthesiology, Stony Brook University, Stony Brook, NY, United States

Pulse wave velocity (PWV) provides a measure of arterial stiffness by quantifying the propagation velocity of the systolic pressure wave along the arterial wall. Prior studies have reported that PWV is elevated in patients with peripheral artery disease (PAD), and here we sought to determine whether the elevation in PWV is correlated with PAD disease severity as measured by the ankle-brachial index (ABI). No correlation was observed between ABI and PWV, suggesting that the systemic nature of atherosclerosis may be contributing to the increase in PWV more than the specific lesions that result in a reduction in ABI.

2774 

3D black-blood DCE-MRI using radial stack-of-stars acquisition and CS reconstruction: application in carotid and femoral arteries

Jasper Schoormans[1], Kang H Zheng[2], Erik S Stroes[2], Gustav J Strijkers[1], Aart J Nederveen[3], and Bram F Coolen[1]

[1]Department of Biomedical Engineering and Physics, Academic Medical Center, Amsterdam, Netherlands, [2]Department of Vascular Medicine, Academic Medical Center, Amsterdam, Netherlands, [3]Department of Radiology, Academic Medical Center

We implemented a high temporal resolution 3D black-blood protocol for DCE imaging of atherosclerotic plaques using a combination of a radial stack-of-stars sampling scheme, motion-sensitised (iMSDE) blood suppression and CS reconstruction. Using this approach, 3D black-blood DCE images with a temporal resolution of 12s could be obtained. In this work, we show the application of our method in patients with femoral and carotid artery plaques.

2775 

Robust fat suppressed direct thrombus imaging (MPRAGE) sequence with a large field-of-view at 3T

Nobuyuki Toyonari[1], Masami Yoneyama[2], Seiichiro Noda[1], Yukari Horino[1], and Kazuhiro Katahira[1]

[1]Kumamoto Chuo Hospital, Kumamoto, Japan, [2]Philips Electronics Japan, Tokyo, Japan

MR plaque imaging is promising for characterizing atherosclerotic plaque. We proposed direct thrombus imaging (MPRAGE), based on mDIXON turbo field-echo sequence, could provide more robust and stable black-blood imaging with a large field-of-view compared with conventional sequences.

2776 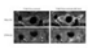

Molecular Magnetic Resonance Imaging of Vascular Myeloperoxidase Activity for the Identification of Unstable Atherosclerotic Plaque

Imran Rashid[1], David Cheng[1], Jihan Talib[1], Ghassan J Maghzal[1], Andre Bongers[2], Ren Minqin[3], and Roland Stocker[1]

[1]Vascular Biology Division, Victor Chang Cardiac Research Institute, Sydney, NSW, Australia, [2]Biological Resources Imaging Laboratory, University of New South Wales, Sydney, Australia, [3]Department of Physics, Centre for Beam Applications, National University of SIngapore, Singapore, Singapore

Non-invasive imaging of unstable atherosclerotic plaques prone to rupture remains an unmet need in clinical cardiology. This is because current imaging modalities provide information on plaque burden, luminal stenosis and calcification, whereas they have limited ability to discern unstable from stable plaques. We used the tandem stenosis mouse model of unstable plaque in conjunction with MRI and a sensor (bis-5-hydroxytryptamide-DTPA-Gd) for the activity of the inflammatory enzyme myeloperoxidase. Our results reveal sustained and greater enhancement of unstable experimental plaque with the targeted sensor compared with its non-targeted analog (DTPA-Gd), and these results were confirmed by separate biochemical and histological analyses.

2777 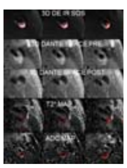

Motion Insensitive 3D Multiple Echo Inversion Recovery Stack of Star(ME IR SOS) technique for measurement of T2* in Intraplaque Hemorrhage (IPH)

Seong-Eun Kim[1], J Rock Hadley[1], J Scott McNally[1], Bradley D Bolster, Jr. [2], Gerald S Treiman[3], and Dennis L Parker[1]

[1]UCAIR, Department of Radiology and Imaging Sciences, University of Utah, Salt Lake City, UT, United States, [2]Siemens Healthcare, [3]Department of Veterans Affairs, VASLCHCS

The purpose of this work was to develop a 3D ME IR SOS technique to reduce off resonance blurring and allow measurement of T2* in Atherosclerotic plaque. In a prior study we observed lower ADC values in symptomatic IPH. We hypothesized that the T2* measurements from 3D ME IR SOS would help identify IPH and further characterize symptomatic and asymptomatic IPH. The 3D ME IR SOS can provide motion insensitive IPH visualization and T2* values simultaneously which may provide important clinical information to detect the plaque progression.

2778 

3D visualization of Vascular Cell Adhesion Molecule-1 (VCAM-1) specific Ultrasmall Superparamagnetic Iron Oxide (USPIO) nanoparticles in the atherosclerotic mouse with accelerated self-navigated radial 4D-MRI.

Kristina Andelovic[1], Patrick Winter[2], Thomas Kampf[2,3], Volker Herold[2], Peter Michael Jakob[2,4], and Wolfgang Bauer[1]

[1]Medizinische Klinik und Poliklinik I, Universitätsklinikum Würzburg, Würzburg, Germany, [2]Experimentelle Physik V, Universität Würzburg, Würzburg, Germany, [3]Institut für Diagnostische und Interventionelle Neuroradiologie, Universitätsklinikum Würzburg, Würzburg, Germany, [4]Fraunhofer IIS, Fraunhofer EZRT, Magnetresonanz- und Röntgenbildgebung (MRB), Würzburg, Germany

USPIO-based, functionalized contrast agents targeting VCAM-1 enable the visualization of inflamed areas in the vessel wall during early atherogenesis. We present a novel 3D technique for coverage of the whole aortic arch at high spatial resolution and a time-resolved detection of nanoparticles with an ECG-free flow-compensated radial 3D-Cine acquisition. T2* weighted 3D-Cines were acquired using two different gradient echoes to provide phase difference maps. The results indicate a reliable detection of the nanoparticles with the new method due to a true 3D coverage of the aorta and the additional phase information.

2779 

Gradient Echo Derived Multi-Contrast Imaging for Carotid Atherosclerosis Assessment

Zechen Zhou[1], Shuo Chen[2], Xihai Zhao[2], Rui Li[2], and Chun Yuan[2,3]

[1]Philips Research China, Shanghai, People's Republic of China, [2]Center for Biomedical Imaging Research, Department of Biomedical Engineering, Tsinghua University, Beijing, People's Republic of China, [3]Vascular Imaging Lab, Department of Radiology, University of Washington, Seattle, WA, United States

In this work, we developed a post processing framework to generate multi-contrast images from a single three dimensional MR scan of multi-echo gradient echo sequence, which can alleviate the registration problem and further improve the scan efficiency with a total scan time of 3min22sec for carotid atherosclerosis imaging. The initial experiments has demonstrated its feasibility for vessel wall delineation and its potential for plaque component characterization.

2780

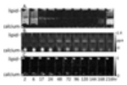

Quantitative characterization of calcified and lipid-laden blood clot in vitro at 3T

Spencer D Christiansen[1,2], Junmin Liu[1], Trevor Wade[1], Joy Dunmore-Buyze[1], Michael B Boffa[3], Luciano Sposato[4], and Maria Drangova[1,2]

[1]Imaging Research Laboratories, Robarts Research Institute, Western University, London, ON, Canada, [2]Dept. of Medical Biophysics, Schulich School of Medicine & Dentistry, Western University, London, ON, Canada, [3]Dept. of Biochemistry, Schulich School of Medicine & Dentistry, Western University, London, ON, Canada, [4]Dept. of Clinical Neurological Sciences, Western University, London, ON, Canada

Thrombus composition in embolic occlusion, particularly the presence of thrombolysis-resistant components such as calcium and fat, can significantly influence treatment efficacy, yet current MR methods for inferring composition are qualitative and sensitive only to red blood cells. We examined the ability of novel post-processing algorithms applied to a tailored GRE acquisition to discriminate and quantify important components within *in vitro* blood clots of varied hematocrit over a nine-day ageing period. Calcium and lard were readily discernable throughout the experiment, while clots were differentiable from one another between two to six days, demonstrating this protocol's potential for thrombus characterization *in vivo*.

2781

Optimization of whole-brain intracranial arterial wall imaging sequence using Bloch equation simulation

Lei Zhang[1], Chao Zou[1], Lijie Ren[2], Dong Liang[1], and Xin Liu[1]

[1]Paul C. Lauterbur Center for Biomedical Imaging, Shenzhen Institutes of Advanced Technology, Chinese Academy of Sciences, Shenzhen, People's Republic of China, [2]Neurology, Shenzhen Second People's Hospital, Shenzhen, People's Republic of China

T1 weighted SPACE has gain popularity in intracranial wall imaging, but its long scan time makes it impractical and its multiple parameters make it very difficult to be optimized. In this study, we looked into the effect of various imaging parameters of T1w SPACE on the signal-to-noise (SNR) and contrast ratio (CR) between vessel wall and cerebrospinal fluid using Bloch equation simulation. An optimized whole-brain intracranial artery wall imaging protocol which had comparable higher CR and SNR within 8min and 0.55mm iso resolution was found. The simulation results were verified by the volunteer study and matched the experiments well.

2782

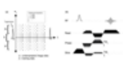

Assessment of Local Pulse-Wave-Velocity Distribution in Mice using k-t BLAST MRI with Semi-Automatic Area Segmentation

Volker Herold[1], Patrick Winter[1], Stefan Herz[2], Fabian Gutjahr[1], Kristina Andelovic[3], Wolfgang Rudolf Bauer[3], and Peter Michael Jakob[1]

[1]Department of Physics, University of Würzburg, Würzburg, Germany, [2]Department of Diagnostic and Interventional Radiology, University Hospital Würzburg, Würzburg, Germany, [3]Department of Internal Medicine I, Division of Cardiology, University Hospital Würzburg, Würzburg, Germany

Arterial stiffness (AS) assessed by pulse wave velocity (PWV) has been shown to represent a valuable biomarker of cardiovascular disease risk. Local elastic properties of the murine aortic vessels such as the pulse-wave-velocity (PWV) can be examined using PC-MRI [1]. In the present study we provide an accelerated method based on a k-t BLAST undersampling scheme combined with a new semi-automatic segmentation algorithm to quantify the distribution of the local PWV along the aortic vessel.

2783

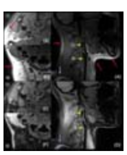

Improvement of fat separation for simultaneous carotid and intracranial vessel wall imaging by dual-echo fat-water imaging

Chao Zou[1], Lei Zhang[1], Chuanli Cheng[1], Xin Liu[1], and Hairong Zheng[1]

[1]Shenzhen Institutes of Advanced Technology, Chinese Academy of Sciences, Shenzhen, People's Republic of China

In this study, we used dual-echo fat-water imaging technique in variable flip angle turbo spin echo sequence for simultaneous carotid and intracranial artery imaging to obtain fat-free vessel wall images. Results show that the technique was promising for simultaneous carotid and intracranial vessel wall imaging to improve the SNR and better delineation of carotid vessel wall.

2784

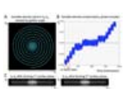

3D Golden-Angle Spiral Sparse Parallel-Imaging for Lumen Area Measurements of the Entire Proximal and Mid-Segments of the Coronary Arteries in a Breath-Hold

Michael Schär[1], Gabriele Bonanno[1,2], Allison G. Hays[2], and Robert G. Weiss[1,2]

[1]Russel H. Morgan Department of Radiology and Radiological Science, Johns Hopkins University School of Medicine, Baltimore, MD, United States, [2]Department of Medicine, Johns Hopkins University School of Medicine, Baltimore, MD, United States

Coronary artery endothelial function (CEF) could historically only be measured with invasive catheterization-based testing. Recently, 2-dimensional cine MRI in combination with isometric handgrip exercise was introduced to quantify CEF noninvasively. However, the MRI technique only assesses CEF at one or two locations in an artery and does not allow assessment of regional heterogeneity present throughout diseased vessels. The aim of this work was to develop high-resolution isotropic 3-dimensional cine coronary MRI that enables measures of coronary lumen area along the entire proximal and mid segments of the coronary arteries in a single breath-hold, a pre-requisite for future 3-dimensional CEF measurements.

2785

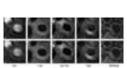

Identification of Carotid Lipid-Rich Necrotic Core by Three-Dimensional Magnetization-Prepared Rapid Acquisition Gradient-Echo Imaging

Huiyu Qiao[1], Dongxiang Xu[2], Feiyu Li[3], William S. Kerwin[2], Lars Johansson[4], Chun Yuan[1,2], and Xihai Zhao[1]

[1]Center for Biomedical Imaging Research, Department of Biomedical Engineering, Tsinghua University, Beijing, People's Republic of China, [2]Department of Radiology, University of Washington, Seattle, WA, [3]Department of Radiology, Peking University First Hospital, Beijing, People's Republic of China, [4]Department of Radiology, Uppsala University Hospital, Sweden

Carotid atherosclerotic lipid-rich necrotic core (LRNC) is associated with ischemic cerebrovascular events. Currently, LRNC was mainly characterized by contrast-enhanced T1 weighted (CE-T1W) or T2 weighted (T2W) imaging. However, CE-T1W imaging needs gadolinium application and T2W imaging is challenging to identify LRNCs with long-T2 components. This study investigated the usefulness of MP-RAGE in identifying carotid LRNC by comparing with CE-T1W and T2W imaging. We found that LRNC had the lowest relative signal intensity against muscle or fibrous tissue on MP-RAGE images among three sequences (P<0.05), indicating that MP-RAGE might be a better non-contrast imaging tool to identify LRNC than T2W imaging.

2786

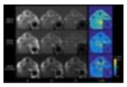

Comparison of black-blood T2 mapping sequences in carotid artery at 3T

Jianmin Yuan[1], Andrew J. Patterson[2], Scott A. Reid[3], Martin J. Graves[1,2], and Jonathan H. Gillard[1]

[1]Department of Radiology, University of Cambridge, Cambridge, United Kingdom, [2]Department of Radiology, Cambridge University Hospitals NHS Foundation Trust, Cambridge, United Kingdom, [3]GE Healthcare, Amersham, United Kingdom

Carotid black-blood quantitative T_2 mapping sequences have the potential to help plaque component segmentation and are more suitable for multi-centre studies across different MRI systems. The purpose of this study is to compare the accuracy of three different black-blood quantitative T_2 sequences in the phantom and healthy volunteers at 3T.

2787

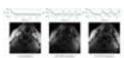

Optimization of 3D black-blood multi-echo T2* weighted sequence in carotid artery

Jianmin Yuan[1], Ammara Usman[1], Pascal Ruetten[1], Andrew J. Patterson[2], Andrew N. Priest[2], Martin J. Graves[1,2], and Jonathan H. Gillard[1]

[1]Department of Radiology, University of Cambridge, Cambridge, United Kingdom, [2]Department of Radiology, Cambridge University Hospitals NHS Foundation Trust, Cambridge, United Kingdom

Carotid T_2* weighted images have multiple applications, including differentiating plaque components and detecting ultrasmall superparamagnetic iron oxide (USPIO) contrast agents. The current work develops and optimizes the three-dimensional black-blood multi-echo T_2* weighted sequence through Bloch simulation and volunteer scans.

2788

Three-dimensional T1-Weighted Black-Blood Turbo Spin-Echo with Navigator Respiratory Gating for the Vessel Wall Imaging: A Novel Approach to Evaluate Plaque in the Aortic Arch

Kenichi Nakagawa[1], Noriyoshi Morimoto[1], Sachi Fukushima[1], and Takashi Tabuchi[2]

[1]Department of Radiological Technology, Kurashiki Central Hospital, Okayama, Japan, [2]Department of Medical Technology, Kurashiki Central Hospital, Okayama, Japan

Complex plaques in the aortic arch on transthoracic echocardiography (TEE) can cause brain embolism. However, TEE, which is associated with a number of complications and contraindications, is not suitable for all patients. Therefore, we focused on contrast evaluation of MRI with 3D T1w black-blood TSE as an adjunct to diagnosis of complex plaques. The aim of this study is to clarify the optimal scan method for 3D T1w black-blood TSE. Our results suggest that 3D T1w black-blood TSE in the aortic arch can reduce the amount of artifact by using the optimal trigger timing by ECG-gating and navigator respiratory gating.

2789

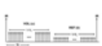

Comparison of Two Different Implementations for the Simultaneous Non-Contrast Angiography and Intraplaque Hemorrhage (SNAP) Sequence

M Louis Lauzon[1,2], Niranjan Balu[3], Chun Yuan[3], and Richard Frayne[1,2]

[1]Radiology and Clinical Neurosciences, Hotchkiss Brain Institute, University of Calgary, Calgary, AB, Canada, [2]Seaman Family MR Research Centre, Foothills Medical Centre, Calgary, AB, Canada, [3]Radiology, University of Washington, Seattle, WA, United States

We compare, using Bloch equation simulation, the relative signal in intraplaque hemorrhage (IPH), arterial wall (Wall) and Lumen (i.e., blood), along with the IPH–Wall contrast for two different implementations of the SNAP sequence. The first implementation is the original version (Ver1) that uses a linear phase-encoding scheme post-IR, whereas the second version (Ver2) uses centric slice-encodes post-IR. We show that, although Ver2 appears to be less time-efficient, it actually provides increased signal and contrast for the same acquisition time.

2790

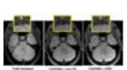

Accelerated multi-contrast high isotropic resolution 3D intracranial vessel wall MRI using a tailored k-space undersampling and partially parallel reconstruction strategy.

Niranjan Balu[1], Zechen Zhou[2], Thomas Hatsukami[1], Mahmud Mossa-Basha[1], and Chun Yuan[1]

[1]University of Washington, Seattle, WA, United States, [2]Philips Healthcare, Beijing, People's Republic of China

Identification and differentiation of intracranial vessel wall pathologies requires multi-contrast high isotropic resolution 3D vessel wall MRI. However scan times for multi-contrast intracranial vessel wall imaging (IVWI) are too long to be tolerated by patients. We have developed a tailored k-space undersampling and partially parallel reconstruction strategy to accelerate 0.5mm 3D isotropic multi-contrast IVWI sequences to five minutes each. We demonstrate an accelerated multi-contrast IVWI protocol that provides similar vessel delineation as fully sampled sequences. Protocol performance was assessed in patients with intracranial atherosclerotic disease and showed clear delineation of vessel wall and atherosclerotic plaque.

2791 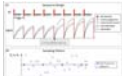

Quantitative 3D Dynamic Contrast Enhanced (DCE) Imaging of Carotid Vessel Wall by Fast T1 Mapping

Nan Wang[1,2], Anthony Christodoulou[1], Yibin Xie[1], and Debiao Li[1,2]

[1]Biomedical Imaging Research Institute, Cedars-Sinai Medical Center, Los Angeles, CA, United States, [2]Department of Bioengineering, University of California, Los Angeles, Los Angeles, CA, United States

Dynamic contrast enhanced (DCE) MRI is a promising technique to quantitatively evaluate the inflammatory status of atherosclerosis noninvasively. However, its demanding sampling requirement leads to sacrifices in slide resolution, coverage, and/or temporal resolution in the applications to vessel wall imaging. In this work we designed accelerated dynamic T1-mapping technique using Low Rank Tensor (LRT) framework to achieve 3D high-resolution quantitative DCE of the carotid arteries.

Traditional Poster

MR Angiography

Exhibition Hall 2792-2823 Thursday 8:15 - 10:15

2792 

Clinical outcomes after magnetic resonance angiography (MRA) compared to computed tomographic angiography (CTA) for pulmonary embolism evaluation

Scott K Nagle[1], Michael D Repplinger[2], John B Harringa[3], Aimee T Broman[4], Christopher R Lindholm[3], Christopher J Francois[1], Thomas M Grist[1], Scott B Reeder[1], and Mark L Schiebler[1]

[1]Radiology, University of Wisconsin, Madison, WI, United States, [2]Emergency Medicine, University of Wisconsin, United States, [3]University of Wisconsin, United States, [4]Biostatistics, University of Wisconsin

In this retrospective case-control study of 1173 subjects with suspected pulmonary embolism, the 6-month rate of major adverse events (venous thromboembolic, major bleeding, or death) was lower following contrast-enhanced magnetic resonance angiography (MRA) (5.4%) than following computed tomographic angiography (CTA) (13.4%, $p < 0.001$). The technical success rate of MRA (92.6%) and CTA (90.5%) performed in a routine clinical setting did not differ significantly ($p = 0.41$). MRA is a clinically effective imaging exam for the primary evaluation of pulmonary embolism.

2793 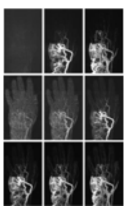

Does TWIST with iterative reconstruction improve diagnostics of AVM of the hand?

Claudia Fellner[1], Walter Wohlgemuth[1], Michaela Schmidt[2], Christoph Forman[2], Christian Stroszczynski[1], and Wibke Uller[1]

[1]Institute of Radiology, University Hospital Regensburg, Regensburg, Germany, [2]Siemens Healthcare GmbH, Erlangen, Germany

Highly accelerated TWIST MRA with standard and iterative reconstruction was compared to a standard TWIST technique in 11 patients with AVM of the hand and/or fingers. Qualitative and quantitative analysis revealed significant advantages for the accelerated protocol with iterative reconstruction: Separation of arterial and venous phase as well as delineation of central and peripheral arterial feeders were significantly improved due to higher temporal resolution compared with our standard protocol while maintaining high spatial resolution.

2794 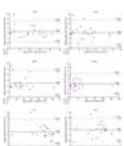

Precision and Reproducibility of Cardiac Phase Resolved Ventricular Volumetry using 4D MUSIC MRI in Congenital Heart Disease

Takegawa Yoshida[1,2], Kim-Lien Nguyen[1,3], Maxine Tang[3], Fei Han[1,2], Peng Hu[1,2], and Paul Finn[1,2,3]

[1]Diagnostic Cardiovascular Imaging Laboratory, David Geffen School of Medicien at UCLA, Los Angeles, CA, United States, [2]Department of Radiology, David Geffen School of Medicien at UCLA, Los Angeles, CA, United States, [3]Department of Medicine, David Geffen School of Medicien at UCLA, Los Angeles, CA, United States

Precise and reproducible quantification of ventricular function and volume, particularly right ventricular volumetry, is important in congenital heart disease. Accurate quantification is highly dependent on accurate delineation of myocardial borders. Ferumoxytol-enhanced MUSIC provides multiphase, high resolution, dynamic 3D imaging of the whole heart. We evaluated the precision and reproducibility of ventricular function and volumetric measurements using a commercial 3D image design and modeling software whose segmentation algorithm takes into account partial volume effects (Mimics, Materialise). We demonstrate that quantification of ventricular function and volumetry for 4D MUSIC images using Mimics is reproducible with high intra-class correlation coefficient.

2795 

Quantification of Cerebrovascular Tortuosity of the SCD Patients using Angiography

Shayan Farzad[1], Adam Bush[2], Damini Dey[3], Natasha Lepore[4], Thomas Coates[5], John Wood[6], Julie Coloigner[4], and Matthew Borzage[7]

[1]Division of Cardiology, University of Southern California, Los Angeles, CA, United States, [2]Biomedical Engineering, University of Southern California, Los Angeles, CA, United States, [3]Cedars-Sinai Medical Center, Los Angeles, CA, United States, [4]Radiology, Children's Hospital of Los Angeles, Los Angeles, CA, United States, [5]Hematology Oncology, Children's Hospital Los Angeles, Los Angeles, CA, United States, [6]Pediatrics and Radiology, Children's Hospital Los Angeles, Los Angeles, CA, United States, [7]Neonatology, Children's Hospital Los Angeles, Los Angeles, CA, United States

Stroke is a critical complication of Sickle Cell Disease (SCD) and is predicted by increased transcranial Doppler velocities. Recent computational fluid dynamic studies demonstrate a combination of high flow and vessel tortuosity are responsible for high TCD velocities. We determined the predictors of vessel tortuosity in control subjects and SCD patients without known vasculopathy. We applied three different tortuosity metrics (distance measure, inflection count, and sum of angles method) to middle cerebral artery segments measured in 19 SCD patients and 13 controls. Both distance and inflection count metrics were increased in SCD patients but the distance metric was more discriminatory. Age and hemoglobin levels were the strongest predictors of tortuosity in SCD patients. Both terms were retained in multivariate analysis, suggesting that chronic anemia exacerbates the normal increase in vessel tortuosity with age.

2796

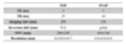

Comparison of Simultaneous Non-Contrast Angiography and intraPlaque Hemorrhage (SNAP) and 3D Time of Flight (TOF) for Non-Contrast Intracranial MR Angiography (MRA)

Qiang Zhang[1], Jia Ning[1], Shuo Chen[1], Zhensen Chen[1], Xihai Zhao[1], Chun Yuan[2], and Huijun Chen[1]

[1]Center for Biomedical Imaging Research, Department of Biomedical Engineering, School of Medicine, Tsinghua University, Beijing, People's Republic of China, [2]Department of Radiology, University of Washington

The purpose of this study is to compare the MRA image contrast of SNAP and TOF sequences in in-vivo cerebral artery images and explore the explanation of the observation by theoretical simulation. We found TOF MRA showed better artery-background contrast than SNAP MRA in proximal large cerebral artery for all cases, but worse in distal small cerebral artery for most of the cases. The theoretical simulation considering the blood velocity and the blood travel distance in imaging slab further validated this observation, suggesting the contrast difference between SNAP and TOF were related to blood velocity and travel distance.

2797

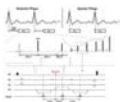

Unenhanced Peripheral MRA with Robust Background Suppression using Chemical-Shift-Encoded Single-Slab 3D GRASE: Decomposition of Angiogram and Fatty Backgrounds

Byungjae Hwang[1,2], Hahnsung Kim[1], Seong-Gi Kim[1,2], and Jaeseok Park[1]

[1]Department of Biomedical Engineering, Sungkyunkwan University, Suwon, Korea, Republic of, [2]Center for Neuroscience Imaging Research, Institute for Basic Science (IBS), Suwon, Korea, Republic of

Unenhanced peripheral MRA, which is based on cardiac-gated fresh blood imaging, exploits a pulsatile nature of arterial blood flow to differentiate arteries from veins and stationary backgrounds by subtracting two sets of images in cardiac diastole and systole, respectively. However, background signals remain substantial after subtraction due to either varying R-R intervals in between the two cardiac phases or subject motion, potentially obscuring the delineation of angiograms. Under the hypothesis that most of bright background signals result from fatty tissues, we develop a novel, unenhanced peripheral MRA method with robust background suppression using chemical-shift-encoded single-slab 3D GRASE to decompose angiograms and fatty background tissues directly from the subtracted, undersampled k-space data between the dual cardiac phases under the framework of compressed sensing.

2798

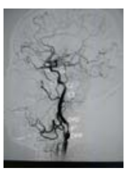

Diagnostic Accuracy Of 3D Head And Neck Joint Black-Blood Vessel Wall Imaging In Patients With Carotid Artery StenosisComparison with DSA

Zhenjia Wang[1], liu wen[2], and yu wei[3]

[1]Department of Radiology, Department of Radiology, Anzhen Hospital, CapitalMedical University, Beijing, China, beijing, People's Republic of China, [2]Department of Radiology, Anzhen Hospital, CapitalMedical University, Beijing, China, [3]Department of Radiology, Anzhen Hospital, CapitalMedical University, Beijing, China, beijing, People's Republic of China

Joint head and neck vessel wall imaging technology with variable flip angle turbo spin echo (SPACE)1 has recently been introduced as a promising MRI method for simultaneous evaluation of extra-cranial and intra-cranial vessel wall. However, this technique is yet to be validated with established imaging techniques. We aim to evaluate the accuracy of this technique using DSA as reference in assessing carotid artery stenosis and plaque morphology.

2799

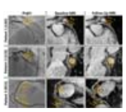

Coronary MRI allows Assessment and Monitoring of Coronary Patency and Blood Flow Velocity Quantification in Patients treated with Bioresorbable Vascular Scaffolds

Simon Reiss[1], Axel Joachim Krafft[1], Marius Menza[1], Lisa Caroline Besch[2], Timo Heidt[2], Christoph Bode[2], Constantin von zur Mühlen[2], and Michael Bock[1]

[1]Department of Radiology, Medical Physics, Medical Center - University of Freiburg, Freiburg, Germany, [2]Department of Cardiology and Angiology I, University Heart Center, Freiburg, Germany

Bioresorbable Vascular Scaffolds (BVS) provide a new and rapidly evolving alternative to drug eluting metal stents (DES) in the treatment of coronary artery disease. Besides potential advantages over DES in the restoration of the vessel function and reduction of post-interventional angina BVS allow for artifact-free coronary MRI of scaffolded arteries. In this study, we demonstrate that MRI for non-invasive monitoring of coronary arteries after BVS implantation is feasible by assessing coronary patency in a group of 11 patients initially and one year post-intervention.

2800

Improving visualization of 4D Flow MRI with four-dimensional angiographic data

Mariana Bustamante[1,2], Vikas Gupta[1,2], Carl-Johan Carlhäll[1,2,3], and Tino Ebbers[1,2]

[1]Department of Medical and Health Sciences, Division of Cardiovascular Medicine, Linköping University, Linköping, Sweden, [2]Center for Medical Image Science and Visualization (CMIV), Linköping University, Linköping, Sweden, [3]Department of Clinical Physiology, Department of Medical and Health Sciences, Linköping University, Linköping, Sweden

We present a technique for the generation of four-dimensional angiographic data from 4D Flow MRI. Using registration between the timeframes of the 4D Flow MRI, the method concentrates information from the entire cardiac cycle into an angiographic dataset at one timeframe. This step is followed by another set of registrations to generate a time-resolved three-dimensional angiography (4D). Visual comparison of the generated data versus conventional techniques resulted in higher scores in all the regions evaluated. The resulting data allow for visualization of the cardiovascular anatomy throughout the cardiac cycle, facilitating anatomical orientation and enhancing visualization of 4D Flow MRI data.

2801

Objective Measurement of Carotid Lumen Using Non-Contrast SNAP MRA

Haining Liu[1], Jie Sun[2], Niranjan Balu[2], Daniel S Hippe[2], Thomas Hatsukami[3], and Chun Yuan[2]

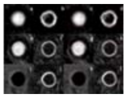

[1]Department of Bioengineering, University of Washington, Seattle, WA, United States, [2]Department of Radiology, University of Washington, Seattle, WA, United States, [3]Department of Surgery, University of Washington

Maximum intensity projection (MIP) is a commonly used tool to measure luminal stenosis. MIP images may underestimate stenosis. Directly measuring lumen size represents an alternative solution, but manual segmentation is laborious and sensitive to flow artifacts and bias. Simultaneous non-contrast angiography and intraplaque hemorrhage (SNAP) imaging affords a novel 3D non-contrast MRA approach. The polarity map available with SNAP makes it less sensitive to flow artifacts and facilitates objective lumen boundary definition. In this study, objective lumen measurements on SNAP and 3D-TOF are compared using CE-MRA as a reference. Results showed good agreement between SNAP and CE-MRA on lumen assessment.

2802

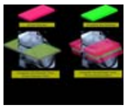

Novel ASL-based flow imaging for cardiovascular hemodynamics and valvular function visualization: comparison with a feasibility study

Yasuhiro Goto[1], Michinobu Nagao[2], Kenji Fukushima[2], Masami Yoneyama[3], Hitoshi Tadenuma[1], Mamoru Takeyama[1], and Shuji Sakai[2]

[1]Department of Radiological services, Tokyo Women's Medical University Hospital, Tokyo, Japan, [2]Department of Diagnostic Imaging & Nuclear Medicine, Tokyo Women's Medical University Hospital, Tokyo, Japan, [3]Philips Electronics Japan, Tokyo, Japan

We developed a novel ASL-based flow imaging (ASL-Flow) with modified flow-sensitive alternating inversion recovery technique and Look-Locker sequence to evaluate cardiovascular hemodynamics and valvular dysfunction. We validate that time-intensity curves of pulmonary artery form ASL-Flow matches for time-velocity curves from 2D phase-contrast MRI. ASL-Flow can visualize more clearly regurgitateion and stenotic jet in valvular diseases than standard cine imaging. The scan time for ASL-Flow is short (15 seconds/slice), and the image reconstruction needs no special software; therefore, this is easy to clinically use. We promise that ASL-Flow is a feasible non-contrast imaging to detect hemodynamics abnormality in structural heart disease.

2803

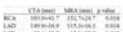

	CTA (mm)	MRA (mm)	p-value
RCA	[illegible]	[illegible]	0.018
LAD	[illegible]	[illegible]	0.018
LCX	[illegible]	[illegible]	0.018

Transluminal Attenuation Gradient in Non-contrast Whole Heart Magnetic Resonance Coronary Angiography (MRA TAG) – Noninvasive Methods for Assessment of Coronary Flow: A Comparison with Coronary Computed Tomography Angiography TAG

Yuki Ohmoto-Sekine[1], Junji Takahashi[2], Takashi Yoshida[2], Rieko Ishimura[3], Makiko Ishihara[4], Yasuji Arase[1], and Mitsue Miyazaki[5]

[1]Health Management Center, Toranomon Hospital, Tokyo, Japan, [2]Radiology Dept., Toranomon Hospital, Tokyo, Japan, [3]Cardiovascular Center, Toranomon Hospital, Tokyo, Japan, [4]Imaging Center, Toranomon Hospital, Tokyo, Japan, [5]Toshiba Medical Research Institute, Chicago, IL, United States

CT coronary angiography (CTA) and non-contrast coronary MRA are established non-invasive methods for anatomical assessment of coronary artery stenosis; however, functional information is limited. Transluminal attenuation gradient (TAG) of CTA predicts a functional significant stenosis. The aim of this study was to access TAG using non-contrast whole heart coronary MRA (MRA TAG) as compared to TAG using CTA (CTA TAG). Preliminary evaluation of MRA TAG provides acceptable prediction of invasive FFR. Further study is required to determine an appropriate prediction of MRA TAG.

2804

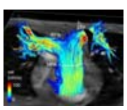

Validation and Error Quantification of Pulmonary Artery 4D Flow-MRI in a digital broadband 3T MR setup

Thekla Helene Oechtering[1], Clara Berlin[1], Malte Sieren[1], Daniel Droemann[2], Joerg Barkhausen[1], and Alex Frydrychowicz[1]

[1]Clinic for Radiology and Nuclear Medicine, University Hospital Schleswig-Holstein, Luebeck, Germany, [2]Medical Clinic III: Pulmonology, University Hospital Schleswig-Holstein, Luebeck, Germany

4D Flow-MRI offers unique possibilities for the diagnosis of pulmonary hypertension. A validation of the sequence on a digital broadband 3T MR system is essential before introduction into clinical routine. This study compared 4D Flow–MRI derived stroke volume (SV) and maximal flow velocity (Vmax) in the pulmonary arteries of 23 healthy volunteers to 2D phase contrast MRI, right ventricular stroke volume (RVSV), conservation of mass-analysis (COM), and to a static phantom for additional error analysis. Results revealed clinically acceptable differences with a trend of phantom correction to improve results except for the COM-analysis.

2805

Breath-hold and Free-Breathing Single-Shot Radial Quiescent-Interval Slice-Selective (QISS) MRA for Evaluation of the Pulmonary Arteries

Robert R. Edelman[1,2], Shivraman Giri[3], Robert Silvers[1], Kiran Thakrar[1], and Ioannis Koktzoglou[4,5]

[1]Radiology, NorthShore University HealthSystem, Evanston, IL, United States, [2]Radiology, Northwestern University, Chicago, IL, United States, [3]Siemens HealthCare, [4]Radiology, NorthShore University HealthSystem, [5]Radiology, University of Chicago

For suspected pulmonary embolism, CTA is the first-line imaging test, with CEMRA a potential alternative. Disadvantages including exposure to ionizing radiation and iodine contrast for CTA, while CEMRA is sensitive to respiratory motion and requires a gadolinium-based contrast agent. As a nonenhanced alternative, we tested breath-hold and free-breathing versions of single-shot radial QISS. Compared with the reference standard, all pulmonary artery branches down to the segmental level were visualized by breath-hold and navigator-gated QISS. With further optimization and validation, radial QISS has the potential to provide a nonenhanced alternative to CTA and CEMRA for the evaluation of suspected pulmonary embolism.

2806

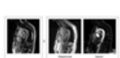

Improved 3D phase contrast MR angiogram calculation using 3D CINE bSSFP and 4D flow MRI

Kelly Jarvis[1,2], Susanne Schnell[1], Alex J. Barker[1], Shivraman Giri[3], Nivedita Naresh[1], James C. Carr[1], Jeremy D. Collins[1], and Michael Markl[1,2]

[1]Department of Radiology, Northwestern University, Chicago, IL, United States, [2]Department of Biomedical Engineering, Northwestern University, Chicago, IL, United States, [3]Siemens Healthcare, Chicago, IL, United States

Improvements in the 3D PC-MRA calculated from 4D flow MRI are needed for better vessel wall depiction and assessment of vascular dimensions. Balanced steady state free precession (bSSFP) is a promising imaging method to combine with 4D flow for an improved depiction of cardiac anatomy and blood-tissue contrast. This study of 10 healthy subjects compares multiple PC-MRA algorithms using bSSFP with 4D flow magnitude and flow images.

2807

Multi-echo sliding interleaved projection reconstruction (SLIPR) imaging of the carotid artery

Jason K Mendes[1], John Roberts[1], Bradley D Bolster, Jr.[2], Seong-Eun Kim[1], J Scott McNally[1], Gerald S Treiman[3], and Dennis L Parker[1]

[1]Radiology and Imaging Sciences, University of Utah, Salt Lake City, UT, United States, [2]Siemens Healthcare, Salt Lake City, UT, United States, [3]Department of Veterans Affairs (VASLCHCS), Department of Veterans Affairs (VASLCHCS), UT, United States

An optimized 3D stack of stars with Sliding Interleaved Projection Reconstruction (SLIPR) provides improved carotid MRA over conventional Time of Flight (TOF) techniques. The stack of stars SLIPR technique takes better advantage of the inflow effect to maximize contrast to noise between blood and tissue. In addition, a multi-echo radial readout minimizes off resonance blurring, allows for fat water separation and shortens acquisition time compared with non-sliding 3D TOF techniques.

2808

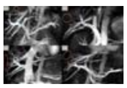

Non-Contrast-Enhanced MRA for Hepatic Vasculature Imaging using Off-Resonance-Robust Velocity-Selective Pulse Train

Lyu Li[1], Qin Qin[2,3], Weibo Chen[1], Ting Li[4], Kangan Li[4], and Hua Guo[5]

[1]Philips Healthcare, Shanghai, People's Republic of China, [2]Radiology, Johns Hopkins University, Baltimore, United States, [3]F.M. Kirby Research Center for Functional Brain Imaging, Kennedy Krieger Institute, Baltimore, United States, [4]Radiology, Shanghai General Hospital, Shanghai, People's Republic of China, [5]Center for Biomedical Imaging Research, Department of Biomedical Engineering, School of Medicine, Tsinghua University, Beijing, People's Republic of China

Preoperative hepatic vascular evaluation is of great importance in a variety of liver surgeries, including tumor resection and transplantation. An accurate depiction of hepatic vascular anatomy can help to prevent the complications and decrease the morbidity and mortality in liver surgeries. However, few studies have reported good image quality in hepatic vasculature imaging using non-contrast-enhanced MR angiography (NCE-MRA) because of the motion and complex structure. In recent years, some studies reported the potential of NCE-MRA with velocity-selective pulse train (VSMRA). In this study, we demonstrated the feasibility of VSMRA for imaging the hepatic vasculature with an off-resonance-robust velocity-selective pulse train at 3T.

2809

A novel method for Background Suppression in Continuous Arterial Spin Labeling (cASL) Angiography

Jianxun Qu[1], Bing Wu[1], and Zhenyu Zhou[1]

[1]MR Research China, GE Healthcare, Shanghai, People's Republic of China

In this work, we implemented background suppression for continuous arterial spin labeling based MR angiography to suppress the noise resulting from the influence of magnetic transfer effect. Pulsed labeling is also incorporated in the background suppression scheme to address the flow void effect in continuous labeling. With the proposed method, the overall vessel clarity was improved without prolonging the scan time.

2810

The Use of Flip Angle Modulation in Zero TE ASL MRA for Improved Angiogram Quality

Jianxun Qu[1], Bing Wu[1], Yu Kang[2], and Zhenyu Zhou[1]

[1]MR Research China, GE Healthcare, Shanghai, People's Republic of China, [2]Radiology Department, Peking University People's Hospital

Time resolved MRA is valuable in study of cerebrovascular disorders. ASL based MRA permits visualization of blood flow without injection of contrast agent. Continuous labeling combined with zero TE readout features maximal labeling efficiency and high angiogram fidelity. However, the constant small flip angle excitation scheme limits its applicability in time resolved visualization. This work performed variable flip angle modulation to improve the quality of angiography in zTE-ASL MRA.

2811

Can non-contrast Fresh Blood Imaging (FBI) provide sufficient pretreatment information of peripheral artery disease (PAD)?

Takashi Okigawa[1], Takashi Fukunaga[2], Akihiko Arakawa[1], Hirohumi Wada[1], Takeshi Oota[1], Kouichi Nakao[2], Joji Urata[3], Katsumi Nakamura[4], and Mitsue Miyazaki[5]

[1]Department of Radiology, Saiseikai Kumamoto Hospital, Kumamoto, Japan, [2]Department of Cardiovascular, Saiseikai Kumamoto Hospital, Kumamoto, Japan, [3]Department of Radiology, Kumamoto city Hospital, Kumamoto, Japan, [4]Department of Radiology, Tobata Kyoritsu Hospital, Fukuoka, Japan, [5]Toshiba Medical Research Institute USA, Japan

Diagnostic accuracy of nonenhanced Fresh Blood Imaging (FBI) was compared with digital subtraction angiography (DSA) or digital angiography (DA), which was performed at percutaneous transluminal angioplasty (PTA), in the evaluation of the peripheral lower-extremity arteries. In the evaluation of 173 segments in 25 patients with peripheral arterial occlusive disease, the sensitivity, specificity, and accuracy of FBI of a consensus reading for detection of 50% or greater stenotic lesions were 100%, 83%, and 88%, respectively. FBI achieves high diagnostic accuracy for the detection of peripheral arterial disease (PAD) in comparison with DSA.

2812

Non-contrast enhanced MR angiography of lower extremity in patients with diabetes: initial experience of using TRANCE technique at 3.0 T

Zhang Lan[1] and Xin Liu[2]

[1]MRI, The 1st affiliated hospital of Henan University of TCM, ZhengZhou, People's Republic of China, [2]ShenZhen Institutes of Advanced Technology, People's Republic of China

There is a clinical need for implementing a Non-contrast enhanced imaging technique for patients with peripheral arterial disease or diabetes and contraindications for the use of contrast medium, especially patients with decline in kidney function or renal artery stenosis. We optimized TRANCE technique combined with VISTA for best performance of NCE-MRA for lower extremity artery at 3.0T MRI.

2813

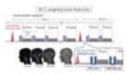

A Novel Technique for 4D Time-of-Flight MR Angiography using Double Adiabatic Inversion Recovery Pulses

Susumu Takano[1], Tetsuo Ogino[2], Shuhei Shibukawa[1,3], Tomohiko Horie[1], Isao Muro[4], Nao Kajihara[1], Toshiki Saito[1], Tetsu Niwa[5], Toshiki Kazama[5], and Yutaka Imai[5]

[1]Department of Radiology, Tokai University Hospital, Kanagawa, Japan, [2]Healthcare department, Philips Electronics Japan, Tokyo, Japan, [3]Graduate School of Medical Sciences, Kanazawa University, Kanazawa, Japan, [4]Department of Radiology, Tokai University Hachiouji Hospital, Tokyo, Japan, [5]Radiology, Tokai University School of Medicine, Kanagawa, Japan

Although previously developed 4D time-of-flight (4D-TOF) at a 3T MR system for evaluating cerebral hemodynamics, this method did not fit at a 1.5T MR system in order to early recovery the brain tissue signals. We proposed a novel 4D-TOF technique using double adiabatic inversion recovery pulse (DIR 4D-TOF) for suppressing background recovery and depiction of intracranial artery at a 1.5T MR system. The results presented show that DIR 4D-TOF with long interval between the first and the second adiabatic inversion recovery pulses could effectively delay T_1 recovery of the brain tissue and improved visibility of intracranial artery.

2814

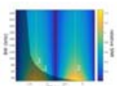

Optimization of signal-to-noise ratio and signal contrast in time-resolved single-echo Dixon imaging

Eric G. Stinson[1], Joshua D. Trzasko[2], and Stephen J. Riederer[2]

[1]Mayo Clinic, Rochester, MN, United States, [2]Radiology, Mayo Clinic, Rochester, MN, United States

Dixon imaging has recently been shown to be useful in contrast-enhanced MR angiography due to motion robustness and improved signal-to-noise ratio. Single-echo Dixon mostly avoids the time penalty associated with multi-echo Dixon imaging, but may incur some time penalty when choosing an echo time to give optimal signal-to-noise ratio (SNR). For dynamic scans, it is beneficial to optimize the imaging parameters for speed, even at the expense of SNR. Additionally, signal contrast can be optimized to further suppress the background water signal. The purpose of this work is to describe optimization of SNR and signal contrast for single-echo Dixon imaging.

2815

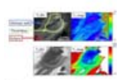

Magnetic resonance imaging discriminates organizing from non-organizing area in deep vein thrombus.

Yasuyoshi Kuroiwa[1,2], Atsushi Yamashita[2], Eriko Nakamura[2], Tosiaki Miyati[3], Auxeisu Fukumi[2], Masaji Maeda[1], Yasushi Kihara[4], Takuroh Imamura[5], and Yujiro Asada[2]

[1]Department of Radiological Technology, Koga General Hospital, Miyazaki, Japan, [2]Department of Pathology, Faculty of Medicine, University of Miyazaki, Miyazaki, Japan, [3]Faculty of Health Sciences, Institute of Medical, Pharmaceutical and Health Sciences, Kanazawa University, [4]Department of Radiology, Koga General Hospital, Miyazaki, Japan, [5]Department of Internal Medicine, Koga General Hospital, Miyazaki, Japan

Deep vein thrombus (DVT) is gradually replaced by fibrous tissue, and is called as organizing reaction. We examined magnetic resonance image (MRI) findings of the organizing DVT in vitro using a 1.5T MR system in autopsy cases with DVT. The organizing area of DVT showed low signal intensity (SI) on T_1 weighted images, in contrast to high SI on T_1 weighted images in non-organizing area. Both areas showed iso to low SI on T_2 weighted image. T_1 SI positively correlated with the erythrocyte content in the thrombus. MRI could discriminate organizing from non-organizing area in DVT.

2816

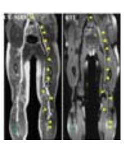

3D MR black-blood thrombus imaging for the diagnosis of acute deep vein thrombosis at 1.5 T: a feasibility study

Guoxi Xie[1,2], Hanwei Chen[3], Xueping He[3], Yufeng Ye[3], Zhuonan He[3], Wei Deng[3], Jianke Liang[3], Debiao Li[2], Xin Liu[1], and Zhaoyang Fan[2]

[1]Shenzhen Institutes of Advanced Technology, Chinese Academy of Sciences, Shenzhen, People's Republic of China, [2]Biomedical Imaging Research Institute, Cedars-Sinai Medical Center, Los Angeles, CA, United States, [3]Department of Radiology, Guangzhou Panyu Central Hospital

Accurate diagnosis of acute deep vein thrombosis (DVT) is relevant for appropriate treatment and avoiding life-threatening events. Recently proposed MR black-blood thrombus imaging (BTI) has demonstrated the potential to provide high sensitive and specific diagnosis of DVT. However, previous studies were performed at 3T and patients investigated were all in subacute to chronic phases. It remains unclear that if BTI could be used for the diagnosis of acute DVT and could work at 1.5T. Therefore, we sought to prospectively assess whether BTI is feasible at 1.5T for diagnosis of acute DVT, using contrast-enhanced MR venography as the standard reference.

2817

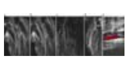

The Diagnostic Value of Sampling Perfection Application with Contrast Optimized Using Variable Flip Angle Evolutions (SPACE MR) in Evaluating Lower Extremity Deep Venous Thrombus

Gang Wu[1], Xu Yan[2], Xiaolei Zhu[3], and Tianjing Zhang[2]

[1]Radiology Department, Tongji Hospital, Wuhan, People's Republic of China, [2]MR Collaboration NE Asia, Siemens Healthcare, Shanghai, People's Republic of China, [3]Siemens healthcare NEA, MR Scientific Marketing, Guangzhou, People's Republic of China

The study evaluate the diagnostic performance of SPACE MR sequence in detecting lower extremity deep venous thrombosis (DVT) and evaluating clot burden, with comparison to ultrasound (US). The result showed that SPACE MR is highly accurate in detecting lower extremity DVT and reliable in the evaluation of clot burden, thus could be considered as an important alternative for patients in whom US cannot be performed.

2818

Clinical utility of the pulmonary artery to ascending aortic ratio by cardiac magnetic resonance in patients with pulmonary hypertension.

Noriko Oyama-Manabe[1], Osamu Manabe[2], Ichizo Tsujino[3], Hiroshi Ohira[3], Tadao Aikawa[4], Kohsuke Kudo[1], and Noriko Oyama-Manabe[1]

[1]Diagnostic and Interventional Radiology, Hokkaido University Hospital, Sapporo, Japan, [2]Nuclear Medicine, Hokkaido University Hospital, [3]First Department of Medicine, Hokkaido University Hospital, [4]Department of Cardiovascular Medicine, Hokkaido University Hospital

Thirty-three patients with pulmonary hypertension (PH) and age-, sex-matched 15 controls were retrospectively evaluated. The pulmonary artery to ascending aortic ratio (PA-A ratio) measured by cardiac MRI was significantly higher in PH patients than that in controls. The patients with pulmonary arterial hypertension showed a significantly higher PA-A ratio compared to patients with other causes of PH. Increased PA-A ratio showed significant correlations with right ventricular (RV) dilatation and decreased RVEF. The PA-A ratio showed high sensitivity and specificity for detection of PH. The PA-A ratio using cardiac MRI is an easy surrogate marker for detection of RV dysfunction and PH.

2819

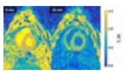

Estimation of Circulating Blood Volume using Ferumoxytol

Rajiv Ramasawmy[1], Miguel Alcantar[1], Jaffar M Khan[1], Adrienne E Campbell-Washburn[1], Anthony Z Faranesh[1], and Robert J Lederman[1]

[1]National Heart Lung and Blood Institute, National Institutes of Health, Bethesda, MD, United States

Clinical assessment of total blood volume is significant for management of patients with decompensated chronic heart failure. We investigate the feasibility of measuring circulating blood volume as part of an interventional cardiovascular MR exam by measuring T_1 changes due to the presence of Ferumoxytol - an intravascular, FDA-approved, iron supplement. Three pigs were scanned prior and twenty minutes post Ferumoxytol administration, from which a mean blood volume of 81.6 ± 1.1 mL/kg was estimated, which approximately overestimates by 15-30% from the literature. This technique has promise as a non-ionizing and non-toxic alternative to measuring patient volume.

2820

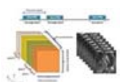

Visibility of the draining location of the thoracic duct to the venous system on balanced turbo field echo with extended k-space sampling

Tetsu Niwa[1], Takakiyo Nomura[1], Shuhei Shibukawa[2], and Yutaka Imai[1]

[1]Radiology, Tokai University School of Medicine, Isehara, Japan, [2]Radiology, Tokai University Hospital, Isehara, Japan

The knowledge regarding the visibility of the thoracic duct draining to the venous system has remained sparse. We assessed the visibility of draining location of the thoracic duct to the venous system in the subclavian region using balanced turbo field echo (bTFE) with extended *k*-space sampling. As a result, a relatively good visibility was achieved in the thoracic duct and the venous branches in the region. This sequence may be useful to grasp the draining location of the thoracic duct to the venous system at the subclavian region.

2821

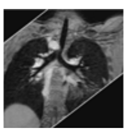

Evaluation of Pediatric Tracheobronchial Anomalies with congenital heart disease using Three-dimensional Turbo Field Echo Magnetic Resonance Imaging Sequence

Yu-min Zhong[1], Ai-min Sun[1], Qian Wang[1], Li-Wei Hu[1], Shi-Yu Wang[1], Qiao-Ru Hou[1], and Min Zhu[1]

[1]Radiology, Shanghai Children's Medical Center affiliated with Shanghai Jiao Tong University school of medicine, Shanghai, People's Republic of China

Tracheobronchial anomalies are common in congenital heart disease (CHD). Cardiovascular anomaly is the principal extrinsic lesion causing tracheobronchial stenosis. MSCT remains an ionizing procedure even though can demonstrate tracheobronchial tree clearly. MRI has the advantage of being non-ionizing and providing excellent soft tissue contrast for the diagnosis of CHD and tracheobronchial anomalies. Spin echo (SE) sequence can demonstrate the tracheobronchial tree but this typically a 2D sequence and therefore difficult to depict the entire tracheobronchial tree optimally. Three-dimensional turbo field echo (3D-TFE) can delineate the entire tracheobronchial tree clearly through post-processing.

2822

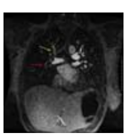

Direct and Indirect Findings of Pulmonary Embolism Using Contrast Enhanced Magnetic Resonance Angiography (CE-MRA)

Donald Benson[1], Scott K. Nagle[1,2,3], Christopher J Francois[1], Scott B. Reeder[1,2,4,5,6], Thomas M. Grist[1,2,6], Michael D. Repplinger[1,5], and Mark L. Schiebler[1]

[1]Department of Radiology, University of Wisconsin-Madison, Madison, WI, United States, [2]Department of Medical Physics, University of Wisconsin-Madison, Madison, WI, United States, [3]Department of Pediatrics, University of Wisconsin-Madison, Madison, WI, United States, [4]Department of Medicine, University of Wisconsin-Madison, Madison, WI, United States, [5]Department of Emergency Medicine, University of Wisconsin-Madison, Madison, WI, United States, [6]Department of Biomedical Engineering, University of Wisconsin-Madison, Madison, WI, United States

Contrast enhanced pulmonary MRA is an important modality for detecting PE in those situations where there are concerns about excess exposure to ionizing radiation or contraindications to iodinated contrast. While most radiologists are experienced in interpreting CT angiographic studies for pulmonary embolus, many are unfamiliar with CE-MRA for the diagnosis of PE. It is important for interpreting physicians to understand both the direct and indirect findings associated with PE. In our retrospective study of 682 patients, we found 136 PE in 61 patients. The prevalence of both direct and indirect findings associated with PE were reviewed in this study.

2823

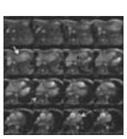

Cardiac manifestations of diffuse lung disease: A pictorial review of cardiac magnetic resonance imaging findings

Donald Benson[1], Scott K. Nagle[1,2,3], Mark L. Schiebler[1], and Christopher J Francois[1]

[1]Department of Radiology, University of Wisconsin-Madison, Madison, WI, United States, [2]Department of Medical Physics, University of Wisconsin-Madison, Madison, WI, United States, [3]Department of Pediatrics, University of Wisconsin-Madison, Madison, WI, United States

Many disease processes associated with diffuse lung disease also have cardiac abnormalities. These cardiac abnormalities can easily be overlooked if one focuses too heavily on the lung findings. The purpose of this educational exhibit is to review the characteristic imaging findings associated with the cardiac manifestations of diffuse lung disease.

Traditional Poster

Flow & Velocity

Exhibition Hall 2824-2861 Thursday 8:15 - 10:15

2824

Voxel-by-Voxel 4D Flow Based Assessment of Retrograde Flow in the Aorta

Xin Shen[1], Kenichiro Suwa[2], Alex J Barker[2], Susanne Schnell[2], Jeremy D Collins[2], James C Carr[2], and Michael Markl[1,2]

[1]Biomedical Engineering, Northwestern University, Chicago, IL, United States, [2]Radiology, Northwestern University, Chicago, IL, United States

Retrograde fraction stratifies the degree of aortic regurgitation (AR) in patients with aortic valve disease. The purpose of this study was to develop 4D flow based voxel-by-voxel regional analysis of forward flow, reverse flow, and retrograde fraction with full volumetric coverage of the aorta. In a study with 10 subjects (5 healthy controls, 5 patients with AR), reverse flow and retrograde fraction maps were used to systematically analyze regional flow patterns and assess differences between standard (plane-wise) and voxel-by-voxel quantification of AR.

2825

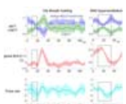

Temporal variation of cerebrovascular transit time measured by BOLD-based time lag mapping

Toshihiko Aso[1] and Shin-ichi Urayama[1]

[1]Human Brain Research Center, Kyoto University Graduate School of Medicine, Kyoto, Japan

A pilot study of perfusion-related signal component in fMRI signal, demonstrates possibility of measuring blood transit time variation by tracking BOLD lag through the vascular structure. Effect of short breath-holding and mild hyperventilation on the time-shift analysis of whole-brain BOLD signals were tested. Temporal variation of the relative BOLD transit time up to ±15% on average were found to be negatively correlated with the global BOLD signal change, which is consistent with the Central Volume Principle under the condition of small CBV change. This relative BOLD transit time is likely to reflect the global CBF/CBV dynamics with high temporal resolution.

2826

An automatic method to estimate 3D Pulse Wave Velocity from 4D-flow MRI data

Joaquin Mura[1], Julio Sotelo[1], Cristian Montalba[1], Bram Ruijsink[2], David Nordsletten[2], Reza Razavi[2], Pablo Irarrazaval[1,3], Cristian Tejos[1,3], Marcelo Andia[1,4], and Sergio Uribe[1,4]

[1]Biomedical Imaging Center, Pontificia Universidad Catolica de Chile, Santiago, Chile, [2]Department of Biomedical Engineering, King's College London, London, United Kingdom, [3]Department of Electrical Engineering, Pontificia Universidad Catolica de Chile, Santiago, Chile, [4]Department of Radiology, School of Medicine, Pontificia Universidad Catolica de Chile, Santiago, Chile

One of the most common and well-accepted biomarkers for Cardiovascular diseases is the Pulse Wave Velocity (PWV), related with the time-shift observed in pressure or flow waveforms along the artery. Some drawbacks in its application can be summarized as data often collected by catheterization or separated 2D flow planes, centerlines do not necessarily coincide with the path followed by wavefronts and, the methods are user-dependent. We propose a novel method for PWV avoiding centerlines by evaluating flows over wavefronts to improve results. A systematic analysis of phantom scans and to a set of volunteers and patients show promising results.

2827

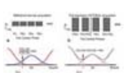

Phase-Contrast MRI with Hybrid One- and Two-sided Flow-Encodings and Velocity Spectrum De-aliasing (HOTDEAL) using Low Spatial Resolution Reference Four-point Phase-Contrast MRI

Da Wang[1,2], Ziwu Zhou[1,3], and Peng Hu[1,2]

[1]Department of Radiological Sciences, David Geffen School of Medicine, University of California, Los Angeles, Los Angeles, CA, United States, [2]Biomedical Physics Interdepartmental Graduate Program, University of California, Los Angeles, Los Angeles, CA, United States, [3]Department of Bioengineering, University of California, Los Angeles, Los Angeles, CA, United States

The proposed technique, phase-contrast MRI (PC-MRI) technique with hybrid one- and two-sided flow-encoding and velocity spectrum de-aliasing (HOTDEAL) using low spatial resolution reference four-point PC-MRI for accelerated blood flow and velocity measurement, is a novel M1-space (gradient first moment space) under-sampling technique for accurate Fourier velocity spectra separation.

2828

Evaluate Systolic and Diastolic Wall Shear Stress of Aorta for Marfan Syndrome by 4D Flow MRI

Pin-Chen Chen[1], Hsin-Hui Chiu[2], Wen-Yih Isaac Tseng[3], and Hsu-Hsia Peng[4]

[1]Institute of Systems Neuroscience, Hsinchu, Taiwan, [2]Department of Pediatrics, Taipei, Taiwan, [3]Institute of Medical Device and Imaging, Taipei, Taiwan, [4]Department of Biomedical Engineering and Environmental Sciences, Hsinchu, Taiwan

We aim to reveal the abnormality of plane-wise and segmental WSS in different cardiac phases of patients with Marfan syndrome (MFS) with dilated aorta. MFS group presented lower plane-wise axial WSS than normal group at ascending aorta and descending aorta during systole. In respect of segmental WSS, either in the whole cardiac cycle or during systole, MFS patients demonstrated reduced values at almost all segments in proximal ascending aorta. In conclusion, the quantitative indices of plane-wise and regional WSS clearly differentiate MFS patients from normal controls. Therefore, quantification of WSS can provide promising approaches for patient managements in the future.

2829

Independent phantom validation of Metric Optimized Gating for fetal cardiovascular phase-contrast flow imaging and application in a second center

Sebastian Lars Bidhult[1,2], Johannes Töger[1], Einar Heiberg[1,2], Erik Hedström[1,3], and Anthony H Aletras[1,4]

[1]Clinical Sciences Lund, Clinical Physiology, Lund University, Skane University Hospital, Lund, Sweden, [2]Biomedical Engineering, Faculty of Engineering, Lund University, Lund, Sweden, [3]Diagnostic Radiology, Lund University, Skane University Hospital, Lund, Sweden, [4]Laboratory of Computing and Medical Informatics, Aristotle University, School of Medicine, Thessaloniki, Greece

Fetal cardiovascular MRI may enhance clinical flow measurements. The lack of fetal ECG for gating however makes phase contrast (PC) flow quantification challenging. Metric Optimized Gating (MOG) overcomes this limitation, but is currently applied only in a single center. We provide independent pulsatile-flow phantom validation of MOG PC-MRI for fetal flow volumes and heart rates, and measurements in human fetuses in a second center. Flow by MOG agrees with timer/beaker and gated flow quantification, and gives pulsatile fetal flow curves in a second center, suggesting MOG PC-MRI as a reliable tool for fetal flow quantification in more centers.

2830

A novel platform to study hemodynamics and morphology in an ex vivo carotid artery model under pulsatile flow conditions

Kristina Andelovic[1], Patrick Winter[2], Thomas Kampf[2,3], Volker Herold[2], Sebastian Schuerlein[4], Jan Hansmann[4], Peter Jakob[2,5], and Wolfgang Bauer[1]

[1]Medizinische Klinik und Poliklinik I, Universitätsklinikum Würzburg, Würzburg, Germany, [2]Experimentelle Physik V, Universität Würzburg, Würzburg, Germany, [3]Institut für Diagnostische und Interventionelle Neuroradiologie, Universitätsklinikum Würzburg, Würzburg, Germany, [4]Deptartment of Tissue Engineering and Regenerative Medicine, Universitätsklinikum Würzburg, Würzburg, Germany, [5]Fraunhofer IIS, Fraunhofer EZRT, Magnetresonanz- und Röntgenbildgebung (MRB), Würzburg, Germany

Biological artery models, cultured in a bioreactor-platform with adjustable pulsatile flow conditions, represent a potential *in vitro* test system for atherosclerosis research and provide a suitable tool for the development of new flow quantification techniques as well as studies of arterial elasticity and flow dynamics *ex vivo* and *in vitro*. A major requirement for these studies is viable motion synchronization in order to achieve time-resolved flow measurements. We present a new platform that uses self-navigation instead of external trigger signals for measurements of 2D- and 4D flow dynamics, vessel wall morphology and quantifications of arterial pulse-wave-velocity and wall shear stress.

2831

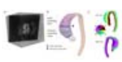

Distribution of 4D flow MRI-derived wall shear stress and oscillatory shear index and its relation with the ascending aorta dilation in bicuspid valve patients.

Lydia Dux-Santoy [1], Andrea Guala[2], José F. Rodríguez-Palomares [2], Julio Sotelo [3], Daniel E. Hurtado [4], Sergio Uribe [5], and Arturo Evangelista [2]

[1]Hospital Universitari Vall d´Hebron, Department of Cardiology. Vall d'Hebron Institut de Recerca (VHIR). Universitat Autònoma de Barcelona. Barcelona. Spain, barcelona, Spain, [2]Hospital Universitari Vall d´Hebron, Department of Cardiology. Vall d'Hebron Institut de Recerca (VHIR). Universitat Autònoma de Barcelona. Barcelona. Spain, [3]Biomedical Imaging Center, Pontificia Universidad Católica de Chile, Department of Electrical Engineering, Pontificia Universidad Católica de Chile, [4]Department of Structural and Geotechnical Engineering, Pontificia Universidad Católica de Chile, [5]Biomedical Imaging Center, Pontificia Universidad Católica de Chile, Department of Electrical Engineering, Pontificia Universidad Católica de Chile.

Elevated WSS is atheroprotective but implies greater medial degradation. Lower WSS degenerates endothelium and determines aneurysm area with lower dilation and rupture risk. OSI distinguishes aneurysm for rupture. Through 4D-flow MRI we analyze WSS and OSI ascending aortic regional differences in 27 BAV patients and 11 controls. Despite average WSS and OSI do not different among TAV and BAV, RL-BAV and RN-BAV and dilated and non-dilated BAV, regional differences have been found. Of most interest, dilated BAVs have partially overlapping regions of lower WSS and high OSI in the distal-anterior ascending aorta which may explain ascending aorta dilation morphotype

2832

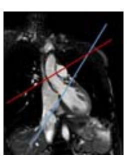

The feasibility of correcting for through-plane heart motion on phase contrast aortic blood flow measurements using feature tracking cine-MRI

Alexander Johansson[1], Frida Svensson[2,3], Åse Johnsson[3,4], and Kerstin Magdalena Lagerstrand[2,3]

[1]Dept of Radiology, Sahlgrenska University Hospital, Gothenburg, Sweden, Sahlgrenska University Hospital, Gothenburg, Sweden, [2]Dept. of Medical Physics and Techniques, Sahlgrenska University Hospital, Gothenburg, Sweden, Sahlgrenska University Hospital, Gothenburg, Sweden, [3]Institute of Clinical Sciences, Sahlgrenska Academy, University of Gothenburg, Gothenburg, Sweden, [4]Dept of Radiology, Sahlgrenska University Hospital, Gothenburg, Sweden, Sahlgrenska University Hospital

Phase contrast measurements are prone to velocity offsets due to through-plane motion of the heart. Here we present a promising method for correction of through-plane heart motion on phase contrast aortic blood flow measurements. The method, which utilizes the inherent information in conventional cine MR images for tracking of the aortic valve, was shown to be both robust and accurate. The reliability, but also the availability of the method makes it an attractive tool for correction of velocity offsets due to through-plane heart motion.

2833

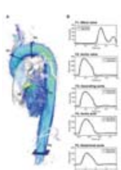

4D Flow MRI and lumped parameter modelling for subject-specific assessment of cardiovascular function

Belen Casas[1,2], Jonas Lantz[1,2], Federica Viola[1], Ann F. Bolger[1,3], Carl-Johan Carlhäll[1,2,4], Matts Karlsson[2,5], and Tino Ebbers[1,2]

[1]Division of Cardiovascular Medicine, Department of Medical and Health Sciences, Linköping University, Linköping, Sweden, [2]Center for Medical Image Science and Visualization (CMIV), Linköping University, Linköping, Sweden, [3]Department of Medicine, University of California San Francisco, San Francisco, CA, United States, [4]Department of Clinical Physiology, Department of Medical and Health Sciences, Linköping University, Linköping, Sweden, [5]Division of Applied Thermodynamics and Fluid Mechanics, Department of Management and Engineering, Linköping University, Linköping, Sweden

Lumped-parameter models of the cardiovascular system can improve the understanding of cardiovascular function and assist treatment planning. The clinical applicability of these models improves when they are subject-specific. This work proposes an approach to personalizing a model of the heart and the systemic circulation using exclusively non-invasive measurements from routine cardiovascular MRI and 4D Flow MRI. Personalized models were constructed for eight healthy volunteers. The model-based pressures and flows agreed well with the in-vivo measurements for each subject. The proposed approach can be used to synthesize medical data into clinically relevant information and estimate parameters that cannot be measured clinically.

2834

Evaluation of Aortic Hemodynamics in Patients with Sievers Type II BAV

Carmen P. S. Blanken[1], Ozair A. Rahman[1], Alex J. Barker[1], Kenichiro Suwa[1], Michael J. Rose[2], James C. Carr[1], Jeremy D. Collins[1], and Michael Markl[1,3]

[1]Radiology, Northwestern University, Chicago, IL, United States, [2]Radiology, Lurie Children's Hospital, Chicago, IL, United States, [3]Biomedical Engineering, Northwestern University, Chicago, IL, United States

Sievers type II bicuspid aortic valve (BAV) is a rare disease that has been associated with more severe aortopathy than the more common type I BAV. To study the relation between aortic valve (AV) morphology and altered aortic hemodynamics in this disease, 4D flow MRI data from 32 type II BAV patients with different AV fusion types were analyzed. The helicity direction of blood flow in the ascending aorta was found to be influenced by AV morphology. Additional research with a larger cohort and comparison to type I BAV should render further insights into the pathophysiologic mechanism underlying BAV aortopathy.

2835

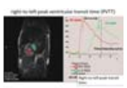

Peak ventricular transit time with first pass perfusion on cardiac MRI is a new marker of right ventricular dysfunction and pulmonary hypertension

Noriko Oyama-Manabe[1], Osamu Manabe[2], Ichizo Tsujino[3], Hiroshi Ohira[3], Tadao Aikawa[4], and Kohsuke Kudo[1]

[1]Diagnostic and Interventional Radiology, Hokkaido University Hospital, Sapporo, Japan, [2]Nuclear Medicine, Hokkaido University Hospital, [3]First Department of Medicine, Hokkaido University Hospital, [4]Department of Cardiovascular Medicine, Hokkaido University Hospital

Thirty-three patients with pulmonary hypertension (PH) and 16 controls were retrospectively evaluated. The right-to-left peak ventricular transit time (PVTT) determined using cardiac first-pass perfusion MRI was prolonged in patients with PH without left ventricular dysfunction. The degree of PVTT prolongation showed a modest association with right ventricular dilatation and dysfunction. Significant positive correlations were observed between PVTT and pulmonary artery pressures. The PVTT showed moderate sensitivity (65%) and high specificity (90%) for detection of PH. PVTT may be an additional simple tool to evaluate right ventricular dysfunction and pulmonary artery pressure in patients with PH.

2836

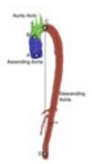

Quantification of helical flow and aortic tortuosity using 4D Flow MRI

Filippa Gustafsson[1,2], Magnus Ziegler[1,2], Martin Welander[1,3], Marcus Lindenberger[1,3], Niclas Bjarnegård[1], Tino Ebbers[1,2], Toste Länne[1,3], and Petter Dyverfeldt[1,2]

[1]Department of Medical and Health Sciences, Linköping University, Linköping, Sweden, [2]Center for Medical Image Science and Visualization (CMIV), Linköping, Sweden, [3]University Hospital Linköping, Linköping, Sweden

Due to the complex anatomy of the heart, its valves, and the aorta, the blood flow in the aorta is similarly complex and can exhibit a swirling, or helical flow pattern. Previous studies have shown that aortic geometry changes with age. As the shape of the aorta is complex and evolves over time, the aim of this study is to examine the relationship between the shape of the aorta and helical flow. The results show that the aorta gets more tortuous with age, and that the increased tortuosity is associated with increased helicity.

2837

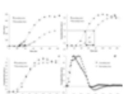

Magnetic Resonance Imaging Reveals Elevated Aortic Pulse Wave Velocity in Overweight Adolescents

Jessica Elizabeth Caterini[1,2], Laura Banks[3,4], Greg D Wells[1,5], Brian McCrindle[4,6], and Mike Seed[4,6]

[1]Physiology and Experimental Medicine, Hospital for Sick Children, Toronto, ON, Canada, [2]Department of Exercise Sciences, University of Toronto, Toronto, ON, Canada, [3]Faculty of Kinesiology and Physical Education, University of Toronto, ON, Canada, [4]Labatt Family Heart Centre, Hospital for Sick Children, Toronto, ON, Canada, [5]Faculty of Kinesiology and Physical Education, University of Toronto, Toronto, ON, Canada, [6]Department of Pediatrics, Faculty of Medicine, University of Toronto, Toronto, ON, Canada

This study provides a comparison of four commonly-used estimates of PWV to evaluate aortic stiffness, and compares these estimates of PWV with factors indicating cardiometabolic risk in obese youth. Hemodynamic parameters and phase-contrast CMR of the aortic arch at 3.0T were measured in 19 participants (12 obese, 7 normal-weight). Four methods of estimating PWV were used (cross-correlation, foot-to-foot, half-peak, area under the curve). There was an association between increasing measures of inflammation (C-reactive protein) and BMI, indicating that aortic PWV may be associated with changes in arterial stiffness in adolescents with subclinical biomarkers of cardiovascular disease. Careful consideration should be given to the method of PWV estimation due to measurement bias.

2838

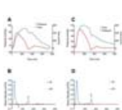

Comprehensive Noninvasive Hemodynamics Using High Temporal Resolution Phase Contrast MR Imaging

Michael A Quail[1], Rebekah Short[1], Bejal Pandya[2], Jennifer Steeden[1], Abbas Khushnood[1], Andrew M Taylor[1], Patrick Segers[3], and Vivek Muthurangu[1]

[1]Centre for Cardiovascular Imaging, University College London, London, United Kingdom, [2]Adult Congenital Heart Disease Department, St Bartholomew's Hospital, London, United Kingdom, [3]IBiTech-bioMMeda, iMinds Medical IT, Ghent University, Gent, Belgium

Implementation of an imaging based technique to perform a non-invasive, comprehensive hemodynamic assessment, using high temporal resolution phase contrast imaging.

2839

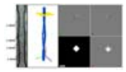

Influence of the k-t Principal Component Analysis acceleration factor on the accuracy of flow measurement in 4D PC-MRI

Gwenaël Pagé[1], Jérémie Bettoni[2], Anne-Virginie Salsac[3], and Olivier Balédent[1,4]

[1]BioFlow Image, University of Picardie Jules Verne, Amiens, France, [2]Maxillo-facial surgery, University Hospital of Amiens, Amiens, FL, France, Metropolitan, [3]Biomechanics & Bioengineering Laboratory, Université de Technologie de Compiègne, Compiègne, France, Metropolitan, [4]Department of image processing, University Hospital of Amiens, Amiens, France, Metropolitan

The main purpose of this phantom study is to assess the influence of k-t Principal Component Analysis reconstruction technique on the 4D PC-MRI velocity measurements through millimetrics vessels. 4D PC-MRI sequence is repeated 4 times with a k-t PCA acceleration factor set at 0, 2, 4 and 8. Flow curves are reconstructed and their mean flow and amplitude are compared. Results shows it is possible to reduce the acquisition time and still maintain a good mean flow measurement accuracy. However, the k-t PCA acceleration factor causes loss of information, resulting in a decrease of the amplitude of the flow curve.

2840

Assessment of global cerebral flow: comparing 2D and 4D flow strategies

Karin Markenroth Bloch[1], Jonas Svensson[2], Mariam Al-Mashat[3], Marcus Carlsson[3], and Danielle van Westen[4]

[1]Lund University Bioimaging Center, Lund University, Lund, Sweden, [2]Dept. of Medical Radiation Physics, Lund University, Lund, Sweden, [3]Lund University, Dept. of Clinical Sciences Lund, Clinical Physiology, Skane University Hospital, Lund, Sweden, [4]Dept. of Diagnostic Radiology, Lund University, Lund, Sweden

Quantifying the total blood supply to the brain and relating that to brain tissue mass gives a measure of global cerebral blood flow (CBF_{glo}). The cerebral blood flow can be measured using phase contrast MRI in the supplying arteries. For accuracy, separate 2D flow measurements for each vessel has been recommended. An alternative is to use one 4D flow measurement that covers all vessels of interest and allows flexible definition of measurement planes. The aim of this work is to compare the flow results obtained from a single 2D flow measurement to those from a 4D flow scan.

2841

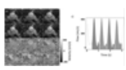

Real-time monitoring of Exercise Stress using Spiral Flow MRI

Rajiv Ramasawmy[1], Anthony Z Faranesh[1], Jaffar M Khan[1], Toby Rogers[1], Robert J Lederman[1], Michael S Hansen[1], and Adrienne E Campbell-Washburn[1]

[1]National Heart Lung and Blood Institute, National Institutes of Health, Bethesda, MD, United States

Interventional cardiovascular MR exams can augment catheter procedures with simultaneous functional measurements. This preliminary work implements an accelerated spiral acquisition to measure real-time, beat-to-beat cardiac output changes during exercise stress induced using a MR-compatible ergometer. At rest, the beat-to-beat variation in cardiac output had a coefficient of variation of 19.1 ± 16.8%. Using this high temporal resolution sequence, a significant increase in cardiac output (5.23 L/min to 8.39 L/min) was measured between rest and exercise sustained at 160-180 W.

2842

Improved Visualization of Common Iliac Artery 3D-cine Phase Contrast Magnetic Resonance Imaging Using Selective Water Excitation

Sachi Fukushima[1], Kenichi Nakagawa[1], Masami Yoneyama[2], Noriyoshi Morimoto[1], Masayuki Kumashiro[1], and Takashi Tabuchi[3]

[1]Department of Radiological Technology, Kurashiki Central Hospital, Okayama, Japan, [2]Philips Electronics Japan, Tokyo, Japan, [3]Department of Medical Technology, Kurashiki Central Hospital, Okayama, Japan

The motion artifacts in the pelvic area using 3D-cine phase contrast (4D PC) MRI may be provide the severity results. The purpose of this study was to demonstrate the usefulness of fat suppression for the common iliac artery (CIA). The study protocol compared 4D PC MRI date without fat suppression to with principle of selective excitation technique (ProSet). We evaluated the streamline visualization, SNR of magnitude images and blood flow volume. ProSet can reduce respiration artifacts. Extending of TR by using ProSet increases SNR. Thus ProSet1-1 is the optimal fat suppression technique to improve vascular visualization.

2843

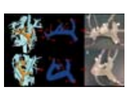

Comprehensive Hemodynamics of Living Donor Liver Transplantion Using MRI-based In-Vitro Experiments and Computational Simulation

David Rutkowski[1,2], Scott B. Reeder[2,3,4,5,6], and Alejandro Roldán-Alzate[1,2,4]

[1]Mechanical Engineering, UW Madison, Madison, WI, United States, [2]Radiology, UW Madison, Madison, WI, United States, [3]Medical Physics, UW Madison, Madison, WI, United States, [4]Biomedical Engineering, UW Madison, Madison, WI, United States, [5]Medicine, UW Madison, Madison, WI, United States, [6]Emergency Medicine, UW Madison, Madison, WI, United States

The purpose of this study was to develop a patient specific experimental methodology to complement computational surgical planning models for living donor liver transplant. 4D flow MRI was performed on one healthy liver donor before and after partial hepatectomy. Physical models of the donor vasculature were created, and experiments were conducted to measure flow and pressure throughout the system. Experimental results were compared with 4D flow measurements and simulation results. Flow measurements were significantly similar between imaging and simulation, and between simulation and experiment. This methodology will be used to improve boundary value assumptions in surgical planning models.

2844

An outlier rejection scheme to improve background phase correction in PC-MRI

Aaron A Pruitt[1], Ning Jin[2], Orlando Simonetti[3], Yingmin Liu[3], and Rizwan Ahmad[3]

[1]The Ohio State University, Columbus, OH, United States, [2]Siemens Healthineers, [3]The Ohio State University

The accuracy of flow quantification in phase contrast MRI (PC-MRI) is limited by the presence of eddy current-induced background phase. A widely reported method to correct background phase relies on polynomial fitting of the pixels within regions of static tissue. However, separating regions with steady flow from static tissue can be challenging because such regions lack temporal variations that are often used to identify and eliminate pixels that are not static. In this work, we present and validate a processing method that identifies and eliminates outliers such as pixels belonging to venous flow and thus improves flow quantification.

2845

Improving Non-Contrast 4D Flow MRI Using Multiple-Thin-Slab Dual-Venc Acquisition

Fatih Suleyman Hafalir[1], Peng Lai[2], Ana Beatriz Solana[3], Anja C.S. Brau[2], Malek Makki[4], Axel Haase[1], and Martin A. Janich[3]

[1]Technical University of Munich, Munich, Germany, [2]GE Healthcare, CA, United States, [3]GE Global Research, Munich, Germany, [4]MRI Research Center, University Children Hospital, Zurich, Switzerland

Dual-venc 4D flow MRI can improve velocity-to-noise ratio (VNR) using a low-venc velocity map to provide a good VNR and a high-venc velocity map to correct the velocity aliasing. However, dual-venc 4D flow MRI significantly lengthens the scan duration to longer than the 10min delayed enhancement wait time and therefore it is difficult to take advantage of T1 shortening immediately after contrast injection. On the other hand, whole volume acquisition saturates blood signal and decreases SNR for 4D flow MRI, especially without contrast agent. Multi Thin Slab (MSLAB) 4D flow MRI acquisition technique provides bright blood imaging with improved SNR and motion robustness. Therefore, by combining dual-venc with MSLAB we propose a more accurate 4D flow method without requirement of contrast agent. In this study, we analyzed our proposed method in a pulsatile flow phantom in terms of VNR and performance in a volunteer.

2846

Volumetric Segmentation-Free Method for Quantitative Visualization of Cardiovascular Wall Shear Stress Using 4D Flow MRI

Evan M Masutani[1], Joseph Y Cheng[2], Marcus T Alley[2], Shreyas S Vasanawala[2], and Albert Hsiao[1]

[1]University of California, San Diego, La Jolla, CA, United States, [2]Stanford University, Stanford, CA, United States

We demonstrate a volumetric technique for calculation and visualization of great vessel wall shear stress (WSS) from 4D Flow MRI data. Traditional methods for WSS have relied on planar sections of the data followed by explicit manual segmentation of vessel boundaries, which can be labor-intensive to perform. We propose a volumetric strategy for computation and visualization of WSS, which may facilitate its clinical translation.

2847

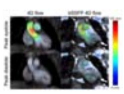

Feasibility of non-contrast-enhanced cardiovascular 4D flow MRI using a balanced SSFP approach

Christopher M. Sandino[1], Marcus T. Alley[2], Joseph Y. Cheng[2], Brian A. Hargreaves[2], and Shreyas S. Vasanawala[2]

[1]Department of Electrical Engineering, Stanford University, Stanford, CA, United States, [2]Department of Radiology, Stanford University, CA, United States

Balanced steady state free precession (bSSFP) phase-contrast sequences have desirable tissue contrast properties that allow for non-contrast-enhanced cardiovascular flow exams. However, they are susceptible to flow-related signal dephasing especially in regions with highly accelerating flow like the heart. To address this, we propose a variable-density radial view-ordered bSSFP 4D flow sequence. Acquired images show reasonable visualization of cardiac anatomy, and similar velocity measurements in aortic regions. Further sequence modifications are suggested to improve its robustness. If proven to be a viable alternative to the standard exam, bSSFP 4D flow would reduce exam costs and greatly improve patient experience.

2848

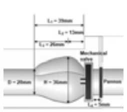

Evaluation of three-dimensional flow characteristics behind the prosthetic mechanical valve under subvalvular pannus formation; in-vitro 4D flow MRI

Hyung Kyu Huh[1], Hojin Ha[1], Sang Joon Lee[1], Namkug Kim[2,3], and Donghyun Yang[3]

[1]Mechanical Engineering, POSTECH, Pohang, Korea, Republic of, [2]Department of Convergence Medicine, Asan Medical Center, [3]Department of Radiology, Asan Medical Center

A pannus formation is a growth of abnormal tissues around the heart valve, which is often found in patients whom underwent heart valve replacement surgery. Significant hemodynamic changes caused by the formation of the pannus may contribute to the failure of the valves even without direct contact to the leaflets. In current study, flow in the sinus if Valsalva under subvalvular pannus formation was analyzed using in vitro phantom and 4D flow MRI. Symmetric pannus causes imperfect opening the valve, which might lead to the heart failure.

2849

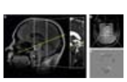

Quantification of cerebrospinal fluid flow through the cerebral aqueduct using 7T MRI

JM Spijkerman[1], JCW Siero[1,2], LJ Geurts[1], MJ Donahue[3], J Hendrikse[1], PR Luijten[1], and JJM Zwanenburg[1]

[1]Department of Radiology, University Medical Center Utrecht, Utrecht, Netherlands, [2]Spinoza Center for Neuroimaging, Amsterdam, Netherlands, [3]Department of Radiology, Vanderbilt University Medical Center, Nashville, TN, United States

In this work the feasibility of recording high spatial resolution quantitative flow (Qflow) measurements in the cerebral aqueduct at 7T was investigated. Five volunteers were scanned, two encoding velocities (v_{enc}) were used: 5 and 13 cm/s. Repeated measurements were performed (v_{enc}=5cm/s: n=4; v_{enc}=13 cm/s: n=5). Mean net CSF flow through the aqueduct (directed towards the spine) was (mean±std) 332±128 ml/day for v_{enc}=5cm/s and 441±149 ml/day for v_{enc}=13cm/s, which is in accordance with values found in literature. Reasonable reproducibility of the measurements was found.

2850

The Magnitude of Static Phantom Corrections for Velocity Encoded Phase Contrast Cine MRI and Clinical Importance

Evan A Nelson[1], Li-Yueh Hsu[1], Anna Noreuil[1], Sara E Berger[2,3], Marcus Y Chen[1], W. Patricia Bandettini[1], Sujata M Shanbhag[1], Shahryar G Saba[4], Giancarlo Serafini[1], Christine Mancini[1], Vandana Sachdev[1], and Andrew E Arai[1]

[1]National Heart, Lung, and Blood Institute, National Institutes of Health, Bethesda, MD, United States, [2]Physiology Department, Northwestern University, Chicago, IL, United States, [3]Computational Neuroscience, IBM / Thomas J Watson Center, Yorktown Heights, NY, [4]Cardiology and Radiology, Hofstra Northwell School of Medicine, Manhasset, NY, United States

The purpose of this study was to investigate the magnitude of ex vivo static phantom corrections affecting Qp, Qs, and the Qp-to-Qs ratio measurements in diagnosing patients with intracardiac shunts. In the patients with Cath as the reference standard, phantom correction improved both the bias as well as the limits of agreement for Qp and the Qp:Qs ratio. For Qs, phantom correction improved the bias but did not significantly change the limits of agreement. While phantom correction appears to improve phase contrast MRI measurements, the main benefit is limited to patients with Qp:Qs close to the important diagnostic threshold selected.

2851 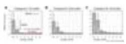

Image-based Background Phase Error Correction in 4D Flow MRI

Julia Busch[1], Daniel Giese[2], and Sebastian Kozerke[1,3]

[1]Institute for Biomedical Engineering, University and ETH Zurich, Zurich, Switzerland, [2]Department of Radiology, University Hospital Cologne, [3]Division of Imaging Science and Biomedical Engineering, King's College London

Background phase errors occurring in 4D Flow MRI are analyzed with respect to their spatial order. Results demonstrate that background errors can range from first up to third spatial order requiring correction with appropriate polynomial orders. While higher order corrections perform well even for low SNR, they are highly sensitive to the amount of stationary tissue present for background phase estimation requiring at least 25%, 60% and 75% of stationary tissue for systems with first, second and third order offsets The amount of stationary tissue available in-vivo, however, limits the use of higher order polynomial models for background phase correction.

2852 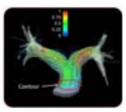

4D flow MR measurements for functional assessment of idiopathic pulmonary arterial hypertension: comparison between patients and healthy volunteers

Xiaole Wang[1], Yunlong Yue[2], Lei Pan[3], Hong Jiang[3], Yunduo Li[1], and Rui Li[1]

[1]Center for Biomedical Imaging Research, Department of Biomedical Engineering, School of Medicine, Tsinghua University, Beijing, People's Republic of China, [2]Department of MR, Beijing Shijitan Hospital of Capital Medical University, [3]Department of Pulmonary Vascular Disease and Geriatric Medicine, Beijing Shijitan Hospital of Capital Medical University

We applied parameter analysis in 4D flow imaging for pulmonary artery hypertension (PAH) and compare the MR parameters between five patients with iPAH and five healthy volunteers. Compared with healthy volunteers, patients with idiopathic PAH have more retrograde flow in MPA, enlarger area of MPA, higher peak acceleration. And Plane-to-plane variations of these parameters were evaluated using the Bland-Altman comparisons, some parameters have relatively low variations which means they can be calculated through 2D flow imaging. In conclusion, MRI results show that the effect of increased pulmonary artery pressure and resistance has influence the flow in MPA.

2853 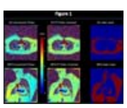

Phase Contrast MRI with Automatic Inline Second Order Background Phase Correction

Gary R. McNeal[1], Timothy C. Slesnick[2], Sassan Hashemi[3], Mehmet Akif Gulsun[4], Andreas Greiser[5], and Ning Jin[1]

[1]Cardiovascular MR R&D, Siemens Healthineers, Chicago, IL, United States, [2]Pediatric Cardiology, Emory University School of Medicine, Children's Healthcare of Atlanta, Atlanta, GA, United States, [3]Cardiovascular Imaging Research Core, Children's Healthcare of Atlanta, Atlanta, GA, United States, [4]Medical Imaging Technologies, Siemens Medical Solutions USA, Inc., Princeton, NJ, United States, [5]Cardiovascular MR R&D, Siemens Healthineers, Erlangen, Germany

This work presents an automatic inline method for correction of background phase errors in 2D PC MRI. Flow images were automatically processed during image reconstruction for background phase correction. Uncorrected and corrected images were compared qualitatively and quantitatively. Quantitative flow measurements were performed by two experienced observers using a fully-manual method and a semi-automated method. Mean Q_p/Q_s of the patient cohort was used as a metric to evaluate the proposed second order background phase correction method.

2854 

4D-flow-MRI in patients with Fontan circulation for evaluation of pulmonary artery blood distribution

Harald Kramer[1,2,3], Anja Lehner[4], Adrian Curta[1], and Robert Dalla-Pozza[4]

[1]Department of Radiology, University of Munich, Munich, Germany, [2]University of Wisconsin - Madison, Madison, United States, [3]DZHK German Center for Cardiovascular Research, Munich, Germany, [4]Department of Pediatric Cardiology and Pediatric Intensive Care, University of Munich, Munich, Germany

4D-flow-MRI can serve as a non-invasive imaging modality to monitor patients with congenital heart disease and status post surgical repair. Patients with Fontan-circulation need to be followed up regularly to identify the right time for re-intervention to avoid pulmonary hypertension or atrophy due to hyper- or hypoperfusion, respectively and the development of protein-losing enteropathy.

2855 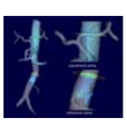

4D-Flow enables depictions and quantitative analysis of the characteristic flow fluctuations in the infrarenal aorta and diastolic suction flow in renal arteries

Masataka Sugiyama[1], Yasuo Takehara[2], Marcus Alley[3], Tetsuya Wakayama[4], Atsushi Nozaki[4], Hiroyuki Kabasawa[4], Takasuke Ushio[1], Yohei Ito[1], and Harumi Sakahara[1]

[1]Radiology, Hamamatsu University School of Medicine, Hamamatsu, Japan, [2]Department of Fundamental Development for Advanced Low Invasive Diagnostic Imaging, Nagoya University, Nagoya, Japan, [3]Radiology, Stanford University School of Medicine, Palo Alto, CA, United States, [4]Applied Science Laboratory Asia Pacific, GE Healthcare Japan, Hino, Japan

4D-Flow can be used to visually and quantitatively evaluate characteristic retrograde flow within the infrarenal abdominal aorta and the diastolic suction flow within the RAs, which might be the initiation factor of degradation of abdominal aortic wall followed by fatal aortic disease.

2856

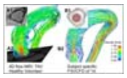

MRI-based Fluid Structure Interaction Simulation of the Bicuspid Aortic Valve using Native Non-linear Valve Properties

Alex J Barker*[1], Anvar Gilmanov*[2], Henryk Stolarski[3], and Fotis Sotiropoulos[4]

[1]Radiology, Northwestern University, Chicago, IL, United States, [2]Saint Anthony Falls Laboratory, University of Minnesota Minneapolis, MN, United States, [3]Department of Civil,Environmental and Geo-engineering, University of Minnesota Minneapolis, [4]Stony Brook University

Limitations of temporal and spatial resolution prevent MRI from visualizing boundary layers and fluid structure interaction (FSI) occurring immediately adjacent to the valve leaflets as well as at the aortic wall downstream from the valve. We make use of CMR image-based patient specific anatomy and boundary conditions to perform computational fluid dynamic (CFD) analysis which incorporates moving boundary conditions. The numerical approach is shown to elucidate complex and dynamic blood and leaflet behavior previously not seen with CMR alone.

2857

Analysis of WSS variability subjected to changes of 4D flow parameters using a realistic aortic phantom.

Cristian Montalba[1], Julio Sotelo[1,2], Jesús Urbina[1,3], Marcelo Andia[1,3], Cristian Tejos[1,2], Pablo Irarrázaval[1,2], Israel Valverde[4,5], and Sergio Uribe[1,3]

[1]Biomedical Imaging Center, Pontificia Universidad Católica de Chile, Santiago, Chile, [2]Electrical Engineering Department, Pontificia Universidad Católica de Chile, Santiago, Chile, [3]Radiology Department, School of Medicine, Pontificia Universidad Católica de Chile, Santiago, Chile, [4]Hospital Virgen del Rocio, Universidad de Sevilla, Seville, Spain, [5]Institute of Biomedicine of Seville, Universidad de Sevilla, Seville, Spain

The purpose of this work was to study the accuracy of the estimation of WSS calculated from 4D flow data acquired at different spatial and temporal resolutions. The data was acquired using a realistic thoracic aortic phantom in nine different hemodynamic conditions. We conclude that WSS measurements are more sensitive to changes in spatial resolution than in temporal resolution.

2858

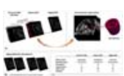

Left Ventricle Strain Estimation using flow MRI

Hernán Mella[1,2], Joquín Mura[1], Julio Sotelo[1,2], Cristian Montalba[1], and Sergio Uribe[1,3]

[1]Biomedical Imaging Center, Pontificia Universidad Católica de Chile, Santiago, Chile, [2]Department of Electrical Engineering, Pontificia Universidad Católica de Chile, Santiago, Chile, [3]Department of Radiology, School of Medicine, Pontificia Universidad Católica de Chile, Santiago, Chile

The stiffness in the myocardium represents a reliable biomarker of cardiac dysfunction or diseases, such as atherosclerosis or cardiac infarction. Actually, there exist methods to retrieve this indicator using MRI, however, they can be very time-consuming, especially for volumetric evaluations. In this work, we propose a novel method to estimate strains using Phase-Contrast or 4D-flow data, where velocity fields are transformed into strain tensors in a numerically simple but robust manner. Preliminary results are promising and we expect to validate our method in volunteers and patients.

2859

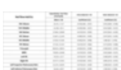

Quantification of blood flow in the great veins and right heart using 4D flow MRI in Chronic Obstructive Pulmonary Disease: A pilot study in the MESA COPD Study

Ozair Rahman[1], Carmen Blanken[2], Pallavi P Balte[3], Bharath Ambale Venkatesh[4], Martin Prince[5], David A Bluemke[6], Oliver Wieben[7], Joao Lima[8], Stephen M Dashnaw[9], James Carr[2], Graham G Barr[3], and Michael Markl[2]

[1]Department of Radiology, Northwestern University, Chicago, IL, United States, [2]Radiology, Northwestern University, Chicago, IL, United States, [3]Epidemiology, Columbia University, New York, NY, United States, [4]John's Hopkins, Baltimore, MD, United States, [5]Radiology, Cornell, New York, NY, United States, [6]Radiology and Imaging Sciences, National Institutes of Health, Bathesda, MD, United States, [7]Radiology, University of Wisconsin-Madison, Madison, WI, United States, [8]Radiology, John's Hopkins, Baltimore, MD, United States, [9]Radiology, Columbia University, New York, NY, United States

Chronic Obstructive Pulmonary Disease is the third leading cause of death in the United States, and affects 24 million Americans with over 65 million people affected world-wide. Up-to 58% of patients develop exertional pulmonary hypertension and right ventricular volume changes. Understanding this phenomenon, known as cor pulmonale can help us gain insight into the complex pathophysiology involved. This pilot study attempts to apply 4D flow MRI in patients with varying degrees of COPD, and assess the feasibility, reproducibility and accuracy of this technique.

2860

Kinetic energy and vorticity in the pulmonary artery in pediatric patients with repaired tetralogy of Fallot using 4D flow MRI

Julio Garcia[1], Silvia Hidalgo Tobon[2,3], Benito de Celis Alonso[4], Manuel Obregon[2], Porfirio Ibanez[2], Julio Erdmenger[2], and Pilar Dies-Suarez[2]

[1]Department of Cardiac Sciences - Stephenson Cardiac Imaging Centre, University of Calgary, Calgary, AB, Canada, [2]Investigacion en Imagen y Resonancia Magnetica Nuclear, Hospital Infantil de Mexico Federico Gomez, Mexico City, Mexico, [3]Physics, Universidad Autonoma Metropolitana, Mexico City, Mexico, [4]Faculty of Physics and Mathematics, Benemérita Universidad Autónoma de Puebla, Puebla, Mexico

Flow alterations in the pulmonary artery (PA) of patients with repaired tetralogy of Fallot (rTOF) may be link with elevated kinetic energy (KE). 4D flow MRI allows for the non-invasive volumetric assessment of flow hemodynamics, vorticity, and KE in pediatric patients with rTOF in the pulmonary (PA). Thus, the aim was to investigate the impact of flow alterations in the PA and its association with KE and vorticity.

2861 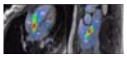 Visualization of atrial septal defects and shunt quantification at multiple locations using 4D Flow MRI in a multicenter pilot study

Raluca Gabriela Chelu[1], Michael Horowitz[2], Dominika Sucha[3], Shreyas Vasanawala[3], Koen Nieman[3], Jean-Francois Paul[4], and Albert Hsiao[2]

[1]Erasmus MC, Rotterdam, Netherlands, [2]UCSD, San Diego, CA, United States, [3]Stanford University, Palo Alto, CA, United States, [4]Institute Mutual Montsouris, Paris, France

4D Flow shows clinical promise for a wide variety of cardiovascular applications. We hypothesized that flow measurements may be valuable across a variety of scanning parameters and field strengths typically used in clinical practice. We therefore established a multicenter clinical study at 4 sites using MRI in patients with atrial septal defects. We investigated the consistency of blood flow measurements obtained along the systemic and pulmonary vasculature. Quantitative data appear robust across multiple observers and measurement locations, from data obtained across multiple sites, representing a step forward in the implementation of 4D Flow in clinical practice.

Traditional Poster

Function

Exhibition Hall 2862-2887 Thursday 8:15 - 10:15

2862 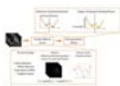 Automated Cardiac Resting Phase Detection in 2D cine MR images for Acquisition Window Selection in High-Resolution Coronary MRI

Davide Piccini[1,2,3], Robin Demesmaeker[1], Gabriella Vincenti[4], Tobias Kober[1,2,3], and Matthias Stuber[2,5]

[1]Advanced Clinical Imaging Technology, Siemens Healthcare AG, Lausanne, Switzerland, [2]Department of Radiology, University Hospital (CHUV) and University of Lausanne (UNIL), Lausanne, Switzerland, [3]LTS5, École Polytechnique Fédérale de Lausanne (EPFL), Lausanne, Switzerland, [4]Division of Cardiology and Cardiac MR Center, University Hospital of Lausanne (CHUV), Lausanne, Switzerland, [5]Center for Biomedical Imaging (CIBM), Lausanne, Switzerland

In MR coronary angiography, the synchronization of the ECG-triggered imaging sequence with periods of minimal diastolic/systolic myocardial motion (resting phases) is essential. The selection of the resting phases is usually performed manually by an expert user. Here, automated detection of the period of minimal myocardial motion is described and tested in 30 cine patient datasets. After normalization of the cine image series, a 1D curve representative of the overall amount of motion for each cine frame is extracted. Frames belonging to diastolic/systolic resting phases are selected from such curve using peak detection and threshold-based region-growing. Testing is performed in comparison to manually expert-selected resting phases.

2863 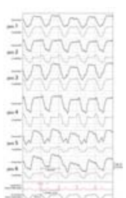 On the link between cardiac action and magnetic field dynamics observed with NMR sensors

Simon Gross[1], Christoph Barmet[1,2], Benjamin E. Dietrich[1], Julia Busch[1], Sebastian Kozerke[1], and Klaas P. Pruessmann[1]

[1]Institute for Biomedical Engineering, ETH Zurich and University of Zurich, Zurich, Switzerland, [2]Skope Magnetic Resonance Technologies Inc., Zurich, Switzerland

Magnetic field dynamics recorded with NMR field sensors located close to beating heart provide detailed access to cardio-vascular action. We present a realistic model that examines the physical pathways which translate mechanical heart activity into observable magnetic field dynamics. It is based on a 4D tissue model obtained from cardiac cine MR images. We confirmed that the observed signals are mainly caused by displacements of blood and muscle tissue. The presented modelling approach is expected to advance the physiological interpretation of the observed signals.

2864  The diagnostic accuracy of cardiac magnetic resonance imaging for the differential diagnosis between the left ventricular non-compaction and the negative heart remodeling in thalassemia intermedia patients

Antonella Meloni[1], Francesca Macaione[2], Vincenzo Positano[1], Andrea Barison[1], Laura Pistoia[1], Salvatore Novo[2], Pasquale Assennato[2], and Alessia Pepe[1]

[1]Fondazione G. Monasterio CNR-Regione Toscana, Pisa, Italy, [2]Università degli Studi di Palermo, Policlinico "Paolo Giaccone", Palermo, Italy

The Grothoff's criteria should be used in the clinical practice in order to improve the specificity of the diagnosis of LVNC and distinguish LVNC and negative heart remodeling in β-TI.

2865  Determining prolate spheroidal modes of cardiac deformation directly from tagged heart images

Walter O'Dell[1] and Shruti Siva Kumar[2]

[1]Radiation Oncology, University of Florida, Gainesville, FL, United States, [2]Biomedical Engineering, University of Florida, Gainesville, FL, United States

An approach was developed to compute modes of left ventricular wall deformation directly from tagged MR images via generation of simulated tagged images undergoing modes of deformation expressed in a prolate spheroidal coordinate system (PSCS). This eliminates the laborious pre-processing step of detecting tags and/or points along tags while employing an efficient and accurate representation of LV wall motion in terms of PSCS modes. The method was tested with simulated and low-quality human image data sets with acceptable initial results. It is hoped that this advancement will help rekindle application of quantitative MR tagging in the clinical and research arenas.

2866

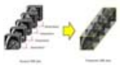

Three-dimensional Bi-ventricular Myocardial Feature Tracking for Congenital Heart Disease Using Standard Cardiac Cine MRI with Interpolation Technique Based on Moving Gradients

Masateru Kawakubo[1], Yuzo Yamasaki[2], Hiroshi Akamine[3,4], and Michinobu Nagao[5]

[1]Department of Radiological Technology, Faculty of Fukuoka Medical Technology, Teikyo University, Omuta, Japan, [2]Department of Clinical Radiology, Graduate School of Medical Sciences, Kyushu University, Fukuoka, Japan, [3]Division of Radiology, Department of Medical Technology, Kyushu University Hospital, Fukuoka, Japan, [4]Department of Health Sciences, Graduate School of Medical Sciences, Kyushu University, Fukuoka, Japan, [5]Department of Diagnostic Imaging & Nuclear Medicine, Tokyo Women's Medical University, Tokyo, Japan

Patients with congenital heart disease (CHD) often have complicated ventricular motion and configuration. Myocardial feature tracking (MFT) MRI can quantitatively analyze 2-dimensional myocardial motion. Although three-dimensional (3D) MFT is required for the patients with CHD, standard cine MRI is limited the setting of thin slice thickness attributed to increasing scan time. In this study, we analyzed bi-ventricular function with 3D MFT using only standard cine MRI datasets reconstructed by moving gradients based image interpolation technique. As the result, 3D MFT is useful to evaluate bi-ventricular function for patients with CHD, and can be easily applied to routine clinical MR examination.

2867

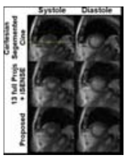

Real-Time Cardiac Functional Imaging Using an Arrhythmia-Robust Radial Imaging Sequence

André Fischer[1,2], Peng Lai[3], James H. Holmes[4,5], Ty A. Cashen[4,5], Kevin M. Johnson[5,6], Anne Menini[1], Christopher J. Francois[5], Anja C.S. Brau[3], and El-Sayed Ibrahim[7]

[1]GE Global Research Europe, Garching bei München, Germany, [2]Cardiac Center of Excellence, GE Healthcare, Garching bei München, Germany, [3]GE Healthcare, Menlo Park, CA, United States, [4]GE Healthcare, Madison, WI, United States, [5]Radiology, University of Wisconsin - Madison, Madison, WI, United States, [6]Medical Physics, University of Wisconsin - Madison, Madison, WI, United States, [7]GE Healthcare, Waukesha, WI, United States

Cardiac cine datasets are difficult to obtain in the presence of arrhythmia or poor gating signal. Here, completely ungated radial real-time imaging may help. Cartesian real-time imaging usually offers compromised spatial resolution to maintain sufficient temporal resolution. Hence, we propose a radial bSSFP-based real-time approach with Golden Angle increment which enables view sharing of temporally adjacent projections. To minimize temporal blurring, a narrow tornado shaped filter, followed by subsequent iterative SENSE reconstruction, was used. Remaining streaking artifacts were reduced by a principal component analysis based technique. Results show good agreement in terms of image quality to a standard Cartesian cine dataset.

2868

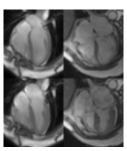

Left Atrial Enlargement and Systolic Failure Measured by Cardiac MRI in Severe Isolated Mitral Regurgitation with Preserved Left Ventricular Ejection Fraction

Xiaoxia Zhang[1,2], Steven Lloyd[3,4], Himanshu Gupta[3,4], Nouha Salibi[1,5], James Davies[3], Louis Dell'Italia[3,4], and Thomas Denney[1,2]

[1]Auburn University MRI Research Center, Auburn University, Auburn, AL, United States, [2]Electrical and Computer Engineering, Auburn University, Auburn, AL, United States, [3]Division of Cardiovascular Disease, University of Alabama at Birmingham, Birmingham, AL, United States, [4]Birmingham Veterans Affairs Medical Center, Birmingham, AL, United States, [5]MR R&D, Siemens Healthcare, Malvern, PA, United States

Mitral regurgitation (MR) from degeneration of the mitral valve (MV) results in a relatively low-pressure form of volume overload caused by excess volume being ejected through a secondary ejection pathway into the left atrium (LA). Optimal timing for MV repair is under debate because a spuriously normal left ventricular (LV) ejection fraction belies severe myocardial damage and that the onset of symptom has increased risk for LV dysfunction post MV repair. LA function measured by cMRI may be an important indicator for timing of MV repair before the onset of symptoms in patients with well-preserved LV systolic function.

2869

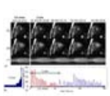

One Minute Free-Breathing 3D Cardiac Cine Imaging with Adaptive Respiratory Self-Gating Efficiencies

Jing Liu[1], Li Feng[2], Karen Ordovas[1], and David Saloner[1]

[1]University of California San Francisco, San Francisco, CA, United States, [2]New York University, New York, NY, United States

Cardiac cine imaging has become the standard for cardiac functional measurements. However, a series of breath-holds are required to acquire 2D cine images covering the whole heart. The capability of children or sick patients to perform consistent breath-holds is limited and often results in non-diagnostic images. We aim to develop a fast and reliable 3D imaging technique for cardiac functional assessment, which only requires one minute of scan time during free breathing. To compensate for respiratory motion, which varies substantially among subjects, we propose to apply adaptive respiratory self-gating efficiencies to generate reliable image quality for 3D cardiac cine imaging.

2870

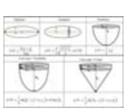

Evaluation of left ventricular (LV) geometric models for estimating LV volumes in 980 children using cardiac cine magnetic resonance imaging

Jiming Zhang[1], Carlo Uribe[2], Benjamin Cheong[1,2], Amol Pednekar[3], Paolo Angelini[2], and Raja Muthupillai[1,2]

[1]Diagnostic and Interventional Radiology, CHI St Luke's Health, Houston, TX, United States, [2]Center for Coronary Artery Anomalies, Texas Heart Institute, Houston, TX, United States, [3]Philips Healthcare, Cleveland, OH, United States

The results from this study that included cine SSFP images of the LV from 980 children show that LV volumes computed using commonly used bi-plane and tri-plane ellipsoidal models deviate significantly when compared to LV volumes estimated from a stack of short axis slices. A cut-cone+cone model of the LV proposed in this manuscript can estimate metrics describing LV function (EDV, ESV, and EF) with just two projections that are comparable to that obtained from an entire stack of short-axis slices.

2871

Feature-Tracking for Volume and Strain with Subtly Tagged SSFP

Eric Schrauben[1], Andreas Greiser[2], Brett Cowan[3], and Alistair Young[3]

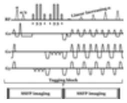

[1]Physiology & Experimental Medicine, University of Toronto, Toronto, ON, Canada, [2]Siemens Healthcare, Erlangen, Germany, [3]Anatomy and Medical Imaging, University of Auckland, Auckland, New Zealand

A novel subtly tagged cardiac acquisition coupled with non-rigid registration is developed and tested in healthy volunteers. The technique produces myocardial strain characterization and ventricular volumetrics within a single scan.

2872

Inter-center reproducibility of left ventricular circumferential strain analysis with spatial modulation of magnetization imaging analysis in healthy and repaired Tetralogy of Fallot patients

Xiaodan Zhao[1], Kathleen Gilbert[2], Hua Zou[1], Ru San Tan[1,3], Wen Ruan[1], Ju Le Tan[1,3], Alistair Young[2], and Liang Zhong[1,3]

[1]National Heart Centre Singapore, Singapore, Singapore, [2]The University of Auckland, New Zealand, [3]Duke-NUS Medical School Singapore, Singapore, Singapore

The aim of this study was to examine inter-center reproducibility of tagging magnetic resonance imaging (MRI) analysis in human patients undergoing either 1.5T or 3.0T MR examinations. A total of 20 subjects, 10 heathy subjects and 10 patients with repaired tetralogy of Fallot (rTOF), aged between 18 and 69 years, underwent either 1.5T or 3.0T MR scans. Circumferential strain (CS) from base, mid, and apex regions were analysed using CIM v8.4 at two centres (NHCS Singapore and University of Auckland). Reproducibility was moderate at the base (ICC 0.765), and excellent at the mid (0.979) and apex (0.982) regions. Overall reproducibility was excellent in both healthy controls and rTOF patients (ICC: 0.956 and 0.932), and at both 1.5T and 3.0T (0.972 and 0.940).

2873

Cardiovascular Magnetic Resonance Imaging Evaluation of Right Ventricular Efficiency in Health and Disease: State of the Art

Christopher J Francois[1], Niti R Aggarwal[2], Alan McMillan[2], and Mark L Schiebler[1]

[1]Radiology, University of Wisconsin - Madison, Madison, WI, United States, [2]University of Wisconsin - Madison, WI, United States

Assessing RV function is complex, particularly in patients with RV dysfunction. Traditional indices, such as RV volumes and ejection fraction, incompletely describe the alterations that occur with changes in RV volume or afterload. New CMR methods of assessing RV efficiency based on strain and energetics have the potential to detect dysfunction earlier than currently used approaches.

2874

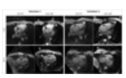

Improved Time Efficiency and Workflow for Fully Self-Gated Non-Contrast 5D Imaging of the Heart

Jerome Yerly[1,2], Davide Piccini[1,3], Lorenzo Di Sopra[1], Jessica AM Bastiaansen[1], Simone Coppo[4], and Matthias Stuber[1,2]

[1]Department of Radiology, University Hospital (CHUV) and University of Lausanne (UNIL), Lausanne, Switzerland, [2]Center for Biomedical Imaging (CIBM), Lausanne, Switzerland, [3]Advanced Clinical Imaging Technology, Siemens Healthcare AG, Lausanne, Switzerland, [4]Department of Radiology, Case Western Reserve University, Cleveland, OH, United States

Current solutions for cardiac and respiratory motion resolved whole-heart MR imaging rely on ECG signal to synchronize data acquisition, sub-optimal strategies for fat suppression which interrupts steady-state magnetization, or contrast agent for anatomical differentiation. To address these hurdles, we present a self-gated framework with bSSFP contrast and binomial spectrally selective excitation pulse which suppresses epicardial fat signal without interrupting steady-state. When compared to existing sequences, the proposed framework reduces energy deposition and acquisition time while preserving or even improving the final image quality.

2875

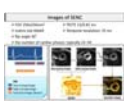

Global and regional wall motion abnormalities detected using strain-encoded MRI in comparison with late gadolinium enhancement in patients with sarcoidosis

Osamu Manabe[1], Noriko Oyama-Manabe[2], Hiroshi Ohira[3], Masanao Naya[3], Tadao Aikawa[3], and Nagara Tamaki[4]

[1]Hokkaido University Graduate School of Medicine, Sapporo, Japan, [2]Hokkaido University Hospital, [3]Hokkaido University, [4]Hokkaido University Graduate School of Medicine

We investigated global and regional myocardial wall motion abnormalities using strain-encoded (SENC) MRI in comparison with late gadolinium enhancement (LGE) in patients with systemic sarcoidosis. Fourteen patients were retrospectively evaluated. We found that global strain assessed using SENC MRI correlated well with global left ventricular (LV) dysfunction and the extent of LGE. In addition, regional longitudinal strain significantly decreased in segments with >10% LGE. SENC MRI has the potential to detect global and regional LV dysfunction and to predict the extent of LGE.

2876

3D left atrial strain imaging based on multi-slice radial cine and feature tracking

Chenxi Hu[1], Nripesh Parulji[1], Haiying Lu[1], Xenophon Papademetris[1], James Duncan[1], and Dana Peters[1]

[1]Yale University, New Haven, CT, United States

Left atrial (LA) strain is an important marker of left atrial remodeling. Two-dimensional atrial strain has been studied using echocardiography and MRI cine. Here we develop a 3D strain method, using volumetric cine data sets at multiple phases. The volumes were registered and 3D strain maps were generated, demonstrating patterns of regional strain in the LA.

2877

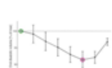

Respiratory variation in left ventricular cardiac function with 3D double-golden-angle whole-heart cine imaging

Karen Holst[1], Martin Ugander[1], and Andreas Sigfridsson[1]

[1]Karolinska Institutet and Karolinska University Hospital, Stockholm, Sweden

Respiratory variation in ventricular volume can potentially provide clinically important information in cardiac diseases involving left ventricular stiffness changes, and can be measured using respiratory resolved imaging. 3D double-golden-angle radial data were acquired during free breathing, and respiratory self-gating signals were extracted from *k*-space. All radial spokes were sorted into 8 respiratory phases and one end-diastolic cardiac phase and left ventricular end-diastolic volume (EDV) was segmented from a short-axis image stack. Respiratory induced changes in EDV were demonstrated and changed 9.0±2.3 % with respect to maximum expiratory EDV.

2878

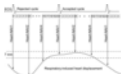

3D-Cine Whole-heart Magnetic Resonance Imaging Using a Novel Prospective Respiratory Self-Gating Technique

Mehdi Hedjazi Moghari[1], Ashita Barthur[1], Matteo Gazzola[1], and Andrew J. Powell[1]

[1]*Cardiology and Pediatrics, Boston Children's Hospital and Harvard Medical School, Boston, MA, United States*

We developed a novel prospective respiratory motion compensation algorithm, Heart-NAV, for free-breathing retrospective electrocardiogram (ECG)-gated 3D-cine steady-state free precession whole-heart magnetic resonance imaging. In 10 patients, there was good agreement between the 3D-cine and conventional breath-hold 2D-cine imaging measurements of ventricular volumes. The mean scan time for the 3D-cine acquisition was 5.9±2.7 minutes. Advantages of the Heart-NAV approach include real-time motion correction allowing for immediate in-line image reconstruction, compatibility with a variety of k-space filling approaches, and utilization of standard scanner hardware/software. Such a 3D-cine approach eliminates the need for breath-holding and simplifies planning for ventricular function assessment.

2879

3D Stack-of-Stars Cardiac Cine MRI: Free-Breathing vs. Respiratory Gated Reconstruction

Jan Paul[1], Yangyang Qu[1,2], and Volker Rasche[1]

[1]*Internal Medicine II, University Hospital of Ulm, Ulm, Germany,* [2]*Department of Cardiology, Zhongda Hospital, Medical School of Southeast University, Nanjing, People's Republic of China*

3D cardiac cine MRI provides consistent data for complete LV analysis in a single scan. As this acquisition is too long for a breathhold, respiratory gating is typically applied.

The aim of this study is to investigate whether respiratory gating is also required for 3D cardiac cine MRI when using a Stack-of-Stars acquisition.

Ungated and Self-Gated reconstructions are compared visually and for LV function parameters.

As no motion artifacts are apparent even in the ungated cine data, and LV function results are comparable to the gated images, ungated reconstruction seems to be feasible for LV analysis.

2880

Improvements in Cardiac MR Elastography Using Reduced FOV Techniques

Yi Sui[1], Arvin Forghanian-Arani[1], Joshua D. Trzasko[1], Shiv Poigai Arunachalam[1], Kevin J. Glaser[1], David S. Lake[1], Kiaran P. McGee[1], Armando Manduca[1], Phillip J. Rossman[1], Richard L. Ehman[1], and Philip A. Araoz[1]

[1]*Radiology, Mayo Clinic, Rochester, MN, United States*

Single-shot spin-echo EPI (SS-SE-EPI) has been utilized for cardiac MR Elastography (cMRE) due to its fast imaging speed and insensitivity to cardiac motion. However, the long echo train in SS-EPI makes it vulnerable to image distortion, which can be prominent in cMRE due to the large susceptibility gradient present at the heart-lung interface. In this study, a reduced phase FOV (rFOV) technique combined with a 2D selective excitation has been implemented in the cMRE. And the results showed that the MRE image quality was improved with reduced image distortions and higher SNR.

2881

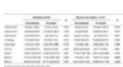

Application of optimized TPAT technique in evaluating arrythmia patients' cardiac function

Hui Chen[1], Xiaohai Ma[1], Lei Zhao[1], Xiaoyong Zhang[2], Guoxi Xie[2], Tianjing Zhang[3], and Zhanming Fan[1]

[1]*Beijing Anzhen Hospital, Beijing, People's Republic of China,* [2]*Shenzhen Institutes of Advanced Technology, Chinese Academy of Sciences, People's Republic of China,* [3]*MR Collaborations NE Asia, Siemens Healthcare, Beijing, China*

Traditional CMR sequences are useful tools for assessing cardiac structure and function, However, the poor image quality and motion artifacts caused by arrhythmia may hamper the diagnostic quality of CMR images. We hypothesized that the optimized temporal parallel acquisition technique (TPAT) may improve this situation by allowing free-breathing of subjects and meanwhile provides a similar diagnostic values for radiologists .

2882

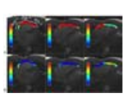

Cardiovascular Magnetic Resonance (CMR) imaging quantification of right and left ventricular strain in repaired Tetralogy of Fallot: Preliminary results in 10 patients and 10 normal volunteers

Donald Benson[1], Mark L. Schiebler[1], Zach Borden[1], and Christopher J Francois[1]

[1]*Department of Radiology, University of Wisconsin-Madison, Madison, WI, United States*

Patients with repaired Tetralogy of Fallot (rTOF) have worsening right and left ventricular function due to their lack of a functional pulmonary valve and the resulting pulmonary insufficiency. Determining the severity of this dysfunction is important for deciding when interventions like pulmonary valve replacement become necessary. Radial and longitudinal myocardial strain is a functional parameter than can aid in this clinical decision. In this small study, myocardial strain was calculated using tissue tracking software applied to axial cine balanced steady-state free precession (bSSFP) images. Significant differences in RV and LV radial and longitudinal strain were found between patients with rTOF and healthy volunteers.

2883 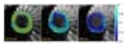

Left Ventricle Circumferential Strain from Radially Tagged Images through CIRCOME combined by SinMod

Fatemeh Rastegar Jouybari[1], Elham Mohammadi[1], and Abbas Nasiraei Moghaddam[1]

[1]Biomedical Engineering, Amirkabir University of Technology (Tehran Polytechnic), Tehran, Iran

Left ventricle function can be evaluated by measuring circumferential strain. CIRcumferential COMpression Encoding (CIRCOME), as a technique for quantification of circumferential strain, needs local frequency and displacement maps during deformation. This study aims to use sine wave modeling approach for estimation of local spatial frequency and displacement maps used in CIRCOME for radially tagged series of images. Circumferential strain computed from proposed method shows expected results in agreement with previous studies.

2884 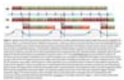

Reducing Specific Energy Deposition in Free Breathing Balanced Steady-State Free Precession (bSSFP) Cine Imaging using Cardio-respiratory Synchronization

Amol Pednekar[1,2], Benjamin Cheong[3], Janie Swaab[4], Melissa Andrews[3], Debra Dees[3], and Raja Muthupillai[2]

[1]Philips Healthcare, Houston, TX, United States, [2]Baylor St. Luke's Medical Center, Houston, TX, United States, [3]Diagnostic and Interventional Radiology, Baylor St. Luke's Medical Center, Houston, TX, United States, [4]Department of Diagnostic and Therapeutic Radiology, Baylor St. Luke's Medical Center, Houston, TX, United States

Free breathing cine bSSFP sequences with minimal compromises in spatio-temporal resolution requirements are highly desirable in patients who can not hold their breath, e.g., sedated patients, patients with poor cardiopulmonary reserve, patients with arrhythmia etc. The results from this prospective clinical study of 14 clinical patients shows that a cardiorespiratory synchronized (CS) sequence can reduce specific energy deposition (0.68 ± 0.24 kJ/kg) by 40% compared to a respiratory gated (RG) sequence (1.2 ± 0.36 kJ/kg) without compromising spatial, temporal, and contrast resolution thus permitting the prescription of bSSFP cine sequences with higher spatial or temporal resolution, and coverage.

2885 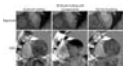

A Comparison Study between the 2D Breath-holding and 3D Free-breathing approaches to in vivo Cardiac Quantitative Susceptibility Mapping

Yan Wen[1,2], Thanh Nguyen[2], Pascal Spincemaille[2], Jiwon Kim[3], Jonathan W. Weinsaft[4], and Yi Wang[1,2]

[1]Meinig School of Biomedical Engineering, Cornell University, New York, NY, United States, [2]Radiology, Weill Cornell Medicine, New York, NY, United States, [3]Medicine, Weill Cornell Medicine, NY, United States, [4]Medicine, Weill Cornell Medicine

Our previous study showed that high quality in vivo cardiac susceptibility maps (QSM) can be obtain using a 2D breath-hold (2DBH) sequence. However, the 2DBH approach is vulnerable to slice misregistration caused by inconsistent breath-holds, which will cause artifacts in the resulting susceptibility maps. Here we introduce a 3D navigator gated sequence (3DNAV) which allows for free-breathing during acquisition, and compare it to the 2DBH approach.

2886 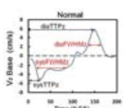

Quantification of Left Ventricular Dyssynchrony and Action Time in Patients with Fabry Disease by Magnetic Resonance Tissue Phase Mapping

Bo-Yan Chuang[1], Ming-Ting Wu[2], Marius Menza[3], Mao-Yuan Su[4], and Hsu-Hsia Peng[1]

[1]Department of Biomedical Engineering and Environmental Sciences, National Tsing Hua University, Hsinchu, Taiwan, [2]Department of Radiology, Kaohsiung Veterans General Hospital, Kaohsiung, Taiwan, [3]Medical Physics, University Hospital Freiburg, Freiburg, Germany, [4]Department of Medical Imaging, National Taiwan University Hospital, Taipei, Taiwan

Recent studies showed that LV dyssynchrony and deceleration time can be recognized as an important predictor of poor outcome in patients. However, the regional myocardial function investigated by MRI is less discussed. In this study, we applied MR tissue phase mapping (TPM) and aim to investigate the myocardial dyssynchrony and action time in LV for Fabry disease (FD). We observed increased longitudinal dyssynchrony and lower systolic action time in FD group. In conclusion, the quantification of LV myocardial dyssynchrony and action time may provide useful information to comprehend the impaired cardiac manifestation and diastolic dysfunction in patients with FD.

2887 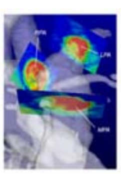

Interaction of Pulmonary Regurgitation Flow and Myocardial Motion Velocity in Patients with Repaired Tetralogy of Fallot

Chin-Wei Liu[1], Ming-Ting Wu[2], Mao-Yuan Su[3], and Hsu-Hsia Peng[1]

[1]Department of Biomedical Engineering and Environmental Sciences, National Tsing Hua University, Hsinchu, Taiwan, [2]Department of Radiology Kaohsiung, Kaohsiung Veterans General Hospital, [3]Department of Medical Imaging Taipei, National Taiwan University Hospital

In this study, we measured pulmonary regurgitation fraction and three-directional myocardial wall motion velocities to establish indices for characterizing cardiac function in patients with repaired tetralogy of Fallot (rTOF). We aim to reveal the interaction of pulmonary regurgitation fraction and myocardial motion velocity and thereby to speculate the myocardial damage in rTOF patients. In conclusion, the pulmonary RF displayed negative correlation with Vz and positive correlation with Vr in the right ventricle of rTOF patients. The analyses of pulmonary flow and myocardial motion velocity can help to comprehend the interaction between pulmonary regurgitation flow and impaired myocardium in rTOF patients.

Traditional Poster

Cancer Diffusion, Perfusion & Other

Exhibition Hall 2888-2910 Thursday 13:00 - 15:00

2888

The Uesfulness of Intravoxel Incoherent Motion Diffusion-weighted Imaging for Predicting the Prognosis of Patients with Acute Myeloid Leukemia

JinLiang Niu[1], HongWei Wang, and XiaoLi Song[2]

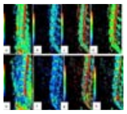

[1]Second Hospital of Shanxi Medical Hospital, Taiyuan, People's Republic of China, [2]Radiology, Second Hospital of Shanxi Medical University, Taiyuan, People's Republic of China

Intravoxel Incoherent Motion (IVIM) is capable of providing both diffusion and perfusion quantification using a single imaging study at the same time, without the need for intravenous contrast injection. acute myeloid leukemia (AML) patients with complete remission and non-complete remission could exhibit different characterizations before treatment in perfusion and tissue cellularity of the lumbar bone marrow. This study was to investigate the usefulness of IVIM parameters in evaluation of prognosis in AML patients.

2889

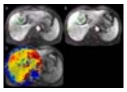

Repeatability of perfusion parameters in free-breathing dynamic contrast-enhanced MRI of malignant hepatic tumors

Bohyun Kim[1], Kyung Won Kim[2], Chang Kyung Lee[3], Nieun Seo[4], Seung Soo Lee[2], and Jeong Kon Kim[2]

[1]Ajou University Hospital, Ajou University School of Medicine, Suwon, Korea, Republic of, [2]Asan Medical Center, Ulsan University College of Medicine, Seoul, Korea, Republic of, [3]Bioimaging Center, Asan Institute for Life Sciences, Asan Medical Center, Seoul, Korea, Republic of, [4]Severance Hospital, Yonsei University College of Medicine, Seoul, Korea, Republic of

In dynamic contrast-enhanced (DCE)-MRI, establishing a high level of repeatability is essential to ensure reliability of changes in perfusion parameters over longitudinal studies in an individual subject. To assess the repeatabilities of perfusion parameters and identify the effect of T1 map on them, we performed two sequential free-breathing DCE-MRI studies in patients with solid hepatic malignancies. Our results showed that K_{ep} had the highest repeatability, and the repeatabilities of all perfusion parameters were boosted when fixed T1 value (800 ms) was used instead of values obtained from T1 mapping.

2890

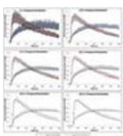

Quantitative evaluation of the effect of temporal resolution and acquisition duration on the accuracy of DCE-MRI measurements in a prostate phantom

Silvin P. Knight[1], Jacinta E. Browne[2], James F. Meaney[1], and Andrew J. Fagan[1]

[1]School of Medicine / National Centre for Advanced Medical Imaging (CAMI), Trinity College University of Dublin / St James's Hospital, Dublin 8, Ireland, [2]School of Physics & Medical Ultrasound Physics and Technology Group, Centre of Industrial Engineering Optics, FOCAS, Dublin Institute of Technology, Dublin 8, Ireland

A novel anthropomorphic prostate phantom test device was used to investigate the effects of temporal resolution (T_{res}) and acquisition duration (AD) on the accuracy of contrast time-intensity curves measured using dynamic contrast-enhanced MRI. When quantitatively compared to ground truth values, large errors in derived pharmacokinetic (PK) parameters (up to 230%) were found for T_{res} values > 8.1 s and AD values < 360 s. The data demonstrate the critical and sensitive dependence of the accuracy of measured PK output parameter values on the acquisition protocol used, while such phantom studies can help identify optimal acquisition parameters for DCE-MRI scans

---

2891

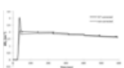

Improved sensitivity for rectal cancer differentiation by T2*-correction in DCE-MRI

Endre Grøvik[1], Kathrine Røe Redalen[2], Tryggve Holck Storås[1], Anne Negård[3], Stein Harald Holmedal[3], Anne Hansen Ree[3], Sebastian Meltzer[3], Atle Bjørnerud[1], and Kjell-Inge Gjesdal[4]

[1]Oslo University Hospital, Oslo, Norway, [2]Akershus University Hospital, Norway, [3]Akershus University Hospital, Lørenskog, Norway, [4]Sunnmøre MR-klinikk, Ålesund, Norway

Quantitative pharmacokinetic analysis from DCE-MRI often neglects CA-induced T2*-effect when converting signal intensity (SI) changes in tissue to CA concentration. The acquired signal may thus be significantly affected by T2* signal attenuation, which in turn results in errors in the DCE-derived parameters. This work utilized a dynamic multi-echo acquisition for extrapolation back to TE=0, thus providing both T2*-corrected and uncorrected measurements of DR1, and investigates the how the correction for T2*-attenuation effects may affect the sensitivity for rectal cancer differentiation by DCE-MRI. The T2*-corrected data showed improved differentiation of rectal cancer.

2892

Enhancement of Lesion Detection through Feature Projection and Classification of Perfusion Parameters

Ramin Jafari[1], Yi Wang[1], Martin R. Prince[2], and Pascal Spincemaille[2]

[1]Cornell University, Ithaca, NY, United States, [2]Weill Cornell Medicine, New York, NY, United States

Perfusion analysis is a powerful tool to quantitatively characterize lesions. This can further be extended to differentiate lesions through comparison perfusion parameters. Typically there is overlap in perfusion parameters which makes it difficult to distinguish lesions. We demonstrate perfusion analysis combined with feature projection and classification enhances lesion detection by increasing separability and extracting features of the lesions simultaneously which can be used in automation of lesion detection.

2893

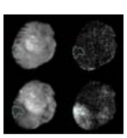

Quantitative Ultra-short Time-to-Echo Contrast-Enhanced Magnetic Resonance Imaging (qUTE-CE MRI) technique use Ferumoxytol as a Positive-Contrast Agent to Delineate Nanoparticle Accumulation in Tumors

Ju Qiao[1], Codi Gharagouzloo[2,3], Liam Timms[4,5], Paraveen Kulkarni[6], Craig Ferris[6], Srinivas Sridhar[4,5], and Anne L van de Ven[4,5]

[1]Mechanical and Industrial Engineering, Northeastern University, BOSTON, MA, United States, [2]Radiology, Massachusetts General Hospital, [3]Radiology, Harvard Medical School, [4]Physics, Northeastern University, Boston, MA, United States, [5]Nanomedicine Science & Technology Center, Northeastern University, Boston, MA, United States, [6]Psychology, Northeastern University, Boston, MA, United States

Here we demonstrate quantitative ultra-short time-to-echo contrast-enhanced magnetic resonance imaging (qUTE-CE MRI) technique, which employs FDA-approved ferumoxytol as a positive-contrast agent to delineate nanoparticle accumulation in tumors.

2894

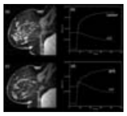

Evaluation of DCE-MRI Exam with High-Temporal Resolution for Breast Cancer Diagnosis in a Biopsy Cohort

Oliver Stewart[1], Laura Heacock[1], Linda Moy[1], and Sungheon Gene Kim[1]

[1]Center for Advanced Imaging Innovation and Research, Radiology, New York University School of Medicine, New York, NY, United States

The purpose of this study was to assess the feasibility of using GRASP DCE-MRI for contrast kinetic analysis to determine lesion malignancy. This IRB-approved retrospective study included 73 women who underwent MRI-guided biopsy scans. The plasma flow in the malignant group was significantly higher than that of the benign group with the area under the curve of 0.77. The results in this study successfully demonstrate that the GRASP DCE-MRI method can be used to acquire adequate high-temporal and high-spatial resolution images of the breast for contrast kinetic analysis.

2895

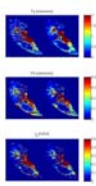

Dynamic Contrast-Enhanced MRI Using Spatial Prior Knowledge

Radovan Jiřík[1], Michal Bartoš[2], Karel Souček[3,4,5], Eva Dražanová[1], Lucie Krátká[1], Lenka Dvořáková[1], Torfinn Taxt[6], and Zenon Starčuk, jr.[1]

[1]Institute of Scientific Instruments of the CAS, Brno, Czech Republic, [2]Institute of Information Theory and Automation of the CAS, Praha, Czech Republic, [3]Department of Cytokinetics, Institute of Biophysics of the CAS, Brno, Czech Republic, [4]Center of Biomolecular and Cellular Engineering, International Clinical Research Center, Brno, St. Anne's University Hospital Brno, Brno, Czech Republic, [5]Department of Experimental Biology, Faculty of Science, Masaryk University, Brno, Czech Republic, [6]Department of Biomedicine, University of Bergen, Bergen, Norway

A method to improve reliability of DCE-MRI is presented. It is based on the assumption that neighboring voxels have similar physiological properties. It is formulated as a total variation regularization of the perfusion parameter maps. The method is applied to the adiabatic approximation of the tissue homogeneity model (ATH). Evaluation was done on data of five tumor bearing mice recorded using two contrast agents with different molecular weights. The resulting perfusion parameter maps were more spatially consistent with preserved edges.

2896

Are radiation-induced perfusion changes in normal appearing brain tissue a confounding factor in tumour response evaluation with DSC-MRI?

Markus Fahlström[1], Tufve Nyholm[2], and Elna-Marie Larsson[1]

[1]Surgical Sciences, Uppsala University, Uppsala, Sweden, [2]Biomedical Technology, Medical Physics and IT, Uppsala University Hospital, Uppsala, Sweden

Radiation-induced brain perfusion changes after radiotherapy have not been studied extensively with DSC-MRI. Tumour perfusion is often normalised to contralateral normal-appearing white matter, why knowledge about radiation effects on perfusion in normal brain tissue is essential. Ten patients were examined with DSC-MRI at 1.5 T before and repeatedly after RT. Multiple volumes were drawn in normal brain tissue. Radiation dose for all volumes were available. Significant CBV and CBF decrease after radiotherapy was visible in grey matter volumes and showed tendency to recover. High radiation dose regions should be avoided when normalising DSC-MRI derived tumour perfusion values.

2897

A population-based digital reference object (DRO) for optimizing dynamic susceptibility contrast (DSC) MRI methods for clinical trials

Natenael B Semmineh[1], Ashley M Stokes[1], Laura C Bell[1], Jerrold L Boxerman[2], and C Chad Quarles[1]

[1]Translational Bioimaging, Barrow Neurological Institute, Phoenix, AZ, United States, [2]Diagnostic Imaging, Rhode Island Hospital, Providence, RI, United States

The standardization of DSC-MRI has been confounded by a lack of consensus on DSC-MRI methodology for preventing potential rCBV inaccuracies, including the choice of acquisition protocols and post-processing algorithms. To address these issues, we developed a digital reference object (DRO) aimed at validating image acquisition and analysis methods for accurately measuring rCBV in glioblastomas. The DRO was developed using trained physiological and kinetic parameters derived from in vivo data, unique voxel-wise 3D tissue structures, and a validated MRI signal computational approach. The DRO's ability to produce reliable signals was validated by comparison to separate cohort of patient data.

2898

Probing infiltration of the normal brain by glioblastoma using magnetic resonance perfusion and permeability techniques

Antoine Vallatos[1], Joanna Birch[2], Lindsay Gallagher[1], Haitham F. I. Al-Mubarak[1], Lesley Gilmour[2], Anthony J. Chalmers[2], and William M. Holmes[1]

[1]Glasgow Experimental MRI Centre, Institute of Neuroscience and Psychology, University of Glasgow, Glasgow, United Kingdom, [2]Translational Radiation Biology, Institute of Cancer Sciences, University of Glasgow, Glasgow, United Kingdom

MRI techniques probing brain perfusion and blood-brain barrier (BBB) permeability were assessed in their ability to detect low tumour invasion in mouse glioblastoma models. A multiple boli Arterial Spin Labeling technique was optimised, achieving high SNR perfusion imaging. Diffusion-weighted arterial spin labelling allowed to separate fast motion vascular components of the signal from slow motion tissue components, providing with BBB permeability weighted maps. Evaluation was performed by comparison with conventional MRI and immunohistochemistry sections (HLA) cut in the MRI plane . Both perfusion weighted maps and BBB permeability weighted maps allowed to identify low tumour regions not detected with conventional MRI techniques.

2899

Application of Monoexponential, biexponential and stretched exponential Diffusion-weighted MR Imaging for Differentiating between Minimal Fat Angiomyolipoma (MFAML) and Papillary Renal Cell Carcinoma (PRCC).

Haojie Li[1], Yao Hu[1], Daoyu Hu[1], and Zhen Li[1]

[1]Radiology, Tongji Hospital, Tongji Medical College, Huazhong University of Science and Technology, Wu Han, People's Republic of China

Accurate preoperative differentiation between MFAML and PRCC is important to determine appropriate treatment strategies.In this study, the preliminary date from our study show that different models of DWI may demonstrate various aspects of tissue properties.fp and α may provide additional information and could lead to improved differentiation with better sensitivity and specificity between MFAML and PRCC compared with conventional imaging parameters.

2900

DDC and α estimates from the stretched exponential model are more robust to variations in b-value selection than ADC estimates, in a cohort of 42 cervical tumours

Jessica M Winfield[1,2], Nandita M deSouza[1,2], Veronica A Morgan[1,2], David J Collins[1,2], and Matthew R Orton[1,2]

[1]*Cancer Research UK Cancer Imaging Centre, The Institute of Cancer Research, London, United Kingdom,* [2]*MRI Unit, The Royal Marsden NHS Foundation Trust, Sutton, United Kingdom*

The influence of b-value selection on fitted parameters from the stretched exponential model (distributed diffusion coefficient DDC, and ‘stretching parameter’ α) and mono-exponential model (apparent diffusion coefficient ADC) was investigated in a cohort of 42 patients with cervical tumours. Diffusion-weighted images images were acquired using 9 b-values between 0 and 800smm^{-2}, and fitted voxel-by-voxel using all b-values (0 to 800smm^{-2}) and b-values n-to-800smm^{-2} (where n is 20,40,60,80,100, or 300smm^{-2}). ADC estimates are highly sensitive to b-value selection, with reduction in ADC when low b-values are excluded, whereas DDC and α are more robust to differences in b-value selection.

2901

Combined analysis of ten DW-MRI studies demonstrates excellent repeatability of apparent diffusion coefficient estimates in extra-cranial soft-tissue tumours

Jessica M Winfield[1,2], Nina Tunariu[1,2], Mihaela Rata[1,2], Keiko Miyazaki[1,2], Neil P Jerome[1,2], Michael Germuska[1,2,3], Matthew D Blackledge[1,2], David J Collins[1,2], Johann S de Bono[4,5], Timothy A Yap[4,5], Nandita M deSouza[1,2], Simon J Doran[1,2], Dow-Mu Koh[1,2], Martin O Leach[1,2], Christina Messiou[1,2], and Matthew R Orton[1,2]

[1]*Cancer Research UK Cancer Imaging Centre, The Institute of Cancer Research, London, United Kingdom,* [2]*MRI Unit, The Royal Marsden NHS Foundation Trust, Sutton, United Kingdom,* [3]*Cardiff University Brain Research Imaging Centre (CUBRIC), School of Psychology, Cardiff University, Cardiff, United Kingdom,* [4]*Drug Development Unit, The Royal Marsden NHS Foundation Trust, Sutton, United Kingdom,* [5]*Division of Clinical Studies, The Institute of Cancer Research, London, United Kingdom*

Repeatability of ADC estimates from ten diffusion-weighted MRI studies in extra-cranial soft tissues (nine patient studies and one healthy volunteer study, with a total of 111 subjects) were analysed in combination using the Radiological Society of North America (RSNA) Quantitative Imaging Biomarkers Alliance (QIBA) framework for assessment of technical performance of imaging biomarkers, in order to investigate factors affecting ADC repeatability. Coefficient of variation was between 2 and 7% for all studies, with no marked differences between imaging protocols or study populations, and better repeatability in large tumours compared with smaller tumours, indicating that ADC is a robust imaging metric with excellent repeatability in extra-cranial soft-tissue tumours.

2902

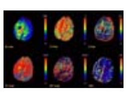

Correlation of Intra-Voxel incoherent motion (IVIM) imaging and Dynamic Susceptibility Contrast (DSC) MRI for high and low grade gliomas

Arush Honnedevasthana Arun[1], Neesha Nagaraj[1], Nithin N Vajuvalli[1], Jitender Saini[2], and Sairam Geethanath[1]

[1]*Dayananda Sagar Institutions, Bangalore, India,* [2]*National Institute of Mental Health, Bangalore, India*

The aim of this study was to validate the feasibility of Intravoxel Incoherent Motion (IVIM) imaging of human brain gliomas; and to differentiate between high grade and low grade gliomas using IVIM parameters (*f, d, D, fD**). These parameters were then compared to CBV maps obtained through DSC-MRI to evaluate the role of non-contrast agent based perfusion imaging. Results obtained showed that IVIM perfusion fraction *f* could be used to differentiate between high and low-grade brain gliomas

---

2903

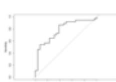

Differential diagnosis of Ocular adnexal lymphoma and idiopathic orbital inflammation：radiomics imaging features and their predictive performance

Guo Jian[1], Xian Junfang[2], Shen Chen[3], Liu Zhenyu[4], and Tian Jie[4]

[1]*Affiliated Tongren Hospital，Capital Medical University, Beijing, People's Republic of China,* [2]*Affiliated Tongren Hospital，Capital Medical University,* [3]*Key Laboratory of Molecular Imaging,Chinese Academy of Sciences, People's Republic of China,* [4]*Key Laboratory of Molecular Imaging,Chinese Academy of Sciences*

Differential diagnosis of Ocular adnexal lymphoma (OAL) and idiopathic orbital inflammation (IOI) is very important due to their quite different therapeutic modalities and prognosis. However, it is not easy for both ophthalmologists and pathologists. Can the emerging radiomics enhance the diagnostic efficiency? This research devoted evidence for this question.

2904

Prognostic Characterization of Prostate Cancer from Benign Tissue MRS

Leo L. Cheng[1], Emily A. Decelle[2], Johannes L Kurth[2], Shulin Wu[3], Taylor L. Fuss[2], Lindsey A. Vandergrift[2], Elita M. DeFeo[2], Elkan F. Halpern[2], Matthias L Taupitz[2], W. Scott McDougal[2], Aria F. Olumi[2], and Chin-Lee Wu[2]

[1]*Molecular Pathology, Massachusetts General Hospital, Charlestown, MA, United States,* [2]*Massachusetts General Hospital, Charlestown, MA, United States,* [3]*Massachusetts General Hospital, Boston, MA, United States*

While serum prostate specific antigen (PSA) testing improved early detection of prostate tumors, implementation of this tool also created a large patient population in which identified cancer lesions were actually indolent. For patients who choose to undergo prostatectomy, cancer aggressiveness can only be determined by post-procedure pathology analysis of cancerous tissue. Additionally, cancer recurrence predictions are often unreliable. As an alternative method to aid decisions regarding treatment, we sought to develop MRS tools which can predict cancer aggressiveness based on the novel use of histologically benign (Hb) tissue.

2905

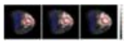

Texture Analysis on Diffusion Weighted MRI in Osteosarcoma

Esha Baidya Kayal[1], Devasenathipathy K[2], Sameer Bakhshi[3], Raju Sharma[2], and Amit Mehndiratta[1,4]

[1]Center for Biomedical Engineering, Indian Institute of Technology, New Delhi, India, [2]Radiodiagnosis, All India Institute of Medical Sciences, New Delhi, India, [3]Medical Oncology, Dr. B.R.Ambedkar Institute-Rotary Cancer Hospital, All India Institute of Medical Sciences, New Delhi, India, [4]Department of Biomedical Engineering, All India Institute of Medical Sciences, New Delhi, India

Texture analysis (TA) uses mathematical approach to characterize the spatial distribution of signal intensity variations in an image, and extracts quantitative information that are otherwise imperceptible qualitatively. Good soft tissue contrast of MRI facilitates TA to produce promising results in diagnosis and prognosis. Diffusion Weighted (DW) MRI based TA might provide additional useful information as DWI captures early cellular changes in tumors in terms of corresponding intensity variations. We computed textural features in patients with Osteosarcoma. Experimental results revealed that textural features show good discrimination among normal and tumour ROI thus might be useful as diagnostic and prognostic marker.

2906

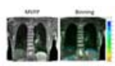

Evaluation of 4D-T2w MRI methods for lung radiotherapy treatment planning with application to an MR-linac

Joshua N Freedman[1,2], David J Collins[1,2], Christopher M Rank[3], Hannah Bainbridge[1], Simeon Nill[1], Marc Kachelrieß[3], Martin O Leach[1,2], Uwe Oelfke[1], and Andreas Wetscherek[1]

[1]Joint Department of Physics, The Institute of Cancer Research and The Royal Marsden NHS Foundation Trust, London, United Kingdom, [2]CR-UK Cancer Imaging Centre, The Institute of Cancer Research, London, United Kingdom, [3]Medical Physics in Radiology, German Cancer Research Center (DKFZ), Heidelberg, Germany

Due to enhanced soft-tissue contrast, 4D-T2w MRI could improve lung tumour target delineation in radiotherapy compared with 4D-CT; reducing planning margins and dose to healthy tissue for treatments on an MR-linac. We have developed a method for generating 4D-T2w MRI, where 3D-T2w MRI is warped using motion vector fields; calculated by image-registration between respiratory phases of 4D-T1w MRI (the MVFP method). Here, 4D-T2w MRI calculated with MVFP and with amplitude-binning of continuously acquired 2D-T2w MRI, are compared. 4D-T2w MRI from the MVFP method exhibited higher image quality and geometrical fidelity than the 2D-binning scheme, but displayed possible motion under-estimation.

2907

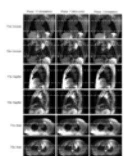

4D-T2 weighted MRI for lung radiotherapy treatment planning

Joshua N Freedman[1,2], David J Collins[1,2], Christopher M Rank[3], Hannah Bainbridge[1], Simeon Nill[1], Marc Kachelrieß[3], Uwe Oelfke[1], Martin O Leach[1,2], and Andreas Wetscherek[1]

[1]Joint Department of Physics, The Institute of Cancer Research and The Royal Marsden NHS Foundation Trust, London, United Kingdom, [2]CR-UK Cancer Imaging Centre, The Institute of Cancer Research, London, United Kingdom, [3]Medical Physics in Radiology, German Cancer Research Center (DKFZ), Heidelberg, Germany

Compared to 4D-CT, 4D-T2w MRI should better characterise respiratory motion in radiotherapy, due to its superior soft tissue contrast. However, 4D-T2w MRI is difficult to acquire due to the long echo and repetition time required. Here, 4D-T2w MRI is obtained by applying motion information from a 4D-T1w volume to a static 3D-T2w volume. For three patients, 4D-T2w MRI was compared to 4D-T1w MRI. Diaphragm positions were consistent to <1.5mm. A method to calculate 4D-T2w MRI, with potential application to an MR-linac, is presented and verified.

2908

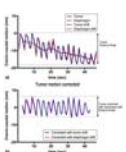

Can diaphragm motion function as a surrogate for motion of esophageal tumors during treatment?

Sophie E. Heethuis[1], Lucas Goense[1,2], Alicia S. Borggreve[1,2], Peter S.N. van Rossum[1,2], Richard van Hillegersberg[2], Jelle P. Ruurda[2], Stella Mook[1], Gert J. Meijer[1], Jan J.W. Lagendijk[1], and Astrid L.H.M.W. van Lier[1]

[1]Department of Radiotherapy, University Medical Center Utrecht, Utrecht, Netherlands, [2]Department of Surgery, University Medical Center Utrecht, Utrecht, Netherlands

Esophageal tumors show large motion in cranio-caudal direction, with a Peak-to-Peak (P-t-P) range of 2.7 to 24.5mm. In case the motion of the tumor could be followed during radiotherapy treatment, this would enable treatment margin reduction. It is researched whether the motion of the diaphragm is correlated with the breathing motion and drift we can detect in esophageal tumors since it could function as surrogate for tumor motion during treatment. A high correlation was found between both motion patterns and correction of the tumor motion using the diaphragm drift resulted on average in a reduction in P-t-P motion in all patients.

2909

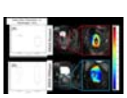

Radiomic features extracted from T2w MRI differentiates KRAS mutational status in rectal cancers: A pilot study

Shanker Raja[1,2], Jacob Antunes[3], Amrish Selvam[3], Anant Madabhushi[3], Sharad George[1], Mazen Alsagri[4], Adnan Hussain[2], Abdullah AlDosary[2], Musa A Fageeh[2], Mohammed AlHarbi[2], and Satish E Viswanath[3]

[1]Radiology, Baylor College of Medicine, Houston, TX, United States, [2]KFMC - Riyadh, Saudi Arabia, [3]Biomedical Engineering, Case Western Reserve University, [4]KFSH - Qassim

Contemporary management of rectal cancer includes consideration of adjuvant anti EGFR therapy; however, KRAS mutational status profiling is mandatory prior to initiation of this therapy. KRAS mutational status is typically assayed on tissue samples (biopsy/surgical specimens). Radiomic features have demonstrated the ability to quantitatively characterize image phenotypic appearance associated with genotype expression in different tumors. We explored the utility of multi-scale, multi-oriented filter banks to define radiomics signatures that distinguish KRAS mutated vs wildtype tumors on T2W MRI. Initial results indicate that macro-scale radiomic features depict significantly different responses between the 2 genotypic groups.

2910

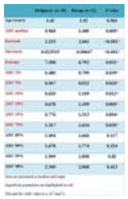

The role of ADC histogram analysis in discriminating between benign and malignant tumours in children

Karen Angela Manias[1,2], Niloufar Zarinabad[1], Emma Meeus[1], Katharine Foster[3], Paul Davies[1], Jan Novak[1], and Andrew Charles Peet[1,2]

[1]Institute of Cancer and Genomic Sciences, University of Birmingham, Birmingham, United Kingdom, [2]Department of Paediatric Oncology, Birmingham Children's Hospital, Birmingham, United Kingdom, [3]Department of Paediatric Radiology, Birmingham Children's Hospital, Birmingham, United Kingdom

We evaluated histogram analysis of ADC maps to differentiate benign from malignant solid paediatric tumours in children and distinguish tumour type. Fifty children (38 malignant, 12 benign tumours) were imaged using multi-b value diffusion-weighted MRI at diagnosis. Whole tumour regions-of-interest (ROIs) were drawn, ADC histograms constructed, and median, 2nd to 98th percentile ADC values, skewness, kurtosis and entropy calculated. ADC histogram parameters were significantly different between malignant and benign lesions, with skewness and kurtosis being the most predictive of malignancy.

Traditional Poster

Cancer Treatment Response & Preclinical

Exhibition Hall 2911-2930 Thursday 13:00 - 15:00

2911

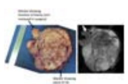

ADC and D from diffusion-weighted MRI correlate with histopathological assessment of nuclear-to-stromal ratio, and histology confirms Dixon fat fraction in retroperitoneal sarcomas

Jessica M Winfield[1,2], Khin Thway[3], Aisha Miah[4], Dirk Strauss[5], David J Collins[1,2], Martin O Leach[1,2], Nandita M deSouza[1,2], Sharon L Giles[1,2], and Christina Messiou[1,2]

[1]Cancer Research UK Cancer Imaging Centre, The Institute of Cancer Research, London, United Kingdom, [2]MRI Unit, The Royal Marsden NHS Foundation Trust, Sutton, United Kingdom, [3]Department of Histopathology, The Royal Marsden NHS Foundation Trust, London, United Kingdom, [4]Department of Radiotherapy, The Royal Marsden NHS Foundation Trust, London, United Kingdom, [5]Department of Surgery, The Royal Marsden NHS Foundation Trust, London, United Kingdom

Soft-tissue sarcomas are often highly heterogeneous tumours. Clinical trials of non-surgical treatments, for example combined radiotherapy and systemic agents, require non-invasive methods for response assessment. Quantitative MRI provides non-invasive response assessment of the whole tumour volume, but metrics require validation against histopathology. In this study, 26 patients with retroperitoneal sarcoma were imaged prior to surgery, with written consent, as part of a prospective single-centre study. Diffusion-weighted MRI parameters (ADC, and D from IVIM) showed correlation with nuclear-to-stromal ratio, and were also related to stroma type and stroma grade. Dixon-derived fat fraction correlated strongly with histopathological assessment of fat fraction.

2912

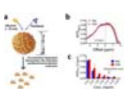

Label-free CEST MRI detection of albumin and albumin-based nanoparticles

Yuguo Li[1,2], Dexiang Liu[3], Jiadi Xu[1,2], Peter C.M. van Zijl[1,2], Shibin Zhou[4], and Guanshu Liu[1,2]

[1]F.M. Kirby Research Center for Functional Brain Imaging, Kennedy Krieger Institute, Baltimore, MD, United States, [2]Department of Radiology, Johns Hopkins University School of Medicine, Baltimore, MD, United States, [3]Department of Radiology, Guangzhou Panyu Central Hospital, [4]Ludwig Center, Howard Hughes Medical Institute and Sidney Kimmel Cancer Center, Johns Hopkins University School of Medicine, Baltimore, MD, United States

Albumin is emerging as one of the most attractive drug carriers for the targeted delivery of therapeutic peptides and drugs. Herein, we developed a label-free MRI approach for monitoring albumin-based drug delivery systems by directly utilizing the inherent CEST signal of albumin. Our in vitro study showed that both human serum albumin (HSA) and albumin-based nanoparticle Nab-paclitaxel (Abraxane) could generate a strong CEST signal at ~2 ppm. Using this inherent CEST signal, we successfully demonstrated the label-free CEST MRI detection of the tumor uptake and distribution HSA and Nab-paclitaxel in a xenograft mouse model.

2913

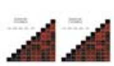

Quantitative ADC as an early imaging biomarker of response to chemoradiation in esophageal cancer

Benjamin Musall[1], Jingfei Ma[1], Brett Carter[1], Penny Fang[1], Amy Moreno[1], Jong Bum Son[1], Brian Hobbs[1], Bryan Fellman[1], and Steven Lin[1]

[1]The University of Texas MD Anderson Cancer Center, Houston, TX, United States

The goal of the study was to investigate if quantitative ADC can be used as an early imaging biomarker for predicting the treatment response to chemoradiation in esophageal cancer. Using pathological findings as the gold standard, our study demonstrated that the change in quantitative ADC from baseline (before treatment) to interim (two weeks after the initiation of treatment) was highly predictive of whether patients had residual tumors at the end of their treatment.

2914

Non-gaussian IVIM imaging biomarkers can non-invasively predict the aggressiveness of small papillary thyroid cancers

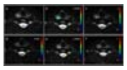

David Aramburu Nuñez[1], Yonggang Lu[2], Vaios Hatzoglou[3], Andre L Moreira[4], Hilda E Stambuk[3], Ramesh Paudyal[1], Yousef Mazaheri[3], Mithat Gonen[5], Joseph O Deasy[1], Ronald A Ghossein[6], Ashok R Shaha[7], Michael Tuttle[8], and Amita Shukla-Dave[1,3]

[1]Medical Physics, Memorial Sloan-Kettering Cancer Center, NEW YORK, NY, United States, [2]Radiation Oncology, Washington University in St. Louis, St. Louis, MO, United States, [3]Radiology, Memorial Sloan-Kettering Cancer Center, NEW YORK, NY, United States, [4]Pathology, NYU Langone Medical Center, NEW YORK, NY, United States, [5]Epidemiology and Biostatistics, Memorial Sloan-Kettering Cancer Center, NEW YORK, NY, United States, [6]Pathology, Memorial Sloan-Kettering Cancer Center, NEW YORK, NY, United States, [7]Surgery, Memorial Sloan-Kettering Cancer Center, NEW YORK, NY, United States, [8]Medicine, Memorial Sloan-Kettering Cancer Center, NEW YORK, NY, United States

There is a need for non-invasive imaging to identify patients with aggressive tumors in papillary thyroid carcinoma (PTC). This study evaluates whether non-gaussian intravoxel incoherent motion (NG-IVIM) DW-MRI has the potential to stratify tumor aggressiveness in PTC. Twenty-four PTC patients underwent pretreatment NG-IVIM DW-MRI at 3T. The apparent diffusion coefficient (ADC), perfusion factor (f), diffusion (D), pseudo diffusion (D*) and diffusion Kurtosis (K) coefficients were calculated from the NG-IVIM model. All patients underwent surgery. Tumor aggressiveness was defined at pathology. ADC and D may be used to distinguish tumors with and without aggressive features in tumor size between 1-2 cm.

2915

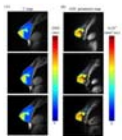

Reproducibility of Quantitative DW-MRI and DCE-MRI of the Breast in the Community Setting: Preliminary Results

Anna G. Sorace[1], Jack Virostko[1], Stephanie L. Barnes[2,3], Jeffrey Luci[4], Debra Patt[5], Boone Goodgame[1,6], Sarah Avery[7], and Thomas E. Yankeelov[1,2,3]

[1]Internal Medicine, University of Texas at Austin, Austin, TX, United States, [2]Biomedical Engineering, University of Texas at Austin, Austin, TX, United States, [3]Institute for Computational Engineering and Sciences, University of Texas at Austin, Austin, TX, United States, [4]Neuroscience, University of Texas at Austin, Austin, TX, United States, [5]US Oncology Network, Austin, TX, United States, [6]Seton Medical Center, Austin, TX, United States, [7]Austin Radiological Association, Austin, TX, United States

Implementation of quantitative DCE-MRI and DW-MRI in the community setting has the potential to impact patient care for a large number of breast cancer patients. Quantitative DW-MRI and DCE-MRI was assessed in phantoms and normal subjects across three sites. In normal subject fibroglandular tissue, the average percent difference in ADC across sites for all subjects was 1.8%, while the average percent difference in the inversion recovery scan and B_1- corrected T_1 map were 14% and 7.3%, respectively. Overall, the results from the phantom and normal subject scans reveal that quantitative MRI can be successfully implemented in the community setting.

2916

Ultra-early ADC (apparent diffusion coefficient) footprint successfully detects tumor irradiation and predicts radiotherapy outcome

Faisal Mahmood[1], Helle Hjorth Johannesen[2], Poul Geertsen[1], and Rasmus Hvass Hansen[2]

[1]Radiotherapy Research Unit, Department of Oncology, University of Copenhagen, Herlev and Gentofte Hospital, Herlev, Denmark, [2]Department of Radiology, University of Copenhagen, Herlev and Gentofte Hospital, Herlev, Denmark

If ultra-early stratification of radiotherapy response was possible it could potentially reduce unnecessary irradiation of normal tissue and improve disease management. In this study repeated diffusion weighted magnetic resonance imaging was conducted along with fractionated radiotherapy in brain metastases patients. It was found that the decrease in the apparent diffusion coefficient (ADC) observed 24 hours after the first radiotherapy fraction may be an indicator of irradiation. Responding patients versus non-responding patients could be differentiated by their corresponding change in ADC seen 48 hours after start of radiotherapy. These findings may have great impact for the emerging hybrid MR – linear-accelerator systems.

2917

Providing improved reliability of plasma volume fraction estimates for monitoring anti-angiogenic effects in liver metastases with DCE-MRI

Mihaela Rata[1], Khurum Khan[1], David Collins[1], Nina Tunariu[1], Dow-Mu Koh[1], James d'Arcy[1], Maria Bali[1], Ian Chau[1], Nicola Valeri[1], David Cunningham[1], Martin O Leach[1], and Matthew Orton[1]

[1]CR-UK Cancer Imaging Centre, The Institute of Cancer Research and Royal Marsden Hospital, London, United Kingdom

Pharmacokinetic modelling of DCE-MRI data allows characterisation of tumour response to anti-angiogenic therapies by estimating the volume transfer constant K^{trans} and the plasma volume fraction Vp. This work assesses the impact on K^{trans} and Vp of treatment changes in an early clinical trial cohort by comparing 4 models: Kety, extended Kety (with two lower limits on Vp), and a new model with Vp proportional to K^{trans}. When K^{trans} is the endpoint of interest, use of the Kety model is sufficient to depict cohort response. If Vp is also of interest, the new model improves the significance of Vp treatment effects.

2918

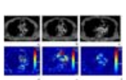

Quantitative Evaluation of Treatment Response to Early Concurrent Chemoradiotherapy with Multi-parametric MRI in Esophageal Cancer

Tieming Xie[1], Guoliang Shao[1], Lulu Liu[2], Jun Yang[3], and Peipei Pang[4]

[1]Radiology, Zhejiang cancer hospital, hangzhou, People's Republic of China, [2]The second clinical medical college, Zhejiang Chinese Medical University, hangzhou, People's Republic of China, [3]Life Sciences, GE Healthcare, Shanghai, People's Republic of China, [4]Life Sciences, GE Healthcare, hangzhou, People's Republic of China

The best dose of concurrent chemoradiotherapy for esophageal cancer exists individual difference because of tumor heterogeneity. The treatment will be more predictable if we can assess the chemoradiotherapy earlier, which will be helpful in early intervention for optimization of treatment plan, treatment time and improvement of overall survival. Multi-parametric MRI is gradually used for evaluating tumor treatment, and provides earlier and more information than conventional MRI. In this study, we used Ktrans value (derived from DCE-MRI) and ADC value (derived from DWI) to assess treatment response after the fifth concurrent chemoradiotherapy in esophageal cancer.

2919

In vivo OE-MRI quantification and mapping of response to hypoxia modifying drugs Banoxantrone and Atovaquone in Calu6 xenografts

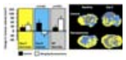

Ross A Little[1], Victoria Tessyman[2], Muhammad Babur[2], Susan Cheung[1], Yvonne Watson[1], Roben Gieling[2], Katherine G Finegan[2], Thomas M Ashton[3], Geoff JM Parker[1,4], W Gillies Mckenna[3], Geoffrey Higgins[3], Kaye J Williams[2,5], and James PB O'Connor[5,6]

[1]Centre for Imaging Sciences, University of Manchester, Manchester, United Kingdom, [2]Manchester Pharmacy School, University of Manchester, Manchester, United Kingdom, [3]CRUK/MRC Oxford Institute for Radiation Oncology and Biology, University of Oxford, Oxford, United Kingdom, [4]Bioxydyn Ltd, Manchester, United Kingdom, [5]Institute of Cancer Sciences, University of Manchester, Manchester, United Kingdom, [6]Department of Radiology, The Christie NHS Foundation Trust, Manchester, United Kingdom

Oxygen-enhanced MRI (OE-MRI) has shown promise as a technique for quantifying and spatially mapping tumour hypoxia. Here we report the first evidence that OE-MRI signals in perfused tumour can non-invasively track therapy-induced changes in hypoxia in vivo in a tumour model. We show that OE-MRI detects (1) reduction in hypoxia and increase in necrosis induced by the hypoxia-activated cytotoxic prodrug Banoxantrone; and (2) reduction in hypoxia and increase in well oxygenated tumour induced by Atovaquone due to increased oxygen availability. These data support first-in-man use of OE-MRI biomarkers in clinical trials of hypoxia-modifying agents.

2920

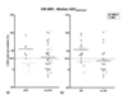

Combining DW- and DCE-MRI for treatment response assessment in patients with esophageal cancer undergoing neoadjuvant chemoradiotherapy

Sophie E. Heethuis[1], Lucas Goense[1,2], Peter S.N. van Rossum[1,2], Alicia S. Borggreve[1,2], Stella Mook[1], Francine E. Voncken[3], Richard van Hillegersberg[2], Jelle P. Ruurda[2], Gert J. Meijer[1], Jan J.W. Lagendijk[1], and Astrid L.H.M.W. van Lier[1]

[1]Department of Radiotherapy, University Medical Center Utrecht, Utrecht, Netherlands, [2]Department of Surgery, University Medical Center Utrecht, Utrecht, Netherlands, [3]Department of Radiotherapy, The Netherlands Cancer Institute-Antoni van Leeuwenhoek Hospital, Amsterdam

Neoadjuvant chemoradiotherapy prior to surgery is often used for treatment of patients with esophageal cancer. Potential benefit could be gained developing a patient tailored treatment, especially for the 29% of the patients who show a pathologic complete response. In this prospective multicenter study it was investigated whether combining DCE- and DW-MRI, which both showed potential for response prediction in previous studies, yields complementary information. It was found that the combination of DCE- and DW-MRI can increase the predictive values and reaches higher ROC_{AUC}.

2921

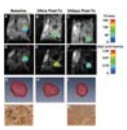

MRI biomarkers for PEGPH20-enhanced treatment of pancreatic ductal adenocarcinoma

Ezekiel Maloney[1], Christopher DuFort[2], Ravneet Vohra[1], Markus Carlson[2], Navid Farr[3], Paolo Provenzano[4], Joshua Park[1], Sunil Hingorani[2], and Donghoon Lee[1]

[1]Radiology, University of Washington, Seattle, WA, United States, [2]Clinical Research Division, Fred Hutchinson Cancer Research Center, Seattle, WA, [3]Medical Devices Research, National Inststitute of Health, Bethesda, MD, [4]Department of Biomedical Engineering, University of Minnesota, Minneapolis, MN

Pancreatic cancer is a devastating disease with poor prognosis. Pancreatic tumor therapy has been ineffective in part because pancreatic tumors have high interstitial fluid pressure (IFP), driven by high hyaluronan concentration, that inhibits penetration of drugs into the tumor. We performed multi-parametric MRI at high resolution to non-invasively assess tumor response in a KPC mouse model to pegylated recombinant hyaluronidase in isolation as well as combined with Gemcitabine. T1 and T2 relaxation as well as diffusion, and 3 dimensional volume measurements were used to characterize the tumors. MR measurements were compared with invasive IFP measurements and histopathological results.

2922

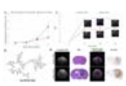

MRI Efficacy Evaluation of AvastinTM in Combination Temozolomide Therapy using GL261 Tumor Bearing Mice

Min-Kyoung Kang[1], Sang-Woo Kim[1], Ig-Jun Cho[1], Joo-Young Kim[1], Zhi Fang[1], Byung-Hwa Hyun[1], and Jae-Jun Lee*[1]

[1]Laboratory Animal Center, Osong Medical Innovation Foundation, Cheongju, Korea, Republic of

The aim of this study was to evaluate of the drug efficacy used by MRI. A mouse were randomly divided into the control and therapy groups for treatment. MRI were performed to compare with two groups and significant differences were observed in the two groups. The volume transfer constant (Ktrans), flux rate constant (kep) and contrast agent (Gd-DOTA-RGD) enhancement were decreased in the therapy group. Apparent diffusion coefficient (ADC) was lower in the control group. Furthermore, histopathologic assessments were in accord with MRI. Based on these results, efficacy evaluation used by MRI can be helped the development of new bio-drug.

2923

Estimation of Contributions to Z-Spectra from CEST and Magnetization Transfer Contrast from Active and Necrotic/Apoptotic Regions of MDA Tumour Xenografts

Wilfred W Lam[1], Jonathan H Klein[1,2,3], Farah Hussein[2], Christine Tarapacki[2], Gregory J Czarnota[1,2,3,4], and Greg J Stanisz[1,3,5]

[1]Physical Sciences, Sunnybrook Research Institute, Toronto, ON, Canada, [2]Radiation Oncology, Sunnybrook Health Sciences Centre, Toronto, ON, Canada, [3]Medical Biophysics, University of Toronto, Toronto, ON, Canada, [4]Radiation Oncology, University of Toronto, Toronto, ON, Canada, [5]Neurosurgery and Pediatric Neurosurgery, Medical University of Lublin, Lublin, Poland

Chemical exchange saturation transfer (CEST) MR imaging has been demonstrated to be able to differentiate active from necrotic/apoptotic regions in MDA tumour xenografts. However, the Z-spectrum reflects not only CEST from dissolved proteins, but also contributions from water saturation and magnetization transfer contrast from semisolid macromolecules. We estimated their individual effect sizes and calculated which significantly contribute to the difference in Z-spectrum amplitude between the two tumour regions. The difference in Z-spectrum amplitude between active and necrotic/apoptotic regions in MDA tumour xenografts is due to the CEST effect with minimal contribution from magnetization transfer contrast and direct water saturation.

2924

In Vivo 3T Clinical Magnetic Resonance Imaging with a Biologically Specific Contrast Agent in Prostate Cancer: A Nude Mouse Model

Christopher Brian Abraham[1,2], Prashant Jani[3], Roxanne Turuba[1,2], Michael Campbell[1,2], Ingeborg Zehbe[1,2], and Laura Curiel[1,2]

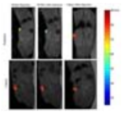

[1]Lakehead University, Thunder Bay, ON, Canada, [2]Thunder Bay Regional Research Institute, Thunder Bay, ON, Canada, [3]Thunder Bay Regional Health Science Center, Thunder Bay, ON, Canada

In this study we characterized in vivo a functional superparagmagnetic iron-oxide magnetic resonance contrast agent that effects the T2 relaxation time in MRI. The agent was developed by conjugating Molday Ion Carboxyl-6 (MIC6), with a de-immunized mouse monoclonal antibody (muJ591) targeting prostate-specific membrane antigen (PSMA). We propose this functional contrast agent as a non-invasive method to detect prostate cancer cells that are PSMA positive to provide increased differentiability from surrounding tissues for treatment. PSMA-positive prostate tumours were induced into 20 immunocompromised mice. The functional contrast agent was injected into 14 mice leaving 6 mice as controls. MR imaging was performed on a clinical 3T scanner using different parameters on a MESE sequence to obtain T2 relaxation time values. Tumour size, signal intensity, and T2 relaxation time were obtained pre and post injection and were found to have a lower value for treated mice compared to controls. ICP confirmed the increased level of elemental iron in treated mice tumours compared to controls. H&E staining showed healthy morphology of all tissues collected. The reduction in T2 relaxation time for the functional contrast agent, combined with its specificity against PSMA suggest its potential as a biologically-specific MR contrast agent.

2925

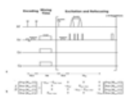

Tumor Progression Monitoring with Hyperpolarized ^{13}C Exchange Spectroscopy in Transgenic Adenocarcinoma of Mouse Prostate Treated with Androgen Deprivation Therapy

Zihan Zhu[1,2], Robert Bok[1], Hsin-Yu Chen[1,2], John Kurhanewicz[1], and Daniel B Vigneron[1]

[1]Department of Radiology and Biomedical Imaging, UCSF, San Francisco, CA, United States, [2]UC Berkeley-UCSF Graduate Program in Bioengineering, UC Berkeley and UCSF, San Francisco, CA, United States

Hyperpolarized ^{13}C MR imaging provides valuable enzyme-kinetic information for investigating disease metabolism. In this work, a new exchange spectroscopic imaging method was applied to a preclinical cancer treatment study and the metabolic information provided by this new method agreed with and proved additional quantitative kinetic metrics over traditional Response Evaluation Criteria in Solid Tumors (RECIST) measures.

2926

In vivo follow-up of colorectal cancer on mice model using endoluminal MRI

Hugo Dorez[1], Raphaël Sablong[1], Hélène Ratiney[1], Laurence Canaple[2], Hervé Saint-Jalmes[3], Sophie Gaillard[1], Driffa Moussata[1,4], and Olivier Beuf[1]

[1]Univ Lyon, INSA-Lyon, Université Lyon 1, UJM-Saint Etienne, CNRS, Inserm, CREATIS UMR 5220, U1206, Lyon, France, [2]Institut de Génomique Fonctionnelle de Lyon, Université de Lyon 1, UMR 5242 CNRS, Ecole Normale Supérieure de Lyon, Lyon, France, [3]LTSI; INSERM U642; Université Rennes 1, Rennes, France, [4]Hôpital Régional Universitaire de Tours - Service hépato-gastroentérologie, Tours, France

For 6 months, 32 mice, chemically treated to induce colorectal cancer, were followed with endoluminal MRI using dedicated endorectal coils. Based on high spatial resolution T1-weigthed images and T1-maps, quantified parameters (colon wall thickness and T1 relaxation time) were measured at each stage of the pathology from healthy tissues to cancer through inflammation. The colon wall thickness was found to be reliable in assessing early stages of the pathology (inflammation from infiltration), where the intrinsic contrast T1 time parameter was reliable for discerning infiltration from tumors. The two biomarkers provide complementary information in the characterization and staging of colorectal cancer.

2927

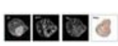

Combined DCE-MRI and immunohistochemical analyses of cervical cancer xenografts reveal differences in the physiological background of prognostic image parameters derived from the Tofts and Brix model

Tiril Hillestad[1], Tord Hompland[2], Anja Nilsen[2], Trond Stokke[1,2], and Heidi Lyng[2]

[1]Department of Core Facilities, Oslo University Hospital, Oslo, Norway, [2]Department of Radiation Biology, Oslo University Hospital, Oslo, Norway

The Tofts and Brix parameters K^{trans} and A_{Brix} , derived from dynamic contrast-enhanced MRI (DCE-MRI), have been suggested as potential markers of hypoxia. This phenotype is associated with poor outcome in cervical cancer treated with chemoradiotherapy. In this study, DCE-MRI was combined with immunohistochemical analysis of cervical cancer xenografts, to better understand the physiological background and prognostic potential of the parameters. Through correlations with hypoxic fraction, vascular and cellular densities, derived from pimonidazole, CD31 and hematoxylin staining of tumor sections, respectively, it was shown that A_{Brix} could be the preferred DCE-MRI parameter for predicting hypoxia related treatment resistance in cervical cancer.

2928

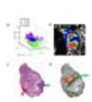

Unraveling osteosarcoma tumor heterogeneity using MRI-defined tumor habitats

SUNING HUANG[1], William Dominguez-Viqueira[1], Epi Ruiz[1], Mikalai Budzevich[1], Bruna v Jardim-Perassi[1], Robert Gillies[1], and Gary Martinez[1]

[1]Imaging and Metabolism, Moffitt Cancer Center, Tampa, FL, United States

We explore heterogeneity in osteosarcoma using imaging “habitats”, which identify different physiological subregions by MRI. We propose a method to establish the relationship between the microenvironmental of a habitat by relating histology to MRI. Computational image analysis was used to cluster tumor habitats with a 3D printing approach to co-register MR images with histology and immunohistochemistry. Compared with H&E and the CA-9, we found that cellular morphology and density were in concordance with the clustered habitats, although there are subtle differences between histology and MRI slices. Thus, identifying tumor habitats in osteosarcoma using multiparametric MRI is feasible and promising.

2929

Multi-parametric MRI of glioblastoma invasion quantitative evaluation using histological stacks

Haitham Al-Mubarak[1], Antoine Vallatos[1], Lindsay Gallagher[1], Joanna Birch[2], Lesley Glmour[2], John Foster[3], Anthony Chalmers[2], and William Holmes[1]

[1]Glasgow Experimental MRI center, University of Glasgow, Glasgow, United Kingdom, [2]Institute of Cancer Sciences, University of Glasgow, Glasgow, United Kingdom, [3]School of medicine, dentistry and nursing, University of Glasgow, Glasgow, United Kingdom

We perform a quantitative histological evaluation of a range of MRI techniques in their ability to probe glioblastoma invasion in a mouse model. Using 3-D histological stacks co-registered with MRI slices allows to achieve high values in Dice, sensitivity and specificity tests (>90%). This approach enables to go beyond the standard evaluation tests, performing direct voxel-to-voxel comparison between MRI and histology, and facilitating the development of multi-parametric analysis models. We also identified promising methods for detecting low tumour concentration regions at the invasion limits.

2930

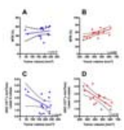

Multi-parametric MRI assessment of tumor progression in a mouse model of pancreatic cancer

Ravneet S Vohra[1], Yak-Nam Wang[2], Joshua Park[1], Kayla Gravelle[2], Stella wHang[2], Joo-Ha Hwang[3], and Donghoon Lee[1]

[1]Department of Radiology, University of Washington, Seattle, WA, United States, [2]Center for Industrial and Medical Ultrasound Applied Physics Laboratory, University of Washington, Seattle, WA, United States, [3]Department of Medicine, University of Washington, Seattle, WA, United States

Pancreatic ductal adenocarcinoma (PDAC) is one of the most common forms of lethal human cancers with poor prognosis. Diagnosis is made usually late in tumor development. There is a dire need to develop sensitive non-invasive biomarkers to diagnose and monitor tumor progression and its associated pathological features. We propose to use multi-parametric MRI (mpMRI) to monitor tumor progression in a genetically engineered KPC mouse model that recapitulates human PDAC. Using mpMRI, we demonstrate that there is a significant correlation between increase in pancreatic tumor volume, Magnetization transfer ratio (MTR), apparent diffusion coefficient (ADC), and chemical exchange saturation transfer (CEST) imaging.

Traditional Poster

Non-Proton MRI & MRS

Exhibition Hall 2931-2965 Thursday 13:00 - 15:00

2931

Highly Accelerated 31P MRSI of Human Calf Muscles combining Flyback Echo Planar Spectroscopic Imaging (EPSI) and Compressed Sensing

Alejandro Santos Diaz[1] and Michael Noseworthy[1,2]

[1]Biomedical Engineering, McMaster University, Hamilton, ON, Canada, [2]Electrical and Computer Engineering, McMaster University, Hamilton, ON, Canada

Very long acquisition times is the most important limitation against performing ^{31}P magnetic resonance spectroscopic imaging (MRSI) in clinic environments. To overcome this limitation we show the feasibility of implementing *in vivo* highly accelerated ^{31}P-MRSI combining flyback echo planar spectroscopic imaging (EPSI) and compressed sensing (CS) achieving a 12x12 matrix over a 24 cm field of view (FOV) in less than 6 minutes. Due to the denoising nature of CS the resultant SNR was also improved using this approach.

2932

Mapping the exchange kinetics of high-energy phosphates in the human calf muscle by direct 31P MRSI at 7T

Andreas Korzowski[1], Sarah Neumann[1], Ludwig Dominik[1], Loreen Ruhm[1], Mark E. Ladd[1], and Peter Bachert[1]

[1]Medical Physics in Radiology, German Cancer Research Center (DKFZ), Heidelberg, Germany

^{31}P MRS allows the non-invasive observation of high-energy phosphate turnover *in vivo*. A model incorporating the effects of exchange processes onto the transverse steady-state magnetization was derived, which allows the direct estimation of relaxation rates from signal intensities in MRSI datasets. Multiple ^{31}P MRSI datasets with different excitation parameters of four healthy were evaluated. Spatially-resolved turnover rates of high-energy phosphates could be estimated and are in agreement with literature values proving feasibility of the proposed approach.

2933

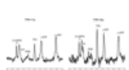

Measurement of human cardiac intracellular pH in vivo using long TR 31P-MRS with adiabatic excitation at 7T

Ladislav Valkovic[1,2], William T Clarke[1], Lucian AB Purvis[1], Matthew D Robson[1], Stefan Neubauer[1], and Christopher T Rodgers[1]

[1]Oxford Centre for Clinical MR Research (OCMR), RDM Cardiovascular Medicine, University of Oxford, Oxford, United Kingdom, [2]Department of Imaging Methods, Institute of Measurement Science, Slovak Academy of Sciences, Bratislava, Slovakia

Determination of human cardiac intracellular pH using ^{31}P-MRS is challenging as the resonance frequency of Pi is concealed by a close resonating 2,3-DPG signal originating from blood. Common short TR and low-flip angle scan used for cardiac ^{31}P-MRS increase the effective SNR/time, but can additionally suppress the Pi signal intensity. We have investigated the feasibility of detecting cardiac Pi and calculating intracellular pH of human heart using long TR 3D-CSI examination with adiabatic excitation at 7T. Comparison to short TR acquisition was performed using interleaved TR measurements. We report robust and repeatable detection of Pi signal in 100% of subjects.

2934

Phosphocreatine T1 in human gastrocnemius muscle at 7T increases during exercise, measured by localized 31P MRS with progressive saturation

Martin Meyerspeer[1], Albrecht Ingo Schmid[1], Fabian Niess[1], Georg Bernd Fiedler[1], Sigrun Goluch[1], Michale Wolzt[2], and Ewald Moser[1]

[1]Center for Medical Physics and Biomedical Engineering, Medical University of Vienna, Vienna, Austria, [2]Department of Internal Medicine III, Medical University of Vienna, Austria

Alterations in T1 have implications on the physiological interpretation of dynamic high-energy phosphate data. Progressive saturation during rest-exercise-recovery experiments was used to simultaneously quantify PCr depletion, recovery and T1 values. The data were acquired using localised 31P MRS in human gastrocnemius. Apparent T1 values increased from 5.0 ± 0.4 s at rest to an average value of 5.8 ± 0.5 s during exercise, with a peak in early exercise and returning towards baseline values before exercise was ceased. These alterations may be explained by changes in the chemical exchange rates of PCr with ATP and Pi.

2935 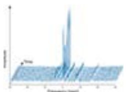

Dynamic 31P spectroscopy during superimposed electrical muscle stimulation and volitional contraction for enhanced metabolic response in the skeletal muscle

Francesco Santini[1,2], Dirk Fischer[3], Oliver Bieri[1,2], and Xeni Deligianni[1,2]

[1]Division of Radiological Physics, University of Basel Hospital, Basel, Switzerland, [2]Department of Biomedical Engineering, University of Basel, Basel, Switzerland, [3]Pediatric Neurology, UniversitätsKinderspital beider Basel (UKBB), Basel, Switzerland

Dynamic 31P spectroscopy of the skeletal muscle can provide useful insight into its energy metabolism. However, in order to see dynamic changes in metabolites, a minimum threshold of physical exercise is necessary. In this work, we present a system that uses electrical muscle stimulation superimposed to volitional muscle contraction in order to enhance the metabolic response of the muscle in the same workload condition. This method can have potential application to patients that are unable to voluntarily exert sufficient work for a dynamic spectroscopy investigation.

2936 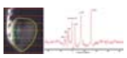

In vivo 31P spectroscopy of ATP levels during a fructose challenge in the liver at 7T

Irene M.L. van Kalleveen[1,2], Jurgen H. Runge[1,3], Wybe J.M. van der Kemp[4], Debra S. Rivera[1,2,5], Jaap Stoker[1], Dennis W.J. Klomp[4], and Aart J. Nederveen[1]

[1]Radiology, Academic Medical Center, Amsterdam, Netherlands, [2]Spinoza Centre, Amsterdam, Netherlands, [3]Division of Imaging Sciences and Biomedical Engineering, King's College London, London, United Kingdom, [4]Radiology, UMC Utrecht, Utrecht, Netherlands, [5]MR Coils, Zaltbommel, Netherlands

The standard evaluation of detecting liver parenchyma is invasive liver biopsy, while MRS is a non-invasive measurement to monitor metabolites. Using ^{31}P spectroscopy it is possible to follow metabolic changes in the liver and the functionality of the liver during fructose uptake by measuring ATP levels. Going to ultra-high field strength, we are more sensitive to ATP levels and are able to use more localized MRS sequences (e.g. 3D CSI). We have shown we are able to monitor ATP levels during fructose uptake in vivo in the liver at 7T and see a decrease in ATP levels during the uptake.

2937 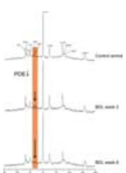

Chronic liver disease in developing brain: an in vivo longitudinal and multiparametric study using 31P MRS, 31P Magnetization transfer and 1H MRS

Veronika Rackayova[1], Vladimir Mlynarik[2], and Cristina Cudalbu[3]

[1]Laboratory for Functional and Metabolic Imaging, EPFL, Lausanne, Switzerland, [2]High Field MR Centre, Department of Biomedical Imaging and Image-Guided Therapy, Medical University of Vienna, Vienna, Austria, [3]Centre d'Imagerie Biomedicale (CIBM), EPFL, Lausanne, Switzerland

Chronic liver disease (CLD) induces irreversible brain alterations, especially in children, probably linked with oxidative stress and energy metabolism perturbations. Our aim was to use combination of NOE enhanced and ^{1}H-decoupled ^{31}P-MRS, ^{31}P-saturation transfer experiment (to estimate mitochondrial creatine kinase rate) and ^{1}H-MRS to study the effect of CLD on developing brain. Our results show significantly reduced $k_{ATP \rightarrow PCr}$ and fluctuating NAD^{+}/NADH ratio indicating perturbation in mitochondrial function, possibly induced by oxidative stress. In addition, altered phospholipid metabolism was observed.

2938 

31P MR spectroscopy of peripheral artery occlusive disease patients with and without diabetes

Petr Sedivy[1,2], Miloslav Drobny[1,2], Monika Dezortova[1], Karel Roztocil[3], Andrea Nemcova[4], Vit Herynek[1], Robert Bem[4], Helena Cermakova[3], Jan Peregrin[5], and Milan Hajek[1]

[1]MR-unit, Institute for Clinical and Experimental Medicine, Prague, Czech Republic, [2]First Faculty of Medicine, Charles University, Prague, Czech Republic, [3]Transplant Surgery Dept., Institute for Clinical and Experimental Medicine, Prague, Czech Republic, [4]Dept. Diabetology, Institute for Clinical and Experimental Medicine, Prague, Czech Republic, [5]Dept. Diagnostic and Interventional Radiology, Institute for Clinical and Experimental Medicine, Prague, Czech Republic

Reduced blood supply limits the oxidative muscle metabolism and causes acidosis due to anaerobic glycolysis. Similar results were found in patients with peripheral artery occlusive disease (PAOD) in which chronic ischemia causes claudication and restricts walking distance. ^{31}P MR spectroscopy of calf muscles of healthy controls and patients show that PAOD significantly influences muscular metabolism which is reflected in dynamic parameters of PAOD patients. The effect of diabetes is significantly pronounced in diabetic PAOD patients at rest compared to controls and PAOD patients without diabetes.

2939 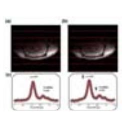

Exogenous NAD+ Enhances Energy Metabolism in Healthy Rat Brains

Ming Lu[1], Xiao-Hong Zhu[1], Yi Zhang[1], and Wei Chen[1]

[1]Center for Magnetic Resonance Research, University of Minnesota, Minneapolis, MN, United States

Decline in NAD^+ availability is tightly linked to many neurological disorders. Our recent study also revealed age dependences of intracellular NAD^+, NADH and total NAD concentrations in healthy human brains. Accumulating evidences have shown that the cellular NAD^+ could serve as a therapeutic target for treating metabolic or age-related neurological diseases and promoting longevity. Therefore, to investigate the effect of exogenous NAD^+ on intracellular NAD metabolism, the *in vivo* ^{31}P-MRS NAD imaging assay developed in our lab was applied in normal rat brains at 16.4 T. Significant increases of cerebral α-ATP, total NAD and NAD^+ levels were observed after the intra-peritoneal infusion of exogenous NAD^+. This study not only demonstrates the feasibility of using exogenous NAD^+ to enhance cerebral ATP and NAD metabolisms, but also provides an opportunity to better understand the roles of NAD metabolism in health and age-related disease.

2940

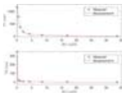

Ferumoxytol as a blood-pool T2 relaxation agent for 7T phosphorus spectroscopy

Jack Julian James Jenkins Miller[1,2,3], Damian John Tyler[1,2], Vicky Ball[1], Oliver Rider[2], and Christopher Rodgers[2]

[1]Department of Physiology, Anatomy & Genetics, University of Oxford, Oxford, United Kingdom, [2]Oxford Centre for Clinical Magnetic Resonance Research, University of Oxford, Oxford, United Kingdom, [3]Department of Physics, University of Oxford, Oxford, United Kingdom

Ferumoxytol is a licensed carbohydrate-coated, superparamagnetic iron oxide nanoparticle indicated in the treatment of anaemia. We show that, in contrast to other agents, it predominantly reduces T_2, is confined to the blood pool for >1 hour post administration, and therefore could improve the efficiency of saturation pulses that aim to remove the 2,3-diphosphoglycerate signal from blood. This proof-of-principle study shows that Ferumoxytol could enable inorganic phosphate detection in vivo, and hence the determination of pH.

2941

Measuring lactate dehydrogenase activity with proton detected 13C hyperpolarization

Felix Kreis[1], Jiazheng Wang[1], Alan Wright[1], and Kevin Brindle[1]

[1]Cancer Research UK Cambridge Institute, University of Cambridge, Cambridge, United Kingdom

Dissolution Dynamic Nuclear Polarized NMR (dDNP NMR) is a promising new tool for assessing metabolism in vivo. The signals of the hyperpolarized substrate and its downstream metabolites are usually detected by direct ^{13}C observation. Here we demonstrate an effective way to repetitively transfer hyperpolarization via indirect couplings from [1-^{13}C] to [3,3,3-$^{1}H_3$] in [1-^{13}C] lactate formed from hyperpolarized [1-^{13}C] pyruvate. The changes in the hyperpolarized [3,3,3-$^{1}H_3$] lactate peak were fitted to a kinetic model. The method sets the stage for dynamic hyperpolarized ^{1}H imaging.

2942

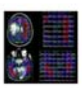

Automated Kinetic Modeling of Hyperpolarized 13C Metabolism in Human Brain Tumors

Jason C Crane[1], Ilwoo Park, Marram P Olson, Daniel B Vigneron, and Sarah J Nelson

[1]UCSF, San Francisco, CA, United States

Methods for dynamic spectroscopic imaging of hyperpolarized (HP) ^{13}C substrates are rapidly evolving and accessible tools are required for reconstructing the data and for validating quantitative kinetic models. This study presents processing tools for automatic analysis of data from dynamic HP ^{13}C experiments. The methods were implemented in the open-source SIVIC software package and applied to the fitting of data from a human brain tumor trial to derive metabolic K_{pl} maps.

2943

Analyzing Reaction Dynamics With Hyperpolarized 13C-NMR

Nicholas Drachman[1], Stephen Kadlecek[1], and Rahim Rizi[1]

[1]Radiology, University of Pennsylvania, Philadelphia, PA, United States

In this study we use hyperpolarized 13C-NMR to probe the dynamics of the decarboxylation reaction of pyruvate via H2O2, commonly used to produce hyperpolarized bicarbonate. Using this method we are able to observe and quantify the dynamics of the intermediate state, 2-hydroperoxy-2-hydroxypropranoate, which has never before been directly observed at room temperature, as well as characterizing a previously overlooked side reaction between the products and reactants of the decarboxylation reaction. This study serves as a template for how to use hyperpolarized 13C NMR to study the dynamics of innumerable other organic reactions with polarizable substrates.

2944

2D Heteronuclear Single-Quantum Coherence MR spectroscopy for in vivo detection of ^{13}C-labeling in rat brain during simultaneous infusion of ^{13}C-labeled substrates

Henk M. De Feyter[1], Kevin L. Behar[2], Douglas L. Rothman[1], and Robin A. de Graaf[1]

[1]Department of Radiology and Biomedical Imaging, Yale University, New Haven, CT, United States, [2]Department of Psychiatry, Yale University, New Haven, CT, United States

We adopted a 2D heteronuclear single-quantum coherence (HSQC) MR spectroscopy method to detect in vivo ^{13}C isotopomers in rat brain through exploiting the high sensitivity of ^{1}H MRS. This method allows for in vivo detection of unique ^{13}C-labeling patterns in brain metabolite pools during simultaneous infusion of different ^{13}C-labeled substrates. We demonstrated that high-quality 2D HSQC MR spectra can be acquired in vivo in a time-resolved manner from rat brain during simultaneous infusion of [U-$^{13}C_6$]-glucose and [2-^{13}C]-acetate. This method can be used to study with high accuracy neuronal and glial metabolism, and the contribution of alternate substrates to brain energy metabolism.

2945

Localized, indirect ^{1}H-[^{13}C] MRS measurement of glutamate and glutamine ^{13}C-labeling in frontal cortex of human brain at 4 Tesla.

Henk M. De Feyter[1], Raimund M. Herzog[2], Peter B. Brown [1], Douglas L. Rothman[1], and Robin A. de Graaf[1]

[1]Department of Radiology and Biomedical Imaging, Yale University, New Haven, CT, United States, [2]Department of Endocrinology, Yale University, New Haven, CT, United States

We present an indirect ^{1}H-[^{13}C] MRS detection method (selective proton-observed, carbon edited (selPOCE) that can be used in the frontal lobe of human brain, allows for separation of overlapping glutamate (Glu) and glutamine (Gln) peaks and provides well-defined spatial localization of the ^{13}C-signal. The method was successfully implemented at 4 Tesla and allowed for the selective detection of ^{13}C-labeling in Glu and Gln in a timely manner (15 min), indicating that the selPOCE can be used for quantitative studies of brain energy metabolism and neurotransmission in a relatively small volume localized in the human frontal lobe.

2946

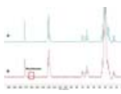

Protocol for investigating in vivo Glucose Metabolism in Human Breast Cancer by 13C MRS at 7T

Sergey Cheshkov[1,2], Ivan E. Dimitrov[1,3], Joseph Rispoli[4], Jiaming Cui[5], Mary McDougall[4,5], Steve Wright[4,5], Stephen Seiler[2], A. Dean Sherry[1,2,6], and Craig R. Malloy[1,2,7]

[1]Advanced Imaging Research Center, UT Southwestern Medical Center, Dallas, TX, United States, [2]Radiology, UT Southwestern Medical Center, Dallas, TX, United States, [3]Philips Medical Systems, Cleveland, OH, United States, [4]Biomedical Engineering, Texas A&M University, TX, United States, [5]Electrical Engineering, Texas A&M University, TX, United States, [6]Chemistry, University of Texas at Dallas, TX, United States, [7]Internal Medicine, UT Southwestern Medical Center, Dallas, TX, United States

Upregulated glucose uptake in cancer is often observed and can be monitored with a radiolabeled analogue of glucose, ^{18}FDG, with detection by PET, however, a well-known constraint is its ionizing radiation. Additionally, except for the trapping of that glucose analogue, PET does not provide information about subsequent glucose metabolism. Here, we demonstrated the feasibility of a simple glucose infusion protocol that allows detection of glucose oxidation in human breast cancer *in vivo* via 7T ^{13}C MRS. The [U-^{13}C]glucose infusion is performed outside of the magnet making the protocol significantly more suitable for patients compared to previous approaches that required prolonged ^{13}C substrate infusions inside the scanner.

2947

Human In Vivo 25Mg Spectroscopy and Imaging at 7T

Nicolas G. R. Behl[1], Armin M. Nagel[1,2], Florian Maier[1], Peter Bachert[1], Mark E. Ladd[1], and Reiner Umathum[1]

[1]Medical Physics in Radiology, German Cancer Research Center (DKFZ), Heidelberg, Germany, [2]Institute of Radiology, University Hospital Erlangen, Erlangen, Germany

^{25}Mg spectroscopy and imaging were performed for the first time in vivo. T_1 and T_2* of ^{25}Mg were evaluated in model solutions and T_2* was additionally estimated in vivo for the human calf. ^{25}Mg spectroscopy of an $MgCl_2$ model solution exhibits a single resonance attributed to free $^{25}Mg^{2+}$ ions, while in vivo spectroscopy of a human calf displays an additional resonance possibly attributable to bound ^{25}Mg. Phantom and in vivo ^{25}Mg imaging of the human calf were performed with a voxel size of 25×25×25 mm^3.

2948

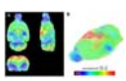

Investigation of Lithium Distribution in the Rat Brain ex vivo using Lithium-7 Magnetic Resonance Imaging at 17 Tesla

Anne-Sophie Hanak[1], Jacques Andrew Stout[2], Lucie Chevillard[1], Boucif Djemaï[2], Patricia Risède[1], Michel Luong[2], Eric Giacomini[2], Joel Poupon[3], David André Barrière[2,4], Frank Bellivier[1,5], Bruno Mégarbane[1,5], and Fawzi Boumezbeur[2]

[1]INSERM UMR-S 1144, Universités Paris-Descartes & Paris-Diderot, Paris, France, [2]Neurospin, CEA, Université Paris-Saclay, Gif-sur-Yvette, France, [3]APHP, GH Saint-Louis-Lariboisière-Fernand Widal, Laboratoire de Toxicologie biologique, Paris, France, [4]Inserm UMR-S 894, Université Paris-Descartes, Paris, France, [5]APHP, GH Saint-Louis-Lariboisière-Fernand Widal, Réanimation Médicale et Toxicologique, Paris, France

Lithium (Li) is the first-line mood stabilizer to treat bipolar disorder patients. However, its mechanisms of action and transport across the blood-brain barrier remain poorly understood. In this study, we aimed at mapping *ex vivo* the cerebral Li distribution of rats treated for 28 days with Li_2CO_3 using ^{7}Li-MRI at 17.2 Tesla. Using a phantom replacement approach, MRI-derived Li concentrations were calculated and validated by comparison to inductively coupled plasma-mass spectrometry (ICP-MS) measurements. Lithium distributions were uneven (normalized lithium content ranging from 0.7 to 1.4) and symmetrical with consistently lower concentrations in the metencephalon and higher ones in the cortex.

2949

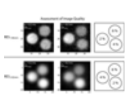

Density-Adapted k-Space Sampling Technique for Fast Relaxing Chlorine-35 Nuclei at 9.4 T

Ruomin Hu[1], Andreas Neubauer[1], Matthias Malzacher[1], Simon Konstandin[2], and Lothar R. Schad[1]

[1]Computer Assisted Clinical Medicine, Heidelberg University, Mannheim, Germany, [2]MR-Imaging and Spectroscopy, Universty of Bremen, Bremen, Germany

Chloride Cl^- as the most abundant anion in mammals is a vital component of biophysical regulatory processes. ^{35}Cl MRI has the potential to visualise Cl^- homeostatic changes during stroke, in tumors and in ionic regulatory diseases. This study aimed at demonstrating the advantages of implementing density-adapted k-space sampling to overcome the instrinsically low SNR associated with ^{35}Cl MRI. We showed that density-adapted k-space sampling yielded distinctively visible improvement of image quality as well as quantitative SNR gain in phantoms with very fast bi-exponential T_2* relaxation over conventional radial sampling.

2950

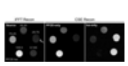

Chemical Shift Encoded (CSE) Image Reconstruction for Spectral Selection in Fluorine-19 MRI

Kai D. Ludwig[1], Diego Hernando[1,2], Nathan T. Roberts[2,3], Ruud B. van Heeswijk[4], and Sean B. Fain[1,2,5]

[1]*Medical Physics, University of Wisconsin - Madison, Madison, WI, United States,* [2]*Radiology, University of Wisconsin - Madison, Madison, WI, United States,* [3]*Electrical and Computer Engineering, University of Wisconsin - Madison, Madison, WI, United States,* [4]*Radiology, Lausanne University Hospital (CHUV) and University of Lausanne (UNIL), Lausanne, Switzerland,* [5]*Biomedical Engineering, University of Wisconsin - Madison, Madison, WI, United States*

In preclinical applications, the high specificity of quantitative ^{19}F MRI may be compromised by non-negligible signal contributions from fluorinated anesthetics (*e.g.* isoflurane). Here, we demonstrate the feasibility of chemical shift encoding (CSE) with multi-resonance fluorine signal modeling and least-squares estimation image reconstruction for ^{19}F MRI. We optimize noise performance (NSA) and use a 3D spoiled gradient-echo acquisition to separate signal contributions from perfluoro-15-crown-5-ether (PFCE) and isoflurane. The method is tested in mixed PFCE/isoflurane phantoms showing effective signal separation. The CSE reconstruction removes isoflurane signal contributions in ^{19}F MR images of PFCE *in vivo*, potentially reducing errors in ^{19}F concentration quantification.

2951

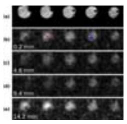

High Resolution Dynamic 31P-MRSI of Ischemia-Reperfusion in Rat Hindlimb at 9.4T Using SPICE

Yuchi Liu[1,2], Bryan Alexander Clifford[3,4], Chao Ma[3,5,6], Fan Lam[3], Zhi-Pei Liang[3,4], and Xin Yu[1,2,7,8]

[1]*Department of Biomedical Engineering, Case Western Reserve University, Cleveland, OH, United States,* [2]*Case Center for Imaging Research, Case Western Reserve University, Cleveland, OH, United States,* [3]*Beckman Institute for Advanced Science and Technology, University of Illinois at Urbana-Champaign, Urbana, IL, United States,* [4]*Department of Electrical and Computer Engineering, University of Illinois at Urbana-Champaign, Urbana, IL, United States,* [5]*Gordon Center for Medical Imaging, NMMI, Department of Radiology, Massachusetts General Hospital, MA, United States,* [6]*Department of Radiology, Harvard Medical School, MA, United States,* [7]*Department of Radiology, Case Western Reserve University, Cleveland, OH, United States,* [8]*Department of Physiology and Biophysics, Case Western Reserve University, Cleveland, OH, United States*

Dynamic ^{31}P-MRSI serves as a non-invasive tool to assess mitochondrial oxidative capacity in skeletal muscle during ischemia-reperfusion or exercise-recovery. However, ^{31}P-MRSI with high spatial resolution requires long acquisition times which render dynamic measurements impractical. In this study, we adapted a recently proposed low-rank tensor-based method for high-resolution dynamic ^{31}P-MRSI in preclinical studies. We present results from an in vivo ischemia-reperfusion experiment on a rat hindlimb with 15 s nominal temporal resolution and 0.75×0.75×1.6 mm^3 nominal spatial resolution, demonstrating the potential of the method for assessing mitochondrial function in different muscle types in small animal models.

2952

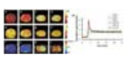

Dynamic Oxygen-17 MR Imaging with Golden-Ratio-Based Radial Sampling and k-Space-Weighted Image Reconstruction

Yuchi Liu[1,2], Yifan Zhang[1,2], Chunying Wu[2], Junqing Zhu[2], Charlie Yi Wang[1,2], Nicholas Tomko[3], Mikhail Linetsky[3], Robert Salomon[3], Yanming Wang[2,4], and Xin Yu[1,2,4,5]

[1]*Department of Biomedical Engineering, Case Western Reserve University, Cleveland, OH, United States,* [2]*Case Center for Imaging Research, Case Western Reserve University, Cleveland, OH, United States,* [3]*Department of Chemistry, Case Western Reserve University, Cleveland, OH, United States,* [4]*Department of Radiology, Case Western Reserve University, Cleveland, OH, United States,* [5]*Department of Physiology and Biophysics, Case Western Reserve University, Cleveland, OH, United States*

This study aimed at developing a 3D dynamic oxygen-17 (^{17}O) MR imaging method to delineate the kinetics of ^{17}O-water uptake and washout in mouse brain with glioblastoma at high temporal and spatial resolution. A 3D imaging method using a stack-of-stars golden-ratio-based radial sampling scheme was combined with k-space weighted image reconstruction to improve the temporal resolution with preserved spatial resolution. The proposed method achieved a temporal resolution of 7.56 s with a voxel size of 5.625 µL in mouse brain at 9.4T. It can also be used to image cerebral oxygen consumption rate in ^{17}O inhalation studies.

2953

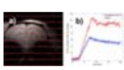

Measurement of $CMRO_2$ in conscious rat with *in vivo* ^{17}O MRS at 16.4T

Hannes Michel Wiesner[1], Yi Zhang[1], Ming Lu[1], Nanyin Zhang[2], Xiao-Hong Zhu[1], and Wei Chen[1]

[1]*CMRR, Radiology, University of Minnesota Medical School, Minneapolis, MN, United States,* [2]*Department of Biomedical Engineering, Pennsylvania State University, University Park, PA, United States*

In this study we performed dynamic in vivo ^{17}O MRS measurements in conscious and isoflurane-anesthetized rat during inhalations of $^{17}O_2$-enriched gas at ultra-high field of 16.4T, ultimately to compare the relation between $CMRO_2$ and brain condition.

2954

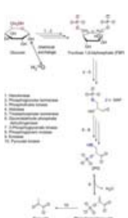

Quantification of Cerebral Metabolic Rates of ^{17}O-Labeled Glucose in Mouse Brain with Dynamic ^{17}O-MRS

Robert Borowiak[1,2,3], Wilfried Reichardt[1,2,3], Dmitry Kurzhunov[1], Christian Schuch[4], Benjamin Görling[5], Dieter Leibfritz[6], Jochen Leupold[1], Thomas Lange[1], Helge Haas[7], Jens Timmer[7], and Michael Bock[1]

[1]*Dept. of Radiology, Medical Physics, Medical Center-University of Freiburg, Germany, Freiburg, Germany,* [2]*German Cancer Consortium (DKTK), Heidelberg, Germany, Heidelberg, Germany,* [3]*German Cancer Research Center (DKFZ), Heidelberg, Germany, Heidelberg, Germany,* [4]*NUKEM Isotopes Imaging GmbH,* [5]*Bruker BioSpin GmbH,* [6]*Faculty of Medicine, University of Tübingen, Germany,* [7]*Institute of Physics, University of Freiburg, Germany*

We studied the chemical exchange kinetics of ^{17}O-labeled glucose at the C1 and the C6 position with dynamic ^{17}O-MRS. A profile likelihood analysis is performed to determine identifiability and confidence intervals of the metabolic rate CMR_{Glc}. The exchange experiments confirm that the C6-^{17}OH label is transferred via glycolysis exclusively by the enzyme enolase into the metabolic end product $H_2{}^{17}O$, while C1-^{17}OH ends up in water via direct hydrolysis as well as via glycolysis. From $H_2{}^{17}O$-concentration time-courses cerebral metabolic rates of CMR_{Glc} = 0.05−0.08 µmol/g/min are obtained which are in of the same order of magnitude as ^{18}F-FDG PET.

2955

Direct Partial Volume Corrected CMRO2 Determination: Simulation assisted Dynamic 17O-MRI

Sebastian C. Niesporek[1], Reiner Umathum[1], Jonathan M. Lommen[1], and Armin M. Nagel[1,2]

[1]Medical Physics in Radiology, German Cancer Research Center (DKFZ), Heidelberg, Germany, [2]Institute of Radiology, University Hospital Erlangen, Erlangen, Germany

A dynamic ^{17}O-MRI inhalation experiment enables localized mapping of the cerebral metabolic rate of oxygen consumption ($CMRO_2$) in the human brain via $H_2{}^{17}O$ quantification. These functional information are tissue viability parameters and can help studying the brain metabolism. In ^{17}O-MRI, accurate quantification and $CMRO_2$-determination is severely biased by partial volume effects caused by low spatial resolution and fast transverse relaxation. A human brain-simulation providing realistic dynamic ^{17}O-data was used to evaluate the performance of a partial volume correction algorithm at different temporal resolution. Findings were then adapted to an in-vivo ^{17}O-MRI inhalation experiment which was conducted in a healthy volunteer.

2956

Proof of concept for the separation of free and bound sodium in human brain through two-TE acquisitions at 3T

Yongxian Qian[1], Tiejun Zhao[2], Karthik Lakshmanan[1], Yulin Ge[1], Yvonne Lui[1], Timothy Shepherd[1], and Fernando E. Boada[1]

[1]Radiology, New York University, New York, NY, United States, [2]Siemens Medical Solutions USA, New York, NY, United States

In human brain, intracellular sodium ions (Na^+) are in slow and restricted motion due to their binding to negatively-charged macromolecules while their extracellular counterparts are in fast and unrestricted motion. This difference in motion properties leads to changes in bi-exponential transverse decay of free and bound sodium ions, which have been explored previously as a means to separate free and bound sodium. In this study, a new approach is proposed to separate free and bound sodium using single-quantum sodium images, without the SNR and SAR limitations as encountered in the triple-quantum filtering approach.

2957

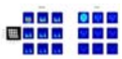

3D Multi-Echo Radial Imaging of $^{23}$Na (3D-MERINA) for time-efficient multi-parameter mapping

Yasmin Blunck[1], Sonal Josan[2], Brad A Moffat[3], Roger J Ordidge[3], Jon O Cleary[3,4], and Leigh A Johnston[1,4]

[1]Electrical & Electronic Engineering, University of Melbourne, Melbourne, Australia, [2]Siemens Healthcare, Melbourne, Australia, [3]Anatomy & Neuroscience, University of Melbourne, Melbourne, Australia, [4]joint senior authors

Challenging imaging characteristics (low SNR, fast bi-exponential decay) have so far limited the application of ^{23}Na-MRI in clinical environments. This work presents 3D Multi-Echo Radial Imaging of ^{23}NA (3D-MERINA), a time-efficient acquisition protocol from which multiple parameter maps (sodium-density, $T_2{}^*{}_{slow}$ and $T_2{}^*{}_{fast}$, free ^{23}NA) can be derived in a single acquisition. Phantom and in-vivo measurements were analysed for the evaluation of parameter mapping and the inference of tissue characteristic based on decay behaviour. All parameters were acquired in a single sodium-density-weighted acquisition under relatively low SAR. Future investigation will exploit 3D-MERINA for SQF-SNR enhancement and the detection of MQF contrasts.

2958

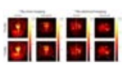

Elliptically-shaped 1Tx4Rx Coil for ^{23}Na Body MRI at 7T

Tanja Platt[1], Nicolas G. R. Behl[1], Thomas M. Fiedler[1], Armin M. Nagel[1,2], Andreas K. Bitz[1], Peter Bachert[1], Mark E. Ladd[1], Mark O. Wielpütz[3], Hans-Ulrich Kauczor[3], and Reiner Umathum[1]

[1]Medical Physics in Radiology, German Cancer Research Center (DKFZ), Heidelberg, Germany, [2]Institute of Radiology, University Hospital Erlangen, Erlangen, Germany, [3]Diagnostic and Interventional Radiology, University Hospital Heidelberg, Heidelberg, Germany

Up to now, only a few abdominal ^{23}Na-MRI studies have been performed at 7T. In this work a ^{23}Na body coil for 7T was enhanced. To achieve an improved homogeneity in the transmit field and in the receive sensitivity, transmit phase settings were optimized and four separate receive channels were implemented. Field distributions in a phantom were obtained for the original and the enhanced configuration. Both setups were applied to the human chest and abdomen. Transmit and receive homogeneity are markedly improved for the enhanced setup. Improvements for *in-vivo* image quality are especially visible in the contour of the body.

2959

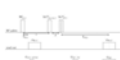

In Vivo Double Quantum Filtered 23Na Imaging of Human Skeletal Muscle

Lena V. Gast[1], Michael Uder[1], and Armin M. Nagel[1]

[1]Institute of Radiology, University Hospital Erlangen, Erlangen, Germany

Double quantum filtered sodium (^{23}Na) MRI represents a way to examine the degree of tissue microstructure but suffers from low signal intensity and therefore long acquisition time. In this work we developed an efficient simultaneous acquisition scheme of single and double quantum images and determined the optimum acquisition parameters for human skeletal muscle. The feasibility of double quantum filtered ^{23}Na images of human lower leg at 3T was shown.

2960

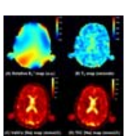

Variable Flip Angle Pipeline for in vivo Sodium Concentration Measurements (VaSCo)

Arthur Coste[1], Fawzi Boumezbeur[1], Alexandre Vignaud[1], Guillaume Madelin[2], Kathrin Reetz[3], Denis Le Bihan[1], Cécile Lerman[1], and Sandro Romanzetti[3]

[1]NeuroSpin, CEA, Paris Saclay University, Gif-sur-Yvette, France, Paris, France, [2]Center for Biomedical Imaging, Department of Radiology, New York University Langone Medical Center, New York, USA, [3]Aachen University Clinic, Neurology Department, Aachen, Germany

This work presents a new method to measure Sodium concentration in human tissue using the Variable Flip Angle method with optimized acquisition parameters. Healthy volunteers were scanned and measures provided concentration values and T1 values in agreement with litterature values.

2961

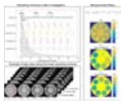

Optimizing the precision and accuracy of sampling schemes for T2* quantification of the fast biexponential decay of sodium MRI

Jonathan M. Lommen[1], Sebastian Flassbeck[1], Nicolas G.R. Behl[1], Mark E. Ladd[1], and Armin M. Nagel[1,2]

[1]*Medical Physics in Radiology, German Cancer Research Center (DKFZ), Heidelberg, Germany,* [2]*Institute of Radiology, University Hospital Erlangen, Erlangen, Germany*

Sodium imaging is mainly performed with spin-density weighted sequences to quantify tissue sodium concentration. However, relaxation weighting can add additional specific information. We pursue appropriate sampling for low SNR and fast biexponential decay. The accuracy and precision of typical T_2^* measurements is determined for different sampling schemes by simulation and phantom measurements. We developed a dedicated sampling scheme for brain parenchyma employing numerical optimization. The results suggest that averaging is preferable to increase reliability compared to denser temporal sampling. In-vivo comparison confirmed the advantage of the optimized patter with increased separation of the decay components.

2962

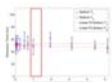

Influences of MRI proton contrast agent on sodium MRI at clinical 3T field strengths

Nadia K Paschke[1], Wiebke Neumann[1], Tanja Gaa[1], Andreas Neubauer[1], Lothar R Schad[1], and Frank G Zöllner[1]

[1]*Computer Assisted Clinical Medicine, Medical Faculty Mannheim, Heidelberg University, Mannheim, Germany*

Sodium MRI enables to measure tissue sodium content (TSC) non-invasively, which provides additional cellular information and can serve as biomarker e.g. for tumor imaging. Thus, sodium imaging can complement standard clinical protocols. Many clinical routine protocols include perfusion scans with proton contrast agents but the influences on sodium relaxation times and therefore quantification accuracies of TSC are unknown. Our preliminary results showed no significant changes in sodium T_1 and only small reductions of T_2 with clinically relevant concentrations of contrast agents. Therefore, proton contrast agents are not expected to influence the TSC quantification in UTE sodium sequences.

2963

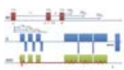

Relaxation in Simultaneously Acquired Single and Triple Quantum Filtered Sodium Imaging

Wieland A. Worthoff[1], Aliaksandra Shymanskaya[1], and N. Jon Shah[1,2]

[1]*Institut of Neuroscience and Medicine - 4, Forschungszentrum Jülich GmbH, Jülich, Germany,* [2]*Department of Neurology, Faculty of Medicine, JARA, RWTH Aachen University, Aachen, Germany*

Sodium imaging delivers valuable information about metabolism and disease. The spin dynamics of sodium are significantly impacted by the environment of the nuclei, multiple quantum coherences might develop via the quadrupole interaction. This allows imaging with multi quantum filters (MQF) to achieve weightings towards different sodium compartments. MQF sodium signals are detected with three consecutive RF pulses, by placing a readout train between the first and second RF pulse, a fully quantitative characterisation of relaxation properties in a two-compartment model is possible from measurements within a single sequence.

2964

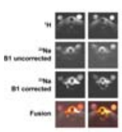

Sodium MRI of the thyroid gland at 7 tesla

Dimitri Welting[1], Wybe van der Kemp[1], Ingmar Voogt[1], Armin Nagel[2,3], Mark Ladd[2], Peter Luijten[1], Alexander Raaijmakers[1,4], Dennis Klomp[1], Nicolas Behl[2], and Mariska Luttje[1]

[1]*Imaging Division, University Medical Center, Utrecht, Netherlands,* [2]*Medical Physics in Radiology, German Cancer Research Center (DKFZ), Heidelberg, Germany,* [3]*Institute of Radiology, University Hospital Erlangen, Erlangen, Germany,* [4]*Biomedical Image Analysis, Eindhoven University of Technology, Eindhoven, Netherlands*

This work shows the potential of sodium imaging of the thyroid gland in vivo at 4mm isotropic resolution integrated to ^{1}H imaging. An optimized setup combined with tuned sequences and B_1 corrections enables quantitative sodium mapping of the thyroid gland and its surrounding tissue. The thyroid gland has the highest concentration of sodium in this part of the neck, estimated to be 64.5 mmol/L in vivo. Sodium imaging might open up the detection of (lymph node) metastases of thyroid cancer, as they are expected to exceed the healthy concentration of sodium detected in the head and neck region.

2965

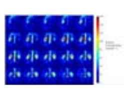

Quantitative Sodium MRI of the Human Kidney at 3T

James Grist[1], Frank Riemer[2], Esben Hansen[3], Mary McLean[4], Rasmus Tougaard[3], Joshua Kaggie[1], Martin Graves[5], Hans Stodkilde-Jorgensen[3], Ferdia Gallagher[1], and Christoffer Laustsen[3]

[1]*Radiology, University of Cambridge, Cambridge, United Kingdom,* [2]*University of Cambridge, Cambridge, United Kingdom,* [3]*MR Research Center, Aarhus University,* [4]*Cambridge Institute, Cancer Research UK,* [5]*MRI, Addenbrooke's Hospital, Cambridge, United Kingdom*

Imaging of the renal system with sodium MRI has gained interest in the past few years, especially in using the technique to quantify, and assess for, changes in the cortio-medullary sodium gradient.

The main hindrance for previous work has been the lengthy scan time required to obtain sodium images. However, utilizing a 3D cones trajectory, the work presented here shows good detection of the cortio-medullary sodium gradient, in a clinically feasible scan time, in a sample of six healthy controls.

Traditional Poster

MRS Applications

Exhibition Hall 2966-2989 Thursday 13:00 - 15:00

2966 

Metabolite levels in hippocampus and temporal lobe using long TE magnetic resonance spectroscopic imaging for epilepsy diagnostics

Francois Lazeyras[1], Maria Toms[1], and Antoine Klauser[1]

[1]Radiology and Medical Informatics, University of Geneva, Geneva, Switzerland

The aim of this study is to obtain normative reference 1H-MRSI data on the ratio of total NAA to total Cho in healthy subjects for subsequent use for clinical diagnosis of epileptic patients. Furthermore, we studied the effect of voxel content, primarily white matter and regional gray matter on metabolic levels.

2967 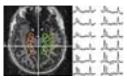

7T MRSI Identifies Neuronal and Axonal Injury in a Limbic Network in MRI Negative Veterans with mTBI and PTSD

Hoby Hetherington[1], Anne VanCott[2], Victor Yushmanov[1], Jodilyn Roberts[3], Daniela Mejia[2], Monique Kelley[4], and Jullie Pan[2]

[1]Radiology, University of Pittsburgh, Pittsburgh, PA, United States, [2]Neurology, University of Pittsburgh, Pittsburgh, PA, United States, [3]Neurology, Pittsburgh Veterans Administration Medical Center, PA, United States, [4]Biostatistics, Pittsburgh Veterans Administration Medical Center, PA, United States

Following mild traumatic brain injury (mTBI) many veterans continue to experience persistent symptoms despite an absence of significant findings on conventional MRI. In this study we acquired MRSI and volumetric data from veterans with a history of mTBI and PTSD, healthy age matched controls and veterans with PTSD without a history of mTBI. Data was acquired from the hippocampus (single slice MRSI) and cingulate (multiband MRSI). Significant declines in NAA/Ch were seen in the hippocampal formation in comparison to healthy controls and veterans with PTSD. Further, reductions in hippocampal NAA/Ch were statistically correlated with reductions in NAA/Ch from the cingulate

---

2968 

Lactate is associated with tumour grading in breast cancer – An ex vivo study on whole breast tumours using multiple quantum coherence (MQC) MRS

Sai Man Cheung[1], Ehab Husain[2,3], Yazan Masannat[3,4], Klaus Wahle[3,5], Steven D Heys[3,4], and Jiabao He[1]

[1]Aberdeen Biomedical Imaging Centre, University of Aberdeen, Aberdeen, United Kingdom, [2]Pathology Department, Aberdeen Royal Infirmary, Aberdeen, United Kingdom, [3]School of Medicine, University of Aberdeen, Aberdeen, United Kingdom, [4]Breast Unit, Aberdeen Royal Infirmary, Aberdeen, United Kingdom, [5]Strathclyde Institute of Pharmacy and Biological Sciences, Glasgow, United Kingdom

Breast cancer is associated with increased lactate production in tumour, known as Warburg effect, that is postulated to enhance cancer cell survival advantage and invasiveness. However, current evidence, mainly based on xenografted animal models or biopsy results, remains controversial, where non-identical biological environments are compared to humans, or partial sampling error may play a role. We therefore examined the role of lactate concentration in whole human breast tumour, and hypothesised that there is a difference in lactate concentration between grade II and III breast cancer. To extract lactate under overwhelming lipid signal, MQC MRS was optimised for robust measurement.

2969 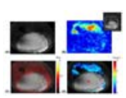

Assessment of Response to Radiation Therapy Using High-Resolution Proton MRSI in Soft Tissue Sarcoma Patients

Chao Ma[1], Yen-Lin Chen[2], Kyung-Wook Jee[2], Ruth Lim[1,2], Ivan A. Chebib[3], Muge Oner Tamam[1], Shuang Hu[1,4], and Georges El Fakhri[1]

[1]Gordon Center for Medical Imaging, Radiology, Massachusetts General Hospital, Harvard Medical School, Boston, MA, United States, [2]Radiation Oncology, Massachusetts General Hospital, Harvard Medical School, Boston, MA, United States, [3]Pathology, Massachusetts General Hospital, Harvard Medical School, Boston, MA, United States, [4]Nuclear Medicine, West China Hospital, Sichuan University, Chengdu, People's Republic of China

As the recent rapid development of radiation therapy techniques glowingly facilitate an individualized adaptive radiation therapy (RT), the roles of imaging as a tool to assess the early treatment response to RT or to tailor the treatment volume are becoming important. Conventional structural MR images have limited specificities in delineating and differentiating between residual/recurrent tumor and treatment effects (e.g., edema, inflammation, and radiation necrosis). This work presents a pilot study to assess response to RT in soft tissue sarcoma (STS) patients using a recently proposed rapid high-resolution MRSI method: SPectroscopic Imaging by exploiting spatiospectral CorrElation (SPICE).

2970 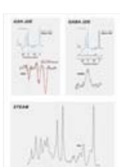

Towards in vivo neurochemical profiling of multiple sclerosis with MR spectroscopy at 7 Tesla: Cross-sectional assessment of frontal-cortex glutathione, GABA, and glutamate in individuals with relapsing-remitting and progressive multiple sclerosis

Kelley M. Swanberg[1,2], Hetty Prinsen[2], Robert K. Fulbright[2], David Pitt[3], Katherine Destefano[3], Mary Bailey[3], and Christoph Juchem[1,2,3,4]

[1]Biomedical Engineering, Columbia University School of Engineering and Applied Science, New York, NY, United States, [2]Radiology and Biomedical Imaging, Yale University School of Medicine, New Haven, CT, United States, [3]Neurology, Yale University School of Medicine, New Haven, CT, United States, [4]Radiology, Columbia University School of Engineering and Applied Science, New York, NY, United States

Multiple sclerosis (MS) is an autoimmune disease that damages the central nervous system and affects an estimated 2.3 million people worldwide. One potential key to understanding MS is investigating the metabolic distinctions between its relapsing-remitting (RR-MS) and progressive courses (P-MS). We obtained single-voxel metabolic ^{1}H spectra at 7 Tesla from the frontal cortex of RR-MS and P-MS patients and controls to explore the effects of disease state on concentrations of brain metabolites like glutathione, GABA, glutamate, and N-acetyl aspartate (NAA). Our results suggest an age- and disease-related decrease in glutamate, as well as a disease-related decrease in NAA, in patients with P-MS relative to RR-MS and controls without MS. No disease-related changes in GSH or GABA were found. Our data underscore the importance of continued investigation into the potential physiological distinctions among various MS subtypes.

2971

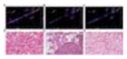

KIDNEY CANCER SUBTYPES, IDENTIFIED BY TWO DIMENSIONAL MR SPECTROSCOPY, MAY EVENTUALLY ALLOW TREAMENT OF CLINICALLY DISTINCT DISEASES.

Aaron James Urquhart[1], Sharon Del Vecchio [1,2], Keng Lim Ng[1,2,3], Hemamali Samaratunga[4], Graham John Galloway[1], Peter Malycha[1], Simon Wood[1,2,3], Glenda C Gobe[1,2], and Carolyn E Mountford[1]

[1]Translational Research Institute, Brisbane, Australia, [2]Centre for Kidney Disease Research, UQDI, The University of Queensland, Brisbane, Australia, [3]Department of Urology, Princess Alexandra Hospital, Brisbane, Australia, [4]Aquesta Pathology, Brisbane, Australia

Small renal masses, such as non-clear cell renal carcinoma (non-ccRCC), can be monitored rather than resected as morbidity is unlikely. The distinction between malignant clear cell RCC (ccRCC) from indolent RCC subtypes and benign renal tumour is not possible by imaging thus some patients undergo unnecessary surgery[1]. Using 2D COrrelated SpectroscopY we report that normal renal tissue, non-ccRCC and ccRCC each has different chemical profile. ccRCC differs from normal tissue with cholesterol and lipid increased by 572% and 481% (P=0.001); decreased alanine 51% (P=0.001); valine 57% (P=0.003) and lysine 46% (P=0.005). When comparing ccRCC to the non-ccRCC there are increases in valine 48% (P=0.004) and lysine 40% (P=0.04).

2972

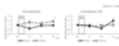

Longitudinal evaluation of neurochemical modulation induced by quadripulse stimulation (QPS) using ultra-short TE STEAM MRS

Hitoshi Kubo[1,2], Takenobu Murakami[2,3], Masafumi Harada[2,4], Noboru Oriuchi[2], Seiichi Takenoshita[2], Shoji Yabuki[1], and Yoshikazu Ugawa[2,3]

[1]Preparing Section for New Faculty of Medical Science, Fukushima Medical University, Fukushima, Japan, [2]Advanced Clinical Research Center, Fukushima Medical University, Fukushima, Japan, [3]Department of Neurology, Fukushima Medical University, Fukushima, Japan, [4]Department of Radiology, The University of Tokushima Graduate School, Tokushima, Japan

To evaluate longitudinal neurochemical modulation induced by rTMS, we used ultra-short TE STEAM MRS. Glx, GABA and 15 other metabolites were measured using 3T MR equipment longitudinally and LCModel was used to calculate these concentrations quantitatively. QPS was employed as rTMS and left M1 was stimulated in each subject. Five healthy male volunteers participated in this study. The long-term depression intervention induced Glx increment, and the long-term potentiation intervention induced GABA decrement. The present results suggested a usefulness of the ultra-short TE STEAM MRS in evaluation of the longitudinal neurochemical modulation induced by rTMS.

2973

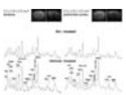

Effect of psychotherapeutic approaches on cortical and striatal neurochemical profile in a juvenile rat model of ADHD: an in vivo 1H MRS study @ 11.7T

Alireza Abaei[1], Francesca Rizzo[2,3], Dinesh K Deelchand[4], Tobias M. Böckers[2], and Volker Rasche[1]

[1]Core Facility Small Animal Imaging, Ulm University, Ulm, Germany, [2]Institute of Anatomy and Cell Biology, Ulm University, Ulm, Germany, [3]Department of Child and Adolescent Psychiatry, Ulm University, Ulm, Germany, [4]Center for Magnetic Resonance Research, University of Minnesota, MN, United States

Proton MRS is employed to assess the effect of systemic administration of aripiprazole and riluzole on the neurochemical profile of distinct functional regions in juvenile rat brain non-invasively *in vivo*. In this study, a dedicated optimized STEAM sequence with single-shot phase and frequency correction, and image-based shimming was applied to quantify subtle changes in the brain metabolites concentration during drug treatment in an ADHD rat model.

2974

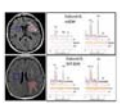

Influence of signal-to-noise, spectral filtering, and Cramér–Rao Lower Bounds for the optimal use of in vivo 2HG MRS to determine glioma IDH mutation status

Sunitha B Thakur[1], Olivia Sutton[1], Samuel R Briggs[1], Ralph Noeske[2], Andrei Holodny[1], Ingo K Mellinghoff[1], and Robert J Young[1]

[1]Memorial Sloan Kettering Cancer Center, New York, NY, United States, [2]GE HealthCare, Berlin, Germany

Cancer-associated mutations in IDH results in overproduction of 2-hydroxyglutarate (2HG). A few studies have evaluated the use of MR spectroscopy (MRS) technology to noninvasively determine IDH mutation status by measuring 2HG concentrations. However, it is unknown how factors such as signal-to-noise ratio (SNR), spectral apodization, and Cramér–Rao Lower Bounds (CRLB) can influence MRS sensitivity and specificity for 2HG detection in gliomas. This study seeks to define the ideal method to define optimal thresholds of CRLB and spectral filtering resulting in improved 2HG detection sensitivity without a drop in MRS specificity.

2975

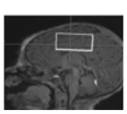

GABA concentration measurements in infants without sedation

Ryan J. Larsen[1], Borjan Gagoski[2], Marie Drottar[2], Thea Francel[2], Alana Matos[2], Clarisa Carruthers[2], Catherine Vu[2], Jonathan Litt[3], Bradley P. Sutton[1,4], and Ellen Grant[5]

[1]Beckman Institute, University of Illinois at Urbana-Champaign, Urbana, IL, United States, [2]Boston Children's Hospital, Harvard Medical School, Boston, MA, United States, [3]Beth Israel Deaconess Medical Center, Boston, MA, United States, [4]Department of Bioengineering, University of Illinois at Urbana-Champaign, Urbana, IL, United States, [5]Boston Children's Hospital, Harvard Medical School, Boston, MA

We report measurements of GABA concentration in infants without sedation using the MEshcher-Garwood (MEGA) sequence. Single-voxel measurements were performed in 114 infants at approximately one month and/or three months of age. Quantification is performed with water scaling, and concentration values are reported in units of mM of NMR-visible water in the brain. For the two scan times, we found the inter-subject coefficient of variation (CV) of GABA to be 8% and 9%, respectively. Average GABA concentration values are 7% higher for the 3 month scan than the 1 month scan, indicating a gradual increase in GABA concentration after birth.

2976

Longitudinal MRS Study following Treatment of Early-Phase Psychosis with N-Acetylcysteine

Andrew M Wright[1], Ruoyun Ma[2], Tom Hummer[3], Michael Francis[3], Andrew Visco[3], Nikki Mehdiyoun[3], Ulrike Dydak[2,4], and Alan Breier[3]

[1]Health Sciences, Purdue University, Lafayette, IN, United States, [2]Purdue University; Indiana University School of Medicine, [3]Indiana University School of Medicine, [4]Health Sciences, Purdue University; Indiana University School of Medicine, Lafayette, IN, United States

This study followed early stage schizophrenia patients undergoing treatment with single voxel MRS in the frontal lobe. Patients were split into a placebo (sugar pills) and treatment (N-acetylcysteine (NAC)) group and followed over the course of a year where they participated in 2-3 MRS scans at regular intervals. Patients show significantly elevated concentrations of Cre and Glx when compared to controls. This significance remained throughout the longitudinal study in intra- and inter-patient comparisons. This unchanged elevation of Glx and Cre contradicts the hypothesis that NAC will work to normalize these metabolite concentrations.

2977

Evaluation of the amygdala and the anterior cingulate cortex by single voxel proton MR spectroscopy in patients with post-traumatic stress disorder after earthquake

Xiaorui Su[1], Weina Wang[1], Qiyong Gong[1], and Qiang Yue[1]

[1]Huaxi MR Research Center, Department of Radiology, West China Hospital of Sichuan University, chengdu, People's Republic of China

In order to explore the changes of metabolites in the amygdala and the anterior cingulate of PTSD after earthquake, MR spectroscopy was applied. MRS showed higher ml and NAA levels in ACC, higher NAA levels in the right amygdala of PTSD group as compared to healthy controls. Besides, both in PTSD and healthy controls, NAA+NAAG levels were higher in the left amygdala than the right. And our results indicate there are some metabolic changes in amygdala and ACC of PTSD subjects. Whether combining depressive disorders, cause of PTSD and types of traumatic causes may have contributed to the inconsistency.

2978

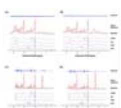

Attenuated excitatory metabolism in the prefrontal Cortex of single prolonged stress model: in vivo and ex vivo proton magnetic resonance spectroscopy

Song-I LIm[1,2], Kyu-Ho Song[1], Chi-Hyeon Yoo[1,2], Dong-Choel Woo[2], and Bo-Young Choe[1]

[1]Department of Biomedical Engineering, and Research Institute of Biomedical Engineering. The Catholic University of Korea College of Medicine, Seoul, Korea, Republic of, [2]Asan Institute for Life Sciences, Asan Medical Center, Seoul, Korea, Republic of

The purpose of the study was to evaluate neurochemical changes in the prefrontal cortex of rats during time-dependent sensitization in the single prolonged stress (SPS) model that reveals pathogenetic neurometabolites characteristic of posttraumatic stress disorder by using *in vivo* and *ex vivo* proton magnetic spectroscopy. After the time-sensitization period, Glu and Cr levels were reduced and Cho and Lac levels were increased in SPS group in comparison with control group. These indicate that SPS induced sustained adaptation of the glutamatergic activity in PFC.

2979

Posterior cingulate gyrus metabolism differs in parkinson's disease patients with and without cognitive impairment

Mingming Huang[1], Xiaobao Li[1], Guiquan Shen[1], and Hui Yu[1]

[1]Department of Radiology, Affiliated Hospital of Guizhou Medical University, Guiyang, China, Guiyang, People's Republic of China

1H-MRS technology combined with Lcmodel software were used to quantitative the concentration of metabolites of posterior cingulate gyrus (PCC) in Parkinson's disease patients with(PDCI) and without cognitive impairment(PDN), and MMSE and MOCA tests were also performed. Compared with controls, the concentration of total creatine (tCr), N-acetylaspartate(NAA), myo-Inositol(mI), Glutathione (GSH), as well as glycerophosphocholine + phosphocholine (tCho) were found significantly decreased in PCC in PDCI group , but no changes were found in PDN. Additionally, correlations between concentration of tCr, GSH, tCho, NAA and MMSE (MoCA) scores can also be found . These results may indicate that the metabolites abnormalities in PCC might be used as a biomarker to track cognitive decline in Parkinson's disease in a clinical setting.

2980

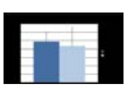

Brain Metabolite Changes During Motor Task: A 3T functional MRS Study

Jay Hennessy[1,2] and Jamie Near[1,2]

[1]Biomedical Engineering, McGill University, Montreal, QC, Canada, [2]Brain Imaging Center, Douglas Mental Health Institute, Montreal, QC, Canada

Previous fMRS studies at 7T have shown changes in brain metabolite levels elicited by different stimuli. This 3T study employed a modified version of PRESS to effectively measure neurochemical changes generated by a finger tapping task during the MRS scan. The results show lactate in the motor cortex increased approximately 11%, while glutamate and aspartate trend toward a 2% increase and 3% decrease respectively. More subjects are required for further validation.

2981

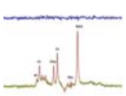

7 Tesla 1H MR Spectroscopy of the Motor Cortex following Transcranial Direct Current Stimulation

Kayla Ryan[1,2], Krzysztof Wawrzyn[3], Joseph Gati[1], Blaine Chronik[1,2,3], Neil Duggal[4], and Robert Bartha[1,2]

[1]Centre for Functional and Metabolic Mapping, Robarts Research Institute, London, ON, Canada, [2]Medical Biophysics, Western University, London, ON, Canada, [3]Physics and Astronomy, Western University, London, ON, Canada, [4]Clinical Neurological Sciences, Division of Neurosurgery, London Health Sciences Centre, London, ON, Canada

Transcranial direct current stimulation (tDCS) is a form of non-invasive brain stimulation that has been used to treat numerous cognitive and motor disorders. However, its mechanism of action is poorly understood, resulting in controversy over its effectiveness. The current study used ultra-high magnetic field (7 Tesla) magnetic resonance spectroscopy to determine if metabolite ratios were altered after the application of tDCS. In this preliminary study of 8 subjects, we found no differences in metabolite ratios in the motor cortex immediately following stimulation.

2982 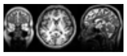

Brain Metabolite Level Estimation at Anterior Cingulate Cortex in Fibromyalgia Using Advanced MRS

JY-KANG ADRIAN LIOU[1,2,3], Tun-Wei Hsu[1,2,3], Wei-Ta Chen[2,4], Chien-Yuan Eddy Lin[5,6], and Jiing-Feng Lirng[1,2,3,4]

[1]RADIOLOGY, TAIPEI VETERANS GENERAL HOSPITAL, Taipei, Taiwan, [2]School of Medicine, National Yang-Ming University, Taipei, Taiwan, [3]School of Biomedical Engineering and Technology, Faculty of Imaging and Radiological Sciences, National Yang-Ming University, Taipei, Taiwan, [4]NEUROLOGY, TAIPEI VETERANS GENERAL HOSPITAL, Taipei, Taiwan, [5]GE Healthcare, Taipei, Taiwan, [6]MR Research China, GE Healthcare, Beijing, People's Republic of China

We apply MEGA-PRESS MRS to measure brain metabolite level of Fibromyalgia patients and healthy controls at anterior cingulate cortex. The results show higher levels of GABA in Fibromyalgia than healthy controls but no significant difference was found in glutamine and glutamate levels.

2983 

Treatments in chronic liver disease induced hepatic encephalopathy: a longitudinal in vivo 1H MRS study of brain metabolism using rifaximin

Emmanuelle Flatt[1], Cristina Cudalbu[2], Olivier Braissant[3], Stefanita Mitrea[2], Valérie McLin[4], Dario Sessa[4], and Rolf Gruetter[5]

[1]Laboratory for Functional and Metabolic Imaging, Center for Biomedical Imaging, Ecole polytechnique Fédérale de Lausanne, Lausanne, Switzerland, [2]Center for Biomedical Imaging(CIBM), Ecole Polytechnique Fédérale de Lausanne, Lausanne, Switzerland, [3]Service of Biomedicine, University Hospital of Lausanne, Lausanne, Switzerland, [4]Swiss Center for Liver Disease in Children, Department of Pediatrics, University Hospitals Geneva, Geneva, Switzerland, [5]Laboratory for Functional and Metabolic Imaging (LIFMET) & Center for Biomedical Imaging (CIBM), Ecole polytechnique Fédérale de Lausanne, Lausanne, Switzerland

Hepatic encephalopathy (HE) is a severe complication of chronic liver disease (CLD). Treatments for HE have focused on reducing plasma ammonia levels implicated in HE pathogenesis. The antibiotic rifaximin reduces the production of gut ammonia which is considered to be the main toxin in CLD-induced HE. Rifaximin is commonly used in the treatment of HE and has been shown to reduce the frequency of HE episodes, but the molecular mechanisms behind this effect are unknown. We assessed, in vivo and longitudinally, the effect of rifaximin on brain metabolites in bile duct ligated rats using high-field proton Magnetic Resonance Spectroscopy.

2984 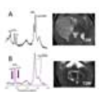

Metabolic Subtypes of Atypical Teratoid Rhabdoid Tumors

Benita Tamrazi[1], Marvin D Nelson[1], and Stefan Bluml[1]

[1]Radiology, Children's Hospital Los Angeles, Los Angeles, CA, United States

Atypical Teratoid Rhabdoid Tumors (AT/RT) are highly malignant pediatric brain tumors distinguished from other primitive/embryonal tumors by alterations of the SMARCB1 gene. Recently, two molecular subtypes have been described for AT/RTs. We have reviewed MR spectra of AT/RT patients and identified two distinct clusters in respect to their metabolic profiles. Should a correlation with genetic subtypes be confirmed, in vivo MRS could potentially play a key role in the initial stratification of patients diagnosed with AT/RT.

2985 

Experimental setup for direct observation of hippocampal glycolysis in rat brain as a marker of cellular health

Dirk Ernst Johannes Cleppien[1], Bernd Lecher[2], Christian Kempe[2], Markus Sack[1], Anja Meier[2], Max Kullack[2], Wolfgang Weber-Fahr[1], and Alexander Sartorius[1]

[1]RG Translational Imaging, Department NeuroImaging, Central Institute of Mental Health, Medical Faculty Mannheim, University of Heidelberg, Mannheim, Germany, [2]mfd diagnostics GmbH, Wendelsheim, Germany

Glycolysis is fundamental for cerebral energy metabolism. The current glycolysis pathway gives direct information about the local cellular health. To investigate hippocampal glycolysis in living rats, we established an experimental setup combining MRS and laser spectroscopy. It provides the opportunity to observe the behavior to the involved substances (glucose, lactate, NADH) for different glycolytic pathways. Under hyperglycemic conditions, blood oxygen limits glucose consumption leading to drops in NADH and lactate. In contrast, NADH and lactate concentrations increase under anaerobic conditions. This corresponds well with known literature and demonstrates the power of the presented setup to characterize hippocampal glycolysis in vivo.

2986 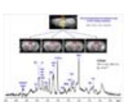

Demyelination of the corpus callosum in a mouse model of mucopolysaccharidosis type I

Ivan Tkac[1], Igor Nestrasil[2], Steven Q Le[3], Jakub Tolar[4], and Patricia I Dickson[3]

[1]Center for Magnetic Resonance Research, University of Minnesota, Minneapolis, MN, United States, [2]Departmant of Pediatrics, University of Minnesota, Minneapolis, MN, United States, [3]Department of Pediatrics, Los Angeles Biomedical Research Institute at Harbor-UCLA Medical Center, Torrance, CA, United States, [4]Pediatric Bone and Marrow Transplantation, University of Minnesota, Minneapolis, MN, United States

Mucopolysaccharidosis type I (MPS I) is an autosomal lysosomal storage disease caused by deficiency of α-L-iduronidase enzyme, which results in glycosaminoglycans accumulation within the lysosomes. MPS I leads to progressive loss of cognitive function and substantial physical disease in children. Abnormal myelin composition and reduced expression of myelin-related genes has been recently reported in a canine model of MPS I. The purpose of this study was to demonstrate whether demyelination of the corpus callosum can be detected also in a mouse model of MPS I using *in vivo* ^{1}H MRS at 9.4 T.

2987 

Investigating metabolic alterations in a depressive-like rat model of chronic forced swimming stress using in vivo proton magnetic resonance spectroscopy at 7T

Chi-Hyeon Yoo[1,2], Kyu-Ho Song[1], Song-I Lim[1,2], Do-Wan Lee[3], Dong-Cheol Woo[2], and Bo-Young Choe[1]

[1]Department of Biomedical Engineering, and Research Institute of Biomedical Engineering, The Catholic University of Korea College of Medicine, Seoul, Korea, Republic of, [2]Asan Institute for Life Sciences, Asan Medical Center, Seoul, Korea, Republic of, [3]Ehwa Brain Institute, Ehwa Woman's University, Seoul, Korea, Republic of

The chronic forced swimming stress (CFSS) depression-like animal model has been widely used to investigate the pathophysiology of depression focusing on the monoamine system. The goal of this study was to investigate the CFSS-induced metabolic effects in the prefrontal cortex (PFC) of animals showing depression-like behavior using high-field and short echo time (TE) in vivo proton magnetic resonance spectroscopy (1H MRS). The results suggest that high-field and short TE in vivo 1H MRS can reliably quantify the key metabolites involved in depression and CFSS-induced behavioral despair and metabolic alterations similar to those found in human patients with depressive disorders.

2988

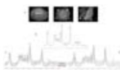

Metabolic Assessment of a Migraine Model using Relaxation-Enhanced 1H Spectroscopy at Ultra-High Field

Nastaren Abad[1,2], Jens T. Rosenberg[1], Tangi Roussel[3], Dillon Grice[2], Michael G. Harrington[4], and Samuel Colles Grant[1,2]

[1]Center for Interdisciplinary Magnetic Resonance, National High Magnetic Field Laboratory, Tallahassee, FL, United States, [2]Chemical & Biomedical Engineering, Florida State University, Tallahassee, FL, United States, [3]Department of Chemical Physics, Weizmann Institute of Science, Rehovot, Israel, [4]Molecular Neurology Program, Huntington Medical Research Institutes, Pasadena, CA, United States

This study evaluates biochemical and metabolic imbalances that may result in a collection of dysfunctional pathways that are distinct in migraineurs. The high sensitivity and spectral dispersion available to ^{1}H MRS at 21.1 T expanded metabolic profiling in an animal model of migraine to include total creatine (tCr), choline (Cho), N-acetyl-aspartate (NAA), myoinositol (mI), lactate (Lac), taurine (Tau), aspartate (Asp), Glx, a mixture of glutamate, glutamine and GABA, and Gly, the latter identified as a mixture of glycine, glutamine, and glutamate. For the migraine analogue, Lac, Gly and Tau increased while tCr decreased temporally and in comparison to saline controls.

2989

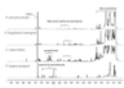

NMR phytometabolomics for evaluation of non-polar chemosensory signatures

Rama Jayasundar[1] and Aruna Singh[1]

[1]Department of NMR, All India Institute of Medical Sciences, New Delhi, India

With increasing interest in the role of taste related fatty acids in food, pharmacology, health and diseases, objective study of this chemosensory parameter has assumed importance. The potential of NMR metabolomics to fingerprint chemosensory properties has been explored in the context of non-polar phytocompounds in this study. Non-polar fractions obtained by dual phase (chloroform-methanol/water) extraction of select dietary plants (n=24) were studied using proton NMR spectroscopy. Partial Least Squares Discriminant Analysis of the spectral data showed distinct chemosensory based clustering. NMR based chemosensory studies of non-polar phytocompounds could open new applications in sensorial sciences related to lipids and fatty acids.

Traditional Poster

MRS Processing & Quantitation

Exhibition Hall 2990-3008 Thursday 13:00 - 15:00

2990

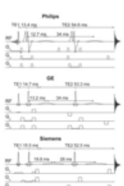

Integrative analysis of GABA-edited MRS data acquired at 19 research sites

Mark Mikkelsen[1,2], Maiken K. Brix[3,4], Pieter F. Buur[5], Kim M. Cecil[6], Kimberly L. Chan[1,2,7], David Y.-T. Chen[8], Alexander R. Craven[9,10], Koen Cuypers[11,12], Niall W. Duncan[13], Ulrike Dydak[14], David A. Edmondson[14], Gabriele Ende[15], Lars Ersland[10,16], Ian Greenhouse[17], Ashley D. Harris[18], Stefanie Heba[19], Tun-Wei Hsu[20], Jacobus F. A. Jansen[21], R. Marc Lebel[22], Chien-Yuan E. Lin[23], Jy-Kang Liou[20], Jiing-Feng Lirng[20], Ruoyun Ma[14], Celine Maes[11], Scott O. Murray[24], Sean Noah[17], Ralph Noeske[25], Michael D. Noseworthy[26], Georg Oeltzschner[1,2], James J. Prisciandaro[27], Nicolaas A. J. Puts[1,2], Timothy P. L. Roberts[28], Markus Sack[15], Napapon Sailasuta[29,30], Muhammad G. Saleh[1,2], Michael-Paul Schallmo[24], Nicholas Simard[31], Stephan P. Swinnen[11,32], Martin Tegenthoff[19], Peter Truong[29], Hans-Jörg Wittsack[33], Vadim Zipunnikov[34], Helge J. Zöllner[33,35], and Richard A. E. Edden[1,2]

[1]Russell H. Morgan Department of Radiology and Radiological Science, The Johns Hopkins University School of Medicine, Baltimore, MD, United States, [2]F. M. Kirby Research Center for Functional Brain Imaging, Kennedy Krieger Institute, Baltimore, MD, United States, [3]Department of Radiology, Haukeland University Hospital, Bergen, Norway, [4]Department of Clinical Medicine, University of Bergen, Bergen, Norway, [5]Spinoza Centre for Neuroimaging, Amsterdam, Netherlands, [6]Department of Radiology, Cincinnati Children's Hospital Medical Center, Cincinnati, OH, United States, [7]Department of Biomedical Engineering, The Johns Hopkins University School of Medicine, Baltimore, MD, United States, [8]Department of Radiology, Taipei Medical University Shuang Ho Hospital, New Taipei City, Taiwan, [9]Department of Biological and Medical Psychology, University of Bergen, Bergen, Norway, [10]NORMENT – Norwegian Center for Mental Disorders Research, University of Bergen, Bergen, Norway, [11]Department of Kinesiology, KU Leuven, Leuven, Belgium, [12]REVAL Rehabilitation Research Center, Hasselt University, Diepenbeek, Belgium, [13]Brain and Consciousness Research Centre, Taipei Medical University, Taipei, Taiwan, [14]School of Health Sciences, Purdue University, West Lafayette, IN, United States, [15]Department of Neuroimaging, Central Institute of Mental Health, Mannheim, Germany, [16]Department of Clinical Engineering, Haukeland University Hospital, Bergen, Norway, [17]Helen Wills Neuroscience Institute, University of California, Berkeley, Berkeley, CA, United States, [18]Department of Radiology, University of Calgary, Calgary, AB, Canada, [19]Department of Neurology, BG University Hospital Bergmannsheil, Bochum, Germany, [20]Department of Radiology, Taipei Veterans General Hospital, National Yang-Ming University School of Medicine, Taipei, Taiwan, [21]Department of Radiology, Maastricht University Medical Center, Maastricht, Netherlands, [22]GE Healthcare, Calgary, AB, Canada, [23]GE Healthcare, Taipei, Taiwan, [24]Department of Psychology, University of Washington, Seattle, WA, United States, [25]GE Healthcare, Berlin, Germany, [26]Department of Electrical and Computer Engineering, McMaster University, Hamilton, ON, Canada, [27]Department of Psychiatry and Behavioral Sciences, Medical University of South Carolina, Charleston, SC, United States, [28]Department of Radiology, Children's Hospital of Philadelphia, Philadelphia, PA, United States, [29]Research Imaging Centre, Centre for Addiction and Mental Health, Toronto, ON, Canada, [30]Department of Psychology, University of Toronto, Toronto, ON, Canada, [31]School of Biomedical Engineering, McMaster University, Hamilton, ON, Canada, [32]Leuven Research Institute for Neuroscience & Disease (LIND), KU Leuven, Leuven, Belgium, [33]Department of Diagnostic and Interventional Radiology, University Düsseldorf, Düsseldorf, Germany, [34]Department of Biostatistics, Johns Hopkins Bloomberg School of Public Health, Baltimore, MD, United States, [35]Institute of Clinical Neuroscience and Medical Psychology, Heinrich-Heine-University Düsseldorf, Düsseldorf, Germany

In this large multi-vendor, multi-site study, we seek to better understand the factors that impact quantitative outcomes of GABA-edited MR spectroscopy. Data from 187 participants from 19 research sites acquired on scanners from the three major vendors were pooled and analyzed using a standard pipeline. Coefficients of variation for GABA measurements acquired on each scanner platform and across the entire cohort were less than 11%. Multilevel linear modelling showed that most of the variance was accounted for by participant-level differences, while vendor-level differences accounted for comparatively more proportional variance than site-level differences.

2991

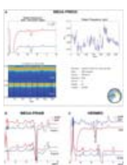

Gannet 3.0: Developing post-processing tools for accelerated J-difference editing

Muhammad Gulamabbas Saleh[1,2], Georg Oeltzschner[1,2], Mark Mikkelsen[1,2], Nicolaas A.J. Puts[1,2], and Richard A.E. Edden[1,2]

[1]Russell H. Morgan Department of Radiology and Radiological Science, The Johns Hopkins University School of Medicine, Baltimore, MD, United States, [2]F. M. Kirby Center for Functional Brain Imaging, Kennedy Krieger Institute, Baltimore, MD, United States

Initially conceived as a MATLAB-based batch-processing tool for GABA-edited MRS data acquired with MEGA-PRESS, Gannet 3.0 has been extended to provide new functionalities that can reconstruct data acquired using accelerated editing techniques of multiple metabolites and regions, perform frequency-and-phase correction (FPC), and perform fitting for GSH-edited spectra. We have demonstrated optimal FPC for MEGA-PRESS, MEGA-PRIAM and HERMES data, and fitting for GSH-edited spectra, rendering Gannet 3.0 a suitable post-processing tool for both conventional and accelerated editing.

2992

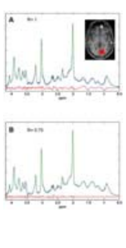

Basis set optimization for quantification of semi-LASER at 9.4T under consideration of CP effect and relaxation

Ioannis-Angelos Giapitzakis[1,2] and Anke Henning[1,3]

[1]High Field Magnetic Resonance, Max Planck Institute for Biological Cybernetics, Tuebingen, Germany, [2]Graduate School of Neural and Behavioural Sciences, Tuebingen, Germany, [3]Institute of Physics, Ernst-Moritz-Arndt University Greifswald, Greifswald, Germany

In this abstract, we evaluated the Carr-Purcell behavior of semi-LASER sequence at 9.4T and we studied the influence of different relaxation times between the different moieties of NAA and NAAG using in-vivo acquired from occipital lobe and simulated spectra. The results indicate that differences in the relaxation time between different moieties can affect the fitting results and the metabolites levels. Moreover, an estimated value for the relaxation time of NAA-aspartate moiety is given. This work indicates that more measurements and investigation should be done, studying more metabolites and brain regions.

2993

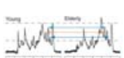

Influence of age-specific macromolecular pattern on MRS quantification

Malgorzata Marjanska[1], J Riley McCarten[2], Dinesh Deelchand[1], Laura S Hemmy[2], and Melissa Terpstra[1]

[1]Center for Magnetic Resonance Research and Department of Radiology, University of Minnesota, Minneapolis, MN, United States, [2]Geriatric Research Education and Clinical Center, Minneapolis VA Medical Center, MN, United States

The resonances originating from high-molecular weight macromolecules (MM) underlie those of metabolites in brain ^{1}H NMR spectra. In humans, MM content and MM pattern have been shown to depend on age of the subject. In this project, the influence of age-specific MM pattern on MR quantification was investigated. The age-associated differences in the MM pattern have a major influence on the quantification of metabolite concentrations in the aging brain which might lead to different interpretation of the data. This important finding suggests that the age-specific MM spectrum should be used in the basis set to obtain accurate concentrations of metabolites.

2994

Influence of broader spectral linewidths generated *in vivo* on metabolite quantification

Malgorzata Marjanska[1], Dinesh Deelchand[1], and Melissa Terpstra[1]

[1]Center for Magnetic Resonance Research and Department of Radiology, University of Minnesota, Minneapolis, MN, United States

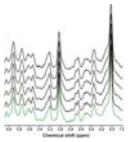

To understand how linewidth impacts the current best practice of quantification, the novel approach was used to measure spectra of several linewidths from each subject in contrast to the traditional approach of mathematically broadening one reference spectrum. Mathematical broadening of an *in vivo* spectrum reproduced the lowering of tCr concentration reported in the past. In contrast, tCr concentrations measured from broader spectra obtained using suboptimal shims tended to be higher than those measured using ideal shims. Further inquiry into the exact source of these artifacts is likely to lead to corrective approaches.

2995

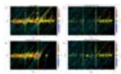

Fitting comparison for 9.4T 1D semi-LASER and 2D-J-resolved semi-LASER data

Tamás Borbáth[1], Ioannis Angelos Giapitzakis[1], Saipavitra Venkateshwaran Murali Manohar[1], and Anke Henning[1,2]

[1]High-Field Magnetic Resonance, Max Plack Institute for Biological Cybernetics, Tübingen, Germany, [2]Institute of Physics, Ernst-Moritz-Arndt University Greifswald, Greifswald, Germany

In this abstract, we present an adapted version of the ProFit-V2 fitting software to fit J-resolved semi-LASER data at 9.4T. Simulated basis sets with ideal pulses show the need to reduce the echo time to account for the spin locking effect of the adiabatic pulses. Further, a comparison of the fitting error estimations using correlation matrices and Cramer-Rao Lower Bounds with a metabolite cycled semi-LASER fitted with LCModel is done.

2996

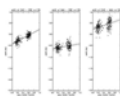

Tissue-type dependence of in vivo chemical shifts of metabolites ?

Jan Willem van der Veen[1], Stefano Marenco[2], Karen Berman[3], and Jun Shen[1]

[1]Magnetic Resonance Spectroscopy Core, NIH, NIMH, Bethesda, MD, United States, [2]NIMH-IRP, [3]Clinical & Translational Neuroscience Branch, NIH, NIMH

Recent high field susceptibility imaging experiments have revealed significant differences in water frequency in different tissue types. We studied the frequency distribution of choline, creatine, NAA, myo-inositol, glutamate, glutamine and GABA from gray matter- and white matter-dominant voxels. Based on data acquired from 135 normal subjects it was found that the best fit frequency of at least several metabolites are significantly dependent on tissue type composition.

2997

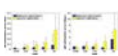

Difference optimization: Automatic correction of relative frequency and phase for 1H MEGA-PRESS spectra

Marianne Cleve[1], Martin Krämer[1], Alexander Gussew[1], and Jürgen R. Reichenbach[1]

[1]Medical Physics Group, Institute of Diagnostic and Interventional Radiology, Jena University Hospital - Friedrich Schiller University Jena, Jena, Germany

We present an automatic routine for alignment of GABA ^{1}H MEGA-PRESS spectra to reduce subtraction artefacts which can compromise reliable GABA quantitation. The algorithm iteratively optimizes relative frequency and phase offsets between the edited and non-edited ^{1}H MEGA-PRESS spectra by minimizing the sum of the magnitude of the difference spectrum. The proposed method was applied to simulated spectra with preset frequency and phase errors and *in vivo* MEGA-PRESS data and compared to spectral registration, an alignment method implemented in the open source FID-A toolbox[1]. Difference optimization demonstrated robust performance without requiring limitation of the input data range or user intervention.

2998

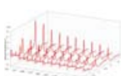

Pinpointing differences in diffusion characteristics of metabolites determined in human gray matter using simultaneous spectral and diffusion modeling

Andre Doering[1], Victor J Adalid Lopez[1], Chris Boesch[1], and Roland Kreis[1]

[1]Depts. Radiology and Clinical Research, University Bern, Bern, Switzerland, CH-3010, Switzerland

A recently described non-water suppressed diffusion-weighting MR spectroscopy sequence was applied in 13 healthy volunteers. The method uses the large water signal to compensate motion-related signal drop for the metabolite signals. 2D signal modeling with FiTAID allows for implementation of different prior knowledge constraints in order to prevent non-physical solutions or to restrict the number of unknown diffusion constants. In gray matter, highly significant differences for ADCs of several metabolites (faster diffusion for glutamate than NAA or myo-inositol) were found and their dependence on prior knowledge constraints investigated.

2999

Absolute Quantification of Brain Metabolites at 3T: Methods and Pitfalls

Simona Nikolova[1], Robert Nikolov[2], and Craig E.L. Stark[1,3]

[1]Department of Neurobiology and Behavior, University of California, UCI, Irvine, CA, United States, [2]Department of Neurology, University of California, UCI, Irvine, CA, United States, [3]Center for the Neurobiology of Learning and Memory, University of California, Irvine, CA, United States

There exist several partial volume correction methods in the literature that often produce similar results. However, various tissue fractions can lead to substantial differences in estimated concentrations. These deviations are greater at longer TEs and greater cerebrospinal fluid contributions. In instances with a 75% WM fraction and no gray matter, the deviations can be up to 37% for TE of 135 ms at 3.0 T. These corrections were then applied to common regions of interest (ROI) in an MRS study involving 5 participants at 3T. By understanding where these methods deviate one can better make cross study comparisons.

3000

In vivo quantification of glutathione T2 in the human brain at 7 Tesla using echo time extension with variable refocusing selectivity and symmetry

Kelley M. Swanberg[1,2], Hetty Prinsen[2], Daniel Coman[2], Robin A. de Graaf [2,3], and Christoph Juchem[1,2,4,5]

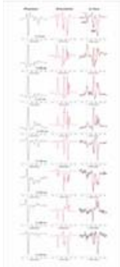

[1]Biomedical Engineering, Columbia University School of Engineering and Applied Science, New York, NY, United States, [2]Radiology and Biomedical Imaging, Yale University School of Medicine, New Haven, CT, United States, [3]Biomedical Engineering, Yale University School of Medicine, New Haven, CT, United States, [4]Radiology, Columbia University School of Engineering and Applied Science, New York, NY, United States, [5]Neurology, Yale University School of Medicine, New Haven, CT, United States

The tripeptide glutathione (L-γ-glutamyl-L-cysteinyl glycine or GSH) is an endogenous antioxidant implicated in many neurological conditions, including multiple sclerosis. Its precise quantification by proton magnetic resonance spectroscopy is, however, hampered by its uncertain T_2. Here, we present a method for the quantification of GSH T_2 in the human brain at 7 Tesla using optimized echo time extension delays and variable refocusing selectivity and symmetry to maximize the intensity and specificity of J-difference-edited GSH signals predicted by a full density matrix description of signal behavior. Using this method, we measured a GSH T_2 of 144.2 ± 5.5 ms that is considerably shorter than that calculated for either of two common reference metabolites NAA (221.9 ± 10.3 ms) or creatine (155.3 ± 5.9 ms), emphasizing the importance of considering T_2 relaxation differences in the spectroscopic measurement of these metabolites at long echo times.

3001

Diurnal effects on brain MRI volume and 1D MR neurospectroscopy

Oun Al-Iedani[1], Karen Ribbons[2], Jameen ARM[3], Jeannette Lechner-Scott[4], and Saadallah Ramadan[3]

[1]Department of Medical Radiation Sciences, Newcastle University, Newcastle, Australia, [2]Department of Neurology, John Hunter Hospital, Newcastle, Australia, [3]Newcastle University, Newcastle, Australia, [4]Hunter Medical Research Institute, Newcastle, Australia

Our major aim of this study was to to evaluate diurnal effects on two key MR metrics; total brain volume and neurometabolite profiles. Repeated 3D-MPRAGE and 1D-MRS were undertaken over a 10-hour period on 10 healthy subjects (aged 36.1±7.7 years). Volumetric analysis, using vendor segmentation software, did not reveal any statistically significant effect of time of day or sex on total brain volume. Spectral data processing and analysis using LCModel showed a mild increase in glycerophosphocholine and total choline levels between 7am and 12pm. Our study suggested a lack of significant diurnal effect on these parameters.

3002

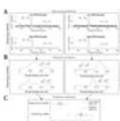

The use of weighted averaging in spectroscopy studies improves statistical power

Jack Julian James Jenkins Miller[1,2,3], Lowri E Cochlin[1,4], Damian John Tyler[1,2], and Kieran Clarke[1]

[1]Department of Physiology, Anatomy & Genetics, University of Oxford, Oxford, United Kingdom, [2]Oxford Centre for Clinical Magnetic Resonance Research, University of Oxford, Oxford, United Kingdom, [3]Department of Physics, University of Oxford, Oxford, United Kingdom, [4]PulseTeq Limited, Surrey, United Kingdom

In vivo MR spectroscopy is often characterised by a spectral signal-to-noise ratio (SNR) that varies highly between experiments, particularly when investigating non-proton nuclei. A common design for spectroscopic studies is to compare the ratio of two spectral peak amplitudes between groups, e.g. individual PCr/γ-ATP ratios in phosphorus MRS, or bicarbonate-to-pyruvate ratios in hyperpolarized ^{13}C MRS. The uncertainty on this ratio is often neglected. We show that the correct propagation of this uncertainty improves statistical power.

3003

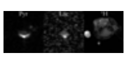

Bounded rate constant estimation in hyperpolarised [1-13C]pyruvate experiments by a Delayed-rejection Adaptive Metropolis Markov-Chain Monte Carlo (DAM-MCMC) Method

Jack Julian James Jenkins Miller[1,2,3], Angus Zoen Lau[1,4], and Damian John Tyler[1,2]

[1]Department of Physiology, Anatomy & Genetics, University of Oxford, Oxford, United Kingdom, [2]Oxford Centre for Clinical Magnetic Resonance Research, University of Oxford, Oxford, United Kingdom, [3]Department of Physics, University of Oxford, Oxford, United Kingdom, [4]Physical Sciences, Sunnybrook Research Institute, Toronto, ON, Canada

Hyperpolarised [1-^{13}C]pyruvate forms an effective probe of metabolism in vivo and has been used extensively to diagnose and prognosticate cancer. Commonly, [1-^{13}C]pyruvate metabolism is quantified by either total metabolite-to-pyruvate integral ("AUC") ratios, or by fitting metabolic models by least-squares methods. Here, we use a modified Markov Chain Monte Carlo (MCMC) method with adaptive sampling and delayed rejection to fit models to hyperpolarised datasets of the healthy rat brain generated by a spectral-spatial EPI imaging sequence . The method is able to statistically discriminates between signal and noise, and returns quantitatively bounded maps of rate constants of interest, such as $k_{\text{Pyruvate}\rightarrow\text{Lactate}}$.

3004

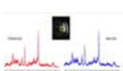

The effect of sex on neurochemical profile quantified from the human brain at 7T

Petr Bednarik[1], Ivan Tkac[1], Lynn Eberly[2], and Silvia Mangia[1]

[1]Department of Radiology, CMRR, University of Minnesota, Minneapolis, MN, United States, [2]School of Public Health, University of Minnesota, Minneapolis, MN, United States

Sex is a critical biological factor that needs to be factored into study designs and analyses. In the present work, we sought to quantify sex-related differences of neurochemical profiles, utilizing 1H MRS data from the visual cortex of 22 healthy females (age 24±6 years) and 27 males (age 26±6 years) acquired at 7 T. Whereas there was a trend of sex-related differences for few metabolites, no statistically significant differences were observed above the attained metabolite sensitivity threshold of 0.2 µmol/g. The results indicate that sex is not a major confounding variable for MRS experiments performed on the visual cortex of young subjects.

3005

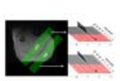

Comparison of metabolic adaptations between endurance- and sprint-trained athletes in two different muscles using a 31P spectroscopic multi-slice sequence

Kevin Moll[1], Alexander Gussew[1], Maria Nisser[2], Martin Krämer[1], and Jürgen R. Reichenbach[1]

[1]Medical Physics Group, Institute of Diagnostic and Interventional Radiology, Jena University Hospital - Friedrich Schiller University Jena, Jena, Germany, [2]Institute for Physiotherapy, Jena University Hospital - Friedrich Schiller University Jena, Jena, Germany

Due to specific training orientations athletes adapt with different metabolic responses to a given exercise. We used a 31P MR multi-slice sequence allowing a non-invasive investigation of high energy changes in two muscles. Different metabolic adaptations were shown within two muscles of different trained athletes. This may help to characterize training specific effects on energy metabolism.

3006

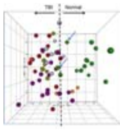

Linear discriminant and principle component analysis of MR spectroscopy data in pediatric mild traumatic brain injury (pmTBI)

Thao T. Tran[1], Marie Csete[2], Brian D. Ross[3], Elizabeth Geesaman[4], John Wilkes[4], and Dan Buzatu[4]

[1]Imaging, Huntington Medical Research Institutes, Pasadena, CA, United States, [2]Huntington Medical Research Institutes, Pasadena, CA, United States, [3]California Institute of Technology, [4]Division of Systems Biology, FDA National Center for Toxicological Research, Jefferson, AR, United States

Pediatric mild traumatic brain injury data is necessary to understanding and predicting recovery of cognitive and psychiatric sequelae as pediatric subjects may take longer to recover than adults. Our study presents MR spectroscopy data acquired in five different brain regions of concussed and non-concussed high school athletes. Data were analyzed utilizing linear discriminant in combination with principal component analysis. Initial results demonstrate reasonable separation of mTBI subjects compared to normal controls. In addition, data from multiple time-points after injury demonstrate a return toward normal pattern and can be used to predict recovery and return-to-play times.

3007

Temperature Calibration and Errors Assessed by Magnetic Resonance Spectroscopy

Bhanu Prakash KN[1], Sanjay K Verma[2], Suresh Sadananthan[3], Venkatesh Gopalan[2], Jadegoud Yaligar[2], Sankar Seramani[2], Andrew A Maudsley[4], and Sendhil Velan S[2]

[1]Signal and Image Processing, Singapore Bioimaging Consortium, Singapore, Singapore, [2]Laboratory of Molecular Imaging, Singapore Bioimaging Consortium, Singapore, Singapore, [3]Singapore Institute for Clinical Sciences, Singapore, [4]Miller School of Medicine, University of Miami, Miami, FL, United States

Whole brain temperature mapping is of great interest for investigating traumatic brain injuries. Single-voxel-spectroscopy (SVS) and CSI approaches provides limited spatial coverage in the brain, whereas 3D Echo-planar spectroscopic imaging (EPSI), covers the entire brain for investigating temperature and metabolism in traumatic brain injury and other studies . Our study focuses on calibration and validation of the temperature measurement in brain phantoms using EPSI and SVS at pre-clinical and clinical scanners, to study and analysis of whole brain temperature in rodents and humans.

3008

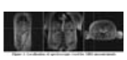

Effect of dietary intervention on liver fat content during the day. A pilot MR study

Miloslav Drobny[1], Petr Sedivy[1], Tereza Blahova[2], Katerina Zemankova[2], Monika Dezortova[1], Jan Kovar[2], and Milan Hajek[1]

[1]MR Unit, Dept Diagnostic and Interventional Radiology, Institute for Clinical and Experimental Medicine, Prague, Czech Republic, [2]Centrum of Experimental Medicine, Institute for Clinical and Experimental Medicine, Prague, Czech Republic

Liver fat content is an important parameter characterizing clinical status of the liver. Steatosis can be measured by magnetic resonance spectroscopy and imaging techniques non-invasively. The group of healthy volunteers was examined by MRS and MRI on three occasions after fat load, fat load with glucose and during whole-day fasting.

Obtained results show that both used MR techniques are suitable for fat content measurements in the liver during dietary intervention. The pilot study results suggest that concentration of NEFA in systemic circulation is a critical factor that determines whether fat accumulates in the liver during the day in healthy insulin sensitive subjects.

Traditional Poster

MRS Acquisition Techniques

Exhibition Hall 3009-3024 Thursday 13:00 - 15:00

3009

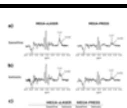

Investigation of the brain energy metabolism by simultaneous detection of lactate and β-hydroxybutyrate using MEGA-sLASER

Michael Dacko[1] and Thomas Lange[1]

[1]Department of Radiology, Medical Physics, University Medical Center Freiburg, Freiburg, Germany

For the detection and quantification of lactate (Lac) and β-hydroxybutyrate (bHB) via 1H-MRS, difference editing methods such as MEGA-PRESS have been proposed. Since MEGA-PRESS suffers from substantial signal loss due to large chemical shift displacement, we propose MEGA-sLASER for simultaneous detection of the two metabolites at 3T. It is demonstrated that the signal-to-noise ratio of the target resonances in the difference spectrum is increased by a factor of two compared to MEGA-PRESS and that quantification accuracy can thus be substantially improved, enabling the robust detection of Lac and bHB in healthy brain.

3010

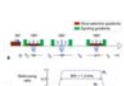

Improved Triple-refocusing 1H MRS at 3T for detection of GABA and Glutamate in human brain in vivo

Zhongxu An[1], Vivek Tiwari[1], Sandeep Ganji[1], and Changho Choi[1]

[1]Advanced Imaging Research Center, University of Texas Southwestern Medical Center, Dallas, TX, United States

Reliable detection of GABA is important for studies in neuro-psychiatric diseases. In vivo 1H GABA resonances are extensively overlapped with the neighboring resonances including glutamate and glutamine. We present a new triple-focusing 1H MRS method which can fully resolve GABA 2.29-ppm and Glu 2.35 ppm signals at 3T.

3011

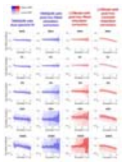

Dual spectral analysis for metabolite quantification in the presence of lipids and macromolecules

Peter J Lally[1,2], Alan Bainbridge[3], and Sudhin Thayyil[1,2]

[1]Imperial College London, London, United Kingdom, [2]Imperial College Healthcare NHS Trust, London, United Kingdom, [3]Medical Physics & Bioengineering, University College London Hospitals NHS Trust, London, United Kingdom

In this study, we aim to reduce the bias inherent in fitting short echo time spectra by performing a two-point saturation recovery experiment. At both points lipid and macromolecule magnetisation is excited from an approximately fully relaxed state and so this signal component is unchanged, thus the fitting model can be constrained. We show that this may be an advantageous strategy in comparison to other common techniques, reducing bias where fitting spectra with narrow linewidths.

3012

GABA editing with reduced sensitivity to B1 inhomogeneity and improved detectability at 7T using MEGA-LASER

Pallab Bhattacharyya[1], Mark Lowe[1], and Ovidiu Andronesi[2]

[1]Imaging Institute, Cleveland Clinic, Cleveland, OH, United States, [2]Radiology, Massachusetts General Hospital, Charlestown, MA, United States

GABA spectroscopy is performed at 7T in vitro and in vivo using MEGA-PRESS and MEGA-LASER sequences. MEGA-LASER is shown to be much less sensitive to B1 inhomogeneity, and having higher signal intensity than MEGA-PRESS. Relative inter- and intra-sequence variabilities with respect to B1 inhomogeneity and regional variation are reported. Higher signal intensity in MEGA-LASER is attributed to reduced chemical shift displacement artifact and less signal loss resulting from spatial effects in phase evolution of J-coupled GABA.

3013

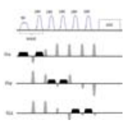

MASE-sLASER, a short TE matched chemical shift displacement error sequence for single voxel spectroscopy at ultrahigh field

Seyedmorteza Rohani Rankouhi[1], Hadrien Dyvorne[2], Donghyun Hong[1], Priti Balchandani[2], and David Norris[3]

[1]Erwin L. Hahn Institute for Magnetic Resonance Imaging, Essen, Germany, [2]Translational and Molecular Imaging Institute, New York, NY, United States, [3]Donders Institute for Brain, Cognition and Behaviour, Nijmegen, Netherlands

Conventional sLASER sequence has different Chemical Shift Displacement Error (CSDE) in one of the three slice selection directions. In this work, a short TE matched CSDE sLASER sequence (MASE-sLASER) has been implemented using the novel MASE pulses for single voxel spectroscopy at 7T. The matched low CSDE of this sequence in all three directions provides more exact representation of the metabolites in the imaged voxel. The short duration of the MASE pulses with acceptable bandwidths have made it possible to achieve a TE as short as 28 ms for the MASE-sLASER sequence despite having one more RF pulse than the conventional sLASER sequence.

3014

Editing of GABA at variable TEs with antiphase J-difference editing approach

Seyedmorteza Rohani Rankouhi[1] and David Norris[2]

[1]Erwin L. Hahn Institute for Magnetic Resonance Imaging, Essen, Germany, [2]Donders Institute for Brain, Cognition and Behaviour, Nijmegen, Netherlands

The most commonly used editing MRS method for measuring GABA is MEGA which works at TE=68 ms and any odd multiples thereof. Here we present a J-difference editing method which makes it possible to measure GABA signal at variable TEs independent of the effect of J-evolution by preserving the two side peaks of GABA in antiphase states at any echo time above 34ms. We also show an application of this editing technique to be measurement of T2 relaxation time of GABA in vivo.

3015

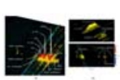

Qualitative Comparison between In Vivo J-Resolved Semi-LASER at 3 T and 9.4 T

Saipavitra Venkateshwaran Murali Manohar[1], Ioannis Angelos Giapitzakis[1], Tamas Borbath[1], Matti Gaertner[2], and Anke Henning[1,3]

[1]High Field Magnetic Resonance, Max Planck Institute for Biological Cybernetics, Tuebingen, Germany, [2]Department of Psychiatry, Charité - Universitätsmedizin Berlin, [3]Institute of Physics, Ernst-Moritz-Arndt University Greifswald, Greifswald, Germany

J-resolved semi-LASER with maximum-echo sampling is optimized at 9.4T and compared with the same implementation at 3T in terms of SNR and spectral resolution. SODA scheme is appreciated for the sequence rather than the MC scheme. SNR at 9.4T (t_1 steps: 85) was approximately 5.8 times greater than at 3T (t_1 steps: 100) and strongly coupled peaks are well-resolved. However, the trade-off between SNR and spectral resolution is explained as lactate (1.32 ppm), a weakly-coupled metabolite, is better resolved at 3T. Higher band-width AFP pulses helped in almost vanishing the J-refocused peaks which made the J-resolved peaks clearly distinguishable. A few interesting downfield peaks and the doublet of NAA (7.82ppm) are observed.

3016

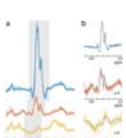

Simultaneous measurement of Aspartate, NAA, and NAAG using HERMES spectral editing at 3 Tesla

Kimberly Chan[1,2,3], Muhammad Saleh[2,3], Georg Oeltzschner[2,3], Peter Barker[2,3], and Richard Edden[2,3]

[1]Biomedical Engineering, Johns Hopkins School of Medicine, Baltimore, MD, United States, [2]Russell H. Morgan Department of Radiology and Radiological Science, Johns Hopkins School of Medicine, Baltimore, MD, United States, [3]F. M. Kirby Research Center for Functional Brain Imaging, Kennedy Krieger Institute, Baltimore, MD, United States

It has previously been shown that the HERMES method ('Hadamard Encoding and Reconstruction of MEGA-Edited Spectroscopy') can be used to simultaneously edit two metabolites (1). Examples of pairs of metabolites edited include N-acetyl-aspartate (NAA) and N-acetyl aspartyl glutamate (NAAG), or glutathione and GABA (2). Here, we demonstrate that HERMES can acquire simultaneously and then separate three overlapping edited signals, for the example of NAA, NAAG and Aspartate (Asp). We optimize this sequence using simulations, and show its feasibility in phantoms and in vivo. We also explore the echo time modulation of the aspartate spin system using simulations and phantom experiments.

3017

Very Short Echo Time MRS for Single Voxel Spectroscopy in Small Voxels

Ariane Fillmer[1], Ioannis Angelos Giapitzakis[2], Ralf Mekle[3], Semiha Aydin[1], Anke Henning[2,4], Bernd Ittermann[1], and Florian Schubert[1]

[1]Physikalisch-Technische Bundesanstalt (PTB), Berlin, Germany, [2]Max Planck Institute for Biological Cybernetics, Tuebingen, Germany, [3]Center for Stroke Research Berlin (CSB), Charité - Universitätsmedizin Berlin, Berlin, Germany, [4]Institute of Physics, Ernst-Moritz-Arndt University Greifswald, Greifswald, Germany

This work presents the combination of metabolite cycling with a non-water-suppressed SPECIAL localization scheme in order to enable improved averaging coherence for very short echo time MRS in small voxels or voxels that suffer otherwise from low SNR or frequency instabilities.

3018

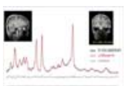

Feasibility and Reproducibility of Neurochemical Profiling in the Human Hippocampus at 7T

Petr Bednarik[1], Ivan Tkac[1], James Joers[1], Alena Svatkova[2], Gulin Oz[1], and Dinesh Deelchand[1]

[1]Department of Radiology, CMRR, University of Minnesota, Minneapolis, MN, United States, [2]Department of Pediatrics, University of Minnesota, Minneapolis, MN, United States

Despite advancements in single-voxel hippocampal ^{1}H MR spectroscopy, low abundant and J-coupled metabolites, which are critically involved in neuro-energetics, memory and excitation/inhibition balance, are still poorly quantified at 3T. Hippocampal ^{1}H MRS at 7T may benefit from higher SNR and better spectral dispersion. Thus, the precision and test-retest reproducibility of quantification achieved at 7T using semi-LASER sequence was compared to the outcome of a similarly designed 3T study. The higher SNR at 7T relative to 3T allowed using smaller voxel for more precise selection of hippocampal gray matter while demonstrating improved quantification of J-coupled and/or low abundant metabolites.

3019

Rapid Diffusion Tensor MR Spectroscopy (DTS) of Metabolites in Human Brain

Chris Hanstock[1], Dana Cobzas[1], and Christian Beaulieu[1]

[1]University of Alberta, Edmonton, AB, Canada

Few studies have focused on metabolite diffusion using ^{1}H-MRS, compared to the vast number observing water diffusion by DWI/DTI. These MRS studies are lengthy, therefore difficult to implement clinically, and use up to three b-values to yield the diffusion spectra. Single exponential signal loss is assumed for metabolites, neglecting the possibility of non-linear decay at high b-values, as has been observed for water. Our goals are: (i) Characterize the metabolite signal decay versus b-value in human white matter to determine the non-linear region. (ii) Develop a rapid diffusion tensor spectroscopy method that can be executed in a clinically useful time.

3020

4-Dimensional spin echo for prostate 1H MRSI at 7T using a multi-transmit system

Nienke D. Sijtsema[1], Arjan D. Hendriks[1], Peter R. Luijten[1], Dennis W.J. Klomp[1], Petra J.W. Pouwels[2], and Catalina S. Arteaga de Castro[1]

[1]Imaging Division, University Medical Center, Utrecht, Netherlands, [2]Department of Physics and Medical Technology, VU University Medical Center, Amsterdam, Netherlands

A 4-dimensional spatially and spectrally selective spin echo sequence was developed for prostate 1H MRSI at 7T. This sequence has intrinsic water and lipid suppression properties due to the limited spectral bandwidth, so only prostate metabolites are measured. The low peak power of the pulses also leads to lower SAR deposition and RF duty cycles. Phantom experiments showed an average water suppression of 99.99% at short TE, with low SAR and RF duty cycle values compared to adiabatic pulses routinely used at higher field strengths. Combined, these properties enable fast prostate MRSI acquisitions without water and lipid artifacts.

3021

In-vivo testing of automatic voxel prescription for high inter-subject reproducibility in single-voxel MR spectroscopy

Young Woo Park[1], Dinesh K Deelchand[2], James M. Joers[2], Brian J. Soher[3], Peter B. Barker[4], HyunWook Park[1], Gülin Öz[2], and Christophe Lenglet[2]

[1]Electrical Enginnering, Korea Advanced Institute of Science and Technology, Daejeon, Korea, Republic of, [2]Department of Radiology, Center for Magnetic Resonance Research, University of Minnesota Medical School, Minneapolis, MN, United States, [3]Department of Radiology, Duke University Medical Center, Durham, NC, United States, [4]Department of Radiology, Johns Hopkins University School of Medicine, Baltimore, MD, United States

In this study, we present the implementation and outcome of a scheme for automatic voxel placement in single-voxel spectroscopy. The scheme is based on transfer of voxels prescribed on an atlas to the subject images during the scanning session and allows fast and reliable placement of voxels for spectroscopy measurements. 1H spectra of three different volumes of interest (VOIs) from multiple subjects were measured with a Siemens 3T scanner following automated and manual VOI placements. MRS data acquired using automatic placement produced spectral quality comparable to manual placement, while yielding better cross-subject spatial consistency than manual placement.

3022

magna cum laude

Automated Voxel Placement: A Linux-based Suite of Tools for Accurate and Reliable Single Voxel Coregistration

Eric Andrew Woodcock[1], Muzamil Arshad[1], Dalal Khatib[1], and Jeffrey A Stanley[1]

[1]Psychiatry and Behavioral Neurosciences, Wayne State University School of Medicine, Detroit, MI, United States

Single-voxel magnetic resonance spectroscopy (MRS) provides quantification of brain metabolite levels in vivo. However, MRS studies suffer from an often overlooked source of error variance: inconsistent voxel placement. It is well-established that metabolite levels vary by brain region and voxel tissue composition. Thus, inconsistent voxel placement increases likelihood of Type I and II errors. To address this problem, we developed and evaluated a novel and automated method of prescribing voxel placements at the time of scanning. Results demonstrated a significant improvement in prescribing accurate and reliable voxel placements between and within subjects compared to manual placement and published methods.

3023

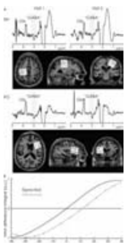

Measuring and minimizing effects of eddy currents on selective spectral editing experiments at 3T

Georg Oeltzschner[1,2], Karim Snoussi[1,2], Nicolaas A.J. Puts[1,2], Mark Mikkelsen[1,2], Ashley D. Harris[3,4,5], Subechhya Pradhan[6,7], Kyrana Tsapkini[8], Michael Schär[1], Peter B. Barker[1,2], and Richard A.E. Edden[1,2]

[1]Russell H. Morgan Department of Radiology and Radiological Science, The Johns Hopkins University School of Medicine, Baltimore, MD, United States, [2]F.M. Kirby Research Center for Functional Brain Imaging, Kennedy Krieger Institute, Baltimore, MD, United States, [3]CAIR Program, Alberta Children's Hospital Research Institute, University of Calgary, Calgary, AB, Canada, [4]Department of Radiology, University of Calgary, Calgary, AB, Canada, [5]Hotchkiss Brain Institute and Alberta Children's Hospital Research Institute, Calgary, AB, Canada, [6]Diagnostic Imaging and Radiology, Children's National Health System, Washington, DC, United States, [7]Department of Radiology, George Washington University, Washington, DC, United States, [8]Department of Neurology, The Johns Hopkins University School of Medicine, Baltimore, MD, United States

Macromolecule-suppressed J-difference-edited MRS of GABA is extremely sensitive to B_0 offsets. Relatively small frequency shifts (~10 Hz) may cause unwanted co-editing of macromolecules, to the extent that the edited 'GABA' signal appears negative in-vivo. We demonstrate an approach to measure transient field shifts arising from gradient-related eddy currents, and present a way to minimize these effects in order to restore correct editing.

3024

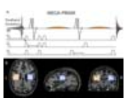

MEGA-PRIAM: Dual-volume excitation and parallel reconstruction for J-difference-edited MR spectroscopy

Georg Oeltzschner[1,2], Nicolaas A.J. Puts[1,2], Kimberly L. Chan[1,2,3], Vincent O. Boer[4], Peter B. Barker[1,2], and Richard A.E. Edden[1,2]

[1]Russell H. Morgan Department of Radiology and Radiological Science, The Johns Hopkins University School of Medicine, Baltimore, MD, United States, [2]F.M. Kirby Research Center for Functional Brain Imaging, Kennedy Krieger Institute, Baltimore, MD, United States, [3]Department of Biomedical Engineering, The Johns Hopkins University School of Medicine, Baltimore, MD, United States, [4]Hvidovre Hospital, Danish Research Center for Magnetic Resonance, Hvidovre, Denmark

A twofold acceleration of MEGA-edited spectroscopy, using Parallel Reconstruction In Accelerated Multivoxel (MEGA-PRIAM) to simultaneously acquire data in two separate locations, is demonstrated. PRIAM separates the signals from two dualband-excited voxels using spatial receiver-coil sensitivity profiles. Phantom experiments show that MEGA-PRIAM separates GABA- and glutathione-edited spectra with low crosstalk between the voxels. In-vivo experiments establish that dual-voxel MEGA-PRIAM increases signal-to-noise ratio (SNR) 40% compared to sequentially acquired single-voxel MEGA-PRESS measurements with the same total duration. GABA and glutathione estimates are consistent between dual-voxel MEGA-PRIAM and single-voxel MEGA-PRESS acquisitions.

Traditional Poster

NMR & EPR Applications

Exhibition Hall 3025-3029 Thursday 13:00 - 15:00

3025

Quantifying pO2-Driven Longitudinal Relaxation of Water 1H Spins in the Presence of Magnetization Transfer: Cross-Linked BSA as a Tissue Mimic

Kelsey Meinerz[1], Tianzhe Li[2], Scott C. Beeman[3], Joel R. Garbow[3,4], and Joseph J.H. Ackerman[2,3,4]

[1]Physics, Washington University, Saint Louis, MO, United States, [2]Chemistry, Washington University, Saint Louis, MO, United States, [3]Radiology, Washington University, Saint Louis, MO, United States, [4]Siteman Cancer Center, Washington University, St Louis, MO, United States

Crosslinked bovine serum albumin phantoms are used as tissue biexponential relaxation surrogates/mimics to investigate the potential of R_1-based tissue-O_2 quantification and to characterize the influence of physiologically relevant variations of temperature and protein concentration on such determinations. The relaxation-rate constant for the rapidly relaxing apparent water population is dominated by magnetization transfer and is insensitive pO_2. The relaxation-rate constant for the slowly relaxing apparent water population is linearly related to pO_2 and provides the basis for a possible MR-Oximetry protocol.

3026 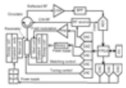

Brain redox imaging using blood-brain-barrier nitroxides by digital EPR imaging system

Miho C Emoto[1], Hideo Sato-Akaba[2], and Hirotada G Fujii[1]

[1]Sapporo Medical University, Sapporo, Japan, [2]Osaka University, Osaka, Japan

Electron paramagnetic resonance (EPR) imaging is a noninvasive imaging method for visualizing the brain redox status using nitroxide compounds as imaging probes. A digital imaging system for three-dimensional continuous-wave EPR imaging of small animals was developed using a high-speed analog-to-digital converter, digital-to-analog converters and field programmable gate array integrated circuits to improve the signal-to-noise ratio (SNR) and visualize the precise brain redox status in mice. Compared to an analog EPR imager, the digital EPR imager obtains a higher SNR of a phantom and produces images with sufficient quality to create a more accurate brain redox map of the mouse head.

3027 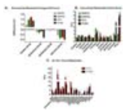

Towards Imaging the Glycolytic and Glutaminolytic Differences in Prostate Cancer Cell Lines that Affects Outcome of Glutaminase Inhibition

Niki Zacharias Millward [1,2], Christopher McCullough[3], Sriram Shanmugavelandy[1], Jaehyuk Lee[1], Youngbok Lee[4], James McHenry[5], Lawrence Jones [6], and Pratip Bhattacharya[7]

[1]Cancer Systems Imaging, MD Anderson Cancer Center, Houston, TX, United States, [2]Bioengineering, Rice University, Houston, TX, United States, [3]Institute for Bioscience and Biotechnology Research, National Institute of Standards and Technology, Rockville, MD, United States, [4]Applied Chemistry, Hanyang University, Korea, Republic of, [5]University of Houston Downtown Campus, Houston, TX, [6]Huntington Medical Research Institutes, Pasadena, CA, [7]MD Anderson Cancer Center, Houston, TX, United States

To understand and image how metabolism changes in prostate cancer (PCa), we determined both extracellular and intracellular metabolic profile of four PCa cell lines with varying degrees of aggressiveness. Differences in metabolism and mechanistic link were further explored using carbon-13 glucose and glutamine feeding studies and hyperpolarized pyruvate metabolic imaging trials with subcutaneous xenograft PC3 and PC3M animal models. We found increased glutamine utilization in the more metastatic cell line PC3M and this increased dependence on glutamine leads to reduction in cell proliferation and ATP when cells are treated with glutaminase inhibitor CB-839. No reduction is seen in PC3 line.

3028 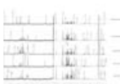

PROTON NMR METABOLIC PROFILING OF CSF REVEALS DISTINCT DIFFERENTIATION OF MENINGITIS WITH NEGATIVE CONTROLS

Tanushri Chatterji[1], Suruchi Singh[2], Ajai Kumar Singh[3], Manodeep Sen[4], and Raja Roy[2]

[1]Departent of Microbiology, Dr. Ram Manohar Lohia Institute of Medical Sciences, Lucknow, India, [2]Centre of Biomedical Research, Lucknow, India, [3]Department of Neurology, Dr. Ram Manohar Lohia Institute of Medical Sciences, Lucknow, India, [4]Department of Microbiology, Dr. Ram Manohar Lohia Institute of Medical Sciences, Lucknow

The chemical composition of cerebrospinal fluid (CSF) in central nervous system (CNS), varies during onset of meningitis, neurodegenerative disorders and in traumatic cases.The study attempted to observe the metabolic variation in meningitis cases, negative controls and positive controls. Further differentiation among the groups was carried out using Principal Component Analysis (PCA) followed by Partial Least Square Discriminant Analysis (PLS-DA).On the basis of metabolic profile it was found that negative control CSF samples are more appropriate for differentiation of meningitis than positive control CSF samples.The biomarkers identified were ketone bodies, amino acids, propylene glycol, citrate and creatine/creatinine.

3029 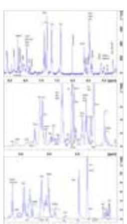

Longitudinal Investigation of the Metabolome of Developing 3D Aggregating Brain Cell Cultures at Different Maturation Stages by 1H HR-MAS NMR

Gaelle Diserens[1], Martina Vermathen[2], Chiara Sartori[3,4], Marie-Gabrielle Zurich[3,4], and Peter Vermathen[1]

[1]Depts. Radiology and Clinical Research, University Bern, Bern, Switzerland, [2]Dept. Chemistry and Biochemistry, University Bern, Bern, Switzerland, [3]Dept. Physiology, Faculty of Biology and Medicine, University of Lausanne, Lausanne, Switzerland, [4]Swiss Center for Applied Human Toxicology (SCAHT), Switzerland

3D rat brain aggregate model is an excellent tool for mechanistic studies including OMICS analysis. However, their metabolic profile have not been yet fully investigated. The aim was to investigate by ^{1}H-HR-MAS NMR the metabolic fingerprint of 3D brain cell cultures at different maturation stages to establish a developmental profile of metabolic changes. Chemometric analysis revealed a clear separation of samples from the different maturation days. Metabolite concentration evolutions could be followed and revealed strong and various metabolic alterations. The strong metabolite evolution emphasizes the brain modelling complexity during maturation, possibly reflecting physiological processes of brain tissue development.

Traditional Poster

Technical Developments in Hyperpolarized 13C MRI/MRS

Exhibition Hall 3030-3046 Thursday 13:00 - 15:00

3030 

Hyperpolarized [6-13C,6-15N3]-Arginine as a Novel Probe to Interrogate Arginase Activity

Andrew Cho[1], Roozbeh Eskandari[1], Jason S Lewis[1], and Kayvan R Keshari[1]

[1]Memorial Sloan Kettering Cancer Center, New York City, NY, United States

Across most cancer types, increased macrophage infiltration is associated with a worsening prognosis. This is because tumor associated macrophages (TAMs) exhibit a variety of pro-tumor effects ranging from vascular recruitment, cell proliferation, extravasation, and immune suppression. A marker of TAMs is arginase-1 expression, which converts arginine to urea and ornithine. It is thought that arginase expression reduces the amount of arginine available to local T-cells, leading to T-cell receptor dysfunction. In this abstract, we outline the synthesis and characterization of novel compound [6-13C,6-15N3]-Arginine as a hyperpolarized 13C MRS probe to interrogate arginase activity, with the potential for in vivo translation.

3031

Hyperpolarization of [4-13C]5-aminolevulinic acid

Stephen J. DeVience[1], Graeme Woodworth[2], Joseph P. Y. Kao[3,4], and Dirk Mayer[1]

[1]Diagnostic Radiology and Nuclear Medicine, University of Maryland School of Medicine, Baltimore, MD, United States, [2]Neurosurgery, University of Maryland School of Medicine, Baltimore, MD, United States, [3]Center for Biomedical Engineering and Technology (BioMET), University of Maryland School of Medicine, Baltimore, MD, United States, [4]Physiology, University of Maryland School of Medicine, Baltimore, MD, United States

We performed the first DNP hyperpolarization of ^{13}C-labeled 5-aminolevulinic acid (5-ALA), achieving 13% polarization at dissolution and measuring a T_1 of 20 s. 5-ALA is used for fluorescent imaging and photodynamic therapy of glioblastoma, and our results suggest it is also a promising substrate for hyperpolarized metabolic imaging of this cancer.

3032

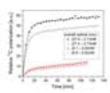

Hyperpolarization of 2-keto[1-13C]isocaproate for in vivo studies with photo-induced radicals

Steffen F. Frank[1], Hikari A. I. Yoshihara[2], Mor Mishkovsky[1], Arnaud Comment[3], and Rolf Gruetter[1,4,5,6]

[1]Laboratory for Functional and Metabolic Imaging, École Polytechnique Fédérale de Lausanne, Lausanne, Switzerland, [2]Institute of Physics of Biological Systems, Swiss Federal Institute of Technology, Lausanne, Switzerland, [3]General Electric Healthcare, Chalfont Saint Giles, United Kingdom, [4]Department of Radiology, University of Lausanne, Lausanne, Switzerland, [5]Department of Radiology, University of Geneva, Geneva, [6]Centre for Biomedical Imaging, École Polytechnique Fédérale de Lausanne, Lausanne, Switzerland

Hyperpolarized 2-keto[1-^{13}C]isocaproate (KIC) provides a means to probe brain nitrogen homeostasis and to assess molecular signatures of tumors. The dynamic nuclear polarization process requires a free-radical polarizing agent, and samples are typically doped with persistent radicals. An alternative is to use photo-induced radicals of α-keto acids that recombine upon dissolution. [1-^{13}C]KIC hyperpolarized with photo-induced radicals could be used to measure the alterations in amino acid metabolism that are linked to neurodegenerative diseases and cancer, and the aim of the present study is to identify the main features that influence the polarization dynamics.

3033

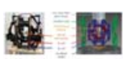

SQUID-based ultralow field nuclear magnetic resonance spectroscopy using the para-H2 based hyperpolarization technique SABRE

Kai Buckenmaier[1], Matthias Rudolph[1,2], Christoph Back[2], Joern Engelmann[1], Juri Rudin[1], Tomasz Misztal[3], Ute Bommerich[4], Klaus Scheffler[1], Dieter Koelle[2], Reinhold Kleiner[2], Hermann Mayer[3], Johannes Bernarding[4], and Markus Plaumann[4]

[1]High-field Magnetic Resonance, MPI for Biological Cybernetics, Tuebingen, Germany, [2]Physikalisches Institut and Center for Quantum Science (CQ) in LISA+, University of Tübingen, Germany, [3]Institue of Inorganic Chemistry, University of Tübingen, Germany, [4]Department for Biometrics and Medical Informatics, Otto-von-Guericke-University Magdeburg, Germany

SABRE is a technique to achieve continuous hyperpolarization for MR measurements by the interaction of para-hydrogen and a substrate via steady ligand exchange on a catalyst. Thus, MR-active nuclei can be hyperpolarized more than only once. At field strengths of mT Faraday coils, commonly used in conventional or high field MRI, become insensitive and SQUIDs performing superior. Since SQUIDs are broadband detectors, the static magnetic field B_0 can be changed easily or multiple nuclei can be measured simultaneously. Here, we successfully demonstrate the advantages of a SQUID based system by showing significant signal enhancement (^{1}H, ^{19}F) by hyperpolarization of 3-fluoropyridine.

3034

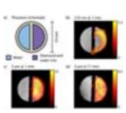

Nanodiamond Imaging with Hyperpolarized 13C MRI

David E. J. Waddington[1], Thomas Boele[1], Ewa Rej[1], Dane R. McCamey[2], Torsten Gaebel[1], and David J. Reilly[1]

[1]ARC Centre of Excellence for Engineered Quantum Systems, School of Physics, University of Sydney, Sydney, Australia, [2]School of Physics, University of New South Wales, Sydney, Australia

Hyperpolarized ^{13}C MRI leverages an over 10 000 times increase in the ^{13}C polarization of biomolecules, enabling new molecular imaging applications. However, metabolic applications are limited to processes on the timescale of a minute by the short lifetime of the hyperpolarized signal. Here, we hyperpolarize nanodiamonds and microdiamonds to achieve large, long-lived ^{13}C polarizations. We then image these particles in phantoms, demonstrating the potential of hyperpolarized nanodiamonds for imaging over long timescales. As nanodiamond has been established as a biocompatible platform for drug delivery, our results will motivate further research into hyperpolarized MRI for tracking nanoparticles in vivo.

3035

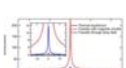

Transport of Hyperpolarized Nanodiamonds

Thomas Boele[1], David E. J. Waddington[1], Ewa Rej[1], Torsten Gaebel[1], and David J. Reilly[1]

[1]ARC Centre of Excellence for Engineered Quantum Systems, School of Physics, University of Sydney, Sydney, Australia

Hyperpolarized ^{13}C MRI using nanodiamond (ND) holds the potential for tailored diagnostic imaging combined with targeted drug delivery in the human body. An obstacle to realizing this potential is the transfer of hyperpolarized ND from the hyperpolarizer to the patient without losing the majority of the ^{13}C polarization as it travels through low magnetic fields before reaching the MRI scanner. We demonstrate that polarization loss is highly dependent on magnetic field and construct a system of transfer magnets that improves the transfer efficiency of our hyperpolarized ND by more than an order of magnitude.

3036

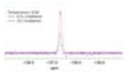

photo-CIDNP for 19F MR amino acid-protein interaction studies in physiological solvents

Frederike Euchner[1], Markus Plaumann[1], Thomas Trantzschel[1], Joachim Bargon[2], Ute Bommerich[1], and Johannes Bernarding[1]

[1]Department for Biometrics and Medical Informatics, Otto-von-Guericke University Magdeburg, Magdeburg, Germany, [2]Institute of Physical and Theoretical Chemistry, University of Bonn, Bonn, Germany

Fluorinated amino acids are of high interest in biochemistry and pharmaceutics. The low ^{19}F MR signal was increased employing hyperpolarization (photo-Chemical Induced Dynamic Nuclear Polarization, photo-CIDNP). 3-Fluoro-tyrosine in physiologic salt solution was hyperpolarized in presence of an albumin derivative using a low cost LED allowing repetitive irradiation and increasing the hyperpolarized signal. A clear ^{19}F signal enhancement could be observed. In comparison to past examinations with a laser system, only small temperature changes caused by LED light irradiation were measured in the current study.

3037

Simultaneous Visualization of Hyperpolarized Fluorinated Amino Acids by Multi Chemical Shift Selective 19F MRI

Tuba Güden-Silber[1], Jürgen Schrader[2], and Ulrich Flögel[1]

[1]Experimental Cardiovascular Imaging, Heinrich Heine University, Düsseldorf, Germany, [2]Molecular Cardiology, Heinrich Heine University, Düsseldorf, Germany

We demonstrate the induction of ^{19}F photo-chemically induced dynamic nuclear polarization (photo-CIDNP) in ^{19}F MR imaging experiments. To this end, we made use of laser-induced hyperpolarization in a system consisting of flavin mononucleotide as a photosensitizer and the fluorinated aromatic amino acids tyrosine and tryptophan, respectively. The induction of ^{19}F photo-CIDNP led to an extensive ^{19}F signal enhancement which could be exploited for simultaneous imaging of both amino acids by ^{19}F multi chemical shift-selective imaging within 20 s. Hence, our approach resulted in a substantial improvement of the intrinsically low ^{19}F MR sensitivity for mono-fluorinated amino acids.

3038

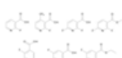

Examination of the hyperpolarizability of fluorinated nicotinic acids and further pyridine carboxylic acids using SABRE

Markus Plaumann[1], Frederike Euchner[1], Rainer Ringleb[1], Sara Hadjiali[2], Joachim Bargon[3], Gerd Buntkowsky[2], Johannes Bernarding[1], and Ute Bommerich[1]

[1]Department for Biometrics and Medical Informatics, Otto-von-Guericke University Magdeburg, Magdeburg, Germany, [2]Eduard-Zintl-Institute for Inorganic and Physical Chemistry, Technical University Darmstadt, Darmstadt, Germany, [3]Institute of Physical and Theoretical Chemistry, University of Bonn, Bonn, Germany

Nicotinic acid and isonicotinic acid are two derivatives of pyridine carboxylic acids. Both substrates are of high interest in medical chemistry. In the current study seven fluorinated derivatives of these pyridine carboxylic acids were chosen for examination of the ^{1}H and ^{19}F hyperpolarizability using the SABRE technique. Influences of the position of the carboxylic group and fluorine as well as the catalyst system concerning the achievable signal enhancements were examined. Furthermore an H/D-exchange could be observed in some cases. The presented data gives important information for future MR imaging studies.

3039

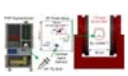

Resolving spin-spin couplings in hyperpolarized in vivo metabolic 13C spectroscopy at low magnetic field following murine tail-vein injection

Aaron M. Coffey[1], Matthew A. Feldman[1], Roman V. Shchepin[1], Milton L. Truong[1], Wellington Pham[1], and Eduard Y. Chekmenev[1]

[1]Radiology, Vanderbilt University Institute of Imaging Science, Nashville, TN, United States

We demonstrate murine whole-body MRS and the ability to resolve the ^{13}C multiplet of hyperpolarized 1-^{13}C-succinate-d_2 in a biplanar magnet with B_0 = 0.0487 T and inhomogeneity <13 ppm over 40 cm DSV. At low magnetic field strength no loss of SNR relative to high field for a well-designed radiofrequency coil occurs, but chemical shift dispersion is potentially insufficient to differentiate hyperpolarized metabolites and contrast agents. However, at sufficiently low field strength, magnetic susceptibility derived B_0 field inhomogeneity *in vivo* becomes negligible. Consequently, direct spectroscopic resolution of spin-spin couplings or *J*-couplings, more commonly performed near zero field, becomes feasible.

3040

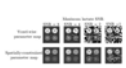

Spatio-temporally constrained reconstruction for hyperpolarized carbon-13 MRI using kinetic models

John Maidens[1], Jeremy W Gordon[2], Murat Arcak[1], Hsin-Yu Chen[2], Ilwoo Park[2], Mark Van Criekinge[2], Eugene Milshteyn[2], Robert Bok[2], Rahul Aggarwal[3], Marcus Ferrone[4], James B Slater[2], John Kurhanewicz[2], Daniel B Vigneron[2], and Peder EZ Larson[2]

[1]Electrical Engineering & Computer Sciences, University of California, Berkeley, Berkeley, CA, United States, [2]Radiology & Biomedical Imaging, UCSF, San Francisco, CA, United States, [3]Medicine, UCSF, San Francisco, CA, United States, [4]Clinical Pharmacy, UCSF, San Francisco, CA, United States

We present a method of generating metabolism maps from dynamic hyperpolarized carbon-13 MRI images. By incorporating prior information into our model-based reconstruction via spatial regularization of the parameter maps, we achieve two qualitative benefits: elimination of non-identifiability in unperfused background regions, and denoising. This method is illustrated on a simulated dataset and a clinical prostate cancer dataset.

3041

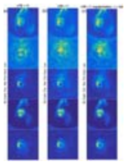

Improved reconstruction for IDEAL spiral CSI

Rie B Hansen[1], Christian Ø Mariager[2], Christoffer Laustsen[2], Rolf F Schulte[3], Jan H Ardenkjær-Larsen[1], and Lars G Hanson[1]

[1]Department of Electrical Engineering, Technical University of Denmark, Kgs. Lyngby, Denmark, [2]MR Research Centre, Aarhus University, Aarhus, Denmark, [3]GE Global Research, Munich, Germany

In this study we demonstrate how reconstruction for IDEAL spiral CSI (spectroscopic imaging scheme developed for hyperpolarized dynamic metabolic MR imaging) can be improved by using regularization with a sparsity constraint. By exploiting sparsity of the spectral domain, IDEAL spiral CSI can achieve chemical shift encoding by acquisition of only few time-shifted echoes. The minimum number of echoes required to avoid noise amplification can be decreased by means of regularization enforcing spectral sparsity, hereby reducing scan time. Improvements achieved by using regularized reconstruction are demonstrated for in vivo data from a hyperpolarized cardiac study of a pig.

3042

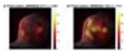

Characterization and flip angle calibration of ^{13}C surface coils for hyperpolarization studies

Rie B Hansen[1], Henrik Gutte[2], Majbrit ME Larsen[3], Annemarie T Kristensen[3], Andreas Kjær[2], Jan H Ardenkjær-Larsen[1], and Adam E Hansen[2]

[1]Department of Electrical Engineering, Technical University of Denmark, Kgs. Lyngby, Denmark, [2]Department of Clinical Physiology, Nuclear Medicine & PET and Cluster for Molecular Imaging, Rigshospitalet, University of Copenhagen, Copenhagen, Denmark, [3]Department of Veterinary Clinical and Animal Sciences, Faculty of Health and Medical Sciences, University of Copenhagen, Frederiksberg C, Denmark

The aim of the present work is to address the challenge of optimal flip angle calibration of ^{13}C surface coils in hyperpolarization studies. To this end, we characterize the spatial profile of the flip angle and demonstrate that it allows for a simple calibration improving the signal-to-noise ratio for hyperpolarized ^{13}C magnetic resonance spectroscopic imaging.

3043

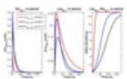

A Preliminary Framework for Validation of HP MRI using Mass Spectrometry

James A. Bankson[1], Keith A. Michel[1], Christopher M. Walker[1], Yunyun Chen[2], Jorge Delacerda[1], Charles Kingsley[1], Philip L. Lorenzi[3], Lin Tan[3], and Stephen Y. Lai[2]

[1]Department of Imaging Physics, UT MD Anderson Cancer Center, Houston, TX, United States, [2]Department of Head & Neck Surgery, UT MD Anderson Cancer Center, Houston, TX, United States, [3]Department of Bioinformatics & Computational Biology, UT MD Anderson Cancer Center, Houston, TX, United States

Dynamic imaging of HP pyruvate shows tremendous promise for offering new insight into tumor metabolism with unprecedented sensitivity, specificity, and spatiotemporal resolution. Imaging constraints due to the finite, nonstationary, and non-renewable signal pool necessitate the use of complex imaging and reconstruction strategies, but current approaches to validation of complex HP MRI measurements are lacking and new methods are critically needed. In this work, we investigate a framework for external validation of quantitative HP MRI biomarkers of tumor metabolism using stable isotope tracer analysis (MS-SITA). We show good agreement between quantitative biomarkers of chemical conversion derived from HP MRI and MS-SITA.

3044

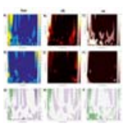

Simulation of Hyperpolarized Perfusion MRI with a Segmented Snapshot Acquisition

Keith A Michel[1], Christopher M Walker[1], Yunyun Chen[2], Jorge Delacerda[1], Stephen Lai[2], and James A Bankson[1]

[1]Department of Imaging Physics, UT MD Anderson Cancer Center, Houston, TX, United States, [2]Department of Head & Neck Surgery, UT MD Anderson Cancer Center, Houston, TX, United States

Metabolically inert hyperpolarized tracers can be used for perfusion measurements *in vivo*. In this work we present a simulation study to compare the performance for measurement of tissue perfusion of a conventional imaging approach to a segmented snapshot acquisition where each segment ends with a 90 degree RF pulse.

3045

Practical Considerations of Quantitative kPL Estimation in Hyperpolarized-13C Imaging in Response to Pulse Sequence Design and Parameters

Hsin-Yu Chen[1,2], Jeremy W. Gordon[1], Robert A. Bok[1], Peng Cao[1], Cornelius von Morze[1], Eugene Milshteyn[1,2], Ralph E. Hurd[3], John Kurhanewicz[1,2], Peder E.Z. Larson[1,2], and Daniel B. Vigneron[1,2]

[1]Department of Radiology and Biomedical Imaging, University of California, San Francisco, San Francisco, CA, United States, [2]UCSF/UC Berkeley Graduate Program in Bioengineering, University of California, San Francisco, San Francisco, CA, United States, [3]GE healthcare, Menlo Park, CA, United States

Hyperpolarized-^{13}C MRI has recently enabled imaging of cancer pathophysiology with high spatiotemporal resolution in humans. Quantitative measure of tumor metabolism can be made possible by estimating conversion rate constants (e.g. k_{PL} for pyruvate-to-lactate). We have identified 3 systematic sources affecting k_{PL} estimation that were introduced by MR acquisition and pulse sequences – an RF-spoiling effect, a T_2*-weighting factor, and a crusher flow-suppression phenomenon. These sources were investigated using a transgenic cancer model and simulations.

3046

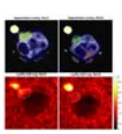

A fuzzy Markov random field approach for the unsupervised segmentation of hyperpolarized 13C MRI data

Charlie J Daniels[1,2] and Ferdia A Gallagher[1,3]

[1]Department of Radiology, University of Cambridge, Cambridge, United Kingdom, [2]Integrated Mathematical Oncology, Moffitt Cancer Centre, Tampa, FL, United States, [3]Cancer Research UK Cambridge Institute, University of Cambridge, Cambridge, United Kingdom

MRI with hyperpolarized ^{13}C-labelled compounds is an emerging clinical technique allowing *in vivo* metabolic processes to be characterized non-invasively. Accurate quantification of metabolism requires a region-of-interest to be defined, which is usually based on spatial information only. However, as the hyperpolarized data is 5-dimensional (spatial, temporal and spectral), it offers the possibility of applying novel segmentation methods to more accurately define this region-of-interest. A novel solution to the problem of ^{13}C image segmentation is proposed here, using a hybrid Markov random field model with fuzzy logic. Performance of the algorithm is demonstrated using in silico and in vivo data.

Traditional Poster

Molecular Imaging & Novel Contrast Agents

Exhibition Hall 3047-3063 Thursday 13:00 - 15:00

3047

magna cum laude

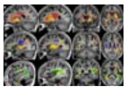

Whole-Brain Visualization of Manganese Deposition in Welders

Chien-Lin Yeh[1,2], Courtney Beth Johnson[3], Ruoyun Ma[1,2], Shalmali Dharmadhikari[4], Sandy Snyder[1], and Ulrike Dydak[1,2]

[1]Purdue University, West lafayette, IN, United States, [2]Indiana University School of Medicine, Indianapolis, IN, United States, [3]Department of Psychiatry, Indiana University School of Medicine, Indianapolis, IN, United States, [4]Department of Radiology and Imaging Sciences, Emory University, Atlanta, GA, United States

While the paramagnetic properties of Mangnaese (Mn) make it useful as a contrast agent for MRI, little is known about the spatial distribution of Mn deposition in the human brain due to occupational Mn exposure. Using a novel approach to analyze and visualize whole brain Mn deposition in welders, Mn was elevated in motor and cognitive associated networks, consistent with respective reports on impaired neuropsychological function. Our Mn maps even reveal the diffusion of Mn along white matter tracts for the first time in humans. These findings help explain how Mn exposure affects the function of particular brain networks.

3048

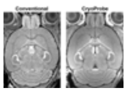

High Resolution MEMRI Reveals the Purkinje Cell Layer as the Source of Contrast in the Mouse Cerebellum

Harikrishna Rallapalli[1,2], Brian J Nieman[3], Aidin Arbabi[3], Dulcie Vousden[3], Jason P Lerch[3], and Daniel H Turnbull[1,2]

[1]Kimmel Center for Biology and Medicine at the Skirball Institute of Biomolecular Medicine, New York University School of Medicine, New York, NY, United States, [2]Biomedical Imaging Graduate Program and Department of Radiology, New York University School of Medicine, New York, NY, United States, [3]Mouse Imaging Centre, The Hospital for Sick Children, Toronto, ON, Canada

Imaging the developing mouse brain with conventional MRI is challenging. Manganese-enhanced MRI (MEMRI) has the potential to provide a noninvasive, *in vivo* approach for analyzing mutant phenotypes in the early postnatal mouse cerebellum. We present preliminary data generated using a CryoProbe (Bruker) suggesting that the primary source of Mn contrast in the mouse cerebellum is the Purkinje cell layer.

3049

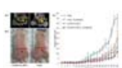

Gd complex of DO3A-benzothiazole conjugate for neutron capture therapy

Ki-Hye Jung[1], Ji-Ae Park[1], Jung Young Kim[1], Yongmin Chang[2,3], Tae-Jeong Kim[4], Hee-Kyung Kim[4], Kyo Chul Lee[1], Joo Hyun Kang[1], and Yong Jin Lee[1]

[1]Division of RI-Convergence Research, Korea Institute of Radiological & Medical Sciences, Seoul, Korea, Republic of, [2]Department of Medical & Biological Engineering, Kyungpook National University, Daegu, Korea, Republic of, [3]Department of Radiology and Molecular Medicine, Kyungpook National University, Daegu, Korea, Republic of, [4]Institute of Biomedical Engineering Research, Kyungpook National University, Daegu, Korea, Republic of

We have presented a strategy for incorporating low-molecular-weight Gd(III) chelate for dual non-invasive MR contrast agent and NCT, without the necessity of loading individual contrast therapeutic drugs, which is usually required in theranostics. The Gd-DO3A-BTA injected and neutron irradiated group, the tumor growth was significantly suppressed. This information could provide a basis for the prospect of obtaining a synergistic or cumulative action of chemotherapy (ChT) and Gd-NCT. We examined the neutron capture irradiation of MDA-MB-231 mice in the presence of Gd-DO3A-BTA. The results indicate that Gd-DO3A-BTA is suitable neutron capture agent for Gd-NCT.

3050

Mn-complex of DO2A-benzothiazole chelate as a new hepatobiliary MRI contrast agent

Soyeon Kim[1], Hee-Kyung Kim[2], Eun-Young Jeon[3], Md. Kamrul Islam[1], Garam Choi[1], Au Reum Baek[1], Bo Kyung Sung[1], Tae-Jeong Kim[3], and Yongmin Chang[1,2,4]

[1]Medical & Biological Engineering, Kyungpook National University, Daegu, Korea, Republic of, [2]Department of Molecular Medicine & BK21 Plus KNU Biomedical Convergence Program, Kyungpook National University, Daegu, Korea, Republic of, [3]Institute of Biomedical Engineering Research, Kyungpook National University, Daegu, Korea, Republic of, [4]Department of Radiology, Kyungpook National University

The purpose of the present work is to design and synthesize a new bifunctional complex for use in Mn(II)-based liver-targeting MR imaging. Its r_1 relaxivity in human serum albumin (HSA) solution is 3.21 $mM^{-1}s^{-1}$, similar to MRI CA such as MnDPDP®. In vivo MR image after injection of Mn-DO2A-BTA by tail vein showed that its excretion is made via kidney and also bile duct, confirming hepatobiliary uptake.

3051

Cyclodextrin-based pseudo-rotaxanes as conjugatable molecular imaging biosensors for hyperpolarized 129Xe MRI

Braedan RJ Prete[1], Simrun Chahal[2], Ashvin Fernando[3], Tao Li[1], Francis Hane[4], Brenton DeBoef[3], and Mitchell Albert[1]

[1]Lakehead University, Thunder Bay, ON, Canada, [2]University of Guelph, [3]University of Rhode Island, [4]Lakehead University, MURILLO, ON, Canada

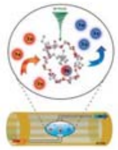

Hyperpolarized (HP) 129Xe molecular imaging technology has recently advanced in the detection of biochemically inactive supramolecular cage-molecules within a living mammalian model. Unfortunately, the natural bio-distribution of these biosensor molecules is non-specific, which makes it difficult to precisely localize them in vivo using HP 129Xe MRI. With the HyperCEST detection of easily conjugated cyclodextrin-based pseudo-rotaxanes, we have identified a critical advancement in 129Xe biosensor design by uncovering a novel biosensor, which has the potential to precisely detect markers of early disease in a human body with comparable sensitivity to PET but with the spatial resolution of MRI.

3052 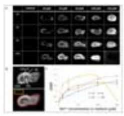

Mn2+ uptake mechanisms in organotypic rat hippocampal slice cultures

Alexia Daoust[1], Galit Saar[1], Steven Dodd[1], and Alan Koretsky[1]

[1]*National Institute of Neurological Disorders and Stroke, National Institutes of Health, Bethesda, MD, United States*

MEMRI can be used for different applications such as tracing neuronal connections or functional imaging. However, Mn^{2+} uptake and transport mechanisms are still unclear. These mechanisms were studied in an organotypic hippocampal slice culture. After adding Mn to the medium, MRI contrast changes were affected by Ca channel manipulation and other metals that use divalent metal transporters. Mn cellular uptake was also affected by both, the presence of glutamate receptor antagonist and a neuronal activity inhibitor. Our results establish hippocampal slice as a system to study the cellular mechanisms related to MEMRI.

3053 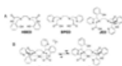

A Janus Chelator Enables Biochemically Responsive MRI Contrast With Exceptional Dynamic Range

Eric M Gale[1], Chloe M Jones[1], Ian Ramsay[1], Christian T Farrar[1], and Peter Caravan[1]

[1]*A. A. Martinos Center for Biomedical Imaging, MGH/ Harvard Medical School, Charlestown, MA, United States*

Mn-JED is a new biochemically responsive MRI contrast agent that provides 9-fold relaxivity change by switching between the Mn(3+) and Mn (2+) oxidation states. The JED chelator is the only chelator that supports both the Mn(3+) and Mn(2+) oxidation states in biological milieu. Rapid interconversion between oxidation states is achieved by peroxidase activity (oxidation) and cysteine (reduction). Peroxidase activity is drastically elevated during acute inflammation. Thiols such as cysteine are overabundant in the microenvironment of proliferative tumors. Mn-JED provides a new paradigm for the design of biochemically responsive MRI contrast agents.

3054 

Diamagnetic imaging agents with a modular chemical design for quantitative detection of β-galactosidase and β-glucuronidase activities with catalyCEST MRI

Gabriela Fernández-Cuervo[1], Kirsten A. Tucker[2], Scott W. Malm[3], Kyle M. Jones[4], and Mark D. Pagel[4]

[1]*Pharmaceutical Sciences, University of Arizona, Tucson, AZ, United States,* [2]*Chemistry and Biochemistry, University of Arizona, Tucson, AZ, United States,* [3]*Pharmacy, University of Arizona, Tucson, AZ, United States,* [4]*Biomedical Engineering, University of Arizona, Tucson, AZ, United States*

We have designed and synthesized new MRI agents that quantitatively detect β-galactosidase and β-glucuronidase activities by measuring changes in chemical exchange saturation transfer (CEST). Based on a modular approach, we incorporated the enzymes' respective substrates to a salicylate moiety with a spontaneously disassembling, chromogenic spacer via a carbamate linkage. This design furnished highly selective diamagnetic CEST agents that detected and quantified enzyme activities of glycoside hydrolase enzymes. Michaelis-Menten enzyme kinetics studies were performed by monitoring catalyCEST MRI signals, which were validated with UV-vis assays.

3055 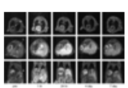

Tumor-targeted alkylphosphocholine chelates for dual-modality PET/MR imaging

Ray R Zhang[1], Christinna L Brunnquell[1], Reinier Hernandez[1], Alan McMillan[1], Anatoly N Pinchuk[1], Paul A Clark[2], Vincent L Cryns[3], John S Kuo[2], and Jamey P Weichert[1]

[1]*Department of Radiology, University of Wisconsin Madison, Madison, WI, United States,* [2]*Department of Neurological Surgery, University of Wisconsin Madison, Madison, WI, United States,* [3]*Department of Medicine - Endocrinology, University of Wisconsin Madison, Madison, WI, United States*

Extensive structure-activity relationships studies have previously shown that alkylphosphocholine (APC) analogs selectively deliver radioiodine and larger fluorophores to a variety of tumor types in rodent models and humans[1-3]. To further explore the payload capacity of APCs, we synthesized several new APC-chelates and assessed their ability to deliver Gd (MRI) and ^{64}Cu (PET) selectively to tumors *in vivo*. Prolonged T1-weighted signal enhancement following Gd-DOTA-APC injection was observed in all tumor models. Clinical PET/MR imaging of U87 flank xenograft at 24h and 48h post-administration of Gd-DOTA-APC and ^{64}Cu-DOTA-APC demonstrated co-localization of T1-weighted signal enhancement and PET activity in the tumor.

3056 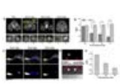

Facile and Novel Synthesis of MR/NIR Dual Modal Contrast Agent for In Vivo Non-invasive Molecular Imaging

Hye Sun Park[1], Mi Young Cho[1], Hyunseung Lee[1], and Kwan Soo Hong[1]

[1]*Bioimaging Research Team, Korea Basic Science Institute, Cheongju-si, Korea, Republic of*

We proposed the phase transferring method of hydrophobic magnetic nanoparticles without any chemical modifications, for use as a magnetic resonance (MR)/near-infrared (NIR) fluorescence bimodal imaging contrast agent. Indocyanine green (ICG) was used both as an optical component and a surfactant for phase transfer with no superfluous moiety. ICG-MNP-labeled dendritic cells presented MR/NIR dual-modal imaging properties with high and sensitive detection ability for a long time. We expect that this novel MR/NIR contrast agent with sensitive detection and simultaneous imaging capability can be used in the imaging and tracking of immune cells to confirm immunotherapeutic efficacy.

3057

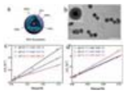

Multifunctional magnetic nanocomposites for T1/T2 Dual-Mode MRI and pH-responsive drug delivery

Xi Huang[1], Shizhen Chen[1], Yaping Yuan[1], Lianhua Liu[1], and Xin Zhou[1]

[1]Key Laboratory of Magnetic Resonance in Biological Systems, State Key Laboratory of Magnetic Resonance and Atomic and Molecular Physics, National Center for Magnetic Resonance in Wuhan, Wuhan Institute of Physics and Mathematics, Chinese Academy of Sciences, Wuhan, People's Republic of China

In this abstract, multifunctional Fe_3O_4@SiO_2@PAA-cRGD nanocomposites were designed and synthesized to load water soluble Mn-porphyrin and anticancer drug doxorubicin, which could realize both pH-responsive drug release and T1/T2 dual-mode MRI capability. In vitro cell fluorescent imagings showed that c(RGDyk)-modified nanocomposites can effectively target A549 cells. Furthermore, in vitro T1-weighted and T2-weighted MR images of A549 cells were observed. For in vivo MRI, T1 and T2 relaxation was significantly accelerated in the tumor after i.v. injection of nanocomposites. These evidences showed that the nanocomposites could be used as pH-responsive T1/T2 dual-mode contrast agent, and have the potential for the tumor-targeted MRI and drug delivery.

3058

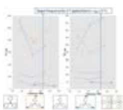

Extrinsic MRI contrast agents based on nuclear quadrupole enhanced relaxation: Principle, requirements and characterization of promising compounds

Christian Gösweiner[1], Danuta Kruk[2], Per-Olof Westlund[3], Fischer Roland[4], Schlögl Martin[4], Markus Bödenler[1], Andreas Petrovic[1], Hermann Scharfetter[1], and Stefan Spirk[5]

[1]Institute of Medical Engineering, Graz University of Technology, Graz, Austria, [2]Faculty of Mathematics and Computer Science, University of Warmia and Mazury in Olsztyn, Poland, [3]Department of Chemistry, Umeå universitet, Sweden, [4]Institute of Inorganic Chemistry, Graz University of Technology, Graz, Austria, [5]Institute for Chemistry and Technology of Materials, Graz University of Technology, Graz, Austria

Quadrupole Relaxation Enhancement is a quantum mechanical effect that can be exploited to create a new generation of extrinsic contrast agents for usage in MRI. In this work we have investigated the physical requirements of such contrast agents have to meet to be useful. Based on our findings concerning nuclear quadrupole resonance-properties, spin relaxation behavior and toxicity we suggest a variety of ^{209}Bi-aryl compounds. The sensitivity of these compounds onto chemical or magnetic field changes equip them with smart properties such as on/off switching of the contrast or molecular imaging.

3059

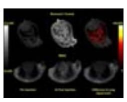

Synthesis of Amplifiable Probe Gd-5-HT-DOTAGA and Application to Molecular Imaging of Pulmonary Inflammation

Aurora Rodriguez-Rodriguez[1], Nicholas Rotile[1], Julian Goding[2], Clemens K Probst[3], Andrew M Tager[3], Alexei Bogdanov, Jr[2], and Peter Caravan[1]

[1]A. A. Martinos Center for Biomedical Imaging, Massachusetts General Hospital, Charlestown, MA, United States, [2]University of Massachusetts Medical School, Worcester, MA, United States, [3]Center for Immunology and Inflammatory Diseases, Massachusetts General Hospital, Boston, MA, United States

We report the synthesis of a new amplifiable MR probe that combines the stability of the macrocyclic Gd-DOTA core with the myeloperoxidase-reactive 5-hydroxytryptamide (5-HT) moiety. The relaxivity of Gd-5-HT-DOTAGA is increased 60% in the presence of myeloperoxidase activity. In a mouse model of bleomycin induced lung injury, the change in lung-to-muscle contrast to noise ratio is increased 50% compared to naïve animals, consistent with 3-fold higher Gd lung concentrations measured *ex vivo*.

3060

Synthesis of hepatocyte-specific manganese complex with high kinetic stability and MR contrast characteristic for liver cancer imaging

Heekyung Kim[1], Garam Choi[2], Md. Kamrul Islam[2], Soyeon Kim[2], Ah Rum Baek[2], Bo Kyung Sung[2], Eunyoung Jeon[3], Tae-Jeong Kim[3], and Yongmin Chang[1,2,4]

[1]BK21 Plus KNU Biomedical Convergence Program, Kyungpook National University, Daegu, Korea, Republic of, [2]Medical & Biological Engineering, Kyungpook National University, Daegu, Korea, Republic of, [3]Institute of Biomedical Engineering Research, Kyungpook National University, [4]Radiology, Kyungpook National University

Novel manganese (II) complex based on EDTA coordination cage bearing benzothiazole aniline (BTA) moiety with high chelation stability was designed and synthesized for use as a liver-specific MRI contrast agent. In addition to forming a hydrophilic, this new hepatobiliary Mn(II) chelate is rapidly taken up by hepatocyte of liver. The magnetic and kinetic properties of Mn(II) complex are higher than commercially available analogue, Mn-DPDP, which was clinically approved MR liver contrast agent. The complex, Mn-EDTA-BTA, was evaluated via in vivo MR imaging to prove high tumor detection sensitivity using animal liver tumor model.

3061

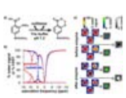

Detection of sulfatase enzyme activity with a catalyCEST MRI contrast agent

Sanhita Sinharay[1], Gabriela Fernández-Cuervo[2], Jasmine P. Acfalle[1], and Mark D. Pagel[3]

[1]Chemistry and Biochemistry, University of Arizona, Tucson, AZ, United States, [2]Pharmaceutical Sciences, University of Arizona, Tucson, AZ, United States, [3]Medical Imaging, University of Arizona, Tucson, AZ, United States

CatalyCEST MRI with a diamagnetic CEST agent, 4-acedamido-2-(sulfoxy)benzoic acid, can detect the activity of sulfatase. An enzyme-responsive CEST signal was compared to an unresponsive CEST signal to determine a reaction coordinate of contrast agent cleavage by sulfatase. This imaging method produced parametric maps of CEST signal amplitudes and the reaction coordinates. Three isoforms of the enzyme were tested in biochemical solutions. catalyCEST MRI with the agent detected sulfatase activity in the media from sulfatase-expressing HEK293 cells but not in the media of sulfatase-deficient BT529 cells.

3062

One-pot microwave synthesis of fluorinated silicon nanoparticles for dual 19F-MRI and fluorescence imaging

Sha Li[1], Shizhen Chen[1], Yaping Yuan[1], Lili Ren[1], Yuqing Yang[1], and Xin Zhou[1]

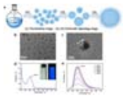

[1]Key Laboratory of Magnetic Resonance in Biological Systems, State Key Laboratory of Magnetic Resonance and Atomic and Molecular Physics, National Center for Magnetic Resonance in Wuhan, Wuhan Institute of Physics and Mathematics, Chinese Academy of Sciences, Wuhan, People's Republic of China

In this study, we have designed a one-pot microwave strategy for facile and rapid synthesis of blue-emitting ^{19}F-SiNPs. The as prepared ^{19}F-SiNPs significantly exhibited ultral small sizes, excellent water solubility and strong fluorescence. Besides, The chemically and magnetically equivalent trifluoromethyl groups grafted on the prepared nanoparticles displayed a single NMR signal, which offered advantages to maximize the generated magnetic resonance signal. In summary, such resultant ^{19}F-SiNPs are particularly suitable for real-time ^{19}F-MRI and fluorescence dual modality imaging.

3063

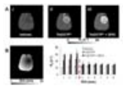

Simultaneous imaging of drug delivery with SPIO-based MRI and drug therapy with pHe readout from BIRDS

Samuel Maritim[1], Daniel Coman[2], Yuegao Huang[2], Jyotsna Rao[2], John Walsh[1], and Fahmeed Hyder[1]

[1]Biomedical Engineering, Yale University, New Haven, CT, United States, [2]Department of Radiology & Biomedical Imaging, Yale University, New Haven, CT, United States

Since acidification of the extracellular environment is a hallmark of cancer pathogenesis, successful therapy may manifest as normalization of pHe. We have shown that quantitative pHe measurement is possible with BIRDS is possible even in the presence of superparamagnetic iron oxide nanoparticles (SPIO-NPs). Because SPIO-NPs have been used to image and track drug delivery, we envisage co-injection of BIRDS agents and NPs, containing drugs and SPIO, as a new protocol that can track drug delivery to tumors, concurrently map tumor location and size (by MRI), and at the same time measure therapeutic efficacy through changes in tumor pH (by BIRDS).

Traditional Poster

Targeted Molecular & Cellular Imaging

Exhibition Hall 3064-3078 Thursday 13:00 - 15:00

3064

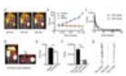

A novel tracer for non-invasive atherosclerotic plaque phenotyping by PET/MR imaging

Max L Senders[1,2], Calvin Yeang[3], Hannah Groenen[1], Francois Fay[1], Claudia Calcagno[1], Simone Green[3], Phuong Miu[3], Thomas Reiner[4], Joseph L Witztum[3], Zahi A Fayad[1], Willem J M Mulder[1], Carlos Perez-Medina[1], and Sotirios Tsimikas[3]

[1]Translational and Molecular Imaging Institute, Icahn School of Medicine at Mount Sinai, New York, NY, United States, [2]Medical Biochemistry, Academic Medical Center, Amsterdam, Netherlands, [3]Division of Cardiovascular Diseases, Sulpizio Cardiovascular Center, Department of Medicine, University of California, La Jolla, San Diego, CA, USA., [4]Department of Radiology, Memorial Sloan Kettering Cancer Center, New York, NY, USA

Atherosclerotic plaques that rupture can cause stroke or myocardial infarction. Oxidation specific epitopes (OSE), as present in oxidized LDL (OxLDL), are hallmarks of vulnerable plaques . We have developed the PET radiotracer ^{89}Zr-LA25 that targets OSE. Integration of ^{89}Zr-LA25 PET imaging with previous validated techniques enables ‘’vulnerable’’ plaque phenotyping by PET/MRI

3065

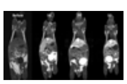

A new highly stable macrocyclic gadolinium complex as a liver targeting MRI contrast agent

Heekyung Kim[1], Ah Rum Baek[2], Soyeon Kim[2], Eun-Young Jeon[3], MD. Kamrul Islam[2], Garam Choi[2], Bo Kyung Sung[2], Tae-Jeong Kim[3], and Yongmin Chang[1,2,3,4]

[1]BK21 Plus KNU Biomedical Convergence Program, Kyungpook National University, Daegu, Korea, Republic of, [2]Medical &Biological Engineering, Kyungpook National University, [3]Biomedical Engineering Research Institue, Kyungpook National University, [4]Radiology, Kyungpook National University

Gd-EOB-DO3A is prepared according to the general synthetic methods, and characterized by spectroscopic analysis. The relaxivities are r1 = 8.07, r2 = 8.57 mM-1s-1. From in vivo T1-weighted MR images, we observe good liver-specific enhancement that can be compared with commercial liver targeting agents, and confirm the biliary excretion via gallbladder. Also the kinetic stability of the gadolinium complex was determined with time-dependent longitudinal relaxation rate (R1,p(t)/R1,p(0)) and the relaxation was maintained above 70% against to initial value during the measurement.

3066

Highly Sensitive Magnetic Nanoprobe for Detection of ErbB2-expressing Cancer

Dan Heo[1,2], Jaemoon Yang[1], and Jin-Suck Suh[1]

[1]Department of Radiology, Yonsei University College of Medicine, Seoul, Korea, Republic of, [2]Nanomedical National Core Research Center, Yonsei University, Seoul, Korea, Republic of

ErbB2, which belongs to the epidermal growth factor receptor (EGFR) family, plays a key role in human malignancies. ErbB2 is overexpressed in approximately 30% of human breast cancers and in many other cancer types, including stomach, bladder, ovarian and lung carcinomas. The objective of this study is the development of anti-ErbB2 aptamer-modified T2 contrast agent based on magnetic nanoprobe (Apt_{ErbB2}-MNP) having high-specificity onto Erbb2-expressing cancer. For confirmation of Apt_{ErbB2}-MNP as T2 contrast agent, T2 relaxivity and hydrodynamic diameter was measured. *in vitro* binding affinity tests were conducted not only recombinant ErbB2 proteins but also the live cells. *in vivo* targeting ability was verified by *in vivo* MRI analysis.

3067

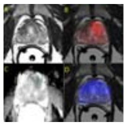

[18F]-DCFPyL standard uptake values correlate with apparent diffusion coefficient and choline measurements on a 3T PET-MRI in prostate cancer

Reggie Taylor[1,2,3], Irina Rachinsky[4], Zahra Kassam[4,5], William Pavlosky[4], Ashley Lozanski[6], John Butler[1], Stephen Pautler[5,6], Aaron Ward[1,3], Joseph Chin[1,5,6], Ting-Yim Lee[1,3,5,7], Glenn Bauman[1,3,4,8], and Jonathan Thiessen[1,3]

[1]Lawson Health Research Institute, London, ON, Canada, [2]Siemens Healthcare Limited, Oakville, ON, Canada, [3]Medical Biophysics, Western University, London, ON, Canada, [4]Medical Imaging, Western University, London, ON, Canada, [5]Oncology, Western University, London, ON, Canada, [6]Surgery, Western University, London, ON, Canada, [7]Robarts Research Institute, London, Canada, [8]London Regional Cancer Program, London, ON, Canada

PET data with the [^{18}F]-DCFPyL PSMA-targeted probe to examine prostate cancer in patients scheduled for radical prostatectomy was acquired concurrently with diffusion weighted imaging and chemical shift imaging using a 3T PET-MRI. Standard uptake values (SUV) were compared to apparent diffusion coefficients (ADC) and choline plus creatine over citrate ratios (CC/C). Positive correlations existed between the SUV and CC/C in voxels with low ADC. Negative correlations existed between the ADC and SUV in voxels with high CC/C, and negative correlations also existed between the ADC and CC/C in voxels with high SUV.

3068

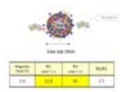

In vitro and in vivo detection of treatment-induced apoptosis using ultrasmall superparamagnetic iron oxide (USPIO)-conjugated Annexin V: A pilot study

Osamu Togao[1], Akihiro Nishie[1], Chihiro Tamura[2], Mayumi Yamato[2], Kazuhiro Ichikawa[2], Satoshi Nohara[3], Yoshio Ito[3], Naoki Kato[4], Satoshi Yoshise[4], and Hiroshi Honda[1]

[1]Clinical Radiology, Graduate School of Medical Sciences, Kyushu University, Fukuoka, Japan, [2]Innovation Center for Medical Redox Navigation, Kyushu University, [3]Meito Sangyo Co., LTD, [4]Guerbet Japan KK

Apoptosis is involved in many pathological processes. Early detection of treatment-induced apoptosis in malignant tumors is clinically useful for a decision making in therapeutic strategy. Phosphatidylserine (PS) expressed on the cell membrane is known to be a marker of apoptosis which can be detected by probes with Annexin V. In this study, we newly synthesized USPIO-conjugated Annexin V and investigated its potential in the use in apoptosis imaging in both in vitro and in vivo studies.

3069

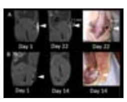

A Bright Contrast Labelling Approach for Non-Invasive MR Imaging of Biomaterials

Daniel Andrzej Szulc[1,2], Tameshwar Ganesh[2,3], Maryam Abdinejad[4], Hanlin Liu[4,5], Xiao-an Zhang[4,5], and Hai-Ling Margaret Cheng[1,2,6]

[1]Institute of Biomaterials & Biomedical Engineering, University of Toronto, Toronto, ON, Canada, [2]Ted Rogers Centre for Heart Research, Translational Biology & Engineering Program, Toronto, ON, Canada, [3]Pharmaceutical Sciences, Leslie Dan Faculty of Pharmacy, University of Toronto, Toronto, ON, Canada, [4]Department of Physical and Environmental Sciences, University of Toronto Scarborough, Toronto, ON, Canada, [5]Department of Chemistry, University of Toronto, Toronto, ON, Canada, [6]Edward S. Rogers Sr. Department of Electrical & Computer Engineering, University of Toronto, Toronto, ON, Canada

Tissue engineered biomaterials have the potential to regenerate almost every tissue type. One difficult aspect to advancing this technology is determining the properties and fate of these materials once introduced in vivo. Non-invasive imaging technology such as MRI holds significant potential for monitoring implanted biomaterials. Few novel approaches to directly image biomaterials have recently been developed; however, most are designed for specific materials or utilize iron oxides with limited specificity. In this study, we investigate a novel approach to labelling biomaterials with a highly efficient T1 agent and a biologically derived adhesive, which allows for accurate and sensitive detection in vivo.

3070

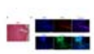

A Specific MRI contrast agent for glioma: Targeted Quadruple Mutant IL-13 (TQM-13) conjugated liposomes encapsulated with Magnevist@

Xiaoli Liu[1], A. B. Madhankumar[2], Patti A. Miller[1], Becky Slagle-Webb[2], Oliver Mrowczynski[2], Akiva Mintz[3], Qing X. Yang[1], and James R. Connor[2]

[1]Radiology, College of Medicine Penn State University, Hershey, PA, United States, [2]Neurosurgery, College of Medicine, Penn State University, Hershey, [3]Radiology and Nuclear Medicine Wake Forest School of Medicine, NC, USA

There is a clinical need for targeted MRI-contrast agents that are more sensitive and specific in detection of glioma than conventional MRI contrast. We use interleukin-13 (IL-13) as targeting ligand because 75% of glioma cells overexpress IL-13Rα2 significantly1. We investigated the relative efficacy of liposomes conjugated with wild type IL-13 to a variant of IL-13, known as Targeted Quadruple Mutant13 (TQM-13) that has been shown to be more selective for the IL-13Rα2 and binds with higher affinity than the wide type. Our targeted MRI agent, TQM-13-liposomes-Gd, produced specific MRI contrast, delineating tumor, inflamed and normal tissues.

3071

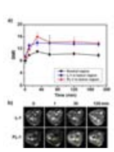

Metastatic Liver Cancer Targeted Liposomal Theranostic Prodrug for in vivo Diagnosis and Therapy

Hyun Min Kim[1], Hyunseung Lee[1], and Kwan Soo Hong[1]

[1]Bioimaging Research Team, Korea Basic Science Institute, Cheongju-Si, Korea, Republic of

Reported here is a new theranostic agent, **1**, which consists of a Gd^{3+}-texaphyrin core conjugated to a doxorubicin prodrug via a disulfide bond undergoing cleavage in the presence of glutathione, a species typically upregulated in cancer cells. To improve the solubility and tumor targeting of **1**, it was loaded into folate receptor-targeted liposomes to produce **FL-1**. **FL-1** was found to selectively produce a greater anti-proliferative effect in the case of the KB and CT26 cell lines as compared to the HepG2 and NIH3T3 cell lines. FL-1 was also found to provide enhanced MR imaging in vivo under conditions of T1 contrast in the early stage of metastatic cancer progression.

3072

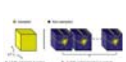

Compressed Sensing with Signal Averaging Reduces Motion Artifacts in Fluorine-19 MRI

Emeline Darçot[1], Jerome Yerly[1,2], Tom Hilbert[1,3,4], Roberto Colotti[1], Maxime Pellegrin[5], Elena Najdenovska[1,2], Tobias Kober[1,3,4], Matthias Stuber[1,2], and Ruud B van Heeswijk[1]

[1]Radiology, University Hospital of Lausanne (CHUV)-University of Lausanne (Unil), Lausanne, Switzerland, [2]Center for Biomedical Imaging (CIBM), Lausanne, Geneva, Switzerland, [3]Advanced Clinical Imaging Technology (HC CMEA SUI DI PI), Siemens Healthcare AG, Lausanne, Switzerland, [4]Signal Processing Laboratory 5 (LTS5), Ecole Polytechnique Fédérale de Lausanne, Lausanne, Switzerland, [5]Angiology service, University Hospital of Lausanne (CHUV)-University of Lausanne (Unil), Lausanne, Switzerland

In addition to conventional signal averaging, compressed sensing (CS) can be applied to fluorine-19 MRI to improve its low signal-to-noise ratio. For a given acquisition time and CS algorithm, an N-averages N-fold-undersampled dataset results in higher sensitivity than a fully sampled non-averaged dataset. However, it is still unclear whether averaging changes the sensitivity to motion artifacts for an undersampled acquisition.We therefore tested the hypothesis that an N-averages N-fold undersampled acquisition is more robust against motion artifacts than a fully sampled non-averaged acquisition when both are reconstructed with CS.

3073

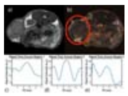

Improved tracking and quantification of SPIO-labeled cells using bSSFP with compressed sensing TurboSPI

Zoe O'Brien-Moran[1,2], Marie-Laurence Tremblay[1], Christa Davis[1], James Rioux[1,2,3], and Kimberly Brewer[1,2,3,4]

[1]Biomedical Translational Imaging Centre (BIOTIC), Halifax, NS, Canada, [2]Physics, Dalhousie University, Halifax, NS, Canada, [3]Diagnostic Radiology, Dalhousie University, Halifax, NS, Canada, [4]Microbiology, Dalhousie University, Halifax, NS, Canada

Understanding immune cell behaviour is important for evaluating therapeutic response in pre-clinical models. We monitor cell migration in a mouse model of cervical cancer by labeling cells with superparamagnetic iron oxide (SPIO). Simultaneous pre-clinical PET/MRI confirmed that the balanced steady-state free precession (bSSFP) sequence lacks specificity to SPIO-labeled cells within the tumor. We tested TurboSPI, a multi-echo single point imaging technique with compressed sensing that provides high temporal resolution 3D R_2* mapping in under 45 minutes. These maps exhibit superior SPIO specificity compared to bSSFP images and enabled us to do both qualitative and quantitative cell tracking.

3074

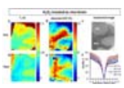

ROS imaging by endogenous contrast MRI: specificity and translational premises

Alessandro M Scotti[1,2,3], Rongwen Tain[1,3], Weiguo Li[4,5], Xiaohong Joe Zhou[1,2,3], and Kejia Cai[1,2,3]

[1]Radiology, College of Medicine, University of Illinois at Chicago, Chicago, IL, United States, [2]Bioengineering, University of Illinois at Chicago, Chicago, IL, United States, [3]3T Research Program, Center for MR Research, College of Medicine, University of Illinois at Chicago, Chicago, IL, United States, [4]Research Resource Center, College of Medicine, University of Illinois at Chicago, Chicago, IL, United States, [5]Radiology, College of Medicine, Northwestern University, Chicago, IL, United States

Detection of the elusive Reactive Oxygen Species is pivotal for understanding and diagnosis of many diseases. Recently ROS has been imaged with endogenous MRI contrasts in biological system by reduction in CEST trough combined T_1 shortening and proton exchange enhancing effects. We here show potential confounding factors such as H_2O_2, molecular oxygen, iron oxidation, pH, and temperature to be negligible in phantom studies. In addition, for the first time, we have imaged ROS by endogenous MRI contrasts under physiological conditions, at clinical MRI field strength and on ex vivo brain tissue, paving the path for clinical translation.

3075

19F MR-Imaging of acute thrombi using a clinically relevant perfluorocarbon nanoemulsion

Sebastian Temme[1], Christoph Jacoby[2], Christoph Grapentin[3], Jürgen Schrader[1], and Ulrich Flögel[1]

[1]Molecular Cardiology, University of Düsseldorf, Düsseldorf, Germany, [2]Division of Cardiology, Pulmonology and Vascular Medicine, University of Düsseldorf, Düsseldorf, Germany, [3]Pharmaceutical Technology and Biopharmacy, University of Freiburg, Freiburg i. Br.

Exact localization of acute thrombi is still a serious problem in the clinical setting. Here we show the feasibility of artefact-free ^{19}F MR-imaging using clinically relevant PFOB-nanoemulsions functionalized with an α2-antiplasmin peptide, specific for early thrombi. Utilizing the isolated CF_3-peak of PFOB in combination with a conventional ^{19}F RARE sequence is suitable for specific and artefact-free imaging of acute thrombi *in vitro* and also *in vivo*.

3076

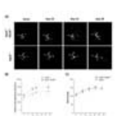

Non-invasive imaging of macrophage accumulation in abdominal aortic aneurysm by 19F MRI

Sebastian Temme[1], Guang Yang [2], Christoph Jacoby[3], Stegbauer Johannes [2], and Flögel Ulrich [1]

[1]Molecular Cardiology, University of Düsseldorf, Düsseldorf, Germany, [2]Department of Internal Medicine/Nephrology, University Hospital Düsseldorf, Düsseldorf, Germany, [3]Division of Cardiology, Pulmonology and Vascular Medicine, University of Düsseldorf, Düsseldorf, Germany

Abdominal aortic aneurysms (AAA) are a relatively common disease, with still unclear etiology that is associated with high mortality due to aortic rupture. Here we show that mice deficient for the Mas-receptor show aggravated AAA formation upon Ang-II treatment and that accumulation of macrophages in bulk aneurysms can be non-invasively visualized by ^{1}H/^{19}F MRI using intravenously applied perfluorocarbon nanoemulsions which are efficiently phagocytosed by macrophages. We conclude that Mas-receptor deficiency leads to increased inflammation with enhanced AAA formation and that ^{19}F MRI-based inflammation imaging will help to further unravel the role of monocytes/macrophages in the course of AAA progression.

3077

Selective acidification and de-energization of melanoma xenografts and sensitization to temozolomide

Kavindra Nath[1], Jeffrey Roman[1], David S Nelson[1], Mary E Putt[1], Kevin Muriuki[1], Stepan Orlovskiy[1], Dennis B Leeper[2], and Jerry D Glickson[1]

[1]University of Pennsylvania, Philadelphia, PA, United States, [2]Thomas Jefferson University, Philadelphia, PA, United States

Using ^{31}P magnetic resonance spectroscopy, we have shown that LND selectively lowers the intracellular pH and decreases ATP levels in human melanoma xenografts. Tumor acidification results from inhibition of lactate export via the monocarboxylic acid transporters and inhibition of pyruvate transport and oxidation via the mitochondrial pyruvate carrier. Energetics is further attenuated by inhibition of electron transport at complex II. Under these conditions, temozolomide accumulates in the tumor as a result of decreases in intracellular pH, which inhibits DNA repair by O^6-alkyltransferase via conversion to dacarbazine and formation of diazomethane, and also inhibits glutathione-S-transferase that deactivates the reactive alkylating intermediate.

3078

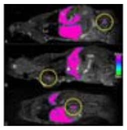

Detection of metastasis-associated macrophages in the lung, lymph nodes and brain using fluorine-19 based MRI cell tracking

Ashley V Makela[1,2] and Paula J Foster[1,2]

[1]Medical Biophysics, Western University, London, ON, Canada, [2]Robarts Research Institute, London, ON, Canada

The escape and invasion of cancer cells and the growth of metastatic tumors is in part due to the role of tumor associated macrophages. The macrophages present in these metastatic sites are called metastasis associated macrophages. This study used ^{19}F-based cellular MRI to detect lymph node, lung and brain metastases arising from breast cancer. A custom built ^{1}H/^{19}F birdcage coil allowed for 'head to toe' mouse imaging, allowing for detection of ^{19}F agent accumulation, with ^{1}H images verifying anatomical location. This information may be useful in understanding the timing and role of macrophages in the metastatic process.

Traditional Poster

Application of Hyperpolarized 13C MRI/MRS

Exhibition Hall 3079-3094 Thursday 13:00 - 15:00

3079

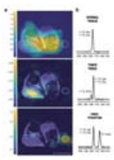

In-vivo imaging of glutamine metabolism to the oncometabolite 2-hydroxyglutarate in IDH1/2 mutant tumors

Lucia Salamanca-Cardona[1,2], Alex J. Poot[1,2], Valentina Di Gialleonardo[1,2], Fabian M. Correa[1,2], Hardik Shah[3], Hui Liu[3], Vesselin Z. Miloushev[1], Kristin L. Granlund[1,2], Justin R. Cross[3], Craig B. Thompson[4], and Kayvan R. Keshari[1,2]

[1]Radiology, Memorial Sloan Kettering Cancer Center, New York City, NY, United States, [2]Molecular Pharmacology Program, Memorial Sloan Kettering Cancer Center, New York City, NY, United States, [3]Donald B. and Catherine C. Marron Cancer Metabolism Center, Memorial Sloan Kettering Cancer Center, New York City, NY, United States, [4]Cancer Biology and Genetics Program, Memorial Sloan Kettering Cancer Center, New York City, NY, United States

2-hydroxyglutarate (2-HG) is an oncometabolite that accumulates in various cancers as a result of mutations in the isocitrate dehydrogenase (IDH1/2) genes and can be used as a biomarker for diagnosis. In this work, we demonstrate the fast conversion of glutamine to 2-HG and use it as a basis for developing a 2-HG *in-vivo* detection method. Using hyperpolarized [1-^{13}C] glutamine and magnetic resonance imaging (MRI), we present the non-invasive unambiguous detection of 2-HG formation with high specificity from glutamine *in-vivo* and real-time in IDH1 and IDH2 mutant tumors.

3080

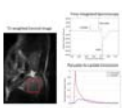

Identifying Immune-Related Metabolic Properties of Pancreatic Cancer via Hyperpolarized Pyruvate Spectroscopic Imaging and NMR Metabolomics

Joseph Weygand[1,2], Prasanta Dutta[1], Jessica Molkentine[3], Yeonju Lee[4,5], Travis Salzillo[1,2], Meifang Yu[3], Jaehyuk Lee[1], Eugene Koay[4], Cullen Taniguchi[4], and Pratip Bhattacharya[1]

[1]Cancer Systems Imaging, University of Texas MD Anderson Cancer Center, Houston, TX, United States, [2]Graduate School of Biomedical Sciences, University of Texas Health Science Center at Houston, Houston, TX, United States, [3]Experimental Radiation Oncology, University of Texas MD Anderson Cancer Center, Houston, TX, United States, [4]Radiation Oncology, University of Texas MD Anderson Cancer Center, Houston, TX, United States, [5]Five Prime Therapeutics, Inc, San Francisco, CA, United States

Although immunotherapy presents an attractive new treatment option for patients with pancreatic cancer, its implementation has been underwhelming. As a critical first step in understanding this failure, we have applied hyperpolarized pyruvate spectroscopic imaging and NMR spectroscopy to interrogate the metabolic properties of pancreatic tumors cultivated in the presence of different immune environments. We observed that the immune environment in which a pancreatic tumor is harvested significantly alters metabolic function and that these metabolic differences exhibit a temporal dependence with respect to tumor development.

3081

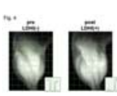

Evaluation of the in vivo on-target effect of a newly developed LDH inhibitor using hyperpolarized 13C Magnetic Resonance Spectroscopic Imaging

Nobu Oshima[1], Shun Kishimoto[2], Keita Saito[2], Dan Crooks[3], Kristin Beebe[3], Kazutoshi Yamamoto[2], Jeffery Brender[2], Ganesha Rai[4], Bryan T Mott[4], David J Maloney[4], James B Mitchell[2], Murali K Cherukuri[2], and Leonard M Neckers[3]

[1]RBB,UOB/NCI, NIH, Bethesda, MD, United States, [2]RBB/NCI, NIH, Bethesda, MD, United States, [3]UOB/NCI, NIH, Bethesda, MD, United States, [4]National Center for Advancing Translational Sciences (NCATS), NIH, Rockville, MD, United States

This study aimed to monitor the impact on metabolic flux in vivo of a newly developed Lactate Dehydrogenase A Inhibitor (LDHI), using hyperpolarized 13C Magnetic Resonance (MR) technology. Using hyperpolarized 13C MR Spectroscopy and Chemical Shift imaging, we found that the LDHI significantly and rapidly suppressed the [1-13C]lactate to [1-13C]pyruvate ratio after single dose administration to mice harboring a MiaPaca (a glycolytic pancreatic cancer cell line) xenograft. These results indicate that the LDHI suppressed lactate production in the tumors. Thus, using Hyperpolarized 13C MRI provides a very useful technology to evaluate in vivo on-target efficacy of LDH inhibitors.

3082 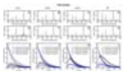

Study of the Tetracycline-controlled Transcriptional Activation of c-Myc in Burkitt Lymphoma B-cell Line P493-6 Using Hyperpolarized [1-13C] pyruvate

Eugen Kubala[1,2,3], Laura Jacobs[4], Julia Kempf[4], Kim A Muñoz Alvarez[1], Rolf F Schulte[3], Steffen J Glaser[2], Markus Schwaiger[1], Marion I Menzel[3], and Ulrich Keller[4]

[1]Department of Nuclear Medicine, Klinikum rechts der Isar, Technische Universität München, Munich, Germany, [2]Department of Chemistry, Technische Universität München, Munich, Germany, [3]GE Global Research, Munich, Germany, [4]III. Medical Department, Klinikum rechts der Isar, Technische Universität München, Munich, Germany

We proved that the transcriptional activation of *c-Myc* expression controlled by tetracycline has a direct influence on lactate dehydrogenase-A (LDH-A) activity in B-cell line P493-6 *in vitro*. Using hyperpolarized [1-^{13}C]pyruvate and ^{13}C magnetic resonance spectroscopy we were able to monitor a reduction of pyruvate to lactate reaction catalyzed by LDH-A. Incubation of the P493-6 cells in a media with 0.1 µg/mL tetracycline for 24 hours reduced the kinetic value of the reaction by 41.8±10.5 %. This proves that the control of *c-myc* has a significant influence on LDH-A activity and can be measured using ^{13}C magnetic resonance spectroscopy with hyperpolarized [1-^{13}C]pyruvate.

3083 

Assessment of lactate dehydrogenase activity in renal cell carcinomas using hyperpolarized 13C pyruvate MR

Renuka Sriram[1], Celine Baligand[1], Hecong Qin[1], Justin DeLos Santos[1], Robert Bok[1], John Kurhanewicz[1], and Zhen Jane Wang[1]

[1]Radiology and Biomedical Imaging, University of California San Francisco, San Francisco, CA, United States

The incidence of renal cell carcinomas (RCCs) has increased significantly over time due to the widespread use of cross-sectional imaging with incidental cancer detection. RCCs vary widely in histological grade and risk of metastasis. However, current imaging techniques cannot reliably differentiate low grade, indolent RCCs from localized but potentially aggressive RCCs, resulting in the over-treatment of many indolent cancers. Increasing evidence has shown that increased glycolysis with lactate production is a dominant metabolic feature of RCCs. In particular, lactate dehydrogenase expression is positively correlated with RCC grade, and a strong predictor of tumor progression and poor prognosis. Hyperpolarized ^{13}C MR allows real time investigation of cellular metabolism, and provides time-resolved metabolic kinetics that reflects flux through enzyme-catalyzed reactions. The purpose of this study is to investigate whether hypeprolarized ^{13}C pyruvate MR can inform on the LDH activity in orthotopic RCC tumor models.

3084 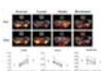

Acute renal metabolic effect of metformin treatment assessed with hyperpolarized magnetic resonance imaging

Haiyun Qi[1], Per Mose Nielsen[1], Marie Schroeder[1], Lotte Bonde Bertelsen[1], Fredrik Palm[2], and Christoffer Laustsen[1]

[1]MR Research Center, Aarhus University, Aarhus N, Denmark, [2]Department of Medical Cell Biology, Uppsala University, Uppsala, Sweden

Metformin is the primary anti-diabetic drug in type-2 diabetes.However, controversy exists on its use in patients with renal impairment.Here we investigated the acute metabolic effects of metformin treatment in rat kidneys,with hyperpolarized ^{13}Cpyruvate and Clark-electrodes.A significantly altered metabolic phenotype was observed 30min post metformin treatment.Anaerobic metabolism was elevated in the cytosol,indicated by increased lactate/pyruvate ratio,and mitochondrial aerobic metabolism was reduced,indicated by decreased bicarbonate/pyruvate ratio.Acute metformin treatment increased renal blood flow with higher O_2 saturation and did not change tubular O_2 consumption.These results indicate that metformin reduces mitochondrial respiration and enhances anaerobic metabolism,even with enough oxygen supply,within only 30min of treatment.

3085 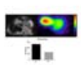

Measuring perfusion in a renal ischemic/reperfusion rat model using hyperpolarized α-Trideuteromethyl[15N]glutamine.

Per Mose Nielsen[1], Rolf F. Schulte[2], Hayuin Qi[1], and Christoffer Laustsen[1]

[1]MR Research Center, Aarhus University Hospital, Aarhus N, Denmark, [2]GE Global Research, Munich, Germany

Renal IRI is a leading cause of AKI in several disease states; currently there are several methods to measure renal perfusion in the clinic, but all suffer under specific drawbacks. Here we present a pilot study using the hyperpolarized perfusion marker α-trideuteromethyl[15N]glutamine in a 40 min unilateral ischemia reperfusion rat model. A reduction of 51% in perfusion was observed in the animal. We therefore believe that α-trideuteromethyl[15N]glutamine is a highly promising molecule in renal perfusion studies.

3086 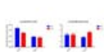

Assessment of metabolism in early renal ischemia/reperfusion injury using hyperpolarized 13C-pyruvate.

Per Mose Nielsen[1], Hayuin Qi[1], and Christoffer Laustsen[1]

[1]MR Research Center, Aarhus University Hospital, Aarhus N, Denmark

Renal IRI is a leading cause of AKI in several disease states; there is a current lack of precise methods to directly assess success of kidney transplant after reperfusion. We here showed how we can measure metabolic function in both the contralateral kidney and post-ischemic 2 min after reperfusion and again after 1 hour of reperfusion. We here saw a very different response compared to metabolic data collected from animals after 24 hours of reperfusion. In this study we induced mild/moderate ischema and it looks like we captured metabolic images in a phase of repair and salvage to maintain normal kidney filtration function in the animals. It seems that severe injury has not yet occurred, or maybe won't occur. Together with perfusion measurements or kidney filtration measurements this method might hold some clinical value.

3087 

Hyperpolarized Imaging of Lithium-Induced Modulation of [1-13C]Pyruvate Metabolism in the Heart

Jonas Steinhauser[1], Grzegorz Kwiatkowski [1], Patrick Wespi[1], and Sebastian Kozerke[1]

[1]Institute for Biomedical Engineering, University and ETH Zurich, Zurich, Switzerland

Lithium is the first-line drug used in bipolar disorder, a chronic psychiatric illness characterized by severe biphasic changes in mood. Lithium has a narrow therapeutic window and has shown cardiac side effects. The present work demonstrates the detectability of lithium induced changes of mitochondrial metabolism in cardiomyocytes by employing hyperpolarized [1-13C]pyruvate magnetic resonance imaging of the in-vivo heart. In healthy rats, lithium is shown to increase mitochondrial metabolism and decrease glycolytic lactate production indicating a potential role of lithium in the heart.

3088 

Influence of Isoflurane Anesthesia on Assessment of Cardiac Metabolism Using Hyperpolarized [1-13C] Pyruvate

Jonas Steinhauser[1], Grzegorz Kwiatkowski [1], Patrick Wespi[1], and Sebastian Kozerke[1]

[1]Institute for Biomedical Engineering, University and ETH Zurich, Zurich, Switzerland

Isoflurane is frequently used in hyperpolarized [1-13C]pyruvate studies. Even though literature suggests direct interaction with mitochondrial metabolism, the influence of the compound on cardiac metabolism has not been assessed in detail yet. In the present study the impact of low versus high isoflurane concentration is examined in a cross-over experiment. Results reveal that cardiac metabolism is modulated by isoflurane concentration showing increased lactate and reduced bicarbonate production during high isoflurane dose relative to low dose.

3089 

Maternal-fetal exchange and metabolism followed in real-time by dynamic hyperpolarized 13C imaging on pregnant rats

Stefan Markovic[1], Anne Fages[1], Tangi Roussel[2], Ron Hadas[3], Michal Neeman[3], and Lucio Frydman[1]

[1]Department of Chemical Physics, Weizmann Institute of Science, Rehovot, Israel, [2]NeuroSpin Centre CEA Saclay, Gif-sur-Yvette, France, [3]Department of Biological Regulation, Weizmann Institute of Science, Rehovot, Israel

Monitoring placental metabolism is of particular interest for the early-detection of complications during pregnancy. This study discusses the use of dynamic nuclear polarization (DNP) enhanced ^{13}C MRSI of hyperpolarized pyruvate, that has been injected into pregnant rats. The enzymatic conversion of pyruvate to lactate was followed in real-time in maternal and fetal compartments –including placentas. Lactate ^{13}C signals in placentas could be observed; they peaked significantly later and were longer-lived than both placental ^{13}C pyruvate and ^{13}C signals in maternal organs. Single-voxel analyses for both metabolites in different organs revealed the T_1 relaxation times and kinetics of the Pyr -> Lac transformation.

3090 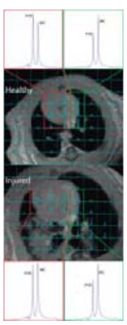

Assessing Gas Exchange via Co-Administration of Hyperpolarized [1-13C] Pyruvate and 13C-Bicarbonate

Nicholas Drachman[1], Stephen Kadlecek[1], Hooman Hamedani[1], Mehrdad Pourfathi[1], Sarmad Siddiqui[1], Yi Xin[1], Harrilla Profka[1], Ian Duncan[1], and Rahim Rizi[1]

[1]Radiology, University of Pennsylvania, Philadelphia, PA, United States

We assess gas exchange in healthy and acutely injured rat lungs by measuring the difference between bicarbonate-to-pyruvate signal-ratio in the right vs. left ventricle of the heart following co-administration of hyperpolarized [1-^{13}C] pyruvate and ^{13}C-bicarbonate.

3091 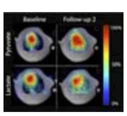

Probing metabolic alterations in lung injury during protective and non-protective ventilation using hyperpolarized [1-13C] pyruvate

Mehrdad Pourfathi[1], Yi Xin[1], Maurizio Cereda[2], Stephen Kadlecek[1], Harrilla Profka[1], Hooman Hamedani[1], Ian Duncan[1], Sarmad Siddiqui[1], Nicholas Drachman[1], Kai Ruppert[1], and Rahim Rizi[1]

[1]Radiology, University of Pennsylvania, Philadelphia, PA, United States, [2]Anesthesiology and Critical Care, University of Pennsylvania, Philadelphia, PA, United States

In this study, hyperpolarized [1-^{13}C]-pyruvate imaging was used to investigate the effect of positive-end expiratory pressure (PEEP) on the stabilization of lung metabolism after injury. Results demonstrated significantly lower lactate-to-pyruvate ratio in rats ventilated with PEEP.

3092 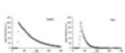

Hyperpolarized 13C-MRI of DMPO and NAC for evaluating oxidative stress in living animal

Keita Saito[1], Deepak Sail[2], Burchelle N. Blackman[2], Hellmut Merkle[3], Rolf E. Swenson[2], James B. Mitchell[1], and Murali C. Krishna[1]

[1]National Cancer Institute, Bethesda, MD, United States, [2]National Heart, Lung, and Blood Institute, [3]National Institute of Neurological Disorder and Stroke

5,5-Dimethyl-1-pyrroline-N-oxide (DMPO) is used to detect reactive oxygen species in vitro, and N-acetyl-L-cysteine (NAC) is an antioxidant. We synthesized ^{13}C-labeled DMPO and NAC, and investigated feasibility of hyperpolarized ^{13}C-DMPO and ^{13}C-NAC for evaluating oxidative stress in mice. Hyperpolarized ^{13}C-DMPO and ^{13}C-NAC provided a single peak at 76 ppm and 174 ppm, respectively, and the T_1 relaxation time was sufficiently long to apply them for mouse imaging. The signals ^{13}C-DMPO and ^{13}C-NAC were also detected in a mouse body after intravenous injection. The results showed ^{13}C-DMPO and ^{13}C-NAC can be applied to some disease models to evaluate oxidative stress in vivo.

3093 Enhancing metabolic imaging of energy metabolism in traumatic brain injury using hyperpolarized [1-13C]pyruvate and dichloroacetate

Stephen J. DeVience[1], Xin Lu[1], Julie Proctor[2], Parisa Rangghran[2], Juliana Medina[2], Elias R. Melhem[1], Rao Gullapalli[1], Gary M. Fiskum[2], and Dirk Mayer[1]

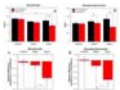

[1]Diagnostic Radiology and Nuclear Medicine, University of Maryland School of Medicine, Baltimore, MD, United States, [2]Anesthesiology and the Center for Shock, Trauma, and Anesthesiology Research, University of Maryland School of Medicine, Baltimore, MD, United States

We investigated the use of dichloroacetate (DCA) in ^{13}C-pyruvate imaging of traumatic brain injury as a way to improve bicarbonate signal strength and to elucidate changes in pyruvate dehydrogenase activity. Rats were injured with a controlled cortical impact and then injected with ^{13}C-pyruvate before and after administration of DCA. Spectrally-resolved imaging was performed on the brain to quantify the resulting pyruvate, lactate, and bicarbonate signals. The bicarbonate signal and bicarbonate-to-lactate ratio were found to be sensitive to traumatic brain injury, and were affected equally by DCA in injured and uninjured hemispheres of the brain.

3094

Hyperpolarized [1-13C]-MRI in an ectothermic reptile

Kasper Hansen[1,2], Per Mose Nielsen[3], Esben Søvsø Szocska Hansen[3,4], Cathrine Williams[1], William Joyce[1], Michael Pedersen[2], Tobias Wang[1], and Christoffer Laustsen[3]

[1]Section for Zoophysiology (Department of Bioscience), Aarhus University, Aarhus C, Denmark, [2]Comparative Medicine Lab (Department of Clinical Medicine), Aarhus University, Aarhus N, Denmark, [3]MR Research Centre (Department of Clinical Medicine), Aarhus University, Aarhus N, Denmark, [4]Danish Diabetes Academy, Odense, Denmark

Many non-mammalian vertebrates hold enormous potential as “model animals” for various fields of basic physiological and biomedical research. Hyperpolarized magnetic resonance imaging (MRI) can provide quantitative *in vivo* information about metabolic processes including major pathways of the citric acid cycle and glycolysis via spectral differences of pyruvate intermediates. The combination of [1-^{13}C]-MRI and model animals exhibiting “selected physiological traits” may be a strong tool for gaining novel insights into relevant metabolic mechanisms. In this pilot study we test, for the first time, the application of [1-^{13}C]-MRI in an ectothermic reptile.
